QC
851
.G73
v.4

Air Ministry
Meteorological Research Committee
MRP 552-652 (non-inclusive)

MRP No.	Title	Author
553	The Formation and Behaviour of Cold Front Waves.	J.S. Sawyer
554	The Upper Air Over Nairobi, 1 degree 16'S 36 degree 51'E 5371 ft. Above M.S.L.	N. Carruthers
556	Wind Forecasts on Empire Air Routes.	C.S. Durst
559	Drop Size distribution in Cloud.	A.C. Best
563	An Analysis of Observations of Humidity in the Upper Troposphere and Lower Stratosphere.	J.K. Bannon
564	The Distance Over which an Aircraft Flying on a Constant Heading May Experience Severe Icing in Convective Cloud Conditions.	R.F. Jones J.G.D. Beimers
566	Report on Charney and Eliassen's One-Dimensional Numerical Method for Calculating Motion of Barotropic Disturbances in a Westerly Airstream.	F.H. Bushby
570	High Level Meteorological Photographic Reconnaissance.	G.W. Hurst
574	Accuracy of Geostrophic Trajectories.	C.S. Durst N.E. Davis
576	A Note on Frost Point Observations in Relation to Aircraft Condensation Trails.	J.K. Bannon
579	Note on the Estimation of Natural Evaporation From Meteorological Data.	F. Pasquill
583	Atmospheric Inhomogeneity on the 50-km. Scale.	R. Frith
591	Report on Zonal, Meridional and Other Indices.	A.G. Forsdyke
593	The Relation Between the Radar Echoes From Cumulus and Cumulonimbus Clouds and the Turbulence Within Those Clouds. (Part II).	R.F. Jones
597	Studies of the Structure of Fronts - Part I.	A.G. Matthewman
598	On the Equation of Diffusion in the Atmosphere.	E. Knighting
601	Index of M.R.P.'s Approved for General Distribution.	

MRP No.	Title	Author
602	The Effect of a Hedge on the Flow of Air.	N.E. Rider
603	The Evaporation of Raindrops.	A.C. Best
604	Notes on the Derivation of True Air Temperature From Aircraft Observations.	D.D. Clark
605	A Test of the Rossby Formula as Applied to the Movement of Long Atmospheric Waves at the 500 mb. level.	E.J. Sumner
609 AD 223003	A Particular Solution of the Power-law Diffusion Equation.	E. Knighting
610	The Occurrence of High Rates of ice Accretion on Aircraft.	A.C. Best
611 AD 223007	Anomalous Sound Reception Experiments, April, 1944 - April, 1945.	R.J. Murgatroyd
612	Day to Day Variations in the Tropopause - Their Causes and Significance.	J.S. Sawyer
613	Thunderstorms of 5th June, 1950 as Seen by Radar.	R.F. Jones
622	Second Report Arising From Charney and Eliassen's Method of Computing Forecast 500 mb. Contour Charts.	F.H. Bushby
624	Forecasting the Formation of Radiation Fog - a Preliminary Approach.	J.M. Craddock D. Pritchard
626	A Study of the Relation between Aerodynamic Drag and Wind Profile Over Grassland.	N.E. Rider
627 AD 223008	Effect of Turbulence on Drop Size Distribution in Cloud.	A.C. Best
631	Severe Clear Air Turbulence Experienced at High Altitude on 2nd and 7th November, 1950.	J.K. Bannon
632	Hemisphere-wide Circulation Patterns and Type Classification.	H.H. Lamb
633	The Distribution of Medium and High Cloud Near the Jet Stream.	J.S. Sawyer B. Ilett
639 AD 223001	Coalescence as a Factor in Drop Size Distribution in Cloud.	A.C. Best
645	Some Statistics of Rate of Rainfall in Southern England.	A.C. Best
646 AD 223018	Seasonal Changes in the Mean Pressure Distribution Over the World and Some Inferences About the General Circulation.	A.H. Gordon

L 5544

M.R.P.601
1st June, 1951.

AIR WEATHER SERVICE
TECHNICAL REFERENCE FILE

AIR MINISTRY

METEOROLOGICAL RESEARCH COMMITTEE

INDEX OF M.R.Ps. APPROVED FOR GENERAL DISTRIBUTION

(Appendix No.8 of M.R.P.200)

M.R.P.	Title	Author
551	Index of M.R.Ps. Approved for General Distribution.	
552	Temperature Inhomogeneity in the Free Air.	R. Frith
553	The Formation and Behaviour of Cold Front Waves	J.S. Sawyer
554	The Upper Air over Nairobi, 1°16'S 36°51'E 5371ft. above M.S.L.	N. Carruthers
556	Wind Forecasts on Empire Air Routes.	C.S. Durst
559	Drop Size Distribution in Cloud.	A.C. Best
563	An Analysis of Observations of Humidity in the Upper Troposphere and Lower Stratosphere.	J.K. Bannon
564	The Distance over which an Aircraft Flying on a Constant Heading May Experience Severe Icing in Convective Cloud Conditions.	R.F. Jones and J.G.D. Beimers
566	Report on Charney and Eliassen's One-Dimensional Numerical Method for Calculating Motion of Barotropic Disturbances in a Westerly Airstream.	F.H. Bushby
574	Accuracy of Geostrophic Trajectories.	C.S. Durst and N.E. Davis
576	A Note on Frost Point Observations in relation to Aircraft Condensation Trails.	J.K. Bannon
579	Note on the Estimation of Natural Evaporation from Meteorological Data.	F. Pasquill
583	Atmospheric Inhomogeneity on the 50-km. Scale.	R. Frith
591	Report on Zonal, Meridional and Other Indices.	A.G. Forsdyke
593	The Relation between the Radar Echoes from Cumulus and Cumulonimbus Clouds and the Turbulence within those Clouds. (Part II).	R.F. Jones
597	Studies of the Structure of Fronts - Part I	A.G. Matthewman

570 we have

[illegible]

G.291651/DC/5/51/170

Incl #11

At the time of issue this report has not been published. Any author desiring to quote this paper should refer to it as "A paper of the Meteorological Research Committee (London).
M.R.P. No.............by Mr.
A copy is available in the Library of the Meteorological Office."

M.R.P. 652
4th August, 1951.

AIR MINISTRY

METEOROLOGICAL RESEARCH COMMITTEE

INDEX OF M.R.Ps. APPROVED FOR GENERAL DISTRIBUTION
(Appendix No. 9 of M.R.P. 200)

M.R.P.	Title	Author
598	On the equation of diffusion in the atmosphere.	E. Knighting
602	The effect of a Hedge on the Flow of Air.	N.E. Rider
603	The Evaporation of Raindrops.	A.C. Best
604	Notes on the Derivation of True Air Temperature from Aircraft Observations.	D.D. Clark
605	A test of the Rossby Formula as applied to the movement of long atmospheric waves at the 500 mb. level.	E.J. Sumner
609	A particular solution of the power-law diffusion equation.	E. Knighting
610	The occurrence of high rates of ice accretion on aircraft.	A.C. Best
611	Anomalous sound reception experiments, April, 1944 - April, 1945.	R.J. Murgatroyd
612	Day to day variations in the tropopause - their causes and significance.	J.S. Sawyer
613	Thunderstorms of 5th June, 1950 as seen by radar.	R.F. Jones
622	Second report arising from Charney and Eliassen's method of computing forecast 500 mb. contour charts.	F.H. Bushby
624	Forecasting the formation of radiation fog - a preliminary approach.	J.M. Craddock and Dorothy Pritchard
625	RESEARCH PROGRAMME 1951/52.	
626	A study of the relation between aerodynamic drag and wind profile over grassland.	N.E. Rider
627	Effect of turbulence on drop size distribution in cloud.	A.C. Best
631	Severe clear air turbulence experienced at high altitude on 2nd and 7th November, 1950.	J.K. Bannon
632	Hemisphere-wide circulation patterns and type classification.	H.H. Lamb
633	The distribution of medium and high cloud near the jet stream.	J.S. Sawyer and Betty Ilett

/639

M.R.P.	Title	Author
639	Coalescence as a factor in drop size distribution in cloud.	A.C. Best
645	Some statistics of rate of rainfall in Southern England.	A.C. Best
646	Seasonal changes in the mean pressure distribution over the world and some inferences about the general circulation.	A.H. Gordon
650	A study of the rainfall of two selected synoptic situations.	J.S. Sawyer

This report has not yet been published and is to be treated CONFIDENTIALLY. Its contents must not be quoted.

553

M.R.P. ~~559~~
S.C.II/51
17th April, 1950.

ATI - 188394

AIR MINISTRY

METEOROLOGICAL RESEARCH COMMITTEE

The formation and behaviour of cold front waves

by

J.S. Sawyer (Meteorological Office)

AIR WEATHER SERVICE
TECHNICAL REFERENCE FILE

SUMMARY

The early stages of the formation of 56 cold front waves are examined with particular emphasis on the associated thickness pattern. The results are studied in relation to various theories of wave depressions. The evidence is found consistent with the hypothesis that frontal zones more than 1200 miles long are unstable for wavelike distortions if none exist; however observed waves are usually initiated by kinematic distortion of the front or by the circulation caused by cyclonic development associated with broad features of the upper flow. It is conjectured that the rate of growth of unstable waves is too slow to permit the growth of very small disturbances to significant dimensions. Kinematic distortion of the front may be either orographic or the result of the flow around adjacent pressure systems. The development of waves which are not the result of such frontal distortion occurs in areas in which cyclonic development should be expected on Sutcliffe's theory.

The movement of the waves and other features of their behaviour in the earlier stages are examined.

Contents

1. Introduction

2. Plan of Investigation

3. The cold front wave of 23rd May, 1948

4. Circumstances under which cold front waves form

5. Characteristics of cold front waves

    (a) Areas of formation

    (b) Direction of motion

    (c) Speed of newly formed waves

    (d) Deepening of newly formed waves

    (e) Other characteristics of cold front waves

6. The theory of wave formation in the light of present results

7. Application of results to forecasting

Appendix

List of waves studied.

/ The

The formation and behaviour of cold front waves

1. Introduction

A difficult problem which frequently presents itself to the forecaster, is whether or not a given cold front will give rise to frontal waves. The present investigation was undertaken in order to discover how far this question can be answered and in the hope that the results may form a useful guide in the construction of "prebaratic" charts. Attention has therefore been directed throughout the work to the earliest stages in the formation of cold front waves, and the results are not intended to apply to the behaviour of waves of substantial amplitude which have been in existence for 24 hours or more.

The classical Norwegian theory of "wave" cyclones has regarded the frontal zone as in unstable equilibrium, and has sought to show that any small perturbation will grow and take on the characteristics of the recognised "wave depressions". The theory was originally put forward by J. Bjerknes and H. Solberg (1) in 1922 and was given its most complete mathematical formulation by V. Bjerknes, J. Bjerknes, H. Solberg and T, Bergeron in 1932 (2). If this view on cyclogenesis is correct it would be inappropriate to search for criteria for the formation of a frontal wave, apart from such criteria as may determine whether or not a front is unstable in this respect; it is also unlikely that any precision would be attainable in specifying the probable area or time of formation of a new wave disturbance.

On the other hand it has been suggested by R.C. Sutcliffe (3) that the formation of a wave on a front is not an accidental effect of frontal instability, but is a consequence of factors, not necessarily associated with the front itself, which lead to cyclogenesis in the area concerned. This view is also implicit in the writing of Sir Napier Shaw (4).

An intermediate point of view has been adopted by many authors, namely that although the wave is an unstable oscillation of the polar front the initial perturbation is not usually a small one. This idea first appears in the analysis of waves on a quasi-stationary front by T. Bergeron and G. Swoboda (5), where the distortion of the front is attributed to an old depression in the polar air. The same point of view is expressed by many other authors, notably by W.C. Kaye and C.S. Durst (6) C.K.M. Douglas (7) and C.J. Boyden (8).

The Current outlook on the problem of the formation of wave depressions is admirably expressed by H.R. Byers (9) who writes:- "The Norwegians have sought to prove that the developments along the fronts in the low levels precede the high level perturbations. Strong evidence is also available to support the opposing argument, that perturbations have their seat in the upper atmosphere .... It is likely that mountains, land and sea temperature contrasts and ocean-current contrasts can affect the air flow and divert it to create a wave. It has also been found that many waves are started by some nearby disturbance. .... Experience has shown that a very important effect comes from the appearance of an upper-level trough of low pressure in a trough line making a considerable angle (approaching 90 deg.) with the front".

If useful criteria are to be established for forecasting the formation of frontal waves it is necessary to decide between these points of view. It is possible that different factors operate on different occasions, but if this is so, it is important that we should know the relative importance of the several processes of cyclogenesis, and the circumstance under which each is dominant.

Before proceeding to describe the scheme of the present investigation, it is convenient to consider in a little more detail the various theories of cyclogenesis on slow-moving fronts.

The mathematical basis of the Norwegian theory of unstable waves on the polar front was based on the assumption of two homogeneous air masses of different temperature separated by a surface of discontinuity. The mathematical treatment shows that unstable waves are possible on such a discontinuity surface with a wavelength in a range from about 500 to 3000 Km, that they resemble cyclone waves, that their instability increases with the shear between the two currents, and that they move with a speed between that of the warm and cold currents but closer to that of the warm air. It is doubtful if any more specific results of the analysis can be regarded as applicable to the atmosphere, particularly as it is now known that only part of the temperature contrast at fronts is concentrated at the frontal surface, and that substantial temperature gradients within the air masses are normal (E. Palmen and C.W. Newton (10)). However, mathematicl studies of wave motion in baroclinic currents without a frontal discontinuity have recently been made by J.G. Charney (11) and E.T. Eady (12). These studies confirm the existence of unstable waves of wavelength about 1000 Km in the oscillations of a steady atmospheric current in which there is a temperature gradient across the stream, corresponding to a broad zone of transition instead of a front. Although the treatments differ in many respects, they agree that the wave motion is more unstable the greater the vertical wind shear and the steeper the vertical temperature lapse. Eady finds it necessary to consider the effect of condensation in warming the upward branch of the circulation in order to explain unstable disturbances on the observed scale, but Charney's results indicate the possibility of unstable disturbances without taking condensation into account.

It has been observed that the distortion of the frontal surface to form a wave is associated with a distortion of the strong flow in the upper troposphere, the "jet stream". J. Bjerknes (13, 14 and 15) regards the upper perturbation as caused by the initial wave on the frontal surface, and uses the non-balanced character of the disturbed upper flow to explain the divergence of air above the wave and consequent deepening - this is a qualitative approach to the instability problem discussed by Charney, but it lends itself to discussion of waves which have grown beyond the stage of small amplitude. Opposed to the viewpoint of Bjerknes, a recent paper by R. Berggren (16) regards the distortion of the jet stream as the primary disturbance, and suggests that the distortion of the surface front is a secondary effect.

R.C. Sutcliffe has suggested that the problem may be (17) approached from an entirely different angle. He has shown theoretically that the main features of the distribution of cyclonic and anticyclonic development may be deduced from the superimposed patterns of flow in the upper and lower troposphere, or more conveniently from the surface isobars and the "thickness pattern" for a layer between two isobaric surfaces extending through most of the troposphere. If the flow at all levels near a front were straight and parallel, there is no reason to expect cyclonic development on Sutcliffe's theory and the method is not directly applicable to discussing the stability of small perturbations. However, although the straight parallel stream is the starting point for most instability theories, nevertheless it is rarely found on the synoptic chart even in approximate form, and the question arises as to whether Sutcliffes theory can be applied to determine areas of cyclogenesis along the front from the configuration of the thickness pattern.

The present investigation was planned with particular emphasis on the use of the thickness pattern together with the surface pressure field as a tool in forecasting the formation and behaviour of frontal waves. This course was chosen because of the advantages of the thickness pattern as a forecasting tool in other respects (18), and because suitable charts are drawn in the course of routine forecasting at C.F.O. and as the basis of the medium range forecast experiment. Sutcliffe's theory is directly applicable to these charts, and some emphasis has been given to testing its practical utility in the present problem.

Careful analysis of synoptic charts will often reveal very small distortions of a slow-moving cold front. These may have an amplitude of only 50 miles and wavelength of only 200-300 miles. Such small waves were noted by T. Bergeron and G. Swoboda (5) and are sometimes referred to by forecasters as "ripples". They can be traced only in a dense network of synoptic stations. The formation of these short-wavelength disturbances has not been studied in the present paper.

2. Plan of the investigation.

In order to obtain a representative set of examples of the formation of cold front waves, it was decided to consider all the waves forming within a definite area during a period of one year. The area selected was that covered by the forecasters main working chart at C.F.O. (Form 2331 - see fig. 13); it covers the eastern half of the Atlantic and Europe. The period studied was February, 1948 to January, 1949. The preliminary selection of examples was made on the C.F.O. working charts, F.2231. All frontal waves appearing on these charts were examined to determine whether or not they originated within the area of the chart. Those waves appearing to develop within the selected area were reanalysed in order to provide a homogeneous and reliable set of examples for further study.

During the reanalysis several cases were rejected for some of the following reasons:-

(a) the frontal analysis was incorrect and the disturbance did not form as a frontal wave (sometimes the disturbance was present before the front),

(b) the wave could be traced back outside the selected area,

(c) the wave did not exist at all.

A few examples were also eliminated because they formed as waves on a warm front and not on a cold front. 56 examples remained in which the formation of a frontal wave was reasonably certain and could be identified over a series of charts. Revised frontal positions were determined where necessary to maintain continuity.

For each of the 56 examples one synoptic (surface) chart was carefully redrawn in conformity with the revised analysis in order to represent the synoptic situation about the time of the first appearance of the wave. The pressure field was converted to give the contours of the 1000 mb. surface which were drawn at 100 foot intervals on a scale of $1:15 \times 10^6$. Superimposed on these were drawn thickness lines for the 1000-500 mb. layer at the same epoch. For this purpose the thickness pattern was obtained from the working charts at C.F.O. by graphical subtraction of the 500 and 1000 mb. contours with some modification to improve the fit with observations; thickness lines were drawn at 100 foot intervals. This series of charts formed the basic material for the numerical evaluation of the vorticity of the thermal wind field, ζ', and the evaluation of Sutcliffe's thermal development term, $V'.\partial\zeta'/\partial s$. The track of the wave was also indicated on these charts for comparison with the pressure field and thickness pattern.

It is well known to forecasters that waves do not form readily on short cold fronts of a few hundred miles in length and, indeed, the theoretical studies suggest that short frontal waves are stable and are therefore unlikely to arise spontaneously. Among the 56 selected cases of wave formation there was none which occurred on a front less than 1200 miles in length. Therefore, when it was decided to study also those cold fronts which did not form waves, attention was confined to fronts more than 1200 miles long. All such fronts without waves which extended across the selected area during the period February 1948 - January 1949 were listed and examined; they provided material for assessing the success of various criteria suggested for predicting the formation or non-formation of waves.

One example has been examined in rather more detail than the others; in this a wave formed over the Bristol Channel at 0600 on 23rd May, 1949. The developments on this occasion are presented in the following section as **they** illustrate many of the features regarded as typical of wave formation and demonstrate the technique employed in study of other cases. The development took place within a close network of surface and upper air observations and lends itself to detailed analysis.

3. The Cold front wave on 23rd May, 1948.

On the 22nd May, 1948, a cold front moved southward over the British Isles and an active wave depression developed on this front. An independent low pressure centre first appeared over th Bristol Channel on the morning of 23rd May, 1948. This centre deepened slowly and moved northeast into the Skagerrak. Before the main wave developed another distortion of the front had appeared over Eastern England, but this moved southeast into the Netherlands and flattened out again.

The synoptic situation before the formation of either disturbance of the front is illustrated by Fig.1 which shows situation at 1500 G.M.T. 22nd May, 1949. It will be seen that the front was not clearly defined on the surface chart by the wind field, pressure tendencies or cloud structure. The rain accompanying the front was slight and irregularly distributed over an area some 150 miles behind the front; probably the only extensive area of rain was over southeast Scotland. Fig.4(a) shows the thickness lines for the layer between the 1000 and 500 mb. surfaces over a wider area. It will be noted that there is a strong concentration of thickness lines lying parallel to the front along the whole of its extent; this indicates that a strong temperature contrast existed across the frontal zone despite the absence of clearly defined frontal phenomena on the surface chart. It will also be seen that a trough-line in the pattern of thickness lines, a "thermal trough", extended from the Norwegian Sea to the west coast of Scotland and that the advection resulting from the flow pattern as given by the 1000 mb. contours (also shown in Fig.4(a)) was tending to extend the trough southward and increase its distortion. This latter effect is the result of the strong southward movement of the air over the British Isles, combined with the slower motion near Iceland and the tendency of the current over the North Sea to turn towards the east into Denmark.

The subsequent developments are illustrated by Figs.2 and 3. The isochrones of frontal position in figure 2 show the rapid appearance of the small distortion over eastern England and its subsequent disappearance over Germany; also the later formation of the longer wave over southwest England and its growth into the form typical of a frontal depression. Figures 3 (a) (b) and (c) illustrates the movement of the rain areas and the isallobaric low associated with the two waves. It is significant that both the rain areas and the isallobaric lows appear to have drifted slowly south with the front for a short initial period; subsequently they moved more quickly eastward soon after the waves were established. The development of the rain area simultaneously with the formation of the wave may also be remarked; and the fact that the rain area and isallobaric low are separated by a distance of 200 to 300 miles in the early stages.

The changes of the thickness pattern accompanying the formation of the waves is indicated by Figs. 4, 5 and 6 which show the situation at 12 hour intervals. These charts have also been used to examine the applicability of Sutcliffe's theory to this case of cyclonic development.

Sutcliffe (17) has shown that, on the basis of certain assumptions, the cyclonic development may be represented by the expression

$$-\frac{1}{l}\left\{V'\frac{\partial\zeta'}{\partial s} + 2V'\frac{\partial\zeta_0}{\partial s}\right\} \qquad \text{............ (1)}$$

in which V' is the thermal wind velocity

ζ' is the vorticity of the thermal wind field

ζ_0 is the vorticity of the low level flow pattern

$\partial/\partial s$ denotes differentiation along the direction towards which the thermal wind is directed

and l is the coriolis parameter $2\omega \sin \phi$. The second term, $2V' \partial\zeta_0/\partial s$ in the expression (1) leads to a field of development which will result in the displacement of existing vorticity systems in the lower atmosphere in the direction of the thermal wind. It cannot itself account for the formation of new centres of vorticity in the lower atmosphere, and is mainly responsible for the motion of pressure systems with the thermal wind. It will be referred to as the "thermal steering term".

On the other hand the first term, $V' \partial\zeta'/\partial s$ in (1) depends only on the thermal field itself and is likely to be significant in producing new centres of vorticity and new pressure centres. It will be referred to as the "thermal vorticity term" and much of the present investigation has been devoted to the study.

Both terms, the "thermal steering" and "thermal vorticity" terms, have been evaluated for the situations illustrated in Figs. 4(a), 5(a) and 6(a) and are displayed in the accompanying figs. (b) separately and (c) added together. For this purpose, geostrophic motion is assumed and the thermal wind is evaluated over the layer 1000 to 500 mbs. It might have been regarded as more appropriate to evaluate the expression over the whole of the tropopause, say 1000-300 mb., but attention was confined to the 1000-500 mb. thickness charts as these are more readily available and in more general use. The effect on the field distribution of the values of expression (1) would not have been large if the layer 1000-300 mb. had been used; the magnitudes of the values would have been increased by about a half and the "thermal vorticity term" would have received slightly greater weight in the distribution of development finally calculated.

It is noteworthy that the formation of the waves took place in very close association with a marked maximum of the "thermal vorticity term" - there are indeed signs of two maxima one associated with each wave. The "thermal steering term" was insignificant at first but rapidly grew as the main wave developed; this is in conformity with the initial slow movement of the area of development and its subsequent acceleration eastward as indicated by the behaviour of isallobaric low and rain areas. In examining Figs. 4, 5 and 6(b) and (c) the uncertainty of the thermal field and the difficulty in making precise measurements of second differentials should be borne in mind; the differences between the expected development areas and those observed certainly lie within the experimental error.

In order to examine the front in more detail, north-south cross-sections have been drawn along longitude 50°W (Fig.7). These illustrate that the front was thermally well defined in the middle and upper troposphere; a "jet stream" of about 100 kts. was present situated in accord with the model suggested by E. Palmen and C.W. Newton (10). No significant change in the thermal or dynamical structure of the front took place during the formation of the waves except for a slight increase in slope from 1 in 100 to 1 in 75.

The jet stream itself underwent a rapid displacement simultaneously with the formation of the wave. The position of the axis of the jet at 300 mbs. and its changes are shown in Fig. 8.

4. The circumstances under which cold front waves form.

During the selection of examples it became apparent that, in a number of the examples of cold front waves, the distortion of the front was the necessary consequence either of the disturbance of the flow round a range of hills, or of the flow pattern imposed near the front by a depression or other synoptic system having no connection with the front itself. Orographic distortion of a front is illustrated in Fig.9 and distortion by neighbouring pressure systems in Fig.10(a) and (b). In some of these cases the wave was only transitory, but in most it persisted and behaved in a manner similar to those waves which appeared to arise spontaneously.

It was considered impractical to devise an objective criterion which would separate those developments which were spontaneous from those which were induced orographically or by other pressure systems; on the other hand, it was considered desirable to search for criteria for wave formation primarily among those cases in which the distortion of the front would not have been anticipated kinematically. The 56 examples of new waves were, therefore, reviewed and classified by inspection as either "induced" (I) or "non-induced" (U). Cases of doubt were placed in the former category, in order that in all examples classified as "non-induced" (U) either there was some real instability or another cause of formation must be sought. 25 waves were classified as "induced" and 31 as "non-induced".

An analysis of the thickness pattern (1000-500 mb.) accompanying the formation of the 56 selected waves was made on the basis of the thickness models presented by R.C. Sutcliffe in M.R.P. 420 (3). This classification was made by inspection of the thickness patterns which were drawn, as described in section 2. The number of cases of wave formation in areas classified by Sutcliffe as anticyclogenetic A and cyclogenetic C is given in Table I, together with those in which the pattern was indeterminate or the formation too near the A/C boundary to permit classification. The table is subdivided according as the formation was associated with ridge or trough, confluence or difluence.

Table I - Classification of thickness patterns associated with the formation of cold front waves.

Type of Wave.	Anticyclogenetic (A)									Indeterminate									Cyclogenetic (C)										
	Trough			Ridge			Straight			Trough			Ridge			Straight			Trough			Ridge			Straight			Sinusoidal	
	Confluent	Difluent	Parallel	Confluent	Difluent	Parallel	Confluent	Difluent	Parallel	Confluent	Difluent	Parallel	Confluent	Difluent	Parallel	Confluent	Difluent	Parallel	Confluent	Difluent	Parallel	Confluent	Difluent	Parallel	Confluent	Difluent	Parallel	Confluent	Parallel
Non-induced (U)	-	2	-	-	-	-	-	-	-	-	-	-	-	-	-	-	-	3	5	5	12	-	1	1	-	-	-	-	2
	2			0			0			0			0			3			22			2			0			2	
Induced (I)	-	-	-	-	-	-	-	-	-	-	-	-	-	1	-	-	-	6	2	3	8	1	1	1	1	1	-	-	-
	0			0			0			0			1			6			13			3			2			0	
Total	-	2	-	-	-	-	-	-	-	-	-	-	-	1	-	-	-	9	7	8	20	1	2	2	1	1	-	-	2
	2			0			0			0			1			9			35			5			2			2	
	2									10									44										

Subsequently, charts of the thermal vorticity, ζ' were constructed for the time and area of the formation of each of the 56 waves; from these the "thermal vorticity" term, $- V' \partial\zeta'/\partial s$ was calculated over an area surrounding the formation of the new wave. It was clear from inspection of the charts that there was an association between the formation of waves and positive areas in the field distribution of the "thermal vorticity term". The new wave tended to appear first towards the edge of the positive area towards which the thermal wind is directed. This is not suprising because the "thermal steering term" is likely to lead to the displacement of newly generated cyclonic vorticity in the direction of the thermal wind. In a considerable number of examples, but not all, a definite local maximum of the "thermal vorticity term" could be associated with the formation of the new wave as in the example of 23rd May, 1948, - see fig.5.

The examples were classified according as to whether or not the area should have been regarded as cyclogenetic on the basis of Sutcliffe's theory, i.e. associated with positive values of $-V' \partial\zeta'/\partial s$. Some allowance was made for the observed tendency for the development to be displayed in the direction of the thermal wind. The results of this analysis are given in Table II,

Table II - Number of waves forming in areas classified as cyclogenetic and non-cyclogenetic on Sutcliffe's theory.
(based on numerical evaluation of the thermal vorticity term).

	In accord with Sutcliffe's theory. $-V' \partial\zeta'/\partial s > 1.0\ hr^{-2}$ or formation near boundary of region of strong + values towards boundary in direction of the thermal wind. (1)	Doubtful $V' \partial\zeta'/\partial s$ small and uncertain (2)	Not in accord with Sutcliffe's theory $V' \partial\zeta'/\partial s < 0$ or definitely not substantially greater than 0 (3)
Non-induced U	22	3	6
Induced I	13	2	10
Total	35	5	16

The results summarised in Table II indicate conclusively that a close association exists between the formation of waves and positive areas of the "thermal vorticity term". The separation of cases into "non-induced" and "induced" was done without reference to the thermal distribution, and the different distribution of positive and negative values of $-V' \partial\zeta'/\partial s$ in the two classes is a strong indication that there is a real distinction between them. From the approximately equal number of positive and negative values of the thermal vorticity term among the examples classified as "induced", we may conclude that the existence of an area of positive values of $-V' \partial\zeta'/\partial s$ is not a major factor in the formation of these waves. On the other hand, the strong preponderance of positive values in association with waves of the "non-induced" class suggests that a positive area of the "thermal vorticity" term is needed for the "spontaneous" development of a wave. The table is not conclusive in this respect because of the existence of six cases apparently in conflict with the theory; however, it must be recalled that the network of upper air observations is not adequate to establish the thickness pattern with certainty and a re-examination of these waves showed that they all formed in a rather open network of observations over the Atlantic. It is considered that several, if not all, of these six cases may be the result of erroneous drawing of the thickness pattern.

We turn now to Table I in which the classification of the thickness pattern into anticyclogenetic and cyclogenetic on Sutcliffe's theory was made by inspection without numerical measurement. As in Table II, a strong association of wave development with cyclogenetic areas on Sutcliffe's theory is observed, less strong in respect of "induced waves" than "non-induced". The cyclogenetic area in the "lee" of a thermal trough is the most common situation for wave development, accounting for 35 out of the 56 waves, but wave development also occurs in other types of cyclogenetic area on Sutcliffe's theory.

The close association between cold front waves and the cyclogenetic area in advance of the thermal trough is made clear by Fig.11, which presents a histogram of the distance of the formation of the wave from the axis of the nearest thermal trough; 35 out of the 56 examples formed between 200 and 600 miles to the "lee" (i.e. normally to the east) of the trough line. However, the structure of a cold front and its role in synoptic systems implies that it usually lies to the east of a cold trough, and the frequency of new waves in such areas cannot be attributed entirely to the cyclogenetic nature of the upper wind field.

In a previous report on the use of thickness patterns in forecasting secondary formation (17), it was noted that slow moving secondaries form on cold fronts in areas just to the left of strongly difluent thermal patterns. Three of the waves selected in the present study were accompanied by such thermal patterns and each of these was slow moving; on the other hand, there were several waves which were slow moving but not associated with a notably difluent thermal pattern.

In a view of the minor discrepancies between Table I and Table II a comparison was made between the visual estimates of the sign of the "thermal vorticity term" and its subsequently calculated value. The comparison is presented in Table III. The definitions of rows (1) and (2) in Table III do not correspond exactly with the definitions adopted in Table II columns (3) and (2) so that total are not the same.

Table III - Comparison between the sign of the thermal vorticity term as estimated from inspection of the thickness pattern and as evaluated numerically.

Calculated \ Estimated			Estimated		
			Not-cyclogenetic		Cyclogenetic
			$-V' \partial \zeta'/\partial s < 0$	$V' \partial \zeta'/\partial s \doteqdot 0$	$-V' \partial \zeta'/\partial s > 0$
Calculated	Not cyclogenetic (1)	$-V' \partial \zeta'/\partial s < 0$	2	2	6
	(2)	$V' \partial \zeta'/\partial s \doteqdot 0$	0	4	7
	Cyclogenetic (3)	$-V' \partial \zeta'/\partial s > 0$	0	4	31

One of the factors which guide the forecaster in placing new waves on a "prebaratic" chart is the spacing of individual pressure systems. Long trailing fronts are regarded as more likely to form waves than short moving cold fronts. The length was measured of all the cold fronts on which new waves formed in the period of study, and the frequency distribution is presented in histogram form in Fig.12. For this purpose the length was measured in a straight line on the chart from the "high pressure" end of the front to the most distant point of the front towards the lower pressure.

It is noteworthy that in no case did a new wave form on a cold front which extended less than 1200 miles forward from the following ridge of high pressure.

It was noted that, among the examples of wave formation studied, there were several in which the first distortion of the front was apparent while it was still moving quickly. No further study was made of the speed of fronts which formed waves.

In order to reach any valid conclusion regarding the conditions under which cold front waves form it is necessary to examine not only those fronts which form waves, but also those which do not. Since no new waves were found on fronts less than 1200 miles long, it was considered unnecessary to study such fronts further; by this means a very large number of cold fronts were eliminated from the study. Over the same period and area as used in the selection of examples of new waves, 39 cold fronts were found which were more than 1200 miles long and on which no new wave formed. The selection was made on the analysed surface chart alone, but the associated thickness pattern was subsequently examined. It was then found that a number of the fronts were only minor or weak features of the thermal field and for that reason might have been regarded as unlikely to form significant disturbances.

In order to separate the thermally significant cold fronts from such minor or less significant features, the following criterion was imposed, viz:-

A. The front should be associated with a thermal gradient approximately at right angles to the front represented by a thermal wind of 25 Kt. or more over the range 1000-500 mb. for a distance along the front of at least 1200 miles.

This criterion was satisfied by all but 3 of the fronts of the previous analysis which formed waves; it was satisfied by only 13 out of the 39 fronts which did not form waves. These results are exhibited in tabular form in Table IV.

Table IV - Analysis of cold fronts extending for more than 1200 miles during period Feb. 1948 - Jan. 1949 - Area of Form 2331.

	Number of fronts satisfying criterion A above.	Number of fronts not satisfying criterion A above.	Total
Fronts forming waves	52	3	55
Fronts not forming waves.	13	26	39
Total	65	29	94

It may be concluded that most thermally significant fronts which exceed 1200 miles in length do form waves. Of the 13 fronts which satisfied criterion A most extended through a thickness pattern which indicated cyclonic development on Sutcliffe's theory. Nevertheless, on some of them it is unlikely that an experienced analyst would have expected wave development because the front was moving quickly forward throughout its length. Inspection of the thickness patterns does not suggest that any rule for wave development can be laid down on the basis of the thickness pattern alone, which will enable the fronts with wave formation to be separated from those without. This does not rule out the possibility that careful measurement of the vorticity field might provide such a distinction.

To summarise the results of this study on the formation of cold front waves we observe that:-

(1) Wave secondaries form only on cold fronts which are defined over a length of 1200 miles and most such fronts form waves.

/ (2)

(2) Some of these waves are the result of the distortion of the front by external influences, ranges of hills or other pressure systems.

(3) Other waves, the majority, can be explained on the basis of Sutcliffe's theory of development.

(4) There are few if any waves which form with neither one or other of the processes (2) or (3) operating, but there are a few cases in which these processes might be expected to operate but no wave forms.

(5) There is no unique form of thickness pattern (trough, ridge, difluence etc.) which is associated with the formation of cold front waves; but formation 200 to 600 miles east of a thermal trough is very common.

5. Characteristics of cold front waves.

In the following sub-sections the data collected during the present study has been used to study the behaviour of the waves during their first 24 hours. The direction of motion, speed and deepening is discussed in relation to the results of other investigators, but it is important to remember that the statistics given here are typical of a special class of waves, those newly formed. Owing to their small amplitude it is difficult to obtain as accurate results from the study of newly formed waves as would have been possible if selected waves of larger amplitude had been used. No attempt has, therefore, been made to discuss the theoretical aspects of the relations observed; it is considered that this should be done on the basis of statistics in respect of disturbances selected with this purpose in view.

5(a) Areas of formation.

Figure 13 presents the positions at which the 56 re-analysed cold front waves first appeared. The selection was restricted to waves forming within the area of Form 2331 and the boundary of this chart is also shown. The occurrence of wave formation appears to be more frequent south of latitude 53°N than to the north; this is even more clear when the "induced" waves are ignored. The distribution is similar to that presented by Gentry (20) in respect of this area.

The formation of waves on fronts after crossing the Alps was ignored in the original selection of cases as primarily due to orographic influences. Fig.13 is therefore not representative over N. Italy and the western Mediterranean.

5(b) Direction of motion.

It was originally pointed out by S. Bjerknes and Solberg (1) that warm sector depressions move in a direction approximately parallel to the isobars in the warm sector; observational verification of this was presented by E. Palmen (21). More recently the motion of depressions has been related to the horizontal temperature distribution and it has been noted that depressions tend to move in the direction of the thermal wind over the centre ("thermal steering") (see Douglas and Harding (22)). Steering of young depressions by upper winds at various levels has also been recognised widely in Germany and America.

In order to examine the value of rules based on these ideas, the motion of the 56 selected waves has been analysed in relation to the warm sector isobars and the thermal wind over the tip of the wave. For this purpose the average motion of the disturbance over the first 24 hours has been used; the position of the centre is determined from the apex of the wave in the earliest stages, but the centre of lowest pressure is used as defining the disturbance when formed. The direction of the warm sector isobars, and thermal winds were measured as nearly as possible to the time of first appearance of the wave.

Histograms are presented as figure 14 and 15 showing the frequency of various directions of motion of the wave relative to the warm sector isobars and thermal wind. In most cases the wave moved within 20 degrees of the directions both of the warm sector isobars and the thermal wind; the scatter about the thermal wind is slightly larger than about the direction of the warm sector isobars, but this is as likely to be due to uncertainty of the thermal wind as to any real difference. The distribution of direction is almost symmetrical with respect to both the thermal wind the warm sector isobars. However, J.E. Miller (23) found that the 24-hour motion of newly formed waves averaged 20° to the left of the 3 Km isobars over the centre at the time of formation, but obtained better agreement with the mean direction of the 3 Km isobars during the 24-hour period.

In order to test whether the relation of the direction of motion to the warm sector isobars could be improved fore forecasting purposes by use of the thermal wind, the departure from the direction of the warm sector isobars (α) has been correlated with the angle between the thermal wind and the warm sector isobars. (β). The correlation coefficient is $+ .37 \pm .11$ and the regression equation

$$\alpha = + .34\,\beta + 0.7$$

(α and β are in degrees)

This suggests that the best estimate of the direction of motion of a newly formed wave lies about halfway between the direction of the warm sector isobars and the thermal wind direction over it.

The relationship with the thermal wind found here for new wave depressions is appreciably closer than found by J.M. Austin (24) for cyclones of all types when comparing their direction of motion with both upper contours and isotherms. The fact that all types of depression were treated together probably also accounts for the failure of W.C. Palmer (25) to establish satisfactory forecasting rules based on steering by upper level currents.

5(c) The speed of newly formed waves.

Figure 16 presents in histogram form the frequency of various speeds among the 56 selected waves. For this purpose the speed used has been an average over the first 24 hours after the wave first formed, but the speed over this period was reasonably uniform in most cases. A wide range of speed is possible; speeds up to 70 knots were observed. The most common speed for the newly formed waves was between 30 and 40 knots. The waves which formed in strongly difluent thermal patterns were all slow moving.

The speed of the wave, V, has a positive correlation both with the geostrophic wind speed in the warm sector, v_o and with the thermal wind, v' over the apex of the wave. The correlation coefficients are + .37 and + .23 respectively and corresponding regression equations.

$$V = 19 + 0.3\,v_o$$

$$V = 21 + 0.24\,v'$$

The partial correlation coefficient between V and v_o is + .32 and between V and v' is +.16. The partial regression equation is

$$V = 16 + 0.26\,v_o + 0.15\,v'$$

In viewing these results it is important to remember that there is considerable observational error both in the geostrophic wind in the warm sector and in the thermal wind, on account of the limitations of the observational network. This is probably greater in respect of the thermal wind.

A scatter diagram presenting the relation between the speed of the wave and the geostrophic wind speed on the warm sector is given in Fig.17. Figure 17 shows that the geostrophic wind speed in the warm sector is probably an over estimate of the speed of a newly formed wave - about 4/5 of the geostrophic speed would be a better estimate.

On the other hand it may be noted that a number of waves appear to have travelled more quickly than the wind speed at low levels in the warm air. That this may happen has been stressed by R. Berggren (16) and by R.M. Poulter (26) both of whom regard the speed of small waves as more **nearly** equal to the wind speed in the middle troposphere.

Palmen (27) gives empirical formulae for the speed of (a) feeble waves and (b) warm sector depressions. If the units of velocity, V (disturbance), and v (geostrophic) wind speed, are converted to knots and the temperature difference ΔT between the air masses is converted to degrees Fahrenheit these relations become

$$(a) \quad V = 8 + 0.7\,v + 6\sqrt{\Delta T}$$

$$(b) \quad V = 2 + 0.6\,v + 5\sqrt{\Delta T}$$

These relations have been superimposed on Fig.17 for differences of temperature of 0 and 10°F between the air masses; the relation for warm sector depressions is the better fit to the present data.

Austin (21) obtained a negligible correlation of the speed of depressions with the upper winds at various levels above them; also with the thermal winds 850-700 mb. and 700-500 mb. When only depressions which were moving in the direction of the thermal wind were considered, Austin found a correlation of +0.18 with the thermal wind 850-700 mb. and +0.30 with that for the 700-500 mb. layer. These figures compare with the value of +.23 obtained in the present study. The partial correlation is +.17 between the speed of the waves in the present study and the thermal wind when the effect of the warm sector wind speed has been eliminated. Although it is uncertain whether this correlation is significant it does suggest that a real relation exists between the speed of the wave and the thermal wind, but on the present data it appears to have little forecasting value.

A brief examination was made to ascertain if the speed of wave secondaries was influenced by their distance from the thermal trough line, but no significant relation was found.

5(d) The deepening of newly formed wave depressions.

The frequency of various changes of central pressure of the newly formed waves is displayed in figure 19. This shows that the

/ central

central pressure usually falls, most commonly with a change of between 5 and 10 mb. in the first 24 hours. The fall of central pressure does not necessarily indicate intensification in the sense of increasing circulation around the wave, but an examination of the vorticity of the flow near the surface showed that this did increase in most cases. Figure 19 is in close agreement with a similar diagram given by Miller (23) for depressions forming off the east coast of America.

An attempt has been made to relate the deepening of the wave depressions to the numerical value of the "thermal vorticity term," $-V' \partial\zeta'/\partial s$ but no relationship sufficiently close to be of forecasting value was found. In order to obtain a representative value of the thermal vorticity term an average value was taken over a length of 300 miles along the thickness line through the point of formation of the wave in a direction opposed to thermal wind. Correlation coefficients of -0.24 and +0.17 were obtained respectively between the thermal vorticity term and the 24-hour change of central pressure of the wave and the 24 hour change of vorticity in the central region. These are of the expected sign, and the failure to obtain higher correlations is probably in part due to uncertainties of measurement etc. but also to the fact that comparison has been made with the 24 hour change in intensity. The "thermal vorticity term" was evaluated for a single epoch at the beginning of the period; it is probably not representative of the value over the wave during its first 24 hours during which period the wave will have moved some 600 miles or more.

It has been suggested by E.J. Sumner (28) that the vertical stability of the air masses near the centre of the new wave exercises an important control on the rate of deepening, and that the presence or absence of reports of "sferic" might be used as indication of this. In order to examine this relationship the occurrence of "sferic" within 300 miles of each of the new waves was noted during its first 24 hours of existence. However, no significant difference was found in the rate of deepening between those systems associated with reports of "sferic" and those which were not (see figure 19(b)); neither was any relationship observed with the change in vorticity near the centre.

5(e) Other characteristics of cold front waves.

It was noted during the course of the investigation that in many of the examples of wave formation, the first indications of development, anomalous pressure tendency and precipitation, did not occur on the front, but within the adjacent air masses. Such development usually took place in the polar air and in 19 cases out of the 56 studied, it led to the appearance of a depression in the polar air, often close to the front. Subsequently the front and depression moved together and later conformed with the conventional model. Attention has recently been drawn to developments of this kind by Postma (29). One case of a depression forming first in the warm air was noted in the present series.

6. The theory of wave formation in the light of the present results.

The results of the present investigation cannot be said to be conclusively in support of any one of the theories of frontal wave outlined in section 1. However, there are certain "pointers" to be derived from them which are worthy of consideration.

First, the facts that no waves were observed to form on fronts less than 1200 miles long and that longer effective fronts nearly always formed waves; these facts point towards the acceptance of a theory of instability in which waves exceeding about 800 miles in length are unstable (the undisturbed front has to accommodate about one an a half wave lengths). If distortion of the front by neighbouring systems or development associated with some broad feature of the upper flow were the only factors to be considered, we might expect short

/ waves

waves to be more heavily damped than longer ones, but we should not expect such a clear limitation on the length of a front which can form waves as is observed.

On the other hand it does appear that within the probable limits of the experiment, the formation of all of the observed waves can be adequately explained either by (1) the distortion of the front by orography or neighbouring pressure systems or (2) by development to be expected on Sutcliffe's theory and associated with the existing upper flow pattern.

How can these two conflicting results be reconciled? A possible explanation may be obtained by considering the rate of growth of frontal waves assumed to be unstable in accord with one or other of the theoretical models. No reliable estimate appears in the literature regarding the theoretical rate of growth, but observation of frontal waves on the synoptic chart suggests that most developing waves take some 24 hours to double their amplitude. If this rate of growth were typical also of the period before the wave reached observable dimensions, then the wave would require 2 days to grow from an amplitude of 25 miles to a detectable amplitude of about 100 miles during which period it would move at normally observed speed along practically the whole length of the front. There is, therefore, some reason to expect that very small perturbations of a front will not have time to grow into waves of the dimensions observed on the weather map and that the observed disturbances must start as waves of finite amplitude.

If this point of view is accepted then the observed relation of the early stages of wave formation with distortion of the front or development on Sutcliffes theory is explained. To summarise; The evidence is consistent with the hypothesis that frontal zones are unstable for waves of length more than 800 miles, but the rate of growth of such waves is slow and observed waves are usually initiated either by the mechanical distortion of the front or by the circulation caused by development associated with features of the upper flow pattern - the occurrence of the latter areas of cyclonic development is in accord with Sutcliffe's theory.

Much remains to be explained. In particular, the method by which the lowest pressure is transferred to the surface front; but this may need to await a full understanding of the structure and dynamics of the frontal zone itself.

7. Application of the results to forecasting.

Certain of the results obtained above are directly applicable to the problem of forecasting. The following working rules are suggested based upon them.

(1) If a cold front extends over a length of 1200 miles or more and is associated with a 25 Kt. thermal wind (1000-500 mb.) over this length, a new wave should be expected on it.

(2) New waves should not be inserted on shorter fronts or fronts not fulfilling condition (1).

(3) On fronts satisfying condition (1) the wave may be expected to develop either.

  (a) where the front is subject to orographic distortion

  (b) where a bulge in the front can be produced by the flow round adjacent pressure systems.

  or (c) where the thermal vorticity term is a maximum.

/ (4)

(4) If direct estimate of the thermal vorticity term is not possible the most probable position for a new wave to form is between 200 and 600 miles **east** of a thermal troughline.

(5) Both the thermal wind and the direction of the warm sector isobars are a good guide to the direction of motion of a newly-formed wave.

(6) The speed of a newly-formed wave is not closely related with the thermal wind speed and probably the most useful estimate is obtained by taking about 4/5 of the geostrophic wind speed in the warm sector.

(7) Waves associated with a markedly difluent thermal pattern move slowly.

(8) No reliable rule is available with regard to the rate of deepening of newly formed waves. The fall of central pressure is commonly about 5 to 10 mb. in the first 24 hours but a wide variation is possible.

(9) The pressure distribution rain and cloud areas during the earliest stages of wave formation do not always agree with the accepted model of the young wave. Frontal analysis should not be amended because the low pressure centre or rain area appears to be detached from the fronts in the early stages of wave development.

/References

References

(1) Bjerknes J. and Solberg H.; Life cycle of cyclones and the polar front theory of atmospheric circulation. Geofy. Publ., Oslo, 3, 1922, No.1.

(2) Bjerknes V., Bjerknes J., Solberg H. and Begeron T.: Physikalische Hydrodynamik Berlin, 1933.

(3) Sutcliffe R.C.; A preliminary note on rules for forecasting based on thickness patterns. Air Ministry, London, 1948, M.R.P. 420.

(4) Shaw, Sir Napier; Manual of Meteorology, Vol.II. Cambridge, 1928, p.288.

(5) Bergeron T. and Swoboda G.; Wellen und Wirbel an einer quasi-stationaren Grenzflache über Europe. Veroff. Geophys. Inst., Leipzig, Ser.2 Bd.3 No.2, p.63.

(6) Kaye W.C. and Durst C.S.: Some examples of the development of depressions which affect the Atlantic. Quart. J.R. met. Soc., London, 58, 1932, p.151.

(7) Douglas C.K.M.: Some factors influencing the development and occlusion of warm sectors. Quart. J.R. met. Soc., 65, 1939, p.525.

(8) Boyden C.J.; The mechanics of the depression - some criticisms and a contribution. Quart. J.R. met. Soc., 64, 1938, p.85.

(9) Byers H.R.; General Meteorology. New York, 1944, p.313-4.

(10) Palmen E. and Newton C.W.; A study of the mean wind and temperature distribution in the vicinity of the polar front in winter. J. Met., Lancaster Pa., 5, 1948, p.220.

(11) Charney J.G.; The dynamics of long waves in a baroclinic westerly current. J. Met., Lancaster Pa., 4, 1947, p.135.

(12) Eady E.T.; Long waves and cyclone waves. Tellus, Stockholm, 1949, 1, No.3, p.33.

(13) Bjerknes J.; Theorie der ausser-tropischen Zykonenbildung. Met. Z., Braunschweig, 52, 1937, p.462.

(14) Bjerknes J.; The deepening of extra-tropical cyclones. Quart. J.R. met. Soc., 66 Supplement, 1940, p.57.

(15) Bjerknes J. and Holmboe J.; On the theory of cyclones. J. Met., Lancaster, Pa., 1, 1944, p.1.

(16) Berggren R., Bolin B. and Rossby C.G.; An aerological study of zonal motion, its perturbations and breakdown. Tellus, Stockholm, 1, 1949, No.2 p.14.

(17) Sutcliffe R.C.; A contribution to the theory of development, Quart. J.R. met. Soc., London, 73, 1947, p.370.

(18) Sutcliffe R.C.; The use of upper air patterns in general forecasting. Met. Mag., London, 77, 1948, p.145.

(19) Sawyer J.S.; Secondary depressions on cold occlusions - the associated thickness pattern and other characteristic features. Air Ministry, London, 1949, M.R.P. 494.

(20) Gentry R.C.; Formation of new-moving centres south of deep lows. U.S. Weather Bureau, Forecast Research Division, Washington, 1944, Research paper No.7.

(21) Palmen E.; Über die Bewegung der ausser-topischen Zyklonen. Societas Scient. Fennica. Phys. Math. Helsingfors, III No.7, 1926.

/ (22)

(22) Douglas C.K.M. and Harding J.; The construction of prebaratic charts - Meteorological Office, London, 1943, S.D.T.M. No.44.

(23) Miller J.E.; Cyclogenesis in the Atlantic coastal region of the United States. J. Met., Lancaster, Pa. 3, 1946, p.31.

(24) Austin J.M.; An empirical study of certain rules for forecasting the movement and intensity of cyclones. J. Met., Lancaster, Pa., 4, 1947, p.16.

(25) Palmer W.C.; On forecasting the direction of movement of winter cyclones. Mon. Weath. Rev., Washington D.C., 76, 1948, p.181.

(26) Poulter R.M.; Forecasting technique in respect of cold fronts crossing the British Isles. Uxbridge (typescript), 1945.

(27) Palmen E.; Zur Frage der Fortsplanzunggeschwindigkeit der Zyklonen, Met. Z., Braunschweig, 43, 1928, p.96.

(28) Sumner E.J.; Cyclonic development and the importance of atmospheric stability and the field of vertical motion in the process. Central Forecasting Office, Dunstable, Typescript, 1949.

(29) Postma K.R.; The formation and development of occluding cyclones - a study in surface weather maps; Koninklijk Nederlands Meteorologisch **Instituut** Mededelingen en Verhandelingen, Serie B., De Bilt, Deel 1, 1948, No.10.

/Appendix

Appendix - List of cold front waves forming within the area of Form 2231.
Period February 1948 - January 1949.

Formation of Wave						Classification
Date	Time G.M.T.	Position		Central Pressure mb	Induced (I) or Non-Induced (U)	Thermal Pattern Anticyclonic A Cyclonic C Indeterminate -
		Lat.	Long			
5 Feb. 1948	1800	51 N	20 W	1007	U	A
29 Feb. "	0600	43 N	35 W	993	U	C
18 March "	0600	51 N	39 W	1007	U	A
28 March "	0600	52 N	20 W	995	I	C
5 April "	0000	50 N	37 W	1012	U	C
9 April "	0000	52 N	25 W	1005	U	C
15 April "	1200	50 N	28 W	1015	U	C
27 April "	0600	63 N	22 W	1017	I	C
29 April "	0600	51 N	IE	1001	U	C
6 May "	0600	47 N	35 W	1010	I	C
9 May "	1200	58 N	12 W	1017	I	C
13 May "	0600	44 N	34 W	1010	U	C
23 May "	0600	51 N	5 W	1008	U	C
25 May "	0600	46 N	9 W	1006	I	C
28 June "	0600	50 N	9 E	1006	U	C
17 July "	1500	48 N	29 W	1006	I	-
18 July "	1800	45 N	24 W	1015	U	C
29 July "	1500	50 N	24 W	1011	I	C
16 Aug. "	1200	48 N	2 E	1015	U	-
17 Aug. "	0600	46 N	0 W	1015	U	C
21 Aug. "	1800	42 N	30 W	1009	U	C
25 Aug. "	1200	38 N	22 W	1018	U	C
30 Aug. "	1200	46 N	21 W	1019	I	-
3 Sept. "	0000	51 N	00 W	1000	I	C
7 Sept. "	1800	43 N	24 W	1017	I	C
10 Sept. "	0600	45 N	10 W	1012	U	C
27 Sept. "	1200	53 N	4 W	1002	I	-
28 Sept. "	0000	50 N	7 W	1007	I	C
29 Sept. "	0300	46 N	39 W	1001	I	-
2 Oct. "	1800	55 N	4 W	1021	I	-
10 Oct. "	0600	55 N	5 W	1015	U	-
10 Oct. "	0000	41 N	22 W	1018	U	C
13 Oct. "	1200	50 N	16 W	1003	U	C
20 Oct. "	1200	61 N	14 W	995	I	C
25 Oct. "	0600	52 N	4 W	1000	I	C
26 Oct. "	2100	54 N	19 E	1009	U	C
5 Nov. "	1800	40 N	18 W	1012	U	C
5 Nov. "	1500	55 N	16 E	989	I	C
12 Nov. "	1500	53 N	10 W	1015	U	C
12 Nov. "	1200	47 N	14 W	1017	I	C
15 Nov. "	0000	53 N	11 W	1009	U	C
21 Nov. "	1500	43 N	25 W	987	I	C
26 Nov. "	1800	40 N	16 W	1011	U	C
2 Dec. "	1800	52 N	5 W	1002	I	-
7 Dec. "	0000	45 N	11 W	1005	I	C
8 Dec. "	0600	40 N	6 W	1015	I	-
16 Dec. "	1200	46 N	31 W	996	I	C
17 Dec. "	1800	39 N	25 W	1011	I	C
27 Dec. "	0000	49 N	12 W	1008	U	C
2 Jan. 1949	0000	41 N	4 W	994	U	C
9 Jan. "	1800	53 N	35 W	1024	U	C
18 Jan. "	1800	46 N	39 W	1014	U	C
19 Jan. "	0000	51 N	29 W	1005	U	C
24 Jan. "	1800	48 N	30 W	985	U	C
27 Jan. "	0600	47 N	22 W	999	U	-
31 Jan. "	1800	55 N	33 W	1003	I	C

G.256772(a)/JDG/4/50/40

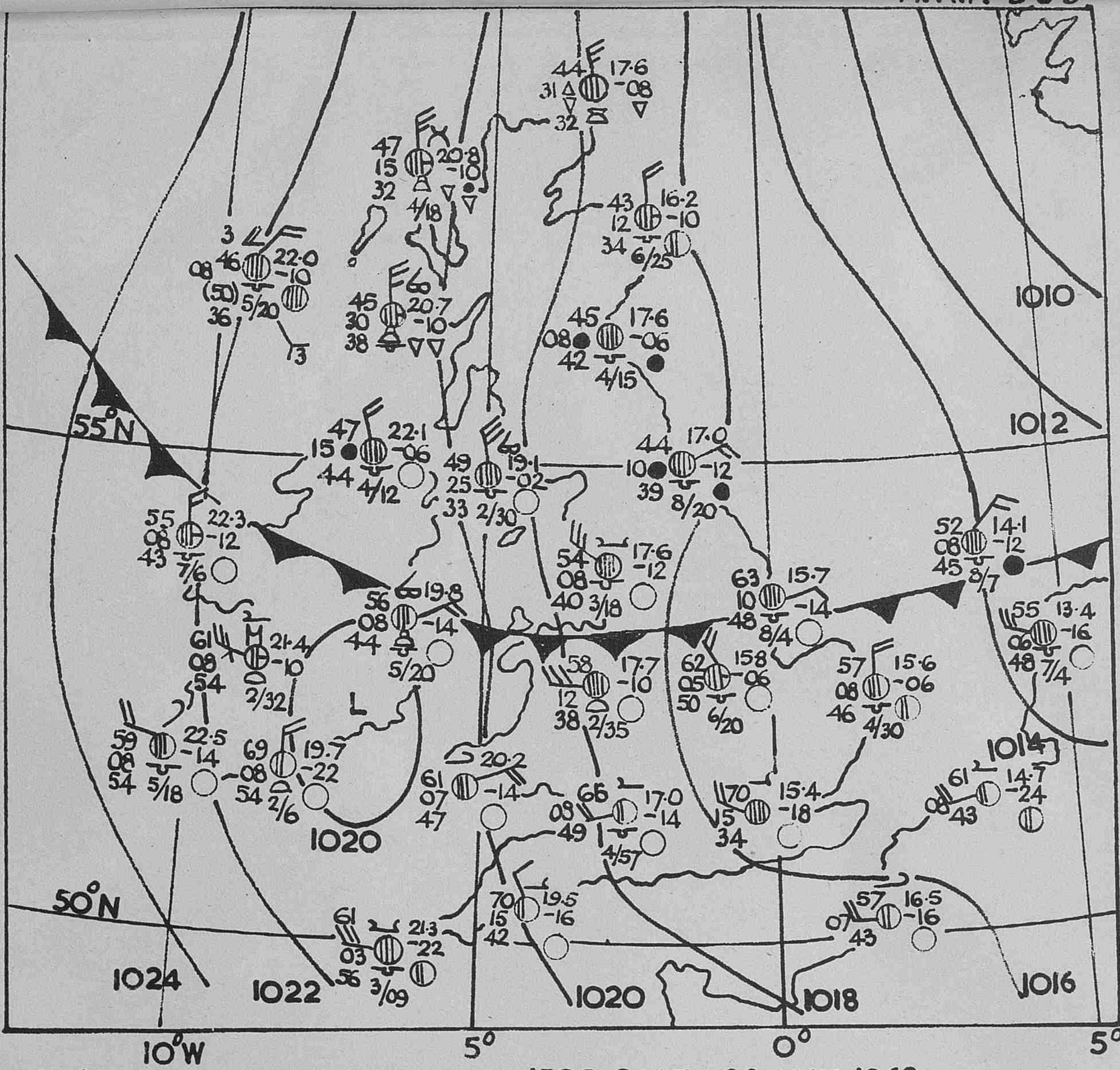
55°N
50°N
1010
1012
1014
1016
1018
1020
1020
1022
1024
L
10°W
5°
0°
5°

Fig. 1. Weather map for 1500 G.M.T. 22. MAY 1948.

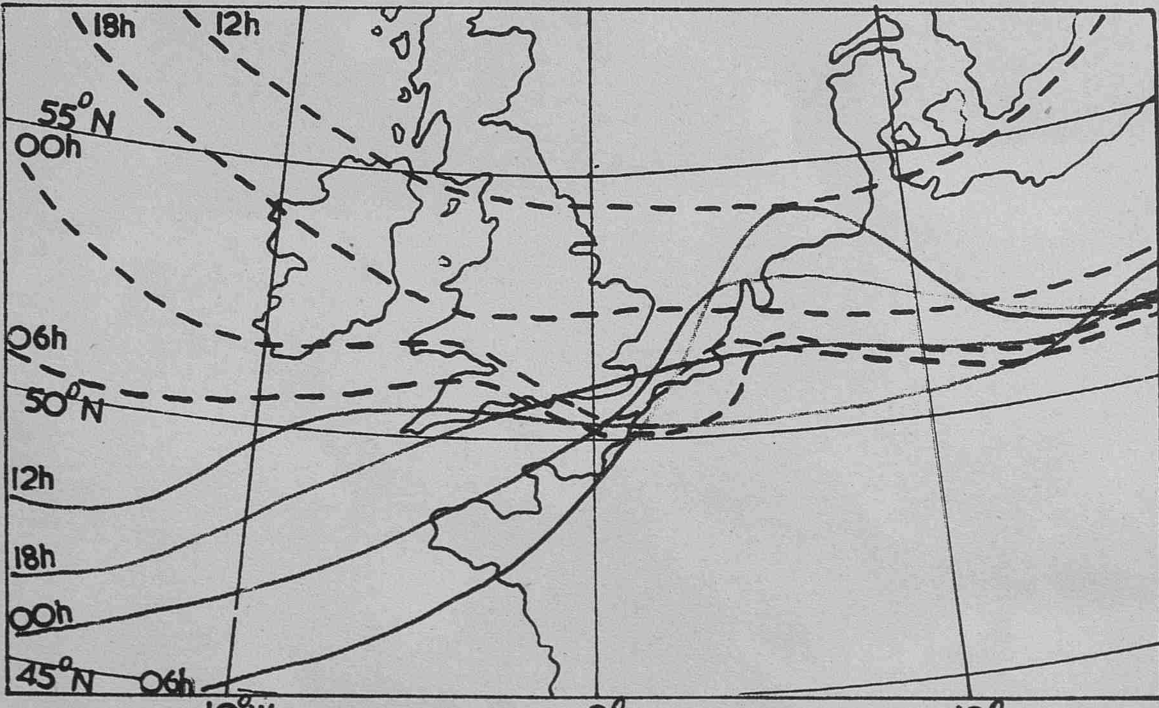
18h
12h
55°N
00h
06h
50°N
12h
18h
00h
45°N
06h
10°W
0°
10°

Fig. 2. Isochrones of cold front position 1200 G.M.T. 22 MAY 1948 to 0600 G.M.T. 24 MAY 1948. (Isochrones up to and including 0600. 23 MAY dashed lines—subsequent isochrones continuous).

Fig. 3. Synoptic charts 1800 G.M.T. 22 MAY to 1800 G.M.T. 23 MAY showing isallobars and rain areas.

3hr. isallobars at intervals of 1mb/3hr. — — — — — —
Track of isallobaric centres. x• • • • • • •x
Rain areas. ▨
Track of rain area. •——•——•
Isobars at 2mb. intervals. ————
Cold front ▼▼ Warm front ●●●

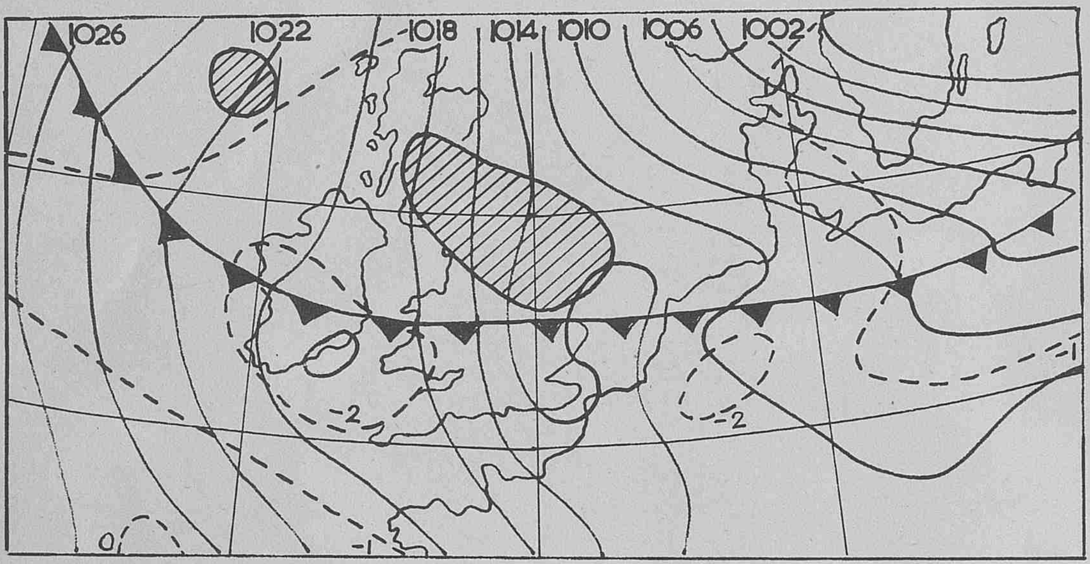
1026
1022
1018
1014
1010
1006
1002
-2
-2
-1
0
-1

Fig. 3(a) 1800 G.M.T. 22 MAY 1948.

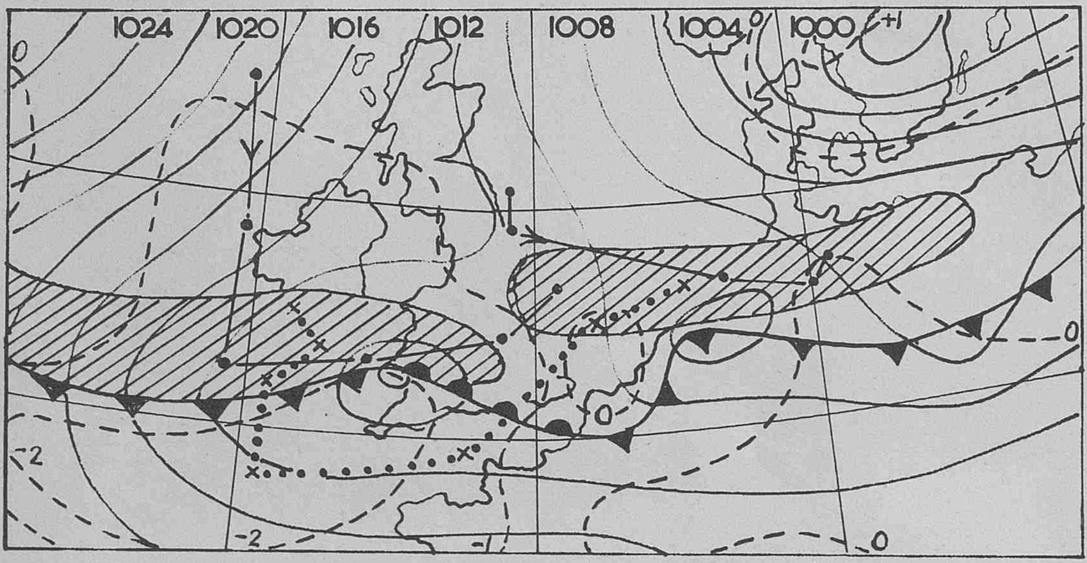
1024
1020
1016
1012
1008
1004
0
1000
+1
0
0
0
-2
-2
-1
-1
0

Fig. 3(b) 0600 G.M.T. 23 MAY 1948.

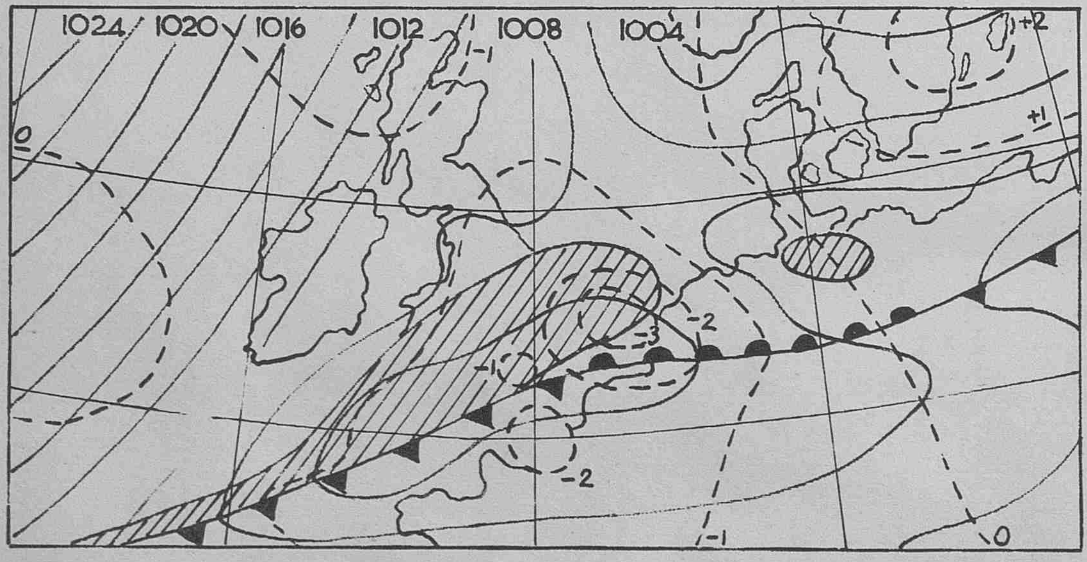
1024
1020
1016
1012
1008
1004
-1
+2
+1
0
-2
-3
-1
-2
-1
0

Fig. 3(c) 1800 G.M.T. 23 MAY 1948.

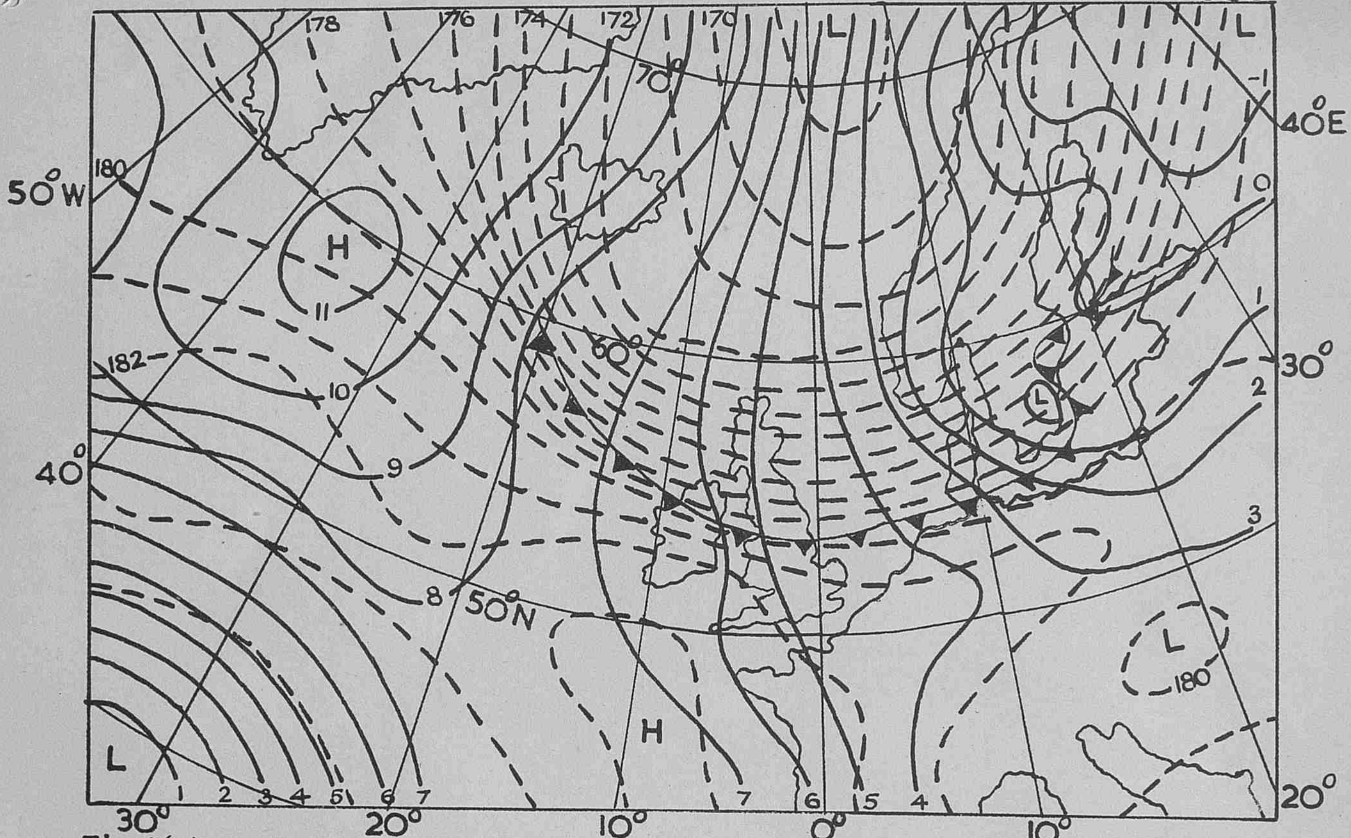
178
176
174
172
170
L
70°
L
40°E
-1
0
50°W
180
H
11
60°
1
30°
182
10
L
2
40°
9
3
8
50°N
L
180
H
L
1
2
3
4
5
6
7
7
6
5
4
20°
30°
20°
10°
0°
10°

Fig. 4(a). Contours of 1000 mb. surface and thickness lines 1000 - 500 mb. at 100 ft. intervals.

1500. G.M.T. 22. MAY, 1948.

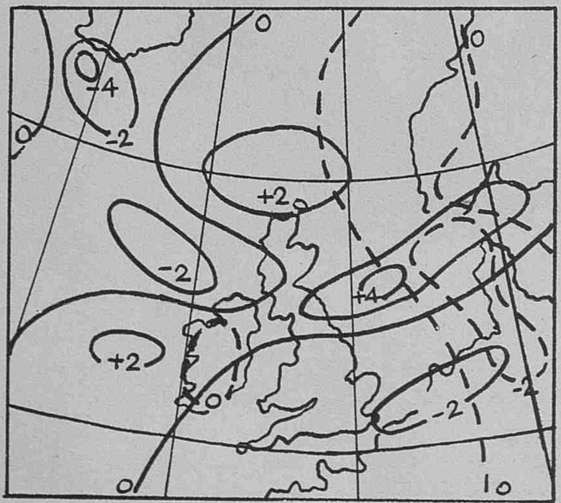
0
0
-4
-2
0
+2
-2
+4
+2
0
-2
-2
0
0

Fig. 4.(b). Isopleths of thermal vorticity term and thermal steering term.

Thermal steering term $- 2V'\frac{\partial \zeta_0}{\partial s}$ (dashed line)

Thermal vorticity term $- V'\frac{\partial \zeta'}{\partial s}$ (continuous line).

(Units hr^{-2}).

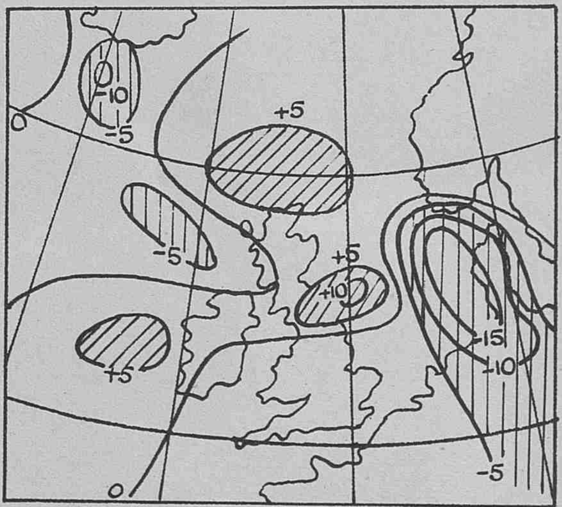
0
-10
0
-5
+5
-5
+5
+10
+5
-15
-10
-5
0

Fig. 4(c). Isopleths of Sutcliffe's expression of the relative divergence.

$$-\frac{1}{\ell}\left(V'\frac{\partial \zeta'}{\partial s} + 2V'\frac{\partial \zeta_0}{\partial s}\right)$$

(Units $hrs^{-1} \times 10^{-2}$)

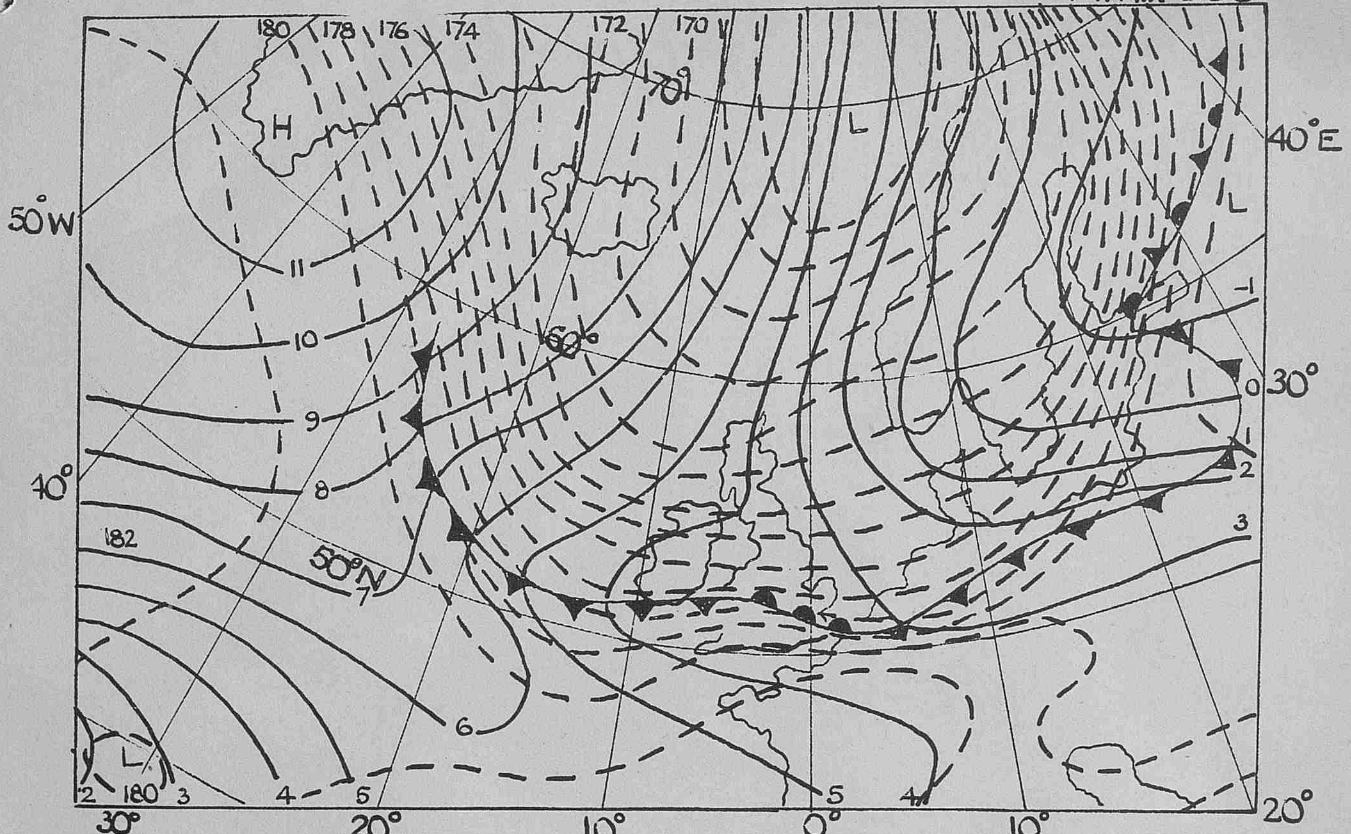
180
178
176
174
172
170
70°
H
L
40°E
50°W
L
11
10
60°
9
-1
0
30°
8
1
2
40°
182
50°N
7
3
6
L
2
180
3
4
5
5
4
30°
20°
10°
0°
10°
20°

Fig. 5 (a). Contours of 1000 mb. surface and thickness lines 1000 - 500 mb. at 100 ft intervals.

0300. G.M.T. 23. MAY, 1948.

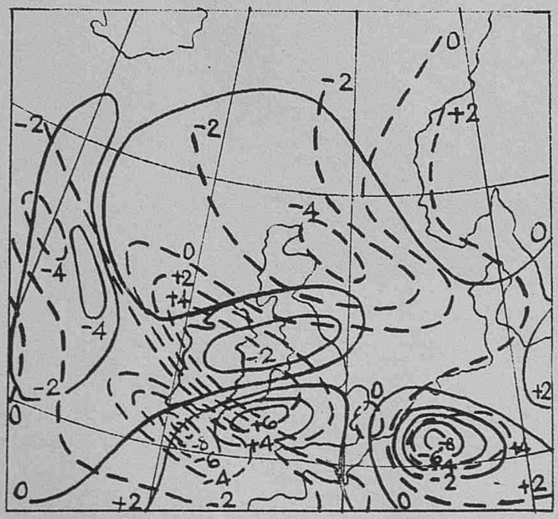
-2
0
+2
-2
-2
-4
-4
0
+2
+4
-4
-2
-4
-2
0
0
+2
+6
+4
-6
-4
-8
-4
0
-2
+2
+4
+2
0
+2
-2
0

Fig. 5 (b) Isopleths of thermal vorticity term and thermal steering term.

Thermal steering term $-2V'\frac{\partial \zeta_0}{\partial s}$ (dashed line).

Thermal vorticity term $-V'\frac{\partial \zeta'}{\partial s}$ (continuous line).

(Units hr^{-2})

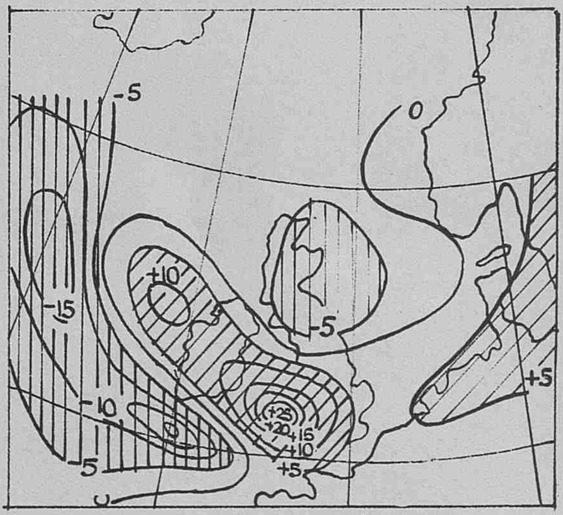
-5
0
+10
5
-15
-5
+5
-10
0
+25
+20
+15
+10
+5
-5
0

Fig. 5 (c). Isopleths of Sutcliffe's expression of the relative divergence.

$$-\frac{1}{\ell}\left(V'\frac{\partial \zeta'}{\partial s} + 2V'\frac{\partial \zeta_0}{\partial s}\right)$$

(Units $hrs^{-1} \times 10^{-2}$)

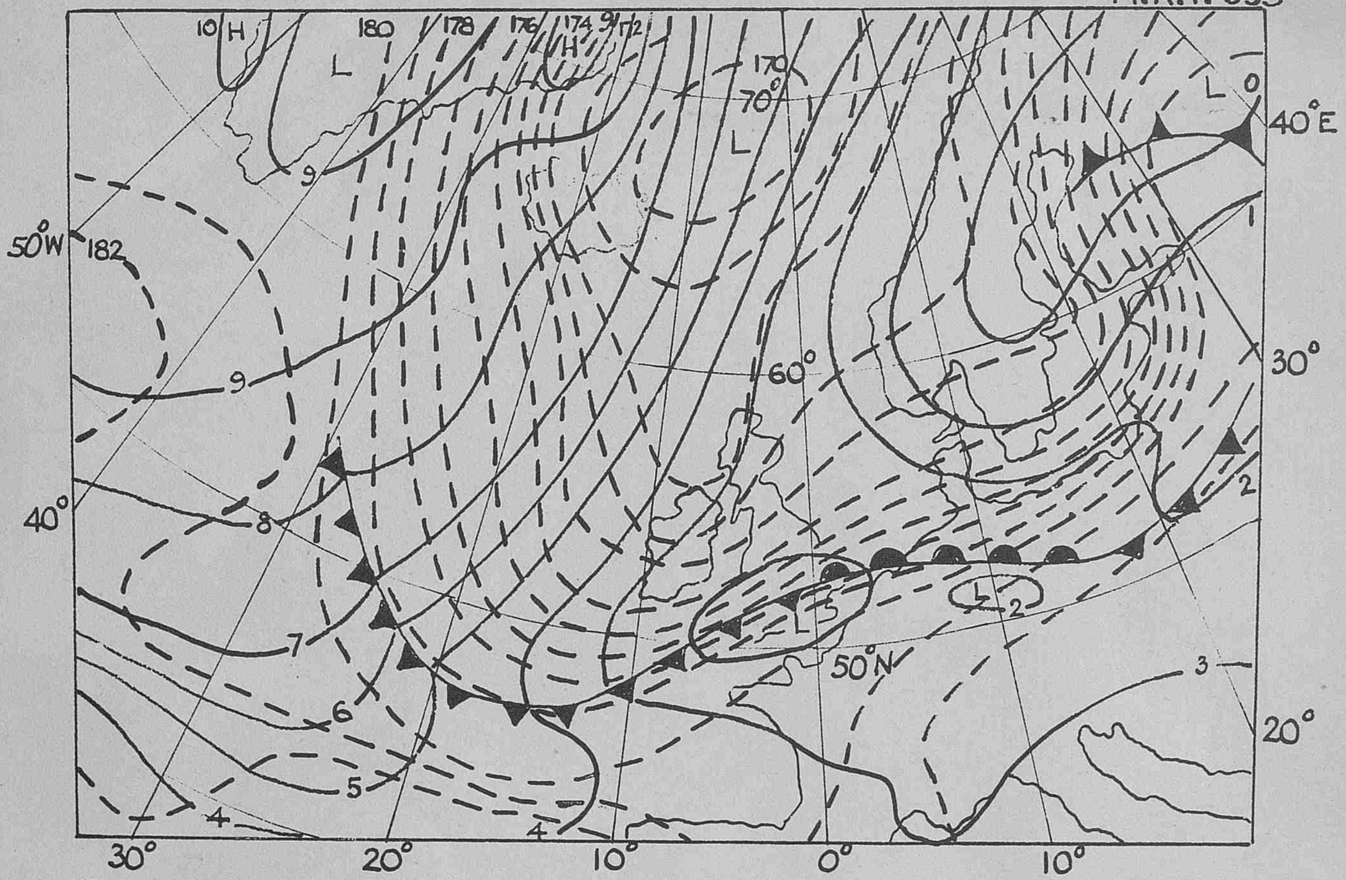
10
H
180
178
176
174
9
172
H
L
170
70°
L
L
0
40°E
9
50°W
182
9
60°
30°
40°
8
2
L
2
L
5
7
50°N
6
3
20°
5
4
4
30°
20°
10°
0°
10°

Fig. 6 (a). Contours of 1000 mb. surface and thickness lines 1000 - 500 mb. at 100 ft. intervals. 1500. G.M.T. 23 MAY, 1948.

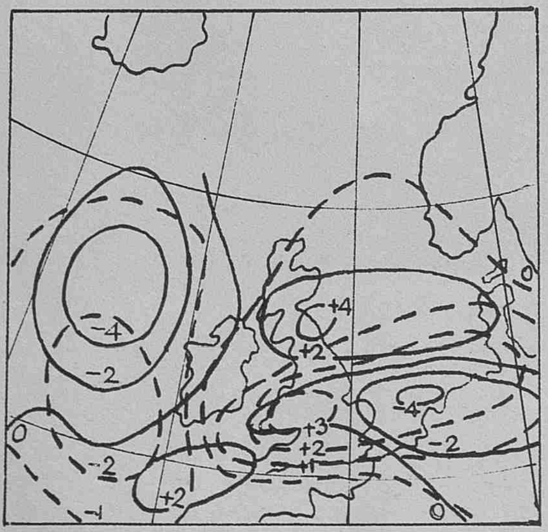
0
+4
+2
-4
-2
+3
+2
-4
-2
0
-2
+2
-1
0

Fig. 6 (b). Isopleths of thermal vorticity term and thermal steering term.

Thermal steering term $-2V'\frac{\partial \zeta_0}{\partial s}$ (dashed line)

Thermal vorticity term $-V'\frac{\partial \zeta'}{\partial s}$ (continuous line)

(Units hr^{-2})

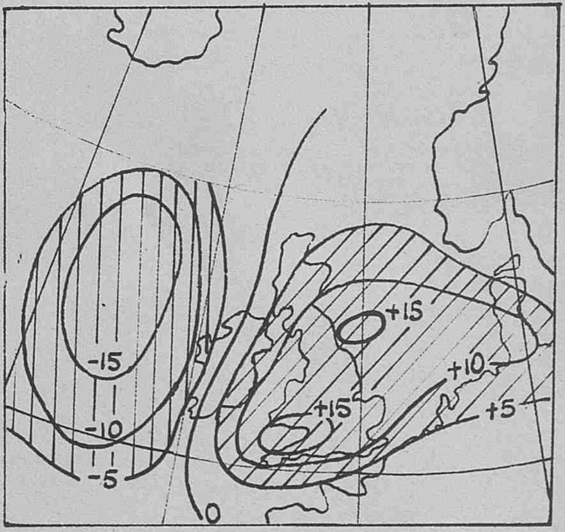
+15
-15
+10
+15
+5
-10
-5
0

Fig. 6 (c). Isopleths of Sutcliffe's expression of the relative divergence.

$$-\frac{1}{\ell}\left(V'\frac{\partial \zeta'}{\partial s}+2V'\frac{\partial \zeta_0}{\partial s}\right)$$

(Units $hrs^{-1} \times 10^{-2}$).

M.R.P. 553

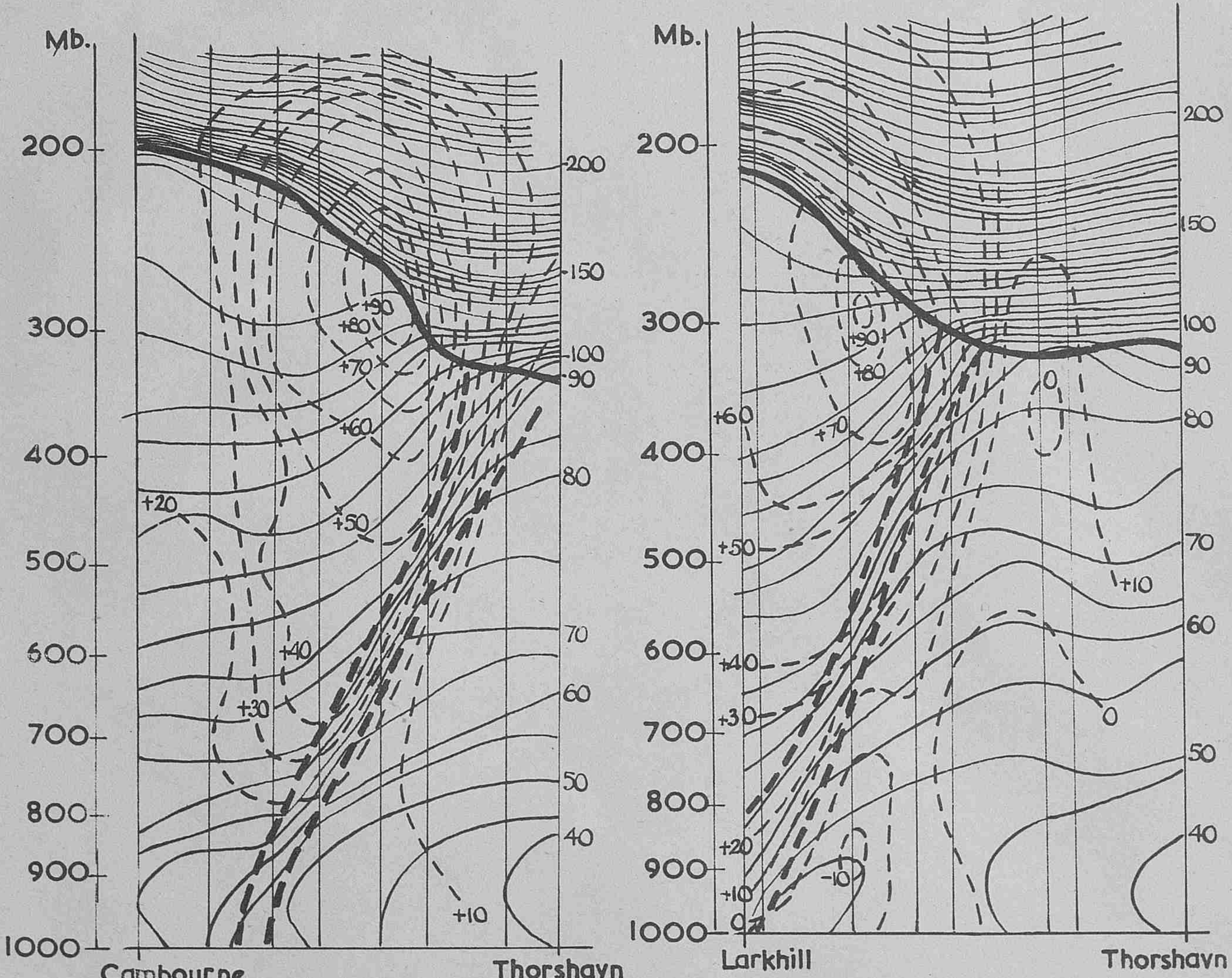

1500 G.M.T. 22 MAY 1948.

1500 G.M.T. 23 MAY 1948.

Fig. 7. South-North cross-sections through front.

Potential temperature – continuous lines (°F).

Isokinetics (lines of equal normal wind speed from observed winds) – dashed lines. (kts).

Tropopause ▬▬▬

Boundaries of frontal zone = = =

M.R.P. 553

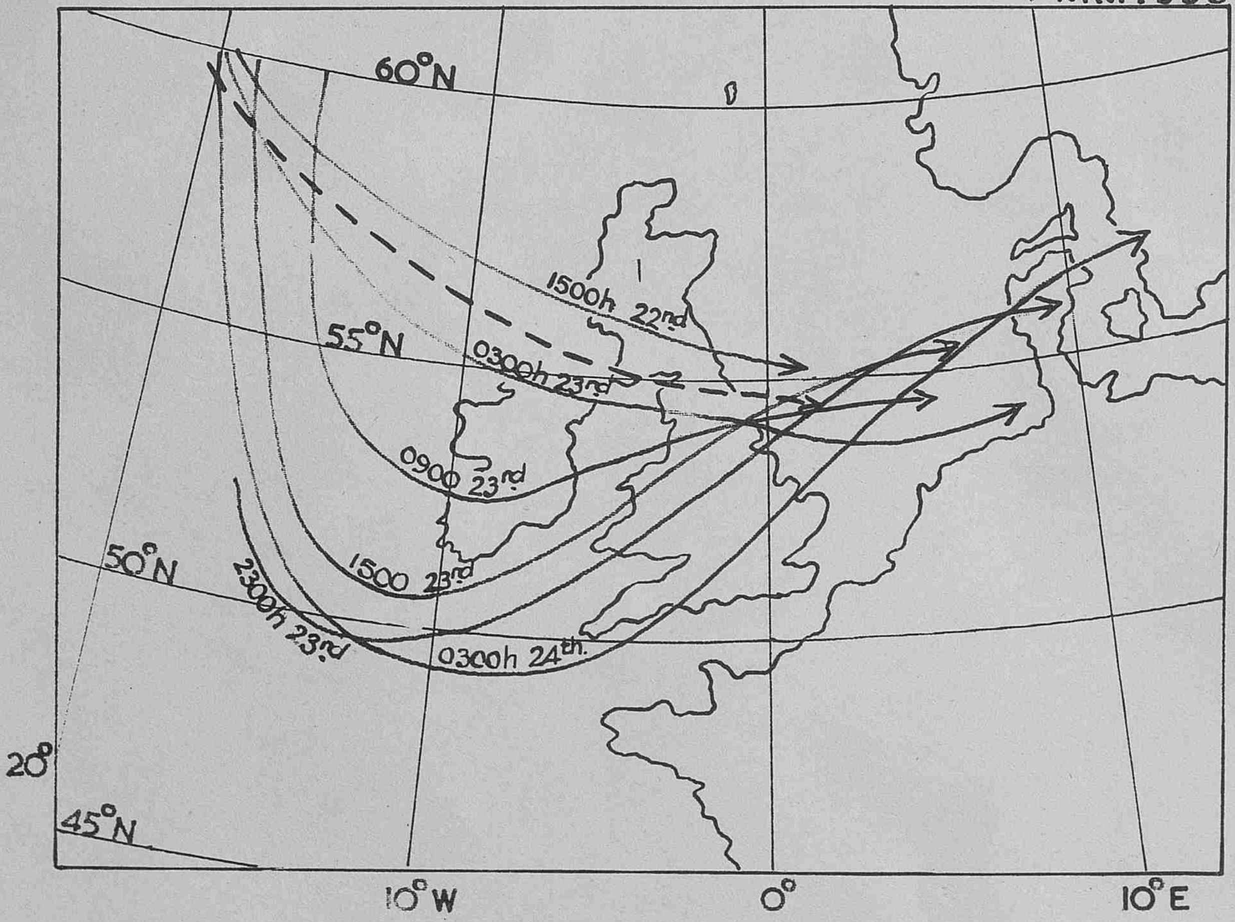
60°N
55°N
50°N
45°N
20°
10°W
0°
10°E
1500h 22nd
0300h 23rd
0900 23rd
1500 23rd
2300h 23rd
0300h 24th

Fig. 8. Changes in location of axis jet stream at 300 mb. during development of wave.

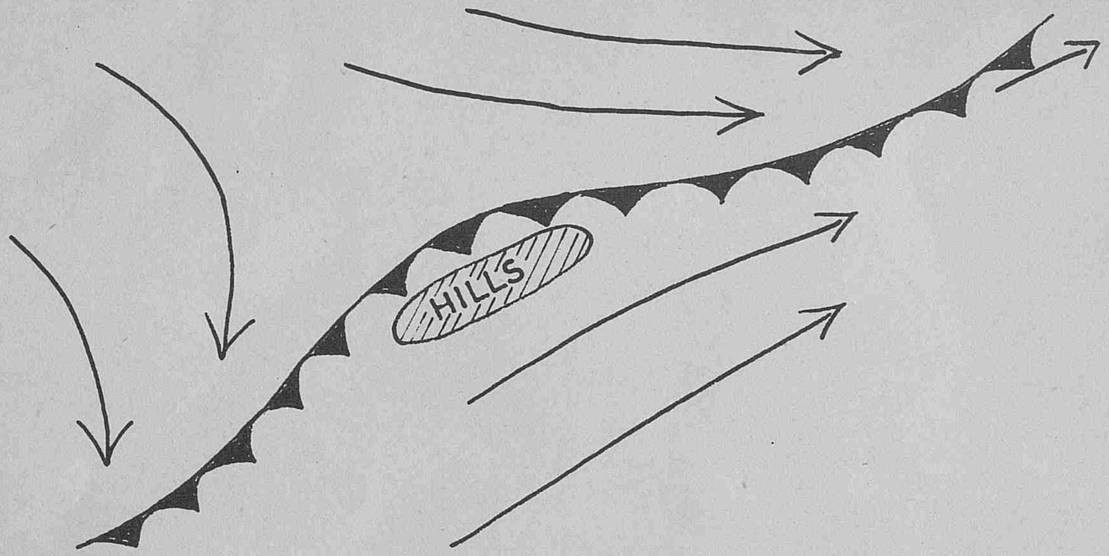

Fig. 9. Illustrating the distortion of a cold front by a range of hills.

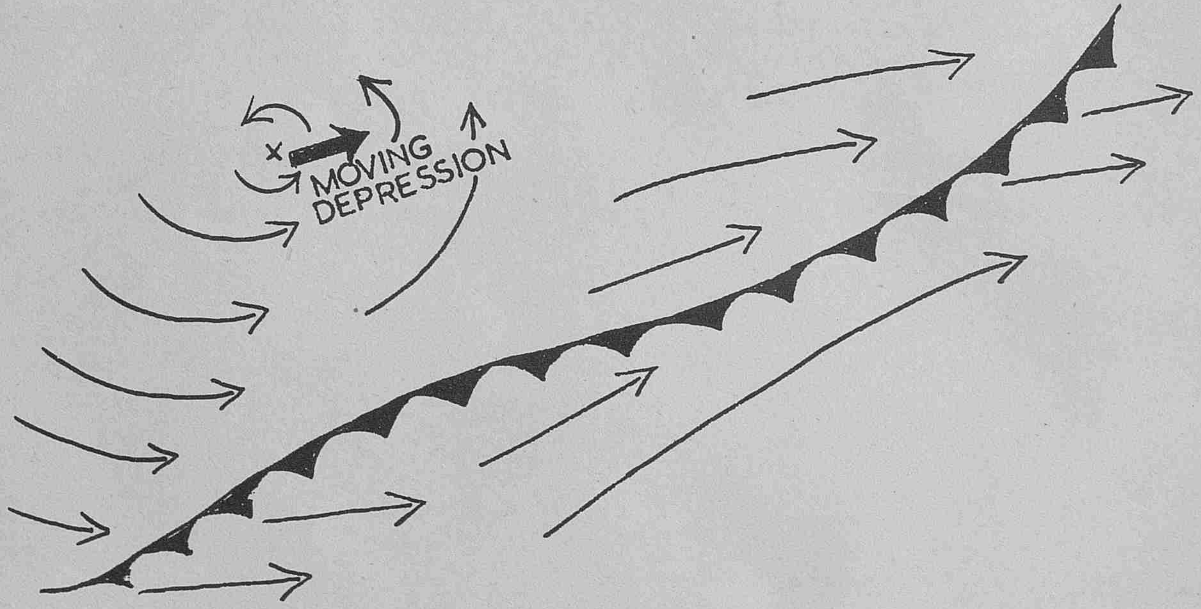
MOVING DEPRESSION

Fig. 10(a). Distortion of a front by a depression in the cold air.

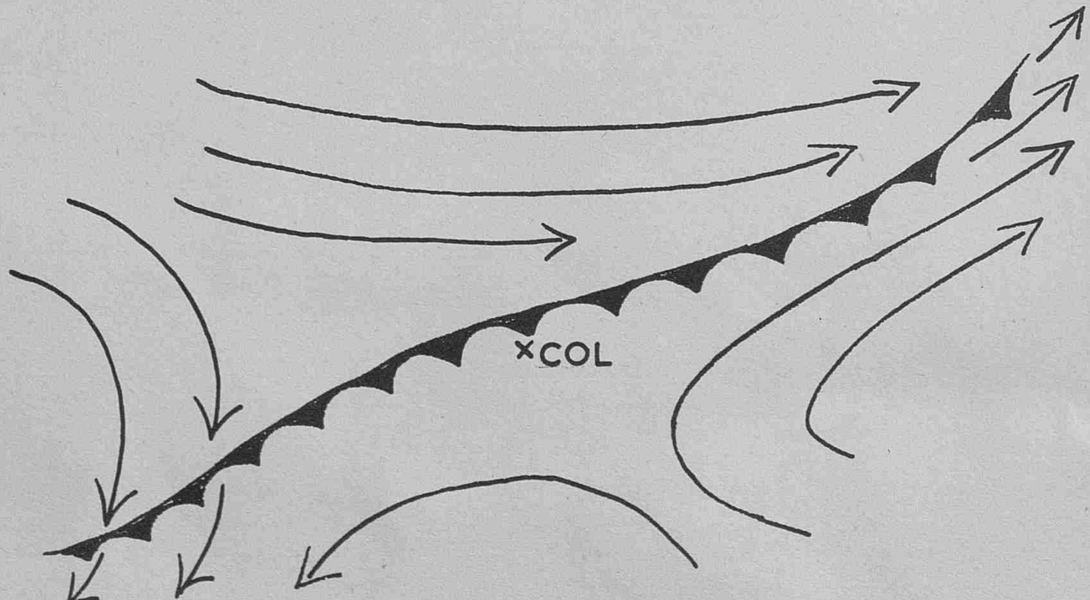

Fig. 10(b). Distortion of a front approaching a col.

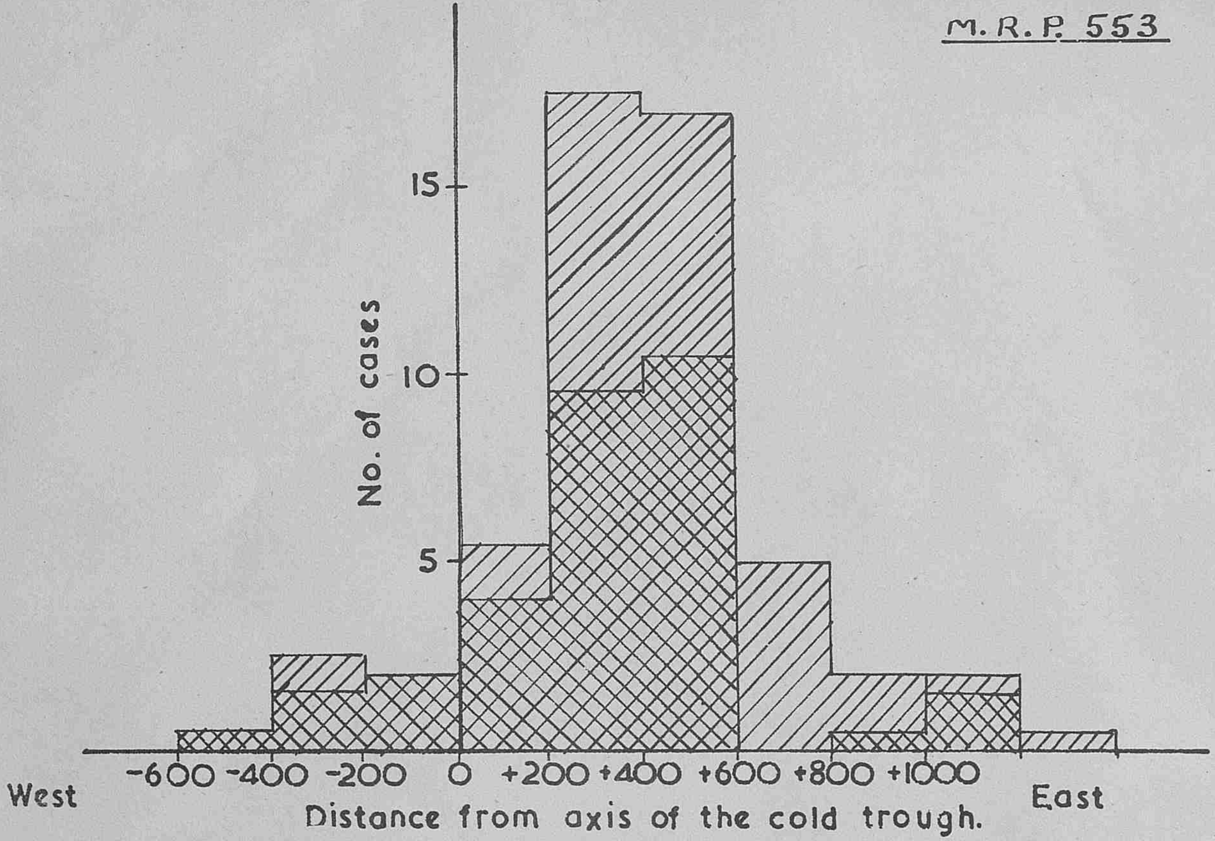

Fig. 11. Histogram illustrating the frequency of formation of cold front waves at various distances to the east of the thermal trough line.

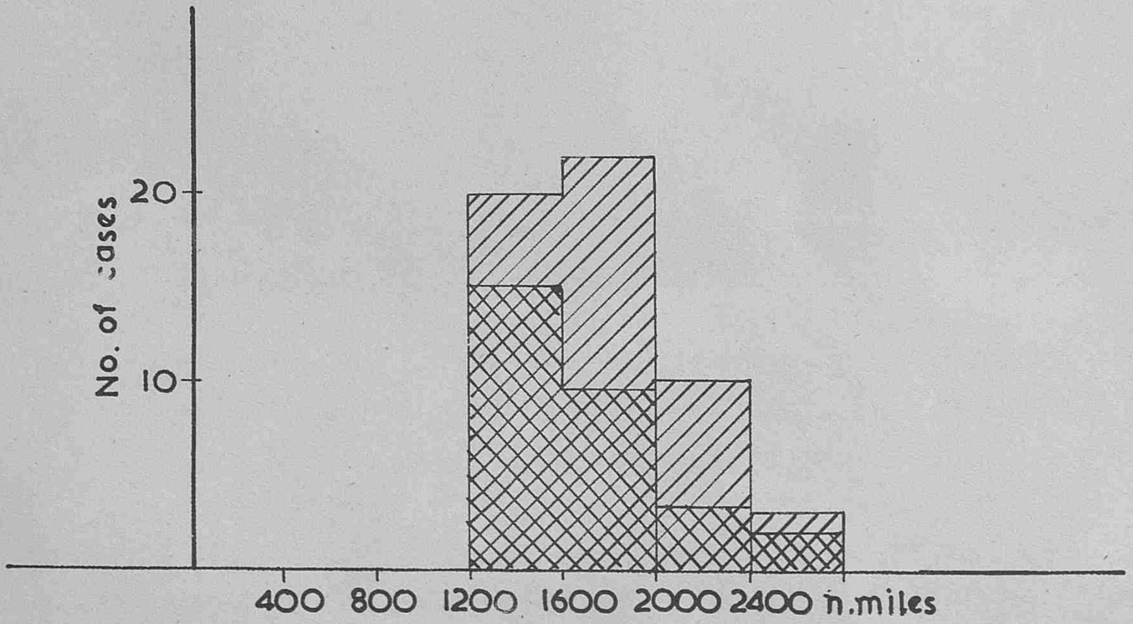

Fig. 12. Histogram illustrating the frequency of various lengths of cold fronts forming waves.

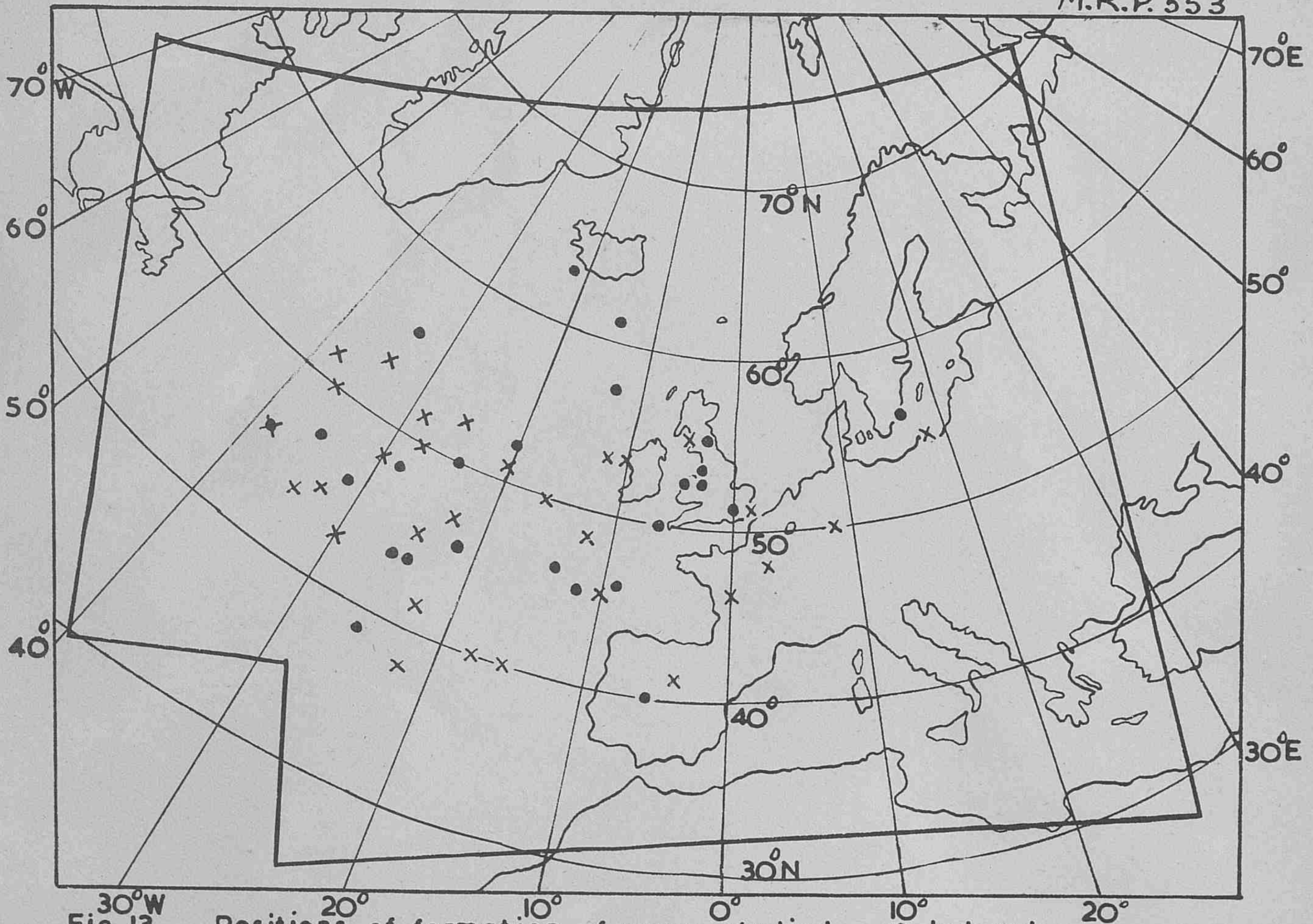
70°W
60°
50°
40°
70°E
60°
50°
40°
30°E
70°N
60°
50°
40°
30°N
30°W
20°
10°
0°
10°
20°

Fig. 13. Positions of formation of waves studied. ● Induced.
× Not induced.

Continuous line is boundary of area of F 2231A- used to limit area of study.

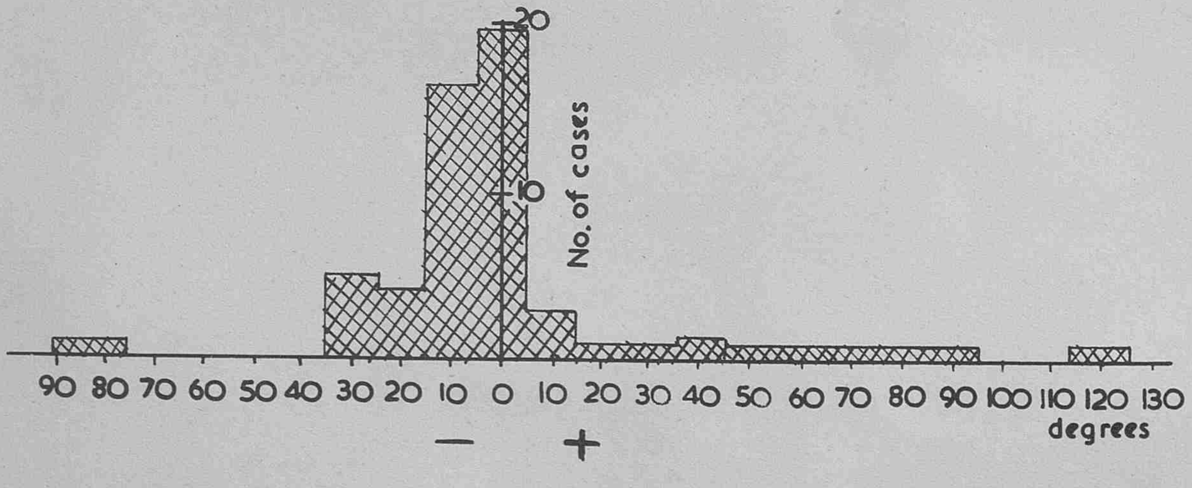

Fig. 14. Histogram illustrating direction of motion with respect to warm sector isobars. (+ indicates deviation towards higher pressure).

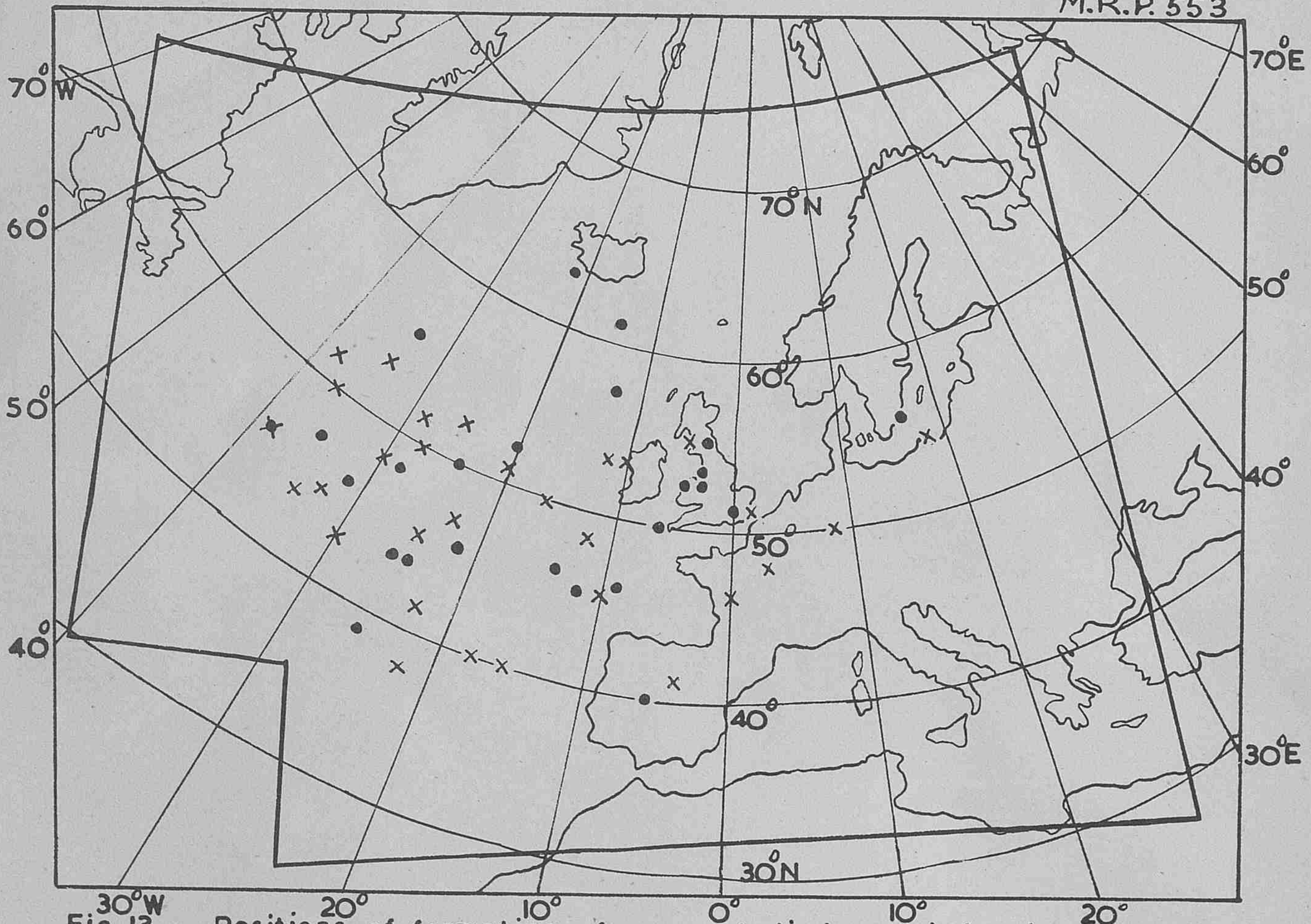
70°W
60°
50°
40°
70°E
60°
50°
40°
30°E
70°N
60°
50°
40°
30°N
30°W
20°
10°
0°
10°
20°

Fig. 13. Positions of formation of waves studied. ● Induced.
× Not induced.

Continuous line is boundary of area of F 2231A - used to limit area of study.

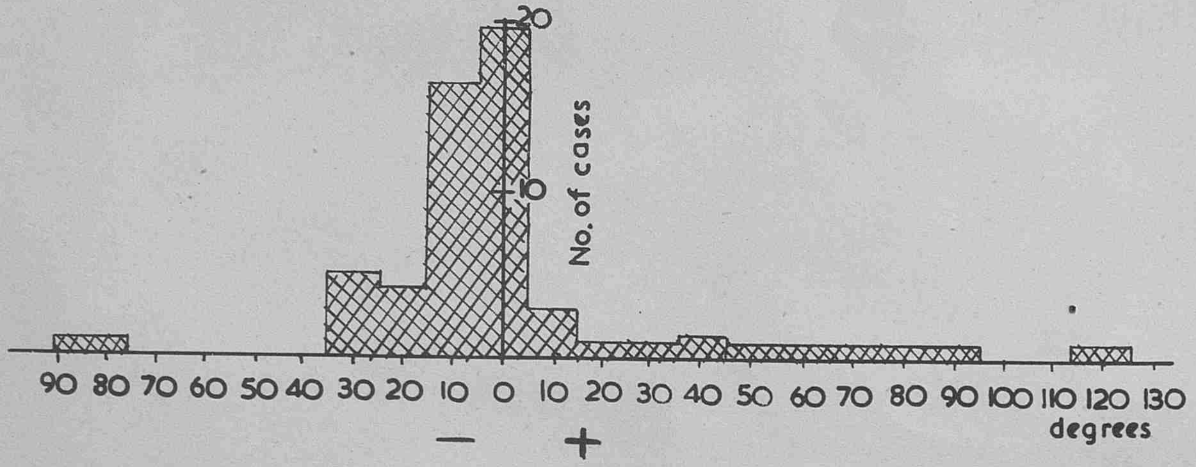

Fig. 14. Histogram illustrating direction of motion with respect to warm sector isobars. (+ indicates deviation towards higher pressure).

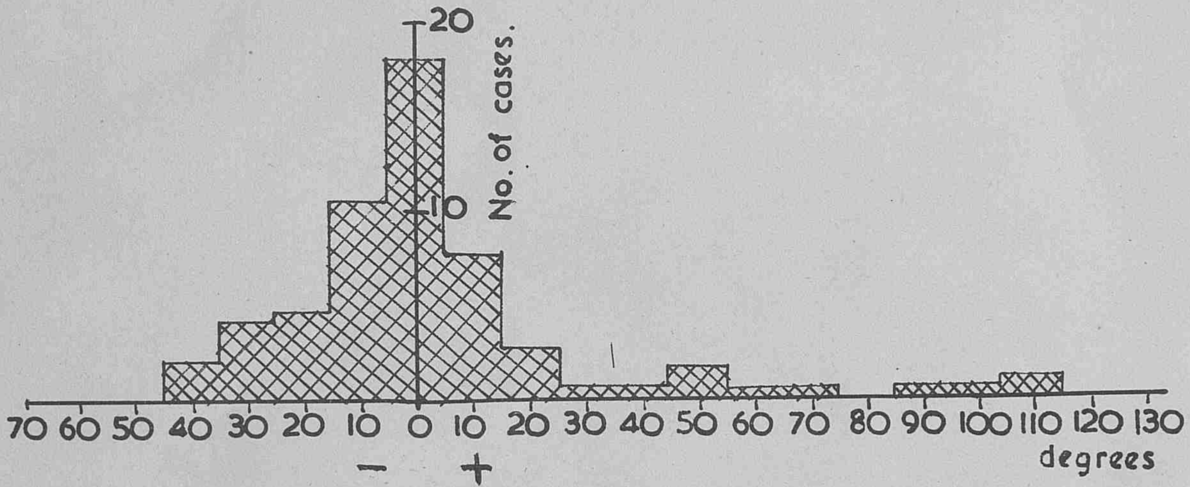

Fig. 15. Histogram illustrating direction of motion with respect to thermal wind direction over newly formed wave. (+ indicates deviation towards warm air).

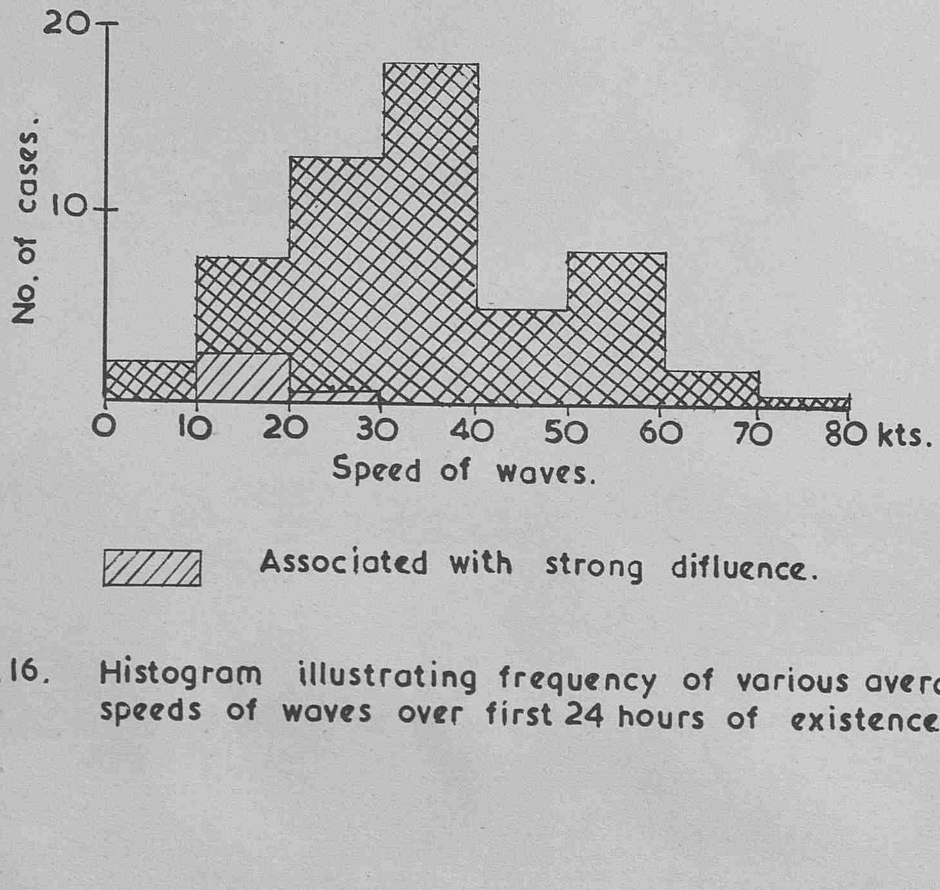

Fig. 16. Histogram illustrating frequency of various average speeds of waves over first 24 hours of existence.

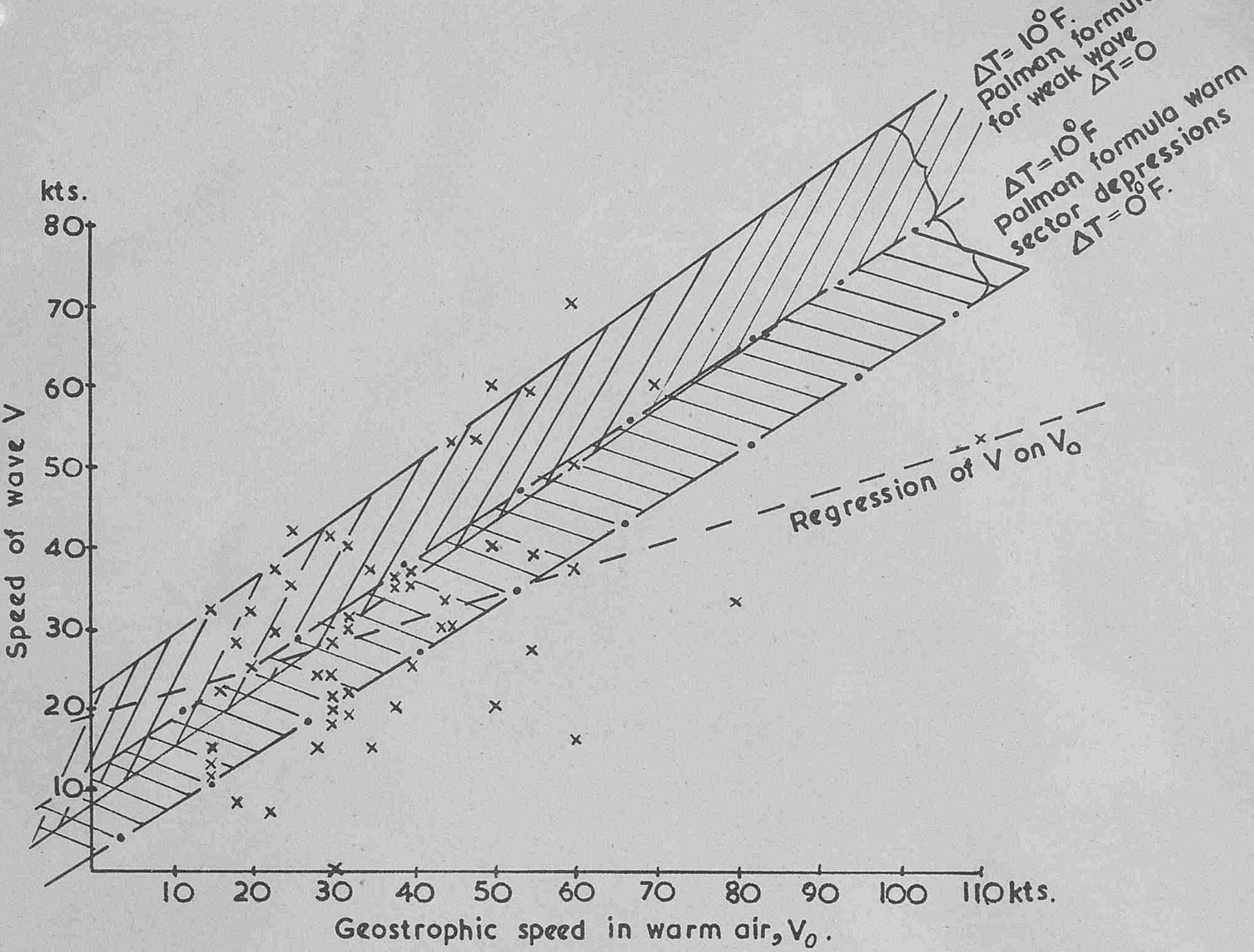

Fig.17. Relation between speed of a wave and the geostrophic wind speed in the warm sector.

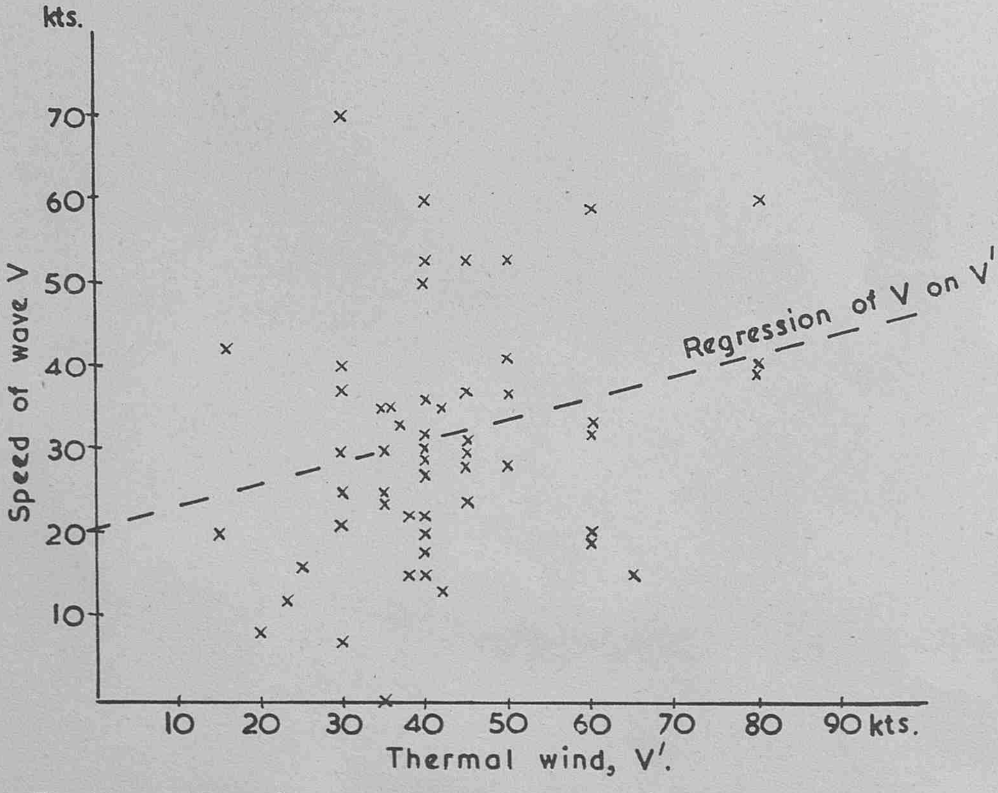

Fig.18. Relation between thermal wind over the centre and speed of a newly formed wave on a cold front.

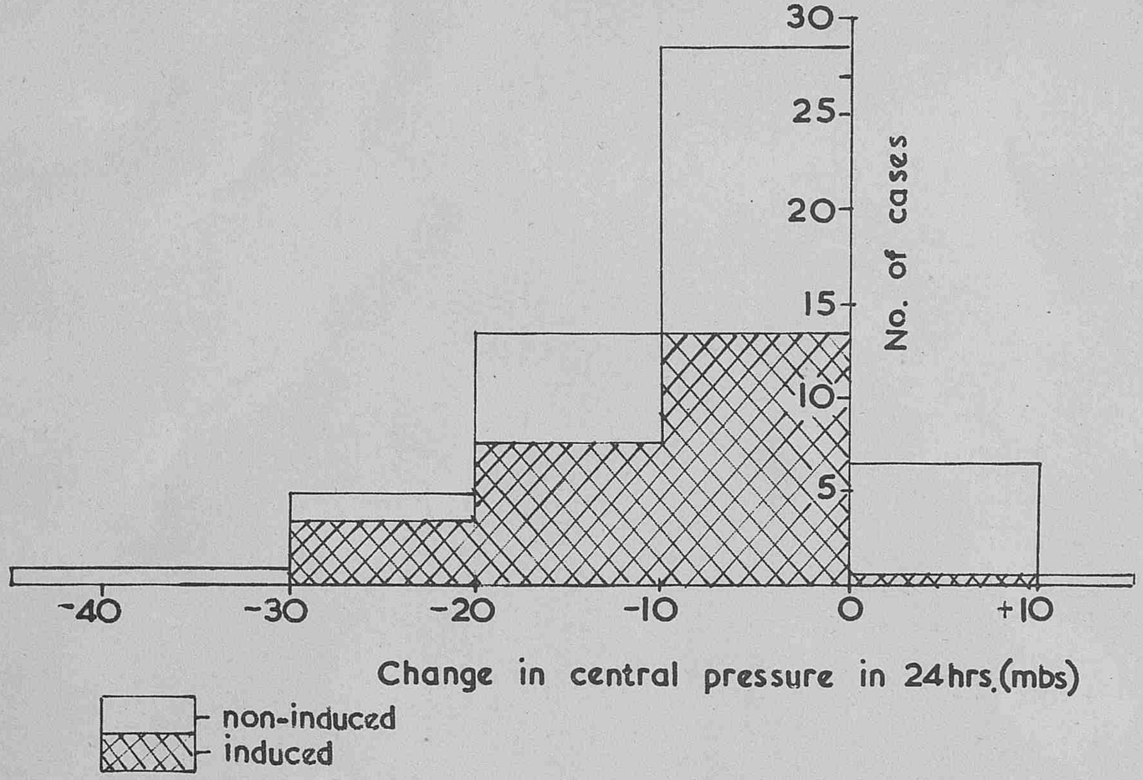

Fig. 19(a) Histogram illustrating the frequency of various changes of central pressure in wave depressions during their first 24hrs, showing separately induced and non-induced waves.

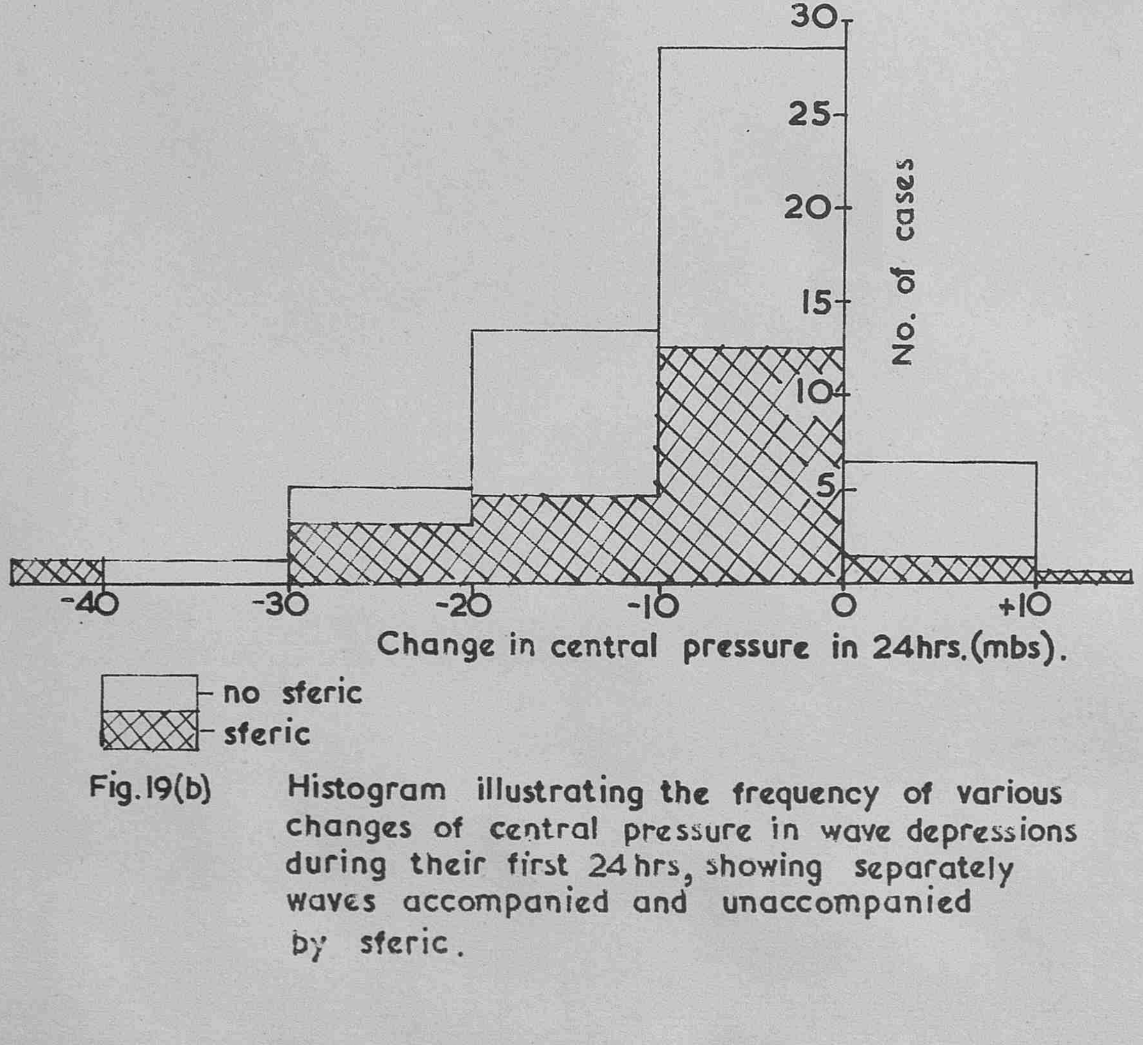

Fig. 19(b) Histogram illustrating the frequency of various changes of central pressure in wave depressions during their first 24hrs, showing separately waves accompanied and unaccompanied by sferic.

and is to be treated
CONFIDENTIALLY. Its
contents must not be quoted.

M.R.P.554
S.C.III/55
18th April, 1950

AIR WEATHER SERVICE
TECHNICAL REFERENCE FILE

AIR MINISTRY

METEOROLOGICAL RESEARCH COMMITTEE

The Upper Air over Nairobi, 1°16'S 36°51'E. 5371 ft. above M.S.L.

A preliminary survey of data to the end of 1949
By N. Carruthers, Meteorological Office.

Introduction.

Radiosonde observations have been made at Nairobi since June, 1947. To begin with, these comprised observations of temperature and humidity only; but observations of wind, by radar, were started in November, 1947.

From January, 1948, the upper air data have been received in M.O.18 in the form of punched (Hollerith) cards; and, since November, 1948, these have been accompanied by the same data on forms A.M.3427a and b (temperature) and 3428 (wind). The use of Hollerith equipment, for sorting and preliminary tabulation, facilitated the extraction of extremes of temperature and the compiling of frequency tables both of temperature and of wind. The two months' wind data prior to January, 1948, not having been punched on cards, are omitted from the present survey; but the seven months' temperature data for 1947, are included. The numbers of morning observations at the different levels for each calendar month are given in Table I. These are at 0600 G.M.T. except for 19 observations at 0300 in April and November 1948. Afternoon ascents, at 1500, were made on 22 days: April 2 to 10 and November 11 to 20, 1948 and June 15 to 17, 1949; but observations from these ascents have not been included for fear of introducing bias into the summaries (especially of wind) by overweighting the conditions prevailing during these groups of consecutive days.

This preliminary survey excludes humidity and the results are grouped under three main headings:

Upper air temperature (Table II, figs.1 and 2)

Upper winds (Tables III and IV)

Distribution of pressure and temperature at the tropopause (Table V).

The relation of tropopause height to wind at different levels has not yet been examined.

In the tables (III, IV and V(a)) in which frequencies are expressed as percentages, a small cross or asterisk denotes "less than 0.5 per cent".

Upper air temperature.

Extreme values of temperature and the average monthly temperature are shown for each calendar month at eight standard levels in Table II. At the lower levels, both the average seasonal variation and the scatter of individual observations are small; but above 200 mb. the scatter is much increased. This is brought out in figs.1 and 2. For the separate months, the range is greatest at 60 mb.: 44°F. in June, 48°F. in February and 49°F. in December. Comparable figures for Larkhill (51°N) in July, but for a longer period of record 1945-49, are:

Pressure (mb.):	500	300	200	150	100
Range at 0600 (°F.):	30	26	40	34	27

/Fig.1

G.256788/MFG/4/50/40

Fig.1 shows percentage frequencies of temperatures in steps of 2°F. at six standard levels over Nairobi in January, April, July and October. In fig.2, temperature (as abscissa) is plotted against pressure on a logarithmic scale. The outer curves show extremes for the year as a whole. The lowest recorded temperature so far was -129°F at the tropopause at 0300 on 12.11.48. This is equivalent to 184°A. The highest in the stratosphere is -54°F or 225°A. The central curve shows average temperature for October. This curve is typical of all the curves of average monthly mean temperature except that at 60 and 40 mb. the temperatures shown are 4°F. and 6°F. higher than the average temperatures for the year at these two levels.

In computing average temperatures, equal weight was given to each year irrespective of the number of observations except where (at 60 and 40 mb.) the number of observations in an individual month was less than 10. In such a case the weight assigned to the monthly mean was one tenth of the number of observations - unit weight being assigned where the number of observations exceeded 10.

It is not possible to assess the extent of diurnal variation of upper air temperature at Nairobi from the scanty data available. On those days for which there are observations at two different hours these are 0300 and 1500 G.M.T., roughly 5h. and 17h. local time, and the difference between the observations at these hours does not give the full diurnal range. Near the ground, in November 1948, temperatures at 1500 exceeded those at 0300 by 9°F. or 10°F. on average; from 700 mb. to 200 mb., average differences were inappreciable; but at 150 mb., on 7 out of 9 days, and at 100 mb. on 5 out of 7, the morning temperature was the higher, average differences (afternoon minus morning) being -4°F. at 150 mb. and -7°F. at 100 mb. This change of sign at high levels is confirmed by similar observations in April, 1948.

Upper Winds

The summaries of Tables III and IV show percentage frequencies of wind direction and speed for May to September and October to April. As will be seen from the discussion which follows, these summaries represent homogeneous wind systems only at the lower levels. The same grouping of the months has been retained for the 200-, 150- and 100- mb. levels also, in order to enable rough comparisons to be made of the general trends of speed and direction with height. Vector mean winds and average wind speeds have been computed only for the lower three levels for October to April, where the wind distribution shown approximates to a normal circular distribution. Frequencies are given to the nearest per cent. Slight adjustments were made to ensure agreement between the percentages for "all directions" and the sums of the percentages for individual directions.

Over Niarobi, as in temperate latitudes, there is a general tendency for wind speeds to increase with height above the ground, at any rate up to some level in the upper troposphere, though wind speeds over the equator are smaller than at comparable levels in higher latitudes. From the records at Nairobi for 1948 and 1949, winds appear to fall off again above the 150-mb. level (about 14 km.); but it is difficult to say to what extent the apparent lack of high speeds is due merely to loss of observations at 100 mb. and above.

Below 300 mb., the predominating winds in all months of the year tend to be easterly. Nevertheless a definite seasonal effect is apparent. From October to April (Table IV), 60 to 70 per cent. of the winds are easterly and only about 20 per cent. of the speeds fall below 10 knots. From May to September (Table III), however, the wind direction varies considerably; and very light winds are the rule, about 60 per cent. of the speeds being below 10 knots.

Above 300 mb., a seasonal effect can still be traced but, as regards speed, it is almost the reverse of that apparent at lower levels. In January, February and March, the easterly regime persists up to about 60 mb. (19 km.) with only moderate increase of wind speed with height. From June to September, on the other hand, there is a very definite easterly current at the 200-, 150- and 100- mb. levels, in marked contrast to the variableness of the wind at lower levels, and speeds tend to be higher than in any other season of the year. For 60 and 40 mb. the observations are insufficient to form a dependable guide; although they suggest that westerly winds predominate from June to September, this appearance may be due merely to a greater loss of easterly, than of westerly, wind observations associated with strong easterly winds at 150 and 100 mb.

In the intervening months also, characteristic wind regimes in the upper levels are evident but speeds tend to be lower than in the seasons already mentioned. In April and May there is much diversity of direction, with east and west winds slightly more frequent than north and south winds. In October and November, the predominating direction is westerly. December is mixed in character showing characteristics of both the October - November and the January - March seasons.

The following table sets out the seasonal variations in the wind regime. An indication of relative speeds is given in section (b) of the table. This shows the percentage frequency of winds of 30 knots or more at 500 mb. and 150 mb., the months being grouped so as to show the changes of regime in the upper troposphere.

Wind Regime over Nairobi

(a) Predominating direction.

Below 300 mb.	October - April Easterly		May - September Variable but easterly directions most frequent.	
Above 300 mb.	Oct.-Nov. Westerly	Jan.-Mar. Easterly up to 60 mb.	April-May Variable	June-Sept. Easterly up to 100 mb. with tendency to W. above.

(b) Percentage frequency of winds of 30 knots or more at representative levels in the lower and upper troposphere.

	October-November	January-March	April-May	June-September
500 mb.	0	7	3	0.5
150 mb.	15	21	11	40

The maximum wind speeds recorded for 1948 and 1949 occur in the upper easterly stream of the season June to September. Those which exceeded 75 knots are listed here.

Date	Pressure level (mb.)	Direction (^{o}E of N)	Speed (knots)
1948 July 29	156	90	78
July 30	139	105	80
1949 June 27	159	80	85
July 7	189	80	77
July 22	111	85	85
Aug. 18	164	80	76
Aug. 19	140	85	82
Sept. 5	155	85	79

/Distribution

Distribution of pressure and temperature at the tropopause.

Percentage frequencies of tropopause pressures taken over the whole year are given in Table V(a). The distribution is approximately normal and this is true also of the distributions for the separate months, with very little shift in general level in different seasons.

Table V(b) shows, for each month, the distribution of frequencies of tropopause temperatures in steps of 2°F.; the value underlined marks the column in which the median temperature lies. Median temperatures are highest in June, July, August and September and lowest in December, January, February, March and April.

Table V(c) shows the frequencies of corresponding values of pressure and temperature at the tropopause in the two groups of four months, December to March and June to September. April was omitted on account of the large scatter on the month. No definite relationship is apparent between pressure and temperature.

April, 1950.

Table I. Number of Observations at 0600 over Nairobi

	Jan.	Feb.	March	April	May	June	July	Aug.	Sept.	Oct.	Nov.	Dec.	Year
(a) Temperature. June, 1947 to December, 1949.													
700 mb.	50	48	45	39	40	65	84	82	76	81	70	74	754
500	50	47	45	39	38	62	84	81	76	81	69	74	746
300	47	45	42	37	34	61	83	77	75	80	65	72	718
200	46	44	40	37	32	61	82	74	73	78	63	71	701
150	45	44	40	37	31	60	81	71	71	78	61	69	688
100	34	40	34	36	31	55	77	64	65	74	57	61	628
60	16	24	18	16	19	37	37	23	19	53	21	31	314
40	4	3	3	4	4	12	7	5	2	16	6	8	74
(b) Wind. January, 1948 to December, 1949.													
700 mb.	48	44	45	47	41	40	53	49	49	51	53	53	573
500	48	43	45	47	39	40	53	49	50	52	52	52	570
300	45	45	43	46	35	39	52	46	49	50	48	51	549
200	44	43	42	46	32	39	52	41	48	50	47	51	535
150	44	43	42	45	27	37	51	40	46	50	46	50	521
100	32	39	35	43	21	33	49	35	42	47	45	43	464
60	10	21	20	8	5	16	18	13	11	32	15	24	193
40	1	2	1	1	-	6	4	6	2	5	4	5	37

Table II. Upper Air Temperature over Nairobi. 0600 G.M.T. June, 1947 to December, 1949.

	Jan.	Feb.	March	April	May	June	July	Aug.	Sept.	Oct.	Nov.	Dec.	Year
Absolute maximum (°F)													maximum (°F)
700 mb.	55	53	54	54	52	51	52	56	53	52	50	52	56
500	28	25	27	27	29	21	26	27	26	26	26	26	29
300	- 11	- 20	- 17	- 13	- 2	- 12	- 17	- 13	- 17	- 16	- 12	- 16	- 2
200	- 47	- 42	- 56	- 48	- 48	- 52	- 55	- 48	- 53	- 53	- 48	- 54	- 42
150	- 70	- 75	- 77	- 72	- 74	- 72	- 71	- 70	- 71	- 66	- 71	- 74	- 66
100	- 97	- 96	- 96	- 89	- 80	- 86	- 85	- 84	- 89	- 90	- 92	- 94	- 80
60	- 82	- 74	- 76	- 78	- 77	- 70	- 73	- 66	- 67	- 74	- 76	- 68	- 66
40	- 67	- 59	- 71	- 76	- 80	- 73	- 68	- 60	- 73	- 54	- 77	- 59	- 54
Average monthly mean Temperature (°F) (Equal weight is given to each year, except where the observations number less than 10)													
x maximum - minimum													Average range of monthly mean temperature (°F)
700 mb.	x49.9	49.5	49.1	49.2	47.3	45.6	45.8	45.2	47.1	47.2	46.2	46.8	4.7
500	21.6	20.5	21.7	x22.3	x22.3	21.0	20.4	20.9	20.9	20.9	22.0	21.5	1.9
300	- 23.9	- 24.8	- 22.9	- 20.7	x- 20.2	- 22.7	- 25.2	- 23.9	- 23.4	- 22.8	- 21.9	- 23.6	5.0
200	- 62.3	- 62.0	- 61.9	- 59.3	x- 58.3	- 61.2	- 64.5	- 63.8	- 63.6	- 62.5	- 60.4	- 61.6	6.2
150	- 84.5	- 85.3	- 85.9	- 83.3	x- 82.5	- 83.4	- 84.2	- 85.0	- 85.9	- 87.2	- 84.7	- 84.7	4.7
100	-107.2	-106.8	-109.3	-106.7	-105.8	x- 99.5	-100.2	-100.2	-104.2	-105.8	-107.7	-107.4	9.8
60	- 98.9	- 98.4	- 95.4	- 97.9	- 96.5	- 94.0	x- 86.6	- 88.0	- 89.3	- 88.9	- 95.2	- 97.7	12.3
40	(- 83.0)	(x- 68.3)	(- 84.3)	(- 87.3)	(- 90.7)	- 83.5	- 79.4	- 74.4	(- 71.0)	- 74.6	- 81.6	- 86.9	(22.4)
Absolute minimum (°F)													minimum (°F)
700 mb.	40	39	44	44	43	39	39	39	37	41	40	41	37
500	17	11	16	16	18	15	14	14	14	16	16	16	11
300	- 31	- 30	- 29	- 30	- 27	- 29	- 36	- 32	- 32	- 29	- 30	- 32	- 36
200	- 72	- 70	- 69	- 69	- 68	- 71	- 82	- 73	- 76	- 72	- 69	- 78	- 82
150	-100	- 94	- 97	- 93	- 91	- 94	- 98	- 96	-103	-100	- 99	- 99	-103
100	-117	-123	-122	-119	-116	-122	-118	-118	-119	-118	-124	-118	-124
60	-122	-122	-118	-121	-115	-114	-110	-106	-106	-109	-118	-117	-122
40	-104	- 81	-103	-126	-111	- 99	- 87	- 96	- 69	- 97	- 86	-101	-126

Table III Winds over Nairobi 1948, 1949

May to September 0600 G.M.T.

Direction (nearest 5°)

	N 350° -15°	20° -45°	50° -75°	E 80° -105°	110° -135°	140° -165°	S 170° -195°	200° -225°	230° -255°	W 260° -285°	290° -315°	320° -345°	All directions
Speed					Frequencies per cent								
kt. 700 mb.	(232 observations)												
0-9													67
10-19	x	2	x	4	9	3	1	1	3	2	3	2	31
20-29		x		1	x			x					2
all Speeds	x	2	x	5	9	3	1	2	3	2	3	2	100
kt. 500 mb.	(231 observations)												
0-9													54
10-19	5	5	6	10	4	3	x	x			2	6	43
20-29	2	x	x	x	x								3
30-39				x									x
All Speeds	7	6	6	11	4	3	x	x	-	-	2	6	100
kt. 300 mb.	(221 observations)												
0-9													38
10-19	1	3	3	4	4	4	5	4	4	4	6	5	47
20-29				3	4	1	1	1	2				12
30-39	x			1		x	x		x				3
All Speeds	2	3	3	8	8	6	6	5	6	4	6	5	100

x Less than ½ per cent.

/Table III (continued)

Table III Winds over Nairobi 1948, 1949

May to September 0600 G.M.T. (continued)

Direction (nearest 5°)

	350° -15°	20° -45°	50° -75°	80° -105°	110° -135°	140° -165°	170° -195°	200° -225°	230° -255°	260° -285°	290° -315°	320° -345°	All directions
Speed						Frequencies per cent							
kt. 200 mb.	(212 observations)												
0-9													19
10-19	1	3	6	7	6	2	2	2	3	1	2	3	38
20-29	1	x	5	10	3	3	2	x	1	2	x	2	31
30-39			3	4	1			x	x	x			9
40-59				3									3
60-79				x									x
All Speeds	2	3	14	24	10	5	4	3	5	4	2	5	100
kt. 150 mb.	(201 observations)												
0-9													13
10-19	x	1	5	4	5	2	2	2	5	3	1	2	32
20-29	x		4	6	3	2	x		x	1	1	x	19
30-39		x	3	8	x	x		x			x		13
40-59			5	13	x		x						19
60-79				4									4
All Speeds	1	1	17	35	9	4	3	3	5	4	3	2	100
kt. 100 mb.	(180 observations)												
0-9													26
10-19	2	2	4	8	8	2	3	3	3	1	3	2	41
20-29		2	3	9	3	x		x	1	1			20
30-39	x		1	4	3								8
40-59			1	3									4
60-79			1	x									1
All Speeds	3	4	10	24	14	2	3	3	4	2	3	2	100

x Less than $\frac{1}{2}$ per cent.

Table IV Winds over Nairobi 1948, 1949

October to April 0600 G.M.T.

Direction (nearest 5°)

	350° -15°	20° -45°	50° -75°	80° -105°	110° -135°	140° -165°	170° -195°	200° -225°	230° - 255°	260° -285°	290° -315°	320° -345°	All directions
Speed					Frequencies per cent								
kt. 700 mb.	(341 observations)												
0-9													25
10-19	5	10	19	11	6	1	x				1	1	54
20-29	1	5	11	2	x								19
30-39		1	1										2
All speeds	6	16	31	13	6	1	x	–	–	–	1	1	100
	Vector Mean: 59°, 11 kt.			Average speed: 15kt.									
kt. 500 mb.	(339 observations)												
0-9													15
10-19	1	2	16	25	9	3	x				1	x	58
20-29		1	7	11	3	1							23
30-39			1	2	1								4
40-59				x									x
All speeds	1	3	24	38	13	4	x	–	–	–	1	x	100
	Vector Mean: 88°, 13 kt.			Average speed: 15kt.									
kt. 300 mb.	(328 observations)												
0-9													28
10-19	3	5	5	8	5	5	3	2	1	1	2	2	42
20-29	1	2	2	7	7	1	1		x	1	x	1	23
30-39			1	3	1	x					x		6
40-59		x		1									1
All speeds	4	7	8	19	13	6	4	2	1	2	3	3	100
	Vector Mean: 92°, 8 kt.			Average speed: 16kt.									

x less than ½ per cent.

/Table IV (continued)

Table IV. Winds over Nairobi

October to April 0600 G.M.T. (continued)

Direction (nearest 5°)

	350° -15°	20° -45°	50° -75°	80° -105°	110° -135°	140° -165°	170° -195°	200° -225°	230° -255°	260° -285°	290° -315°	320° -345°	All directions
Speed				Frequencies per cent									
kt. 200 mb. (323 observations)													
0-9													18
10-19	2	2	3	5	4	1	3	3	5	6	2	2	38
20-29	x	1	1	5	5	2	1		2	3	2	x	22
30-39	1		1	1	7	1	x	x	1	x	1	x	14
40-59			x	3	3	x							7
60-79					1								1
All Speeds	3	3	5	14	20	4	5	3	8	9	5	3	100
kt. 150 mb. (320 observations)													
0-9													15
10-19	2	4	4	4	4	4	3	1	4	4	5	3	42
20-29	1	1	1	4	3	2	1	1	3	4	2	1	24
30-39	x		1	3	2	x	x		2	2	2	x	13
40-59				1	1		x				1	x	4
60-79				1	x								2
All Speeds	3	5	6	13	11	6	5	2	9	10	10	5	100
kt. 100 mb. (284 observations)													
0-9													18
10-19	1	3	4	7	5	4	2	3	2	5	5	2	43
20-29	1	4	2	8	5	2		1	1	3	x	x	28
30-39	x	1	1	4	1				x	1	1	x	10
40-59			x	x							1		1
All Speeds	3	8	7	19	11	6	2	4	3	9	7	3	100

x Less than ½ per cent.

G.256788/MFG/4/50/40

Table V. Tropapause over Nairobi 1948, 1949 at 0600

(a) Distribution of tropopause pressures (416 observations)

Pressure (mb):	50-59	60-69	70-79	80-89	90-99	100-109	110-119	120-129	130-139	140-149
Frequency (%):	x	7	12	21	27	20	9	2	1	x

(b) Distribution of tropopause temperatures (actual numbers of observations)

Temperature °F.	-129 -128	-127 -126	-125 -124	-123 -122	-121 -120	-119 -118	-117 -116	-115 -114	-113 -112	-111 -110	-109 -108	-107 -106	-105 -104	-103 -102	-101 -100	-99 -98	-97 -96	-95 -94	-93 -92	-91 -90	-89 -88	Total
January			1	2	5	3	8	3	2	1		2				1						28
February				3	4	7	6		5	1	2	4	1	1		1						35
March			1	6	6	5	2	3		2	1	1		1								28
April	1			2	3	4	8	2	3	4		1		1			1				1	31
May			1	2		5	2	6	4	5	3			1	1							30
June		1					3	1	3	4	7	-	6	6	5			1			1	38
July						2	1	2	2	4	5	1	5	7	6	8		1	1			45
August						1			2	5	2	5	6	5	3	1		1				31
September							2	2	4	3	10	4	5	3	2	1	1					37
October				1		2	4	6	8	9	6	2	1	3	2	1	1					46
November			2	1	1	5	3	1	6	2	1	3	2	2								29
December			1	2	3	4	8	6	5	1	3	3	2									38
Year	1	1	6	19	22	38	47	32	44	41	40	26	28	30	19	13	3	3	1		2	416

Note:- The frequency underlined indicates the column in which the median temperature lies.

/Table V (continued)

Table V (continued)

(c) Frequencies of related tropopause pressures and temperatures.

Temperature °F.	-129 -128	-127 -126	-125 -124	-123 -122	-121 -120	-119 -118	-117 -116	-115 -114	-113 -112	-111 -110	-109 -108	-107 -106	-105 -104	-103 -102	-101 -100	-99 -98	-97 -96	-95 -94	-93 -92	-91 -90	-89 -88	Total
Pressure (mb)						December to March																
50-59											1											1
60-69				2	1	2	4	2			1	2										14
70-79			1	1	3	5	7	1	2			2										22
80-89			2	3	6	6	6	3	4	1	1	2	2									36
90-99				3	5	3	5	2	3	2	3	3										29
100-109				4	1	2	1	3	1	1			1									14
110-119					1	1	1	1	1	1		1		1		1						9
120-129					1				1					1								3
130-139																1						1
140-149																						-
Total	-	-	3	13	18	19	24	12	12	5	6	10	3	2		2						129
						June to September																
50-59											1											1
60-69										1	2			1								4
70-79							2	1	2	3			2	3				1			1	15
80-89						1	1	1	2	2	2		5	1	1	1		2	1			20
90-99		1				1	2	1	4	8	8	2	6	5	5	4	1					48
100-109						1			3	2	6	4	6	6	7	3						38
110-119							1	2			3	3	2	3	2	2						18
120-129												1	1		1							3
130-139											2			2								4
140-149																						-
Total	-	1	-	-	-	3	6	5	11	16	24	10	22	21	16	10	1	3	1	-	1	151

Note:- The frequency underlined indicates the column in which the median temperature lies.

G.256788/MFG/4/50/40

M.R.P. 554

FIG. 1

FREQUENCIES OF 2-DEGREE RANGES OF TEMPERATURE °F. AT NAIROBI

PERIOD: JUNE 1947 – DECEMBER 1949
HOUR OF OBSERVATION: 0600 or 0300 G.M.T.

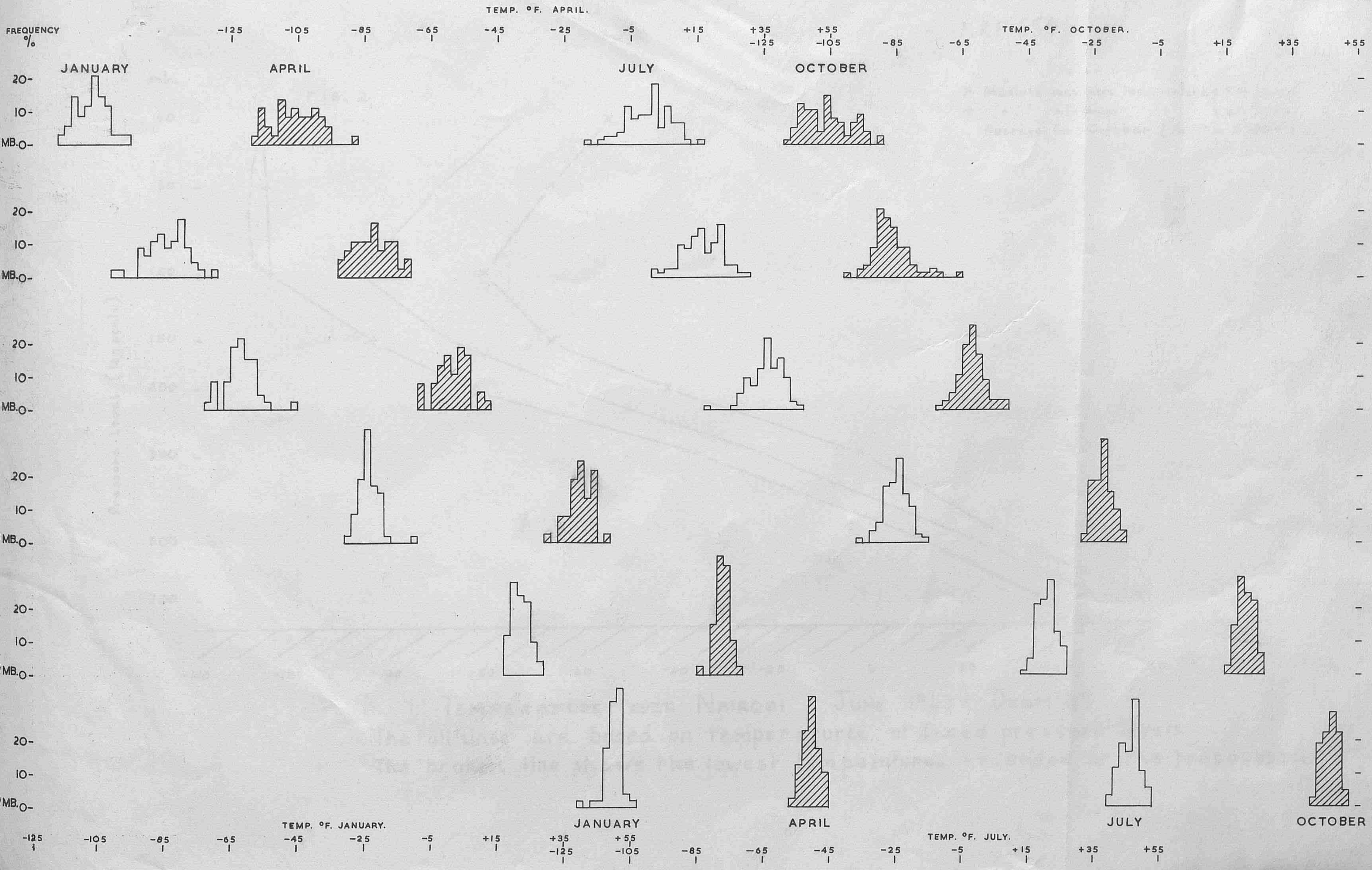

M.R.P. 554

FIG. 2

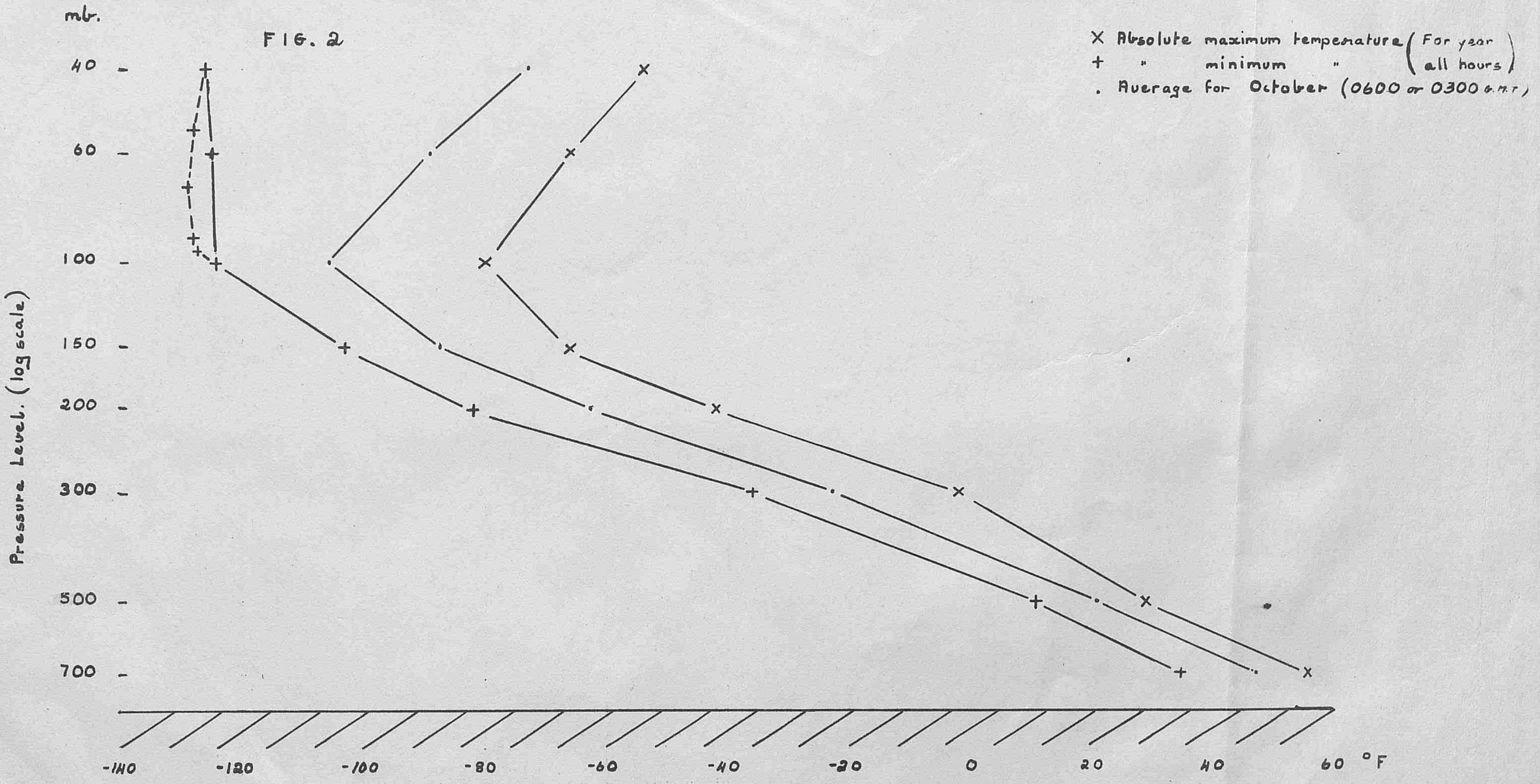

TEMPERATURE OVER NAIROBI JUNE 1947 - DEC 1949

The full lines are based on temperatures at fixed pressure levels.

The broken line shows the lowest temperatures recorded at the tropopause.

This report has not yet be published and is to be treated CONFIDENTIALLY. Its contents must not be quoted.

AS ATI No 88403

. 556
I/53
April, 1950.

METEOROL

Wind Forecasts on Empire Air Routes

by

C.S. Durst (Meteorological Office)

AIR WEATHER SERVICE
TECHNICAL REFERENCE FILES

Summary

The purpose of this paper is to endeavour to find out what are the probable magnitudes of the errors in wind forecasts which will occur on Empire Air Routes. As a yard stick for this is taken the probable error of a forecast made by purely statistical methods. For instance if we knew nothing about the present wind field the best estimate of the future wind we can give for any particular place is the average for the season. On the other hand, if we have a recent observation at that place this gives additional information. The best estimate of the future wind is then a weighted mean between the recent observation and the seasonal average the weighting factor being based on statistics of previous observations; in this the weight given to the recent observation decreases with the length of the forecast. An analysis indicates that in temperate latitudes the current synoptic methods of forecasting are appreciably more accurate than this statistical method, at any rate when practised by expert forecasters with every facility. In subtropical regions it is almost certainly not so, with techniques in use at present.

In this paper it is not intended in any way to detract from the importance of the synoptic chart, for it is the weapon by which advance must be made, nor is it wished to minimise the necessity of up to the minute observations, but in our present state of knowledge high altitude winds cannot be forecast in the tropics without tremendous effort in men, material and communications. It is believed, however, that statistical devices may be of material help in forecasting winds over parts of the empire air routes and statistical information certainly forms a means whereby measure can be made of the advances achieved.

In the following paper comparison has been made between the point forecasts for 24 hours ahead made at C.F.O. with actual winds. The result showed that the probable vector error of 24 hour forecasts made by present synoptic methods was 12 to 17 knots at 10,000 feet, 17 to 23 knots at 18,000 feet and 28 to 35 knots at 30,000 feet; it may be expected to be about 20 to 30 knots at 38,000 feet. The errors are smaller in summer than in winter. The same exactitude of determination cannot be obtained in low latitudes but by comparison of the temporal correlation coefficients of wind it is possible to give upper limits to the standard vector errors of 12 hour and 24 hour forecasts which would be made in other latitudes. These are set out for points on the route to Australia in Table VII. At 30,000 feet the standard vector errors of 24 hour forecasts will be something less than 40 to 45 knots in winter at points over France and the western Mediterranean and will decrease to under 20 knots over Malaya. In summer at points over most of the route the standard errors are likely to be less than 20 knots at that height.

Over a route as a whole the forecast errors will be appreciably less than at the individual points on the route. In general the longer the route the smaller the average error.

Comparison has been made between certain forecasts made across the Atlantic with statistical probabilities, and on the basis of this the probable errors have been derived of the forecasts of track winds over certain empire air routes. In the calculation of these the spatial correlation coefficients of wind are found to be important and these have been calculated. It is found that there are important differences in the spatial correlation of wind in tropical and in temperate latitudes.

In Table XVIII are set out the probable errors which would arise in the track winds, if no forecasts were given but the aircraft flew on comparatively long flights using only the normal winds for navigating. The probable errors

at 18,000 feet and 38,000 feet are of the magnitude of 5 to 10 knots for flights of 1,000 to 1,400 miles and are less still for longer flights.

Recommendations are made as to how the needs of aircraft flying on the empire routes should be met at the present time.

An appendix is added setting out statistically the errors which arise in assuming that the mean wind derived from a number of observations scattered along a route is an accurate representation of the true mean wind over that route. Errors of 5 knots occur in the tropics even with wind stations every 500 miles.

Introduction

Wind forecasts fall under two main heads those for a point and those for route. In the latter case they are usually required in the form of the track component or better of the equivalent head wind (this latter takes beam wind into account as well as headwind).

The following paper is divided into parts. Part I deals with winds at a point, Part II with winds over a route, Part III contains recommendations of a practical nature.

Part I. Forecasts for a Point

1. Statistical testing of C.F.O. Forecasts

From June, 1948 forecasts have been made as a routine at the Central Forecast Office twice a day for the heights 300 mb., 500 mb., and 700 mb., for a period 24 hours ahead and during the months May and June, 1949, in addition forecasts for 6 hours and 12 hours ahead were made for the heights 500 mb., and 700 mb.

For the year June, 1948 to May, 1949 the 24 hour forecasts* were examined statistically for accuracy by the calculation of the Standard Error and the 6 hour and 12 hour forecasts for the two months available were similarly treated.

The results are shown in Tables I and II.

Table I. Errors in 24 hour Forecasts June, 1948 to May, 1949

		Vector mean wind	Standard Vector Deviation	24 hour Standard Vector Difference	24 hour Standard F/C error	24^R	$24^R F$
Spring	300	294° 24	51	48	36	0.57	0.75
	500	293° 18	36	33	23	0.57	0.79
~~Summer~~	700	290° 12	27	23	19	0.65	0.76
Summer	300	278° 34	46	46	33	.50	0.75
	500	274° 24	30	29	20	.54	0.79
	700	268° 17	21	19	14	.61	0.78
Autumn	300	276° 35	43	49	35	0.34	0.66
	500	264° 27	28	33	22	0.32	0.70
	700	262° 20	21	22	16	0.44	0.70
Winter	300	278° 27	58	62	42	0.43	0.74
	500	277° 21	41	40	28	0.56	0.78
	700	265° 17	31	28	20	0.58	0.78

In this and the following table t^R is the correlation coefficient of wind with that t hours earlier and t^{RF} is the correlation coefficient of the forecast wind with the actual, the forecast being for t hours.

---

*Footnote: Throughout this paper a 12 hour (or 24 hour) forecast means a forecast of an occurrence 12 hours (or 24 hours) after the hour of the chart or observation on which the forecast is based.

/Table II

Table II. Errors in 6, 12 and 24 hour Forecasts May, June, 1949

	May, 1949					June, 1949				
	Standard Vector Deviation	Standard Vector Difference	Standard Error	t^R	$t^R F$	Standard Vector Deviation	Standard Vector Difference	Standard Error	t^R	$t^R F$
500 mb.										
6 hour f/c.	33	18	13	0.85	0.92	25	12	10	0.88	0.92
12 hour f/c.		25	17	0.72	0.86		15	14	0.80	0.85
24 hour f/c.		28	22	0.64	0.77		22	16	0.61	0.79
700 mb.										
6 hour f/c.	24	12	11	0.86	0.90	19	8	7	0.90	0.92
12 hour f/c.		15	12	0.81	0.87		11	11	0.81	0.81
24 hour f/c.		18	17	0.70	0.74		16	12	0.63	0.78

It was difficult to make the 6 and 12 hour forecasts very exactly because the prebaratics and the prontours at the C.F.O. are made for 0000, 0600, 1200 and 1800 G.M.T. whereas the observations at the upper wind stations are made at 0300, 0900, 1500 and 2100. The forecaster made his forecast immediately after the completion of the appropriate prontour and then obtained a forecast for the precise time at which a Larkhill observation would be made by interpolation with the latest completed actual map. For example to make a forecast for 1500 on a particular day, the 0000 actual surface and contour charts would be available; a prebaratic and prontour for 1800 would be drawn and the forecast derived by interpolation between the contour for 0000 and the prontour for 1800. Thus the forecast is more nearly for 15 hours than for 12 hours. The broad conclusions from Tables I and II are:-

(i) The errors in the forecasts vary with season and with height in direct relation to the standard deviation and to the 24 hour variance of wind; the result is that the correlation coefficient between the 24 hour forecast and actual wind is fairly constant with season and height between about 0.70 and 0.80 in temperate latitudes, at least to 300 mb. It is likely to be about the same at 200 mb. also.

(ii) The actual (50%) errors of a 24 hour forecast are shown in Table III below for 300 mb., 500 mb., and 700 mb.

Table III. Fifty per cent errors in forecasts at different heights

Height	Fifty per cent errors.
200 mb.	(20 kts. to 30 kts.)
300 mb.	28 kts. to 35 kts.
500 mb.	17 kts. to 23 kts.
700 mb.	12 kts. to 17 kts.

In the first line of this table estimates have been made for 200 mb. from the assumption of a correlation coefficient of 0.70 and the knowledge that the standard deviation at that height varies from about 35 kts. in spring to about 48 kts. in autumn. In Table III the larger figure refers to winter the smaller to summer. Thus in summer at 700 mb. (10,000 feet) half the 24 hour forecasts will be accurate within 12 kts. but in winter at 300 mb. (30,000 feet) an accuracy cannot be expected greater than 35 kts. on the majority of occasions.

(iii) The months May and June, 1949 appear to have been ones in which the temporal correlation coefficients $({}_tR)$ were high, particularly for periods of 24 hours.

If account is taken for the 6 hour and 12 hour forecasts being more nearly 9 hour and 15 hour forecasts the correlation coefficient between forecast and actual winds is seen to have almost a linear-relationship with the period of the forecast.

Moreover in Statistics of Wind (M.R.P.408) it appeared that the values of the temporal correlation coefficients also decreased linearly with time. So as a rough estimate we can set down the values in Table IV.

Table IV. Values of temporal wind correlation coefficients (R_t) and of wind forecasting correlation coefficients (${}_FR_t$) for various periods and standard errors (ϵ) of wind forecasts in terms of standard deviation (σ), and also the standard vector difference (η) in terms of standard deviation.

Period (hours)	0	6	12	18	24
R_t	1.00	0.88	0.75	0.65	0.55
${}_FR_t$	1.00	0.94	0.87	0.81	0.75
ϵ (kts.)	0	0.35σ	0.51σ	0.62σ	0.71σ
η (kts.)	0	0.49σ	0.71σ	0.84σ	0.95σ

The interpretation of the last line but one is that the standard error of 12 hour forecasts made with every facility available (as at C.F.O.) is likely to be about half the standard vector deviation and of a 24 hour forecast to be about 7/10 of the standard deviation.

2. The definition of success

In M.R.P. 222 Priestley has discussed the accuracy of forecasts of temperature and wind. He considered that if S is termed the success of a forecast it can be represented by the formula

$$S^2 \equiv \eta_t^2 - \epsilon_t^2 - E^2(1 - k) \qquad \text{..........} \; (1)$$

Here η_t is the standard vector difference, at the appropriate height, during the time t, ϵ_t is the standard error in the forecast during the period t, E is the standard error of observations and K is an adjustment factor representing the quality of the analysis. Priestley deduces that k may be reasonably put as unity and so

$$S^2 \equiv \eta_t^2 - \epsilon_t^2 \qquad \text{..........} \; (2)$$

Further he proposes that the correct comparison of the success S should be with the standard vector difference and writes the percentage success $100S/\eta_t$

$$\text{as} \qquad 100\sqrt{1 - \epsilon_t^2/\eta_t^2} \qquad \text{..........} \; (3)$$

From this last expression it is seen that if the conclusions reached above are right the percentage success falls off from about 70 for a 6 hour forecast to 66 for a 24 hour forecast, the value for 12 hours being 69.

Priestley gave values of the 12 hour percentage success for the months August to December, 1944, for the heights 750, 500 and 300 mb., the average values being 64 for 750 mb., 56 for 500 mb. and 58 for 300 mb. Hence it would seem that there has been a material improvement in the wind forecasts during the post war years, which is probably to be attributed to the greater information provided by weather ships to the westward and to the improvements which have been made in the drawing of prebaratics and prontours.

3. The Accuracy of Forecasts north of Latitude 45°N.

The forecasts discussed above are probably the most accurate which can be effected at the present time; for over the British Isles, the network of upper air observations is as close as anywhere in the world, and the forecasters who make these prognostics are some of the most expert available. Moreover, and this is very important, at the C.F.O. the forecasters are not subjected to the demands for special services to which many forecasters at airports are liable.

One may therefore assume that the C.F.O. errors are the minimum likely to be attainable. An upper limit can be set by the errors which would be made by a purely statistical method of using a regression equation dependent on the temporal correlation coefficient. Using the values of $_tR$ given in Table IV we get the following comparison of the probable error (50% ~~circle) of forecasts~~ made with every facility and by statistical methods.

Table V. Probable errors (50% circle) of forecasts made by C.F.O. methods and statistical methods.

Period (hours)	6	12	18	24
By C.F.O. methods	0.29σ	0.42σ	0.51σ	0.59σ
By statistical methods	0.39σ	0.56σ	0.63σ	0.69σ

The values of σ have been plotted in Geophysical Memoir No. 85 for all parts of the world. However it is not to be expected that Table V will show the accuracy attainable except in latitudes above 45°N. Regarding other latitudes more will be said later.

4. Statistical Forecasts over the British Isles

In order to find out how far the temporal correlation of wind could be improved by taking into account the wind field as represented by neighbouring stations the following procedure was carried out. A circulation index was derived by calculating the general pressure gradient at 500 mb. over an area bounded by Latitudes 45°N. and 60°N. and Longitudes 0° and 20°W. Taking this circulation index into account with the gradient of wind components between Liverpool and Aldergrove, Liverpool and Lerwick (and also in some examples Liverpool and Weather ship Item and well as Liverpool and Leuchars) the correlation coefficient was calculated between the wind at Liverpool and at the same place 12 hours (and 24 hours later). The results are shown in Table VI. (It may be pointed out that with large probable errors, such as occur in these data, the exact form of the regression equation is comparatively unimportant.)

Table VI. Temporal correlation coefficients at Liverpool

(Wind at Liverpool with wind at Subsequent time)

Months	June - July, 1948				Dec., 1948 - Jan., 1949			
Height	700 mb.		300 mb.		700 mb.		300 mb.	
Period of Time	12h	24h	12h	24h	12h	24h	12h	24h
Without regard to general field	0.71	0.56	+0.69	+0.53	0.76	0.62	+0.64	0.43
Taking account of north south circulation (Lerwick)	0.73	0.57	+0.70	+0.54	+0.79	+0.64	+0.67	+0.43
Taking account of east west circulation (Aldergrove)	0.75	0.59	+0.74	+0.58	+0.80	+0.65	+0.69	+0.48
Taking account of both north south and east west circulation (Lerwick and Aldergrove)	+0.77	+0.60	+0.75	+0.58	+0.83	+0.66	+0.72	+0.48
Taking account of both north south and east west circulation (Lerwick, Leuchars, Aldergrove and Item)	+0.78	+0.60	+0.77	+0.61	+0.87	+0.71	+0.73	+0.57

In Table VII is shown the standard errors of the forecasts deduced from a regression equation that takes account of the events at one point only and and those deduced from a regression equation that takes account of the wind at neighbouring points. The percentage success is also shown by figures in brackets.

Table VII. Standard Errors (knots) of Statistical Forecasts.

	June - July, 1948				Dec., 1948 - Jan., 1949			
	700 mb.		300 mb.		700 mb.		300 mb.	
	12h	24h	12h	24h	12h	24h	12h	24h
When no account is taken of the general field.	17(37)	20(45)	36(40)	43(49)	21(35)	25(44)	42(44)	49(48)
When account is taken of both north-south and east-west circulation.	15(56)	19(51)	32(59)	40(58)	16(71)	23(59)	37(59)	45(60)

The standard errors in this table are calculated from the formula $\epsilon = \sigma\sqrt{1 - R^2}$ where ϵ is the standard error, σ the standard deviation and R the appropriate correlation coefficient.

From this it seems the improvement is quite material particularly in Winter. The improvement in the 12 hour forecasts is greater than in the 24 hour forecasts. Possibly the field which covered about 650 miles to the westward was not sufficiently great for the 24 hour forecasts.

The forecasts derived from a regression equation involving the relationship between the wind at, say, Liverpool with winds at Lerwick, Aldergrove and weather ship, Item, are not as accurate as those made by the Central Forecasting Office, for which the percentage success is about 69 for a 12 hour forecast and 66 for a 24 hour forecast. It is not to be expected that statistical forecasts (in an elementary state) should be, since they cannot at present take development into account. It is however conceivable that with greater knowledge of the physical processes involved in the travel of wind systems development could be included.

For a rapid forecast the statistical method has advantages. The circulation index can be calculated sufficiently accurately from a previous chart and that being done the forecast of the wind at say 300 mb. could be deduced a few minutes after the observations were received. To make prontour charts and a forecast would take a matter of an hour from the time the observations were received.

5. Values of Temporal Correlation coefficients of wind in Various Latitudes.

Correlation coefficients have been calculated for certain places which are set out in Table VIII. In most cases they were calculated from a years observations.

From this table it may be concluded that at 500 mb. the coefficients of the correlation of wind with time in 12 and 24 hours do not vary greatly from place to place, but at 300 mb. there is an indication that the coefficients are higher over the Mediterranean and the sub-tropics than over the British Isles. This is not unnatural since the tropopause is more frequently below the 300 mb. level in the latitude of the British Isles than further to the south, and when the tropopause is in the neighbourhood of this level the variations of wind with time are most likely to be great.

However the essential feature of the table is that there does not seem to be any radical and fundamental difference in the statistical law of variation of wind with time between the latitudes of the British Isles and elsewhere, except perhaps that the coefficients at Nairobi are small.

Thus the magnitudes of the 12 hour and 24 hour standard vector differences of wind are dependent on the standard deviations. These standard deviations have been mapped in Upper Winds over the world (G.M.85) and hence those maps show at once where winds are most liable to considerable changes in 12 or 24 hours.

The maps in G.M.85 were largely extrapolated but the figures in Table VIII are in substantial agreement with those maps except that in the tropics the values on the maps particularly at 200 mb. are decidedly too big.

6. The accuracy of point forecasts in low latitudes

No forecasts have been made for latitudes South of 50°N which can be compared with actuals - at any rate at the higher levels. The degree of accuracy is a vital question however to those designing future air routes. It is possible however to give some estimation from the data in Table VIII and the information given earlier on what can be done over the British Isles.

Let us assume that the correlation of wind with time is 0.70 for 12 hours and .53 for 24 hours, for all latitudes from say 45° to 20° and is, say 0.65 for 12 hours and 0.45 for 24 hours in the tropics. Then from the standard deviations given in G.M.85 (modified in the light of the data in Table VIII) we can calculate the standard vector differences (η) and the standard errors (ϵ) due to statistical forecasts as in Table IX.

Values such as those in Table IX give the upper limit to the errors in accuracy of forecasts of the wind at a point (as against the wind over a route) in some cases synoptic charts will give increased accuracy. The interpretation of the statistics of Table IX is as follows:-

(i) For places where no observations are made the forecaster can only deduce the winds from neighbouring stations. If he cannot make such deductions the best forecast he can make is the normal vector mean wind derived from G.M.85. In that case the standard error will be the standard vector deviation (σ) in Table IX.

(ii) If there are observations made at the point he can give the observation as a forecast; in that case the standard error of the forecast after a lapse of 12 hours is given by η_{12} and after 24 hours by η_{24}.

It may be seen that η_{24} is but little less than σ and is even greater than σ in the tropics. (Hence to give an observation 24 hours old as a forecast is generaly unsound.)

(iii) As an alternative the forecaster can take the actual observation and use a regression equation as described in M.R.P.456. The standard error in that case will be ϵ_{12} or ϵ_{24} after intervals of 12 hours and 24 hours respectively.

(iv) The forecaster may be able to draw contour maps of the upper air and construct a prontour for the appropriate time. His percentage success will not be higher than 70 for a 24 hour forecast even over the British Isles with present techniques. If the value of percentage success dropped to 50 over the Mediterranean and Iraq there would be no gain over statistical forecasts.

(v) It would seem improbable that without great expenditure of effort in establishing a close network of radio wind stations all along the route a success of much more than 50% could be attained in the lower extratropical latitudes.

(vi) In the tropics it is extremely improbable that the percentage of success of orthodox forecasts would be as high as 50% and there a method based on statistics would be the only way of improving on the use of the normal vector mean wind as the forecast.

(vii) It is seen that with a delay of 24 hours the use of a regression equation does not give great improvement over the use of the vector mean wind but with a delay of less than 12 hours the improvement is appreciable.

Table VIII. Variation of Wind with time

Station	Dates	Vector Mean Wind		Winter				Spring						Summer						Autumn						Mean value of correlation coefficient	
				Standard Vector Deviation	Number of Obs.	12 Hour Correlation Coeff.	24 Hour Correlation Coeff.			Standard Vector Deviation	Number of Obs.	12 Hour Correlation Coeff.	24 Hour Correlation Coeff.			Standard Vector Deviation	Number of Obs.	12 Hour Correlation Coeff.	24 Hour Correlation Coeff.			Standard Vector Deviation	Number of Obs.	12 Hour Correlation Coeff.	24 Hour Correlation Coeff.	12h.	24h.
500 mb.																											
Larkhill	July'46-June'47	305°	20	39	-	0.76	0.53	283°	15	33	-	0.72	0.50	273°	19	29	-	0.74	0.57	281°	19	36	-	0.74	0.58	0.74	0.55
Gibraltar	1948	295°	15	32.6	175	0.71	0.47	246°	14	29.2	181	0.79	0.60	256°	21	19.8	169	0.69	0.39	280°	10	23.3	170	0.76	0.61	0.74	0.52
Malta	1948	300°	23	35.8	180	0.62	0.45	296°	17	25.3	121	0.79	0.66	291°	23	19.3	92	-	0.45	291°	13	21.8	137	0.69	0.59	0.66	0.54
Habbaniya	1948	262°	35	25.8	179	0.60	0.47	253°	33	20.0	182	0.61	0.36	263°	14	15.9	140	0.72	0.61	260°	22	17.6	129	0.63	0.68	0.64	0.53
Bahrein	1948	274°	39	22	61	-	0.69	264°	33	20	48	-	0.74	18°	4	13	79	-	0.42	268°	13	20	89	-	0.71		0.64
San Juan	1947	278°	14	18.6	164	0.71	0.53	225°	1	14.1	172	0.73	0.59	96°	7	9.9	174	0.47	0.31	24°	4	13.5	153	0.68	0.43	0.65	0.47
Nairobi	1948	86°	13	11.7	74	-	0.52	90°	13	9.7	50	-	0.37	27°	7	11.0	56	-	0.40	84°	12	11.1	66	-	0.63		0.48
300 mb.																											
Larkhill	July'46-June'47	309°	31	56	-	0.65	0.58	288°	22	46	-	0.70	0.36	278°	27	46	-	0.63	0.37	293°	27	57	-	0.83	0.63	0.70	0.49
Gibraltar	1948	300°	25	39.4	145	0.62	0.37	257°	18	40.7	161	0.69	0.54	267°	23	27.7	158	0.69	0.49	292°	12	34.4	157	0.74	0.61	0.69	0.50
Malta	1948	297°	34	46.6	172	0.67	0.47	294°	26	38.4	118	0.70	0.57	276°	33	22.6	90	-	0.41	294°	17	29.1	133	0.67	0.46	0.68	0.48
Habbaniya	1948	264°	63	41.7	174	0.75	0.54	256°	60	33.5	181	0.71	0.57	265°	26	23.9	136	0.85	0.71	258°	44	30.7	122	0.77	0.69	0.77	0.61
Bahrein	1948	268°	72	31	44	-	0.47	258°	43	26	23	-	0.62	13°	3	19	76	-	0.49	258°	28	31	86		0.79		0.59
San Juan	1947	294°	22	27.6	141	0.71	0.53	279°	24	26.9	165	0.76	0.63	266°	7	16.0	160	0.71	0.55	320°	10	24.5	139	0.72	0.53	0.73	0.56
Nairobi	1948	87°	11	14.6	73	-	0.28	93°	10	14.2		-	0.45	143°	5	15.9		-	0.32	126°	6	13.0		-	0.59		0.41
200 mb.																											
Larkhill	July'46-June'47	308°	33	46	-	0.80	0.58	290°	21	35	-	0.66	0.53	280°	27	39	-	0.76	0.60	295°	26	48	-	0.82	0.62	0.76	0.58
Habbaniya	1948	266°	75	27	123	0.70	0.49	258°	75	26	125	0.67	0.41	259°	26	19	81	0.80	0.68	259°	53	24	48	0.65	0.74	0.71	0.58
Bahrein	Nov.'48-Oct.'49	270°	100	28	63		0.39	258°	69	37	68		0.68	98°	12	15	73		0.58	259°	30	20	86		0.67		0.58
Nairobi	1949	110	20	19	52		0.34	90	4	18	44		0.59	90	11	18	48		0.43	250	7	15	47		0.50		0.47

Note: There is an uncertainty in the mean annual correlation coefficients of about 0.01 in the case of Larkhill, 0.02 in the cases of Gibraltar, Malta, Habbaniya and San Juan, and 0.03 in the cases of Bahrein and Nairobi for 24 hours.

/ Table IX

Table IX. Statistics of Variation of Wind in 12 and 24 hours

(a) at 500 mb. (18,000 feet)

Position	Winter (D.J.F.)					Spring (M.A.M.)					Summer (J.A.J.)					Autumn (S.O.N.)				
	Standard Deviation	12 hours		24 hours		Standard Deviation	12 hours		24 hours		Standard Deviation	12 hours		24 hours		Standard Deviation	12 hours		24 hours	
	σ kts.	η_{12} kts.	ϵ_{12} kts.	η_{24} kts.	ϵ_{24} kts.	σ kts.	η_{12} kts.	ϵ_{12} kts.	η_{24} kts.	ϵ_{24} kts.	σ kts.	η_{12} kts.	ϵ_{12} kts.	η_{24} kts.	ϵ_{24} kts.	σ kts.	η_{12} kts.	ϵ_{12} kts.	η_{24} kts.	ϵ_{24} kts.
S. France	38	29	27	37	32	31	24	22	30	26	23	18	16	22	20	25	19	18	24	21
Malta	36	28	26	35	31	25	19	18	24	20	20	15	14	19	17	23	18	16	22	20
Cairo	24	19	17	23	20	20	15	14	19	17	17	13	12	16	14	21	16	15	20	18
Bahrein	22	17	16	21	19	20	15	14	19	17	13	10	9	13	11	20	15	14	19	17
Karachi	21	16	15	20	18	18	14	13	17	15	15	12	11	15	13	20	15	14	19	17
Calcutta	20	15	14	19	17	18	14	13	17	15	15	12	11	15	13	18	14	13	17	15
Rangoon	13	12	10	14	12	15	13	11	16	13	13	11	10	14	12	18	15	13	19	16
Singapore	12	10	9	13	11	15	13	11	16	13	11	9	8	11	10	15	13	11	16	13
Darwin	20	17	15	21	18	17	14	13	18	15	15	13	11	16	13	17	14	13	18	15
Sydney	26	20	19	25	22	28	22	20	27	24	29	23	21	28	25	26	20	19	25	22
(b) at 300 mb. (30,000 feet)																				
S. France	45	35	32	44	38	43	33	31	42	37	34	26	24	33	29	40	31	29	39	34
Malta	47	37	34	46	40	38	29	27	37	32	23	18	16	22	20	29	23	21	28	25
Cairo	40	31	29	39	34	32	25	23	31	27	20	15	14	19	17	27	21	19	26	23
Bahrein	31	24	22	30	26	26	20	19	25	22	20	15	14	19	17	31	24	22	30	26
Karachi	33	26	24	32	28	30	23	21	29	25	22	17	16	21	19	27	21	19	26	23
Calcutta	30	23	21	29	25	26	20	19	25	22	22	17	16	21	19	25	19	18	24	21
Rangoon	20	17	15	21	18	25	21	19	26	22	20	17	15	21	18	25	21	19	26	22
Singapore	17	14	13	18	15	18	15	14	19	16	16	13	12	17	14	15	13	11	16	13
Darwin	25	21	19	26	22	27	23	21	28	24	27	23	21	28	24	23	19	17	24	21
Sydney	37	29	26	36	31	40	31	29	39	33	40	31	29	39	34	37	29	26	36	31
(c) at 200 mb. (38,000 feet)																				
S. France	38	29	27	37	32	33	26	24	32	28	30	23	21	29	25	35	27	25	34	30
Malta	30	23	21	29	25	30	23	21	29	25	25	19	18	24	21	30	23	21	29	25
Cairo	30	23	21	29	25	35	27	25	34	30	20	15	14	19	17	33	26	24	32	28
Bahrein	28	22	20	27	24	37	29	26	36	31	15	12	11	15	13	20	15	14	19	17
Karachi	30	23	21	29	25	35	27	25	34	30	17	13	12	17	14	25	19	18	24	21
Calcutta	30	23	21	29	25	32	25	23	31	27	20	15	14	19	17	25	19	18	24	21
Rangoon	30	25	23	31	27	30	25	23	31	27	20	17	15	21	18	30	25	23	31	27
Singapore	20	17	15	21	18	20	17	15	21	18	20	17	15	21	18	20	17	15	21	18
Darwin	30	25	23	31	27	37	31	28	39	33	32	27	24	33	29	30	25	23	31	27
Sydney	35	27	25	34	30	35	27	25	34	30	35	27	25	34	30	35	27	25	34	30

/ Part II

Part II. Forecasts for a route

1. The Magnitude of forecast errors for air routes.

The forecasts which have been discussed in the previous sections are forecasts made at a point. If forecasts are made for aircraft the wind given is usually the head wind in a number of zones which are passed through on the flight, sometimes with the forecast of the head wind of the whole flight also. It can easily be seen that the standard deviation of a head wind along a route is less than the standard deviation of the head wind component at a single point on the route. This decrease depends on the correlation between winds at different points on the route, the smaller the correlation between neighbouring points (and the longer the zone or route) the smaller will be the standard deviation of the mean wind over the route. This fact is brought out in the discussion of the theory of equivalent head winds.

Since the standard errors of wind forecasts are found to be nearly proportional to the standard deviations of the winds, it is fairly certain that the standard errors of forecasts of equivalent head winds over an air route will be smaller than the forecast of the equivalent head wind at a point.

2. Statistical variation of Route Winds

To show the sort of magnitude of this effect Tables X and XI are reproduced. These values were derived from an examination which was made of the contour charts for 225 mb. printed in the German D.W.R.s during the war. The routes height and period were chosen because they were ones for which the war time German data were most readily accessible.

Table X. Statistics of wind variation with time on an East-West route 1,200 miles long at a height of 225 mb.

Season	Standard Vector deviation of wind at a point (derived from S.D.T. M.118)	Standard Vector deviation of wind over route	24 hour standard vector difference of wind over route	24 hour Temporal Correlation Coefficient
Winter 1942-3	45 kts.	27 kts.	21 kts.	0.69
Summer 1943	36 kts.	30 kts.	19 kts.	0.79

Table XI. Statistics of wind variation with time on the route London to Sicily (1,000 miles) at a height of 225 mb.

Season	Standard Vector deviation of wind at a point (derived from S.D.T. M.118)	Standard Vector deviation of wind over route	24 hour standard vector difference of wind over route	24 hour Temporal Correlation Coefficient
Winter 1942-3	43 kts.	31 kts.	23 kts.	0.72
Summer 1943	34 kts.	29 kts.	26 kts.	0.60

Comparing Table VIII with Tables X and XI it is seen that the correlation coefficient between the wind averaged over a route at one time and at a subsequent time is materially greater than that at a point particularly if the route is east west. The 24 hour temporal correlation coefficient at a point is about 0.55 so it is clear that the gain is very appreciable in addition to the gain due to the reduction in standard deviation over the route.

From this it follows that the average error of a route forecast estimated from statistics is materially less than that made for a point and it may be expected that a route forecast made by orthodox methods from a prontour map will also be materially more accurate than that made for a single point.

The measurements in Tables X and XI were derived from measurements of contour gradient over a strip about 400 miles in breadth. Such a width is too great to take account of narrow jet streams which would affect an aeroplane. On this account the correlation coefficients are likely to be on the high side when compared with winds accurately observed by aircraft flying at constant height on successive days.

3. Comparison of route forecasts

Some comparisons were made at London Airport of 12 hour forecasts on the Great Circle Track from London to Gander using (a) prontour charts prepared as routine at London Airport and (b) a statistical method previously laid down. There were unfortunately certain difficulties in the timing of the prontour charts, which had the effect of reducing the accuracy of the prontour winds particularly over the Western Atlantic but tended to increase the accuracy of the prontour winds over the Eastern part of the route. The comparison was made over a period of 20 days and included 160 comparisons (20 at each of 8 points). Comparisons were made at 500 mb. and 700 mb. The forecast winds were deduced by the forecasting staff at London Airport.

The results are summarised in Tables XII and XIII. In Table XII the lines marked "8 positions simultaneously" represent values when the errors at all the 8 positions were meaned vectorially along the route on each of the 20 occasions; "all cases together" means that each of the 160 comparisons was taken on its own merits. Similarly in Table XIII but in that case the 8 positions were meaned algebraically.

The difference is not great. The decrease in error when a route forecast is made of a wind component stands out strikingly in both methods.

It is satisfactory to see that the prontour method is more accurate than the statistical, but in this it is well to notice the comparison of times taken to prepare the forecast. The prontour forecasts were estimated to take 217 minutes, the statistical forecasts 160 minutes, a gain to the statistical method of nearly an hour. Against this must be set the fact that the prontour method gives forecasts for other routes with little trouble and enables comparisons to be made between times of flight on different routes. If on the other hand forecasts for different times are needed, the whole process of drawing prontours has to be repeated but the statistical forecast is measured at once.

4. Accuracy of Route Forecasts according to length of route and locality

(a) Introductory

The aviator requires a forecast of the wind over the route he will follow at the height at which he will fly. This forecast may be given:-

(i) as a number of forecast winds at points along the route,

(ii) as the average (vector mean) of these forecast winds thereby giving an average wind over the route,

(iii) as an average of the head wind component over the route,

(iv) as an equivalent head wind along the route.

Both (ii) and (iv) enable allowance to be made for the lateral drift of the aircraft, (iii) does not, (i) and (ii) are in terms of vectors (iii) and (iv) are in scalars.

In Meteorological Report No.7 Sawyer has shown the relationship between the (scalar) standard deviation of the equivalent head wind and the mean vector standard deviation of wind derived from the maps which are being published in Geophysical Memoirs 85.

/Table XII

TABLE XII. Magnitudes of vector errors (knots) of forecasts on route London Airport to Gander

Height 700 mb.	Method	Mean error kts.	Max. error kts.	Min. error kts.	No. of cases		
					(a) better than (b)	(b) better than (a)	(a) equals (b)
8 positions simultaneously	(a) Prontour	17	25	0			
	(b) Statistical	18	25	0	13	6	1
All cases together	(a) Prontour	17	75	0	88	68	4
	(b) Statistical	18	53	0			
Height 500 mb.							

Table XIV. Correlation with distance

Period	Height	Places	Distance Miles	Stretch Vector Correlation Coefficient	Number of Obs.	Probable error of Correlation Coefficient
July-Oct.1946)	500 mb.	Larkhill-Liverpool	160	0.86	183	0.01
Jan.-Apr.1947)	500 mb.	Larkhill-Lerwick	650	0.37	209	0.04
"	300 mb.	Larkhill-Liverpool	160	0.78	136	0.02
"	300 mb.	Larkhill-Lerwick	650	0.35	175	0.04
"	200 mb.	Larkhill-Liverpool	160	0.86	99	0.02
"	200 mb.	Larkhill-Lerwick	650	0.37	129	0.05
June-July 1948	300 mb.	Liverpool-Aldergrove	160	0.75	122	0.03
"	300 mb.	Aldergrove-Jig	600	0.17	122	0.06
"	300 mb.	Liverpool-Jig	700	0.16	122	0.06
Dec.1948-Jan.1949	300 mb.	Liverpool-Aldergrove	160	0.78	124	0.02
"	300 mb.	Aldergrove-Jig	600	0.33	124	0.05
"	300 mb.	Liverpool-Jig	700	0.13	124	0.07
Jan.-Apr.1947) Nov.-Dec.1947)	45000 ft.	Various over British Isles	150 approx.	0.88	759	0.01
May-Oct.1947	45000 ft.	" "	150 approx.	0.86	847	0.01
Summer 1949	500 mb.	Miami-Tampa	185	0.62	74	0.05
Winter 1948/49	500 mb.	Miami-Tampa	185	0.71	56	0.05
Summer and } 1949 Winter }	200 mb.	Miami-Tampa	185	0.48	20	0.12
		Weighted Mean	185	0.63	150	0.03
Winter 1948-49	200 mb.	New Orleans-Brownsville	530	0.53	22	0.10
Winter 1948-49	200 mb.	Miami-Havana	250	0.68	68	0.04
Summer 1949	200 mb.	New Orleans-Brownsville	530	0.39	106	0.05
Summer 1949	200 mb.	Brownsville-San Antonio	230	0.63	114	0.04
		Weighted Mean	(240	0.65	182	0.03
			(530	0.41	128	0.05
Summer 1948	300 mb.	Bahrein-Habbaniya	720	0.26	71	0.07
Autumn 1948	300 mb.	Bahrein-Habbaniya	720	0.22	81	0.07
Winter (Dec.)1948	300 mb.	Bahrein-Habbaniya	720	0.10	27	0.13
		Weighted Mean	720	0.23	189	0.05
June-Dec.1949	300 mb.	Malta-Whelus Field	220	0.57	133	0.04
June-Dec.1949	200 mb.	Malta-Whelus Field	220	0.60	67	0.05
		Weighted Mean	220	0.57	200	0.03

His analysis is equally applicable to the average (vector mean) wind over a route and if we call the standard vector deviation of this route wind $\bar{\sigma}$ and the mean standard vector deviation derived from the charts $[\sigma^2]^{1/2}$ we get the following expression.

$$\frac{\bar{\sigma}}{[\sigma^2]^{1/2}} = \sqrt{\left[\frac{2}{S^2}\int_0^S \int_0^S R(x)\, dx\, ds\right]} \qquad \ldots\ldots\ldots\ldots(4)$$

where R(x) is the correlation coefficient between winds at one point and those x miles away. The value of R(x) is therefore of great importance.

(b) Correlation Coefficients of wind with distance

In Table XIV there are given some values of the spatial correlation coefficients between points at various distances apart over the British Isles, some from over the Mediterranean and Middle East and also some derived from data published in the American Upper Air Bulletins.

These data may be summarised in Table XV which is supplemented by some further data set out in M.R.P.408.

Table XV. Correlation of wind with distance

	Distance (miles)	Mean correlation coefficient
British Isles	150 approx.	0.87
	160	0.81
	600 - 700	0.27
Mediterranean and) Middle East Area)	220	0.57
	720	0.23
Southern U.S.A. and) West Indies)	185	0.63
	240	0.65
	530	0.41
South Africa	30	0.88
	115	0.76
	270	0.63
Malaya	200	0.62

These points have been plotted in Figure I and two curves have been drawn, one representing temperate latitudes, the other subtropical latitudes (including the Mediterranean region).

There is an undoubted difference between the two curves which may be attributed to the magnitudes of those eddies that have the most influence in the different regions. Clearly in regions where the eddies (depressions) are of the order of 500 or 1000 miles the correlation coefficients at 200 or 300 miles are higher than in those regions where the eddies are of 100 or 200 miles for in the latter case the winds at points 200 or 300 miles apart are unlikely to be affected in the same sense.

On Figure I a curve has also been added which represents a generalisation of that given by Sawyer in the report on Equivalent head winds. This curve lies considerably above both those curves now derived. The reason for this is that Sawyer's curves were all derived from geostrophic winds and in all measurements of geostrophic winds a considerable element of smoothing is introduced, in fact the geostrophic wind represents an average of all winds which occur during perhaps 6 hours in time and 200 miles in space. Therefore it is natural that geostrophic winds at distances of the order of 500 miles should be more highly correlated than winds measured during one or two minutes at a spot defined in dimensions of a mile or so.

It is proposed to pursue this topic in a further paper.

It should also be remembered that (as is seen in Section I, 5) there is ground for believing the temporal as well as the spatial correlation coefficients are smaller in the subtropics than in extra tropical latitudes. On both these accounts an observation of wind in the tropics is less respresentative of the wind field both in space and time than it would be in extra tropical latitudes and forecasts made on scattered observations are likely to be more widely in error in the tropics than over Europe (vide Appendix).

(c) The Standard Deviation of Route Winds

The curves given in Figure I show the value of $R(x)$ for various values of x. We are now in a position to calculate the values of

$$\frac{\overline{\sigma}^2}{\left[\sigma^2\right]}$$

from equation (i). This has been done, the curves being shown in Figure III, as well as curves for

$$\int_0^S R(x)\,dx \qquad \text{(Figure II).}$$

In Table XVI there are given for convenience values of some typical values of

$$\frac{\overline{\sigma}}{\left[\sigma^2\right]^{1/2}}$$

Table XVI. Values of the ratio of the standard vector deviation of winds averaged over routes of various lengths to the average standard deviation of the wind.

Length of route	250	500	1000	1500	2000 miles
Tropical	.90	.84	.74	.66	.59
Temperate	.96	.90	.80	.70	.63

If we require the standard deviation of the track component along the route we must multiply these ratios by o.707.

In Table XVII there are set out some estimates of the standard vector deviations of winds in winter and summer on certain routes; the majority are for flights of 1000 to 1400 miles but by way of contrast two routes are added for flights of 2200 miles.

(It should be noted that the standard deviations used are based in the main on Geophysical Memoir 85 but are modified for the higher levels in the tropics where it appears that the maps show excessively high values.)

Table XVII. Standard Vector Deviation (kts.) of Route winds between certain places.

Route	Length miles	Winter (Dec. to Feb.) 500 mb. $[\sigma^2]^{\frac{1}{2}}$	$\bar{\sigma}$	300 mb. $[\sigma^2]^{\frac{1}{2}}$	$\bar{\sigma}$	200 mb. $[\sigma^2]^{\frac{1}{2}}$	$\bar{\sigma}$	Summer (June to Aug.) 500mb. $[\sigma^2]^{\frac{1}{2}}$	$\bar{\sigma}$	300 mb. $[\sigma^2]^{\frac{1}{2}}$	$\bar{\sigma}$	200 mb. $[\sigma^2]^{\frac{1}{2}}$	$\bar{\sigma}$
London-Malta	1300	38	28	48	35	38	28	25	18	35	26	32	24
Malta-Cairo	1400	30	21	42	33	30	21	19	13	22	15	27	19
Cairo-Bahrein	1200	23	16	34	24	29	21	15	11	20	14	18	13
Bahrein-Karachi	1100	21	15	33	24	29	21	14	10	18	13	16	11
Cairo-Khartoum	1000	19	14	32	24	22	16	15	11	18	13	18	13
Khartoum-Nairobi	1200	14	10	18	13	20	14	12	8	16	11	18	13
Nairobi-Salisbury	1200	13	9	17	12	20	14	13	9	17	12	20	14
London-Cairo	2200	34	20	45	27	34	20	23	14	29	17	30	18
Cairo-Nairobi	2200	16	9	25	14	21	12	14	8	17	9	18	10

(d) An estimate of the forecast errors

We can now get an estimate of the upper limit of the random errors of wind on these routes; for if no forecast service at all were available but accurate maps of normal winds had been prepared, the navigator would fly on those normal winds and from Table XVII we can calculate that the error in the track component would be as shown in Table XVIII.

Table XVIII. Errors in track components of wind which would be exceeded on 50% and 20% of time if the normal winds only were used.

Route	Length Miles	Winter (Dec. to Feb.) 500 mb. 50%	20%	300 mb. 50%	20%	200 mb. 50%	20%	Summer (June to Aug.) 500 mb. 50%	20%	300 mb. 50%	20%	200 mb. 50%	20%
London-Malta	1300	13	25	17	31	13	25	9	16	12	23	11	22
Malta-Cairo	1400	10	19	16	30	10	19	6	12	7	13	9	17
Cairo-Bahrein	1200	8	14	11	22	10	19	5	10	7	13	6	12
Bahrein-Karachi	1100	7	13	11	22	10	19	5	9	6	12	5	10
Cairo-Khartoum	1000	7	13	11	22	8	14	5	10	6	12	6	12
Khartoum-Nairobi	1200	5	9	6	12	7	13	4	7	5	10	6	12
Nairobi-Salisbury	1200	4	8	6	11	7	13	4	8	6	11	7	13
London-Cairo	2200	10	18	13	24	10	18	7	13	8	15	9	16
Cairo-Nairobi	2200	4	8	7	13	6	11	4	7	4	8	5	9

(Note: In this table it is assumed that the errors in the forecast of track components will be distributed according to the normal scalar law of errors. This may not be precisely true but the discrepancy should not be great.)

The interpretation of this table is, for example, that if aircraft are flying on the route Cairo to Khartoum at 200 mb. with no forecast service except the knowledge of the normal wind they would encounter head winds of more than 8 knots above that they expected on 25% of occasions in winter and of 14 knots above that they expected on 10% of occasions. In summer such winds would be even less frequent.

It must be emphasised that these are upper limits and any sound scheme for forecasting will certainly reduce the errors. For instance on the route from the British Isles ot Cairo with the facilities at present available it would undoubtedly be possible to draw prontour maps for 200 mb. which would effect an improvement. How much improvement this would mean can to some extent be judged from Table XI for it seems that the 24 hour temporal correlation of wind over the route London to Sicily is about 0.65, which means that the forecast for 24 hours ahead would have a probable error of about two thirds of the standard vector deviation. If the standard vector deviation of the route ($\overline{\sigma}$) at 200 mb. is 28 kts. in winter and 24 kts. in summer the probable error of the track component of forecast wind would be less than 10 kts. in winter and 8 kts. in summer as against 13 kts. in winter and 11 kts. in summer if no forecast service were available.

/Part III.

Part III. Conclusions and Recommendations.

The object of this paper has been to make some estimates of the errors in wind forecasts to which the Civil Aircraft operator will have to submit.

It may be presumed that when the time comes to operate jet aircraft flying at 40,000 feet a meteorological forecasting service will be in operation from the British Isles to Egypt, Iraq and on to India. With the present network of Upper Air Stations it will be possible to construct contour maps at 200 mb. from which route winds could be measured which would be more representative than the mean values of the observed winds on the route.

However the technique of making forecasts at that height is not known and as an interim measure until such a technique has been formed, it is recommended that a statistical method of deriving route wind forecasts should be adopted on the strength of data given in Part II, Section 2. (It must be emphasised that any forecast issued by a statistical method would be subject to amendation by the forecaster if there was an obvious reason for doing so.)

In the region between the Tropic of Cancer and the Tropic of Capricorn orthodox methods of forecasting are impracticable. It is recommended that aircraft should fly on the normal winds for the seasons and that no attempt should be made to make forecasts, until far mor observations are available and more is known of the mechanism of the atmosphere. It is found that the errors involved in this procedure will not be excessive.

It is however essential that the normal maps on which the aircraft operate shall be as correct as possible and on this account it is necessary that the maps of Geophysical Memoir 85 should be revised, particularly in regard to the intertropical region.

/These

$$\sqrt{\sum_{1}(U^2 + V^2) \sum_{1}(U'^2 + V'^2)}$$

$$\text{or} \qquad R = \frac{1}{\sigma\sigma'}\sum_{1}^{r}(UU' + VV') \qquad \ldots\ldots \quad (8)$$

$$\text{where} \quad \bar{\sigma}^2 \equiv \frac{1}{r}\sum_{1}^{r}(U^2 + V^2) \quad \text{and} \quad \sigma'^2 \equiv \frac{1}{r}\sum_{1}^{r}(U'^2 + V'^2) \quad \ldots\ldots \ (9)$$

Then ϵ, the standard error of the observed route wind, is given by

$\sigma\,(1 - R^2)^{1/2}$

and tells us the degree of inaccuracy engendered by having observing stations at finite distances apart.

/Using

These recommendations must be looked on only as temporary expedients to be reviewed from time to time as research proceeds on the mechanism of the atmosphere at high altitude in low latitudes.

/Part III.

APPENDIX

The Representative Character of Upper Wind Observations

Let u_o, v_o be the departures from normal of the components of wind at one end of an air route of length D, and let u_p, v_p be the departures from normal of the components of wind at any observing station on the route distant P from the starting point. Let u, v be the departures from normal of the components of wind at any other point on the route.

If there are a number of observing stations n spaced equidistantly along the route, n = D/P and we have the mean departures of wind components as derived from these stations

$$\frac{1}{n+1}\sum_{o}^{n} u_p \quad , \quad \frac{1}{n+1}\sum_{o}^{n} v_p$$

which we will call U' and V'

Moreover the true mean departures of wind components along the route are

$$\frac{1}{D}\int_{o}^{D} u\,dx \quad , \quad \frac{1}{D}\int_{o}^{D} v\,dx$$

which we will call U and V

If R is the stretch correlation coefficient between the mean wind derived from the observing stations and the true mean wind we have by definition

$$R = \frac{\sum_{1}^{r}(UU' + VV')}{\sqrt{\sum_{1}^{r}(U^2 + V^2)\sum_{1}^{r}(U'^2 + V'^2)}} \quad \text{......} \quad (7)$$

or

$$R = \frac{1}{\sigma\sigma'}\sum_{1}^{r}(UU' + VV') \quad \text{.....} \quad (8)$$

where

$$\sigma^2 \equiv \frac{1}{r}\sum_{1}^{r}(U^2 + V^2) \quad \text{and} \quad \sigma'^2 \equiv \frac{1}{r}\sum_{1}^{r}(U'^2 + V'^2) \quad \text{....} \quad (9)$$

Then ϵ, the standard error of the observed route wind, is given by

$\sigma(1 - R^2)^{1/2}$

and tells us the degree of inaccuracy engendered by having observing stations at finite distances apart.

Using the method adopted by Sawyer in Appendix II to Met. Report 7 it is seen that

$$\bar{\sigma}^2 = \frac{2\sigma^2}{D^2}\int_0^D\int_0^S R(x)\ dx\ ds \qquad \ldots\ldots\ (10)$$

where R(x) is the correlation coefficient between winds at distances x apart and

$$\sigma^2 = \frac{1}{r}\left\{\sum_1^r u^2 + \sum_1^r v^2\right\}$$

The value of this expression is shown in Fig.III.

Now

$$\sigma'^2 = \frac{1}{r}\sum_1^r \frac{1}{(n+1)^2}\left(\sum_0^n u_p\right)^2 + \frac{1}{r}\sum_1^r \frac{1}{(n+1)^2}\left(\sum_0^n v_p\right)^2 \qquad \ldots\ldots\ (11)$$

$$= \frac{\sigma^2}{n+1} + \frac{2n\sigma^2}{(n+1)^2}R_{0,1} + \frac{2(n-1)}{(n+1)^2}\sigma^2 R_{0,2} + \ldots + \frac{2}{(n+1)^2}\sigma^2 R_{0,n} \qquad \ldots\ldots\ (12)$$

where $R_{0,1}$ is the correlation coefficient between the winds at two stations distant P apart, $R_{0,2}$ between two stations 2 P apart and so on.

Moreover

$$\sum_1^r \frac{u_pU}{\sigma^2} + \sum_1^r \frac{v_pV}{\sigma^2} = \frac{1}{D}\int_0^D \sum_1^r \frac{u_pu}{\sigma^2}\ dx + \frac{1}{D}\int_0^D \sum_1^r \frac{v_pV}{\sigma^2}\ dx \qquad \ldots\ (13)$$

$$\text{or} \quad = \frac{1}{D}\int_0^{D-P} R(x)\ dx + \frac{1}{D}\int_0^P R(x)\ dx \qquad \ldots\ldots\ (14)$$

So that $\sum_1^r (UU' + VV')$ which is $\sum_1^r \left\{\frac{1}{n+1}\sum_0^n u_pU + \frac{1}{n+1}\sum_0^n v_pV\right\}$

$$= \frac{2}{D}\frac{\sigma^2}{n+1}\sum_0^n \int_0^{\frac{pD}{n}} R(x)\ dx \qquad \ldots\ldots\ldots\ (15)$$

Hence we can write R as

$$\frac{2}{D}\,\frac{\sigma}{\bar{\sigma}}\;\frac{\sum_{0}^{n}\left\{\int_{0}^{\frac{pD}{n}} R(x)\,dx\right\}}{\sqrt{(n+1) + 2nR_{0,1} + 2(n-1)R_{0,2} + \dots + 2R_{0,n}}} \quad \ldots\ldots (16)$$

In Section 4(c) of Part II the various quantities in this expression have been calculated and so in Table XIX the values of R are shown for typical routes in the tropics and temperate regions.

Table XIX. Values of R when routes are of various lengths and observing stations are at various distances apart

Distance between observing station(Miles)		250	500	1000	2000 miles
Tropics					
Length of route	1000 miles	0.963	0.90	0.76	
	2000 miles	0.980	0.91	0.78	0.52
Temperate Zone	1000 miles	0.980	0.94	0.80	
	2000 miles	0.997	0.96	0.83	0.54

We can now calculate the standard vector error (ϵ) of the route wind determined from n stations from $\bar{\sigma}\sqrt{1 - R^2}$ or since we know the ratio of $\bar{\sigma}$ to σ from expression (10) we can calculate ϵ in terms of σ. This is done in Table XX.

Table XX. Values of standard error (in terms of mean standard vector deviation $[\overline{\sigma^2}]^{1/2}$ due to observations being spaced out at various distance along routes of certain lengths.

Distance between observing stations		250 miles	500 miles	1000 miles	2000 miles
Tropics					
Length of route	1000 miles	0.20σ	0.32σ	0.48σ	
	2000 miles	0.12σ	0.24σ	0.37σ	0.50σ
Temperate Zone					
Length of route	1000 miles	0.16σ	0.27σ	0.48σ	
	2000 miles	0.05σ	0.18σ	0.35σ	0.53σ

To interpret this into concrete examples:-

On the London Malta route in winter at 200 mb. a mean wind over the route based on observations every 250 miles is going to have a vector probable error of about 5 knots. If observations were only available at the two ends the vector probable error would be about 15 knots. Of course in this case it would be possible to obtain more accurate results by drawing contour charts, but the meaning of contour charts becomes increasingly doubtful in lower latitudes. On the route Khartoum to Nairobi and thence to Salisbury (where the normal standard vector deviation of wind is about 20 kts. at 200 mb.) if there were wind finding stations Khartoum, Nairobi and Salisbury, the probable error of the route wind for flights of 1000 miles would be about 8 knots and for a flight of 2000 miles about 6 knots. Even if there were wind finding stations every 500 miles there would still be a probable vector error in the route wind of 5 knots.

Fig. I. Correlation of wind with distance (R(x))

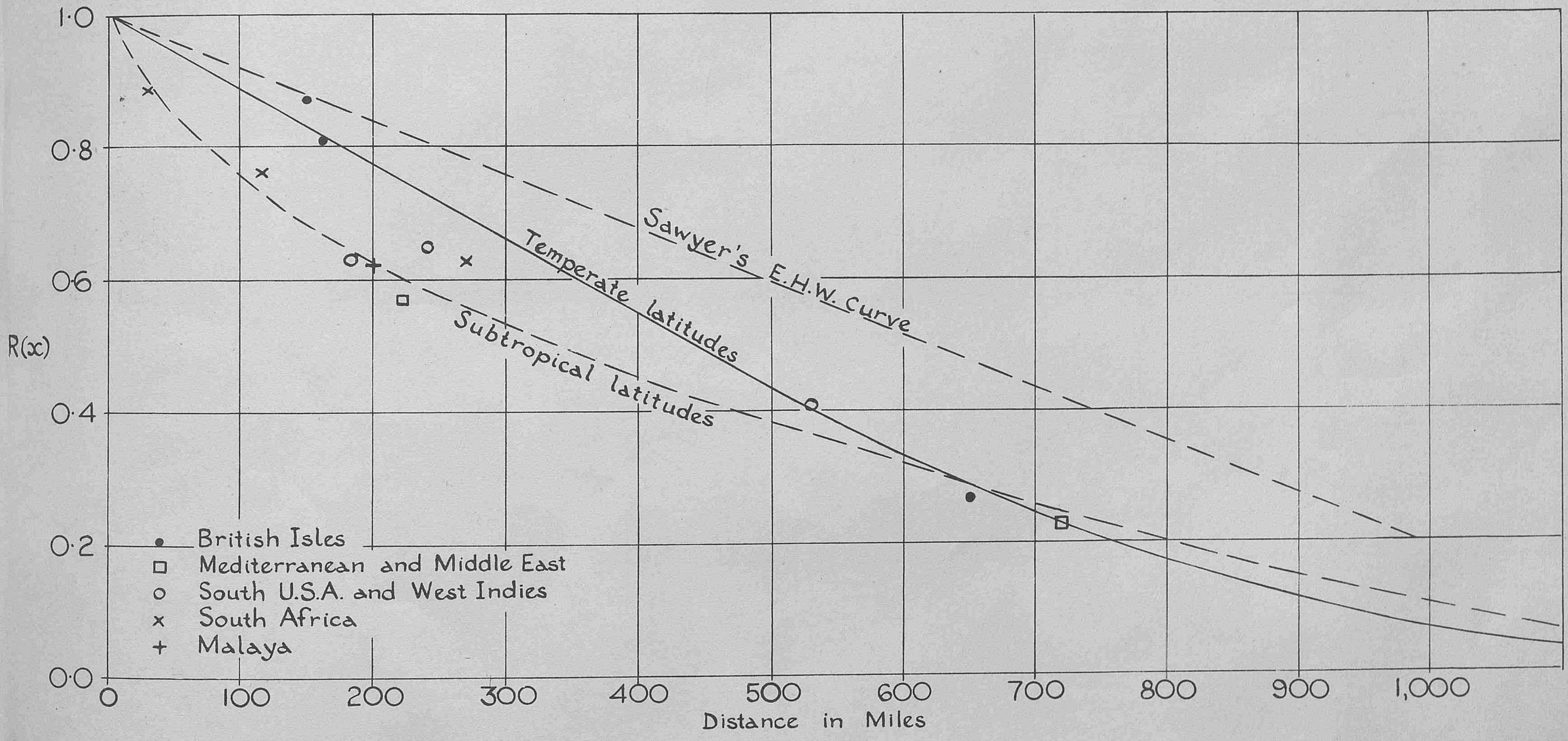

Fig. II. Variation of $\int_0^s R(x)dx$ with distance.

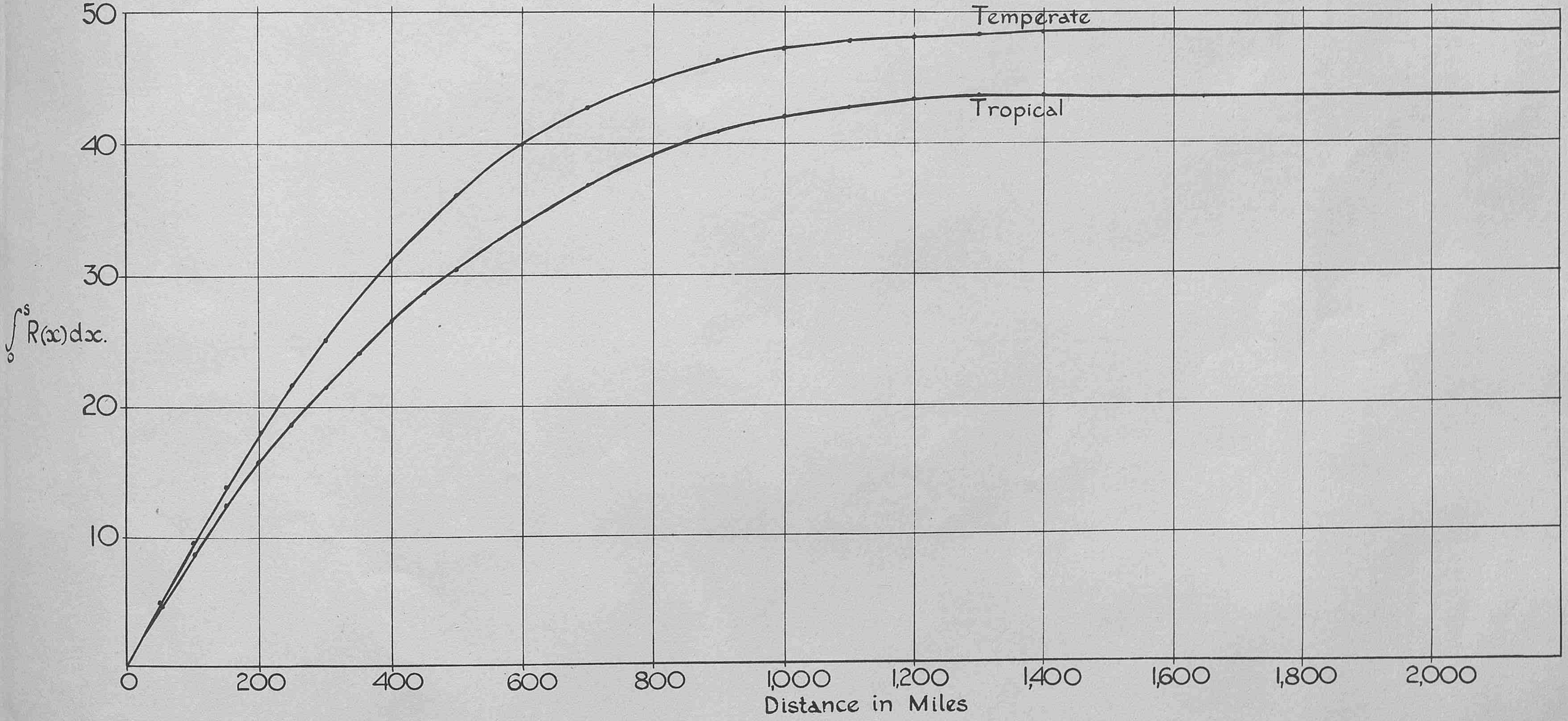

Fig. III. Variation of $\frac{\bar{\sigma}^2}{\sigma^2}\left[=\frac{2}{D^2}\int_0^D\int_0^s R(x)\,dx\,ds\right]$ with distance.

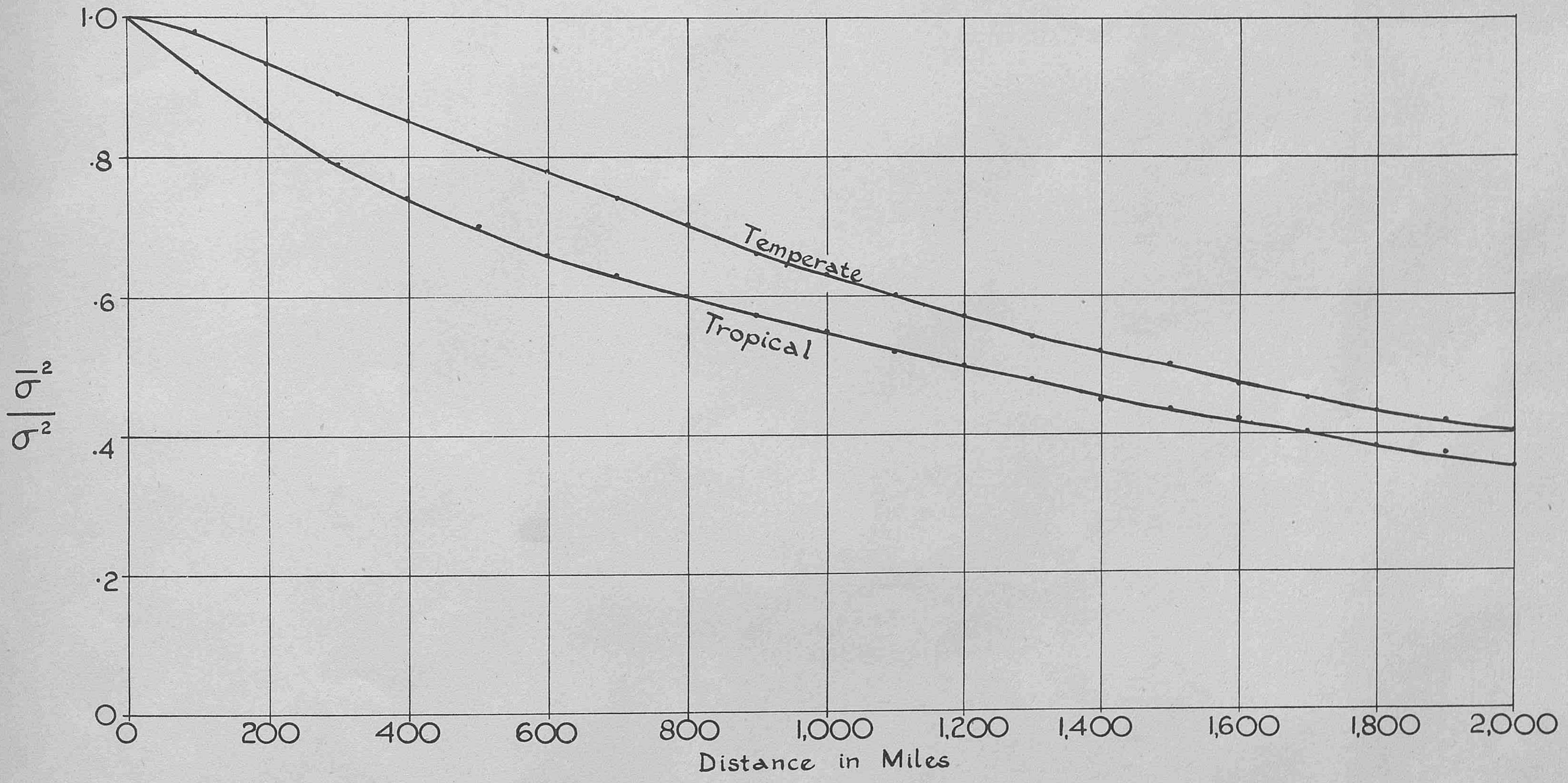

CONTROL NUMBER

mats

This report has not yet been published and is to be treated CONFIDENTIALLY. Its contents must not be quoted.

M.R.P.559
S.C.III/56
5th May, 1950.

AF218662 — 1

AIR MINISTRY

METEOROLOGICAL RESEARCH COMMITTEE

Drop Size Distribution in Cloud

by

A. C. Best. (Meteorological Office)

Classification Cancelled
by authority of Chief AWS
By PSB
Date 4 Oct 50

AIR WEATHER SERVICE
TECHNICAL REFERENCE FILES

1. Summary

Some experimental measurements of drop size distribution in cloud are examined and it is shown that the size distribution of cloud drops can be described by the equation

$$1 - F = \exp\left[-(x/a)^n\right]$$

where F is the fraction of liquid water in the air comprised by drops with diameter less than x. In any one cloud a and n are constants. The value of a increases as the liquid water content of the cloud increases. The parameter n varies from about 2 to 5 in different clouds with a mean value of about 3.2; it is not clear what factors govern the variation of n. Finally the relationships between the various ways of expressing the average size of cloud drops are examined.

2. Introduction

Although there are many published data for the mean drop size in clouds there appears to be but little available information on drop size distribution. Cloud structure on a micro scale is frequently far from homogeneous and for some purposes a knowledge of drop size distribution is required. Moreover different investigatiors have used different parameters in describing the mean drop size. For example Bricard (1934) has given the following mean drop diameter based upon measurements made on Pic-du-Midi.

Nimbostratus	22 microns	(5 measurements)
Stratosumulus	16 ..	(5 ..)
Cumulus	13 ..	(4 ..)
Stratus	10.6 ..	(2 ..)

Lewis and Hoecker (1949) have published a large number of measurements of 'mean effective drop diameter' from which the following averages have been extracted

Cumulus	19 microns	(98 measurements)
Cumulonimbus	24 ..	(89 ..)
Altocumulus	22 ..	(65 ..)
Altocumulus/Altostratus	19 ..	(42 ..)
Stratocumulus	16 ..	(19 ..)

/Bricard's

518662

Bricards's measurements were made by catching the drops in oil. Lewis and Hoecker used the rotating cylinder method. It is clear that the values quoted above do not refer to the same quantity - Bricard's figures refer to the arithmetical mean of the drop diameters whereas Lewis and Hoecker's mean effective diameter must be related in some way to the quantity of water corresponding to drops of a particular size. Without some knowledge of the drop size distribution it is not possible to compare the two sets of values.

Inspection of the small amount of data on drop size distribution known to the writer suggested that drop size distribution in cloud might be adequately represented by an equation of the form

$$1 - F = \exp\left[-(x/a)^n\right]$$

where F = fraction of liquid water in the air comprised by drops with diameter less than x.

n and a are constants.

We shall see later that this formula does in fact adequately describe certain data. Two advantages follow immediately. The numerical values found for the constants a and n facilitate a quantitive comparison of different sets of data. The application of an appropriate formula enables one to assess the relation between the various kinds of mean drop size which may be quoted.

3. The experimental measurements available

The data which form the basis of this note fall into two groups. During the period January 1943 to May 1944 a number of measurements of the size of cloud particles were made from an aircraft by Dr. J. Mazur (Mazur (1943), see also Best (1946)) using an instrument known as the Aircraft Impactor. This instrument consists essentially of a glass plate with a covering of a uniform film of either oil to trap the water droplets which impinge on it or alternatively of magnesium oxide in which impinging particles make craters. There was a shutter arrangement whereby the plate was exposed to the airstream for a known short period of time. The plates were examined through a microscope after the flight and the drop sizes assessed. Mazur normally took three or four samples in each cloud, the plates being usually, but not always, exposed at different heights in the cloud. The data available to the writer included

Height

Cloud type

Number of drops with diameters falling bewteen specified limits

(the limits were not the same for each sample)

Number of drops per cubic centimetre of air.

The second group of data covers results published by Diem in two papers (Diem, 1942 and 1948). The second paper is essentially a continuation of the first and we shall not distinguish between them. Diem used three methods of measuring drop size viz. the 'glory' method, deposition of ice on cylinders and a third method similar in many respects to that of Mazur. The first two methods give only mean drop sizes and we shall be concerned here only with the results obtained by the third method which gives information about drop size distribution. Diem's second paper gives mean curves for drop size distribution in various types of cloud. Both papers give percentage drop size distribution for individual samples in the form of small block diagrams. For each sample

/the

218662

the total number of drops assessed was stated and, usually, the liquid water content of the air (g/cm^3) based upon these measurements.

The data from Mazur's work and from the first paper of Diem have previously been reported (Best 1946) but the present analysis, besides including the additional data from Diem, differs in some ways from that adopted earlier.

4. Method of analysis

(a) Mazur's data A difficulty associated with Mazur's data arose from the fact that occasionally a sample included a very few large drops. On a few occasions these large drops had diameters up to about 100 microns. A very few large drops may have a very great influence on the shape of the drop size distribution curve if the latter is based upon volume, instead of number, of drops between specified diameter limits. At the same time the number of large drops may be so small (e.g. up to five per cent of a total number of several hundred) that one can place little reliance upon the measured frequency of occurrence. Moreover it is doubtful whether one should regard such drops as cloud droplets or as precipitation elements. Finally there is the possibility that the large drops may have originated in the water being blown off the measuring instrument onto the plate. With these considerations in mind it was decided to discard all samples containing drops with a diameter exceeding 60 microns. This limit was chosen quite arbitrarily. It led to discarding 18 samples out of 114, the 18 samples having been obtained on 11 out of 26 flights. The discarded samples usually contained less than five large drops (out of several hundred). Next the samples obtained in any one cloud were added together and the function F evaluated for the various diameters used in assessing the drop sizes. It was not yet practicable to group samples obtained in different clouds since the ranges of x within which the drops had been counted originally were not the same for all clouds. Accordingly F was plotted against x for each cloud and from the graph so obtained the value of x corresponding to the values 0.05, 0.10, 0.25, 0.50, 0.75, 0.90 and 0.95 of F were read. For the selected values of F the logarithms of x were averaged over groups of clouds, the grouping being done by cloud type and liquid water concentration in the cloud.

(b) Diem's data. The procedure in dealing the Diem's data was simplified by the fact that all the block diagrams giving percentage number drop size distribution were based upon the same diameter limits. The work of reading values from the small scale block diagrams was very laborious however and was attempted only for those diagrams which were based upon samples containing more than 100 drops. Some of these selected diagrams were grouped according to cloud type and liquid water content and corresponding values of x and F were obtained. Diem, in his second paper, gives some volume distribution curves, averaged over all his samples, for various cloud types irrespective of liquid water content. From these mean curves values of F for various values of x were also obtained.

5. Presentation of results

If equation 1 represents the drop size distribution then a plot of $\log_{10} x$ against $\log \log_{10} 1/(1-F)$ should approximate closely to a straight line. Figure 1 shows such plots for each group of data described above. In each case the best straight line has been drawn by eye and the values of n and a determined from this line. Table 1 shows the values of n and a so obtained and also gives certain auxiliary data which are relevant to an assessment of the reliability of the results. From figure 1 and the tabulated values of a and n we may draw the following conclusions

(i) Equation 1, with suitable values for the two parameters, represents the drop size distribution in cloud with reasonable accuracy. In this connection it should be mentioned that, when drawing the straight lines, the points corresponding to log $\log_{10} 1/(1-F)$ less than $\bar{2}.66$ or greater than 0.0 have been ignored. This is equivalent to neglecting the 10 per cent of water comprised by the smallest drops and the 10 per cent comprised by the largest drops. The worst fit is, perhaps, obtained from clouds with small water content. For practical applications however it is more important that the clouds with substantial water content do conform to the formula.

(ii) In general the value of a increases as the liquid water content of the cloud increases. In figure 2 $\log_{10}$ a has been plotted against $\log_{10}W$ and it can be seen that, very approximately, a increases as the square root of W.

(iii) If n is plotted against W it will be seen that the two variables appear to be quite independent. The variation of n with cloud type (in table 1) is not well marked though there does appear to be a tendency for smaller values of n to be associated with layer type clouds (groups 1, 2, 3, 7, 8, 9, 10, 12 and 17) than with convective clouds (groups 4, 5, 6, 15 and 19). There are anomalies here however in groups 14, 16 and 18. A high value for n corresponds to little variation in cloud particle size and vice versa and one might therefore expect the shorter lived clouds to exhibit large values for this parameter. On the whole it seems safer to conclude that some other factor apart from those mentioned above influence the value of n.

(iv) Table 1 contains 20 values for n though there is a certain amount of overlapping of the data upon which they are based. The mean of these 20 values is 3.20 with a standard deviation of 0.78. It will be recalled that a similar analysis to that described above was applied to some measurements made by the Meteorological Research Flight; Best, 1949, resulting in nine values for n. The mean of those nine values was 3.06 with a standard deviation of 0.72. Until more is known of the factors which influence the value of n it seems reasonable to accept a value of about 3.2. In passing it may be noticed that when equation 1 was applied to raindrop size distribution (Best, 1948) a value of 2.25 was obtained for n.

/Table 1

218662

Table 1

Experimental data on drop size distribution in cloud

Group	Cloud	Liquid water content, W. g/m³	No. of Samples	No. of Clouds	Total No. of drops	No. of drops per cm³	n	a microns
Mazur								
1	Sc	0.07	14	4	6940	306	2.17	12.9
2	..	0.15	12	3	6830	267	2.60	17.5
3	..	0.35	12	3	9075	453	2.91	22.6
4	Cu	0.07	18	6	9311	250	3.51	11.3
5	..	0.13	5	3	2863	311	4.65	13.9
6	..	0.22	7	3	4066	275	3.77	19.5
7	St	0.13	10	3	5068	317	1.85	25.1
Diem								
8	Sc	0.05	2	2	348		3.24	12.3
9	..	0.15	3	3	359		2.90	11.6
10	..	0.23	3	3	567		3.06	24.7
11	..	0.48	2	2	646		4.94	18.0
12	As	0.13	5	5	1584		2.53	18.1
13	Ns	0.30	4	3	599		4.17	26.5
14	Cu	0.20	4	3	1084		2.01	21.0
15	Cu(1)		10				3.52	12.9
16	As		31				3.55	16.8
17	St		19				2.75	27.8
18	Sc		26				3.28	13.0
19	Cu(2)		8				3.31	25.6
20	Ns		27				3.31	27.0

Notes. (a) A few of Mazur's results have been omitted because, either on account of cloud type or liquid water content, the results would refer to groups consisting of one cloud only.

(b) In groups 8 to 14 the number of drops per cubic centimetre have been omitted because some of Diem's results were inadequate to permit this computation.

(c) Groups 15 to 20 are computed from Diem's 1948 mean curves and so are based upon all his individual measurements irrespective of liquid water content and including the results given in groups 8 to 14.

6. The average size of cloud particles

Having established that equation 1 represents drop size distribution in cloud with reasonable accuracy we may now consider the relation between the various ways of ecpressing the average drop size.

We define four average diameters as follows:-

D_p The predominant diameter is the diameter corresponding to the maximum volume of water.

D_p The mode diameter is the diameter corresponding to the maximum number of drops.

D_m The mean diameter is the sum of all the drop diameters divided by the number of drops.

/D_v

218662

D_v The mean volume diameter is the diameter of a drop whose volume is equal to the average drop volume.

In any experimental measurements of drop size in cloud there is a minimum drop size to which the measuring apparatus will respond and the numerical value of D_m and D_v will clearly depend upon the minimum measurable diameter z. In the appendix formulae are developed for the computation of the four average diameters on the assumption that equation 1 adequately represents the drop size distribution, for three different values of the minimum measurable diameter z and for various values of n. In equation 1 x occurs only in the ratio x/a and it is to be expected therefore that z is important only as a fraction of a and that the four average diameters should be expressible as fractions of a, the fractions depending upon n and, for D_m and D_v, upon z/a. In table 2 the numerical values of D/a are given for various values of n and z/a.

Table 2

Values of the four mean diameters

z/a =	Any value		0.05		0.1		0.2	
n	D_p/a	D_d/a	D_m/a	D_v/a	D_m/a	D_v/a	D_m/a	D_v/a
1.5	0.481	-	0.112	0.228	0.201	0.331	0.282	0.494
2.0	0.707	-	0.148	0.301	0.243	0.391	0.393	0.527
2.5	0.815	-	0.210	o.393	0.301	0.464	0.396	0.551
3.0	0.874	-	0.301	0.492	0.376	0.541	0.488	0.617
3.5	0.908	-	0.410	0.585	0.460	0.613	0.544	0.664
4.0	0.931	-	0.516	0.663	0.543	0.677	0.599	0.707
4.5	0.946	0.614	0.605	0.723	0.617	0.729	0.650	0.746
5.0	0.956	0.725	0.672	0.767	0.678	0.770	0.697	0.779

We see from this table that D_p is but little affected by variations in n and, of course, is independent of z. On the other hand D_v and particularly D_m show considerable variation with n and, except at the larger values of n, a substantial variation with z. We see also that with a small value for z D_m may be only about one third of D_p. There are no values for D_d when n equals four or less because the number distribution curve then has no mode.

7. Conclusions

The drop size distribution in cloud can be described with reasonable accuracy by means of an equation of the form of equation 1. The values of the parameter a increases with the liquid water content of the cloud but it is not clear what are the factors which govern the value of n. A reasonable mean value for n seems to be about 3.2.

If a single average size is used to described the average size of cloud drops it seems preferable to quote the predominant diameter since this is less liable to variation with n and the limitations of the measuring equipment than some of the other average sizes which may be quoted.

References

Best, A. C.	1946.	M.R.P. 309.
..	1948.	M.R.P. 452.
..	1949.	M.R.P. 483.
Bricard, J	1943.	La Meteorologie, Jan-June, p. 57.
Diem, M.	1942.	Ann. Hydr., 70. p. 142.
..	1948.	Met. Rund., No. 9/10
Lewis, W. and Hoecker, W.H.	1949.	N. A. C. A. Tech. Note 1904.
Mazur, J	1943.	M.R.P. 109

218662

Appendix.

Computation of the Average Size of Cloud Drops.

We suppose that at diameters greater than the minimum measurable size the drop size distribution is described by equation 1.

The volume of water comprised by drops with diameter between x and x+Δx is

$$W \frac{\partial F}{\partial x} \Delta x = W \frac{n\, x^{n-1}}{a^n}\, e^{-(x/a)^n}\, \Delta x \qquad \dots\dots\dots\dots\dots\dots(2)$$

and the number of drops with diameter between x and x+Δx is

$$\frac{6W}{\pi x^3} \frac{\partial F}{\partial x} \Delta x = \frac{6W}{\pi} \frac{n x^{n-4}}{a^n}\, e^{-(x/a)^n}\, \Delta x \qquad \dots\dots\dots\dots\dots(3)$$

Now D_p and D_d are the values of x which make the right hand sides of equations 2 and 3 respectively maxima. We thus get

$$D_p = a\left(1 - \frac{1}{n}\right)^{1/n} \qquad \dots\dots\dots\dots\dots\dots\dots\dots\dots(4)$$

$$D_d = a\left(1 - \frac{4}{n}\right)^{1/n} \qquad \dots\dots\dots\dots\dots\dots\dots\dots\dots(5)$$

It is clear also that

$$D_m = \frac{\dfrac{6Wn}{\pi a^n} \displaystyle\int_z^\infty x^{n-4}\, e^{-(x/a)^n}\, x\, dx}{\dfrac{6Wn}{\pi a^n} \displaystyle\int_z^\infty x^{n-4}\, e^{-(x/a)^n}\, dx}$$

and

$$\frac{\pi D_v{}^3}{6} = \frac{W}{\dfrac{6Wn}{\pi a^n} \displaystyle\int_z^\infty x^{n-4}\, e^{-(x/a)^n}\, dx}$$

where z is the diameter of the smallest measurable drop. Putting $(x/a)^n = t$ we get

$$D_m/a = \frac{\displaystyle\int_{(z/a)^n}^\infty e^{-t}\, t^{-2/n}\, dt}{\displaystyle\int_{(z/a)^n}^\infty e^{-t}\, t^{-3/n}\, dt} \qquad \dots\dots\dots\dots(6)$$

$$D_v/a = \left[\frac{1}{\displaystyle\int_{(z/a)^n}^\infty e^{-t}\, t^{-3/n}\, dt}\right]^{1/3} \qquad \dots\dots\dots(7)$$

21862

We wish to compute the values of these four average diameters for various values of n and z/a. If we write

$$X_2 = \int_{h^n}^{\infty} e^{-t}\, t^{-2/n}\, dt \qquad X_3 = \int_{h^n}^{\infty} e^{-t}\, t^{-3/n}\, dt$$

where h = z/a the computation of D_m and D_v will depend upon the evaluation of X_2 and X_3. At first sight these appear to be easily obtainable from tables of the Incomplete Gamma function. However we have seen that a is likely to have a value from 10 to 30 microns and experimental measurements appear to be reliable down to z = 1 or 2 microns. Thus h may have a value of the order 0.05 and the only tables known to the writer do not deal with such small values of the limit. In order to ensure that significant quantities were not neglected the formulae for X_2 and X_3 were put into the following form by repeated integrations.

$$X_2 = -A_2(h^{n-2} + B_2) + C_2\left[1 - I(u_2,p_2)\right] \qquad \text{...........(8)}$$

$$X_3 = -A_3(h^{n-3} + B_3) + C_3\left[1 - I(u_3,p_3)\right] \qquad \text{...........(9)}$$

where

$$A_2 = \frac{e^{-h^n}}{1 - \frac{2}{n}} \qquad A_3 = \frac{e^{-h^n}}{1 - \frac{3}{n}}$$

$$B_2 = \frac{h^{2n-2}}{2 - \frac{2}{n}} \qquad B_3 = \frac{h^{2n-3}}{2 - \frac{3}{n}}$$

$$C_2 = \frac{\Gamma(3 - \frac{2}{n})}{(1 - \frac{2}{n})(2 - \frac{2}{n})} \qquad C_3 = \frac{\Gamma(3 - \frac{3}{n})}{(1 - \frac{3}{n})(2 - \frac{3}{n})}$$

$$u_2 = \frac{h^n}{\sqrt{(3 - \frac{2}{n})}} \qquad u_3 = \frac{h^n}{\sqrt{(3 - \frac{3}{n})}}$$

$$p_2 = 2 - \frac{2}{n} \qquad p_3 = 2 - \frac{3}{n}$$

$$I(u,p) = \frac{\int_0^{u\sqrt{(p+1)}} e^{-t}\, t^p\, dt}{\Gamma(p+1)}$$

From equations 6 and 7 we have

$$D_m = a\,\frac{X_2}{X_3} \qquad D_v = a\left[\frac{1}{X_3}\right]^{1/3} \qquad \text{........(10)}$$

The advantage of equations 8 and 9 is that the function I is tabulated in Pearson's table of the Incomplete Gamma Function and the values of the parameters are such that, although I cannot be evaluated from the tables the latter show that the values of I with which we are concerned are small (less than 0.02) in the cases considered compared with unity and so can be neglected.

Equation 8 fails when n = 2 since A_2, B_2 and C_2 become infinite. Similarly equation 9 fails when n = 1.5 or 3 for similar reasons. It is clear that when n = 2 or 3 respectively

$$X_2 = \int_{h^2}^{\infty} \frac{e^{-t}}{t}\, dt = ei(h^2)$$

$$X_3 = \int_{h^3}^{\infty} \frac{e^{-t}}{t}\, dt = ei(h^3)$$

and to evaluate the exponential integral in these cases we use the expansion (Mathematical Physics, H. and B. S. Jeffreys, p. 441)

$$ei(y) = -\gamma - \log_e y + y - \frac{y^2}{2.\ 2!} + \frac{y^3}{3.\ 3!} - \ldots.$$

To compute X_3 when $n = 1.5$ we use

$$X_3(n=1.5) = \frac{e^{-h^{1.5}}}{h^{1.5}} - ei(h^{1.5})$$

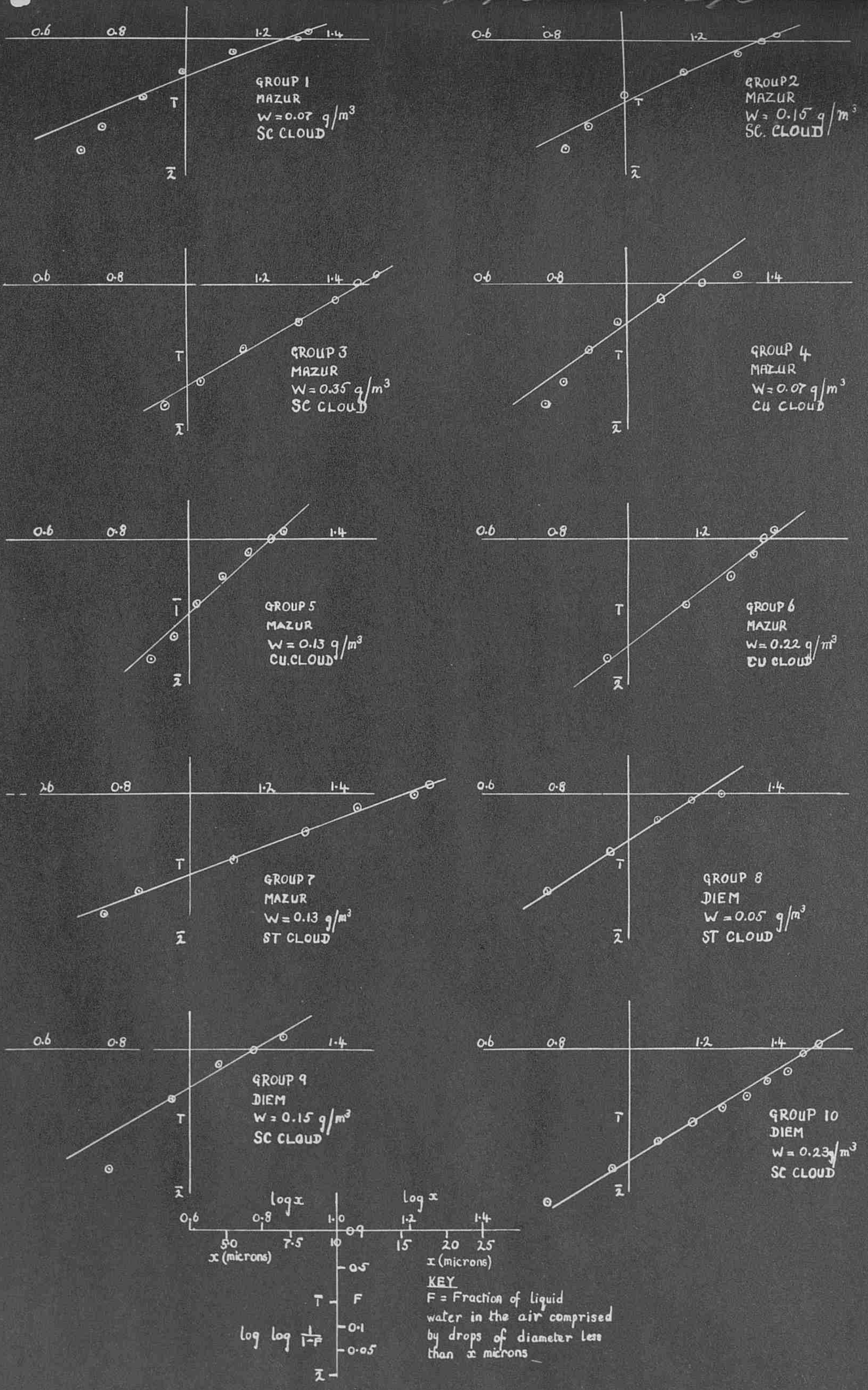

FIG. 1a FRACTION OF VOLUME OF WATER AS A FUNCTION OF DROP SIZE.

218662-11

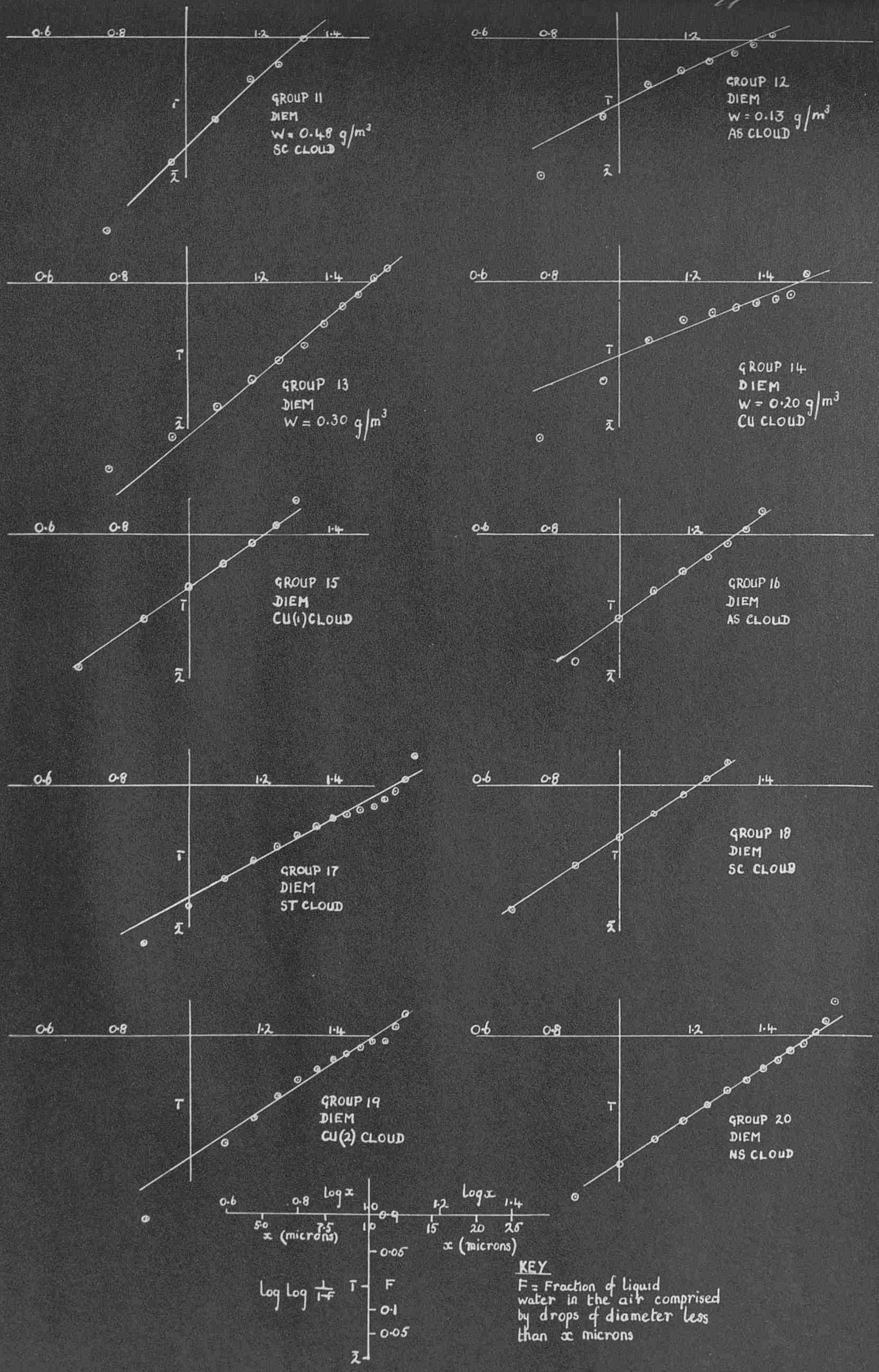

FIG 1 b FRACTION OF VOLUME OF WATER AS A FUNCTION OF DROP SIZE.

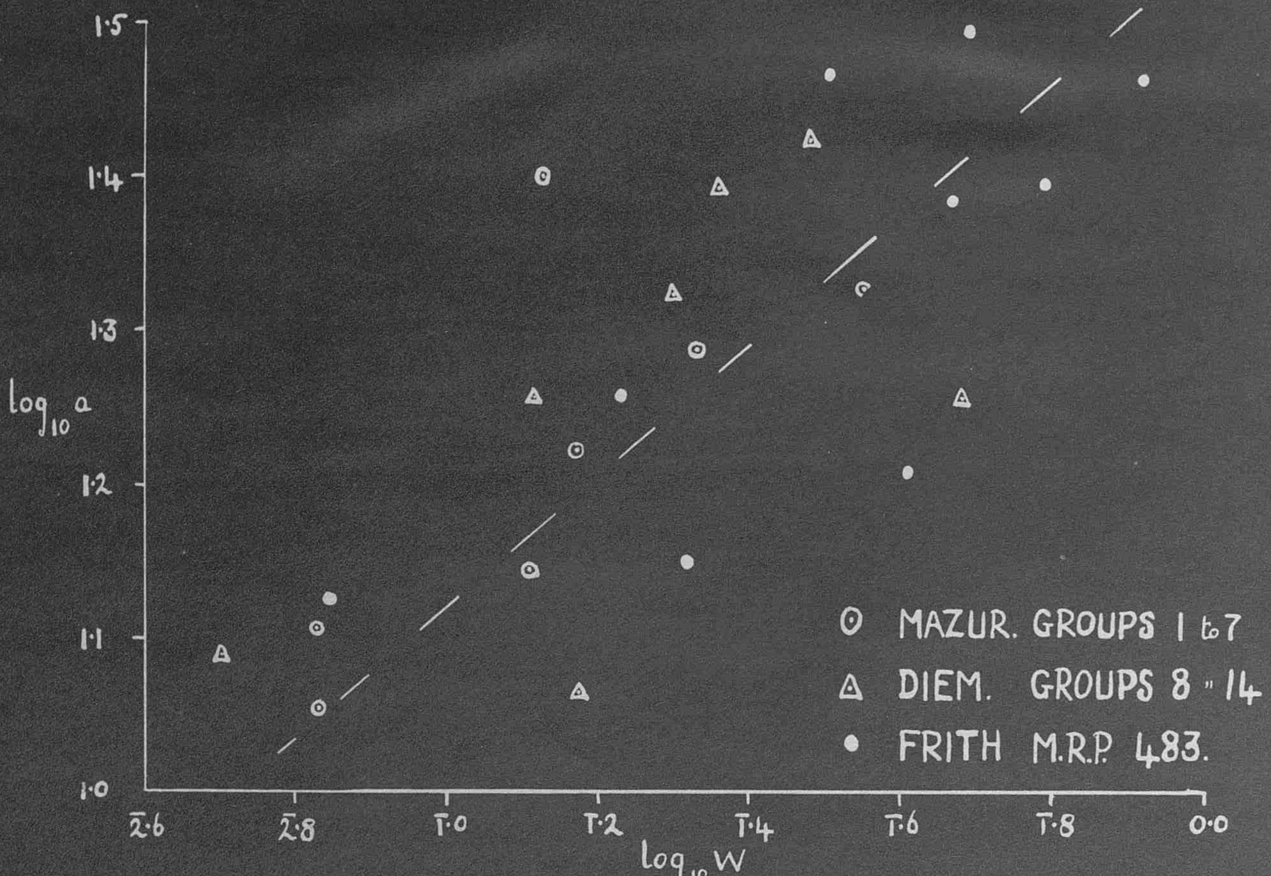

Fig. 2 Relation between "a" and liquid water concentration in cloud.

218662-12

This report has not yet been published and is to be treated CONFIDENTIALLY. Its contents must not be quoted.

.P.563
S.C.III/59
17th May, 1950

AIR MINISTRY

METEOROLOGICAL RESEARCH COMMITTEE

An analysis of observations of humidity in the upper troposphere and lower stratosphere

by

J.K. Bannon (Meteorological Office)

AIR WEATHER SERVICE
TECHNICAL REFERENCE FILES

Summary

Following Shellard's (1) general analysis of humidity observations at high altitudes the 96 series of frost point observations made by the Meteorological Research Flight in the upper troposphere and lower stratosphere up to the end of 1949 have been analysed with respect to the weather situation and the time of year. The number of observations is much too few for definite conclusions in most cases. The following are some tentative results.

Ascent of air above the level 325 - 250 mb over anticyclones and descent above the same level over cyclones would explain observed moisture distributions in the vertical in many cases.

In cyclonic conditions if there is a marked discontinuity in lapse rate of frost point with height it usually occurs at the tropopause.

Frost point near the tropopause increases more than temperature at the same level between winter and summer, the largest part of the change being between winter and spring.

There is usually a marked change in frost point characteristics on penetrating a frontal surface in the upper troposphere.

The level of the axis of a jet stream is usually moister than neighbouring levels. Frost point observations support the idea that the air in jet streams sinks from ridge to trough and rises from trough to ridge.

1. Introduction

All water vapour in the troposphere and lower stratosphere presumably has its origin at the earth's surface. The distributing mechanism is first convection and turbulence and secondly the large scale circulations in the atmosphere, anticyclones, depressions, trade winds and so on, and their associated vertical air movements. The processes of condensation and precipitation are always tending to return the water to the earth again.

Considerable bodily sinking and rising of air occur in the upper troposphere and lower stratosphere and often follow each other at comparatively short intervals. For example air in the upper troposphere in moving over the top of a typical temperate depression sinks or subsides on the east side of the ridge, rising again after passing through the upper trough, and all this may occur within 12 to 24 hours. Such subsidence and ascent must have a marked effect on the distribution of water vapour in the vertical.

The degree of convective or mechanical turbulence in the atmosphere also varies enormously since the thermal stability of the air and the wind shear vary within wide limits. The rate of diffusion of water vapour therefore also has wide variations.

It is thus not surprising that large and somewhat irregular variations of water vapour content are observed in the upper troposphere and lower stratosphere. Indeed it has not yet been possible to detect any very definite relation between the synoptic situation and the pattern of water vapour distribution in the vertical at these levels except in a few broad respects, though this may be because the number of observations available for study is small.

The results of 96 ascents by the Meteorological Research Flight have been used in the present analysis; these include the observations from 1943 onwards described by Shellard (1), (omitting those for 19th and 20th January, 1948, which Shellard says are doubtful), and also some further observations made in the latter part of 1949. Frost point is again used as the parameter defining the amount of water vapour present in the atmosphere.

2. Frost-point and tropopause height

Shellard (1) found significant correlations between the height (pressure) of the tropopause and the frost points at the 200, 250 and 300 mb levels, these being the most marked relations between the height of the tropopause and humidity. The correlation coefficients between pressure at the tropopause and F_{200} (frost point at 200 mb), F_{250} and F_{300} for the data used here were -0.62, -0.67, -0.61 respectively as compared with the values -0.67, -0.67, -0.62 found by Shellard for the smaller number of observations. Accordingly it was decided to sub-divide the observations according to tropopause height, thus eliminating one factor and so facilitating comparison of observations. Pressure intervals corresponding to 2,000 ft. in the ICAN atmosphere, (see e.g. Meteorological Air Observers Handbook, M.O.470, 1945), were used to classify tropopause heights, the tropopause being defined in the same way as in (1).

Table I sets out all the observations divided according to tropopause height;[x] temperatures and frost points are given for the levels 450, 400, 350, 325, 300, 275, 250, 225, 200, and 188 mb, when available. In a few instances the frost point was reported as greater than the dry bulb temperature; as cloud was present in each case at the same level it seems unlikely that there could have been any appreciable super-saturation and the frost points have therefore been tabulated as equal to the temperature. The weather situation was specified broadly (column 3) as anticyclonic (a), cyclonic, (c) or intermediate, (i). It sometimes happened that though the circulation was, say, anticyclonic near the earth's surface, it was cyclonic at the 300 mb level; when the lower and upper circulations differed note was taken of this fact, the second entry referring to the upper circulation. The air mass was also noted in column 4; the usual abbreviations P = polar, A = arctic, T = tropical, with post-scripts C = continental, M = maritime, were used. When the ascent intersected a frontal surface between two air masses the upper type is noted first and an asterisk in the table denotes the lowest observation in this air mass. The classification into circulation and air mass types is necessarily somewhat arbitrary.

The observations were divided seasonally, the seasons being taken as:-

Winter	January to March
Spring	April to June
Summer	June to September
Autumn	October to December

as in reference (1).

3. Cyclonic, intermediate and anticyclonic circulations

To facilitate comparison of the different seasons and circulation types (at 300 mb) Table II has been prepared from Table I, giving the mean values of temperature and frost point for the various categories when there were sufficient observations to justify this. It is probable, in view of the

/ remarks

---

[x] When the tropopause as found by the ascent was at one of the end heights of a height category, the category in which it was placed was decided by the general tropopause level shewn by adjacent radio-sonde observations.

remarks in section 1, that only by considering mean values will it be possible to determine relations between the water vapour distributions in the various categories, (seasonal etc.). It must be emphasised, however, that the paucity of data makes almost all the results tentative rather than definite in nature. Five or ten times the data would probably be required to give a true picture.

(a) Vertical motion.

It is seen that there is the following broad distinction between cyclonic and anticyclonic cases with intermediate cases between. The cyclonic cases are warmer and have lower frost points than the anticyclonic cases with similar tropopause heights for a considerable depth below the tropopause and into the stratosphere; often the cyclonic cases are colder and have higher frost points at about the 400 mb level than the anticyclonic cases. These broad differences are consistent with the following scheme of vertical motions:- general ascent in anticyclonic cases above a level somewhere in the 325 - 250 mb layer and general subsidence in cyclonic cases above a similar level.

Examples of this pattern are the cases in tropopause heights 262 - 238 mb; for the summer observations the three c cases are warmer and moister at 400 mb than the four i cases, colder and drier from 325 - 275 mb but warmer and with lower frost points at 250 mb and at greater heights. In the next category, tropopause heights 238 - 216 mb, the summer i and a classes agree with the postulated principle as do the winter and spring observations for the 216 - 197 mb tropopause category. In some cases however the observations do not agree with the principle. For example for the spring observations in the 287-262 mb tropopause range the c cases are warmer and moister on the whole than the i cases, above the 450 mb level; however this may not be significant as the average date for the c cases was exactly a month later than for the i cases. The spring observations for tropopause range 238 - 216 mb do not confirm the model either, the one c case having the very high frost point of - 79°F at 188 mb. This frost point was only once exceeded at this level in the whole series of observations and the level was then in the troposphere; for this reason the observation cannot be considered representative. The most serious contradiction to the proposed general scheme is the summer series of observations in the tropopause range 197-179 mb where the mean frost points for the a cases are lower than for the i cases. Altogether from the observations available there are six series of observations which confirm the proposed general broad distinction, three which partly confirm it, and two which contradict it. If only those cases of Type I tropopause, (i.e. more clearly defined tropopause heights) are considered, the same general result is obtained.

The Table A below indicates the evidence for and against the proposed general pattern of temperatures and frost points.

Table A

Synopsis of evidence for and against proposed temperature and frost point pattern in the upper air.

(Numbers and classifications of the observations in brackets)

Season	Tropopause height range				
	287-262 mb	262-238 mb	238-216 mb	216-197 mb	197-179 mb
Winter	Agrees (2 i, 1 c)	Agrees mainly: FP of a 2°F less than of i. (1a,1i,1c)			Agree FP not temperature. (5a, 2i)
Spring	Disagrees (3i, 3c)	Agrees (3i, 1c)	Agrees partly not case c. (2a,3i,1c)	Agrees (1a, 1i)	Agrees (3a, 1i)
Summer		Agrees (4i, 3c)	Agrees (2a, 7i)		Disagrees (2a, 3i)

Figures 1, 2 and 3 show mean temperature and frost point curves for tropopause ranges 262 - 238 mb (summer), 238 - 216 mb (spring and summer). It will be noted that there is no great permanent change in lapse rate of frost point with height at the tropopause in these mean curves as has been pointed out by Frith (2).

(b) Marked discontinuity in lapse rate of frost point with height

On many occasions there is a marked steepening of the lapse rate of frost point with height at a level not far from the tropopause. Table III gives some details of the relation of this level with the tropopause. It is seen that the more cyclonic the situation the more likely that the frost point lapse discontinuity, if it occurs, will be at the tropopause. (Only one c case in eight occurred with the discontinuity not at the tropopause). Conversely the more anticyclonic the situation the more likely that the discontinuity is some distance below the tropopause. The type of tropopause did not appear to affect the result.

It was noticed that the presence of a frontal surface in the upper troposphere did not appear to have any effect on these frost point discontinuities.

4. Air Mass Differences

In the lower troposphere the dew point varies widely between air mass types. In the upper troposphere and lower stratosphere it is difficult to make comparisons of water vapour content (as shewn by frost point) since water vapour content varies with tropopause height. Indeed analysing the observations with respect to tropopause height as is done in Table I shows that air mass type appears to have little effect on the frost point, at any rate in the vicinity of the tropopause; (at much lower levels, say about 400 mb, the frost points vary widely presumably because of subsidence or ascent). For example the summer frost points for tropopause range 262-238 mb, at the levels 275, 250 and 225 mb do not show any systematic trend from lower to higher values as one progresses from polar, through polar continental, polar maritime to tropical air. This rather surprising result is of course due to the method of analysis.

The tropopause height is governed by two main factors, the air mass type (or temperature) and the circulation type. The former is well illustrated by the high correlation (0.79) which Dines (3) found between height of the tropopause and the mean temperature up to a height of 9 km, confirmed by Priestley (4); the latter is shewn by the high correlation between tropopause height and surface pressure (0.68) or pressure at 9 km, (0.84) also found by Dines. In the same way the frost point at say 300 mb level would be expected to be related to the air mass type (or temperature) and also to the circulation type. The former relation is obvious; tropical air would be expected to have high and polar air low water vapour content. The latter relation follows from the association of vertical motions with the various circulation types, to which reference will be made later. Presumably the two factors, air mass type (temperature) and circulation type, both aid in the relation between tropopause height and frost point at a fixed level, found by Shellard (1).

It is clear that comparing frost points of different air masses having similar tropopause heights will mean comparing frost points in different circulation types; with the same tropopause height tropical air will have a more cyclonic circulation than polar air.

Perhaps a better comparision of frost points in different air masses may be made by classifying occasions according to circulation type. Table IV shows mean temperatures and frost points at the 400, 300 and 200 mb levels for various air masses and seasons, when there were sufficient observations for comparison purposes; the observations at 200 mb are divided according to whether they were in the troposphere or stratosphere. These means are based on small numbers of observations and the classification into air mass and circulation types is rather arbitrary so that the figures given cannot be claimed to be necessarily representative. Observations at a particular level varied greatly. An increase of frost point going from P through PM to T can be noted in many instances (especially at the 300 mb level) but there are exceptions; the frost point differences between air masses usually do not appear to be large. It is emphasised again, however, that because of the small number of observations and the other limitations of the analysis the results may be misleading.

The fact that there is little difference in frost point between air masses with the same tropopause height in the upper troposphere and lower stratosphere is consistent with the hypothesis put forward in section 3 above, namely that anticyclonic circulations are associated with ascent and cyclonic with subsidence in upper levels. For example, suppose height H is below average tropopause height for tropical air but above average for polar air; then those cases, tropical and polar, with tropopause height H will be cyclonic and anticyclonic respectively, in the mean. That is, on the hypothesis of section 3, the tropical air will have subsided and will thus have lower frost point, the polar air will have ascended thus having higher frost point that is usual for these air masses at the level H: thus the effects of air mass type and circulation type on frost point will tend to cancel each other.

5. Seasonal variation in frost point

The same difficulties arise in comparing frost points in different seasons as in different air masses; since there is a seasonal variation in tropopause height it is not strictly appropriate to compare cases with the same tropopause height in different seasons.

Dewar and Sawyer (5) give seasonal mean heights of the tropopause over Southern England based on three years (1943-45) daily observations by radio-sonde and various other irregular observations by balloon-sonde over many years; they are as follows:-

Winter (December - February)	35,000 ft.
Spring (March - May)	34,500 ft.
Summer (June - August)	37,500 ft.
Autumn (September - November)	37,000 ft.

These figures are interpolated from the charts of mean tropopause height and are only accurate, therefore, to about 500 ft. The weather characteristics of a particular season probably have a great influence on the mean tropopause height; e.g. Priestley (4) gives mean tropopause heights for Larkhill for 1944 as follows:-

Winter	37,000 ft.
Spring	36,300 ft.
Summer	37,000 ft.
Autumn	34,800 ft.

However, it would seem that the seasonal range of tropopause height is small, about 3,000 ft. In Table I the tropopause height ranges are of 2,000 ft. so that in a comparison of observations in different seasons but having the same tropopause height, the error due to seasonal variation in tropopause height should not be large and in some cases, when tropopause height change between seasons is less than 2,000 ft., should be zero.

Figures 4, 5, 6 and 7 show seasonal comparisons, (winter, spring, summer), of temperature and frost point for four ranges of tropopause height for polar maritime air and intermediate type circulation; data were insufficient to make comparisons for other air masses. (In one or two cases other categories were included in the mean curves in the figures; e.g. in Figure 4 the 3 spring cases include one which was classified cyclonic but whose temperatures and frost points were very similar and in most cases intermediate to the other two 'i' cases. Since the classification into circulation types and air masses is somewhat arbitrary it was considered that the inclusion of one or two cases just outside the given categories was justiable in view of the small number of observations available). It will be seen that the greatest differences in frost point and temperature are between the winter and spring seasons. Roughly, frost point increases 11°F and temperature 9°F between winter and spring in the neighbourhood of the tropopause; from spring to summer the increases are about 4° and 3°F respectively.

6. Effect of frontal surfaces on frost point distribution

There were 15 cases in which the M.R.F. ascent penetrated a frontal surface at or above the 450 mb level. Table V gives details of these 15 occasions. The height of the frontal surface was determined by considering available neighbouring upper air observations as well as the aircraft sounding; usually this height was in little doubt, within 25 mb. In the last column of the table is given the decrease in the depression of the frost point below the dry bulb temperature in passing through the frontal surface, upwards, defined as the change in depression in a 50 mb interval covering the frontal zone or the zone of frost point lapse change, whichever is the smaller. On three occasions frost point observations were not available below the frontal surface. The change in frost point depression below dry bulb temperature has been taken as a suitable indicator of change in humidity in passing through the frontal surface. Normally both frost point and dry bulb temperature fall off with height in the troposphere, but the lapse of dry bulb temperature is much more steady, even when passing through frontal surfaces. (Since water vapour is conveyed from one level to another by falling hydrometeors it is not surprising that the distribution of water vapour content, as shewn by frost point, is irregular compared with that of temperature). Thus change in frost point depression is usually a good measure of the change of lapse rate of frost point. It is noted from Table V that there are often large changes of frost point depression through a frontal surface; the mean of the figures given in column 5 is 15.5°F.

It was noted that in six of the cases, (1st, 2nd, 4th, 12th, 14th and 15th), the frost point appeared to be abnormally low, just below the frontal surface, compared with the general trend of frost point distribution with height in the lower air mass. A typical example is shewn in Figure 8. In each of these cases the ascent was made in the vicinity of a jet-stream. It may be that this apparent dryness below the frontal surface is caused by a vertical circulation associated with the front though this is difficult to visualise.

7. Lapse of frost point in the stratosphere

As Shellard (1) has pointed out, there is often, but not invariably, a sharp increase in the lapse rate of frost point with height on entering the stratosphere. The mean differences in lapse rate of frost point over the 50 mb intervals of height above and below the tropopause are given in Table VI.

Table VI

Mean differences in lapse rate of frost point in the 50 mb intervals above and below the tropopause, in °F per 1,000 ft.

	Circulation Type			Total
	Cyclonic	Intermediate	Anticyclonic	
Mean difference °F/1,000 ft.	2.3	2.0	0.4	1.6
Number of observations	14	36	12	62

No relation between tropopause height and this discontinuity in the lapse rate of frost point could be discovered.

It is immediately obvious from the Table that the circulation type has a large effect on the steepening of the frost point lapse rate above the tropopause. Since all of the early observations used by Dobson (6) were in cyclonic or intermediate circulations the very rapid fall in frost point on entering the stratosphere, to which he drew attention, is explained.

Shellard has shewn (1) that the lapse rate of frost point above the tropopause is partially related to the sharpness of the tropopause, i.e. the rate of increase of temperature with height in the lower stratosphere. This is consistent with subsidence in the lower stratosphere being the cause of the increased lapse rate of frost point in cyclonic conditions.

The steepening of the lapse rate of frost point with height just above the tropopause occurs in a shallow layer, however. As pointed out by Frith (2) and as seen in Figures 1, 2 and 3 there is no great permanent change in lapse rate of frost point at the tropopause.

The very rapid fall in frost point with height on entering the stratosphere above depressions can be explained by the mechanism given by Goldie (7). According to this, (see, for example, his Figures 1 and 2), the formation (or travel) of a depression involves removal of a quantity of air from the depression to the anticyclone in the levels between about the 400 mb level and the tropopause, together with subsidence in the stratosphere above the depression. This removal in effect creates a discontinuity in the vertical direction by bringing together layers which were separated by possibly 4,000 to 6,000 ft. It must thus result in a steeper step down in frost point in the region of the tropopause over depressions than is found in the originally undisturbed atmosphere, assuming that in the undisturbed atmosphere there was a steady fall of frost point with height.

8. Observations in the neighbourhood of jet streams

There were 17 observations in the neighbourhood of the narrow zones of high winds in the upper troposphere which are usually called jet streams; the occasions, (data in Table I), are listed under:- 3.5.44, 7.2.45, 9.2.45, 8.6.45, 23.10.45, 6.2.48, 24.5.48, 20.1.49, 21.1.49, 21.2.49, 1.3.49, 18.3.49, 26.4.49, 26.7.49, 12.8.49, 17.8.49, 27.10.49. (The definition of a jet stream is necessarily rather arbitrary; about 100 kt or more for the maximum wind speed was taken as the criterion).

Some interesting points became apparent in the analysis of these cases.

The first is that the level of the axis of the jet stream, (the core of fastest moving air) is usually moister than levels above and below: this holds for some distance (several hundreds of miles) on either side of the jet axis.

Three different types of frost point distribution with height were noted:-

Comparatively dry upper troposphere becoming moister in the neighbourhood of the tropopause and then drier again above	Type K
Comparatively dry upper troposphere becoming moister at a level below the tropopause and then drier again above this level	Type H
Becoming steadily drier upwards	Type L

Table VII gives details of the general characteristics of the jet stream frost point observations. Cases were considered to be 'well marked' if there was a variation in depression of frost point below dry bulb temperature, above the 450 mb level, such that the ratio maximum to minimum was 3/2 or more. Examples of Type K and H are given in Figures 9 and 10.

Palmen and Nagler (8) have suggested that there are vertical circulations associated with jet-streams with a nul level in the neighbourhood of 300 mb and, in a North Westerly current, (i.e. on the west side of an upper trough), rising motion above this level on the warm side of the jet and sinking on the cold side, with the reverse circulation below this level; the directions of the circulations are reversed when the current is South Westerly, (i.e. on the east side of the upper trough). It is seen that the frost point distributions found by the M.R.F. do not confirm these circulations though, of course, without additional information they cannot be taken as conclusive evidence against the hypothesis.

Berggren et alia (9) and Palmen and Nagler (8) have pointed out that the axis of a jet stream which has a sinusoidal plan over the earth's surface is lowest at the bottom (southern part) of a trough in the upper air and the latter authors say that there is a general sinking of the air in the jet from ridge to trough and a general ascent again from trough to ridge. Bannon (10) has also noted the decrease in height of the axis of a northerly jet towards the south. There were no frost point observations at or near the top of a ridge, associated with a jet stream, but there were 6 observations near the trough and 7 between trough and ridge in which there was a minimum of the depression of frost point below dry bulb temperature at a certain level (usually near the level of the jet axis); the mean of these minima depressions was 16°F for the trough observations and 4°F for the observations between trough and ridge. The evidence from the frost point observations thus confirms the sinking of air in a jet stream from ridge to trough.

9. Conclusions

These first observations of humidity (frost point) in the upper troposphere and lower stratosphere have been very valuable and good use has been made of them. (See, for example, references (6) and (1) and Brewer (11)).

The present study has shown, however, that the 100 odd isolated observations can only give rough indications of the variation of humidity in the upper atmosphere between the different types of weather system which affect the British Isles. A much greater volume of data would help in this direction, a statistical study then being possible. The results given in this note can only be considered tentative or approximate, at best. More satisfying and conclusive results can only be obtained when observations are available comparable with the British radio-sonde net-work in area and regularity.

The usefulness of a net-work of frost point observations in the upper air is obvious. For example it would be possible to extend to high altitudes the analysis of the vertical motions of the air, (about which information is sadly lacking), from a study of the conservative properties of its water vapour content after the manner of Hewson (12).

The isolated observations available now should prove useful in synoptic investigations of particular occasions as an addition to other upper air information. Because of the great variations in humidity in the upper air a study of individual ascents is probably the best way to make the most of the observations.

se stated)

References

1. Shellard, H.C. 1949 M.R.P.486

2. Frith, R. 1949 Weather, Vol.4, October 1949, pp. 330-1.

3. Dines, W.H. 1919 Geophysical Memoir No. 13

4. Priestley, C.H.B. 1945 S.D.T.M. No.104

5. Dewar, D. and J.S. Sawyer 1947 M.R.P.334

6. Dobson, G.M.B. with A.W. Brewer and B.M. Cwilong 1946 Proc. Roy. Soc. Vol.A 185, pp. 144-175.

7. Goldie, A.H.R. 1944 M.R.P.213
   or 1949 Weather, Vol.4, pp.346 - 350 and pp. 393-399.

8. Palmen, E. and K.M. Nagler 1949 Journal of Meteorology, Vol.6, No. 4, pp. 223-242.

9. Berggren, R. B. Bolin and C-G. Rossby 1949 Tellus, Vol.1, No. 2, pp.14-37.

10 Bannon 1950 A.R.C. Report No.12, 877

11. Brewer, A.W. 1949 Q. Journal Roy. Met. Soc., Vol.75, pp. 351-363.

12. Hewson, E.W. 1938 Q. Journal Roy. Met. Soc., Vol.64, pp. 407-418.

G.269094/JDG/5/50/40

---

25. 4.45	275I	c; i	P3	57	103		
30. 5.45	275I	i	P5	53	119		
29. 6.48	285II(240I)	i; c	PM8	45	99		
5. 5.49	285II	i; c	PM2	51	100		
18. 5.49	262I	c	P4	54	108		
19. 7.45	280I	c	P6	49	103		
18. 7.49	262I	i; c	P0	48	106		
262 - 238 mb.							
9. 2.45	260II	i	PM				
26. 2.48	260II(215I)	i; c	A9	59	112	61	119
17. 2.49	250II	a	T5	65	91	63	92
22. 4.45	250II	i	P8	71	102	71	106
24. 5.48	238I	i	PM6	55	104	56	111
25. 4.49	250II	i; c	PM3	49	103		
26. 4.49	250I	a; i	PM5	60	108		
7. 7.49	262I	i; c	P6	51	111		
8. 7.49	250II	i	P2	54	94		
14. 7.49	250I	c; i	P1	51	101		
15. 7.49	238I(260II)	c	P1	48	102		

/ 8. 8.49

G.269094(a)/JMB/5/50/40

Table I. Temperatures and Frost Points (°F, negative unless otherwise stated) s specified levels, arranged according to tropopause height (ranges of 2,000')

Notes: (i) When tropopause is double the secondary height is given in (
(ii) The circulation type at 300 mb. if different from that at the earth's su ace, is quoted after the surface type (c = cyclonic; a = anticyclonic; i = intermediate)
(iii) When two air masses are present the upper is quoted first. An * indicates the first observations within the upper air mass if this level is above 450 mb.
(iv) Tropopause heights are given in mb. to the nearest 1,000', for convenience of analysis. The aircraft observations were usually at height intervals of 1,000' so that these tropopause heights are not accurate to the nearest millibar. (Tropopause heights in M.R.P.486 are given to nearest 5 mb). Height categories in doubtful cases were decided by reference to adjacent radio-sonde observations.

Date	Tropopause Height (mb) and Type	Circulation Type	Air Mass	450 mb.		400 mb.		350 mb.		325 mb.		300 mb.		275 mb.		250 mb.		225 mb.		200 mb.		188 mb.	
				T	FP	T	FP	T	FP	T	FP	T	FP	T	FP	T	FP	T	FP	T	FP	T	FP
Range 410 - 376 mb.																							
5. 5.44	400 II	c	P	33	42	47	55	47	89	51	91	51	96										
376 - 344 mb.																							
8.12.47	345II(310I)	c	PM			47	65	53	85	55	90	55	95	53	96	53	100						
4. 4.48	360I	c	P					45	94	45	99	44	104	47	109	48	110						
344 - 315 mb.																							
17. 2.48	344II(276II)	a; c	P/A							57	79	59	87	61	92	60	97	58	108				
19.10.48	330II	i	PM/P	31	40	42	47	53*	59*	58	63	53	85	50	100	50	104	50	110	49	114		
315 - 287 mb.																							
7. 2.45	300I	i	PM/P	22	65	32	69	46	72	52	75	59	80	55	91	55	101	57	106				
22. 1.48	315II(270I)	c; i	PM							54	85	56	91	58	94	52	99	51	102				
8. 6.45	300I	i	P	21	39	33	53	43	59	48	69	53	81	50	92	47	101	50	110				
22. 8.43	300I	c	P	12	30	23	43	35	55	42	64	49	72	47	84								
5. 7.49	300II	i; c	T/P	14	46	26	47	38	61	40	67	44	81	45	84	46	86	48	97	49	101		
22.12.43	300II	i; c	P	22	48	32	53	45	50	50	62	60	71	55	92	51	108	46	117				
23.10.45	300I	c; in	P	21	46	29	71	39	73	48	78	57	85	57	86	51	95	55	102	51	109		
287 - 262 mb.																							
8. 1.48	280I	c; i	PM/P			40	75	47	70	52	71	57	88	63	99	57	103						
6. 2.48	280II(250I)	i; c	PM/P			39	57	51	78	53	84	54	93	61	98	61	102	57	109				
20. 2.48	276II	i	A									45	102	49	104	43	101	47	99				
27. 2.48	285II(220I)	i; c	A									62	63	69	72	66	89	71	102	66	115	62	110
11. 2.49	276I	a; i	P	26	32	38	38	50	55	55	71	62	86	67	88	67	96	65	95	55	96	58	97
3. 5.44	275II	i	PM/P	19	63	29	65	41*	55*	47	61	53	69	61	71	62	95						
25. 4.45	275I	c; i	PM	18	30	31	43	45	49	53	54	61	64	70	72	68	86	62	103	57	103		
30. 5.45	275I	i	PM	21	26	32	39	47	52	55	61	61	65	70	71	62	100	56	105	53	119		
29. 6.48	285II(240I)	i; c	PM/P	18	27	26	36	36*	46*	42	50	47	58	55	74	54	73	46	98	45	99		
5. 5.49	285II	i; c	PM/P	14	29	26	40	40	54	46	60	52	67	56	74	57	82	53	92	51	100		
18. 5.49	262I	c	P	18	51	26	47	39	50	47	57	55	62	64	69	65	82	57	94	54	108		
19. 7.45	280I	c	PM	7	49	19	44	33	54	42	60	51	62	56	73	49	88	47	96	49	103		
18. 7.49	262I	i; c	P	12	30	24	40	39	45	47	52	54	55	63	63	58	79	50	100	48	106		
262 - 238 mb.																							
9. 2.45	260II	i	PM/P	23	60	33	51	46	64	53	73	58*	82*	63	77	65	82						
26. 2.48	260II(215I)	i; c	A	23	81	31	78	45	86	49	90	52	87	58	92	59	97	61	109	59	112	61	119
17. 2.49	250II	a	T											63	79	70	84	68	85	65	91	63	92
22. 4.45	250II	i	P	9	44	21	42	36	56	42	61	49	67	59	73	69	73	72	88	71	102	71	106
24. 5.48	238I	i	PM/P	23	47	32	62	42*	61*	47	56	53	61	61	67	66	74	64	86	55	104	56	111
25. 4.49	250II	i; c	PM/P	15	80	28	70	39	68	44	78	45	84	42	94	50	95	50	103	49	103		
26. 4.49	250I	a; i	PM/P	21	50	30*	65*	39	60	44	68	52	70	56	87	61	99	57	105	60	108		
7. 7.49	262I	i; c	P	8	27	19	35	35	41	43	48	52	54	58	70	59	90	56	96	51	111		
8. 7.49	250II	i	P	7	27	20	39	35	56	42	59	49	63	55	67	61	74	57	82	54	94		
14. 7.49	250I	c; i	PM	8	9	19	20	31	46	39	49	47	54	53	61	59	73	54	91	51	101		
15. 7.49	238I(260II)	c	PM	7	16	20	34	32	46	40	53	47	67	55	70	58	77	51	91	48	102		

Date	Tropopause Height (mb) and Type	Circulation Type	Air Mass	450 mb.		400 mb.		350 mb.		325 mb.		300 mb.		275 mb.		250 mb.		225 mb.		200 mb.		188 mb.	
				T	FP	T	FP	T	FP	T	FP	T	FP	T	FP	T	FP	T	FP	T	FP	T	FP
20. 7.49	188II	a; i	T/PM	1	3	10	17	25	27	32	36	37	45	47	50	55	61	64	70	73	79	76	79
22. 7.49	197II	a; i	PM	0	13	10	40	24	44	32	46	40	41	49	50	55	61	64	66	71	72	72	90
25. 7.49	185II	a	T/PM	+6	12	5	22	20	30	27	39	36	44	43	55	53	59	62	65	72	81		
17. 8.49	180I	a; i	PM/P	+2	7	9	14	19	23	28	31	37	42	46	54	56	60	65	66	74	78	76	86
28. 9.49	185II	a	PM	5	44	15	53	25	62	34	58	39	63	48	73	56	76	65	82	72	88	75	91
179 - 162 mb.																							
25. 1.49	170I	i	PM	20	80	26	92	37	99	43	97	48	96	53	95	63	97	64	102	70	103	74	107
27. 4.49	180I	a; i	PM	6	58	17	68	30	83	37	85	45	94	53	97	62	96	70	79	79	85	84	92
20. 6.49	170-	a	PM	1	18	12	65	25	60	34	55	42	61	51	64	59	72	66	80	73	88	77	87
15. 8.49	170II	a	T	+6	41	6	27	21	32	29	45	36	47	45	50	55	61	64	67	75	78	78	90
19. 8.49	165II	a	PM	+5	40	5	56	19	52	27	57	35	59	43	64	53	71	63	74	73	81	76	81
162 - 147 mb.																							
26. 7.49	160I	a; i	T/PM	1	41	13	46	27	51	27	55	32*	38*	39	46	48	49	54	74	62	85	66	92
12. 8.49	160I	a	PM/P	+2	14	9	18	24	34	32	42	39	41	47	47	56	56	64	66	71	82	73	88
Above 147 mb.																							
4. 8.49	120I	a	T	+1	11	12	19	23	40	32	45	39	48	47	59	51	78	56	82	60	91	63	95

Table II

Mean temperatures and frost points in various tropopause height ranges
and for various seasons and upper circulation types (°F, negative values unless otherwise stated)
Figures in ( ) give the total range in °F.

Tropopause Range	Season and number of observations	Air Mass Type and Upper Circulation Type	450 mb.		400 mb.		350 mb.		325 mb.		300 mb.		275 mb.		250 mb.		225 mb.		200 mb.		188 mb.	
			T	FP	T	FP	T	FP	T	FP	T	FP	T	FP	T	FP	T	FP	T	FP	T	FP
287-262 mb.	Winter (2)	PM and P; i			39 (2)	67 (37)	49 (3)	63 (15)	53 (3)	71 (0)	59 (5)	87 (2)	65 (4)	93 (11)	62 (10)	99 (7)						
	(1)	c			39	57	51	78	51	84	54	93	61	98	61	102	57	109				
	Spring (3)	PM; i	19 (3)	40 (37)	31 (3)	49 (36)	44 (6)	52 (6)	52 (8)	59 (7)	58 (8)	66 (5)	67 (9)	71 (1)	64 (6)	93 (14)	59 (6)	104 (2)				
	(3)	PM and P c	17 (4)	36 (24)	26 (0)	41 (11)	38 (4)	50 (8)	45 (5)	56 (10)	51 (8)	62 (9)	58 (9)	72 (5)	59 (11)	79 (9)	52 (11)	95 (8)	50 (9)	102 (9)		
	Summer (2)	P and PM c	9 (5)	39 (19)	21 (5)	42 (4)	36 (6)	49 (9)	45 (5)	56 (8)	53 (3)	59 (7)	59 (7)	68 (10)	53 (9)	83 (9)	49 (3)	98 (4)	49 (1)	105 (3)		
262-238 mb.	Spring (3)	P and PM i	17 (14)	47 (6)	28 (11)	56 (23)	39 (6)	59 (5)	44 (2)	61 (12)	51 (4)	66 (9)	59 (5)	76 (20)	65 (8)	82 (26)	64 (15)	93 (19)	62 (16)	105 (6)		
	(1)	PM c	15	80	28	70	39	68	44	78	45	84	42	94	50	95	50	103	49	103		
	Summer (3)	P, PM, PC c	6 (4)	22 (11)	18 (3)	34 (3)	32 (5)	43 (5)	40 (5)	53 (10)	48 (7)	61 (13)	55 (6)	69 (2)	58 (3)	82 (13)	53 (5)	91 (10)	50 (3)	106 (9)		
	(4)	P and T i	7 (5)	35 (46)	19 (3)	41 (37)	32 (6)	49 (18)	39 (5)	51 (22)	46 (6)	57 (18)	53 (5)	63 (13)	59 (10)	73 (10)	56 (10)	88 (13)	52 (2)	99 (8)		
238-216 mb.	Spring (3)	PM, i	9 (9)	40 (31)	20 (7)	42 (15)	33 (7)	52 (20)	41 (7)	63 (10)	48 (5)	66 (6)	56 (3)	69 (4)	61 (3)	78 (2)	68 (4)	83 (8)	65 (8)	98 (8)	66 (11)	107 (18)
	(2)	PC, a	9 (2)	39 (20)	21 (1)	53 (7)	36 (2)	61 (7)	43 (3)	67 (3)	51 (2)	70 (4)	57 (0)	77 (5)	65 (3)	77 (2)	73 (1)	82 (2)	73 (1)	95 (5)	71 (0)	103 (11)
	(1)	PM, c			28	39	38	55	46	63	52	66	57	66	65	72	66	80	59	88	54	79
	Summer (7)	P and PM i	6 (9)	24 (24)	18 (9)	38 (28)	29 (9)	48 (13)	36 (11)	51 (24)	45 (12)	61 (18)	54 (11)	65 (15)	61 (12)	69 (7)	65 (22)	82 (12)	61 (13)	98 (17)		
	(2)	PM, a	3 (1)	31 (7)	13 (1)	28 (2)	26 (4)	41 (6)	34 (2)	48 (12)	42 (2)	49 (7)	51 (1)	56 (0)	61 (3)	63 (2)	67 (7)	78 (14)	63 (15)	91 (11)		
216-197 mb.	Winter (5)	P and T i	15 (12)	34 (42)	26 (13)	41 (19)	39 (10)	51 (31)	46 (9)	60 (23)	53 (12)	67 (24)	60 (12)	74 (27)	68 (13)	83 (27)	76 (16)	89 (22)	80 (21)	98 (17)	78 (18)	102 (13)
	Summer (4)	P and T i	2 (6)	19 (21)	13 (9)	27 (28)	25 (6)	43 (24)	32 (6)	51 (27)	39 (6)	55 (17)	47 (9)	65 (14)	55 (8)	71 (7)	61 (12)	77 (8)	66 (10)	85 (12)		

/197-179 mb.

G.269094(b)/MFG/5/50/40

Table III

Marked discontinuities in lapse rate of frost point with height, in neighbourhood of the tropopause.

1 Circulation type	2 Total No. of observations	3 No. of cases with F.P. discontinuity	4	5 Mean tropopause height for cases in Col.3 and 4 (mb)	6 Range of tropopause heights (mb)	7 Mean of difference in heights of tropopause and F.P. discont. (ft.)	8 Range of differences in Col.7. (ft.)	9 No. of cases with zero differences in Col.7.	10
		Type I tropop.	Type II tropop.					Type I tropop.	Type II tropop.
a	33	8	2	204	160-250	2,150	11,000	1	0
i	47	12	5	260	197-330	380	5,400	6	2
c	16	7	1	267	230-375	375	3,000	6	1

G.269094(c)/DC/5/50/40

Me

Season and Circulation Type	Air Mass	200 mb. oposphere T	FP
Winter; i	P		
	PM	(3)	102
	T		
Spring; c	P		
	PM		
i	P		
	PM	(2)	87
a	PC		
	PM	(3)	85
	T	(1)	79
Summer; c	P		
	PC		
	PM		
i	P		
	PM	(3)	76
	T	(2)	82
a	PM	(3)	84
	T	(2)	79

F

G.269094(d)/MFG/5/

Table IV

Mean temperatures (T) and frost points (FP)
in various air masses (°F, negative)

Season and Circulation Type	Air Mass	400 mb.		300 mb.		200 mb. (stratosphere)		200 mb. troposphere	
		T	FP	T	FP	T	FP	T	FP
Winter; i	P	35(2)	43	60(2)	82	70(2)	97		
	PM	30(10)	56	56(11)	78	79(4)	101	79(3)	102
	T	21(2)	30	49(2)	59	79(2)	91		
Spring; c	P	26(1)	47	55(1)	62	54(1)	108		
	PM	27(3)	50	49(4)	69	51(4)	97		
i	P	27(2)	47	51(2)	74	71(2)	102		
	PM	24(8)	52	52(11)	69	62(8)	103	77(2)	87
a	PC	21(2)	53	51(2)	70	73(2)	95		
	PM	16(4)	49	45(4)	62	71(1)	94	77(3)	85
	T	-	-	39(1)	43			71(1)	79
Summer; c	P	22(3)	39	52(3)	60	49(2)	109		
	PC	16(1)	32	45(1)	61	50(1)	104		
	PM	19(2)	39	49(2)	65	49(1)	103		
i	P	19(2)	41	47(2)	58	56(2)	101		
	PM	16(12)	33	43(13)	55	62(8)	95	72(3)	76
	T	15(3)	30	38(4)	53	56(2)	93	67(2)	82
a	PM	11(5)	37	39(5)	52	62(2)	91	72(3)	84
	T	5(2)	25	36(2)	45			73(2)	79

Figures ( ) are the number of observations.

Table V

Frost point characteristics of Frontal surfaces in upper troposphere.

Date	Type of **front**	Height of frontal surface (mb.)	Tropopause Height (mb.)	Decrease in frost point depression through the **front** (thro' 50 mb. or the main change) °F
3. 5.44	W	350	275	21^x
9. 2.45	W	300	260	11^x
6. 2.48	W	450	280	-
24. 5.48	C	350	238	21
29. 6.48	W	375	285	0
19.10.48	W	350	330	0
21. 1.49	W	425	240	31
1. 3.49	C	450	227	-
18. 3.49	C	450	240	15
22. 4.49	W	225	188	3^x
25. 4.49	C	450	250	-
26. 4.49	W	400	250	20^x
27. 6.49	W	375	188	17
26. 7.49	W	320	160	27^x
8. 8.49	C	425	238	20

W = warm frost

C = cold frost

^{x}This decrease, the main change, occurred in less than 50 mb.

Table VII

General characteristics of Frost Point distribution with height near jet streams.

	Cold Side of Jet Stream		Warm Side of Jet Stream	
	All	Well Defined	All	Well Defined
No. of observations	7	6	10	8
Type K	4	3	3	2
Type H	0	0	6	5
Type L	2	2	0	0
Indeterminate	1	0	1	1
Mean difference in height moistest level - jet axis level	800'	0	1500'	100'

G.269094(f)/JDG/5/50/40

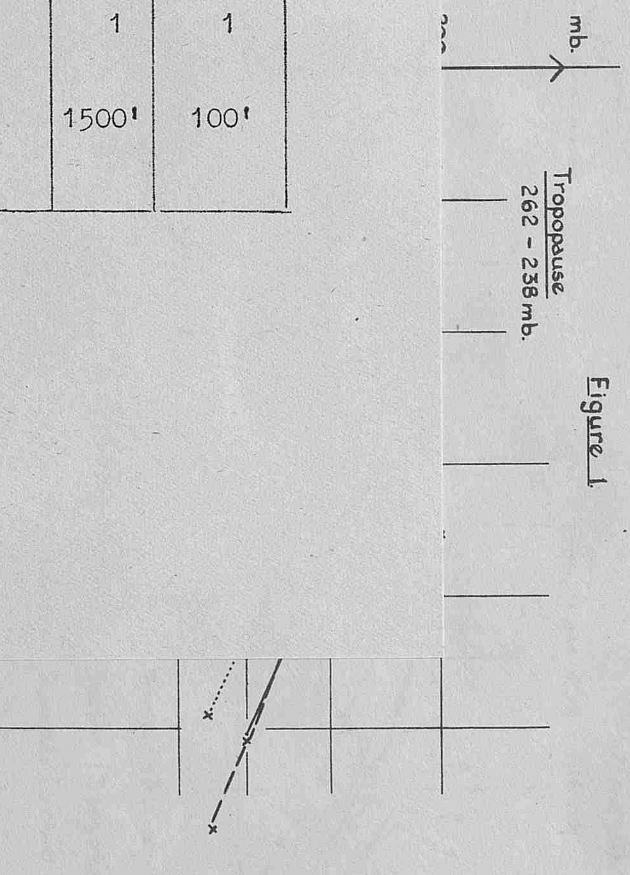

Figure 1.

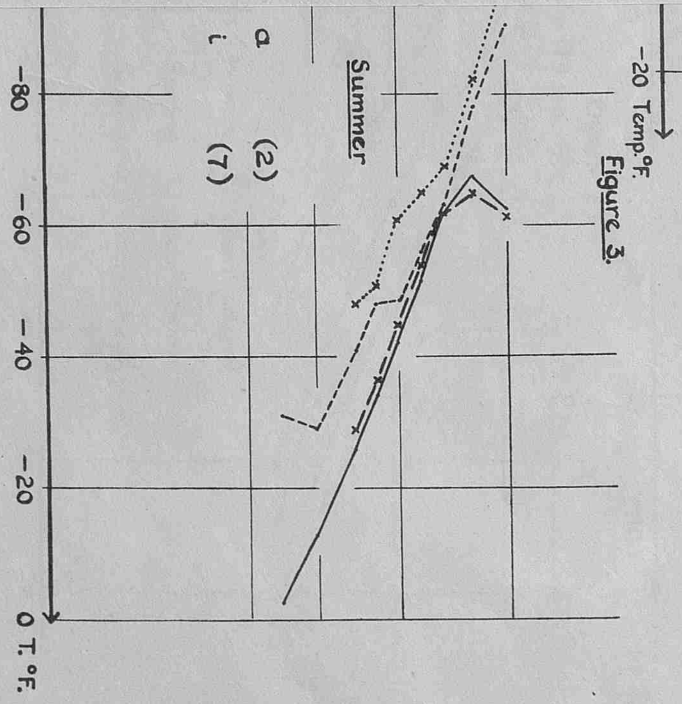

Figure 3.

MRP 563

Figure 1.

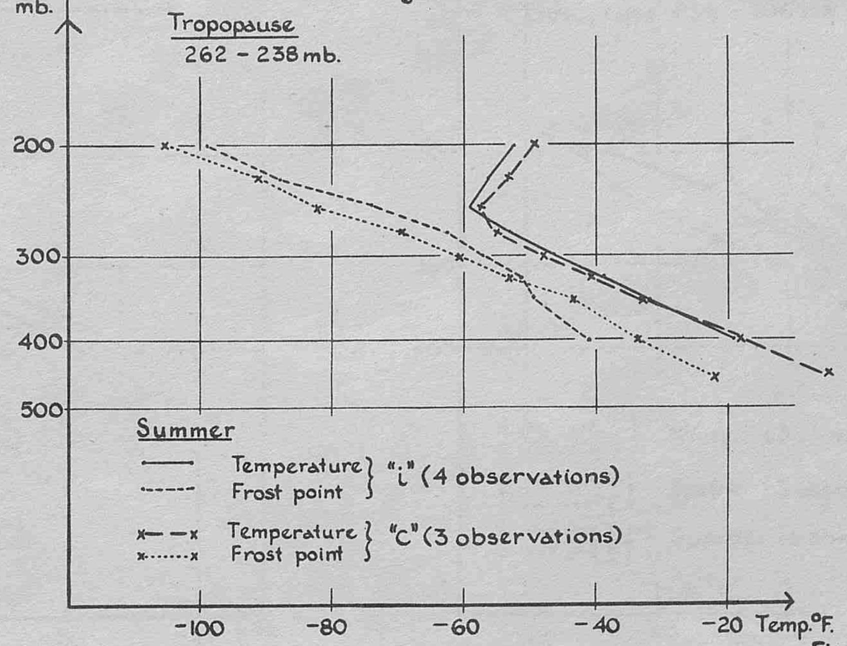

Figure 2.

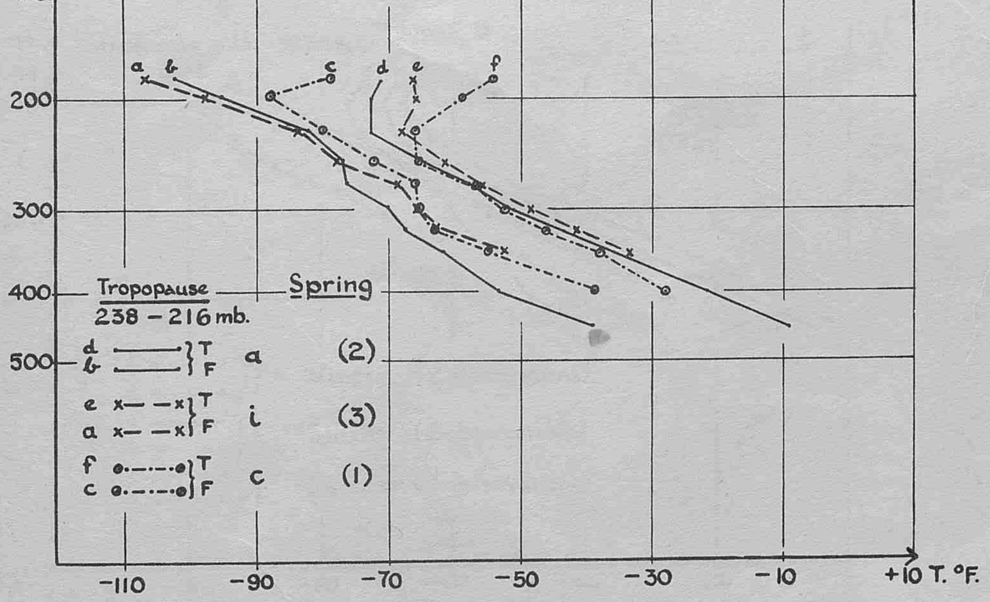

Figure 3.

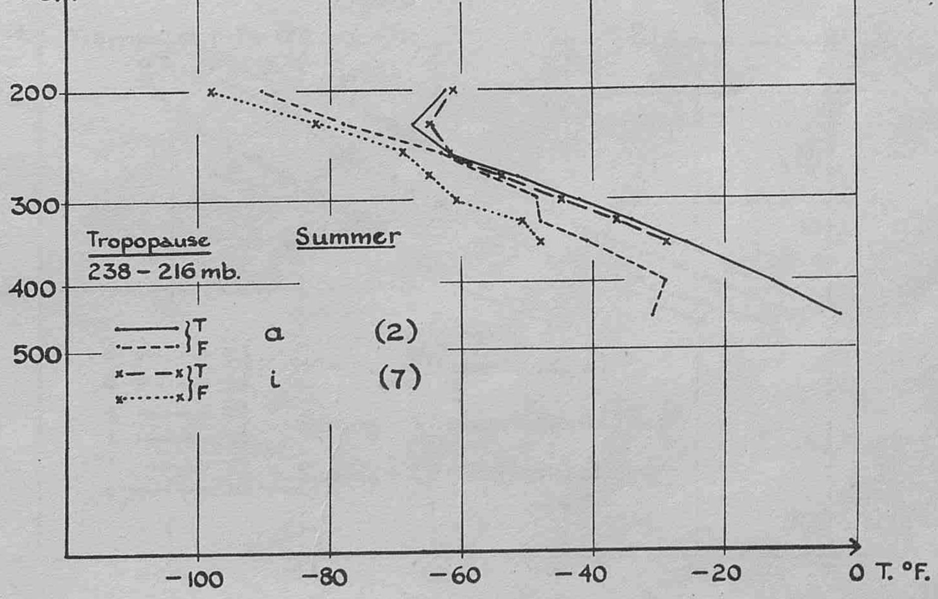

Figure 4.

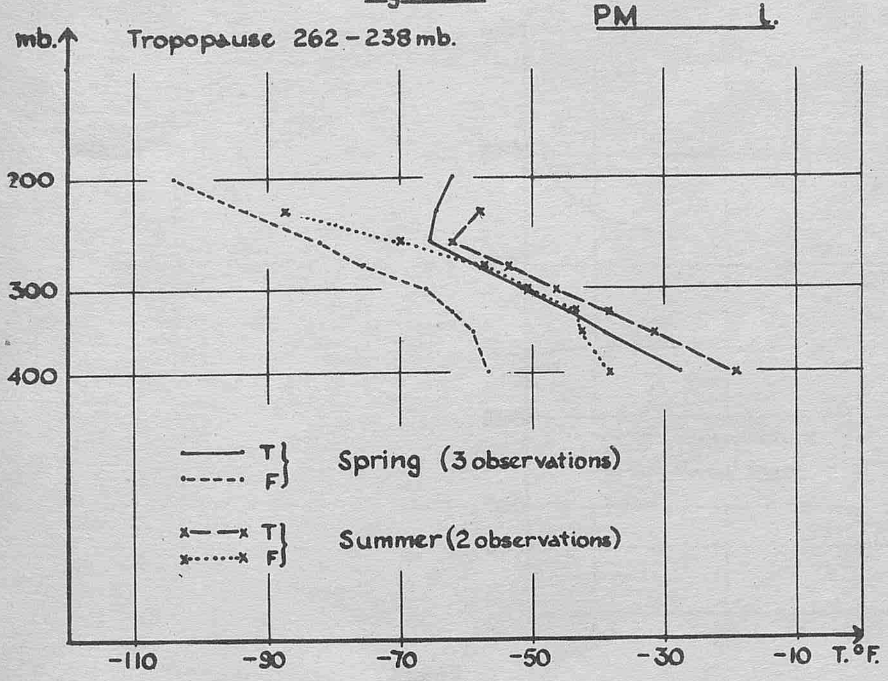

Figure 5.

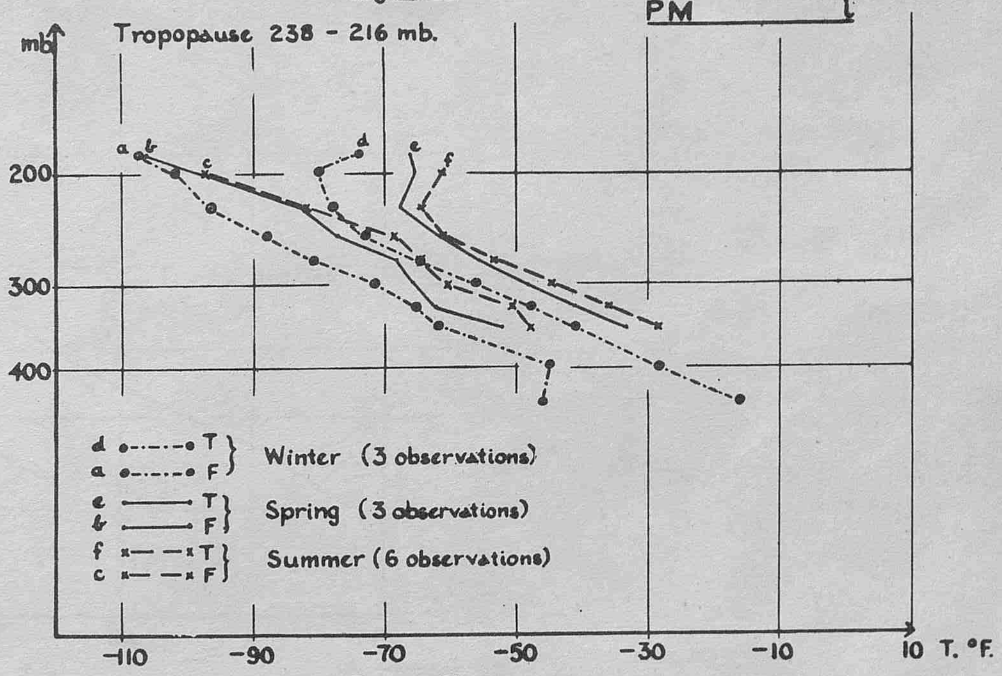

Figure 6.

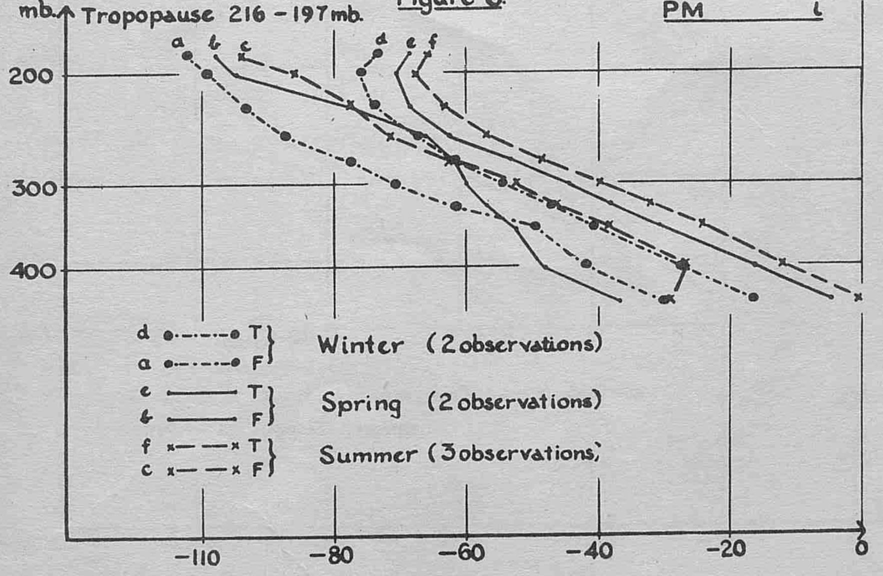

Figure 7.

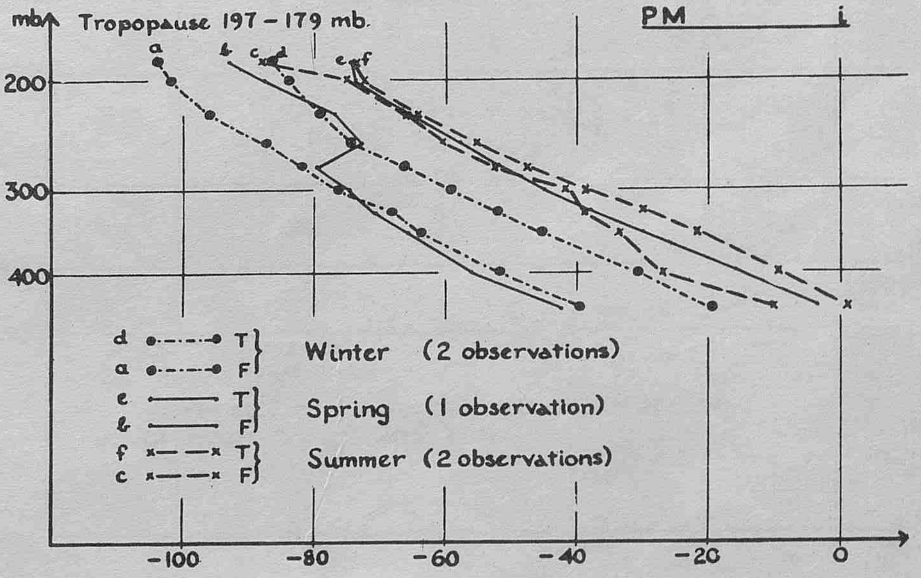

Figure 8.
26th. April, 1949

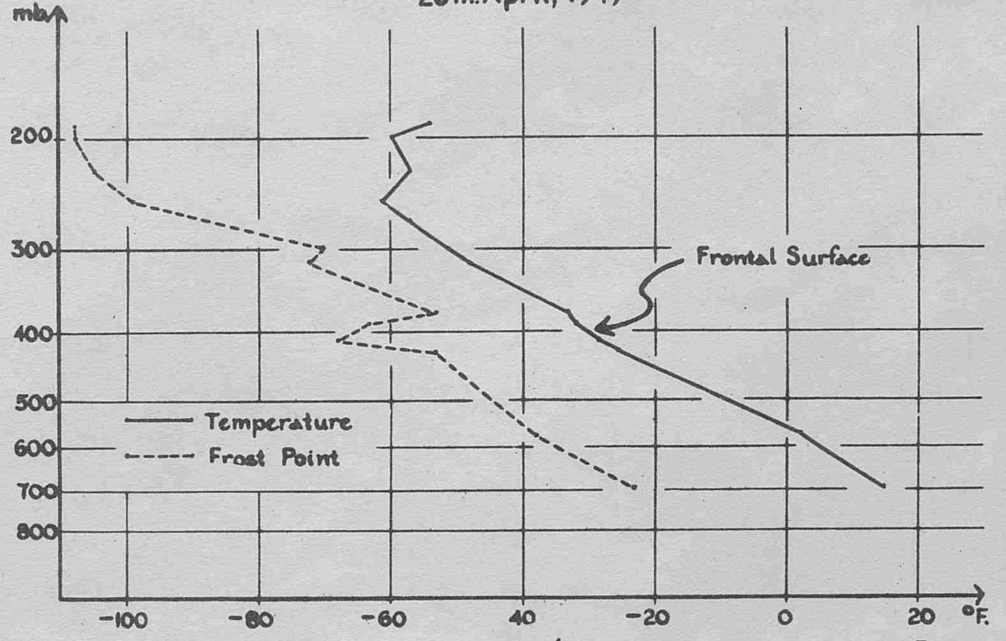

Figure 9.
7th. February, 1948.

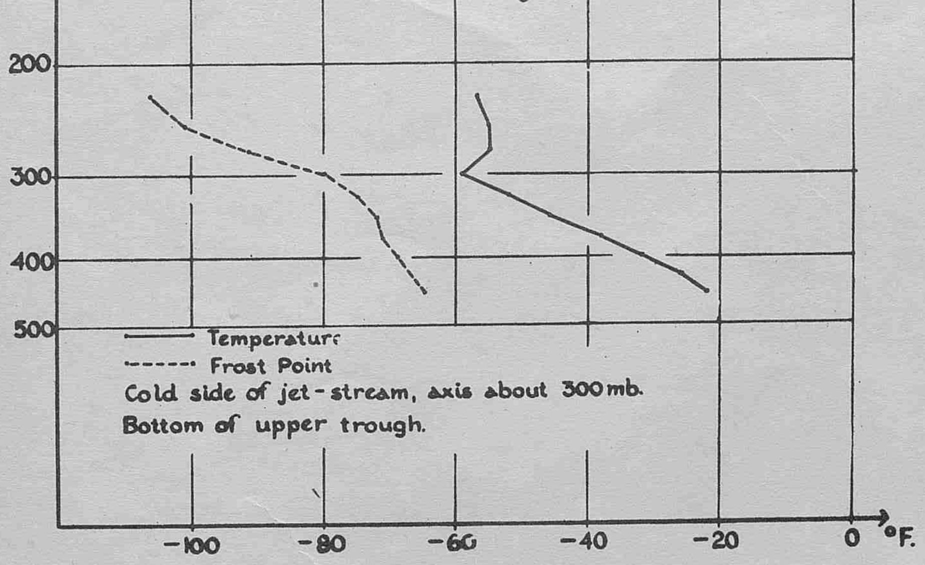

Cold side of jet-stream, axis about 300 mb.
Bottom of upper trough.

Figure 10.
12th. August, 1949.

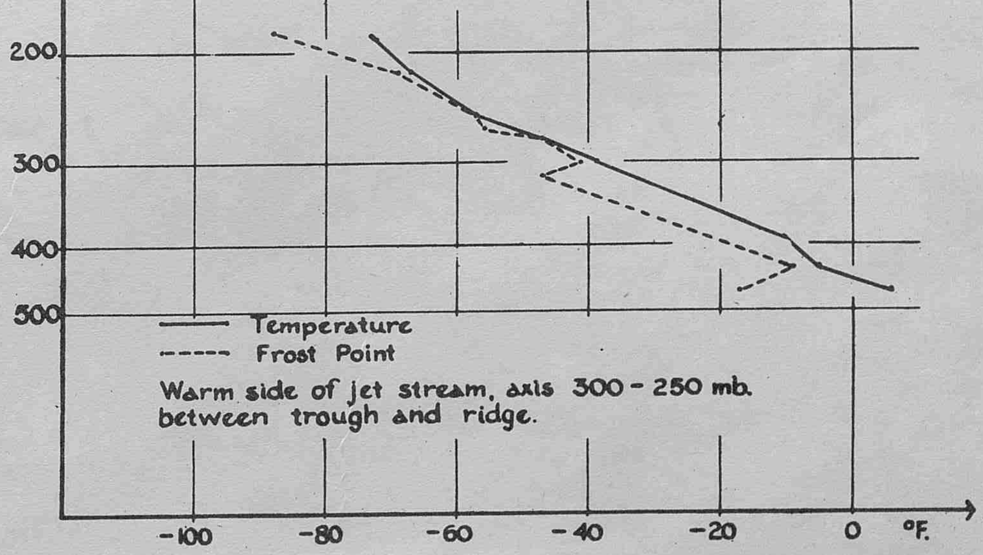

Warm side of jet stream, axis 300 - 250 mb.
between trough and ridge.

published and is to be treated
CONFIDENTIALLY. Its
contents must not be quoted.

M.R.P.564.
S.C.III/60.
31st May, 1950.

AIR MINISTRY

METEOROLOGICAL RESEARCH COMMITTEE

AD223159

The distance over which an aircraft flying on a constant heading may experience severe icing in convective cloud conditions.

by

R.F. Jones and J.G.D. Beimers (Meteorological Office)

Introduction

AIR WEATHER SERVICE
TECHNICAL REFERENCE FILE

In considering aircraft icing problems it has long been recognized that the cumulonimbus cloud is the cloud in which, owing to the large amount of free water available in the supercooled state, icing is likely to be the most severe. Cumulonibus clouds, however, are isolated and of varying sizes and information has been lacking on the frequency with which such clouds, and therefore potentially severe icing, will be encountered on an aircraft flight at a constant heading, and on the length of time an aircraft might be exposed to the risk of continuous severe icing. Answers to both these problems would be of value in assessing the general icing risk to aircraft and would assist in the design of aircraft de-icing equipment.

Recent papers (1,2) have discussed the radar echoes received from precipitating cumulus and cumulonimbus clouds, using a 10cm radar equipment, The echoes received from levels above the freezing level have been interpreted as coming from that part of the cloud which contains a large enough concentration of supercooled waterdrops of raindrop size. Although 10cm radar equipment will not therefore define the whole volume of the cloud (3), it will indicate the part of the cloud in which the free water concentration is greatest and therefore the part of the cloud in which the icing may be expected to be most severe. The P.P.I. display of such an equipment gives a projection of the echoing volume of the cloud on a nearly horizontal plane. The horizontal dimensions of a cumulonimbus echo do not vary considerably with height (4), except near to the echo top, nor is the echo column at any time appreciably inclined to the vertical, so that the width of an echo on the P.P.I. display along a particular bearing can with reasonable accuracy be taken to represent the distance over which an aircraft, flying on this bearing above the freezing level and below the echo top, would be exposed to the risk of severe icing.

An analysis of P.P.I. display tube photographs taken on showery days may therefore give useful data towards the solution of the problems set out in the first paragraph above and the present paper gives the results of such an analysis.

2. Data available and method of analysis

P.P.I. display tube photographs, taken at East Hill, are available for many different weather situations and those photographs relating to days wich isolated showers were extracted. Days on which the showers appeared to be associated with well-marked troughs or cold fronts, leading to a long line of almost continuous echo extending along one bearing only, were not considered.

On each photograph the largest aggregate length of echo intercepted on a straight line through the station (the centre of the photograph) was measured, so that this line gave the heading an aircraft flying over the station would take to experience the greatest icing risk, at the time the photograph was taken,

/The

G.269174/DC/6/50/40

The line covered a total range of 120 miles with the station at its centre but, to exclude errors due to permanent echoes and observations made at excessively short ranges, all echoes lying within 10 miles of the station were ignored, leaving a total length of 100 miles to be examined. In additon the longest distance continuously within echo on this bearing was also measured.

A total of 290 photographs taken on 39 days in the period 13th May, 1947 to 17th May, 1949 inclusive was analysed in this way. The number of photographs taken on any one day was not the same but, as the number of individual days was so small and the choice of a representative picture for a particular day impossible, all the available photographs, taken at intervals of not less than five minutes, have been used in the analysis. The maximum readings for each day have been extracted and are set out in Table I. It should be remembered that photographs may not have been taken at the most favourable time on every day, so that the value of the information in Table I is limited.

3. Presentation of the results of the analysis

The information, obtained as described in Section 2 above, from all the 290 photographs is presented in Figures I and II in the form of frequency curves.

In Fig.I the frequency of occurrence of various aggregate echo-intercepts on the line of flight of 100 miles across the station which intercepted the most echo is shown as a percentage of the total number (290) of such flights.

Fig.II shows the frequency of occurrence of maximum lengths of continuous flight in echo in the 100-mile flights of Fig.I, expressed as a percentage of the total number of flights.

The same information is displayed in Figs.III and IV in a different form. Fig.III shows the percentage number of occasions when specified values of aggregate distance within echo were exceeded on a flight of 100 miles across the station, while Fig.IV shows the percentage frequency with which, during a 100-mile flight, specified maximum distances of continuous flight within an echo would be exceeded.

4. Interpretation and discussion of the results of the analysis

On the assumption that flight in the echo part of cloud (above freezing level) is associated with severe icing, Fig.I may be interpreted as refering to the greatest proportion of a flight, at a particular instant on a showery day, during which severe icing may be encountered and the frequency with which that proportion would be met on a large number of flights, provided all the flights were made above the freezing level.

The maximum frequency occurs for a proportion of 10 miles (aggregate) of probable severe icing in every 100 miles of flight, but the mean value is 10.5 miles and an important number of occasions would occur when severe icing would be encountered over greater distances than this. This point is brought out more clearly in Fig.III from which it will be seen that, although the maximum frequency occurs at 10 miles (where the slope of the curve is greatest), 40% of all flights would be likely to experience severe icing over an aggregate distance greater than 10 miles in every 100 miles and 1 flight in 10 may get severe icing for 17 miles or more.

Fig.II indicates that the greatest distance on a particular flight over which continuous icing is likely to occur is most frequently 5 miles, but the mean value is 8.3 miles and there is a very considerable number of occasions when continuous icing may occur for greater distances than 5 miles. Thus, from Fig.IV, 70% of all flights would experience continuous icing for more than 5 miles and 1 flight in 10 would be liable to get continuous icing for about 13 miles or more.

It would appear from Fig.III that icing for more than about 25 miles (aggregate) in every 100 miles is very unlikely but it should be remembered that this is true only for isolated shower conditions such as occur, for example, in polar air in summer in the East and SE of England. On some occasions, however, large masses of thunderstorms and areas of thundery rain move North or NE from the continent across England and in such conditions it would not be unlikely for there to be more than 30 miles of continuous echo along a straight line, with the virtual certainty of severe icing above the freezing level. The freezing level in such conditions, however, is usually high and flight in this country beneath the freezing level would not be impossible. On other occasions, associated with cold fronts or well-marked polar troughs, long lines of echo may also occur exceeding the limits of Figs.I and II, but in such conditions the belt of echo is likely to be relatively narrow and the position of the belt can probably be forecast with reasonable accuracy. Further examination of the single occasion in Fig.II when the distance in continuous echo was 32 miles revealed it to be associated with storms moving North from the continent, the freezing level being about 12,000 feet. The occasion of 28 miles, on the other hand, in the same figure was associated with polar air moving around a depression over Lancashire and the freezing level was at about 5,000 feet.

Comparison between Figs.III and IV reveals that by far the greater proportion of the total echo on a single flight of 100 miles is likely to be contributed by one single continuous echo. Thus, from Fig.III, while 40% of all flights would be through more than 10 miles of echo, Fig.IV indicates that for the same percentage of flights there would be more than 8 miles of continuous echo. Similar results are to be observed for other values of the percentage of flights.

Table I indicates that, by taking only the extreme values for each day of the 39 days, there are 28 days out of the 39 when the distance of severe icing would be between 5 and 19 miles in every 100 miles, the mean distance for all days being 16 miles, and 35 days out of the 39 when the maximum continuous echo would lie between these limits, the mean value being 13 miles. As mentioned previously, however, it cannot be assumed that the worst conditions of each day were photographed on the display tube.

5. Limitations to the application of the results

While it is probable that the results here described give some information which has not previously been available and give a general indication of the extent of the icing hazards in cumulonimbus flying, only limited use of the detailed results and values quoted should be made for the following reasons.

(i) The analysis covers a period of only two years during which the frequency of occurrence, and severity when it did occur, of shower activity may have been less than the long term average.

(ii) The analysis is only strictly applicable to a limited area of the Midlands of England and may not apply to other areas, even of England. In particular the results may not be applicable to coastal areas where the shower frequency is high in winter nor to mountainous regions where orographic effects are added to the normal surface heating effect.

(iii) The analysis does not include frontal effects, including the effect of well-marked troughs, which can usually be forecast, but applies to the random distribution of shower activity in unstable air.

(iv) No allowance is made in the measurements for the effect of the range at which the radar echoes were observed. Distant echoes, due to attenuation by range, will appear smaller on the P.P.I. display tube than an echo due to a similar cloud at shorter ranges.

Without a detailed knowledge of the way the raindrop distribution varies horizontally through the particular cloud no useful correction can be made for range. In general, however, the nature of the cumulonimbus echo, which indicates the probability of an abrupt change in echo intensity on entering the precipitation core of the cloud, makes it unlikely that any serious correction would be necessary for the majority of echoes examined. In any case the echo observed would still be the volume of maximum icing risk within the cloud at whatever range it was viewed.

(v) The echo as seen on the P.P.I. display, being the projection of the whole volume of echo on an almost horizontal plane, may on some occasions over-estimate the extent of the echo at the line of flight above the freezing level.

6. Summary

An analysis of the radar echo distribution from showers as seen on the P.P.I. display of a 10cm radar equipment is used to give an indication of the frequency with which severe icing conditions may be encountered on a flight at a constant heading on a day when isolated showers are occurring.

Undue weight cannot be attached to the detailed results but it would appear that in showery weather severe icing conditions may occur at the worst on about 40% of all flights in the Midlands of England for more than 10 miles in every 100 miles but on only about 4% of all flights for more than 20 miles in every 100 miles. Continuous icing is likely to occur at the worst on about 40% of all flights for more than 8 miles in 100 miles but on only about 4% of all flights for more than 17 miles in 100 miles.

7. References

1. Jones, R.F.: The heights and temperatures at the tops of radar echoes associated with various cloud systems. M.R.P. No.458, Air Ministry, Meteorological Research Committee, London, 1949.

2. Meteorological Office: Detection of icing conditions by radar. M.R.P. No.482, Air Ministry, Meteorological Research Committee, London, 1949.

3. Jones, R.F.: The horizontal dimensions of cumulonimbus clouds at various heights. M.R.P. No.535, Air Ministry, Meteorological Research Committee, London, 1950.

Table I

Maximum total distances which would be flown in echo on each day on a constant heading across the station and maximum distances continuously in echo - frequencies of occurrence.

Echo extent (miles)	Total echo distance No. of occurrences	Continuous echo No. of occurrences
0 - 4	1	1
5 - 9	7	8
10 - 14	11	18
15 - 19	10	9
20 - 24	5	1
25 - 29	3	1
30 - 34	2	1
TOTALS	39	39

G. 269174/ABC/6/50/40

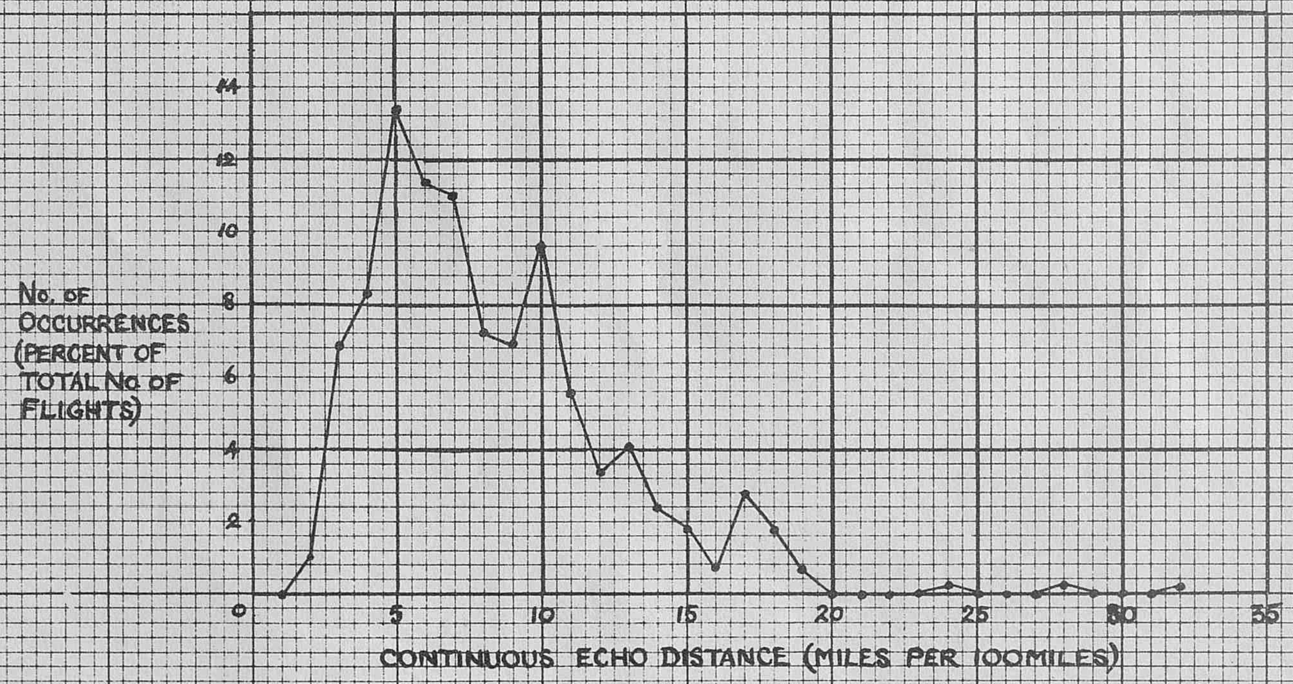

FIG II FREQUENCY WITH WHICH AN AIRCRAFT WOULD HAVE BEEN CONTINUOUSLY IN ECHO FOR SPECIFIED DISTANCES IN THE 100MILES OF FLIGHT OF FIG. I.

G. R.

M.R.P.564

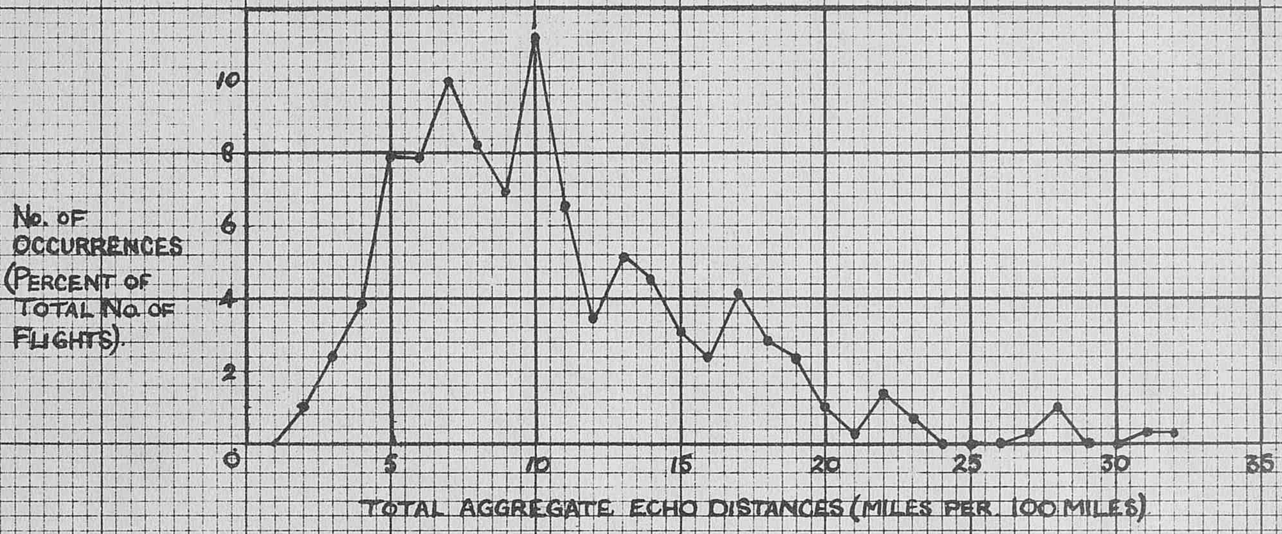

FIG. I FREQUENCY OF OCCURRENCE OF VARIOUS ECHO INTERCEPT DISTANCES ON THE LINE OF FLIGHT OF 100 MILES, WHICH INTERCEPTED MOST ECHO

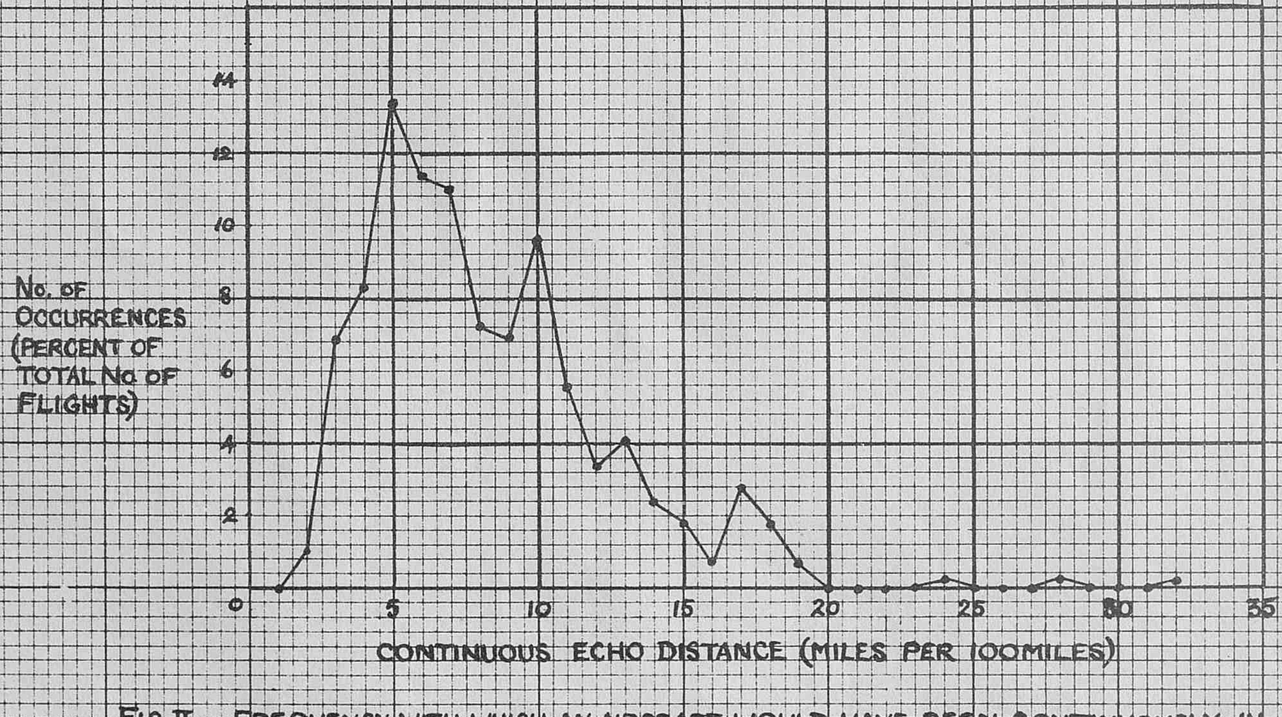

FIG. II FREQUENCY WITH WHICH AN AIRCRAFT WOULD HAVE BEEN CONTINUOUSLY IN ECHO FOR SPECIFIED DISTANCES IN THE 100 MILES OF FLIGHT OF FIG. I.

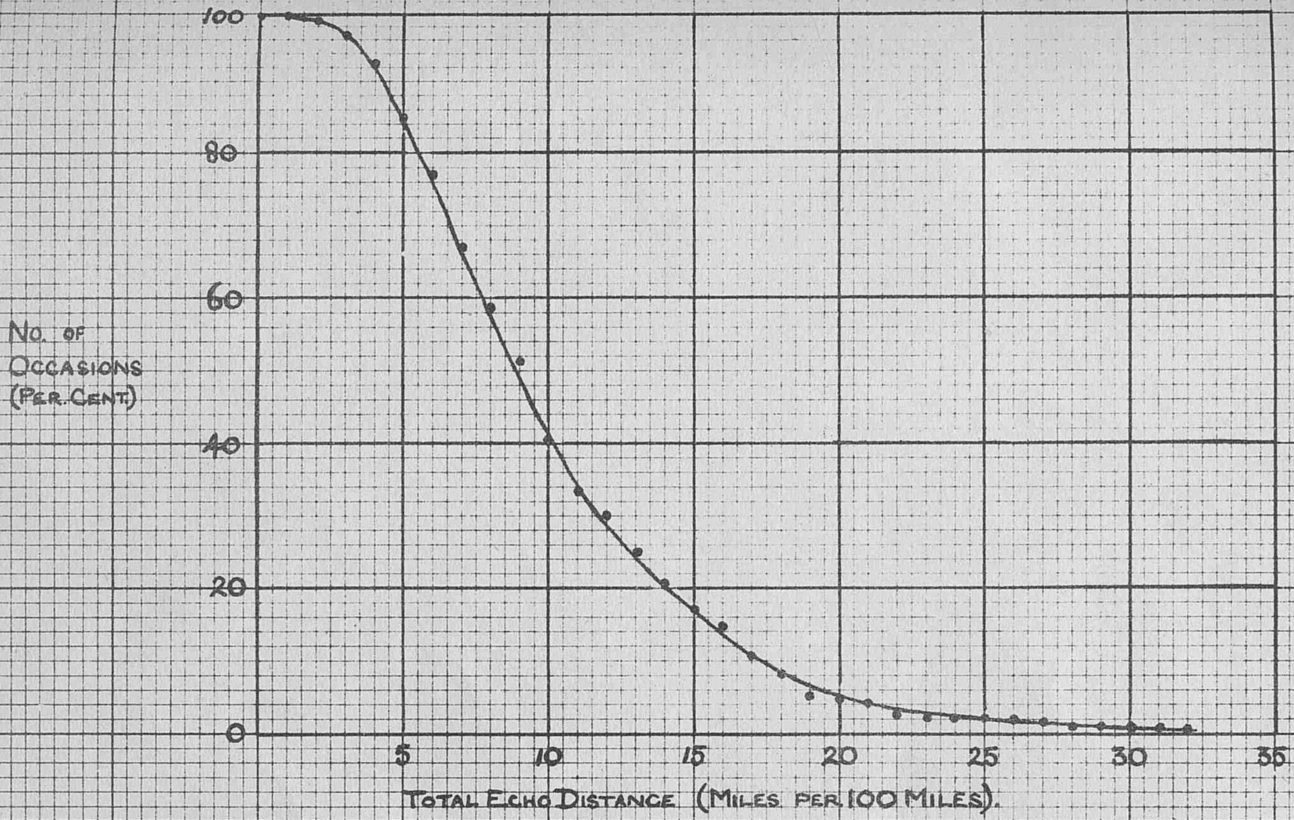

Fig. III Percentage number of occasions when a certain aggregate distance within echo was exeeded on the 100 mile flights of Fig. I

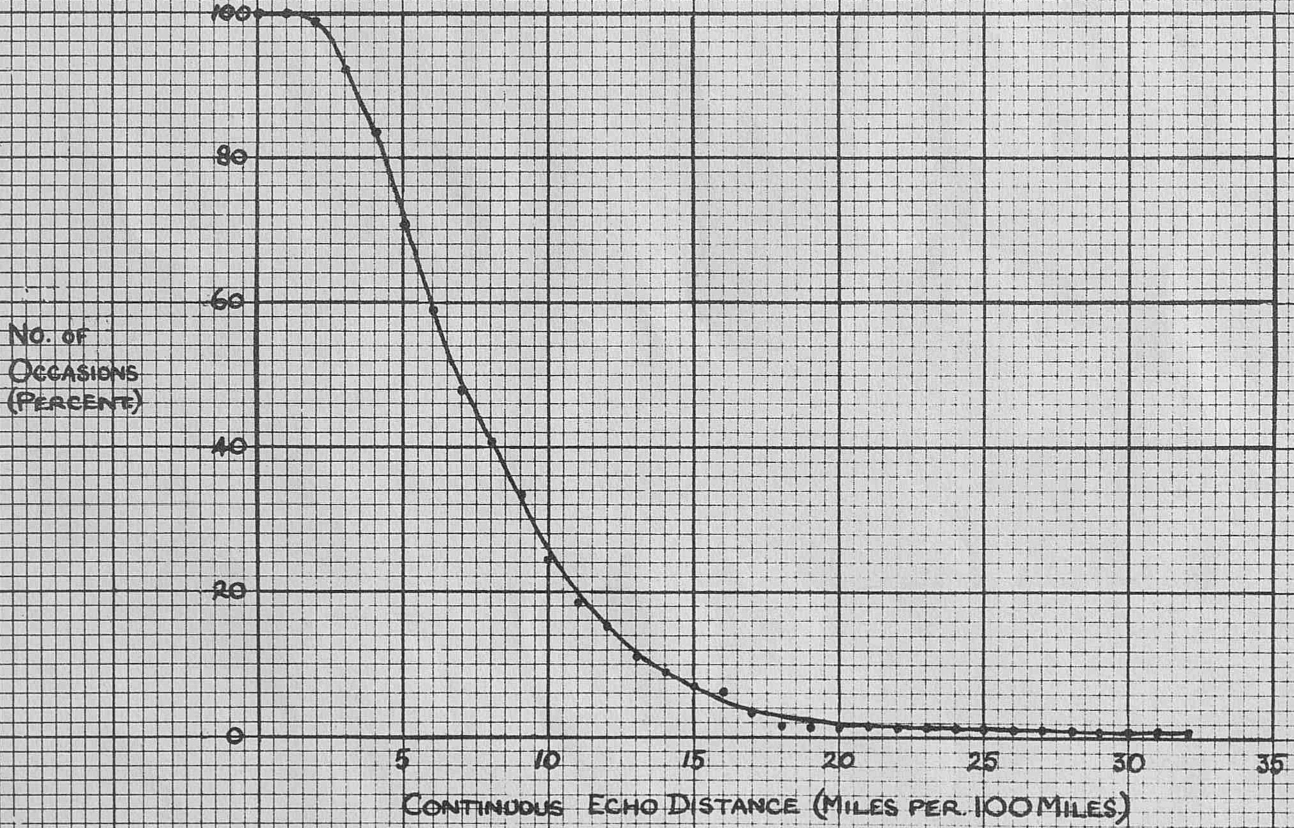

Fig IV Percentage number of occasions when an aircraft would have been continuously in echo for a greater distance than the specified distance on the 100 mile flights of Fig. I

CONFIDENTIALLY. Its
contents must not be quoted.

M.R.P. 566
S.C.II/57
1st July, 1950.

AIR MINISTRY

METEOROLOGICAL RESEARCH COMMITTEE

Report on Charney and Eliassen's One-Dimensional Numerical Method for Calculating Motion of Barotropic Disturbances in a Westerly Airstream

by

F.H. Bushby (Meteorological Office)

Introduction

Numerous writers in America have suggested that the changes in the atmospheric flow in the middle troposphere can be treated as though the atmosphere was a barotropic fluid, i.e. a fluid in which pressure is a function of density alone. Recently Charney and Eliassen (1) have given a numerical method of computing changes caused by small perturbations superimposed on a uniform zonal current. The treatment is essentially one dimensional and was regarded by the authors as a preliminary study to an attack on the more general two-dimensional problem. However, the authors claimed that the one-dimensional method could produce results in forecasting comparable with existing techniques and it was considered worth examination in the Forecast Research Division at Dunstable.

The present report records the first results of such an examination. A summary of the theoretical basis of the original paper is given so that reference to the original is not essential. Charney's method has been applied daily to the 0300 G.M.T. 500 mb. profiles along latitudes 45° North and 60° North for the month of November, 1949, and the results compared with forecasts produced by other methods. An attempt has been made to formulate certain objective rules which would specify the regions in which Charney's method would probably give an erroneous result.

Summary of Theory

The one-dimensional method depends upon several assumptions, the main ones being as follows:-

1. The existence of an equivalent barotropic level at approximately 500 mbs.
2. That the motion can be considered as consisting of small perturbations superimposed upon a zonal current constant with respect to time and longitude.
3. The height perturbation is assumed to have a sine dependency on the North-South co-ordinate.

Charney commences his theoretical approach by starting with the well-known Rossby vorticity equation which relates changes of vorticity to the divergence in a horizontal layer of the atmosphere.

$$\frac{d}{dt}(f+\zeta) + \frac{f}{\rho}\left\{\frac{\partial}{\partial x}(\rho u) + \frac{\partial}{\partial y}(\rho v)\right\} = 0 \qquad \ldots\ldots \quad (1)$$

where

ζ = vertical vorticity component relative to the earth.

f = Coriolis parameter.

/u =

u = component of velocity in x direction (east).

v = component of velocity in y direction (north).

ρ = density.

Charney averages this equation in the vertical direction with respect to pressure throughout the atmosphere, and utilising the tendency equation, obtains

$$\overline{\frac{d}{dt}(f+\zeta)} = \frac{f}{p_o}\frac{\partial p_o}{\partial t} - \frac{f}{H}w_o \quad \text{.........(2)}$$

where the bar denotes average value

subscript "o" denotes surface values

p = pressure

T = temperature

H = $\frac{RT_o}{g}$, where R = Specific gas constant.

w = vertical velocity component.

Charney assumes that the shape of the streamlines is the same at all levels and that the increase of wind with height is similar along all verticals. The velocity field can then be written.

$$u = \bar{u}(x,y,t)\,A(p) \qquad v = \bar{v}(x,y,t)\,A(p) \quad \text{(3)}$$

and (2) becomes

$$\frac{\partial\bar{\zeta}}{\partial t} + \left(\bar{u}\frac{\partial}{\partial x} + \bar{v}\frac{\partial}{\partial y}\right)\left(f + \overline{A^2}\bar{\zeta}\right) = \frac{f}{p_o}\frac{\partial p_o}{\partial t} - \frac{f}{H}w_o \quad \text{........(4)}$$

There must be a certain level p = $\bar{p}$, where u = $\bar{u}$, v = $\bar{v}$, $\zeta = \bar{\zeta}$ and at this level (4) becomes

$$\frac{\partial\zeta}{\partial t} + \left(u\frac{\partial}{\partial x} + v\frac{\partial}{\partial y}\right)\left(f + \overline{A^2}\zeta\right) = \frac{f}{p_o}\frac{\partial p_o}{\partial t} - \frac{f}{H}w_o \quad \text{..........(5)}$$

In a barotropic fluid A(p) $\equiv$ 1, and $\overline{A^2}$ = 1, so that equation (5) (with $\overline{A^2}$ = 1) holds at all levels, and can be interpreted as indicating that a level p = $\bar{p}$ exists at which the motion of the baroclinic atmosphere corresponds to the motion of an equivalent barotropic atmosphere. This level is defined as the "equivalent barotropic level" and for convenience is taken as being 500 mbs; although Charney (2) has stated that the value lies between 550 and 600 mbs., and a proper value for $\overline{A^2}$ in the Atmosphere is 5/4.

In order that equation (5) should imply the existence of an equivalent barotropic atmosphere, it is necessary to approximate $\overline{A^2}$ to 1. It has been shown in reference (3) that replacing assumption (3) by the more general assumption.

$$u = \bar{u} + B(p)u', \qquad v = \bar{v} + B(p)v' \quad \text{........ (6)}$$

where

/ u' =

u' = thermal wind component in x direction per unit thickness. $\overline{A^2}$ will normally vary between 1 and 4/3, but although locally $\overline{A^2}$ may increase to as much as 2, on those occasions $\frac{\partial \zeta}{\partial t}$ will be small.

The results obtained by Charney would seem to justify this approximation of $\overline{A^2} = 1$, and the consequent existence of an equivalent barotropic level, even though on theoretical grounds the approximation does in certain cases seem to be rather coarse.

Introducing the geostrophic approximation into the vorticity equation (5), considering small perturbations on a constant zonal current U, and taking into account the effect of topography and friction, Charney obtains the following linear differential equation.

$$\left(\frac{\partial}{\partial t} + U\frac{\partial}{\partial z} + \mu F\right)\left(\frac{\partial^2 z}{\partial x^2} - m^2 z\right) + \beta\frac{\partial z}{\partial x} - \lambda^2\frac{\partial z}{\partial t} = -\mu\lambda^2 U\frac{\partial h}{\partial x} \qquad \text{.........} (7)$$

where the unsuffixed variable now refers to the 500 mb. level.

U = zonal current.

$\mu = u_{g_o}/u$ where suffix g_o refers to top of friction layer.

$F = \frac{\sin 2\alpha}{\sqrt{2}} \frac{\sqrt{Kf}}{H}$

α = angle between isobars and the surface wind.

K = eddy diffusivity.

z = height of 500 mb. surface.

$\beta = \frac{\partial f}{\partial y}$

$\lambda^2 = \frac{f^2}{gH}$

$h(x)$ = mountain profile along latitude circle in question

A sine variation of the z perturbation with y has been assumed, given by

$$\frac{\partial^2 z}{\partial x^2} = -m^2 z \qquad \text{.........} (8)$$

In the computations the units used were x in radians of longitude, t in days. This gives

$\beta = 4\pi \cos^2\phi$

$\lambda^2 \doteqdot 2.5 \sin^2 2\phi$

/ Comparison

Comparison of observed and computed stationary wavelengths over oceans suggested that m^2 was approximately 15, but the value of m^2 does not make a vital difference to the computations.

Integration of (7) by Fourier Analysis gives

$$z(x + Ut,t) = z(x,o) + \int_o^{2\pi} z(\alpha,o)\, I_{a^2}(x - \alpha,t)\, d\alpha + \mu\lambda^2 \int_o^{2\pi} h(\alpha)\, J(x - \alpha,t)\, d\alpha \quad \ldots\ldots (9)$$

where

$$I_{a^2}(x,t) = \frac{1}{2\pi} \sum_{-\infty}^{\infty} \left\{ \exp\left(\frac{inbt}{n^2 + a^2}\right) - 1 \right\} \exp(inx) \quad \ldots\ldots (10)$$

$$J(x,t) = \frac{1}{2\pi} \sum_{-\infty}^{\infty} \left\{ \exp(inUt) - \exp\left(\frac{inbt}{n^2 + a^2}\right) \right\} \frac{\exp(inx)}{n^2 - s^2} \quad \ldots\ldots (11)$$

$$a^2 = m^2 + \lambda^2 \qquad\qquad b = \beta + \lambda^2 U$$

By computing functions I and J, Charney showed that for t = 1 day J is small compared with I and can be neglected. Also, it is possible to take a limited influence region for the summation of I. This is apparent from graphing I with respect to x. Equation (9) then becomes

$$z(x + Ut,t) = z(x,o) + \int_{x-x_1}^{x+x_2} z(\alpha,o)\, I_{a^2}(x - \alpha,t)\, d\alpha \quad \ldots\ldots (12)$$

$a^2 = m^2 + \lambda^2$ and was taken $\div$ 18.

For a one day forecast

$$z(x + U,1) = z(x,o) + \int_{x-x_1}^{x+x_2} z(\alpha,o)\, I_{18}(x - \alpha,1)\, d\alpha \quad \ldots\ldots (13)$$

Charney (2) has calculated and tabulated the function I_{18}

$$\int_{x-x_1}^{x+x_2} z(\alpha,o)\, I_{18}(x - \alpha,1)\, d\alpha$$

can be evaluated by Simpson's Rule from the observed initial profile z(x,o) taking intervals of 10° longitude.

For latitude 45° North, values of $I_{18}(x,1)$ are given in reference (2). These values are reproduced in Table I. In obtaining these values b is taken as 7. Taking $x_1 = 80$, $x_2 = +40$, and integrating (13) by Simpson's Rule,

/ z

$$z(x + U,1) = z(x,o) + \sum_{-4}^{8} A_N\, z(x + 10N,o)$$

$$= z(x,o) + \sum_{-3}^{7} A_N\, z(x + 10N,o)$$

as A_8 and A_{-4} are negligible. Coefficients A_N are given in table II.

For latitude 60° North, values of $I_{18}(x,1)$ were computed for a value of $b = 4.5$. (On the month's charts considered, a more accurate value would have been $b = 4$). In the expression $I_{a^2}(x,t)$ in (10)b only occurs in a product term containing t. Values for $I_{18}(x,t)$ are tabulated in the Journal of Meteorology for $b = 7$, $t = 1, 2, 3....7$. As a value for I_{18} for $b = 4.5$, $t = 1$, was required, the values of $I_{18}(x,t)$ given for $bt = 7, 14, 21....49$ were interpolated by means of Newton's forward difference formula to obtain $I_{18}(x,t)$ for $bt = 4.5$. In the interpolation use was made of the identity $I_{18}(x,o) \equiv o$. These values are tabulated in Table I.

Integration by Simpson'ssRule was again carried out taking $x_1 = 60$, $x_2 = +40$ giving

$$z(x + U,1) = z(x,o) + \sum_{-4}^{6} B_N\, z(x + 10N,o)$$

$$= z(x,o) + \sum_{-3}^{6} B_N\, z(x + 10N,o)$$

as coefficients B_6 and B_{-4} are negligible. Coefficients B_N are given in Table II.

Table I

	b = 7		b = 4.5	
x	$I^{*}_{18}(x,1)$	$I^{*}_{18}(-x,1)$	$I_{18}(x,1)$	$I_{18}(-x,1)$
0°	-4.301	1.999	-3.02	1.55
10°	-1.506	1.239	-.94	.86
20°	-0.529	0.777	-.45	.50
30°	-0.167	0.457	-.15	.27
40°	-0.048	0.275	-.06	.17
50°	-0.016	0.161	-.02	.09
60°	0.002	0.091	.00	.04
70°	-0.003	0.057	.00	.03
80°	0.003	0.028	.00	.01
90°	-0.001	0.020	.00	.01
100°	0.001	0.008	.00	.00
110°	0.001	0.007	.00	.01
120°	-0.002	0.004	.00	.00
130°	0.002	0.001	.00	.00
140°	-0.002	0.003	.00	.00
150°	0.002	-0.002	.00	.00
160°	-0.001	0.002	.00	.00
170°	0.001	-0.001	.00	.00
180°	0.001	0.001	.00	.00

/ Table II

Table II

N	A^*_N	B_N
-3	-.039	-.035
-2	-.062	-.052
-1	-.351	-.219
0	-.134	-.086
1	.289	.200
2	.091	.058
3	.106	.063
4	.032	.020
5	.038	.021
6	.011	
7	.013	

*These coefficients are slightly different from those published in Telus Vol.1 No. 2, but are based on figures given in the more complete table in reference (2).

Method of Investigation

The practical application of the forecast formula is a simple mechanical process, which is described in Appendix I. The formula was first applied to the 500 mb. profiles along latitude 45° North for the 0300 G.M.T. charts of November 1949. The forecast change in the profile was plotted on a graph, and compared with the actual change. Also plotted on the graph were the changes forecast by Forecast Division Dunstable on their routine 500 mb. prontours over the range from 35° West to 35° East. The forecast thickness lines for the first days of the Research Division "four day forecasts" were gridded with the actual 1,000 mb. contours for the appropriate day, and the results also plotted. From the results obtained it was found possible to make certain objective rules which specify the synoptic regions in which Charney's formula will not give a reasonably good forecast.

The formula was then applied to the 500 mb. profile along latitude 60° North for the same month's charts, and the results again compared with the Forecast Division's prontours.

Before the numerical forecast changes were examined, the objective rules were applied to specify those areas where an accurate forecast was not expected.

Summary of Results

The results for latitude 45° North were first analysed. A comparison was made between the numerical forecast change and the actual change (See Table III line 1). The following notation was used:-

A. Good agreement over the whole range.

B. Good agreement over most of range.

BC. Good agreement over about half of the range

C. Poor agreement over most of the range

D. Poor agreement over whole range.

Good agreement was taken as meaning a difference of 200 feet or less.

Secondly, a comparison was made of the difference between the numerical forecast change and the actual change, and the difference between the Forecast Division's forecast and the actual change (See Table III line 2). The following notation was used:-

/ A.

A. The numerical method better than Forecast Division over whole range.

B. The numerical method better than Forecast Division over most of range.

BC. Little to choose between the numerical results and Forecast Division's results.

C. Forecast Division better than the numerical method over most of range.

D. Forecast Division better than the numerical method over whole range.

Thirdly a comparison was made between the results obtained by the numerical method and the results obtained by utilising the "pre-thickness" pattern produced on the first days of the "four day" forecast produced in the Research Division at Dunstable (See Table III line 3). These were classified using the notation described for comparing the numerical forecast with the Forecast Division's forecast. It must be remembered, however, that no attempt had been made in the Research Division's Experimental forecasts to forecast the actual contours.

Table III

Comparison	A	B	BC	C	D
Charney's forecast change and actual change	1	12	1	13	3
Charney's forecast change and Forecast Divisions forecast change.	2	4	9	9	5
Charney's forecast change and "pre-thickness" forecast change.	1	4	2	1	1

Charney's method gave a reasonably accurate forecast at about half the positions for which the computations were carried out, although the correlation coefficients for the forecast changes and the actual changes was only .34. The correlation coefficient between the actual change and the forecast change obtained by assuming an eastward displacement of the pressure profile equivalent to one day's zonal flow was .27. Thus the more elaborate features in the theory do improve the forecast appreciably.

Nearly all the cases when the numerical method gave an error greater than 200 ft. occurred when one of the following criteria applied, each of which meant that Charney's original assumptions were not fulfilled. In the first 3 cases the error in the forecast is generally displaced downstream a distance equivalent to one day's zonal flow.

1. The presence of a closed circulation in the 500 mb. contour pattern during forecast period.

2. A trough or ridge in the 500 mb. contour pattern whose axis is inclined at an appreciable angle to the meridian, or a U shaped trough or ridge whose axis is parallel to a maridian, but with strong meridional flow along its sides.

3. A flat area of insignificant pattern in the 500 mb. contour patterns.

4. A strong thermal field with surface isobars at right angles to it (generally wave depressions on an active front).

The closed circulation in the 500 mb. pattern usually has a fairly local effect, and elsewhere along the latitude circle the results are good unless any other factors are present to cause further discrepancies. The presence of a closed circulation means that the motion can no longer be regarded as a small perturbation on a constant zonal current, and that there is not a sine dependency on the y (North-South) co-ordinate. The forecast for 0300Z on 3rd November, 1949, based on the 0300Z chart on 2nd November, 1949, shows the discrepancies due to a closed circulation. (See figs. 1a, 2a, 2b).

In the case of the trough or ridge in the 500 mb. pattern whose axis is inclined to the meridian, once again the effect is also usually relatively local. The motion can no longer be regarded as a small perturbation on constant West-East zonal currents, and in a large number of cases there will be an East-West rather than West-East component of the actual motion. There is also no sine dependency on the y co-ordinate of the height perturbation. A U-shaped trough or ridge with strong meridional flow along its sides also cannot be regarded as a small perturbation on a West-East zonal current, and again there is no sine dependency on the y co-ordinate. The forecast for 0300Z on 9th November, 1949, shows a good example of the discrepancies due to an upper trough whose axis is inclined to a meridian. Here the discrepancy in the forecast is about 15 degrees of longitude further East than the axis of the quasi-stationary trough (See figs. 1b, 3a, 3b).

A flat area of insignificant pattern means that the actual zonal flow in that area is very much less than the average flow over the hemisphere. (See figs. 1c, 4a, 4b).

The main errors from 20th November to 25th November, 1949, over the Atlantic were caused by the meridional advection of a strong W-E thermal field on the North side of a frontal belt lying parallel to the 45° North latitude. This advection took place near developing waves on the fronts and did not cause a big distortion in the sinusoidal pattern, but rather a general increase (or decrease) in the 500 mb. level over a wide area. (See figs. 1d, 5a, 5b, 5c, 5d). Charney's method assumes the shape of the streamlines in approximately the same at all levels, and that the increase of wind with height is similar along all verticals. This is certainly not the case here. (See reference (3)).

A correlation coefficient was computed for the Forecast Division's forecast change and the actual change, and compared with a similar correlation coefficient for the numerical method of the same range. The correlation coefficient was .48 for the Forecast Division's method and .37 for the numerical method, but it must be remembered that in several of the cases considered, Charney's original assumptions were not fulfilled.

It was not possible to determine the actual number of independent observations on which the correlation coefficients were based, as there is a certain correlation between changes at neighbouring points along the profile, and also between changes on consecutive days. However, on the data examined, the numerical forecast applied to a total of 500 points, and the Forecast Division's forecast applied to a total of 300 points. Even allowing for a degree of dependence of certain of the forecast changes upon each other, it was estimated that the correlation coefficients obtained were still significant, having an error of not greater than ±.1 from the true value. By examining further data the correlation coefficients could be obtained more accurately, but whilst the present coefficients are not conclusive, it is considered that they are significant.

Before Charney's forecast formula was applied to the 500 mb. profile along 60° North, the surface, 500 mb. and 1,000-500 mb. thickness charts were carefully examined, and in accordance with the four criteria stated above, certain points were specified as being regions where the numerical method was not expected to apply. The correlation coefficient between the numerical forecast change and the actual change for the whole range was .37, whilst the correlation coefficient for the points left after certain regions had been excluded was .47.

When the Forecast Division's prontours at 60° N were examined, the correlation coefficient between the change they forecast, and the actual change was .56. This was increased to only .59 when the points specified above were left out. The correlation coefficient between the numerical forecast change and the actual change for the points in the Forecast Division's range after the points specified had been left out was .45.

Throughout the range from 75° W to 85° E, it was found that 62% of the the points were points where the numerical method could be expected to apply. As during the month considered the main train was usually further south than 60° North, a higher percentage of points had to be left out than would be the case if the method was applied to latitudes further south.

Conclusion

The results of the test show significant success but the standard obtained is less than that achieved by conventional methods.

From the study of the month's charts it would seem that the assumptions in Charney's formula are too great for the formula to be applied as a routine measure to all areas of the chart. However, by applying the formula to areas of the chart which are not affected by the following criteria:

1. A closed circulation in 500 mb. contour pattern.
2. A trough or ridge whose axis is inclined at an appreciable angle to the meridian, or a U-shaped trough or ridge whose axis is parallel to the meridian, but with a strong meridional flow along its sides.
3. A flat area of insignificant pattern in the contour pattern.
4. A strong thermal field with surface isobars at right angles to it, one would expect a forecast which was almost as accurate as the routine forecasts produced by conventional methods. Before conclusive results about the relative accuracy of Charney's one-dimensional method, and the conventional thickness method could be obtained, further investigation would be necessary but it is considered that on the results so far obtained the method deserves further study both from the practical and theoretical aspects.

Acknowledgements

I wish to acknowledge the assistance given by Miss K. Dyson in carrying out the computations involved in producing the report.

References

1. Charney J.G. and Eliassen A. A numerical method for predicting the perturbations of the middle latitude westerlies. Tellus Volume 1, No. 2, 1949, p.38.
2. Charney J.G. On a physical basis for numerical prediction of large scale motions in the atmosphere. Journal of Meteorology Vol. 6, No. 6, 1949, p.371.
3. Bushby, F.H. M.O.21 Technical Note No. 14.

Table IV

Multiples of coefficients A_N for latitudes 45° North (b = 7)

N	A_N	50	100	150	200	250	300	350	400	450	500	550	600	650	700	750	800	850	900	950	1000	1050	1100	1150	1200
-3	-.039	-2	-4	-6	-8	-10	-12	-14	-16	-18	-20	-21	-23	-25	-27	-29	-31	-33	-35	-37	-39	-41	-43	-44	-46
-2	-.062	-3	-6	-9	-12	-16	-19	-22	-25	-28	-31	-34	-37	-40	-43	-47	-50	-53	-56	-59	-62	-65	-68	-71	-74
-1	-.351	-17	-35	-53	-70	-88	-105	-123	-140	-158	-176	-193	-211	-228	-246	-263	-281	-298	-316	-333	-351	-369	-386	-404	-422
0	-.134	-7	-13	-20	-27	-33	-40	-47	-54	-60	-67	-74	-80	-87	-94	-101	-107	-114	-121	-127	-134	-141	-147	-153	-160
1	+.289	14	29	43	58	72	87	101	116	130	145	159	173	188	202	216	231	246	260	275	289	303	318	332	346
2	.091	5	9	14	18	23	27	32	36	41	45	50	55	59	64	68	73	77	82	86	91	96	100	105	110
3	.106	5	11	16	21	27	32	37	42	48	53	58	64	69	74	79	85	90	95	101	106	111	117	122	128
4	.032	2	3	5	6	8	10	11	13	14	16	18	19	21	22	24	26	27	29	30	32	34	35	37	38
5	.038	2	4	6	8	9	11	13	15	17	19	21	23	25	27	29	30	32	34	36	38	40	42	44	46
6	.011	1	1	2	2	3	3	4	4	5	5	6	7	7	8	8	9	9	10	10	11	12	12	13	14
7	.013	1	1	2	3	3	4	5	5	6	7	7	8	8	9	10	10	11	12	12	13	14	14	15	16

Table V

Multiples of coefficients B_N for latitude 60° North (b = 4.5)

N	B_N	50	100	150	200	250	300	350	400	450	500	550	600	650	700	750	800	850	900	950	1000	1050	1100	1150	1200
-3	-.035	-2	-3	-5	-7	-9	-11	-12	-14	-16	-17	-19	-21	-23	-25	-26	-28	-30	-31	-33	-35	-37	-39	-40	-42
-2	-.052	-3	-5	-8	-10	-13	-16	-18	-21	-23	-26	-29	-31	-34	-36	-39	-42	-44	-47	-49	-52	-55	-57	-60	-62
-1	-.219	-11	-22	-33	-44	-55	-66	-77	-88	-99	-109	-120	-131	-142	-153	-164	-175	-186	-197	-208	-219	-230	-241	-252	-263
0	-.086	-4	-9	-13	-17	-21	-26	-30	-34	-39	-43	-47	-52	-56	-60	-65	-69	-72	-77	-82	-86	-90	-95	-99	-103
1	.200	10	20	30	40	50	60	70	80	90	100	110	120	130	140	150	160	170	180	190	200	210	220	230	240
2	.058	3	6	9	12	15	17	20	23	26	29	32	35	38	41	43	46	49	52	55	58	61	64	67	70
3	.063	3	6	9	13	16	19	22	25	28	31	35	38	41	44	47	50	54	57	60	63	66	69	72	76
4	.020	1	2	3	4	5	6	7	8	9	10	11	12	13	14	15	16	17	18	19	20	21	22	23	24
5	.021	1	2	3	4	5	6	7	8	9	11	12	13	14	15	16	17	18	19	20	21	22	23	24	25

Table VI

Application of Charney's formula to profile along 45° North on 8/11/49, producing a forecast profile for 0300Z on 9/11/49. (See Fig.1b)

x =	-120	-110	-100	-90	-80	-70	-60	-50	-40	-30	-20	-10	0	10	20	30	40	50	60	70	80	90	100	110	120
z(x,o) =	18200	18600	18550	18450	18200	17900	17750	17850	18150	18550	18850	18600	18150	17600	17750	18500	18800	18700	18500	18200	18100	18500	18450	18150	18000
z(x,o) - 18000	200	600	550	450	200	-100	-250	-150	150	550	850	600	150	-400	-250	500	800	700	500	200	100	500	450	150	0
A_{-3} = -.039				-8	-23	-21	-18	-8	4	10	6	-6	-21	-33	-23	-6	16	10							
A_{-2} = -.062				-37	-34	-28	-12	6	16	9	-9	-34	-53	-37	-9	25	16	-31							
A_{-1} = -.351				-193	-158	-70	35	88	53	-53	-193	-298	-211	-53	140	88	-176	-281							
A_0 = -.134				-60	-27	13	33	20	-20	-74	-114	-80	-20	-54	33	-67	-107	-94							
A_1 = .289				58	-29	-72	-43	43	159	246	173	43	-116	-72	145	231	202	145							
A_2 = .091				-9	-23	-14	14	50	77	55	14	-36	-23	45	73	64	45	18							
A_3 = .106				-27	-16	16	58	90	64	16	-42	-27	53	85	74	53	21	11							
A_4 = .032				-5	5	18	27	19	5	-13	-8	16	26	22	16	6	3	16							
A_5 = .038				6	21	32	23	6	-15	-9	19	30	27	19	8	4	19	17							
A_6 = .011				6	9	7	2	-4	-3	5	9	8	5	2	1	5	5	2							
A_7 = .013				11	8	2	-5	-3	7	10	9	7	3	1	7	6	2	0							
Positive				18531	18243	17988	17942	18172	18535	18901	19080	18704	18264	17828	18247	18982	19129	18919							
Negative				-339	-310	-205	-78	-15	-38	-149	-366	-481	-444	-195	-32	-73	-283	-406							
F/Cz(x+17,1)				18192	17933	17783	17864	18157	18497	18752	18714	18223	17820	17633	18215	18909	18846	18513							

U (zonal current) = 17° long. per day.

Appendix One

Method of Tabulation

It was found convenient to represent negative values in red and positive values in blue ink, and to use "vertically ruled paper". The simplest method of tabulation is as follows:-

1. Write horizontally along the top row the values of x (longitude) at 10° intervals, beginning with value x = -120 (120° W), and ending with the value x = +120.

2. Write horizontally along 2nd row the values of z (x,o) along the appropriate latitude circle at 10° intervals from x = -120 to x = +120.

3. Write horizontally along 3rd row the values z (x,o) - 18,000 under the appropriate longitude.

4. Commencing on the 4th row and to the left of the previous 3 rows, write the values of A_N for N = -3 to N = +7 vertically beneath each other (For latitude 60° North use coefficients B_N for N = -3 to N = +5).

5. Commencing with the value (Z (-120,o) - 18,000), multiply it by A_{-3}, and place the result in the row A_{-3}, column x = -90.

   Next with the value (z (-110,0) - 18,000), multiply it first by A_{-3}, placing result in row A_{-3}, column x = -80. Then multiply (z (-110,0) - 18,000) by A_{-2}, placing result diagonally downwards and to the left of previous result. Continue with value (z (-100,0) - 18,000), multiplying in turn by A_{-3}, A_{-2}, A_{-1}, placing first result in row A_{-3} column x = -70 and subsequent results diagonally downwards to the left.

   Continue until table is complete.

6. Add each column, including the value of z(x,o) but not value of (z(x,o) - 18,000). This gives forecast value of z(x + U, 1).

As Northern Hemisphere charts were used, (scale 1:30,000,000) it was only possible to measure z to the nearest 50 feet. In carrying out "operation 5" above, it was found convenient to use a table of multiples of coefficients A_N and B_N at intervals of 50 from 0 to 1200. These tables are given as tables IV and V.

A worked example is shown in table VI, forecasting the 500 mb. profile along latitude 45° North for 0300 G.M.T. on November 9th, 1949, using data from the corresponding chart one day earlier. With practice, a competent assistant should be able to work out a forecast profile along one line of latitude from 70° W to 70° E in 20 minutes.

The zonal current was obtained by measuring zonal indices on the 500 mb. chart on which the forecast was based for the half hemisphere from 120° W to 60° E. The zone 35° North to 55° North was taken to obtain the zonal current for 45° North, and the zone 55° North to 70° North was used to obtain the zonal current at 60° North. If the method were being applied in a forecasting office, this may not be practicable but as the zonal current is fairly conservative the error in using the previous day's value would not be very great.

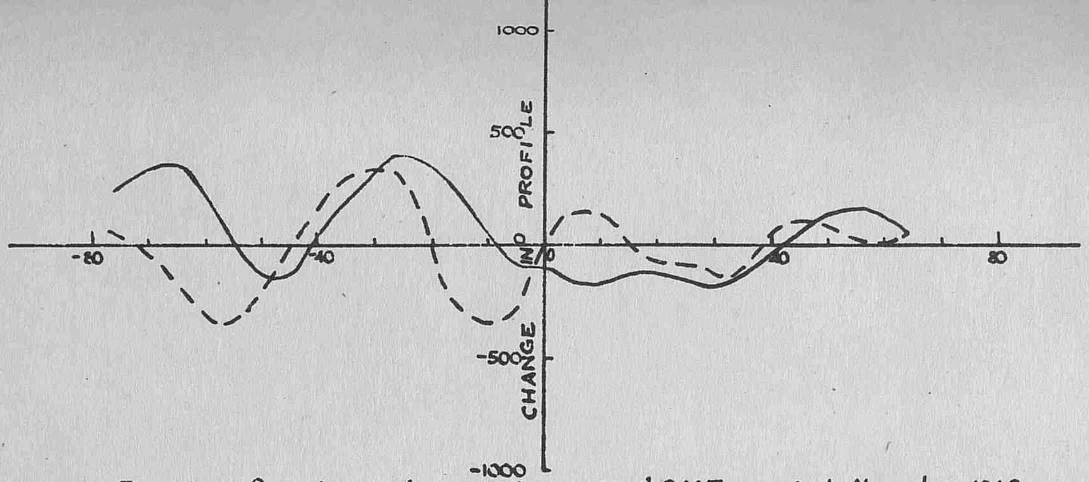

Fig. 1(a) One day changes from 0300h.G.M.T. on 2nd. November 1949.

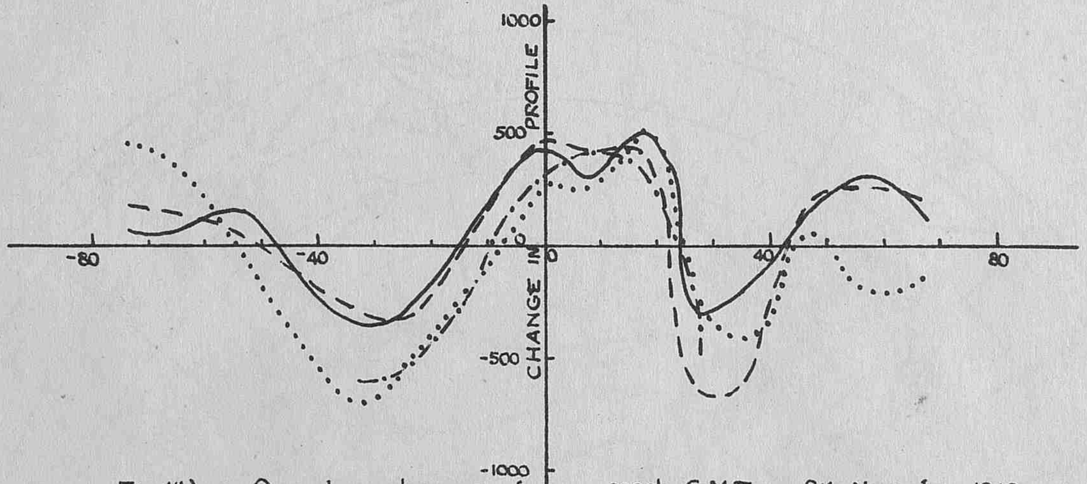

Fig. 1(b) One day changes from 0300h. G.M.T. on 8th. November 1949.

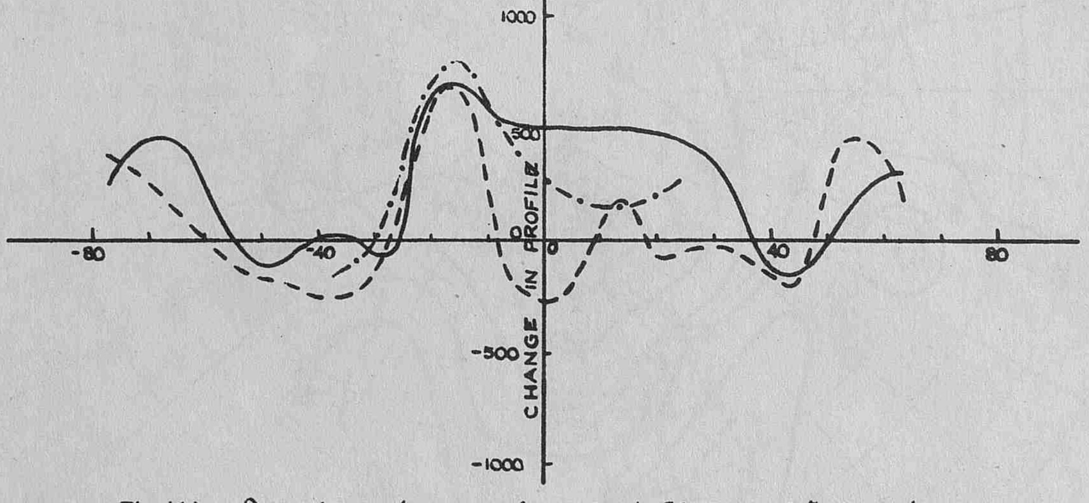

Fig. 1(c). One day changes from 0300h G.M.T. on 28th. November. 1949.

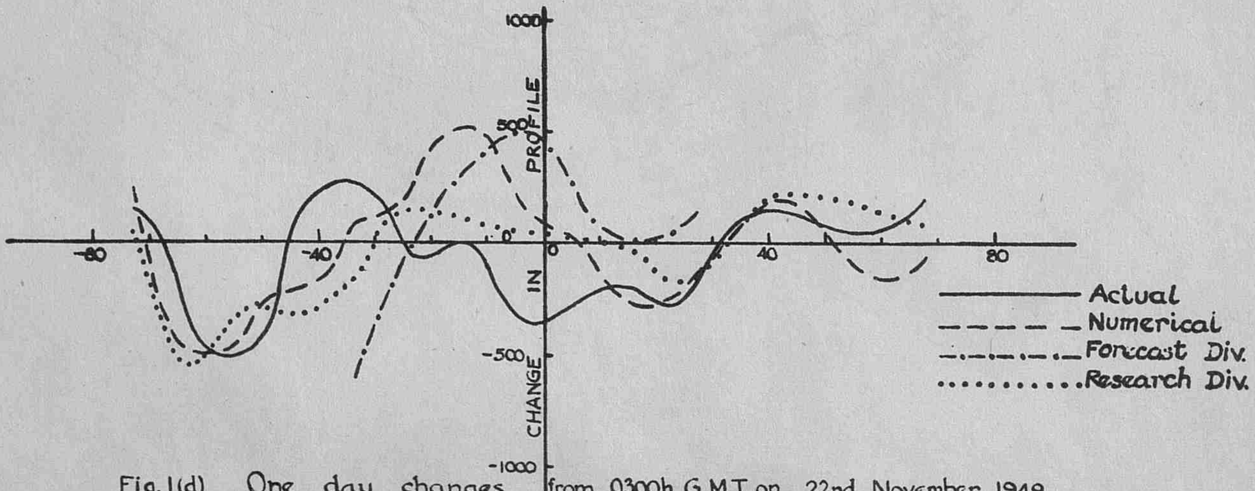

Fig. 1(d) One day changes from 0300h G.M.T on 22nd November 1949.

Fig. 1. Actual and forecast one day changes of some 500mb. profiles.

M.R.P. 566

2·11·49 0300 G.M.T.
500 mb.

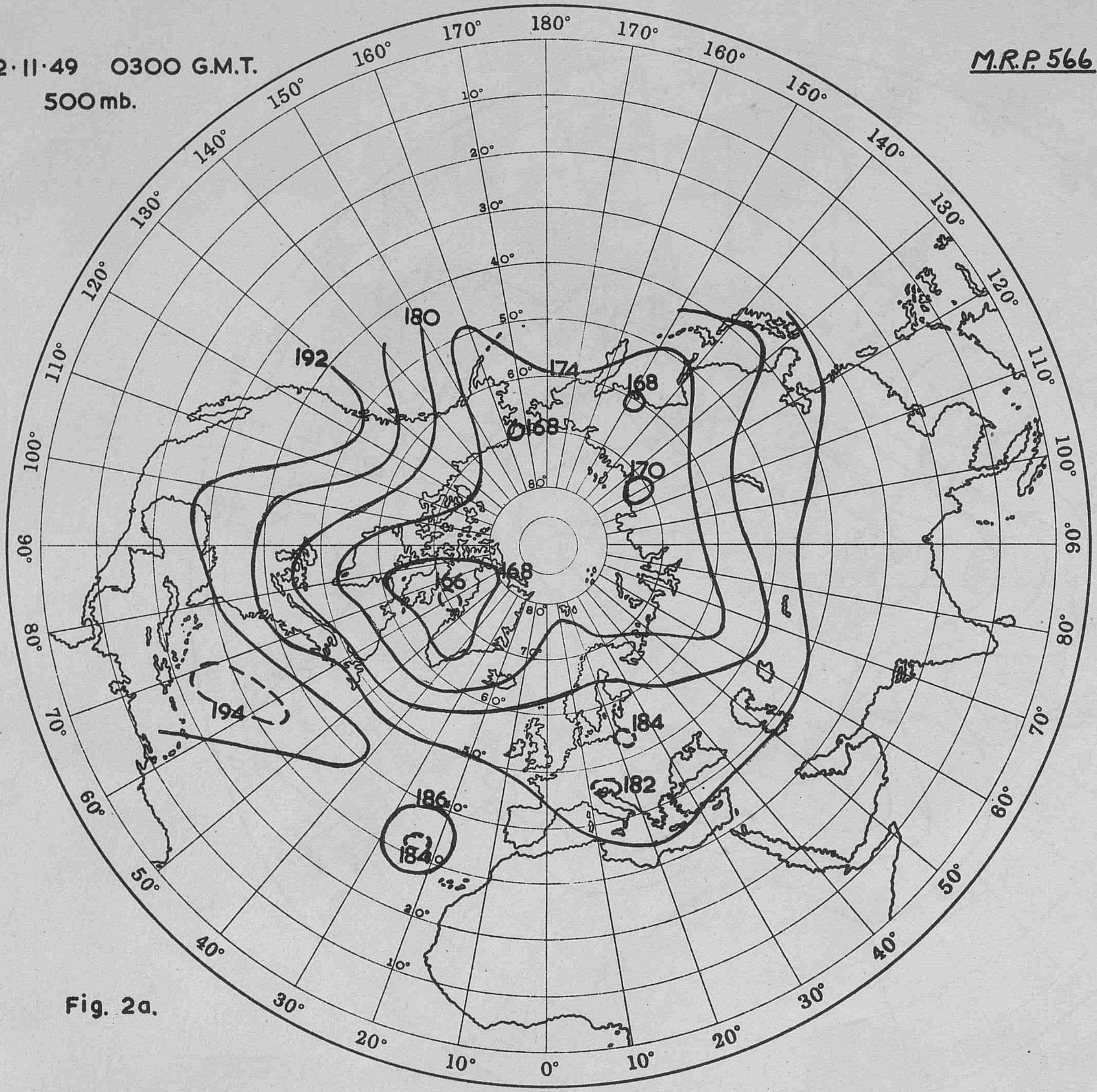

180°
170°
160°
150°
140°
130°
120°
110°
100°
90°
80°
70°
60°
50°
40°
30°
20°
10°
0°
192
180
174
168
168
170
166
168
194
184
182
186
184

Fig. 2a.

3·11·49 0300 G.M.T.
500mb.

M.R.P. 566

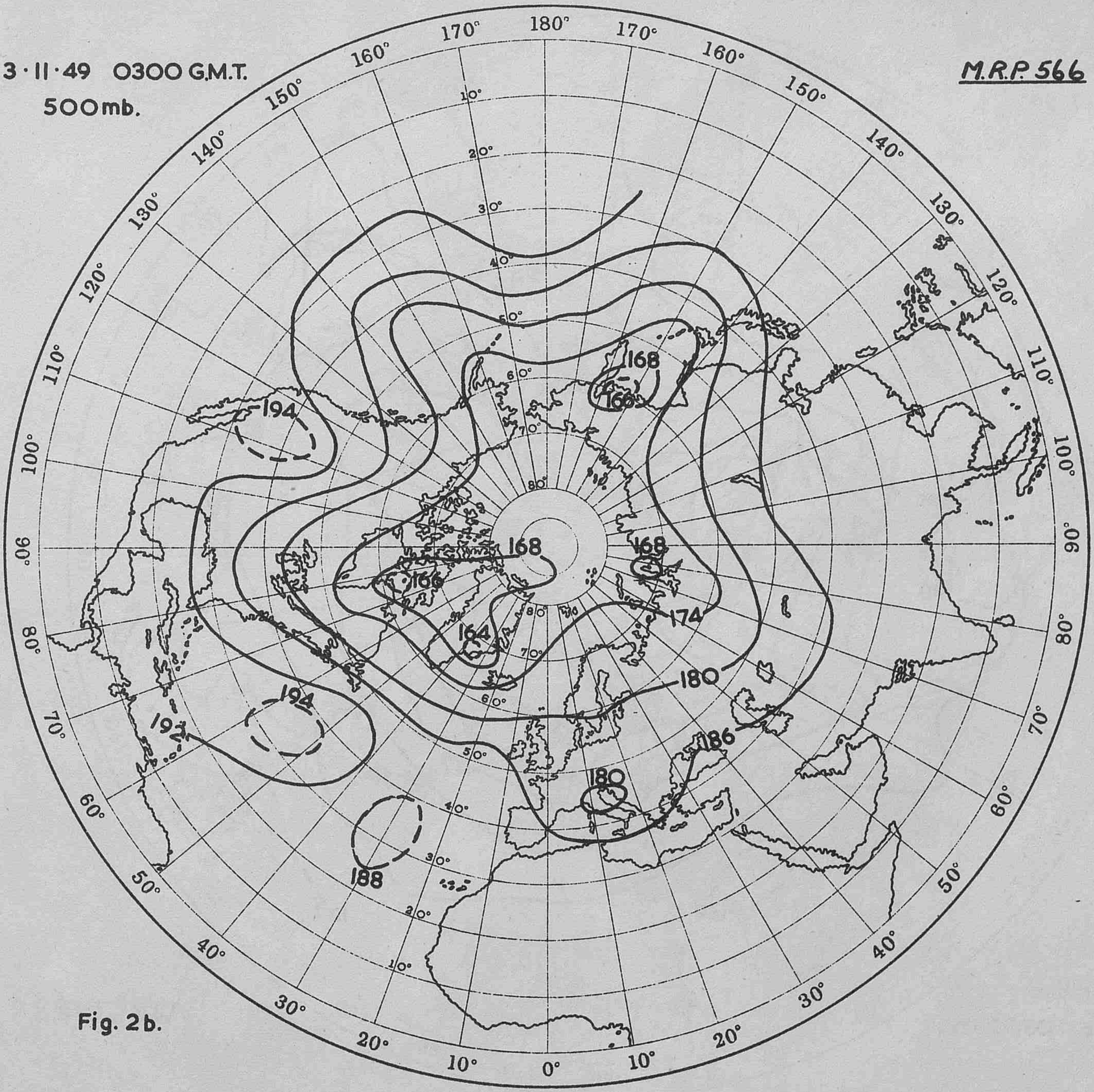
194
194
191
188
168
168
168
166
166
164
174
180
180
186
180°
170°
160°
150°
140°
130°
120°
110°
100°
90°
80°
70°
60°
50°
40°
30°
20°
10°
0°
10°
20°
30°
40°
50°
60°
70°
80°

Fig. 2b.

8 · 11 · 49 0300 G.M.T.
500mb.

M.R.P. 566

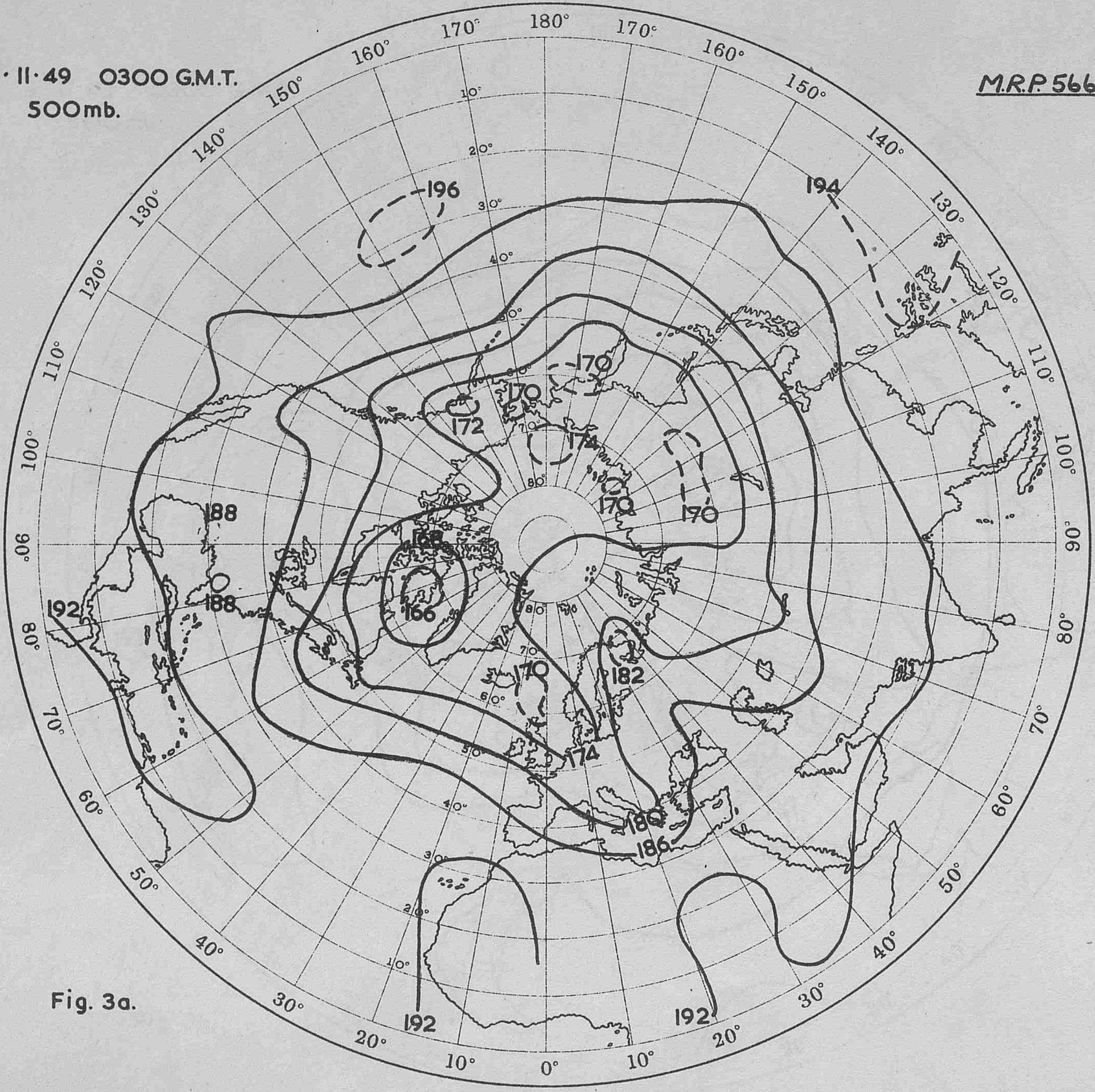
196
194
192
188
186
182
180
174
172
170
166
168
180°
170°
160°
150°
140°
130°
120°
110°
100°
90°
80°
70°
60°
50°
40°
30°
20°
10°
0°
10°
20°
30°
40°
50°
60°
70°
80°

Fig. 3a.

M.R.P. 566

9·11·49 0300 G.M.T.
500 mb.

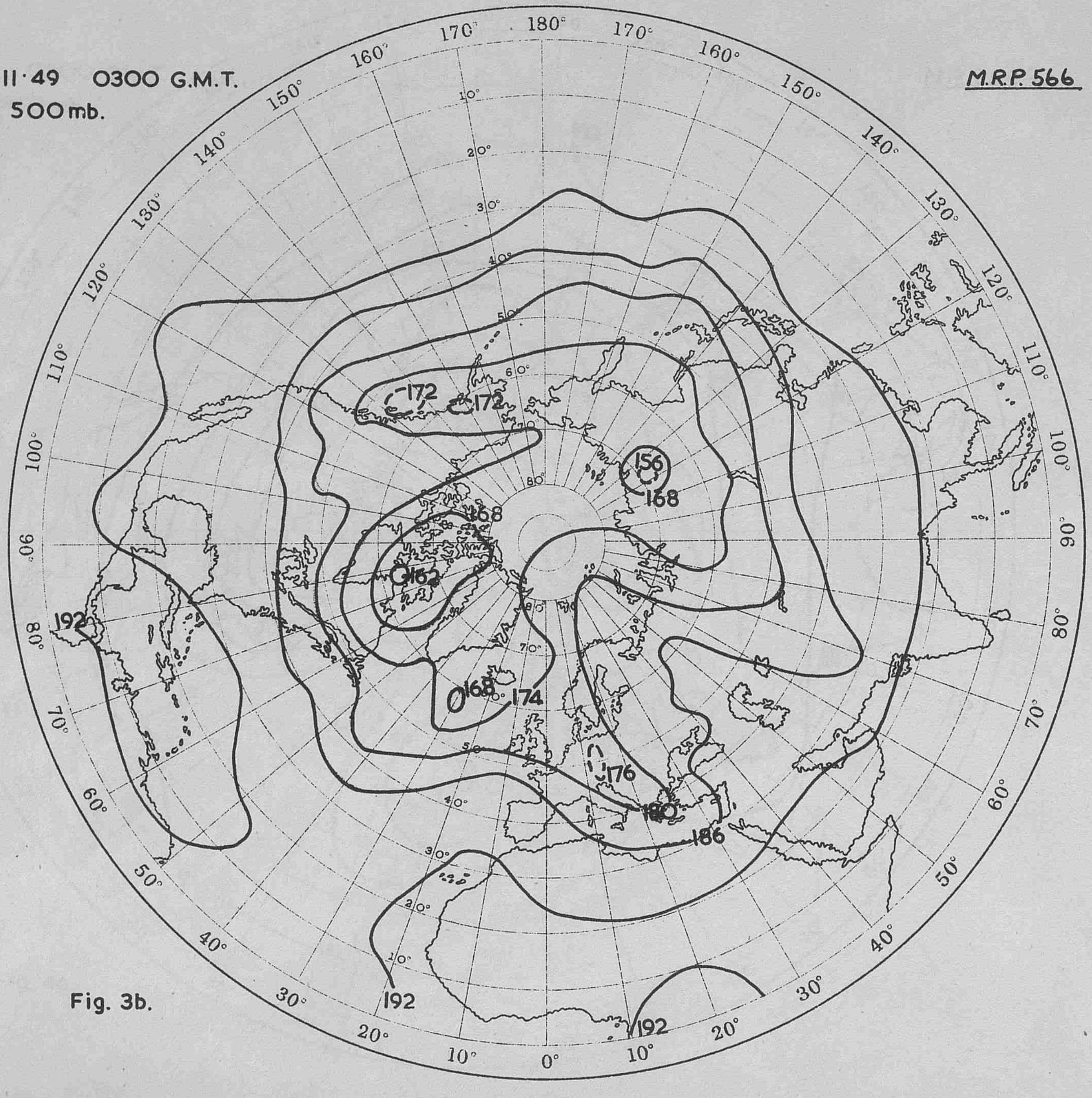

192
186
180
176
174
172
172
168
168
168
162
156

Fig. 3b.

28·11·49 0300 G.M.T.
500 mb.

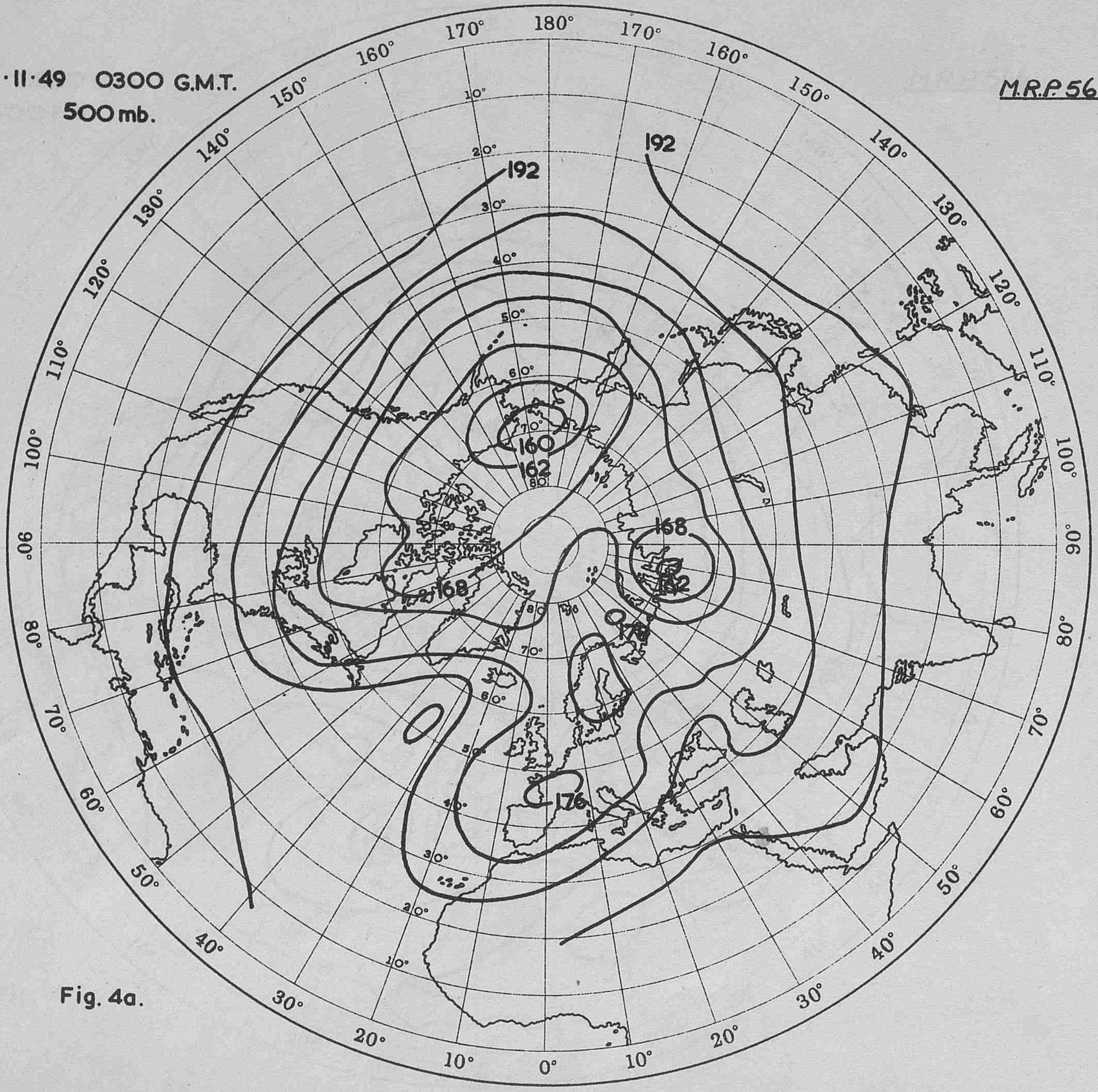
180°
170°
160°
150°
140°
130°
120°
110°
100°
90°
80°
70°
60°
50°
40°
30°
20°
10°
0°
192
192
160
162
168
168
162
176
176
10°
20°
30°
40°
50°
60°
70°
80°

Fig. 4a.

29-11-49. 0300 G.M.T.
500 mb.

M.R.P. 566

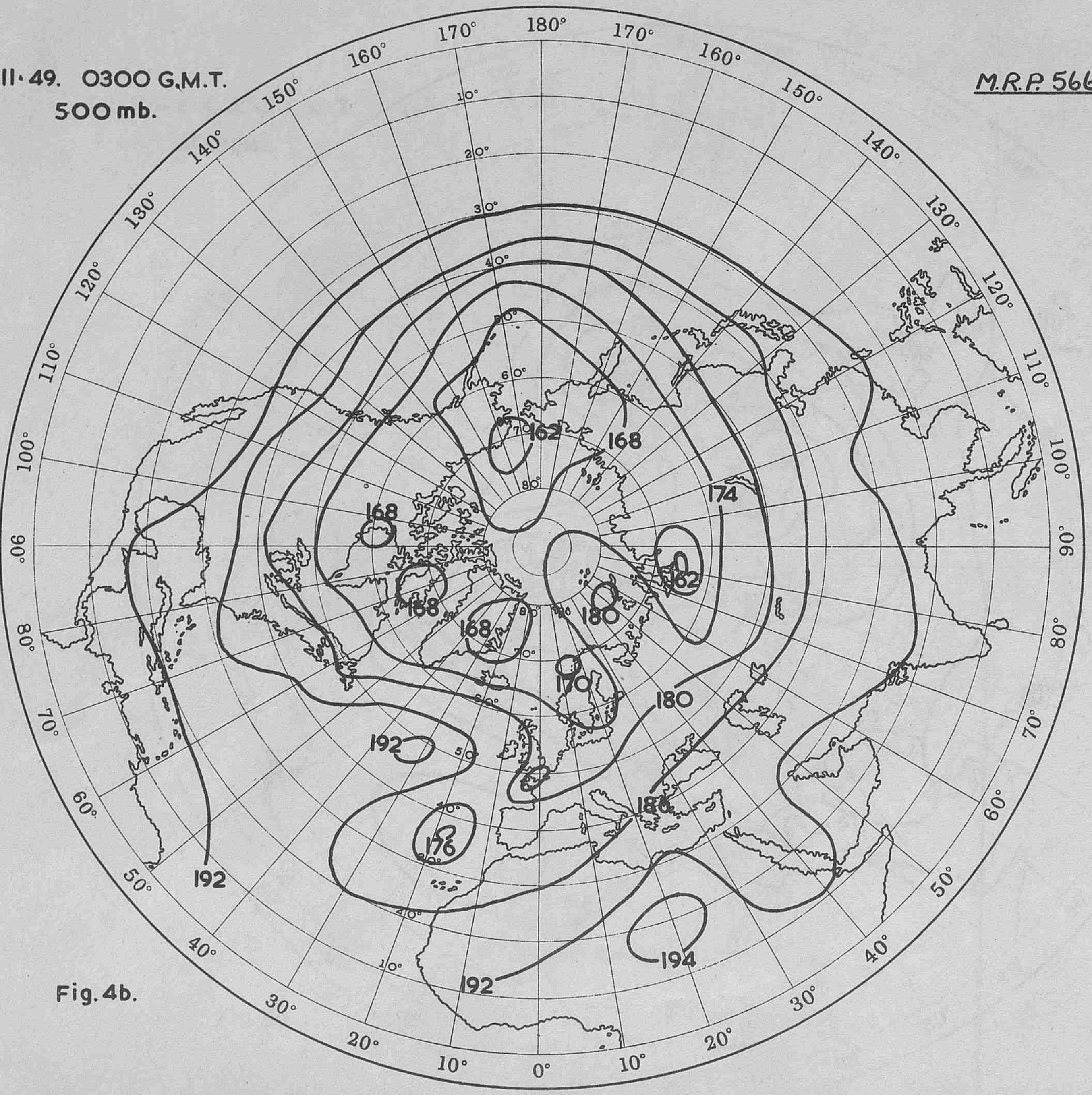

180°
170°
160°
150°
140°
130°
120°
110°
100°
90°
80°
70°
60°
50°
40°
30°
20°
10°
0°
162
168
174
180
186
192
194
176
170

Fig. 4b.

M.R.P. 566

22·11·49 0300 G.M.T.

500 mb.

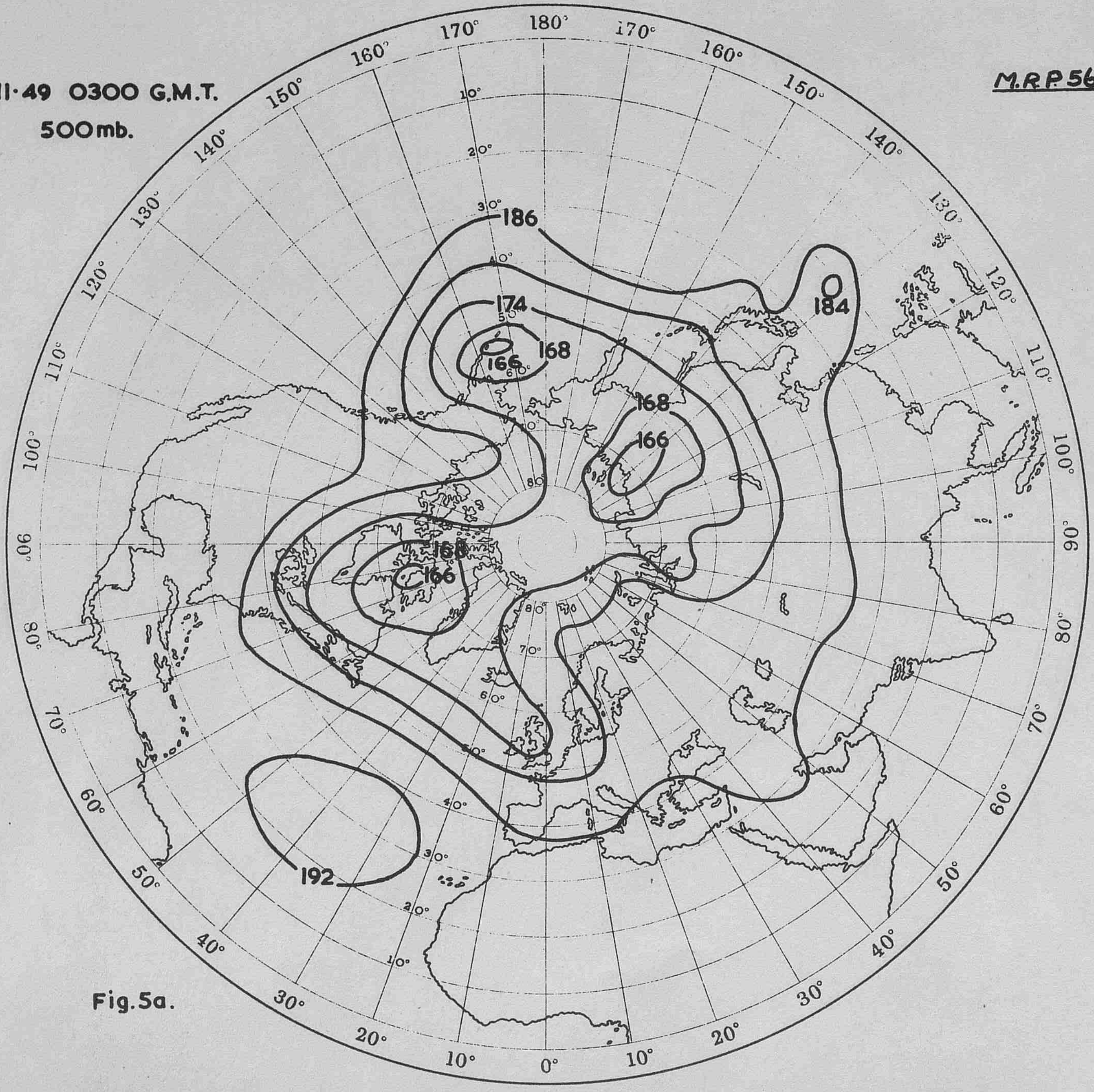
186
184
174
168
166
168
166
168
166
192
180°
170°
160°
150°
140°
130°
120°
110°
100°
90°
80°
70°
60°
50°
40°
30°
20°
10°
0°

Fig. 5a.

22·11·49 0300 G.M.T.
500mb.

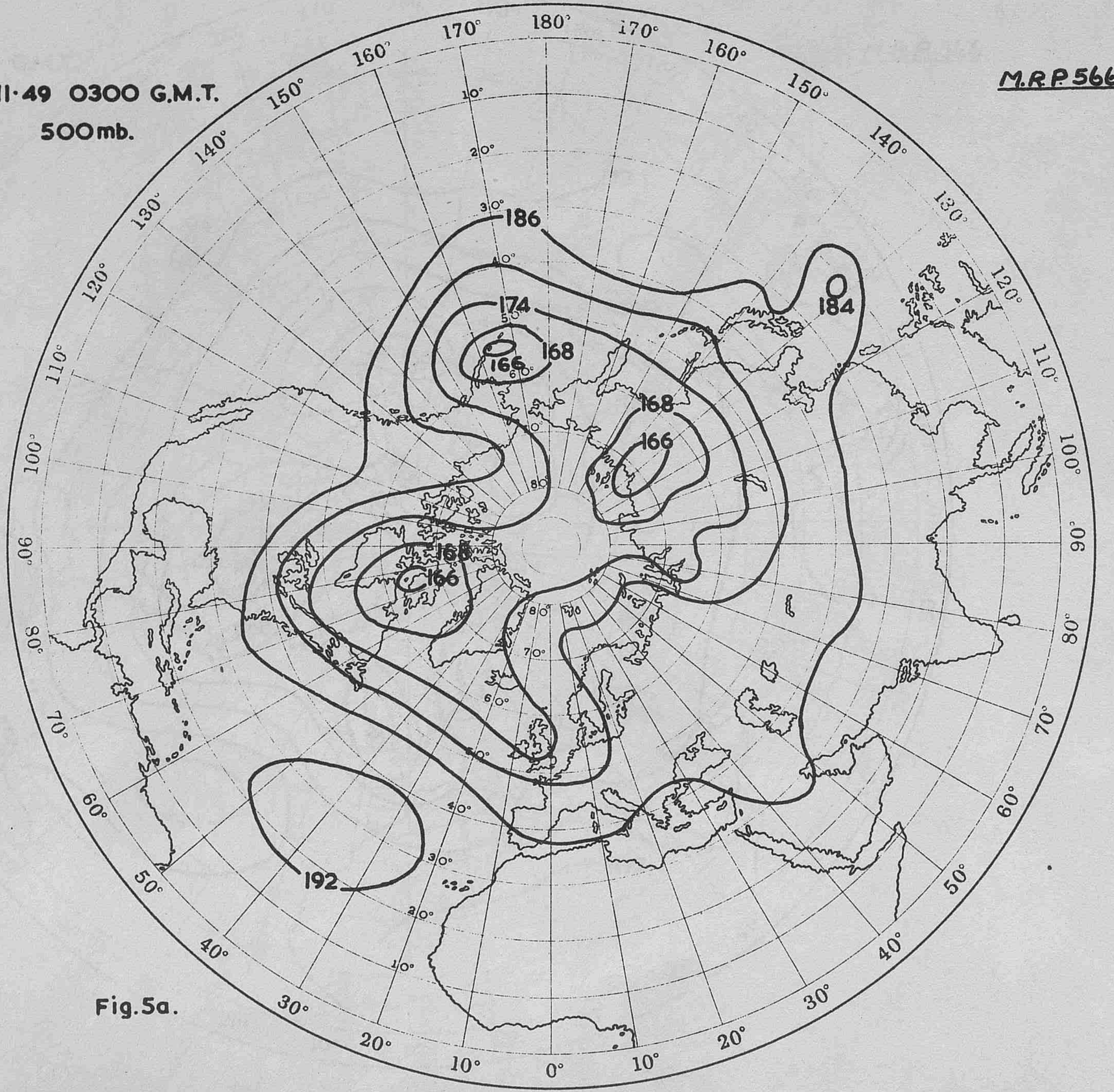
186
184
174
168
166
168
166
168
166
192
180°
170°
160°
150°
140°
130°
120°
110°
100°
90°
80°
70°
60°
50°
40°
30°
20°
10°
0°
10°
20°
30°
40°
50°
60°
70°
80°

Fig. 5a.

23·11·49 0300 G.M.T.
500mb.

M.R.P. 566

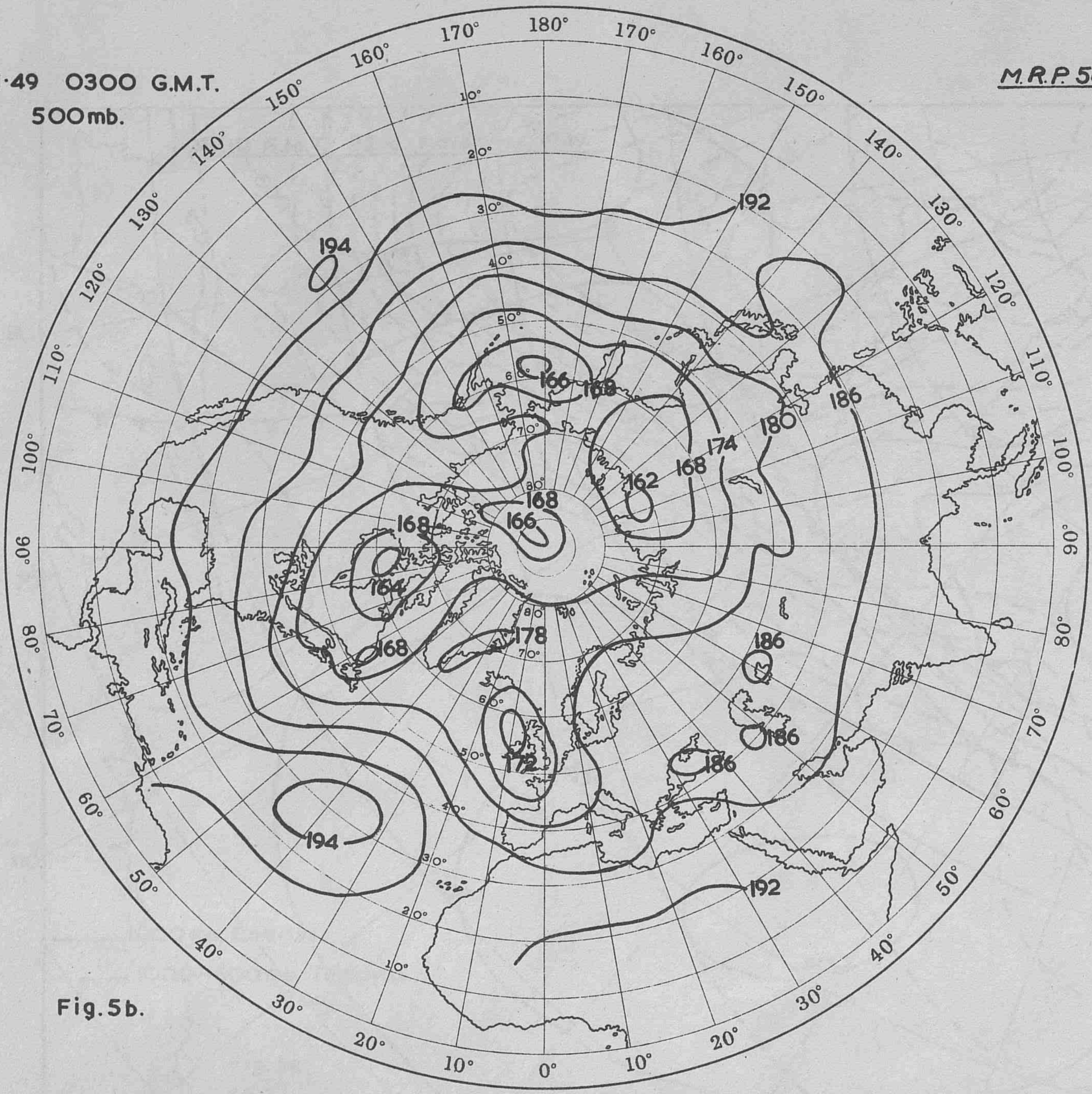
180°
170°
160°
150°
140°
130°
120°
110°
100°
90°
80°
70°
60°
50°
40°
30°
20°
10°
0°
194
192
186
180
174
168
166
162
164
178
172

Fig. 5b.

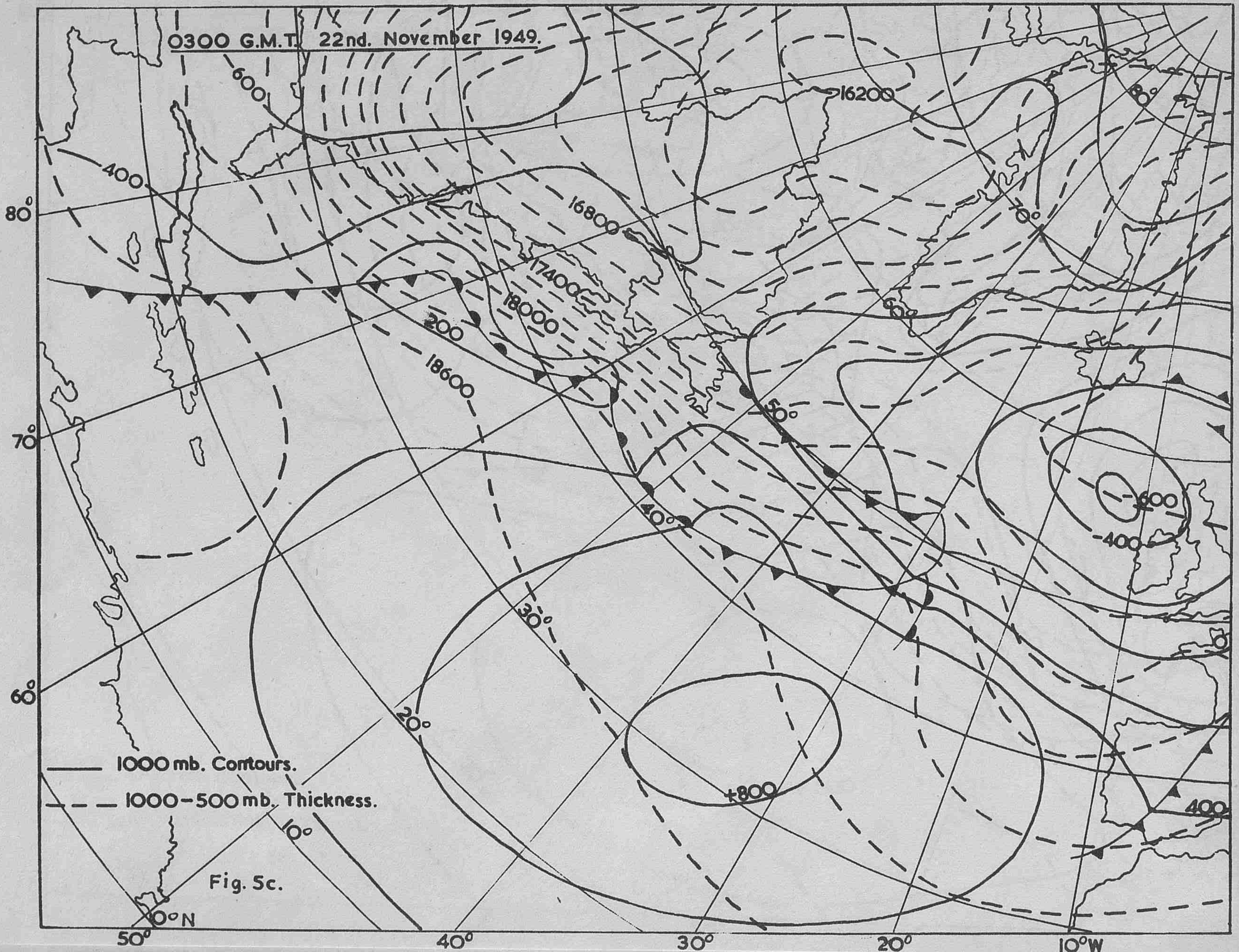

0300 G.M.T. 22nd. November 1949.

600
400
16200
16800
17400
18000
18600
200
+800
-600
-400
400
80°
70°
60°
50°
40°
30°
20°
10°
0°N
50°
40°
30°
20°
10°W
1000 mb. Contours.
1000–500 mb. Thickness.

Fig. 5c.

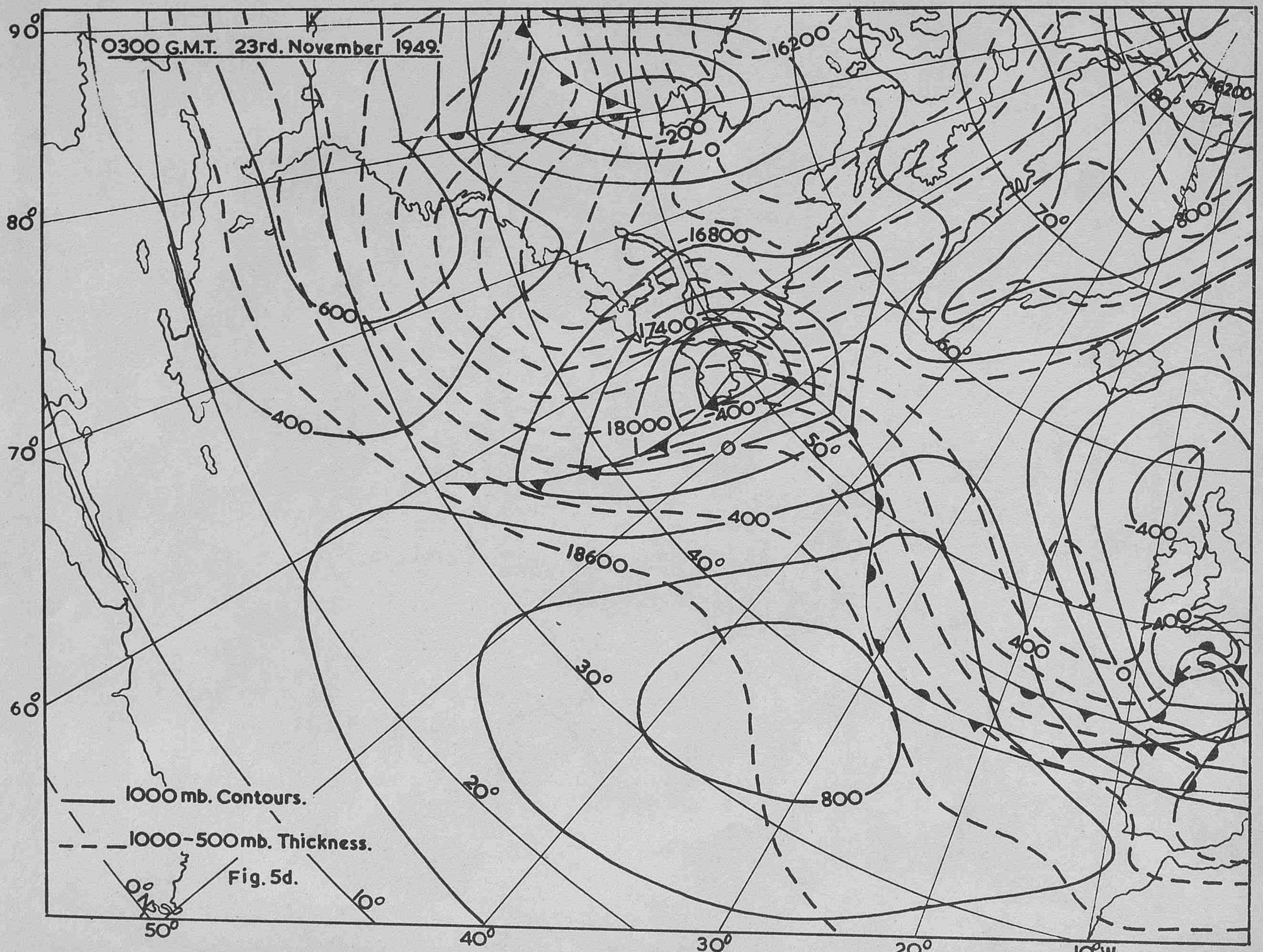

0300 G.M.T. 23rd. November 1949.

1000 mb. Contours.
1000-500 mb. Thickness.
16200
16200
16800
17400
18000
18600
-200
0
-400
0
400
600
400
800
-400
400
0
400
800
90°
80°
70°
60°
50°
40°
30°
20°
10°W
0°
10°
20°
30°
40°
50°
60°
70°
80°

Fig. 5d.

CONFIDENTIALLY. Its contents must not be quoted.

M.R.P. 570
S.C. II/60
20th July, 1950.

AIR MINISTRY

METEOROLOGICAL RESEARCH COMMITTEE

HIGH LEVEL METEOROLOGICAL PHOTOGRAPHIC RECONNAISSANCE

by
G.W. Hurst (Meteorological Office)

High level aircraft reconnaissance is perhaps the only method of obtaining comprehensive weather information over many ocean or desert areas, and of weather systems as a whole. The most desirable thing would be for the reconnaissance aircraft to carry experienced meteorological observers, but many factors (e.g. restricted nature of aircraft involved) will contribute in most cases to prevent this. The alternatives are therefore either to train pilots and/or navigators to interpret cloud sheets and the general visible weather pattern as seen from 40,000 feet and above in the light of their experience, followed by a detailed "debriefing" with a competent meteorologist on return; or to install suitable cameras in these aircraft to take photographs which can be interpreted by meteorological personnel on return; these would supplement personal "debrief". In either event, a wide background of comparative photographic material must be made available, and tentative experimental work has been started at Benson on these lines.

A number of sorties have been made from Benson on specially chosen days, normally those with a more or less active front visible within about 200 miles of the station. They have been performed by either Spitfires or Mosquitoes, mainly the former. Spitfires have the advantage of being able to operate at a distinctly greater maximum height, and several of the photographs taken were from about 43,000 feet true; Spitfire can, however, only carry either a port facing oblique camera, or vertical cameras. Mosquitoes on the other hand can carry and use simultaneously port facing, side facing and vertical cameras, but can only attain an operational height of about 37,000 feet true. Most of the photographs have been taken by Spitfires with port facing cameras. Two separate techniques of photography were adopted: panorama and across - frontal flights.

Panorama photographs taken by Spitfire aircraft were made by taking a series of photographs over approximately a fixed point, successive photographs being taken at appropriate intervals as the aircraft turned through 360°. The finished prints could be assembled into a continuous strip, and by choosing the location it was possible to include the whole run of the frontal edge for several hundred miles. These photographs showed the frontal edge, the upper surface of the frontal cloud and gave an indication of the characteristics of the pre-frontal (or post-frontal) air mass. Attempts were made in some cases to construct a cloud map from these data.

Across-frontal photographs, taken by Mosquito aircraft using all available cameras, were made by the aircraft flying at right angles to the lie of the front, the intention being for the aircraft to start photography over the clear air ahead of the front and complete photography in the clear air behind or vice versa.

The photographs taken to date do little more than outline the problem, and perhaps give an indication of lines upon which development might take place. Preliminary results indicate that fronts, provided they are well marked and fairly active, can be fairly readily identified and photographed, but that the interpretation and classification of the photographs cannot easily be done except by an expert. In some cases rather surprising results emerged, such as the discovery that frontal cloud in what had been a well marked, though weakening, cold occlusion extended only up to about 8,000 feet. An obvious difficulty in interpretation is that whilst the upper surface of a front can be fixed with a high degree of accuracy, the same is not true of the ground level section (except possibly a cold front, which would no doubt show up readily with cumulus heads above a stratified layer).

/ Experience

G.269466/JMB/7/50/40

1074072

INCLOSURE 1 TO IR-192-57
AIR ATTACHE, LONDON

57-186C

2941

RWS:

Experience so far has suggested very interesting and promising possibilities, and much must be gained by the build up of a standard set of high level photographs of meteorological situations. It is thought possible that a standard technique of panorama and cross-frontal photography might be developed, and that a standard height (preferable 50,000 feet) might be adopted to make all photographs mutually comparable, and to make measurement and assessment of distances more uniform. A height of 50,000 feet would give a range of vision of up to 275 miles from the point of observation.

The following are the occasions when sorties were attempted, with notes of the experience encountered:-

(1) 8th November, 1949, 541 Squadron flying a Spitfire. A frontal linkage extended from a wave which had given some rain and drizzle in southwest England and Wales to a deep and active centre in the Atlantic which gave subsequent general rain over the British Isles. The linkage extended at 1500 G.M.T. from 100 miles southwest of Ireland to Nantes. The pilot took a good set of panorama photographs at approximately 1410 G.M.T. from the St. Eval area.

(2) 18th November, 1949, 540 Squadron flying a Mosquito. A cold occlusion over the east coast of England was moving east. It had been fairly active, with rain or drizzle over a wide area. The pilot was briefed to climb to maximum height, and to make good a track of 070° from base, taking photographs (side facing and forward facing obliques, and verticals) until the clear air ahead of the front was reached. The aircraft took off at 1100 G.M.T. and climbed to 35,000 feet, was still in cloud, and at this level surging on one engine was encountered. The pilot estimated the cloud tops were probably a further 2,000 feet above him, and in view of the very narrow clearance this would give below the aircraft at maximum height, together with the roughness of one engine, he decided to abandon the attempt.

(3) 1st December, 1949, 541 Squadron flying a Spitfire. A rather weak cold front extended at 0600 G.M.T. from Flamborough Head to just south of Cork which was moving south at 10 - 15 knots. A warm front from Calais - Cherbourg - W.S.W. was drifting slowly south; this front too was weak, but with much moister surface air coming in from the west. The pilot was briefed to climb to 40,000 feet and perform panoramic photography in the Bedford area. The pilot took off at 1045 G.M.T. climbed to 20,000 feet, could not see any front and therefore from that height took photographs which he thought of interest in the area. In fact they suggest photography from 40,000 feet might well have been profitable. In these photographs there were several shots of a fault in a cloud sheet very similar to that discussed by R. Frith (Nature, Vol. 165, p.899).

(4) 1st December, 1949, 541 Squadron flying a Spitfire. Situation as in 3. The pilot was briefed to perform high level panoramic photography in the Portland Bill area. He carried a vertical and not a port facing oblique camera, the intention being to take photographs with a 70° bank. He took off at 1400 G.M.T. and found this impracticable, as the aircraft could not maintain a height of 40,000 feet with this bank, and he kept slipping into the Cirrostratus layer. The attempt was therefore abandoned; the Squadron Commander, Sqn.Ldr. Colston, expressed the view that loss of height, with such a bank, could not be avoided at above 35,000 feet.

(5) 8th December, 1949, 541 Squadron flying a Spitfire. At 1200 G.M.T. a cold occlusion from south of Zuider Zee - Rouen - Rennes was moving south at 5 - 10 knots; it was a fairly active front with a pronounced surface wind veer. The pilot was briefed to perform two sets of panoramic photographs, one from near the Lincolnshire coast and the other from the South Midlands area. He took off at about 1100 G.M.T. and took two excellent sets of photographs, 13 to each set from south/south through 360°; the aircraft was levelled for each bearing.

/(6)

57-186C

(6) 22nd December, 1949, 541 Squadron flying a Spitfire. At 1200 G.M.T. a warm front from Chester - St. Athan - Lizard was moving east at 10 - 15 knots. The rain area associated with it was somewhat narrow, but there was a marked rise in the surface dew point to its west. The pilot took off at 1030 G.M.T. and attempted a modified panorama photograph, in the S.E. Kent area taking photographs continuously whilst maintaining a bank of 70° in a rate ¼ turn to port. He started photography at 43,000 feet but had to descend about 5,000 feet due to engine trouble; he completed a 360° turn at the lower level. This is perhaps the simplest method of performing panoramic photography, but the angle of bank should be rather less in order to avoid losing the horizon at times.

(7) 28th February, 1950, 540 Squadron flying a Mosquito. At 0600 there was a double occlusion, the first from Carlisle - Sealand - Channel Islands, and the second Aldergrove - Pembroke Dock - Lizard both moving slowly east in the north, almost stationary in the south; a centre south of the Lizard was moving away S.S.E. At 1200 G.M.T. there was little change and the edge of the frontal cloud remained visible, almost unmoved, though dissipating slightly, in the south western sky at Benson all day. The crew was briefed to do a full across frontal flight to the clear air beyond the second front, and to continue photography on the return flight. The aircraft took off at 1204 G.M.T. but, unfortunately, the time intervals selected were far too short and a continuous record was not obtained. However side facing obliques were taken intermittently to the turning point, and a most interesting set of photographs emerged.

/(8)

(8) 4th April, 1950, 58 Squadron flying a Mosquito. At 0600 G.M.T. an occlusion extended from Malin Head - Cork - 50°N. 9½°W. moving east at about 30 knots; there was a cold front in the C.F.O. analysis about 50 miles to the west of this. At 1200 G.M.T. there was a single cold occlusion from Leuchars - Bristol - Brest and at 1800 G.M.T. from Spurn Head - Greenwich - 48°N. 00°. There were local showers near the front in south, some rain in the north. Stations were reporting a cumulus type of cloud behind the occlusion. The pilot was briefed to take a panorama photograph of the front, then to fly along the edge and take further photographs at maximum heights. He took off at 1500 G.M.T., and discovered that at 8,000 feet he was above cloud. He took a number of photographs to prove this and returned to base.

The photographs obtained on the sorties 1, 5 and 6 have been mounted in strips and will be available for exhibition; the photographs on sorties 3, 7 and 8 did not lend themselves to mounting in strip form, and will be available for exhibition as series of separate prints.

7

Appendix to M.R.P.570. - High Level Photographic Meteorological Reconnaissance

To illustrate the type of strip photograph which can be obtained from 40,000 feet a reproduction has been made on a reduced scale. This reproduction is of one of a pair of panoramic sets taken by the same pilot. The second set, available for exhibition, was taken half an hour later over East Lincs. Explanatory notes are given below:

Thame (Oxon) 8th September, 1949

Sortie detail. 8.12.49 at 1130, prints 0001-0013.

Situation. A deep depression (centre about 962 mbs) just E of the Faroes was moving NE and at 1200 a cold occlusion extended from the centre to Denmark thence to just SE of the Zuider Zee, and on to Rouen and the SW. The airstream to the NW of this front was fairly unstable, particularly when well into the cold air behind; the frequent showers over the Irish Sea and off N. Ireland were penetrating inland to E. Yorks and the NE Midlands. The front itself was well marked with both wind change and weather, and the surface air ahead was much moister than in the cold air.

Brief. The pilot was briefed to fly at above 40,000 ft. and take panoramic photographs of the north west edge of the occlusion from two fairly widely separated points. He was left to select these points as he thought appropriate, recommended areas being to the north of Benson and somewhere over Lincolnshire.

Execution and Pilot's comments. The pilot performed the photography from 42,000 ft. on the lines planned, first near Thame and secondly near Spilbury/Horncastle. He took photographs every 30°, the first and last exposures in each set of panoramic photographs being taken with the camera pointing due South, so that each set comprised 13 prints. He levelled and straightened at each bearing before photography. The pilot reported top of the frontal cloud sheet as about 22,000 ft. and the thickness 10,000 ft. Except for some cirrus, mainly to the south west he saw no cloud above 22,000 ft. Below this layer there was a 2/8 Sc sheet at 2,000 ft., 5-600 feet thick.

Photograph Analysis. Prints 0001-0013. The front is seen in prints 0001-5 and 0011-13. The appearance of the front is normal, with a rather ragged leading (or trailing, in this case) edge and extensive holes in the foreground. The undulating nature of the upper cloud sheet will be noted, especially in 0002. 0006-8 show the cold air and bring out well the appearance of cumulus cloud from about 40 miles and 40,000 ft. The cumulus cloud was responsible for very local showers only - approximately a third of the reporting stations in the Midlands area reported showers during the day, and in these cases amounts of precipitation were small. No Cu or Cb heads can be seen to the SE, and the conclusion may be drawn that there were none near the line of the occlusion over NE France with tops above 22,000 ft.

2nd October, 1950.

G.278024/DC/10/50/40

CATALOGED BY ASTIA
AS ATI No 146535

M.R.P. 574
S.C.III/66
16th August, 1950.

DEC 8 1950

METEOROLOGICAL RESEARCH COMMITTEE

Accuracy of Geostrophic Trajectories

by

C.S. Durst and N.E. Davis (Meteorological Office)

AIR WEATHER SERVICE
TECHNICAL REFERENCE FILES

1. The accuracy of measurement of wind from isobars

In a paper on Convergence and Divergence in the Atmosphere (Q.J.R. Met. S.66 1940, p.171), estimates have been made of

(a) the magnitude of the ageostrophic wind, and

(b) the magnitude of the error that is likely to be made in measuring a pressure gradient.

These magnitudes were obtained for a height of about 1,500 feet over S.E. England. At that height in that locality the ageostrophic winds are probably on the high side and the errors in measurement are certainly far lower than at greater heights and in less accurately surveyed areas.

The root mean square value of the ageostrophic wind in January 1938 was about 9 knots, and thus taking account that the ageostrophic wind is probably less in summer and possibly less at higher levels, we may expect the probable value of the ageostrophic wind during the year as a whole to be of the order of 5 knots; a magnitude of 10 knots was found by Bannon (Q.J.R. Met. S.75 1949, p.131) for the ageostrophic winds at 10,000 feet, so we can say that 5 knots is a conservative estimate. We may moreover expect that the average duration of such ageostrophic winds is 6 hours in view of their being usually associated with the passage of depressions and fronts.

The probable error in measurement of the geostrophic wind was found to be 2 mi/hr along and across the isobars, i.e. a probable vector error of about 2½ knots. This will certainly rise to 3 or 4 knots at greater heights and may well be 10 knots or more over the less well known areas of the globe. On the average let us assume an error of 5 knots in the measurement of the geostrophic wind.

2. The departure of the geostrophic trajectory from the true trajectory

Combining the two we can assume that the vector error involved in assuming the geostrophic wind to be the true wind is of the order of 7 knots. This means that in 6 hours the end of the geostrophic trajectory is likely to be 40 nautical miles away from the true position of the air parcel to which it is supposed to refer.

It is reasonable to suppose that the departures will increase as the square root of the duration of the trajectory, and on this basis we get in Table I the probable departures from true position of the ends of the geostrophic trajectories after different intervals of time.

TABLE I Estimated departures (statute miles) from true position of ends of geostrophic trajectories after specified times:

Time	6 hr.	24 hrs.	2 days	4 days	8 days
Probable Departure	50	100	130	200	260

/ 3.

CONFIDENTIALLY. Its
contents must not be quoted.

M.R.P. 574
S.C.III/66
16th August, 1950.

AIR MINISTRY

METEOROLOGICAL RESEARCH COMMITTEE

DEC 8 1950

Accuracy of Geostrophic Trajectories

by

C.S. Durst and N.E. Davis (Meteorological Office)

1. The accuracy of measurement of wind from isobars

In a paper on Convergence and Divergence in the Atmosphere (Q.J.R. Met. S.66 1940, p.171), estimates have been made of

AIR WEATHER SERVICE
TECHNICAL REFERENCE FILES

(a) the magnitude of the ageostrophic wind, and

(b) the magnitude of the error that is likely to be made in measuring a pressure gradient.

These magnitudes were obtained for a height of about 1,500 feet over S.E. England. At that height in that locality the ageostrophic winds are probably on the high side and the errors in measurement are certainly far lower than at greater heights and in less accurately surveyed areas.

The root mean square value of the ageostrophic wind in January 1938 was about 9 knots, and thus taking account that the ageostrophic wind is probably less in summer and possibly less at higher levels, we may expect the probable value of the ageostrophic wind during the year as a whole to be of the order of 5 knots; a magnitude of 10 knots was found by Bannon (Q.J.R. Met. S.75 1949, p.131) for the ageostrophic winds at 10,000 feet, so we can say that 5 knots is a conservative estimate. We may moreover expect that the average duration of such ageostrophic winds is 6 hours in view of their being usually associated with the passage of depressions and fronts.

The probable error in measurement of the geostrophic wind was found to be 2 mi/hr along and across the isobars, i.e. a probable vector error of about $2\frac{1}{2}$ knots. This will certainly rise to 3 or 4 knots at greater heights and may well be 10 knots or more over the less well known areas of the globe. On the average let us assume an error of 5 knots in the measurement of the geostrophic wind.

2. The departure of the geostrophic trajectory from the true trajectory

Combining the two we can assume that the vector error involved in assuming the geostrophic wind to be the true wind is of the order of 7 knots. This means that in 6 hours the end of the geostrophic trajectory is likely to be 40 nautical miles away from the true position of the air parcel to which it is supposed to refer.

It is reasonable to suppose that the departures will increase as the square root of the duration of the trajectory, and on this basis we get in Table I the probable departures from true position of the ends of the geostrophic trajectories after different intervals of time.

TABLE I Estimated departures (statute miles) from true position of ends of geostrophic trajectories after specified times:

Time	6 hr.	24 hrs.	2 days	4 days	8 days
Probable Departure	50	100	130	200	260

/ 3.

3. The dispersion of air masses due to eddies

It is well known through the work of Richardson (Beitr Physik fr Atmos 15 24-29) and others that two parcels of air initially near together will drift apart owing to the operation of the eddies. This effect was investigated by tracking air from 4 points over the British Isles and measuring their distance apart after 6, 12, 13, 24, 30 and 36 hours. The points chosen were London, 50, 150 and 350 miles due north and the tracks were followed at a height of 700 mb during the month of February 1948, one set of tracks being commenced at midnight each day for a period of 20 days.

Table II gives the mean distance $\bar{l}$ (statute miles) apart after time t (hours) of pairs of parcels initially at a distance of l_o (statute miles).

TABLE II

l_o miles	t in hours					
	6	12	18	24	30	36
50	74	118	131	148	169	200
100	138	159	220	279	313	332
150	198	259	319	391	439	484
200	255	320	397	484	581	653
300	371	428	589	729	837	926
350	438	549	671	820	956	1070

If we consider the relation between $\bar{l} - l_o$ and t for each l_o we find a linear regression of the form

$$\bar{l} - l_o = A(l_o).t$$

with highly significant correlations $\geqslant 0.99$ (See figure 1). Further if we consider the relation between l_o and $A(l_o)$ we find a linear regression between log l_o and log $A(l_o)$ with highly significant correlation > 0.995 leading to the relation

$$A(l_o) = 0.13\, l_o^{0.86}$$

(see figure 2)

Hence the dispersion of pairs of particles is carried out according to the law

$$\bar{l} - l_o = 0.13\, l_o^{0.86} . t$$

Using this relation, Table III gives the mean distance apart after t' days of two particles initially l_o (statute miles) apart.

/ TABLE III

TABLE III

l_0 miles	t' in days							
	1	2	3	4	5	6	7	Increase per day
50	143	236	328	421	514	607	700	+97
100	268	437	605	774	942	1111	1279	+168
200	506	812	1117	1423	1729	2035	2341	+306
300	733	1167	1600	2033	2467	2900	3334	+433

4. The magnitude of the errors in plotted trajectories

The figures given in Tables I and III may be looked on in this way. The inherent inaccuracy of geostrophic trajectories will lead to a small departure of the plotted trajectory from the true trajectory. This departure will be enhanced rapidly by the eddy effect and one can surmise that the order of departure of the plotted trajectory from the true after a week will be 1,000 miles, after 10 days 2,000 miles, and after a fortnight 3,000 miles. It must moreover be remembered that these values are the radii of the 50% circles, and on half the occasions the errors will be greater.

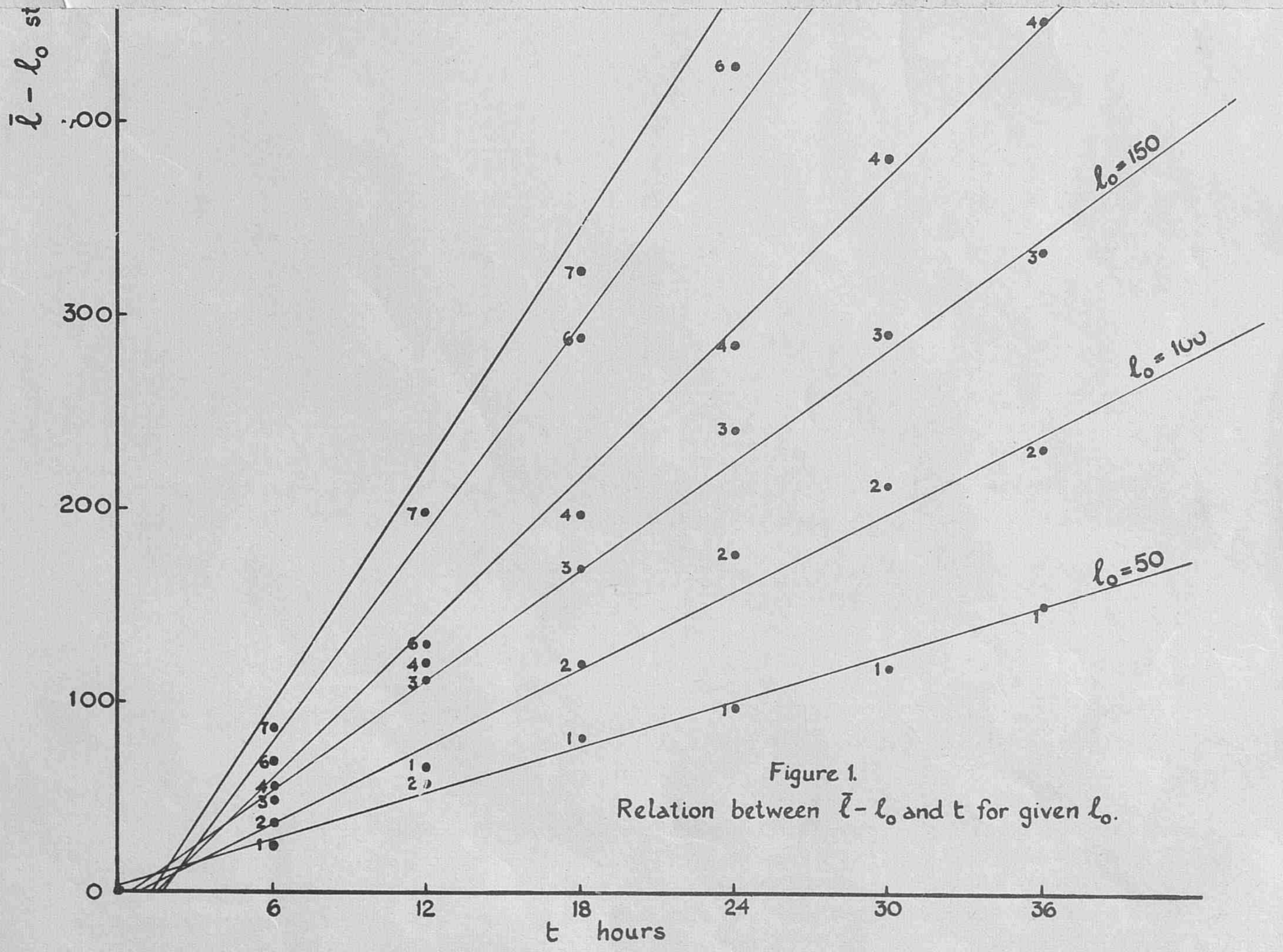

Figure 1.
Relation between $\bar{l} - l_0$ and t for given l_0.

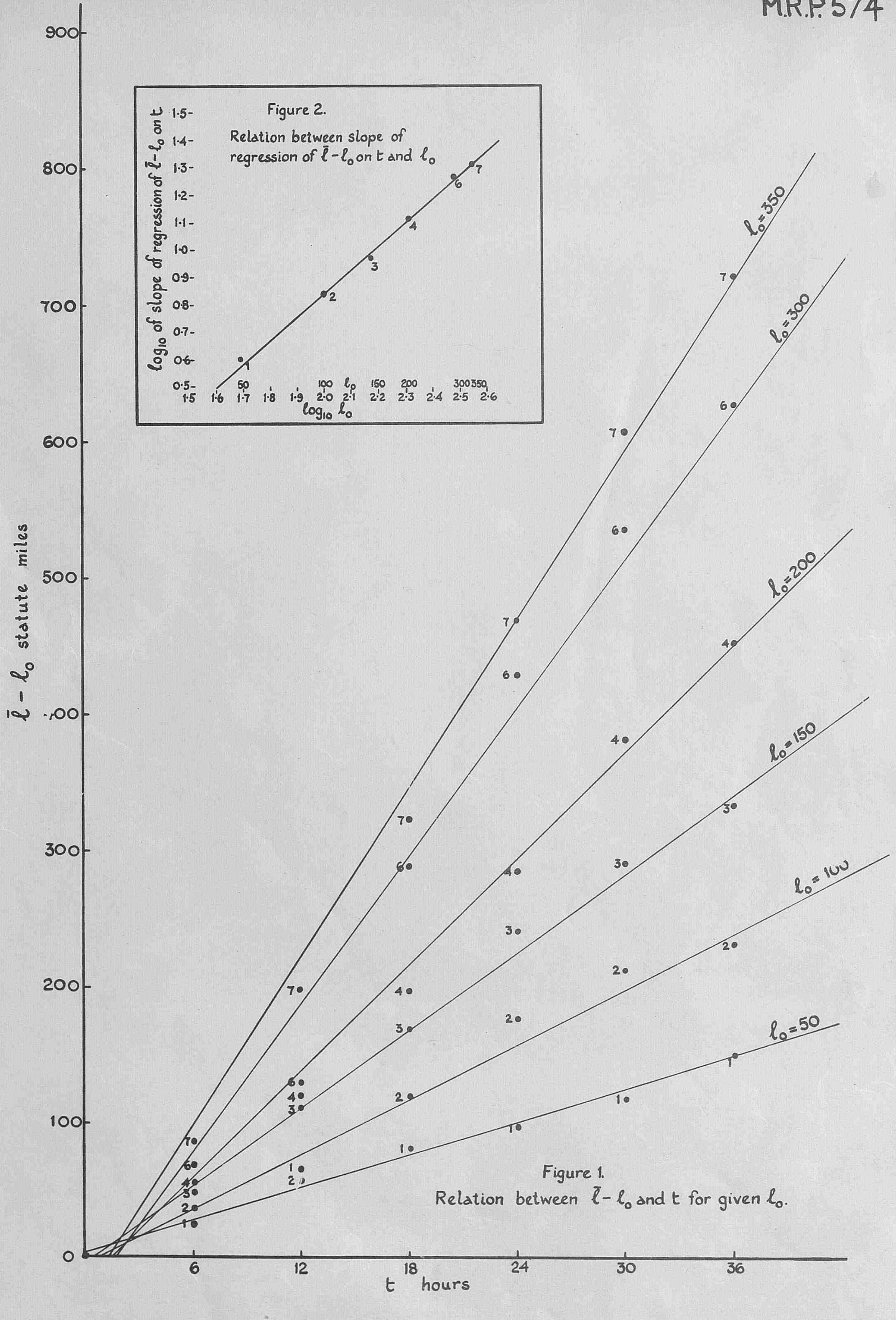

Figure 2.

Relation between slope of regression of $\bar{l} - l_0$ on t and l_0

Figure 1.

Relation between $\bar{l} - l_0$ and t for given l_0.

This repo
published
CON
contents

CATALOGED BY ASTIA
AS ATI No. 103532

.R.P.576
.C.III/68
August, 1950.

DEC 8 1950

AIR MINISTRY

METEOROLOGICAL RESEARCH COMMITTEE

A Note on frost point observations in relation to aircraft condensation trails

by

J.K. Bannon (Meteorological Office)

AIR WEATHER SERVICE
TECHNICAL REFERENCE FILE

Summary

The occurrence of condensation trails, persistent and non-persistent, on high altitude ascents made by the Meteorological Research Flight appears to bear little relation to observed humidities.

1. Introduction

On the high altitude flights made by the Meteorological Research Flight to observe the water vapour content in the upper troposphere and lower stratosphere exhaust condensation trails are often observed and note is taken of their persistence, density (on a rough qualitative scale) and the levels at which they occur.

The occurrence of condensation trials, according to theory, is related to the relative humidity and temperature of the air as well as to other factors. (See M.O. 479, Condensation Trails from Aircraft, 1943). This note sets out the results of an analysis of the occurrence of condensation trails with respect to the simultaneous observations of frost point and temperature.

2. Data available

From 20th January, 1949, when detailed observations on condensation trails were commenced, to mid-June, 1950, persistent condensation trails were observed from the sounding aircraft on 25 flights and trails of some kind on 86 flights. The total number of flights made was 96. The flights usually reached a height of between 200 and 175 mb. pressure.

The aircraft making the trails were, in every case, Mosquito P.R.34's which have Merlin engines. (The experiments described in M.O. 479 were made by Spitfire aircraft also with Merlin engines though of a different Mark).

The persistence of condensation trails is difficult to assess from the aircraft which is making the trails; usually the trails dissipate within a few seconds but if they persist for say two minutes they appear to stretch to the horizon. The Meteorological Research Flight ascents are usually made in a spiral and a trail is called persistent when it can be seen bending round on the horizon; this means that it has at least two to three minutes persistence. Quite often the trails formed on ascent are seen again on descent but this fact is not always noted.

3. Persistent Trails

(a) Frost Point depression below air temperature

Persistent condensation trails were observed with widely varying humidities. Table I gives the frequency of occurrence of condensation trails with frost point depressions below air temperature in various ranges. (The frequencies do not add up to the total number of occasions as each observation of a trail usually extended over a range of frost point depressions as the aircraft was ascending or descending and so would count

/ more

This report has
published and is to be treated
CONFIDENTIALLY. Its
contents must not be quoted.

M.R.P.576
S.C.III/68
August, 1950.

DEC 8 1950

AIR MINISTRY

METEOROLOGICAL RESEARCH COMMITTEE

A Note on frost point observations in relation to aircraft condensation trails

by

J.K. Bannon (Meteorological Office)

AIR WEATHER SERVICE
TECHNICAL REFERENCE FILE

Summary

The occurrence of condensation trails, persistent and non-persistent, on high altitude ascents made by the Meteorological Research Flight appears to bear little relation to observed humidities.

1. Introduction

On the high altitude flights made by the Meteorological Research Flight to observe the water vapour content in the upper troposphere and lower stratosphere exhaust condensation trails are often observed and note is taken of their persistence, density (on a rough qualitative scale) and the levels at which they occur.

The occurrence of condensation trials, according to theory, is related to the relative humidity and temperature of the air as well as to other factors. (See M.O. 479, Condensation Trails from Aircraft, 1943). This note sets out the results of an analysis of the occurrence of condensation trails with respect to the simultaneous observations of frost point and temperature.

2. Data available

From 20th January, 1949, when detailed observations on condensation trails were commenced, to mid-June, 1950, persistent condensation trails were observed from the sounding aircraft on 25 flights and trails of some kind on 86 flights. The total number of flights made was 96. The flights usually reached a height of between 200 and 175 mb. pressure.

The aircraft making the trails were, in every case, Mosquito P.R.34's which have Merlin engines. (The experiments described in M.O. 479 were made by Spitfire aircraft also with Merlin engines though of a different Mark).

The persistence of condensation trails is difficult to assess from the aircraft which is making the trails; usually the trails dissipate within a few seconds but if they persist for say two minutes they appear to stretch to the horizon. The Meteorological Research Flight ascents are usually made in a spiral and a trail is called persistent when it can be seen bending round on the horizon; this means that it has at least two to three minutes persistence. Quite often the trails formed on ascent are seen again on descent but this fact is not always noted.

3. Persistent Trails

(a) Frost Point depression below air temperature

Persistent condensation trails were observed with widely varying humidities. Table I gives the frequency of occurrence of condensation trails with frost point depressions below air temperature in various ranges. (The frequencies do not add up to the total number of occasions as each observation of a trail usually extended over a range of frost point depressions as the aircraft was ascending or descending and so would count

/ more

more than once in the table). The five occasions when the trails were formed in pre-existing cloud are also indicated.

Table I

Frequencies of occurrence of persistent condensation trails with various values of temperature (T) minus frost point (FP)

	T - FP (°F)									
	0 - 4	4- 8	8 -12	12-16	16-20	20-24	24-28	28-32	Over 32	
All occasions	12	14	12	11	7	5	4	3	1	69
	17	20	17	16	10	7	6	4	1	
With cloud	4	3								(7)

Total number of occasions of persistent trails 25

Total number of occasions of persistent trails with cloud 5

For comparison with Table I, Table Ia gives the percentage frequency of occurrence of various ranges of temperature minus frost point for 91 ascents, irrespective of the occurrence of condensation trails, for the two levels 275 and 250 mb. when both these levels were in the troposphere.

Table Ia

Percentage frequencies of occurrence of various ranges of temperature (T) minus frost point (FB).

Level	T - FP (°F)									
	0 - 4	4 - 8	8 -12	12-16	16-20	20-24	24-28	28-32	Over 32	
275 mb.	7	12	24	19	11	14	2	4	7	100%
250 mb.	10	16	19	28	10	5	4	1	7	100%

Number of observations 91.

It will be noted that the modes of the two distributions in Table Ia are higher than for the distribution in Table I confirming that persistent condensation trails do tend to form in conditions moister than average.

It has been suggested that the degree of turbulence present in the free atmosphere in a trail producing layer must be important in determining whether the trail will be persistent or not; if the atmosphere is not saturated a trail in turbulently mixed air would be expected to dissipate more quickly than if the air were non turbulent. Those cases of persistent condensation trails occurring in layers where turbulence was noticeable as bumps to the investigating aircraft have been separated and the frequences of occurrence of condensation trails with frost point depression in various ranges for these cases are given in Table II. Allowing for the small number of observations it is seen that there is no significant difference in the characters of Tables I and II.

Table II

Frequencies of occurrence of persistent condensation trails with various values of T - FP; bumpy occasions

	T - FP (°F)							
	0 - 4	4 - 8	8 -12	12-16	16-20	20-24	24-28	28-32
All occasions	3	3	5	2	2		1	2
With cloud	1	1						

Total number of occasion of persistent trails, with bumps 13
Total number of occasion of persistent trails, with bumps, with cloud 2

Two cases are of special interest. On the first, 22nd July, 1949, though the frost point depression below air temperature was only 1°F at 300 mb. and the air temperature was 5°F below the Mintra temperature, (the immunity temperature for the Spitfire aircraft above which trails will never form and below which trails may form provided the air is moist enough; see M.O. 479), no trails occurred. ≠/

On 13th May, 1950, persistent trails, formed on ascent near the tropopause at the 250 mb level, were still found to be thick by the time that level was reached on the descent some 15 minutes later. Measured on descent the frost point was 8°F below air temperature, (more than 8°F above and below this level). Temperature (-73°F) was 33°F below the Mintra temperature.

(b) Air Temperature

In every case of persistent trail formation the air temperature was below the Mintra temperature. Table III gives the frequencies of occurrence of these trails with Mintra minus air temperature in various ranges, (Mintra for sublimation to ice), where the temperature is that of the base of the trail bearing layer.

Table III

Frequencies of occurrence of persistent trails with Mintra - T (T is air temperature at base of trail layer) within various ranges.

Mintra - T (°F)								
0 - 4	4 - 8	8 -12	12-16	16-20	20-24	24-28	28-32	Over 32
0	1	1	4	7	1	4	3	4

(c) Depth of layers of persistent trails.

Table IV gives the frequency of occurrence of various depths of persistent trail bearing layers as found by the Meteorological Research Flight, row (a) gives the total figures and row (b) those in which the top of the layer was not reached.

Table IV

Frequencies of occurrence of various depths of persistent trail producing layers.

	Depths in thousands of feet						
	Less than 1	1 - 3	3 - 5	5 - 7	7 - 9	9 - 11	Over 11
(a) All	3	9	1	4	4	1	3
(b) Top not reached	-	1	1	3	3	1	2

25 tot

11 not reac

/ 4.

≠/ The Mintra temperatures normally used are those assuming sublimation to ice when saturation with respect to an ice surface is reached; the Mintra temperature for condensation to super-cooled water at saturation with respect to a water surface, is about 4°F below the ice Mintra.

4. First formation of trails

It has been suggested, (M.R.P. 489, Condensation Trails from Jet Aircraft), that the first formation of non-persistent trails might be used as a method of estimating the humidity of the air when the air temperature is known; the nearer the air temperature to the Mintra temperature the moister the air. Accordingly the depression of air temperature below the Mintra and the depression of frost point below air temperature have been extracted for the 71 cases in which the first formation of trails on ascent were well marked and are plotted on figure 1; when bumpiness was noted at the same level, (16 occasions), the observation is marked with a 'B', the other observations being marked by crosses.

Figure 2 shows the plot of depression of air temperature below Mintra against depression of frost point below dry bulb for the first appearance of persistent trails, on ascent. The four bumpy cases are marked 'B'.

From these two diagrams it is seen that air temperature below Mintra temperature at first trail formation has little relation to the humidity of the air as indicated by frost point temperature.

5. Conclusions

It seems clear from the facts set out in section 3 that much remains to be learnt of the nature of condensation trails. There is a very rough correspondence between the occurrence of trails, (persistent or ephemeral), and the humidity of the air; on those occasions when no trails were formed the air was extremely dry. But it is seen that persistent trails can form in quite dry air (Table I) and that their persistence is not because of lack of turbulent mixing (Table II). Presumably the accuracy of the temperature and frost point measurements is not in doubt and it is concluded that an ice cloud, (which may originally be a super-cooled water cloud - see M.R.P 489), can persist in a dry atmosphere at these levels, (usually at pressure less than 300 mb. and temperature below - 40°F).

Brewer, (Weather, Vol.1, 1946, page 34) has stated that"really persistent trails are almost always associated with the super saturation in the upper air". He may call "really persistent" trails those which thicken after formation but there is no doubt that he (and most others, including the present writer until recently), assumes that ordinary persistent trails occur with a high humidity.

Since the humidity of the air appears to affect the occurrence of trails so little, the formation of trails and their persistence must be governed by some factor or factors other than humidity and temperature; the other obvious variable is condensation or sublimation nuclei.

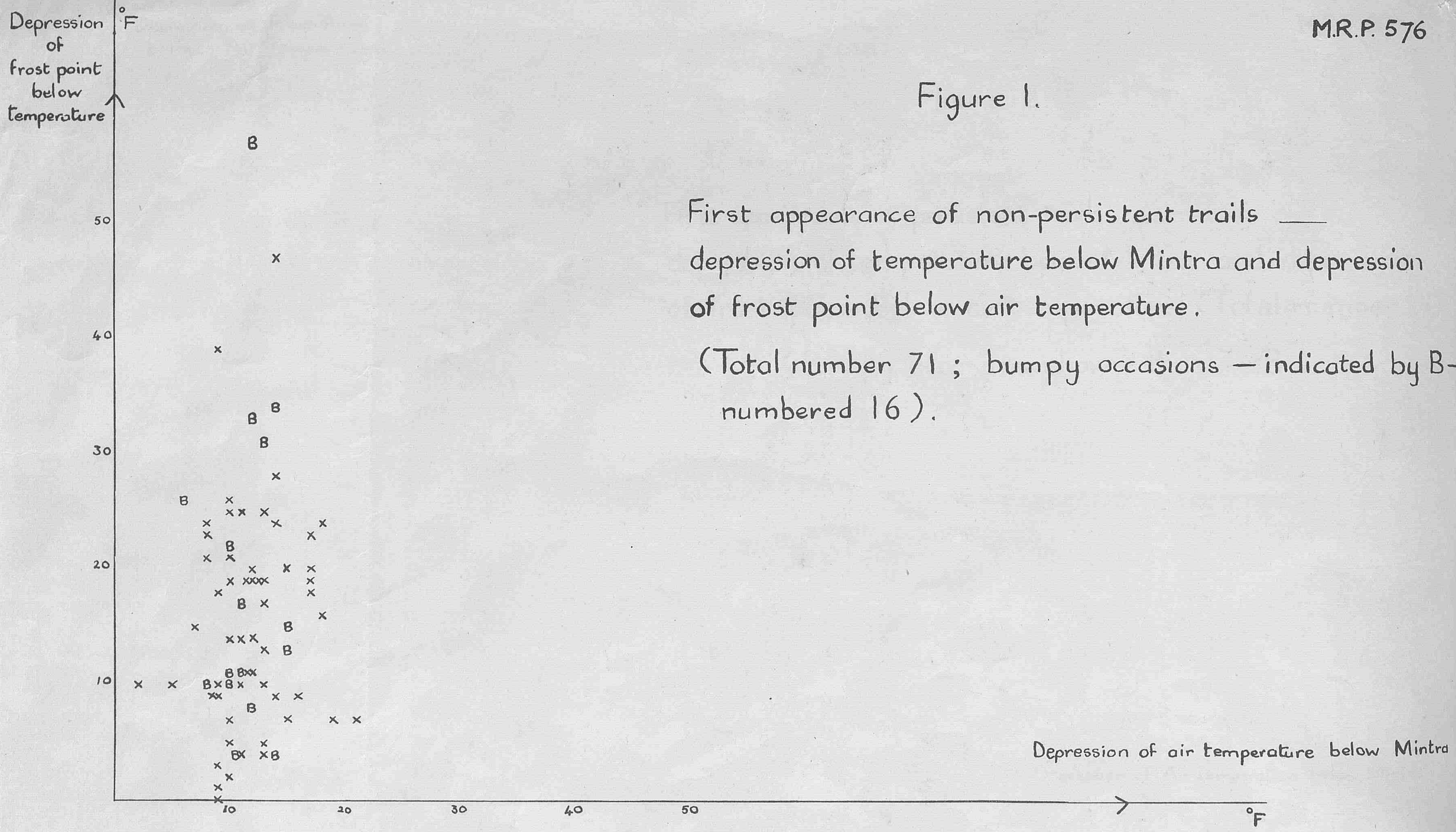

Figure 1.

First appearance of non-persistent trails — depression of temperature below Mintra and depression of frost point below air temperature.

(Total number 71 ; bumpy occasions — indicated by B — numbered 16).

M.R.P. 576

Figure 2.

First appearance of persistent trails —— depression of temperature below Mintra and depression of frost point below air temperature. (Total number 25).

(Bumpy occasions shown thus — B).

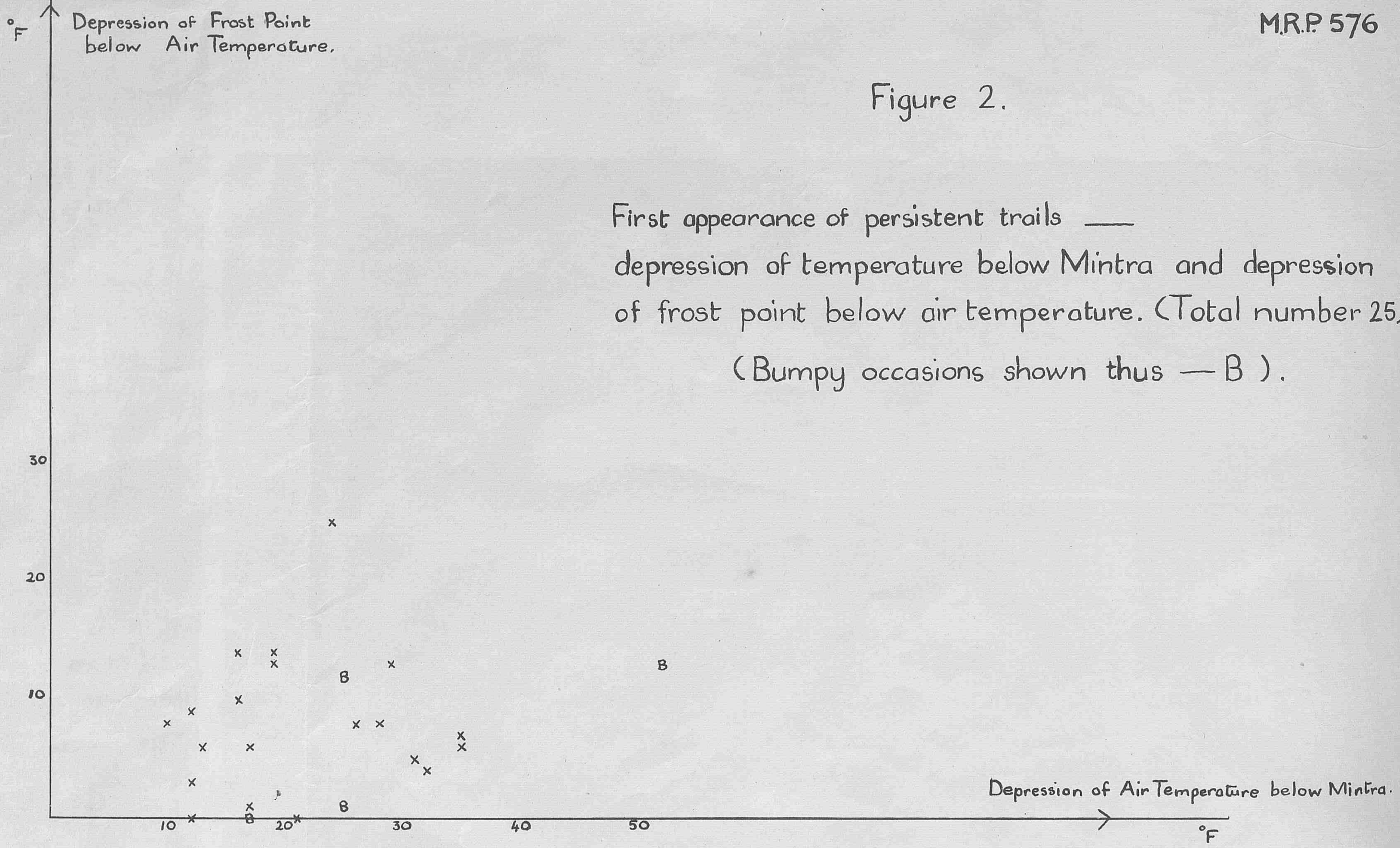

Mats

DEC 12 1950

This report has not yet been published and is to be treated CONFIDENTIALLY. Its contents must not be quoted.

M.R.P.576
S.C.III/68
August, 1950.

AIR MINISTRY

METEOROLOGICAL RESEARCH COMMITTEE

AF251450-1

A Note on frost point observations in relation to aircraft condensation trails

by

J.K. Bannon (Meteorological Office)

on p.2 of classification log -- RTF

Summary

The occurrence of condensation trails, persistent and non-persistent, on high altitude ascents made by the Meteorological Research Flight appears to bear little relation to observed humidities.

1. Introduction

On the high altitude flights made by the Meteorological Research Flight to observe the water vapour content in the upper troposphere and lower stratosphere exhaust condensation trails are often observed and note is taken of their persistence, density (on a rough qualitative scale) and the levels at which they occur.

The occurrence of condensation trials, according to theory, is related to the relative humidity and temperature of the air as well as to other factors. (See M.O. 479, Condensation Trails from Aircraft, 1943). This note sets out the results of an analysis of the occurrence of condensation trails with respect to the simultaneous observations of frost point and temperature.

2. Data available

From 20th January, 1949, when detailed observations on condensation trails were commenced, to mid-June, 1950, persistent condensation trails were observed from the sounding aircraft on 25 flights and trails of some kind on 86 flights. The total number of flights made was 96. The flights usually reached a height of between 200 and 175 mb. pressure.

The aircraft making the trails were, in every case, Mosquito P.R.34's which have Merlin engines. (The experiments described in M.O. 479 were made by Spitfire aircraft also with Merlin engines though of a different Mark).

The persistence of condensation trails is difficult to assess from the aircraft which is making the trails; usually the trails dissipate within a few seconds but if they persist for say two minutes they appear to stretch to the horizon. The Meteorological Research Flight ascents are usually made in a spiral and a trail is called persistent when it can be seen bending round on the horizon; this means that it has at least two to three minutes persistence. Quite often the trails formed on ascent are seen again on descent but this fact is not always noted.

3. Persistent Trails

(a) Frost Point depression below air temperature

Persistent condensation trails were observed with widely varying humidities. Table I gives the frequency of occurrence of condensation trails with frost point depressions below air temperature in various ranges. (The frequencies do not add up to the total number of occasions as each observation of a trail usually extended over a range of frost point depressions as the aircraft was ascending or descending and so would count

/ more

0803
AWS:

C.D. 8053

By safe hand

more than once in the table). The five occasions when the trails were formed in pre-existing cloud are also indicated.

Table I

Frequencies of occurrence of persistent condensation trails with various values of temperature (T) minus frost point (FP)

	T - FP (°F)								
	0 - 4	4 - 8	8 -12	12-16	16-20	20-24	24-28	28-32	Over 32
All occasions	12	14	12	11	7	5	4	3	1
With cloud	4	3							

Total number of occasions of persistent trails 25

Total number of occasions of persistent trails with cloud 5

For comparison with Table I, Table Ia gives the percentage frequency of occurrence of various ranges of temperature minus frost point for 91 ascents, irrespective of the occurrence of condensation trails, for the two levels 275 and 250 mb. when both these levels were in the troposphere.

Table Ia

Percentage frequencies of occurrence of various ranges of temperature (T) minus frost point (FB).

Level	T - FP (°F)								
	0 - 4	4 - 8	8 -12	12-16	16-20	20-24	24-28	28-32	Over 32
275 mb.	7	12	24	19	11	14	2	4	7
250 mb.	10	16	19	28	10	5	4	1	7

Number of observations 91.

It will be noted that the modes of the two distributions in Table Ia are higher than for the distribution in Table I confirming that persistent condensation trails do tend to form in conditions moister than average.

It has been suggested that the degree of turbulence present in the free atmosphere in a trail producing layer must be important in determining whether the trail will be persistent or not; if the atmosphere is not saturated a trail in turbulently mixed air would be expected to dissipate more quickly than if the air were non turbulent. Those cases of persistent condensation trails occurring in layers where turbulence was noticeable as bumps to the investigating aircraft have been separated and the frequences of occurrence of condensation trails with frost point depression in various ranges for these cases are given in Table II. Allowing for the small number of observations it is seen that there is no significant difference in the characters of Tables I and II.

25/45d-2

Table II

Frequencies of occurrence of persistent condensation trails with various values of T - FP; bumpy occasions

	T - FP (°F)							
	0 - 4	4 - 8	8 -12	12-16	16-20	20-24	24-28	28-32
All occasions	3	3	5	2	2		1	2
With cloud	1	1						

Total number of occasion of persistent trails, with bumps 13
Total number of occasion of persistent trails, with bumps, with cloud 2

/ Two

0803

MS: ______

Two cases are of special interest. On the first, 22nd July, 1949, though the frost point depression below air temperature was only 1°F at 300 mb. and the air temperature was 5°F below the Mintra temperature, (the immunity temperature for the Spitfire aircraft above which trails will never form and below which trails may form provided the air is moist enough; see M.O. 479), no trails occurred. ≠/

On 13th May, 1950, persistent trails, formed on ascent near the tropopause at the 250 mb level, were still found to be thick by the time that level was reached on the descent some 15 minutes later. Measured on descent the frost point was 8°F below air temperature, (more than 8°F above and below this level). Temperature (-73°F) was 33°F below the Mintra temperature.

(b) Air Temperature

In every case of persistent trail formation the air temperature was below the Mintra temperature. Table III gives the frequencies of occurrence of these trails with Mintra minus air temperature in various ranges, (Mintra for sublimation to ice), where the temperature is that of the base of the trail bearing layer.

Table III

Frequencies of occurrence of persistent trails with Mintra - T (T is air temperature at base of trail layer) within various ranges.

Mintra - T (°F)								
0 - 4	4 - 8	8 -12	12-16	16-20	20-24	24-28	28-32	Over 32
0	1	1	4	7	1	4	3	4

(c) Depth of layers of persistent trails.

Table IV gives the frequency of occurrence of various depths of persistent trail bearing layers as found by the Meteorological Research Flight, row (a) gives the total figures and row (b) those in which the top of the layer was not reached.

25/450 -3

Table IV

Frequencies of occurrence of various depths of persistent trail producing layers.

	Depths in thousands of feet						
	Less than 1	1 - 3	3 - 5	5 - 7	7 - 9	9 - 11	Over 11
(a) All	3	9	1	4	4	1	3
(b) Top not reached	-	1	1	3	3	1	2

/ 4.

≠/ The Mintra temperatures normally used are those assuming sublimation to ice when saturation with respect to an ice surface is reached; the Mintra temperature for condensation to super-cooled water at saturation with respect to a water surface, is about 4°F below the ice Mintra.

4. First formation of trails

It has been suggested, (M.R.P. 489, Condensation Trails from Jet Aircraft), that the first formation of non-persistent trails might be used as a method of estimating the humidity of the air when the air temperature is known; the nearer the air temperature to the Mintra temperature the moister the air. Accordingly the depression of air temperature below the Mintra and the depression of frost point below air temperature have been extracted for the 71 cases in which the first formation of trails on ascent were well marked and are plotted on figure 1; when bumpiness was noted at the same level, (16 occasions), the observation is marked with a 'B', the other observations being marked by crosses.

Figure 2 shows the plot of depression of air temperature below Mintra against depression of frost point below dry bulb for the first appearance of persistent trails, on ascent. The four bumpy cases are marked 'B'.

From these two diagrams it is seen that air temperature below Mintra temperature at first trail formation has little relation to the humidity of the air as indicated by frost point temperature.

5. Conclusions

It seems clear from the facts set out in section 3 that much remains to be learnt of the nature of condensation trails. There is a very rough correspondence between the occurrence of trails, (persistent or ephemeral), and the humidity of the air; on those occasions when no trails were formed the air was extremely dry. But it is seen that persistent trails can form in quite dry air (Table I) and that their persistence is not because of lack of turbulent mixing (Table II). Presumably the accuracy of the temperature and frost point measurements is not in doubt and it is concluded that an ice cloud, (which may originally be a super-cooled water cloud - see M.R.P 489), can persist in a dry atmosphere at these levels, (usually at pressure less than 300 mb. and temperature below - 40°F).

Brewer, (Weather, Vol.1, 1946, page 34) has stated that "really persistent trails are almost always associated with the super saturation in the upper air". He may call "really persistent" trails those which thicken after formation but there is no doubt that he (and most others, including the present writer until recently), assumes that ordinary persistent trails occur with a high humidity.

Since the humidity of the air appears to affect the occurrence of trails so little, the formation of trails and their persistence must be governed by some factor or factors other than humidity and temperature; the other obvious variable is condensation or sublimation nuclei.

25/452-4

M.R.P. 576

Figure 1.

First appearance of non-persistent trails — depression of temperature below Mintra and depression of frost point below air temperature.

(Total number 71 ; bumpy occasions — indicated by B — numbered 16).

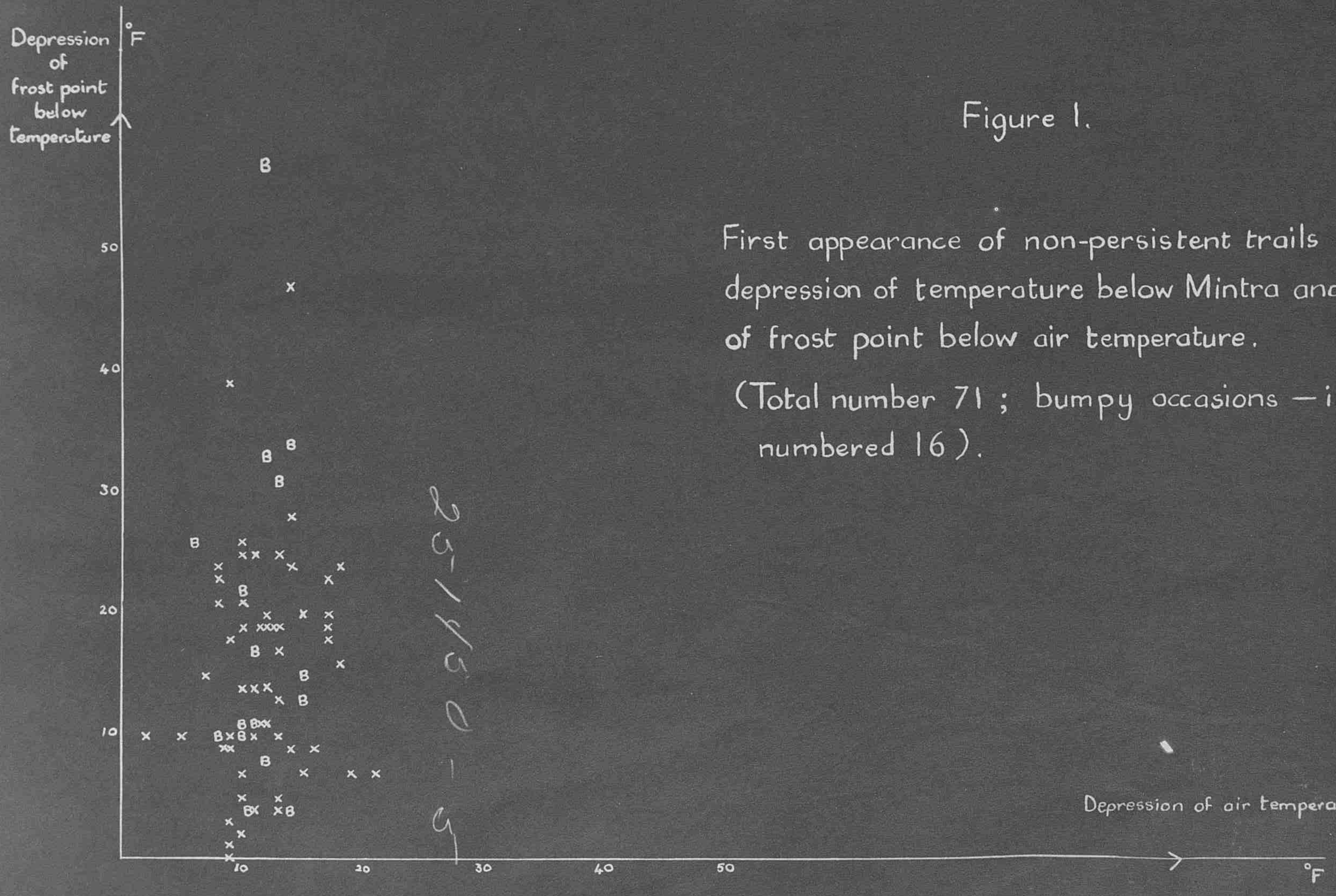

25/450 – 5

M.R.P. 576

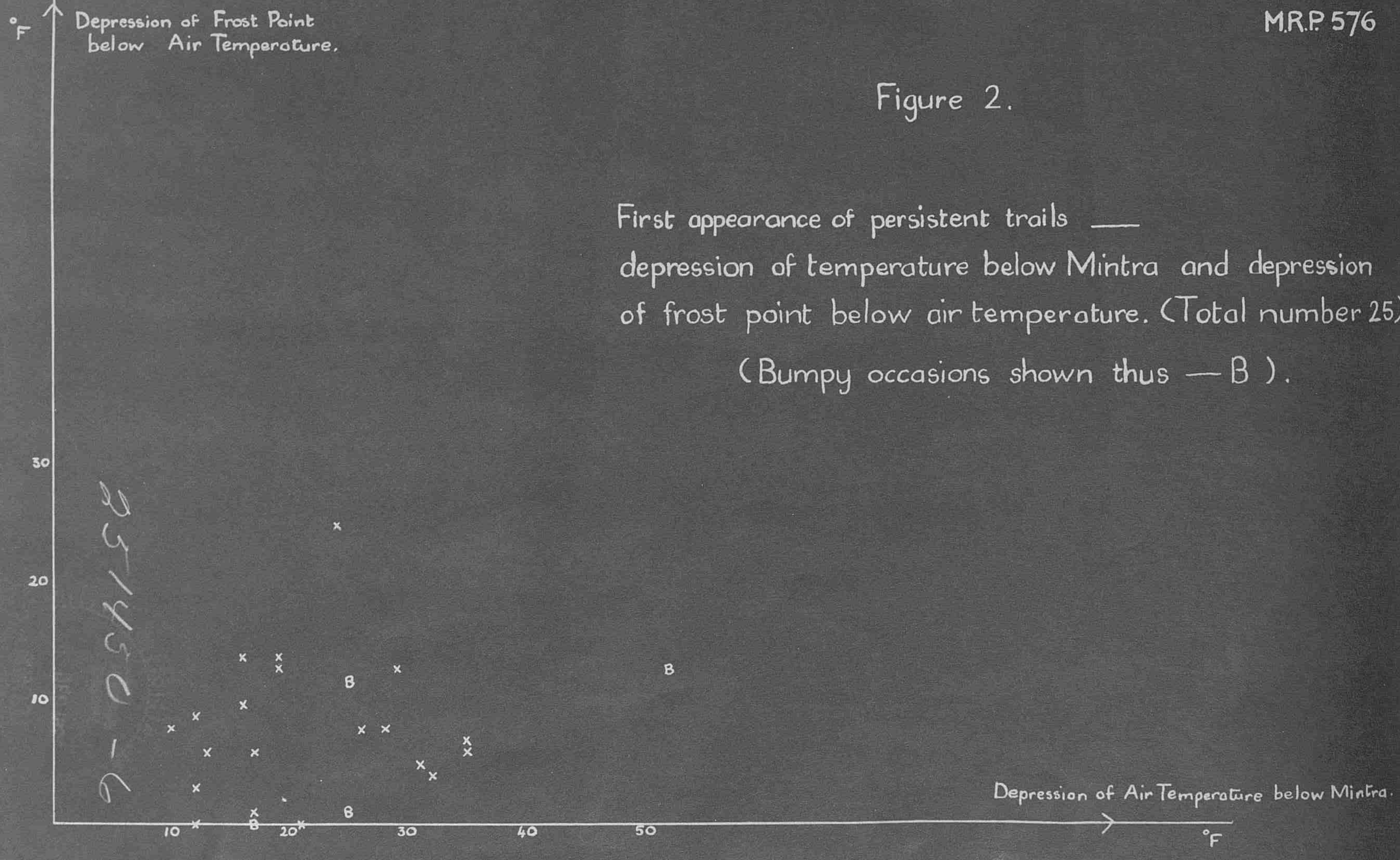

Figure 2.

First appearance of persistent trails — depression of temperature below Mintra and depression of frost point below air temperature. (Total number 25).

(Bumpy occasions shown thus — B).

25/450 - 6

CONFIDENTIALLY. Its contents must not be quoted.

M.R.P. 579
S.C.III/69
21st September, 1950.

AIR MINISTRY

METEOROLOGICAL RESEARCH COMMITTEE

DEC 8 1950

AIR WEATHER SERVICE
TECHNICAL REFERENCE FILE

NOTE ON THE ESTIMATION OF NATURAL EVAPORATION FROM METEOROLOGICAL DATA

by

F. Pasquill

Summary

Two different approaches to the problem of estimating natural evaporation from meteorological data, developed recently by Penman and the present writer respectively, are reviewed and discussed. Both methods are empirical, but whereas the former appeals basically to open water tank performance, the latter is supported by principles and aerodynamic data which have provided satisfactory quantitative interpretations of a variety of diffusion phenomena in the lower atmosphere in adiabatic conditions.

A quantitative examination in the light of the latter approach indicates that in so far as open water tank performance appears to lead to the correct magnitude of natural evaporation in certain circumstances, the result is merely accidental and a consequence of the combined influences of the artificial features of an evaporation tank. The adoption of the conventional evaporation tank as a starting point in the natural evaporation problem should accordingly be regarded as a limited and generally unsatisfactory form of empiricism.

A physically acceptable application of the principle of Penman's "combined sink strength and heat balance" method for evaluating tank evaporation in terms of readily available meteorological data is now put forward for a saturated natural surface, i.e., wet ground. It is demonstrated, however, that a transpiring vegetated surface cannot generally be regarded as effectively saturated, and the extension of the method to surfaces which are not visibly wet requires the accumulation of data (as suggested) on the effective degree of saturation of natural surfaces.

As regards the broad estimation of long term natural evaporation it is demonstrated, for the British Isles and Sweden, that the assumption of negligible net transfer of sensible heat to the air leads simply to estimates of evaporation which are in reasonable agreement with catchment area data and which, moreover, are identical with those provided for the British Isles by Penman's more complex empirical method. This implies that the ultimate test of Penman's method against catchment area data is concerned with a limiting case and cannot be regarded as a convincing general verification.

1. Introduction

The problem of relating local evaporation from a natural land surface to measurable meteorological quantities has recently been considered along two distinct lines. One of these approaches, followed by the writer (1949, a, and 1950, b) has attempted to take into account the aerodynamics underlying the process of diffusion near the earth's surface and to express the rate of evaporation in terms of the detailed vertical structures of humidity, wind speed and temperature representative of the surface. Although the study of this method was carried out over grassland, the ultimate relation is not basically restricted to any one particular site or type of surface, though for its full application, it requires measurements of a rather exacting nature over reasonably level unobstructed terrain, and if extended to the evaluation of long term water loss it would, in its present form, involve lengthy computations. As an example of its application in this direction the daily water losses from a pasture during a week of fair spring weather have been evaluated (Pasquill, 1949, b).

The other approach, due to Penman (1948), starts with the evaporation from an open water tank and its dependence (ultimately) on the meteorological factors normally specified in routine climatological observations. The evaporation from an open water tank is then related empirically to that from nearby tanks containing long-settled soil, either left bare or with a turf growth, with an artificial water supply arranged to keep the bare soil surface continuously wet and the turf transpiring at the maximum rate. The method was finally applied to the estimation of the annual evaporation from catchment areas and the result found to be in encouraging agreement with rainfall and run-off data.

Both approaches are essentially empirical though the types of empiricism employed are very different. The purpose of the present note is to emphasise this difference and its implications in the general problem of indirectly evaluating natural evaporation. The first part of the note is accordingly a review of previous work, but in later sections certain specific features are discussed in greater detail than hitherto and attention is thereby focussed on existing limitations and future observational requirements.

2. Preliminary Features

All existing approaches depend on one or the other (or both) of two relations, one expressing evaporation in terms of the distribution of vapour and the diffusive power of the air above the surface, the other expressing the balance of heat exchange processes at the surface. Both involve, explicitly of implicitly, a specification of the vertical flux of water vapour or heat in an atmosphere which is characteristically turbulent. On existing concepts, following the classical "mixing length" models of turbulent mixing, or merely by direct appeal to an analogy with molecular processes, this flux is written in the form

$$\rho K \frac{\partial S}{\partial Z}$$

where K is the so-called eddy diffusivity (cm^2, sec^{-1}) and ρ the density of of the atmosphere. $\frac{\partial S}{\partial z}$ is the vertical gradient of the property undergoing transport, S being the content of the property per unit mass of air. The basis for writing the flux in this form is essentially intuitive or empirical and final justification for it must be sought in the results to which it leads.

We may then write, neglecting the variation of ρ with height;

$$E = -\left(K_v \frac{\partial X}{\partial z}\right)_{z=0} \qquad \ldots\ldots\ldots\ldots\ldots\ldots(1)$$

$$H = -L\left(K_v \frac{\partial X}{\partial z}\right)_{z=0} - \rho c_p \left(K_h \frac{\partial \theta}{\partial z}\right)_{z=0} \qquad \ldots\ldots(2)$$

in which E is the local rate of evaporation, $\frac{\partial X}{\partial z}$ and $\frac{\partial \theta}{\partial z}$ the vertical gradients of absolute humidity and potential temperature, H the net incoming radiant energy minus that absorbed in the heating of the earth's crust, L the latent heat of vaporization, ρ and c_p the density and specific heat of the air. The subscripts v and h refer to the transport of vapour and heat. Actually, in expressing the above limiting values of the turbulent flux terms consideration should be given to the possibility of a transition region very close to the surface in which molecular motion assumes an importance comparable with that of the turbulent motion, and, at the surface itself, becomes the dominant process. Such ideas have been followed by Montgomery (1940) and Sverdrup (1937) in treating the evaporation from extensive water surfaces. These considerations, especially in their application to a rough surface, are exceedingly complex from both analytical and observational points of view, and it is clearly desirable, where possible, to avoid specifically introducing conditions at the surface itself. Where this is not possible in the present note, it will be assumed, as by many other workers, that the characteristic turbulent regime extends right down to the surface.

In considering the local vapour and heat transfer from an extensive area, the most reasonable and tractable assumption to make is that of horizontally uniform steady conditions. This appears to be an acceptable assumption for a shallow surface layer of the atmosphere, not more than a few metres deep, except presumably at the junctions of surfaces extremely dissimilar in their aerodynamic, thermal and evaporative properties. Where a variety of such surfaces are involved the assumption can only have significance in an average (spatial) sense. The result of this assumption is that (1) and (2) may be rewritten as:-

$$E = -\left(K_v \frac{\partial X}{\partial z}\right)_{z\ \text{small}} \qquad \ldots\ldots\ldots\ldots\ldots\ldots\ldots\ldots(3)$$

$$H = -L\left(K_v \frac{\partial X}{\partial z}\right)_{z\ \text{small}} - \rho c_p \left(K_h \frac{\partial \theta}{\partial z}\right)_{z\ \text{small}} \ldots(4)$$

3. Penman's Approach

In Penman's investigation of the daily water losses from an open water tank, consideration is given to the application of an existing hydrodynamical treatment of the evaporation from an area of finite extent downwind. This application will not, however, be discussed here, since Penman ultimately concludes this "aerodynamic" approach to be unsuccessful and in all subsequent applications adopts an empirical equation of the familiar form.

$$E = (a + bu)(e_o - e) \qquad \ldots\ldots\ldots\ldots\ldots\ldots\ldots\ldots\ldots(5)$$

where E is the daily evaporation, in mm. depth of water, u is the wind speed in miles per day (m.p.d.) at a height of 2 m, e_o is the daily mean saturation vapour pressure (in mm. Hg.) at the "surface" temperature of the water and e the daily mean vapour pressure at screen level. The values of a and b given by Penman are somewhat different for the two tanks which he considers, viz.:

	a	b
'cylinder O'	0.30	4.26×10^{-3}
'tank MO'	0.35	3.43×10^{-3}

but in view of a suspected local exposure effect on the results for 'cylinder O' he adopts the 'tank MO' values as giving the more reliable general guide.

The same results are then tested against the classical "heat balance" method, assuming heat transfer from the tank to the air to be prescribed by a relation similar to that for evaporation, but with the vapour content of the air replaced by it's sensible heat content. This is equivalent to assuming $K_v = K_h$ in equations (2) and (4) and in effect it means that we may write

$$E = (X_o - X)\, f(u)$$

$$H = L(X_o - X)\, f(u) + \rho c_p(\theta_o - \theta)\, f(u)$$

or eliminating the function f(u) from the latter equation -

$$H = LE + \rho c_p E \frac{(\theta_o - \theta)}{(X_o - X)} \qquad \text{........................(6)}$$

Thus E may be estimated from measurements or estimates of temperature and vapour pressure at one height (say screen level) and at the evaporating surface, and of H. Neglecting the absorption of heat by the tank and its surround, so that H is given by the net incoming radiation, Penman found the estimates of daily evaporation from 'tank MO' to be too big in mid-summer but to improve later in the year. Subsequently, in considering the mean daily evaporation over longer periods at various times during 1944 and 1945 it was concluded that the estimates for 'cylinder O' were almost invariably too low while those for 'tank MO' were reasonably good. The 'cylinder O' results were considered to be spurious owing to the fact that this tank (together with the soil tanks) was situated on the edge of an open pit 8 ft. deep and 20 ft. diameter, whereas 'tank MO' was completely surrounded by soil.

Adopting the empirical equation (5) with constants appropriate to 'tank MO', and the classical heat balance equation (6), as adequately established for an evaporation tank, Penman then combined the two so as to eliminate θ_o and e_o (or X_o), since for the open water surface e_o (or X_o) may be expressed as a known function of θ_o. The difficult measurement of the "surface" temperature of the tank water was thus avoided and the daily water loss E_o from a 'tank MO' prescribed in terms of air conditions and known constants only. The relations finally given by Penman for practical use are as follows:-

$$E_o = (H\Delta + 0.27E_a)/(\Delta + 0.27) \text{ mm/day} \qquad \text{............(6a)}$$

$$E_a = 0.35(1 + 9.8 \times 10^{-3}\, u_2)(e_a - e_d) \text{ mm/day} \qquad \text{........(6b)}$$

$$H = (1 - r)R_A(0.18 + 0.55\, n/_N) - \sigma T_a{}^4(0.56 - 0.092\sqrt{e_d})(0.10 + 0.90\tfrac{n}{N}) \qquad \text{..............(6c)}$$

where the symbols have the following meanings and units:-

e_a and e_d	saturation vapour pressures at air temperature ($T_a{}^o$) and dewpoint temperature respectively, in mm. Hg.
U_2	wind speed at 2 m. in miles per day.
Δ	$de/_{dT_a}$ in mm/^{o}F at Ta.
R_A	short wave radiation through a completely transparent atmosphere, in evaporation equivalent of mm/day.

/ r

r	short wave radiation reflexion coefficient (taken to be 0.05 for an open water tank).
$\frac{n}{N}$	ratio of actual/possible hours of sunshine.
σ	Stefan's constant.

Up to this stage the situation is straightforward in as much as the above considerations provide an empirical rule for estimating the daily water loss from a conventionally exposed evaporation tank in terms of readily available climatological data. The difficulty lies in suitably adjusting such estimates so as to correspond to natural evaporation. Regarding the measurements of absolute evaporation loss from the soil tanks as probably spurious owing to the presence of the open pit, Penman assumes the ratios of evaporation from 'cylinder O' and the soil tanks to be unaffected by this feature. Application of these ratios (E_B/E_o for bare soil and E_T/E_o for turf) to values of E_o evaluated as above is then presumed to give the evaporation losses from soil cylinders with a complete soil surround and these are further implicitly assumed to represent the local evaporation from an extensive area of similar surface, with, of course, the original limitations regarding water supply to the surface. Provisional values of the above ratios for Southern England are given by Penman as follows:-

E_B/E_o	all seasons	0.9
E_T/E_o	Midwinter	0.6
	Spring and Autumn	0.7
	Midsummer	0.8
	Whole Year	0.75

Penman finally tests this procedure by evaluating long period mean annual evaporation losses from "cropped soil" at various positions in the British Isles and demonstrating that these estimates are in reassuring agreement with those provided independently by rainfall and run-off data for various catchment areas. Thus, over long periods, the empirical steps adopted by Penman appear to be justified. Later in these notes we shall reconsider this justification and examine to what extent it implies a justification for the application of the method over shorter periods and to smaller areas.

4. The estimation of evaporation in adiabatic conditions on the basis of aerodynamic data

In this section a brief review will be given of the method followed by the writer (1949, a, and 1950, b) and since a generalized basis for this method is to be found in well-established laboratory data for turbulent flow through pipes and over flat plates, an outline will first be given of these data and their application to problems of diffusion in the atmosphere near the earth's surface.

The first direct application to the atmosphere of a laboratory formula for the resistance of a pipe appears to have been made by Prandtl and Tollmien (1925), who quote a formula due to Hopf and Fromm for flow in a rough pipe and apply it to an analysis of the vertical distribution of wind and the resistance of the earth's surface. They point out, however, that the application to heights well above the surface cannot be considered rigorous. Since then an extensive body of information has been made available on the mean properties of turbulent flow in pipes and over flat plates (see Goldstein, 1938) and the direct application of this to certain problems of diffusion in the lower atmosphere in adiabatic conditions has recently been considered in great detail by Calder (1949). Calder's presentation of the general argument will be followed here.

/ The

The laboratory experiments distinguish between two types of flow, so-called "aerodynamically smooth flow" in which the drag exerted on the boundary is a function of the Reynolds number only and "aerodynamically rough flow" in which the drag is independent of the Reynolds number and is proportional to the square of the velocity of the fluid. In more detail, the distribution of mean velocity with distance from the boundary and its relation to the drag exerted on the boundary are represented accurately, except very close to the surface, by the equations given below. In these equations the symbols have the following meanings:-

u	velocity at distance z from the boundary (z measured from the base plane of the roughness elements in the case of a rough surface),
v_*	$\sqrt{\frac{\tau_0}{\rho}}$
τ_0	tangential shearing stress per unit area of the boundary,
ρ	fluid density,
ν	kinematic viscosity of fluid,
k	a constant equal to 0.4, the so-called von Kàrmàn's constant,
z_0	a "roughness parameter" dependent only on the size, shape and disposition of the roughness elements,
d	a "zero-plane displacement", taking into account the raising of the effective boundary (above the base surface) owing to the finite volume of the roughness elements.

The equations are:

Smooth flow $$\frac{u}{v_*} = \frac{1}{k}\log_e\left(\frac{v_* z}{\nu}\right) + 5.5 \qquad \text{.....................(7)}$$

Rough flow $$\frac{u}{v_*} = \frac{1}{k}\log_e\frac{(z-d)}{z_0} \qquad \text{.......................(8)}$$

Criteria on the existence of rough or smooth flow over a particular surface, or of an intermediate flow regime (transitional flow) have been given by Schlichting (1936) as follows:-

rough $$\frac{v_* z_0}{\nu} > 2.5$$

transitional $$2.5 > \frac{v_* z_0}{\nu} > 0.13$$

smooth $$0.13 > \frac{v_* z_0}{\nu}$$

the parameter z_0 being deduced from velocity profile observations at sufficiently high Reynolds numbers to give fully rough flow.

In the problems treated by Calder (see later) the transcendental functions lead to insuperable mathematical difficulties and to avoid these Calder makes use of power law formulae (well known in smooth flow results) approximating to the above. These are:-

Smooth flow $$\frac{u}{v_*} = q\left(\frac{v_* z}{\nu}\right)^{\alpha} \quad \ldots\ldots\ldots\ldots\ldots\ldots\ldots\ldots(9)$$

Rough flow $$\frac{u}{v_*} = q'\left(\frac{z - d}{z_o}\right)^{\alpha} \quad \ldots\ldots\ldots\ldots\ldots\ldots\ldots\ldots(10)$$

in the application of which the values of q, q' and α are chosen so as to give the best agreement between (9) (or (10)) and the more accurate formula (7) (or (8)) over the height range on which interest is concentrated.

The aerodynamic generality of the above relations suggests that they might be expected to hold near the surface of the earth, as long as the flow in this case is dominated by the surface drag, that is, in the absence of buoyancy effects due to thermal stratification of the atmosphere. Abundant evidence is now available (see especially Deacon (1949)) that the wind velocity profiles in the first few metres of the atmosphere in adiabatic conditions are accurately represented in most cases by the functional form of equation (8) for fully rough flow. The exceptions are in the cases of geometrically smooth surfaces (e.g. level snow, mud flats, ice sheets), when transitional or aerodynamically smooth flow is to be expected over the normal range of wind velocities, and in the case of flow over the sea (Rossby, 1936) for moderately light winds. As regards the explicit validity of equation (8) in the lower atmosphere direct measurements of the local aerodynamic drag of grassland have recently been made (Pasquill, 1950, a), using a modification of a technique developed by Sheppard (1947), and encouraging agreement found (actually, equation (8) was found to be satisfied with $k = 0.37$, which, in keeping with the general accuracy of the measurements, was as good agreement with the laboratory value of 0.4 as could be expected). From the evidence so far available it appears, therefore, that the laboratory expressions may be applied with confidence in an adiabatic lower atmosphere.

Proceeding now to the application to diffusion problems, if we write the flux of momentum, or horizontal shearing stress, (τ), in the usual form

$$\tau = \rho K_m \frac{\partial u}{\partial z}$$

and take $\tau = \tau_o$ (proved by Ertel (1933) to hold in the first 30 m. of the atmosphere) then it follows from equations (7) and (8) that

$$K_m = k v_* z \quad \ldots\ldots\ldots\ldots\ldots\ldots\ldots\ldots(11)$$

for both rough and smooth flow. From the approximate power law forms (9) and (10), following Calder (loc. cit.),

$$K_m = \left(\frac{\epsilon}{\alpha}\right) \delta^{2\alpha\beta} u_1^{2\beta-1} z_1^{\alpha(1-2\beta)} z^{(1-\alpha)} \quad \ldots\ldots\ldots\ldots\ldots\ldots(12)$$

where for smooth flow

$$\beta = \frac{1}{1 + \alpha}, \quad \delta = \nu, \quad \epsilon = \left(\frac{1}{q}\right)^{\frac{2}{1+\alpha}}$$

and for fully rough flow

$$\beta = 1, \quad \delta = z_0, \quad \epsilon = \frac{1}{q'^2}$$

with, as pointed out previously, q, q' and α chosen to fit the more accurate relations (7) and (8), and in the case of rough flow, with a zero plane correction to z and z_1.

On the assumption that the eddy diffusivity for any other conservative property of the air is identical with that for momentum (K_m) the above forms for K_m have been employed in treatments of various diffusion problems. Such treatments lead to expressions for diffusion which are free from adjustable constants and which, evaluated from known physical constants and measurable quantities, have been shown to be in excellent agreement with observations of the following features. The wind profile equation applicable is indicated in each case.

(a) The total rate of evaporation from a free-liquid surface of finite extent, in a wind tunnel (Pasquill, 1943) - equation (9)[*]

(b) The total rate of evaporation from a free liquid surface of finite extent (about 20 cm. diameter) exposed in the open at ground level with wind velocities ranging from 1 - 9 m/sec. (measurements by Sheppard, unpublished, and Pasquill, unpublished, referred to by Sutton, 1947, p.272 - 3) - equation (9)[*]

(c) The diffusion of smoke from an infinite crosswind line source at ground level, for distances of travel of 100 - 1000 m. over downland with grass 20 - 70 cm. high, in adiabatic conditions, (Calder, 1949) - equation (10).

(d) The distribution of vapour over and immediately downwind of short grass downland areas (10 or 30 yds. in downwind extent) sprinkled with liquid, in adiabatic conditions. (Calder, 1949) - equation (10).

(e) The natural evaporation from grassland in adiabatic conditions, as indicated by direct measurements of the water loss from isolated but otherwise naturally exposed sections of the surface layers of a clayland pasture (Pasquill, 1949, a, and 1950, b) - equation (8).

The main purpose of the discussion given so far in this section is to emphasise two points, firstly, the generality of the basic aerodynamic data, secondly, the invariable success which has attended its adoption in treatments of the diffusion of matter in turbulent adiabatic flow in diverse circumstances. The inference to be drawn is that although the general method adopted is basically empirical, it may be extended with confidence to circumstances other than those tested above, provided the necessary aerodynamic and thermal conditions are satisfied. In other words, it may safely be assumed that a formula so derived for natural evaporation, and tested against measurements on a surface of specific nature and geographical situation, will apply with equal validity to other natural surfaces and situations.

/Turning

Footnote[*]

In these cases the experimental results were in fact compared with a solution of the two-dimensional problem of evaporation obtained by O.G. Sutton on the basis of a formulation of the Taylor correlation coefficient and "mixing length" concepts. Calder (loc. cit., p.173) has pointed out that for aerodynamically smooth flow the corresponding solution based on equations (7) and (9) of the present notes is identical with that previously obtained by Sutton.

Turning in more detail to the natural evaporation problem the analytical steps are as follows. For effectively steady, horizontally uniform conditions we write, as before

$$E = -K_v \frac{\partial X}{\partial z} \quad \ldots\ldots\ldots\ldots\ldots\ldots\ldots(13)$$

and take

$$K = K_m = \left(\text{from equation (11)}\right) k v_*(z - d)$$

Integrating equation (13) over an arbitrary height range, z_1 to z_2, so as to avoid analytical and observational difficulties associated with conditions at the boundary,

$$X_1 - X_2 = \frac{E}{k v_*} \log_e \frac{(z_2 - d)}{(z_1 - d)}$$

Substituting for v_* from equation (8) and re-arranging

$$E = \frac{k^2 (X_1 - X_2)(u_2 - u_1)}{\left(\log_e \dfrac{z_2 - d}{z_1 - d}\right)^2} \quad \ldots\ldots\ldots\ldots\ldots\ldots(14)$$

This formula was first employed in the evaluation of natural land evaporation by Thornthwaite and Holzman (1942), though at that stage the above generalised basis had not been outlined and no direct examination of the accuracy and limitation of the formula had been provided.

Measurements by the writer (1949, a, and 1950, b) of the water loss by evaporation from a level, well exposed clayland pasture in the early stages of seasonal drying and of the corresponding vertical profiles of wind velocity and vapour pressure up to a height of 2 m, in adiabatic conditions, were compared with equation (14). Water losses over periods of 1 hour were measured by weighing simple soil evaporimeters containing samples (usually 4 inches in diameter and depth) of the surface layer of the pasture, set out so that the surfaces of the samples were exposed as in the original undisturbed state. Control tests indicated that over the period of use of the samples the isolation from underlying soil had not significantly influenced the rate of loss of water from the surface but there was a suggestion that the measurements might slightly underestimate the true evaporation owing to the relatively small cross-sectional area of the samples and the unavoidable disturbance of root and soil continuity at the perimeters of the samples. A summary of about 40 comparisons made, with wind speed ranging from 3 - 9 m/sec. (Pasquill, 1950, b), shows that these measured rates of evaporation agree with those computed from equation (14), on the average to within 1%. For individual hourly values an agreement within ± 20% may be expected on more than 70% of occasions. Bearing in mind the widely established basis of equation (14) this may be taken to mean that the slight uncertainty remaining in the validity of the measurements is of no practical importance and that the true rate of evaporation was measured to a satisfactory approximation and is adequately specified by the treatment based on equation (8).

5. Evaporation and Heat Transfer in non-adiabatic conditions

Attempts have been made to investigate the effects of thermal stratification on the properties of turbulent flow in the laboratory, but with little success as far as application to atmospheric conditions is concerned. The difficulty appears to be in the fact that for the appreciable development of buoyancy influence the required vertical depth of characteristic flow is greater than that which can be achieved in wind tunnels of practical size, except at very low air speeds, when the customary measurements are in any case somewhat unreliable. For the extension of the method of the preceding section to thermally stratified flow we have, therefore, to rely on direct observations in the atmosphere. One point of immediate interest is that the measurements of evaporation from a small free liquid surface at ground level (Pasquill, unpublished, Sutton, 1947, p.273) appeared to be mainly unaffected by variations in thermal stratification and were generally consistent with the expression applicable to aerodynamically smooth flow in adiabatic conditions. The inference is that the evaporation in this case was dominated by the very shallow (few cm. thick) boundary layer characteristic of the small free liquid area itself, in which, as in wind tunnel flow, buoyancy effects were negligible as compared with frictional effects.

The observations of natural evaporation and associated vertical profiles mentioned in the previous section (Pasquill, 1949, a) were also carried out in a range of conditions of thermal stratification. These indicated a variation of eddy diffusivity (K_V) in the anticipated sense, i.e., an increase in unstable conditions and a decrease in stable conditions, but the main interest lay in the indication of a systematic variation of K_V with the Richardson number.

$$Ri = \frac{g}{T} \frac{\left(\frac{\partial\theta}{\partial z}\right)}{\left(\frac{\partial u}{\partial z}\right)^2}$$

which thus appeared to be a unique indicator of the influence of thermal stratification on diffusion. This immediately led to a result of practical importance as follows:

In adiabatic conditions (Ri = o) it follows from (8), (11) and (13) that

$$\frac{-E}{(z-d)^2 \frac{\partial u}{\partial z} \frac{\partial X}{\partial z}} = k^2 = 0.16 \qquad \text{...........(15)}$$

where $\frac{\partial u}{\partial z}$ and $\frac{\partial X}{\partial z}$ are the vertical gradients evaluated at height z.

The values of the above parameter, computed at z = 150, 75 and $37\frac{1}{2}$ cm., were found to increase with increasing negative Ri and to decrease with increasing positive Ri in a manner independent of the heights involved. Now the Richardson number decreases rapidly as the ground is approached and indeed it appeared that at the lowest of the above heights, a substantial departure from adiabatic conditions produced only about 30% departure from the relation in (15). It follows, therefore, that except in conditions of very light wind and marked vertical temperature gradient the relation (15) may be applied generally as a reasonable approximation provided the gradients $\frac{\partial u}{\partial z}$ and $\frac{\partial X}{\partial z}$ are deduced for an effective height somewhat below 50 cm. This is, of course, assured by making the profile measurements of u and X within the height range 0 - 50 cm. but it may be reasoned that where "surface" values are specifically or implicitly employed in conjunction with values of u and X at one height above 50 cm., the necessary condition may still be approximately satisfied. The observational evidence, (e.g. Deacon, 1949, Pasquill, 1949, a) points to the fact that in non-adiabatic conditions the u (or X), log z profiles are of a simple curved form (whereas they are linear in adiabatic conditions). Thus the application of equation (14) to observations at two particular heights z_1 and z_2 means in effect that the gradients are being reasonably correctly specified at a height in the region of the geometric mean of z_1 and z_2 (i.e. the mean logarithmic height). If this geometric mean height is below 50 cm. then on the previous basis we may assume the approximation involved in applying (14) to be acceptable. Thus if we take values of u and X at z_o (i.e. effectively surface values) and z_1 then the effective height of application is $\sqrt{z_o z_1}$. With, for example, z_o 1 cm. (a reasonable value) and z_1 200 cm. this amounts to 14 cm.

An alternative empirical application, which is more accurate, but less convenient in application in that extremely careful wind velocity profile observations are required, follows from an application of Deacon's (1949) generalised wind profile law for non-adiabatic conditions. Deacon found that extensive wind profile measurements in the first few metres could be represented generally by the law

$$\frac{\partial u}{\partial z} = a\, z^{-\beta}$$

with $\beta > 1$, $= 1$ and < 1 in unstable, adiabatic and stable conditions respectively. Integrating this expression and appealing to the observed decrease of stability influence on the profile as the ground is approached (i.e. assuming (8) to apply universally for $z \to 0$) Deacon deduced the wind profile equation

$$u = \frac{v_*}{k(1-\beta)} \left[\left(\frac{z}{z_o}\right)^{1-\beta} - 1 \right] \quad \ldots\ldots\ldots\ldots\ldots(16)$$

From this it follows that

$$K_m = k v_* z_o^{1-\beta} z^{\beta} \quad \ldots\ldots\ldots\ldots\ldots (17)$$

Assuming $K_m = K_v$ this expression was found to give good agreement with the evaporation and profile observations (Pasquill, 1949, a) in unstable conditions but not in stable conditions. For full application in practice wind profile observations in adiabatic conditions (in order to specify z_o from equation (8)) are required, as well as those in unstable conditions, which specify β. For practical purposes, at any rate where the necessary height limitations may be satisfied, the simpler approximate method given above is probably adequate, especially if it is desired to employ wind velocity data at a single height with an assumed nominal value of z_o.

Turning to the problem of the turbulent transfer of heat, which is involved in the "heat balance" method of evaluating evaporation, we may recall that the classical application required equality in K_v and K_h. On classical considerations of turbulent transport there appeared to be no reason to doubt that this equality would hold in the atmosphere but the considerations put forward by Priestley and Swinbank (1947) amend this view. The essence of their argument is that in a thermally stratified atmosphere buoyancy effects lead to a discriminatory mixing term (additional to the indiscriminatory mixing term on the classical approach) which produces an additional component of heat flux always directed upward irrespective of the direction of the mean vertical gradient of potential temperature. Extended to the transport of a property other than heat content this also implies that the transport of this property (measured against the corresponding gradient) may be different from that corresponding to heat by an amount depending on the extent to which the two properties are correlated. As a simple example, consider the vapour and heat transport above a surface consisting of alternate wet and dry patches. It is reasonable to assume that air leaving the wet patches will possess a higher absolute humidity and lower temperature than that leaving the dry patches. Due to the buoyancy discrimination effect on the vertical mixing process there will accordingly be a tendency for a systematic upward movement of relatively warm relatively dry air. If the mean gradients of temperature and humidity are similarly directed this implies opposing effects on the heat and vapour fluxes respectively, the heat flux being increased. On the other hand, if the gradients are oppositely directed, then similarly directed effects would be exerted on the two flux quantities.

A distribution of surface properties such as that discussed above may be expected to exist, in a rough way, on any patchy vegetated surface in dry weather, the transpiring surfaces being the wet, cool patches and the intermediate soil areas the warm, dry patches. The evaporation and profile observations previously discussed (Pasquill, 1949, a) included a limited number of simultaneous measurements of the relevant heat balance factors over a rather patchy clayland pasture. These observations indicated values of the eddy diffusivities for heat and vapour (at a height of 75 cm.) entirely in accord with the above arguments, i.e. with lapses of both temperature and humidity K_h was substantially greater than K_v, whereas with a lapse of humidity and an inversion of temperature K_h and K_v were virtually identical. It followed that in lapse conditions classical heat balance estimates of evaporation may be over-estimates to a considerable extent. As far as the writer is aware, no other direct observations of this feature are available, though a less direct test provided by observations in which evaporation was not independently measured has by claimed by Robinson[*] to support the classical assumption of $K_v = K_h$. This may be due to a difference in surface conditions at the two sites of observation (Kew and Cambridge); it may also be associated with the fact that the profile observations employed in the Kew test were confined to heights below 30 cm., in which region a less marked buoyancy influence is to be expected. Until further critical observations are available, it is considered that the classical "heat balance" method of estimating evaporation cannot be applied with confidence except possibly in terms of observations very close to the ground. On the basis of the discussion earlier in this section, it follows that the latter condition may be approximately satisfied where use is made of surface values and values at some convenient height of 1 or 2 metres.

6. The Interpretation of Open Water Tank Evaporation Measurements

Owing to the difficulties inherent in the direct measurement of natural evaporation as a routine matter, the open water evaporation tank has for long been the only standard reproducible instrumental device for specifying "evaporation" as a climatological feature. The implication is that an instrument of this type does reflect in some way the true natural evaporation and indeed, as we have seen, the indications of such an instrument have been adopted by Penman as a starting point in developing a method for the indirect estimation of natural evaporation. It is evident on the simplest considerations, however, that the meteorological interpretation of evaporation tank performance is somewhat controversial[†], and it seems desirable in the present note to give some further discussion of the matter in the light of the physical considerations advanced in preceding sections.

/ Let

Footnote[*] referred to in Met. Mag., 79, 1950, Meteorological Office Discussion

Footnote[†] See Royal Meteorological Society Discussions as reported in Q.J.R. Met. Soc. 73, p.276, 1947, and 76, p.103, 1950, and Meteorological Office Discussion as reported in Met. Mag. 79, p.81, 1950.

Let us first consider the local evaporation from an extensive surface. On the treatment outlined in section 4 we may obtain an expression for this in terms of the wind and vapour profiles over the surface and in order to effect direct comparison with empirical laws for tanks, and at the same time avoid substantial error due to the neglect of the influence of thermal stratification, we may frame this expression in terms of surface conditions and values of wind speed and vapour pressure at some convenient height above ground, say 2 m. . If we integrate equation (13) (applicable to steady horizontally uniform conditions) using for u and K the approximate power law forms given by Calder (loc. cit.) in equations (9), (10) and (12), with the boundary condition

$$u = o, X = X_o \text{ at } z = o$$

we obtain the following expression,

$$E = \frac{X_o - X}{z^{\alpha}} \epsilon \delta^{2\alpha\beta} z_1^{\alpha(1-2\beta)} u_1^{2\beta-1} \quad \text{..............}(18)$$

where X is the abolute humidity at z and u_1 the wind velocity at z_1, applicable to both aerodynamically smooth and aerodynamically rough flow when ϵ, δ, β are given the appropriate values as previously specified and α, q and q' are chosen to fit the accurate profile laws (7) and (8) over the height range of interest. Since, however, we are not specifically interested in the variation of X with z, we may simplify the above equation by setting $z = z_1$ and substituting for v_* from the power law forms (9) and (10) with the result that

$$E = \frac{v_*^{2}(X_o - X_1)}{u_1} \quad \text{........................}(19)$$

where v_* may then be evaluated from the more accurate equations (7) and (8), so short-circuiting the procedure of choosing appropriate values of α , q and q'. From the variation of v_* with u implicit in these equations it is immediately evident that equation (19) gives E varying linearly with u in rough flow but somewhat less rapidly than directly with u in smooth flow. Indeed for smooth flow (18) gives E varying with

$$u_1^{\frac{1-\alpha}{1+\alpha}}$$

and since (see Calder, loc. cit., p.164) α = 0.095 fits equation (9) to equation (7) over the greater part of the layer up to 200 cm., we have the approximate result:

$$E \propto u_{200}^{0.83}$$

In obtaining absolute values from equation (19) we take

(a) for smooth flow $\nu = 1/7$

(b) for rough flow $d = 0 \quad z_o = 0.20$ cm.

(c) for rough flow

u_{200} m/sec.	d, cm.	z_o, cm.
1.45	15	15.9
2.7	16	8.8
4.0	21	5.6
5.8	32	3.0

The above parameters for rough flow are given by Calder (loc. cit., p.157) on the basis of Deacon's wind profile measurements, (b) corresponding to very short cropped grass and (c) to grass 60 - 70 cm. long. For (c) note the variation of d and z_0 with wind velocity, ascribed to the progressive bending over of the grass blades as wind velocity increases. The following table summarises the results in practical units.

Table I. Computed local evaporation from an extensive surface Eo, in mm. day, per unit vapour pressure difference, $(e_0 - e_{200})$, in mm. Hg. against wind velocity at 200 cm. in miles per day.

Wind velocity at 200 cm.					
	(m.p.d.)	78	145	215	311
	(m/sec.)	1.45	2.7	4.0	5.8
$\frac{E \text{ mm/day}}{(e_0 - e_{200}) \text{ mm. Hg.}}$	Smooth	0.17	0.29	0.40	0.55
	Rough (b)	0.44	0.82	1.23	1.76
	Rough (c)	3.5	4.3	4.9	5.2

It is emphasised that the above results refer, not to E, but to $E/(e_0 - e_{200})$, that is to say, they really represent the diffusive power of the air flowing over various surfaces, and it is immediately seen that an enormous variation occurs for surfaces encountered in practice. It is also noteworthy that while for a short grass surface a linear variation of E with u occurs (following of course from (19) and the constant value of z_0), for the long grass surface the variation of E is much less rapid than linearly with u, owing to the assumed decrease of z_0 with increase in wind velocity.

The results may now be compared with the empirical formulae for open water tank evaporation as quoted by Penman (loc. cit.). Penman's values are also related to wind speed at 200 cm. and vapour pressure at the surface, as in the present case, but to vapour pressure in the air at screen level instead of 200 cm. in the present case. On the basis of equation (18) the difference thus involved may be neglected for the order of magnitude comparison intended here. From this comparison, shown graphically in Fig.1, it appears that evaporation from an open water tank (expressed per unit value of $(e_0 - e_{200})$ does not correspond to that from a smooth sheet of water but approximately to that from a short grass surface. Alternately one may say that the actual evaporation from a tank corresponds to evaporation from an even rougher natural surface at the same temperature but with some appropriate departure from saturation at the surface. On this basis it is evident that open water tank evaporation may be expected to indicate the order of magnitude of natural land evaporation and indeed it may be noted that Robinson[*] has already pointed out that rates of evaporation evaluated by the heat balance method for a short grass surface at Kew show reasonable agreement with a nearby tank in the daytime when the grass is in a fresh condition. The physical reasons for this coincidence, however, have yet to be given; the following considerations seem to provide a plausible explanation.

Apart from any deficiencies in aerodynamic exposure one would expect the flow conditions over the water surface to be those appertaining to an aerodynamically smooth surface except possibly in the event of the surface being excessively disturbed and broken by strong winds. The fact that no marked transition appears in the observed E, u relationships for open water tanks suggests that this has not occurred to a sufficient extent over the range of wind speeds considered. One is thus led to expect, on first considerations, an evaporation rate corresponding to an aerodynamically

/ smooth

Footnote[*] Meteorological Office Discussion, Met. Mag. 79, p.85, 1950.

smooth surface, i.e. about $\frac{1}{3}$ of that actually observed. However, the tank water surface departs from a true sample of an extensive sheet of water in two other respects. Firstly, it is surrounded by a surface at which the vapour pressure will in general be different from that at the water surface itself, and probably lower except in decidedly wet conditions. A surface surrounded at a lower vapour pressure would lead to an increased rate of evaporation from the tank but to an extent which it is not easy to estimate. Secondly, the water surface is surrounded by a projecting rim and the order of magnitude influence of this is one which may be estimated with some confidence from previous experimental data, since the effect of a sharp ridge on the evaporation from a surface downwind of the ridge has been investigated in a wind tunnel by Powell (1942).

Powell measured the rates of evaporation from cylindrical saturated surfaces of various lengths with the axis of the cylinder lying along the wind and with ridges in the form of thin collars fitted at the upwind edges of the wet surfaces. Since any effects observed are due to the "bluff body" resistance imposed by the ridges and the resulting stationary eddy formation downwind of the ridge, the result so observed may be expected to apply approximately in the open atmosphere provided geometrical similarity in the ridge heights and evaporating surface lengths is satisfied. One of the tanks employed by Penman (described as 'tank MO') was exposed so that the water surface was at or near ground level, the rim of the tank projecting 3 in. above this, while the other tank (cylinder 'O') is described as having a higher effective rim. These tanks were both 2 ft. 6 in. in diameter so giving "ridge height/evaporating surface length" ratios of 0.1 or more. For a ratio of 0.1, with evaporating surfaces 30 - 100 cm. long Powell's results show the evaporation to be increased by 70 - 80%, a result which goes some way towards explaining the difference between the evaporation from the tanks and that expected from an ideally exposed water surface.

The general inference to be drawn from the above considerations is that although open water tank evaporation performance may in certain circumstances appear to represent the order of magnitude of natural evaporation, it is almost certain that this is accidental and a result of the combined influences of the various artificial features of the arrangement. The conventional evaporation tank undoubtedly provides a convenient form of measurement but its adoption as a starting point for natural evaporation studies is a complex and limited form of empiricism which disregards the physical principles now known to be operative in natural flow phenomena near the earth's surface. The application of such an approach outside the actual circumstances of direct experimental test should be regarded as fundamentally unreliable.

7. Evaporation from saturated and unsaturated land surfaces

In the case of a saturated surface the equations representing evaporation as a function of the vertical distribution of vapour and as a balance of the remaining heat exchange components may be combined, following Penman (1948), so as to eliminate the surface temperature and leave evaporation expressed in terms of air conditions only. Penman applies this procedure to evaporation from an open water tank, for which the assumption of saturation conditions at the surface is entirely reasonable. The same assumption, however, seems to be implicit in Penman's discussion of evaporation from wet bare soil and turf with a plentiful water supply and in his ultimate application to evaporation from catchment areas.

For a saturated rough surface the same procedure may be adopted, using equation (19), the basis of which is quite general and widely established in adiabatic conditions, instead of the empirical equation (6b) for an open water tank, the doubtful significance of which has been discussed in the previous section. The equations (6a) and (6c) remain unaltered, while (6b) is replaced by

$$E_a \text{mm/day} = \frac{0.27(e_a - e_d)\, u}{\left(\log_e \frac{z - d}{z_o}\right)^2} \qquad \ldots\ldots\ldots\ldots\ldots\ldots(21)$$

where $e_a - e_d$ is in mm. Hg. and u in miles per day, and z is the height (preferably 2 m. or less) at which these quantities are measured. As discussed in section (6) this equation gives magnitudes similar to those from equation (6b) when z_o is taken to be 0.20 and d = 0, i.e. values corresponding to a very short grass surface. For rougher or smoother surfaces equation (21) will give results respectively higher or lower than those from equation (6b). Appealing to the argument previously given for the neglect of the effects of thermal stratification when "surface" values of vapour pressure and temperature are implicitly involved, equations (6a), (6c) and (21) may be applied generally to a natural surface for which saturation conditions at the surface may be assumed and for which an estimate of the appropriate value of z_o may be made. The latter estimate can probably be made with sufficient accuracy for most purposes (see Sheppard, 1947, p.216, and Deacon, 1949, p.92) and the main restriction is provided by the required condition of saturation at the surface. The condition may confidently be assumed to hold only on thoroughly wet ground, though Penman's discussion of the problem implies that it also effectively holds for a freely transpiring vegetated surface. The general validity of the latter assumption in respect of vegetated surfaces in practice is thought to be uncertain, however, and some independent test seems desirable. A more critical test than any hitherto provided is made possible by the recent indirect evaluation of natural evaporation from a pasture, employing equation (14) and observations of the vertical distribution of humidity and wind velocity (Pasquill, 1949, b).

If there is no change of temperature with height and if the surface is saturated, then in equation (19)

$$\text{i.e.} \qquad E = \frac{v_*^2 (X_o - X_1)}{u_1}$$

X_o is simply the saturation value at air temperature. Comparison of rates of evaporation so derived with those based on equation (14) will reveal the extent to which the assumption of saturation is justified. The observations referred to were carried out in fair spring weather with a fairly uniform cover of fresh grass and clover, the latter growing from 3 - 5 cm. high to 5 - 10 cm. during the several days of continuous observation. Bare patches, usually dry, were estimated to occupy only 5 - 10% of the area.

In fact, the observations were associated with a characteristic diurnal variation of vertical temperature gradient and no single observation (corresponding to a period of 15 minutes) exactly satisfied the condition of zero gradient of temperature. The device used, therefore, is to select observations for which the temperature gradient lay between small positive and negative limits, the criterion actually used being

$$0.2 > T_{50} - T_{25} > -0.2^\circ F$$

T_{50} and T_{25} being the air temperatures at 50 and 25 cm. above the ground. With E representing the "actual" rate of evaporation as previously computed (Pasquill, 1949, b) and E_s the corresponding value computed on the assumption of surface saturation and zero temperature gradient (with z_o = 0.7 cm., d = 4 cm., and u as given in the latter paper[*]), then for a given degree of saturation at the surface E/E_s should apparently decrease

/ with

Footnote[*] The required values of T_{50}, from which values of X_o (assumed equal to the saturation value at T_{50}) are derived, and those of $T_{50} - T_{25}$, are not given in the paper referred to but have been extracted from the original observational data.

with increasing positive value of $T_{50} - T_{25}$ (since effectively the surface temperature will be correspondingly over-estimated) and the value interpolated for zero value of $T_{50} - T_{25}$ (i.e. T(surface) = $T_{50} = T_{25}$ implied) should indicate the true value of E/E_s. Of the observations carried out 8 - 12 May, 1947, 23 satisfy the adopted criterion. The corresponding data are given in Table 2 (appended) and the ultimate values of E/E_s are also shown graphically in Fig. 2 against $T_{50} - T_{25}$. There is a clear indication of a slow systematic decrease of E/E_s with increase of $T_{50} - T_{25}$ and for all days except the 9th the correct value of E/E_s (i.e. for $T_{50} - T_{25} = 0$) appears to be close to 0.45. For the day excepted, on which incidentally the highest values of E were obtained, E/E_s appears to be nearer 0.25.

The above considerations refer to a situation of practical interest in which, in the absence of data to the contrary, it might have seemed reasonable to assume saturation conditions at the surface. The test presented here indicates that evaporation estimates so based would be over-estimations to an extent of 100% or more. Although this is only one example there is no reason to suppose that it is not fairly typical of growing pasture in general in fair weather, and it is clear that the assumption of saturation conditions cannot generally be adopted for an apparently healthy and reasonably well covered vegetated surface. The convenient method discussed earlier in this section, in which evaporation is related to readily available meteorological data, cannot therefore be applied reliably without some a priori knowledge of the effective degree of saturation at the surface. In the present state of knowledge there does not appear to be any satisfactory way of specifying this feature other than by a previous application of the indirect procedure demonstrated above. In other words, there is a need for extensive observations of the vertical profiles of wind velocity, temperature and humidity above natural surfaces in various conditions of vegetation cover and weather, so that in due course "normal" values may be prescribed for the effective state of saturation at the ground.

8. The Approximate Estimation of Long Term Natural Evaporation on simplified Heat Balance considerations.

In the "heat balance" application made by Penman the net amount of heat absorbed below the surface of the tank is assumed to be negligible "over a period of several days and frequently over a single day". This seems to be a very reasonable assumption and one which may be expected to hold also for a natural surface over long periods. The heat loss due to evaporation is then simply equal to the difference between the net gain of heat from radiation processes and the heat absorbed in and transported away by the air. Over a period of a whole year, or even a period less than a year, as long as this period begins and ends with similar conditions of air temperature, it may reasonably be assumed that the net absorption of sensible heat by the air is negligible, so leaving only an advection component. Over the periods specified, in which relatively local advection effects may be expected to compensate, the resultant advection component is presumably that associated with the meridional transport of heat through the agency of the general circulation. Although the absolute magnitude of the meridional flux of heat has recently been evaluated (Priestley, 1949) for one position (Larkhill), we require for present considerations to know the rate of change of this meridional flux of heat with latitude. Direct information on this latter feature is at present not available but on general considerations of the heat balance of the earth one expects this meridional flux to increase with latitude in low latitudes and to decrease in high latitudes. A condition of negligible rate of change of flux with latitude and hence of negligible local heat loss to the air is thus likely to be approximately satisfied for some range of middle latitudes, in which case long term evaporation should be equivalent to the net incoming radiation over the same period.

As a test of the above considerations the annual value of H (net incoming radiation) has been evaluated from equation (6c) for three regions in the British Isles, one in N.W. Germany and one in Sweden, for all of which annual rainfall-runoff data are available, and for Siwa in Egypt, for which natural evaporation is presumed to be nil. For the British Isles the necessary annual means of air temperature, vapour pressure and sunshine were extracted from Annual Summaries of the Monthly Weather Report and rainfall-runoff figures from those given by Penman (loc. cit., p.144). For the German area climatological data were extracted from Klima Atlas von Deutschland (Berlin 1921) and rainfall-runoff data from Fischer (1930). For Stockholm the climatological data were taken from Appendix I to Observations Mèteorologiques Suèdoises, 1908, and from Wallèn (1930). The latter also gives rainfall-runoff data for a basin to the S.W. of Stockholm. Appropriate data for Siwa were found in Climatological Normals for Egypt and the Sudan (Physical Department, Ministry of Public Works, Egypt, 1922). In evaluating H from equation (6c) it is necessary to specify the magnitude of r, the natural reflection coefficient for short wave radiation. This cannot be done with any great precision but, fortunately, except for water and snow, the reflection coefficients of natural surfaces do not vary enormously (see Brunt, 1939, p.113) and a figure of 0.2, as adopted by Penman for turf, would appear to be a reasonably average annual figure for a generally vegetated land area and has been used in the present calculations for the British Isles and Germany. For Sweden a value of 0.75 (appropriate to a snow covering) was assumed to apply through the winter months and 0.15 (appropriate to a vegetated area with a proportion of lakes) for the rest of the year. The only figures found for sand were those given by Shaw (Vol. 3, p.144) and of these the one given for "grey sand" (i.e. 0.18) was adopted rather than the alternative figure of 0.09 for "wet sand".

The essential climatological data and computed values of H are reproduced in Table 3, with the available rainfall-runoff data and, in the case of the British Isles, evaporation loss estimates provided by Penman. The latter figures are, in fact, Penman's figures for E_o (open water) multiplied by his suggested overall correction factor of 0.75 in order to convert to cropped soil transpiring at maximum rate.

Table 3. Estimates of Annual Net Incoming Radiation and Evaporation

Stations	Dalwhinnie	Hutton & Stonyhurst	Rothamsted & Greenwich	Luneberg Oldenburg Erfurt	Stockholm	Siwa
Latitude °N	57	54	51	52 (av.)	59	29
Period of weather data	1936	1932-7	1928-36	-	(i) 1859-1925	1911-20
Annual means of Air Temperature, °F	43.1	48.5	49.3	46.6	42	70.5
Vapour pressure, mm. Hg.	6.1	7.4	7.6	7.1	6.2	(iii) 10.8
Fraction of possible sunshine	0.23	0.30	0.33	(iv) 0.35	(ii) 0.30, 0.41	(iv) 0.86
H (from equation (6c)) inches water/year	13	15	17	17	(vi) 13	52
E - cropped soil - Penman inches water/year (v)	13	15	17	-	-	-
Rainfall-run off inches water/year	10	17	19	18	14	assumed 0
Catchment area and period	Spey 1936	Rivington 1932-8	Lea 1928-36	Weser 1896-1915	Nyköpingsån	-

Notes (i) For temperature only - period for rest of data not known.
(ii) For winter months and rest of year respectively.
(iii) Based on 8 a.m. observations only.

(iv) Based on average cloud amount.

(v) Penman, 1948, Table 13, p. 144. These figures are based on 1930-39 climatological data throughout.

(vi) Radiation data given by Wallèn (loc. cit., p. 12) lead to a figure of 16 inches but it is not clear to what extent this data taken into account the reflection of short wave radiation from the ground.

From Table 3 it is seen that, except for Siwa, the computed values of H are in fair agreement with the evaporation losses indicated by the catchment area data. The difference in the case of Siwa is not surprising in view of the relatively low latitude. The most striking feature from the present point of view, however, is the fact that for the British Isles these values of H are identical with the estimates of natural evaporation provided by Penman's empirical method based on open water tank performance.

These results have two important consequences. In the first place, they suggest that the long term identity of net incoming radiation and heat loss due to evaporation does hold to a reasonable approximation in the British Isles and in similar latitudes elsewhere in Europe, in which case, in the absence of catchment area data, the correct order of mean annual evaporation may be estimated very easily from climatological data without any assumptions regarding the evaporative conditions at the surface. In the second place, the results have an immediate bearing on the significance of the ultimate test which the catchment area data provide for Penman's method for estimating natural evaporation. The whole point of the latter method reduces to the specification of the amount of heat carried away by the air but it follows from the above considerations that the test is concerned with circumstances in which this heat term is of a negligible order. The test is thus, in fact, a very limited one and cannot be regarded as a justification for the application of Penman's method in general, e.g., to shorter periods of time and for specific localities, when heat transfer to the air is not necessarily negligible.

9. Recapitulation

A number of features have been discussed in this note and it is perhaps appropriate to conclude by summarising the situation which, in the writer's view, now exists in the problem of estimating natural land evaporation from meteorological data. The problem may be considered in three categories, according to the definition and accuracy required.

(a) The accurate estimation of local evaporation for specific ground and weather conditions.

For this requirement the aerodynamically based method outlined in sections (4) and (5) appears to be the only dependable method at present available. The full application of the method admittedly requires careful observations of the vertical distribution of wind velocity and humidity near the ground and this procedure is one which can be economically adopted only in special research problems. We may include in the latter category the testing of more general and less exacting estimations; in other words, it is suggested that the method may be regarded as a standard for specifying evaporation when, as is usually the case, the directmeasurement of evaporation is impracticable. The method is, of course, only dependable and practicable in open country away from obstructions and marked variations in contour.

(b) The estimation of land evaporation as a broad climatological feature in terms of standard climatological data.

The method developed by Penman, based initially on open water tank performance and requiring only mean values of air temperature, vapour pressure, amount of sunshine and wind speed, is justified by annual rainfall-runoff data for the British Isles. However, in view of the restricted empirical basis of the method and the special circumstances of the ultimate test it seems doubtful that the method can be applied with confidence outside the circumstances of test. Moreover, the considerations of section (8) suggest that, at any rate for the British Isles and similar latitudes elsewhere in Europe, the application of the method to the broad estimation of annual land evaporation is no more reliable than a simple and more direct approach in which, on the average spacially and temporally, evaporation is equated to the net income of radiant energy. The latter method may be applied in terms of data on air temperature, vapour pressure and sunshine only, with an estimate of the reflection coefficient appropriate to the terrain involved.

(c) The approximate estimation of local evaporation for specific ground and weather conditions, without observations of a special character.

This is a requirement mid-way between (a) and (b) and except for the special case of wet ground there appears to be no reliable mid-way procedure for dealing with it. However, the method here suggested for wet ground, a physically acceptable extension of Penman's "combined sink strength and energy balance" method for tank evaporation, could, in due course, be extended to other ground surfaces following the accumulation of data on the effective state of saturation of such surfaces, by systematic application of the method for (a). The meteorological data otherwise required are air temperature, vapour pressure and wind speed at a standard height near the ground, amount of sunshine (or cloud cover) and an estimate of the "roughness parameter" of the surface.

References

Calder, K.L., 1949, Quart. J. Mech. App. Math. II, Pt. 2, p. 154.
Deacon, E.L., 1949, Quart. J.R. Met. Soc., 75, No. 323, p. 89.
Ertel, H., 1933, Met. Z., 50, p. 386.
Fischer, K., 1930, 111 Hydrologische Konferenz der Baltischen Staaten, Warszawa, 1930.
Goldstein, S., 1938, Modern Developments in Fluid Dynamics, (Oxford).
Montgomery, R.B., 1940, Pap. Phys. Oceanogr. Met., Mass. Inst. Tech., 7, 4.
Pasquill, F., 1943, Proc. Roy. Soc. A, 182, p.75
1949, a, Proc. Roy. Soc., A, 198, p.116.
1949, b, Quart. J.R. Met. Soc., 75, No. 325, p.249
1950, a, Proc. Roy. Soc., A, 202, p. 143.
1950, b, Quart. J.R. Met. Soc., in press.
Penman, H.L., 1948, Proc. Roy. Soc., A, 193, p.120.
Powell, R.W., 1942, Trans. Inst. Chem. Eng., 18, 36.
Prandtl, L., & Tollmien, W., 1925, Z.f.Geophys, 1, 47.
Priestley, C.H.B. & Swinbank, W., 1947, Proc. Roy. Soc., A, 189, p.543.
Rossby, C.G., 1936, Pap. Phys. Oceanogr. Met., Mass. Inst. Tech., 4, 3.
Schlichting, H., 1936, Ingen. Arch., 7, 1.
Shaw, N., Manual of Meteorology.
Sheppard, P.A., 1947, Proc. Roy. Soc., A, 188, p.208.
Sutton, O.G., 1947, Q.J.R. Met. Soc., 73, No. 317-318, p.257.
Sverdrup, H.U., 1937, J. Marine Research, 1, 3.
Thornthwaite, C.W., & Holzman, B., 1942, Tech. Bull. U.S. Dept. Agric., No. 817.
Wallèn, A., 1930, Stat. Met. Hydrog. Anstalt, Stockholm, No. 279.

Table 2. Computed Rates of Evaporation from a Clayland Pasture in selected near-isothermal conditions

Date	G.M.T.	u_{50} cm/sec.	$e_{25} - e_{50}$ mm. Hg.	e_{50} mm. Hg.	T_{50} °F.	$T_{50} - T_{25}$ °F.	$10^5 E$ gm/cm^{2}sec.	$10^5 Es$ gm/cm^{2}sec.	E/E_s
8.5.47	0900	344	0.46	11.4	65.0	-0.19	0.78	1.34	0.58
	1000	436	0.47	11.5	68.1	-0.15	1.02	2.38	0.43
	1100	279	0.40	12.0	67.6	-0.08	0.56	1.34	0.42
	1200	328	0.46	12.6	69.6	+0.17	0.75	1.79	0.42
	1400	332	0.39	11.0	67.4	+0.18	0.64	1.84	0.35
9.5.47	1200	509	0.53	10.3	74.9	-0.14	1.34	5.48	0.24
	1400	552	0.52	9.8	75.9	+0.07	1.42	6.53	0.22
10.5.47	0700	154	0.20	10.1	59.0	+0.12	0.15	0.38	0.39
	0800	234	0.28	10.5	60.9	-0.07	0.33	0.68	0.49
	1300	386	0.23	10.2	59.2	+0.10	0.44	0.95	0.46
	1400	339	0.09	10.7	56.7	-0.01	0.15	0.34	0.44
	1500	291	0.11	10.3	57.0	+0.10	0.16	0.42	0.38
	1600	245	0.12	9.2	55.0	+0.13	0.14	0.40	0.35
	1700	303	0.17	9.4	56.2	+0.10	0.26	0.58	0.45
	1800	243	0.12	9.6	56.0	+0.11	0.14	0.42	0.33
11.5.47	0600	260	0.12	7.6	50.0	+0.03	0.15	0.38	0.39
	1400	234	0.59	8.5	64.1	-0.19	0.68	1.54	0.44
12.5.47	0500	133	0.11	8.5	52.3	+0.14	0.07	0.19	0.37
	0600	124	0.13	9.0	53.3	+0.02	0.08	0.16	0.50
	0800	198	0.30	8.9	58.3	-0.04	0.29	0.65	0.45
	0900	209	0.26	9.2	59.1	+0.01	0.27	0.70	0.39
	1500	304	0.30	9.5	66.2	+0.09	0.45	1.93	0.23
	1600	285	0.34	9.8	65.6	+0.18	0.48	1.63	0.29

u_{50} wind velocity at a height of 50 cm.
e_{25}, e_{50} vapour pressures at heights 25 and 50 cm.
T_{25}, T_{50} air temperatures at heights 25 and 50 cm.
E rate of evaporation computed from the established formula (14) with $z_2 = 50$ cm., $z_1 = 25$ cm. $u_1/u_2 = 0.81$, $d = 4$ cm. (See Pasquill, 1949, b)
Es rate of evaporation computed from equations (19) and (8) (effectively the same as equation (14)) with $z_o = 0.7$ cm., $d = 4$ cm., and assuming X_o to be the saturation value at temperature T_{50}.

G.269826/JMB/9/50/40

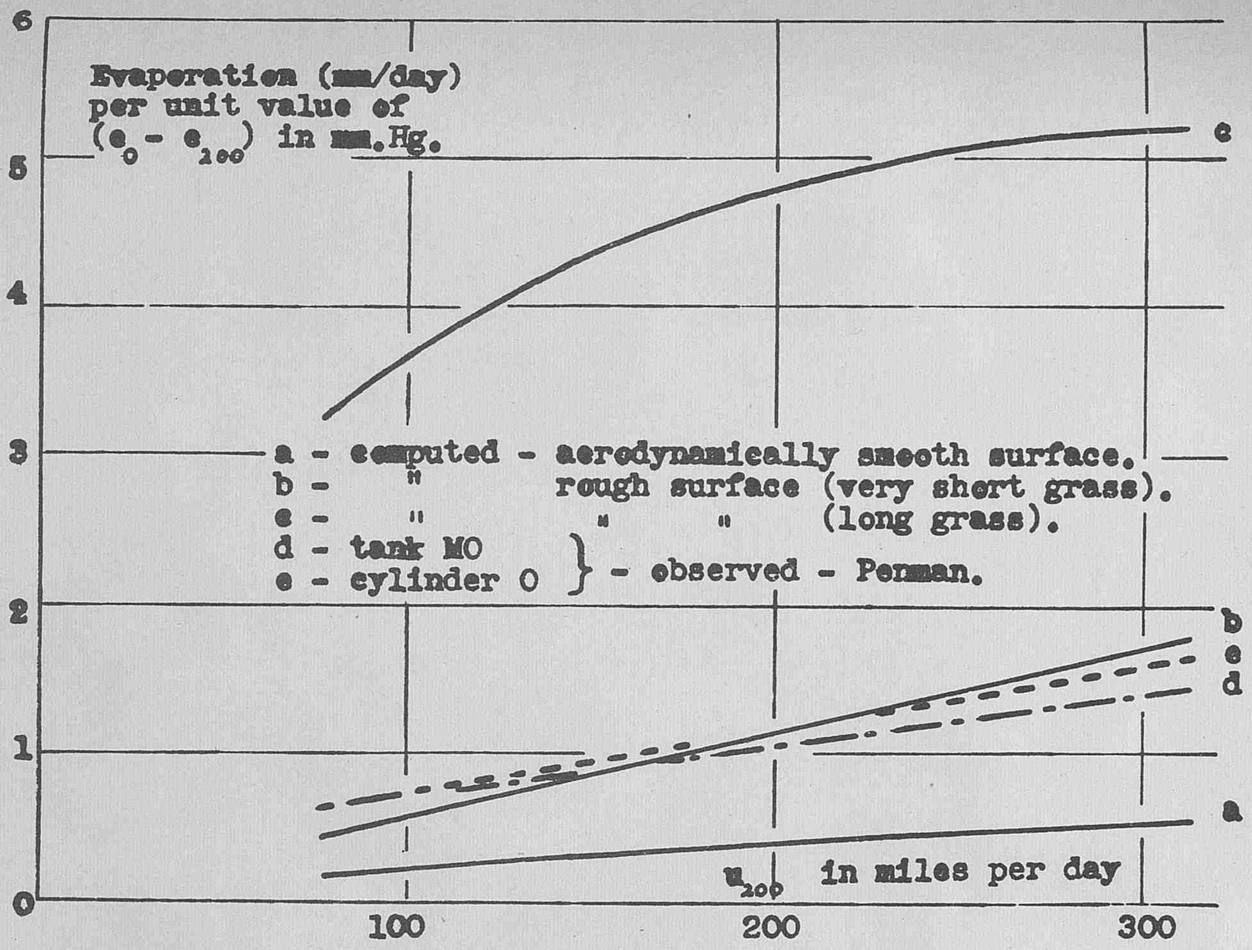

Fig.1. Comparison of computed evaporation from extensive smooth and rough surfaces with open water tank evaporation observed by Penman.

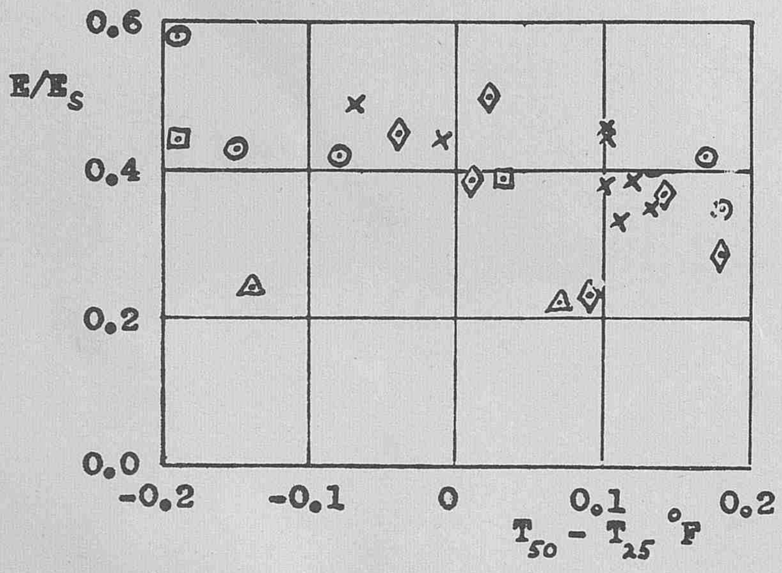

Fig.2. E/E_s for a growing pasture in fair spring weather, where E is the rate reliably computed from humidity and wind profile observations and E is the rate computed assuming that the surface is saturated and that isothermal conditions exist. The symbols ⊙ ◬ × ⊡ ⟐ refer to observations on 8, 9, 10, 11 and 12 May 1947 respectively.

CATALOGED BY ASTIA
AS ATI No. 103791

C 8 1950

SERVICE
ENCE FILES

Atmospheric inhomogeneity on the 50 - km Scale

by

Ronald Frith (Meteorological Office)

Many reports have been published analysing convective patterns in the so-called "convective" layer of the atmosphere. M.R.P. 402 contained the first description of similar patterns in air at levels which are normally considered to be well above convective processes. These patterns were revealed by measuring, and mapping, temperature and humidity at a large number of points on an isobaric surface.

The observations were made from an aeroplane and were, of course, not synchronous. As a rule 30-60 minutes elapsed between the first reading and the last. In Part II of the present paper we show that the changes which take place in 30-60 minutes may be large; but as a rule the broad picture remains the same.

M.R.P. 402 gave full details of three such maps. The general conclusions drawn were that well defined temperature and humidity patterns, with a horizontal scale of the order of 50 km, and an amplitude of the order of one degree in temperature and 10 degrees in frost point, exist in the free air, and also that there can be a close resemblance between the isotherms and the frost point isopleths - warm air being dry and cold air moist.

Some 50 maps have now been obtained at levels up to 20,000 ft and the results of the first few flights amply confirmed. The purpose of the present note is:

(a) to show that the temperature and humidity patterns are associated with vertical air motion (Part I);

(b) to provide information on the vertical dimensions of the patterns; and to discuss the changes which take place in time (Part II);

(c) to illustrate results obtained using a slightly different investigational technique (Part III).

In an appendix we discuss the statement that the variations of indicated aircraft speed which we have analysed, are not due to non-meteorological factors (e.g. variations of engine power).

/PART I

contents must not be quoted.

M.R.P. 583
S.C.II/71
26/9/50

DEC 3 1950
AIR WEATHER SERVICE
TECHNICAL REFERENCE FILES

AIR MINISTRY

METEOROLOGICAL RESEARCH COMMITTEE

Atmospheric inhomogeneity on the 50 - km Scale

by

Ronald Frith (Meteorological Office)

Many reports have been published analysing convective patterns in the so-called "convective" layer of the atmosphere. M.R.P. 402 contained the first description of similar patterns in air at levels which are normally considered to be well above convective processes. These patterns were revealed by measuring, and mapping, temperature and humidity at a large number of points on an isobaric surface.

The observations were made from an aeroplane and were, of course, not synchronous. As a rule 30-60 minutes elapsed between the first reading and the last. In Part II of the present paper we show that the changes which take place in 30-60 minutes may be large; but as a rule the broad picture remains the same.

M.R.P. 402 gave full details of three such maps. The general conclusions drawn were that well defined temperature and humidity patterns, with a horizontal scale of the order of 50 km, and an amplitude of the order of one degree in temperature and 10 degrees in frost point, exist in the free air, and also that there can be a close resemblance between the isotherms and the frost point isopleths - warm air being dry and cold air moist.

Some 50 maps have now been obtained at levels up to 20,000 ft and the results of the first few flights amply confirmed. The purpose of the present note is:

(a) to show that the temperature and humidity patterns are associated with vertical air motion (Part I);

(b) to provide information on the vertical dimensions of the patterns; and to discuss the changes which take place in time (Part II);

(c) to illustrate results obtained using a slightly different investigational technique (Part III).

In an appendix we discuss the statement that the variations of indicated aircraft speed which we have analysed, are not due to non-meteorological factors (e.g. variations of engine power).

/PART I

PART I

To show that the temperature and humidity patterns are associated with vertical air movement

With few exceptions our flights followed the general pattern described in M.R.P. 402. Parallel legs of 10-15 minutes duration (30-50 miles) and some five miles apart, were flown so as to cover a rectangular area, roughly square. The pilot was instructed to maintain a constant pressure height. Fluctuations from this fixed height rarely exceeded ± 30 ft or lasted for more than half a minute ($1\frac{1}{2}$ miles). Readings were taken of indicated air speed, indicated height and indicated temperature every 10 seconds (about 1,000 yards). Readings of the frost point were made as rapidly as possible. The rate depended upon the dryness of the air, the variability of the frost point, and upon the skill of the observer. Normally on "ON" and an "OFF" reading (frost increasing and frost decreasing) could be obtained every 30-60 seconds.

The readings of the frost point hygrometer required no correction. The indicated temperature requires correction for speed. The true airspeed may be obtained from the indicated airspeed by correcting for the density of the air; but in the present analysis, for reasons given in the appendix, it is necessary to use the indicated air speed as it stands.

2. Methods of Analysis

Since it takes 30 to 60 seconds to obtain a frost point reading, humidity fluctuations of period less than a minute cannot be measured. In fact the frost point readings reveal the 20-50 km scale patterns practically undisturbed by smaller scale fluctuations. This is not the case with either the temperature or the airspeed, both of which are subject to quite large short period fluctuations. We therefore decided to group the observations on any one flight according to the frost point.

For each flight five humidity groups were defined so as to contain approximately the same number of observations in each. For each group the mean temperature (corrected for airspeed) and the mean indicated airspeed were calculated. The table below shows a typical analysis:-

Frost Point	19 to $20\frac{1}{2}$	21 to 22	$22\frac{1}{2}$ to $23\frac{1}{2}$	24 to 25	26 to 28°F
Mean Temp:	44.37	44.24	43.91	43.59	43.25°F
Mean I.A.S.	181.5	181.4	181.6	181.6	181.3 kts.

Table I

The relation between frost point and temperature is clear. From this particular example there seems to be little correlation between frost point and i.a.s. We do find that the correlation between frost point and air-speed is less well marked than that between frost point and temperature. Nevertheless there is a correlation. The table below shows the results of combining the data obtained from 50 flights:-

Mean Frost Point	-4	-7	-9	-11	-15	°F
Mean Temp. $\bar{T}$ +	-0.19	-0.04	+0.02	+0.10	+0.12	°F ± 0.02
Mean i.a.s. $\bar{v}$ +	-0.3	0.0	0.0	0.0	+0.3	kts ± 0.2

Table II.

The relation between F.P. and temperature remains clear, But the difference of mean temperature between the extreme groups is less than one third of the difference in the single case quoted above. This is due partly to the fact that some of the areas mapped were clearly cut by a frontal surface - with moist, warm air on one side and dry, cold air on the other.

The table makes it clear that, on the whole, the aircraft has a higher i.a.s. in dry (warm) air than in moist (cold) air. In an appendix we give reasons for deciding that this difference in airspeed is not due to any change in the performance of the aircraft - either on account of the change in humidity or the change in temperature or density of the air. This being so then a higher airspeed (the aircraft being held at a constant pressure height) means either that the aircraft is descending the slope of an isobaric surface or that the aircraft is in a region of ascending air and is, in effect, descending in order to remain at the same level. There is a third possibility:- that the horizontal winds are varying and that the aircraft, slow to respond to a change of horizontal wind on account of its momentum, shows, for example, an increased i.a.s. for a time after running into a stronger head wind. However, bearing in mind that the temperature and humidity patterns are distributed quite at random relative to the aircraft courses, it is difficult to see how changes of horizontal wind could give rise to the correlation found.

Variations in the height of the pressure surface, on the other hand, must occur - since the density is variable. But an aircraft, at a point on a sloping pressure surface, may be ascending or descending according to which way the aircraft is flying. Since the aircraft courses are not related to the patterns there should be no correlation, on this account, between airspeed and humidity. Moreover the slopes of the pressure surface due to the patchiness of temperature may be shown to be too small to have any significant influence upon the airspeed.

It seems, then, that the changes in indicated airspeed are due to vertical motion of the air.

If an aircraft, flying at a fixed pressure level, encounters air which is ascending it will "descend" in order to keep level. Therefore its speed will increase. An estimate of the response of the aircraft to various rates of ascent has been obtained as follows:- The aircraft, a Halifax, was flown at a constant speed and height, then without any adjustment of engine controls, it was made to climb at such a rate that the indicated airspeed remained constant at some other, lower, value. The rate of climb was found to be practically constant (after the first 20 seconds), as follows:-

Speed	160	155	150	145	140 kts.
Rate of ascent	0	80	140	180	260 ft/min.
Speed	160	165	170	175	180 kts.
Rate of descent	0	120	200	300	440 ft/min.

Table III

During the first 20 seconds the mean rate of ascent was three to four times as great as these figures indicate.

We shall ignore the difference between ascent and descent and assume a round figure of 1 kt for 20 ft/min.

Thus if the aircraft flies suddenly into an up-current of n ft/min there will be little change of airspeed at first but within 20 seconds the speed will have increased by about $\frac{n}{20}$ kts.

Referring back, now, to table II we see that the mean i.a.s. is greater in warm, dry, air than in cold, moist, air - and the difference is about 0.5 kt. On the basis of the arguments used above this indicates that warm, dry air tends to be ascending and cold, moist air tends to be descending - the mean relative motion being of the order of 10 ft/min.

Since the warm dry air is lighter than cold moist air this result is not difficult to accept. It implies that "turbulence", on this scale, results in a mean flux downwards of water vapour.

/Appendix

APPENDIX

The speed of an aircraft held in level flight depends upon the following factors:-

The engine thrust.
The weight of the aircraft.
The drag of the aircraft.
The air density.

During normal flying the variations in the weight of the aircraft and the drag are very slight and are certainly not related to variations in the frost point or temperature of the air.

There are slight variations in engine thrust due to temperature changes of the air but these effects are extremely small. Casual variations of engine thrust are unlikely to occur and in any case, these would be unrelated to the frost point.

Variations in the density of the air, at a fixed pressure level, arise from variations in temperature (variations of humidity at the levels we are studying have a negligible effect on density). It is known that, other things being equal, the true airspeed of an aircraft is greater the less dense the air. But in these circumstances it is practically true to say that the indicated airspeed is independent of the density of the air. For this reason the indicated airspeed, instead of the true airspeed, has been used in the analysis in this paper.

/Hence

Figure 2 shows a vertical grid made in the second way between heights 9,000 - 15,000 ft. The first half of the grid was flown from South to North: the second half on a reciprocal course. The lag of the temperature element is serious when the aircraft is ascending or descending rapidly. Some attempt has been made to correct for this but it must be recognized that the temperatures are not very accurate.

Here, as in Figure 1, an inversion of variable intensity is revealed with a close association, both in the inversion and elsewhere, warm-dry and cold-moist.

It is difficult to read into these pictures anything resembling wave motion. It seems far more likely that we are investigating discrete bubbles of air some 20 km across and some 2,000 ft in depth.

23rd FEBRUARY, 1949

When two aircraft are available, some information about the vertical structure can be obtained by flying one of the aircraft vertically above the other. One of the aircraft is generally a Mosquito and it is not practicable for the single observer to take rapid readings of temperature, airspeed and humidity. We are therefore able to compare only temperature and airspeeds. We find, generally, that the temperatures agree quite well so long as the aircraft are not more than 500 ft apart. With increasing separation the similarity decreases and when the aircraft are 2,000 ft apart there is generally little resemblance between the records.

In Figure 3 we show temperature and speeds obtained when flying the Halifax at 9,000 ft and the Mosquito, vertically above, at 9,250 ft. On this occasion a grid of four 10-minute legs was covered twice - the last leg

/of

PART II

Special flights have been made to obtain an idea of the vertical structure of the turbulence patterns we have been studying and also to see how the structure in the horizontal changes with time.

1. The Vertical Structure

Several techniques have been tried out to obtain a picture of the vertical structure of the atmosphere. The two most useful are

(1) A 'grid' similar to the horizontal grid, but with the legs as near by as possible in a vertical plane.

(2) A grid obtained by causing the aircraft to maintain a constant heading - but alternatively ascending and descending through the chosen layer of the atmosphere.

26th JULY, 1948

Figure 1 shows a vertical grid of the first type - covering the layer 650 to 550 mbs (approx. 12,000 to 16,000 ft.) The flight took about 1½ hours to complete.

It will be seen that there was a marked inversion in the eastern end of the section and it is interesting to note how local is this strong inversion. The example illustrates how unrepresentative an isolated upper air-sounding may be; and how circumspect one must be in applying the details of such soundings in forecasting or analytical technique.

4th AUGUST, 1948

Figure 2 shows a vertical grid made in the second way between heights 9,000 - 15,000 ft. The first half of the grid was flown from South to North: the second half on a reciprocal course. The lag of the temperature element is serious when the aircraft is ascending or descending rapidly. Some attempt has been made to correct for this but it must be recognized that the temperatures are not very accurate.

Here, as in Figure 1, an inversion of variable intensity is revealed with a close association, both in the inversion and elsewhere, warm-dry and cold-moist.

It is difficult to read into these pictures anything resembling wave motion. It seems far more likely that we are investigating discrete bubbles of air some 20 km across and some 2,000 ft in depth.

23rd FEBRUARY, 1949

When two aircraft are available, some information about the vertical structure can be obtained by flying one of the aircraft vertically above the other. One of the aircraft is generally a Mosquito and it is not practicable for the single observer to take rapid readings of temperature, airspeed and humidity. We are therefore able to compare only temperature and airspeeds. We find, generally, that the temperatures agree quite well so long as the aircraft are not more than 500 ft apart. With increasing separation the similarity decreases and when the aircraft are 2,000 ft apart there is generally little resemblance between the records.

In Figure 3 we show temperature and speeds obtained when flying the Halifax at 9,000 ft and the Mosquito, vertically above, at 9,250 ft. On this occasion a grid of four 10-minute legs was covered twice - the last leg of the first run being the first leg of the second. Thus there were 7 legs in all - the seventh being not very far away from where the first was flown, but about an hour later. Readings were made every 15 seconds - but in order to reduce the effect of the short period temperature fluctuations, running means over one minute (five readings) have been taken.

The similarity of the temperature traces is obvious, and needs no comment.

The readings of airspeed have not been meaned. Many of the short period fluctuations are due to inadvertent changes of height by the pilot. But it is obvious that there are larger period fluctuations of speed - amounting to more than 5 knots - which are similar for the two aircraft. No clear correlation between temperature and air speed is revealed.

It seems practically certain that these fluctuations of airspeed are caused by vertical motion in the atmosphere. Previous analysis has shown, as was to be expected, that, on the whole, warm air is ascending and cold air descending but it is clear that, in any particular case, warm air may be going up or down.

According to the figures given in Part I of this paper, the strength of the vertical drafts revealed in this flight is of the order of 100 ft/min.

The change with time

Our Halifax aircraft are fitted with so-called Air Position Indicators. These instruments are controlled by the compass bearing and the airspeed. Using the A.P.I. it would be possible, if the wind were uniform and steady, to return repeatedly to exactly the same spot in the air. In fact, of course, the winds are neither uniform nor steady so that it is impossible to return to any given spot. However, over areas 50 x 50 miles and time intervals of less than an hour, the variations of wind, on a synoptic scale, will not cause errors greater than one or two miles. Therefore if the same square of air is flown over twice changes of pattern larger than can be accounted for by the synoptic wind variations must be due to fluctuations of wind on a smaller scale, or due to vertical motion. In the presence of the vertical motion which we believe we have shown to exist, there must be horizontal eddy-motion on a similar scale; but no method is known of measuring this.

3rd DECEMBER, 1948

Figure 4 shows a typical repeated square in which an area some 30 miles square was flown over twice, the last leg of the first grid being the first leg of the second grid. The last reading was made about two hours after the first.

This example has been selected because of the interesting observations of bumpiness. Bumpiness was reported at every observation in the shaded areas. There is a clearly defined lane of bumpiness which is drifting towards the west - relative to the air. It lies, on both maps, along the western slopes of a "trough" of moist air.

The changes in the temperature and frost point patterns are greater than usual. It seems almost certain that large changes such as these can only be due to vertical advection.

/PART III

PART III

Recent Work

1. Since the scale of the "turbulence" pattern we are examining is of the order of 50 km it is clear that a 50 km square is quite inadequate to investigate the intensity and nature of the "turbulence" present. Larger squares are out of the question. We have therefore adopted a new technique. We fly for about 200 miles in a straight line, at a constant pressure height. To avoid any bias the flight is always out to the N.W. at 500 mbs (in a Halifax) or 200 mbs (in a Mosquito) and back on the reciprocal course at 700 mbs or 300 mbs. Typical examples of the results obtained from such flights were given and discussed in M.R.P. 552, and are not reproduced here. Instead we shall discuss results obtained from a somewhat earlier flight, made on slightly different lines. This flight is chiefly interesting in that it provides a good example of the evidence of true periodicity which is sometimes found.

11th AUGUST, 1949

Figure 5 shows the results of a flight in which the legs were 100 miles long. This example is of exceptional interest.

On the first leg, at 18,000 ft, there is a marked fall of frost point from -50 to -60°F. There is also a rise of temperature from -3° to + 5°F but whereas the humidity fall takes place entirely within 5 miles the temperature change is spread uniformly over 90 miles. In spite of this the humidity change is accompanied by a remarkable excursion of the airspeed (from 146 to 158 kts and back again to 145 kts). The sense of this change indicates that immediately prior to the humidity change the air was ascending (rate of ascent of the order 200 ft/min) and that the drier air was apparently descending. (Note both temperature and speed readings have been smoothed by taking running means over $1\frac{1}{2}$ minutes).

Throughout the steady rise of temperature one can trace a periodic fluctuation - indicated by letters 'M' - of length about 10 miles; and closely matched to this is a fluctuation of the airspeed, with high temperature corresponding to high speed (indicating ascent of air).

Towards the end of the run there are two clear waves of temperature and airspeed, marked 'N', also well matched. In Figure 6 we show the Upper Air observations over the Southern half of the country at 0900 and 1500h on this day (the flight was made at about 1200z). The 0900h Liverpool and Larkhill show a strong wind shear at 500 mbs but this has disappeared at 1500h and is not present at other stations. It seems likely that the two waves 'N' are evidence of Helmholtz waves caused by this wind shear.

On the second leg, at 90° to the first, the aircraft passed back into the cool moist air. Again the frost point change takes place far more quickly than the temperature change and again it is accompanied by a speed excursion - but in the opposite direction.

The 3rd and 4th legs were flown at 9,000 ft. The fourth leg provides another example of an abrupt change of frost point (+10 to -20°F in less than one minute ≑ 3 miles) accompanied by a much more gradual rise of temperature and by a marked excursion of air speed. In each of these cases (legs 1, 2 and 4) the graphs of air speed show sharp turning points coincident with the more or less abrupt frost point change.

These fluctuations of airspeed may be due either to fluctuations in the height of the pressure surface; or due to fluctuations in the vertical component of the wind.

Variations in the height of the pressure surface would be caused by density variations; but the speed fluctuations are not particularly well matched to the temperature distribution curve. We feel justified in suggesting that here, in a particular case - as we have suggested earlier from a general analysis - the speed fluctuations are due primarily to vertical air movement.

If this is the case it implies that where the aircraft crossed the front on leg 1 there was a strong up-current, but where it crossed it on leg 2, a strong down-current. This would imply vigorous wave motion, in the vertical, on the frontal surface itself. Since the upper surfaces of inversions, and the tropopause, are known to be undulating it seems most probable that a frontal surface is also in wave motion.

M.R.P. 583

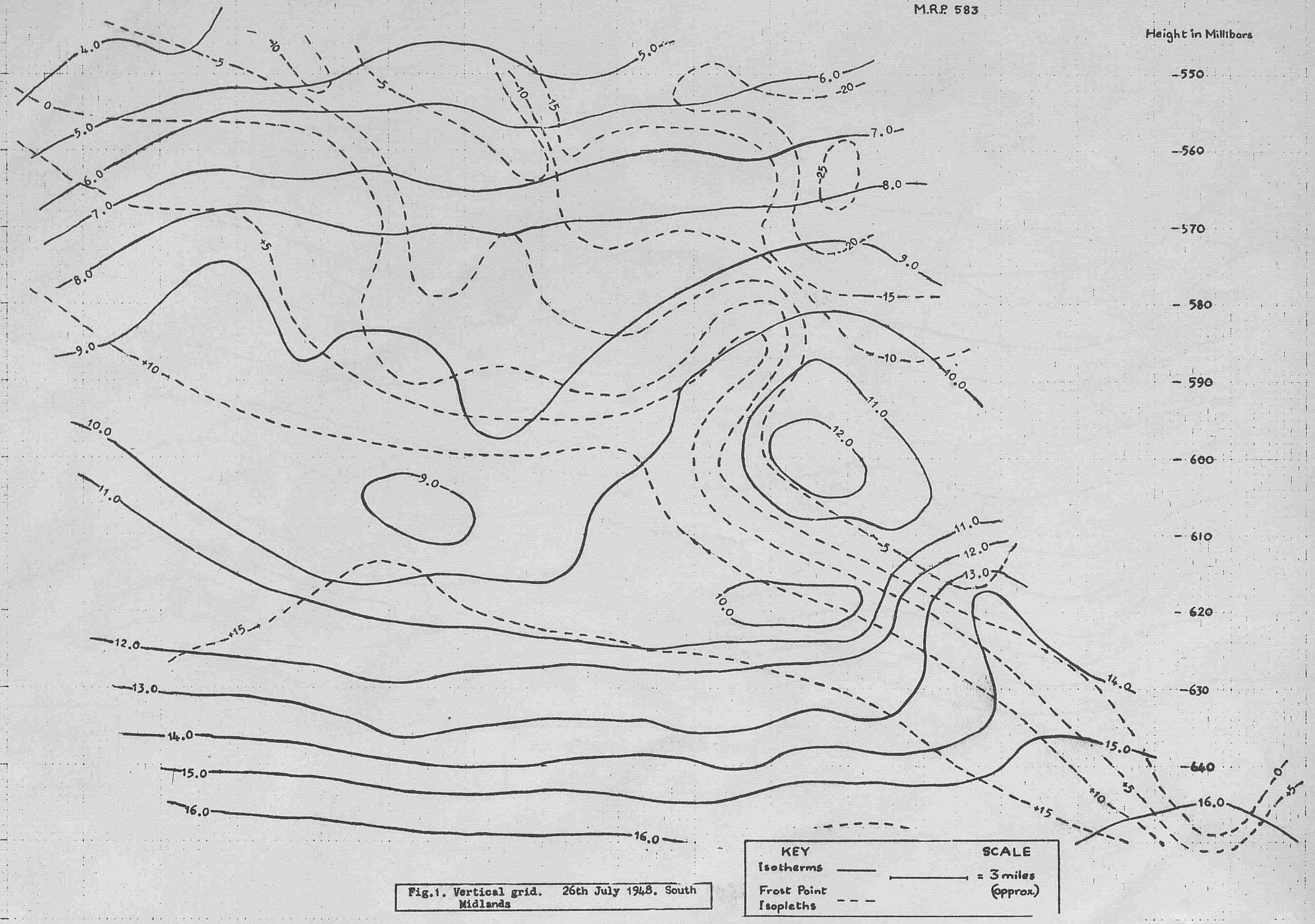

Fig.1. Vertical grid. 26th July 1948. South Midlands

MRP. 583.

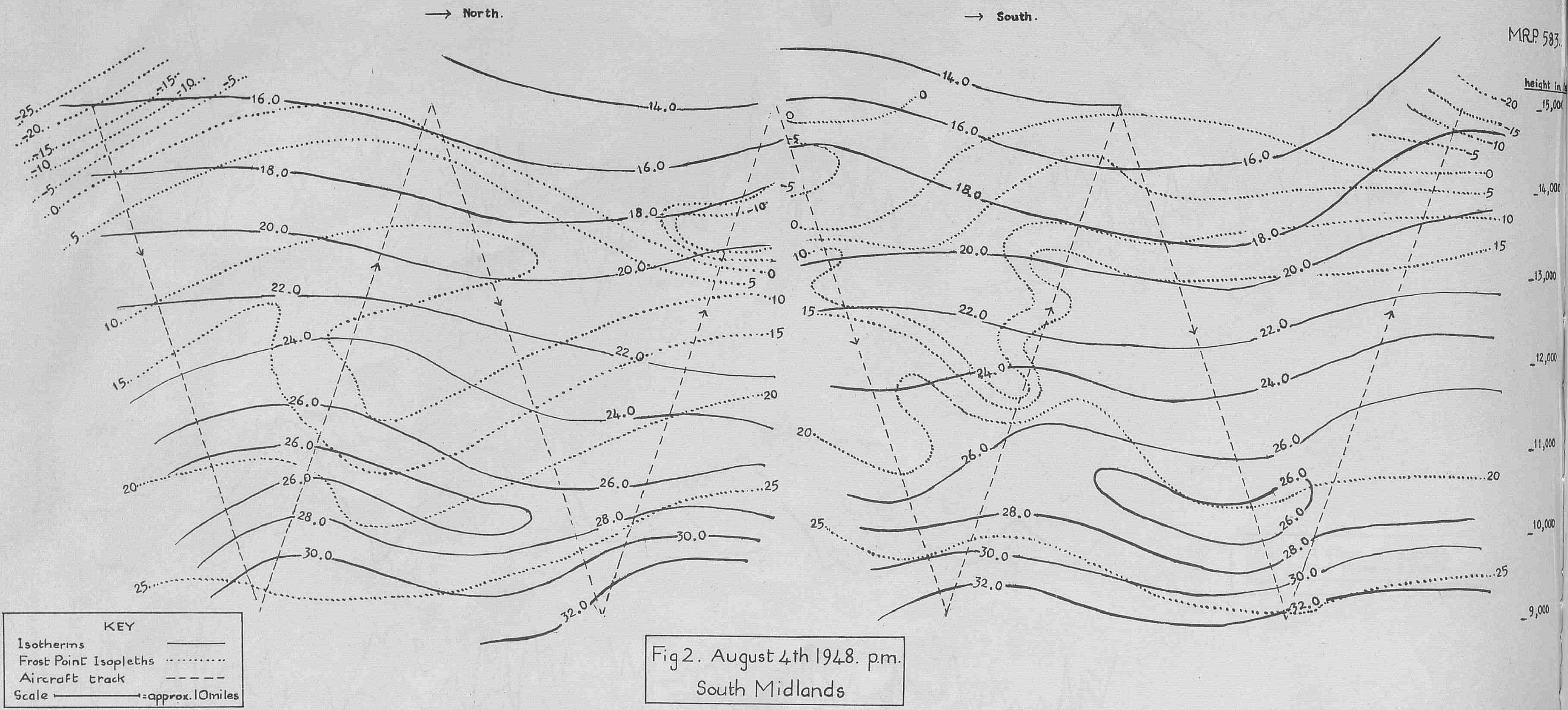

Fig 2. August 4th 1948. p.m.
South Midlands

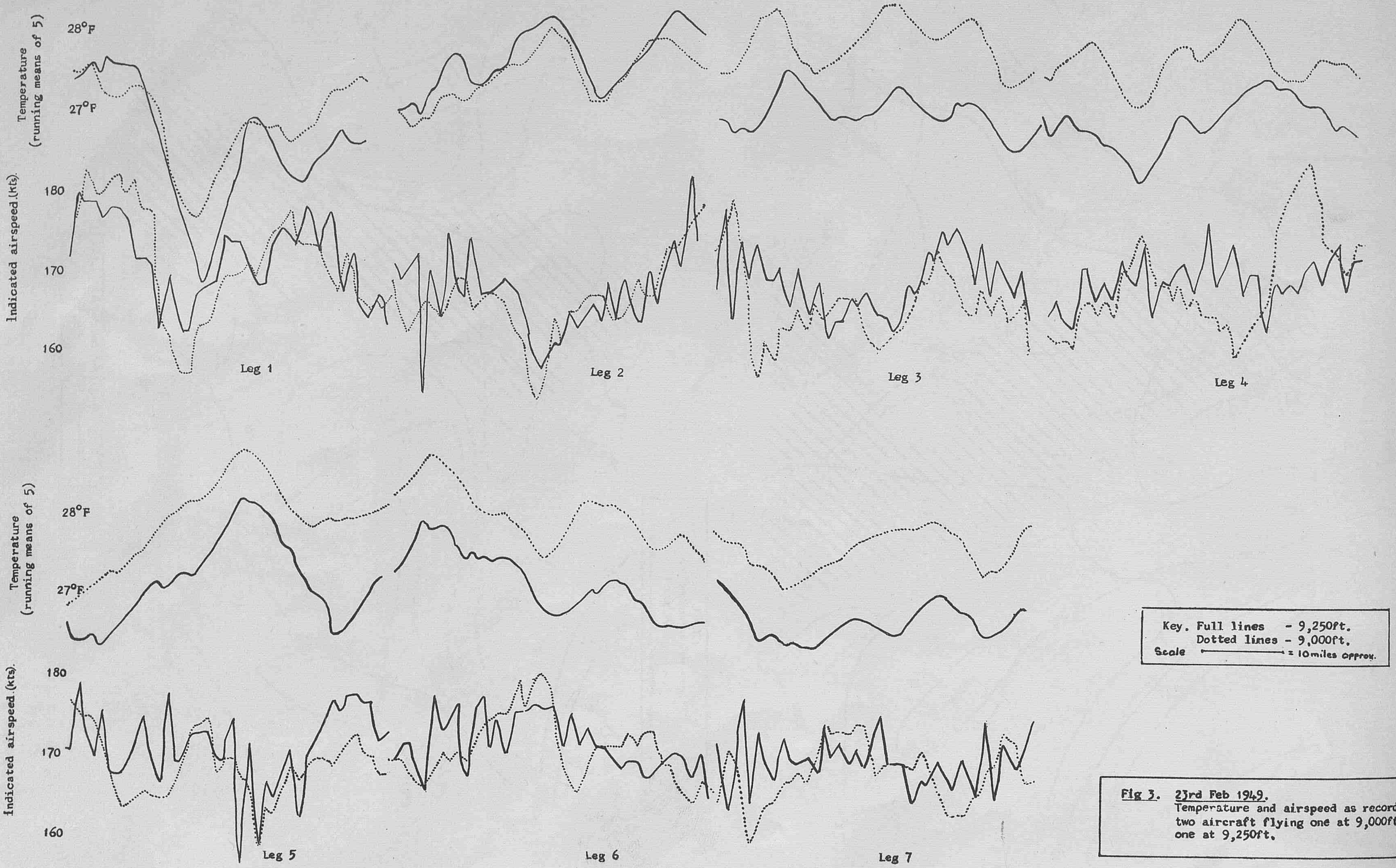

Fig 3. 23rd Feb 1949. Temperature and airspeed as recorded in two aircraft flying one at 9,000ft and one at 9,250ft.

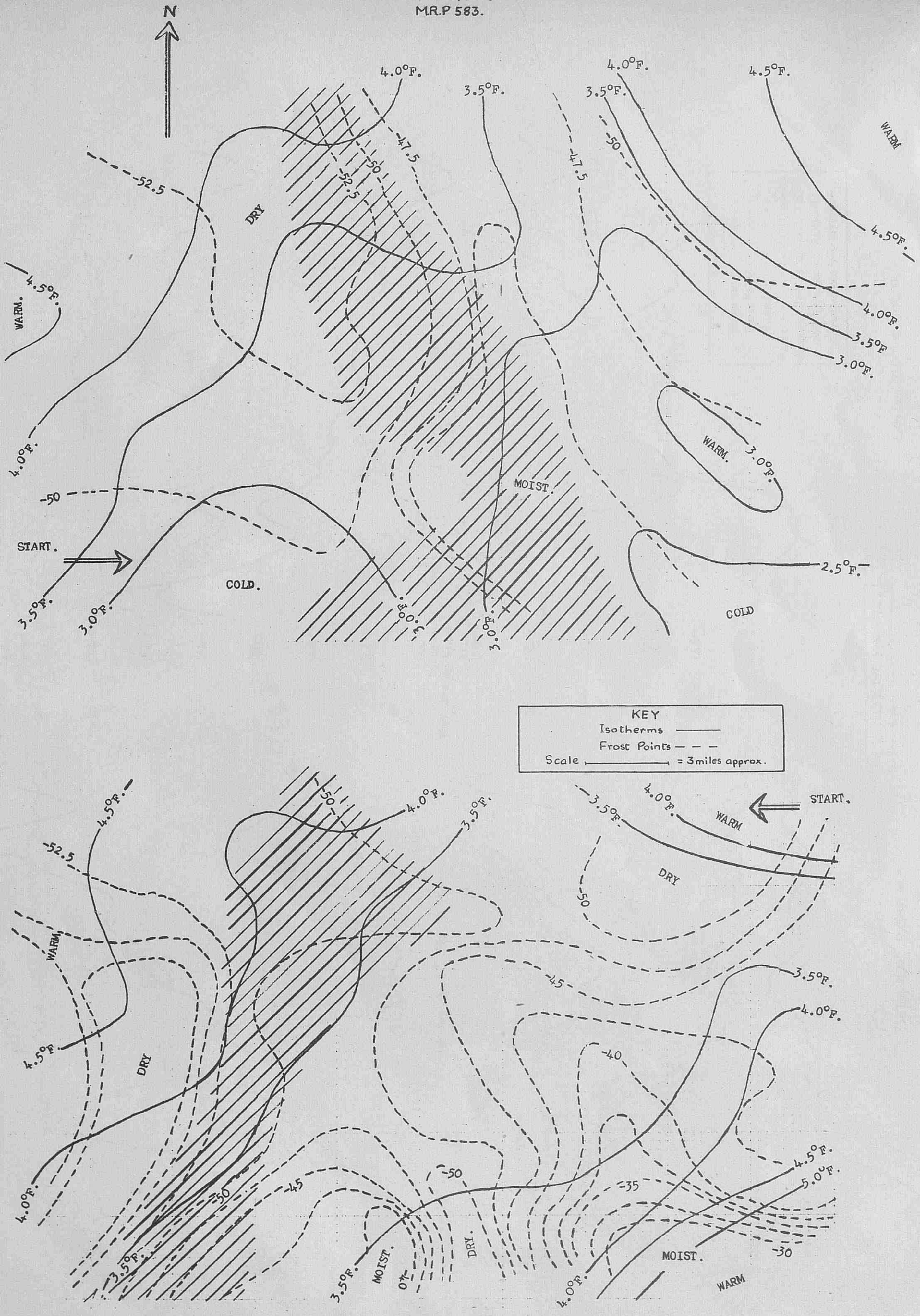
N
4.0°F.
3.5°F.
4.0°F.
3.5°F.
4.5°F.
WARM
-52.5
-47.5
-50
-52.5
-47.5
-50
DRY
4.5°F.
4.5°F.
WARM.
4.0°F.
3.5°F.
3.0°F.
4.0°F.
WARM.
3.0°F.
MOIST.
-50
START.
COLD.
2.5°F.
COLD
3.5°F.
3.0°F.
3.0°F.
3.0°F.
KEY
Isotherms
Frost Points
Scale = 3 miles approx.
4.5°F.
-50
4.0°F.
3.5°F.
3.5°F.
4.0°F.
START.
WARM
-52.5
DRY
-50
WARM
-45
3.5°F.
4.0°F.
4.5°F.
DRY
-40
4.5°F.
5.0°F.
-50
-50
-45
-35
4.0°F.
3.5°F.
MOIST.
0°F.
DRY.
MOIST.
-30
3.5°F.
4.0°F.
WARM

Fig.4. Repeated horizontal grid at 520 mb. South Midlands. Dec. 3rd. 1948

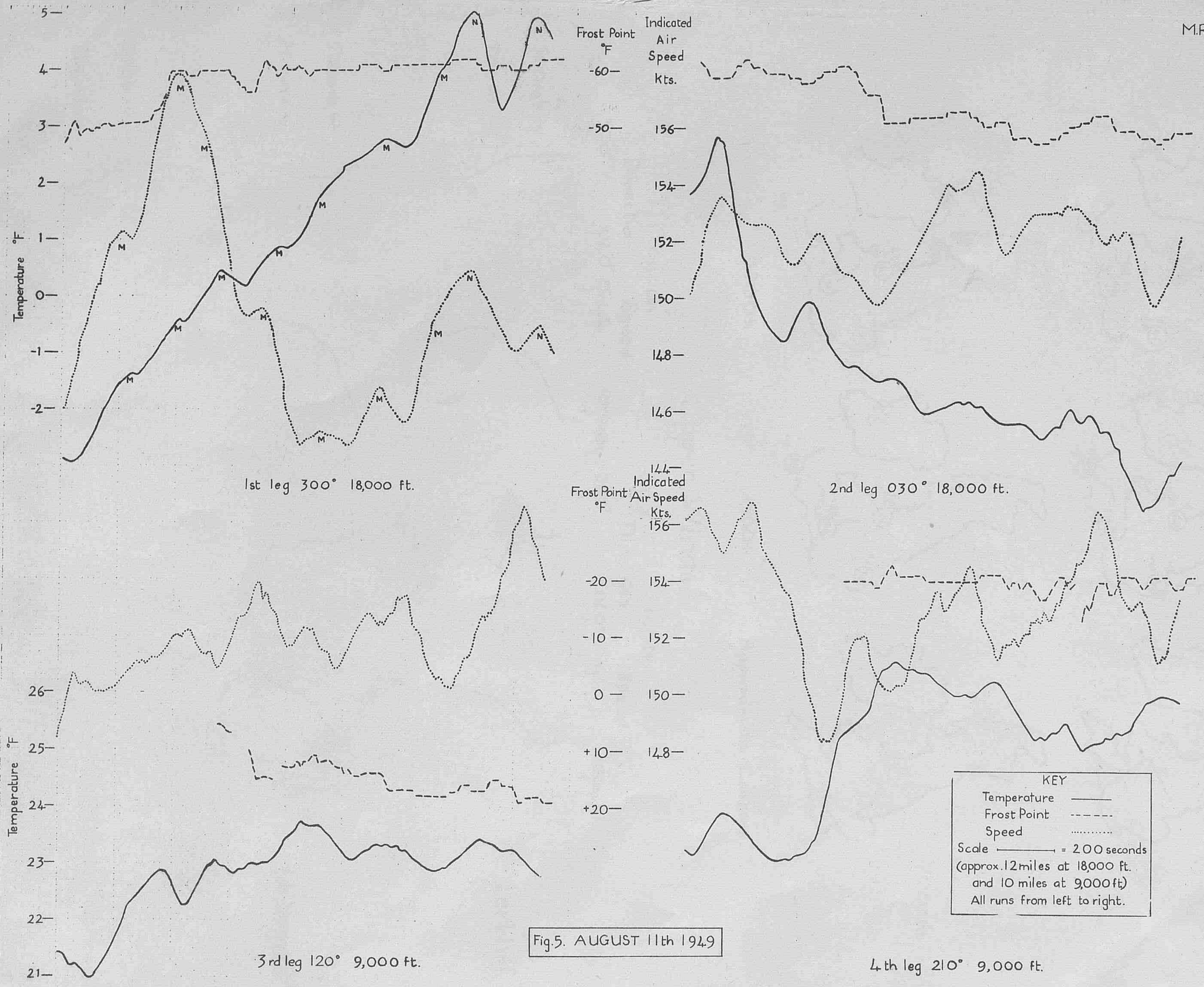

Fig.5. AUGUST 11th 1949

1st leg 300° 18,000 ft.

2nd leg 030° 18,000 ft.

3rd leg 120° 9,000 ft.

4th leg 210° 9,000 ft.

Temperatures, Frost Points and Winds.

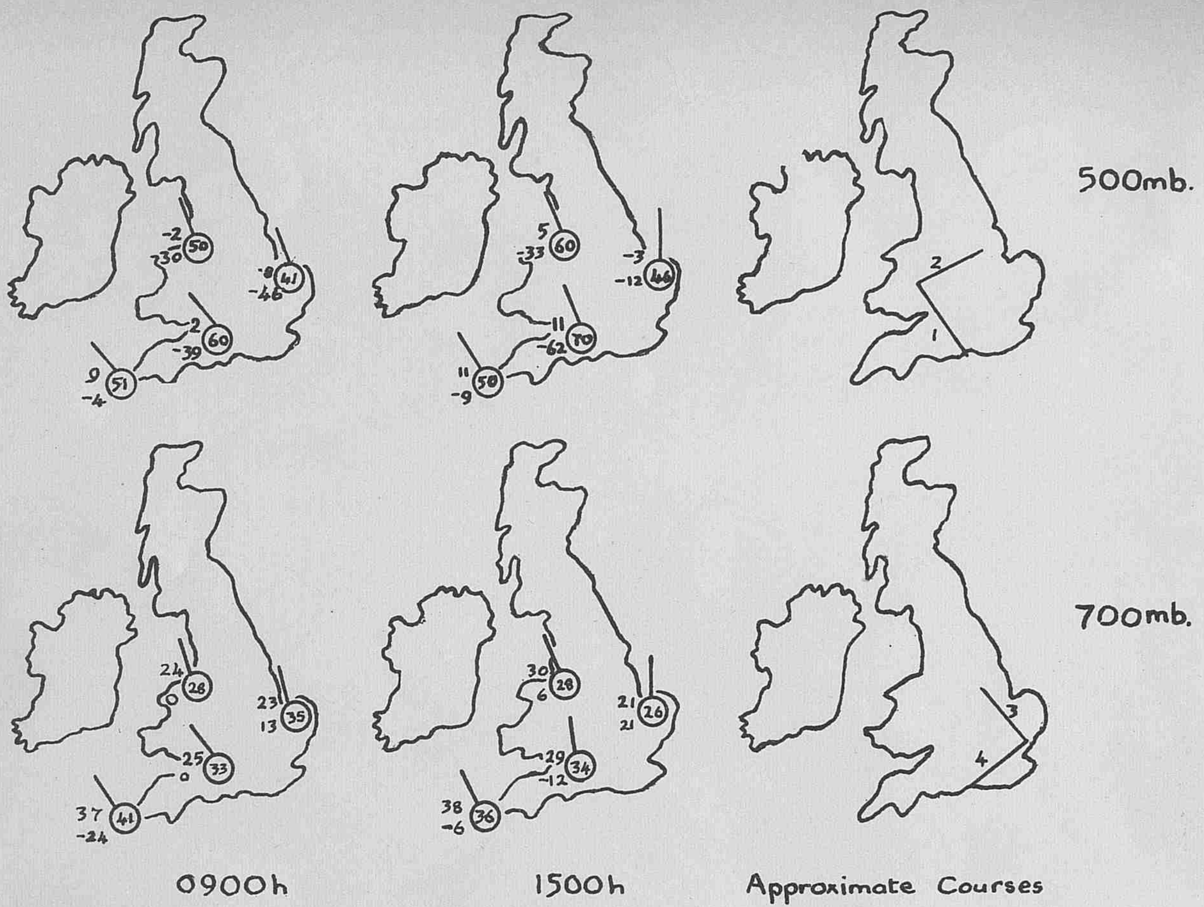
500mb.
700mb.
0900h
1500h
Approximate Courses
-2
-30
50
-8
-46
41
2
-39
60
9
-4
51
5
-33
60
-3
-12
46
11
-62
70
11
-9
58
2
1
24
0
28
23
13
35
25
0
33
37
-24
41
30
6
28
21
21
26
29
-12
34
38
-6
36
3
4

Upper Winds

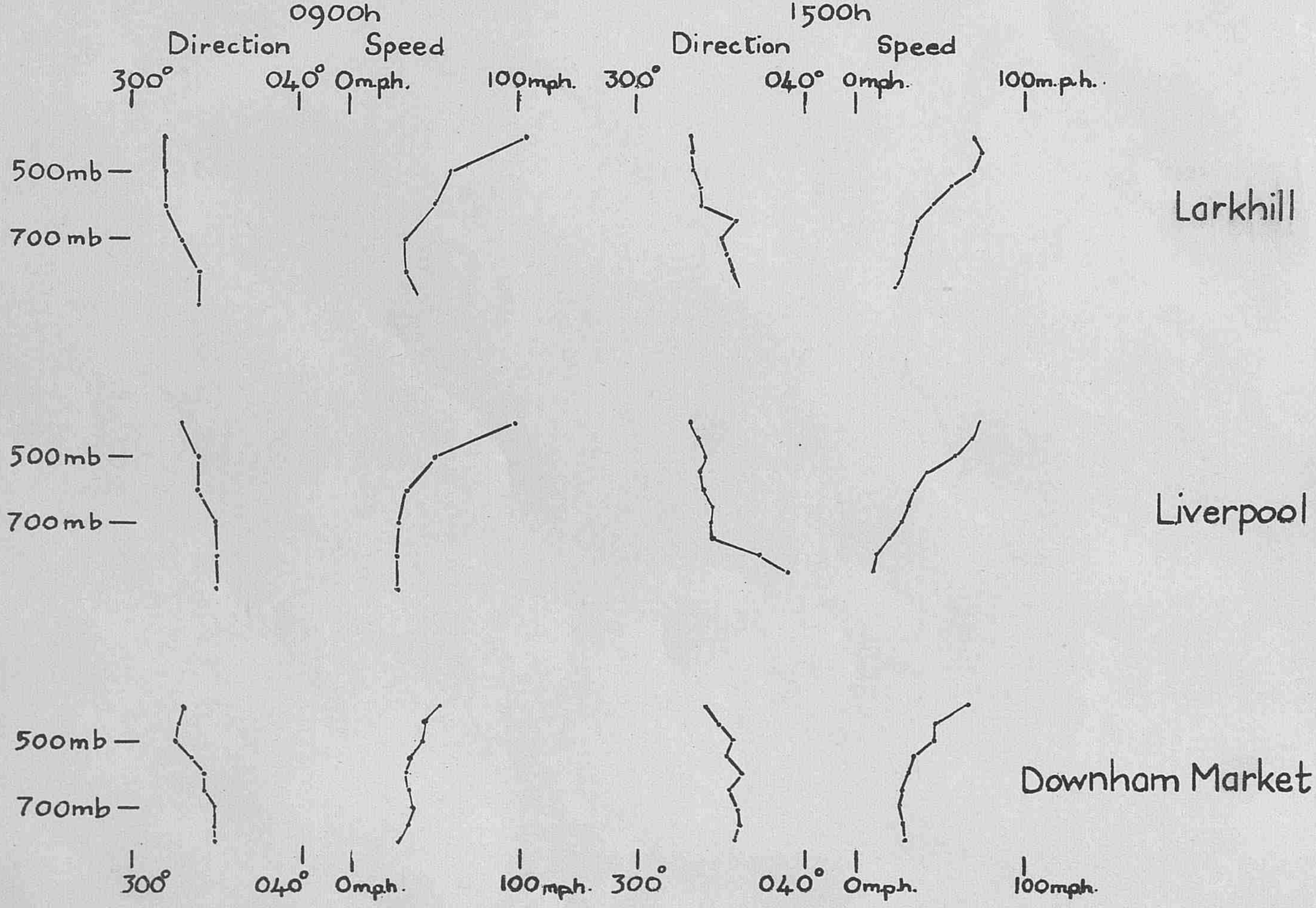

Fig. 6. August 11th 1949

At the time of issue this report has n
been published. Any author desiring t
quote this paper should refer to it as
paper of the Meteorological Res
Committee (London),
M.R.P. No .... by Mr. ....
A copy is available in the
the Meteorological

CATALOGED BY ASTIA
AS ATI No. 110 143

[illegible] REFERENCE FILE
JUN 6 1951

RE

by

A.G. Forsdyke

(Based for the most part on a more detailed report prepared in the Forecasting Research Division by Mr. E.J. Sumner).

1. Introduction. One of the problems in the M.R.C. research programme relating to medium range forecasting is entitled "Zonal, meridional and other indices." This problem was included in the programme because:

(i) there was a considerable literature on the subject, mainly American;

(ii) some use was being made of certain indices in extended forecasting in America;

(iii) such indices were not being used in current British forecasting practice, and it was desirable to decide whether their use could be recommended.

2. Definition: Indices in general. In this context an index is a number, usually derived by a process of averaging, expressing some large-scale property or process in the atmosphere. It is expressed numerically to make it suitable for quantitative treatment.

Indices were used by a number of early workers in statistical investigations connected with long range forecasting. Walker, for example, among many other indices, made use of the "North Atlantic oscillation," a linear combination of mean values, taken over a specified period, of pressure and/or temperature at selected stations in the North Atlantic. He correlated this quantity with numerous others expressing seasonal weather characteristics for particular places or regions. Similar statistical work with indices was described by Exner, Defant, Baur, and Brooks, in many original papers, references to which are to be found in Shaw, Manual of Meteorology, Vol.II, Chapter VIII.

3. Circulation Indices.

(a) General. In recent years numerous indices have been used as measures of the atmospheric circulation. Goldie (1936), for example, used the annual mean pressure differences between certain stations in Scotland as indices of the mean S.-N. and W.-E. air flow over the British Isles. He found interesting relations between these indices and the broad weather characteristics for the British Isles, years of maximum W.-E. flow for example corresponding to warmer and drier conditions than the average. More recently Jones (1943) used the daily difference of pressure between the Azores high and Iceland low as a measure of the strength of the westerlies on the NE. Atlantic. There was some suggestion of periodicities (ranging from 6 to 72 days) in the recurrence of extreme values of this index, but no clear association was found between it and the pressure types proposed by Goldie and used by Jones as a basis of classification.

(b) Zonal indices. During the last few years a large amount of work has been done, chiefly in the U.S.A., on indices devised to represent the strength of the circulation over the whole, or a large part, of the

/northern

~~At the time of issue this ... been published. Any author ... quote this paper should refer to ... paper of the Meteorological Res... Committee (London). M.R.P. No.......... by Mr.......... A copy is available in the Library of the Meteorological Office."~~

M.R.P.591
S.C.II/64
25th October, 1950.

AIR MINISTRY

METEOROLOGICAL RESEARCH COMMITTEE

REPORT ON ZONAL, MERIDIONAL AND OTHER INDICES

AIR WEATHER SERVICE
TECHNICAL REFERENCE FILE
JUN 6 1951

by

A.G. Forsdyke

(Based for the most part on a more detailed report prepared in the Forecasting Research Division by Mr. E.J. Sumner).

1. Introduction. One of the problems in the M.R.C. research programme relating to medium range forecasting is entitled "Zonal, meridional and other indices." This problem was included in the programme because:

(i) there was a considerable literature on the subject, mainly American;

(ii) some use was being made of certain indices in extended forecasting in America;

(iii) such indices were not being used in current British forecasting practice, and it was desirable to decide whether their use could be recommended.

2. Definition: Indices in general. In this context an index is a number, usually derived by a process of averaging, expressing some large-scale property or process in the atmosphere. It is expressed numerically to make it suitable for quantitative treatment.

Indices were used by a number of early workers in statistical investigations connected with long range forecasting. Walker, for example, among many other indices, made use of the "North Atlantic oscillation," a linear combination of mean values, taken over a specified period, of pressure and/or temperature at selected stations in the North Atlantic. He correlated this quantity with numerous others expressing seasonal weather characteristics for particular places or regions. Similar statistical work with indices was described by Exner, Defant, Baur, and Brooks, in many original papers, references to which are to be found in Shaw, Manual of Meteorology, Vol.II, Chapter VIII.

3. Circulation Indices.

(a) General. In recent years numerous indices have been used as measures of the atmospheric circulation. Goldie (1936), for example, used the annual mean pressure differences between certain stations in Scotland as indices of the mean S.-N. and W.-E. air flow over the British Isles. He found interesting relations between these indices and the broad weather characteristics for the British Isles, years of maximum W.-E. flow for example corresponding to warmer and drier conditions than the average. More recently Jones (1943) used the daily difference of pressure between the Azores high and Iceland low as a measure of the strength of the westerlies on the NE. Atlantic. There was some suggestion of periodicities (ranging from 6 to 72 days) in the recurrence of extreme values of this index, but no clear association was found between it and the pressure types proposed by Goldie and used by Jones as a basis of classification.

(b) Zonal indices. During the last few years a large amount of work has been done, chiefly in the U.S.A., on indices devised to represent the strength of the circulation over the whole, or a large part, of the northern hemisphere. These indices are computed from the pressure at a number of points regularly spaced along circles of latitude bordering a specified zonal band. The indices are typified by Rossby's (1939, 1941) zonal westerly index, which is the mean speed of the surface westerlies between lats. 35° and 55°N., calculated by taking the mean pressure difference between those latitudes at equally spaced longitudes and converting by means of the geostrophic relation. Corresponding indices for the other main branches of the planetary circulation have been defined, the three principal surface zonal indices being:

Polar easterlies 55° - 70°N.,

Prevailing westerlies 35° - 55°N., (often referred to as the Zonal Index).

Subtropical easterlies 20° - 35°N.

There are corresponding indices for the upper levels used as standard levels in synoptic meteorology. In America attention has been concentrated chiefly on the 700 mb. level and mean values for the zonal indices at the surface and this level have been computed for use in extended forecasting (Namias 1947).

Modification of these zonal indices are obtained by varying the width or the location of the latitude bands for which they are computed. Thus the so-called Max.-Min. indices are taken for the whole band between the maximum and minimum on the mean pressure profile from equator to pole. The modified Max.-Min. indices are taken for the 20° latitude band covering the greatest pressure differences on the same mean profile.

(c) Meridional indices. The meridional index is a measure of the total exchange of air across any specified parallel of latitude. It is computed by reading off, in sequence, the maximum and minimum values of pressure (or contour height) along the selected parallel; this divides the parallel into a number of segments along which the pressure increases or decreases alternately in a given direction. The sum of the pressure differences along either set of alternate segments is a measure of the meridional exchange of air.

4. Other indices. Among other indices the following may be mentioned as having been devised because of their possible bearing on the problem of medium-range forecasting.

(i) Solenoidal index, computed in the same way as a zonal index but using the thickness (or mean virtual temperature) for a specified pressure interval. This is in effect a thermal wind index and may alternatively be obtained from the difference between the zonal indices for the two levels.

(ii) Kinetic energy and momentum indices, respectively expressing the total kinetic energy and momentum of the air within a given latitude band.

(iii) Transport indices, providing measures of the resultant flux across a specified latitude of physical properties such as momentum and heat content of the air.

(iv) Total mass index, expressing the total mass of air in the northern hemisphere or selected latitude bands. This is computed from the integral of surface pressure over the area considered.

/(v)

(v) Thermal indices have been computed in connexion with the medium range forecasting experiment in the Meteorological Office. They show the daily value of mean latitude of certain standard 1000-500 mb. thickness lines, taken over a whole or half hemisphere. They also show the mean thermal gradient and the total area covered by air having thickness less than the selected standard values.

5. Indices in relation to the atmospheric circulation.

(a) Relation of indices to general circulation types. It has long been recognised that indices of some kind are an essential aid to a study of the nature and mechanism of the general circulation of the atmosphere, and most of the work on indices is concerned with this aspect of the subject. This wide field is, however, outside the scope of this report. It is to be expected, however, that indices might have some more restricted uses in connexion with hemispherical circulation types and type changes, which are widely regarded as of fundamental importance in medium range forecasting.

It would be an obvious advantage if particular values or ranges of values of an index could be recognisably associated with characteristic types of large-scale circulation; this is possible but only to a very limited extent. For example, a high value of the zonal westerly index is associated with low pressure near latitude 55°N. and high pressure near 35°N. over a large part of the hemisphere: the Icelandic and Aleutian lows and the subtropical high pressure cells are all well developed. A very low or negative value of this index is associated with a type in which pressure systems are elongated in the N.-S. direction or with an "inverted" type, with easterly winds over a large part of the middle latitude belt. These associations have been pointed out by Namias (1947). Thorp (1947) and Willett (1949). These typical patterns are commonly referred to as "high" and "low" index types. But Willett also quickly realised that the use of an index as a type indicator is limited to the few occasions when it takes extreme values; any intermediate value may be associated with a number of different circulation types, or indeed a pattern having no semblance of type or order at all.

It is worth remarking that the above index and type associations apply to surface indices only, a fact not realised in the early studies of these indices. The upper westerlies often reach their greatest strength when the surface zonal index is low (Namias 1950). This is confirmed by the small correlation coefficients between the surface and upper indices found by Willett (1946). In this connexion Namias (loc.cit.) remarks that the terms "high" and "low" index type appear to be misnomers. Certainly, the use of these terms as implying vigorous or weak circumpolar westerlies throughout the troposphere, introduced in earlier American works, now seems improper.

(b) Index Correlations. Apart from relating indices directly to the large scale circulation, some understanding of the working of the circulation may be sought through possible correlations among the various indices. Much work in this field has been carried out as a joint project of the U.S. Weather Bureau and the Massachusetts Institute of Technology, and is described in a series of unpublished reports (Willett 1946, 1947, 1949). It is summarised in a typescript report prepared by Mr. E.J. Sumner in the Forecasting Research Division.

Willett computed contemporary and lag correlations for almost every possible combination of index pairs amounting to many thousands in all. The coefficients obtained were almost invariably low, the highest absolute values lying between about 0.30 and 0.40, apart from one or two isolated exceptions. Correlation coefficients of this magnitude have less than a one per cent probability of occurring by chance, so that they are probably not without significance, but nevertheless, they have little practical value.

Some of the more important of Willett's results are summarised below.

(i) Various zonal and meridional indices were correlated, daily, five-day mean and monthly values being considered separately. The contemporary and lag correlation coefficients obtained were, in the main, quite low. Furthermore the removal of seasonal trend reduced these coefficients to complete insignificance.

(ii) Auto-correlation for zonal and meridional indices for varying periods of lag up to about 12 weeks yielded no significant results.

(iii) No significant correlations were found between monthly mean values of certain indices computed separately for the northern and southern hemisphere.

(iv) Circulation indices and indices of certain solar phenomena (sunspot number, monthly mean pyrheliometric value) also gave correlations of no significance.

(v) Willett also correlated the zonal indices with certain other indices expressing the total mass of air in the northern hemisphere. Significant negative correlations were obtained between changes in the strength of the surface westerlies and the total mass of air, (mean surface pressure) suggesting that as the circumpolar vortex speeds up air tends to be thrown out of the hemisphere. When, however, the upper instead of the surface flow was considered , the correlation became insignificant. Significant correlations were also found between the zonal indices and the total mass of air within certain latitude circles; this is, however, perhaps to be expected since the zonal indices themselves are derived, through the geostrophic relation, from the pressure distribution.

(vi) As regards transport indices, the statistical investigations so far reported by Willett are rather limited in scope. Theoretical work by Prof. V.P. Starr (unpublished) having indicated the likelihood of a connexion, Willett investigated the contemporary correlation between the pressure deficit from normal poleward of latitude 45°N and the transport of heat across the same parallel. The resulting correlation coefficients averaged 0.52, substantially higher than most coefficients hitherto found for circulation indices. This result is in conformity with the view that transport indices are useful aids towards an understanding of the mechanism of the general circulation. Moreover, from the point of view of extended forecasting, the transport of heat and momentum across a given circle of latitude are obvious factors to consider as effecting the strength of the circulation and the intensity of the "cold pole" at higher latitudes. Considerable attention is being given to these processes by workers in several countries but the application to forecasting is not yet apparent.

6. The use of indices in medium range forecasting.

(a) Indices as definitive parameters. The prominence given to circulation indices in recent years has been largely on account of their study in connexion with the extended forecasting project in the U.S.A. (R.A. Allen and collaborators, 1940). In the earlier reports on this project it was implied if not explicitly stated that certain indices, in particular zonal indices, were sufficiently precise indicators of circulation types for their forecasting to be a worth-while problem in itself. It must, however, be reiterated that it is only when the indices take extreme values that they give any indication of the associated circulation pattern (para.5(a)).

Nevertheless considerable attention has been given to the problem of forecasting indices. For this purpose it has been the practice in America, and for a time also in connexion with the four day forecasting experiment in this country, to prepare graphs showing the time variation of certain indices, and also, for comparison purposes, of their average values. Almost invariably the graphs show large and irregular day to day fluctuations. No method of forecasting these changes has yet been put forward apart from the ordinary statistical rule that the forthcoming change will, on probability, be in the direction of the normal. The work of Willett (para.5(b) above) shows that there are no significant lag correlations nor periodicities. It is evident that attempts to forecast indices statistically are not likely to be profitable.

It has been claimed that it is occasionally possible to see long period trends in indices which may be indicative of impending type changes. Evidence on this point is, however, far from convincing both in our own experience and in the literature, and it is doubtful whether the detection of such trends is a sufficiently objective process. An index trend might perhaps be useful in giving added weight to a conclusion already arrived at by other reasoning.

In the course of the work outlined in para.5(b) above, Willett investigated contemporary and lag correlations between circulation indices calculated for the separate quandrants of the hemisphere. The results showed nothing significant, indicating that little help is to be got from the application of indices to the idea that bands of strong zonal circulation tend to be propagated eastwards from sector to sector.

As regards the significance for extended forecasting of the general low values of the correlation coefficients between indices (para.5(b)(i)) Willett's conclusions (1947) are very discouraging. He writes "As far as the week to week irregular fluctuations are concerned we must look for a control which is either outside the portion of the atmosphere studied or which is entirely external to the atmosphere (solar)..........."

"If this conclusion is justified, then with the present available data, extended forecasting must continue to be essentially empirically statistical." On this point, however, it is well to recognise, as indeed Willett himself does, that indices calculated on the basis of a geometrical spacing of points, without regard to geographical features, are unreal. Moreover, owing to the process of averaging by which they are computed, these indices cannot specify important details of the prevailing circulation. It is difficult to believe that the fluctuations of the atmospheric circulation are without some degree of internal control: it appears, however, that these indices are not a suitable means of revealing it.

A similar conclusion regarding the unsuitability of indices computed on a geometrical basis follows from the results quoted in para.5(b), (ii), (iii) and (iv) above. The first of these appears to indicate the absence of any periodicities in the short term fluctuations of the strength of the general circulation. On the other hand Jones (para.3(a) above) did find some evidence of periodicities in an index based on the variable positions of large scale pressure features. As to the possible influence of solar phenomena, this is in itself a wide field of research and though inappropriate to this report it is not to be dismissed owing to a lack of correlation between the phenomena and somewhat artificial circulation indices.

(b) Indices as parameters in wave length considerations. Apart from their direct use as discussed in the preceding paragraph, indices have some application as parameters in forecasting the movement of long waves (Rossby waves). Rossby (1939) derived the formula:

$$C = U - \frac{\beta L^2}{4\pi^2}$$

for the movement of these waves, where C is the wave velocity, U the general W. - E. velocity of the air stream, β the rate of change northwards of the Coriolis parameter and L the wave length. This formula, or modifications of it, has been used in the medium range forecasting problem, sometimes quantitatively but more often to give a very rough approximation to the "stationary wave length" (c = o, unchanging wave pattern). A report on an investigation into the use of the Rossby wave formula is nearing completion and will not be anticipated here; it is sufficient to remark that the quantity U in the formula is conveniently taken as one of the zonal indices.

7. Conclusion. We may conclude from the preceding discussion that:

(i) Indices providing numerical measures of properties or processes in the atmosphere on a large scale are an obvious and even essential aid to the study of general circulation problems.

(ii) Zonal, meridional and similar indices have so far shown little value for either synoptic classification or forecasting and there is no basis for recommending the introduction of such indices into forecasting practice at present. A possible exception is the use of some suitable zonal index in connexion with "long waves in the westerlies."

References.

Allen, R.A., Fletcher R., Holmboe, J., Namias, J., Willett, H.C.	1940	Report on an experiment in five day weather forecasting. Papers in Physical Oceanography and Meteorology, Vol.VIII, No.3.
Goldie A.H.R.	1936	Quart. Journal R. Met. Soc. Vol.62 p.81.
Jones F.M.	1943	Air Ministry, Meteorological Research Paper No.80 (unpublished).
Namias J.	1947	Extended forecasting by mean circulation methods. Washington U.S. Weather Bureau.
-	1950	Journal of Meteorology, Lancaster, Pa., U.S.A. Vol.7, No.2 pp. 130-139.
Rossby C.G.	1939	Journal of Marine Research, Newhaven, Conn., U.S.A. Vol.2 p.38.
-	1941	U.S.A. Year Book of Agriculture pp.599-655.
Thorp J.R.	1947	Air Ministry, Meteorological Research Paper No.475 (unpublished).
Willett H.C.	1946	Final Report of the Weather Bureau Massachusetts Institue of Technology, Extended Forecasting Project, for the Fiscal Year July 1945 - June 1946.
	1947	" July 1946 - June 1947.
	1949	" July 1948 - June 1949.

been published. Any author desiring to quote this paper should refer to it as "A paper of the Meteorological Research Committee (London), M.R.P. No .... by Mr............... A copy is available in the Library of the Meteorological Office."

M.R.P. 593
S.C.III/76
30th November, 1950

ATI-110140 JUN 6 1951
AIR WEATHER SERVICE
TECHNICAL REFERENCE FILE

AIR MINISTRY

METEOROLOGICAL RESEARCH COMMITTEE

The Relation between the Radar Echoes from Cumulus and Cumulonimbus clouds and the Turbulence within those clouds

Part II

by R.F. Jones

Report on the second year's cumulonimbus trials at the Meteorological Office radar station at East Hill in co-operation with aircraft from the Royal Aircraft Establishment at Farnborough

1. Introduction

In a previous report (1) the writer has described the results obtained in a series of experiments undertaken to investigate the relationship between the radar echoes received from cumulus and cumulonimbus clouds and the turbulence within those clouds. The experiments there described covered the period August 1947 to October 1948. Since that period the experiments have been continued and the purpose of the present report is to extend those results to cover a second thunderstorm season with observations obtained in the period 9th December, 1948 to 2nd June, 1949.

It is assumed that the two reports will be read in conjunction, thus avoiding unnecessary duplication in this second report. Comparison between the results of the two reports will however be made as occasion demands.

In addition the opportunity has occurred to examine some aircraft flights in greater detail and the present report contains the results of integrating some of the accelerometer records obtained in the aircraft, with a view to assessing the magnitude of the vertical currents on particular flights.

2. The procedure adopted and equipment used.

In carrying out the experiments the same procedure was adopted as described in the first report (1) (section 4). The radar equipment and aircraft instruments also remained the same (Sections 2 and 5).

3. Data available

The year was not a good one for cumulonimbus development in the Midlands of England and this is reflected in the amount of data available for analysis.

A total of eight sorties, for which accelerometer records are available, was made involving 38 traverses of clouds and a total distance flown in cloud of 259 miles. Details of the sorties are given in Table I.

The data available are therefore much less than for the first report and in addition the mean vertical extent of the echoes was also much less. For traverses through clouds containing echoes extending more than 9,000 ft. above the freezing level the mean vertical extent of the echo was 18,500 ft. compared with 25,000 ft. in the first report.

The methods of analysis used were similar to those employed in the original report.

/4.

4. The statistical analysis of the data

(a) Relation between the vertical extent of the echo and the maximum gusts encountered in the cloud containing the echo

Figure I shows the result of plotting the maximum up-gust encountered in flights which went through the echo against the height of the echo top above the freezing level. A similar analysis for the maximum down-gusts is shown in Figure II.

No results were available for echoes extending to a greater height than 17,900 ft. above the freezing level and the evidence confirms that of the previous report in suggesting that, except for the echoes of very great vertical extent (more than 20,000 ft. above the freezing level) the maximum down-gust likely to be experienced is probably largely independent of the vertical extent of the echo. There is little indication also, from Figure I of this report, of any marked correlation between maximum up-gust and vertical extent of the echo.

It is noteworthy however that, from both reports, flight through echoes extending less than 5,000 ft. above the freezing level did not experience gusts greater than +0.5g and -0.4g, although both these values were exceeded in clouds which failed to give an echo (Figure I of first report). The inference is, of course, that the cumulonimbus echoes investigated extending to heights less than 5,000 ft. above the freezing level were from decaying cumulonimbus clouds in which the turbulent activity had decreased considerably. It would be unwise to assume that a developing cumulonimbus echo which had not yet reached a height of 5,000 ft. above the freezing level would exhibit such small turbulence. The speed with which such echoes grow and the fact that most echoes in this country develop to heights greater than 5,000 ft. above the freezing level, combined with the time taken to manoeuvre the aircraft makes it unlikely, with the technique used, that a newly developing isolated echo of such small vertical extent would be investigated.

(b) The appearance of the echo in relation to the maximum gusts encountered in the cloud containing the echo

In Table II is given a general description of the appearance of the echo at the time of the flights through the echo which gave the maximum gusts i.e. the data used for Figures I and II.

The evidence there presented is in agreement with the conclusions drawn in the first report (1) (Section 7(b)), in that the type of echo which gives the greatest up-gusts in the cloud containing the echo is the type which has clear cut edges and tops and sometimes a number of columns and troughs. Relatively smooth conditions are encountered in clouds containing echoes having diffuse edges and tops. The correlation of down-gust magnitude with echo appearance is not so well marked.

Up-gusts greater than 0.5g were only associated with clouds having echoes exhibiting clear cut edges or more than one column. It should be remembered however that in the previous report an up-gust of 0.6g was encountered in a cloud which failed to give any echo and no such runs were made in the period covered by this report.

Evidence of a bright band in an echo, or part of an echo, in the vicinity of the freezing level was usually an indication that the turbulent activity of the cloud, or of the part of the cloud containing the bright band echo, was small and large gusts did not occur. On some occasions when the echo consisted of a diffuse part with a bright band followed or preceded by a well-marked column of echo the larger gusts were associated with the columns of echo and only little turbulence was met in the diffuse echo.

/(c)

(c) Frequency of occurrence of gusts of various magnitudes

As in the previous report a distinction has been drawn between flights made through clouds containing an echo extending more than 9,000 ft. above the freezing level and those containing an echo of less vertical extent.

The heights at which flights took place have, as before, been divided into intervals of 2,000 ft. above or below the freezing level as reference level and the analysis expressed in the form of the average number of yards flown in cloud before encountering a gust of specified magnitude. The results of this analysis are given in Table III.

Comparison of this Table with Table III of the first report indicates that, at almost all heights, the distances flown for this report were considerably less than for the first report. As distinct from the first report there seems little to choose between those echoes extending more than 9,000 ft. above the freezing level and those of less vertical extent as regards the turbulence at those heights for which comparison is possible. Indeed in this report there would appear to be a tendency for the smaller echoes to be the more turbulent. This is due to an increase in turbulence in the clouds containing the smaller echoes compared with the previous report and a decrease in turbulence in the clouds containing the larger echoes. It is emphasised, however, that the distances flown in clouds containing echoes of small vertical extent is small at all heights and the total distance is only about one-sixth of the distance in the previous report.

The decrease in turbulence, in the clouds containing the echoes of large vertical extent, from the first report to this report is a reflection of the generally decreased cumulonimbus activity referred to in Section 3.

It is not considered therefore that great significance can be attached to the discrepancies between Tables III of the first and this report except as a demonstration of the very different cumulonimbus activity which may exist in this country from year to year.

Figure III shows the result of plotting the gust frequency for all flights irrespective of height, distinction being drawn between those flights through clouds containing echoes extending more than 9,000 ft. above the freezing level and those through clouds containing echoes of less vertical extent. In this case it is seen that for gusts up to about 0.7 - 0.8g in magnitude the frequency of occurrence is somewhat greater in the clouds containing the smaller echoes but that the frequency of the gusts greater than 0.7 - 0.8g is probably greater in the clouds containing the larger echoes.

(d) Variation of gust frequency with height

In the previous report it was suggested that the correlation between the height of the zone of maximum turbulence found by the Americans with the freezing level was fortuitous and that the height represented an average height above mean sea level, in the more uniform clouds of the tropical regions, at which the turbulence reached a maximum value. The additional information set out in Table III supports this view in that there is again no evidence of a zone of maximum turbulence near the freezing level.

As in the previous report the data have been re-assessed in terms of the height above mean sea level at which the observations were made for those clouds which contained an echo extending 9,000 ft. or more above the freezing level. This information is shown in Table IV. The smoothed values obtained by plotting the values in Table IV have been used to obtain Figure IV which shows the variation of gust frequency with height above mean sea level. No readings were available for heights greater than 20,000 ft. but it will be seen that there is again a progressive decrease in frequency of gusts with descent below the 16,000 - 14,000 ft. layer (vide p.8 para. 2 of 1st report)

/which

16 of the 20 gust sequences were therefore associated with marked discontinuities in the echo (edges, peak or trough between columns of echo) and if we associate echo discontinuities with discontinuities in the vertical current speed we see that a high proportion of the gust sequences are associated with marked vertical current discontinuities.

The changes in vertical current speed on passing through a cumulonimbus cloud are therefore likely to be frequently associated with a transitional turbulent zone which may have a width varying from 50 yards to about 850 yards, the mean value being about 300 yards.

Such a possibility is illustrated in the first report (Section 8(d)) and it is considered that the evidence here presented tends to confirm this interpretation.

The occurrence of an appreciable number of positive gusts at the trailing edge, and of negative gusts at the leading edge, of a column of echo - if we accept the interpretation in the first report of a well-marked column of echo indicating a marked up-current - is therefore explained in that gusts of both signs are equally likely in the turbulent zone surrounding the echo column.

Two gust sequences from accelerometer records used in this report are illustrated in Figures V and VI.

Figure V shows a sequence of three major gusts within four seconds (approximately 400 yards) which occurred in the trough between two columns of echo. The two major positive gusts are of 0.4g and 0.6g respectively while the major negative gust is 0.4g. Also shown is the integrated curve for this interval of time which shows that the aircraft experienced a vertical velocity increment of about 19 ft/sec. due to this gust sequence.

Figure VI shows a sequence of two gusts which occurred in a time interval of about three seconds the values being +0.4g and -0.6g. This sequence occurred before entry into the echo but beneath an overhanging echo. The integrated curve shows that no increment in vertical velocity of the aircraft resulted from this sequence and suggests the existence of a single narrow up-current within the cloud of magnitude about 12 ft/sec. and only some 200 yards wide.

7. Integrations of the accelerometer records for five flights

The accelerometer records obtained in the aircraft, being records of the accelerations experienced by the aircraft against time, should be capable of integration to yield the upward and downward velocities experienced by the aircraft in the traverse of a cumulonimbus cloud. While it is possible that the aircraft may not always be in an upward air current for a sufficiently long time for it to take up the whole of the air velocity, the integrations should nevertheless give valuable indications of the magnitude of the up and down air currents encountered.

The accelerometer record is obtained on 35 mm film and for integration purposes it was necessary to trace the curve under an enlarger and integrate the curve so obtained. This was a lengthy and laborious task but was achieved for five traverses and the results are given in sections A to E below.

A. Flight at 14,000 ft. on 10th June, 1948

In Section 8(a) (ii) of the first report a flight through a cumulonimbus cloud at 14,000 ft. on 10th June, 1948 was analysed in detail and, from the gust data from the accelerometer record, an indication of the vertical velocity profile of the air was deduced and given in Figure XXI of that report.

It was emphasised that the profile so obtained was only very approximate and did not give actual, or necessarily relative, values of the vertical air current speeds.

The writer is indebted to Mr. W.G.A. Port of the Royal Aircraft Establishment, Farnborough for the graph of vertical velocity against distance through the cloud, obtained by integration of the accelerometer record, given in Figure VII.

The close correspondence between the integrated curve and that of Figure XXI of the first report (shown dotted on Figure VII) is very satisfactory and strongly supports the conclusions of Section 8(a) (ii) of the first report. Some difficulties arise in the interpretation of the curve, however, and are considered in sections (i) to (iv) below.

(i) In obtaining the integrated curve of Figure VII the curve was adjusted on the reasonable assumption that the conditions on leaving the cloud were similar to those on entry and that the vertical velocity before entering and after leaving the cloud was zero. The corrections necessary to achieve this were within the liability to experimental error of the accelerometer record (involving a change of the base line of the recorder of a few thousandths of an inch).

The curve so obtained obviously leads to a considerable excess of negative velocity for the whole flight giving to the aircraft a mean rate of loss of height of 38 ft/sec. The aircraft would therefore be expected to have left the cloud at a much lower height (about 8,000 ft. for the flight of 208 seconds) than it went in. There is no evidence of this although there is no conclusive evidence to the contrary since the aircraft was lost on the radar tubes towards the end of the flight. The pilot however remarked on the radio-telephone immediately after leaving the cloud that he would stay on 14,000 ft. until he heard further from East Hill, implying that no noticeable change of height had actually occurred.

There is some evidence to suggest that the pilot may have switched off his accelerometer seven seconds before leaving cloud while in the final strong column of echo. He would therefore probably have finished his accelerometer record in an upward current so that the final point of the integration curve should show a positive velocity.

(ii) The sloping line from zero velocity at zero distance on Figure VII to -75 ft/sec. at the end of the flight represents a zero line for zero change of height during the run. This leaves the aircraft with a strong positive velocity (about 75 ft/sec.) at the end of the accelerometer record. Consideration of the last paragraph of (i) above, that the accelerometer may have been switched off seven seconds before leaving cloud, agrees with this idea and if we extend the integrated curve by extrapolation for seven seconds (equivalent to 763 yards and shown by _._ ._._ on Figure VII) we find that it is readily possible to achieve zero velocity on leaving cloud.

This assumption makes the final peak of vertical velocity 100 ft/sec compared with 53 ft/sec. for the first major peak while the second and third major down-currents, in the order in which they were met by the aircraft, are 65 ft/sec. and 40 ft/sec. respectively i.e. the bigger down-current immediately followed the smaller up-current.

(iii) The general form of the integrated curve suggests that error may have been introduced by a false magnitude to the initial down-current before entering the echo. A horizontal line at about -38 ft/sec. would give zero change of height for the flight provided we again assume that the accelerometer was switched off in an upward current before leaving cloud. This suggests that the aircraft was climbing when it entered cloud; this is possible since the pilot had limited space for manoeuvring and did in fact have to climb from 10,000 ft. to 14,000 ft. before entering cloud. If the aircraft entered cloud with an upward component of 38 ft/sec. and levelled out just after switching on the accelerometer this would explain the large negative gusts in the first 1000 yards and give a more symmetrical appearance to the integrated curve. (Alternatively something may have occurred to cause the accelerometer to stick and read a false negative acceleration in the first few seconds of the flight.) The upward speeds in the two major columns of echo at the beginning and end of the flight would then be 66 and 65 ft/sec. respectively, while the downward speeds in the two major troughs would be 57 and 64 ft/sec., giving ratios of up to down currents of 66/57 = 1.16 and 65/64 = 1.01 in good agreement with American measurements (2) of 1.14 for the ratio of mean draft speeds at 16,000 ft.

(iv) Either of the interpretations made in Sections (ii) and (iii) above agree in giving relatively small upward currents in the central broad column of echo which was less intense and more diffuse than the two outer columns.

It is considered that the interpretation given in Section (iii) is, on the whole, the most satisfactory; in this case the extrapolated curve must reach the -38 ft/sec. zero line at the end of the cloud either directly or probably after a relatively small down-current.

B. Flight at 10,500 ft. on 1st June, 1949

The integrated curve for this flight is shown in Figure VIII before the application of any corrections. It was realised that the method of tracing introduced the probability of a constant zero error, so that the high value of positive velocity at the end of the flight was not surprising. If we assume that the aircraft was experiencing no upward or downward velocity before entering cloud and again after leaving cloud, this constant zero error can be eliminated by joining the beginning and end of the curve by a straight line and using this line as the true zero. This line is shown dotted in Figure VIII.

It is immediately obvious that such a line leads to a considerable excess of downward velocity over the whole traverse and the net loss of height of the aircraft if it had experienced these velocities would have been 2,760 ft. Photographs (i) to (v) indicate with certainty that a loss of height of this magnitude did not occur and that little or no loss of height occurred at any stage of the traverse. The radar is not sufficiently accurate to indicate small changes of height but the experiences of the pilots agree that the aircraft in fact experiences very little change of altitude over the whole traverse of a cloud, any gain of height in one part of the cloud being compensated by a loss of height at some other part of the traverse. Without a recording altimeter it is impossible to say what changes of altitude did occur but it would appear that the best approximation to actual conditions may be obtained by assuming zero change of height throughout the run, together with the assumption of zero upward velocity at the beginning and end of the traverse.

The simple zero line shown dotted in Figure VIII is certainly not true because of the great loss of height involved and examination of the curve suggests a zero line of the form shown by the full line. This meets the requirement of zero gain of height in the whole traverse and also zero gain of height for the first half of the flight for which the photographs indicated no appreciable change in height by the aircraft.

/A

A zero line of this character implies the existence of a variable zero correction which may be brought about by instrumental error since an error as small as 1/1000th of an inch on the original accelerometer record will have an appreciable effect on the integrated curve. It is clear that for full and accurate use to be made of the accelerometer record information should be available of the actual changes of height of the aircraft during the traverse to enable the zero correction to be applied for a number of intervals of the integrated curve.

It is however considered that the zero line for zero change of height throughout can give a useful indication of the magnitude of the up and down currents and the corrected curve so obtained is given in Figure IX.

Correlation between this curve of vertical velocities and the echo flown through can be obtained from the series of photographs (i) to (v). On four of the five photographs the aircraft position relative to a fixed range marker on the display can be measured and can be plotted against the same time scale as the accelerometer record. Salient features of the radar echo can also be plotted in this way and are shown in Figure IX in their appropriate positions.

The outstanding feature is the exact correlation between the final column of echo (i.e. the column of echo at shortest range - see photograph (v)) and the strong upward current experienced by the aircraft. The peak of this final echo column was fairly broad and extended over 12 seconds, from 93 to 105 seconds, (equivalent approximately to 1200 yards) and throughout this range the vertical velocity curve shows the upward current to be in excess of 14 ft/sec. with a maximum value of 34 ft/sec. The sequence of photographs shows this column to be a newly developing column within the echo.

The column of echo first encountered by the aircraft (see photograph (iii)) was not so sharply defined nor was its edge vertical while the sequence of photographs shows a decrease in vertical extent during the traverse. It seems probable that this column was in a part of the cloud in the decaying stage with the major activity of the cloud transferred to the newly developing column. Correlation with the vertical current profile shows that the peak of this column coincides exactly with a maximum of upward velocity at 69 seconds but that the up-current is only about 9 ft/sec.

Between the two columns of echo there would appear to have been a well-marked down-current which reached a maximum value of 21 ft/sec.

Prior to entry into the echo at the height of the aircraft but while flying above echo (see photographs (ii) and (iii)) there would appear to have been up and down currents of the order of 8 ft/sec., but a similar feature is to be observed in that part of the cloud entirely clear of echo at any height. There seems therefore to be little correlation between echo appearance and vertical velocity except when the aircraft itself is within the radar echo.

All the major gusts of ± 0.4g or greater are seen to have occurred in the final well defined column of echo, three (2 positive, 1 negative) close to the leading edge of the column, two (both positive) beneath the first part encountered of the echo peak, two (both negative) beneath the last part of the echo peak and two (1 negative, 1 positive) close to the final edge of the echo.

C. Flight at 12,000 ft. on 2nd June, 1949

The integrated curve for this flight, which was through a cumulonimbus cloud having a large anvil head, is shown in Figure X, after correction for constant zero error.

This curve would have led to a net loss of height by the aircraft of some 300 ft. but further correction, as in flight B, has not been made since the photographs - see photographs (vi) and (vii) - indicate the possibility of such a small loss of height although, as mentioned previously, discrimination to the accuracy required is not possible from the radar.

From photographs (vi) and (vii) and from a further photograph taken 57 seconds prior to switching on the accelerometer it is possible to plot a curve indicating the aircraft position relative to a fixed range marker on the display against the same time scale as the accelerometer record. The salient features of the radar echo, which photographs (vi) and (vii) show to be ill-defined, can also be plotted in this way and are shown in Figure X in their appropriate positions.

It will be seen that immediately on entry into the rather diffuse edge of the echo the aircraft experienced a well-marked down-current some 1200 yards across which reached a maximum value, or, more accurately, caused the aircraft to reach a maximum velocity, of 26 ft/sec. downwards. A similar down-current of about the same horizontal extent but with a maximum value of about 12 ft/sec. was encountered immediately before leaving the radar echo. The photographs (vi) and (vii) show a tendency towards a weak column inside the echo evidenced by the weak top protruding about 1000 ft. above the general echo top. This column was also (from a photograph taken at reduced receiver gain) the column of maximum intensity in the echo. It will be seen that this column is associated with the major part of the up-current within the cloud, which up-current has a horizontal extent of about 2500 yards and attains a maximum value of about 13 ft/sec.

The radar evidence suggests, and it is confirmed by the pilot, that the cloud was already in the decaying stage - the presence of the well-defined anvil is also probably contributory evidence. The small value of the up-current is not therefore surprising but the two well marked and relatively narrow down-currents still within the echo are of interest. The initiation of down-currents by precipitation has already been suggested (3) and the evidence here certainly supports this view. The down-currents, however, are not general throughout the cloud nor is the maximum intensity of the echo associated with the down-current. The presence of a large anvil head was remarked by the pilot and the spreading out of the echo at high levels to give a diffuse echo with a predominantly level top is almost certainly associated with this. The level top is broken however by the column of echo already referred to, which is also the part of the echo of maximum intensity and correlates with the volume of up-current within the cloud. It is suggested that the down-currents are associated with and probably accentuated by snowfall from the anvil part of the cloud while the up-currents and greater radar response are associated with that part of the cloud which still remains active - although less active than in its early stages - and probably characterised by the appearance of a cumuliform top bulging through the anvil surrounding it. The interpretation here given is shown schematically in the diagram below:- (Figure XI)

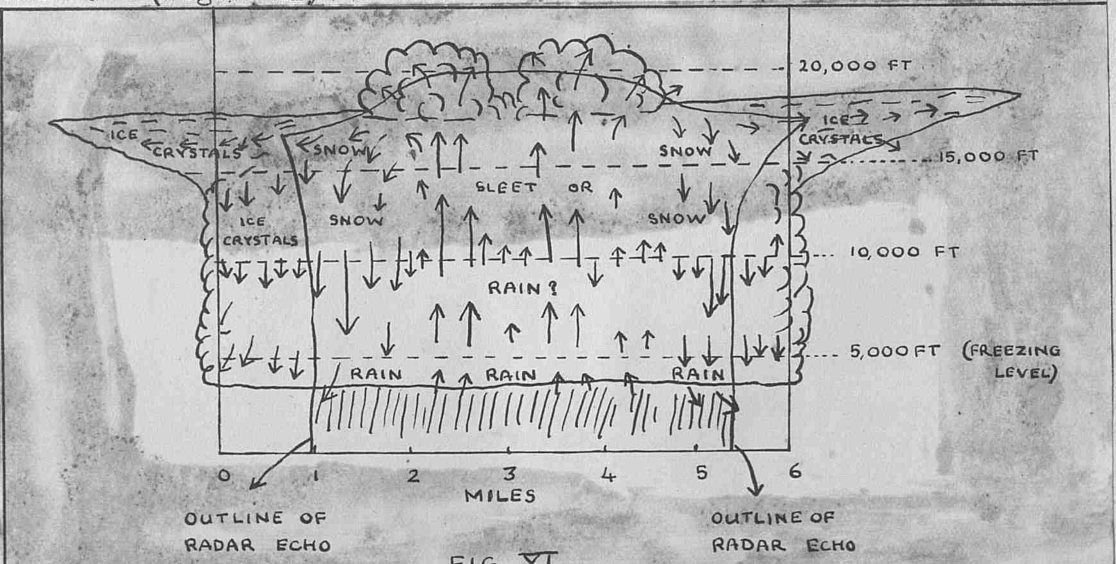

FIG. XI

The three large gusts of ± 0.4g or greater occurred at 27.5 seconds (+0.4g), 28.5 seconds (-0.4g) and 39.5 seconds (-0.5g), the first two on the approach to the column of echo after the major down-current and the last within the column of maximum intensity but before the upward velocity had reached its maximum value.

D. Flight at 8,000 ft. on 18th May, 1949

The integrated curve for this flight, which was through a cumulonimbus cloud having a top at 15,500 ft., is shown in Figure XII before the application of any corrections.

In this case the zero line obtained by joining the beginning and end of the curve, and shown dotted in Figure XII, clearly leads to a large excess of negative velocity and if true would imply that the aircraft lost some 1900 ft. in height between 55 and 120 seconds. Radar photographs which show the aircraft during the cloud traverse are available (see photographs (viii) to (xii)) and in particular photographs taken at 62 seconds and 122 seconds ((x) and (xii) respectively). From these latter two photographs it is quite clear that little or no change of height occurred on passing through the echo (if any, a small gain of height is indicated). The whole series of five photographs indicate that at no stage of the flight was there any appreciable change of height. The simple zero line of Figure XII therefore cannot be true and a zero line must be constructed which gives no appreciable change of height at any stage of the traverse.

Examination of Figure XII suggests the possibility that discontinuities occurred in the zero line at 55 - 58, 80½ - 88 and 113 - 119½ seconds. During these discontinuities it is suggested that the accelerometer registered a false negative acceleration for the first two and a false positive acceleration for the last respectively. Except for these breaks the accelerometer behaved correctly so that we have parallel zero lines displaced by the change of velocity which the integrated false accelerations imposed. Such zero lines give approximately zero change of height for the run, or a small gain of height, and it is considered that the corrected velocity curve so obtained, and shown in Figure XIII, is a reasonable picture of the velocities experienced by the aircraft.

Photographs (viii) to (xii) make it possible to plot a curve of aircraft position and salient features of the radar echo relative to a fixed range marker on the display against the same time scale as the accelerometer record. The salient features of the radar echo are shown in Figure XIII at their appropriate positions.

The photographs show the echo to have a diffuse top overhanging the main echo column and suggestive of an anvil to the cloud. From the point of entry until just after the 20 mile range marker (at 84 seconds on the accelerometer time-scale) the echo was quite weak and it was possible to see the aircraft within the echo. This part of the velocity profile (52 - 84 seconds) is characterised by generally weak up and down currents, nowhere exceeding 7 ft/sec. The more intense part of the echo is associated with two strong up-currents with about 20 ft/sec. as their maximum value and two strong down-currents of about 18 ft/sec. These up and down currents are all of very narrow horizontal extent of the order of 800 yards.

A marked trough in the echo is visible on the photograph negative extending from 100 - 109 seconds and this almost coincides with one of the downward currents (from 105 to 113 seconds) while the final column of echo extends from 109 to 124 seconds and includes one of the marked upward currents, although the peak of the final column from the photographs would appear to have been at 114 seconds.

The end of the echo corresponds very closely with a decrease in the upward velocity to almost zero. Correlation between echo column and up-current and echo trough and down-current is not quite exact but this may be due to the very narrow horizontal extent of these up and down currents and the difficulty of measuring accurately distances on the photograph positives. An A-scope photograph taken 75 seconds after the end of the traverse shows the presence of two peaks of high echo intensity in the final part of the echo as traversed by the aircraft and these two peaks were measured as 25 seconds apart. It will be seen that the peaks of upward velocity towards the end of the traverse were 26 seconds apart. The strong up-current at 43 seconds, prior to entry into the echo, is beneath the overhanging echo top but has no obvious echo characteristics associated with it. Four large gusts (3 of +0.4g, 1 of -3.6g) were experienced before entering the echo and the remaining large gusts (1 of +0.5g, 1 of +0.6g, 1 of -0.6g) were all associated with the final more intense part of the echo.

It is of interest to note that the pilot reported the precipitation as rain freezing into granulated ice. The same description was applied to runs through the same cloud at heights of 9,000, 10,000 and 12,000 ft. with the icing reported as more severe at 12,000 ft. than elsewhere. On the run at 9,000 ft. however the VHF aerial was snapped off due to icing. According to the relevant tephigram (Downham Market 1500 GMT) the freezing level was at 5,800 ft.

A further point of interest is that on the following run through the same cloud five minutes later at 5,000 ft. lightning was reported by the pilot - an unusual phenomenon with the cloud top as low as 15,500 ft. (tephigram temperature 0°F).

E. Flight at 4,000 ft. on 23rd April, 1948

This run was made close to the base of an isolated cumulus cloud the top of which was at 8,500 ft. No radar echo was received from the cloud which was at a range of about 23 miles. The freezing level from the relevant tephigram was at 4,900 ft. and the temperature at the top of the cloud, 20°F. Only slight rime icing was reported on one run at 8,000 ft. and no precipitation was reported on any of four runs through the cloud.

The integrated accelerometer record for this flight, after correction for constant zero error, is shown in Figure XIV. As will be seen this gives predominantly negative velocity which would amount to a loss of height by the aircraft on the traverse of about 300 ft. The form of the curve and the consideration that there was probably little change in height on the traverse suggests a zero line of the form shown by the straight lines on Figure XIV. The velocity curve corrected according to this zero line is shown in Figure XV.

The interest in this velocity curve associated with a non-precipitating cumulus cloud lies in the demonstration of the existence within the cloud of up and down currents similar in form to, but weaker than, those existing in a precipitating cloud. It seems virtually certain that within this cloud down-currents of the order of 10 to 15 ft/sec. did occur.

It has been suggested (3) that the down-currents in a cumulonimbus cloud are initiated by the precipitation but the evidence here presented suggests that the down-currents may already be in existence before precipitation starts. It is appreciated that this analysis applies to a cloud which never did precipitate, nor is it known what stage of development the cloud had reached, but the fact remains that localised down-currents of the order of 10 - 15 ft/sec. had developed in the cloud for some cause other than precipitation and it is at least plausible to imagine that the down-currents in the larger and more active clouds are not initiated by the precipitation, although they may be reinforced. It would appear possible that all clouds of the cumulus type, whether precipitating or not, are characterised by the existence within the cloud of up and down currents of similar magnitude in close proximity to each other, although the magnitude of the up and down currents may be greater at some time in some parts of a precipitating cloud than at any time in any part of a non-precipitating one.

/8.

8. Shortcomings of the radar in defining the vertical cross-section of the radar echo from cumulonimbus clouds

In the foregoing it has been implicitly assumed that the vertical cross-section of the radar echo as seen on the height-range tube display is a true cross-section of the radar echo in the vertical plane enclosing the line of flight of the aircraft. This is not strictly true, principally for two reasons.

(i) The aircraft may not fly directly along the radar beam throughout the radar echo and

(ii) the radar beam is not a narrow pencil beam but a divergent beam having a beam width (measured to half power) of $7\frac{1}{2}^{\circ}$ in the horizontal and $1\frac{1}{2}^{\circ}$ in the vertical.

The effect of (i) above was minimised by giving the pilot a course to steer through the echo which would bring him either directly towards or directly away from the station and hence cause him to fly along the radar beam. Occasionally however the effect of wind drift or other causes may cause him to deviate slightly from the course given. This effect was not considered to have been serious in the great majority of the traverses made.

The effect of (ii) above, however, is potentially more serious in regard to the horizontal beam width of $7\frac{1}{2}^{\circ}$. At 20 - 30 miles range, at which range the majority of traverses were made (see Tables I of this and the previous report), the beam width will vary from about $2\frac{1}{2}$ miles at 20 miles range, with a depth of 2600 ft., to four miles at 30 miles range and a depth of 4,200 ft. By keeping the aircraft response at its maximum value it was usually possible to be reasonably sure that the aircraft was in the centre of the beam and therefore that it flew along the centre of the beam. The weather response, however, is very much larger than that of the aircraft in both horizontal and vertical extent and usually more than filled the beam. The response shown on the height-range tube at a fixed range and height therefore was the sum of all the responses at that range from the part of the echo within the beam i.e. from a width of $2\frac{1}{2}$ miles and vertical extent of 2,600 ft. at 20 miles range to a width of four miles and vertical extent of 4,200 ft. at 30 miles range. The response from a certain volume distribution of raindrops at the centre of the beam will, of course, be greater than that from the same volume distribution towards the edge of the beam so that the portion of the cloud intercepted near the centre of the beam will frequently have a predominant effect on the response as seen on the height-range tube at that range. Nevertheless there may be occasions when a higher concentration of rain drops of greater size exist towards the edge of the beam than in the centre. On these occasions the response on the height-range tube will be partly, and perhaps sometimes principally, due to the response from a part of the cloud not in the centre of the beam and not therefore on the aircraft track. An aircraft may therefore on some occasions appear to go through a strong echo on the height-range tube when it is in fact only skirting the volume responsible for the echo or perhaps, in extreme cases, missing the volume altogether. That the cumulonimbus echo is characterised by considerable variation in intensity in the horizontal is well known and evidenced by the appearance of cells or "cores" within the echo, these cells being associated with a column of echo of high intensity. It seems possible therefore that the height-range tube picture may, on some occasions, be misleading. It has been shown however (4) that the mean diameter of the columns of echo in a large number of multi-column echoes is 1.8 miles so that, with the range of beam width of $2\frac{1}{2}$ to 4 miles already mentioned, it seems likely that, if an aircraft appears to enter a strong column of echo, it will in fact be going through some part of that high concentration of raindrops giving the column of echo although not necessarily through the most intense part. Exceptionally it would seem possible for the echo in which the aircraft appears to be to have no connection with the volume of cloud which the aircraft is traversing at that moment, although in these circumstances it is doubtful whether the echo would be characterised as a "strong" column.

/In

top protruding through the anvil. Indeed the anvil in these circumstances does not extend right across the cloud top, which it usually appears to do when seen from the ground, but rather surrounds the towering cumulus at some distance below its top.

It appears that anvil formation and its associated diffuse echo can only take place when the vertical component of the air current has been reduced to a small value but that as long as the vertical component is large the cloud will maintain its characteristic "cauliflower" structure and associated well defined strong column of echo.

The nature of the echo therefore, as has been indicated in Table II, is a very useful guide to the vertical current structure of the cloud and provides a means of identifying those parts of the cloud where the up-currents are strong. As the integration of the accelerometer records suggests that the strong up-current is always bounded by a down-current of comparable magnitude, the presence of strong columns of echo is an indication of the existence of neighbouring strong up and down currents with the likelihood of severe turbulence. Diffuse parts of the echo on the other hand may be expected to be associated with only weak up-currents or with down-currents and correspondingly less turbulence.

10. Summary

The turbulence encountered in flying through a cumulonimbus cloud is shown to be associated with the existence within the cloud of neighbouring up and down currents of comparable magnitude. Speeds of these currents may exceed 50 ft/sec. on some occasions. These up and down currents are frequently separated by a turbulent zone extending over a mean horizontal distance of about 300 yards in which large up and down gusts occur.

The existence of such up and down currents can be inferred from the appearance of the cumulonimbus radar echo as seen in the vertical cross-section, but similar up and down currents - although probably not of such great speeds - exist in cumulus clouds which fail to give a radar echo.

It is probable that in an active cloud the greatest turbulence is likely to be encountered within the echo but, if the turbulence is severe within the echo, there may also be some substantial gusts in the part of the cloud which fails to give an echo. The most severe gusts are associated with marked echo discontinuities especially the edges of the echo when they are clearly defined.

No interval of height is indicated in which maximum turbulence may be expected but turbulence is probably at a minimum in the lowest levels of the cloud and increases upwards until a height of rather less than half the vertical extent of the cloud is reached, whereafter the turbulence remains approximately the same, probably until near the cloud top.

11. Acknowledgements

It is a pleasure to acknowledge once more the ready co-operation of the pilots of the Spitfire aircraft of the Aerodynamics Flight, Royal Aircraft Establishment, Farnborough.

Acknowledgement is also made to Mr. W.G.A. Port of the same flight for the analysis of the accelerometer records and for the integration of a complete record given in Section 7A above.

12. References

1. Jones, R.F.: The relation between the radar echoes from cumulus and cumulonimbus clouds and the turbulence within those clouds. M.R.P. No.484, Air Ministry, Meteorological Research Committee, London, 1949.

/2.

2. Thunderstorm Project: A report on thunderstorm conditions affecting flight operations. Tech. Paper No.7 (Table 5, p.13), Washington, April, 1948.

3. Byers and Braham: Thunderstorm structure and circulation. J. Met., Milton, Mass., Vol.5, No.3, June, 1948.

4. Jones, R.F.: The horizontal dimensions of cumulonimbus clouds at various heights. M.R.P. No. 535, Air Ministry, Meteorological Research Committee, London, 1950.

0.7g	1.0g	Fairly broad column of echo with well defined edges but generally diffuse top.
0.6g	0.7g	Single column, later (and possibly at first) showing signs of bright band.
0.5g	0.4g	Rather strong extensive echo (about 20 miles long), more of frontal character, exhibiting columns but probably also bright band.
0.3g	0.2g	Single column, clear edges, somewhat diffuse top. Evidence of bright band.

D. Echoes extending 4,000 - 8,000 feet above freezing level

0.6g	0.6g	Block of echo 20 miles long (frontal?) exhibiting marked narrow columns.
0.6g	0.4g	Diffuse echo with bright band followed by narrow column with clear edges and top.

E. Echoes extending 0 - 4,000 feet above freezing level

0.5g	0.4g	Diffuse echo with bright band.

TABLE II

General appearance of echo at time of flights through the echo which gave the maximum gusts

A. Echoes extending 16,000 - 20,000 feet above freezing level

Maximum up-gust	Maximum down-gust	Description of echo
0.8g	0.4g	Broad column with diffuse anvil top and new column at side probably developing. Edge and top of new column well defined, edge of major column (with anvil top) diffuse.
0.5g	0.4g	Diffuse echo with evidence of bright band - some evidence of stronger column but no clear edges or top.
0.4g	0.5g	Two very narrow clearly defined columns with narrow clear space between - possibility of bright band.

B. Echoes extending 12,000 - 16,000 feet above freezing level

0.6g	0.6g	Very broad echo showing evidence of column structure (similar to cold front or occlusion echo) but tops and edges generally diffuse.
0.4g	0.5g	Column with clear cut edges at first but gradually becoming more diffuse. Top becoming more diffuse during flights. Pilot reported cloud top going down.
0.3g	0.3g	Echo with generally diffuse edges and top.
0.3g	0.3g	Two very narrow clearly defined columns with very narrow clear space between.

C. Echoes extending 8,000 - 12,000 feet above freezing level

0.7g	1.0g	Fairly broad column of echo with well defined edges but generally diffuse top.
0.6g	0.7g	Single column, later (and possibly at first) showing signs of bright band.
0.5g	0.4g	Rather strong extensive echo (about 20 miles long), more of frontal character, exhibiting columns but probably also bright band.
0.3g	0.2g	Single column, clear edges, somewhat diffuse top. Evidence of bright band.

D. Echoes extending 4,000 - 8,000 feet above freezing level

0.6g	0.6g	Block of echo 20 miles long (frontal?) exhibiting marked narrow columns.
0.6g	0.4g	Diffuse echo with bright band followed by narrow column with clear edges and top.

E. Echoes extending 0 - 4,000 feet above freezing level

0.5g	0.4g	Diffuse echo with bright band.

G.278260/ABC/11/50/40

TABLE III

Average distances flown in cloud at different levels above the freezing level before encountering gusts of specified magnitude. (Distances in yards)

A. Clouds containing echoes extending to less than 9,000 feet above the freezing level.
B. Clouds containing echoes extending to more than 9,000 feet above the freezing level.

Height above freezing level (feet)		Gust Values										Total distance flown at height shown (yards)
		±0.1 to 0.2g	±0.2 to 0.3g	±0.3 to 0.4g	±0.4 to 0.5g	±0.5 to 0.6g	±0.6 to 0.7g	±0.7 to 0.8g	±0.8 to 0.9g	±0.9 to 1.0g	±1.0 to 1.1g	
-2,000 to	A	285	517	2065	2753	8260	–	–	–	–	–	8,260
-4,000	B	–	–	–	–	–	–	–	–	–	–	–
0 to	A	–	–	–	–	–	–	–	–	–	–	–
-2,000	B	482	1054	2190	4067	28470	28470	–	–	–	–	28,470
0 to	A	487	6013	9020	2255	9020	9020	–	–	–	–	18,040
2,000	B	421	1332	4758	8327	11103	–	–	–	–	–	33,310
2,000 to	A	–	–	–	–	–	–	–	–	–	–	–
4,000	B	557	811	1748	3631	18158	15132	–	–	–	–	90,790
4,000 to	A	508	1329	1551	6985	27940	13970	–	–	–	–	27,940
6,000	B	614	1121	2524	3924	8827	70620	23540	23540	–	70620	70,620
6,000 to	A	534	634	1128	1450	5588	10151	20303	–	–	–	20,303
8,000	B	834	1019	2824	4591	36730	–	–	–	–	–	36,730
8,000 to	A	517	1723	–	–	–	–	–	–	–	–	5,170
10,000	B	890	1922	9930	11916	–	59580	59580	–	–	–	59,580
10,000 to	A	1000	–	–	–	–	–	–	–	–	–	2,000
12,000	B	713	1016	3351	3046	33510	–	33510	–	–	–	33,510
12,000 to	A	–	–	–	–	–	–	–	–	–	–	–
14,000	B	1783	7133	–	–	–	–	–	–	–	–	21,400
All flights	A	477	801	1945	2816	9079	13619	81713	–	–	–	81,713
at all hts.	B	638	1133	2902	4810	19700	41601	74882	124803	–	374410	374,410

G.278260/ABC/11/50/40

TABLE IV

Average distances flown in clouds containing echoes extending more than 9,000 feet above the freezing level at different levels above mean sea level before encountering gusts of specified magnitude
(Distances in yards)

Height above mean sea level (feet)	Gust Values										Total distance flown at heights shown (yards)
	±0.1 to 0.2g	±0.2 to 0.3g	±0.3 to 0.4g	±0.4 to 0.5g	±0.5 to 0.6g	±0.6 to 0.7g	±0.7 to 0.8g	±0.8 to 0.9g	±0.9 to 1.0g	±1.0 to 1.1g	
2,000 to 6,000	492	1331	3283	8207	12310	49240	-	-	-	-	49,240
6,000 to 9,000	577	893	2780	5256	47300	11825	-	-	-	-	47,300
10,000 to 14,000	588	945	2018	3552	14853	54460	54460	54460	-	163380	163,380
14,000 to 18,000	923	1716	6716	8209	73880	73880	73880	-	-	-	73,880
18,000 to 22,000	884	1693	8122	5801	-	-	40610	-	-	-	40,610

TABLE V

Places of occurrence of gusts of ±0.4g or greater relative to the weather echo

Gust Value	Position of gust									Any other positions	Total
	Clear of all echo (none beneath)	Leading edge of echo column	Beneath or in peak of column	Trailing edge of echo column	Above echo	In part of echo with decreasing top	In part of echo with increasing top	In narrow column of echo	Trough between columns of echo		
-0.4g	0	8	10	13	0	5	6	0	5	0	47
-0.5g	0	3	4	5	0	0	2	0	0	0	14
-0.6g	0	0	0	3	0	0	1	0	0	1 - clear of echo but under overhanging top	5
-0.7g	0	0	0	0	0	0	0	0	1	0	1
-0.8g	0	0	0	0	0	0	1	0	0	0	1
-0.9g	0	0	0	0	0	0	0	0	0	0	0
-1.0g	0	0	0	0	0	0	1	0	0	0	1
0.4g	0	11	10	7	0	5	7	0	1	4 - 3 clear of echo but under overhanging top. 1 in overhanging top.	45
0.5g	0	2	2	3	0	0	1	1	1	0	10
0.6g	0	1	3	2	0	0	0	0	1	0	7
0.7g	0	1	2	0	0	0	2	0	0	0	5
0.8g	0	0	0	1	0	0	0	1	0	0	2
Total -ve gusts	0	11	14	21	0	5	11	0	6	1	69
Total +ve gusts	0	15	17	13	0	5	10	2	3	4	69
Total all gusts	0	26	31	34	0	10	21	2	9	5	138

G.278260/ABC/11/50/40

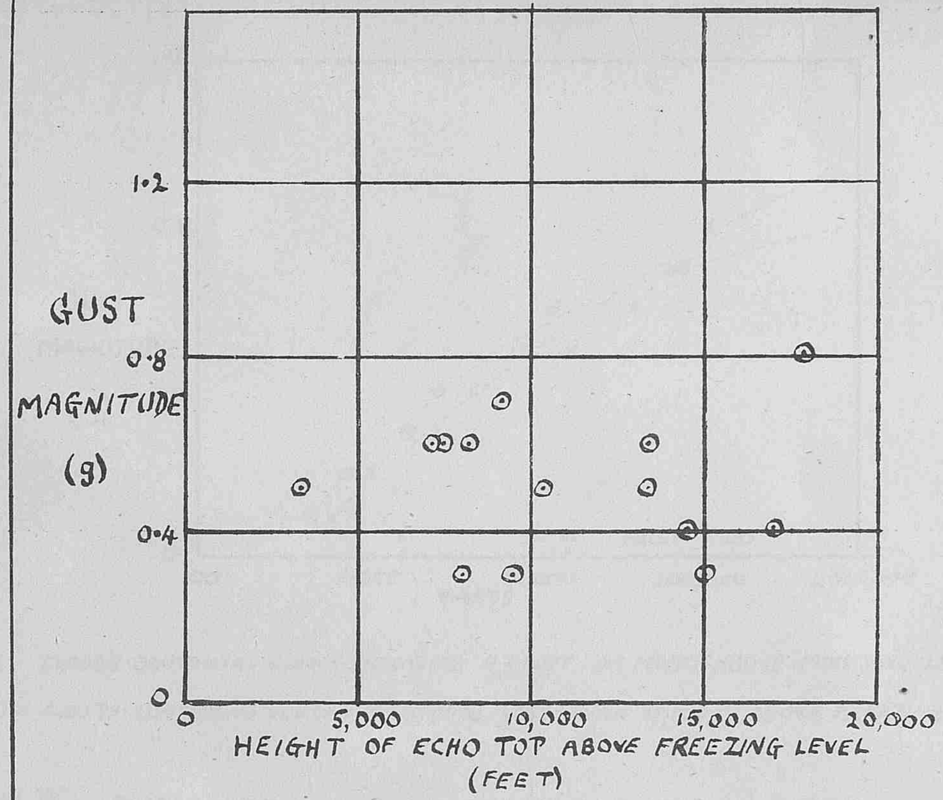

FIG I: VERTICAL EXTENT OF ECHO AND MAXIMUM GUSTS ENCOUNTERED IN CLOUD CONTAINING ECHO - UP-GUSTS

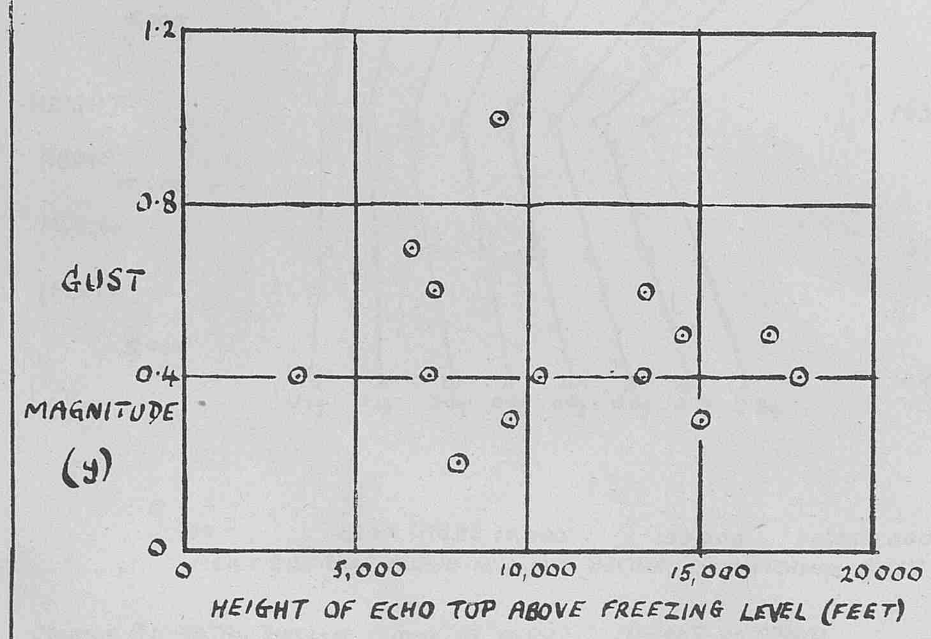

FIG II: VERTICAL EXTENT OF ECHO AND MAXIMUM GUSTS ENCOUNTERED IN CLOUD CONTAINING ECHO - DOWN-GUSTS

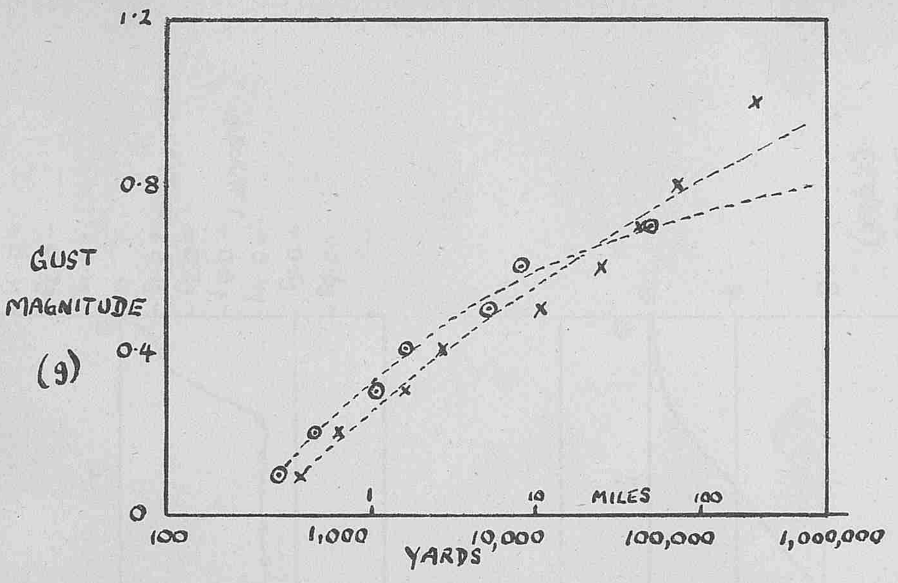

x - CLOUDS CONTAINING ECHOES EXTENDING 9,000 FT OR MORE ABOVE FREEZING LEVEL

⊙ - CLOUDS CONTAINING ECHOES EXTENDING LESS THAN 9,000 FT ABOVE FREEZING LEVEL

FIG III: DISTANCE FLOWN IN CLOUD BEFORE ENCOUNTERING GUST OF SPECIFIED MAGNITUDE. ALL FLIGHTS AT ALL HEIGHTS.

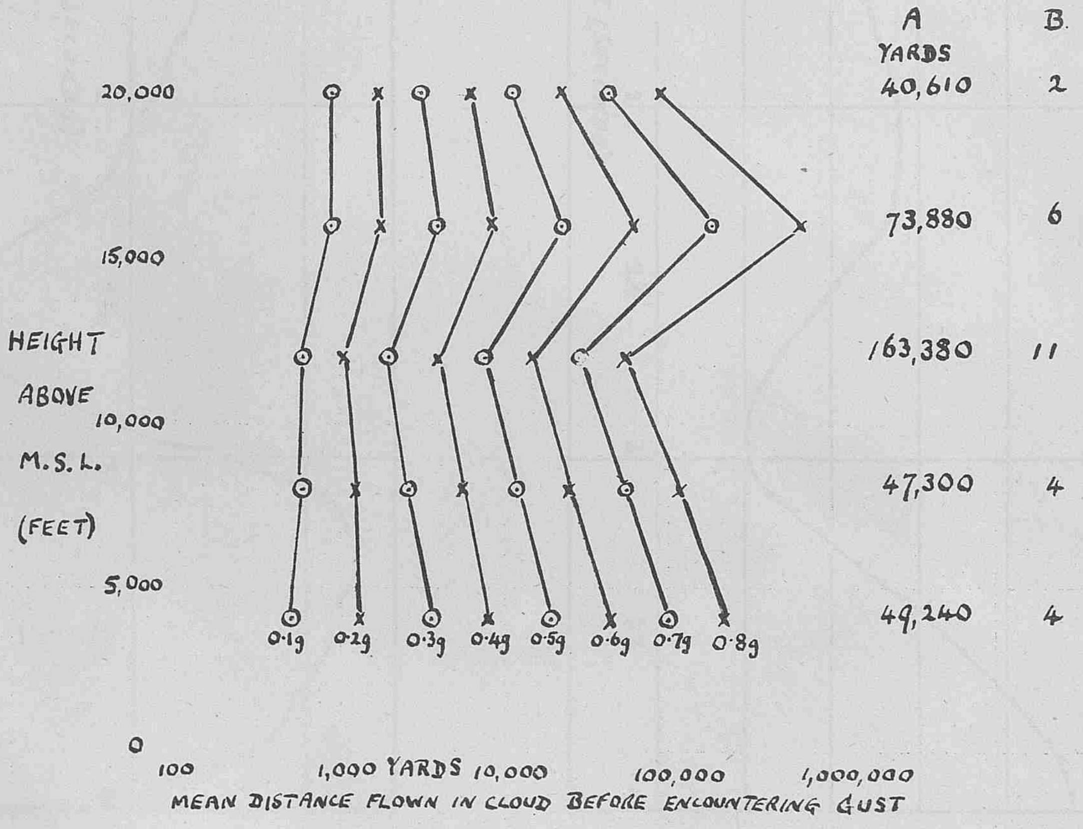

COLUMN A: TOTAL DISTANCE FLOWN IN 4,000 FT HEIGHT INTERVAL

COLUMN B: NUMBER OF FLIGHTS IN 4,000 FT HEIGHT INTERVAL

FIG IV: VARIATION OF GUST FREQUENCY WITH HEIGHT ABOVE MEAN SEA LEVEL FOR VARIOUS GUST MAGNITUDES

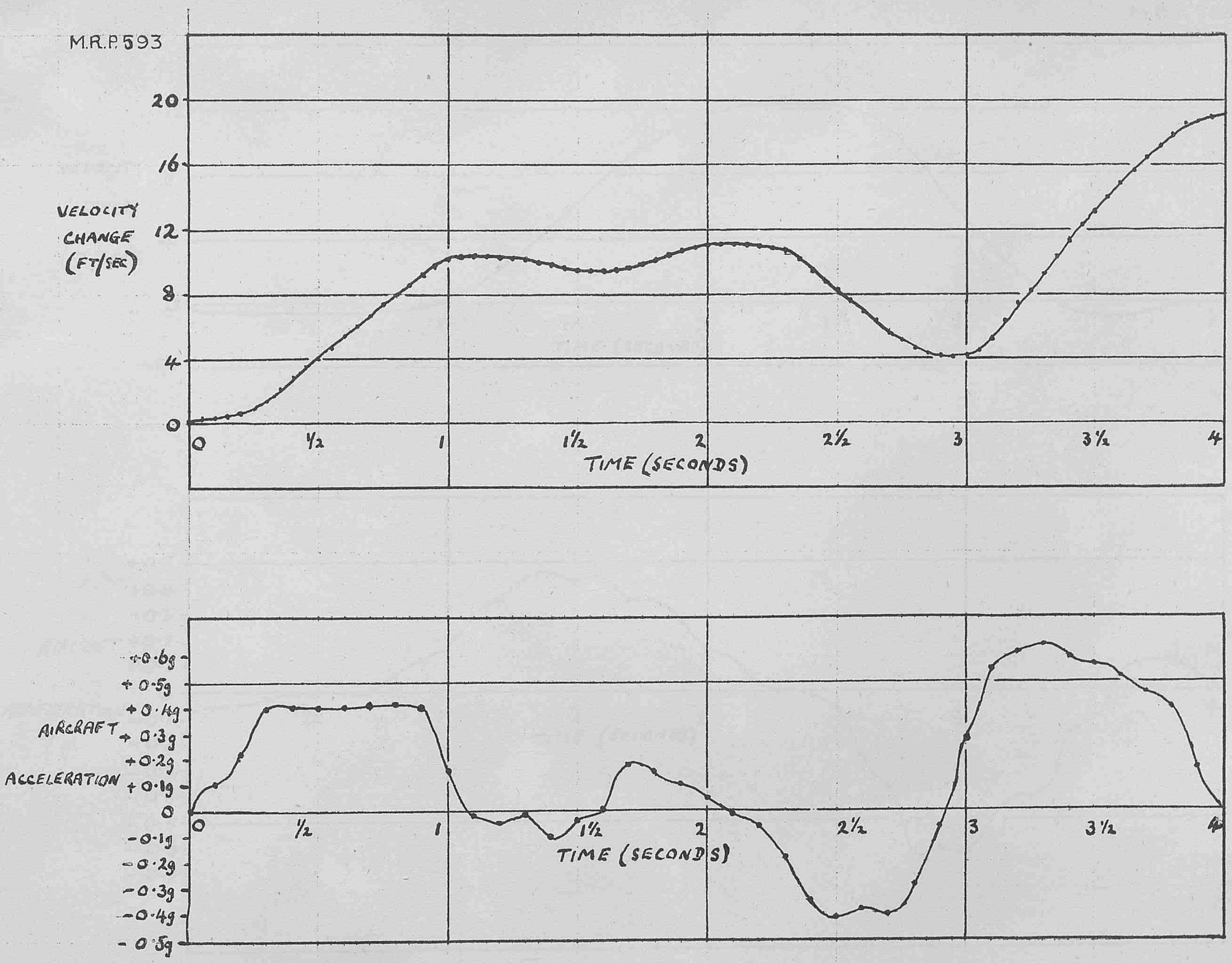

FIG V: SEQUENCE OF THREE MAJOR GUSTS FROM AIRCRAFT ACCELEROMETER RECORD AND (ABOVE) INTEGRATED CURVE SHOWING RESULTANT VELOCITY CHANGE

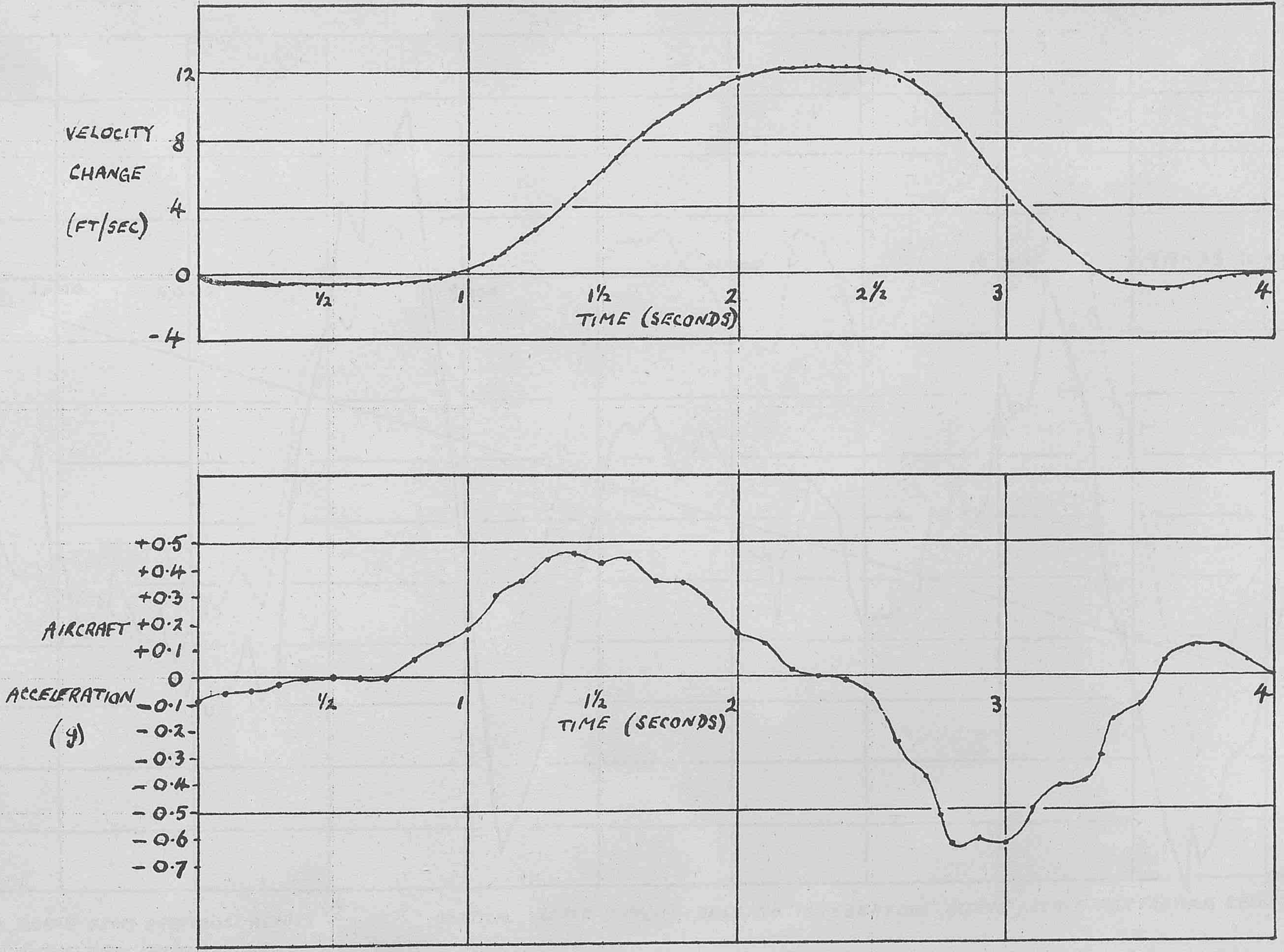

FIG VI: SEQUENCE OF TWO MAJOR GUSTS FROM AIRCRAFT ACCELEROMETER RECORD AND (ABOVE) INTEGRATED CURVE SHOWING RESULTANT VELOCITY CHANGE

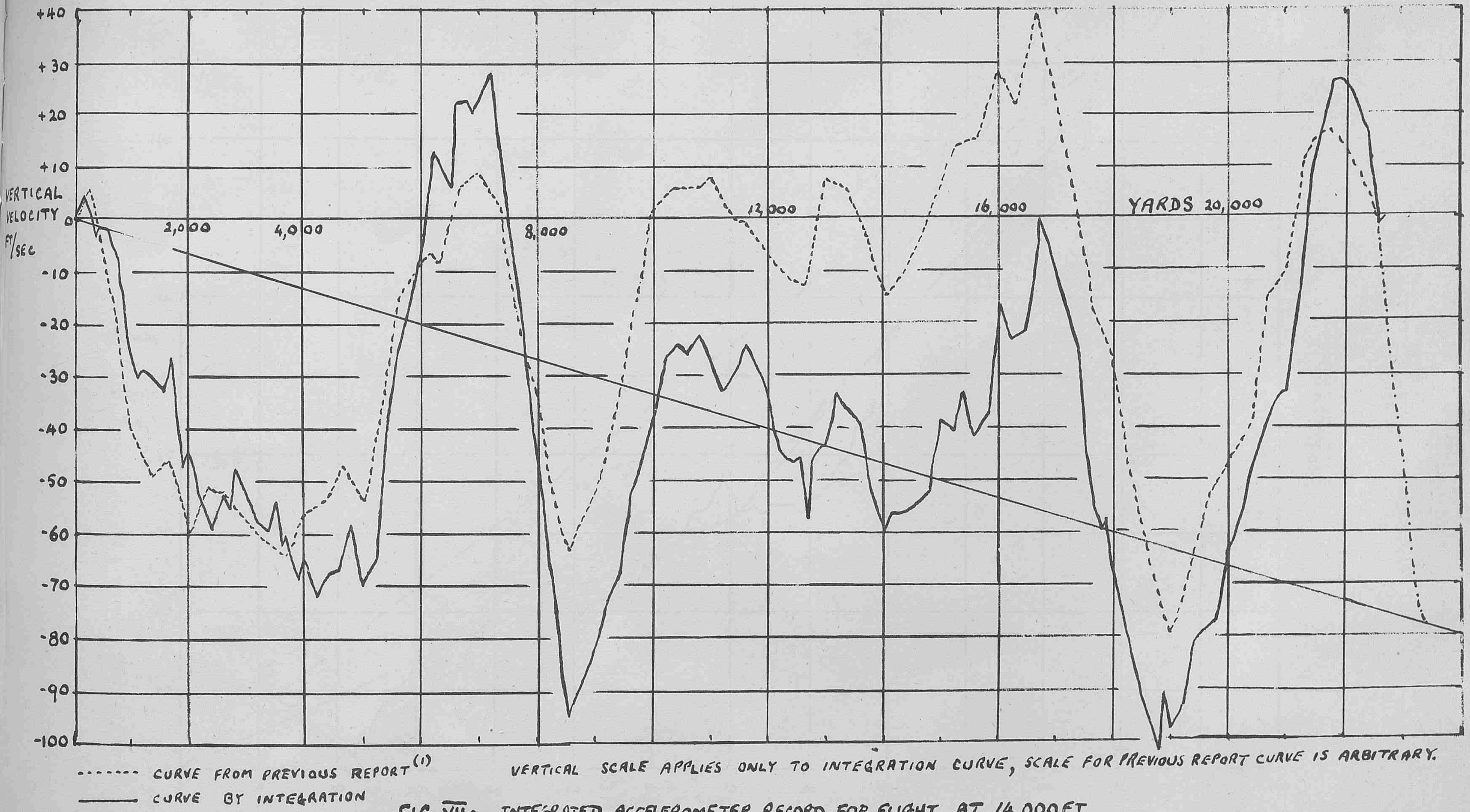

VERTICAL SCALE APPLIES ONLY TO INTEGRATION CURVE, SCALE FOR PREVIOUS REPORT CURVE IS ARBITRARY.

FIG VII: INTEGRATED ACCELEROMETER RECORD FOR FLIGHT AT 14,000 FT

10TH JUNE 1948

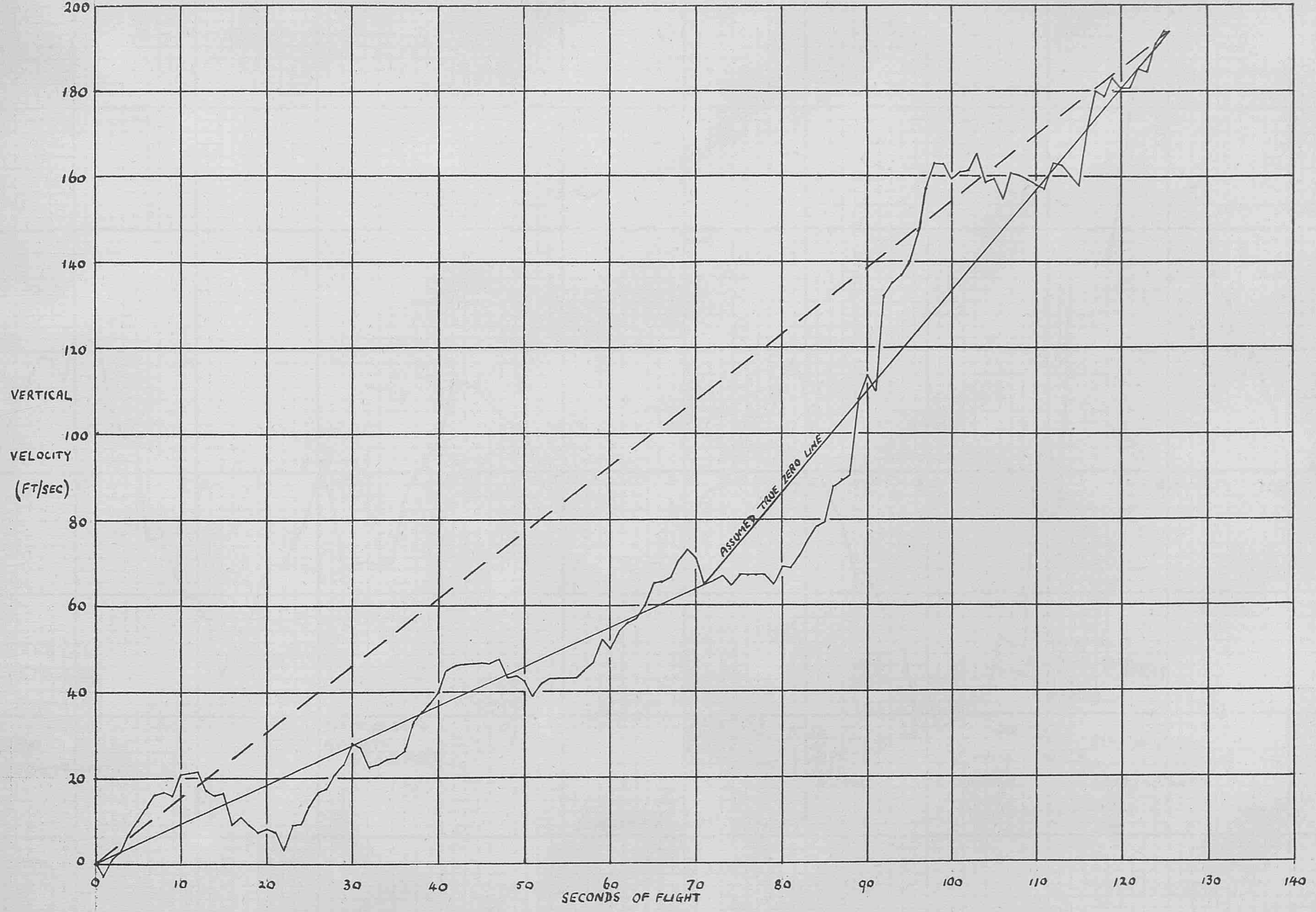

FIG VIII: INTEGRATED ACCELEROMETER RECORD (BEFORE CORRECTION) FOR FLIGHT AT 10,500FT, 1ST JUNE 1949

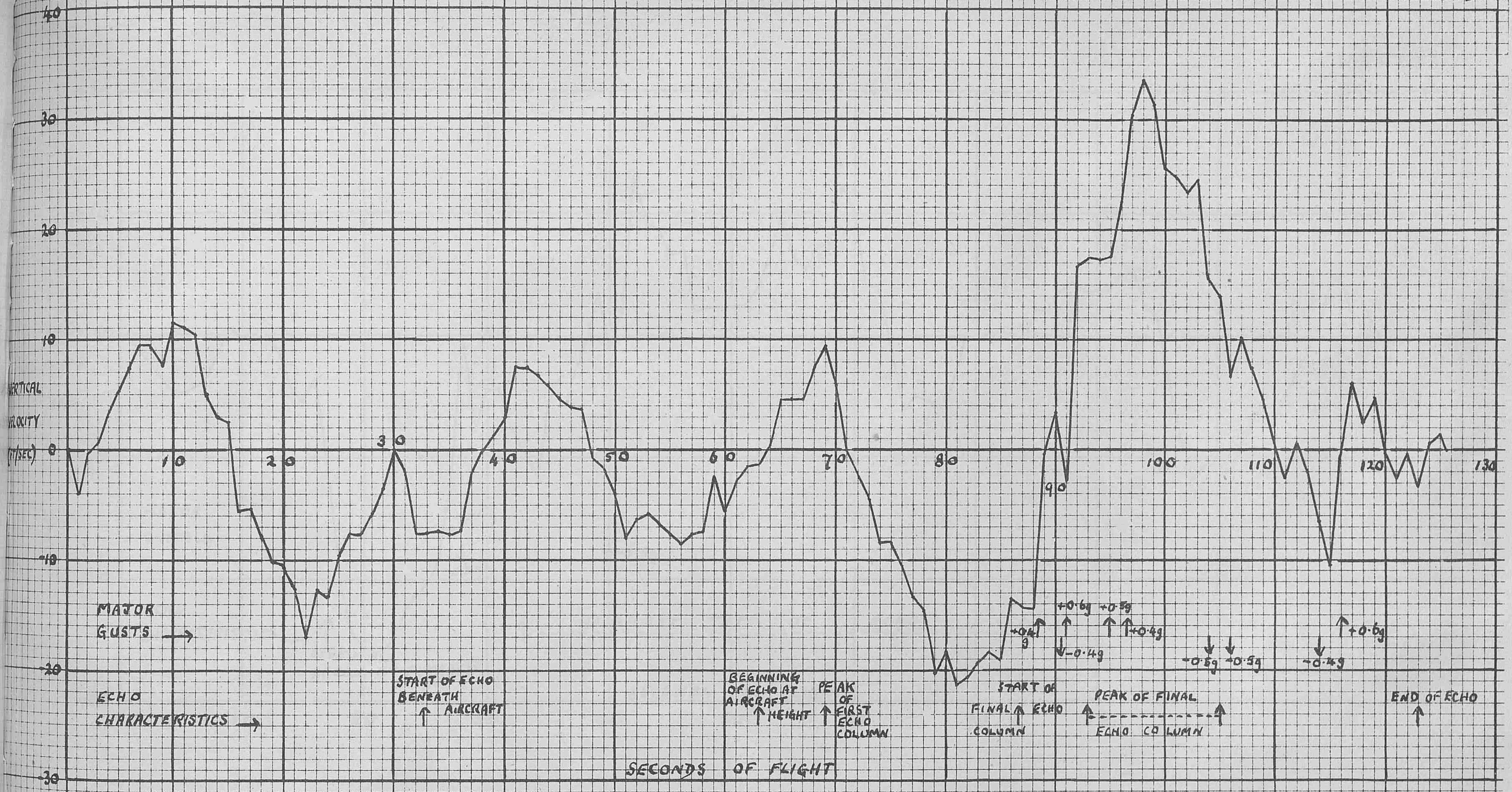

FIG IX: INTEGRATED ACCELEROMETER RECORD, CORRECTED ACCORDING TO ZERO LINE OF FIG VIII, FOR FLIGHT AT 10,500FT, 1ST JUNE 1949
AND MAJOR ECHO AND GUST FEATURES

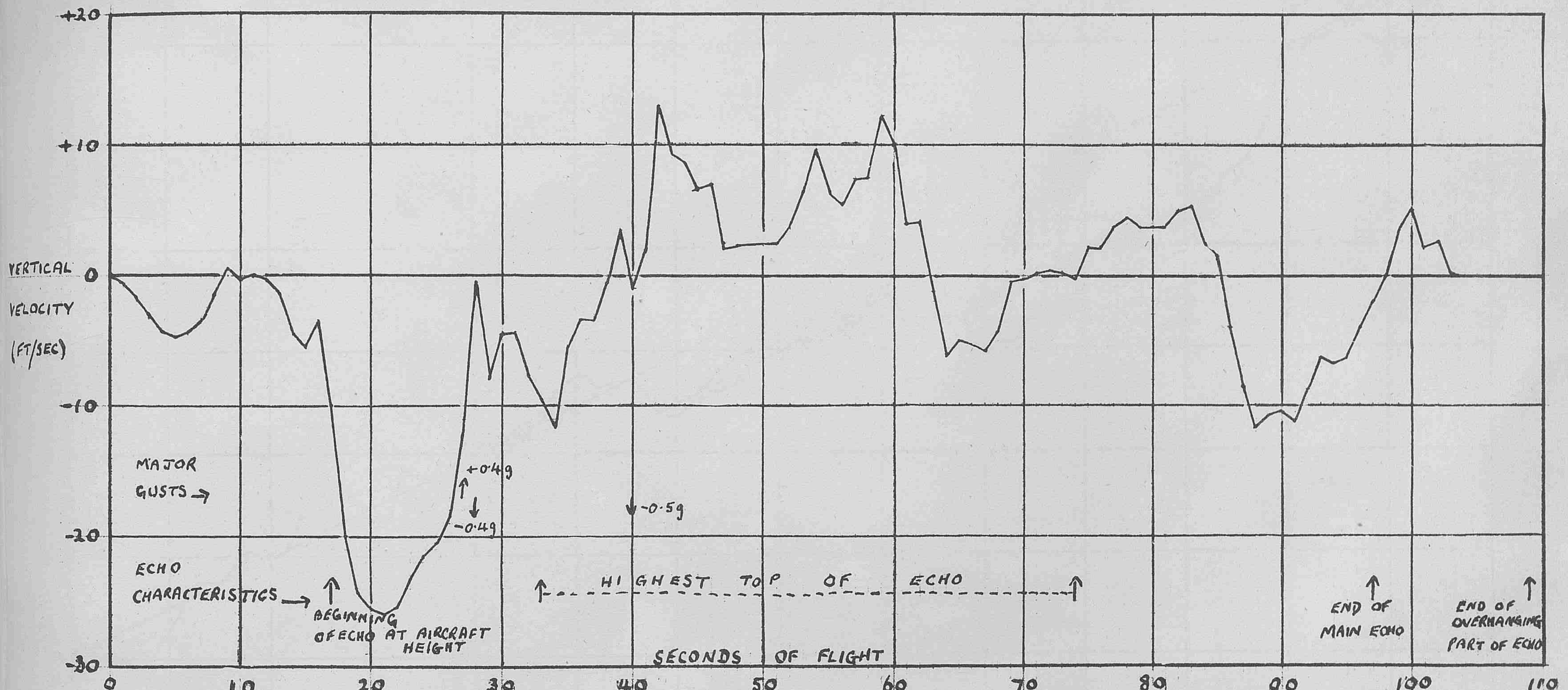

FIG X: INTEGRATED ACCELEROMETER RECORD, CORRECTED FOR CONSTANT ZERO ERROR, FOR FLIGHT AT 12,000 FT, 2ND JUNE 1949 AND MAJOR ECHO AND GUST FEATURES

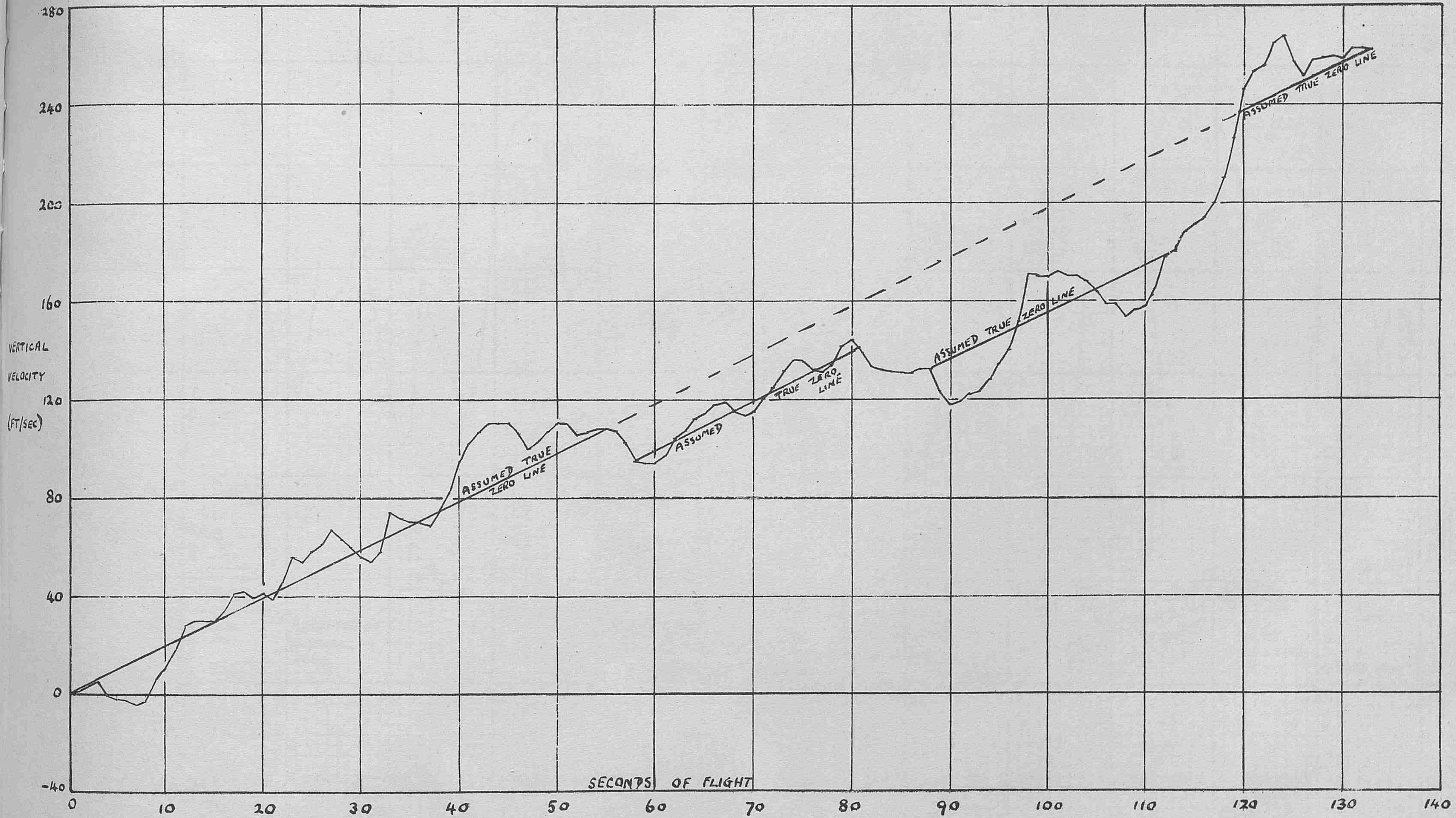

FIG XII : INTEGRATED ACCELEROMETER RECORD (BEFORE CORRECTION) FOR FLIGHT AT 8,000 FT, 18TH MAY 1949

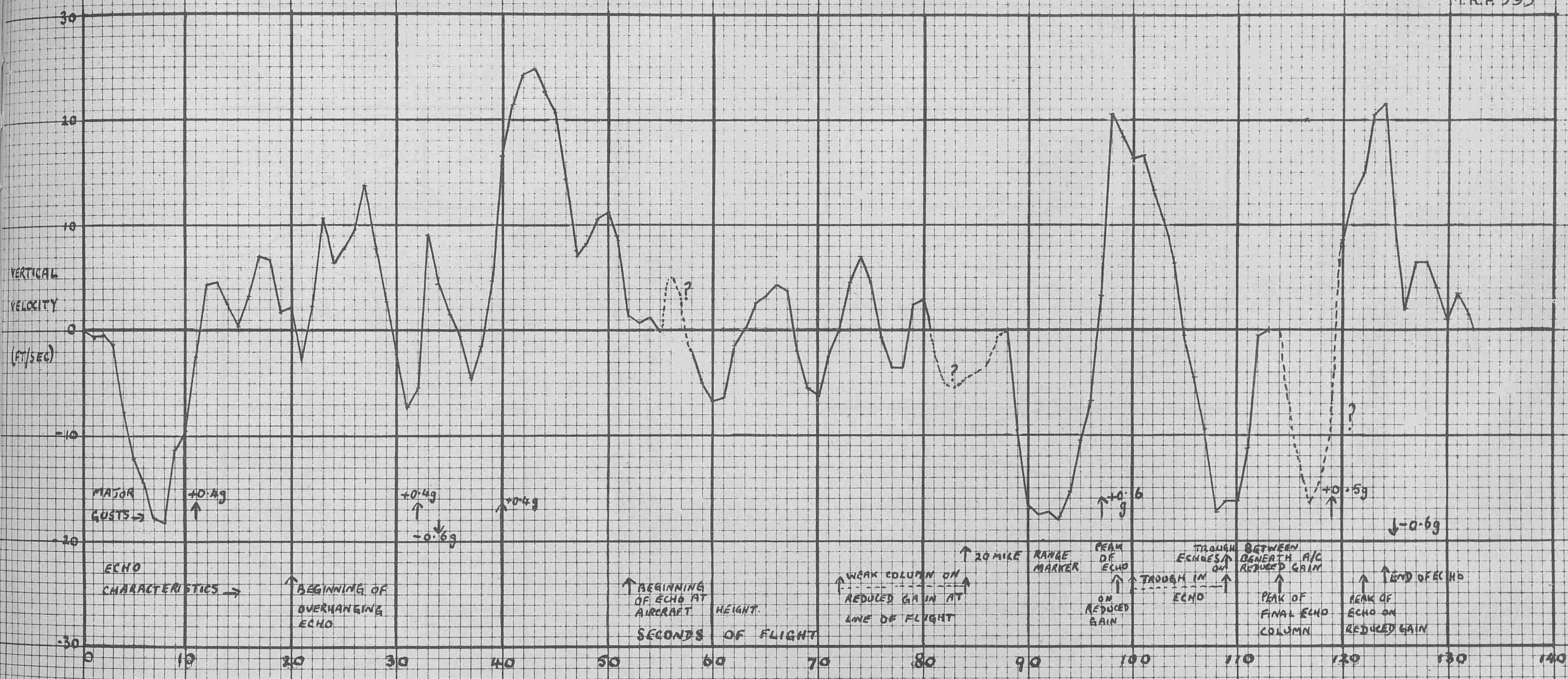

FIG XIII: INTEGRATED ACCELEROMETER RECORD, CORRECTED ACCORDING TO ZERO LINES OF FIG XV, FOR FLIGHT AT 8,000 FT, 18TH MAY 1949

AND MAJOR ECHO AND GUST FEATURES

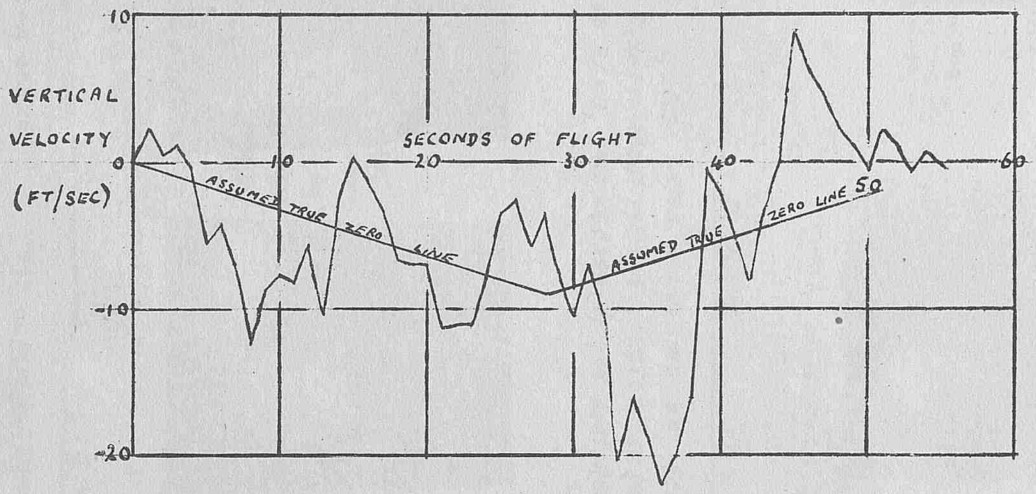

FIG XIV : INTEGRATED ACCELEROMETER RECORD, AFTER CORRECTION FOR CONSTANT ZERO ERROR, FOR FLIGHT AT 4,000 FT, 23RD APRIL 1948

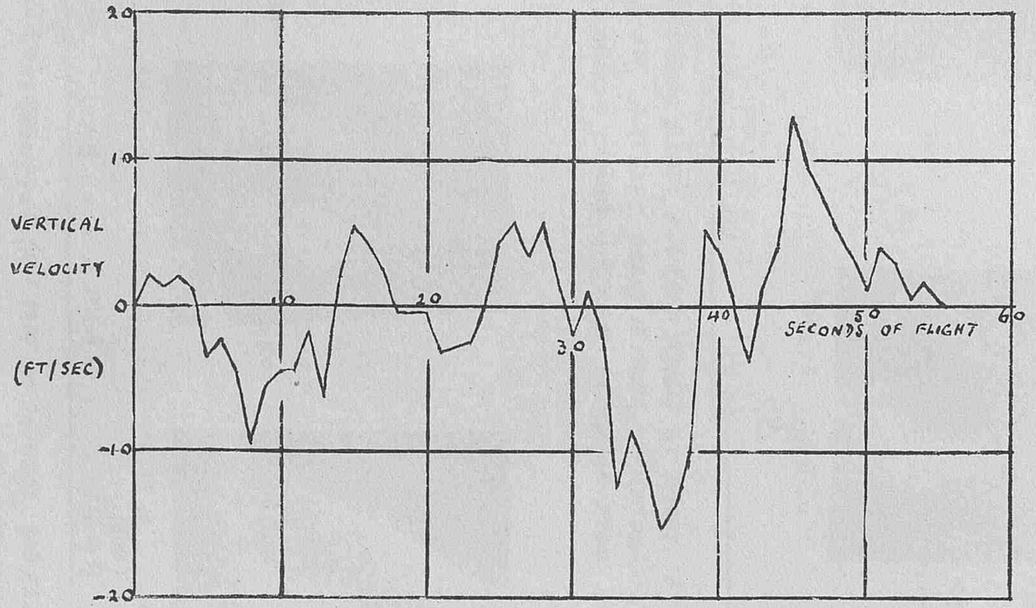

FIG XV : INTEGRATED ACCELEROMETER RECORD CORRECTED ACCORDING TO ZERO LINE OF FIG XVIII, FOR FLIGHT AT 4,000 FT, 23RD APRIL 1948

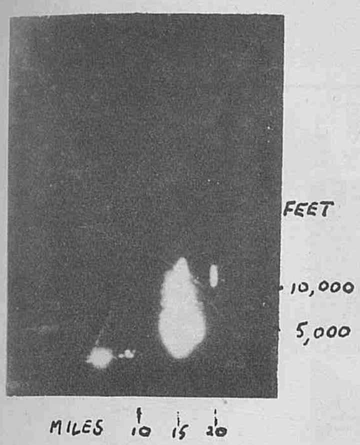
FEET
10,000
5,000
MILES 10 15 20

(i)

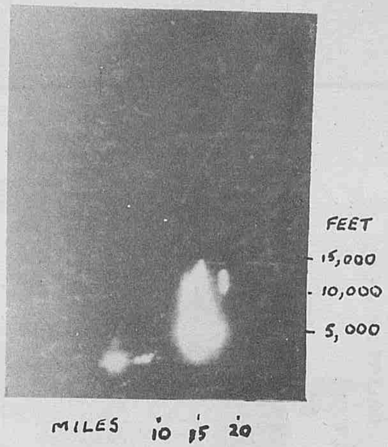
FEET
15,000
10,000
5,000
MILES 10 15 20

(ii)

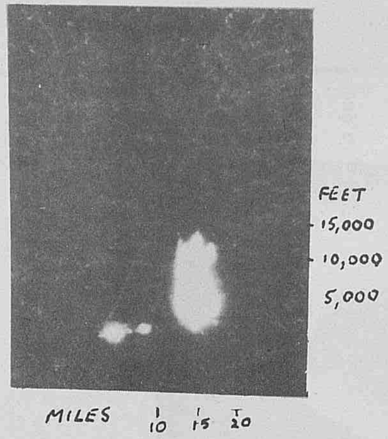
FEET
15,000
10,000
5,000
MILES 10 15 20

(iii)

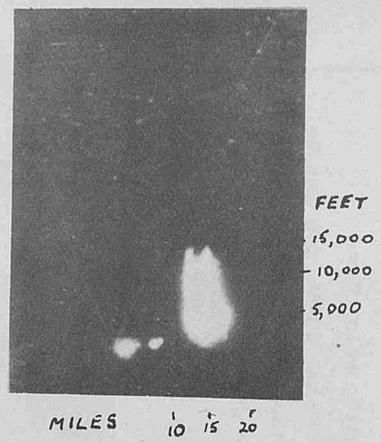
FEET
15,000
10,000
5,000
MILES 10 15 20

(iv)

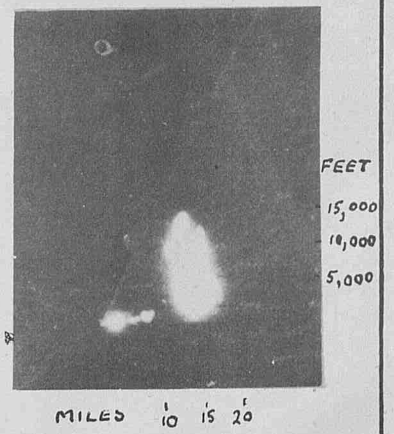
FEET
15,000
10,000
5,000
MILES 10 15 20

(v)

← FLIGHT AT 10,500 FT 1ST JUNE 1949 →

PHOTOGRAPH (i) TAKEN 9 SECS AFTER SWITCHING ON ACCELEROMETER (I.E. 9 SECS AFTER ENTERING CLOUD), AIRCRAFT VISIBLE AT ABOUT 18 MILES, PHOTOGRAPH (ii) 29 SECS AFTER SWITCHING ON, AIRCRAFT ABOUT 17 MILES, PHOTOGRAPH (iii) 48 SECS AFTER SWITCHING ON, AIRCRAFT ABOUT 15 MILES, PHOTOGRAPH (iv) 68 SECS AFTER SWITCHING ON, AIRCRAFT IN EDGE OF ECHO, PHOTOGRAPH (v) 135 SECS AFTER SWITCHING ON (9 SECS AFTER LEAVING CLOUD), AIRCRAFT CLEAR OF ECHO AT ABOUT 10 MILES

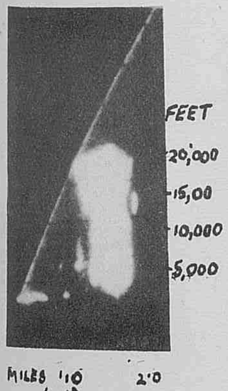
FEET
20,000
15,00
10,000
5,000
MILES 10 20

(vi)

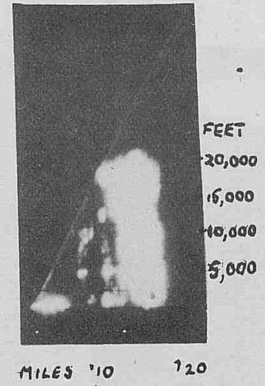
FEET
20,000
15,000
10,000
5,000
MILES 10 20

(vii)

FLIGHT AT 12,000 FT 2ND JUNE 1949

PHOTOGRAPH (vi) TAKEN 2 SECS BEFORE SWITCHING ON ACCELEROMETER (AIRCRAFT VISIBLE AT 18 MILES), PHOTOGRAPH (vii) 121½ SECS AFTER SWITCHING ON (AIRCRAFT AT 11 MILES)

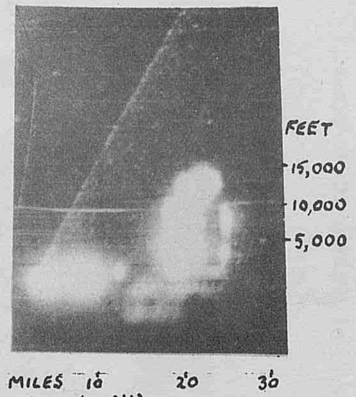
FEET
15,000
10,000
5,000
MILES 10 20 30

(viii)

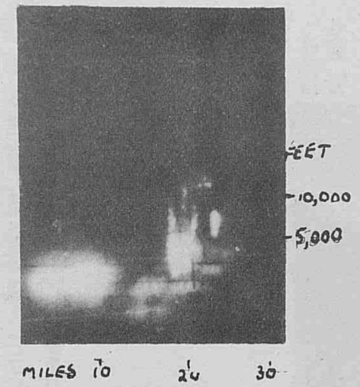
FEET
10,000
5,000
MILES 10 20 30

(ix)

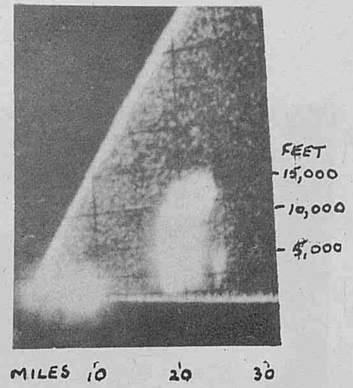
FEET
15,000
10,000
5,000
MILES 10 20 30

(x)

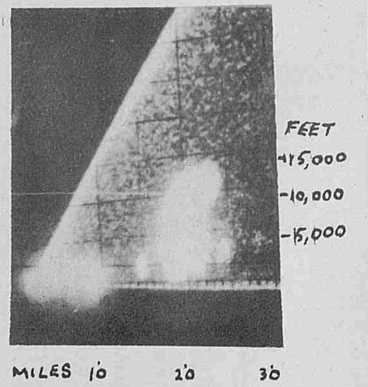
FEET
15,000
10,000
5,000
MILES 10 20 30

(xi)

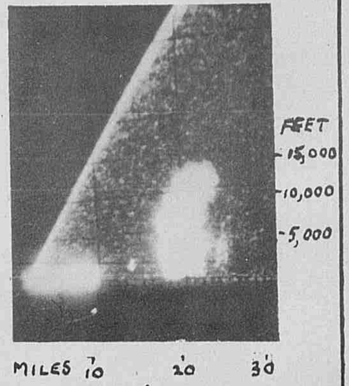
FEET
15,000
10,000
5,000
MILES 10 20 30

(xii)

← FLIGHT AT 8,000 FT 18TH MAY 1949 →

PHOTOGRAPH (viii) TAKEN 9½ SECS AFTER SWITCHING ON ACCELEROMETER (AIRCRAFT AT 24 MILES), (ix) REDUCED GAIN PHOTOGRAPH AT 32 SECS (AIRCRAFT AT 23 MILES), (x) AT 62 SECS (AIRCRAFT IN EDGE OF ECHO - VISIBLE ON NEGATIVE - AT 21½ MILES), (xi) AT 102 SECS (AIRCRAFT IN ECHO - VISIBLE ON NEGATIVE - AT 19 MILES), (xii) AT 122 SECS (AIRCRAFT JUST LEAVING ECHO AT 17½ MILES)

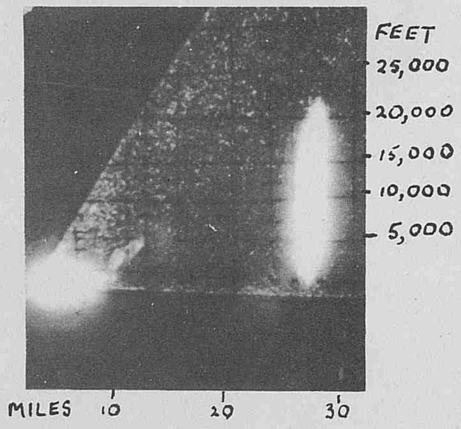

(xiii)

TYPICAL RADAR ECHO FROM CUMULONIMBUS IN ACTIVE STAGE

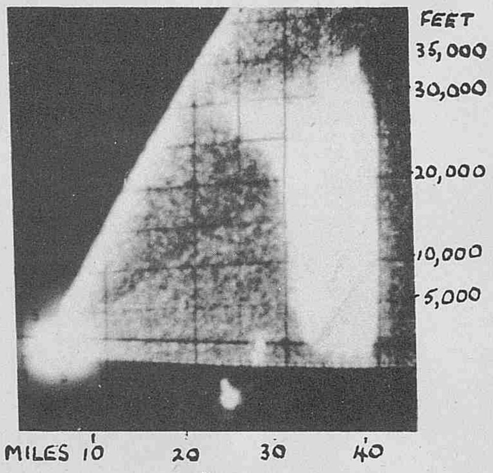

(xiv)

ECHO FROM CUMULONIMBUS SHOWING DIFFUSE ECHO FROM ANVIL

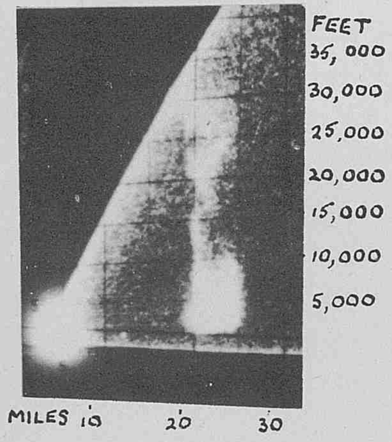

(xv)

ECHO FROM DECAYING CUMULONIMBUS. NOTE DIFFUSE ECHO 10,000 - 30,000 FT AND EVIDENCE OF BRIGHT BAND CENTRED AT 5000 FT.

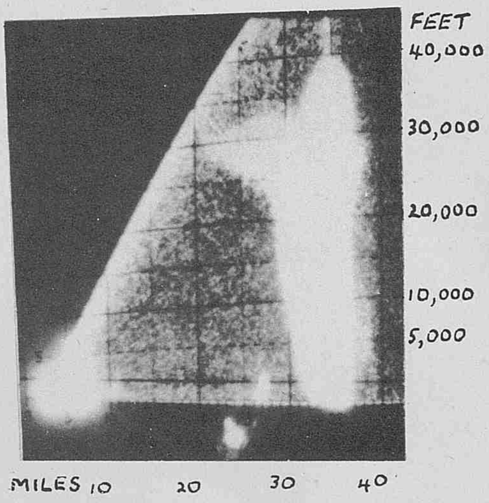

(xvi)

ECHO FROM CUMULONIMBUS SHOWING ACTIVE COLUMN OF ECHO EXTENDING ABOUT 7,000 FT ABOVE THE TOP OF THE DIFFUSE ANVIL ECHO

paper of the Meteorological Research
Committee (London).
M.R.P. No........... by Mr.........................
A copy is available in the Library of
the Meteorological Office.

M.R.P.597
S.C.II/65
28th November, 1950

ATI-146975

AIR MINISTRY

METEOROLOGICAL RESEARCH COMMITTEE

Studies of the structure of fronts - Part I

by

A.G. Matthewman (Meteorological Office)

AIR WEATHER SERVICE
TECHNICAL REFERENCE FILE
JUN 6 1951

1.0. Introduction

In the course of studies on the structure of fronts now in hand in the Forecasting Research Division of the Meteorological Office a considerable number of frontal situations in the neighbourhood of the British Isles are being studied. At a later stage it is hoped to be able to present general conclusions of value in analysis and forecasting. The present short note is intended only to illustrate the nature of the problem. There is nothing essentially new in the results but it is believed that some of the points brought out will not be familiar to many meteorologists who have not themselves attempted to construct cross sections carefully from the observational data.

Although fronts have now been studied for over thirty years, although many detailed analyses have been published and although the standard textbooks show apparent agreement on many aspects, there still remain difficulties of a fundamental nature - indeed there is no satisfactory definition of the term "front" which will cover its wide connotation in synoptic practice or ensure that two analysts will inevitably arrive at the same representation. We shall not however, at this stage, attempt to discuss fundamentals of definition or analysis but shall by studying the data merely indicate some of the difficulties.

1.1. The data used.

The observations used here are the radio-sonde reports of winds, temperature and humidity, from the British Isles and neighbouring areas. In some cases we have had access to the fuller information available in the original records and have not restricted attention to the necessarily incomplete information contained in synoptic reports. The study of these fuller reports is seen to have some importance. It is obvious that the consideration of observational errors may be essential to the proper interpretation of the reports but digression into this difficult field has been left for later attention.

1.2. The mode of representation.

There is a very wide choice of possible parameters to use for the representation of the fields of wind, temperature and humidity. The method here used is as follows:-

1.2.1. The vertical co-ordinate.

Pressure is taken as the basic variable. The corresponding I.C.A.N. height is taken as linear co-ordinate.

1.2.2. Winds.

The vector wind is represented by components as nearly as practicable parallel and at right angles to the front at the surface.

/1.2.3.

1.2.3. Temperature. On the diagram showing temperature in vertical cross-sections, isopleths of dry-bulb temperature on the ordinary Fahrenheit scale are drawn at intervals of 10°.

On the diagram showing temperature on individual vertical soudings, it was considered useful to plot what Bleeker (1) has called the "saturated-potential temperature", namely the temperature at 1000 mbs. in the saturated adiabatic through the observational plots of dry-bulb temperature on the tephigram. It is evident that conditional stability and instability is readily seen in this mode of representation of dry-bulb temperature, and also that at high levels the saturated-potential temperature tends closely to the corresponding wet-bulb potential temperature. The choice here of saturated-potential temperature was guided chiefly by the consideration that (i) the form of this temperature-height graph preserves the form of the corresponding graph of ordinary dry-bulb temperature - in particular jumps in the vertical gradients are preserved - and (ii) a convenient graphical relationship exists between saturated-potential temperature, wet-bulb potential temperature and humidity.

1.2.4. Humidity. The depression of the wet-bulb potential temperature below the saturated-potential temperature has been used in vertical soundings. It will be seen that this gives a clear indication of the humidity and taken alongside the representation of temperature provides by simple subtraction the wet-bulb potential temperature, which is probably the best simple indicator of air mass differences. It is considered that in this mode of representation the essentials are displayed most readily in a minimum of curves.

2.0. The warm front affecting the British Isles, March 31st. 1948.

In figures 1(a) and (b) the surface synoptic situation for 31st March, 1948 at 03.00 and 09.00 G.M.T. is shown. The main surface warm front, cold front and occlusion, the isobars, and present weather precipitation⌿ are shown conventionally. These require no further explanation.

In figures 2(a) and (b) the soundings* for Penzance 03.00, Larkhill 09.00, Penzance 09.00 and Downham 09.00 are represented. The two former are shown on the same diagram as they are in similar positions relative to the advancing surface warm front.

2.1. Analysis of the temperature and humidity soundings.

On a broad view, a single frontal zone with well-marked boundaries is revealed by the Penzance 09.00 temperature soundings (see Fig. 2(b)). The upper boundary of this frontal zone, i.e. the lower boundary of the warm air-mass, is shown by a (pecked) arrow marked "front."

It is evident that the corresponding boundary of the warm air-mass, even at heights in the upper troposphere, may be readily located on the other temperature soundings shown in figures 2(a) and 2(b), as shown by the arrows marked "front."

The lower boundary of the frontal zone, that is, the upper boundary of the main cold air-mass, is very clear on the Penzance sounding for 09.00 and fairly clear on the other soundings shown, but the minor complexities within (and at Downham also below) the main frontal zone are considerable. Probable correspondences of zones of lesser lapse-rate are indicated by numbers in figures 2(a) and 2(b). It is obvious that the correspondences are neither perfect nor beyond dispute.

/On

⌿ For explanation of symbols see appendix.

* Soundings are normally begun one hour before the time stated.

On the Penzance 09.00 sounding a further zone of reduced lapse-rate at high levels is also indicated in figure 2(b).

The humidity readings at Penzance 03.00 are strongly suggestive of subsidence having occurred around 600 mbs. At Larkhill there is similar suggestion of subsidence in the zones marked 4 and 5 and to some extent in 3 although the minimum humidity is greater and is registered rather above the upper boundary of 3. The minor irregularities of the Downham temperature curve, marked 3, 4 and 5, correspond only very slightly to variations in the humidity graph.

2.2. Analysis of the associated wind-soundings.

Associated wind-soundings were available at Downham and Larkhill and these are shown in figures 2 (a) and 2 (b). Minute-average values, centred at the dots and joined by straight lines, give the actual wind components in knots resolved along and perpendicular to the line Penzance - Larkhill - Downham, this line being approximately perpendicular to the surface warm front.

The component quasi-parallel to the front shows a strong increase with height mainly in the upper troposphere to a little below the tropopause. At Downham this increase commenced somewhat above the level regarded as the lower boundary of the broad frontal zone in the temperature field, and extended to the upper boundary of that zone, marked "front" in fig. 2(b). This increase was particularly marked in the sub-zone corresponding to 1 and part of 2. At Larkhill the increase with height in the same component is irregular. It is particularly strong in the sub-zone corresponding to 1, 2, though the rate of increase is only slightly less just above the "front." Some of the variations in the rate of increase with height would appear significant, but detailed correspondences between the various other zones of lesser lapse-rate and zones of greater increases of wind component with height cannot be satisfactorily established.

The line Penzance - Larkhill - Downham is quasi-perpendicular to the surface front. The corresponding component of wind should not be treated as accurately perpendicular to the front at any level, but it may be significant that at Larkhill there is a broad (though irregular) slight decrease with height in this component to about the level of the "front" and a zone of marked increase just above. In the case of Downham, however, a similar decrease upwards to about the middle of the troposphere changes over to a zone of marked increase well below the "front."

2.3. Main features of the soundings shown in figures 2(a) and 2(b)

2.3.1. On a broad scale the four temperature soundings in figures 2(a) and 2(b) ahead of the surface warm front show homogeneously a broad frontal zone, occupying at Penzance (09.00) some 12,000 feet and increasing towards Downham to some 23,000 feet. In detail, the correspondences between soundings of singularities in the vertical temperature gradient within the frontal zone are not obvious.

2.3.2. The component of wind quasi-parallel to the front indicates a jet-stream with a maximum, between Larkhill and Downham, of probably about 135 knots. At Downham the whole of the increase with height in the component is contained within the broad frontal zone defined by the temperature sounding. At Larkhill, on the opposite side of the jet, more than half of the total increase occurs above the front defined by the temperature sounding.

/2.3.3.

2.3.3. The component of wind quasi-perpendicular to the front at Larkhill and Downham shows a broad similarity of structure with height but not similar in relation to the location of the frontal zone on the temperature soundings. The average speed of the surface warm front along the line Penzance - Larkhill - Downham over the six hours 03.00 to 09.00, namely 25-30 knots, may be compared with the component at Larkhill 09.00. At 03.00 the corresponding Larkhill component was 5 to 10 knots lighter, up to 600 mbs.

2.3.4. Correspondences between the singularities in the curves of wind, temperature and humidity on the same sounding are sometimes lacking, or not all obvious, and do not necessarily occur at approximately the same pressure-levels.

3.0. The wave depression affecting the British Isles, October 24th-25th, 1949.

3.1. The surface synoptic situation.

In figs.3 to 6 the mean-sea-level isobars at 4 mbs. intervals and present weather precipitation are displayed for 03.00 and 15.00 G.M.T. on October 24th and 25th, 1949.

The main frontal zones are shown hatched between pecked lines. The minor frontal zones within the main warm sector are left unhatched. The main emphasis of the analysis is on the British Isles area particularly along the line of the vertical cross-sections.

Fig.3 shows at 03.00 October 24th a pronounced wave centred north of the Azores on a frontal zone separating cold polar-maritime air, with a relatively direct track, from warm polar-maritime air which had passed for some time over much warmer sea. This frontal zone at the surface coincided with the main trough lines in the mean-sea-level isobars and carried the centre of the lowest pressure. S.E. of the centre, a second frontal zone separated this warm polar-maritime from the tropical maritime air to south. The temperature contrast across this second zone was rather feeble. This double frontal structure complicates both the surface and upper-air analysis.

In the present example the occlusion process was accompanied by only minor and temporary deepening of the centre of about 8 mbs.

3.2. Upper-air data.

3.2.1. The vertical cross-sections. Two quasi-parallel vertical cross-sections, each quasi-perpendicular to the main warm front of the wave, have been chosen through the radio-sonde stations:

(i) Ship 66°N 02°E, Lerwick, Leuchars, Liverpool, Larkhill, Gibraltar, and

(ii) Jan Mayen, Thorshavn, Stornoway, Aldergrove, Camborne, Brest, Lisbon.

By no means all of these stations reported every six hours wind, temperature and humidity; nevertheless a sufficient number were available particularly in the neighbourhood of the fronts to obtain a series of cross-sections consistent in space and time, as in figs.15 to 27, which illustrate the structure of the fronts as regards dry-bulb temperature (ordinary Fahrenheit scale), (pseudo) wet-bulb potential temperature, and the actual and geostrophic wind fields perpendicular to the cross-sections. Present weather precipitation as reported by stations on or close to the line of the cross-sections and some details of cloud as observed from these ground stations are also entered below the cross-sections, together with a scale of distance from Larkhill.

3.2.2. The individual soundings. The individual soundings for Larkhill at six hour intervals from 03.00 October 24th to 15.00 October 25th are displayed in figures 7 to 13.

The line of the cross-sections Gibraltar - Bordeaux - Larkhill - Liverpool - Leuchars - Lerwick - 66°N 02°E is not quite straight, and although it does not vary much from south - north throughout its length, at Larkhill the directions along and perpendicular to the cross-sections are (about) 160° and 250° respectively. The winds reported by Larkhill have accordingly been resolved in these directions. Marked by crosses are the usual reported winds at 50 mbs. intervals (which are based on 2 or 3-minute averages according as the 50 mbs. pressure level falls or does not fall within 0.2 minutes of the mid-point of the successive 1-minute intervals at which the balloon is located). These crosses have been joined by straight segments of pecked lines. In addition, some greater detail is shown in figs.7 to 10, in which the corresponding 1-minute-average winds are denoted by dots at the mid-point of the 1-minute intervals. These dots have been joined by segments of full straight lines.

The two sets of wind averages illustrate some of the intrinsic difficulties in dealing with radio-sonde observations of wind. Besides instrumental errors, which since the advent of radar are considered to be in general very small - probably less than 2 or 3 knots even up to a slant range of order 66,000 yards - there are usually minor fluctuations say of order 3 to 5 kts. which are probably of no interest except in study of turbulence. If these errors and turbulent fluctuations are reduced by averaging over 2 or 3 minutes instead of over 1-minute intervals the question remains whether averages at successive 50 mbs. pressure-levels (up to 200 mbs., then additional levels) are appropriate and sufficient and whether these 50 mbs. observational points are properly to be joined by straight lines.

As an example of the difficulty consider the graph of the 250° component at 03.00 October 24th. This suggests in the 1 minute-averages joined by straight lines, three frontal zones, which are more or less supported, though not always in quite the corresponding pressure-levels, by the dry-bulb curve. The 2 or 3 minute-averages at 50 mbs. intervals, joined by straight lines, shift the pressure-levels of the quasi-discontinuities in the vertical gradient, "sharpen" the frontal zone 700 to 600 mbs., and replace by one, between 500 and 350 mbs., the two zones suggested by the 1-minute averages. It is a further complication that the pseudo-wet-bulb potential temperature graph derived by subtraction of the humidity from the dry-bulb readings at the various pressure-levels suggests 700 mbs. as a level at which the vertical gradient changes rather rapidly.

3.3. Analysis of the Larkhill soundings.

Between 03.00 October 24th and 03.00 October 25th, 1949 (figs.7 to 11) on a broad scale there are clear indications on the dry-bulb curves of a warm air-mass above a cold air-mass, separated by a warm frontal zone of relatively small lapse-rate with associated relatively large wind-shear quasi-parallel to the frontal zone. By 09.00 October 25th (fig.12) the warm air had replaced the cold down to the ground but at 15.00 October 25th (fig.13) fairly cold air appeared in the lowest layers, as a cold frontal zone passed Larkhill at the surface. Reversion to the more direct polar-maritime air on the Larkhill soundings is not evidenced until after the end of the period here discussed, namely 09.00 26th October.

Thus on a broad scale the frontal analysis is clear. But in detail there is considerable complexity. It is evident that there are sometimes considerable discrepancies between the pressure levels at which the frontal zone appears to be located according to the dry-bulb temperature and wind curves.

In some cases the discrepancies can be attributed to the fusion of an apparently subsided zone with the frontal zone itself - as for example in fig.10 below the chosen lower boundary of the frontal zone. Here the zone of relatively strong wind-shear corresponds more closely with the zone of relatively strong gradient of wet-bulb potential temperature as may be seen in fig.10, by subtracting the humidity from the dry-bulb temperature readings at the relevant pressure levels.

In other cases, the cause of the discrepancies is not known. In fig.11 for example, the chosen upper-boundary of the warm front appears well-defined in the dry-bulb temperature field, but in the one-minute averages of wind quasi-parallel to the front, the corresponding boundary of the marked shear occurs about 60 mbs. higher.

It is evident that the existence of these discrepancies introduces an arbitrariness into the precise location of the frontal boundaries.

It should be pointed out that the temporary appearance of a very dry layer in the middle troposphere at 09.00 25th has been here associated with a minor front, indicated in fig.12, behind a returning wave of tropical maritime air, but this interpretation is doubtful.

3.4. Main features of the cross-sections.

3.4.1. The pattern of isotherms in figs.15 to 21 and 26, 27 exhibits a main frontal zone with relatively small lapse-rate associated with relatively strong baroclinity. The boundaries of the zone are generally well-defined even at high levels in the troposphere, but are at times diffuse and somewhat arbitrary. There is often fairly strong baroclinity in one or both of the surrounding air-masses near the frontal zone, and some latitudinal fall of temperature northwards along the isobaric surfaces.

3.4.2. The tropopause above the warm air has been drawn continuous with the warm boundary of the frontal zone, and the tropopause above the cold air continuous with the cold boundary of the frontal zone. This is unconventional and uncertain.

3.4.3. The isopleths of (pseudo) wet-bulb potential temperature figs.22 to 25 exhibit the well-known tendency to parallelism with and within the frontal zone up to 400 or 300 mbs..

3.4.4. The values of geostrophic wind component perpendicular to the cross-sections, figs.22 to 25, are derived from the geostrophic wind at mean-sea-level and the thermal wind relation. The relatively strong thermal within the frontal zone as defined by the temperature field is associated with a relatively strong shear in the geostrophic component. The pattern of isopleths exhibits a well-marked westerly jet within the warm air and just below the tropopause. This jet moves north rather faster than the surface front while a secondary westerly jet appears farther south. There is a kind of easterly jet in the cold air ahead of the warm front near the ground.

3.4.5. The patterns of isopleths of the corresponding actual wind component perpendicular to the cross-sections similarly exhibit a relatively strong shear within the frontal zone, and well-marked jet-streams corresponding fairly closely in probable location and probable central-maximum value with the geostrophic jets. The behaviour of the actual westerly jets is summarised in fig.14. It should however be pointed out that the decreasing maximum speed of the main westerly jet between 15.00 October 24th and 15.00 October 25th is partly due to the general backing of the winds in the neighbourhood of the jet. Thus while the azimuth of the cross-section in the north at Lerwick and Leuchars is 190°-010°, at 15.00 October 25th the actual wind reported at Lerwick at 250 mbs. was 233° 130 knots. The speed of the 280° component is only 90 kts. and the maximum speed of the northern jet in the same component, which is estimated in the cross-section as nearly 110 knots (see fig.21)is correspondingly less than the total wind-speed at that place. Again the marked ridge on the isopleths of the 280° component wind-speed near Leuchars (fig.21) does not imply light total wind speeds in the area at high levels. The actual wind reported at Leuchars at 250 mbs. was 216° 116 knots.

The second westerly jet to south in fig.21 is located at about 250 mbs. and at about the latitude of the surface cold front. But this cold front, which was thermally rather weak, was aligned at the surface from about 330° to 150° near Larkhill (see fig.6) and the associated frontal zone at Larkhill occupied only the lower troposphere (about 950 to 750 mbs. in fig.13). At Larkhill, where the azimuth of the cross-section backs to 160°-340°, there is in the upper troposphere (450 to 250 mbs. fig.13) a marked increase in the 250° component of wind perpendicular to the cross-section and quasi-perpendicular to the cold front. Thus the southerly jet does not appear to be directly ascribable to geostrophic shear at the cold front. The corresponding geostrophic jet appears to be related rather to the marked baroclinity evident in the warm air between Larkhill and Liverpool. The typical jet structure of pronounced maximum with marked falling off in speed on either side appears to be related on the southern side to the contrary thermal within the cold frontal zone and on the northern side to the easterly jet in the cold air ahead of the warm front.

3.4.6. The following comparisons of these cross-sections with various published studies of temperature and wind fields, may be pointed out. Nyberg (2) has indicated frontal zones extending into the stratosphere through breaks in the tropopause on either side. Berggren, Bolin and Rossby (3) have given an example (for February 12th, 1948) of a frontal zone which was well-marked and seemed "to extend into the lower stratosphere over the Shetlands." The tropopause over the cold air was drawn continuous with the cold boundary of the frontal zone. A trough in the isotherms extended northwards and downwards from the tropopause over the warm air towards the warm boundary of the warm front but the tropopause was not drawn in this region. The associated zonal wind-field showed a single jet but with two troughs in the isopleths to south and to north. In a similar way, average meridional structure based on 12 polar fronts (Palmén and Newton (4)) indicates troughs approaching the upper defined boundaries of the frontal zone but no tropopauses were indicated. In this latter example the primary jet just below 250 mbs. is vertically above the front at around 500 mbs. There is an indication of a minor secondary jet at a higher level (about 200 mbs.) and 7° or 8° of latitude farther south. Durst and Davis (5) have shown an example of a jet stream vertically above the frontal surface at a much higher level than 500 mbs.

Crossman (6) has shown the existence of double jet-streams, averaged over the American area, in which the general tendency of the individual jets was to move south, but there is a northward movement of one jet from 50° to 57°N over the two days 27th to 29th March, 1948. The two jets were generally widely separated from one another but the separation varied from 22° to 8° of latitude.

Phillips (7) has described an investigation into jet-streams mainly over North America at 80° longitude, in which a double jet (23rd January 1948) is succeeded by a single jet associated with a well-developed frontal zone, e.g. 28th January, 1948 but later e.g. 3rd February, 1948, the double jet structure is again apparent. The individual jets as they moved irregularly south showed an (irregular) increase in the potential temperature and an (irregular) decrease in pressure at the centre of the jet which may be contrasted with the behaviour here of the centre of the main jet which moved north at almost constant potential temperature (fig.14).

4.0. Conclusions.

4.0.1. The wind, temperature and humidity soundings over the periods discussed reveal a main warm frontal zone of classical type, extending nearly up to and perhaps above the tropopause. The temperature field exhibits a zone within which the isobaric gradients are relatively large and lapse rates relatively small. The field of actual wind component quasi-parallel to the zone and also the field of pseudo-wet-bulb potential temperature exhibit associated zones within which the gradients are relatively large. At the boundaries of a zone, the various gradients usually change quasi-discontinuously.

4.0.2. Along any one vertical sounding, the boundaries of the main frontal zone indicated by the temperature field occur usually at nearly the same pressure levels as the boundaries of the associated zone indicated by the actual wind field and also with those indicated by the pseudo-wet-bulb potential temperature field. But discrepancies in the pressure levels at which the boundaries occur in the various fields are sometimes considerable, 50 or 100 mbs. or so. Although in some cases the discrepancies may be attributed to the fusion of a subsided zone with the frontal zone, in other cases the cause of the discrepancies is not known⁄.

4.0.3. The field of actual wind component quasi-parallel to the main frontal zone exhibits a well-marked jet-stream with central maximum located in the vertical near but below the tropopause, and in the horizontal at the latitude of the main warm front between about 475 and 350 mbs. Late in the sequence, this jet-stream having moved north, with, but somewhat faster than, the main warm front, a second jet-stream appears to the south at about the latitude of the surface cold front.

⁄ C/f Brewer A.W. M.R.P. No.548.

REFERENCES

(1) BLEEKER, W.	Q.J.R. Met. S. Oct.1939 Vol.65, No.282
(2) NYBERG, A.	Statens Met.-Hydrografiska Anstalt, Commun. Series No.48.
(3) BERGGREN. R., BOLIN B., ROSSBY C-G.	Tellus Vol.1 No.2 May 1949.
(4) PALMÉN E. and NEWTON C.W.	Journal of Met. Vol.5 No.5 October 1948.
(5) DURST C.S. and DAVIS N.E.	Journal Inst. Navigation Vol.2 No.3 July 1949.
(6) CROSSMAN, G.P.	Journal of Met. Vol.7 No.1 February 1950.
(7) PHILLIPS, N.A.	Tellus Vol.2 No.5 May 1950.

G.278340/DC/11/50/40

Thin (semi-transparent) altocumulus in bands or in a layer gradually spreading over the sky and usually thickening as a whole; it may become partly opaque or double-layered.

Altocumulus formed by the spreading out of cumulus.

Any of the following cases:-
- (a) double-layered altocumulus usually opaque in parts, not increasing.
- (b) a thick (opaque) layer of altocumulus, not increasing.
- (c) altostratus and altocumulus both present at the same or different levels.

Altocumulus in the form of cumulus-shaped tufts or altocumulus with turrets.

Form of high cloud.

Filaments or strands of cirrus, scattered and not increasing, often "mares tails."

Dense cirrus in patches of twisted sheaves usually not increasing, possibly but not certainly the remains of the upper part of cumulonimbus.

Cirrus, often anvil-shaped, either the remains of the upper portions of cumulonimbus or part of a distant cumulonimbus the rest of which is not visible. If there is doubt as to the cumulonimbus origin or association, code figure 2 is used.

Cirrus (often hook-shaped) gradually spreading over the sky and gradually thickening as a whole.

Cirrus and cirrostratus, often in bands converging toward the horizon, or cirrostratus alone, in either case gradually spreading over the sky and usually thickening as a whole, the continuous layer exceeding 45° altitude.

Cirrostratus covering the whole sky.

Cirrostratus not increasing and not covering the whole sky; cirrus and cirrocumulus may be present.

Cirrocumulus alone or cirrocumulus with some cirrus or cirrostratus but the cirrocumulus being the main cirriform cloud present. Cirrocumulus may be present in $C_H=1$ to $C_H=8$.

Form of low cloud.

⌓	Cumulus with little vertical development and seemingly flattened.
△	Cumulus of considerable development, generally towering, with or without other cumulus or stratocumulus, bases all at the same level.
⟁	Cumulonimbus with tops lacking clear-cut outlines but distinctly not cirriform or anvil-shaped, with or without cumulus, stratocumulus, or stratus.
⍜	Stratocumulus formed by the spreading out of cumulus; cumulus also often present. Since the spreading out of the scattered parcels of air that have been warmed by the surface may take place, as in stratocumulus vesperalis, as soon as the condensation level is reached, observers are warned that, though cumulus may normally have been seen earlier, the formation of a particular piece of stratocumulus vesperalis may not come from a cumulus.
〜	Stratocumulus not formed by the spreading out of cumulus.
—	Stratus or fractostratus or both, but not fractostratus of bad weather.
---	Fractostratus and/or fractocumulus of bad weather ("scud")., usually under nimbostratus. By "bad weather" is meant the conditions usually prevailing before, during, or after precipitation.
〜⌓	Cumulus and stratocumulus other than those formed by the spreading out of cumulus, with bases at different levels.
⧗	Cumulonimbus having clearly fibrous (cirriform) top, often anvil-shaped with or without cumulus, stratocumulus, stratus or "scud."
⫽	Nimbostratus, base below 10000 ft.

Form of medium cloud.

⫽	Thick altostratus. Through portions of the sheet the position of the sun or moon may be indicated by a light patch.
ω	Thin (semi-transparent) altocumulus, cloud elements not changing much, at a single level.
ℓ	Thin (semi-transparent) altocumulus in patches (often almond-or fish-shaped), cloud elements continually changing and/or occurring at more than one level.
ɷ	Thin (semi-transparent) altocumulus in bands or in a layer gradually spreading over the sky and usually thickening as a whole; it may become partly opaque or double-layered.
ϫ	Altocumulus formed by the spreading out of cumulus.
ɞ	Any of the following cases:- (a) double-layered altocumulus usually opaque in parts, not increasing. (b) a thick (opaque) layer of altocumulus, not increasing. (c) altostratus and altocumulus both present at the same or different levels.
M	Altocumulus in the form of cumulus-shaped tufts or altocumulus with turrets.

Form of high cloud.

ᒧ	Filaments or strands of cirrus, scattered and not increasing, often "mares tails."
ᒧᑐ	Dense cirrus in patches of twisted sheaves usually not increasing, possibly but not certainly the remains of the upper part of cumulonimbus.
ᒣ	Cirrus, often anvil-shaped, either the remains of the upper portions of cumulonimbus or part of a distant cumulonimbus the rest of which is not visible. If there is doubt as to the cumulonimbus origin or association, code figure 2 is used.
/	Cirrus (often hook-shaped) gradually spreading over the sky and gradually thickening as a whole.
2	Cirrus and cirrostratus, often in bands converging toward the horizon, or cirrostratus alone, in either case gradually spreading over the sky and usually thickening as a whole, the continuous layer exceeding 45° altitude.
ᒧᒧ	Cirrostratus covering the whole sky.
⸧	Cirrostratus not increasing and not covering the whole sky; cirrus and cirrocumulus may be present.
ᘔ	Cirrocumulus alone or cirrocumulus with some cirrus or cirrostratus but the cirrocumulus being the main cirriform cloud present. Cirrocumulus may be present in $C_H=1$ to $C_H=8$.

Precipitation.

,,	Drizzle, not freezing, continuous (Slight at time of observation).
, ,,	Drizzle, not freezing, continuous (Moderate at time of observation).
● ,	Drizzle and rain (Slight).
)●(	Precipitation within sight, reaching the ground but distant (Estimated 5 Kms. from station).
(●)	Precipitation within sight, reaching the ground, near but not at station.
●	Rain, not freezing, intermittent (Slight at time of observation).
●●	Rain not freezing, continuous (Slight at time of observation).
● ●●	Rain not freezing, continuous (Moderate at time of observation).
● ▽	Rain shower(s), slight.
● ▽	Rain shower(s) moderate or heavy.

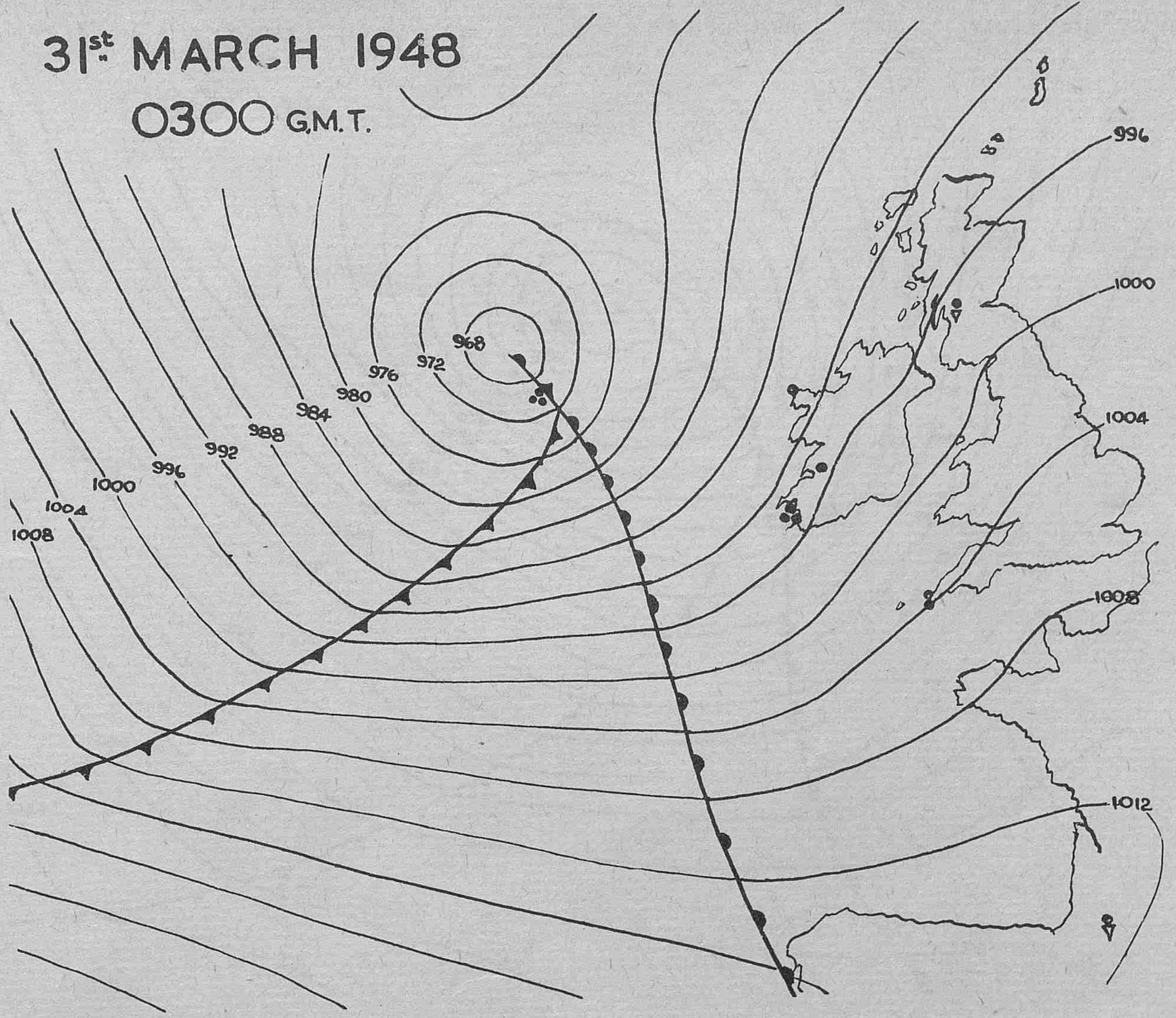
31st MARCH 1948
0300 G.M.T.

968
972
976
980
984
988
992
996
1000
1004
1008
996
1000
1004
1008
1012

Fig. 1 (a)

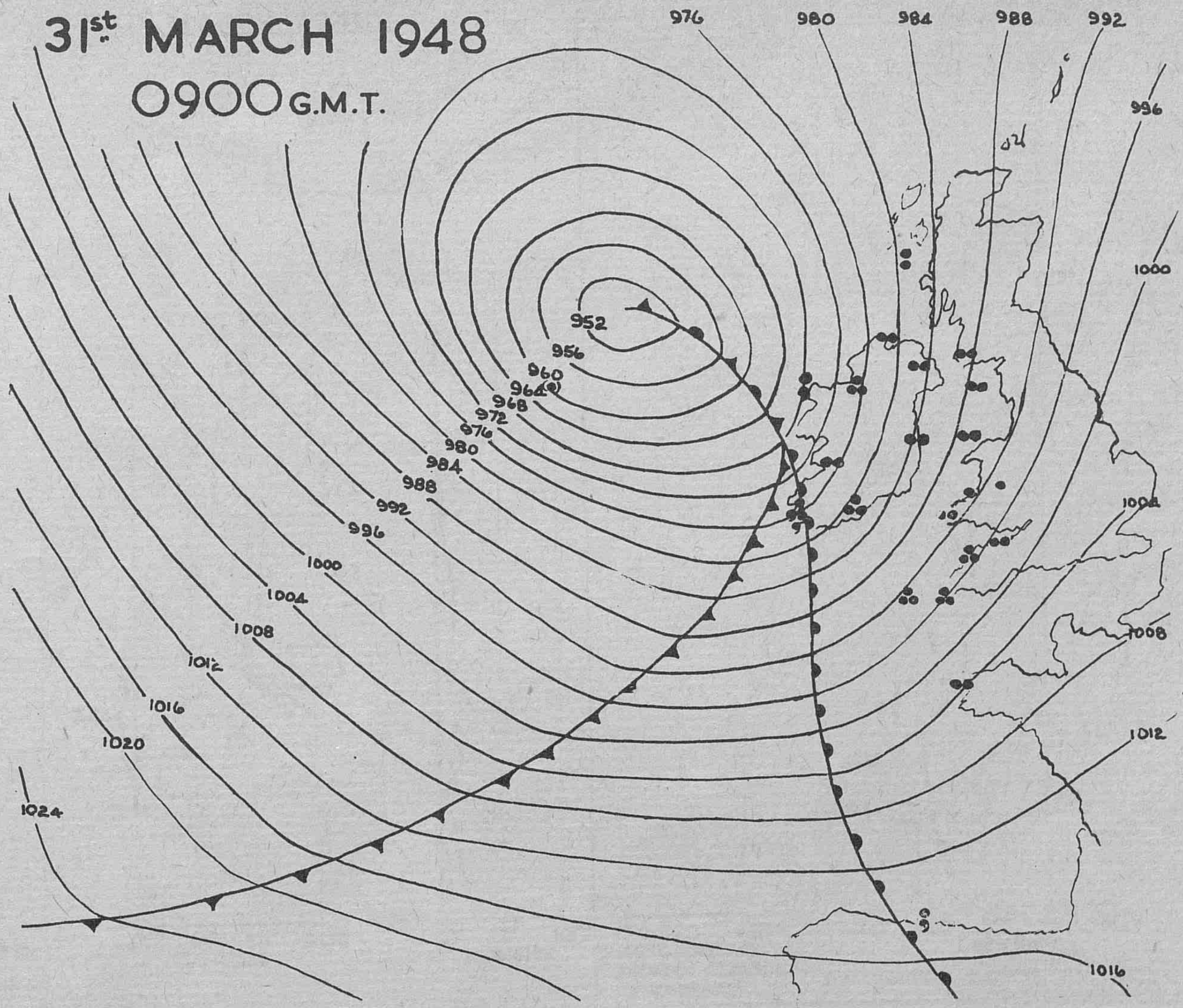

31st MARCH 1948
0900 G.M.T.

952
956
960
964
968
972
976
980
984
988
992
996
1000
1004
1008
1012
1016
1020
1024

Fig. 1 (b).

M.R.P. 597

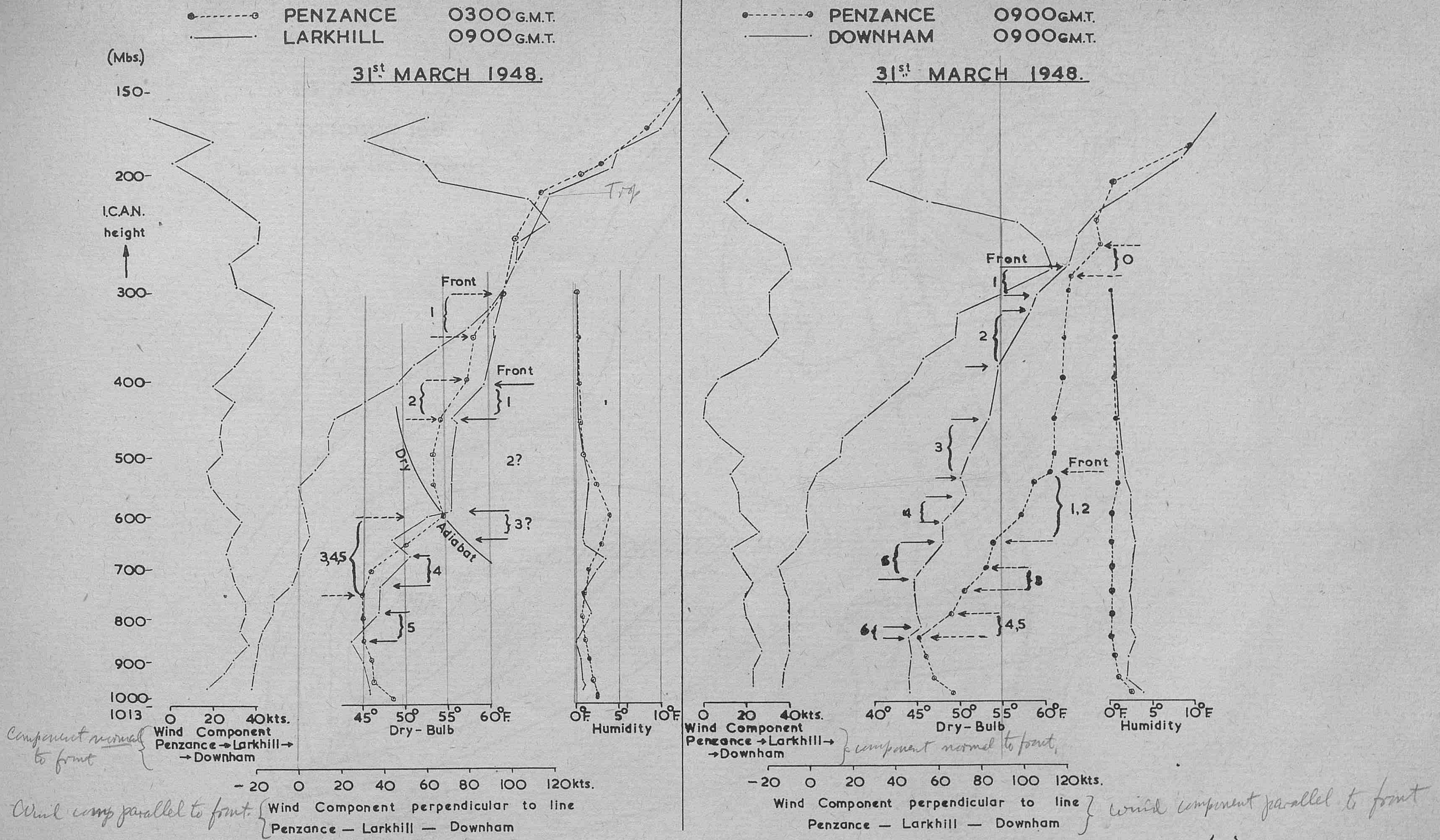

Actual Wind Components, Dry-Bulb Temp. (°F.) on Saturated Adiabatic Scale, Depression of Wet Bulb Potential Temperature (°F)

Fig. 2(a).

Fig. 2(b).

! Penzance - Larkhill ≈ 150 NM   Larkhill - DHM MKT ≈ 120 mi.

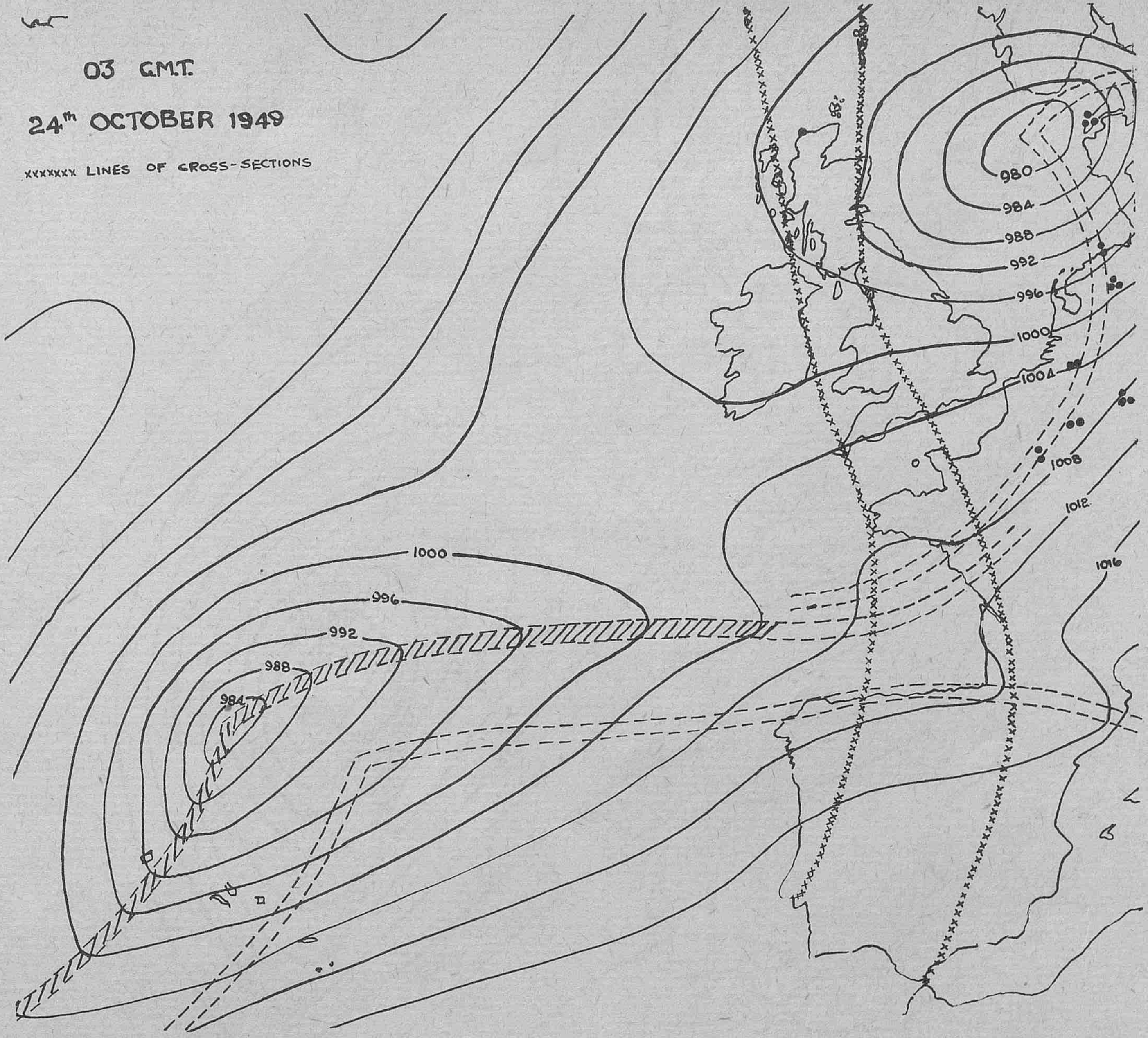

03 G.M.T.

24th OCTOBER 1949

xxxxxxx LINES OF CROSS-SECTIONS

980
984
988
992
996
1000
1004
1008
1012
1016
1000
996
992
988
984

Fig. 3

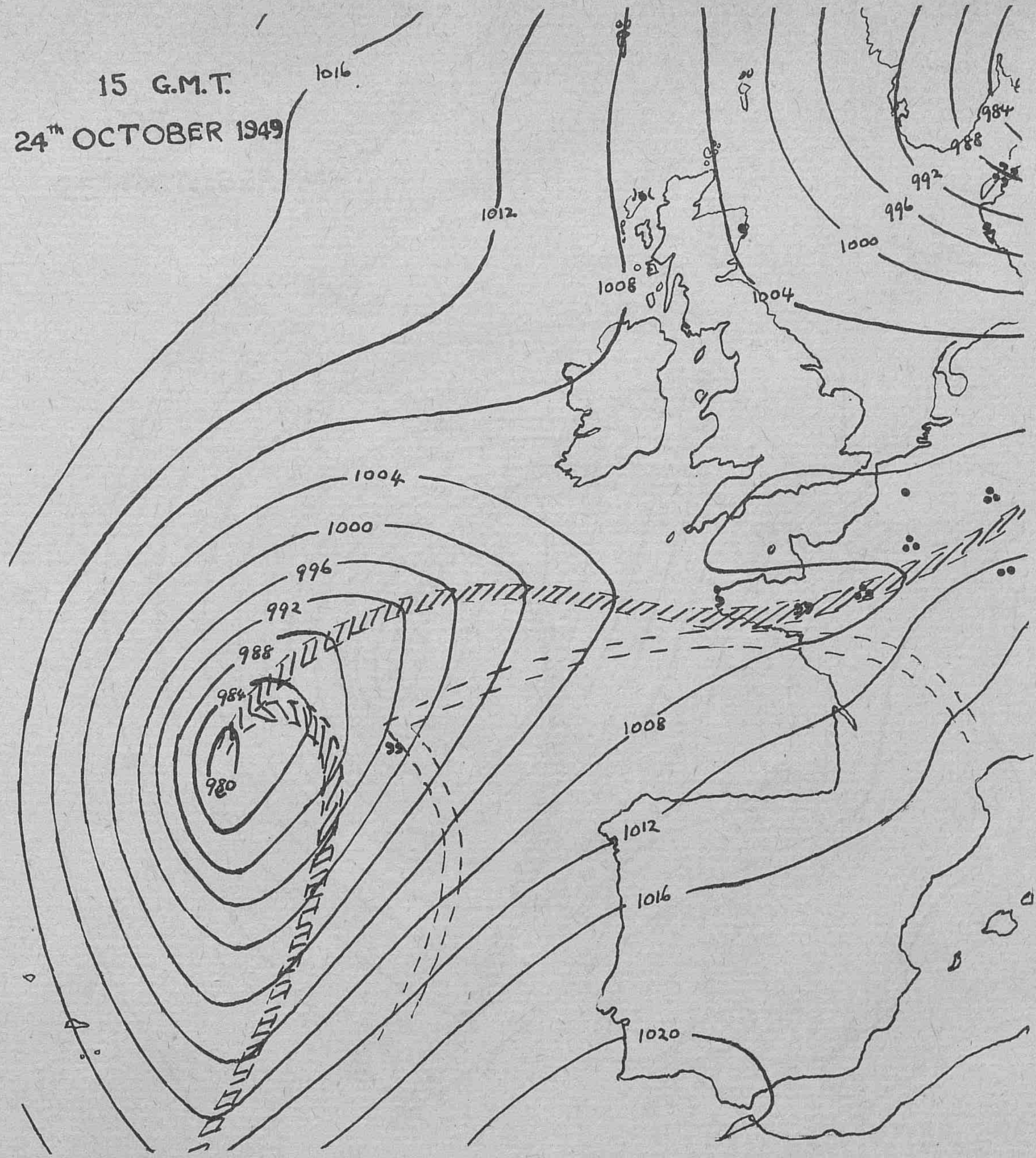

15 G.M.T.
24th OCTOBER 1949

1016
1012
1008
1004
1000
996
992
988
984
980
1004
1000
996
992
988
984
1008
1012
1016
1020

Fig. 4

M.R.P. 597

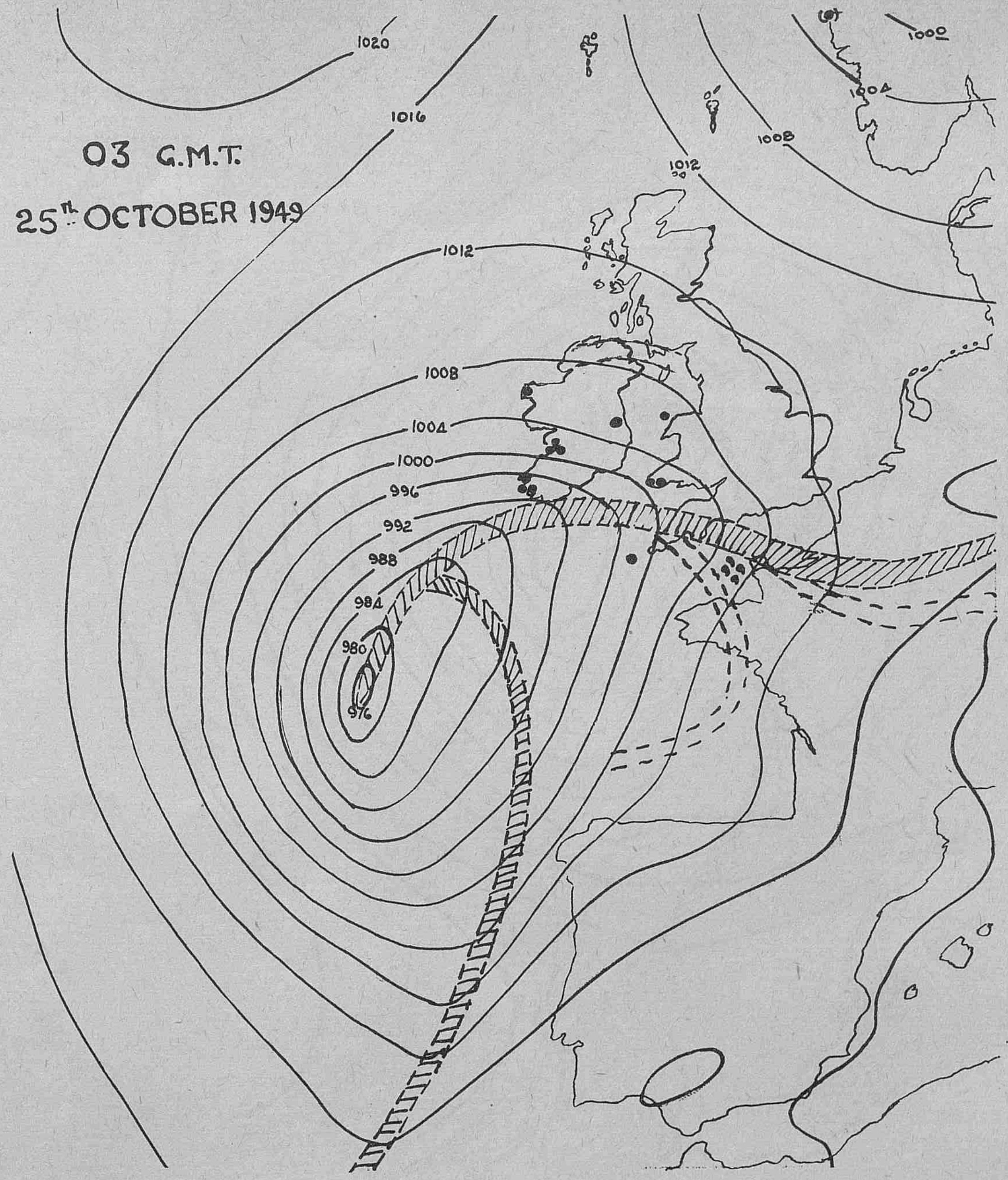

03 G.M.T.

25th OCTOBER 1949

1020
1016
1012
1008
1004
1000
996
992
988
984
980
976
1012
1008
1004
1000

Fig. 5

M.R.P. 597

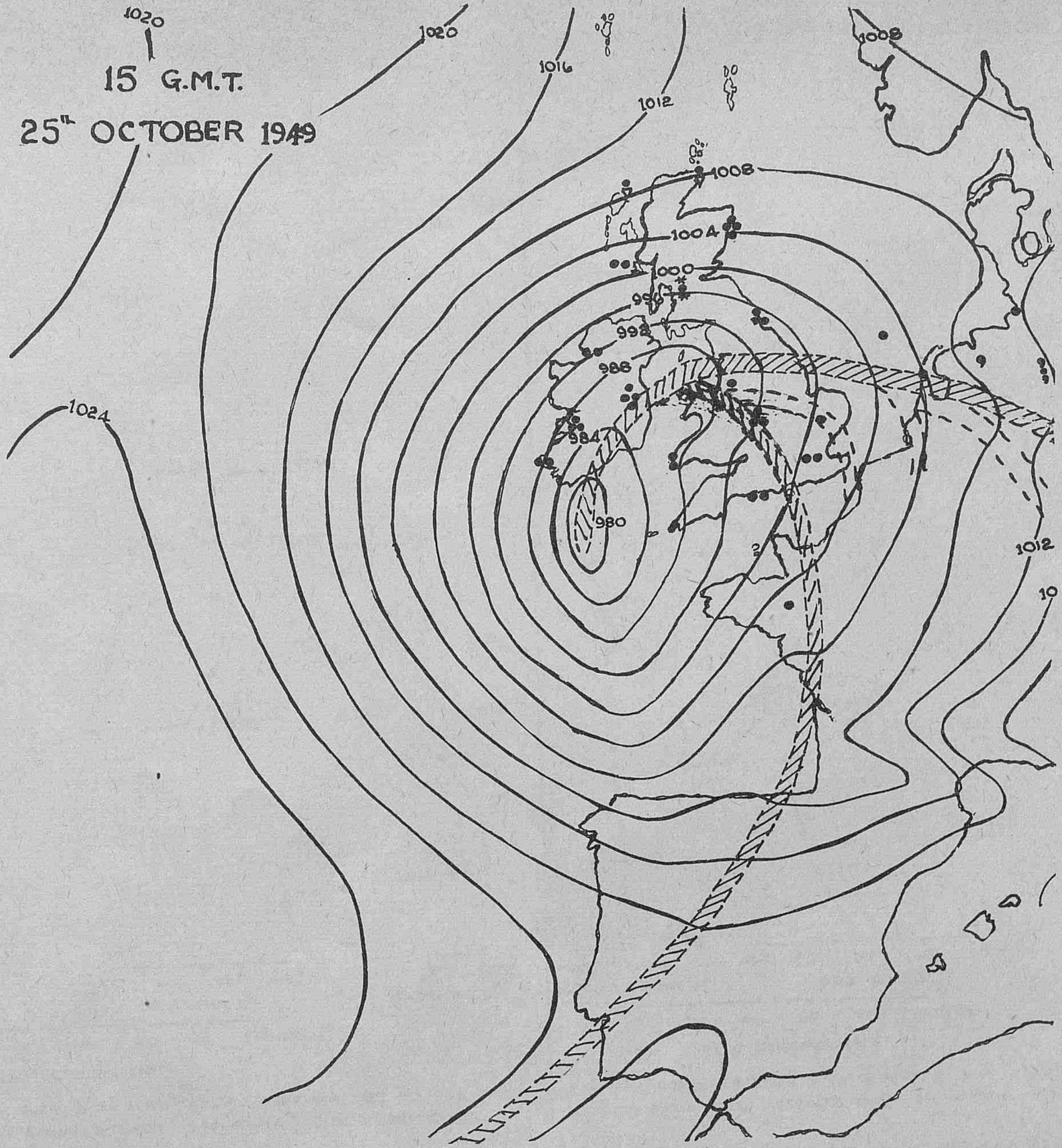

15 G.M.T.
25th OCTOBER 1949

1020
1020
1016
1012
1008
1008
1004
1000
996
992
988
984
980
1024
1012
10

Fig. 6

M.R.P. 597

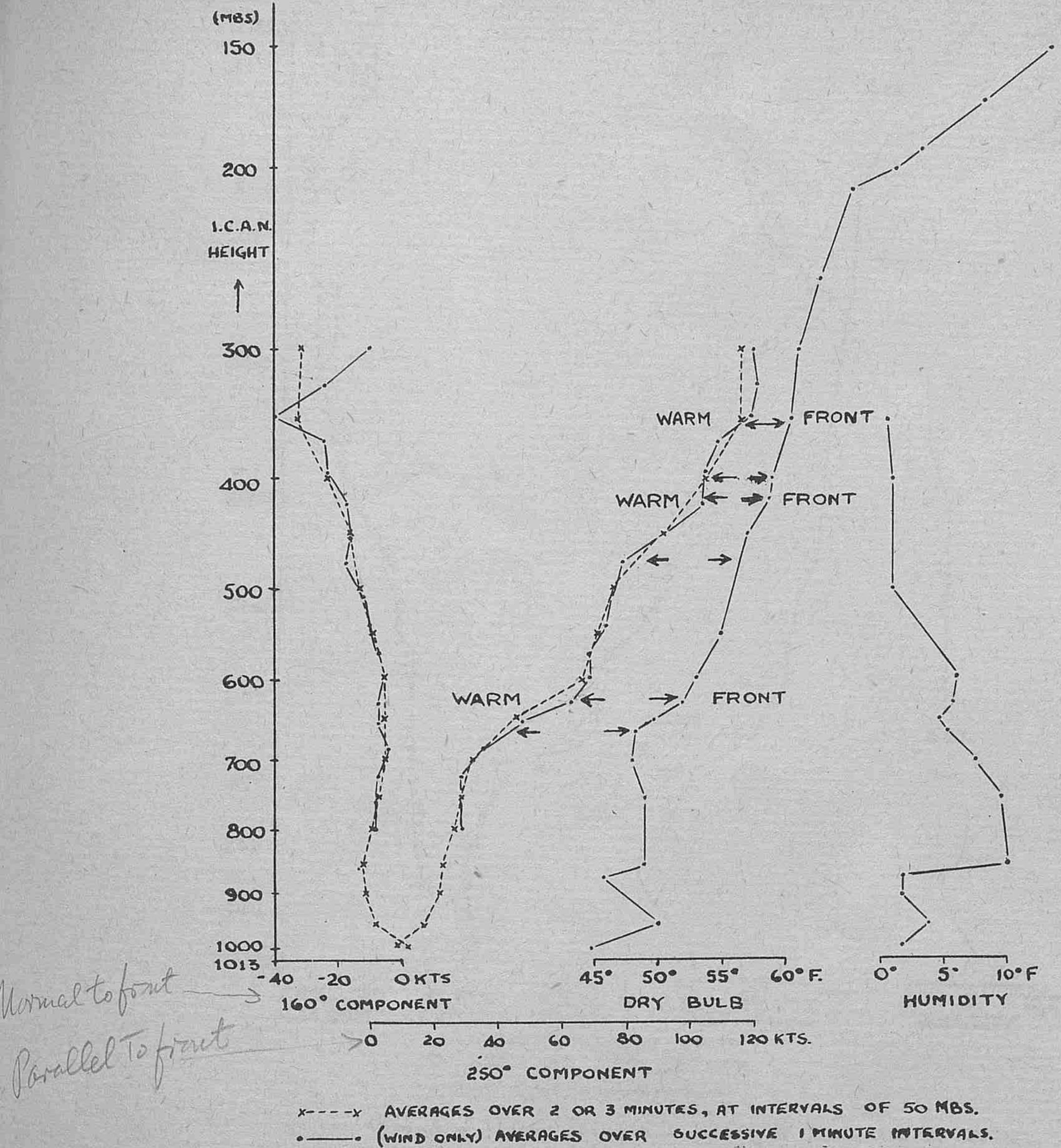

LARKHILL 0300 G.M.T.
24th. OCTOBER 1949.

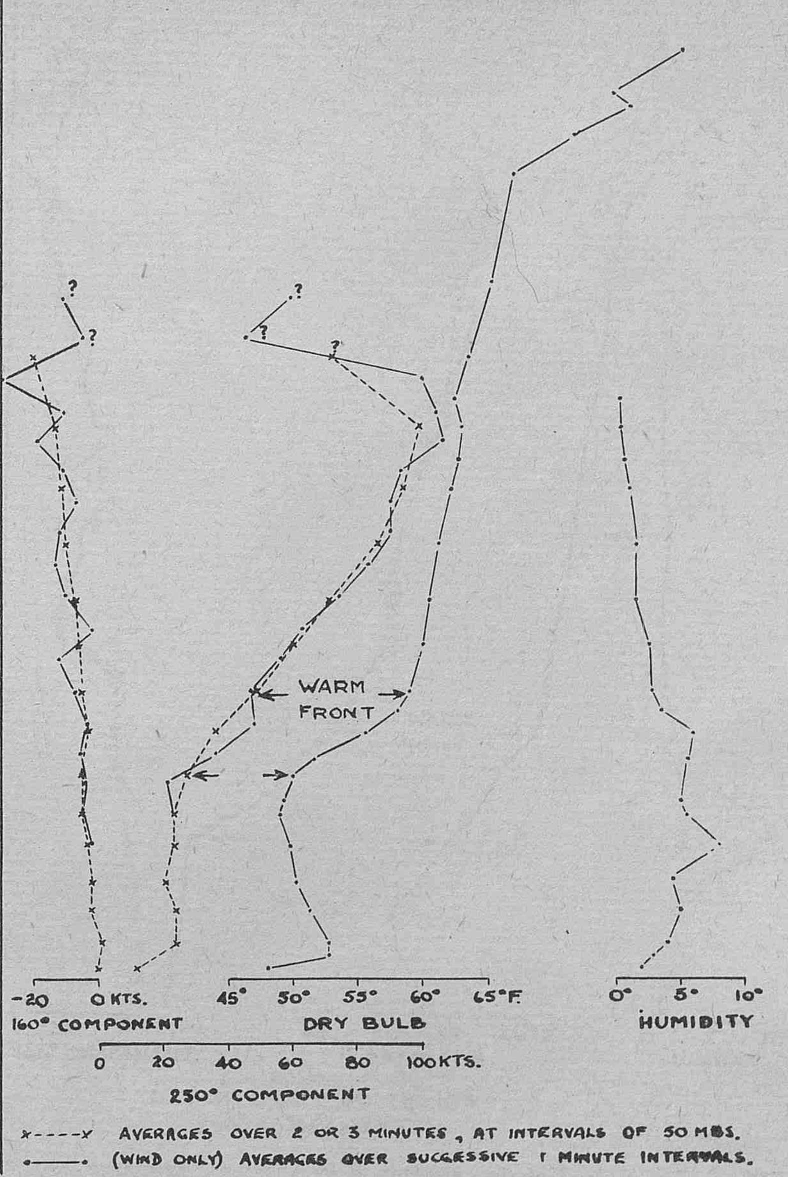

LARKHILL 0900 G.M.T.
24th. OCTOBER 1949.

Actual Wind Components (knots), Dry-Bulb Temp. (°F.) on Saturated Adiabatic Scale, Depression of Wet-Bulb Potential Temperature (°F).

Fig. 7.

Fig. 8.

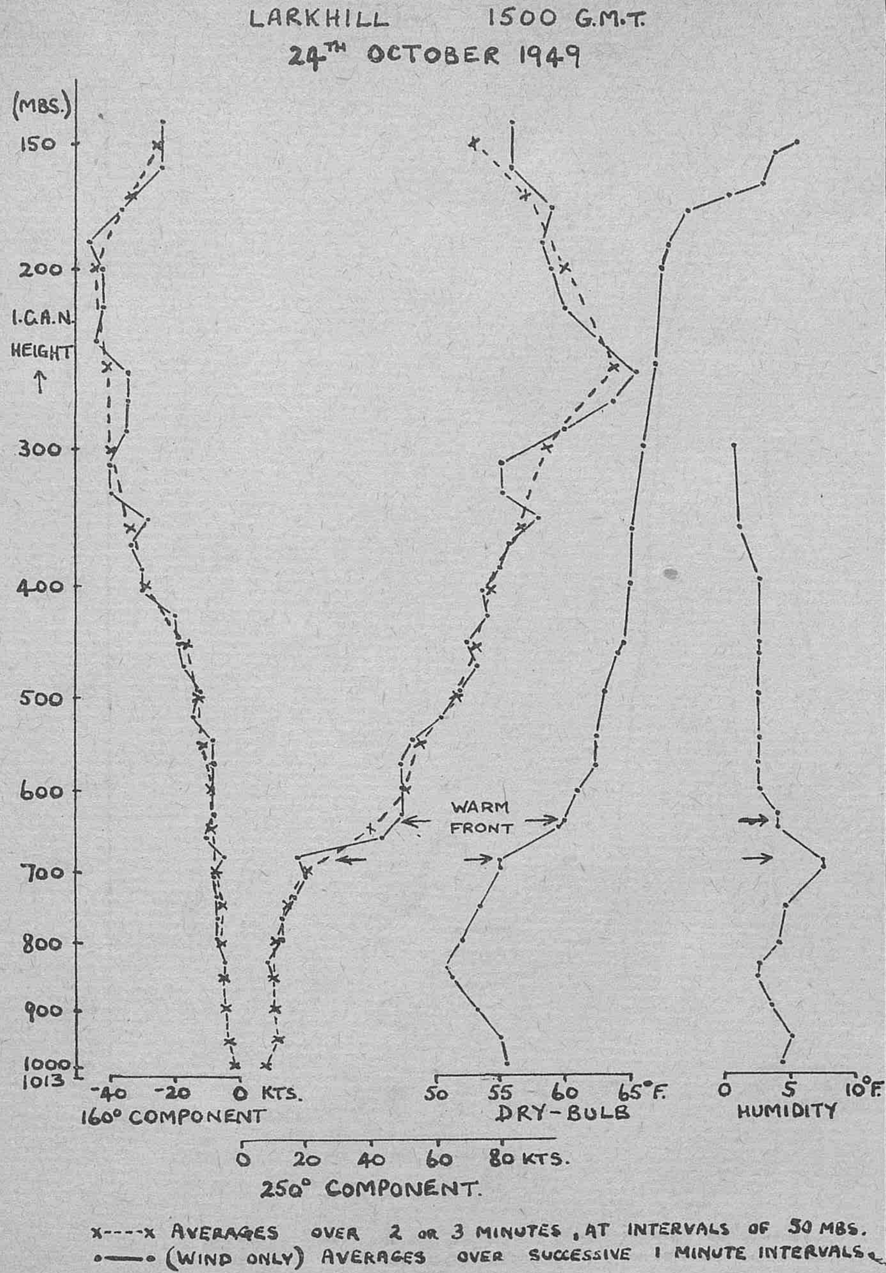

Fig. 9.

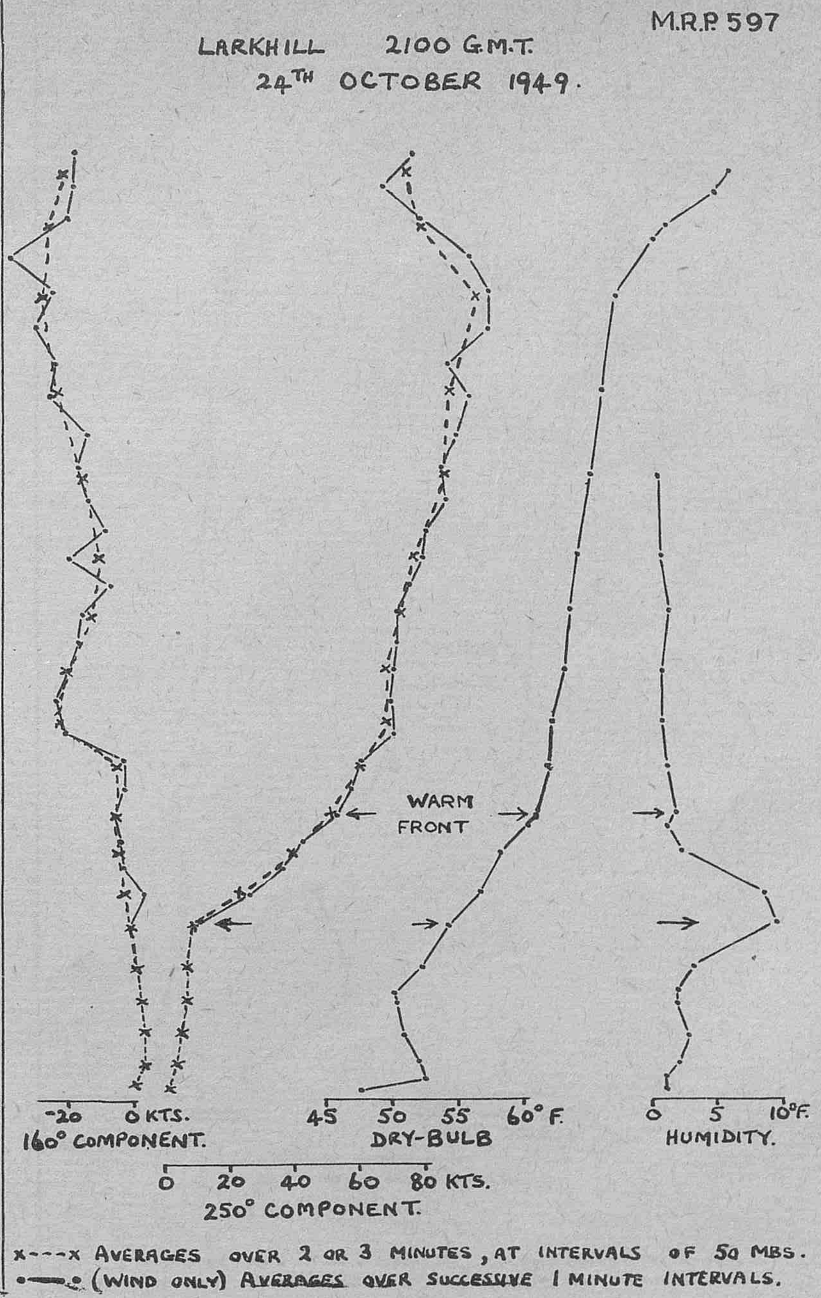

Fig. 10.

Actual Wind Components (knots), Dry Bulb Temperature (°F) on Saturated Adiabatic Scale, Depression of Wet Bulb Potential Temperature (°F)

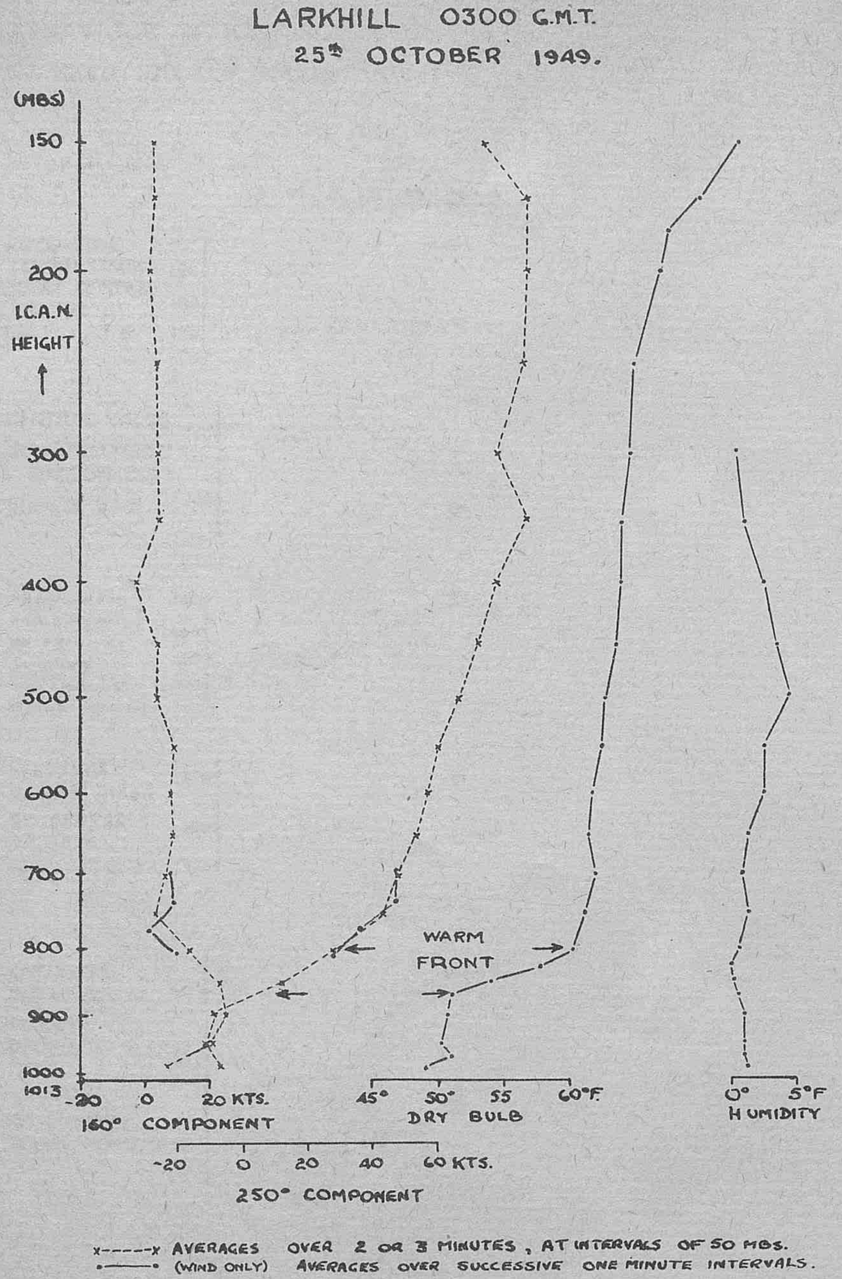

Fig. 11

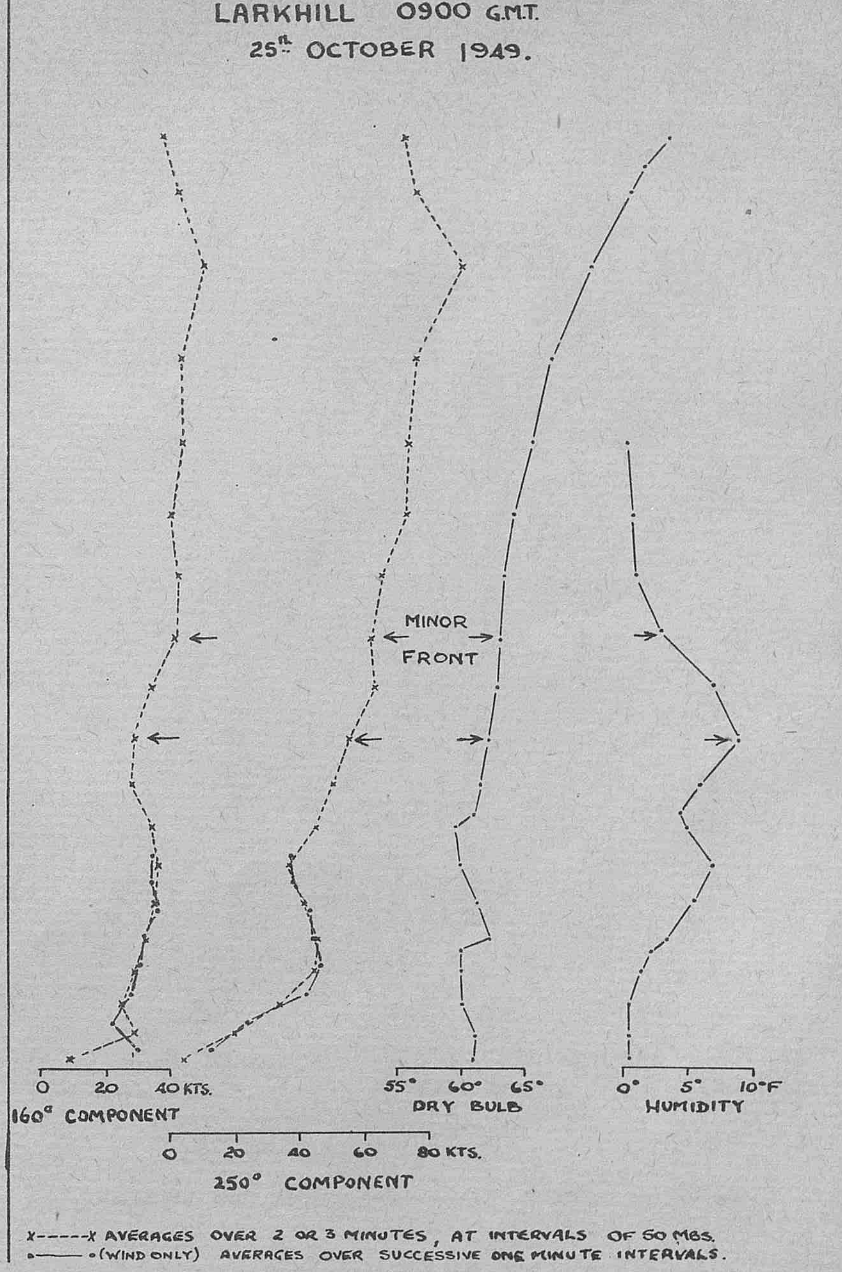

Fig. 12.

ACTUAL WIND COMPONENTS, DRY BULB TEMP. (°F) ON SATURATED ADIABATIC SCALE, DEPRESSION OF WET-BULB POTENTIAL TEMP. (°F)

BEHAVIOUR OF WESTERLY JETS
IN RELATION TO WARM FRONT

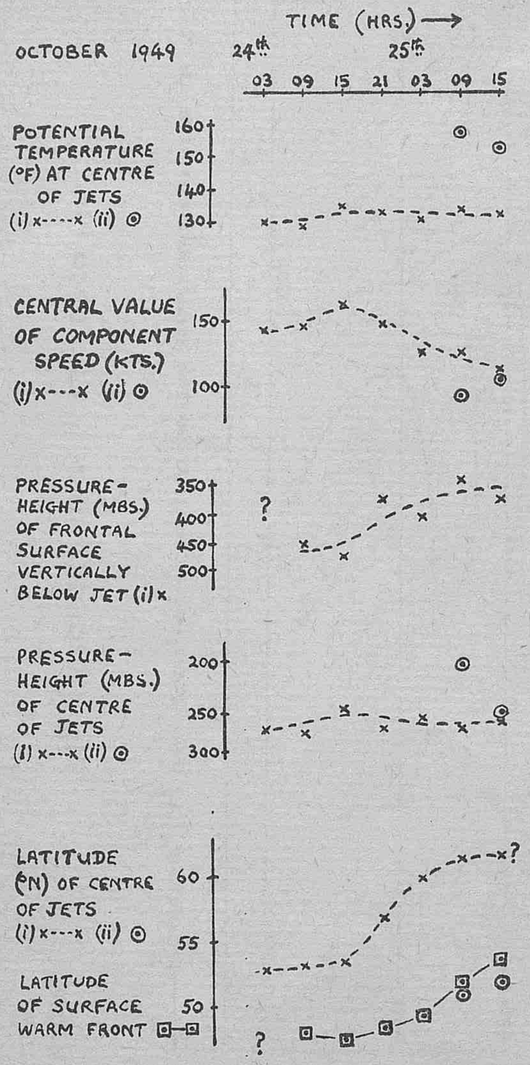

FIG. 14.

LARKHILL 1500 G.M.T.
25TH OCTOBER 1949.

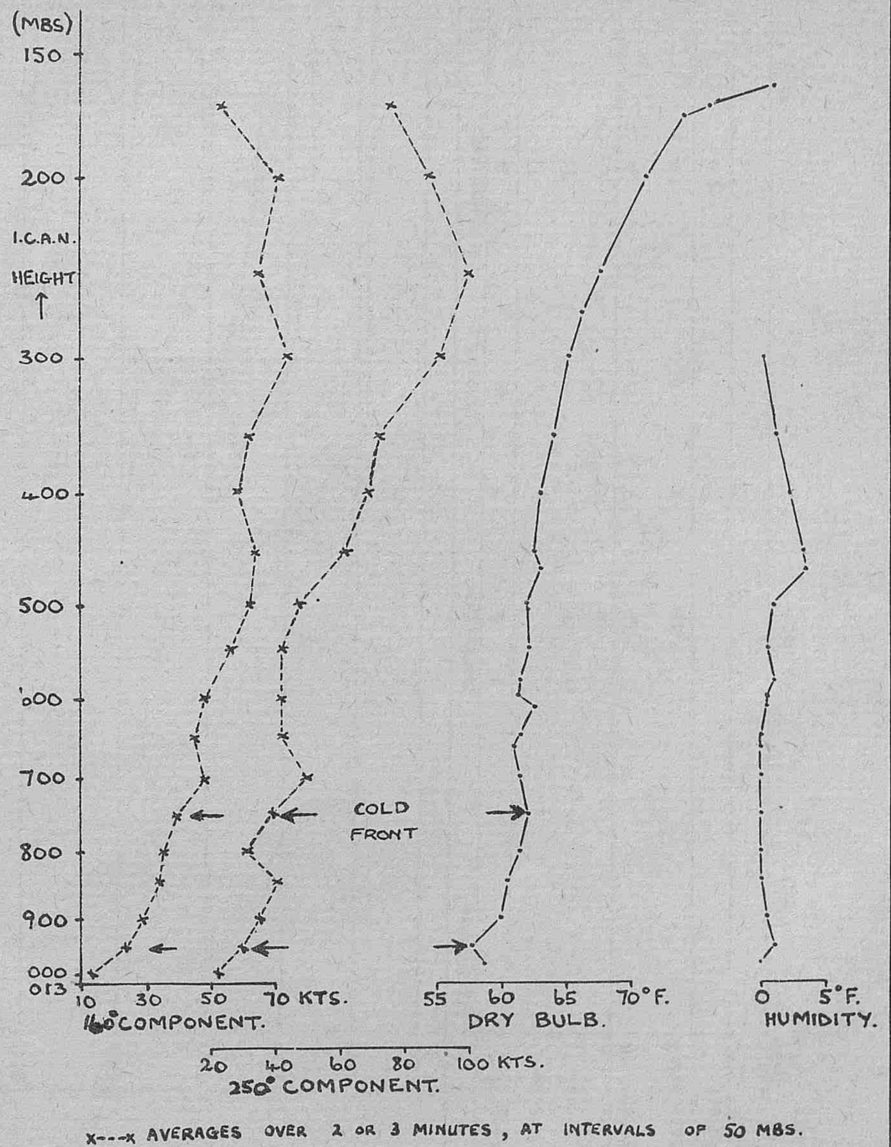

Actual Wind Components (knots) Dry Bulb Temp. (°F) on Saturated Adiabatic Scale, Depression of Wet Bulb Potential Temperature (°F)

Fig. 13.

M.R.P. 597

24th OCTOBER 1949 AT 0300 G.M.T.

——— ISOTHERMS (°F) AND ISOPLETHS OF WIND COMPONENT (KNOTS) PERPENDICULAR TO X-SECTION -------

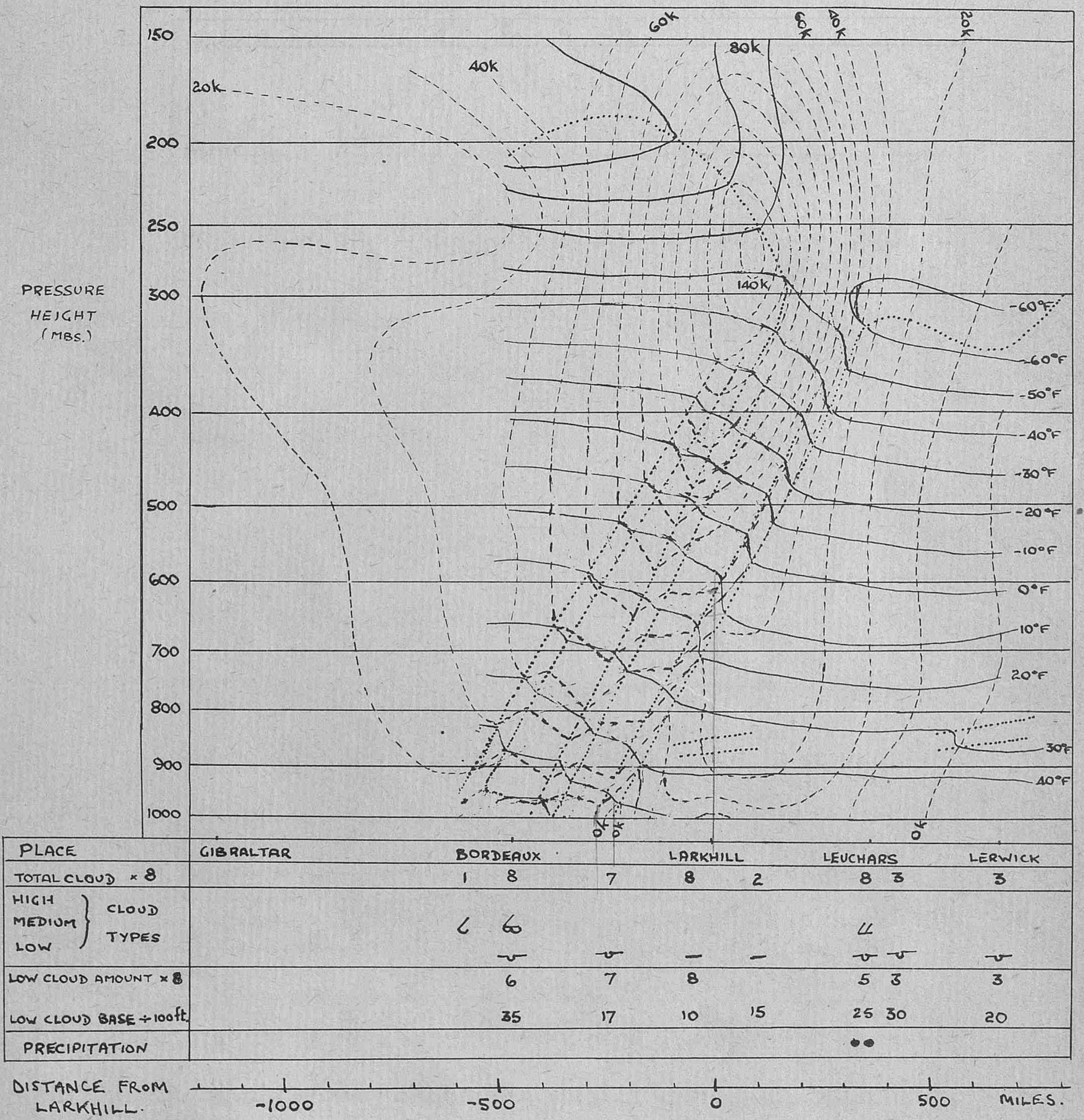

PLACE	GIBRALTAR		BORDEAUX		LARKHILL		LEUCHARS		LERWICK
TOTAL CLOUD × 8		1	8	7	8	2	8	3	3
HIGH MEDIUM } CLOUD TYPES LOW		ℓ	ϭ ◡	◡	—	—	ℒ ◡	◡	◡
LOW CLOUD AMOUNT × 8			6	7	8		5	3	3
LOW CLOUD BASE ÷ 100ft.			35	17	10	15	25	30	20
PRECIPITATION							••		

FIG. 15

M.R.P. 597

24th October 1949 at 0900 G.M.T.

——— Isotherms (°F) and isopleths of wind component (knots) perpendicular to X-section - - - - - -

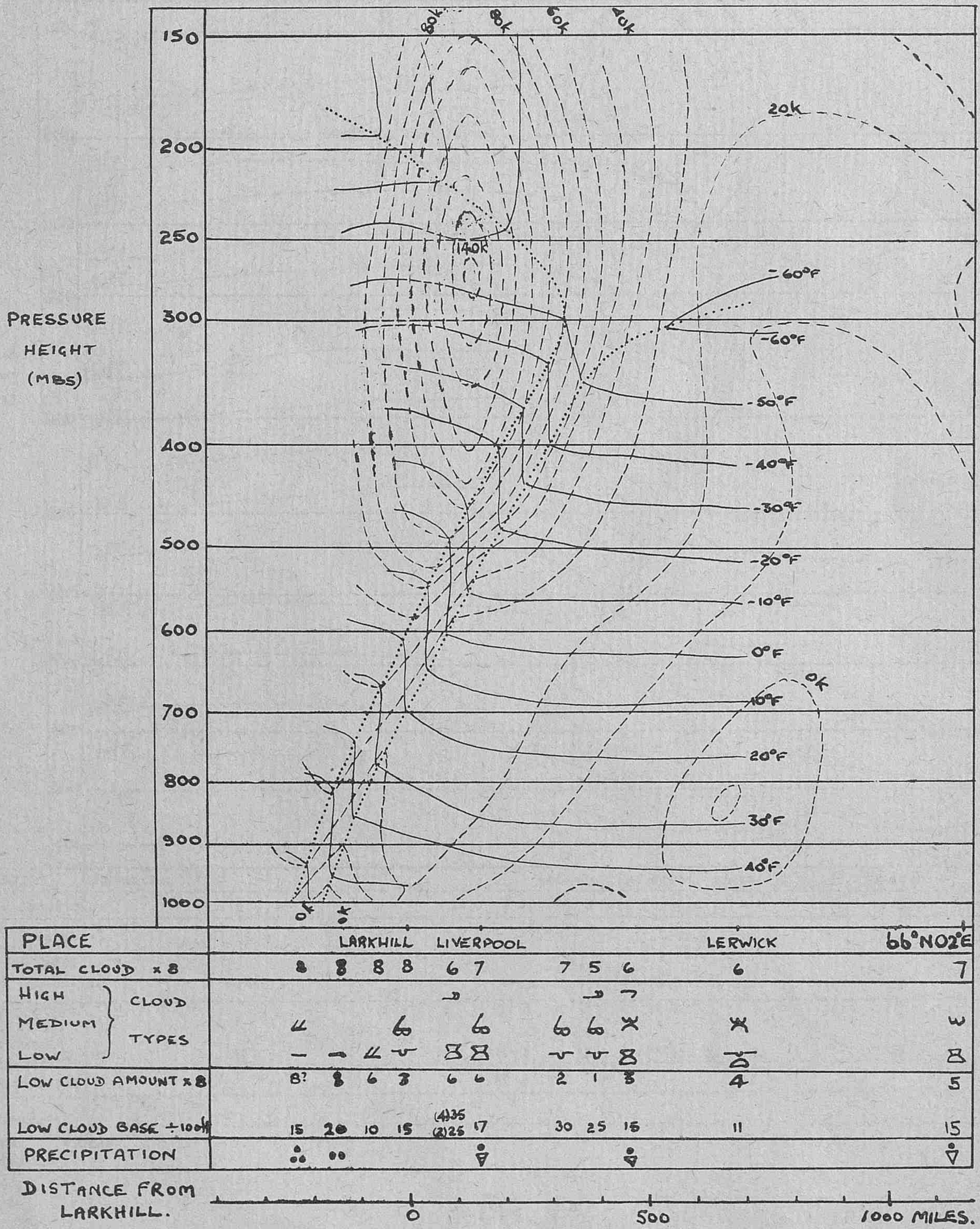

Fig. 16

M.R.P.597 24th October 1949 at 1500 G.M.T.

Isotherms (°F) and Isopleths of wind component (knots) perpendicular to X-Section

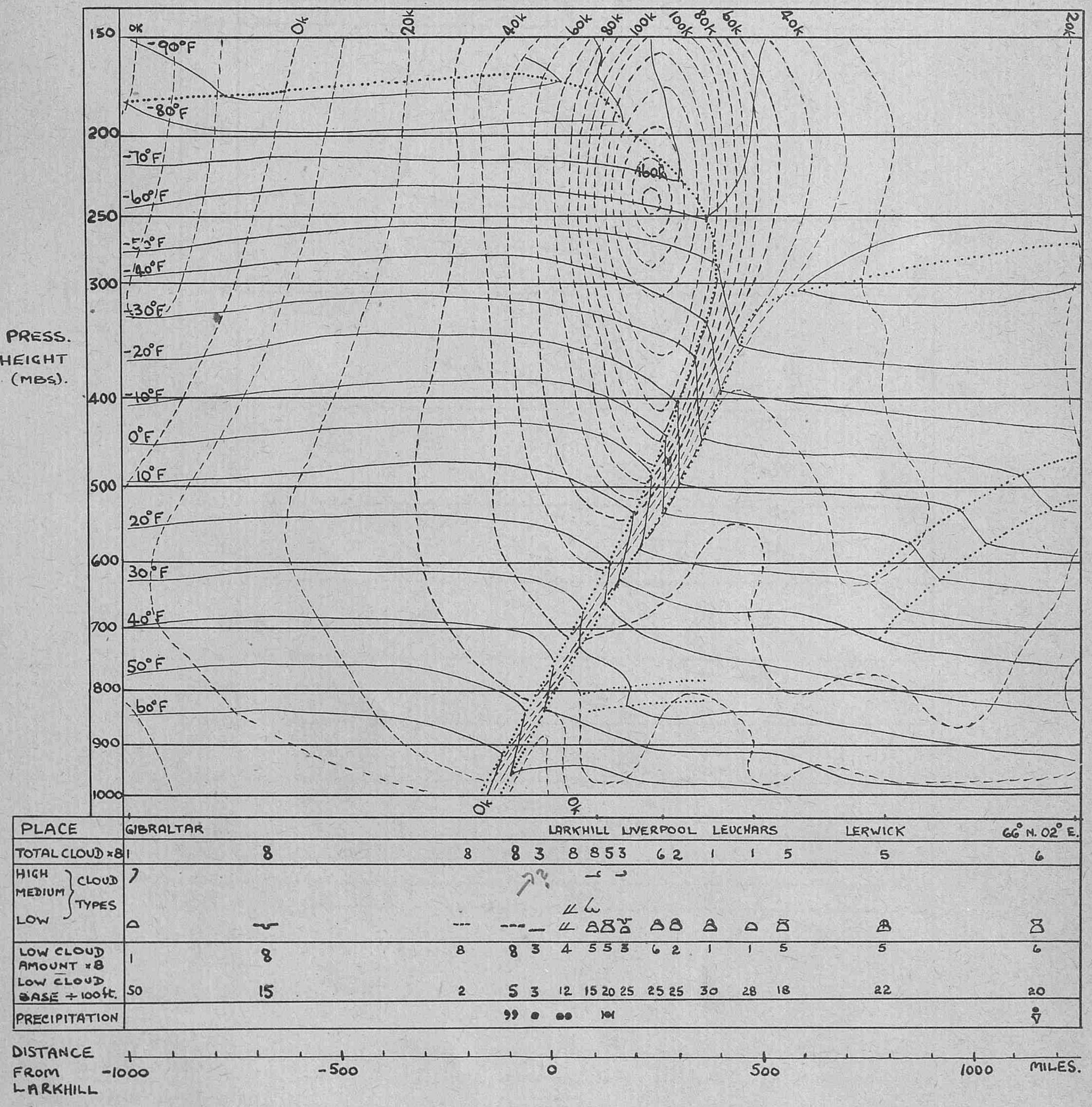

Fig. 17

M.R.P. 597 24th October 1949 at 2100 G.M.T.

——— Isotherms (°F) and isopleths of wind component (knots) perpendicular to X-section - - - - -

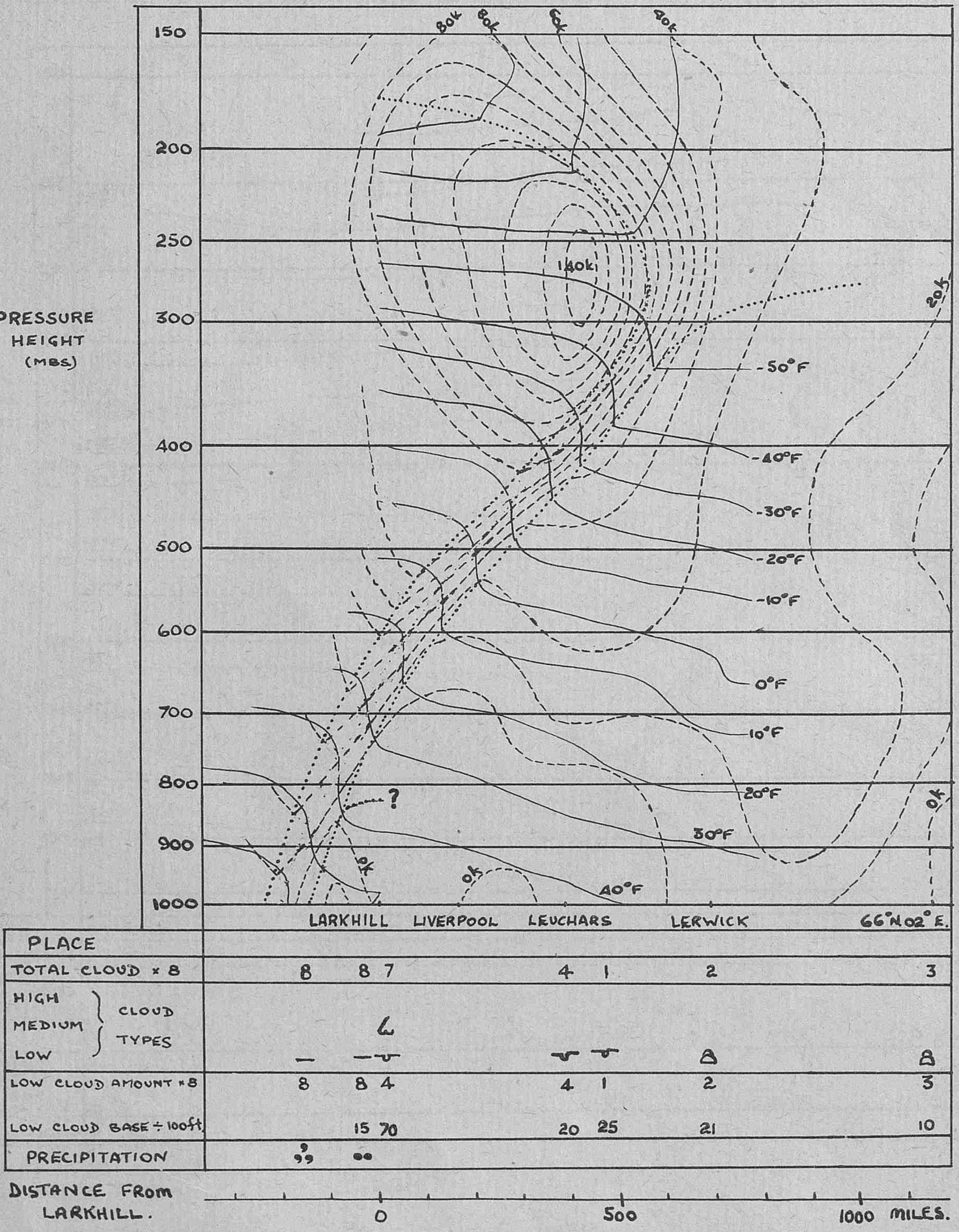

PLACE							
TOTAL CLOUD × 8	8	8	7	4	1	2	3
HIGH / MEDIUM / LOW } CLOUD TYPES	—	— ʖ	ᴗ	ᴗ	ᴗ	ᗣ	ᗣ
LOW CLOUD AMOUNT × 8	8	8	4	4	1	2	3
LOW CLOUD BASE ÷ 100ft		15	70	20	25	21	10
PRECIPITATION	,,,	●●					

FIG. 18

25th OCTOBER 1949 AT 0300 G.M.T. M.R.P. 597

——— ISOTHERMS (°F) AND ISOPLETHS OF WIND COMPONENT (KNOTS) PERPENDICULAR TO X-SECTION -------

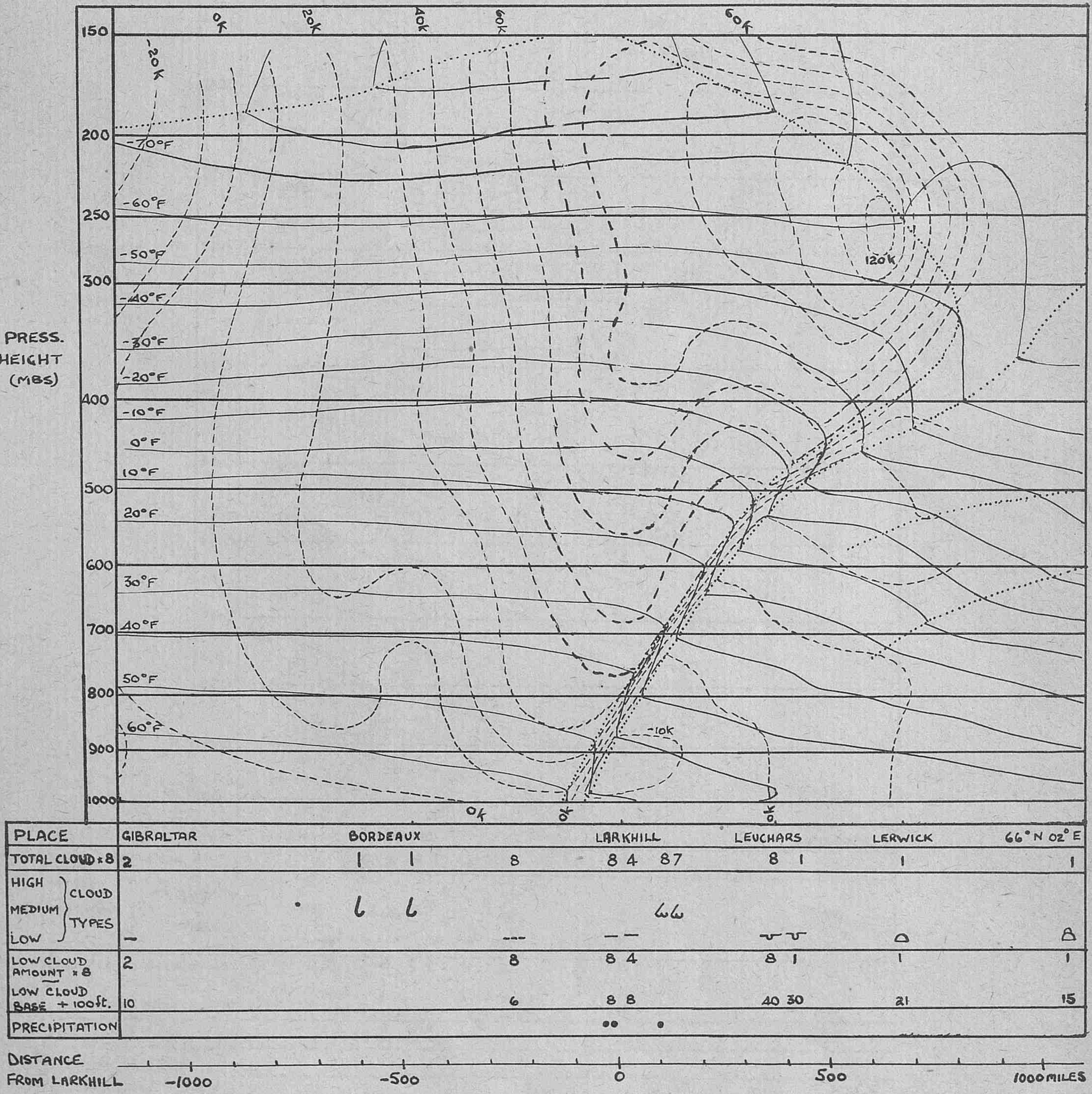

FIG. 19

25th October 1949 at 0900 G.M.T. M.R.P. 597

——— ISOTHERMS (°F) AND ISOPLETHS OF WIND COMPONENT (KNOTS) PERPENDICULAR TO X-SECTION ----

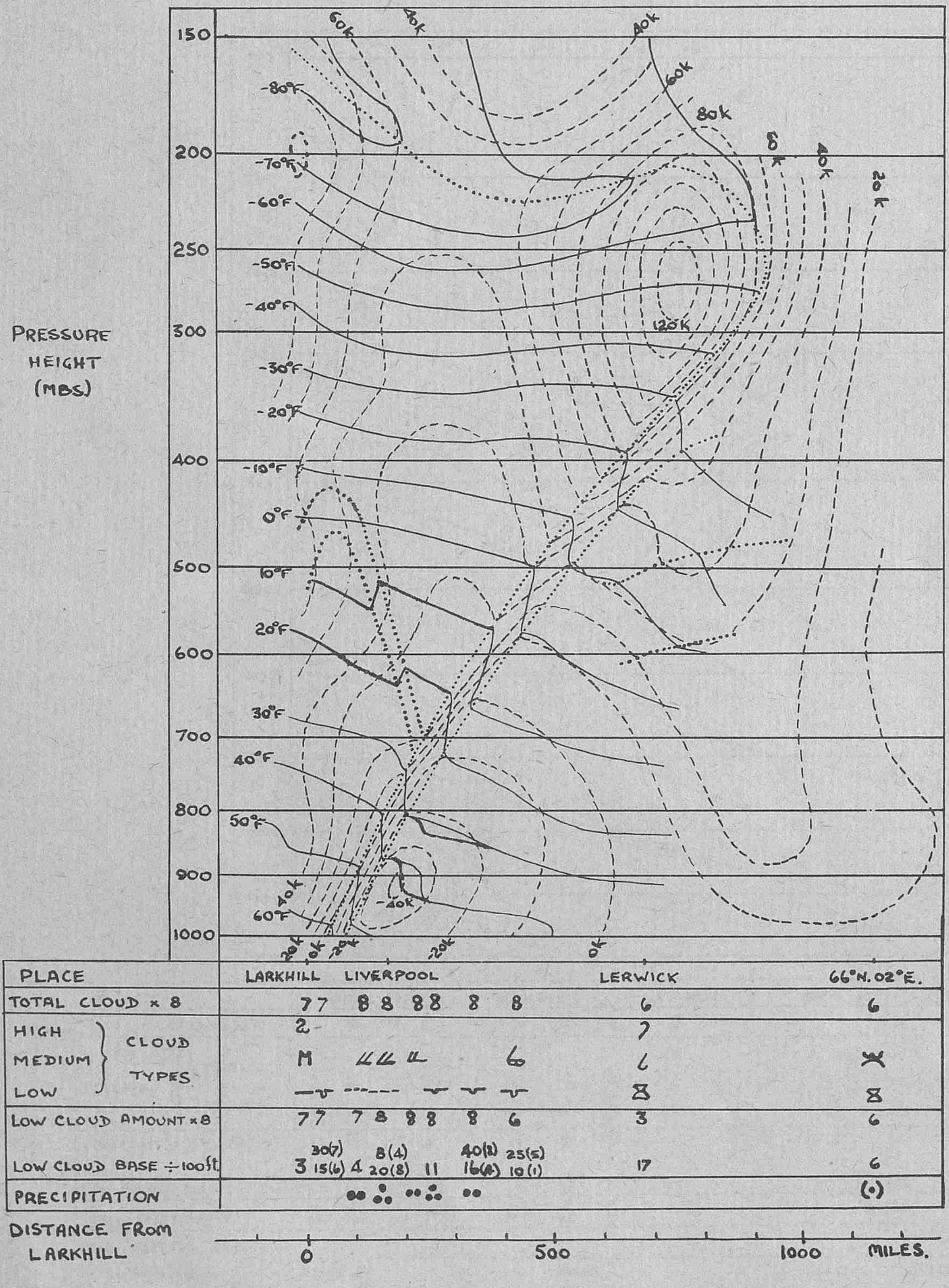

FIG. 20

25th OCTOBER 1949 AT 1500 G.M.T.

——— ISOTHERMS (°F) AND ISOPLETHS OF WIND COMPONENT (KNOTS) PERPENDICULAR TO X-SECTION - - - - - -

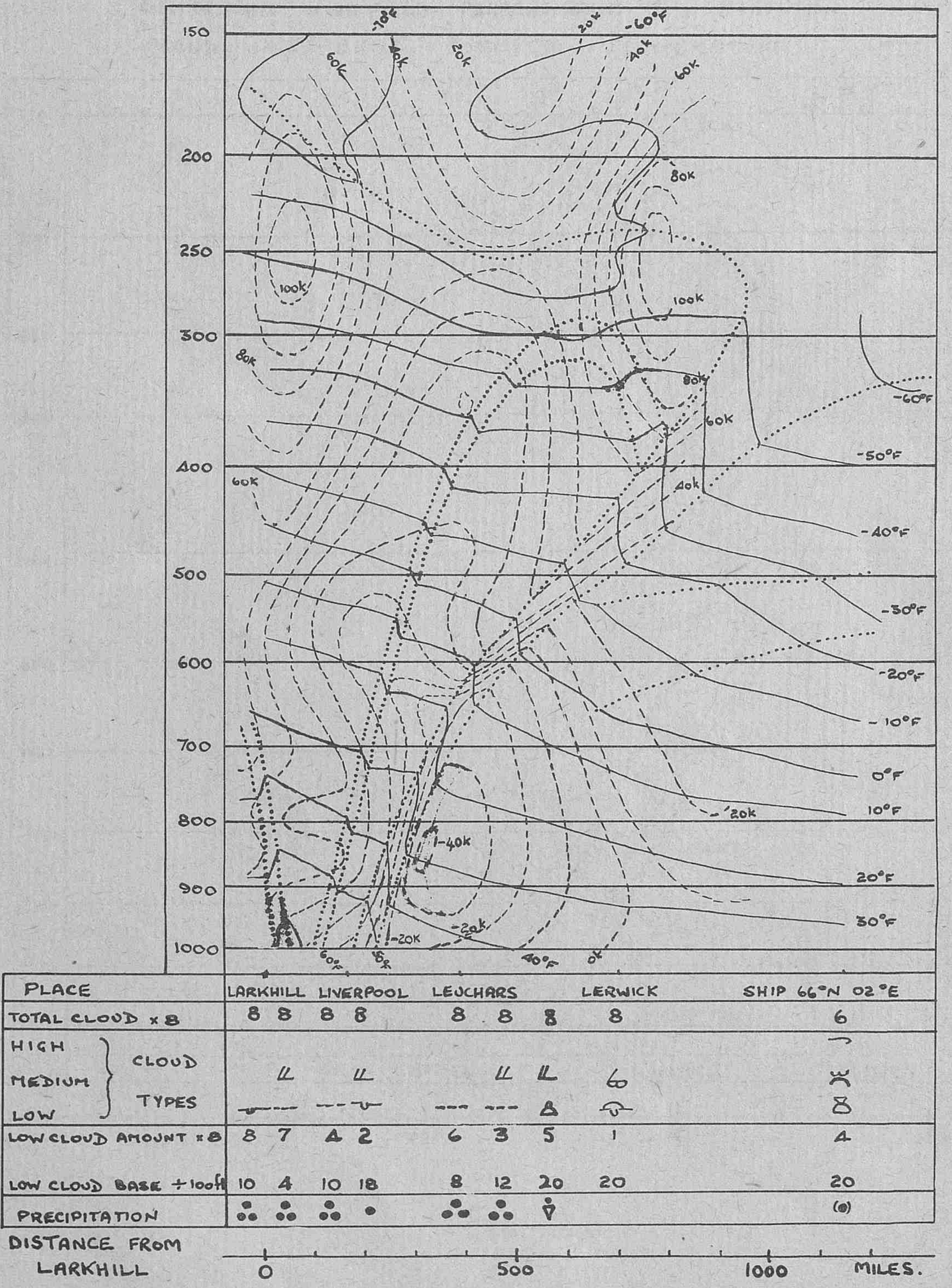

PLACE	LARKHILL		LIVERPOOL		LEUCHARS			LERWICK	SHIP 66°N 02°E
TOTAL CLOUD × 8	8	8	8	8	8	8	8	8	6
HIGH CLOUD TYPES									⌐
MEDIUM CLOUD TYPES		ʟʟ		ʟʟ		ʟʟ	ʟʟ	ɕ	ж
LOW CLOUD TYPES	–v–	–––	–––	–v–	–––	–––	Δ	⌒	8
LOW CLOUD AMOUNT × 8	8	7	4	2	6	3	5	1	4
LOW CLOUD BASE ÷ 100 ft	10	4	10	18	8	12	20	20	20
PRECIPITATION	∴	∴	∴	•	∴	∴	•▽		(•)

FIG. 21

24th October 1949 at 0300 G.M.T.

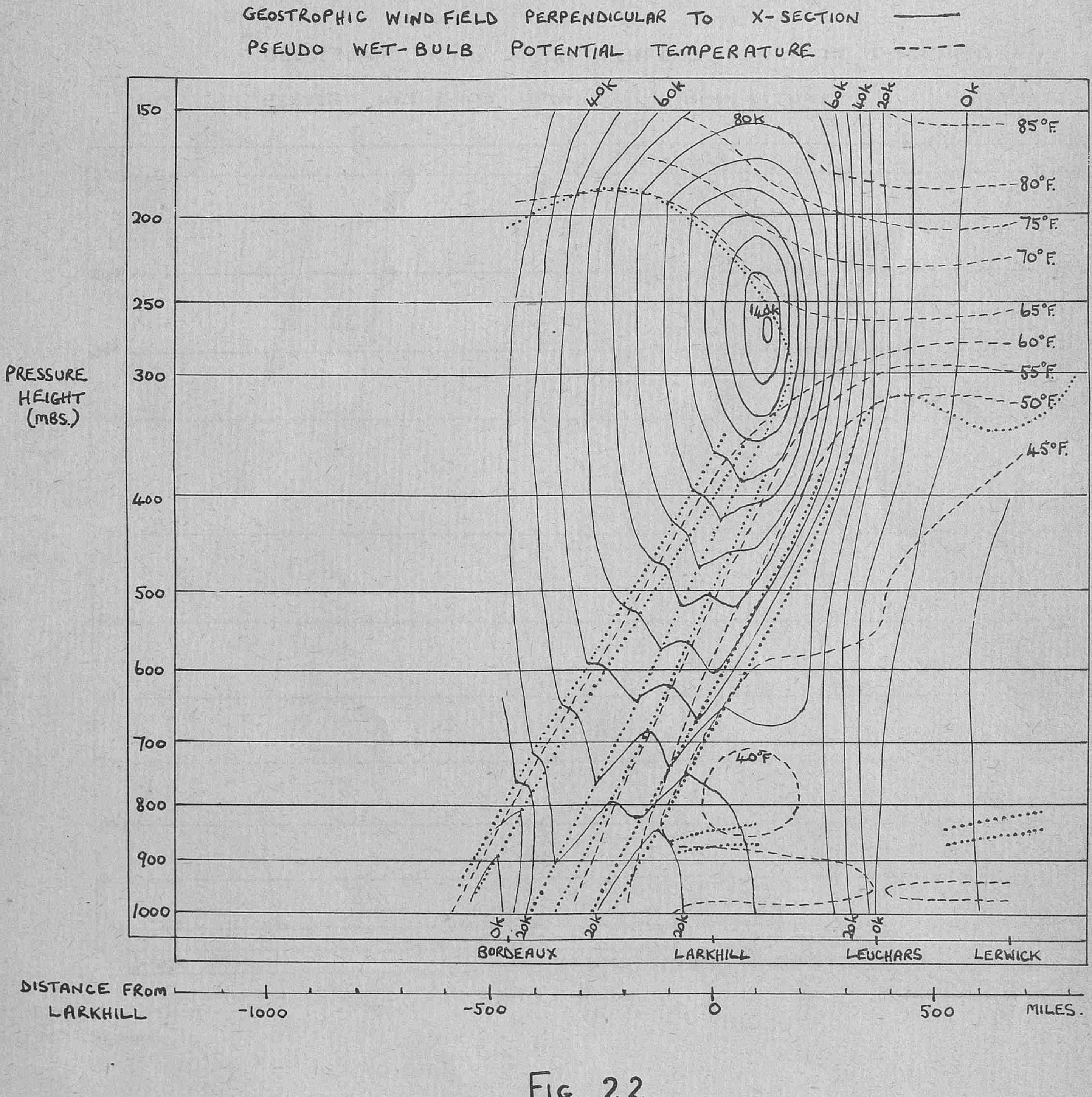

FIG. 22.

M.R.P. 597

24th October 1949 at 1500 G.M.T.

GEOSTROPHIC WIND FIELD PERPENDICULAR TO X-SECTION. ———

PSEUDO WET-BULB POTENTIAL TEMPERATURE - - - - - -

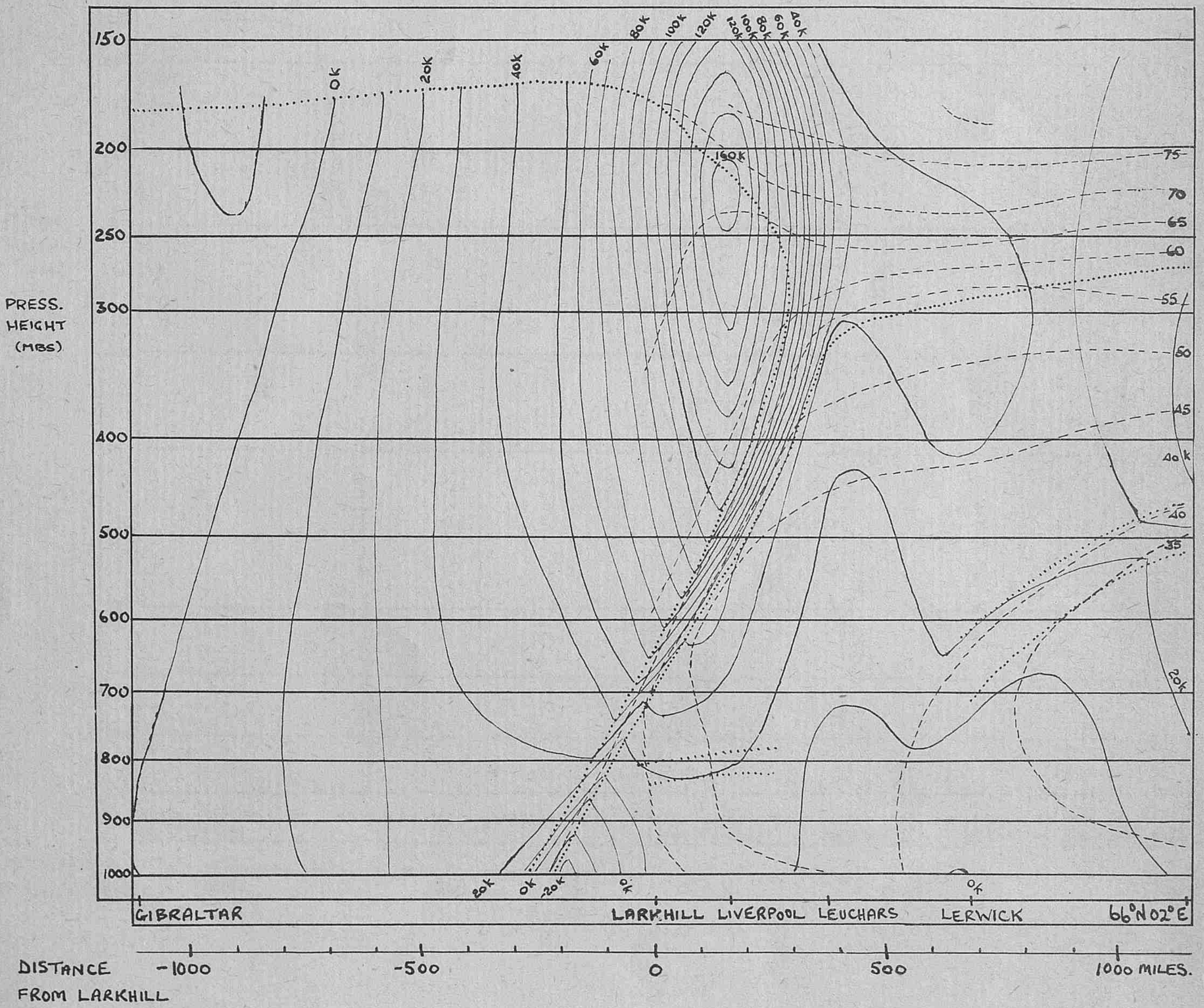

FIG. 23

25th October 1949 at 0300 G.M.T. M.R.P. 597

GEOSTROPHIC WIND FIELD PERPENDICULAR TO X-SECTION. ———

PSEUDO WET-BULB POTENTIAL TEMPERATURE ------

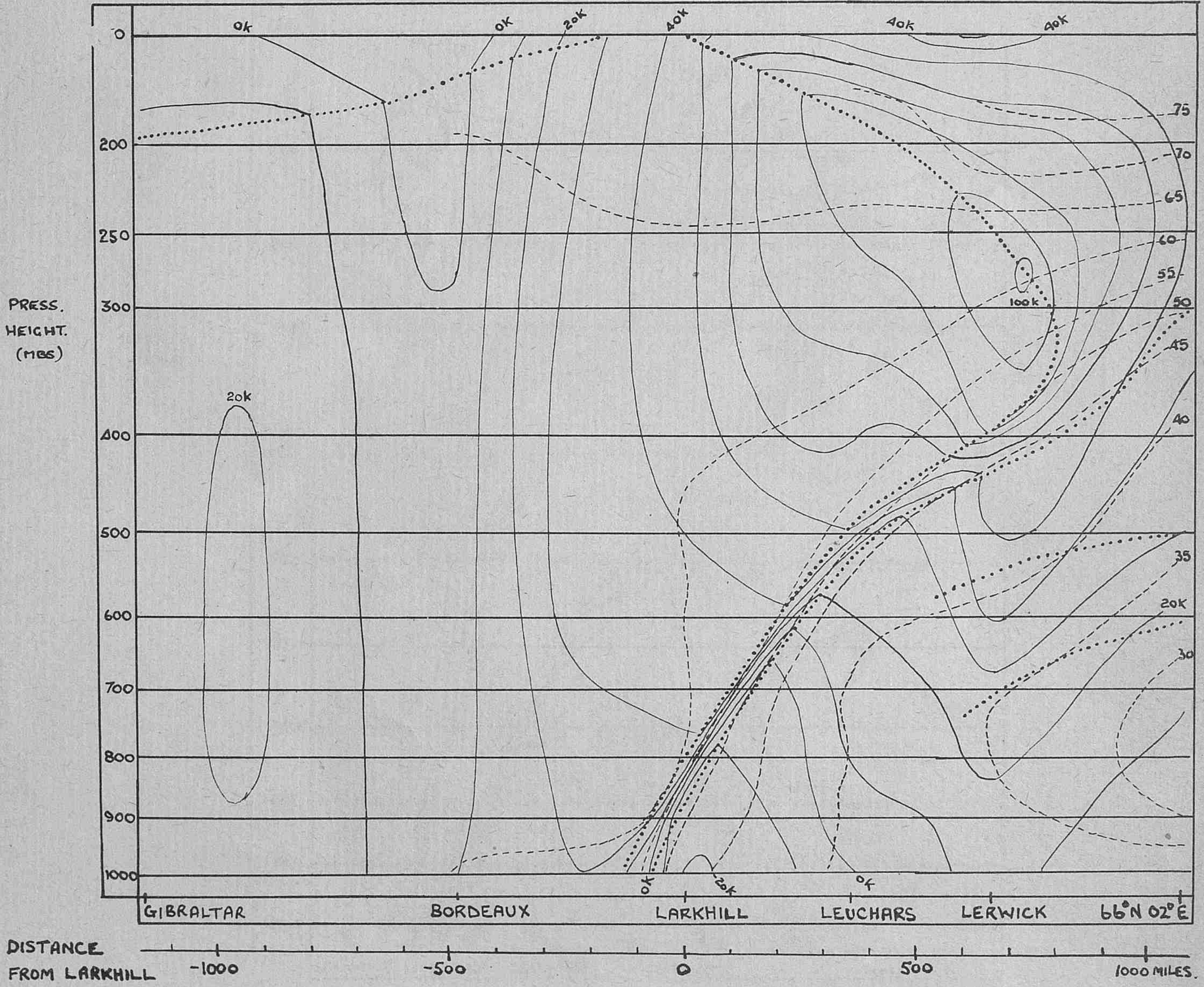

FIG. 24

25th October 1949 at 1500 G.M.T.

Geostrophic wind field perpendicular to X-section ——

Pseudo wet-bulb potential temperature ------

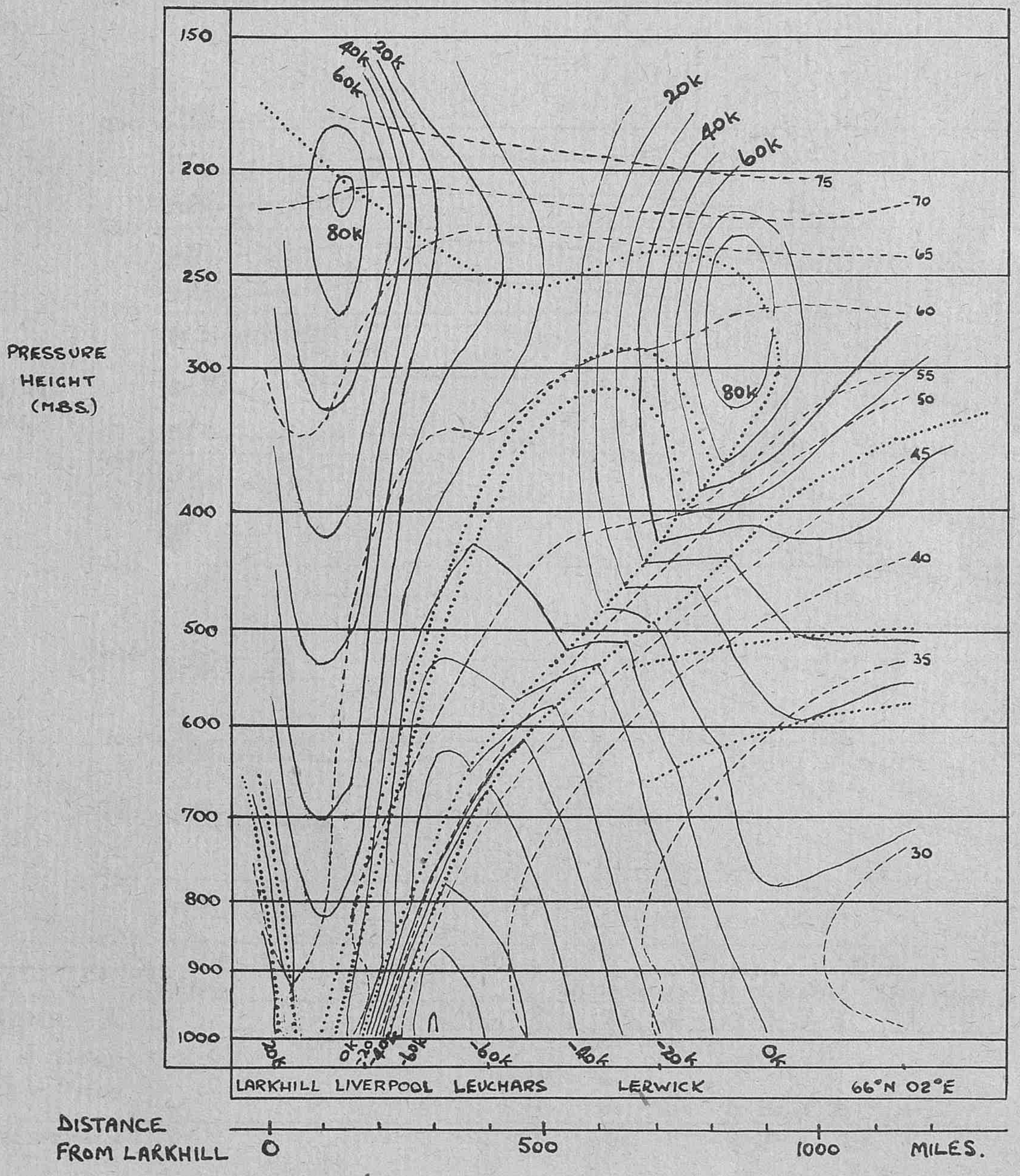

Fig. 25

M.R.P. 597

24th OCTOBER 1949 AT 1500 G.M.T.

——— ISOTHERMS (°F) AND ISOPLETHS OF WIND COMPONENT (KNOTS) PERPENDICULAR TO X-SECTION - - - -

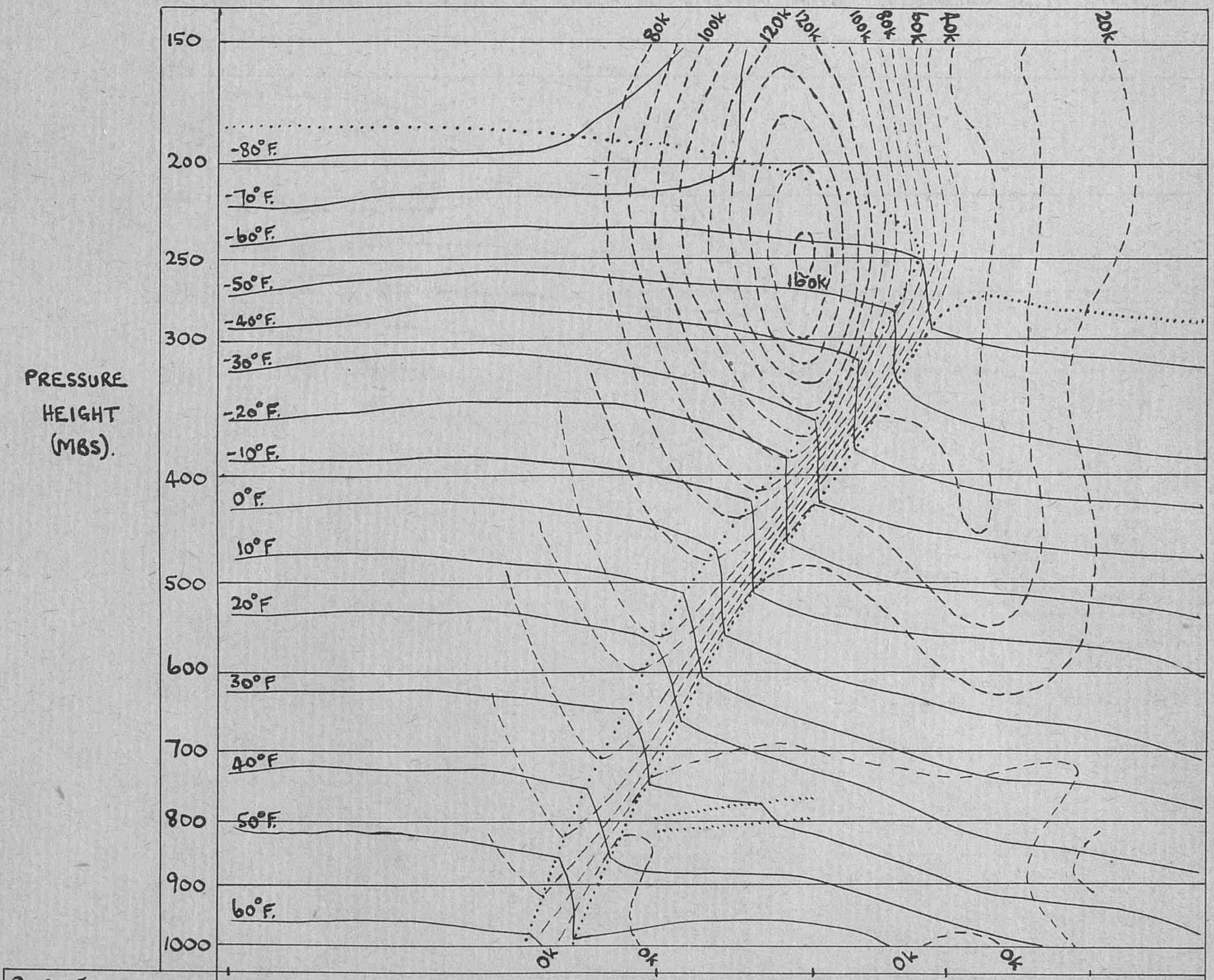

PLACE	LISBON			CAMBORNE		ALDERGROVE				STORNOWAY	THORSHAVN
TOTAL CLOUD × 8	7	7	8	2	4	1	4	7	7	3	3
HIGH CLOUD TYPES		2c		2	—						
MEDIUM CLOUD TYPES			6	6							
LOW CLOUD TYPES	~		---	⌓	~	⌓	△	△	△	△	△
LOW CLOUD AMOUNT × 8	7		6	2	3	1	4	7	7	3	3
LOW CLOUD BASE ÷ 100 FT	15		08	15	25	20	25	36	20	20	15
PRECIPITATION			;					▽	▽	(•)	

DISTANCE FROM CAMBORNE. 500 0 500 1000 MILES.

FIG. 26

25th OCTOBER 1949 AT 0300 G.M.T.

——— ISOTHERMS (°F.) AND ISOPLETHS OF WIND COMPONENT (KNOTS) PERPENDICULAR TO X-SECTION - - - - - -

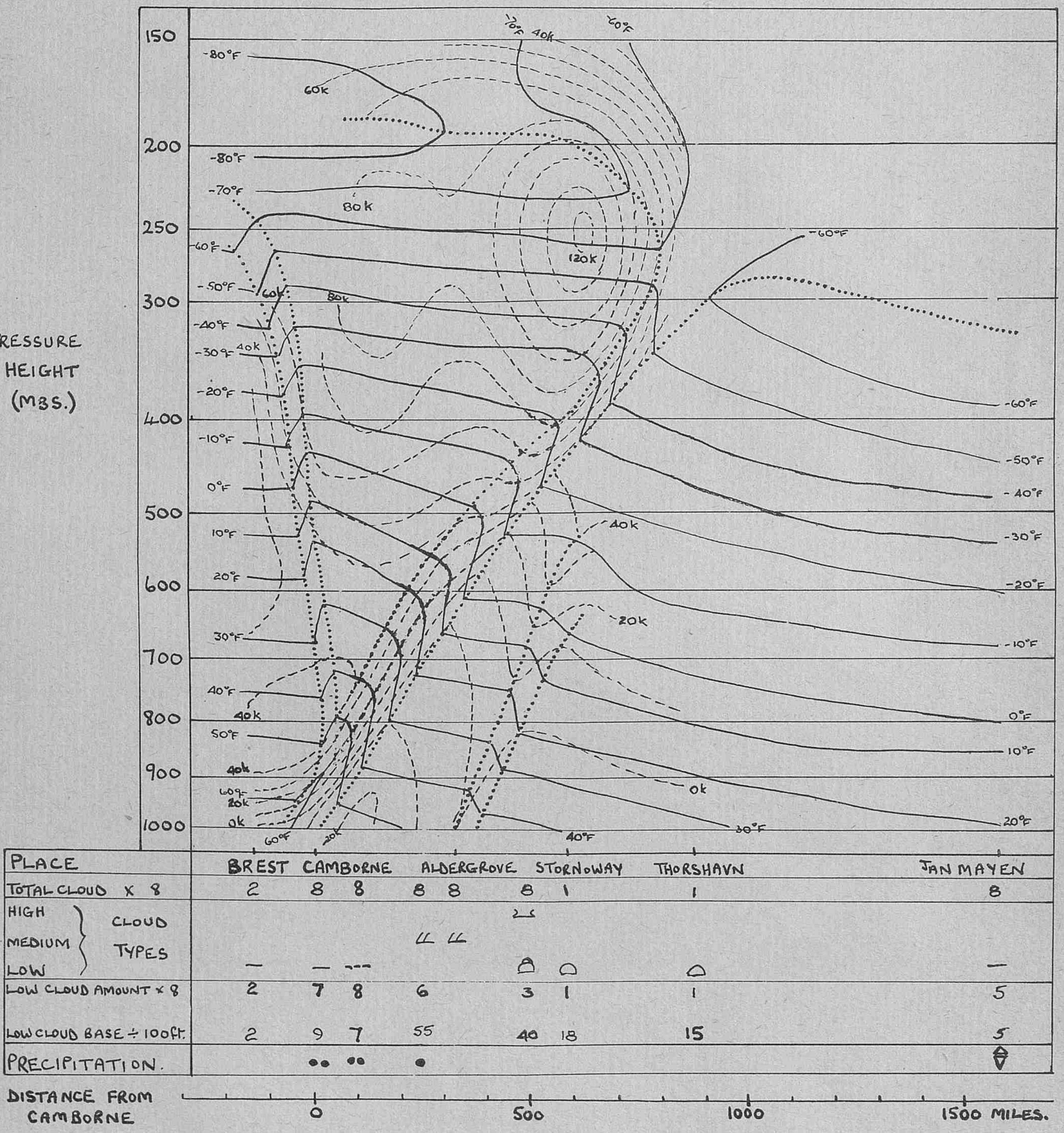

FIG. 27

paper of the Meteorological Research Committee (London),
M.R.P. No .... by Mr ....
A copy is available in the Library of the Meteorological Office."

S.C. III/78
6th December, 1950

MRP 598

ATI - 116112

AIR MINISTRY

METEOROLOGICAL RESEARCH COMMITTEE

On the equation of diffusion in the atmosphere

by E. Knighting, Meteorological Office

Summary.

An analysis is made of the Fickian Equation in two dimensions with the diffusion coefficient proportional to a power of the height above a given datum level, nominally the surface.

1. Introduction.

In considering turbulent transfer in the vertical in the atmosphere, the differential equation often used is

$$\frac{\partial}{\partial z}\left(a z^{1-m}\frac{\partial v}{\partial z}\right) = \frac{\partial v}{\partial t'} + u\frac{\partial v}{\partial x}$$

where x, z and t' are the horizontal, vertical and time coordinates, u the horizontal velocity and v is the entity under discussion; a and m are constants in a particular meteorological situation. Sutton (1943), among other writers, has discussed this equation in the case when $\partial v/\partial t' = 0$ and $u \propto z^n$, following the lines of the classical treatment of the conduction of heat. The equation in which $u = 0$ has been treated in special cases by various writers, e.g. Frost (1948), Knighting (1950).

It is proposed to give here a fairly complete account of the solutions of the equation under the boundary conditions which are normally met with in meteorological problems and to make these solutions readily available to meteorologists. A generalisation of the equation is made in order that the two cases quoted above may be dealt with at the same time. The possible values that n may take are also stressed, since sufficient attention has not always been paid to these values in meteorology, e.g. in the assigning of negative values to m at about midday in summer.

2. Some formulae.

In order that this note shall be self-contained some of the mathematical formulae used are collected here for easy reference.

$$\text{If} \quad \bar{f}(p) = p\int_0^\infty \exp(-pt).f(t)\,dt \qquad \text{.........(1)}$$

$$\text{then we write} \quad f(t) \supset \bar{f}(p) \qquad \text{.......(2)}$$

$I_n(x)$, $K_n(x)$ are the modified Bessel functions of order n. In particular

$$I_n(x) = \sum \frac{(x/2)^{n+2j}}{\Gamma(j+1)\Gamma(n+j+1)} \quad (j = 1, 2, \ldots\ldots \infty) \qquad \text{....(3)}$$

$$x^n K_n(x) = 2^{n-1}\int_0^\infty \exp(-\rho - x^2/4\rho)\rho^{n-1}\,d\rho \qquad \text{....(4)}$$

$$\frac{d}{dx}x^n I_n(x) = x^n I_{n-1}(x), \quad \frac{d}{dx}x^n K_n(x) = -x^n K_{n-1}(x) \qquad \text{....(5)}$$

$$K_n(x) = K_{-n}(x) \qquad \text{.....(6)}$$

$$f(t-h) \supset \exp(-hp)\,\bar{f}(p) \quad t > h \qquad \text{.......(7)}$$

/ $pI_n(\alpha p^{1/2})$

$$pI_n(\alpha p^{1/2})K_n(\beta p^{1/2}) \quad \sqsubset \quad \frac{1}{2t}\exp\left(-\frac{\alpha^2+\beta^2}{4t}\right)I_n\left(\frac{\alpha\beta}{2t}\right), \quad n > 0 \qquad \ldots(8)$$

Of these equations, which are scattered in texts, (1), (2), (7), and (8) are to be found in texts on the operational calculus, while (3), (4), (5) and (6) are to be found in standard treatises on Bessel functions.

3. The equation and the boundary conditions.

The equation which is treated here is

$$\frac{\partial}{\partial z}\left(az^{1-m}\frac{\partial v}{\partial z}\right) = kz^l\frac{\partial v}{\partial t_1} \qquad \ldots\ldots(9)$$

where t_1 is either x or t', k and l are constants. Clearly with proper choice of k and l equation (9) covers both the cases mentioned above; moreover, if the conjugate power law does not hold, but u is still proportional to a power of z, then this equation provides the solution for steady motion. The substitution

$$\begin{aligned} t &= at_1/k = at' \text{ in the time equation} \\ &= ax/k \text{ in the space equation} \end{aligned}$$

removes the parameters and (9) becomes

$$\frac{\partial}{\partial z}\left(z^{1-m}\frac{\partial v}{\partial z}\right) = z^l\frac{\partial v}{\partial t} \qquad \ldots\ldots(10)$$

In meteorological applications we are usually given the distribution of v with z at $t = 0$, and the variation of v with t at the surface, $z = 0$. In addition the value of v is required to remain finite everywhere, in particular as $z \to \infty$. It is under these boundary conditions that we shall solve the problem. Other boundary conditions which may arise, such as a given value of v over a finite strip as in evaporation problems, may be dealt with equally effectively by the method of solution adopted here. Many of the boundary conditions other than those treated here may be replaced by specifying v at a given height h; Jaeger (1945) has dealt with problems of this type.
In the solution of the equations v will be measured from its constant value at $z = \infty$. The boundary conditions that we use are therefore

$$v \to f(t) \quad \text{as} \quad z \to 0 \qquad \ldots\ldots\ldots(11.1)$$

$$v \to \emptyset(z) \quad \text{as} \quad t \to 0 \qquad \ldots\ldots\ldots(11.2)$$

$$v \to 0 \quad \text{as} \quad z \to \infty \qquad \ldots\ldots\ldots(11.3)$$

The solution of equations (10) and (11) breaks up into two natural parts. If U satisfies the equations with $\emptyset(z) = 0$, and V satisfies the equations with $f(t) = 0$, then $v = U + V$ satisfies the equations as given, as is easily seen.

In the solution of these equations the following abbreviations are used to avoid a plethora of symbols.

$$n = \frac{m}{l+m+1} \qquad \ldots\ldots\ldots\ldots(12.1)$$

$$2r = l+m+1 \qquad \ldots\ldots\ldots\ldots(12.2)$$

$$\lambda = \alpha p^{1/2} = \frac{2z^{\frac{l+m+1}{2}}p^{1/2}}{l+m+1} = \frac{z^r p^{1/2}}{r} \qquad \ldots\ldots(12.3)$$

$$\mu = \beta p^{1/2} = \frac{y^r p^{1/2}}{r} \qquad \ldots\ldots(12.4)$$

where y is a value of z to be defined later.

4. Solution of the equations for U.

Applying the transformation, equn. (1), to equns. (10) and (11) with $\emptyset(z) = 0$ we find the system of equations

/equn. (13.1)

$$\frac{\partial}{\partial z}\left(z^{l-m}\frac{\partial \overline{U}}{\partial z}\right) \quad = \quad z^{l}p\overline{U} \qquad \ldots\ldots\ldots(13.1)$$

$$\overline{U} \quad \rightarrow \quad \overline{f}(p) \quad \text{as } z \rightarrow 0 \qquad \ldots\ldots\ldots(13.2)$$

$$\overline{U} \quad \rightarrow \quad 0 \quad \text{as } z \rightarrow \infty \qquad \ldots\ldots(13.3)$$

Jaeger (1945) has developed a solution from these equations with $l = m$, $f(t)$ = a constant, proceeding in a rather different manner from that given here. The basic solutions of (13.1) are

$$\overline{U} \;=\; \lambda^{n}I_{n}(\lambda), \quad \overline{U} \;=\; \lambda^{n}K_{n}(\lambda) \qquad \ldots\ldots(14).$$

Equation (13.3) shows that only the K-form is applicable and

$$\overline{U} \quad = \quad A\lambda^{n}K_{n}(\lambda) \qquad \ldots\ldots(15)$$

while from equns. (4) and (13.2)

$$\overline{f}(p) \quad = \quad A2^{n-1}\Gamma(n) \qquad \ldots\ldots(16)$$

Equns. (4), (15) and (16) give

$$\overline{U} \quad = \quad \frac{1}{\Gamma(n)}\int_{0}^{\infty} \exp(-\rho - z^{2r}p/4r^{2}\rho)\rho^{n-1}\overline{f}(p)\,d\rho \qquad \ldots.(17).$$

We may use equn. (7) directly on this expression, giving

$$U \quad = \quad \frac{1}{\Gamma(n)}\int_{\frac{z^{2r}}{4r^{2}t}}^{\infty} \exp(-\rho)\rho^{n-1}f(t - z^{2r}/4r^{2}\rho)\,d\rho \qquad \ldots(18).$$

In the derivation (v. equn.(16)) the infinite integral defining $\Gamma(n)$ requires that

$$n \quad = \quad \frac{m}{l+m+1} \quad > \quad 0 \qquad \ldots\ldots\ldots(19.1)$$

$$n \quad > \quad 0, \qquad l+m+1 \quad > \quad 0 \qquad \ldots\ldots\ldots(19.2)$$

$$m \quad < \quad 0, \qquad l+m+1 \quad < \quad 0 \qquad \ldots\ldots\ldots.(19.3)$$

$\underline{l}$ is normally required to be positive or zero, otherwise in the steady state case the wind speed at the surface becomes infinite.

Defining the flux at height $\underline{z}$ by

$$\text{Flux} \quad = \quad \Delta F(z,t) \quad = \quad \Delta F(z) \quad = \quad -\Delta z^{l-m}\frac{\partial v}{\partial z} \qquad \ldots.(20)$$

where Δ is to be determined according as the meteorological variable denoted by $\underline{v}$ (if $\underline{v}$ is the temperature, $\Delta = \rho c_{p}$ where $\underline{\rho}$ is the air density and c_{p} the specific heat at constant pressure), and we write $F(z)$ for brevity. By equns. (15) and (16) and considering the flux of U

$$\overline{F}(z) \quad = \quad -z^{l-m}\frac{\partial \overline{U}}{\partial z} \quad = \quad -z^{l-m}\frac{2^{1-n}}{\Gamma(n)}\frac{\partial}{\partial z}\lambda^{n}K_{n}(\lambda)\overline{f}(p) \qquad ..$$

$$= \quad \frac{2^{n}}{\Gamma(n)}\cdot\frac{m}{n(2r)^{2n}}\cdot\lambda^{1-n}K_{1-n}(\lambda)p^{n}\overline{f}(p) \qquad \ldots\ldots(21).$$

Since $\underline{n}$ is usually fractional it is seen that for real values of the flux $\underline{r}$ must be positive; hence equn. (19.3) is not applicable and $\underline{n}$ must be positive. The flux at $z = 0$ is given by

$$/\ \overline{F}(0) \quad =$$

$$\overline{F}(0) \quad = \quad \frac{m\Gamma(1-n)}{n\Gamma(n)}\,(2r)^{-2n}p^{n}\overline{f}(p) \qquad \ldots\ldots\ldots(22)$$

$$F(0) \quad = \quad \frac{n}{n\Gamma(m)}\,(2r)^{-2n}\frac{d}{dt}\int_{0}^{t}(t-\sigma)^{-n}f(\sigma)d\sigma \quad \ldots\ldots(23).$$

By writing equn. (23) in this form we avoid some difficulties at the upper limit of integration arising from the presence of a term $(t - \sigma)^{-n-1}$ in the integrand.

A special well-known case, the conduction of heat, arises by putting $l = 0$, $m = 1$, so that $n = 1/2$ and $r = 1$. Setting $f(t) = \text{constant} = T$, then equns. (18) and (23) reduce to

$$U \quad = \quad T\,\text{erfc}(z/2t^{1/2})$$

$$F(0) \quad = \quad T/(\pi t)^{1/2}$$

which are well-known formulae. (Carslaw and Jaeger 1947).

In a practical case it is better to use equn. (22), expanding $\overline{f}(p)$ in negative powers of p and interpreting by the rule

$$p^{-n} \qquad \frac{t^{n}}{\Gamma(n+1)}\ .$$

For example, if $f(t) = \sin \omega t$, $\overline{f}(p) = \omega p/(p^2+\omega^2)$,

$$\overline{F}(0) \quad = \quad \frac{m\Gamma(1-n)}{n\Gamma(n)}.\omega(2r)^{-2n}p^{n-1}(1 - \omega^2/p^2 + \ \ldots)$$

$$F(0) \quad = \quad \frac{m\Gamma(1-n)}{n\Gamma(n)}.\omega(2r)^{-2n}\left\{\frac{t^{1-n}}{\Gamma(2-n)} - \frac{\omega^2 t^{3-n}}{\Gamma(4-n)} \ \ldots.\right\}$$

The most significant equations from a meteorological point of view are equations (18) and (23), with the condition that n is positive. If n exceeds unity it appears from equation (10) that $\partial U/\partial z$ at the surface, $z = 0$, is infinite, which may or may not be acceptable from a meteorological point of view and indeed is a point that cannot be tested experimentally. The flux at the surface remains finite in this case.

After a sufficiently long time equation (18) may be replaced by

$$U \quad = \quad \frac{1}{\Gamma(n)}\int_{0}^{\infty}\exp(-\rho)\rho^{n-1}f(t - z^{2r}/4r^2\rho)d\rho \qquad \ldots.(24),$$

but a warning is necessary. Most of the contribution towards this integral is concentrated near the lower limit, owing to the presence of the exponential term, and it is necessary to show that the neglected part, the integral from 0 to $z^{2r}/4r^2t$, is very much smaller than the infinite integral. For diurnal heating in the period from dawn to dusk an approximation to the form of f(t) is $\sin \omega t$, where the period of the wave is 24 hours. Between dawn and midday only one-quarter of a wave has passed and the asymptotic form of equation (24) may not be a good approximation.

5. Solution of the equations for V.

Applying the transformation of equation (1) we find the system

$$\frac{\partial}{\partial z}\left(z^{1-m}\frac{\partial \overline{V}}{\partial z}\right) \quad = \quad z^{l}p(\overline{V} - \phi(z)) \qquad \ldots\ldots(25.1)$$

$$\overline{V} \longrightarrow 0 \text{ as } z \longrightarrow 0 \qquad \ldots\ldots\ldots(25.2)$$

$$\overline{V} \longrightarrow 0 \text{ as } z \longrightarrow \infty \qquad \ldots\ldots\ldots(25.3)$$

To solve we write the solution with $\phi(z) = 0$ as $w(z)$ where

$$w(z) = w(1) = A\lambda^n I_n(\lambda), \qquad 0 < z < y. \text{ i.e. } 0 < \lambda < \mu \quad \ldots.(26.1)$$

$$= w(2) = B\lambda^n K_n(\lambda), \qquad y < z. \text{ i.e. } \mu < \lambda \quad \ldots.(26.2)$$

for these two solutions satisfy the boundary conditions, equns. (25.2) and (25.3). In addition we require that

$$w(1) = w(2) \quad \text{at } z = y, \ \lambda = \mu \quad \ldots\ldots\ldots.(27.1)$$

$$\frac{\partial}{\partial z} w(1) - \frac{\partial}{\partial z} w(2) = z^{m-1} \quad \text{at } z = y, \ \lambda = \mu \quad \ldots\ldots\ldots(27.2)$$

These last two equations serve to define A and B and it is easily found that

$$w(1) = \frac{\mu^{1-n}\lambda^n K_n(\mu) I_n(\lambda)}{y^{1-m}} \frac{dy}{du}$$

$$w(2) = \frac{\mu^{1-n}\lambda^n I_n(\mu) K_n(\lambda)}{y^{1-m}} \frac{dy}{du}$$

and it follows that the solution of equns. (25) is

$$\overline{V}(z) = \int_0^z py^1\phi(y)w(1)dy + \int_z^\infty py^1\phi(y)w(2)dy \quad \ldots(28).$$

The first integral, $\overline{L}(1)$, reduces, using equns. (12), to

$$\overline{L}(1) = \int_0^\alpha \alpha^n \beta^{1-n} \phi(y) p I_n(\beta p^{1/2}) K_n(\alpha p^{1/2}) d\beta .$$

The second integral is similar, with I_n and K_n reversed, the limits being (α, ∞). Using equn. (8)

$$V = \frac{\alpha^n \exp(-\alpha^2/4t)}{2t} \int_0^\infty \exp(-\beta^2/4t)\beta^{1-n}\psi(\beta) I_n(\alpha\beta/2t) d\beta \quad \ldots(29)$$

$$\text{where } \phi(y) = \psi(\beta).$$

The proviso in the interpretation of $\overline{L}(1)$ is again that n is positive. The flux is most easily obtained from equn.(29) and gives

$$F(0) = \frac{-m}{2\Gamma(n+1)} \cdot (2r)^{-2n} t^{-n-1} \int_0^\infty \beta\psi(\beta) \exp(-\beta^2/4t) d\beta \quad \ldots(30),$$

and we see that r must be positive.

Turning again to the special values of the parameters for the conduction of heat, we recover the familiar formula

$$F(0) = -T/(\pi t)^{1/2}.$$

It is interesting to calculate the two fluxes when $f(t) = \phi(z) = T$, for then v is everywhere constant and equal to T and there should be no total flux. From equn. (23), with $z = 0$,

$$\text{Flux for U} = \Delta m(2r)^{-2n} t^{-n}/n\Gamma(n)$$

while from equn. (30)

$$\text{Flux for V} = -\Delta m(2r)^{-2n} t^{-n}/n\Gamma(n)$$

Showing that the two fluxes are equal and opposite.

For large values of t, V tends to zero whatever $\psi(\beta)$ may be, providing that $\psi(\beta)$ is such that the integral in equn. (30) exists, which means that after a long time the distribution of v at $t = 0$ is immaterial, the transfer being determined by the impressed variation at $z = 0$, and $v \sim U$.

The solution for V is very well adapted to calculation if $\phi(z) = \psi(\beta)$ is a polynomial, for then we may expand $I_n(\alpha\beta/2t)$ in powers of β, by means of equn. (3), and perform the successive integrations. If z is small, a first approximation is given by the first term of the Bessel expansion, and writing

$$\phi(z) = \psi(\beta) = \theta(\beta^2)$$

then

$$V = \frac{\alpha^{2n}\exp(-\alpha^2/4t)}{(4t)^{n+1}\Gamma(n+1)}\int_0^\infty \exp(-\beta^2/4t)\theta(\beta^2)d\beta^2.$$

If

$$\theta(\beta^2) = \sum a_s\beta^{2s}$$

then

$$V = \sum a_s \frac{\alpha^{2n}\Gamma(1+s)}{(4t)^{n-s}\Gamma(n+1)} \exp(-\alpha^2/4t) ,$$

and in particular, if $\phi(z) = z = (\beta^2)^{1/2r}$

$$V = z\left\{\frac{\alpha^2}{4t}\right\}^{\frac{n-1}{l+m+1}} \frac{\Gamma(1 + 1/l+m+1)}{\Gamma(1 + n/l+m+1)} \exp(-\alpha^2/4t)$$

This result has been given by Frost (1949) for $l = n$, except that Frost omits the term $\exp(-\alpha^2/4t)$, which is nearly unity for small values of z.

6. Discussion of the solutions.

The solution of equations (10) and (11) is now complete and

$$v = U + V.$$

We have dealt only with the formal solution, and where infinite integrals occur have assumed that they exist; e.g. in equation (18) it is assumed that f(t) is such a function that the right hand side of the equation exists. The proof that equations (18) and (29) do satisfy the differential equation and the boundary conditions can easily be supplied. No proof that these solutions are unique is attempted and indeed such proofs would be out of place in a practical paper of this kind.

Some remarks upon the applicability of the solutions is not out of place. It should be recognised that the diffusion law has been assumed to hold to great heights, indeed to $z \to \infty$. In practice it is scarcely likely that this is true and the solutions are approximately true in a layer extending up to some level h; it should also be noted that the larger z is in the interval (0,h) the poorer the approximation, and great caution is necessary in applying asymptotic forms in z, (the caution necessary in using asymptotic forms in t has already been noted), lest the asymptotic form be not a good representation of the facts in the upper part of the range (0,h).

A second important point is that if the experimental results are analysed by means of the solutions given above and lead to values of m which are negative, then the solutions are not applicable. Alternatively, if experimental result in values of m which are negative, no use having been made of the solutions, then the equations are invalid. In either case the diffusion equation cannot represent the motion.

References.

Carslaw, H.S. and Jaeger, J.C. 1947 Conduction of Heat in Solids. Oxford University Press.

Frost, R. 1948 Prof. Notes, Met. Off., London, No. 95.

/1949

Frost, R. 1949 Proc. roy. Soc., London, A198, p. 27.

Jaeger, J.C. 1945 Quart. app. Maths., 3, p. 210

Knighting, E. 1950 Quart. J. R. met. Soc., London, 76, p. 173.

Sutton, W.G.L. 1943 Proc. roy. Soc., London, A182 , p. 48.

MRP's 662, 603, 604, 605

At the time of issue this report has not been published. Any author desiring to quote this paper should refer to it as "A paper of the Meteorological Research Committee (London), M.R.P. No.......... by Mr.......................... A copy is available in the Library of the Meteorological Office."

M.R.P. 602
S.C.III/79
3rd January, 1951.

AIR MINISTRY

METEOROLOGICAL RESEARCH COMMITTEE

AUG 23 1951

The Effect of a Hedge on the Flow of Air

by

N.E. Rider (Meteorological Office)

AIR WEATHER SERVICE
TECHNICAL REFERENCE FILES

1. Introduction

A survey of the influence of a hedge, of the type often found as a border to gardens and fields, on the horizontal wind speed both up wind and down wind from the hedge was undertaken as a preliminary investigation to test the suitability of a site for experiments concerned with certain aspects of the turbulent exchange process. It has been suggested that the results of this survey should be made available as they may hold some interest for those concerned with the microclimatological effects of such obstacles.

2. The Site and Apparatus

The site was a sports field covered with a surface of short grass which was surrounded to the south and west by a field of wheat stubble throughout the period of the experiments. Between the two fields and separating them was a hawthorn hedge. The general characteristics and the dimensions of the site are shown in fig. 1. Fig. 2 is a photograph of the hawthorn hedge taken from the sports field side. It will be noted that the hedge is somewhat open from the ground to a height of approximately 25 cm., but from this height to its top it presents a very dense barrier to the flow of air. The height of the hedge decreased fairly uniformly from 2 m. at the N.W. corner of the sports field to 1.5 m. at the S.W. corner, and its height at the point B (see fig. 1) was 1.68 m.

The instruments employed were sensitive cup anemometers of the Sheppard type which were calibrated in a wind tunnel during the course of the measurements. Masts were available on which the anemometers could be exposed at three heights, namely 2, 1, and $\frac{1}{2}$ m.

3. Measurement of the Unobstructed Wind

The purpose of the measurements was to determine the distances up and down wind from the hedge at which anemometers could be exposed and be expected to yield results which were not influenced by the presence of the hedge. A further aim was to obtain some indication of the pattern of horizontal wind speed between these positions and the hedge. To this end it was necessary to expose anemometers at various distances from the hedge and to compare their readings of wind speed at these distances with the free or unobstructed wind. It was therefore first essential to decide where the free wind should be measured. Throughout the experiments measurements were only made when westerly wind directions which were within fifteen degrees of the normal to the hedge at B. occurred, and a few preliminary measurements served to show that, as far as the upwind direction was concerned, no difficulty arose as anemometers sited at position C. (fig. 1) which was 30.5 m. from the hedge gave the same indications (up to 2m.) as anemometers sited further up wind. It was therefore decided to measure the free wind at this position when investigating the up wind effect of the hedge.

Down wind of the hedge reference to fig. 1 will show that there was a uniform surface of short grass for 147 m. and then a second hedge of the same type as that concerned in the survey. As far as possible it was necessary to choose a point within this 147 m. of uniform surface at which neither hedge had an effect on the pattern of horizontal wind speed. After a few measurements it was decided to measure the free wind when working on the down wind side of the hedge at the point A. (fig. 1) 107 m. from the hedge. We shall see later that this choice was a compromise in so far as there was an indication that the hedge might still have a small effect on the wind at 2 m. in this position.

4. Experimental Procedure

Twelve anemometers only were available so it was possible to use no more than four masts at any one time. In view of this it was decided to keep one mast stationary at either position A or C and move the other three along the line AB or BC as required. The mast which was placed at A or at C will be referred to as the reference mast.

The procedure for any one experiment was as follows:

The four masts were placed in position with three anemometers on each. The anemometers were then started at 5 sec. intervals and allowed to run for 15 min. They were then read and interchanged in such a way that the anemometer exposed to the highest wind at a particular height was afterwards exposed to the lowest wind at the same height. In practice this involved changing the anemometer at 2 m. on the reference mast, i.e. the mast furthest removed from the hedge and therefore exposed to the greatest wind, with that at 2 m. on the mast nearest the hedge, interchanging the anemometers at 2 m. on the intermediate masts, and repeating the process at the other two heights. A second 15 min. run was then taken and the indicated individual wind speeds at each height in each position during the two runs meaned. In this way it was hoped to minimise any instrumental error.

A series of experiments was performed in which the spacing between the masts was reduced as the hedge was approached. Thus the wind speeds at the three heights, in a number of positions within the limits set by the appropriate reference mast position and the hedge, were obtained together with the wind speed at the reference mast position in every case.

5. Method of Presentation of the Results

Since the experiments were conducted on a number of occasions the absolute values of the wind speeds at the reference positions varied. In view of this the wind speeds at the three heights in the various positions were expressed as a percentage of the wind speed at the corresponding heights at the reference position. This seemed to be the best method to adopt in the circumstances. The results up and downwind from the hedge are set out in tables I and II respectively. It is usual in this type of work to express the distances from the barrier in terms of the height of the barrier, and this has been added in the tables. From these results two figures have been drawn. Fig. 3 shows the horizontal wind speed experienced at each of the three heights upwind from the hedge as a percentage of the horizontal wind speed at the corresponding height 18.2 hedge heights (30.5 m.) upwind of the hedge. Fig. 4 is a similar representation of the horizontal wind speeds as a percentage of the corresponding horizontal wind speeds at 63.6 hedge heights (107 m.) downwind from the hedge. In both cases the distance scale is logarithmic.

In order to construct figs. 5 and 6, which show on a vertical section lines of equal horizontal wind speed, up and downwind from the hedge, it was necessary to express the wind speeds at all the individual positions in terms of the free wind at 2 m. at the appropriate reference position. This was done in the following way. The values of the wind speeds at the three heights for all occasions of observation at each reference position were meaned and the ratios

$$\frac{\text{horizontal wind speed at 1 m.}}{\text{horizontal wind speed at 2 m.}} \text{ and } \frac{\text{horizontal wind speed at } \frac{1}{2} \text{ m.}}{\text{horizontal wind speed at 2 m.}}$$

for the upwind and downwind reference positions obtained. The percentages shown in tables I and II for the 1 m. and $\frac{1}{2}$ m. heights were then reduced in these ratios. It was to be expected, as proved to be the case, that these ratios would not be the same for the two positions since the characteristics of the two surfaces differed. The surface of the sports field was unusually smooth for a natural surface and had a grass length of about 3 cm. On the other hand the field of wheat stubble was rough and the length of the stubble was about 15 cm. There were also a few taller weeds.

6. Examination of the Results

(A) Upwind from the Hedge

A study of the figures will show that the effect of the hedge started to be felt at the 2 m. and 1 m. heights at approximately 15 hedge heights in front of the hedge. At the $\frac{1}{2}$ m. height the corresponding distance was about 10 hedge heights. At the 2 m. height there was a steady decrease in the wind speed as the hedge was approached and finally an increase. For the other two lower heights the decrease continued up to the nearest point of measurement, the decrease becoming more rapid as the hedge was approached, except that very near the hedge the rate of decrease diminished. It would be expected that if the hedge had been dense right down to the ground the decrease at the $\frac{1}{2}$ m. height would have been more marked.

(B) Downwind from the Hedge

The most striking feature of the results is the indication that the effect of the hedge extended to about the same distance for the $\frac{1}{2}$ m. and 1 m. heights. This was unexpected as it has been generally accepted that for a height of x m. objects or changes in surface characteristics outside a distance of about 100 x m will have no influence on the measured wind speed at x m. We should therefore expect that after a fetch of about 50 m. (30 hedge heights) there would be no further increase in the measured wind speed at $\frac{1}{2}$ m., whereas the further increase was in the region of 10 %. At 1 m. the wind speed appeared to have attained its unobstructed value well within the expected distance. There is an indication that the wind at 2 m. may not have regained its unobstructed value at the furthest point of measurement, but it certainly must have almost done so. +It should be remembered that the hedge was only 1.68 m. high, and the 2 m. level was well above its top.

At the 1 m. and $\frac{1}{2}$ m. heights there appeared to be two positions at which the wind speed reached a minimum value, and further at a distance of approximately 2 hedge heights the absolute value of the wind speed at $\frac{1}{2}$ m. was greater than that at 1 m. These effects were almost certainly due to the interaction of the air coming over the top of the hedge and that coming through the hedge at its relatively open base.

(C) General

The available literature on the effects of wind breaks indicates that the effectiveness of a barrier depends on the absolute value of the free wind, the effect extending to greater distances with increasing wind speed. No attempt has been made here to investigate this statement as a much more comprehensive survey would be required. The mean wind speed at 2 m. for the downwind reference position was 3.64 m./sec. over all the downwind runs, with extremes of 2.57 m./sec. and 5.54 m./sec. The corresponding values for the upwind reference position were 2.98, 2.32, 4.15 m./sec.

/ One

+The shape of the mean profile at the reference mast position was approximately logarithmic, indicating that, since the measurements were made in stability conditions which could not have been very different from neutral, the influence of the hedge must have been very slight over the whole height range at this position.

One would also expect the stability of the atmosphere within the layer investigated to have some small result on the detailed pattern. Although no measurements of temperature gradients were made during the course of these measurements, all occasions had overcast skies and a moderate wind speed and it is certain that the stability of the atmosphere, as indicated by the Richardson Number, did not differ greatly from neutral.

The detailed pattern of the lines of equal wind speed near the hedge as shown in figs. 5 and 6 is to some extent imaginary, but they have been inserted as representing the most likely pattern indicated by the measurements that were made.

TABLE I.

Horizontal Wind Speeds Upwind from the Hedge as a percentage of that at the Corresponding Height at 30.5 metres (18.2 hedge heights) Upwind from the Hedge

Distance		Heights		
Metres	Hedge Heights	2 m.	1 m.	½ m.
.76	.45	88	69	66
1.52	.91	84	73	72
2.29	1.36	90	83	82
3.05	1.82	92	84	87
3.82	2.46	94	85	89
4.57	2.73	94	88	90
6.10	3.63	95	91	93
7.63	4.50	96	92	92
9.16	5.46	96	94	94
10.7	5.99	97	93	94
12.2	7.26	95	94	94
13.7	8.15	97	95	95
15.3	9.09	97	97	98
18.3	10.8	98	97	100
22.9	13.6	100	101	100
30.5	18.2	100	100	100

Ratio of wind speeds at 30.5 metres from the hedge for all occasions of observation.

2m. : 1 m. : ½ m.

100 : 89 : 75

/ TABLE II

TABLE II

Horizontal Wind Speeds Downwind from the Hedge as a percentage of that at the Corresponding Heights at 107 metres (63.6 hedge heights) Downwind from the Hedge

Distance		Heights		
Metres	Hedge Heights	2 m.	1 m.	$\frac{1}{2}$ m.
.76	.45	70	21	19
1.52	.91	55	12	20
2.29	1.36	56	12	27
3.05	1.82	57	14	23
3.82	2.46	58	15	14
4.57	2.73	60	23	20
6.10	3.63	63	36	30
7.63	4.50	62	39	38
9.16	5.46	64	44	44
11.4	6.80	65	47	37
15.3	9.09	69	61	58
18.3	10.8	73	67	64
22.9	13.6	76	73	66
30.5	18.2	84	84	83
45.9	27.3	92	90	91
61.2	36.4	94	95	94
76.4	45.5	97	97	96
91.6	54.6	99	101	100
107.	63.6	100	100	100

Ratio of Wind Speeds at 107 metres from the Hedge for all Occasions of Observation

2m. : 1 m. : $\frac{1}{2}$ m.

100 : 92 : 83

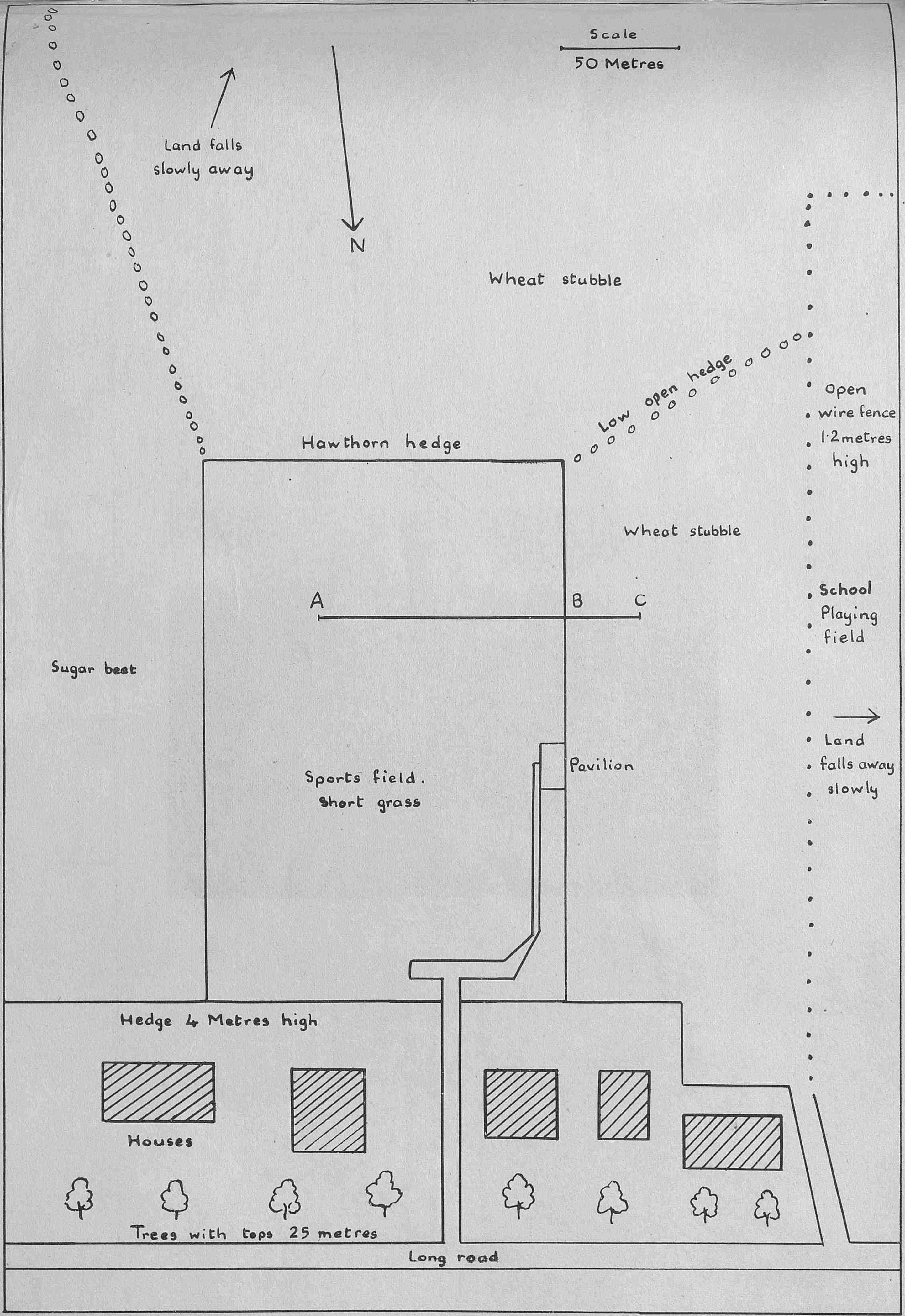
Scale
50 Metres
Land falls slowly away
N
Wheat stubble
Low open hedge
Hawthorn hedge
Open wire fence 1·2 metres high
Wheat stubble
A
B
C
School Playing field
Sugar beet
Land falls away slowly
Pavilion
Sports field. Short grass
Hedge 4 Metres high
Houses
Trees with tops 25 metres
Long road

Downing College Sports Field
and Surroundings

FIG. 1

M.R.P. 602.

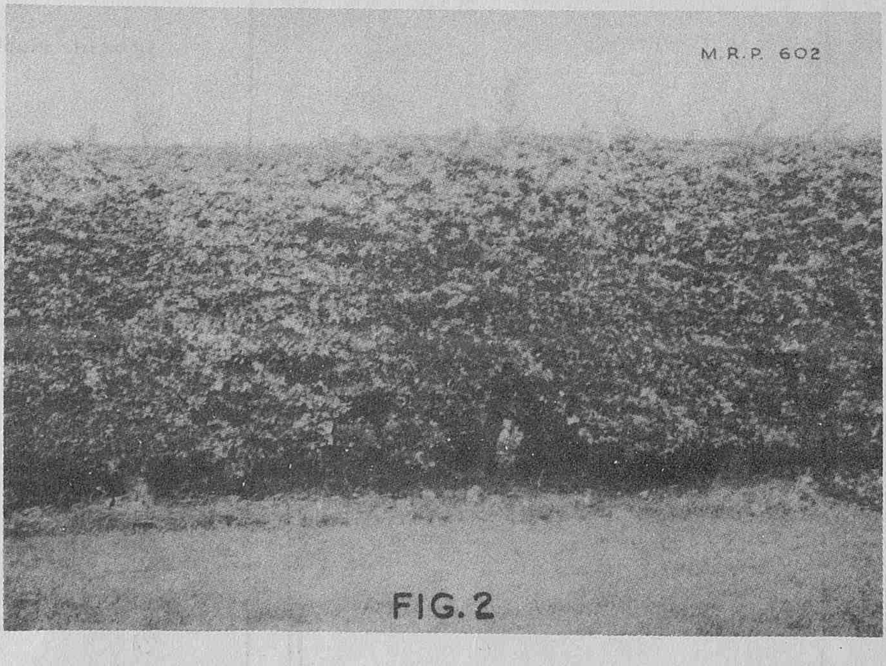

FIG. 2

FIG. 3

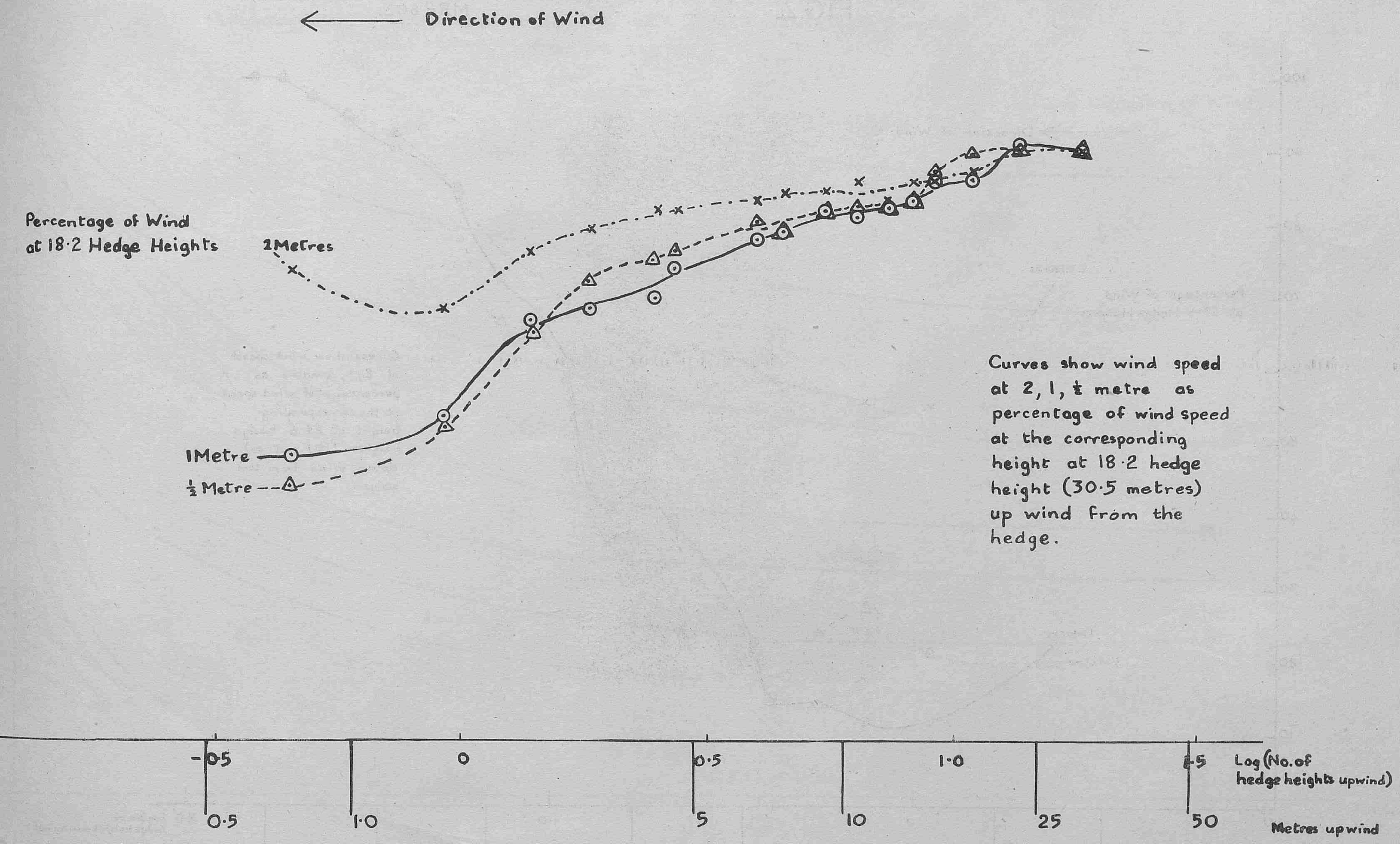

Curves show wind speed at 2, 1, ½ metre as percentage of wind speed at the corresponding height at 18·2 hedge height (30·5 metres) up wind from the hedge.

FIG. 4

M.R.P. 602.

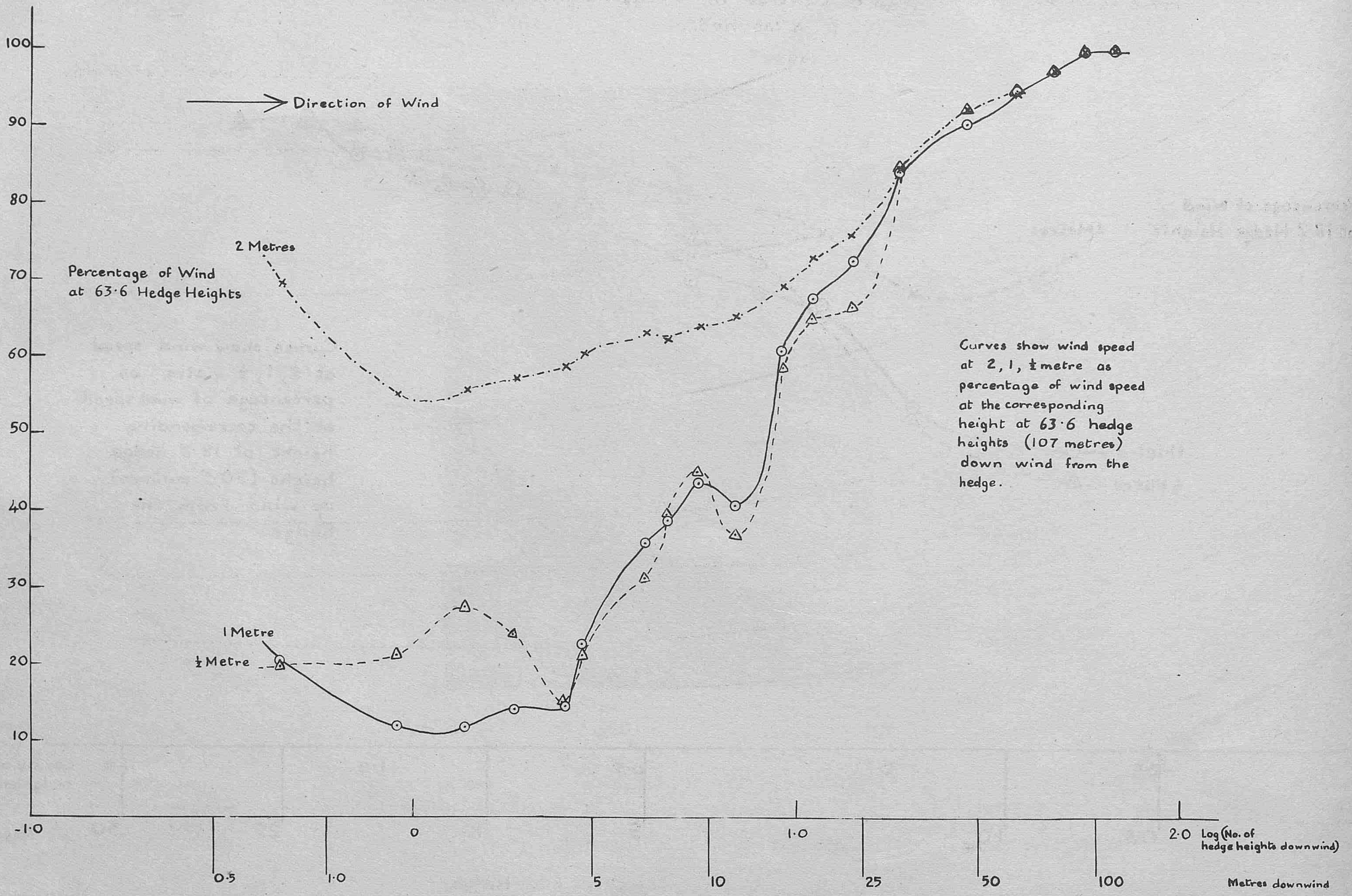

Curves show wind speed at 2, 1, ½ metre as percentage of wind speed at the corresponding height at 63·6 hedge heights (107 metres) down wind from the hedge.

FIG. 5

Vertical section showing lines of equal wind speed up wind from the hedge. Percentages are of wind speed at 2 metres 18·2 hedge heights (30·5 metres) from the hedge.

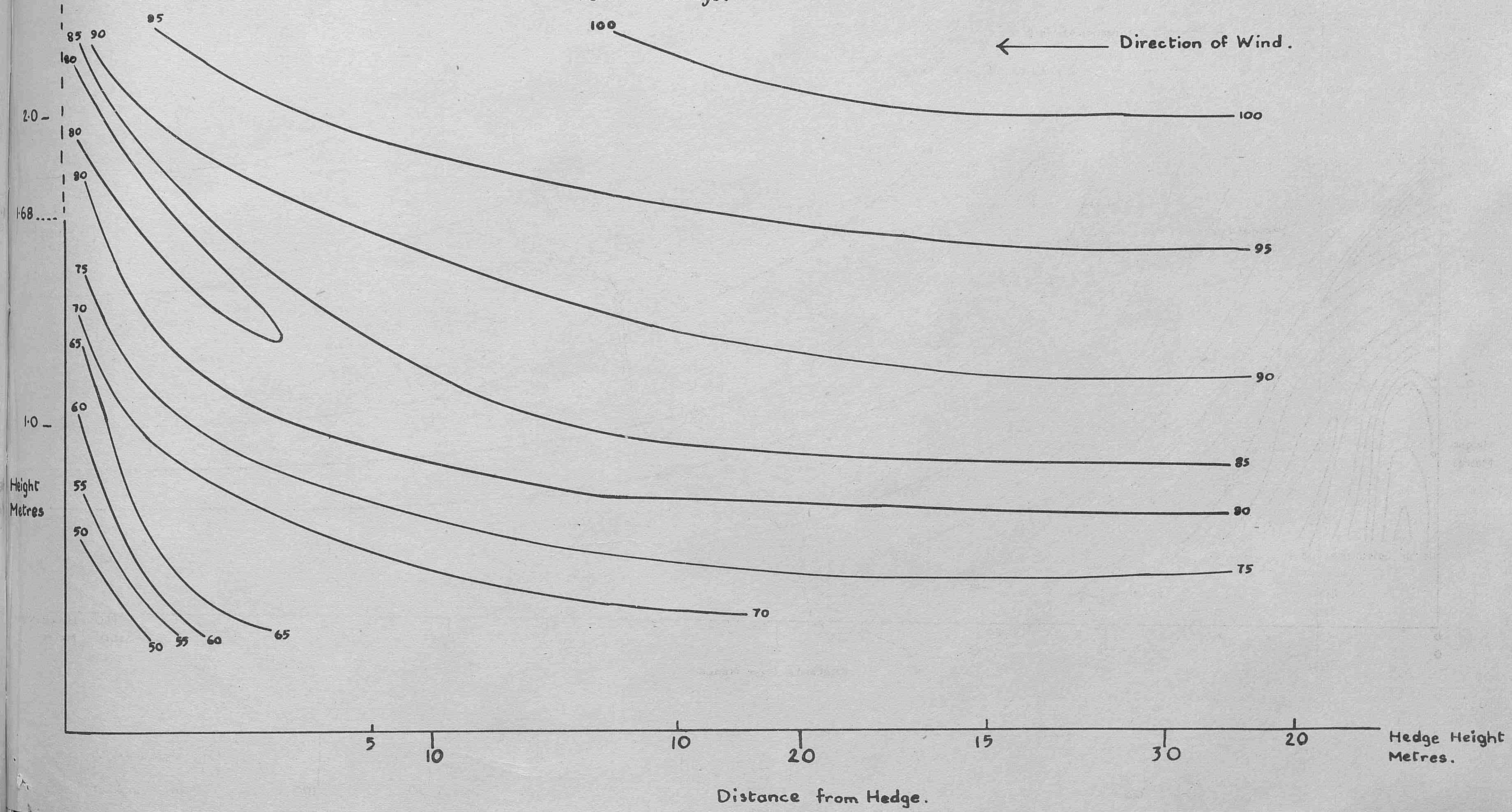

FIG. 6

Vertical section showing lines of equal wind speed down wind from the hedge
Percentages are of wind speed at 2metres 63·6 hedge heights (107 metres)
from the hedge

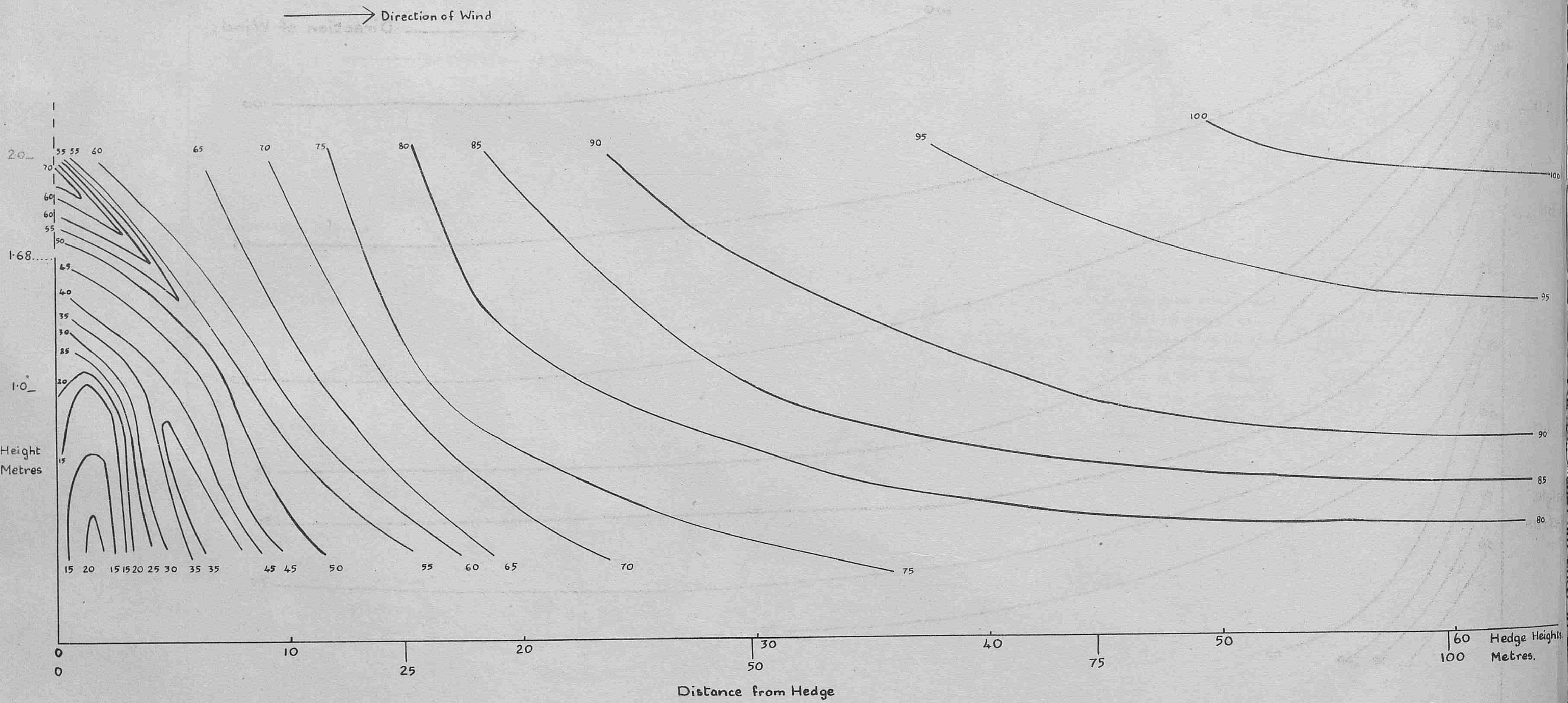

paper of the Meteorological Research Committee (London),
M.R.P. No........... by Mr..........................
A copy is available in the Library of the Meteorological Office."

AF359486

M.R.P. 603
S.C.III/80
11th December, 1950

File in 1-1

AWS

ATI-145272

AIR MINISTRY

METEOROLOGICAL RESEARCH COMMITTEE

The Evaporation of Raindrops

by
A. C. Best
(Meteorological Office)

Summary

From an examination of the available experimental evidence on the ~~the~~ transfer of heat and of water vapour between the surface of a moving sphere and the ambient fluid it is concluded that the transfer co-efficients for vapour and heat are the same. On this basis the rate of evaporation of a single drop of water falling through an atmosphere in which the temperature structure corresponds to the I.C.A.N. standard or the Summer Tropical standard is examined. It is assumed that the rate of increase of the temperature of the drop as it falls into warmer air (degrees per kilometer) is the same as the rate of increase of the temperature of the ambient air but it is shown that this assumption is unlikely to introduce any serious error.

The second part of the paper is devoted to an examination of the effects of evaporation on a collection of water drops (i.e. rain) falling through the two standard atmospheres on the assumption that the characteristics of the air - temperature and humidity - are not changed by the evaporation of the drops. The effects of evaporation on size distribution of raindrops, liquid water content of the air, radar response and rate of precipitation are considered.

The last part of the paper discusses the effect of the evaporation of raindrops on the temperature and humidity of the ambient air at ground level. Curves are given for the temporal variation of air temperature and humidity when rain of a specified intensity falls into it.

1. Introduction

The evaporation of a drop of water in an air stream is determined by the rate of transfer of heat and water vapour between the drop surface and the ambient air. If these transfer processes are governed by molecular diffusion the appropriate equations take a well known form. If there is a substantial relative velocity between the drop and the medium - or more correctly if Reynolds' Number is not small - the transfer processes are governed by eddy diffusivity. In such circumstances it is customary to insert a velocity co-efficient into the transfer equations, We shall show that the experimental evidence is not adequate to distinguish between the velocity co-efficients for heat and water vapour.

The formulation of the appropriate equations for the evaporation of water drops presents little difficulty. Exact solution of the equations is not so easy. In the following paragraphs awkward expressions in the equations are replaced by expressions having a simpler form in order to permit integration of the equations. The simpler forms are derived by evaluating the inconvenient expressions and fitting simpler formulae to them by empirical methods. The results may lose slightly in accuracy but it then becomes possible to express the effects of evaporation in terms of familiar everyday variables.

When dealing with a collection of drops - i.e. rain - no account has been taken of such factors as downdrafts which are associated with thunderstorm rains.

/Part I

G.278573/ABC/12/50/40

PART I

The Evaporation of a single drop in a constant atmosphere

2. Heat Balance equation for a falling drop

In a stagnant medium the usual processes of molecular diffusion of heat and vapour lead to the following equations for an evaporating drop of liquid

$$\frac{dm}{dt} = -\frac{4\pi MDa}{R\phi}(p_T - fp_\theta) \quad \ldots\ldots\ldots\ldots\ldots\ldots\ldots(1)$$

$$\frac{dH}{dt} = 4\pi ka(\theta - T) \quad \ldots\ldots\ldots\ldots\ldots\ldots\ldots\ldots\ldots(2)$$

where

m = mass of drop
t = time
M = molecular weight of liquid (= 18 for water)
D = coefficient of diffusion of water vapour in air ($\text{cm}^2\ \text{sec}^{-1}$)
R = gas constant (= $8.314\ 10^7$ erg $\text{deg}^{-1}\ \text{mol}^{-1}$)
p_T, p_θ = saturation vapour pressure at temperature T, θ.
fp_θ = vapour pressure in ambient air
θ = temperature of ambient air
T = surface temperature of drop
H = heat received by drop by conduction
k = thermal conductivity of air ($\text{cal. cm}^{-1}\ \text{sec}^{-1}\ \text{deg.}^{-1}$)
ϕ = $(\theta + T)/2$
a = drop radius

If there is significant relative motion between the drop and the medium let us write

$$\frac{dm}{dt} = -\frac{4\pi MDa}{R\phi}(p_T - fp_\theta)\,G_1 \quad \ldots\ldots\ldots\ldots\ldots\ldots\ldots(3)$$

$$\frac{dH}{dt} = 4\pi ka(\theta - T)\,G_2 \quad \ldots\ldots\ldots\ldots\ldots\ldots\ldots\ldots(4)$$

where G_1 and G_2 are still to be determined. G_2 of course is the Nusselt Number. If now we neglect any effects due to radiation and assume that the surface temperature of the drop is equal to the mean drop temperature (and that the density of water is unity) we have

$$\frac{4}{3}\pi a^3 \frac{\partial T}{\partial t} = 4\pi ka(\theta - T)\,G_2 - \frac{4\pi MDaL}{R\phi}(p_T - fp_\theta)\,G_1 \quad \ldots .(5)$$

where L is the latent heat of vaporisation of water. If we write V for the terminal velocity of the drop we have $\partial T/\partial t = \alpha V$ where α is the lapse rate of temperature of the drop (positive if T increases downwards) and

$$\alpha a^2 V = 3k(\theta - T)\,G_2 - \frac{3MDL}{R\phi}(p_T - fp_\theta)\,G_1 \quad \ldots\ldots\ldots(6)$$

It is physically obvious that α must exceed zero and it is equally obvious that α cannot exceed the lapse rate of θ. Later we shall need to assume a particular temperature structure for the atmosphere through which the drop falls and we shall select a structure with the I.C.A.N. lapse rate. We shall show (table 3 below) that, if α is put equal to the I.C.A.N. lapse rate, the term on the left hand side of equation 5 is small compared with the terms on the right hand side. The solution to equation 5 therefore depends largely upon the velocity coefficients G_1 and G_2.

/In

In connection with the assumption that the mean drop temperature is equal to the surface temperature of the drop we may note that it can be shown that (e.g. see "Operational Methods in Applied Mathematics", H.S. Carslaw and J.C. Jaeger, p. 235, Ex. 15) if a sudden temperature change is applied to the surface of a drop of water of 1 mm radius the temperature at the centre will have taken up 55 per cent of the change after 1 second and 89.6 per cent after 2 seconds. If the drop has a radius of 3 mm 61.7 per cent of the change is communicated to the centre after 10 seconds and 92.5 per cent after 20 seconds.

3. The Velocity Coefficients G_1 and G_2

Frossling $^{(1)}$ has published experimental results for the evaporation of drops of liquid in an air stream from which he deduced - for water drops.

$$G_1 = 1 + 0.2335\sqrt{Re} \qquad (7)$$

where Re is Reynolds' Number. The experimental results covered the range (for water) $18 < Re < 770$. Takahashi (2) has also published measurements made on the evaporation of water drops for the range $0.2 < a < 1$ mm and $1 < v < 6.5$ m/sec. From his published figures it is not possible to compare his results directly with those of Frossling since the data given by Takahashi do not permit the calculation of Re. However Frossling shows that Takahshi's results as published do not contradict his own.

McAdams $^{(3)}$ gives a small diagram which summarises the information available on the transfer of heat to or from a sphere moving in a fluid and it is convenient to refer to McAdams' nomenclature. He writes

$$\text{Rate of heat transfer} = h\,A\,(\Theta - T)$$

where A is the area of the surface and h is the surface coefficient of heat transfer. Thus for a sphere we have

$$\text{Rate of heat transfer} = 4\pi\, a^2 h(\Theta - T)$$

and by comparison with equation 4 we get

$$G_2 = \frac{a\,h}{k} \qquad (8)$$

McAdams plots (logarithmically) experimental values of $2G_2$ against Re. The Reynolds Number of a falling raindrop has values up to about 3000 and the relevant part of McAdams' diagram is shown, with some additional information, in Figure 1. McAdams states, and indeed it is obvious from his diagram, that in the range $20 < Re < 150{,}000$ the experimental data fit the line

$$2\,G_2 = 0.33\,(Re)^{0.6} \qquad (9)$$

This line is represented by AA' in fig. 1 and it is apparent that it is a good fit to the experimental points though there is some scatter at the small values of Re. Comparison of equations 1 and 2 with equations 3 and 4 suggests that both G_1 and G_2 should approach unity as Re approaches zero, that is that $\log_{10}2G_1$ and $\log_{10}2G_2$ should approach 0.3 as $\log_{10}$ Re approaches minus infinity. Accordingly there are good reasons for suspecting that equation 9 cannot hold at small values of Re. Now in figure 1 the experimental values for small values of Re are all due to Johnstone, Pigford and Chapin $^{(4)}$ and reference to their original paper shows that they deduced a theoretical relationship between G and Re which is represented by the line BB' in figure 1 and that they gave reasons for the discrepancy between the theoretical curve BB' and the experimental points at low Re. The reasons advanced implied that the experimental points were in error. We are thus left in some doubt as to the value of G_2 at low Re. In figure 1 $\log_{10}2G_1$ has been plotted against $\log_{10}$Re from equation 7 and is represented by the line DD'. Over the range of Re for which data are available for the transfer both of heat and of water vapour it appears that the discrepancy between G_1 and G_2 is no greater than the scatter of the experimental points. We note also from the scale of drop radius in figure 1 that a great deal of the range of Re in which we are interested lies outside the range in which experimental results for both heat and vapour are available. In view of the similarity of the mechanisms of heat and vapour transfer it is now difficult to avoid the suggestion that within the limits of experimental error G_1 and G_2 are the same. Accordingly identity between these two functions has now been assumed and both will be denoted by G.

We still have to determine the relationship between G and Re for values of the latter up to about 3000. The evidence consists of Frossling's results over the range $18 < Re < 770$, the experimental results on heat transfer quoted by McAdams but with some doubt about the values at low Re and the implication that the curve should be asymptotic to $\log_{10} 2G = 0.3$ when Re is very small. Bearing in mind these considerations it was decided to adopt the line CC' in figure 1 as representing the best relation between G and Re. This particular line is represented by

$$G = 1 + 0.141\,(Re)^{0.6} \qquad \text{.........} \quad (10)$$

The precise form of the relationship was selected to fit a tractable formula (equation 10) and to satisfy the evidence mentioned above. It must be made clear that no theoretical justification is claimed for equation 10.

4. Calculation of variation of drop size with height

If we now rearrange equation 6 and put $G_1 = G_2 = G$ we get

$$f = \frac{1}{p_\Theta}\left\{p_T - \frac{R\Theta k}{MDL}\left[(\Theta - T) - \chi\right]\right\} \quad \text{.........}(11)$$

where

$$\chi = \frac{\alpha a^2 V}{3Gk}$$

and ϕ has been replaced by Θ as a close approximation. (We shall see later in table 4 that this approximation is justifiable in the present connection.) If Θ and $(\Theta - T)$ are specified we can obtain p_Θ and p_T from the usual tables. If the barometric pressure is also specified the physical characteristics of the air can be evaluated.* Formulae for V have been given elsewhere by the present writer (5). If we also put α equal to the lapse rate in the I.C.A.N. atmosphere ($= 6.5\ 10^{-5}$ °C/cm.), (we discuss the validity of this step more fully in section 5 below) we can then use equation 11 to compute the relative humidity (100f) corresponding to selected values of a. If $(\Theta - T)$ is then plotted against f we can determine the values of $(\Theta - T)$ for selected values of f. This procedure was followed for various heights in the I.C.A.N. and Summer Tropical atmospheres (see appendix for specification of these atmospheres) and various drop sizes. Having obtained $(\Theta - T)$ for specified values of a, f and z we can evaluate $(p_T - fp_\Theta)$. Now reverting to equation 3 we note that

$$\frac{dm}{dt} = 4\pi a^2 \frac{da}{dt} = -4\pi a^2 V \frac{da}{dz}$$

and accordingly, replacing ϕ by Θ

$$a\frac{da}{dz} = \frac{MDG}{R\Theta V}(p_T - fp_\Theta) \quad \text{.......................}(12)$$

---

* The formulae used are given in the appendix.

Using equation 12 the value of ada/dz was computed for a = 0.015, 0.025, 0.035, 0.05, 0.1, 0.15, 0.20, 0.25 cm., for f = 0.95, 0.9, 0.8, 0.7, 0.6, 0.5, and 0.4 and for z = 0, 1, 2, 3, 4, and 5 km in both the I.C.A.N. and Summer Tropical atmospheres. Table 1 is typical of the results obtained which all followed the same general pattern.

Table 1

Values of 10^{10}ada/dz (c.g.s.) in I.C.A.N. atmosphere at 2 km.

f a(cm)	0.95	0.90	0.80	0.70	0.60	0.50	0.40
0.015	5.25	10.7	23.5	35.4	46.5	59.5	72.0
0.025	4.35	8.83	18.2	28.0	38.4	49.3	59.5
0.035	4.07	8.26	17.0	26.2	36.0	46.1	55.8
0.05	4.00	8.10	16.7	25.8	35.3	44.2	54.6
0.10	2.97	7.53	17.0	27.0	37.6	47.5	58.9
0.15	0.27	6.99	17.8	29.3	40.0	52.6	64.5
0.20	-1.43	4.49	16.8	29.9	43.6	56.5	70.1
0.25	-5.48	1.24	15.2	29.9	45.4	59.9	75.2
Mean value above broken line							
	4.42	8.68	18.1	28.9	40.3	51.9	63.8

It can be seen that at low relative humidities ada/dz is large for small values of a, diminishes at first as a increases and then increases again. At high relative humidities however the increase at large values of a does not occur. The most important variation of ada/dz occurs as f varies.

The negative values in the bottom left hand corner of the table occur as a result of the assumption that the the lapse rate of drop temperature is equal to the lapse rate of air temperature. When large drops fall through a nearly saturated atmosphere the evaporation is small and so the heat required to balance the loss of heat of vaporization is small. Owing to the size of the drop however the heat required to raise the drop temperature as it falls into warmer air may be large. Thus the assumption that the left hand side of equation 5 is small compared with each term on the right hand side may no longer be justified. It is convenient at this stage to examine this point more closely.

5. The lapse rate of drop temperature

It is not practicable to solve equation 5 without some assumption about the term dT/dt. It is of interest however to consider the case of a non-evaporating drop. The heat balance equation is then equation 5 with the omission of the second term on the right hand side. This reduces to

$$\frac{dT}{dz} = \frac{3kG}{a^2V}(\theta - T)$$

If we put $\theta = \theta_0 + \beta z$ (measuring z downwards) and assume that the drop starts at a height $z = 0$ with temperature $T = \theta_0$ and that kG/a^2V is independent of z the solution to this equation gives

$$\theta - T = \frac{\beta a^2V}{3kG}(1 - e^{-Az})$$

where

$$A = \frac{3kG}{a^2V}$$

Calculation shows that A varies very slowly with z but very rapidly with a. Taking values appropriate to 2 km in the I.C.A.N. atmosphere we have

Table 2

Data relating to a non-evaporating drop

a(cm)	0.015	0.05	0.1	0.15	0.25
$10^5 A$	1170	80	22	11	5
z(90)m	1.97	28.8	105	208	460
β/A(°C)	0.0055	0.081	0.29	0.59	1.30
Critical R.H.	100	99.4	97.9	95.9	91.1

The quantity $(\theta - T)$ clearly approaches asymptotically the value β/A and reaches 90 per cent of that value after a fall of 2.3/A cm. This quantity, in metres, is denoted by z(90) in table 2. Thus we see that a small drop very rapidly approaches a steady value for $(\theta - T)$ but a large drop falls a much greater distance before achieving a similar value. These figures apply to a non-evaporating drop: a drop of water falling in a nearly saturated atmosphere approaches this condition. The value which $(\theta - T)$ approaches asymptotically, viz β/A, was denoted by χ when we were discussing in evaporating drop (equation 11). Computation shows that χ differs by less than 3 per cent in the I.C.A.N. and S.T. atmospheres. Its value increases with height, by about 25 per cent for a radius 0.015 cm and about 50 per cent for a radius 0.3 cm as the height increases from 0 to 5 km. The variation of χ with drop size is extremely rapid and table 2 shows some values appropriate to 2 km in the I.C.A.N. atmosphere.

The data of table 2 serve to demonstrate the fact that, owing to the lag of drop temperature behind ambient air temperature as the drop falls into warmer air, evaporation may not occur even though the air is unsaturated. If the drop temperature is below the ambient dew point condensation will take place instead of evaporation. The critical depression of the dew point is given by the values of β/A. The last line of table 2 shows the relative humidity corresponding to these critical values of β/A. We see that the effect is negligible for very small drops but significant for large drops. The result of neglecting this effect is that the rate of evaporation of the larger drops, particularly in nearly saturated air, is over estimated.

In a non-saturated atmosphere it is not legitimate to use the preceding arguments to justify the assumption of identity between the air temperature lapse rate and the drop temperature lapse rate. However we may still regard equation 6 with α replaced by the I.C.A.N. lapse rate as being a reasonable approximation to equation 5 provided the left hand side is small in numerical value compared with each term on the right hand side, i.e. provided the heat required to raise the drop temperature is small compared with the heat required to evaporate the water. This condition amounts to ensuring that $\chi/(\theta - T)$ is small. This quantity is tabulated in table 3 for the conditions appropriate to table 1. The pattern of values is typical of other heights and of the Summer Tropical Atmosphere.

Table 3

Values of $\chi/(\theta - T)$ for 2 km in the I.C.A.N. atmosphere

f a (cm)	0.95	0.90	0.80	0.70	0.60	0.50	0.40
0.015	0.014	0.0069	0.0037	0.0024	0.0017	0.0014	0.0011
0.025	0.047	0.023	0.012	0.0078	0.0058	0.0047	0.0038
0.035	0.097	0.049	0.024	0.016	0.012	0.0097	0.0079
0.05	0.20	0.10	0.051	0.034	0.025	0.020	0.016
0.10	0.59	0.33	0.17	0.12	0.089	0.070	0.059
0.15	0.84	0.59	0.33	0.23	0.17	0.14	0.11
0.20	1.16	0.77	0.46	0.33	0.26	0.21	0.17
0.25	1.30	0.93	0.59	0.43	0.34	0.28	0.23

Now in equation 11 we have not neglected the heat required to raise the temperature of the drop as it falls into warmer air; we have approximated to it. Accordingly it is not necessary to restrict our argument to cases when χ is negligibly small. We need only ensure that the left hand side of equation 6 is of less importance than the terms on the right hand side. After consideration of these factors it was decided, arbitrarily, to accept all cases in which $\chi/(\Theta - T)$ was less than 0.5. The broken line in tables 1 and 3 divide the acceptable cases from the remainder. It will be noted that, broadly, this means that the results will not be applicable to large drops falling through a nearly saturated atmosphere. At heights greater than 2 km the dividing line in tables 1 and 3 was extended towards the bottom right hand corner, drops of 0.25 cm radius being excluded at 50 per cent relative humidity at 5 km.

6. Variation with height of size of large drops

We see that in the acceptable region of table 1 the variation of ada/dz with a is small. Accordingly values above the broken line were averaged. It is apparent that ada/dz increases rapidly as a decreases below 0.015 cm and accordingly the average values should be used only to compute the fall distance for evaporation from some larger radius to 0.015 cm. We shall return to a consideration of small drops in section 7.

Having obtained mean values of ada/dz for each height $\log_{10}(10^{10}\ ada/dz)$ was plotted against z for each value of f and for each standard atmosphere in figures 2 and 3. The plotted points approximate reasonably closely to families of parallel straight lines and for ease of computation there are advantages if these straight lines fit formulae of convenient type. The straight lines in figures 2 and 3 have been drawn from the formulae.

$$\text{I.C.A.N.}\qquad 10^{10}\, a\, da/dz = 199.5(1 - f)^{1.13}\, e^{-2.90\ 10^{-6} z} \qquad ......(13)$$

$$\text{S.T.A.}\qquad 10^{10}\, a\, da/dz = 354.8(1 - f)^{1.13}\, e^{-1.98\ 10^{-6} z} \qquad ....(14)$$

In some instances the line shown may not be the line of best fit for the plotted points. In order to separate the variables in equations 13 and 14 it was necessary to treat the lines as a family and not individually. It can be seen that the plotted points approximate reasonably closely to these lines except perhaps above 4 km in the I.C.A.N. atmosphere.

It may appear strange that there should be so much scatter amongst the points corresponding to large values of f. The explanation is that $(\Theta - T)$ is then small (e.g. about 0.7°C when $f = 0.95$ in S.T.A.); but $(\Theta - T)$ was obtained graphically and was read to only 0.1°C. Thus the error in determining $(\Theta - T)$ may lead to a significant error in $(p_T - fp_\Theta)$ and hence in ada/dz for large values of f.

7. Variation with height of size of small drops

We saw above (table 1) that ada/dz increases as a diminishes below 0.015 cm and for that reason it was not justifiable to average ada/dz when dealing with small drops. In passing we may note here that $a = 0.015$ cm was also found (5) a convenient size at which to divide the range of drop sizes when considering formulae for V. Since this size also corresponds to the generally accepted idea of the largest size for drizzle drops we shall refer to drops with diameter less than 0.3 mm by this term.

The procedure chosen for dealing with drizzle drops was based upon the fact that, as shown by the typical figures in table 3, the value of $\chi/(\Theta - T)$ becomes very small for such drops. This was taken as justification for neglecting the term on the left hand side of equation 6 and evaluating $(\Theta - T)$

on the assumption that the heat required to raise the drop temperature as it falls into warmer air can be ignored in comparison with the heat required to balance the evaporative loss. We see then from equation 6 that (Θ - T) will be independent of drop size. In fact the computations for the larger drops had already shown that (Θ - T) never varied by more than 0.1°C as a varied from 0.015 to 0.05 cm. Accordingly the values of (Θ - T) already computed for a = 0.015 cm were used for drizzle drops. As a matter of interest these values are given in table 4. In passing it may also be of interest to note that as the drop size increases to large raindrop size in the I.C.A.N. atmosphere these values might increase by 20 per cent or 10 per cent at very high or very low humidities at the surface and by nearly 50 per cent at all humidities at 5 km. In the S.T.A. the corresponding figures were 10 per cent and 2 to 3 per cent at the surface, and 10 per cent at 5 km.

Table 4

Depression of drop temperature (°C) below air temperature for a drop of radius 0.015 cm.

f z(km)	0.95	0.9	0.8	0.7	0.6	0.5	0.4
			I.C.A.N.				
0	0.5	1.0	2.1	3.3	4.5	5.7	7.0
1	0.5	0.9	1.9	2.8	3.8	4.9	5.9
2	0.4	0.8	1.5	2.3	3.2	4.0	4.9
3	0.3	0.6	1.3	1.9	2.6	3.2	3.9
4	0.2	0.5	1.0	1.5	2.0	2.5	3.1
5	0.2	0.4	0.7	1.1	1.5	1.9	2.3
			S.T.A.				
0	0.8	1.7	3.5	5.5	7.7	10.1	12.8
1	0.7	1.6	3.3	5.1	7.1	9.3	11.6
2	0.7	1.5	3.0	4.7	6.5	8.5	10.5
3	0.7	1.3	2.8	4.3	5.9	7.6	9.4
4	0.6	1.2	2.4	3.8	5.2	6.7	8.3
5	0.5	1.1	2.2	3.3	4.6	5.9	7.2

The air temperature at the surface in the I.C.A.N. atmosphere (15°C) is the same as the air temperature at 4 km in the S.T.A. The different values of (Θ - T) for these two conditions is attributable to the effect of barometric pressure on D.

Returning to the problem of the rate of change of size with height of a drizzle drop we see that equation 12 can be written

$$a\frac{da}{dt} = \frac{M}{R}\,\frac{D(p_T - fp_\theta)}{\theta}\,\frac{G}{V}$$

and that in this equation the first factor on the right hand side is an absolute constant and the second factor is independent of a. The third factor, G/V, depends upon both z and a but is independent of f. Following inspection of the data this equation was rewritten in the form

$$10^{10}\,a\frac{da}{dz}\left[\frac{G}{V}\right]_{0.015}\Big/\frac{G}{V} = \frac{M}{R}\,\frac{10^{10}\,D(p_T - fp_\theta)}{\theta}\left[\frac{G}{V}\right]_{0.015} \qquad \ldots\ldots.(15)$$

where $(G/V)_{0.015}$ denotes the value of G/V for drops of radius 0.015 cm and varies with z. The right hand side of equation 15 was computed for various heights and values of f in both the standard atmospheres. The results are shown plotted in figures 4 and 5. The straight lines which have been fitted to the plots were computed from the formulae

$$\text{I.C.A.N.}\qquad 10^{10}\,a\frac{da}{dz}\left[\frac{G}{V}\right]_{0.015}\Big/\frac{G}{V} = 214.8\,(1-f)^{1.062}\exp(-2.79\;10^{-6}z) \quad \ldots(16)$$

/It

$$\text{S.T.A.} \quad 10^{10}\, a \frac{da}{dz} \left[\frac{G}{V}\right]_{0.015} \Big/ \frac{G}{V} = 386.4\,(1-f)^{1.062} \exp(-1.74\; 10^{-6} z) \quad \ldots\ldots\ldots\ldots\ldots\ldots\ldots\ldots (17)$$

It can be seen that these lines are reasonably good fits except perhaps above 4 km at low humidities in the I.C.A.N. atmosphere.

The next step was to evaluate $(G/V)_{0.015}/(G/V)$. This quantity varies with drop size and with height but it was found that the variation with z was negligible. The variation from 0 to 5 km was about 5 per cent for a = 0.0025 cm in both atmospheres and about 1 per cent for a = 0.0125 cm. Accordingly the values were meaned for all heights and finally these mean values were used to plot figure 6. It can be seen that for drop radii from 0.015 to 0.005 cm the difference between the two atmospheres is negligible. The straight line drawn in figure 6 represents the relation

$$\frac{G}{V} = \left[\frac{G}{V}\right]_{0.015} \frac{0.0145}{a} \quad \ldots\ldots\ldots\ldots\ldots\ldots\ldots\ldots (18)$$

and is clearly a good approximation for drop radii from 0.015 to 0.005 cm. Below this size the index of a in the denominator on the right hand side of equation 18 should be increased but the drops are now becoming of the sixe of cloud particles and are outside the range of consideration of the present paper.

If we combine equation 18 with 16 and 17 we obtain

$$\text{I.C.A.N.} \quad 10^{10}\, a^2 \frac{da}{dz} = 3.115\,(1-f)^{1.062} \exp(-2.787\; 10^{-6} z) \quad \ldots (19)$$

$$\text{S.T.A.} \quad 10^{10}\, a^2 \frac{da}{dz} = 5.603\,(1-f)^{1.062} \exp(-1.741\; 10^{-6} z) \quad \ldots (20)$$

These two equations correspond to 13 and 14 for large rain drops.

8. Graphs of variation of drop size with height

The computations described above were deliberately framed to produce, if possible, formulae which could be easily integrated to give the change of drop size with height. From equations 13 and 14, 19 and 20 we see that, if a drop of radius a_1 at height z_1 evaporates to a radius a_2 at height z_2 the relation between the four quantities is given by equations 21 to 24.

Raindrops

$$\text{I.C.A.N.} \quad a_1^2 - a_2^2 = 137.5\; 10^{-4} (1-f)^{1.13} \left[\exp(-2.90\; 10^{-6} z_2) - \exp(-2.90\; 10^{-6} z_1)\right] \quad \ldots\ldots (21)$$

$$\text{S.T.A.} \quad a_1^2 - a_2^2 = 358.4\; 10^{-4} (1-f)^{1.13} \left[\exp(-1.98\; 10^{-6} z_2) - \exp(-1.98\; 10^{-6} z_1)\right] \quad \ldots\ldots (22)$$

Drizzle drops

$$\text{I.C.A.N.} \quad a_1^3 - a_2^3 = 3.35\; 10^{-4} (1-f)^{1.062} \left[\exp(-2.79\; 10^{-6} z_2) - \exp(2.79\; 10^{-6} z_1)\right] \quad \ldots\ldots\ldots (23)$$

$$\text{S.T.A.} \quad a_1^3 - a_2^3 = 9.65\; 10^{-4} (1-f)^{1.062} \left[\exp(-1.74\; 10^{-6} z_2) - \exp(-1.74\; 10^{-6} z_1)\right] \quad \ldots\ldots\ldots (24)$$

/10

The evaporative process must be considered in two stages of course, separated by the height at which the radius is 0.015 cm. Furthermore equations 23 and 24 must not be applied to drops smaller than 0.005 cm radius. Equations 21 to 24 have been used to construct the curves in figures 7 and 8. These show the variation of drop size with height for drops of six different sizes starting to fall from 6 km through either the I.C.A.N. or S.T. atmosphere and with a relative humidity of either 50, 70 or 90 per cent. Curves for other sizes, starting heights or humidities obviously can be interpolated.

Although we are not concerned here with the evaporation of cloud particles we may note that figure 6 shows that for such small drops the index of the radius on the left hand side of equations 23 and 24 would be greater than three and the fall distance for evaporation would be correspondingly diminished.

/PART 2

PART 2

The evaporation of rain in a constant atmosphere

9. Effect of evaporation on drop size distribution and liquid water concentration in rain

We have seen that the amount by which a drop evaporates while falling through the atmosphere depends upon the length of the fall path, the ambient temperature and humidity and the pressure. Equations 21 and 22 show that the change in surface area of a drop as it falls a specified distance through the air is a function only of these characteristics of the air and of the heights at the beginning and end of the fall, that is the change in surface area is independent of the drop size. (We shall ignore the implications of equations 23 and 24 since only a small amount of water in rain is associated with drops of radius less than 0.015 cm.) If then we write

$$a_1^2 - a_2^2 = K^2 \quad \text{.........} (25)$$

we see that K is the initial radius of the drop which will just evaporate completely while falling between specified heights and through one of the standard atmospheres having a specified relative humidity. In fact K is a convenient measure of the amount of evaporation which will take place over a specified fall path. We shall call K the 'vanishing radius' corresponding to a particular fall path through an atmosphere of specified characteristics. The numerical value of K is obtained by equating K^2 to the right hand side of equations 21 or 22 as appropriate. It is useful to examine the order of magnitude of K. If, in equation 22, we put $f = 0.5$, $z_1 = 6$ km and $z_2 = 0$ km we get $K^2 = 0.01139$ and so K varies from 0 to about 0.1 cm.

It is obvious that the effects of evaporation will depend upon the initial drop size distribution. Let us suppose that at the initial height the drop size distribution is given by

$$1 - F = \exp -(2a/b)^n \quad \text{.........} (26)$$

where F is the fraction of liquid water in the air composed of drops with radius less than a, and b and n are constants. It has been shown elsewhere (6) that this form of distribution is in reasonable agreement with measurements at ground level. We shall also use the symbol W to denote the liquid water concentration (g/cc) at the initial height. We notice that b has the dimensions of a length. In fact the value of n determines the shape of the distribution curve represented by equation 26 but the value of b determines the drop size about which the sizes are distributed. We may regard b as a scale diameter for the distribution represented by equation 26. We have dealt with this matter in some detail because, as we shall see below, the effects of evaporation on rain are conveniently measured not in terms of the vanishing radius K but rather in terms of the ratio of the vanishing radius K to the scale diameter b, i.e. in terms of K/b. For any specified fall path and value of b the ratio is easily evaluated, as already explained, with the help of equations 21 or 22.

It is easily shown from equations 25 and 26 that at some height, less than the initial height and where the vanishing radius has a value K

$$\begin{array}{l}\text{Total volume of drops}\\ \text{with radius less}\\ \text{than } \sqrt{(r^2 - K^2)}\end{array} = Wn\left(\frac{2}{b}\right)^n \int_K^r a^{n-4}(a^2-K^2)^{3/2}\exp\left[-(2a/b)^n\right] da \quad \text{....} (27)$$

The actual height in the atmosphere is clearly unimportant. The significant variable is K. Let W(K/b) denote the liquid water concentration at a point where the vanishing radius is K and let F(r/b, K/b) denote the fraction of liquid water, at the same height, composed of drops with radius less than r.

Then from equation 27 we easily get

$$W(K/b) \quad = \quad Wn2^n \int_{K/b}^{\infty} H(u)\,du \quad \dots\dots\dots\dots\dots\dots\dots (28)$$

$$F\left(\frac{r}{b},\frac{K}{b}\right) \quad = \quad \int_{K/b}^{\sqrt{\frac{r^2}{b^2}+\frac{K^2}{b^2}}} H(u)\,du \Bigg/ \int_{K/b}^{\infty} H(u)\,du \quad \dots\dots (29)$$

where

$$H(u) \quad = \quad u^{n-4}\left(u^2 - \frac{K^2}{b^2}\right)^{3/2} \exp\left[-(2u)^n\right] \quad \dots\dots\dots\dots (30)$$

We note that K and b occur in these expressions only in the form of the ratio K/b. It is for this reason we have adopted the particular nomenclature. It has been shown (6) that b is of the order 0.1 to 0.3 (cm) so that K/b varies from 0 to 1.

The integrals in equation 29 cannot be evaluated explicitly. They have been computed graphically for a selection of values of n and of K/b.

Let us suppose that at a height where the vanishing radius is K the drop size distribution has the same general form as that represented by equation 26. Let us write

$$1 - F\left(\frac{r}{b},\frac{K}{b}\right) \quad = \quad \exp\left[-(2r/bc)^m\right] \quad \dots\dots\dots\dots\dots\dots (31)$$

then we have

$$\log\log\left[1/\left(1 - F\left(\frac{r}{b},\frac{K}{b}\right)\right)\right] \quad = \quad \log\log e + m\left(\log\frac{2r}{b} - \log c\right) \quad \dots (32)$$

where all the logarithms are to base 10. Thus, if our supposition about the form of the drop size distribution is correct, we should get a straight line by plotting log log $(1/[1 - F(r/b, K/b)])$ against log (2r/b) and from the constants of this straight line we should be able to evaluate m and c. This procedure has been followed using values of F(r/b, K/b) computed graphically (equation 29). The results are shown in figures 9a to 9d for four values of n.

In the interests of clarity it was thought better to plot the computed points in figure 9b and to draw the line only for K/b = 0. For the same reason the scale of figures 9b and 9c is different from that adopted for figures 9a and 9d.

The lines in figures 9a to 9d are substantially straight if we disregard the 10 per cent of water comprised by the smallest drops and the 10 per cent comprised by the largest drops, that is for values of log log $(1/[1 - F(r/b,K/b)])$ between $\bar{2}.66$ and 0. Accordingly the best straight line has been fitted in each case by the method of least squares. For this purpose five points were interpolated on each curve for equally spaced values of the ordinate between $\bar{2}.66$ and 0.0 inclusive. From these straight lines the values of m and c were determined. These are tabulated in tables 8 and 9.

It will be appreciated that graphical evaluation of F(r/b, K/b) inevitably leads to the introduction of small errors which are difficult to estimate.

This probably accounts for small irregularities in tables 8 and 9. Obviously when K/b = 0 we have m = n and c = 1.

Table 8

Effect of evaporation on distributive index in drop size distribution

	Values of m			
n	2	3	4	5
K/b				
0.0	2	3	4	5
0.1	2.38	3.13	4.05	4.91
0.2	2.68	3.45	4.01	4.78
0.3	2.98	3.59	4.05	4.73
0.4	3.11	3.58	3.99	4.36
0.5	3.23	3.56	3.92	4.16
0.6	3.36	3.68	4.01	3.83

Table 9

Effect of evaporation on scale diameter in drop size distribution

	Values of c			
n	2	3	4	5
K/b				
0.0	1	1	1	1
0.1	1.09	1.01	1.00	0.99
0.2	1.16	1.03	0.98	0.96
0.3	1.24	1.03	0.94	0.90
0.4	1.30	1.03	0.90	0.83
0.5	1.34	1.03	0.84	0.74
0.6	1.40	0.99	0.79	0.65

We see from these tables that the variation of the distributive index m depends very much upon the initial value. Broadly it appears that the effect of evaporation is to bring m to a value between 3.5 and 4.0. It should perhaps be remarked that the calculations mentioned were rather laborious and those for higher values of K/b were probably less accurate than those for low values.

From table 9 we get the rather surprising result that the scale diameter, bc, is increased by evaporation for small values of the distributive index but is decreased for large values of n. It has been shown (9) that with drop size distribution represented by equation 26 the ratio of the mean diameter to bc, whatever reasonable interpretation is placed upon the word 'mean', depends upon m and may depend upon the smallest measurable size. This ratio however is always independent of bc and increases as m increases. Now considering tables 8 and 9 together we see that if m has an initial value 2 both m and bc increase with K/b and so the mean diameter increases. If m has an initial value 5 both m and bc decrease as K/b increases and so the mean diameter decreases. For the intermediate cases of n = 3 or 4 m increases with bc practically constant or m is almost constant but with decreasing bc. Thus for n = 3 the mean diameter increases and with n = 4 the mean diameter decreases. In brief then evaporation increases the mean diameter if n = 2 or 3 and decreases it if n = 4 or 5.

The liquid water concentration corresponding to vanishing radius K is given by equation 28. The values of W(K/b)/W have been computed and are given in table 10.

/Table 10

Table 10

Effect of evaporation on liquid water concentration

Values of W(K/b)/W

K/b \ n	2	3	4	5
0.0	1	1	1	1
0.1	0.81	0.88	0.90	0.92
0.2	0.56	0.62	0.67	0.68
0.3	0.35	0.37	0.38	0.40
0.4	0.20	0.18	0.17	0.16
0.5	0.11	0.069	0.050	0.038
0.6	0.052	0.021	0.0089	0.0037

Here again we see that early evaporation of the small drops in a wide distribution (n small) causes an early reduction in W but subsequently the large drops in the wide distribution slow down the total rate of evaporation. It is rather interesting that W(K/b)/W is independent of n when K/b has a value about 0.35.

10. Effect of evaporation upon radar response from falling rain

The radar response from a cloud of falling drops is proportional to $\sum a^6$ where the summation is taken over all the drops in unit volume. If the drop size distribution after evaporation is represented by equation 31 it is easily shown that

$$\sum a^6 = \frac{3\, W(K/b)\, b^3\, c^3}{32\,\pi}\, \Gamma\left(\frac{m+3}{m}\right) \qquad \text{..................(33)}$$

If now we write Z(K/b) for the value of $\sum a^6$ after an evaporation path K/b, and Z for the same quantity at the initial height we have, using the nomenclature of the preceding section

$$\frac{Z(K/b)}{Z} = \frac{W(K/b)\, c^3\, \Gamma(1 + \frac{3}{m})}{W\, \Gamma(1 + \frac{3}{n})} \qquad \text{.......................(34)}$$

Using the numerical values from tables 8, 9 and 10 table 11 has been computed to show the effect of evaporation on radar response.

Table 11

Effect of evaporation on radar response from falling rain

Values of Z(K/b)/Z

K/b \ n	2	3	4	5
0.0	1	1	1	1
0.1	0.899	0.892	0.898	0.893
0.2	0.701	0.645	0.630	0.604
0.3	0.503	0.381	0.315	0.293
0.4	0.325	0.186	0.124	0.093
0.5	0.194	0.0711	0.0298	0.0157
0.6	0.103	0.0190	0.0044	0.00105

We see that the slow rate of evaporation of the large drops in a wide distribution more than balances the rapid evaporation of the small drops and leads to a slower rate of decrease of Z than occurs in rain composed of more uniform drops.

/11.

11. Effect of evaporation upon rate of precipitation

In section 9 we considered the effect of evaporation upon the concentration of liquid water in the air. The rate of precipitation, i.e. the rate at which rain falls on a horizontal surface is a function both of the liquid water concentration and of the drop size distribution and since evaporation affects both these characteristics it is not immediately obvious how the rate of precipitation will be affected. If the liquid water concentration and the drop size distribution are known the rate of precipitation can be computed from a knowledge of the terminal velocities of drops of different sizes. It is clear also that if the drop size distribution is constant the rate of precipitation will be directly proportional to the liquid water concentration.

If the drop size distribution is defined by equation 26 it is easily shown that

$$I = 7.2\ 10^{-2}\ \frac{n}{b^{n}}\ W \int_{0}^{\infty} V\ (2a)^{n-1}\ e^{-(2a/b)^{n}}\ da \quad \ldots\ldots\ldots\ldots\ldots(35)$$

where I is the rate of precipitation in mm/hr, W is the liquid water concentration in g/m^3 and V is the terminal velocity (cm/sec) of a drop of radius a. The integral on the right hand side of equation 35 has been evaluated graphically for a selection of values of b and n using the values of V appropriate to the surface in a Summer Tropical atmosphere (5). Values of I/W are given in table 12.

Table 12

Ratio of rate of precipitation (mm/hr) to liquid water content of air (g/m^3)

n b(cm)	2	3	4	5
0.05	6.2	6.3	6.5	6.5
0.10	11.9	12.2	12.5	12.8
0.15	16.5	17.2	17.5	17.7
0.20	19.9	20.9	21.4	22.0
0.25	22.6	24.0	24.5	25.0

Table 12 demonstrates that the influence of n on I/W is practically negligible but that the ratio I/W is very materially affected by the value of b. From tables 8, 9, 10 and 12 it is possible to compute the effect of evaporation on the rate of precipitation in any specified case.

For subsequent use the values in table 12 have been averaged for all values of n and log I/W has been plotted against log b in figure 10. The plotted points depart but little from a straight line over the range of b from 0.1 to 0.25. It has been shown (5) that this is a reasonable range of values for b and the straight line in figure 10 has accordingly been drawn ignoring the point for b = 0.05 cm. The equation to this line is

$$I = 67\ W\ b^{0.73}$$

In a discussion of measurements of the size distribution of raindrops (6) it was shown that b and W are proportional to I raised to some power. Using the numerical values of the constants given in that paper (and which apply primarily to temperate latitudes) it can be shown that after making allowance for the different units employed here

$$I = 58\ W\ b^{0.664}$$

in reasonable agreement with the computed result now obtained.

/PART 3

PART 3

The effect of the evaporation of rain on the ambient air

12. Basic equations

So far we have dealt only with the evaporation of drops into an atmosphere the characteristics of which are not affected by the evaporation. In practice of course the temperature and humidity of the air are influenced - sometimes largely - by the evaporation of raindrops falling through the air. As the drops evaporate their temperature falls and heat is then supplied to the drops from the air, thereby lowering the air temperature. The evaporation of the drops also increases the humidity of the air and this in turn reduces the rate of evaporation. We shall now consider the variation with time of the temperature and humidity of the air through which rain is falling. For simplicity we shall confine this part of the work to conditions at the surface.

Let the number of drops per unit volume of air and having radius between a and a+da be Nda. The rate of gain of heat by each drop is (equation 4) $4\pi\ Ka(\Theta - T)G$. Integrating this over all the drops and equating to the rate of loss of heat from the air we get

$$c_p\,\sigma\,\frac{d\theta}{dt} = -\int_0^{\infty} 4\pi ka(\theta - T)GN\,da \qquad \ldots\ldots\ldots\ldots\ldots\ldots(36)$$

where c_p is the specific heat of air at constant pressure and σ is the air density.

If ρ is the ambient vapour density we obtain in a similar way (equation 3) an equation representing the conservation of water, viz

$$\frac{d\rho}{dt} = \int_0^{\infty} \frac{4\pi MDa}{R\theta}\,(p_T - fp_\theta)GN\,da \qquad \ldots\ldots\ldots\ldots\ldots\ldots(37)$$

The term Ø in equation 3 has been replaced by Θ as a close approximation.

Equations 36 and 37 are the basic equations the solution to which will show how the temperature and humidity of the air will vary as a result of the evaporation of raindrops falling through the air. Before we can solve these equations we must examine the two integrals.

13. Relation between temperature and vapour density in air through which rain is falling

Let us consider the quantity $(\Theta - T)$. As already indicated in section 7 $(\Theta - T)$ is almost independent of drop size. Table 13 is given to illustrate this.

Table 13

Value of depression of drop temperature below air temperature at a pressure 1013.2 mb and for an air temperature 301°A.

f a(cm)	0.95	0.9	0.8	0.7	0.6	0.5	0.4
0.015	0.7	1.4	2.9	4.5	6.15	8.0	9.9
0.025	0.7	1.4	2.9	4.5	6.2	8.0	9.95
0.035	0.7	1.4	2.95	4.5	6.2	8.0	9.95
0.05	0.7	1.45	2.95	4.55	6.2	8.0	9.95
0.10	0.75	1.5	3.0	4.6	6.25	8.1	10.0
0.15	0.85	1.55	3.05	4.65	6.3	8.15	10.1
0.20	0.90	1.6	3.1	4.7	6.35	8.2	10.15
0.25	0.95	1.65	3.2	4.8	6.45	8.3	10.2

The values in the bottom left hand corner of the table correspond to cases when $\chi > 0.5(\theta - T)$. Excluding these cases we see that there is very little variation in $(\theta - T)$ with a and that we can justifiably take mean values. Similar results were obtained at other temperatures from 288° to 314°A. Table 14 shows the mean values of $(\theta - T)$ for values of a up to and including 0.25 cm and for which $\chi < 0.5(\theta - T)$, for a pressure 1013.2 mb and various temperatures.

Table 14

Mean values of $(\theta - T)$

f θ(°A)	0.95	0.9	0.8	0.7	0.6	0.5	0.4
288	0.52	1.10	2.24	3.42	4.63	5.84	7.15
294.5	0.63	1.27	2.63	3.98	5.44	6.97	8.57
301	0.71	1.47	3.01	4.60	6.26	8.09	10.02
307.5	0.80	1.62	3.34	5.09	7.04	9.13	11.43
314	0.86	1.73	3.56	5.57	7.75	10.16	12.89

(In passing we may note here that Byers, Moses and Harney (7) state that the rain temperature may initially be up to 10°C lower than the ambient air temperature. The conditions they were discussing - summer thunderstorms in Ohio - would correspond to θ = about 302°A and f = 0.5 to 0.7. The initial temperature difference presumably occurs - at least sometimes - before downdraft has started and from table 14 we should expect $(\theta - T)$ to be 5 to 8°C in such circumstances.)

Now if $(\theta - T)$ is independent of a it follows that $(p_T - fp_\theta)$ is also independent of a. Accordingly a companion table to table 14 was computed giving mean values of $(p_T - fp_\theta)$ (not reproduced here). The next step was to evaluate the ratio $[k(\theta - T)/\sigma]/[D(p_T - fp_\theta)/\theta]$ for each case tabulated in table 14. The results showed some systematic variation of the ratio with both f and θ but the variation was small. The mean of the 35 values was 0.1176 with a mean absolute deviation of 0.0062 and a standard deviation of 0.0080. We shall accordingly adopt the mean value 0.1176. Then from equations 36 and 37 it follows that

$$\frac{d\theta}{dt} = -\frac{0.1176\, R}{c_p M} \frac{d\rho}{dt}$$

or, putting in the numerical values of the constants and integrating

$$\theta = A' - 2.263\; 10^6 \rho \text{.............................} (38)$$

where A' is a constant which depends upon the initial conditions.

We may note also that since $(\theta - T)$ and $(p_T - fp_\theta)$ are independent of a, equations 36 and 37 can be written in the form

$$\frac{d\theta}{dt} = -\frac{4\pi}{c_p}\frac{k}{\sigma}(\theta - T)\, X \text{ ....} (39)$$

$$\frac{d\rho}{dt} = \frac{4\pi M}{R}\frac{D}{\theta}(p_T - fp_\theta)\, X \text{ ....} (40)$$

$$X = \int_0^\infty aGN\, da \text{ ....} (41)$$

In order to determine the variation of θ with time we must integrate equation 39. Now X is a function only of the drop size distribution and of the number of drops, i.e. it is independent of θ and t provided G is independent of θ. We shall show below that this is approximately true. Thus, in order to integrate equation 39, we must express $\frac{k}{\sigma}(\theta - T)$ in terms of θ and ρ .

14. Variation of velocity factor G with θ and with a.

The velocity factor G is given by equation 10. Values were computed for several different drop sizes using the terminal velocities appropriate to $\theta = 288^{o}$A and $\theta = 314^{o}$A and a pressure 1013.2 mb (5). The value of G varied from 1.94 to 1.87 as the temperature increased from 288°A to 314°A for a drop radius 0.015 cm. For a drop radius 0.25 cm the corresponding figures were 18.5 and 17.2. The variation is so small that it was decided to treat G as independent of θ over the range 288 to 314°A and to use the means of the values for these two temperatures. Values for several different drop sizes were computed in this way. G is thus a function only of a. We shall consider the evaluation of X below and for this purpose it is useful to know an explicit form of the relationship between G and a. Using the mean values of G for the two temperatures 288 and 314° log G has been plotted against log a in figure 11. The resulting points approximate closely to a straight line the equation of which is

$$G = 61.1\ a^{0.85} \qquad (42)$$

15. Relation between $(\theta - T)$, θ and ρ .

In table 14 we have expressed $(\theta - T)$ as a function of θ and of f. Now f can be expressed in terms of ρ and ρ_{θ}, the saturation value of ρ at temperature θ. Moreover ρ_{θ} is a function only of θ and, from equation 38, we see that ρ is also a function of θ. Since k/σ is also a function of θ (for the given atmospheric pressure 1013.2 mb) we see that $\frac{k}{\sigma}(\theta - T)$ can be expressed as a function of θ and equation 39 can then be integrated. Examination of the numerical values of $\frac{k}{\sigma}(\theta - T)$ suggested that this quantity could be expressed in the form

$$\frac{k}{\sigma}(\theta - T) = 1.905\ 10^{9}\ (\rho_{\theta} - \rho)^{1.064} \exp(-0.0343\ \theta)\ \ldots.(43)$$

That this is so is shown in figure 12 where the plotted points have been computed from the values in table 14 and the straight lines have been computed from equation 43. From equations 39 and 43 and putting in numerical values for the constants we can now write

$$9.96\ 10^{10}\ t = -\frac{1}{X}\int_{\theta_1}^{\theta_2} \frac{e^{0.0343\theta}}{(\rho_{\theta} - \rho)^{1.064}}\ d\theta \quad \ldots\ldots\ldots.(44)$$

and, from equation 38

$$\rho = A - 4.419\ 10^{-7}\ \theta \quad \ldots\ldots\ldots\ldots\ldots\ldots\ldots.(45)$$

where A is determined by the initial conditions of temperature and humidity and t is the time (in seconds) for the temperature to fall from θ_1 to θ_2 owing to evaporation of the raindrops. The shape of the temperature time curve is thus determined by the integral on the right hand side of equation 44 but the time scale is determined by X. The shape of the humidity time curve is related to the shape of the temperature time curve. Thus the problem is now reduced to two parts; the evaluation of the integral on the right hand side of equation 44 to determine the shape of the temperature time and humidity time curves and the evaluation of X to determine the time scale. We deal with these separately below.

/16

16. Shape of the temperature time and humidity time curves

Let the initial values of f, ρ and θ before the rain begins to fall be denoted by f_o, ρ_o and θ_o respectively. These values determine the value of A in equation 45 and from that equation we see that

$$\rho_\theta - \rho \quad = \quad \rho_\theta + 4.419\ 10^{-7}\theta - (f_o\rho_o + 4.419\ 10^{-7}\theta_o) \quad \ldots\ldots\ldots(46)$$

Evaporation from the falling raindrops continues until $\rho_\theta = \rho$. For convenience write

$$u \quad = \quad \rho_\theta + 4.419\ 10^{-7}\ \theta$$

$$v_o \quad = \quad f_o\rho_o + 4.419\ 10^{-7}\ \theta_o$$

Then u is a function only of θ and v_o is completely determined by the initial conditions. Moreover

$$\rho_\theta - \rho \quad = \quad u - v_o$$

and so

$$f \quad = \quad 1 - \frac{u - v_o}{\rho_\theta} \quad \ldots\ldots\ldots\ldots\ldots\ldots\ldots\ldots\ldots\ldots\ldots(47)$$

Equation 47 relates the relative humidity to the temperature, The steady state temperature θ_1 is reached when f = 1 and $u = v_o$. By evaluating the right hand side of equation 47 for various values of θ we determine the values of θ for selected values of f. Values of $(\theta_o - \theta_1)$ obtained in this way for nine sets of initial conditions are shown in Table 15.

Table 15

Depression of steady state temperature below initial temperature $(\theta_o - \theta_1)$ for various initial conditions

f_o \ θ_o(°A)	293	303	313
0.5	6.66	8.46	10.18
0.7	3.81	4.75	5.64
0.9	1.20	1.50	1.76

Returning now to equation 44 we can write

$$Y \quad = \quad 9.96\ 10^{10}\ t_\theta\ X \quad = \quad -\int_{\theta_o}^{\theta} \frac{e^{0.0343\theta}}{(u - v_o)^{1.064}}\ d\theta \ \ldots\ldots(48)$$

where t_θ is the time required for the temperature to fall from the initial value θ_o to θ. The function Y is a direct measure of t_θ but the time scale can be determined only after X has been evaluated from a consideration of the number and size distribution of the raindrops. The integral on the right hand side of equation 48 has been evaluated graphically for various values of θ, for three values of θ_o and three values of f_o. These computations gave temperature time curves, the time being expressed in terms of Y. Humidity time curves were then obtained by the method already indicated (equation 47).

The results are shown in figures 13 and 14. It can be seen that, as would be expected on intuitive grounds, the excess of temperature above the steady state value θ_1 diminishes exponentially and the excess of relative humidity over the initial value increases exponentially. The initial relative humidity has no effect on the temperature time curve and the initial temperature has no effect on the humidity time curve (within the range of these variables represented in figures 13 and 14). The initial temperature does however have a very slight effect on the temperature time curve and the initial relative humidity has a slightly greater effect on the humidity time curve though in each case it has not been considered worth while drawing more than one line on the figures.

The points depart from straight lines in figures 13 and 14 after the change in temperature or humidity has reached about 0.8 to 0.9 times its ultimate value. This may be due to the inevitable inaccuracies in the computations at high relative humidities already mentioned though this seems rather unlikely. For practical purposes however the effect does not seem important.

Table 15 shows the ultimate change in temperature for each set of initial conditions. Over the range of variables considered it appears that to a close approximation $(\theta_o - \theta_1)$ is a linear function of θ_o and, with less accuracy, a linear function of f_o.

The equations to the lines in figures 13 and 14 are

$$\frac{\theta_o - \theta_1}{\theta - \theta_1} = \exp\,(2.74\ 10^{-11}\ Y)$$

$$\frac{1 - f_o}{1 - f} = \exp\,(2.39\ 10^{-11}\ Y)$$

17. The time scale of temperature time and humidity time curves

Finally we turn to the evaluation of X, defined by equation 41. Of the three factors in the integrand aGN the first needs no discussion and G has already been discussed in section 14.

If at some fixed level above the surface the number of drops per unit volume of air with radius between a and a + da, Nda, is constant with time then at any lower level Nda will vary with time as a result of evaporation below the fixed level. To introduce such considerations here however would lead to great complexity as it implies that N varies according to conditions above the surface and we shall therefore consider only the value of X when N is constant with time.

If the drop size distribution is defined by equation 26 then we can easily show that (using also equation 42)

$$aGN = \frac{183.3\ Wn}{4\pi}\left(\frac{2}{b}\right)^{n} a^{n-2.15}\, e^{-(2a/b)^{n}}$$

and from this it easily follows that

$$X = \frac{101.6\ W}{\pi\ b^{1.15}}\,\Gamma\left(1 - \frac{1.15}{n}\right) \qquad \ldots\ldots\ldots\ldots\ldots\ldots\ldots\ldots(49)$$

The parameter W is not convenient for the present considerations and we shall now replace it by $I.10^{-6}/67.b^{0.73}$ from section 11 (remembering that here W must be measured in g/cc). We still have the parameter b in the expression for X and since b is not normally measured and our aim is to interprete the temperature and humidity time curves in terms of familiar variables we shall use the experimental result $b \approx 0.13\ I^{0.232}$ (6). With these substitutions equation 49 becomes

$$X = 22.27\ 10^{-6}\ I^{0.564}\,\Gamma\left(1 - \frac{1.15}{n}\right) \qquad \ldots\ldots\ldots\ldots\ldots\ldots(50)$$

where I is measured in mm/hr. Now the values of $\Gamma(1 - \frac{1.15}{n})$ for n = 2, 3, 4 and 5 are 2.08, 1.45, 1.28 and 1.20 respectively. We shall adopt a value of 1.6, corresponding approximately to n = 2.5 this being about the mean value obtained in reference (6). Then from equation 48 we have

$$Y = 3.55 \cdot 10^6 \, I^{0.564} \, t_\theta \quad \ldots\ldots\ldots\ldots\ldots\ldots\ldots (51)$$

The coefficient of t_θ in equation 51 has the following values

I	$3.55 \ 10^6 \ I^{0.564}$
1 mm/hr	$0.355 \ 10^7$
5 "	0.880 "
10 "	1.301 "
25 "	2.180 "
50 "	3.221 "

These figures determine the time scale of the curves in figures 13 and 14. For example we see that if rain falls at 10 mm/hr and the air at the surface is initially at a temperature of 303°A and relative humidity 50 per cent the temperature will fall eventually to (303 - 8.46)°A = 294.5°A. The temperature will have reached (303 - 8.46 x 0.8) = 298.23°A after $59 \ 10^9/1.3 \ 10^7$ = 4530 seconds and the relative humidity will have risen to (50 + 50 x 0.8) = 90 per cent after $67.5 \ 10^9/1.3 \ 10^7$ = 5190 seconds.

In practice of course the rate of change of the surface temperature and humidity would be somewhat more rapid than indicated (even with no downdraft) if the value of I is measured at the onset of precipitation. As the rain continues the evaporation in the upper air diminishes and so the rate of precipitation at all lower levels increases. The time scale however varies inversely approximately only as the square root of I.

18. Comparison with Dolezel's work

Dolezel (8) has considered the effect of falling rain on the temperature and humidity of the ambient air. He was concerned primarily with conditions which exist near a warm front and selected a particular set of circumstances for examination. His treatment was less general than that given here inasmuch as he considered only one air temperature - 10°C (though he did deal with three different lapse rates of air temperature) and only one drop size distribution. Dolezel's basic equations were similar to those employed here though he seems to have assumed identity between the velocity coefficients for heat and vapour on the basis of analogy.

Despite various minor differences in the two treatments values deduced from the present general treatment should be of the same order as those obtained by Dolezel for his special cases. From figure 6 of Dolezel's paper we select some results corresponding to θ_o = 283°A and f_o = 0.5. The ambient air was assumed to be isothermal. These results are given in table 16 together with corresponding values obtained from the present treatment. The value of $\theta_o - \theta_1$ for the present treatment was obtained by extrapolation from table 15. The remaining figures were obtained by inserting values for I in equation 51 and then using figures 13 and 14.

Table 16

Comparison of Dolezel's results with those from the present treatment for θ_o = 283°A and f_o = 0.5

			After 1 hr.		After 2 hr.	
	I mm/hr	$\theta_o - \theta_1$ °C	$\theta_o - \theta$ °C	f	$\theta_o - \theta$ °C	f
Dolezel	3.56	4.7	3.0	0.79	4.1	0.92
Figs. 13 and 14	3.56	4.9	2.5	0.73	3.7	0.87
Dolezel	1.78	4.7	1.7	0.65	2.8	0.76
Figs. 13 and 14	1.78	4.9	1.9	0.67	3.0	0.79

It is considered that the agreement between the two sets of figures is as good as could be expected.

APPENDIX

The formulae used for calculating the various physical properties of air and water were as follows

$$L = 597 - 0.552\ t \quad \text{cal.gm}^{-1}$$

$$D = 0.219\ \frac{1013.2}{P}\left(\frac{T}{273}\right)^{1.853} \quad \text{cm}^2\ \text{sec}^{-1}$$

$$k = 5.72\ 10^{-5}\ (1 + 0.00298t) \quad \text{cal cm}^{-1}\ \text{sec}^{-1}\ \text{temp}^{-1}$$

$$\mu = 1715\ 10^{-7}\ \frac{273 + 117}{T + 117}\left(\frac{T}{273}\right)^{3/2} \quad \text{gm cm}^{-1}\ \text{sec}^{-1}$$

where t and T are temperature in °C and °A respectively and P is barometric pressure in mb.

The authorities for these formulae are

L. Above 0°C values calculated from this formula agree with values quoted by Dorsey (Properties of ordinary water substance - Reinhold Publishing Corporation). Below 0°C the formula is that assumed by Whipple (Monthly Weather Review, March, 1927) and leads to calculated values of saturation vapour pressure in good agreement with those published by Washburn.

D. This formula is given by Dorsey. (Properties of ordinary water substance).

k. This is in agreement with the published measurements of Hercus and Sutherland. (Proc. Roy. Soc. A.145, 1934, 599).

μ See Tables of Physical and Chemical Constants, Kaye and Laby, 9th Ed., p. 40.

The I.C.A.N. standard atmosphere is defined by a pressure 1013.2 mb and a temperature 15°C at the surface and a constant lapse rate of temperature up to 11 km of 6.5°C per km.

The Summer Tropical Atmosphere (See Meteorological Glossary, 3rd Ed, p. 179, H.M.S.O., London) has the same surface pressure and temperature lapse rate as the I.C.A.N. atmosphere but has a surface temperature of 41°C.

/References

References

1. Frossling N., 1938, Gerlands Beitr. z. Geophys, 52, p.170.

2. Takahashi Y., 1936, Geophysical Mag., Tokyo, 10, p.321.

3. McAdams W.H., 1942, Heat Transmission, 2nd Edn., McGraw Hill Book Co. New York and London, p.236.

4. Johnstone H.F.
Pigford R.L. and
Chapin J.H. 1941, Trans. Am. Inst, Chem. Engrs., 37, p. 95.

5. Best A.C., 1950, Q.J. Roy. Met. Soc. London, 76, p.302.

6. Best A.C., 1950, Q.J. Roy. Met. Soc. London, 76, p.16.

7. Byers H.R.
Moses H. and
Harney P.J. 1949, J. Met., 6, p.51.

8. Dolezel 1944, J. Met., 1, p.89.

9. Best A.C. 1950, M.R.P. 559.

G.278573/ABC/12/50/40

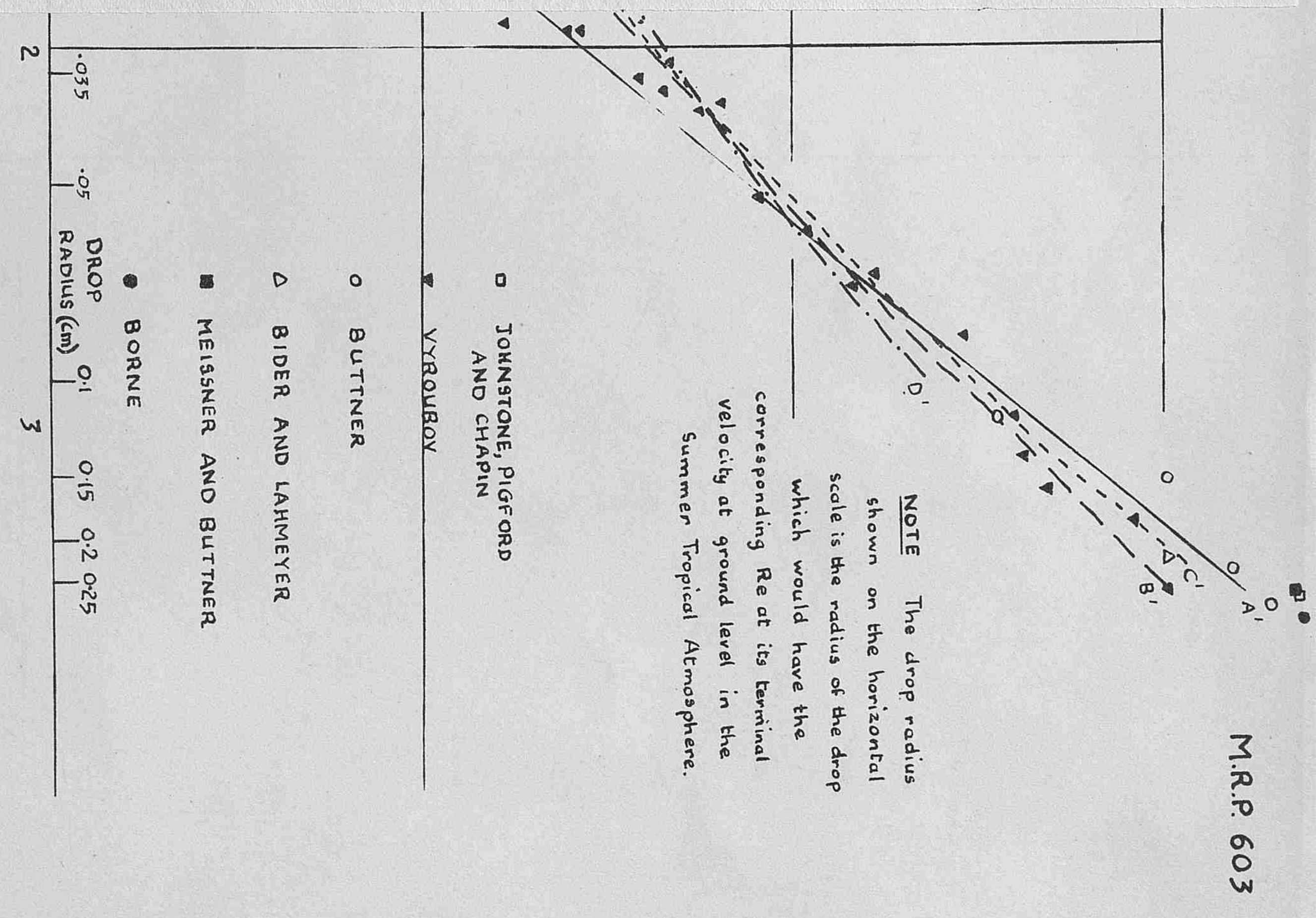

ocity Coefficient with Re.

M.R.P. 603

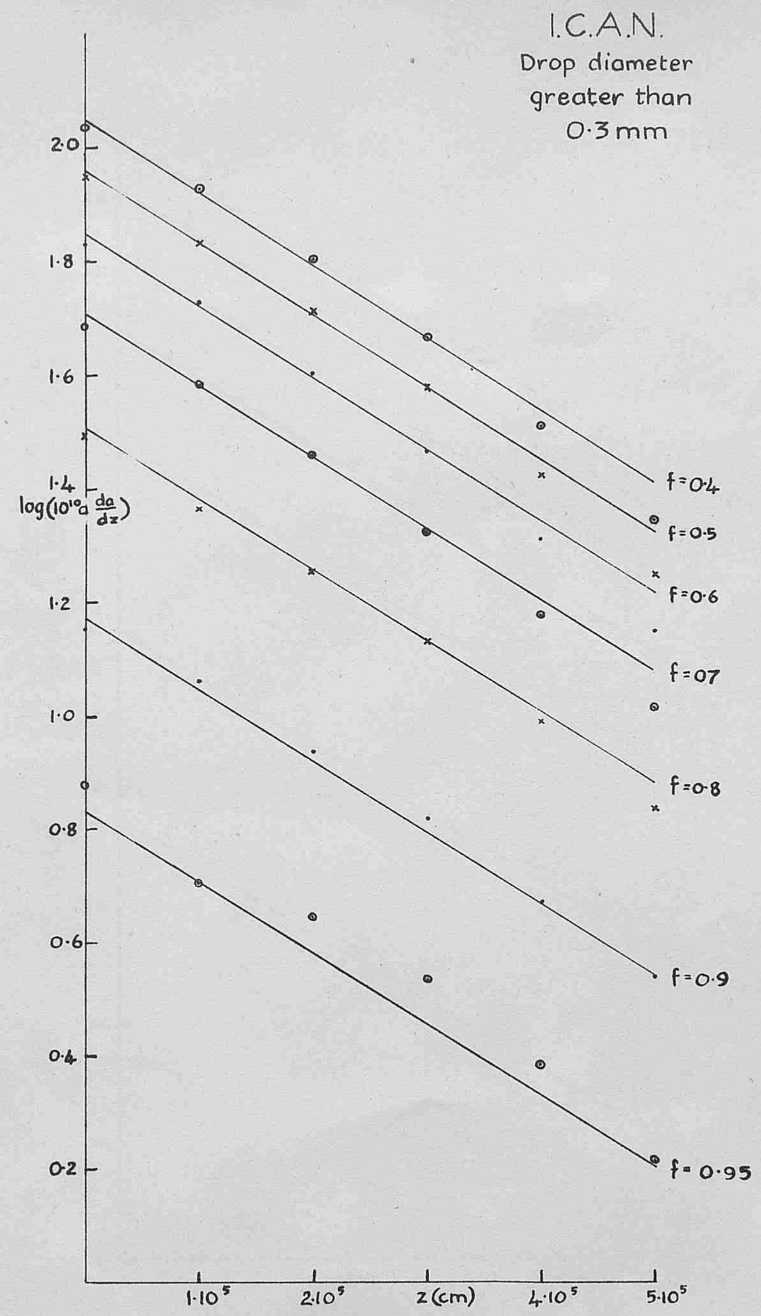

Fig.2

Rate of variation of surface area of rain drop with height as a function of height (I.C.A.N. Atmosphere).

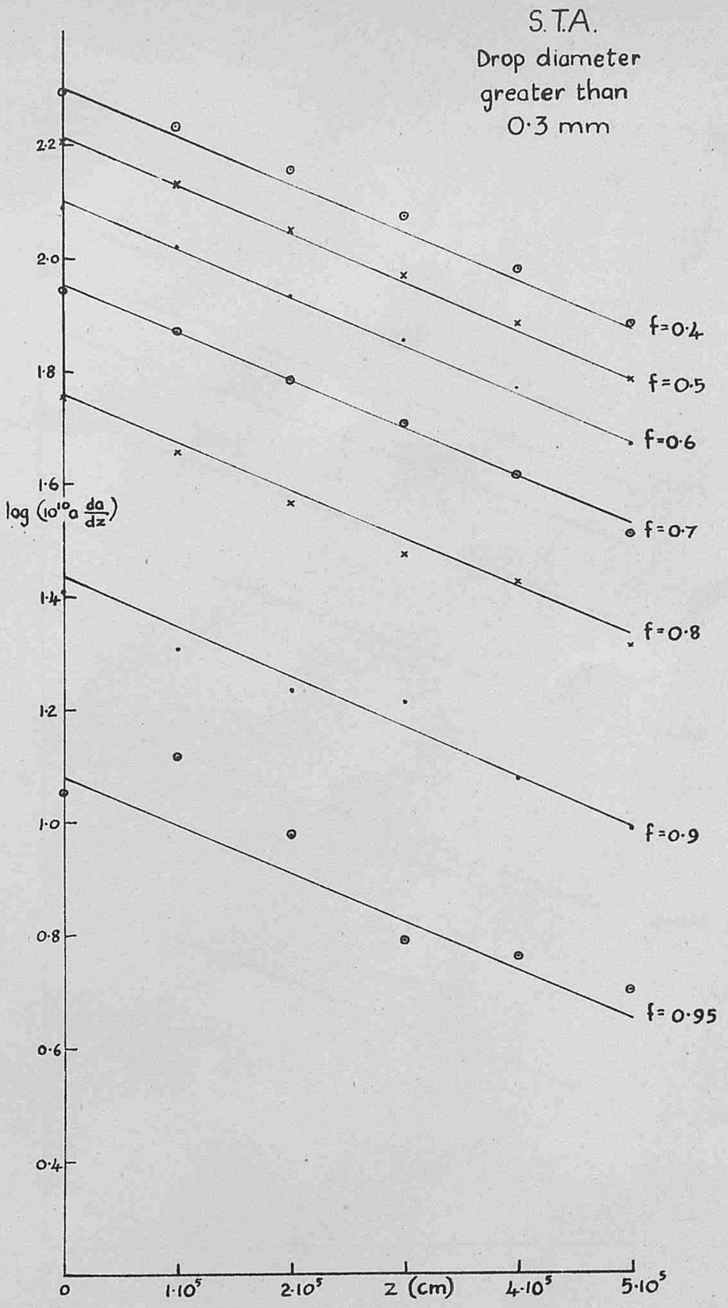

Fig.3

Rate of variation of surface area of rain drop with height as a function of height (Summer Tropical Atmosphere)

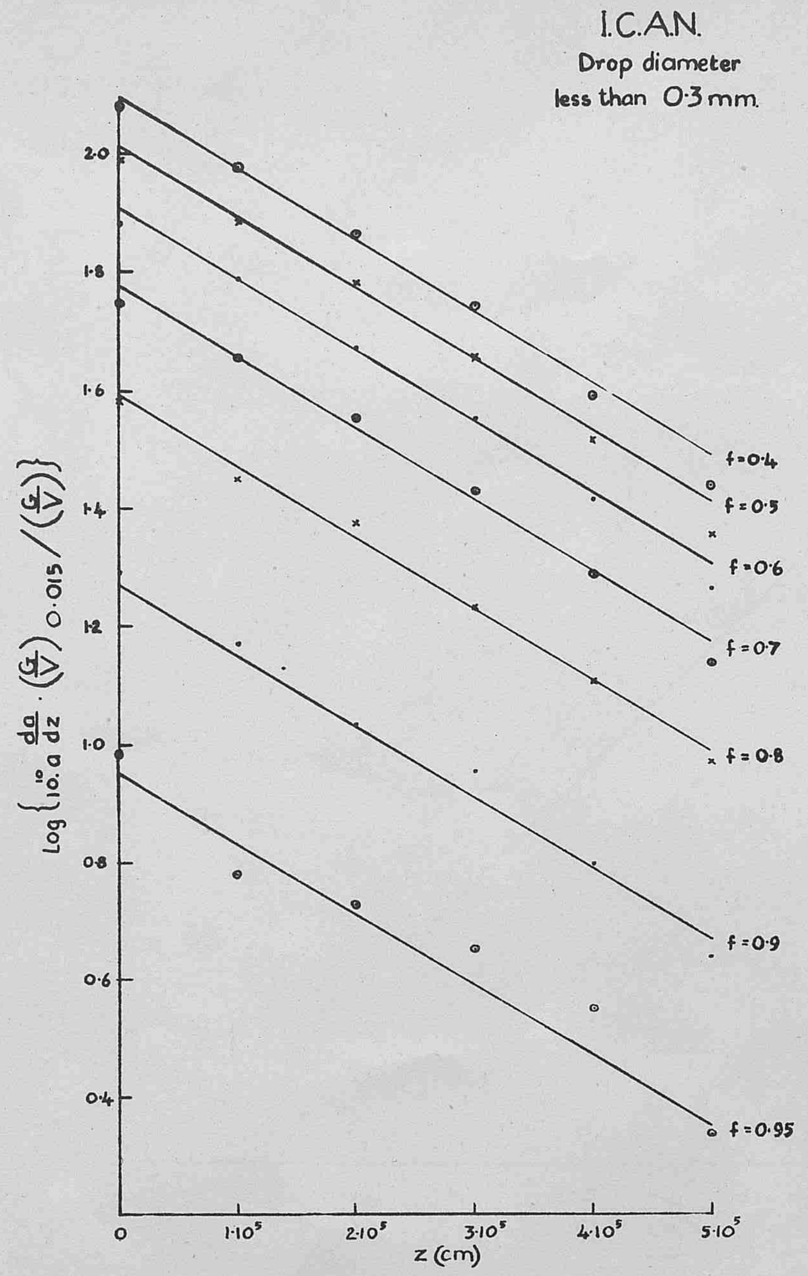

FIG. 4
Rate of variation of surface area of drizzle drop with height as a function of height (I.C.A.N. atmosphere)

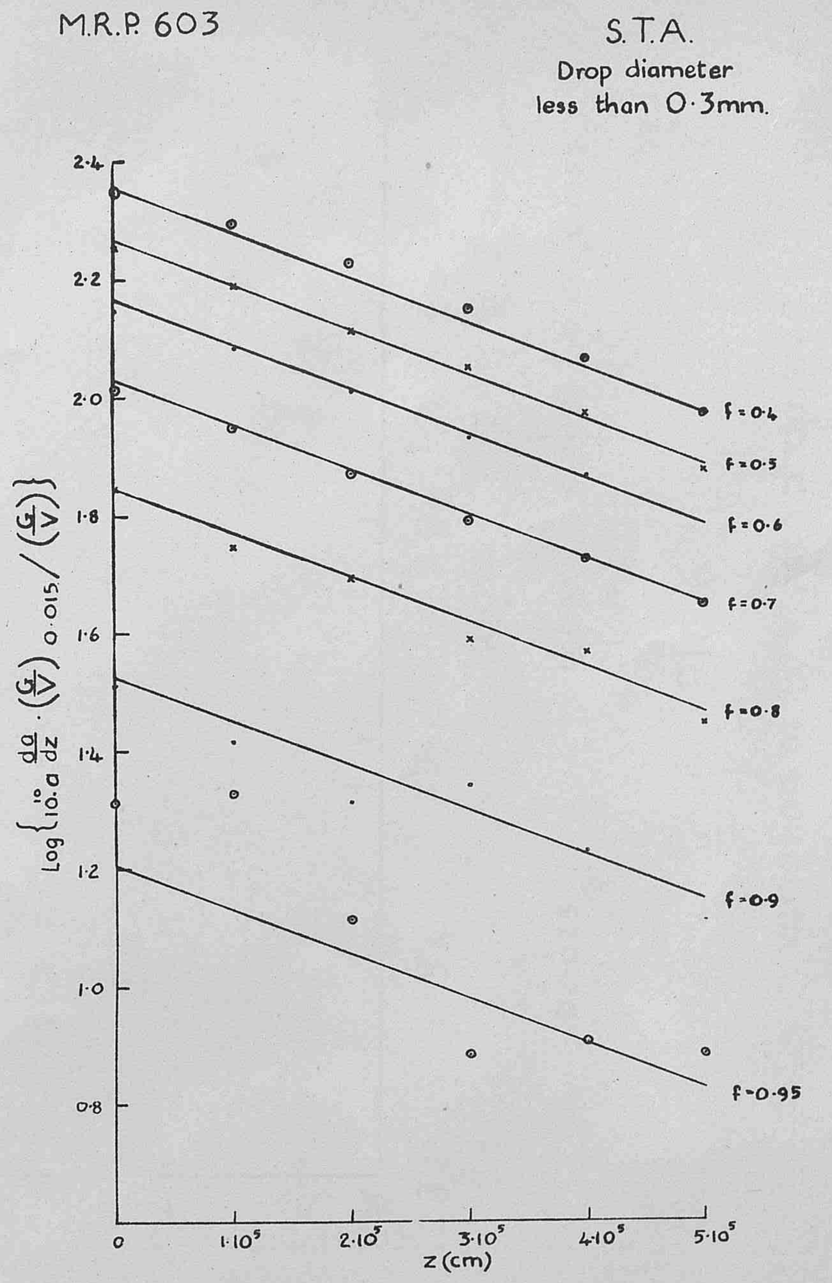

FIG. 5
Rate of variation of surface area of drizzle drop with height as a function of height (Summer Tropical Atmosphere)

M.R.P. 603

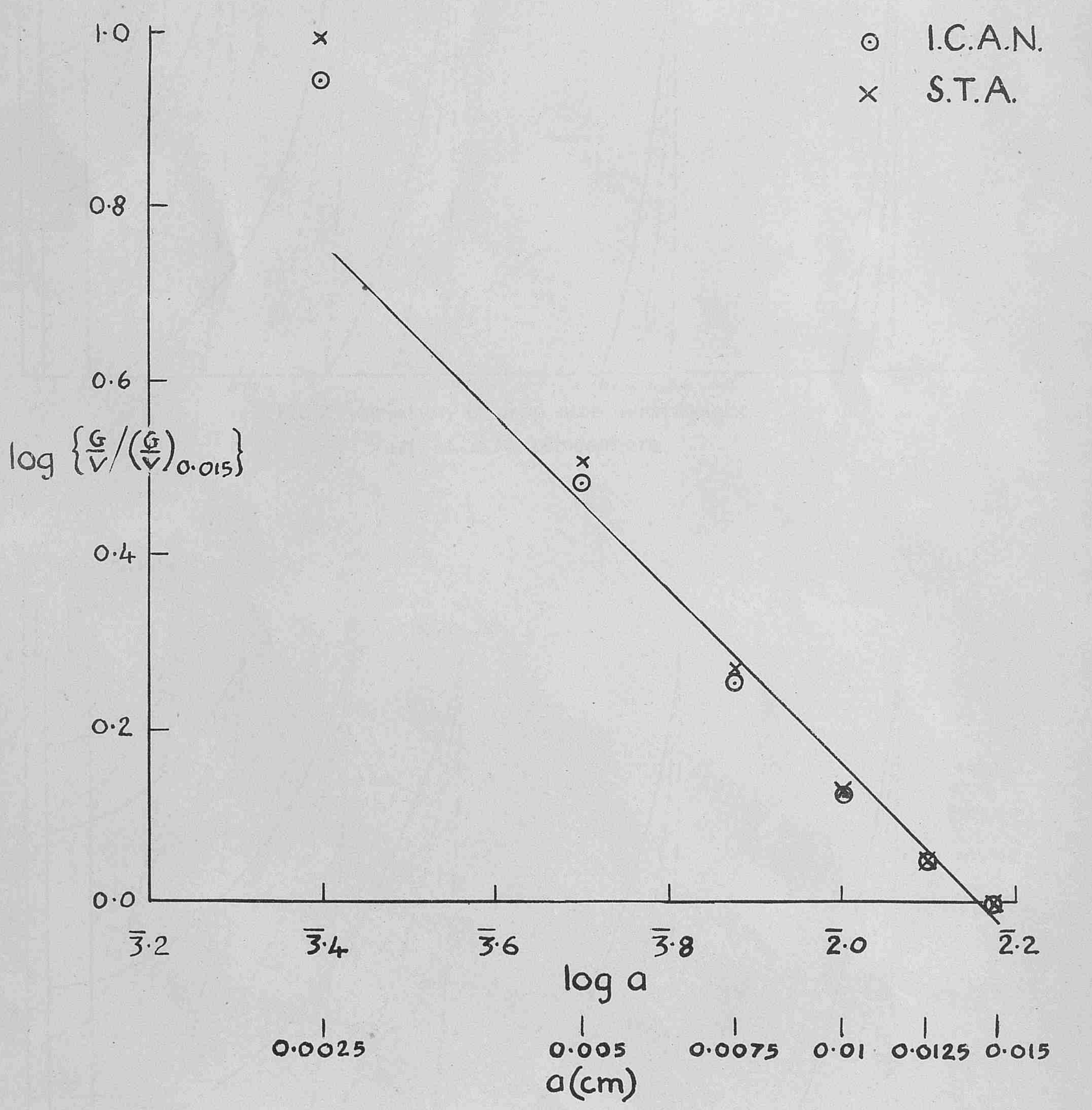

FIG. 6

Variation of G/V with drop size

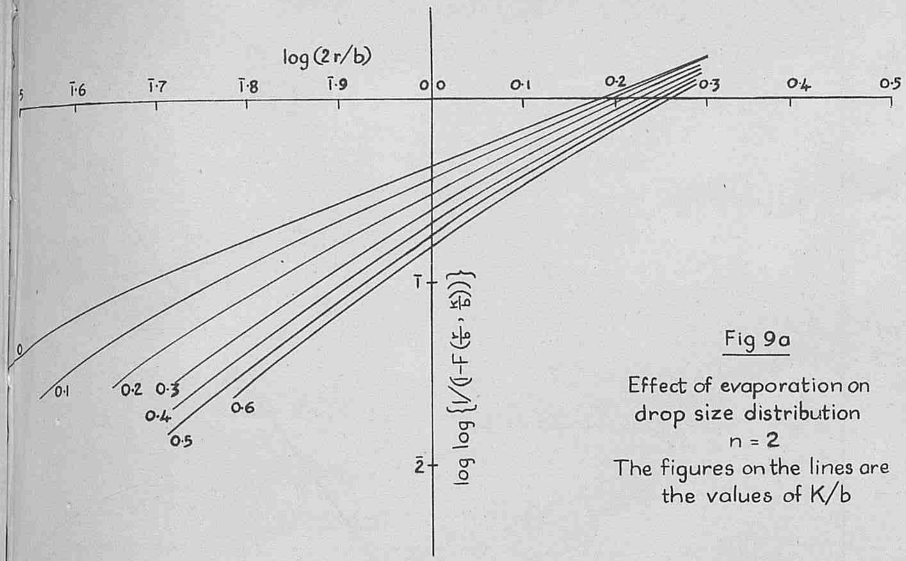

Fig 9a

Effect of evaporation on drop size distribution
n = 2
The figures on the lines are the values of K/b

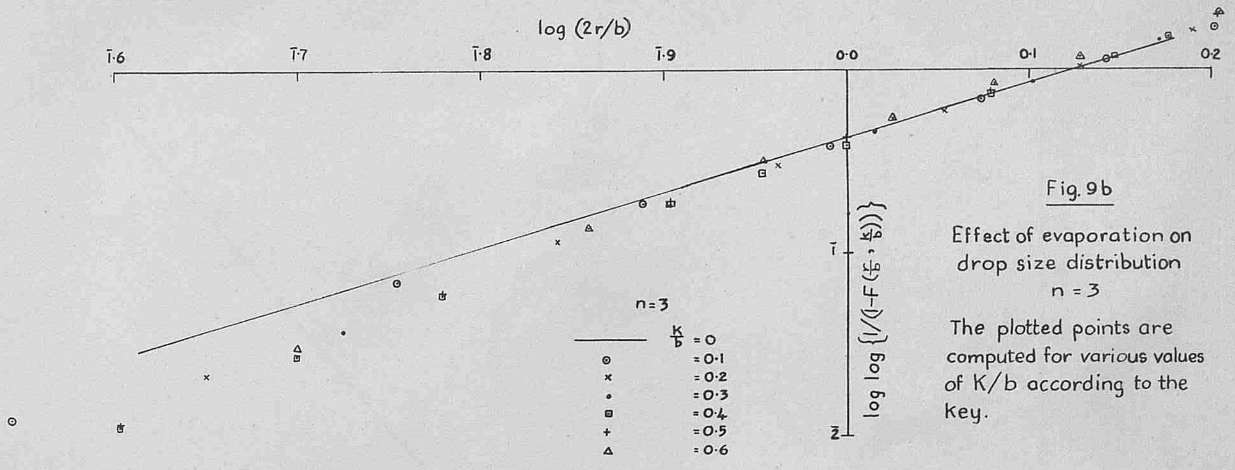

Fig. 9b

Effect of evaporation on drop size distribution
n = 3

The plotted points are computed for various values of K/b according to the key.

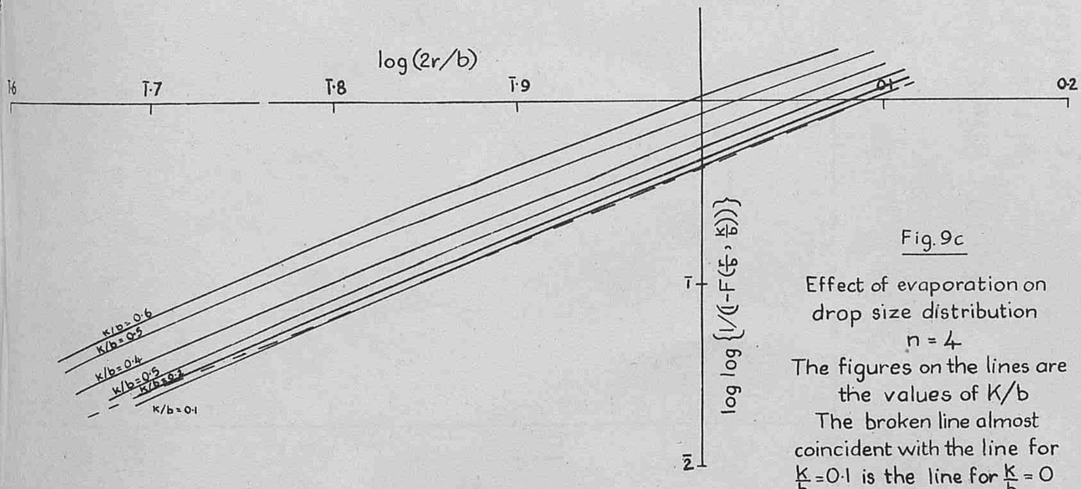

Fig. 9c

Effect of evaporation on drop size distribution
n = 4
The figures on the lines are the values of K/b
The broken line almost coincident with the line for $\frac{K}{b}$ = 0·1 is the line for $\frac{K}{b}$ = 0

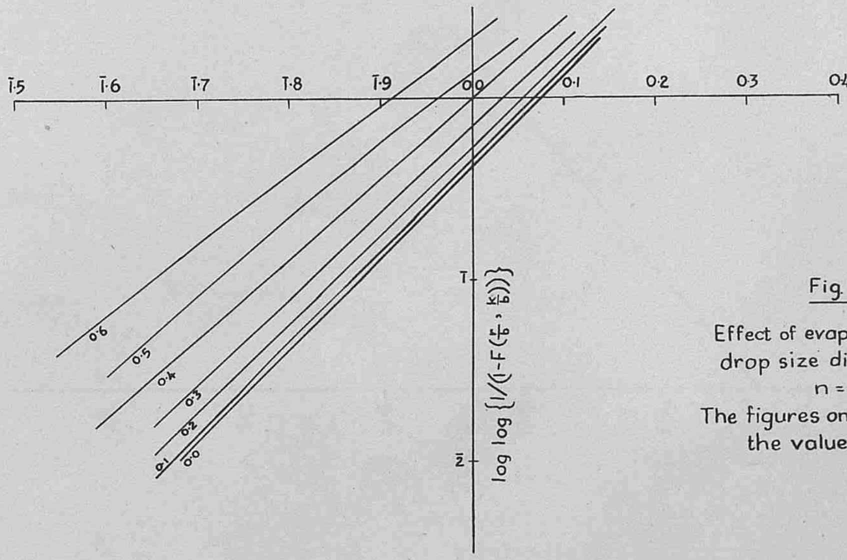

Fig. 9 d

Effect of evaporation on drop size distribution
n = 5
The figures on the lines are the values of K/b

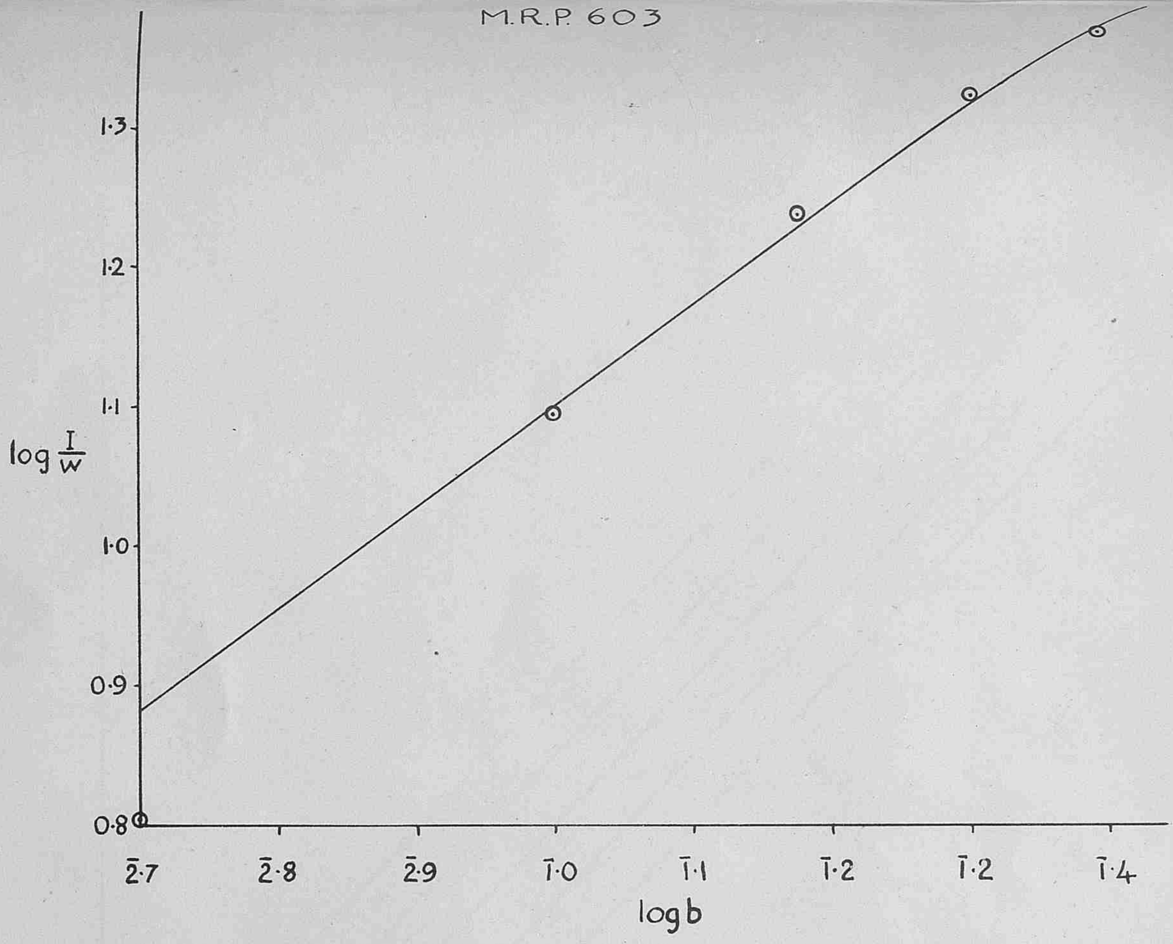

Fig. 10. Effect of drop size distribution on ratio of rate of precipitation to liquid water content of air.

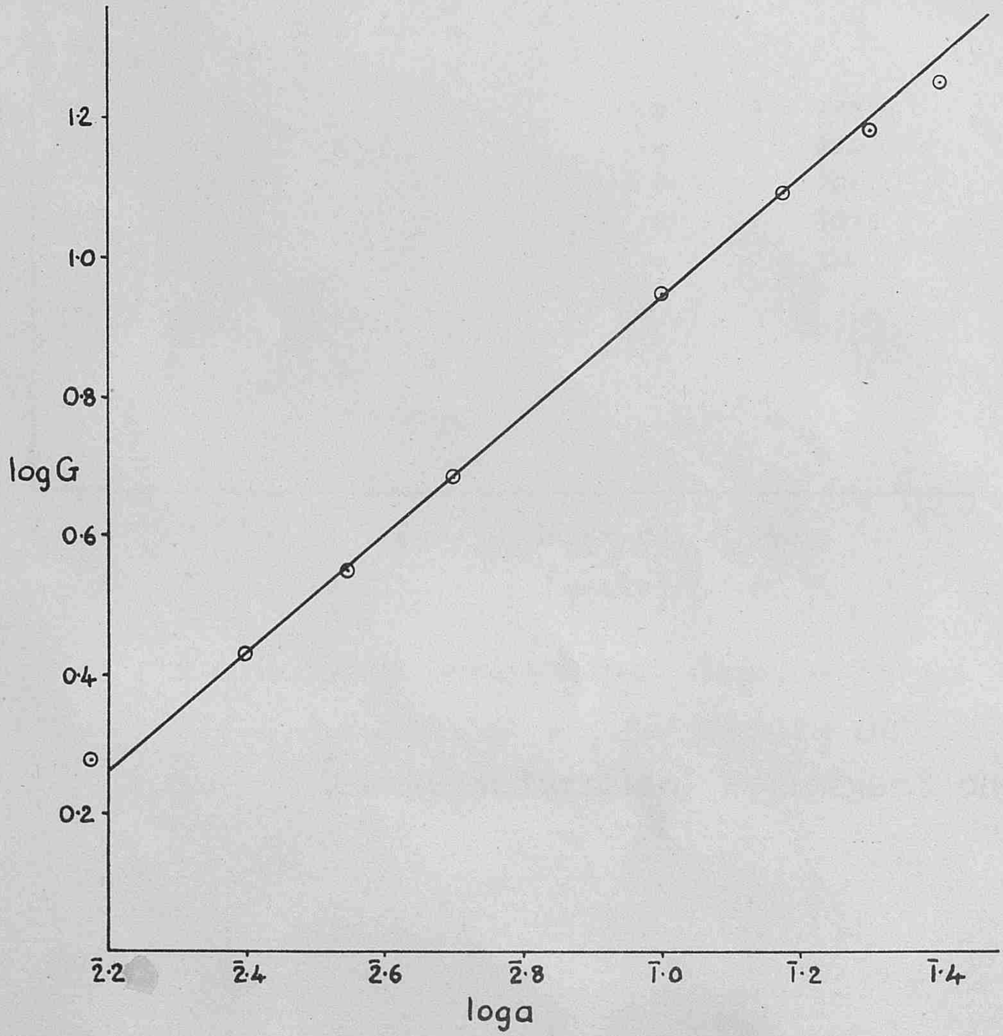

Fig. 11. Relation between velocity factor G and drop radius a when drop is falling through atmosphere.

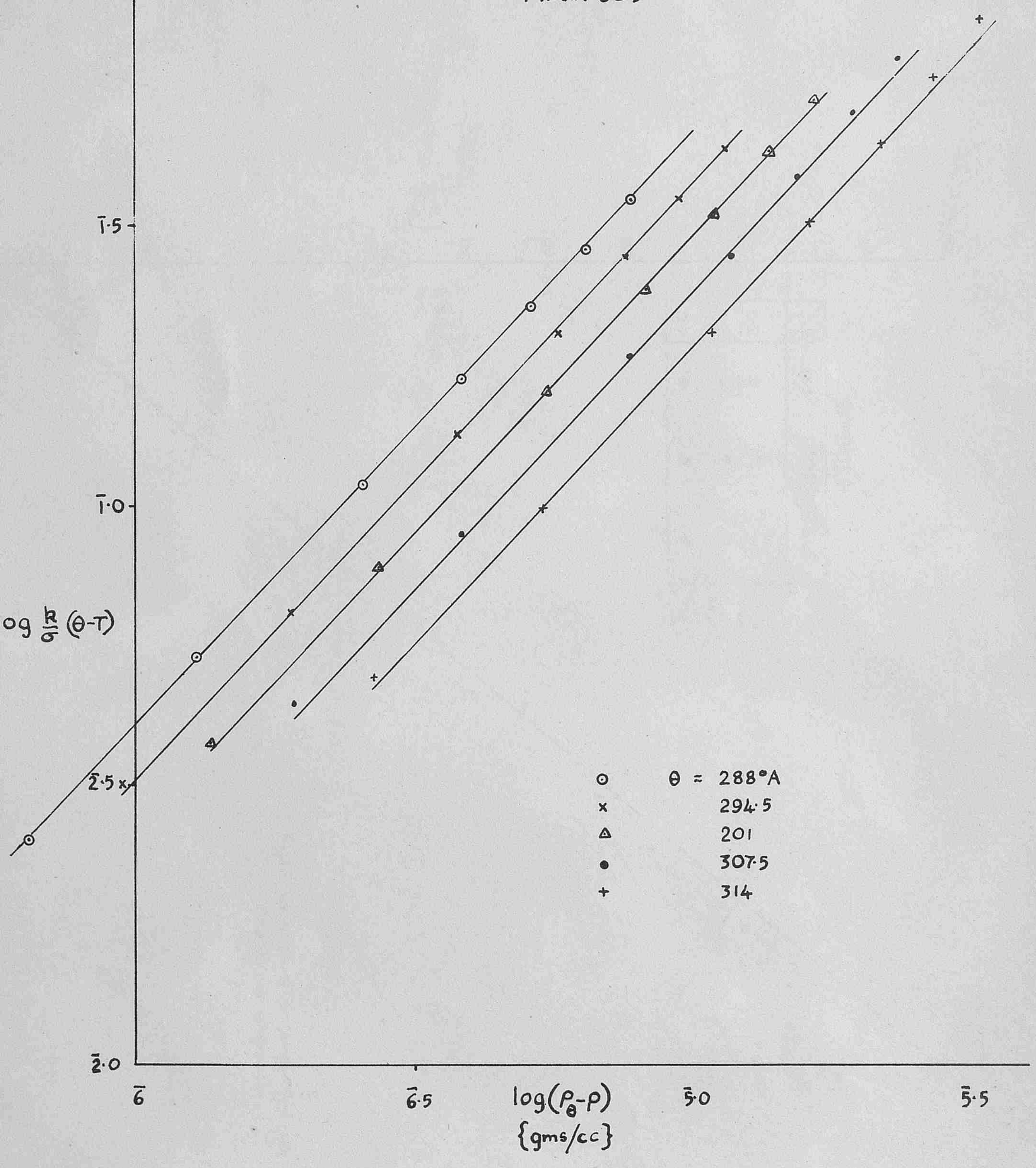

Fig.12. Drop temperature depression as function of vapour density deficit (below saturation) in ambient air.

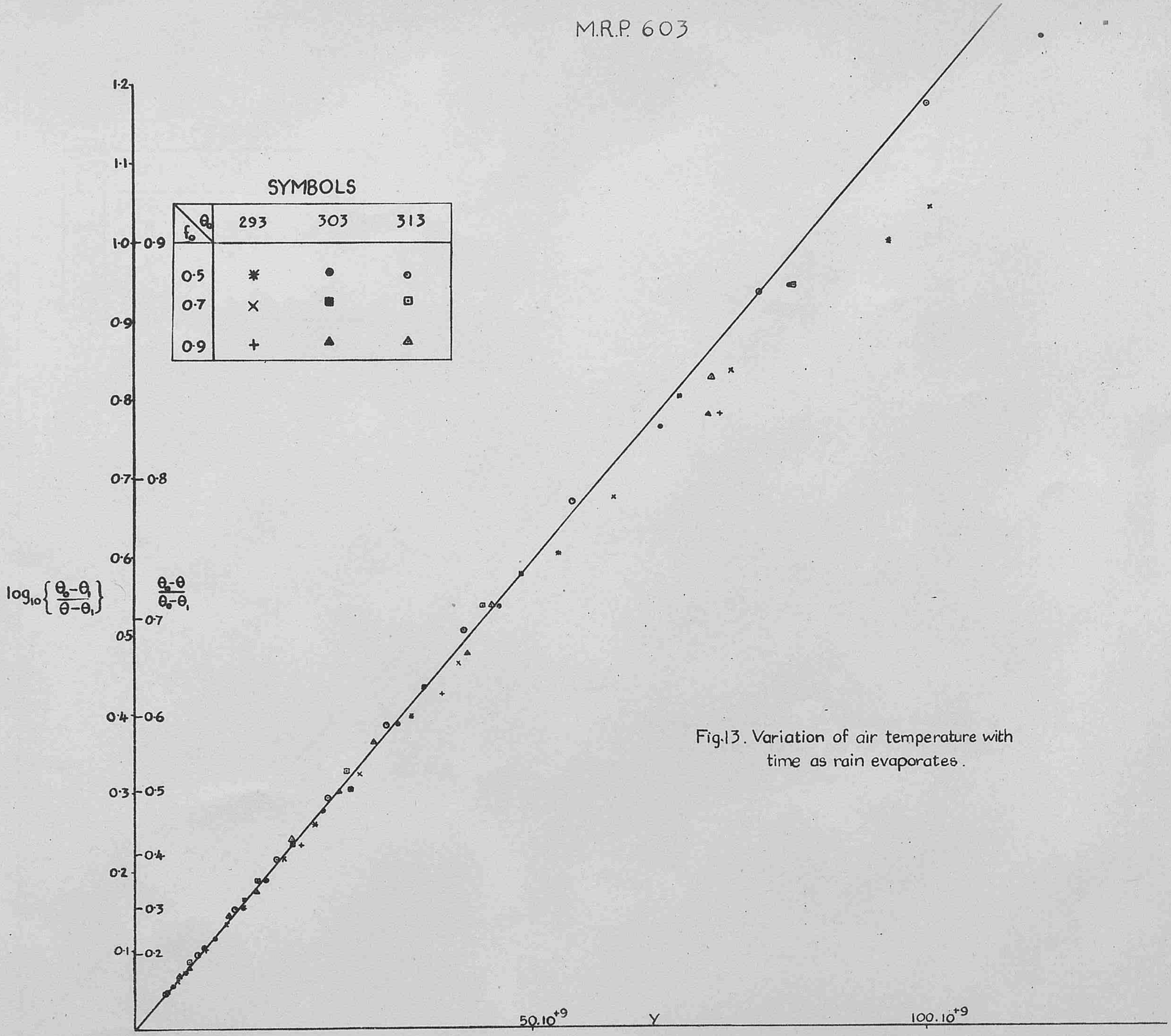

Fig.13. Variation of air temperature with time as rain evaporates.

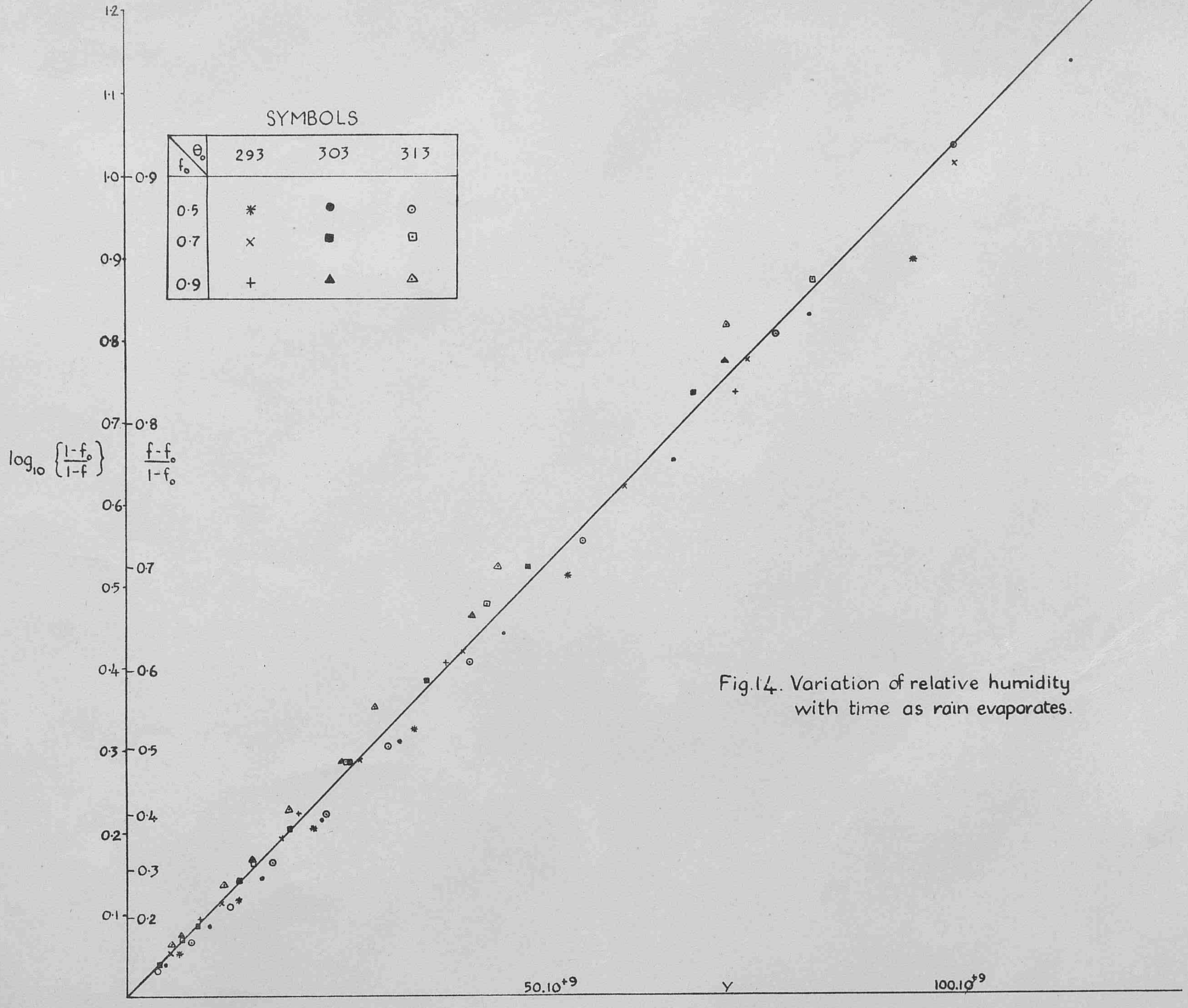

Fig. 14. Variation of relative humidity with time as rain evaporates.

177 TUESDAY 9 OCT P.M.

been
quot
pape
Com
M.R.
A copy is available in the Library of
the Meteorological Office."

ASTIA FILE COPY

M.R.P. 604
S.C.I/48
12th Dec. 1950

AIR MINISTRY
METEOROLOGICAL RESEARCH COMMITTEE

ATI-200027

Notes on the derivation of True Air Temperature from Aircraft Observations.

by

D. D. Clark.
(Meteorological Office)

AIR WEATHER SERVICE
TECHNICAL REFERENCE FILE
JUN 6 1951

Definition of terms used.

T_s = true air temperature
T_i = the indicated temperature
P_s = the static air pressure in the absence of position error (the true air pressure)
P_t = the total air pressure or the pressure of the air if brought to rest relative to the aircraft
q = $P_t - P_s$ the pressure rise
V = the true air speed
V_i = the indicated air speed if referred to slow aircraft but now called the 'equivalent air speed' if the compressibilty of the air is significant.
V_r = the reading of the air speed indicator in the absence of position error.
P_o = the M.S.L. pressure, 1013.2 mb. ICAN
T_o = the M.S.L. temperature, 288°A ICAN
ρ_o = the M.S.L. density, 1.226×10^{-3} gm/cm^3 ICAN
ρ = air density at the level considered.
α = the air speed correction factor

$$T_i - T_s = \frac{\alpha}{K^2}\left(\frac{V}{100}\right)^2$$

where K is the factor converting from knots to cm/sec.

λ defined in the equation

$$T_i - T_s = \lambda \frac{V^2}{2c_p}, \quad 0 < \lambda < 1$$

a = speed of sound, $a_o = 3.40 \times 10^4$ cm/sec.
m = Mach Number = V/a
k^2 = convertion factor knots^2 to (cm/sec)^2 = 2.65×10^3
γ = ratio of specific heat at constant pressure to specific heat at constant volume for air = 1.402

Accentuation of a symbol indicates that it has the value corresponding to the immediate neighbourhood of the static source, e.g. P_s' is the static pressure before the application of position error correction. All units unless stated are given in cm. gm. sec.

~~quote this paper
paper of the Meteorological Research
Committee London),
M.R.P. No .... by Mr..........................
A copy is available in the Library of
the Meteorological Office."~~

M.R.P. 604
S.C.I/48
12th Dec. 1950

ATI-200027

AIR MINISTRY
METEOROLOGICAL RESEARCH COMMITTEE

AIR WEATHER SERVICE
TECHNICAL REFERENCE FILE
JUN 6 1951

Notes on the derivation of True Air Temperature from Aircraft Observations.

by

D. D. Clark.
(Meteorological Office)

Definition of terms used.

T_s = true air temperature
T_i = the indicated temperature
P_s = the static air pressure in the absence of position error (the true air pressure)
P_t = the total air pressure or the pressure of the air if brought to rest relative to the aircraft
q = $P_t - P_s$ the pressure rise
V = the true air speed
V_i = the indicated air speed if referred to slow aircraft but now called the 'equivalent air speed' if the compressibilty of the air is significant.
V_r = the reading of the air speed indicator in the absence of position error.
P_o = the M.S.L. pressure, 1013.2 mb. ICAN
T_o = the M.S.L. temperature, 288°A ICAN
ρ_o = the M.S.L. density, 1.226×10^{-3} gm/cm³ ICAN
ρ = air density at the level considered.
α = the air speed correction factor

$$T_i - T_s = \frac{\alpha}{K^2}\left(\frac{V}{100}\right)^2$$

where K is the factor converting from knots to cm/sec.

λ defined in the equation

$$T_i - T_s = \lambda \frac{V^2}{2c_p}, \quad 0 < \lambda < 1$$

a = speed of sound; $a_o = 3.40 \times 10^4$ cm/sec.
m = Mach Number = V/a
k^2 = convertion factor knots² to (cm/sec)² = 2.65×10^3
γ = ratio of specific heat at constant pressure to specific heat at constant volume for air = 1.402

Accentuation of a symbol indicates that it has the value corresponding to the immediate neighbourhood of the static source, e.g. P_s' is the static pressure before the application of position error correction. All units unless stated are given in cm. gm. sec.

Review of existing practice.

If we start with the simple relation connecting the temperature rise with the air speed

$$T_i - T_s = \frac{\lambda V^2}{2c_p} \quad \ldots\ldots\ldots\ldots\ldots\ldots\ldots\ldots(1)$$

or its equivalent form

$$T_i - T_s = \frac{\alpha}{K^2}\left(\frac{V}{100}\right)^2 \quad \ldots\ldots\ldots\ldots\ldots\ldots(2)$$

then, given T_i and V, T_s can be found.

T_i is read off directly from the temperature indicator corrected for instrumental error, and, for slow aircraft, V is derived from the equation

$$V = V_i\sqrt{\frac{\rho_o}{\rho}} \quad \ldots\ldots\ldots\ldots\ldots\ldots\ldots\ldots(3)$$

$$= V_i\sqrt{\frac{P_o}{T_o}}\sqrt{\frac{T_s}{P_s}} \quad \ldots\ldots\ldots\ldots\ldots\ldots(4)$$

as described in the Meteorological Air Observer's Handbook p.42. In this case V_i is taken to be identical with the air speed indicator reading corrected for instrument and position errors. It is not necessary, however, to extract V separately and T_s is obtained by combining (1) and (4) in the form

$$T_i - T_s = \frac{\lambda}{2c_p}\,\frac{V_i^2 P_o T_s}{T_o P_s} \quad \ldots\ldots\ldots\ldots\ldots\ldots(5)$$

$$\text{or} \qquad T_s = \frac{T_i}{\left(1 + \frac{\lambda}{2c_p}\,\frac{V_i^2 P_o}{T_o P_s}\right)} \quad \ldots\ldots\ldots\ldots(6)$$

As speeds increase these simple relationships no longer hold and it is necessary to distinguish between V_i, sometimes called the 'equivalent air speed' and defined as V_i in (3) or (4), and V_r which is the reading on the air speed indicator, corrected for instrumental error.

The energy equation under adiabatic conditions can be written

$$\frac{q}{P_s} = \left\{1 + \frac{\gamma-1}{2}\left(\frac{V}{a}\right)^2\right\}^{\frac{\gamma}{\gamma-1}} - 1 \quad \ldots..(7)$$

or using (3) where V_i now stands for the 'equivalent air speed'

$$\frac{q}{P_s} = \left\{1 + \frac{\gamma-1}{2}\,\frac{P_o}{P_s}\left(\frac{V_i}{a_o}\right)^2\right\}^{\frac{\gamma}{\gamma-1}} - 1 \quad \ldots(8)$$

Expanding the R.H.S. of(8) and remembering that $a_o = \gamma P_o/\rho_o$ we get

$$q = \frac{\rho_o V_i^2}{2}\left\{1 + \frac{P_o}{4P_s}\left(\frac{V_i}{a_o}\right)^2 + \frac{2-\gamma}{24}\left(\frac{P_o}{P_s}\right)^2\left(\frac{V_i}{a_o}\right)^4 + \ldots\right\} \ldots(9)$$

Now, in U.K. air speed indicators are calibrated according to the formula

$$q = \frac{\rho_o V_r^2}{2}\left\{1 + \frac{1}{4}\left(\frac{V_r}{a_o}\right)^2\right\} \quad \ldots\ldots\ldots\ldots\ldots\ldots\ldots(10)$$

In the absence of position error, when V_r would refer to the reading of the air speed indicator in the free air stream, (9) and (10) together give the relation between V_i and V_r, namely,

$$V_r^2 \left(1 + \frac{V_r}{4a_o{}^2} \right) = V_i{}^2 \left(1 + \frac{P_o}{4P_s} \left(\frac{V_i}{a_o}\right)^2 + \frac{2-\gamma}{24} \left(\frac{P_o}{P_s}\right)^2 \left(\frac{V_i}{a_o}\right)^4 + \ldots \right) \ldots(11)$$

Many sets of tables are available giving the values of V_i corresponding to values of V_r, and the conversion from V_r to V_i is termed 'correcting for the compressibility error'.

If in (4), V_r were used as V_i, then the value of V which would be obtained would be too large by an amount ΔV where, if all terms containing $(V_i/a_o)^8$ or smaller be neglected,

$$\Delta V = 0.285 \sqrt{\frac{\rho_o}{\rho}} \left(\frac{P_o}{P} - 1 \right) \left(\frac{V_i}{100} \right)^3 \ldots\ldots\ldots(12)$$

$$= 0.285 \frac{P_s T_o}{P_o T_s} \left(\frac{P_o}{P} - 1 \right) \left(\frac{V}{100} \right)^3 \ldots\ldots\ldots\ldots(13)$$

In table 1 are given some of the values of ΔV from (13) for three selected air speeds and three altitudes, T_s being assumed to have the values corresponding to an ICAN atmosphere. The table also shows the errors in T_s which would arise from using V_r for V_i in (4) assuming $\lambda = 10^{-4} \times 2c_p/K^2$ (i.e. $a = 1$). The temperature errors have been converted to °F for convenience.

Table 1.

Pressure Altitude mb.	True air speed in knots 200 error in air speed knots	 error in temperature °F	 300 error in air speed knots	 error in temp. °F	 400 error in air speed knots	 error in temp. °F
500	1.28	0.09	4.3	0.46	10.2	1.5
300	2.0	0.14	6.7	0.66	16.0	2.3
150	2.6	0.19	8.6	0.87	20.5	2.9

When the position error has to be taken into account then, assuming the position error to be in the form of a static pressure correction ΔP_s the value of V_r should first be adjusted by applying the correction ΔV_r corresponding to ΔP_s obtained by differentiation of (10)

$$\Delta V_r = - \frac{\Delta P_s}{\rho_o V_r'(1 + V_r'^2/2a_o^2)} \ldots\ldots\ldots\ldots(14)$$

In this expression accents indicate values referred to the neighbourhood of the static source, i.e. before the position error has been applied. If desired, the tables or graphs giving V_i in terms of V_r from (11) can be modified with the aid of (14) to give V_i directly from V_r' thus combining the two steps $V_r' \rightarrow V_r$, $V_r \rightarrow V_i$ into one.

Charnley and Fleming (Ref.1) however prefer to insert the correction for position error after the correction for compressibility which means working with elaborate correction formulae but which, since the two steps are finally combined, comes to the same in the end.

In the method of approach to the true air temperature outlined above, the introduction of such terms as the 'indicated air speed' and the 'equivalent air speed' produces artificial errors which have thenceforth to be eliminated by manipulating awkward mathematical formulae. It is therefore more logical and much simpler not to employ the terms V_r and V_i but to use instead the pressure terms from which they are derived, namely q and P_s. In the method which will now be described this course has been adopted and a much neater analysis is obtained which leads to a more rapid derivation of the true air temperature.

Re-writing (1)

$$T_i - T_s = \frac{\lambda V^2}{2c_p}$$

and putting $a^2 = \gamma(c_p - c_v)T_s$ we get

$$T_i - T_s = \frac{\lambda V^2 (\gamma - 1) T_s}{2a^2} \quad \ldots\ldots\ldots\ldots(15)$$

or

$$T_s = \frac{T_i}{1 + \lambda(\gamma - 1)m^2/2} \quad \ldots\ldots\ldots(16)$$

It will be seen that (15) and (5) and (16) and (6) are equivalent forms. Now from (7) remembering that $m^2 = V^2/a^2 = V^2\rho/\gamma P$

$$\frac{\gamma - 1}{2} m^2 = \left(1 + \frac{q}{P}\right)^{\frac{\gamma - 1}{\gamma}} - 1 \quad \ldots\ldots(17)$$

For purposes of reference denote either side of this equation by F

$$\text{i.e. } F\left(\frac{q}{P}\right) = \left(1 + \frac{q}{P}\right)^{\frac{\gamma - 1}{\gamma}} - 1$$

Equation (16) can now be written

$$T_s = \frac{T_i}{1 + \lambda\left[\left(1 + \frac{q}{P_s}\right)^{\frac{\gamma - 1}{\gamma}} - 1\right]} \quad \ldots\ldots(18)$$

Equation (18) gives a direct expression for T_s in terms of the known quantities q, P_s and T_i for a thermometer of known λ, and incorporates all the steps represented by equations (5) to (11). If, in addition, q/P_s be treated as one variable, T_s could be obtained from one set of tables involving T_i and q/P_s, given λ.

It follows from what is discussed in the Appendix that, if interpolation is allowed, tables of this type could be constructed having some eighty-four entries of q/P_s against, say, two hundred entries of temperature in degrees Fahrenheit, and that a separate set of such tables would be required for each value of λ. If these figures were represented graphically then several curves corresponding to several values of the parameter λ could be drawn and the whole set of information would be contained on one graph.

To give the required degree of accuracy, however, without interpolation, the tables would have to contain at least ten times as many entries of q/P_s and at least twice as many entries of T_i which would make them unwieldy for normal observing duty. It is better therefore, in computing T_s from equation (18), first to form the function F(q/P) by the aid of tables and then to complete the calculation by slide rule. Table II, which is described in detail in the Appendix, gives values of F(q/P) in terms of q/P and Figure 1 shows F(q/P) graphically.

The use of q in these calculations raises the question of whether it is worth having instruments calibrated in terms of q instead of V_r as at present. Meanwhile, however, q can be obtained readily by a straight conversion from V_r using equation (10). The pressure equivalents, q, of values of V_r over the range 200-600 knots are given in table III.

The successive steps in both methods are compared below, it being assumed that all instrumental readings have been corrected for instrumental errors.

Existing method using V_i

(i) Apply the position error correction.
(ii) Convert V_r to V_i by applying the compressibility correction.
(iii) Using (5) or (6) obtain T_s by slide rule

OR

(i) Apply the compressibility correction to V_r.
(ii) Apply the position error correction to the result of (i) to get V_i

(iii) As before.

As already mentioned, steps (i) and (ii) may be combined but, as this means the manipulation of three variables V_r, P_s and the position error to give V_i, the combination can only be rendered graphically.

Alternative method using q.

(i) Apply position error corrections to q' and P_s'.
(ii) Form the function $F(q/P)$ from tables.
(iii) Use (18) and obtain T_s by slide rule.

Discussion.

In the first method, the application of the position error (if we do not wish to use the multitudinous graphs which result from combining steps (i) and (ii),) entails making some side calculations or using subsidiary graphs or tables based on equation (14) or similar. Also, in the step to V_i, the pressure occurs as an additional parameter which, even if the applications of position error and compressibility error are separated, means taking account simultaneously of P_s and V_r, whereas, in the alternative method, the replacement of V_r by q, eliminating V_r from the argument, allows the ratio q/P_s to appear as an independent variable, thus simplifying the analysis.

Furthermore step (iii) in the first method still contains the extra variable P_s, in addition to V_i, and is therefore longer than the corresponding step (ii) in the alternative method which contains only $F(q/P)$.

Reference.

(1) CHARNLEY W. J. and FLEMING I, Corrections applied to air-speed indicator and altimeter readings for position error and compressibility effects.
R.A.E. Report No. Aero 2299, February 1949.

Appendix.

The pressure rise which we have called q could be obtained either directly from the airspeed indicator or else from a second aneroid measuring the total pressure P_t. The proportional error in the first case, (obtained by logarithmic differentiation of (18), assuming $\lambda = 1$ and $\Delta T_i = 0$ to simplify the formulae) is given by

$$\left(\frac{\Delta T_s}{T_s}\right)_q = \frac{\gamma - 1}{\gamma}\,\frac{\frac{q}{P_s}}{1 + \frac{q}{P_s}}\left(\frac{\Delta P_s}{P_s} - \frac{\Delta q}{q}\right) \quad \ldots\ldots\ldots(19)$$

i.e.

$$\left|\left(\frac{\Delta T_s}{T_s}\right)_q\right|_{max} = \frac{\gamma - 1}{\gamma}\,\frac{\frac{q}{P}}{1 + \frac{q}{P}}\left(\left|\frac{\Delta P_s}{P_s}\right| + \left|\frac{\Delta q}{q}\right|\right) \quad \ldots\ldots(20)$$

Likewise in the second case from (18) putting $1 + \frac{q}{P_s} = \frac{P_t}{P_s}$

$$\left(\frac{\Delta T_s}{T_s}\right)_{P_t} = \frac{\gamma - 1}{\gamma}\left(\frac{\Delta P_s}{P_s} - \frac{\Delta P_t}{P_t}\right) \quad \ldots\ldots\ldots\ldots\ldots(21)$$

i.e.

$$\left|\left(\frac{\Delta T_s}{T_s}\right)_{P_t}\right|_{max} = \frac{\gamma - 1}{\gamma}\left(\left|\frac{\Delta P_s}{P_s}\right| + \left|\frac{\Delta P_t}{P_t}\right|\right) \quad \ldots\ldots\ldots(22)$$

If ΔP represents a position error then $\Delta P_s = -\Delta q$, $\Delta P_t = 0$ which makes (19) and (21) identical. If, however, ΔP is an instrumental error then $\left|\frac{\Delta P_s}{P_s}\right| = \left|\frac{\Delta P_t}{P_t}\right|$ and to the same order also $= \left|\frac{\Delta q}{q}\right|$ so that the ratio

$$\left|\left(\frac{\Delta T_s}{T_s}\right)_q\right|_{max} \Big/ \left|\left(\frac{\Delta T_s}{T_s}\right)_{P_t}\right|_{max} = \frac{\frac{q}{P}}{1 + \frac{q}{P}} < 1$$

From which it follows that it is advantageous to measure q directly in preference to P_t.

Present types of aneroid altimeters and airspeed indicators after correction for instrumental errors are accurate to one per cent and if great care is taken and corrections applied also for changes with temperature then one half per cent can be obtained. For our purpose we will take the figure one per cent as representing the accuracy of altimeters and air-speed indicators.

Now for any small variation in q/P of value $\Delta(q/P)$ the corresponding proportional variation in T, namely $\Delta T_s/T_s$ is, from (18) by differentiation, assuming $\lambda = 1$, and omitting any variation in T_i for the moment,

$$\frac{\Delta T}{T} = -\frac{\gamma - 1}{\gamma}\,\frac{\Delta\left(\frac{q}{P}\right)}{1 + \frac{q}{P}} \quad \ldots\ldots\ldots\ldots\ldots(23)$$

Also $$\Delta\left(\frac{q}{P}\right) = \frac{q}{P}\left(\frac{\Delta q}{q} - \frac{\Delta P}{P}\right) \quad \ldots\ldots\ldots\ldots\ldots\ldots(24)$$

So that $$\left|\Delta\left(\frac{q}{P}\right)\right|_{max} = \frac{q}{P}\left(\left|\frac{\Delta q}{q}\right|_{max} + \left|\frac{\Delta P}{P}\right|_{max}\right) \quad \ldots\ldots\ldots\ldots(25)$$

If we take $$\left|\frac{\Delta q}{q}\right|_{max} = \left|\frac{\Delta P}{P}\right|_{max} = 0.01$$

then from (24) $$\left|\Delta\left(\frac{q}{P}\right)\right|_{max} = \frac{q}{P}(0.02)$$

and hence $$\left|\frac{\Delta T}{T}\right|_{max} = 0.02\,\frac{\gamma - 1}{\gamma}\,\frac{\frac{q}{P}}{1 + \frac{q}{P}}$$

$$= 0.00572\,\frac{\frac{q}{P}}{1 + \frac{q}{P}} \quad \ldots\ldots\ldots\ldots\ldots\ldots(26)$$

The values of $|\Delta(q/P)|_{max}$ and $|\Delta T/T|_{max}$ for different values of q/P are given below.

q/P	0.1	0.2	0.3	0.4	0.5	0.6	0.7	0.8	0.9
$\lvert\Delta(q/P)\rvert_{max}$	.002	.004	.006	.008	.010	.012	.014	.016	.018
$\lvert\Delta T/T\rvert_{max} \times 10^3$	.52	.95	1.32	1.63	1.90	2.14	2.35	2.54	2.71

As would be expected the accuracy falls off at the higher speeds and higher altitudes which correspond to larger values of q/P. At a M.S.L. temperature of 15°C (288°A) and q/P = 0.1, $\Delta T = 0.15°C$ (0.27°F) and at - 53°C (220°A) and q/P = 0.8, $\Delta T = 0.56°C$ (1°F).

The values for $|\Delta(q/P)|_{max}$ in the second line suggest that if a table for F(q/P) were being constructed it would be sufficient for entries of q/P to be made at intervals of 0.001 which would then provide values of T to within the limits of instrumental accuracy.

For a pressure range of 1000 - 100 mb. approx. and indicated air speeds between 200 and 600 knots, but for true air speed not exceeding the speed of sound, the values of q/P vary between 0.06 and 0.893, tables for F(q/P) for values of q/P, spaces at intervals of 0.001 would contain 833 entries but would give the desired precision without the need for interpolation. A coarser table with steps in q/P of 0.01 would contain 84 entries, but, to get the required degree of accuracy, intermediate values would have to be interpolated which would not be practical when converting numerous temperature readings.

The limits of accuracy in the derived value of the true air temperature also depend, of course, on the accuracy in the reading of T_i. With a good aircraft thermometer using a null-reading type indicator the reading can be made to 0.1°F, and, with pointer indicators or with recorders, the best accuracy that can be expected from existing equipment is ± 0.5°F. Adding these errors to the others arising from the pressure instruments gives, with null reading type indicators, for q/P = 0.1 and T = 15°C (59°F) an accuracy to about ± 0.4°F, and at the other end of the scale for q/P = 0.8 and T = - 53°C (-63°F) an accuracy to about ± 1.1°F while with pointer indicators or recorders these figures would be larger by 0.5°F. In all cases it is assumed that λ is known and that no error arises from variations in λ.

									.08	.09
									22	.025
									48	.052
									74	.076
									96	.099
									.19	.121
									.40	.142
									.61	.162
.7	.165	.166	.168	.170	.171	.174	.176	.178	.180	.181
.8	.184	.185	.188	.190	.191	.193	.195	.196	.199	.200

/TABLE III

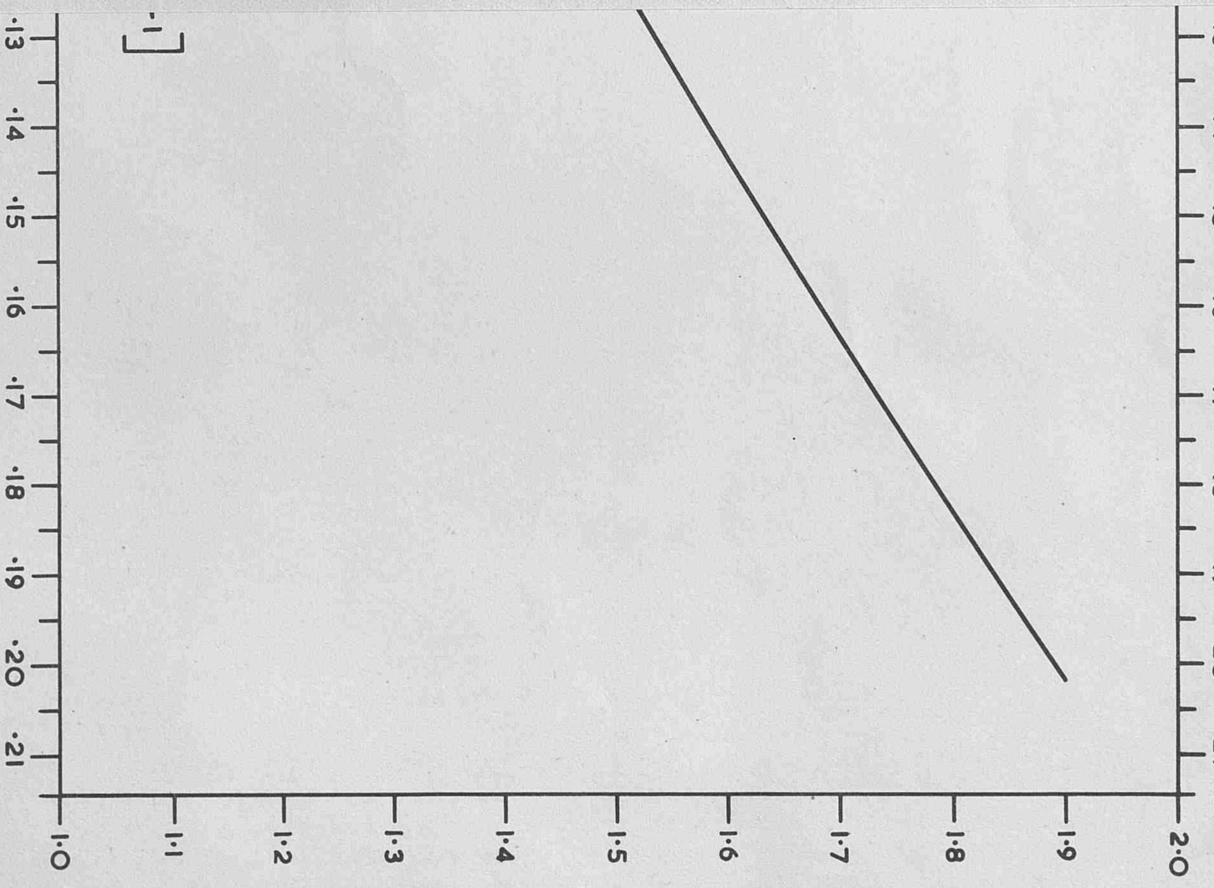

TABLE II

$$F\left(\frac{q}{p}\right) = \left(1 + \frac{q}{p}\right)^{\frac{\gamma-1}{\gamma}} - 1$$

q/p	0	.01	.02	.03	.04	.05	.06	.07	.08	.09
.0							.017	.020	.022	.025
.1	.028	.030	.033	.035	.039	.041	.043	.046	.048	.052
.2	.054	.056	.059	.061	.064	.066	.069	.071	.074	.076
.3	.078	.080	.082	.085	.087	.090	.092	.094	.096	.099
.4	.101	.104	.106	.108	.110	.113	.114	.117	.119	.121
.5	.123	.126	.127	.129	.132	.134	.136	.139	.140	.142
.6	.144	.147	.148	.150	.153	.154	.156	.158	.161	.162
.7	.165	.166	.168	.170	.171	.174	.176	.178	.180	.181
.8	.184	.185	.188	.190	.191	.193	.195	.196	.199	.200

/TABLE III

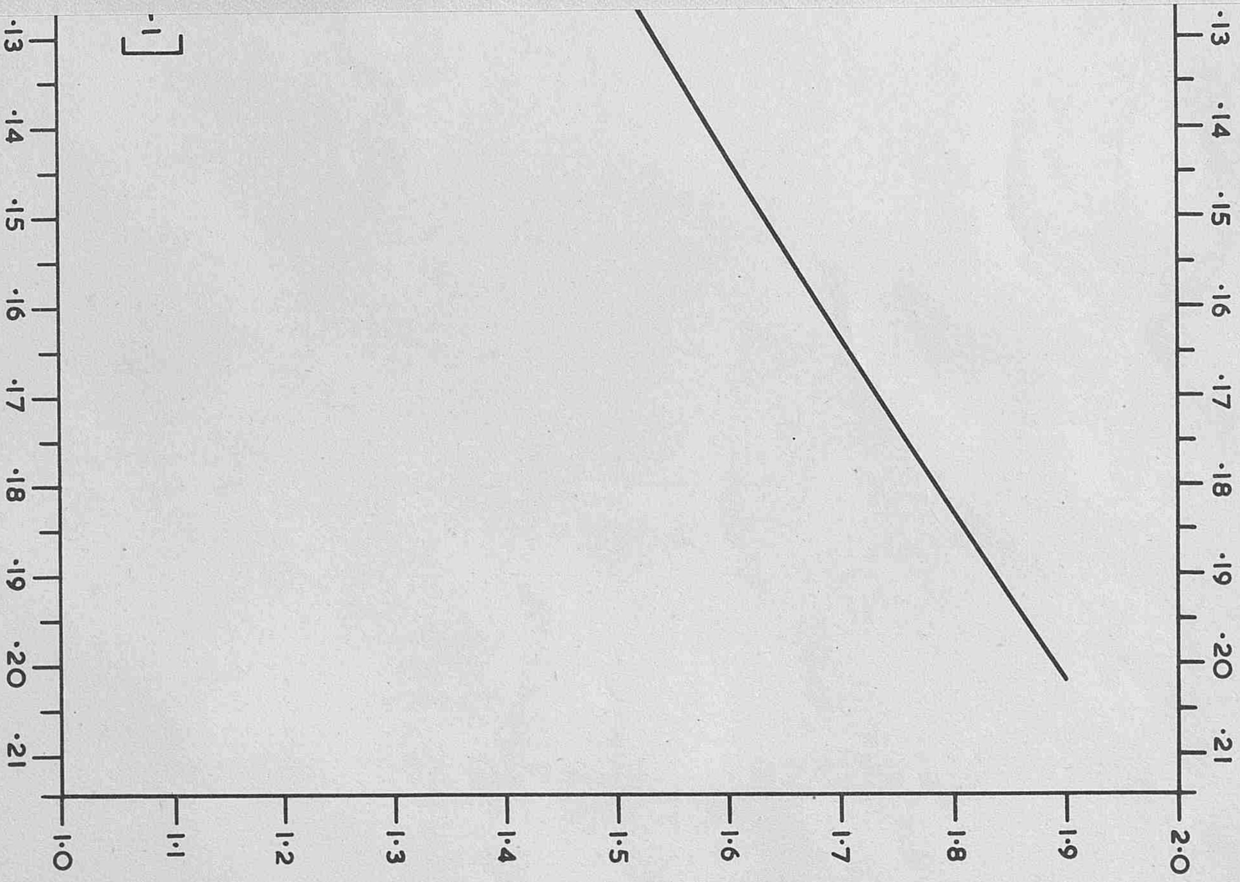

TABLE III

V_r Knots	q mb.	V_r knots	q mb.
200	66.466	400	283.694
210	73.443	410	299.312
220	80.801	420	315.495
230	88.529	430	332.199
240	96.647	440	349.402
250	105.153	450	367.109
260	114.052	460	385.325
270	123.361	470	404.055
280	133.062	480	423.677
290	143.187	490	443.465
300	153.715	500	464.187
310	164.680	510	485.475
320	176.075	520	507.335
330	187.906	530	529.774
340	200.200	540	552.796
350	212.925	550	576.408
360	226.129	560	600.615
370	239.800	570	625.952
380	253.923	580	651.386
390	268.550	590	678.000
		600	705.271

G.278584/ABC/12/50/40

The values of $|\Delta(q/P)|_{max}$ and $|\Delta T/T|_{max}$ for different values of q/P are given below.

q/P	0.1	0.2	0.3	0.4	0.5	0.6	0.7	0.8	0.9
$|\Delta(q/P)|_{max}$	.002	.004	.006	.008	.010	.012	.014	.016	.018
$|\Delta T/T|_{max}$ x 10^3	.52	.95	1.32	1.63	1.90	2.14	2.35	2.54	2.71

As would be expected the accuracy falls off at the higher speeds and higher altitudes which correspond to larger values of q/P. At a M.S.L. temperature of 15°C (288°A) and q/P = 0.1, ΔT = 0.15°C (0.27°F) and at - 53°C (220°A) and q/P = 0.8, ΔT = 0.56°C (1°F).

The values for $|\Delta(q/P)|_{max}$ in the second line suggest that if a table for F(q/P) were being constructed it would be sufficient for entries of q/P to be made at intervals of 0.001 which would then provide values of T to within the limits of instrumental accuracy.

For a pressure range of 1000 - 100 mb. approx. and indicated air speeds between 200 and 600 knots, but for true air speed not exceeding the speed of sound, the values of q/P vary between 0.06 and 0.893, tables for F(q/P) for values of q/P, spaces at intervals of 0.001 would contain 833 entries but would give the desired precision without the need for interpolation. A coarser table with steps in q/P of 0.01 would contain 84 entries, but, to get the required degree of accuracy, intermediate values would have to be interpolated which would not be practical when converting numerous temperature readings.

The limits of accuracy in the derived value of the true air temperature also depend, of course, on the accuracy in the reading of T_i. With a good aircraft thermometer using a null-reading type indicator the reading can be made to 0.1°F, and, with pointer indicators or with recorders, the best accuracy that can be expected from existing equipment is ± 0.5°F. Adding these errors to the others arising from the pressure instruments gives, with null reading type indicators, for q/P = 0.1 and T = 15°C (59°F)

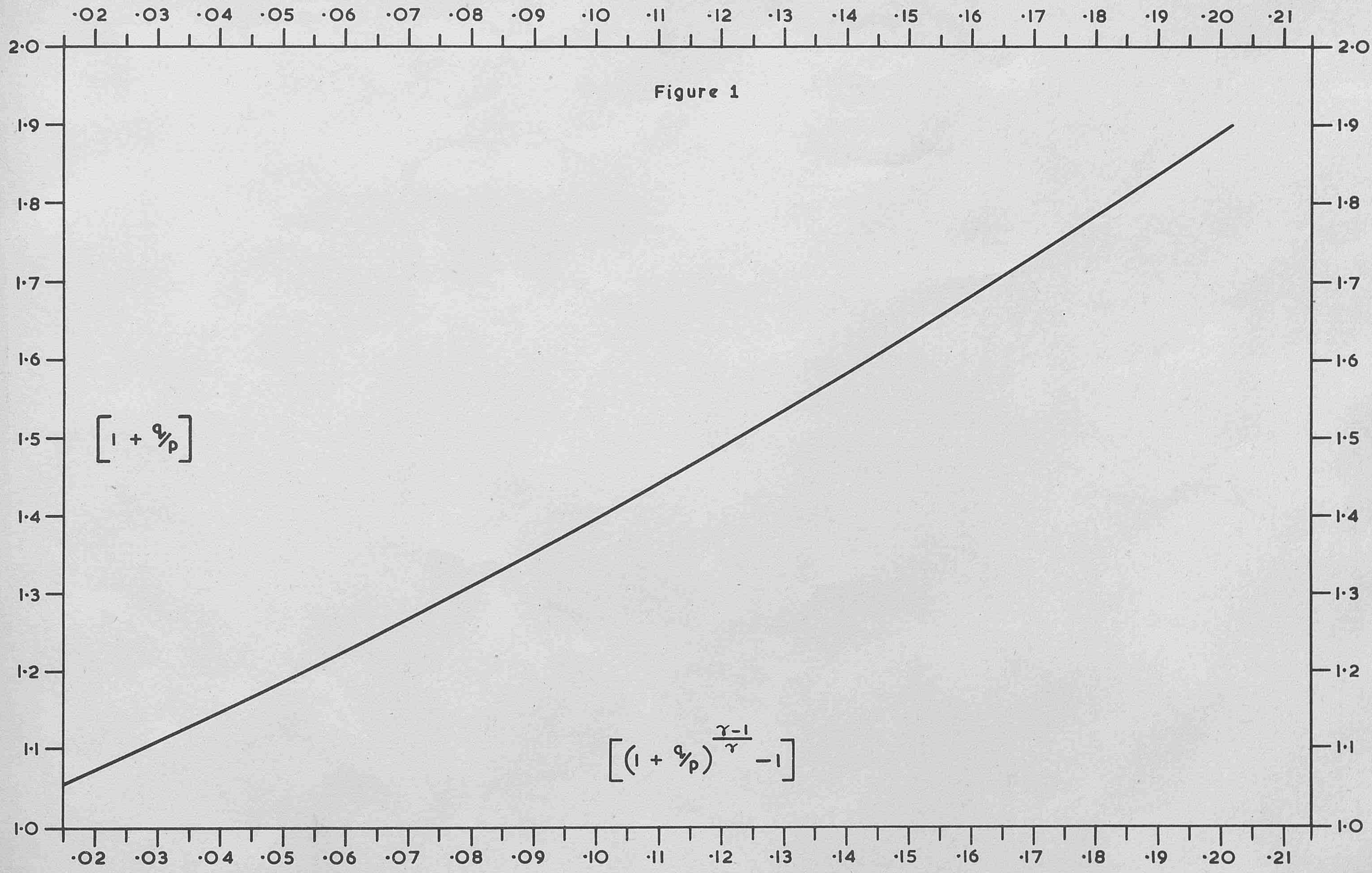

Figure 1

$\left[1 + q/p\right]$
$\left[\left(1 + q/p\right)^{\frac{\gamma-1}{\gamma}} - 1\right]$
·02
·03
·04
·05
·06
·07
·08
·09
·10
·11
·12
·13
·14
·15
·16
·17
·18
·19
·20
·21
1·0
1·1
1·2
1·3
1·4
1·5
1·6
1·7
1·8
1·9
2·0

quote this paper shou
paper of the Meteo
Committee (London),
M.R.P. No........... by
A copy is available in the Library of
the Meteorological Office."

ASTIA FILE COPY

M.R.P.605
S.C.II/66
10th January, 1951.

IR MINISTRY

METEOROLOGICAL RESEARCH COMMITTEE

ATI-200026

AIR WEATHER SERVICE
TECHNICAL REFERENCE FILE
JUN 6 1951

A Test of the Rossby Formula as applied to the movement of Long Atmospheric waves at the 500 MB. level

by
E.J. Sumner (Meteorological Office)

Table of contents

1. Introduction.

2. Existing tests of the Rossby wave formula.

RESEARCHES CARRIED OUT AT DUNSTABLE.

3. General procedure.

4. Preliminary test of the Rossby wave formula.

5. A more accurate test of the Rossby formula.

6. The effect of other factors on the movement of atmospheric waves.

7. Short-range forecasting test.

8. Medium-range forecasting test.

9. Conclusions.

Summary.

Various measurements appertaining to long atmospheric waves are made on one year's 500 mb. charts. The 24-hour zonal displacements of these waves, considered as trough-pairs, are correlated with estimates based on the Rossby formula, the parameters involved being computed in accordance with a definite procedure. The correlations for the warmer seasons are small, while those for the cooler seasons are only moderately good. However, when the data are smoothed, to reduce random errors the correlation coefficients are considerably improved. In all cases the formula has to be modified by means of regression coefficients in order to secure the best fit to the data.

The mean zonal velocity and the wave-length parameters as measured here are shown to be important factors in determining the speed of long waves, but the effect of latitude is not established.

The modified Rossby formula is tested on independent data; no improvement on current short- and medium-range forecasting techniques is effected.

1. Introduction.

1.1 The wave-like flow patterns which occur in the prevailing westerlies of the middle and upper troposphere are often sufficiently conserved, sometimes over a period of days, to be identifiable in broad features on successive synoptic charts. They are associated directly or indirectly with typical weather phenomena and it is of some importance in short- and medium-range forecasting to be able to anticipate their speed or propagation.

/The

paper of the Meteorological Research
Committee (London),
M.R.P. No.......... by Mr.........................
A copy is available in the Library of
the Meteorological Office."

M.R.P.605
S.C.II/66
10th January, 1951.

IR MINISTRY

METEOROLOGICAL RESEARCH COMMITTEE

ATI-200026

A Test of the Rossby Formula as applied to the movement of Long Atmospheric waves at the 500 MB. level

by

E.J. Sumner (Meteorological Office)

AIR WEATHER SERVICE
TECHNICAL REFERENCE FILE
JUN 6 1951

Table of contents

1. Introduction.

2. Existing tests of the Rossby wave formula.

RESEARCHES CARRIED OUT AT DUNSTABLE.

3. General procedure.

4. Preliminary test of the Rossby wave formula.

5. A more accurate test of the Rossby formula.

6. The effect of other factors on the movement of atmospheric waves.

7. Short-range forecasting test.

8. Medium-range forecasting test.

9. Conclusions.

Summary.

Various measurements appertaining to long atmospheric waves are made on one year's 500 mb. charts. The 24-hour zonal displacements of these waves, considered as trough-pairs, are correlated with estimates based on the Rossby formula, the parameters involved being computed in accordance with a definite procedure. The correlations for the warmer seasons are small, while those for the cooler seasons are only moderately good. However, when the data are smoothed, to reduce random errors the correlation coefficients are considerably improved. In all cases the formula has to be modified by means of regression coefficients in order to secure the best fit to the data.

The mean zonal velocity and the wave-length parameters as measured here are shown to be important factors in determining the speed of long waves, but the effect of latitude is not established.

The modified Rossby formula is tested on independent data; no improvement on current short- and medium-range forecasting techniques is effected.

1. Introduction.

1.1 The wave-like flow patterns which occur in the prevailing westerlies of the middle and upper troposphere are often sufficiently conserved, sometimes over a period of days, to be identifiable in broad features on successive synoptic charts. They are associated directly or indirectly with typical weather phenomena and it is of some importance in short- and medium-range forecasting to be able to anticipate their speed or propagation.

The best known formula is that of Rossby (1939) who showed the velocity (c) of plane non-divergent waves in an autobarotrophic atmosphere is given by

$$c = U - \frac{\beta L^2}{4\pi^2} \qquad \text{.........} \quad (1)$$

where U is the mean zonal velocity (assumed uniform everywhere), L the wave-length and β the rate of change of Coriolis parameter with latitude. The waves form an equally spaced, uniformly progressive, harmonic train of pertubations extending to infinity in all directions. As was pointed out by Neamtan (1946) the formula also applies under the same conditions to finite amplitude waves.

Various modifications of equation (1) have been suggested based on a model more in keeping with synoptic experience. For example, account has been taken of the finite width of atmospheric disturbances (Haurwitz, 1939; Neamtan, 1946), lateral shear in the basic zonal current (Thompson, 1948), and the inclination of the axes of the individual troughs and ridges to the direction of movement of the train as a whole (Machta, 1949).

1.2. Although quasi-permanent wave forms do occur on synoptic charts they are always baroclinic in some degree and the barotropic assumption is thus perhaps the most unrealistic feature of the analysis. Apart from any general objections to the neglect of baroclinity, the change in wind velocity with height in the real atmosphere raises the practical problem of deciding which level (if any) is most suitable for computing the zonal velocity. Charney (1947) has indicated that the Rossby formula may be applied to baroclinic wave pertubations provided the mean zonal velocity throughout the depth of the atmosphere is used for U in equation (1). In winter, at least, this mean velocity is on an average approximately equal in value to the actual zonal velocity in the vicinity of the 600 mb. level, though in individual cases considerable departures must often arise. In a later publication (1949) this "equivalent - barotropic level" is given as between 550 and 600 mb.

2. Existing Tests of the Rossby wave formula.

2.1 Cressman (1948) has made a specific test on daily charts. He showed that the simple wave formula (equation 1) "may by applied on daily maps to the long stationary or progressive waves in a broad current of upper westerlies, with am error not greater than errors inherent in computation and vertification." This test was for the limited period from autumn, 1946, to spring, 1947, and for the area 170°E eastward to 50°W; also it only applied to well-marked sinusoidal wave trains which are conserved for several days on successive charts, cases of retrogression being excluded.

The wave-length used in the computations was the trough-to-trough distance on 700 mb. charts, but the zonal velocity was computed from the estimated meridional pressure profile at the 600 mb. level. Each 24-hour movement was observed at every 5 degrees of latitude, both at the beginning and the end of the day, and meaned for two successive troughs. The actual observed motion of the pair of troughs and the estimated 24-hour displacements were averaged over a period of several days.

Using this procedure, the average of the absolute values of the errors was about 2° longitude a day and the distribution of errors was symmetrical "indicating that the 600 mb. surface was at approximately the optimum height for the determination of the zonal wind speed."

2.2 In a later paper, Cressman (1949) has taken into account the variation of wave length with longitude and its effect on the speed of propagation. Under similar restrictions as above fifty cases for an unstated period were studied and the average error, irrespective of sign, between the actual and computed displacements of the waves (taking account of wave-length variations) was about 6° of longitude. The error using the straight-forward Rossby wave equation, the initial zonal velocity and wave-length being assumed constant throughout, was 11° of longitude for the 3-day displacements. This compares with 13° of longitude obtained by simply extrapolating a previous 24-hour movement for the 3-day period.

RESEARCHES CARRIED OUT AT DUNSTABLE

3. GENERAL PROCEDURE.

3.1 Selection of data.

It is evident from the previous section that periods can be found during which well-defined and steadily moving sinusoidal wave trains move more or less in accordance with the Rossby wave formula. The present test is concerned with the question of how far this formula is applicable prognostically to a more general class of wave-like disturbances, showing varying degrees of distortion and complexity, and to determine any likely empirical modifications which may suggest themselves. The emphasis throughout is on the practical possibilities of numerical application as a routine to short- and medium-range forecasting. For this purpose we are limited to the standard levels used in normal synoptic practice and of these the 500 mb. level was chosen as that for which charts covering the greatest area were available. This level has the virtue of being closest to the equivalent-barotropic level of Charney (1949) to which the Rossby formula seems to be more applicable.

This study was confined to one year's charts only, viz. 1st September, 1948 to 31st August, 1949, and the half-hemisphere from 120°W eastward to 60°E, the data being segregated into seasons. The observational coverage generally ruled out any consideration of a more extended area, but there were occasions when troughs were followed eastward beyond the Urals or were picked up west of the Rockies. The patterns were selected entirely without reference to any other isopleths or any other levels, the sole criterion being a 500 mb. chart with anything resembling a coherent wave train represented by at least two distinct troughs separated by a ridge. The waves (troughs) were considered in over-lapping pairs: n waves gave (n - 1) pairs which were each treated as a separate case. Closed centres sometimes occurred in association with the flow patterns, and the ridges between the troughs were sometimes vestigial. Cases of both retrogression and progression were included.

3.2 Specification of the position and character of waves.

In order to locate the wave train as a whole a latitude was selected (to the nearest 5°) which was central to the pattern. The logitudinal position of the troughs and ridges with respect to this datum latitude was determined by where the axes (defined as lines joining the lowest or highest latitudes of individual contours of the troughs and ridges, respectively) cut the selected latitude. An example of an actual wave-pair showing the axes and the selected latitude is given in Fig.1.

In addition to these measurements the individual troughs were classified as tilted or not, the precise direction of tilt being noted, and their amplitude measured in accordance with a definite procedure. The amplitude of a particular trough-pair was taken as the average of the amplitude of troughs comprising it.

3.3. The determination of the various parameters in the Rossby wave formula.

The Rossby wave formula requires some measure of U the basic zonal velocity, L, the wave-length and the parameter β . The latter was taken as the appropriate value at the selected latitude, and L was defined as the trough-to-trough distance between the points where their respective axes cut the selected latitude.

The determination of the value of U presents more difficulty. In the simple model originally used by Rossby this parameter is the mean zonal flow over any width containing the wave since the basic current is constant over the entire field. However, atmospheric waves are always finite in width and have some lateral shear, so that averaging gives different values for different zonal widths. It was therefore decided to compute U in a number of different ways in order to decide which gave the best results under test.

The first two parameters computed, U_1 and U_2, were respectively determined by the mean zonal flow (expressed as the geostrophic equivalent of the mean pressure gradient) and for the two bands 10° and 20° of latitude in width, 5° and 10° on either side of the selected latitude. Those values were computed only for the restricted sector comprising a particular pair of waves.

Since the selected patterns often contained closed centres, a certain amount of easterly flow occurred which effectively reduced the values of the above parameters, particularly U_2. It was therefore decided to use certain additional indices following the main flow round the troughs and ridges. A line judged to be more or less central to the flow was followed and pressure differences for 10° and 20° ranges of latitude were read off at given points along the profiles. The geostrophic equivalent of the mean of these readings determined the two indices U_3 and U_4, respectively.

The zonal index for the fixed latitude band 35 - 55°N, and for a sector from 120°W to 60°E, has been computed as a routine in the Forecasting Research Division and conveniently provides an alternative index U_5.

4. PRELIMINARY TEST OF THE ROSSBY WAVE FORMULA.

4.1 Procedure and presentation of results.

In the test 24-hour displacements were estimated by means of equation (1), using all of the five values of the zonal parameter (as computed above) in turn, together with the relevant values of β and L. Each of these was correlated with the actual subsequent 24-hour displacements of the upwind and downwind troughs of particular trough-pairs separately, and with the average displacements of both troughs of a pair. For U_2 and U_4 these computations were done for the four seasons individually and for the entire year collectively, but, for reasons which will appear later, only the correlations for the cooler seasons (winter and spring) were worked out for U_1, U_3 and U_5. The data were further segregated into one class comprising all the data without discrimination, and another for which there were no complications, either apparent before the event or occurring during the ensuing 24 hours, due to new developments, sudden intensifications, minor-waves, cut-offs and marked lack of a through-flow connecting the two troughs in question.

Table 1 shows these linear correlation coefficients together with the coefficients (a, b) for the regression of the actual displacements (A) on the estimated (E) in the form $A' = aE + b$, so that A' is the best fit with actuality which can be obtained from a given estimate. The correlations for data based on U_1, U_2,———U_5, are designated by r_1, r_2,————r_5, respectively. The average values of the zonal parameters and the wave-lengths used in these computations are show in the appendix.

Table 1. Showing the correlation coefficients and regression coefficients corresponding to various categories of data.

		Zonal parameter		Band fixed with respect to selected latitude.						Band following the flow						Fixed latitude (33-55°) 20° band width - U_5		
				10° width - U_1			20° width - U_2			10° width - U_3			20° width - U_4					
Displacements	Season/	No. of Observations	Type of Data	r_1	a	b	r_2	a	b	r_3	a	b	r_4	a	b	r_5	a	b
Upwind trough	Autumn	16	Selected				0.07	0.06	5.3				-0.10	-0.02	5.8			
		23	All				0.10	0.11	5.7				0.01	0.02	6.2			
	Winter	14	Selected	0.36	0.25	2.4	0.35	0.30	1.5	0.48	0.32	-1.0	0.21	0.19	2.1	-0.03	-0.04	4.4
		18	All	0.34	0.25	2.9	0.41	0.37	2.9	0.39	0.28	0.0	0.17	0.16	2.5	-0.04	-0.06	4.1
	Spring	48	Selected	0.34	0.27	5.8	0.44	0.36	5.3	0.41	0.37	3.2	0.45	0.46	3.4	0.37	0.44	6.3
		55*	All	0.27	0.27	6.3	0.35	0.36	5.8	0.41	0.45	2.4	0.42	0.54	2.9	0.34	0.49	6.3
	Summer	55	Selected				0.27	0.31	2.3				0.17	0.26	1.8			
		77	All				0.21	0.23	1.9				0.18	0.27	1.1			
	Year	133	Selected				0.44	0.40	3.3				0.40	0.45	1.7			
		173*	All				0.41	0.41	3.1				0.42	0.53	0.9			
Downwind trough	Autumn	16	Selected				0.23	0.27	3.7				0.62	1.43	-8.9			
		23	All				0.41	0.56	3.2				0.64	1.43	-7.8			
	Winter	14	Selected	0.68	0.59	2.2	0.69	0.69	1.7	0.81	0.69	-5.3	0.80	0.82	-4.3	0.67	1.03	-1.1
		18	All	0.64	0.56	2.9	0.66	0.66	2.3	0.77	0.66	-4.0	0.76	0.83	-3.7	0.50	1.03	-0.7
	Spring	48	Selected	0.52	0.56	3.1	0.58	0.65	3.1	0.56	0.68	-1.0	0.57	0.81	0.0	0.49	0.78	5.1
		55*	All	0.47	0.53	3.6	0.51	0.60	3.7	0.45	0.57	0.6	0.52	0.78	0.1	0.45	0.75	5.1
	Summer	54	Selected				0.32	0.29	2.6				0.37	0.45	1.9			
		76	All				0.34	0.30	2.5				0.35	0.43	1.1			
	Year	132	Selected				0.58	0.58	2.6				0.61	0.77	-0.8			
		172*	All				0.54	0.54	2.9				0.59	0.74	-0.5			
Mean Displacement of both troughs of a pair	Autumn	16	Selected				0.33	0.17	4.5				0.61	0.64	-0.8			
		22	All				0.32	0.25	4.7				0.34	0.54	1.0			
	Winter	14	Selected	0.62	0.39	2.8	0.66	0.47	2.6	0.77	0.47	-2.2	0.72	0.52	1.3	0.51	0.55	1.2
		18	All	0.71	0.44	3.1	0.63	0.45	1.8	0.70	0.43	-1.2	0.60	0.51	-0.7	0.47	0.54	1.7
	Spring	48	Selected	0.57	0.41	4.5	0.68	0.51	4.2	0.71	0.57	0.4	0.67	0.63	1.8	0.55	0.59	5.9
		55*	All	0.51	0.39	5.1	0.60	0.49	4.9	0.64	0.55	0.8	0.65	0.66	1.6	0.54	0.61	5.7
	Summer	54	Selected				0.36	0.25	2.6				0.33	0.30	1.7			
		76	All				0.35	0.24	2.3				0.30	0.28	1.5			
	Year	132	Selected				0.66	0.48	3.0				0.66	0.60	0.6			
		171*	All				0.61	0.47	3.1				0.63	0.61	0.4			

/ The seasons are defined as follows:-
Autumn the three month September - November inclusive
Winter, the three months December - February etc..

*Subtract one for r_3 and r_4.

/4.2

4.2 General remarks on the results.

A complete discussion of these results is not attempted here but the following points are noted:-

(a) The correlation coefficients are appreciably higher in the cooler seasons (winter and spring) than for the warmer seasons. They also show a large increase in value for the downwind as compared with the upwind troughs.

The formula is considered to have no practical forecasting value in the summer or for the upwind member at any season, the particular zonal and wave-length parameters used here being more appropriate to the downwind troughs. There therefore seemed little point in computing the coefficients for r_1, r_3 and r_5 for the summer season or for the few rather dubious results of this particular autumn.

(b) The correlations for the mean displacements are greater than those for either of the individual features, presumably owing to the partial elimination of random errors by the meaning process.

(c) Under the same circumstances of season and type of trough, the difference between the correlations r_1, ________ r_4 are small. This suggests that there is no optimum width over which one should mean the basic flow. However, a computation of the partial correlations between the actual 24-hour mean displacements and the individual zonal parameters suggested that none of the zonal indices used here makes any appreciable contribution to the success of the formula (but see section 5.4).

The values of r_5 are usually the lowest in the table, and the appropriate partial correlations showed that U_5 makes no contribution to the formula at all.

(d) There is a consistent increase for the "selected" data but in general this is negligibly small.

(e) In all cases the simple Rossby formula has to be modified by means of appropriate regression coefficients which vary in value from one set of data to another (mainly on a seasonal basis) and more especially with the zonal parameter used.

5. A MORE ACCURATE TEST OF THE ROSSBY WAVE FORMULA.

The preceding section was concerned with a crude practical test of the Rossby wave formula. The data used are affected by errors of drawing and measurement[*], apart from the possible short-period effect of such factors as topography and friction. Moreover, the general form of the equation was accepted without comment. A rigorous test of the formula requires that the effect of these disturbances should be eliminated or, at least, effectively reduced, and, in order to assess the validity of the theory the importance of the individual parameters in the equation must be considered.

5.2 Smoothing procedure and initial results.

In order to smooth out the various errors as much as possible a verification procedure similar to that of Cressman (1948) was adopted. Occasions on which a particular wave-pair was conserved for three days were chosen and the average displacements of the troughs in deg. long./day were correlated with the averages of the three daily estimates (using U_2 for convenience).

---

[*] A practical test showed that the average error due to drawing and measurement was about 2-3° long. at all seasons.

Preliminary calculations using this smoothing technique showed a definite increase in the values of the correlation coefficients at all seasons. For the mean trough displacement, for example, the r_2-correlation for the cool seasons collectively (38 cases) was 0.82, and 0.63 for the warmer seasons (61 cases). The partial correlations (cool seasons) were as follows: mean displacement with U_2, 0.32; mean displacement with the expression βL^2 , - 0.85. The lowness of the first partial correlation confirms the lack of importance of these zonal parameters (section 4.2(c)) in determining the wave velocity. However, it seemed so unlikely a *priori* that the strength of the zonal current was of such little significance that it was decided to repeat some of the above computations making a more accurate determination of the central latitude.

5.3 A more accurate central latitude.

The individual daily values for the 38 3-day periods (cool seasons) described in section 5.2 were carefully recomputed, the selected latitude was now being to the nearest whole degree. The parameter U2 was calculated as before, i.e. for a 20° band and for a sector just containing the wave-pair in question. It was also considered worth while to evaluate a new zonal index (U_6) for a 30° band-width. The troughs were positioned with respect to this datum latitude, but as it was felt that a single-point location was perhaps insufficient they were also positioned by means of the two additional points at which their axes cut the latitude lines 10° on either side of the datum latitude. The three longitudinal values for each trough were meaned to give a representative position.

Table 2 sets out the results of this work for the r_2 - correlations. Apart from the usual symbols the partial correlations ρ_1 (actual displacement with U_2) and ρ_2 (actual displacement with βL^2) are shown for the individual features and the mean trough displacement. The corresponding figures for the latter, with the troughs positioned by three intersections, are given at the bottom of the table. The last column contains the appropriate correlations (r) using all the 64 daily values making up the 3-day periods.

Table 2. Showing the r_2-correlations, regression coefficients, and partial correlations for data based on 3-day averages; the selected latitude is to the nearest degree and troughs are positioned at one or three points, respectively. Cool seasons only.

Trough	No. of cases	r_2	a	b	ρ_1	ρ_2	r (based on daily values)
Upwind	38	0.72	0.52	4.1	0.26	-0.71	0.40
Downwind	38	0.90	0.76	2.2	0.64	-0.82	0.65
Mean displacement	38	0.93	0.64	3.1	0.65	-0.90	0.71
Mean displacement, troughs positioned at 3 points.	38	0.91	0.60	3.5	0.62	-0.84	0.62

Except for the upwind trough, there was a noticeable increase in the values of r_2, compared with the previous results (section 5.2) which seemed to be effected mainly by the presumably more representative determination of the zonal index. The increase in ρ_1 is particularly notable;[*] although still smaller than ρ_2 it now represents a useful contribution to the success of the formula. The average departure of the actual displacements from the line of best fit is 1.4 deg. long./day for the mean trough displacements, which is well within the limits of error of drawing and measurement.

---

[*] In this connection, the value of ρ_1 for the general parameter U_4, everything now being with respect of the more accurate selected latitude, was only 0.33 for the corresponding data, which justifies the use of U_2 throughout in this main section.

The smallness of both partial coefficients for the upwind trough is perhaps what one would expect. The simple type of interaction envisaged by the Rossby theory is a downwind effect the pressure field progressively adapting itself to the field of motion while the individual air particles follow constant vorticity trajectories. The very low value of ρ_1 implies that it is the zonal index rather than the wave-length that is least representative of conditions further upwind on which its rate of propagation may be expected to depend.

The corresponding correlations when the troughs were positioned at three points (mean trough only) are all lower than when the normal procedure was adopted although the difference is small, and, evidently, nothing is to be gained by the more elaborate measurements.

Table 3 shows the results for the zonal parameter U_6, the corresponding correlation coefficient being designated by r_6, and the partial correlation with this index by ρ_3. The axes of the troughs are positioned at one point (top line) and three points (bottom line), respectively.

Table 3. Showing the r_6-correlations, regression coefficients and partial correlations for the same data as in the preceding table (mean displacement only).

No. of cases	r_6	a	b	ρ_3	ρ_2
38 (one point)	0.92	0.69	4.3	0.61	-0.91
38 (three points)	0.91	0.69	4.9	0.53	-0.88

Here again there is little significant difference between any of the corresponding correlations in this and the previous table. These findings confirm that there is no optimum width over which one should mean the basic zonal flow in order to achieve the best results.

5.5 The effect of latitude.

The variation of Coriolis parameter (l) with latitude, viz., β , is of fundamental importance in the Rossby wave theory, and it was therefore decided to attempt an assessment of the significance of β in the formula. For the 38 "smoothed" data considered in section 5.3 the value of $4\pi^2(c - U_2)/L^2$

(β' , say), obtained by solving for β in equation (1), was found in each case and compared with what it should be at the datum latitude in question. This latter was taken as the average of the three latitudes for the individual days comprising a 3-day spell. The values of β and β' were then plotted graphically on the same scale. There was little discernible relationship between them. It must be pointed out, however, that all the 38 datum latitudes lay between 41° and 59°N (27 of them between 50° and 59°N), and it is considered that, owing to the smallness of the variations of β over the range encountered, the data are not sufficiently accurate to show the effect looked for.

6. THE EFFECT OF OTHER FACTORS ON THE MOVEMENT OF ATMOSPHERIC WAVES.

6.1 The general importance of the zonal velocity and the wave-length (especially the latter) in determining the speed of atmospheric waves has been established by the above results. Moreover, it is evident that under ideal conditions for which a wave-train (or pair) is conserved for at least a 3-day period, an equation of the form $a(U - \beta L^2/4\pi^2) + b$ provides a remarkably good fit to the actual wave speed. However, in view of the possible effect of various other parameters, such as lateral shear and tilt of the axes, and also of departure from the "equivalent-barotropic level" a certain amount of modification of the individual parameters of the Rossby equation is to be expected. Treating U and βL^2 as independent variables (for the 38 smoothed data, downwind troughs and for U_2, only) the following multiple regression equation was obtained:

$$A' = 0.80\, U_2 - 0.72\, \frac{\beta L^2}{4\pi^2} + 1.0$$

The appropriate partial correlation coefficients are given in Table 2. As was expected, both terms had to be reduced by different numerical factors.

6.2 Following on this an attempt was made to assess the importance of various likely parameters on the movement of these waves. This was confined to the winter and spring data and to the downwind troughs only. However, the results were inconclusive and difficult to interpret.

There were some positive indications that waves with tilted axes tend to move faster than waves with axes more or less parallel to the meridians, other things being equal, which is in keeping with Machta's (1949) theory , but the magnitude of the effect was such that no absolute significance could be attached to the results.

The possible effect of lateral shear of the mean zonal current was not in evidence at all, possibly owing to a systematic compensation by the width parameter (see Thompson's formula, 1948). It was felt that a more specific test than we could attempt was required in order to assess the importance of lateral shear and width of the wave disturbance which would be very difficult in practice since it is almost impossible to delineate the precise boundaries of a particular wave train. However, it is as well to bear in mind that such factors as the above, apart from being of great importance in particular cases, may be sufficiently variable over longer periods and from one set of data to another to alter radically the values of the regression coefficients in an equation which ignores them.

The effect of amplitude or of simple "confluence" or "difluence" of the basic zonal current were not in evidence in these data. The lack of effect of amplitude conforms with Neamtan's (1946) demonstration that equation (1) does in theory apply to waves of any amplitude.

6.3 It is concluded from the above that insofar as the movement of long atmosphere waves is explicable on the basis of the equivalent-barotropic assumption, the appropriate model is by no means a simple one.

7. SHORT-RANGE FORECASTING TEST.

7.1 A rough comparison with the routine results obtained by the Forecasting Division (Meteorological Office, M.O.2., Dunstable) for the same period as for this investigation suggested that the Rossby formula improved slightly on present forecasting methods provided regression coefficients obtained from the data themselves were used. In order to assess the practical value of the above work a test on independent data is necessary. Ideally, regression coefficients based on many years' data are required to provide workable estimates, but failing a lengthy computation one of the regression formulae already obtained was used.

/7.2

7.2 Test on independent data.

The period chosen was from January to May, 1950, and only troughs that were preceded by another (i.e. downwind troughs) were selected (46 cases in all) the datum latitude being to the nearest whole degree. The regression coefficients it was thought best to use, were those for U_2 based on the 64 daily data comprising the 38 3-day periods (section 5.3), viz., a = 0.69, b = 2.3. For the routine forecasts the standard and mean deviations of the differences between forecast and actual displacements were 4.7 and 3.6 deg. long./day respectively. Using the above regression coefficients the corresponding figures for our own estimates based on the above coefficients were 5.6 and 4.8 deg. long./day. The average 24-hour displacement of these troughs was approximately 6.0 deg. long./day. Both results leave much to be desired, even though part of the discrepancy is due to errors of drawing and positioning. The comparative failure of the estimates based on the Rossby formula is partly due to using inappropriate regression coefficients. For the data in question, the line of best fit is obtained by putting a = 0.57 and b = 0.1 compared with 0.69 and 2.3 actually used; the correlation r_2 was 0.66, which is as high as any obtained for similar data.

7.3 Conclusion.

It is concluded from these results that no particular improvement on the standard of accuracy at present attained by routine forecasting techniques can be expected by an application of the modified Rossby wave equation. If regression coefficients based on a much longer period were available, and if in addition some segregation (for example, into simple and tilted wave forms) were attempted, it is very probable that the above figures for our estimates would be improved, but it is by no means certain that the improvement would be sufficient to better the routine results.

8. MEDIUM-RANGE FORECASTING TEST.

8.1 Preliminary check for all seasons.

During the year studied one or more wave-pairs within the half-hemisphere from the Rockies eastwards were sufficiently developed to permit measurements of the sort dealt with in the previous sections on more than one day in three. In view of the importance attached to forecasting the position of these features several days ahead, and because of their relative frequency, an investigation into the possibilities of applying the Rossby wave formula numerically in medium-range (4-day) forecasting was attempted. It is evident from later statistics (see Appendix 1) that once a definite wave-pair appears on synoptic charts it will either degenerate quickly, or, more often, persist in some recognizable form for three or four days at least.

The medium-range forecasting experiment, at present being tried out in the Research Division at Dunstable, is based on three successive 24-hour prebaratic and 1000 - 500 mb. pre-thickness charts (prepared twice a week) from which the general character of the weather over the British Isles for four days in advance is deduced. From these forecast charts the 500 mb. contour charts up to three days ahead can be obtained and a 3-day estimate of the displacement of the troughs at 500 mb. on such occasions as they appear would therefore provide a useful check on the forecast.

A trial computation of the correlations between the actual 3-day displacement of troughs and that estimated from equation (1) using the initial value of U_2 and L was made. Only the values for the cool season and the downwind troughs were considered to show sufficient promise to warrant the application of the formula numerically. The results for these data were: $r_2 = 0.89$, $a = 0.73$ and $b = 2.6$ deg. long./day.

8.2 Test on independent data and conclusion.

An attempt to apply the Rossby formula to the period January-May, 1950, using the above coefficients, gave a mean error of 12 deg. long./3 days for the only six cases, coinciding with the periods of the medium-range forecasts, for which the wave train which had been forecast to persist did so (four more, out of a total of 37 forecasts, did not). The mean error of the experimental forecasts was only 6 deg. long./3 days (the average trough displacement being 20 deg. long. in the 3 days) but the number of cases is too small to permit of a conclusive comparison.

In order to increase the number of cases the same period was reviewed, without being tied to forecast periods, and 25 3-day periods (some of them over-lapping) were found. For these data the average error was 13.0 deg. long., the corresponding mean 3-day displacement of all the downwind troughs concerned being 20 deg. long.

These results are considered to be too poor to justify the use of such simple regression formulae in medium-range forecasting.

The actual regression coefficients obtained from the data in question were $a = 0.43$ and $b = 2.8$, while r_2 was 0.55. The latter value is much lower than that previously found; even when three particular doubtful cases, involving a cutting-off and a subsequent re-intensification of the troughs, were eliminated, the correlation was only increased to 0.65. The disparity between the coefficient "a" obtained from these data and that previously obtained (viz., 0.43 as compared with 0.75) is also large.

9. Conclusions.

The main conclusions of this study may be summarized as follows:-

(a) The mean zonal velocity and the wave-length are important factors in determining the speed of long atmospheric waves. The effect of latitude is not established.

(b) There is some evidence that, under the same circumstances, tilted waves move faster tham simple wave forms. The amplitude seems to be unimportant; moreover, the possible effect of lateral shear is not apparent in the results.

(c) In all cases considered the Rossby equation had to be modified by means of empirical adjustments to secure the best fit to the data. For the same zonal parameter these regression coefficients vary sensibly from season to season and year to year.

(d) The results of a specific test are not considered to justify the use of simple wave-formulae of the Rossby type numerically in short- and medium- range forecasting practice.

Acknowledgement.

I am grateful to Dr. R.C. Sutcliffe and to the Heads of M.O.21 and M.O.22 (Research Division, Meteorological Office, Dunstable) for suggestions and criticisms received during the preparation of this report, and also to Mr. J.M. Craddock for some advice on the statistical procedures used herein. I am also indebted to Miss P. Lutt, of the same division, for considerable assistance in the computational and other work involved in the investigation,

/BIBLIOGRAPHY

BIBLIOGRAPHY

Charney J.G., 1947 - The dynamics of long waves in a baroclinic westerly current. J. Meteor., Vol. 4, No. 5, 135 - 162.

Charney J.G., 1948 - On the Scale of Atmospheric Motions. Geofysiske Publikasjoner. Vol.XVII, No. 2.

Cressman G.P., 1948 - On the forecasting of long waves in the upper westerlies. J. Meteor., Vol. 5, No. 2, 44 - 57.

Cressman G.P., 1949 - Some effects of wave-length variations of the long waves in the upper westerlies. J. Meteor. Vol. 6, No.1, 56 - 60.

Haurwitz B., 1939 - The Motion of Atmospheric Disturbances. Sears Found. Jour. Mar. Res.

Machta L., 1949 - Dynamical characteristics of a tilted-trough model. J. Meteor, Vol.6, No.4, 261 - 265.

Neamtan S.M., 1946 - The motion of harmonic waves in the atmosphere. J. Meteor., Vol.3, No.2, 53 - 56.

Rossby C.G., 1939 - Relations between Variations inthe Intensity of the Zonal Circulation and the Displacement of the Semi-permanent Centres of Action. J. Marine Res., Vol.II, No.1.

Thompson P.D., 1948 - The propagation of permanent type waves in horizonal flow. J. Meteor., Vol.5, No.4, 166-- 168.

/APPENDIX

Appendix.

The following statistics relate to the 500 mb. flow patterns studied within the period September 1st, 1949, to August 31st, 1949, inclusive.

The total number of days (occasions) in the year on which a wave train (represented by at least two troughs and a ridge) appeared was 165 and the total number of trough-pairs involved (there being more than one pair on some charts) was 246. On 10 occasions, involving 13 trough-pairs, one or both of the troughs comprising a pair were not identifiable on a subsequent 24-hour chart. There were also 11 spells (25 occasions, 32 pairs) on which the wave-pairs were conserved for one or even two days, but which for various reasons (such as lack of observations or great complexity virtually prohibiting measurements) were not used. Thus the total number of days actually studied in the above test was 130 and the total number of trough pairs was 202. The following table gives a complete list of all the occasions used in connection with these latter.

Table of Spells used in the Computations

Period		Duration of spell (in days)
From	To	
September 8th	September 12th, 1948	5
September 30th	October 5th, 1948	6
October 8th	October 11th, 1948	4
October 18th	October 21st, 1948	4
November 9th	November 11th, 1948	3
November 23rd	November 26th, 1948	4
November 30th	December 9th, 1948	10
January 2nd	January 5th, 1949	4
January 11th	January 12th, 1949	2
January 24th	January 28th, 1949	5
March 15th	March 19th, 1949	5
March 21st	March 23rd, 1949	3
April 4th	April 7th, 1949	4
April 11th	April 14th, 1949	4
April 20th	April 26th, 1949	7
April 29th	May 7th, 1949	9
May 27th	June 1st, 1949	6
June 14th	June 29th, 1949	16
July 5th	July 10th, 1949	6
July 14th	July 16th, 1949	3
August 3rd	August 23rd, 1949	21

Figure 2 shows a frequency diagram of the persistence of wave-like patterns in days. A spell of n days, say, is one in which a wave-pair (not necessarily the same wave pair) was present on n successive charts. Allowing half a day on either side on an average for the pattern to form and decay, this figure may be taken as representing the approximate duration of the spell.

2. Mean values of the zonal parameters (in deg. long./day), and the wave-length (in deg. long.)

Season	No. of Observ-ations	U_1	U_2	U_3	U_4	Wave-length
Autumn	23	17.8	15.8	23.3	19.8	69
Winter	18	16.3	16.9	26.6	23.3	83
Spring	55	19.4	17.7	23.1[*]	19.6	60
Summer	77	9.9	9.7	14.3	8.7	62
Year	173	14.6	13.8	19.7[*]	16.8[*]	64

[*] Subtract one observation from total.

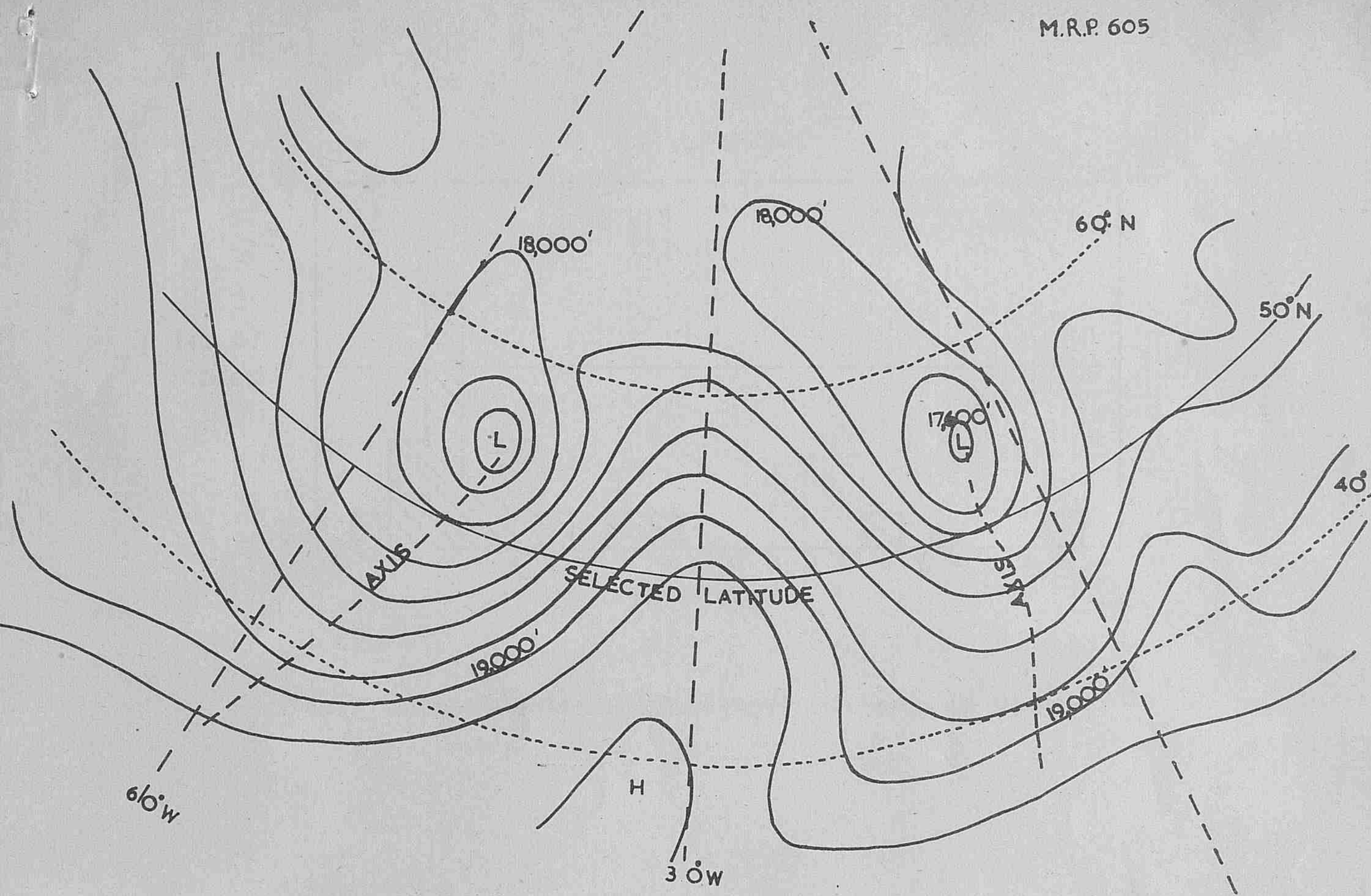
18,000'
18,000'
60° N
50° N
40° N
L
L
17,400'
AXIS
AXIS
SELECTED LATITUDE
19,000'
19,000'
H
60° W
30° W
GREENWICH

FIG. I. Showing the axes and selected latitude of an actual wave-pair

The diagram is part of the 500 mb. circumpolar contour chart for 3rd September 1948 (0300z)

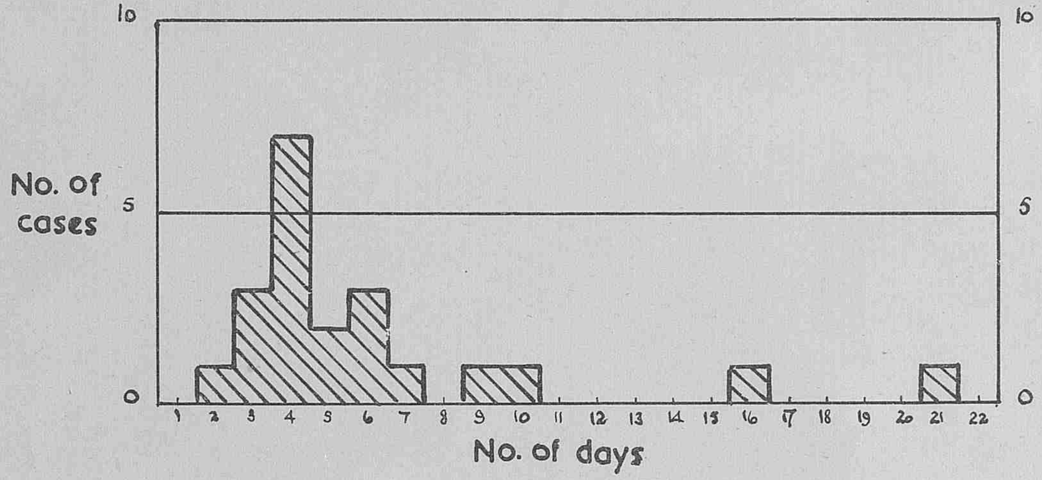

FIG.2. Showing persistence of wave patterns in days

At the time of issue this report has not been published. Any author desiring to quote this paper should refer to it as "A paper of the Meteorological Research Committee (London).
M.R.P. No.......... by Mr..............................
A copy is available in the Library of the Meteorological Office."

SEP 26 1955
AIR WEATHER SERVICE
TECHNICAL REFERENCE FILES

M.R.P. 609
S.C.III/83
2nd. January, 1951.

AD-223003

AIR MINISTRY

METEOROLOGICAL RESEARCH COMMITTEE

A particular solution of the power-law diffusion equation.

by E. Knighting, Meteorological Office.

Summary.

A solution of the power-law diffusion equation is obtained for the case in which the surface variation is of the form of a sine wave. The solution is somewhat different from those previously published and it is shown that the method hitherto used for the estimation of the index in the power law is open to criticism.

1. Introduction.

The power-law diffusion equation has been much used to describe changes taking place in the lower atmosphere. Sutton (1949) and Calder (1948) have given solutions of the equation with the variation at the surface represented by a sine curve; these solutions are approximate and refer to conditions after a long period of time and at heights well above the surface, and have been used to estimate the index of the power law by comparison with an empirical law found by Best (1935). This empirical law is that from the surface up to a height of 17 m. the lag of the maximum of temperature at a height z on a clear summer day satisfies the relation

$$\text{lag} = \text{const. } z^{0.19}$$

and the same law is valid to rather greater heights. Sutton and Calder develop the oscillatory part of the solution of the diffusion equation and, by comparing the lag given by their solution with that found by Best, estimate the index of the power law. We wish to develop a more exact solution and to show that this method of estimating the index is open to criticism.

2. The solution of the equations.

The physical problem may be stated as follows. At a given zero of time an entity v is constant at all heights; there is an impressed variation at the surface which follows the form of a sine wave, and it is assumed that at very great heights there is very little variation in the value of the entity; the diffusion coefficient is proportional to a power of the height above the surface. It is required to find the subsequent distribution of the entity. The entity considered by Sutton and Calder is potential temperature and the conditions of the problem are approximately obeyed, for at about 0600 on a clear summer day potential temperature is approximately constant with height and the surface variation with time is approximately given by a sine curve.

We use the notation of M.R.P. 598 and denote by U the change in the value of the entity v from its constant value at zero time. The analysis determining the variation of $\overline{U}$ has been developed in M.R.P. 598, and here we are considering the time case in which $l = 0$. We proceed from equations (15) and (16) of that paper which give

$$\overline{U} = \frac{2^{1-n}}{\Gamma(n)} \lambda^n K_n(\lambda) . \overline{f}(p) = A\frac{2^{1-n}}{\Gamma(n)} \lambda^n K_n(\lambda) . \frac{\sigma p}{p^2+\sigma^2} \qquad .....(1)$$

where the surface variation has been written in the form

$$f(t') = A \sin \omega t' = A \sin \omega t/a = A \sin \sigma t \qquad .....(2).$$

For sufficiently large values of λ we may use the asymptotic expansion of the Bessel function and write equation (1) in the form

$$\overline{U} = A \frac{2^{1-n}}{\Gamma(n)} \lambda^{n-1/2} \left(\frac{\pi}{2\lambda}\right)^{1/2} \exp(-\lambda) \frac{\sigma p}{p^2+\sigma^2}$$

To interpret equation (3) we use the inversion theorem (Carslaw and Jaeger 1941) and writing, as in M.R.P. 598,

$$\lambda = \alpha p^{1/2}$$

we obtain

$$U(z,t) = \frac{A2^{1-n}\sigma}{2\pi i\Gamma(n)}\left(\frac{\pi}{2}\right)^{1/2}\int_{c-i\infty}^{c+i\infty}\exp(pt - \alpha p^{1/2})\alpha^{n-1/2}p^{(2n-1)/4}\frac{dp}{p^2+\sigma^2} \qquad ..(4).$$

The integrand in equation (4) has a singularity at $p = 0$ and poles at $p = \pm\sigma i$; the integration is carried out around the typical contour of Figure 1. If $n > -3/2$ there is no contribution from the small circle and we find

$$U(z,t) = A\frac{2^{1-n}}{\Gamma(n)}\left(\frac{\pi}{2}\right)^{1/2}\alpha^{n-1/2}\left\{\exp\left(-\alpha\left(\frac{\sigma}{2}\right)^{1/2}\right)\sigma^{(2n-1)/4}\sin\left(\sigma t + \frac{(2n-1)\pi}{4} - \alpha\left(\frac{\sigma}{2}\right)^{1/2}\right)\right.$$
$$\left. + \frac{\sigma}{\pi}\int_0^\infty \exp(-\rho t)\rho^{(2n-1)/4}\sin\left(\alpha\rho^{1/2} - \frac{2n-1}{4}\pi\right)\frac{d\rho}{\rho^2+\sigma^2}\right\} \qquad ..(5).$$

If we put $n = 1/2$ in equation (5) the problem is equivalent to one in the conduction of heat, and it is also noted that with this value of $\underline{n}$ the asymptotic expansion of the Bessel function is exact so that the solution holds for all values of the height $\underline{z}$. Writing also $\sigma = \omega/K$ to conform with the usual notation used in the conduction of heat, equation (5) reduces to

$$U = A\left\{\exp(-z(\omega/2K)^{1/2})\sin(\omega t' - z(\omega/2K)^{1/2})\right.$$
$$\left. + \frac{\omega}{\pi}\int_0^\infty \exp(-\rho t')\sin z(\rho/K)^{1/2}\frac{d\rho}{\rho^2+\omega^2}\right\} \qquad ......(6)$$

which is a known result (Carslaw and Jaeger 1941).

3. The estimation of $\underline{n}$.

Equation (5) differs from that given by Sutton and Calder in the appearance of the term $(2n-1)\pi/4$ in the sine term and in giving an explicit form for the non-oscillatory term in the solution.

(a) The oscillatory term.

The presence of the term $(2n-1)\pi/4$ emphasizes that we have used an asymptotic expansion and that the solution is valid only if $\underline{\alpha}$ is sufficiently large. Putting $\alpha = 0$ and neglecting the non-oscillatory term, as Sutton and Calder do, we find that the time of maximum value of $\underline{U}$ at the surface is given by

$$\sigma t + \frac{2n-1}{4}\pi = \omega t' + \frac{2n-1}{4}\pi = \frac{\pi}{2}.$$

This is incorrect, for we know from the form of $f(t')$ that the correct time is givin by

$$\omega t' = \pi/2 .$$

All that we can deduce from equation (5) is that the time of maximum at a height $\underline{z}$ is given by $\underline{t}'$ where

$$\omega t' + \frac{2n-1}{4}\pi - \alpha\left(\frac{\sigma}{2}\right)^{1/2} = \frac{\pi}{2}$$

providing that $\underline{\alpha}$ is sufficiently large, and that if this is true the lag in times of maximum between levels z_1 and z_2 is

$$\omega(t_1' - t_2') = (\alpha_1 - \alpha_2)\,(\sigma/2)^{1/2}.$$

Now α is given by

$$\alpha = \frac{2z^{(1+m)/2}}{(1+m)a^{1/2}}$$

and without knowing the values of m and a it is not possible to assert that α is sufficiently large to ensure that the asymptotic expansion is a good approximation. Best's empirical law cannot be applied without a pre-knowledge of the answer that we are seeking.

(b) The non-oscillatory term.

Sutton and Calder neglect the non-oscillatory term in comparison with the oscillatory term. For sufficiently large values of t the integral will become small, the integrand being swamped by the negative exponential. In order to find if the integral is in fact small compared with the oscillatory term it is necessary to know the value of σ (=ω/a). The value of a is, however, unknown.

4. Conclusion.

From these considerations it is concluded that the estimation of the index in the power law from the lag is a more difficult question than has hitherto been considered, and that conclusions reached are open to criticism.

References.

Best, A.C.	1935	Geophys. Mem. No. 65. Met. Off. London.
Carslaw, H.S. and Jaeger, J.C.	1941	Operational Methods in Applied Mathematics. Oxford University Press, London.
Calder, K.L.	1948	The Diffusive Properties of the Lower Atmosphere. Permanent Records of Research and Development, No. 9-401 Ministry of Supply, London.
Sutton, O.G.	1949	Atmospheric Turbulence. Methuen. London.

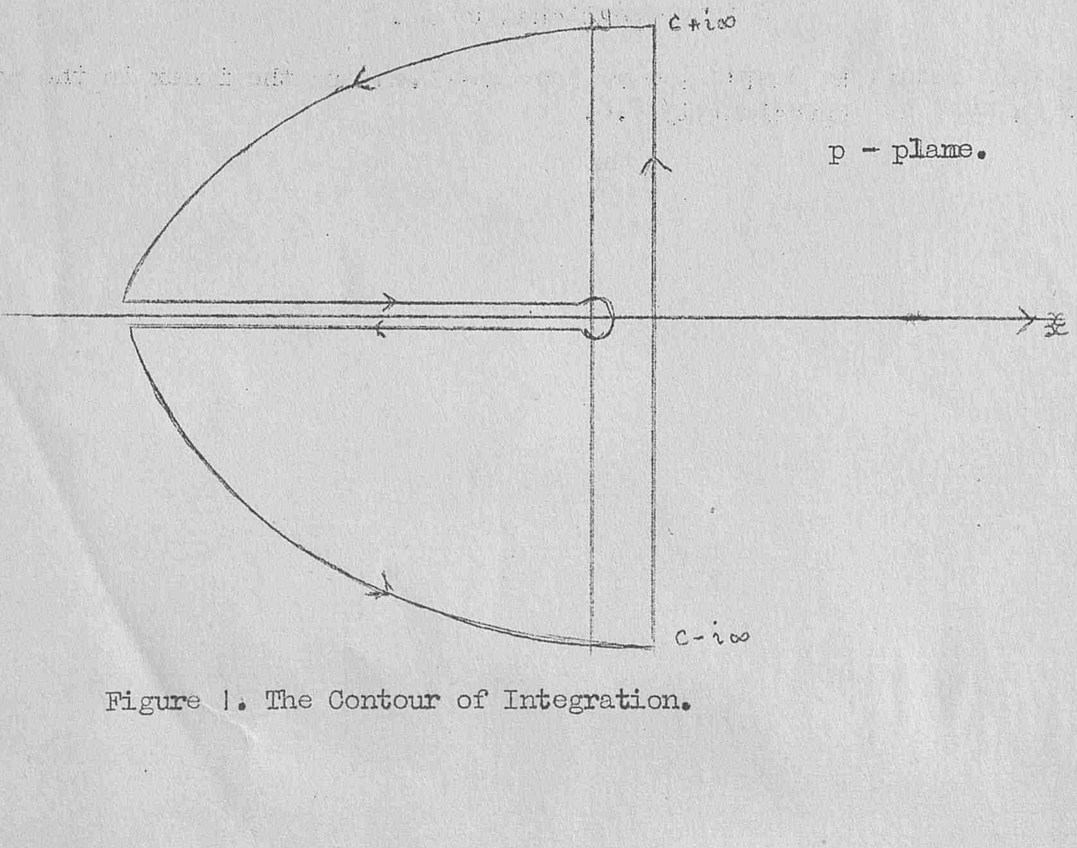

Figure 1. The Contour of Integration.

Appendix.

As an illustration of the differing results which may be obtained according as $\underline{\alpha}$ is treated as large or small, we suppose $\underline{\alpha}$ to be small (instead of large, as above). Then assuming $n < 1$, the first two terms in the expansion of $\lambda^n K_n(\lambda)$ are

$$\lambda^n K_n(\lambda) = \frac{\pi\lambda^n}{2\sin n\pi}\left\{I_{-n}(\lambda) - I_n(\lambda)\right\} = \frac{\pi 2^{n-1}}{\sin n\pi}\left\{\frac{1}{\Gamma(1-n)} - \frac{(\lambda/2)^{2n}}{\Gamma(1+n)}\right\}$$

The expression for $\overline{U}$ is now, from equation (1),

$$\overline{U} = \frac{\pi}{\sin n\pi\,\Gamma(n)}\left\{\frac{1}{\Gamma(1-n)} - \frac{(\alpha/2)^{2n}p^n}{\Gamma(1+n)}\right\}\frac{\sigma p}{p^2+\sigma^2}$$

The oscillatory term is easily found to be

$$U = \sin\sigma t - \frac{(\alpha/2)^{2n}\pi\sigma^n}{\sin n\pi\,\Gamma(n)\Gamma(1+n)}\sin(\sigma t + n\pi)$$

Now $\sigma t = \omega t'$, and writing $\omega t' = \pi/2 + \omega\mu$, where $\underline{\mu}$ is the time lag of the maximum value of $\underline{U}$ at height $\underline{z}$, then by differentiation we find that μ is given by

$$\sin\omega\mu = \frac{(\alpha/2)^{2n}\pi\sigma^n}{\sin n\pi\Gamma(n)\Gamma(1+n)}\sin(\omega\mu + n\pi).$$

Taking $\underline{\alpha}$ sufficiently small and expanding $\sin(\omega\mu + n\pi)$ we get the approximate equation

$$\sin\omega\mu = \text{const.}\ (\alpha/2)^{2n}\cos\omega\mu$$

or

$$\tan\omega\mu \sim \omega\mu \sim \text{const.}\ (\alpha/2)^{2n}$$

From the definition of $\underline{\alpha}$ and since $n = m/(m+1)$ we have for the lag $\underline{\mu}$

μ is proportional to z^m.

Applying this result to Best's law we have $m \sim 0.2$, and the index in the power law, $1 - m$, must be approximately 0.8.

quote this paper should refer to it as "A
paper of the Meteorological Research
Committee (London).
M.R.P. No.......... by Mr.........................
A copy is available in the Library of
the Meteorological Office."

M.R.P. 610
S.C.III/84
24th January, 1951.

ATI - 200025
AUG 23 1951
AIR WEATHER SERVICE
TECHNICAL REFERENCE FILES

AIR MINISTRY

METEOROLOGICAL RESEARCH COMMITTEE

THE OCCURRENCE OF HIGH RATES OF ICE ACCRETION ON AIRCRAFT

BY

A.C. BEST (Meteorological Office)

SUMMARY

Measurements of liquid water content in strongly convective cloud at great heights in America are compared with theoretical values and good agreement is found. The same method of computing the amount of liquid water in clouds with much higher temperatures at the base is thus justified. After taking account of the variation with drop diameter of the temperature of spontaneous freezing of small drops the probability of an aircraft encountering various concentrations of supercooled liquid water in strongly convective cloud in low latitudes is assessed.

1. Introduction. The present-day tendency for airline operators to plan in terms of jet or gas turbine engined aircraft flying at greater heights than has hitherto been common practice has concentrated attention on the maximum rates of ice accretion which are of probable occurrence. The problem of ice accretion is not new, of course, but hitherto it has been encountered more frequently in temperate regions than in low latitudes and more frequently in winter than in summer. This has been because in low latitudes, or in temperate latitudes in summer, many types of aircraft can conveniently operate at heights below the freezing level. The newer type of aircraft are designed to operate at greater heights and it appears that many aircraft of the future will operate at heights where the temperature is frequently below 0°C. even in tropical regions.

It is generally accepted that the highest rates of ice accretion occur in strongly convective cloud and it is clear that the free water content of a convective cloud will increase as the cloud base temperature increases, other things being equal. One would therefore expect the highest rates of ice accretion to occur in convective cloud in the tropics. During recent years there have been many observations made of liquid water content and mean effective drop diameter in cloud. Most of these measurements have been made in the United States of America during winter or spring. The results so obtained have direct application to the operation of present day aircraft in temperate latitudes but it is not immediately obvious how these results should be modified for application to future aircraft or to other latitudes.

It is the purpose of this note to summarize the information on rates of ice accretion available from certain American sources and then to consider how the results should be modified when assessing the maximum rate of ice accretion (anywhere in the world) against which an aircraft of the future should be protected. A similar task has already been performed by Jones and Lewis (9) for present-day aircraft operating in America. Much of the data and of the theoretical treatment in the present paper derives from the publications of the second of these two authors.

2. The experimental data available. The experimental data used in the present note comprise measurements of liquid water content and of mean effective drop diameter published in various N.A.C.A. Technical Notes (1, 2 and 3). The areas and seasons in which the measurements were made were as follows:-

N.A.C.A. Tech. Note No.	Place	Time	Cloud Types
1424	Mainly northern states of U.S.A.	Winter 1946-47	Mainly Strato-cumulus.
1793	Great Lakes and surrounding states.	Winter 1947-48	Stratus and Stratocumulus.
1904	Northern U.S.A.	Jan. to May 1948	Mainly convective.

It can be seen that the results of these measurements may faithfully represent conditions during winter in temperate regions but will need modification before they are applied to summer flying or to flying in low latitudes.

The authors of these three papers have of course discussed their measurements in their respective papers. However the purpose of the present note - to get some guidance regarding icing rates in low latitudes - is different from that of the original authors. It has therefore seemed desirable to use only the tabulated data in the three Technical Notes, to combine them and to examine certain aspects of them, bearing in mind the present requirement.

We shall accordingly examine the frequency distribution of values of W (the liquid water content of the air), the frequency distribution of drop size and then, on the basis of the method of assessing the icing rate as described in Appendix 1, the frequency distribution of various rates of icing.

We may note that the experimental data were obtained on experimental flights carried out for research purposes during which icing conditions were sought. The frequency of encounter with icing conditions would thus bear no relation to the frequency with which an airline aircraft would encounter icing conditions. It is likely however that this dissimilarity would not be so marked with regard to the relative frequency of various rates of icing.

3. The observed frequency distribution of W in temperate latitudes

(a) Convective cloud

The data were taken from T.N.s No. 1904 and 1424. (Except where stated otherwise the value denoted by W_1 in T.N. No. 1904 has been used since this corresponds to W in the other papers). Preliminary examination indicated that the value of W was not related to the temperature at the same height except that there was a suggestion that, in cumulonimbus cloud, large values of W were more frequent at the lower temperatures. The data in T.N. 1904 however clearly showed that large values of W are more frequent in cumulus than in cumulonimbus cloud. For example the percentage number of observations of W exceeding 0.6 g/m^3 was 27.3 for cumulus cloud (99 observations) but only 8.5 for cumulonimbus cloud (94 observations). The data are too few to justify dividing into groups according to all the parameters which might be significant. Accordingly results from all measurements in cumulus and cumulonimbus clouds given in both reports have been grouped together to give the cumulative percentage frequency figures in table 1.

Table 1

Cumulative percentage frequency distribution of W (g/m^3)

Cloud Type	No. of Obs.	Value of W (g/m^3) 0.1	0.2	0.3	0.4	0.5	0.6	0.7	0.8	0.9	1.0	1.2	1.4	1.63
		Percentage number of measurements < W												
Convective	215	17.2	34.0	51.1	61.4	72.5	82.8	88.3	90.6	94.5	97.2	99.0	99.5	100
Layer	156	19.2	53.8	76.9	91.0	98.1	100							
Medium	140	59.3	91.5	98.6	100									

The convective cloud in table 1 refers to well developed convective cloud since it is clear that an aircraft seeking icing conditions would not examine small cumulus clouds.

Later in this note we shall need to pay some attention to the greatest value of W measured in these flights. The value 1.63 g/m^3 quoted in table 1 was the greatest value averaged over the period of exposure, generally a few minutes, of the rotating cylinders (the instrument used for measuring W). A somewhat higher value - 1.72 g/m^3 - was obtained as the highest average over any single period during which the aircraft was in cloud. The authors of T.N. 1904 also quote the highest value of W averaged over 10 secs. found on each flight. The two greatest values in this category were 1.88 and 2.0 g/m^3.

We shall also need at a later stage to consider the temperature and height at which these large values of W were obtained. The values 1.63 and 1.72 g/m^3 were obtained (on the same occasion, flight 179) when the aircraft was at a height of 14,500 feet and the temperature was 6°F. (in cumulonimbus cloud). The form in which the data are presented does not permit one to determine with certainty the temperature and height at which the 10-second values of 1.88 and 2.0 g/m^3 were measured but it seems probable that the value of 2.0 g/m^3 for W was obtained at the same time as the values 1.63 and 1.72 (flight 179) already quoted and that the value 1.88 g/m^3 was obtained at about 15,000 feet and a temperature of about -10°F. (flight 201).

One further comment on the figures in table 1 is desirable. The rotating cylinder method of measuring W has been criticised on the ground that at temperatures only slightly below freezing point the cylinders do not collect all the supercooled water. Of the 215 measurements summarized in table 1 only 13 were obtained at a temperature above 19°F. so that the frequency distribution is not likely to be seriously in error on this account.

(b) Layer cloud

Data relating to stratus and stratocumulus cloud are given in all three Technical Notes. Grouping the data together there was definite evidence that the frequency of large values of W decreases as the temperature decreases. For example at temperatures from 29 to 10°F. 26.1 per cent of the observations indicated a value of W exceeding 0.3 g/m^3 (134 measurements) but at temperatures below 10°F. (22 measurements) only 4.5% gave W greater than 0.3 g/m^3.

If the effect of temperature is ignored the figures in table 1 for cumulative percentage frequency are obtained.

(c) Medium type cloud

Data relating to altocumulus, altocumulus castellatus, altostratus and altocumulus embedded in altostratus cloud (from T.N. 1904 and 1424) were grouped under this heading. The range of W was small and with the unit of W employed here (viz. 0.1 g/m^3) no effect of temperature on the distribution of W was apparent. Cumulative percentage frequencies as given in table 1 were obtained.

4. The frequency distribution of mean effective drop size

(a) Convective cloud

There was no evidence that temperature has any effect on the frequency distribution of d (mean effective drop diameter – i.e., the median volume diameter) either in cumulus or cumulonimbus cloud but T.N. 1904 shows that large values of d occur more frequently in cumulonimbus than in cumulus cloud. For example the mean effective drop diameter exceeded 24 microns in 14.4 per cent of the measurements in cumulus cloud (total number 97) but in 39.4 per cent in cumulonimbus cloud (total number 89).

Grouping all convective cloud together the cumulative percentage frequencies in table 2 were obtained.

Table 2

Cumulative percentage frequency distribution of mean effective drop diameter d (microns)

Cloud Type	No. of Obs.	Value of d (microns)												
		6	9	12	15	18	21	24	27	30	35	40	45	50
		Percentage number of measurements $<$ d												
Convective	208	-	2.4	11.0	25.0	40.4	57.6	76.4	89.9	93.2	95.6	-	97.5	98.1
Layer	159	1.9	20.1	51.0	74.3	85.5	93.1	96.2	97.5	98.8	99.4	100		
Medium	135	0.7	5.2	17.0	37.0	54.9	69.6	84.5	88.9	90.4	91.1	-	-	97.1

(Note. The totals in this table differ from those in table 1 because W and d were not always both quoted).

/ (b)

(b) Layer cloud

The small number of observations at low temperatures makes it difficult to be certain of the effect of temperature on the frequency distribution of d for layer type cloud but there was a suggestion from the data that large values of d do not occur at very low temperatures.

Ignoring any possible temperature effects and grouping all the observations together, the results in table 2 were obtained.

(c) Medium type cloud

Again the data suggested that very large values of d occur more frequently at higher temperatures than at low temperatures but the evidence was not conclusive. Table 2 gives the frequency distribution of d for medium type cloud.

5. The frequency distribution of computed rate of icing in temperate latitudes

The rate of ice accretion on an aircraft depends upon the liquid water content of the air and the drop size, the shape and size and rate of airflow past the affected part of the airframe and - to some extent - upon the physical characteristics of the air. The meteorologist can take account only of meteorological factors and in Appendix 1 the rate of ice accretion - in grams per hour per square centimetre of cross section - of a hypothetical ice collector is examined. This hypothetical collector consists of a cylinder of three inches diameter placed with its axis perpendicular to an airstream of 200 miles per hour in which the characteristics of the air correspond to a height of 3 km. in the I.C.A.N. atmosphere. It is shown that the rate of ice accretion R_g on this hypothetical collector can be assessed numerically from a knowledge of the liquid water content and drop size and that R_g is a convenient numerical measure of the rate of ice accretion likely to be experienced by an aircraft.

For each occasion on which both liquid water content and mean effective drop diameter are quoted in the three N.A.C.A. Technical Notes the rate of icing R_g has been assessed by the method described in Appendix 1.

The results for cumulus and cumulonimbus from the data of T.N. 1904 were examined but there appeared to be no significant difference between the two cloud types in the frequency distribution of R_g (icing rate as defined in Appendix 1). It appears that the greater frequency of large values of W in cumulus cloud is balanced by the greater frequency of large values of d in cumulonimbus cloud already noted.

The effect of temperature was also examined. The data for convective cloud covered a reasonably large number of observations at temperatures down to -10°F. but there was no evidence of a significant correlation between temperature and frequency distribution of R_g. In layer type cloud the number of observations was small at very low temperatures but there was a definite indication of a decrease in frequency of large values of R_g at lower temperatures. In medium type cloud it was not possible to be confident of the importance of temperature. Grouping together the results for all temperatures, table 3 was obtained to show the cumulative percentage frequency of various values of R_g.

/ Table 3

Table 3

Cumulative percentage frequency distribution of Rate of Icing Rg (as defined in Appendix 1)

Cloud Type	No. of Obs.	0.5	1.0	1.5	2.0	3	4	5	6	7	8	10
		Percentage number of measurements $<$ Rg										
Convective	198	-	17.7	-	29.3	-	49.5	-	69.1	-	76.7	86.4
Layer	155	18.7	38.1	56.7	65.7	87.1	91.5	96.7	98.6	99.4	100	
Medium	137	35.0	51.1	67.9	74.5	88.3	94.9	98.5	99.2	100		

Rg	12	14	17	21	33
Convective	93.5	96.5	98.0	99.0	100
Layer					
Medium					

6. Comparison of observed and theoretical values of liquid water content.

If one could specify in detail the mechanism by which a convective cloud is formed it would doubtless be an easy matter to compute exactly the liquid water content. Since we cannot specify this mechanism exactly we have recourse to describing a model of a convective cloud which corresponds as closely as possible to what we know of the mechanism by which such clouds are formed. In Appendix 2 we have described three models of which, it is believed, model 3 corresponds reasonably closely to what happens in practice. This model assumes that

(a) The convective cloud is formed by a current of air ascending through an environment of which the relative humidity is 70 per cent.

(b) The ascending current entrains air from the environment at such a rate that the mass of the cloud is doubled during ascent through a pressure height of 400 mb.

(c) The temperature of the air inside the cloud is equal to that at the same level outside the cloud and the lapse rate of temperature is adjusted, rather artificially, to be slightly greater than the saturated adiabatic lapse rate.

With this model of a convective cloud the liquid water content and temperature are computed for various heights above cloud base (assumed to be at 950 mb) and for three different cloud base temperatures.

The results of the computations show that there is a temperature and height at which the liquid water content has a maximum value and that for a considerable depth of cloud centred at this height of maximum W the value of W varies but little. The results are given in detail in Appendix 2 but it is convenient to summarize them briefly here as follows:-

Cloud Base Temperature	Max. value of W	Temperature at max. value of W	Height at max. value of W
°F.	g/m^3	°F.	ft.
38	2.07	-7.1	11500
70	4.2	20.5	17500
82	5.1	27.5	20700

In Appendix 3 we have computed the liquid water content in layer type cloud on the assumption that the condensed water results from bodily rising of the air along the saturated adiabat through a height of 3,000 feet. The liquid water content of the air resulting from such lifting can be expressed as a function of the temperature at the top of the layer of cloud as follows:-

Temp. at top of Cloud (°F.)	32	14	-4	-22	-40
W (g/m^3)	1.59	1.05	0.65	0.39	0.18

In deriving these figures it is assumed that the pressure at the top of the cloud is 900 mb.

Turning now to the observations made in America, consideration of layer type cloud may be dismissed very rapidly. The greatest values quoted for W in layer type cloud are 0.53 g/m^3 (at 19°F.) and 0.57 g/m^3 (at 20°F.) in T.N. 1424. These values confirm the suggestion in Appendix 3 that the value of W is seldom more than half the value obtained by adiabatic lifting through 3,000 feet.

In T.N. 1904 Lewis and Hoecker quote measurements of liquid water content measured during a number of flights in convective cloud. Corresponding to each measurement of W the temperature at the same height in the cloud is also given. For obvious reasons the tabulated data do not give the temperature and height of base of cloud. For many flights W and the corresponding temperature are given for several different heights in, apparently, the same cloud. Some of these flights were made in weather conditions near the western seaboard of the U.S.A. in which one would expect a cloud base at about 950 mb and a near wet adiabatic lapse rate in the cloud. Eight such flights were selected (Nos. 154, 155, 171, 175, 176, 179, 200 and 201) and the temperature at the cloud base estimated. The estimate was made by using the observed temperature at a stated height and tracing a wet adiabat from the corresponding point on the tephigram to the 950 mb level. In practice two estimates were made for each selected flight, using the highest and lowest temperatures (at different heights of course) measured in the particular cloud. The difference between the two estimates exceeded 3°F. for one flight only (No. 154 - with a difference of 5°F.) The mean of the two estimates varied from 31°F to 47.5°F. with an average value of 38°F. For this reason 38°F. was chosen for numerical computation in Appendix 2. On the two flights on which the greatest values of W were observed, Nos. 179 and 201, the estimated cloud base temperatures (as described above) were 47.5°F. and 39°F. respectively. Interpolation in the theoretical values quoted above for convective cloud suggests that with these cloud base temperatures the maximum values of W should be about 2.6 and 2.1 g/m^3 respectively; the comparable measured 10-second values were 2.0 and 1.88 g/m^3 respectively. It is considered that this agreement is reasonable, in view of all the approximations involved, and that the agreement justifies the calculations in Appendix 2, and the use of cloud model 3 with an ambient relative humidity of 70 per cent.

The height and temperature at which the maximum values of W were measured are also in reasonable accord with expectations based upon the theoretical values when it is borne in mind that the theoretical heights are above cloud base at 950 mb, that the value of W shows very little variation with height in the neighbourhood of the height at which the maximum value occurs and that on flight 179 the cloud base temperature was about 10°F. higher than that adopted in the calculations.

7. The frequency distribution of W: generalization

Now, as already explained, the main difficulty lies in the fact that there are no data giving the frequency distribution of W for high cloud base temperatures such as may occur in low latitudes. The close agreement between computed and measured values for maximum W with low cloud base temperatures justifies the same computational method for assessing the maximum value of W with high cloud base temperatures. Of the 215 measurements of W in convective cloud summarised in table 1, only 17 were made at a temperature outside the range 19°F. to -20°F. Now reference to table 7 of Appendix 2 shows that with cloud model 3, 70 per cent. ambient relative humidity and cloud base temperature 38°F. W varies only between about 1.65 and 2.07 g/m^3 in this temperature range. To a reasonable approximation, therefore, the large majority of measurements were made at a temperature at which W might be expected to have a value close to the maximum value. In fact, of course, the measurements gave a frequency distribution of W as indicated by table 1. We shall now assume that the frequency distribution of W, expressed as a fraction of the maximum value corresponding to the cloud base temperature, is independent of cloud base temperature. With this assumption the frequency distribution in table 1 for convective cloud (layer and medium cloud are clearly unimportant in this connection) has been plotted in figure 1, W being expressed as a fraction of 2.07 g/m^3 the maximum value of W for a cloud base temperature of 38°F, cloud model 3 and 70 per cent ambient relative humidity from table 7 of Appendix 2. The shape of the curve in the upper parts must obviously be unreliable owing to the small number of observations involved but it seems likely to be reliable up to about W/W max. = 0.4.

8. Frequency distribution of Icing Rate: generalization

We have now devised means of assessing the frequency distribution of W in convective cloud, using cloud base temperature as the independent variable. As explained in Appendix 1, however, drop size is also of importance in determining icing rates. It might be possible to devise means of assessing the frequency distribution of drop size on lines similar to those employed for W but this would be of little help unless the relation between drop size distribution and W were known. Fortunately it appears that a simpler procedure is suitable.

In figure 2, two curves have been plotted. One is the frequency distribution of Rg for convective cloud, based upon table 3. The other is the frequency distribution of R^1g where R^1g is the icing rate which would have existed for all convective cloud occasions used in table 1 if the mean effective drop diameter had been equal to the median drop diameter for convective cloud obtained from table 2 (19.7 microns). It can be seen that the two curves are practically identical. The utility of this lies in the fact that the frequency distribution of icing rate can thus be assessed from the frequency distribution of W (which we have discussed in section 7 above) and an assessment of the median mean effective drop diameter. Since this paper is concerned with the maximum icing rate we need scarcely consider layer or medium type cloud any more for, as we have seen, both W and the median value of the mean effective drop diameter are appreciably greater in convective cloud than in cloud of any other type.

9. Conditions in low latitudes

It is not unusual for the mean vapour pressure, at the surface, to have values between 30 and 33 mb. at places such as Calcutta, Lagos and Singapore. When convective cloud occurs in such circumstances the cloud base temperature is likely to be not far removed from the surface dew point, i.e. 75 to 78°F.

The effect of temperature upon mean drop size is somewhat difficult to assess. Howell (4) has dealt with drop size in convective cloud but only for a cloud base temperature of 32°F. The present writer (5) has considered the factors, including temperature, which determine the size of the drops in layer type cloud. Both treatments probably over-simplify the problem but it is reasonably certain that higher temperatures lead to larger drops though it is difficult to say how much larger. We shall not over-estimate the icing rate if we assume a mean effective drop diameter of 20 microns.

If we now assume a maximum cloud base temperature of 76°F. - a conservative figure in view of the dew points quoted above - and a drop diameter of 20 microns we can, using figures 1 and 4, make the following inferences about the liquid water content and icing rates likely to be encountered in low latitudes in well developed convective cloud.

Maximum liquid water content - about 4.6 g/m^3
(Interpolated from Table 7 of Appendix 2)

On 75% occasions W > 4.6 x 0.07 = 0.32 g/m^3 (using Figure 1)
Rg > 4.5
On 50% occasions W > 4.6 x 0.15 = 0.69 g/m^3
Rg > 9.9
On 25% occasions W > 4.6 x 0.25 = 1.15 g/m^3
Rg > 16.5
On 10% occasions W > 4.6 x 0.36 = 1.65 g/m^3

On 5% occasions W > 4.6 x 0.44 = 2.02 g/m^3

The slow variation of W with temperature in table 7 of Appendix 2 also suggests that these values of W would not be reduced below about three quarters of the quoted value even at temperatures as low as -40°F. In deriving these figures we have made certain assumptions about the temperature structure of the cloud. For this reason it would probably be unwise to apply the reduction factor of 3/4 at low temperatures. However at temperatures as low as -40°F. we must reconsider the physical processes implied by Appendix 2.

10. The freezing of small droplets

It now seems to be generally accepted that clouds at a temperature near -10°C. (14°F.) probably contain a few ice nuclei. At still lower temperatures the number of ice nuclei increases and at -32°C. (-25.6°F.) there is a marked increase in the number of ice nuclei (in air which has not been carefully cleaned). At -41°C. (-41.8°F.) there is a further large increase in the number of ice nuclei. The experiments upon which these results are based were laboratory experiments but nevertheless they do indicate a probability that in the atmosphere the number of ice nuclei may increase markedly as the temperature falls to -40°F. If there are sufficient ice nuclei present the amount of liquid water is likely to decrease by sublimation and so the icing risk to aircraft diminishes. Unfortunately the laboratory work mentioned above gives no guide to the amount of water which is likely to remain liquid at various temperatures. Accordingly, beyond noting the probability that serious icing is unlikely at temperatures below -40°F, we shall now consider the laboratory work of Dorsch and Hacker (6). Heverley (7) had shown that the temperature at which a drop of water freezes spontaneously is lower for the smaller drops. Dorsch and Hacker extended this work and showed that the temperature of spontaneous freezing of a droplet is not uniquely determined by the size of the drop. There is, in fact, a range of temperature at which freezing occurs for each drop size. If the number of drops (all of the same size) which freeze at a specified temperature is plotted against the temperature, a frequency curve approximating to the conventional "normal" shape is obtained, the peak occurring at a temperature which depends upon the drop size. The standard deviation of temperature of spontaneous freezing for a given drop size is of the order of 5°F. Dorsch and Hacker give the average temperature of spontaneous freezing for a number of drop sizes and table 4 is based upon their results.

Table 4

Average temperature of spontaneous freezing
as a function of drop diameter

Drop Diameter (microns)	90	35	18.5	13	10.5	6.5	4.5	4.0
Temp. of spon. freezing (°F.)	-12.5	-15.0	-20	-22	-25	-30	(-35)	(-40)

The two bracketed values for very small drops are obtained by extrapolation and are probably very uhreliable.

We propose to apply these results to clouds in the atmosphere. There are, of course, obvious objections to doing this. The conditions of the laboratory experiments are not those of the free atmosphere and moreover table 4 ignores the fact that drops of the same size do not all freeze at the same temperature. Nevertheless there seems no other way of forming a numerical estimate of the decrease of liquid water at very low temperatures.

It has been shown elsewhere (8) that the distribution of drop size in cloud can be represented by

$$1 - F = \exp\left[-(d/a)^n\right] \quad \ldots\ldots\ldots\ldots\ldots\ldots\ldots\ldots(1)$$

where F is the fraction of free water in the cloud comprised of drops with diameter less than d. n and a are constants, the former having a value about 3.3. We shall assume that this distribution law is valid at temperatures above -12.5°F. and that thereafter, as the drops are carried up in the rising air current, the vapour pressure is so small that the major factor affecting the liquid drop size distribution is the successive freezing of the larger liquid drops as the temperature falls. To evaluate "a" we note that from equation 1 it is easily shown that 50 per cent of the water is comprised of drops with diameter less than 0.892a. Let us assume that a reasonable value for this diameter is the median value from table 2, i.e. 20 microns; from this we get $a = 22.4\,\mu$ However since there is some uncertainty about the appropriate value of "a" we shall also consider the result of putting 0.892a equal to 15 and 25 microns, leading to $a = 16.8\,\mu$ and $28.0\,\mu$ respectively. Then using equation 1 and table 4 we deduce the figures in table 5.

Table 5

Fraction of free water which remains liquid

Temp. (°F.) >		-12.5	-15	-20	-22	-25	-30	-35	-40
Liquid	$a = 28\,\mu$	1.0	0.88	0.22	0.076	0.038	0.008	(0.002)	(0.002)
Fraction	$a = 22.4\,\mu$	1.0	0.99	0.41	0.15	0.079	0.017	(0.005)	(0.004)
	$a = 16.8\,\mu$	1.0	1.0	0.75	0.35	0.19	0.043	(0.013)	(0.009)

The figures quoted for temperatures of -35 and -40°F. are unreliable since they were obtained by extrapolating the data of Dorsch and Hacker.

We see that in each case the fraction of water remaining liquid decreases markedly at temperatures below -15°F., becoming almost negligible at -30°F. Within this temperature range the rate of decrease with decreasing temperature is rather sensitive to the value of a. Now we noted above that with higher cloud base temperatures the drop size (and hence a) is likely to be greater, and larger drops are likely to lead to greater rates of icing. From table 5 however we see that larger drops lead to a smaller fraction of water remaining liquid. Since we are concerned here with maximum rates of icing and safety considerations are involved it therefore seems reasonable to adopt the values corresponding to $a = 22.4\,\mu$ in table 5.

11. Significance of the numerical icing rate

The question of whether a particular combination of circumstances leads to "severe" icing can be answered only by the pilot of the aircraft and so the answer must, to some extent, be subjective. On the other hand a numerical scale of icing is of little use unless it can be interpreted in terms used by the pilot. Lewis (12) has suggested that the ranges 0 to 1 to 6 to 12 g/cm^2 hour for Rg should be classified as light, moderate and heavy but for our present purpose it seems better to take advantage of some comments in a report by B.E.A. This report (Viking Fluid De-icing Trials, Winter 1949/50, P. and D. Report No. AD/2) lists the liquid water content and drop size measured in a number of flights into icing clouds. The text of the report contains remarks which, on a few occasions, classify the icing as severe or approaching severe. The value of Rg has been determined from figure 4 of Appendix 1 for these occasions. The results were as follows:-

W (g/m^3)	d (microns)	Rg	Remarks in Report
.35	11	2.0	Severe
.35	10	1.6	Approaching severe
.32	18	4.0	Severe
.33	10	1.5	Severe
.28	13	2.2	Approaching severe
.82	12	5.5	Severe
.74	15	7.3	

From these comments by an experienced aircrew it would seem reasonable to assume that on any occasion when Rg exceeds 4.0 the rate of icing would be regarded as severe.

12. A design specification - Comparison with specification in N.A.C.A. Technical Note No. 1855

Probably it is impracticable to protect an aircraft against ice accretion in the worst possible combination of circumstances which can be envisaged. If that is so the duty of the meteorologist is to advise the aircraft designer of the frequency of the various degrees of severity. It is then incumbent upon the designer and/or operator to decide what risk shall be taken.

In the present paper we have been concerned primarily with the greatest rate of ice accretion which is probable in strongly convective cloud. It is now proposed to construct a table showing the severity of icing which is likely to be exceeded only in a specified percentage number of occasions of icing in strongly convective cloud in low latitudes. We do this by combining the percentage frequencies in section 9 with the correction factors for a = 22.4 microns in table 5. Since safety considerations are involved it has seemed desirable to increase these correction factors to 0.5, 0.2, 0.1 and 0.05 for -20°F., -22°F., -25°F. and -30°F. respectively. For example from section 9 we see that on 10 per cent of occasions W exceeds 1.65 g/m3, but at -25°F. only 0.1 of this amount, i.e. 0.17 g/m3, remains liquid. As the range of sizes of drops remaining liquid diminishes the mean size approaches more and more closely to the maximum size still liquid. Bearing in mind again that safety considerations are involved it is therefore desirable to couple the maximum size of drop still in the liquid state with the values of W. We thus get table 6.

Table 6

Value of liquid water content exceeded on a specified percentage number of occasions of icing in strongly convective cloud

Temp. °F.	Drop Diameter μ	Percentage number of icing occasions in convective cloud 75%	50%	25%	10%	5%	0%
		Minimum value of W (g/m^3)					
32 to -15	20	0.35	0.7	1.2	1.7	2.1	4.6
-20	19	0.18	0.35	0.6	0.85	1.05	2.3
-22	13	0.07	0.14	0.24	0 34	0.42	0.9
-25	11	0.04	0.07	0.12	0.17	0.21	0.5
-30	7	0.02	0.04	0.06	0.09	0.11	0.25
-40	7	0.02	0.04	0.06	0.09	0.11	0.25

It is of course clear that these figures apply to low latitudes since a cloud base temperature of 76°F. is assumed.

Jones and Lewis (9) have proposed specifications of icing severity in various circumstances. They considered not only the severity in strongly convective cloud but also conditions in areas in which there is widespread convection and in layer type cloud. Their icing condition designated as "Instantaneous Maximum" corresponds approximately to the last column of table 6 and indeed the results are very similar. It seems desirable therefore to compare and contrast their treatment with that adopted above. Jones and Lewis computed the theoretical value for W appropriate to a cloud base temperature of 85°F. at 950 mb. using cloud model 3 of Appendix 2 with a 70 per cent relative humidity (the conception of cloud model 3 in Appendix 2 derives of course from the work of Jones and Lewis). They do not describe the method of computation in detail but the numerical results obtained are very similar to those for 82°F. cloud base temperature in Appendix 2. Having obtained these theoretical values Jones and Lewis then scale them down at very low temperatures but it appears that the reason for so doing is based upon the increase in the number of ice crystals at these low temperatures. There does not appear to be any quantitative argument in support of the values they give.

If we examine the values in table 6 in conjunction with figure 4 of Appendix 1 we see that Rg will be less than 4 on 95% occasions at -22°F. and on 100% occasions at -25°F. In fact the spontaneous freezing of droplets should lead to a marked absence of high rates of icing on the airframe at temperatures below a critical value which is in the neighbourhood of -32°C. (-25.6°F.) It is not clear whether the similarity between this temperature and the temperature at which the number of ice nuclei increases markedly is more than a coincidence.

13. The relative frequency of severe icing in various parts of the world

In the preceding sections we have been concerned only with the percentage frequency distribution of various rates of icing. We have not hitherto considered the actual frequency of high icing rates. However we have seen that the very severe rates of icing (e.g. Rg > about 8) occur only in strongly convective cloud and that even occasions of Rg = 4 are very much more frequent in strongly convective cloud than in layer or medium type cloud. From this it is a reasonable inference that the frequency of very severe icing over various routes is proportional to the frequency of thunderstorms over those routes. Now a considerable amount of information exists on the frequency of thunderstorms at various places and it thus appears that this information might be used as a guide to the relative frequency of high rates of icing. This method of approach does not, of course, give any information about the absolute frequency of high icing rates, about the height at which icing occurs or about the lower rates of icing, but it should lead to a reliable estimate - for planning purposes - of the relative frequency of very severe icing conditions.

Appendix 1.

14. Quantitative assessment of icing rate.

The rate of ice accretion experienced by an aircraft flying through a cloud of supercooled water drops may vary over a very wide range and there is an obvious need for some means of forming a numerical assessment of the icing rate in specified conditions. A method of doing this has apparently been adopted by the Weather Bureau of U.S.A. but since the literature describing the basis of the method is not very accessible and since also it is desired to examine the extent to which the method fulfils the requirements an outline of the procedure is given below.

The rate of ice accretion depends upon the liquid water concentration in the air, the drop size, the air speed past the aircraft, the size of the affected part of the aircraft and the efficiency of catch of the affected part. By efficiency of catch we mean the ratio of the amount of water caught to the amount of water in the swept path.

The problem of the efficiency of catch of a solid object moving through a drop laden atmosphere was first considered by Glauert (10) and later extended by Langmuir (11). Glauert considered the efficiency of catch of aerofoils and of circular cylinders; Langmuir dealt with circular cylinders, spheres and ribbons. The parts of an aircraft have various shapes and for simplicity we shall here confine attention to circular cylinders. Langmuir has shown that the efficiency of catch E of a circular cylinder is related to a quantity k by curves of the type shown in figure 3 where

$$k = \frac{2\rho}{9\mu}\frac{a^2U}{R} \quad \ldots\ldots\ldots\ldots\ldots\ldots\ldots\ldots\ldots(2)$$

and

a = drop radius.
U = air speed.
R = radius of cylinder.
ρ = density of drops (=1 for water)
μ = coefficient of viscosity of air.

There are several curves in figure 3 and the precise curve to use depends upon another parameter ϕ defined by the relation

$$\phi = \frac{18\,\sigma^2}{\mu\rho}RU \quad \ldots\ldots\ldots\ldots\ldots\ldots\ldots\ldots\ldots(3)$$

where

σ = density of air.

The variables fall naturally into three groups, viz. those characteristic of the air (σ and μ), those related to the ice collector (R and U) and those related to the cloud (ρ and a). Let us standardize the atmospheric characteristics by assuming that the aircraft is flying at a height of 3 km in the I.C.A.N. atmosphere. Then we put $\sigma = 0.9095\ 10^{-3}$ g/cc and $\mu = 1.692\ 10^{-4}$ poise. If, at the same time, we change the units for drop radius to microns and for air speed to miles per hour equation 2 reduces to

$$k = 5.87\ 10^{-4}\frac{a^2U}{R} \quad \ldots\ldots\ldots\ldots\ldots\ldots\ldots\ldots(4)$$

In passing we may note that Langmuir adopted average conditions at the top of Mount Washington and put $\mu = 1.658\ 10^{-4}$ poise and $\sigma = 1.040\ 10^{-3}$, thus getting 5.99 for the numerical coefficient on the right hand side of equation 4.

We now standardize the ice collector by defining it as a cylinder of diameter 3 inches moving at 200 mi/hr through the air and equation 4 becomes

$$k = 0.0308\ a^2 \quad \ldots\ldots\ldots\ldots\ldots\ldots\ldots\ldots\ldots(5)$$

with a measured in microns. In the same conditions we get

$$\phi = 2994 \sim 3000 \quad \ldots\ldots\ldots\ldots\ldots\ldots\ldots\ldots(6)$$

Equation 6 determines the curve in figure 3 which will be used (the curve for $\phi = 3000$ has been interpolated from Langmuir's original curves) and equation 5 defines k in terms of drop size. Having evaluated k the value of E, the efficiency of catch, can be read from the curve for $\phi = 3000$ in figure 3.

If the liquid water concentration in the air is W g/cc it is easily seen that the rate of ice accretion Rg is given by

$$Rg \quad = \quad 3600\ UWE\ \text{g/cm}^2 \text{ per hour} \quad \ldots\ldots\ldots\ldots\ldots (7)$$

where U is measured in cm/sec. Putting U = 8940 cm/sec (= 200 mi/hr) we get

$$Rg \quad = \quad 3.218\ 10^7\ WE \text{ g/hour per unit area of cross section} \quad \ldots\ldots\ldots\ldots\ldots (8)$$

Using equation 7 isopleths of Rg have been plotted in figure 4 on a drop size - liquid water content diagram. This diagram emphasizes the sensitivity of Rg to variation in drop size when the drops are small.

The theory indicates that no deposition occurs on the collector when k falls below a critical value which, for a cylinder, is 1/8. This implies that, for our standard ice collector, no ice accretion will occur if $a < 2.03$ microns.

15. Effect of variation from standard conditions.

Our standard collector has been defined as a three inch diameter cylinder moving at 200 mi/hr through the I.C.A.N. atmosphere at a height of 3 km. We must now assess the variations to be expected when the conditions depart from standard.

We may note first that variations in ϕ have a small effect on E. For example if a = 10 microns then we have k = 3.08. The values of E are then 0.50, 0.44 and 0.38 for ϕ = 1000, 3000 and 10000 respectively.

Variations in R and U correspond to variations in the structure of the aircraft and in its speed. It is rather outside the province of the meteorologist to take account of such factors but we may note here that equation 2 indicates the reason for the greater tendency of small objects, such as aerial masts, to collect ice and also the greater tendency for high speed aircraft to suffer from icing. The latter tendency is additional to the effect of the greater volume of the swept path per unit of time. In fact the two aspects are represented by the occurrence of the two factors U and E on the right hand side of equation 7.

Variations in k owing to variations in the characteristics of the atmosphere arise from the effect of the latter on $1/\mu$ (for k) and σ^2/μ (for ϕ). We tabulate below the ratio of these quantities at various heights in the I.C.A.N. and Summer Tropical atmospheres to the corresponding values (denoted by subscript zero) at 3 km in the I.C.A.N. atmosphere.

Atmosphere	I.C.A.N.			S.T.A.	
Height (km)	1	3	10	5	10
$(1/\mu)/(1/\mu)_0$	0.97	1.0	1.17	0.97	1.06
$(\sigma^2/\mu)/(\sigma^2/\mu)_0$	1.44	1.0	0.24	0.58	0.23

We see that the variation in ϕ may be by a factor of 4 at great heights but we have already seen that if a = 10 microns a factor of 3 in ϕ increases E by only about 14 per cent. The variation in k arising from the variations in $1/\mu$ will obviously have only a small effect on E.

Bearing in mind the other sources of uncertainty in this kind of work (such as estimation of W and a, the assumption that the drops are of uniform size etc) it appears that little would be gained by trying to make allowance for the temperature and density of the air at the height of the aircraft. Accordingly figure 4 will be regarded as providing a reasonable numerical assessment of the icing rate in all circumstances.

Appendix 2.

The liquid water content of convective cloud.

16. Three models of a convective cloud.

The simplest model of a convective cloud consists of a vertical current of air in which water condenses as a result of cooling by ascent, the temperature falls with height at the saturated adiabatic lapse rate and the cloud is isolated from its surroundings so that no air is entrained from outside the cloud. There is little doubt that such a model is much oversimplified except in a very few cases which are probably of transitory existence. A more elaborate model is obtained if one assumes that air is entrained into the cloud from its surroundings and this seems likely to approximate more closely to reality provided a suitable rate of entrainment is postulated. With this second model any calculations involve some assumption concerning the lapse rate of temperature in the cloud. Here again the simplest assumption is that the temperature follows the wet adiabatic lapse rate. This however is inconsistent with the assumption of unsaturated air being entrained from outside. We thus arrive at the third model in which air is entrained into the cloud and the lapse rate of temperature in the cloud is adjusted to some value intermediate between the dry and saturated adibatic lapse rates.

Although the three models we have described seem unlikely to be equally probable there are advantages in computing W according to each model. The first model (no entrainment) will give an upper limit which W cannot exceed, it may correspond to the core of a strongly convective cloud for a short period of time. The second model may correspond to some inner part of the cloud (but not the core).

We shall, of course, assume that all condensed water is carried up in the rising air current.

17. Symbols.

At any height z above cloud base let

T = temperature (°A)
P = barometric pressure (mb)
p = saturation vapour pressure (mb) of water at T°A.
ρ = saturation vapour density (g/m^3) of water at T°A.
σ = air density at pressure P and temperature T.
W = liquid water concentration (g/m^3).

and let the suffix zero denote the conditions at the base of the cloud.

18. No entrainment.

Let unit volume of air at the cloud base rise to height z above the cloud base. The volume then increases to P_oT/PT_o.

The mass of water vapour required to saturate the new volume is $\rho P_oT/PT_o$. The mass of vapour in the original unit volume was ρ_o. Thus the condensed water in the volume P_oT/PT_o is $(\rho_o - \rho P_oT/PT_o)$ and

$$W = \frac{PT_o}{P_oT}\left(\rho_o - \rho\,\frac{P_oT}{PT_o}\right) \quad \ldots\ldots\ldots\ldots\ldots\ldots\ldots\ldots (9)$$

Now if p is measured in mb and ρ in g/m^3 we have

$$\rho = 216.7\,\frac{p}{T}$$

and substituting in equation 9 we get

$$W = \frac{216.7}{T}\left\{\frac{P}{P_o}p_o - p\right\} \quad \ldots\ldots\ldots\ldots\ldots\ldots\ldots (10)$$

If the values of T_o and P_o are known the value of T at any pressure level P can be found from the tephigram by following the ascent along the wet adiabat and values of W can thus be computed. Corresponding values of z can also be found from the tephigram.

19. With entrainment.

We must define the rate of entrainment of the outside air. Consider an element of cloud having mass M (i.e. M is the mass of the air in the element of cloud) and suppose it increases by an amount dM as it rises from pressure level P to level P + dP. We define the rate of entrainment by

$$\frac{dM}{M} = -c\,dP \quad \dots\dots\dots\dots(11)$$

where c is a constant whose value is still to be determined. Integrating equation 11 between the two levels P_1 and P_2 we get

$$\log\frac{M_2}{M_1} = -c(P_2 - P_1) \quad \dots\dots\dots\dots(12)$$

We now assume that the rate of entrainment is such that the mass of the cloud is doubled as it ascends between two pressure levels 400 mb apart (That this rate of entrainment is reasonable is shown in The Thunderstorm (13)) We thus get

$$\log 2 = 400\,c \quad \dots\dots\dots\dots(13)$$

to determine c.

If the relative humidity of the air outside the cloud is 100f, and if the temperature of the ambient air is the same as the cloud temperature at the same level then the mass of water vapour added to the cloud element as it passes from P to P+dP is

$$f\rho\frac{dM}{\sigma} = -c\frac{f\rho M}{\sigma}dP$$

The original vapour content of the cloud element was ρ_0/σ_0 and the water vapour required for saturation at the level P is $M\rho/\sigma$, the volume of the element now being M/σ. Hence we have

$$W = \frac{\sigma}{M}\left\{\frac{\rho_0}{\sigma_0} - \frac{M\rho}{\sigma} + c\int_P^{P_0}\frac{f\rho M}{\sigma}dP\right\} \quad \dots\dots\dots\dots(14)$$

$$= \frac{\rho_0 T_0}{P_0}\;\frac{P}{MT} - \rho + \frac{P}{MT}fc\int_P^{P_0}\rho\frac{MT}{P}dP \quad \dots\dots\dots\dots(15)$$

where M is defined by

$$\log M = c(P_0 - P) \quad \dots\dots\dots\dots(16)$$

from equation 12 and c is given by equation 13. The integral on the right hand side of equation 15 must be evaluated graphically. The value of T at any level is obtained by following a wet adiabat (with respect to water) on the tephigram from the point corresponding to the base of the cloud.

20. Entrainment with adjusted lapse rate in the cloud.

As pointed out above the rate of decrease of temperature with height must exceed the saturated adiabatic lapse rate in a convective cloud in which entrainment occurs. There is, however, very little reliable information available about the lapse rate in convective cloud or about the difference between the temperature in a convective cloud and the ambient temperature at the same level. Accordingly the following artificial expedient was adopted in order to define the lapse rate of temperature in the cloud. It was assumed that entrainment took place only at multiples of 50 mb and that the temperature of the entrained air was given by dry adiabatic ascent from the preceding entrainment level. Now from equation 12 we can show that if $P_1 - P_2 = 50$ mb then $M_2/M_1 = 1.09$. Thus if T_w is the temperature reached at P_2 along the saturated adiabat from P_1 and T_d the temperature reached along the dry adiabat then the cloud temperature at P_2 will be given by $T_d + (T_w - T_d)/1.09$.

It must be emphasized that this artificial expedient was adopted only for the purpose of defining the temperature lapse rate in the cloud. Obviously it gives a rate of decrease of temperature slightly greater than the saturated adiabatic lapse rate and to that extent is likely to correspond more closely to reality. For the computation of water vapour brought into the cloud by the entrained air it is still assumed that the ambient air temperature is equal to the cloud temperature at the same height.

21. Some numerical results.

The methods indicated above have been used to compute W at various heights for three different cloud base temperatures (38°F, 70°F and 82°F) all at 950 mb. The results are given in table 7. All heights are above cloud base. Model 1 is the case of no entrainment, model 2 allows entrainment as indicated above but with the saturated adiabatic lapse rate in the cloud. At a given pressure level the height (above cloud base) and temperature will be the same in model 2 as in model 1. Model 3 takes account of the adjustment of lapse rate in the cloud. The entries in the various parts of the table terminate at a level where the temperature is substantially below -40°F.

Table 7
Values of liquid water content W(g/m³) in various models of convective cloud.

Cloud model	1			2		3			
Ambient R.H.				70°/o	100°/o			70°/o	100°/o
P(mb)	z(ft)	T(°F)	W	W	W	z(ft)	T(°F)	W	W
Cloud base temperature 38°F at 950 mb. 3°C									
950	0	38.0	0	0	0	0	38.0 3.3	0	0
900	1433	33.3	0.72	0.54	0.67	1433	32.9 .5	0.61	0.74
800	4501	22.8	1.89	1.35	1.63	4496	21.9 -5.6	1.46	1.74
700	7896	10.4	2.71	1.82	2.15	7884	8.8 -12.9	1.94	2.27
600	11704	-5.3	3.18	2.00	2.31	11676	-7.1 -21.7	2.07	2.37
500	16036	-25.2	3.27	1.89	2.15	15988	-27.3 -32.9	1.91	2.16
400	21068	-50.0	3.01	1.55	1.74	20996	-52.8 -47.1	1.55	1.73
Cloud base temperature 70°F at 950 mb. 20°C									
950	0	70.0	0	0	0	0	70.0	0	0
900	1526	66.5	1.08	0.59	1.00	1526	66.0	0.89	1.30
800	4811	58.7	3.19	1.78	2.74	4810	57.6	2.22	3.15
700	8473	49.5	4.91	2.72	3.92	8460	47.3	3.29	4.45
600	12618	38.6	6.14	3.33	4.54	12583	35.4	3.96	5.12
500	17406	24.9	6.91	3.70	4.78	17339	20.5	4.19	5.20
400	23082	5.8	7.18	3.77	4.63	22949	0.7	4.05	4.88
300	30042	-21.8	6.58	3.27	3.89	29819	-29.0	3.37	3.96
250	34212	-42.0	5.99	2.84	3.35	33909	-50.1	2.88	3.36
Cloud base temperature 82°F at 950 mb. 27°C									
950	0	82.0	0	0	0	0	82.0	0	0
900	1561	78.6	1.44	0.75	1.37	1560	78.1	1.13	1.73
800	4923	71.6	3.70	1.56	3.16	4917	69.9	2.67	4.05
700	8683	63.8	5.43	2.44	4.26	8659	60.7	3.87	5.59
600	12951	54.9	6.76	3.05	4.94	12899	50.1	4.51	6.27
500	17911	43.2	7.91	3.72	5.48	17799	36.5	5.05	6.64
400	23811	27.6	8.50	4.14	5.59	23607	18.6	5.09	6.36
300	31141	6.5	8.17	4.09	5.06	30777	-6.6	4.50	5.43
250	35611	-9.0	7.66	3.72	4.59	35105	-24.8	3.99	4.74
200	40861	-30.8	6.87	3.26	3.94	40153	-49.0	3.31	3.90

Comparison of the various columns in the table shows that cloud model 1 leads to a much higher value of W than models 2 and 3. The two latter models do not differ very greatly but if one is concerned to know the greatest probable value of W it seems preferable to use model 3 both because this leads to somewhat higher values of W and also because the model seems likely to approximate more closely to reality.

If the maximum value of W for any given cloud model is plotted against cloud base temperature it will be seen that the resulting points approximate reasonably closely to a straight line so that the maximum value of W for other cloud base temperatures can be obtained with fair accuracy by linear interpolation.

Appendix 3.

22. The liquid water content of layer type cloud.

We consider here clouds such as stratocumulus which are formed by turbulence - not by bodily lifting of the whole air mass. An upper bound to the liquid water content is given by assuming that the air is lifted - by eddies - along the wet adiabatic ascent curve from the base of the cloud to the top. It is clear however that this value will seldom be attained since the value is appropriate only to the top of the cloud and, by definition, the cloud is being continuously mixed by turbulence. It has been suggested by Lewis, Kline and Steinmetz (1) that a practical upper limit to the concentration of free water is given by half the value computed on the basis of adiabatic lifting from base to top.

Clouds of this type are seldom more than about 3000 feet deep though they may extend horizontally for many miles. The following table shows the liquid water content of air which has risen along the saturated adiabat through a height of 3000 feet above the cloud base to reach a temperature T (as shown in the table) at a pressure level 900 mb (computed from equation 10 of appendix 2)

Liquid water content (g/m^3) in Layer Cloud.
Cloud depth 3000 feet.

Temp. at top of cloud (°F)	32	14	-4	-22	-40
W (g/m^3)	1.59	1.05	0.65	0.39	0.18

At lower pressures the liquid water content is less. For example an ascent of 3000 feet above the cloud base to a temperature of 32°F at 700 mb leads to a free water content of 1.47 g/m^3.

References.

1. Lewis, W., Kline, D. B., and Steinmetz, C. P., N.A.C.A. Tech Note No. 1424.
2. Kline, D. B., N.A.C.A. Tech. Note No. 1793.
3. Lewis, W., and Hoecker, W. H., N.A.C.A. Tech. Note No. 1904
4. Howell, W. E., J. Met. Amer. Met. Soc. 6, 1949, p. 134.
5. Best, A. C., M.R.P. 538.
6. Dorsch, R. G., and Hacker, P. T., 1950, N.A.C.A. Tech. Note No. 2142(1).
7. Heverly, J. R., 1949, Trans. Amer. Geophys. Union, 30, p. 205.
8. Best, A. C., M.R.P. 559.
9. Jones, A. R., and Lewis, W., N.A.C.A. Tech. Note No. 1855.
10. Glauert, M., A.R.C. Technical Report, R. and M. No. 2025, 1940.
11. Langmuir, I., and Blodgett, K. B., Army Air Force Technical Report No. 5418, Air Materiel Command, Dayton, Ohio, 1946.
12. Lewis, W., N.A.C.A. Tech Note No. 1393.
13. - - , The Thunderstorm, Washington, D.C., 1949, p. 37.

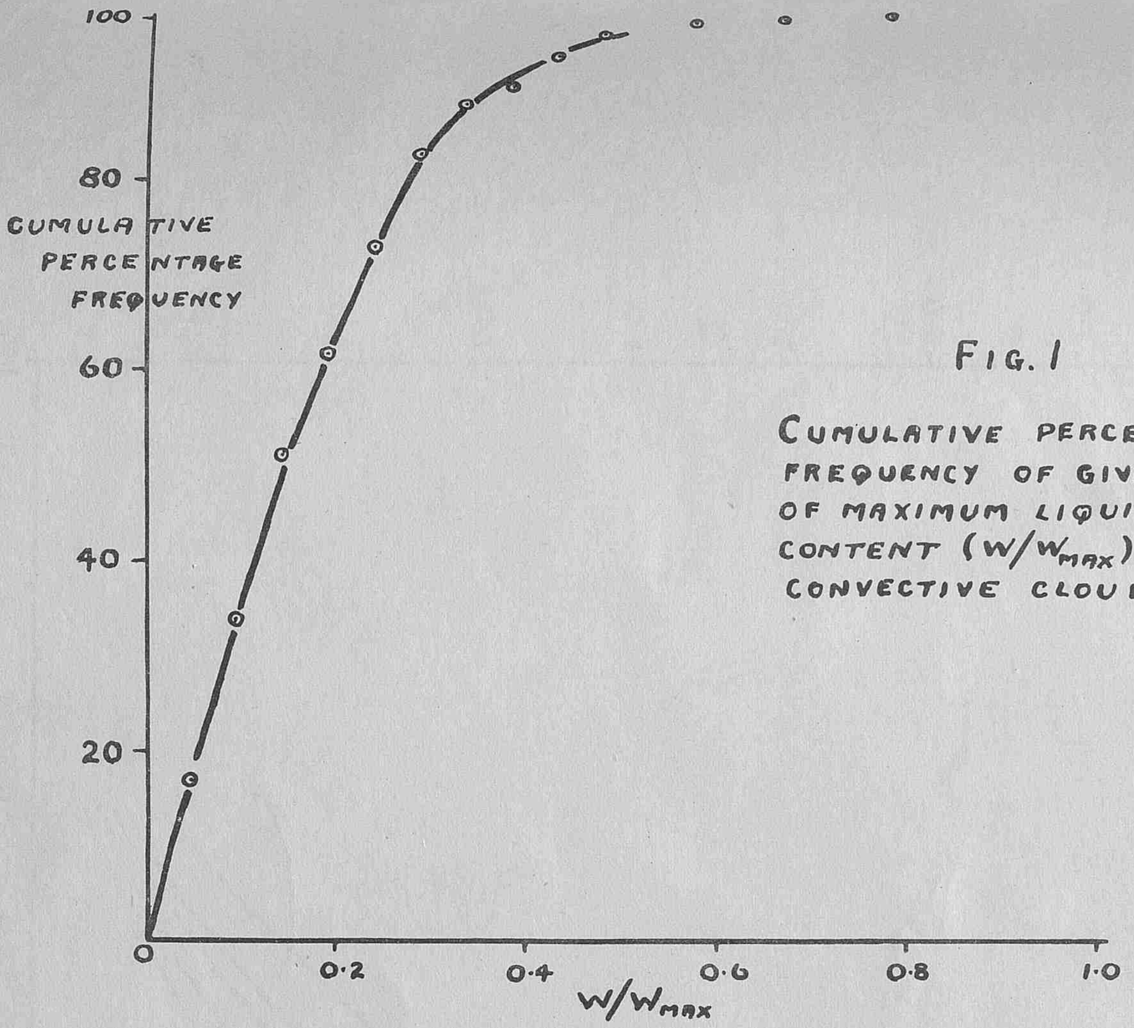

FIG. 1

CUMULATIVE PERCENTAGE FREQUENCY OF GIVEN FRACTION OF MAXIMUM LIQUID WATER CONTENT (W/W_{MAX}) IN CONVECTIVE CLOUD.

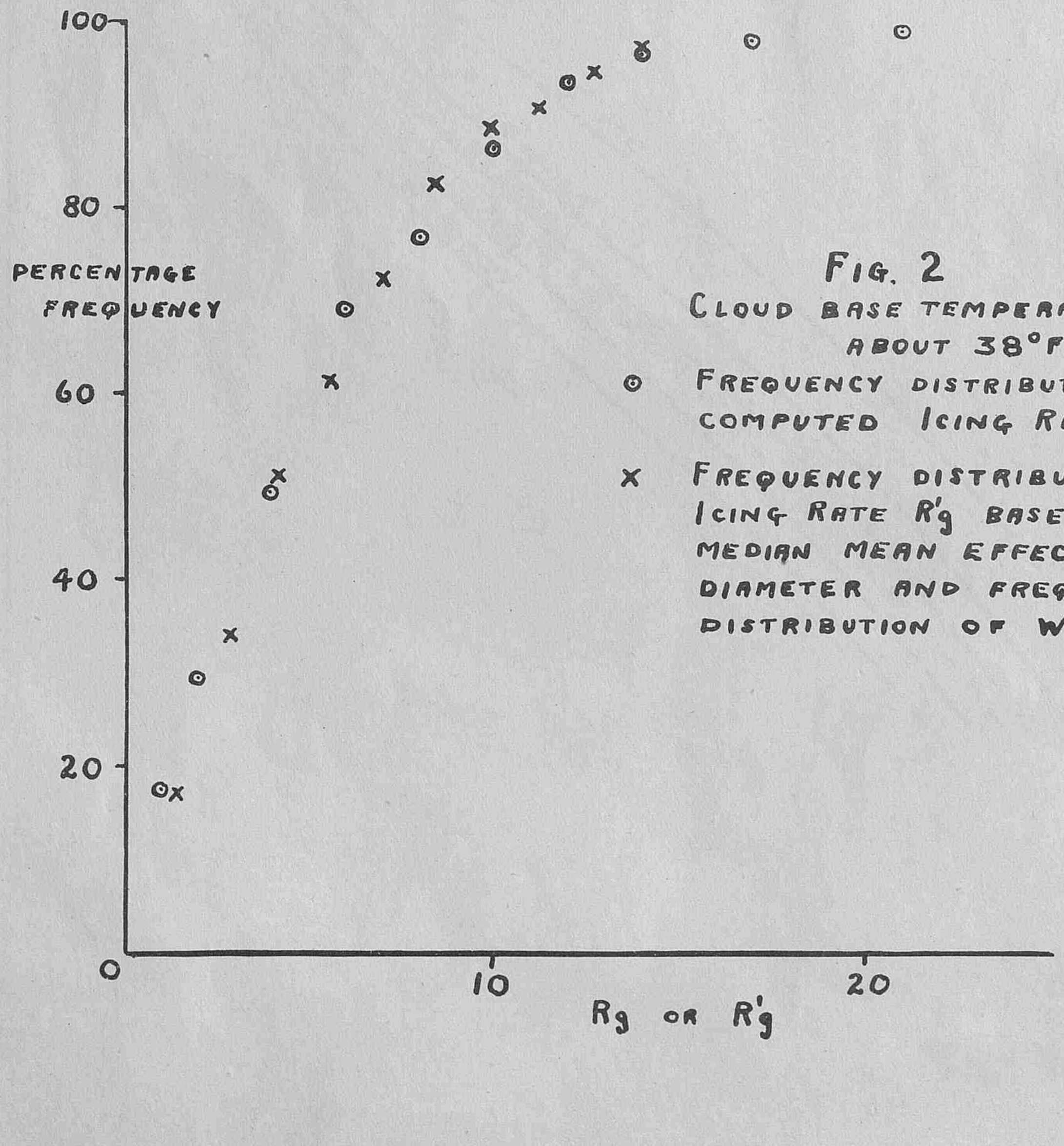

FIG. 2

CLOUD BASE TEMPERATURE ABOUT 38°F

⊙ FREQUENCY DISTRIBUTION OF COMPUTED ICING RATE R_g.

x FREQUENCY DISTRIBUTION OF ICING RATE R'_g BASED UPON MEDIAN MEAN EFFECTIVE DROP DIAMETER AND FREQUENCY DISTRIBUTION OF W.

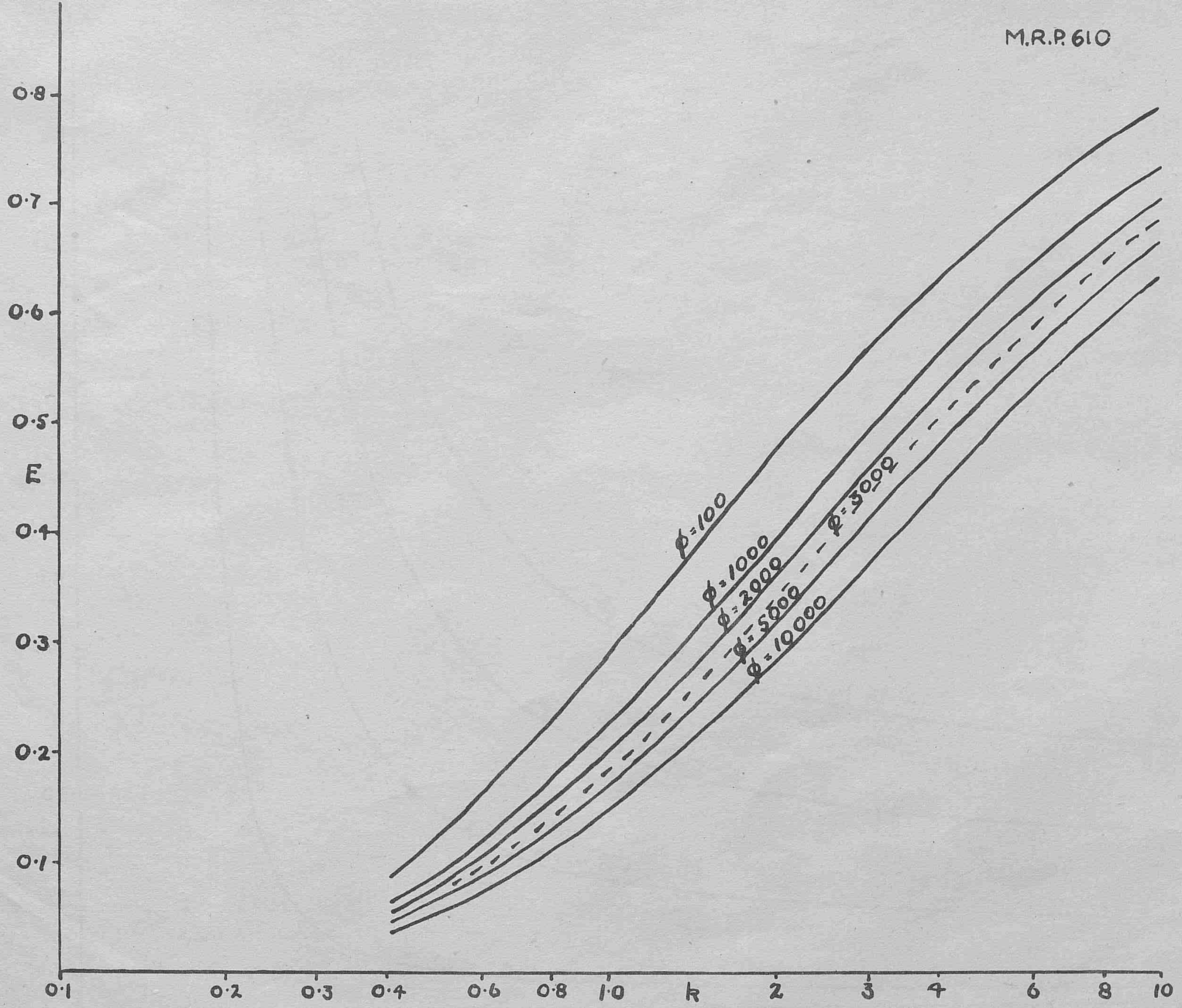

FIG 3. COLLECTION EFFICIENCY OF A CYLINDER E AS A FUNCTION OF k

M.R.P. 610

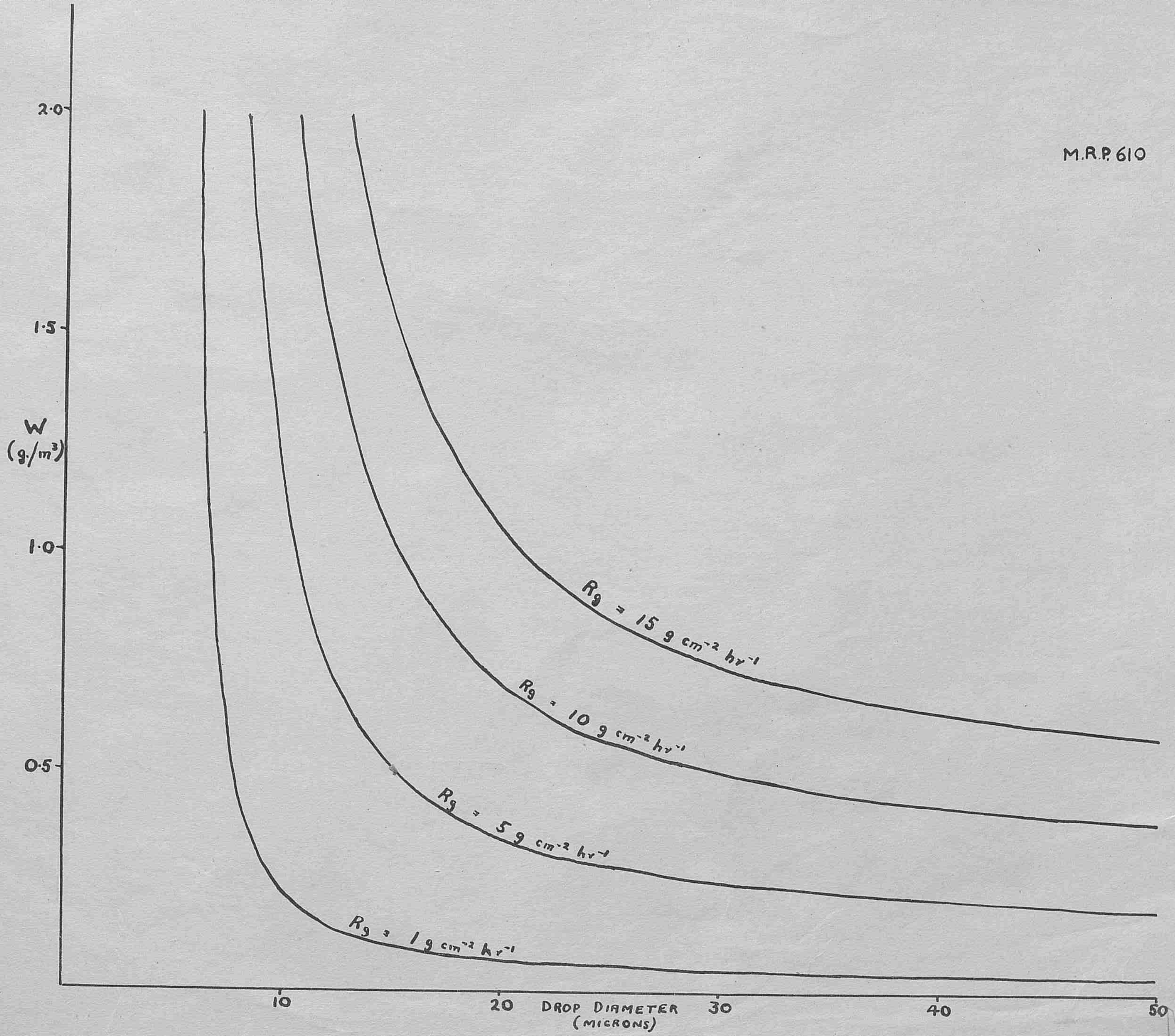

FIG 4. ICING RATE R_g AS A FUNCTION OF DROP SIZE AND LIQUID WATER CONTENT.

24th February, 1951

MRP 611

SEP 26 1955

AIR WEATHER SERVICE
TECHNICAL REFERENCE FILES

AD 223007

AIR MINISTRY

METEOROLOGICAL RESEARCH COMMITTEE

Anomalous Sound Reception Experiments April 1944 - April 1945

by

R.J. Murgatroyd (Meteorological Office)

Summary.

The results of the seven most successful experiments described in M.R.P.346 have been re-calculated. The simplifying assumption of parabolic variation of sound speed with height has been replaced by an assumption that the "unknown" portion of the atmosphere which was investigated can be treated as a "two straight line" structure with a dividing level at a height of 35 km. The new method leads to a more satisfactory way of treating the data mathematically and allows full use to be made of the sideways deflection of the sound path by crosswind effects.

The final values of wind and temperature up to about 50 km height are broadly similar to those obtained by the methods of M.R.P. 346 with the exception that the low temperatures at a height of about 30 km are not so noticeable. It is concluded that this feature of M.R.P. 346's results was to some extent due to the use of the parabolic assumption.

Introduction.

When M.R.P. 346 was examined by the Meteorological Research Committee it was considered that the variations of temperature with height shown in Fig.4 of this paper were improbable. It was suggested that the results given may have been conditioned by the nature of the mathematical assumption (parabolic variation of sound speed with height). This question was dealt with in M.R.P. 470 by Dr. E.T. Goodwin who found that an assumed exponential variation of sound speed with height would produce results of a more probable nature. The problem of calculating winds and temperatures in the stratosphere or ozonosphere is reconsidered in the report below and a new method has been used for recalculating the major results of M.R.P. 346. The new results are presented in the attached Figs. 4, 5 and 6 corresponding to the Figs. 4, 5 and 6 of M.R.P. 346.

Reconsideration of the Methods of M.R.P. 346.

There are at least three points in which an improvement is desirable in the methods used in M.R.P. 346:-

(a) If possible the results obtained should be acceptable without making recourse to any particular mathematical assumption. It would be better to obtain mean values of winds and temperatures for portions of the height range rather than assume a continuous law of variation through the whole range unless there are good grounds for assuming that the structure should correspond reasonably with the mathematical assumption made. The parabolic form was not satisfactory as, although its integrated effect was correct, it gave wide variations from what was expected at given levels - e.g. lower temperatures than were expected between 20 and 35 km.

/presumably

G.278685/DC/1/50/40

At the time of issue this report has not been published. Any author desiring to quote this paper should refer to it as "A paper of the Meteorological Research Committee (London), M.R.P. No.......... by Mr.......................... A copy is available in the Library of the Meteorological Office."

presumably compensated by higher temperatures than would otherwise have been obtained between 35 and 50 km., say. It may be that an exponential assumption will give more plausible results in the 20 to 35 km range, but the basic difficulty that there are no grounds for using this assumption in preference to others remains. In fact, as was pointed out in M.R.P. 470, only the most general conclusions about the wind and temperature conditions at these levels can possibly be drawn from this work and if we have any data on the 20 - 35 km range, say, it would be better to assume values to the 30 or 35 km level and then use the observations from these experiments to obtain semi-quantitative values for the greater heights.

For these reasons and also the fact that an exponential law could not easily be handled to satisfy (b) and (c) below, no further work was done on the basis of this assumption.

(b) An unsatisfactory feature of M.R.P. 346 (and of all similar work known to the author on this problem) is the failure to make adequate use of the change in apparent direction of the sound propagation due to cross-wind components. This is just as fundamental a feature of the measurement of the sound wave at the receiving microphone lattice as is the apparent sound speed and it should therefore be made full use of in the calculation of the results. This point was mentioned in connection with equations (15) and (28) of M.R.P. 346 and a limited use was made of this data in equations (29) to (32). The method given below succeeds in making better use of this piece of information.

(c) Figs. 4, 5 and 6 of M.R.P. 346 give a number of separate determinations (thin lines) based on individual observations and a mean value (thick line) which is taken as the final result of each experiment. The incidence of random errors in this work is very high and the thin lines show a large scatter. It would be more satisfactory statistically to combine all the observations at an earlier stage and produce the most probable result based on a Least Squares calculation. This was also done in the method below.

Method of Treatment.

The difficulty in producing mean values for portions of the height ranges is that these cannot be used in connection with the refraction equations. The next best thing is to assume linear variations throughout the layers concerned provided that they are regarded merely as indications of the general values within the layer and not as values at a particular height.

The number of layers to be used could be varied with the amount of data available, although of course the smaller the number of layers used the better the statistical determination of the values within these layers. It was finally decided to use two layers only - the first from 18 km (height of radio sonde values) to 35 km and the second from 35 km to the maximum heights available (about 50 km). There is no special reason for using 35 km as the dividing level. It divides the "unknown layer" into two roughly equal sub-layers. It is however possible that somewhere above 30 km there is in fact a region of extensive change in the wind and temperature structure perhaps comparable with the tropopause. From 20 km upwards the stratosphere as far as the limit of measurement by balloon ascents has been shown to be roughly isothermal while other indirect evidence indicates considerably higher temperatures at

50 km so that somewhere between there must be a region of change of lapse rate. The data on winds has indicated a change to a "monsoon" regime between 25 and 30 km but very little is known about winds at higher levels. The division into two layers at 35 km, although somewhat arbitrary, probably has a certain amount of physical reality, and variations of a few kilometers from this level for the actual transition layer will not be important as we are only expecting to get a general idea of mean values between 18 km and 35 km and also between 35 km and 50 km.

The effect of using two layers and different sub-division levels was examined in one experiment (Expt.8) and is shown in TABLE I below.

TABLE I

An illustrative case from some of the Expt.8 (13th Sept, 1944) calculations of calculated temperatures °C. assuming different dividing levels.

Dividing Level	28 km	33 km	35 km	37 km
Heights				
24	- 73	- 59	- 58	- 54
30	- 77	- 68	- 61	- 55
36	- 51	- 58	- 66	- 55
42	- 24	- 30	- 33	- 33

The results in the case shown in TABLE I were not varied greatly particularly at the higher levels by choosing values other than 35 km as the dividing level. It was therefore decided that the best method would be to proceed as follows:-

(a) Assume that the region considered could be treated as two main layers - the lower from 18 to 35 km height and the upper from about 35 to 50 km height.

(b) Assume that within these layers temperature and the two wind components varied approximately linearly with height (actually sound speed was used as the linear variable instead of temperature).

Although these are somewhat arbitrary assumptions they represent in the writer's view the best that can be done with the problem. They allow all the data to be used in an orderly manner and the results they give have an accuracy as great as seems attainable in this type of work.

Comparison with other methods.

When M.R.P.346 was written it was stated that previous workers had not been able to obtain results which permitted a satisfactory separation of wind and temperature effects. This has now been done in recent American experimental work (Stratosphere Winds and Temperatures from Acoustical Propagation Studies. A.P. Crary. Journal of Meteorology Vol.7, No.3, pp.233 - 242). In this article which gives results of work in Alaska, Bermuda and the Canal Zone a somewhat similar method of calculation was used. No measurements of the sideways deflection of the sound ray were made and hence only observations of the timings were available. From these a calculation of the variation of sound velocity with height was made on the assumption of linear variations within two layers with a dividing level. The dividing level was made variable (instead of the writer's assumption of a fixed value of 35 km) and the range of velocities at different heights for extreme positions of this dividing level was found. Another assumption was then made that the sound velocity could be represented by (a + w) instead of (a cos ψ + w) (a = sound speed, w = following wind component, ψ = inclination of the sound 'ray' to the horizontal). Then for any given height knowing the velocity range on several azimuths a Least Squares determination of a and w, and hence temperature and wind components, was made. The results obtained are impressive and their accuracy is probably as good as the results quoted below although the method of working up the results here appears to be more satisfactory.

/Mathematical Methods

Mathematical Methods.

(a) Use of the Range and Time equations.

Using the nomenclature of M.R.P. 346 the equations below are repeated:-

$$n_1 = \frac{a_o}{2X}\left\{ 3T - 3X + 3X\left\{ \frac{A}{a_o} - 1 \right\} - \sqrt{\frac{32\,n_o}{a_o}}\;h_1 \right\} \quad \ldots\ldots\ldots\ldots(20)$$

$$h_2 = \sqrt{\frac{n_1}{a_o}}\left\{ \frac{X}{2\sqrt{2}} - \frac{h_1}{\sqrt{\frac{n_1}{a_o}} - \sqrt{\frac{n_o}{a_o}}} \right\} \quad \ldots\ldots\ldots\ldots\ldots\ldots\ldots\ldots\ldots(21)$$

$$\left.\begin{aligned} n &= A - a - D_N \cos\theta - D_E \sin\theta \\ n_1 &= A - a_1 - D_{N_1} \cos\theta - D_{E_1} \sin\theta \end{aligned}\right\} \quad \ldots\ldots\ldots\ldots\ldots\ldots\ldots\ldots(22)$$

If we put $h_1 = 17$ km equation (20) allows n_1 to be found at a height of 35 km above the earth's surface, and $h_1 + h_2$ gives the height at which $n = 0$.

(b) The linear variation of a, D_N and D_E with height.

(i) Between $h = 0$ and $h = h_1$

$$\left.\begin{aligned} a &= a_o + \frac{h}{h_1}(a_1 - a_o) \\ D_N &= D_{N_o} + \frac{h}{h_1}(D_{N_1} - D_{N_o}) \\ D_E &= D_{E_o} + \frac{h}{h_1}(D_{E_1} - D_{E_o}) \end{aligned}\right\} \quad \ldots\ldots\ldots\ldots\ldots\ldots\ldots\ldots(43)$$

These satisfy the conditions at $h = 0$, $a = a_o$, $D_N = D_{N_o}$, $D_E = D_{E_o}$ and at $h = h_1$, $a = a_1$, $D_N = D_{N_1}$, and $D_E = D_{E_1}$ with linear variation with height between and using (22):-

$$n = n_o + \frac{h}{h_1}(n_1 - n_o) \quad \ldots\ldots\ldots\ldots\ldots\ldots\ldots\ldots\ldots\ldots(44)$$

(ii) Between $h = h_1$ and $h = h_1 + h_2$

$$\left.\begin{aligned} a &= a_1 + (h - h_1)\cot\alpha \\ D_N &= D_{N_1} + (h - h_1)\cot\beta \\ D_E &= D_{E_1} + (h - h_1)\cot\gamma \end{aligned}\right\} \quad \ldots\ldots\ldots\ldots\ldots\ldots\ldots\ldots(45)$$

and hence

$$n = n_1 - (h - h_1)\ (\cot\alpha + \cot\beta\cos\theta + \cot\gamma\sin\theta)$$

$$0 = n_1 - (h_2)\ (\cot\alpha + \cot\beta\cos\theta + \cot\gamma\sin\theta) \quad \ldots\ldots\ldots\ldots\ldots\ldots\ldots\ldots\ldots\ldots(46)$$

If $h_3 = 15$ km say

$$\left.\begin{aligned} \cot\alpha &= \frac{a_3 - a_1}{h_3} = \frac{a_2 - a_1}{h_2} \\ \cot\beta &= \frac{D_{N_3} - D_{N_1}}{h_3} = \frac{D_{N_2} - D_{N_1}}{h_2} \\ \cot\gamma &= \frac{D_{E_3} - D_{E_1}}{h_3} = \frac{D_{E_2} - D_{E_1}}{h_2} \end{aligned}\right\} \quad \ldots\ldots\ldots\ldots\ldots(47)$$

$$\frac{n_1}{h_2} = \frac{1}{h_3}\left\{(a_3 - a_1) + (D_{N_3} - D_{N_1})\cos\theta + (D_{E_3} - D_{E_1})\sin\theta\right\} \quad \ldots\ldots\ldots\ldots\ldots\ldots\ldots\ldots(48)$$

Since θ, n_1, h_2, h_1 and h_3 are known the only unknowns in this equation are a_1, D_{N_1}, D_{E_1}, a_3, D_{N_3} and D_{E_3}.

Hence from observations of A, T and X on three azimuths the temperature and wind at a height of 50 km could be estimated.

Similarly since n_1 is known the values a_1, D_{N_1} and D_{E_1} can be found for the height of 35 km. Intermediate values are readily determined as the variation between these heights is linear.

So far there is little difference from the 'two straight line' structure method described in M.R.P 346. The equations however can be used in connection with the sideways deflection data.

(c) Use of the deflection value Y.

The cross-wind value $W^1 = D_E\cos\theta - D_N\sin\theta$.
Hence between $h = 0$ and $h = h_1$ from (43)

$$W^1 = W^1{}_0 + \frac{h}{h_1}(W^1{}_1 - W^1{}_0) \quad \ldots\ldots\ldots\ldots\ldots\ldots\ldots\ldots(49)$$

Between $h = h_1$ and $h = h_1 + h_2$

$$\left.\begin{aligned} W^1 &= W^1{}_1 + (h - h_1)(\cot\gamma\cos\theta - \cot\beta\sin\theta) \\ &= W^1{}_1 + \frac{h}{h_2}(W^1{}_2 - W^1{}_1) \\ &= W^1{}_1 + \frac{h}{h_3}(W^1{}_3 - W^1{}_1) \end{aligned}\right\} \quad \ldots.(50)$$

From equation (15) we have

$$\frac{Ya_o}{\sqrt{2a_o}} = \int_o^{h_1} \frac{W^1}{\sqrt{n}}\,dh + \int_{h_1}^{h_1+h_2} \frac{W^1}{\sqrt{n}}\,dh \quad \ldots\ldots\ldots\ldots(51)$$

Equations (44) and (49) for W^1 and n respectively can be substituted in the first integral and equations (46) and (50) in the second integral. Hence

$$\frac{Y_o}{\sqrt{2a_o}} = \frac{2}{3}\,\frac{h_1}{n_1-n_o}\left\{(W^1{}_1\sqrt{n_1} - W^1{}_o\sqrt{n_o}) + \frac{2(W^1{}_o\,n_1 - W^1{}_1\,n_o)}{\sqrt{n_1}+\sqrt{n_o}}\right\}$$

$$+ \frac{2}{3}\frac{h_2}{\sqrt{n_1}}\left\{2W^1{}_2 + W^1{}_1\right\} \quad \ldots\ldots\ldots\ldots\ldots\ldots\ldots(52)$$

In this equation the only unknowns at this stage are $W^1{}_1$ and $W^1{}_2$ and from (50) $W^1{}_3$ is simply obtained from $W^1{}_2$.

The position therefore is that another equation is now available containing linear terms in D_{N_1}, D_{E_1}, D_{N_3} and D_{E_3}.

Hence for any one azimuth there are three basic equations (22), (48) and (52) available and six unknowns i.e. a_1, D_{N_1} and D_{E_1} at the first selected height 35 km and a_3, D_{N_3} and D_{E_3} at the second selected height say 50 km above the earth's surface.

It can readily be seen what is a reasonable height to use for h_3 from examination of the values of h_2 obtained from the equations (21) for the different azimuths used.

Theoretically when the cross-wind deflection data are used in this manner good receptions on two azimuths only are sufficient to produce a result from an experiment. In practice however the equations are very sensitive to the errors in observation due to difficulties of determining exactly the initial times of sound reception at the recording microphones and it was found feasible to consider only the experiments in which receptions on three or more azimuths were available. Thus for 3 azimuths 9 equations in six unknowns are available, for 4 azimuths 12 equations and so on. The determination of the most probable values by Least Squares methods then becomes possible and errors of observations consequently can be reduced. The results shown in Figs.4, 5 and 6 are the most probable values found by this method.

Discussion of Results.

The results obtained are shown in Figs.4, 5 and 6 and TABLES V and VI which correspond to the similar Figures and Tables of M.R.P. 346. The following conclusions were obtained:-

(a) TEMPERATURE

1. There is a large inversion of temperature in the region of 40 - 50 km height and probably at about 50 km values of temperature exist which are roughly equal to surface values.

2. From about 20 - 30 km at least the temperature is roughly isothermal but there is some evidence for rather lower temperatures towards the top of this layer than have been found at the bottom.

3. At any given level at 40 km or above there is evidence for a large annual variation of temperature. Approximately 40°C is suggested for the amount of this variation at 50 km height.

(b) WIND

4. The wind at levels of 30 to 40 km is predominantly westerly in winter and easterly in summer. The winter westerly components may attain values of 50 - 60 m/sec. but the summer easterly components have maximum values of 20 - 30 m/sec. There is some evidence that at levels higher than 50 km the wind may be westerly during both winter and summer although speeds are likely to be considerably greater in the winter.

5. North-south components of wind are less than east-west components at these high levels. There is some evidence that a mainly northerly component is probable in winter and a southerly component in summer.

Most of the above conclusions have been arrived at in other work. Other work on anomalous sound receptions, calculations from meteor observations, calculation of direct absorption of solar radiation by ozone, work on atmospheric oscillations, and direct measurements from the V2 rocket trials in U.S.A. all give support to the existence of a region of high temperature at a height of about 50 km. as in 1. above.

As far as is known all evidence so far available suggests that the atmosphere remains roughly isothermal from the tropopause until an inversion starts somewhere above about 30 km. The suggestion of a region of lower temperature between about 20 and 35 km in 2. above was therefore thought to be unlikely. However, the effect is not well marked in these recalculations as it was in M.R.P.346 and the evidence is now regarded as inconclusive on this point. Perhaps the fact that all these experiments were done at night may be important.

The large annual variation in temperature in 3. above is supported by the American work in Alaska. It is reasonable to suppose that with these high temperatures being caused by direct solar absorption the value attained would be less in winter than in summer. This would however be complicated by the ozone's annual variation. If there is more ozone at higher levels in winter all the absorption could take place at higher levels in winter than in summer. In this case the maximum temperature might occur at greater heights in winter than in summer and this result was actually obtained in Alaska.

The "monsoon" effect of wind described in 4. is now fairly well established. The evidence given for this in M.R.P. 346 has since been strengthened by direct measurements by balloon in both England and the U.S.A. and is also confirmed in the American work in Alaska. The reason must be the differential heating between poles and equator in summer and winter with the atmosphere at 30 km or so becoming very cold during the polar night but becoming warmer than that above the tropics in summer. The tendency for a return to westerly winds at all seasons about 50 km would seem to indicate that 50 - 60 km may be the level of the efective top of the ozone layer.

The evidence for 5. is not well supported and more information will be required before anything can be said with any confidence on the meridional circulation at these levels.

Conclusions

The re-examination of the problem of determining winds and temperatures from recordings of anomalous sound propagation has produced a more satisfactory method of dealing with the observations. There are still some unsatisfactory aspects, in particular the selection of the constant dividing level of 35 km. The next step in improving the system would be to retain the "two straight line" structure formulae above but make the dividing level variable and deal with the outside limits of "a + w" thus produced. This would have the effects of removing the objections to both the system described above and the American system discussed. The statistical and computational problems raised would be considerable but certainly capable of solution. It is thought however that with the comparatively large errors of observations present and the broad physical assumptions made, further refinement of the mathematical treatment is not justified and that the system above represents a good practical solution.

TABLE V

Westerly Wind Components m/sec. at Different Heights

Expt.No.	Date	25 km	30 km	35 km	40 km	45 km	50 km
5	27/7/44	- 5	- 12	- 20	- 15	- 9	- 4
6	8/8/44	- 8	- 17	- 25	- 18	- 11	- 4
8	13/9/44	- 4	- 8	- 13	- 3	+ 6	+ 15
11	6/12/44	+ 34	+ 44	+ 54	+ 54	+ 53	+ 53
12	6/1/45	+ 19	+ 29	+ 39	+ 38	+ 37	+ 37
15	6/3/45	+ 27	+ 40	+ 53	+ 51	+ 48	+ 46
16	6/4/45	- 3	- 4	- 5	- 2	+ 1	+ 4

Southerly Wind Components m/sec. at Different Heights

5	27/7/44	- 1	- 3	- 5	0	5	10
6	8/8/44	- 7	- 4	- 1	- 1	1	2
8	13/9/44	0	- 1	- 2	- 3	- 4	- 5
11	6/12/44	5	11	17	14	12	9
12	6/1/45	- 29	- 28	- 27	- 33	- 40	- 46
15	6/3/45	- 20	- 20	- 19	- 23	- 29	- 33
16	6/4/45	- 5	- 5	- 5	- 8	- 12	- 16

TABLE VI

Temperatures °A at Different Heights

Expt. No.	Date	25 km	30 km	35 km	40 km	45 km	50 km
5	27/7/44	222	222	220	248	278	310
6	8/8/44	216	212	208	240	278	310
8	13/9/44	217	214	210	241	271	300
11	6/12/44	206	199	193	217	242	268
12	6/1/45	206	205	204	223	243	269
15	6/3/45	206	202	197	224	252	283
16	6/4/45	214	212	211	236	263	290

G. 278685/DC/1/51/40

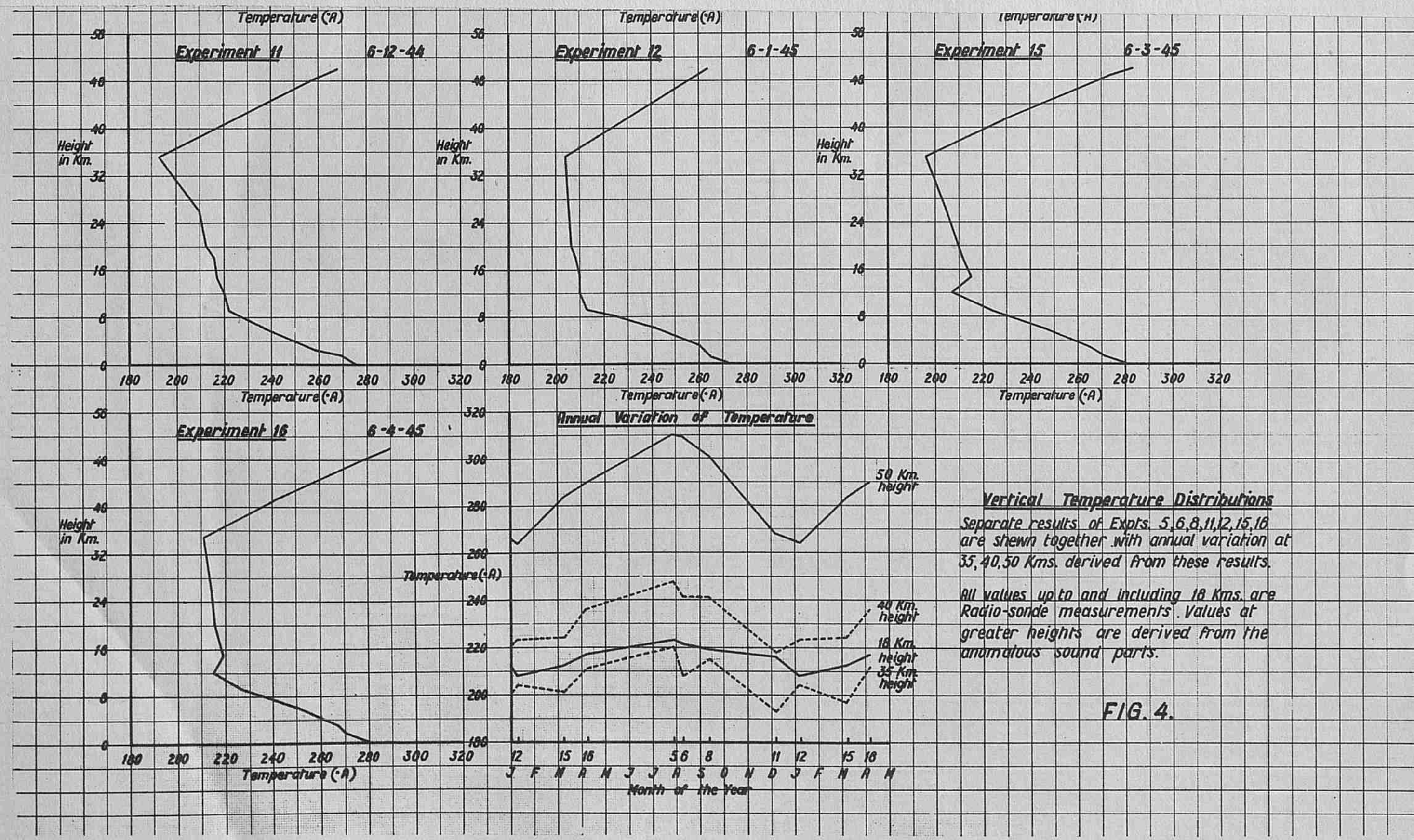

Vertical Temperature Distributions

Separate results of Expts. 5,6,8,11,12,15,16 are shewn together with annual variation at 35,40,50 Kms. derived from these results.

All values up to and including 18 Kms. are Radio-sonde measurements. Values at greater heights are derived from the anomalous sound parts.

FIG. 4.

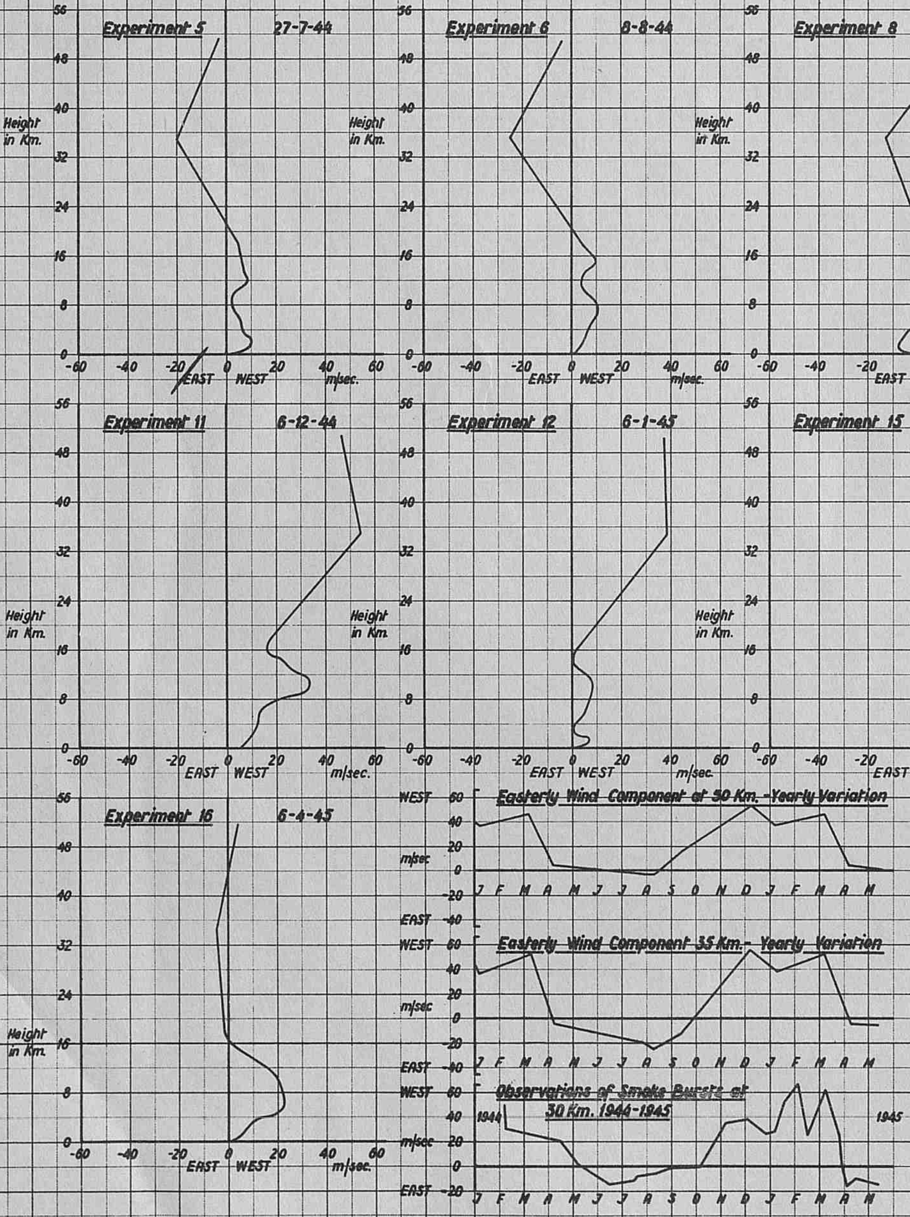

EAST-WEST Wind Component
Results of separate Experiments.

Values below 16 Km. are Radio-sonde observations. Values above are deduced from Anomalous Sound Recordings.

Yearly variations are compared with direct observations of smoke drifts at 30 Km.

FIG. 5.

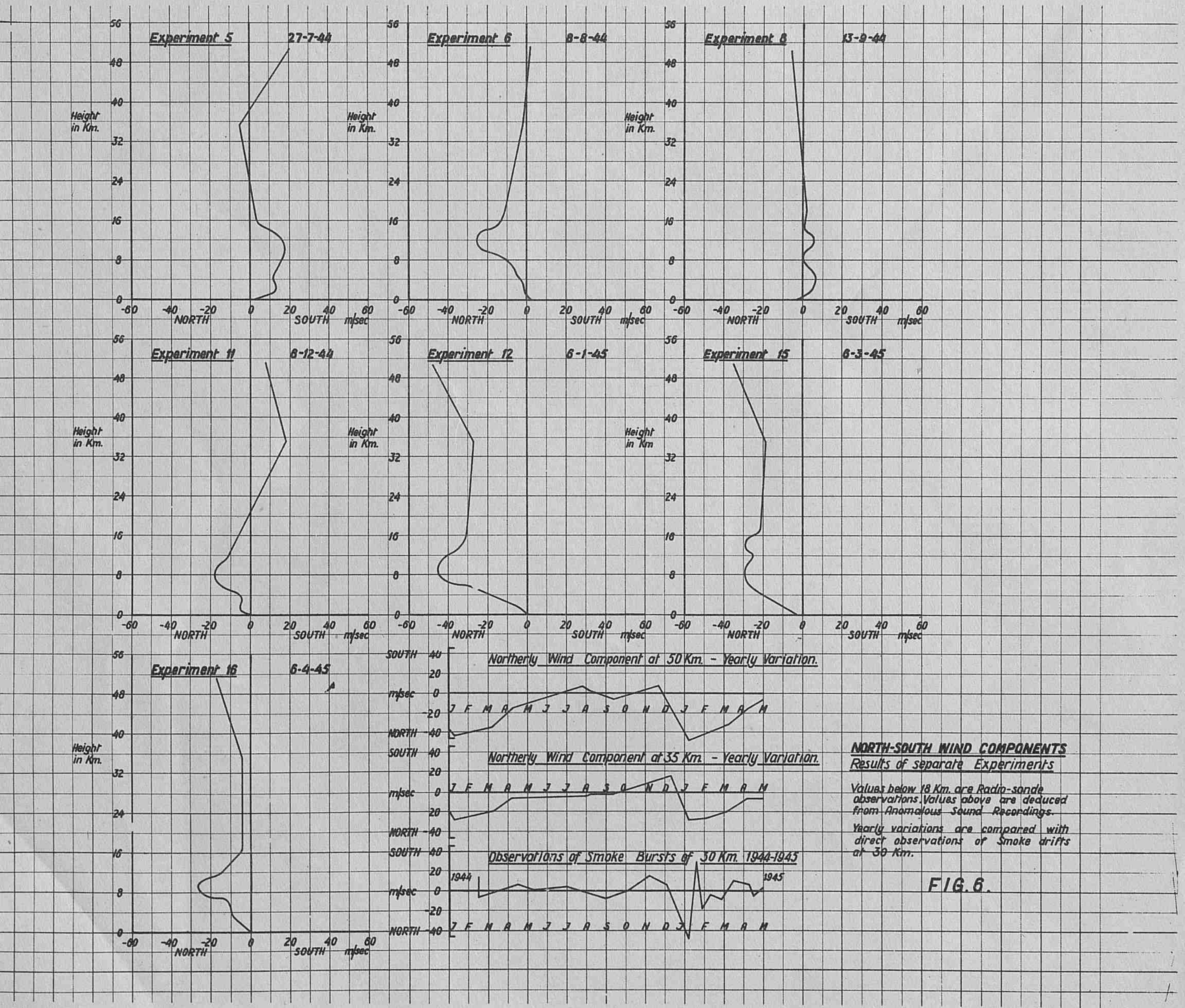

NORTH-SOUTH WIND COMPONENTS

Results of separate Experiments

Values below 18 Km. are Radio-sonde observations. Values above are deduced from Anomalous Sound Recordings.

Yearly variations are compared with direct observations of Smoke drifts at 30 Km.

FIG. 6.

paper of the Meteorological Research
Committee (London).
M.R.P. No........... by Mr.............................
A copy is available in the Library of
the Meteorological Office."

Personal Copy
M.R.P. 612
S.C.II/69
14th February, 1951

AIR MINISTRY

A T I - 172126

METEOROLOGICAL RESEARCH COMMITTEE

Bob -
My charts constructed at South Ruislip in 1951-52 and MacDill in 1949-50 bear out most of the statements made in this paper.
Durbin

Day to Day Variations in the Tropopause - Their Causes and Significance

by
J.S. Sawyer
(Meteorological Office)

Sawyer gave this to me in Aug. 51.

1. Introduction

The increasing amount of flying at levels of 30,000 to 40,000 feet has drawn attention to the need for an improvement in our knowledge of the structure and dynamics of the upper troposphere and lower stratosphere. The tropopause is an important feature of this layer of the atmosphere and an understanding of the nature of the changes which it undergoes and their relation to other features of the weather situation is essential to the proper analysis and forecasting of meteorological conditions around 35,000 ft. !! The present investigation has therefore been directed to the study of day to day variations of the tropopause and to their relation with the recognisable weather systems which are followed during the course of routine weather analysis.

During the Second World War (1939 - 45) an extensive network of radiosonde observations was established over Europe and N. America and has been maintained since with the addition of observations from "weather ships" in the N. Atlantic. Most of these soundings reach the tropopause so that the material is now available for the drawing of comprehensive charts of the topography and structure of the tropopause; it is possible to draw charts at 12 hr. intervals over a wide area and at 6 hr. intervals in the immediate vicinity of the British Isles. Prior to 1939 upper air soundings which reached the tropopause had been irregular and generally unrelated in time or space. Analysis of them had therefore been primarily on a statistical basis following the pioneer work of W.H. Dines (1). Strong correlation was found between the height of the tropopause, the pressure at 9 km and the temperature in the middle troposphere and a smaller correlation with surface pressure. However, as will be seen, these relations are of only limited use in predicting short term fluctuations of the tropopause.

In addition to the statistical treatment of observations of tropopause height, several analyses have been published of data obtained from sequences of aerological soundings at short intervals of time and of soundings on international aerological days. Such aerological analyses, notably those of J. Bjerknes (2), E. Palmen (3) and A. Nyberg (4), have drawn attention to certain features of tropopause behaviour in relation to the weather systems of the troposphere. However, no comprehensive synoptic analysis based on the routine radiosonde ascents of the post war years appears to have been published. The results of such an analysis of the topography of the tropopause for one month (May, 1949) are described in the following paper. The aims of the investigation have been to ascertain whether a self-consistent analysis of the tropopause is possible, to recognise and describe characteristic modes of behaviour of the tropopause and to relate them to the synoptic situation in the troposphere, and finally to seek the physical processes responsible for the observed day to day changes. It was hoped that the results of this study would be of theoretical value in improving our understanding of the physical nature of the tropopause and also of practical value in the problem of forecasting the temperature structure of the air near the tropopause level. Thus indirect assistance in the important problem of forecasting high level winds was sought. The study is to be regarded as a preliminary to further investigation; the various modes of tropopause behaviour require further study on more extensive data, and the present paper is intended primarily to indicate the lines on which such work might proceed. It may also form a basis for relating physical research on the tropopause to synoptic studies.

In the following section, various theoretical and practical ideas will be outlined in order to present a brief survey of present knowledge regarding the tropopause. Subsequently the scheme of the investigation will be described in section 3, followed by some statistical results in section 5. Various modes of behaviour of the tropopause are described in section 7 and the relation of present results to earlier investigations and to theoretical problems is discussed in section 8.

2. Theoretical and Observational Knowledge of the Tropopause.

(a) The reasons for stratosphere and tropopause

The accepted explanation of the division of the atmosphere into troposphere and stratosphere was given by E. Gold (5) and W.J. Humphreys (6) who regarded the stratosphere temperature as determined essentially by the requirements of radiative balance and the troposphere as a region in which the turbulent transfer of heat upward was dominant. On this basis it would be natural to regard the tropopause as the upper limit of convective turbulent exchange, and the sharp change of lapse rate at the tropopause as a change from a lapse determined by turbulence to one determined by radiation. However, although usually steep, the lapse immediately below the tropopause is not normally suitable for penetrative convection either of dry or moist air, and moreover although turbulence has been reported by aircraft at these levels it appears to be the exception rather than the rule. It, therefore, seems unlikely that penetrative convection is proceeding actively and continuously at levels immediately below the tropopause as it is, for example, below the inversion which limits convection in the lower layers of a summer anticyclone.

In the absence of persistent convection from below, it would be surprising that the change of lapse rate should remain as sharp as it is found to be, if there were no other factors operative. In an atmosphere with homogeneous radiative properties radiation as well as turbulence would tend to smooth such a discontinuity. Evidence as to the detailed structure of the lapse rate near the tropopause is not available, but it is noteworthy that the radio-soundings which observe temperature at levels separated by approximately 5 mb (450 ft.) fail to detect any departure from a discontinuous change in lapse rate on the majority of occasions. (More detailed temperature soundings by specially designed equipment might provide valuable information).

It may be argued that the temperature lapse rate in the troposphere is to be regarded as determined primarily by a form of turbulence in which the turbulent elements are not the individual cloud cells but the depressions and anticyclones of the large scale circulation which result in an oblique upward and downward exchange of air from low levels in low latitudes to high levels in high latitudes (as described by E.T. Eady (7)). However, the exchange of air in the region immediately below the tropopause by this process would seem to be too slow to account for the sudden change of lapse at the tropopause. Moreover, the lower stratosphere is known to take part in the circulation of depressions and anticyclones and it is not clear why the large scale turbulent process should have a sharply defined upper limit.

R.M. Goody (8) has recently discussed the radiative conditions at the tropopause and shown that a sudden change of lapse or inversion is possible provided that we postulate a constant lapse rate in the troposphere maintained up to the tropopause by turbulent transfer of heat. However, in view of the preceding considerations it seems doubtful if this assumption can be justified. It would seem more natural to attribute the sudden change in lapse rate at the tropopause to an abrupt change in the radiative properties of the atmosphere at the tropopause level. A rapid decrease upward of humidity of the air is known to be a feature of the lower stratosphere although not always identifiable with the tropopause (Shellard (9)); a sudden change in the haze content has also been observed (Brewer (10)). The different radiative loss from a moist or hazy troposphere compared with the overlying drier cleaner air may well account for the sharp change of lapse at the tropopause (see F. Möller (11)). The cause of the low water content of the temperate stratosphere is still undetermined. Frost points measured within the stratosphere are normally found to lie between -80°F and -120°F (Shellard (9)). There is laboratory evidence that below -70°F the nuclei for ice formation become fewer and that larger crystals form than at higher temperatures and would consequently fall more rapidly (Dobson (12)). Thus if the air is cooled to these low temperatures drying will be rapid, but so far as is known temperatures below -110°F occur regularly only near the tropopause in the equatorial belt and this has led A.W. Brewer (13) to suggest that air is transferred from troposphere to stratosphere in the equatorial belt and re-absorbed in the troposphere in the temperate regions, thus maintaining the dryness of the temperate stratosphere. J.K. Bannon and A.H.R. Goldie have suggested a similar circulation for slightly different reasons (14). However, temperatures below - 80°F do occur at the tropopause over England from time to time at all seasons (Dewar (15)) and if the transfer of air from the troposphere is a fairly rapid process it might also occur in temperate and sub-tropical latitudes and the derivation of part of the stratospheric air in this way is not ruled out.

To summarise the explanations of the tropopause:-

The broad features of vertical temperature distribution within the atmosphere may be regarded as determined by the requirement of radiative equilibrium in the upper layers (the stratosphere) and of convective and turbulent transfer of heat in the lower layers (the troposphere). Whether this explanation can be pressed to explain the sudden change in lapse rate at the tropopause is more doubtful and an alternative explanation lies in the different radiative properties from troposphere and stratosphere associated with their different dust and water contents, the sharp change of lapse being associated with the rapid transition in these properties. The choice between these two interpretations has some bearing on the interpretation of the daily changes in the tropopause because on the latter we should expect the tropopause to move up and down with the air itself whereas on the former we might expect to find evidence of the tropopause moving downward with respect to the air as turbulence slackened and radiative balance extended to lower levels, and moving upward as turbulence increased in the troposphere.

(b) The statistical properties of the tropopause

The statistical method has proved well adapted to codifying knowledge regarding the behaviour of the tropopause. The high correlation between the tropopause height and temperature and conditions within the troposphere was first emphasised by W.H. Dines (1) in 1919. Since then the broad correctness of the results has been confirmed by several investigators and probably the most reliable evaluation of the correlation coefficients is that by C.H.B. Priestley (16). The statistical relation between tropopause height and the synoptic situation was also investigated by C.S. Durst and W.C. Swinbank (42). The most important relations are

(a) positive correlation between tropopause height and temperature in the middle troposphere (e.g. at 500 mb) (+ 0.65)

(b) positive correlation between tropopause height and surface pressure (+ 0.49) ?

(c) positive correlation between temperature at the tropopause and pressure at the tropopause (+ 0.75)

Bostiks correlation between trop ht + 500-1000 thickness?

Values in brackets are the correlation coefficients evaluated by Priestley.

Although these correlations are substantial, about 40 per cent of the variance of the tropopause height remains unexplained. Moreover, most of the correlation of the tropopause height with the 500 mb temperature and surface pressure arises from the association of these three factors in the "long wave pattern" of the hemispherical flow. This is brought out in Figure 1 and Figure 2 which show the contours of the tropopause (Figure 1) and the contours of the 500 mb surface (the long wave pattern) over a wide area. The correlations are therefore representative of the oscillations of the tropopause which occur over wide areas and over periods of several days. The correlations are not necessarily representative of the smaller-scale variations (on the scale of individual depressions and less, nor of the short period changes in tropopause height, 24 hours or less). The contribution to the correlations of the longer period oscillations is illustrated in Figure 3 in which are plotted the 6 hour values of tropopause height, and height and temperature of the 500 mb. level at Larkhill in May 1949.

Nevertheless, E. Björkdal (18) has suggested the use of the regressions between tropopause height and temperature in the middle troposphere (5 km) for the purpose of completing contour charts of the tropopause over areas of limited observations. The method is however probably restricted to delineating the broader features of the long wave pattern, and, although it may be valuable for completing the fringes of a chart, it is doubtful if it can provide any help for the improvement of the finer detail of tropopause topography within a network of observations as complete as that over Europe and the British Isles.

Priestley (16) has also made use of statistical method in order to predict 12-hour changes in the height of the tropopause. He does not quote the correlation coefficients between the 12-hour change in tropopause height and the 12-hour changes in 500 mb temperature or surface pressure and it is probable that these correlations are smaller than those between the original data of heights and temperature. Nevertheless Priestley's table suggests that if the change of 500 mb temperature and surface pressure can be correctly predicted the sign of the change in tropopause height can be correctly given from the statistical relations on about 50 per cent of occasions and would be incorrectly given on about 15 per cent - the remainder being undetermined. Priestley realises that such relationships alone are inadequate for the forecasting of the changes in the tropopause and it is the purpose of the present paper to collate some of the additional knowledge which is required on the day to day disturbances of the tropopause.

Another limitation of the linear correlation technique as applied to the tropopause problem is illustrated by the fact demonstrated by Palmen (19) that as surface pressure decreases below 990 mb. the corresponding average height of the tropopause ceases to decrease and commences to increase. The average height of the tropopause corresponding to certain surface pressures is given by Palmen as follows:-

Surface Press.	976mb	987mb	993mb	1007mb	1017mb	1025mb	1034mb
Trop. Height	8.46	7.89	7.72	8.67	9.95	10.81	11.55 km

(c) Synoptic studies of the tropopause

Even before a coverage of upper air soundings was available which permitted the study of the tropopause on a synoptic basis, W.H. Dines (20) had deduced from the nature of the correlations between pressure and temperature at the tropopause and in the troposphere that the observed variations in the tropopause height must be the result of both horizontal and vertical motions. The analyses of the tropopause from the subsequent serial ascents and "aerological day" data owed much to the influence of E. Palmen. Palmen (19) emphasises the importance of vertical motion as well as horizontal advection in displacing the tropopause, but also introduces the idea of the reformation and dissipation of the tropopause by dynamical convergence and divergence.

The various views on the causes of variations of tropopause height are probably best made clear by a consideration of the tropopause oscillation in association with a system of progressive troughs and ridges. One of the first aerological analyses of such a system was given by J. Bjerknes (2). He attributes the tropopause oscillation primarily to horizontal advection of high tropopause in association with warm air from low latitudes and low tropopause with cold air from high latitudes. Bjerknes was studying a depression with an open warm sector and he recognises that vertical motion may have more influence on the tropopause in occluding depressions. Bjerknes also finds that the tropopause ridge lies ahead of the surface pressure trough and the tropopause trough is ahead of the surface pressure ridge but the tropopause wave is in phase with the pressure wave in the upper troposphere which is displaced backwards with respect to the pressure oscillation at lower levels. !! Bjerknes' model of the tropopause oscillation in association with a warm sector depression is illustrated diagrammatically in Figure 4 and has been widely reproduced. The basis of this analysis is a single continuous tropopause but in later papers Bjerknes has followed the technique of Palmen which will now be described.

Palmen's earlier studies, (21), (19), (3), (22) and (23), were mainly concerned with deep, rapidly occluding depressions. Palmen found that the tropopause behind a deep and active depression was often at a lower level and lower potential temperature than in the original cold air mass. He concluded that not only was vertical motion of the air important in lowering the tropopause behind a depression, but also that the tropopause dissolved at its old level and reformed at a new lower level behind a deep depression. Support for the idea of the reformation of the tropopause at a lower level also came from the ill defined nature of the tropopause on some of the ascents in these deep depressions; these soundings showed several levels of change of lapse rate which could be interpreted as tropopauses in process of formation and decay. The process of reformation of the tropopause at a new level was regarded by Palmen as the result of dynamical effects, horizontal divergence combined with vertical convergence. Such a system results in upward motion and an increasing lapse rate below the new tropopause level and downward motion above the new tropopause with a decreasing lapse rate or increasing inversion above it. The vertical circulation envisaged by Palmen in association with developing depressions and anticyclones is illustrated in Figure 5. The vertical circulation is additional to the horizontal movements of the tropopause. J. Bjerknes and Palmen (24) have jointly published some further observations regarding the depression of 26 - 28th December, 1928 and concluded that in the later stages of this depression vertical motion had an important influence on the tropopause although Bjerknes' original analysis (2) stressed only the advective effect. A.H.R. Goldie (25) has also stressed the importance of the vertical circulation in distorting the tropopause but in contrast to Palmen he appears to regard the tropopause as a continuous and persistent material surface. C.K.M. Douglas (26) has also regarded all three processes, advection, vertical motion and reformation, as operative in determining the configuration of the tropopause, but he has stressed radiation and turbulence as factors likely to lead to the dissipation and reformation of the tropopause rather than dynamical divergence and convergence stressed by Palmen. A. Refsdal (27) has also emphasised the radiative effect.

The idea that the tropopause may reform and dissipate dynamically and thus result in two or more discontinuities of lapse rate at the lower boundary of the stratosphere has led to the introduction into aerological analyses of the "multiple", "foliated" or "laminated" tropopause. The most complete exposition of this analytical technique is given by J. Bjerknes and E. Palmén (28). They regard every discontinuity of lapse rate near the base of the stratosphere as a "tropopause" and where there is more than one such discontinuity the tropopause is regarded as "multiple". As a "working hypothesis" it is assumed that each individual tropopause has a constant potential temperature throughout its extent and the potential temperature is thus used to identify individual tropopause sheets. When descending air motion takes place it is supposed that the lowest tropopause sheet will be intensified and become dominant and when upward motion takes place the upper tropopause is expected to become dominant. Individual tropopause sheets are therefore regarded as incipient discontinuities of lapse rate which can be intensified into a well defined discontinuity in a suitable divergent horizontal wind field. Palmen and Bjerknes are very tentative in regard to the origin of the series of tropopause layers but appear to regard them as probably formed by irregular penetration of convection to various levels in the equatorial belt; they also consider an explanation based on radiation to be possible.

Observational evidence from soundings reaching the tropopause does show that more than one change of lapse rate is not unusual. However, "multiple tropopauses" do not appear to be nearly so widespread as the Bjerknes and Palmen analysis would suggest and, indeed, the evidence within this paper seems a little forced.

True !!

This form of analysis with multiple tropopauses has been adopted in several other analyses by various authors including J. van Mieghem and A. Nyberg. These are listed among the references (references (29) to (35)) but the main interest of these papers lies in the tropopause behaviour found to be associated with particular synoptic systems.

More recently meridional atmospheric cross-sections have been prepared extending over a wider area than any of the earlier studies, and in these the authors have analysed the tropopause of the northern hemisphere into two or three discontinuous sheets. For example E. Palmen and K.M. Nagler (36) recognise three distinct tropopause sheets on some vertical cross-sections which they have drawn, viz:- a "real tropical tropopause" south of latitude 40°N and at level near 100 mb, an "extra-tropical tropopause" between latitudes 35° and 47°N and at level between 300 and 200 mb and a "polar tropopause" at about the 300 mb level further north. The southern of these two discontinuities had been recognised over northern India by K.R. Ramanathan and K.P. Ramakrishnan (37) as early as 1933, and attributed by them to a large scale folding of the tropopause resulting from meridional circulations in the vertical plane. The northern discontinuity noted by Palmen and Nagler is associated with the "jet stream" and will be discussed further in section 7(a).

These discontinuities in tropopause level shown on meridional sections are on a much greater scale than the separation of individual tropopause laminae on the earlier model of Palmen; the separation is usually 5,000 to 10,000 feet in height and 40 to 80°F in potential temperature for the former compared with 3,000 ft. and 10°F for the latter. The various treatments of the tropopause in meridional sections are made clear in Figure 6(a) on which are shown the mean tropopause according to Ramanathan (38) with an indication as to how folding may give rise to a discontinuity; this may be compared with Figure 6(b) in which an outline of an individual section by Palmen and Nagler is given. It is interesting to note that recent evidence from high altitude radio sondes (F.J. Scrase (39) and B. Gutenberg (40)) has shown that temperature in the stratosphere frequently begins definitely to increase upward at a level of about 60,000 feet in extratropical latitudes. This is about the same level as the equatorial tropopause and the discontinuity may indeed be more or less continuous with it. This level is rather lower than the previously accepted level of the base of the upper warm "ozone" layer, but it does not appear necessarily desirable to regard this change of lapse from isothermal or slight lapse to inversion as a high level tropopause in temperate latitudes as Scrase (39) appears to do.

(d) Definitions of the tropopause

It will be clear from the preceding account of the various treatments of the tropopause problem that different authors have defined the tropopause in different ways and that some of the differences between their results arise from this. It was one of the aims of the present investigation to provide a background against which the revision of present definitions of the tropopause within the Meteorological Office could be considered. It is therefore convenient to list some of the methods used by investigators to define the tropopause.

In recent Meteorological Office practice the position of the tropopause has been determined according to the following convention which differs slightly from that given by W.H. Dines (1).

Type I - When the stratosphere commences with an abrupt change in lapse rate to an inversion, the tropopause is at the base of the inversion.

Type II - When the stratosphere commences with an abrupt change to a lapse rate of less than 2°C per Km or to isothermal, the tropopause is at the height of that change.

Type III - When there is no abrupt change of lapse rate, the tropopause is taken as the height of the point at which the lapse rate first becomes less than 2°C per Km, provided that it does not subsequently exceed this value for any subsequent kilometer.

These definitions of the level and the type of the troposphere were intended primarily for statistical purposes but have also been applied in the drawing of synoptic charts of tropopause topography. They are not entirely unambiguous particularly in respect of the emphasis to be put on the requirement of an "abrupt" change. There has been a tendency in interpretation to consider a tropopause as Type I when an inversion exists whether abrupt or not when perhaps greater emphasis on the requirement of an abrupt change would have placed the tropopause at such a change at a lower level.

Although a rigid definition of the tropopause ~~is~~ required for statistical analysis it may be possible to adopt a more subjective view when synoptic analysis is undertaken; this may be desirable in order to maintain continuity in space and time. J. Bjerknes (2) writes "On first sight one would place the tropopause simply where the lowest temperature occurs, while the true tropopause, which is lower down, passes for an insignificant feature in the upper troposphere. To arrive at a coherent system it is necessary to admit the diminution of the vertical lapse rate of temperature as a sign of the true tropopause". In the later paper J. Bjerknes and E. Palmen (28) regard all sudden decreases of lapse rate in the upper troposphere and lower stratosphere as defining a characteristic point of the tropopause. Recently H. Flohn and R. Penndorf (41), accepting Palmen's analysis of laminated tropopauses, have suggested that no attempt should be made to define a single tropopause level but that a tropopause layer should be substituted extending downward a conventional distance from the level at which isothermal conditions are reached.

3. The present series of tropopause charts

In order to make a study, as unbiassed as possible, of the day to day changes in the tropopause, it was decided to plot and analyse a month's series of contour charts of the tropopause with considerably greater attention to continuity and detail than is possible during routine analysis. Contours of the tropopause are drawn daily at C.F.O. and published in the Daily Aerological Record, but these charts are drawn only at 24-hour intervals and full advantage is not made of continuity with intermediate soundings. A subsequent comparison of the two sets of charts revealed few differences in respect of the broad distribution of high and low tropopause but there were significant differences in detail.

The present series of charts were plotted and analysed for 6-hour intervals. Plotted data were (a) the pressure at the tropopause, (b) the potential temperature at the tropopause and (c) the observed wind at the reported level nearest to the tropopause. The topography of the tropopause was delineated by means of isobars drawn at 20 mb intervals. The charts also contained an analysis of the surface pressure field and surface fronts in order to assist in relating the tropopause changes to ordinary synoptic developments. One month's charts were plotted, those for May 1949. The month was selected on account of the availability of data but proved to contain an interesting variety of weather types.

In order to assist in maintaining the continuity in the sequence of tropopause charts, trajectories of the air at tropopause level were drawn based on the observed winds and on a specially constructed series of 200 mb charts. Trajectories were estimated for 24 hours centred on each upper air sounding within the British Isles made at either 0300 or 1500 G.M.T. All data for the plotting of the charts were taken from the tephigrams plotted at C.F.O. from the telegraphic messages received. The placing of the tropopause was reconsidered in respect of each sounding and all significant changes in lapse rate near the tropopause level were recorded. In order to facilitate easy reference to the data small plots of pressure against temperature were made for each sounding and displayed in the appropriate geographic position on maps of the area studied.

In the drawing of the isobars on the tropopause, soundings which appeared discordant with the requirements of continuity in time or space were re-examined and, if two or more discontinuities of lapse rate existed, that which gave better continuity was accepted as the tropopause, irrespective of whether or not this accorded strictly with the Meteorological Office convention quoted in para. 2(d). In areas without observations the trajectories were used to complete the chart on the assumption that the tropopause was a material surface moving with the air.

In the drawing of the tropopause charts it was found difficult to regard the tropopause as a continuous surface. Discontinuities of level were therefore accepted and indicated where they were believed to exist. Evidence for the existence of real discontinuities lies in the disappearance of the tropopause at one level and reappearance at another in a sequence of soundings together with intermediate soundings showing changes of lapse rate at both levels. A useful criterion for the existence of such a discontinuity is a substantial change of potential temperature at the tropopause. The nature and origin of these discontinuities will be further discussed in later sections.

4. The accuracy of the data regarding the tropopause

Before examining the results of the investigation it is convenient to consider the magnitude of the errors to be expected in the determination of the tropopause pressure and potential temperature from a radio-sounding. D.N. Harrison (42) has stated that, apart from systematic errors due to radiation and affecting all instruments in the same way, the probable error of the observed pressure in the high troposphere and lower stratosphere is about 5 mb and of the observed temperature about 1° F. (These errors refer to the pressure and temperature at the position of the instrument at the time and do not refer to the errors of pressures computed hydrostatically nor to temperatures on pressure surfaces).

The diurnal variation of pressure and potential temperature at the tropopause has been evaluated for the individual sounding stations during the month concerned. The mean of the tropopause pressure and potential temperature for the standard hours averaged over the five stations making 4 daily soundings is given in Table I. The absence of any systematic variation in the mean pressure between the synoptic hours suggests that systematic errors in pressure are negligible. The small variation in potential temperature may be real or instrumental. It implies a diurnal oscillation of temperature with an amplitude of 3 to 4°F. This variation is however smaller than random errors.

/Table I

Table I - Mean pressure p, and potential temperature, θ, at the tropopause averaged over all soundings at Aldergrove, Liverpool, Downham, Larkhill and Camborne for each synoptic hour - May 1949

Hour of observation (GMT)	0300	0900	1500	2100
Pressure, p, (mb)	243 ✓	243 ✓	240 ✓	244 ✓
Potential temperature, °F	127 ✓	130 ✓	132 ✓	128 ✓

During the course of a radio-sounding, observations of pressure, ? temperature and humidity are made once during each rotation of the fan-operated switch. This leads to discreet observations of temperature for about every 5 mb change of pressure near the tropopause. On account of the discreet nature of the observations a probable error of about 3 mb would be expected in the pressure at the tropopause and combining this with the 5 mb probable error of the pressure element we derive an estimate of 6 mb for the total probable error of the pressure at the tropopause.

The temperature at the tropopause is subject to no other error than the 1°F probable instrumental error noted above. However, the potential temperature is derived from both the temperature and pressure observations and will be affected by errors in both. At the levels where the tropopause occurs, a change of 1 mb in pressure (at constant temperature) results in a change of 0.75°F in the potential temperature and a change of 1°F in temperature (at constant pressure) results in a change of potential temperature of about 1.5°F. Combining the effects of the uncertainties in pressure and temperature at the tropopause we obtain an estimate of the probable error of the potential temperature at the tropopause as about 5°F.

In the following section we shall be concerned more with the errors of the difference of pressure and potential temperature at the tropopause in two soundings. We may therefore summarise the estimates of errors in this section as follows:-

Estimated root mean square error in tropopause pressure = 9 mb.
Estimated root mean square error in difference of two tropopause pressures = 13 mb.
Estimated root mean square error in tropopause potential temperature = 7°F.
Estimated root mean square error in difference of two potential temperatures = 10°F.

5. The advective contribution to short period changes in the tropopause

As indicated in section 3, trajectories were drawn of the estimated air movement during 24 hours centred on each of the available tropopause observations in the British Isles for each of the main hours of observation, 0300 and 1500 G.M.T. A total of some 460 trajectories were drawn, based on observed winds whenever possible, but often on the contours of the 300 mb or 200 mb surfaces. Geostrophic motion was then assumed and interpolation made as appropriate.

These trajectories have been used to assess the importance of advection in causing the observed changes in the tropopause, by comparing the magnitude of the changes of pressure and potential temperature of the tropopause following the air trajectory with the changes taking place at fixed points. In making use of the trajectories in this way it is important to realise that they have been used in order to maintain consistency in the drawing of the

/tropopause

tropopause charts themselves. The changes in tropopause pressure and potential temperature might therefore appear to be smaller than is in fact so. In order to minimise this effect only those trajectories have been used upon which it was possible to establish reasonably reliable values of pressure and potential temperature from soundings close to the track of the air.

Table II gives the root mean square values of the change in potential temperature and pressure at the tropopause over 6, 12 and 24-hour periods.

This is given both for fixed points (the figures are averages for the 9 sounding stations in the British Isles) and also for points along the estimated horizontal trajectory of air at the tropopause level. These figures are displayed graphically in Figure 7.

Table II - Root mean square values of the 6, 12 and 24-hour change of pressure and potential temperature at the tropopause
(a) following the air motion
(b) at a fixed point

Data for May 1949

Period	6 hr.	12 hr.	24 hr.
Pressure (mb)	(a) 15.4 (8.0) (b) 29.5 (26.1)	(a) 20.2 (15.5) (b) 36.1 (34.0)	(a) 26.1 (23.0) (b) 41.6 (39.6)
Potential Temperature (°F)	(a) 7.4 (b) 15.1 (12.0)	(a) 8.7 (b) 16.9 (14.3)	(a) 8.6 (b) 19.1 (16.8)
Number of trajectories	343	391	78

It will be noted that the changes following the air motion are substantially smaller than those at a fixed point, and it follows that advection plays an important part in the bringing about of the observed changes. Advection probably accounts for about half of the observed change of tropopause pressure at a point and almost all the observed changes in potential temperature apart from the effects of instrumental error.

The changes in potential temperature following the air motion show little significant increase with the length of the period. They are also slightly smaller than the estimated instrumental error of 10°F (see section 3). It is concluded that the differences in potential temperature along the trajectory which are observed are primarily due to instrumental errors and that the real changes are too small to be detected statistically. There are indeed a small number of cases of larger changes and these are discussed in section 7(d).

The figures in brackets in Table II represent the root mean square value of the pressure changes when allowance has been made for m.s.e's of 13 mb and 10°F due to observational uncertainty (see section 4). Following the air motion these figures increase rapidly with time at first but later more slowly, showing that the vertical motion tends to retain the same sign over at least 12 hours. An average vertical velocity of about 5 mb per hour is suggested as normal at the tropopause level.

6. Comparison with original records for Larkhill

In order to ascertain how far the tropopause as determined from telegraphic reports and adjusted to meet the requirements of continuity also represented a singular point in the temperature and wind soundings, the original records from the Larkhill soundings were examined, in relation to the tropopause level used to draw the chart series. It was found that the tropopause was normally associated with a sudden change of lapse rate which was indistinguishable from a true discontinuity by the instrument. The level selected as the tropopause from the plotted tephigrams and used in the drawing of the tropopause charts was found to coincide with a sudden change in lapse rate on 108 out of the 123 soundings which reached the tropopause during the period. There was no sharp change of lapse rate on 13 of the remaining soundings but on two soundings a sharp change existed at a level which, although appearing to define the tropopause, was inconsistent with the tropopause maps which had been drawn on the basis of continuity.

Examination of the wind soundings showed that significant changes of wind usually occur at or near the tropopause. However, the nature of these changes and their relationships to the level of the tropopause varied a great deal from one sounding to another and it does not seem likely that wind structure can be used to identify the tropopause. The converse ?

7. Characteristic features of the tropopause charts

In the following section various recurrent features of the tropopause charts will be briefly described. With only a month's charts as a basis the discussion cannot be conclusive but it is regarded as adequate to distinguish the main types of tropopause behaviour. The various features deserve further study and might provide useful synoptic models which can be introduced into the analysis of tropopause charts in association with the related developments in the troposphere even when observations are insufficient to be conclusive. These models may also assist in analysing and forecasting upper winds at levels near or just above the tropopause.

7(a). Folding of the tropopause

It has been noted by several authors, notably J. Bjerknes and Palmen (28) and by Kraus (43), that in advance of a warm front the level at which tropical air first replaces the polar air may lie above the tropopause in the cold air - this is the highest level at which the tropical air is warmer than the polar - and in the stratosphere the front, if it exists, must have cold front characteristics. The structure near the tropopause of at least some warm fronts is therefore believed to be as indicated in Figure 8. On this basis a sounding at point D would be expected to lie within the troposphere from D to C and again from B to A. It would show two tropopause levels, C and A. The same structure is also described by Nyberg and Palmen (33), Nyberg (35), Van Mieghem (44). Probably the earliest reference to this structure was due to A.H.R. Goldie (45).

Some 12 distinct examples of folds in the tropopause of essentially similar type were found on the tropopause charts for May, 1949, in association with warm front systems. In addition one similar fold was observed to form behind a cold front and another occurred without any associated surface frontal systems. In fact, folded tropopause occurred with all of the major warm front systems for which adequate observational coverage was available during the period, although the folded structure did not necessarily extend throughout the length of the front. The relationship of the fold or discontinuity in the tropopause to the front is displayed pictorially in Figures 9. These diagrams are intended only to bring out what are regarded as the significant features; the details varied considerably from case to case.

The first formation of the folded tropopause appears to take place from 500 to 1000 miles ahead of the surface warm front and to be well to the right of the track of the depression centre. Subsequently the folded structure may become more extensive and the line of the discontinuity tends to conform to the shape of the front but to be displaced 600 to 1000 miles ahead of it. The limit of the high level tropopause often appears to undergo a process analagous to occlusion; this will be described in the following sub-section. The "fold" has been found to lie above a variety of pressure systems but is usually east of the axis of the ridge of surface high pressure. It does not seem possible to identify its position by any feature of the surface synoptic chart.

There is a close association between the folded tropopause and the jet stream. The cases noted all occurred in association with a "jet stream" and most of them first appeared near the axis of the central part of the jet. There may be some tendency for the tropopause discontinuity to be a little to the left of the axis of the jet. It is quite probable that the folding process is closely associated with the dynamics of the "jet". Namias and Clapp (46) have shown that it might be expected that the entrance to a jet stream should be associated with a transverse component in the circulation as represented in the schematic transverse section Figure 10. This is on account of the fact that air entering the jet is strongly accelerated and therefore deflected across the isobars to the left to a greater extent than the less accelerated air above and below.

The confluent entrance to the jet brings together air from widely different localities; often arctic and tropical air come into close juxtaposition. This leads to an increase in the slope of the tropopause in the vicinity of the jet as indicated by the dashed line in Figure 10. The transverse circulation such as indicated in the figure would create an additional distortion of the tropopause to the final position indicated by the solid line, and thus would result in the folded structure observed. Reported wind soundings have been examined for evidence of the transverse flow necessary to produce the folded structure but the observations are inconclusive. In some cases there appears to be a component of wind across the general slope of the tropopause which is greater at the higher level of the tropopause than at the lower, but the difference is of the order of 5 to 10 knots and is therefore difficult to distinguish from errors in the soundings. A transverse component of this magnitude would however be quite adequate to produce the observed folded structure.

An example of a folded tropopause is that of 19th May, 1949. Figure 11 shows the surface positions of the fronts and isobars at 1500 superimposed upon the contours of the tropopause. The fold in the tropopause extends from N.N.W. to S.S.E. parallel to the warm frontal systems some 700 miles to the west. Figure 12 shows the contours of the 300 mb. surface and the position of the associated jet stream. Figure 13 shows a sequence of upper air soundings from Larkhill. Wind soundings from Larkhill and Camborne do not give any indication of the transverse current round the jet stream which has been suggested as a possible cause of the folded tropopause. However, the possibility remains that the folding process had already taken place upstream. A sounding at Aldergrove on the 6th May, 1949, is reproduced in hodograph form in Figure 14. It illustrates this possibility. This sounding was taken in the central part of a "jet stream" during the period when the formation of a folded tropopause was first detected. The fairly uniform direction of shear from 700 to 300 mb. can be regarded as defining the thermal gradient and the axis of the jet. The small component of the wind at 250 mb. transverse to this axis may indicate a circulation through the jet at this level. However, the detailed study of a large number of wind soundings through "jet streams" would be needed to establish this.

Routine soundings at 6-hour intervals are inadequate to investigate the rapidity of the change of tropopause level in association with the folded structure. Nyberg and Palmen (33) noted changes of 2 to 4 km in the level of the tropopause in two hours in a situation of this type.

7(b). "Occlusion" of tongues of high tropopause

In the preceding section it has been indicated that a discontinuity of the tropopause often arises by "folding" in association with a jet stream.

The discontinuity (here regarded as defined by the limit of the high tropopause sheet) usually lies slightly to the left of the axis of the jet. At the exit from the "jet stream" or sometimes at a marked troughline in the flow, the limit of the upper tropopause sheet is distorted as indicated schematically in Figure 15(a), (b) and (c), leading to a rather narrow tongue of high tropopause extending from the left exit of the jet stream. Such tongues were noted eight times on the tropopause charts for May, 1949. With one exception they were short lived features with a life of only a little over 12 hours, and were subject to a process of destruction very similar to the manner in which warm tongues disappear during the occlusion process of depressions.

An examination of the changes in tropopause height following the estimated air movement suggested that the tropopause within the tongue descended, and became less well defined, while at the same time a new tropopause at a lower level became more definite, probably forming out of the lower branch of the folded tropopause. The examination of a series of soundings through approximately the same air column as it moved along, indicated that this process could be the result of approximately adiabatic air movements in which the air at the level of the "high" tropopause descended and air at the level of the lower tropopause underwent little change of level.

Such a system of air movements requires vigorous divergence of the air between the two levels and indeed such divergence is to be expected dynamically to the left of the exit from a slow moving jet stream because the air on the left side of the jet has considerable cyclonic vorticity which must be lost at the exit (if the air moves faster than the characteristic configuration of contours).

The whole process appears to transfer relatively small volumes of air from the tropopause to the stratosphere.

An example of the formation and "occlusion" of a tongue of high tropopause is given in the charts for 0300, 1500 G.M.T. 5th May, and 0300 G.M.T. 6th May, 1949. A folded tropopause had developed in association with a jet stream extending from N.N.W. to S.S.E. off the west coasts of the British Isles and the approximate limit of the "high" tropopause is indicated by the "black and white" line on the chart for 0300 5th May, (Figure 16(a)). The corresponding limit has been indicated on the next chart (Figure 17(a)) for 1500 5th May, 1949, and could have been reached by motion following the observed and estimated winds at that level. However, on the third chart (Figure 18(a) for 0300 6th May) the high tropopause was no longer a significant feature over a large part of the area which should have been reached by air initially within the high tropopause area and the tongue has been shown as correspondingly reduced. Some estimated trajectories of air at tropopause level are shown in Figure 19. Contours of the 200 and 300 mb. surface corresponding to Figures 2, 3 and 4 are given in Figures 16, 17 and 18(b).

The dissolving of the high level tropopause by subsidence and its replacement by a lower tropopause is illustrated in Figure 19 by means of temperature soundings from a selection of stations plotted on a thermodynamic diagram (log pressure against temperature). Valentia may be regarded as typical of a sounding with a high tropopause near to the fold before the distortion commenced. The Liverpool and Downham Market soundings were taken in the tongues of high tropopause and those at Sola and Jever in the area which it would have been expected to reach had it not dissolved. The soundings at Sola still show traces of the upper tropopause at a potential temperature close to that at which it was previously observed.

7(c). Tropopause "Funnels"

Any sequence of charts of the contours of the tropopause reveals the presence of centres of low tropopause. These features have been discussed in several synoptic studies, notably by Palmen (23) and (19), Bjerknes and Palmen (28), Bjerknes, Mildner, Palmen and Weickmann (32) and J. Van Mieghem (44). Centres of low tropopause develop frequently in association with

/vigorously

vigorously deepening depressions and subsequently become centred over the old depression when it becomes slow moving and fills.

As has been indicated in section 2, Palmen has suggested that the formation of such areas of low tropopause is the result both of the descent of the air at the tropopause level together with the dissolution of the tropopause and its reformation at a lower level as the result of vigorous horizontal divergence. Palmen uses the expression "tropopause-trichter" (tropopause funnel) to describe the resulting systems of low tropopause which have several characteristic features.

The tropopause contour charts for May 1949 contained 12 centres of low tropopause. These were all persistent features with a life of from 2 to $7\frac{1}{2}$ days. All of the examples during this period were associated with descent of the tropopause during their initial stages. In some, but not all, of them there was evidence of a reformation of the tropopause at a lower level from the fact that the potential temperature at the tropopause in the centre of the tropopause depression became substantially lower than previously observed anywhere on the tropopause in the region of formation.

Out of the 12 examples of tropopause "funnels" studied, nine formed in association with active but rather slow-moving depressions - it is probable that depressions developing close to the tip of a cold trough or to the left of a difluence in the thermal pattern are particularly likely to lead to the development of a tropopause depression. Three of the examples studied were not initially associated with any recognisable surface pressure system. With two exceptions the tropopause low later became associated with a cold pool in the troposphere and an associated slow-moving depression.

The formation of tropopause funnels appears to be (more) closely associated with the flow pattern near the tropopause level. Nine of the twelve cases were associated initially with well defined troughs at 300 mb which subsequently developed closed circulations in several cases; the remaining examples were associated with closed 300 mb circulations from the earliest traceable stage. Evidence from the trajectories drawn for air at tropopause level suggest that the air usually subsides as it approaches the trough line from the west and ascends as it leaves the area on the eastern side. However, there usually appears to be a central core in which the air remained near the upper troughline and moved with it, even when no closed 300 mb contours were present. The structure is indicated schematically in Figure 20. It seems probable that the central core consists of essentially the same air at tropopause level through much of its history and that its movement is primarily due to horizontal advection. On the other hand the air passes through the outer regions of the tropopause depression which is maintained in these areas by the dynamical descent and ascent associated with the flow pattern.

In its later stages a tropopause "funnel" is often associated with a closed "low" at 300 mb but in the cases studied it appears to have been situated sufficiently eccentrically for its motion to be explained by advection. Motion of the centres of fully established tropopause funnels was generally slow, 20 kt or less, and often tortuous. In their earlier stages when associated with an open trough at 300 mb speeds of up to 45 kt appear to be normal.

An important feature of the structure of tropopause funnels is the presence of a very low tropopause in the central region - usually well below the 300 mb level and sometimes below 400 mb. The potential temperature at this tropopause is usually between 80 and 95°F which is often well below the potential temperature at the tropopause in any of the air masses entering into the original circulation. It is not possible to say on the present evidence whether radiational cooling in the upper atmosphere could be sufficiently rapid to bring about this change but examination of the potential temperature change along the large number of trajectories drawn at tropopause level (see Section 5) suggests that the radiational effect is normally much smaller than this. It is also significant that the low central tropopause appears to be continuous with the lower boundary of an adjacent cold front in many cases. The tropopause is apparently well defined within the central core but on its fringes is often difficult to place; this also is consistent with a discontinuous structure as shown schematically in Figure 21.

The tropopause funnel with a closed wind circulation appears to be a dynamically stable system. Collapse of the system is often associated with the over-running of a higher tropopause associated with the approach of a vigorous warm-frontal system. When this occurs the decay of the tropopause funnel is rapid and it may effectively disappear from the charts in 12 to 24 hours. The process appears to be associated with the rapid descent of air in the tropopause funnel and its ultimate absorption into the troposphere.

The structure and behaviour of a tropopause "funnel" is illustrated by the system of 15 to 21st May, 1949. Charts of the pressure at the tropopause are reproduced at 24-hour intervals (Figures 22 to 26) together with charts of the 300 mb contours. Surface isobars and fronts are superimposed on the tropopause charts. This example was selected because it was well observed over the British Isles, but the 300 mb trough is not as clearly defined in the early stages as in many examples.

The sequence of soundings from Larkhill in Figure 27 presents typical soundings in various regions of a tropopause funnel. The arrows indicate the positions of the tropopause and the discontinuity in lapse in the upper troposphere. Continuous arrows have been used to indicate the level which has been accepted as the tropopause in the construction of contour charts.

Two cross sections through this funnel in perpendicular directions are shown in Figures 28 and 29 and illustrate the structure. The isokinetics, lines of equal normal wind velocity, have been based on both geostrophic measurements and observations; they show a jet stream to the north and east of the tropopause funnel and a less well defined maximum of wind to the south and west.

The over-running of a tropopause funnel is also illustrated in Figure 26 over the west coast of France where a "funnel" which has moved in from the Atlantic is collapsing beneath the high tropopause encroaching in association with the Atlantic frontal system. There is insufficient evidence to indicate whether a typical central core existed in the tropopause funnel over western France.

7(d). Reformation of the tropopause at a new level

On the tropopause charts for May 1949 there are several situations in which the tropopause appears to have been replaced simultaneously over a fairly wide area by a new tropopause at a different level.

There were five occasions on which the tropopause over the British Isles appears to have been displaced downward in this manner and one rather doubtful case in which it appears to have been transferred upward. This excludes developments in association with folded tropopauses or tropopause funnels as described in preceding section and also some cases which depended on the interpretation of a single sounding and may be attributable to instrumental error. The selection of the cases was made from the air trajectories at tropopause level and every occasion on which the tropopause potential temperature appeared to change by 10°F or more following the trajectory was examined.

The change in tropopause level was usually not large; 20 to 40 mb seems common with a corresponding change of potential temperature of 10 to 20°F. (smaller changes would have been eliminated by the method of selection). It is difficult to prove whether the change of tropopause level is continuous or discontinuous but comparison of soundings along a trajectory suggests in most cases that a discontinuity of lapse rate develops at a new level and subsequently becomes the dominant discontinuity, the potential temperature at both levels being approximately conserved meanwhile. This was also found by Palmen (17).

The surface synoptic chart showed no features which could be connected directly with these developments; several of the cases occurred on the fringes of anticyclonic areas. If the process is a quasi-adiabatic one, considerable horizontal divergence would have been required between the old and the new tropopause levels in order to transfer the tropopause downward as observed. In most of the examples the original tropopause which was replaced covered only a limited area 300 to 500 miles in width and its elimination resulted in an essentially simpler tropopause distribution and probably the flow pattern was also simplified. A dynamical cause is therefore possible.

An example is given by three successive soundings at Larkhill from 08 to 2100 on 21st May, 1949 (Figure 30). The winds were light at the tropopause level and the soundings can be regarded as representing essentially the same air column. That advection was unimportant is also brought out by the existence of similar simultaneous changes at Liverpool and Downham Market. The original high level tropopause disappears after the first sounding, but was continuous with a high tropopause previously identified at Camborne. The new lower level tropopause is indicated on the first sounding and appears to rise during the process while air at higher levels subsides. The synoptic situation is illustrated in Figure 31 together with the topography of the tropopause.

7(e) Minor Discontinuities of the Tropopause

Several of the charts of the tropopause show minor discontinuities of the tropopause at which the pressure level of the tropopause changes by about 20 mb and the potential temperature by some 10 or 15°F. Such discontinuities are recognised by J. Bjerknes and Palmen (28) in their diagrams of laminated tropopause. These discontinuities are persistent and can be traced on the tropopause charts over periods of one or two days at least. The discontinuous nature of the change is suggested by the frequent observation of double tropopause near the boundary.

An example of such a discontinuity appears on the tropopause chart for 5th May 0300 (Figure 16(a)) preceding the advance of a folded tropopause from the west. In this case the change in tropopause level seems to be associated with a change in the source of the air at that level; on the 4th the air over Southern England had approached from the southeast over France but on the 5th this was replaced by a westerly current from the Atlantic. The existence of a frontogenetic "col" at the 200 and 300 mb. level is clear from the 300 mb. contour chart for 5th May 0300 (Figure 16(b)).

The successive soundings at Larkhill from 2000 G.M.T. on 4th to 0800 G.M.T. on the 5th are reproduced in Figure 32. The changes in this example are somewhat obscured by the general descent of the air at tropopause level which was taking place, but the original tropopause can still be identified on the last sounding at Larkhill having descended from 225 mb to 267 mb but changing in potential temperature only from 123°F to 127°F. The occasion is interesting because an ascent by a Met. Research Flight aircraft was made at Farnborough (Figure 33) using a frost-point hygrometer. It is noteworthy that the original lower tropopause is the more striking feature of the temperature curve at Farnborough although the upper new tropopause is also indicated by a small irregularity. On the frost-point curve the upper new tropopause is marked by a rapid decrease in frost-point upward (Figure 33).

8. Results of the present investigation in relation to the structure of the tropopause

The results described in paragraph 4 indicate that at most times the tropopause may be regarded as a material surface moving with the air, but that at infrequent intervals the tropopause dissipates at one level and reforms at another. During the investigation no indication was found of steady motion of the tropopause upward or downward relative to the air and usually the tropopause is found to retain its potential temperature within the limits of measurement over 24 hours. Thus over such periods behaviour of the air near the tropopause level may be treated as adiabatic. The results of the trajectory analysis also indicate that vertical motion of the air at the tropopause level is of similar importance to horizontal advection in producing the changes of tropopause level at a given point.

Although the tropopause moves with the air as a material surface it is not continuous, but the discontinuities do not appear to be as numerous as some of the analyses by Palmen would suggest. On the tropopause charts drawn in the present investigation, there seemed to be no strong evidence that the potential temperature was strictly uniform along a single tropopause sheet and the use of this convention seems to have caused Palmen to depict an unnecessarily complex tropopause structure. Some of the discontinuities in the tropopause arise by a process of "folding" over, but other processes may also be operative. In particular the tropopause structure in sub-tropical latitudes and the connection between the tropopause in the equatorial belt and in the temperate regions requires further investigation.

It is possible to recognise certain characteristic disturbances of the tropopause. These lead to the transfer of air both from troposphere to stratosphere (in the occluding of high tropopause) and from stratosphere to troposphere (in the collapse of tropopause funnels).

The investigation gives no direct answer to the problem of the reason for the existence of the tropopause, but it does draw attention to the fact that the tropopause is maintained as a distinct feature during complicated distortions and displacements which might have been expected to destroy it. Moreover it acts as a material surface during the process. It therefore seems likely that some factor is operative which tends to maintain the discontinuity in lapse rate at the tropopause in association with particular material layers of air. The different radiation from moist and dry air seems a possible factor, although different dust content might also affect radiation and have a similar influence. The occurrence of anomalous occasions when the humidity discontinuity and tropopause appear to be at different levels may perhaps be accounted for by complex structure as described in section 7(e) and Figure 33 or by the displacement of the tropopause from the level of minimum temperature during the course of dynamical developments such as described in other paragraphs of section 7.

9. Practical application of the present results

It appears to be possible to prepare a self-consistent analysis of the tropopause in which the tropopause is treated as material surface embedded in the atmosphere and moving with it. It is necessary to admit the existence of discontinuities in the surface and of occasions when it reforms at a new level. It is considered that these should be incorporated in any system of tropopause analysis. It does not appear likely that any definition of the tropopause can be formulated which will permit it to be determined unambiguously on every individual temperature sounding, but if in fact the existence of the tropopause is associated with a change in radiative properties of the air, it would be desirable to give considerable weight to the abruptness of the change of lapse rate. For this purpose it might prove desirable in practice for the most distinct change in lapse rate to be indicated by the radio sounding station where the complete plot of the observations is available.

Forecasting of high-level winds requires a full analysis and understanding of dynamical developments in the upper troposphere and lower stratosphere. Analysis of the topography of the tropopause may prove useful in bringing out the vertical motions of the atmosphere at these levels as well as assisting the analysis of the temperature structure. A recognition of the modes of behaviour of the tropopause would be desirable for both purposes and it is considered that the modes of behaviour investigated briefly in section 7 should receive further attention.

REFERENCES

REFERENCES

1. Dines W.H. — The characteristics of the free atmosphere. Geophys. Mem., No. 13, London, Vol. 2, 1919, p.45.
2. Bjerknes J. — Exploration de quelques perturbation atmospherique à l'aide de sondages rapprochés dans les temps. Geofys. Publ., Oslo, Vol. IX, No. 9, 1930.
3. Palmen E. — Registrierballonaufsteige in einer tiefer Zyklone. Mitteilungen Instituts der Universität Helsingfors, No. 26, 1935.
4. Nyberg A. — Synoptic - aerological investigation of weather conditions in Europe 17 - 24 April, 1939. Meddelanden, Serien uppsater No. 48, Statens Meteorologisk - Hydrografiska Anstalt, Stockholm, 1945.
5. Gold E. — The isothermal layer of the atmosphere and atmospheric radiation. Proc. Roy. Soc. A, London, Vol. 82, 1909, p. 47.
6. Humphreys W.J. — Vertical temperature gradients of the atmosphere especially in the region of the upper inversion. Astroph. Journ., Vol. 29, 1909, p. 14.
7. Eady E.T. — Contribution to the Symposium on the General Circulation of the Atmosphere; 30th March, 1950, at Oxford. (Not yet published).
8. Goody R.M. — The thermal equilibrium of the tropopause and the temperature of the lower stratosphere. Proc. Roy. Soc. A., London, Vol. 197, 1949, p. 487.
9. Shellard H.C. — Humidity of the Lower Stratosphere - Met. Mag., London, Vol. 78, 1949, p. 341.
10. Brewer A.W. — The measurement of visibility of the upper air. Air Ministry, London, 1950, M.R.P. 548.
11. Möller F. — Die Wärmestrahlung des Wasserdamfes in der Atmosphäre. Gerlands Beiträge zur Geophysik, Leipzig, Vol. 58, 1941, p. 49.
12. Dobson G.M.B. — Ice in the Atmosphere - Quart. J.R. Met. Soc., London, 75, p. 117.
13. Brewer A.W. — Evidence for a world circulation provided by measurements of helium and water vapour in the stratosphere. Quart. J.R. Met. Soc., London, 75, 1949, p. 351.
14. Bannon J.K. & Goldie A.H.R. — The Stratosphere - Met. Mag., London, Vol. 78, 1949, p. 98.
15. Dewar D. — Frequencies of tropopause temperatures over Larkhill from June 1945 to December 1947. Met. Mag., London, Vol. 79, 1950, p. 27.
16. Priestley C.H.B. — Characteristics of the tropopause over Southern England, 1944. Meteorological Office, London, S.D.T.M. No. 107, 1945.

/17.

17. Durst C.S. & Swinbank W. — The relationship between the height of the tropopause and the wind in the neighbourhood of the tropopause particularly in regard to the synoptic situation. Met. Office, London, S.D.T.M., No. 18, 1941.

18. Björkdal E. — On the correlation between the geopotential of the tropopause and the temperature of the middle troposphere. Geofys. Publ., Oslo, Vol. XII, No. 15, 1940.

19. Palmen E. — Aerologische Untersuchungen der Atmophärischen Storungen mit besonderer Berucksichtigung der stratophärischen Vorgänge - Mitteilungen des Meteorologischen Instituts der Universität, Helsingfors, No. 25, 1933.

20. Dines W.H. — The correlation between pressure and temperature in the upper air with a suggested explanation. Quart. J.R. Met. Soc., Vol. 51, 1925, p. 31.

21. Palmen E. — Die Beziehung zwischen troposphärischen und stratosphärischen Temperature - und Luftdruckschwankungen - Beitrage zur Physik der freien Atmosphäre, Leipzig, Vol. 17, 1931, p. 102.

22. Palmen E. — Registrierballon aufsteige in einer tiefen syklone. Mitteilungen des Meteorologischen Instituts der Universität, Helsingfors, No. 26, 1935.

23. Palmen E. — Zur Frage der Temperature, Druck, und Wind verhältnisse in den höheren Teilen einer okludierten Zyklone. Met. Z., Braunchweig, Vol. 53, 1936, p. 17.

24. Bjerknes J. & Palmen E. — Aerologische analyse einer Zyklone - Beitrage zur Physik der Freien Atmosphäre, Vol. 31, 1934, p. 53.

25. Goldie A.H.R. — On the dynamics of cyclones and anticyclones, Part II. Weather, London, Vol. 4, 1949, p. 393.

26. Douglas C.K.M. — Some facts and theories about the upper atmosphere. Quart. J.R. Met. Soc., London, Vol. 61, 1935, p. 53.

27. Refsdal A. — Zur Thermodynamik der Atmosphäre. Geofys. Publ., Oslo, Vol. IX, No. 12, p. 56 - 57.

28. Bjerknes J. & Palmen E. — Investigation of selected European cyclones by means of serial ascents. Case 4. Feb. 15 - 17, 1935. Geofys. Publ., Oslo, Vol. 12, No. 2, 1937.

29. Mieghem J. van. — Analyse aerologique d'un front froid remarquable. Institut Royal Metéorologique de Belgique, Memoires, Vol. 7.

30. Mieghem J. van. — Sur l'existence de l'air tropical froid et de l'effet de foehn dans l'atmosphere libre - Institut Royal Metéorologique de Belgique, Memoires, Vol. 12, 1939.

31. Mieghem J. van. — Analyse aerologique du Cyclone due 17 - 19 Decembre 1936 sur l'Europe Occidentale. Institut Royal Metéorologique de Belgique, Memoires, Charleroi, Vol. 10, 1939.

/32

32.	Bjerknes J., Mildner P., Palmen E. & Weickmann L.	Synoptische-aerologische Untersuchung der Wetterlage während der Internationalem Tage vom 13, bis 18, Dezember 1937. Ver. Geophys. Inst. Univ. Leipzig, Vol. 7, Part 2, 1939.
33.	Nyberg A. and Palmen E.	Synoptische-aerologische Bearbeitung der Internationalem registrierballon aufsteige in Europa in der Zeit 17 - 19 Oktober. Geogr. Ann., Stockholm, 1942, No. 1 & 2.
34.	Mieghem J. van & Dufour L.	Analyse aerologique de la situation atmospherique du 7 au 9 Oct. 1938 sur l'Europe Occidentale et Centrale. Institut Royal Météorologique de Belgique, Memoires, Brussels, Vol. 14, 1942.
35.	Nyberg A.	Synoptic-aerological investigation of weather conditions in Europe 17 - 24 April 1939. Meddelanden, Serien uppsater No. 48, Statens Meteorologisch - Hydrografiska Anstalt, Stockholm, 1945.
36.	Palmen E. & Nagler K.M.	An analysis of the wind and temperature distribution in the free atmosphere over North America in a case of approximately westerly flow. J. Met, Lancaster, Pa., Vol. 5, No. 2, 1948.
37.	Ramanathan K.R. & Ramakrishnan K.P.	Distortion of the tropopause due to meridional movement in the substratosphere. Nature, London, Vol. 132, 1933, p. 932.
38.	Ramanathan K.R.	Discussion of results of sounding balloon ascents at Agra during the period July 1925 to March 1928 and some allied questions. Memoirs of Indian Met. Dept., Vol. 25, Part V, Calcutta, 1930, p. 163.
39.	Scrase F.J.	Measurements of wind and temperature up to 100,000 ft. by radio-sonde and radar. Met. Mag., London, Vol. 78, 1949, p. 284.
40.	Gutenberg B.	New data on the lower stratosphere. Bull. Amer. Met. Soc., Milton, Mass., Vol. 30, 1949, p. 62.
41.	Flohn H. & Penndorf R.	The stratification of the atmosphere. Bull. American Met. Soc., Milton, Mass., Vol. 31, 1950, p. 71.
42.	Harrison D.N.	The accuracy of Mk. II radio-sonde observations, Air Ministry, London, M.R.P. 422, 1948.
43.	Kraus E.	The formation of a laminated tropopause and the mass exchange between the stratosphere and the troposphere. Met. Mag., Vol. 78, 1949, p. 322.
44.	Mieghem J. van	Le premier example d'analyse d'un cyclone dans l'espace et le temps. Institut Royal Met. de Belgique, Miscellanées Fasc., II.
45.	Goldie A.H.R.	Circumstances determining the distribution of temperature in the upper air under conditions of high and low barometric pressure - Quart. J.R. Met. Soc., Vol. 49, 1923, p. 16.
46.	Namias J. & Clapp P.F.	Confluence theory of high tropospheric jet stream. J. Met., Lancaster, Pa., Vol. 6, 1949, p. 330 - 336.

Fig. 1. Contours of the tropopause 0300 G.M.T. 7 May 1949.

Level of the tropopause indicated by isobars at 20mb. intervals.

▬ ▬ ▬ Discontinuity in tropopause surface.

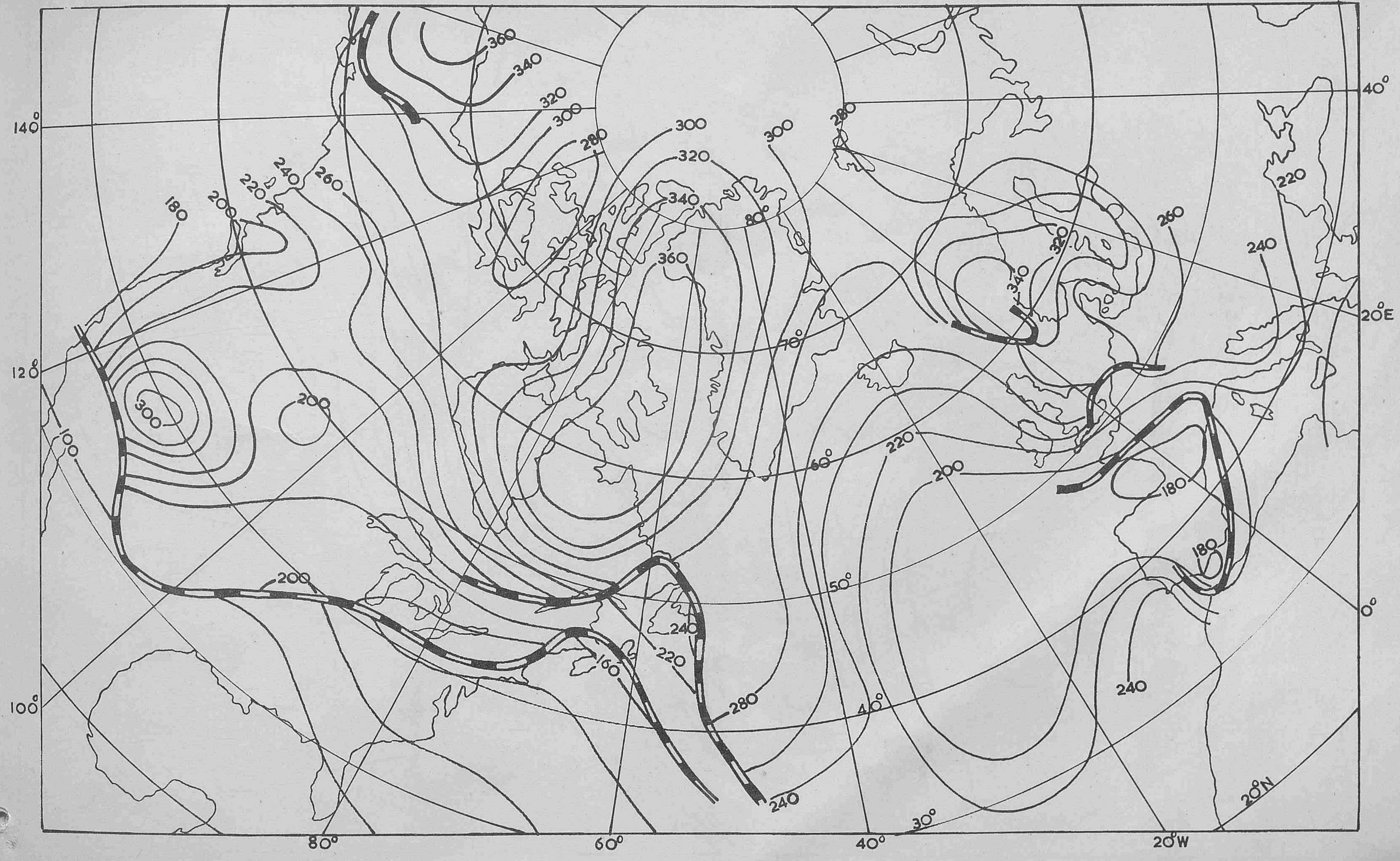

140°
120°
100°
80°
60°
40°
20°W
0°
20°E
40°
30°
40°
50°
60°
70°
80°
20°N
100
180
200
220
240
260
280
300
320
340
360
300
200
200
160
220
240
280
240
300
320
340
360
300
280
220
200
260
320
340
240
220
180
180
240

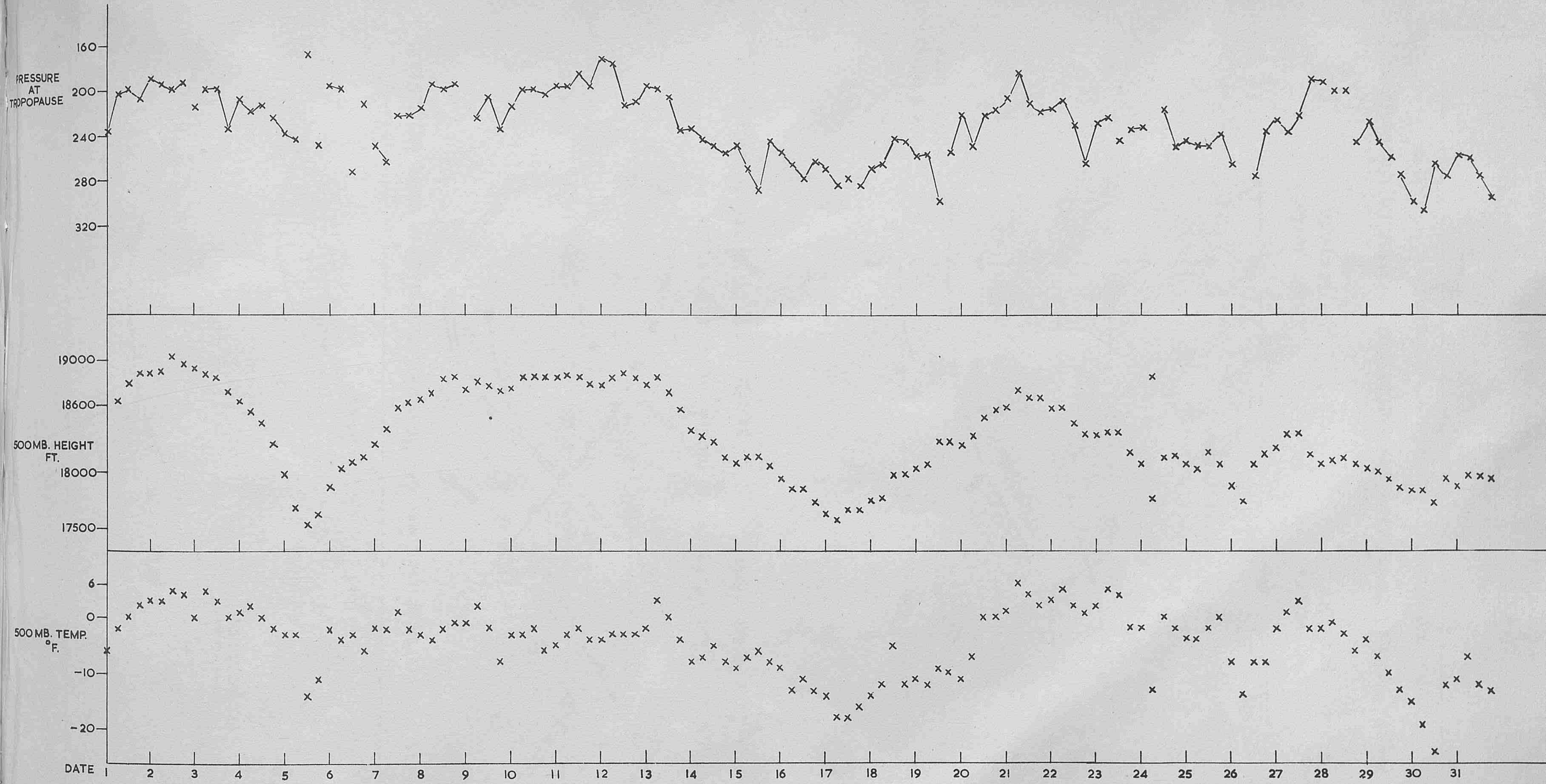

Fig. 3. Pressure at the tropopause, height of 500mb. surface and temperature at 500mb. at 6h. intervals. (Date against 0300 G.M.T. observation).

LARKHILL. May 1949.

(In the upper diagram points have been joined by a line where they have been treated as lying on a continuous tropopause surface during the analysis — gaps indicate tropopause discontinuities.)

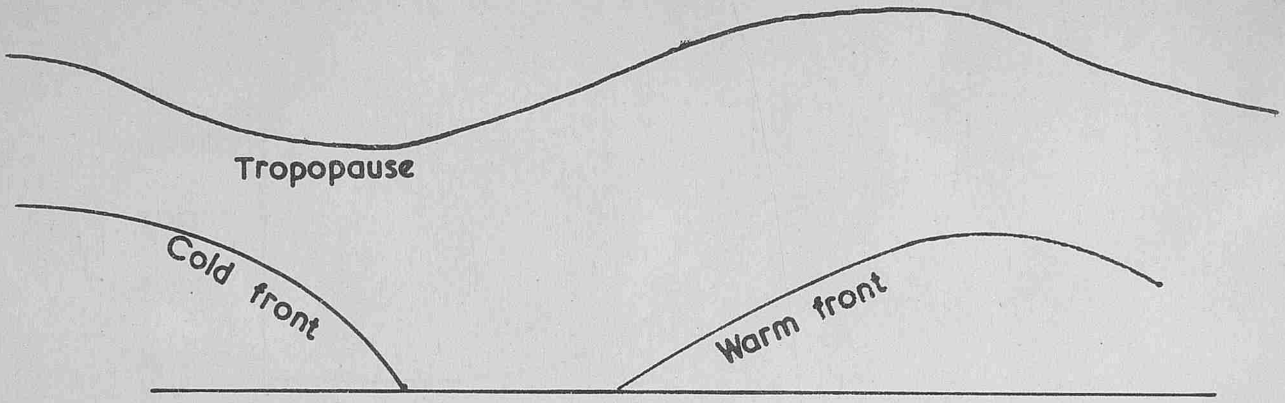
Tropopause
Cold front
Warm front

Fig. 4(a). Vertical section of Bjerknes model of a wave depression

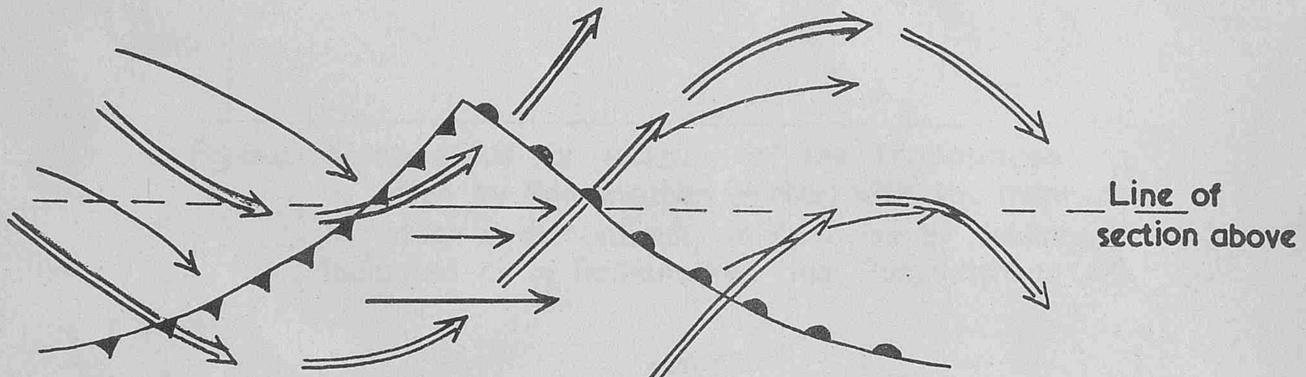
Line of section above

Fig. 4 (b). Plan of Bjerknes model wave depression

→ Low level flow ⟹ Flow in upper troposphere

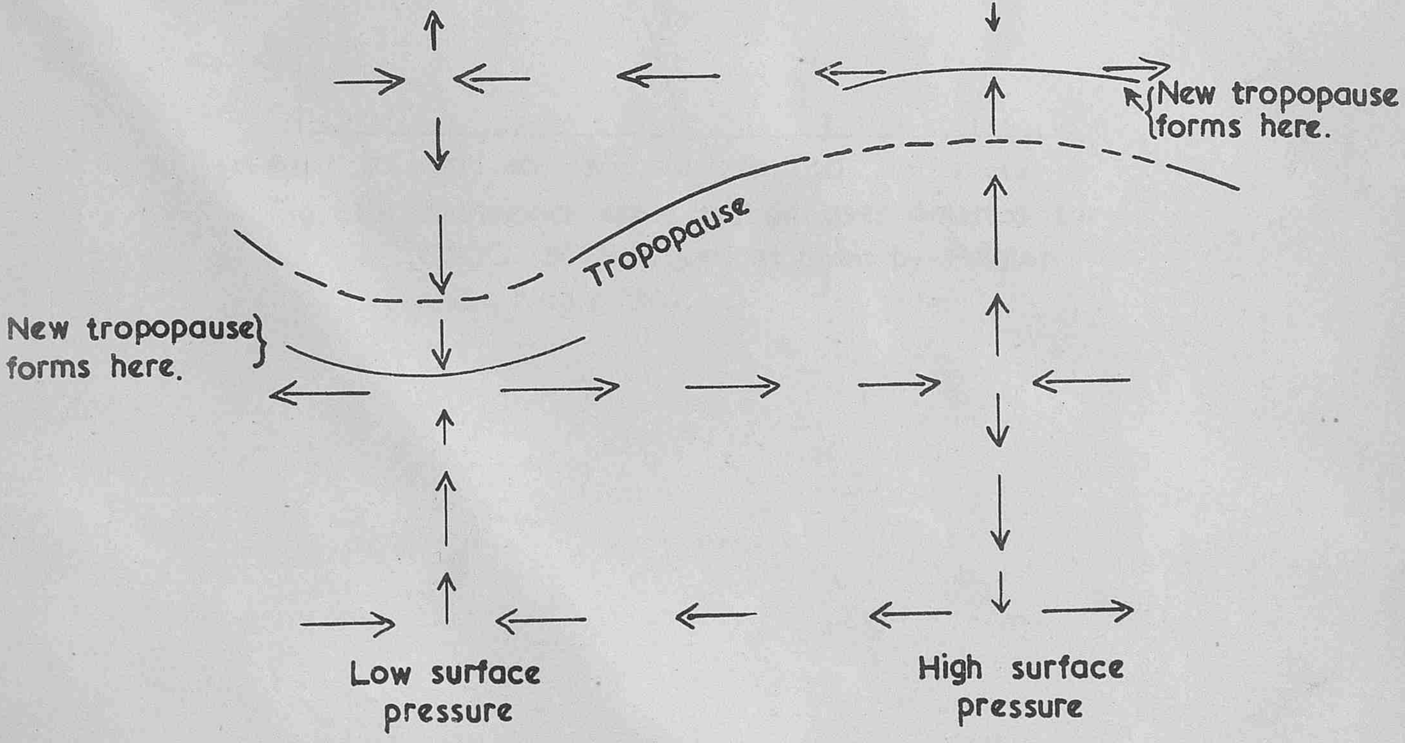
New tropopause forms here.
Tropopause
New tropopause forms here.
Low surface pressure
High surface pressure

Fig. 5. Vertical circulation associated with developing depressions and anticyclones according to Palmen.

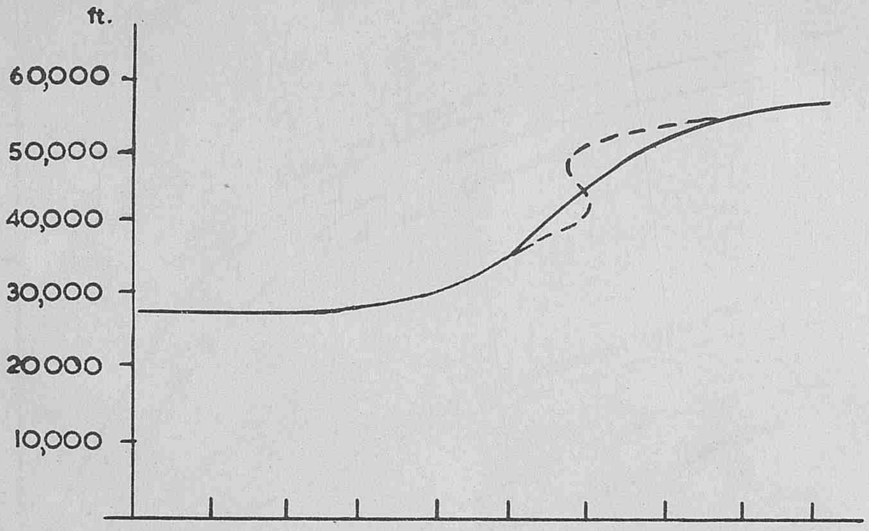

Fig.6(a). Mean latitudinal variation of the Tropopause as given by Ramanathen (Winter) with the manner in which a discontinuity might arise by folding indicated as by Ramanathen and Ramakrishnan (37).

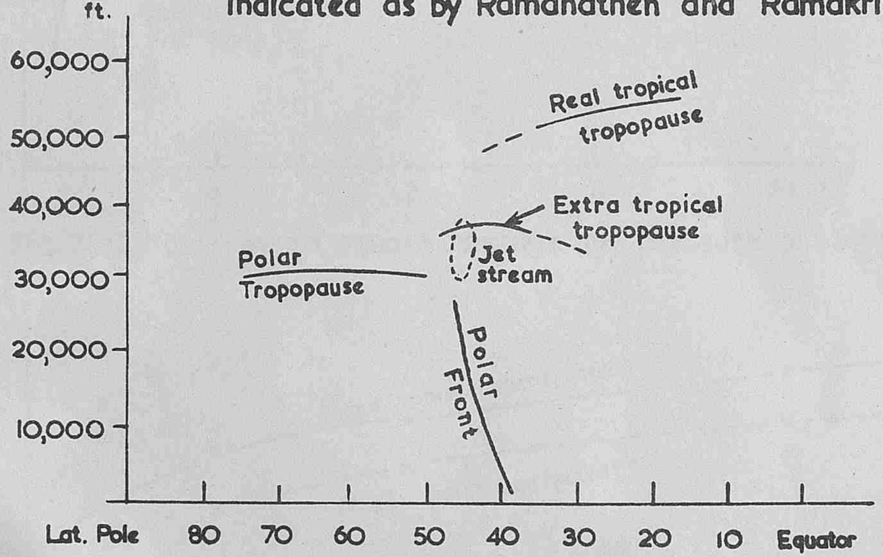

Fig. 6(b) Meridional cross section over America for 0300 30 Nov. 1946 as given by Palmen and Nagle (36).

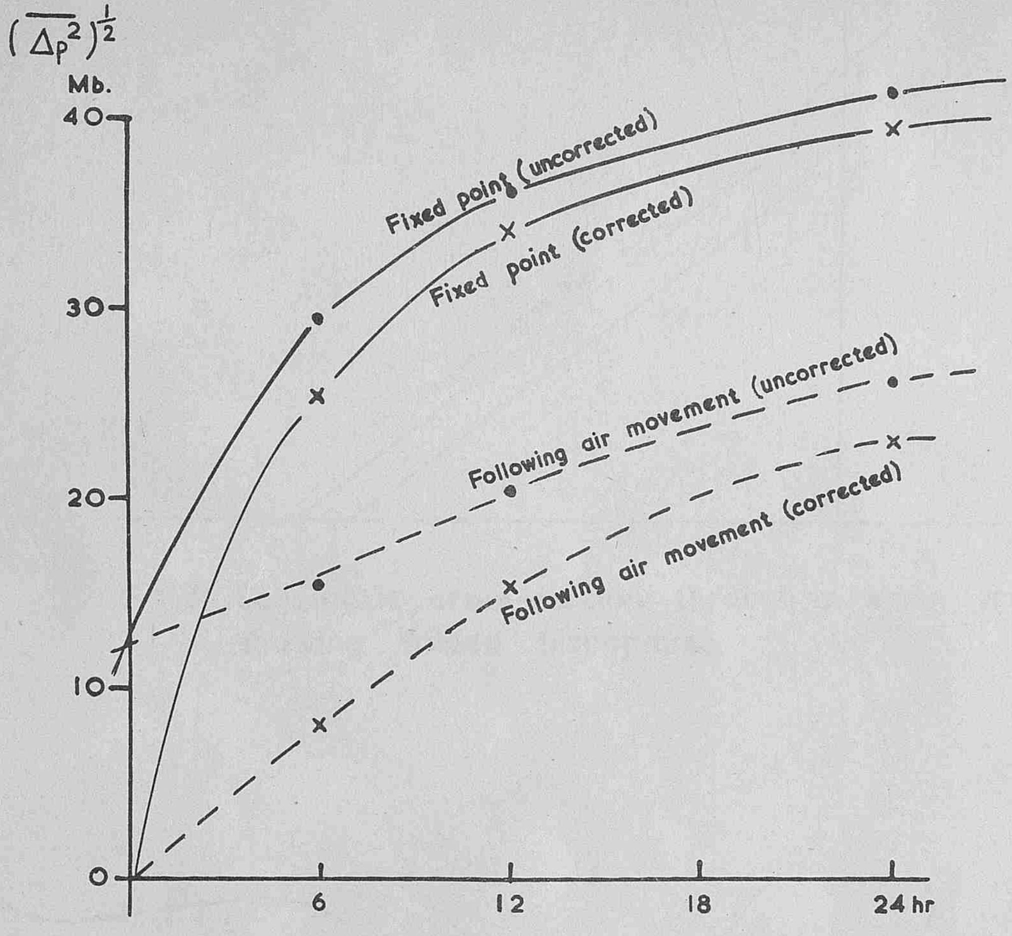

Fig. 7(a) Root mean square change of pressure at tropopause.

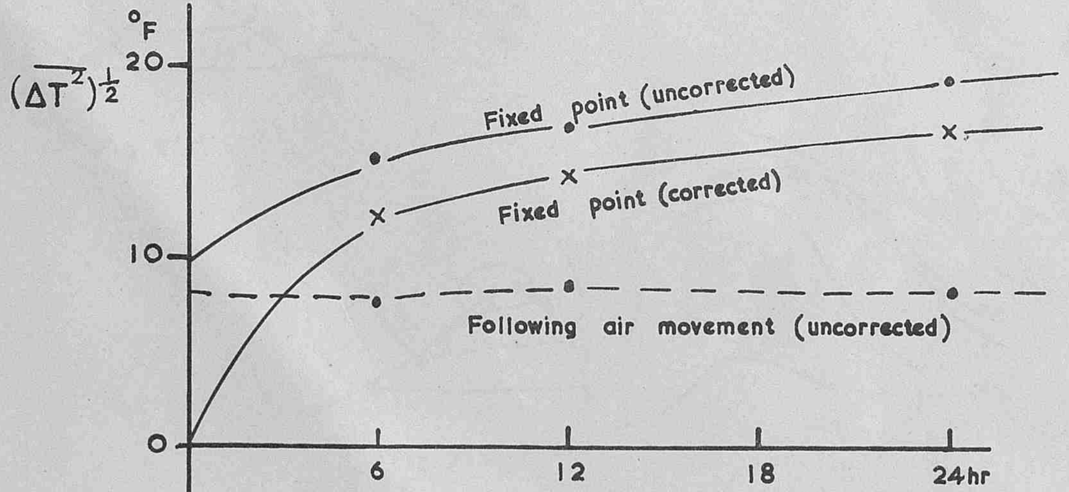

Fig. 7(b). Root mean square change of potential temperature at tropopause.

Fig. 7. Root mean square change of pressure and potential at the tropopause as a function of the time interval. Variation at a fixed point and following the air movement are given. Lower curves are corrected for instrumental error — upper curves are not.

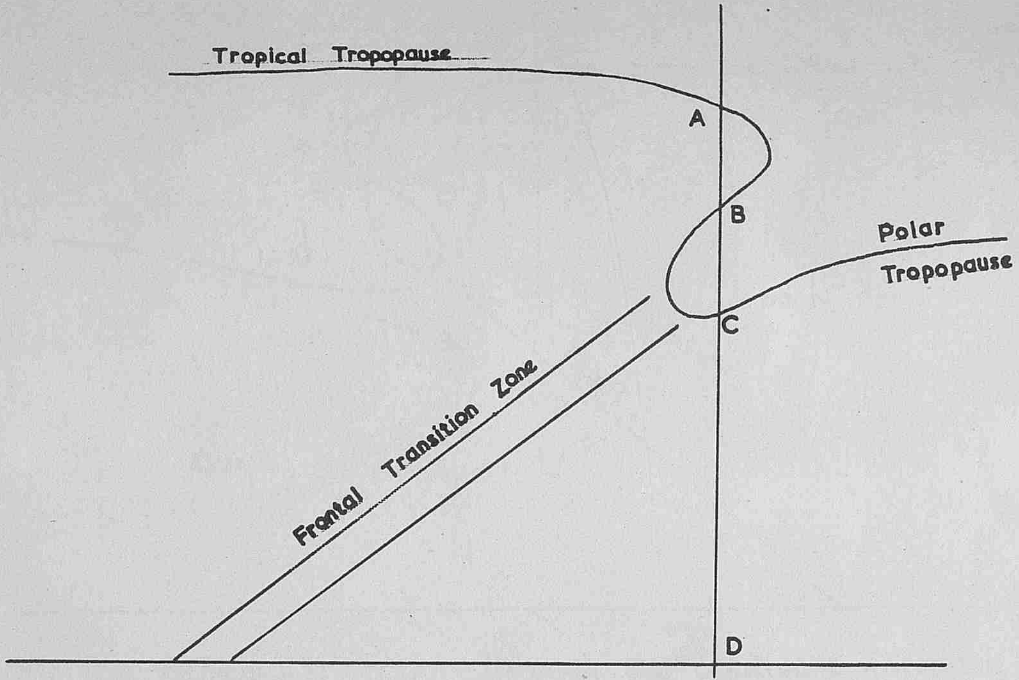
Tropical Tropopause
A
B
Polar Tropopause
C
Frontal Transition Zone
D

Fig. 8. Schematic cross-section through a warm front showing folded tropopause.

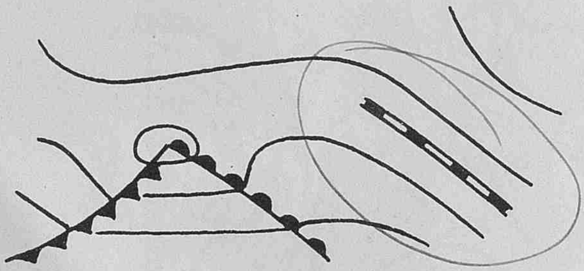

"These are breaks"

Fig. 9(a)

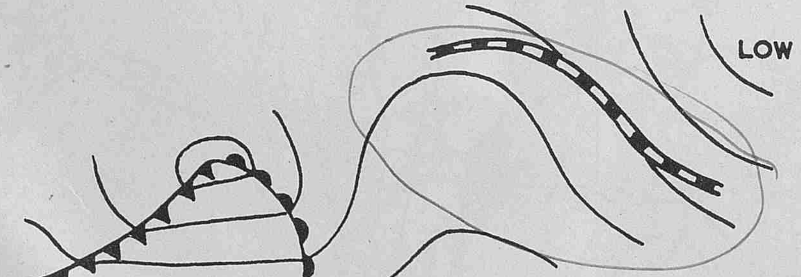

Fig. 9 (b)

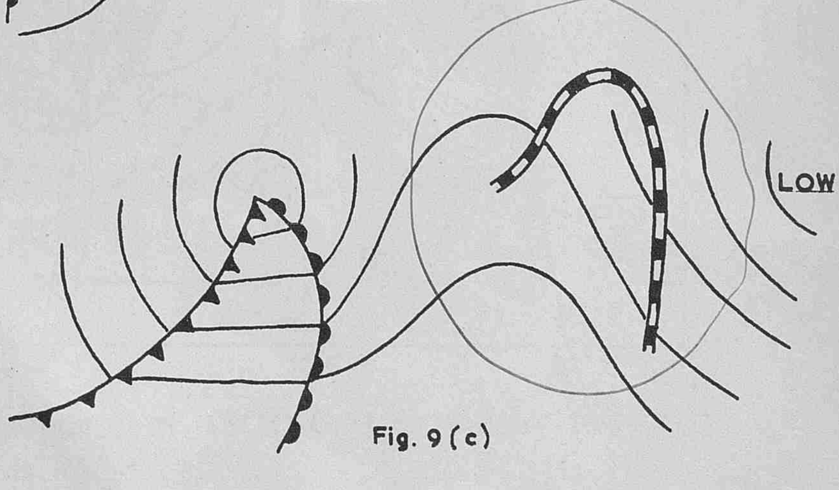

Fig. 9 (c)

Fig. 9.
Schematic relation of folded tropopause to frontal system in the horizontal.

Fold in tropopause ▬▭▬▭▬

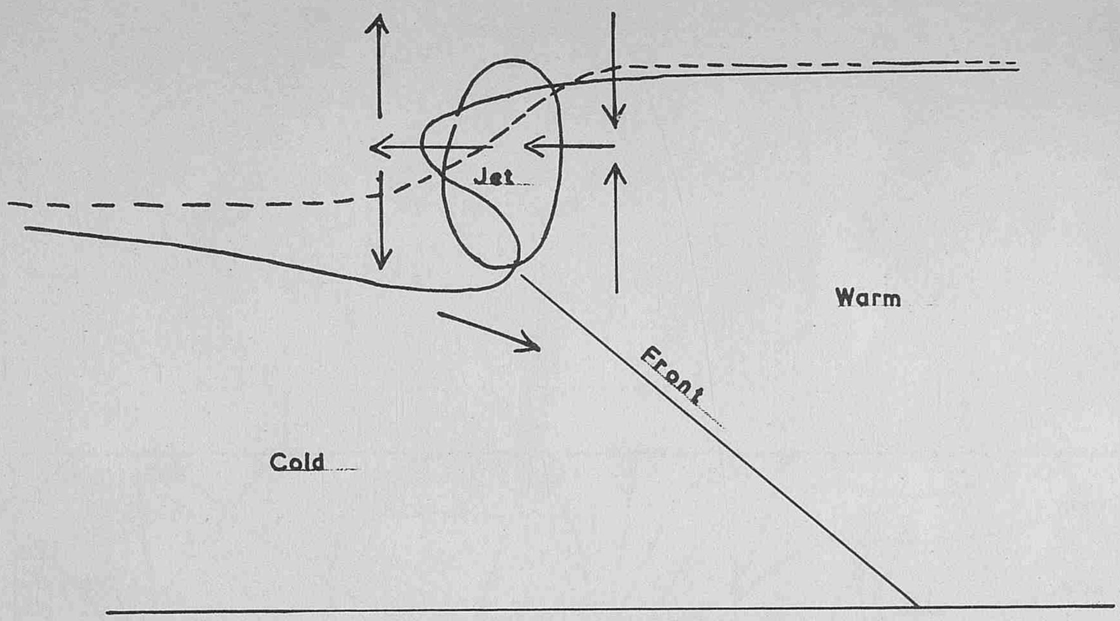
Jet
Warm
Front
Cold

Fig. 10. Schematic section through the confluent entrance to a jet stream. (looking east).

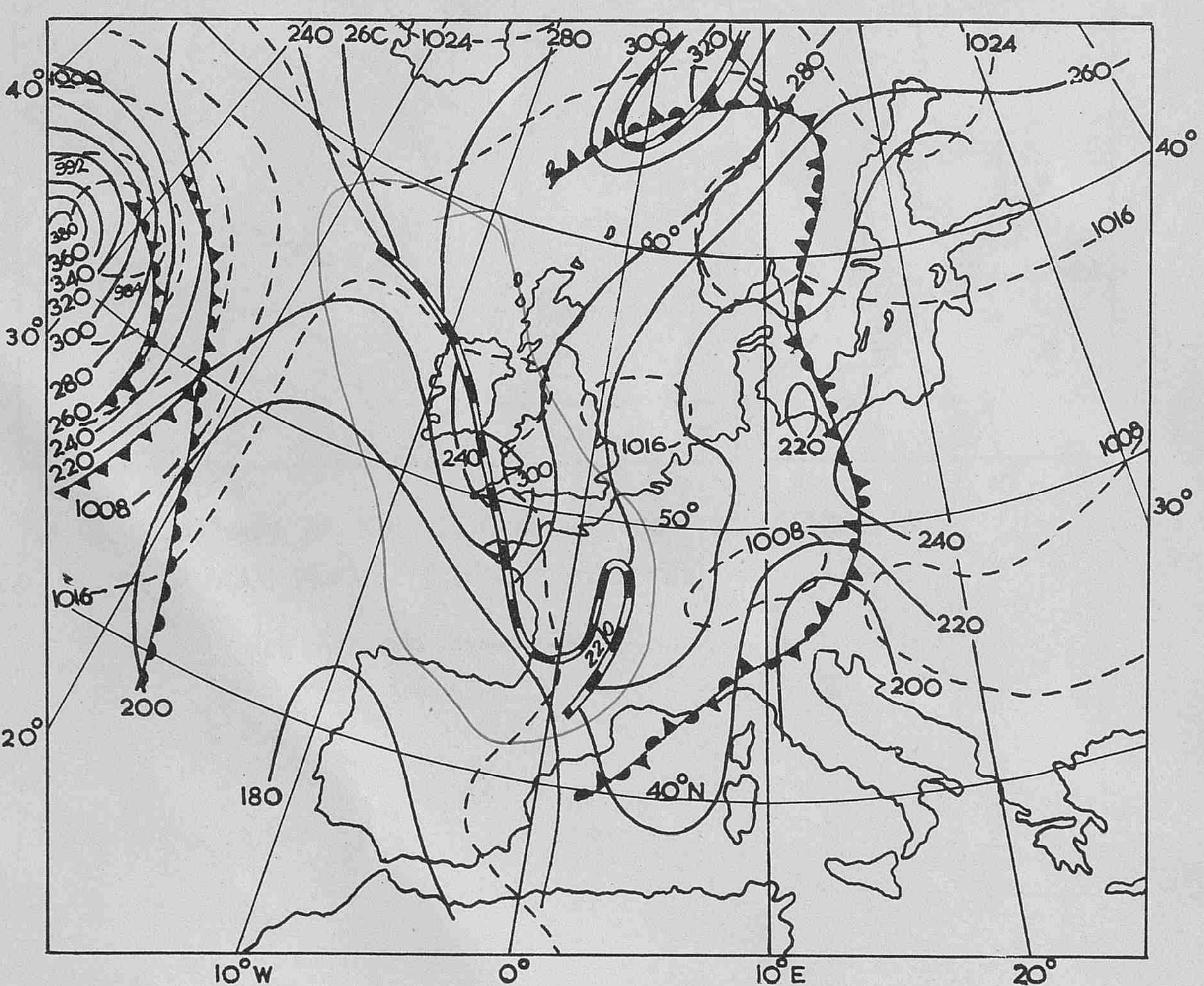
240
260
1024
280
300
320
280
1024
260
40°
1016
1000
992
384
380
360
340
320
300
280
260
240
220
1008
30°
20°
60°
1016
240
300
220
1008
30°
50°
1008
240
220
200
220
1016
200
180
40°N
10°W
0°
10°E
20°

Fig. 11. Isobars on the tropopause at 1500 G.M.T. 19 MAY 1949 at 20mb. intervals.

Discontinuity in tropopause ▬▬▬

Surface isobars at 8mb. intervals and surface fronts - - - - -

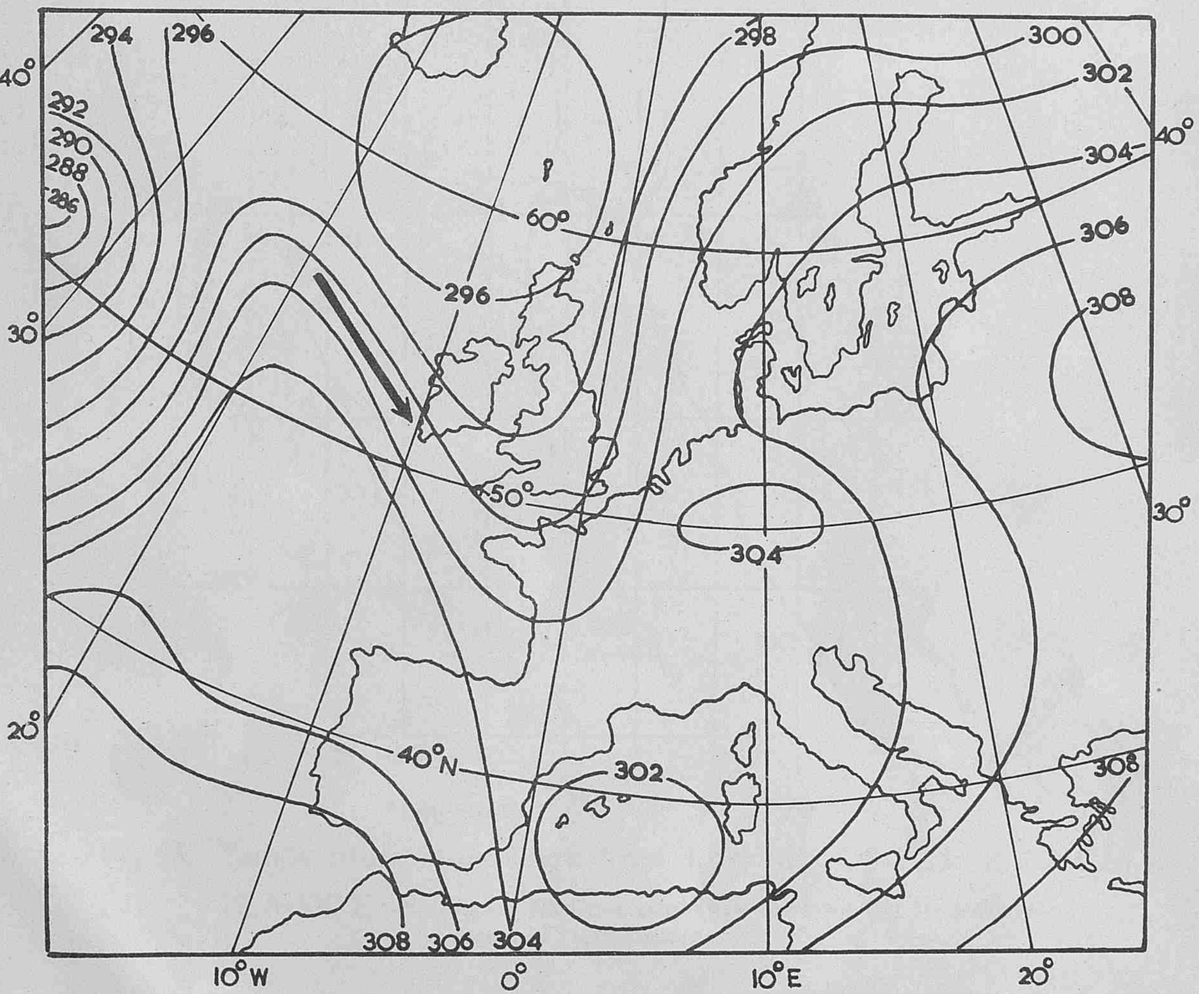
294
296
298
300
302
304
306
308
292
290
288
286
296
60°
50°
40°N
304
302
308
308
306
304
40°
30°
20°
40°
30°
10°W
0°
10°E
20°

Fig. 12. Contours of the 300 mb. surface at 1500 G.M.T.
19 MAY 1949. (200 ft. intervals).

Jet Stream ⟶

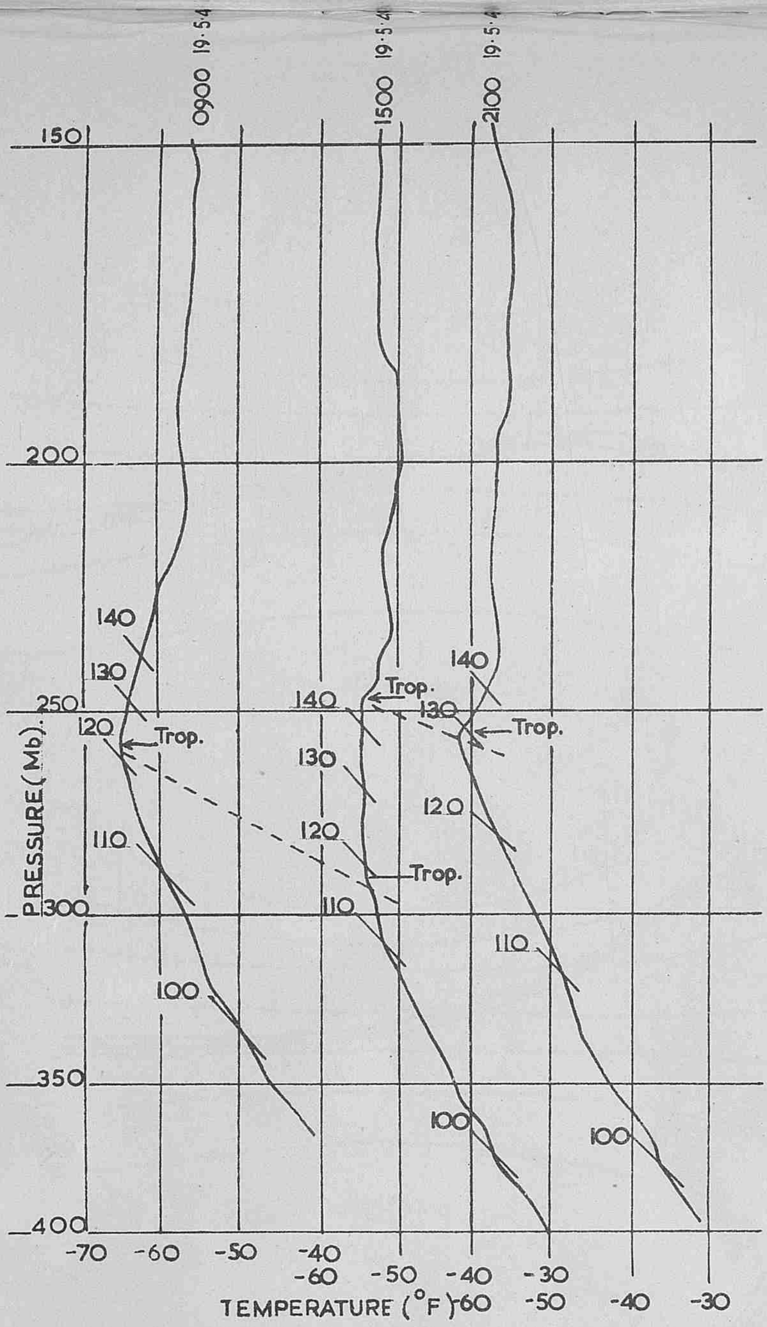

Fig. 13. Temperature soundings from Larkhill. 0900 to 2100 G.M.T. 19 MAY 1949. (sloping lines are adiabatics corresponding to indicated potential temperatures).

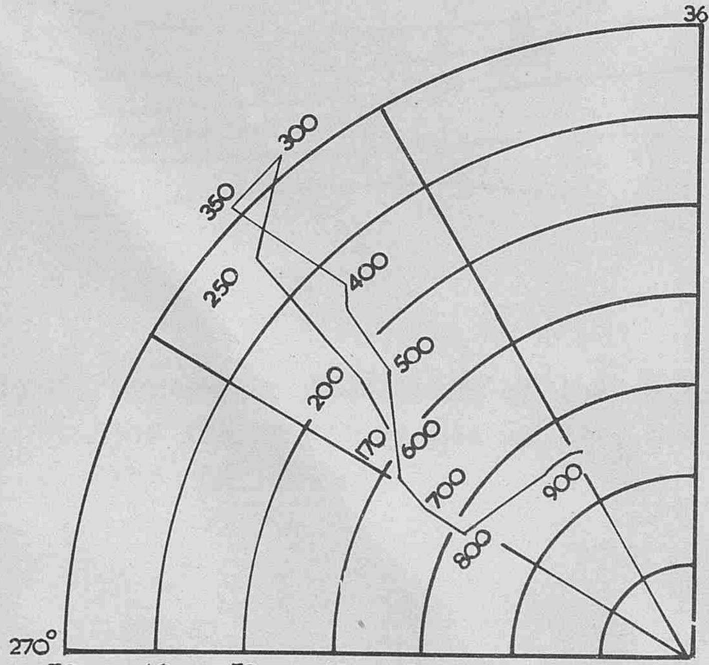

Fig. 14. Hodograph of wind sounding at Aldergrove 2100 G.M.T. 6 MAY 1949.

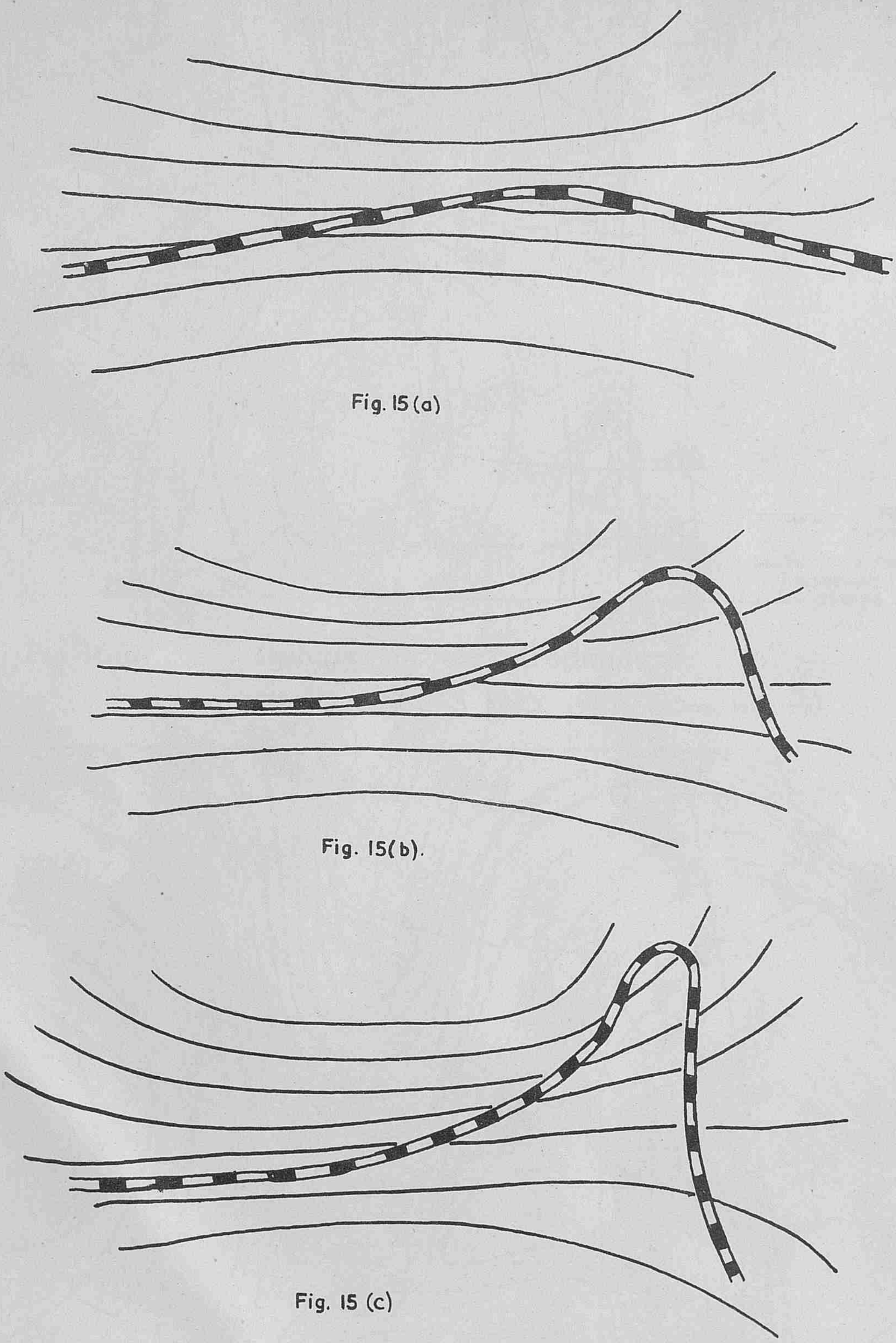

Fig. 15 (a)

Fig. 15(b).

Fig. 15 (c)

Fig. 15. Schematic illustration of the distortion of the folded tropopause at the exit from the jet stream.

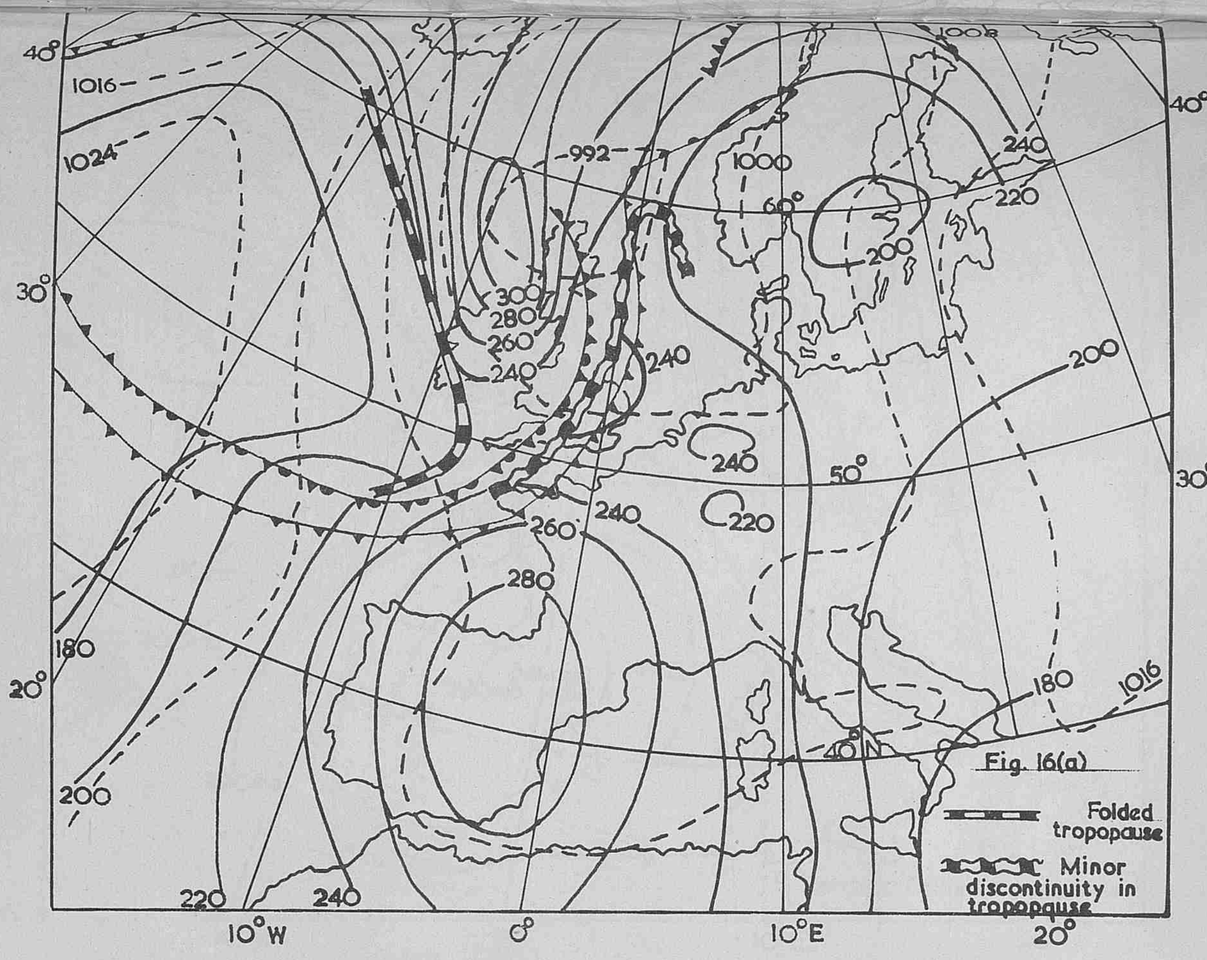
40°
1016
1024
992
1000
1008
60°
240
220
200
30°
300
280
260
240
240
240
200
50°
30°
260
240
220
280
180
20°
180
1016
40°N
Fig. 16(a)
200
Folded tropopause
Minor discontinuity in tropopause
220
240
10°W
0°
10°E
20°

Fig 16(a) Isobars on the tropopause.

0300 G.M.T. 5 MAY 1949. (20 mb. intervals)

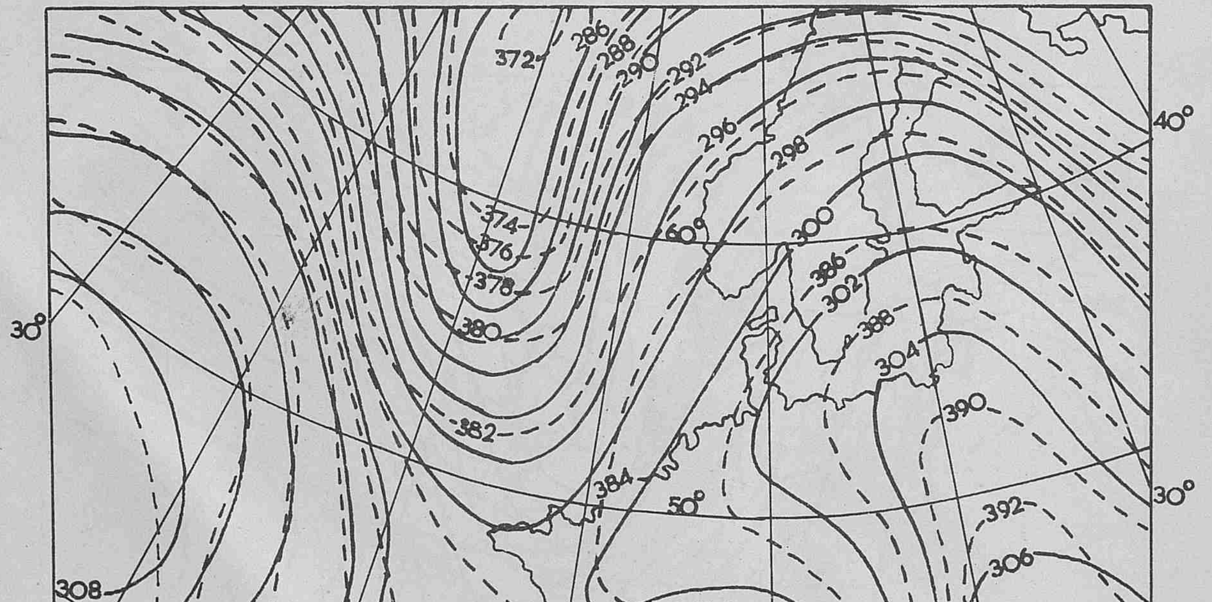
372
286
288
290
292
294
296
298
40°
374
376
378
60°
300
386
302
388
30°
380
304
382
390
384
50°
30°
392
306
308
308
20°
306
394
388
40°N
296
298
300
392
304
390
302
10°W
0°
10°E
20°

Fig. 16(b) Contours of 200 and 300 mb. surfaces.

0300 G.M.T. 5 MAY 1949.

——— 300 mb. - - - - 200 mb.

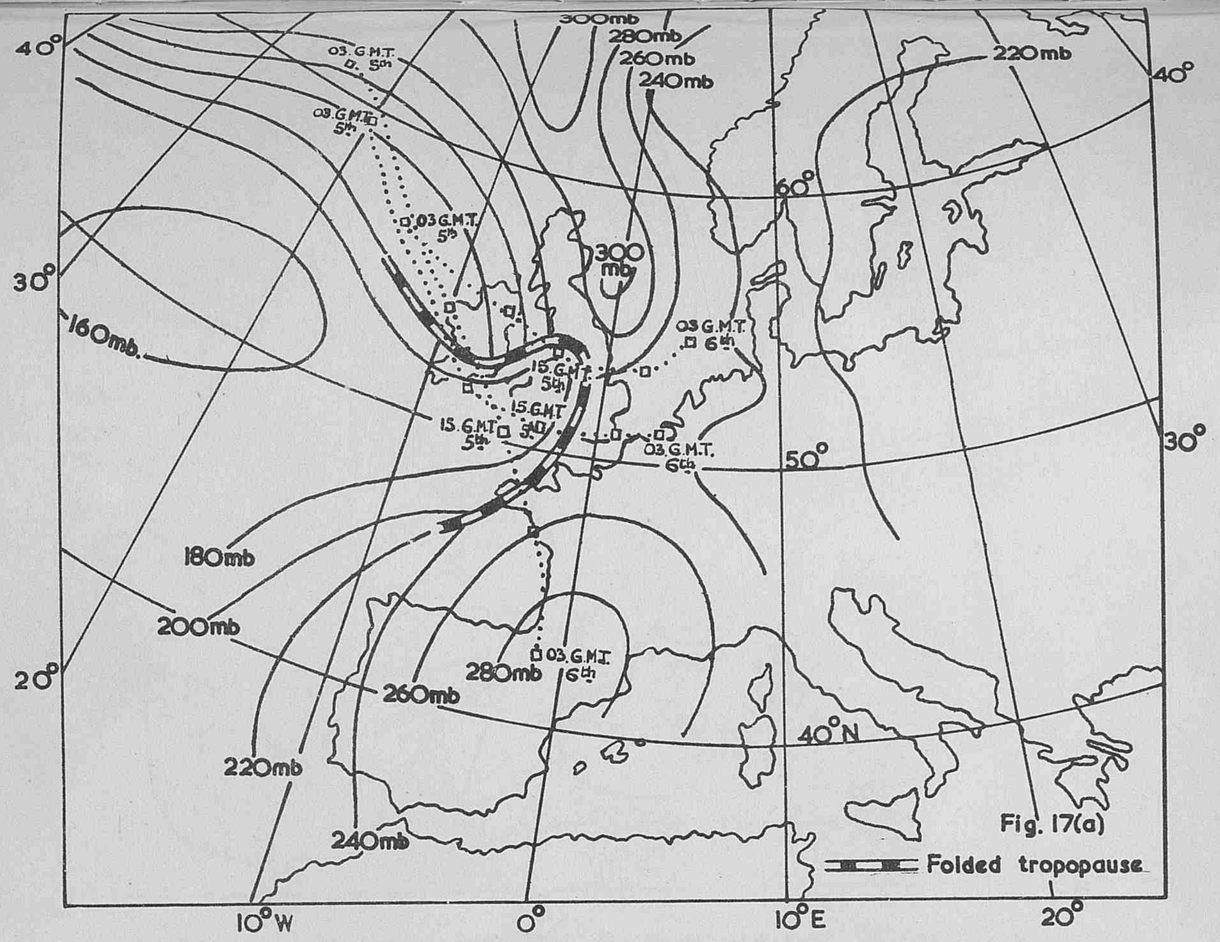
300mb
280mb
260mb
240mb
220mb
03 G.M.T. 5th
03 G.M.T. 5th
03 G.M.T. 5th
300 mb
03 G.M.T. 6th
15 G.M.T. 5th
15 G.M.T. 5th
15 G.M.T. 5th
03 G.M.T. 6th
03 G.M.T. 6th
160mb.
180mb
200mb
260mb
280mb
220mb
240mb
60°
50°
40°N
40°
30°
20°
10°W
0°
10°E
20°
Fig. 17(a)
Folded tropopause

Fig. 17(a). Isobars on the tropopause

1500 G.M.T. 5 MAY 1949 (20 mb. intervals)

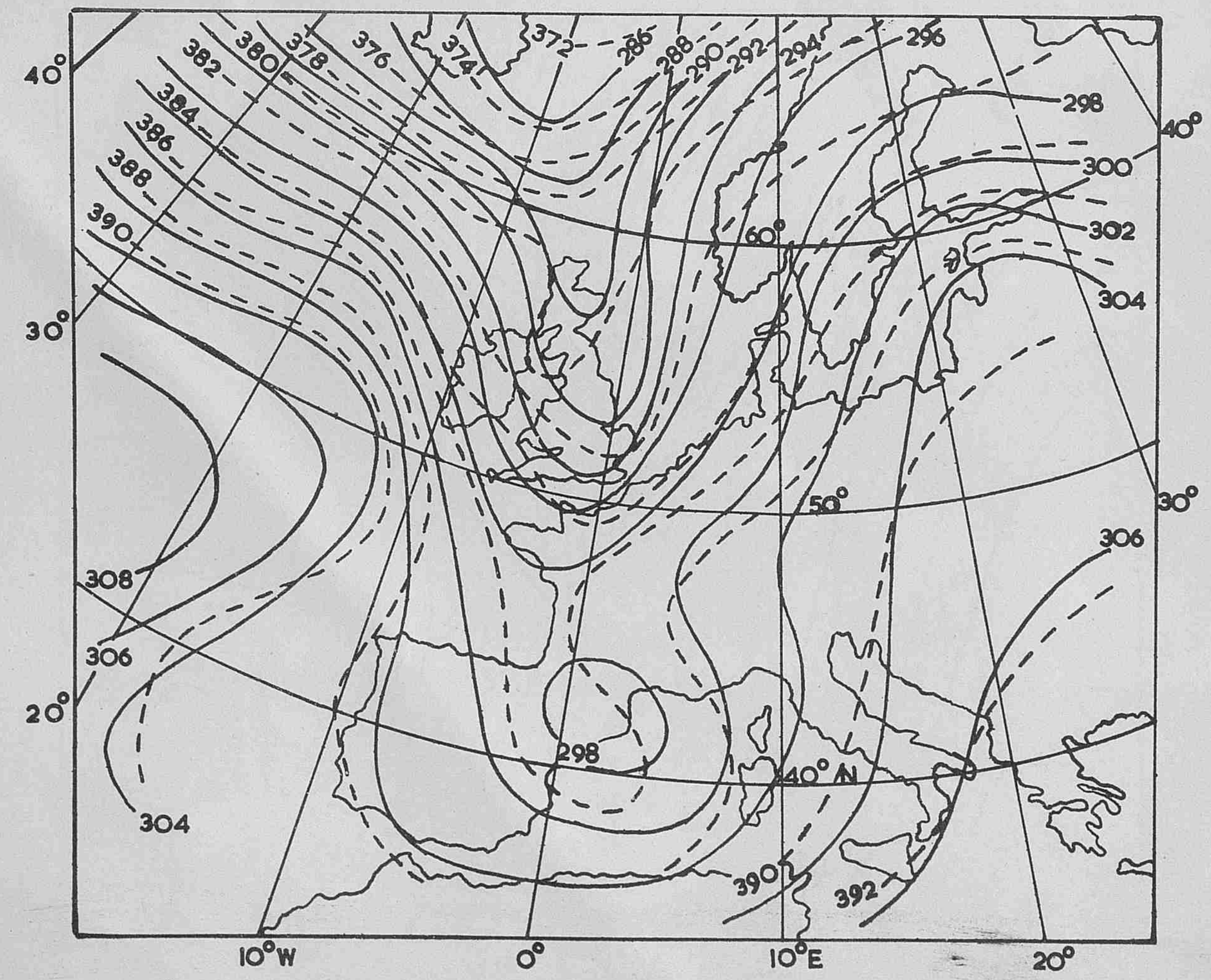
372
374
376
378
380
382
384
386
388
390
286
288
290
292
294
296
298
300
302
304
306
308
306
304
298
390
392
60°
50°
40°N
40°
30°
20°
10°W
0°
10°E
20°

Fig. 17(b) Contours of 200 and 300mb. surfaces

1500 G.M.T. 5 MAY 1949

——— 300mb. - - - - 200mb.

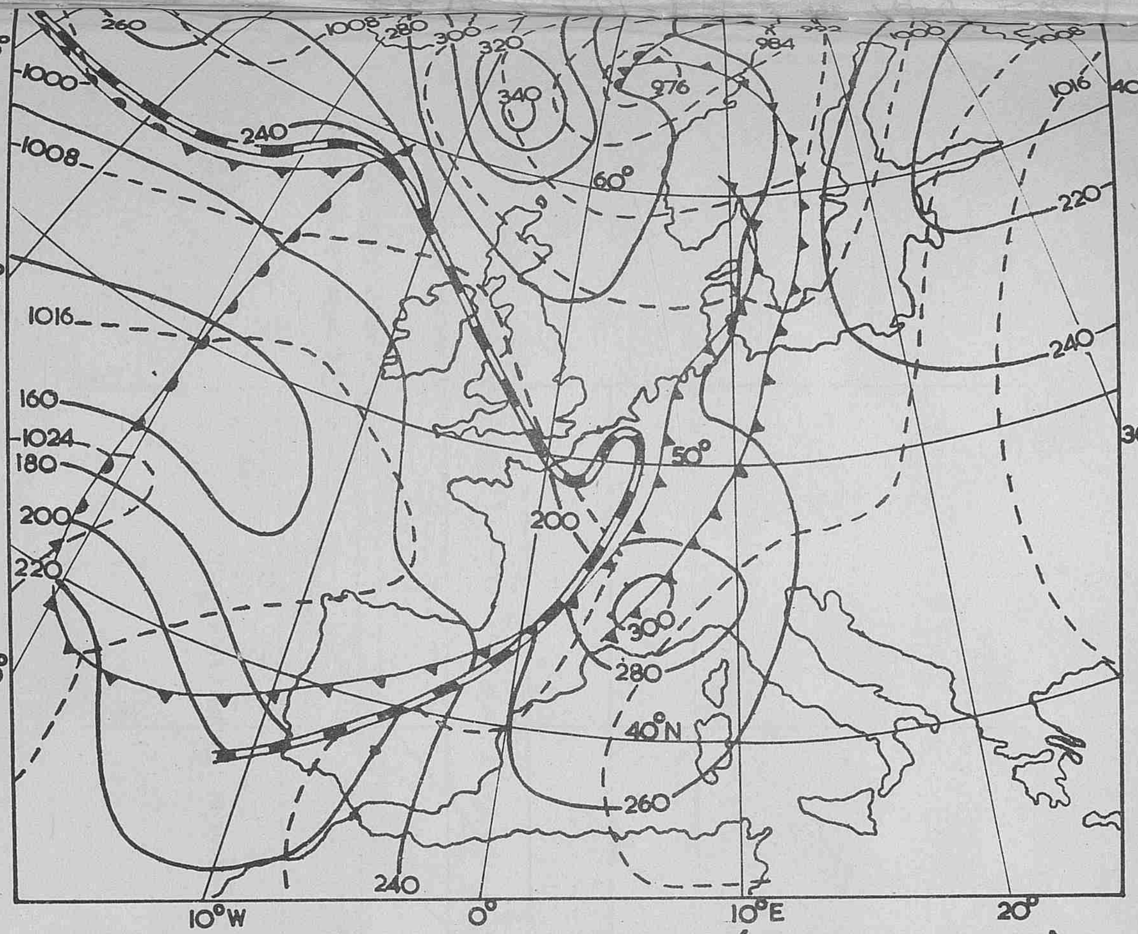
40°
30°
20°
10°W
0°
10°E
20°
1000
1008
1016
1024
160
180
200
220
240
260
280
300
320
340
992
984
976
1000
1008
1016
220
240
60°
50°
40°N
200
300
280
260
240
40°
30°

Fig. 18(a) Isobars on the tropopause (at 20mb intervals)
0300 G.M.T. 6 MAY 1949
Surface isobars - - - - and fronts

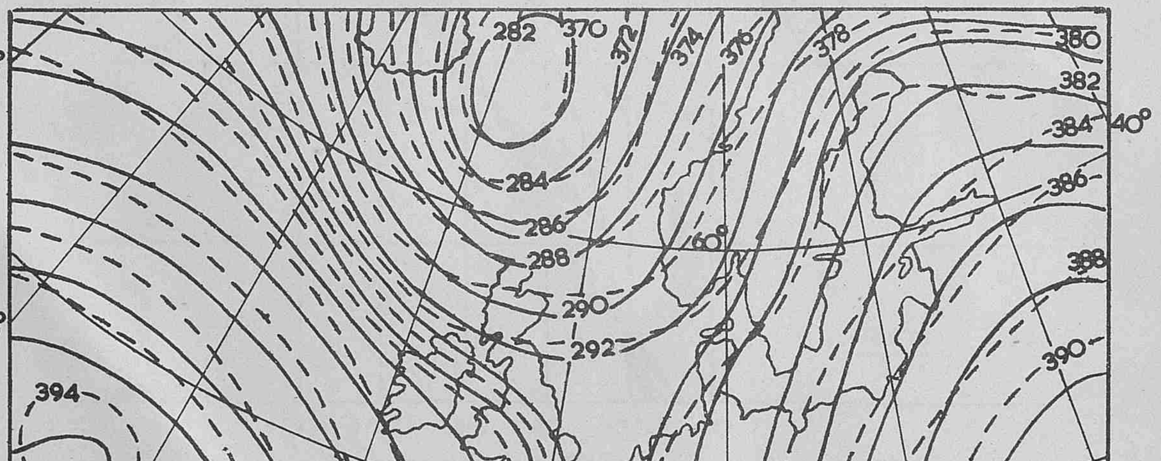
40°
30°
20°
10°W
0°
10°E
20°
282
370
372
374
376
378
380
382
384
386
388
390
284
286
288
290
292
60°
50°
40°N
394
392
390
388
308
306
304
302
380
294
294
296
298
300
302
302
304
306
40°
30°

Fig. 18(b). Contours of 300 and 200 mb. surfaces
(at 200 ft. intervals).
——— 300 mb. - - - - 200 mb.

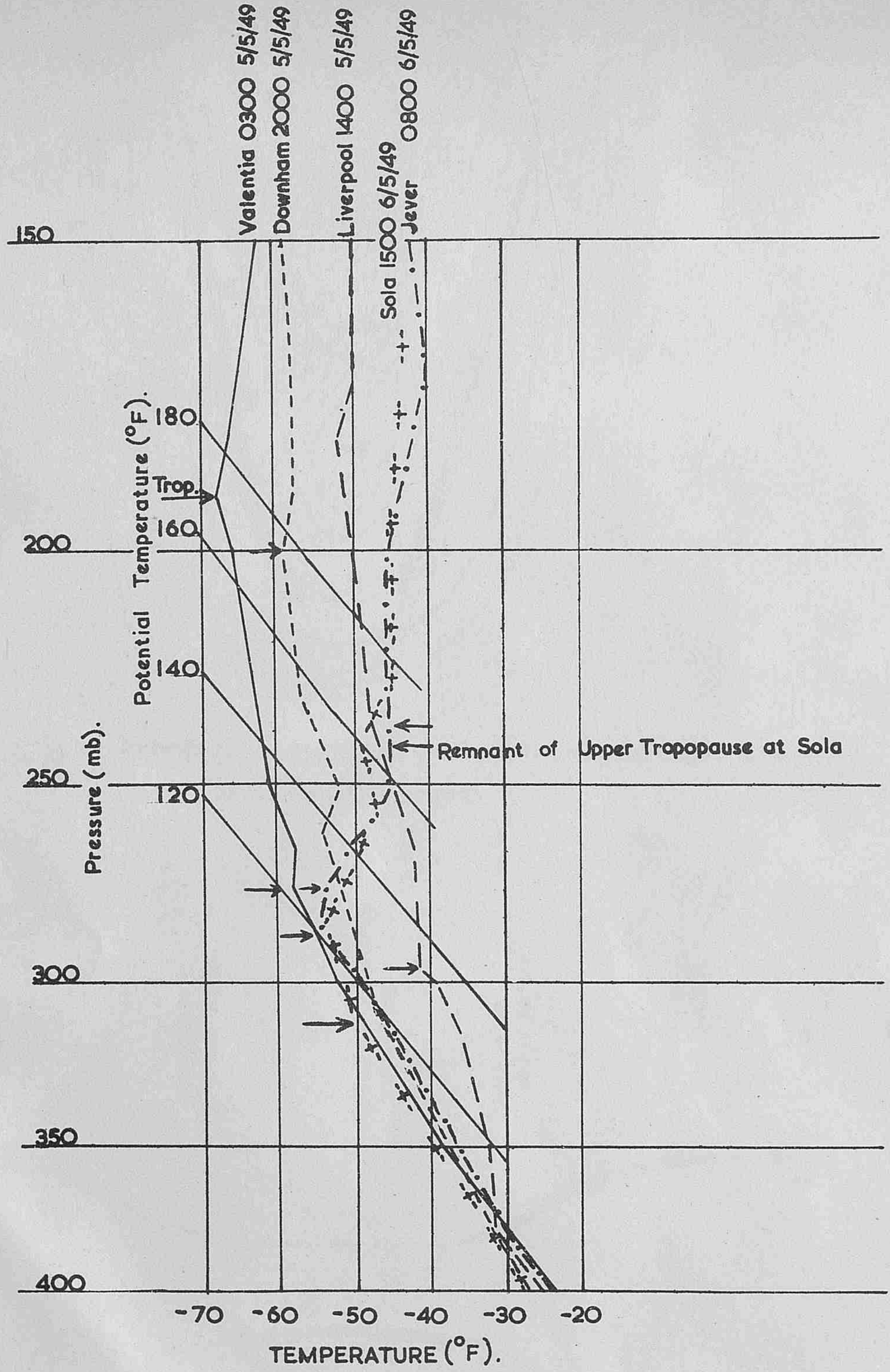

Fig. 19 Temperature soundings 5-6 MAY 1949 illustrating the "occlusion" of a high level tropopause.

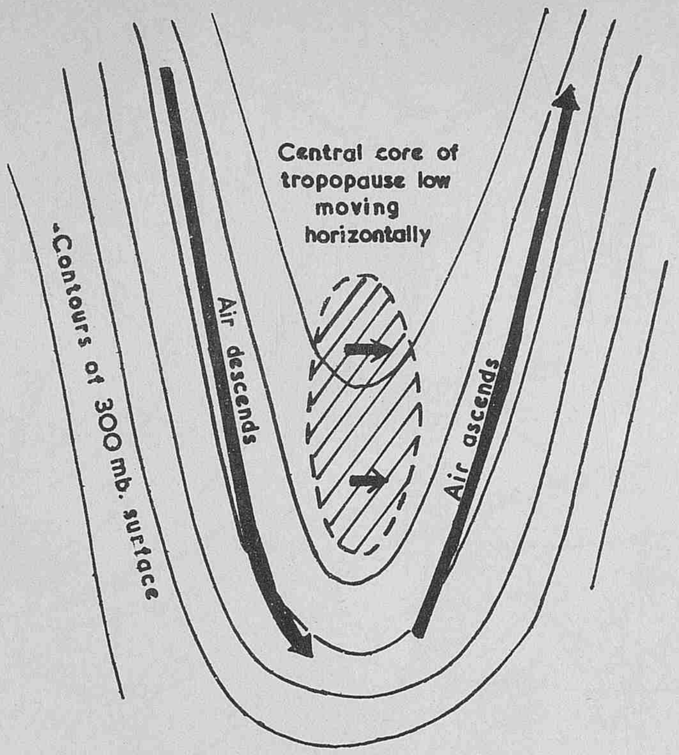
Central core of tropopause low moving horizontally
Air descends
Air ascends
Contours of 300 mb. surface

Fig. 20 Schematic relation between tropopause low and 300 mb. contours.

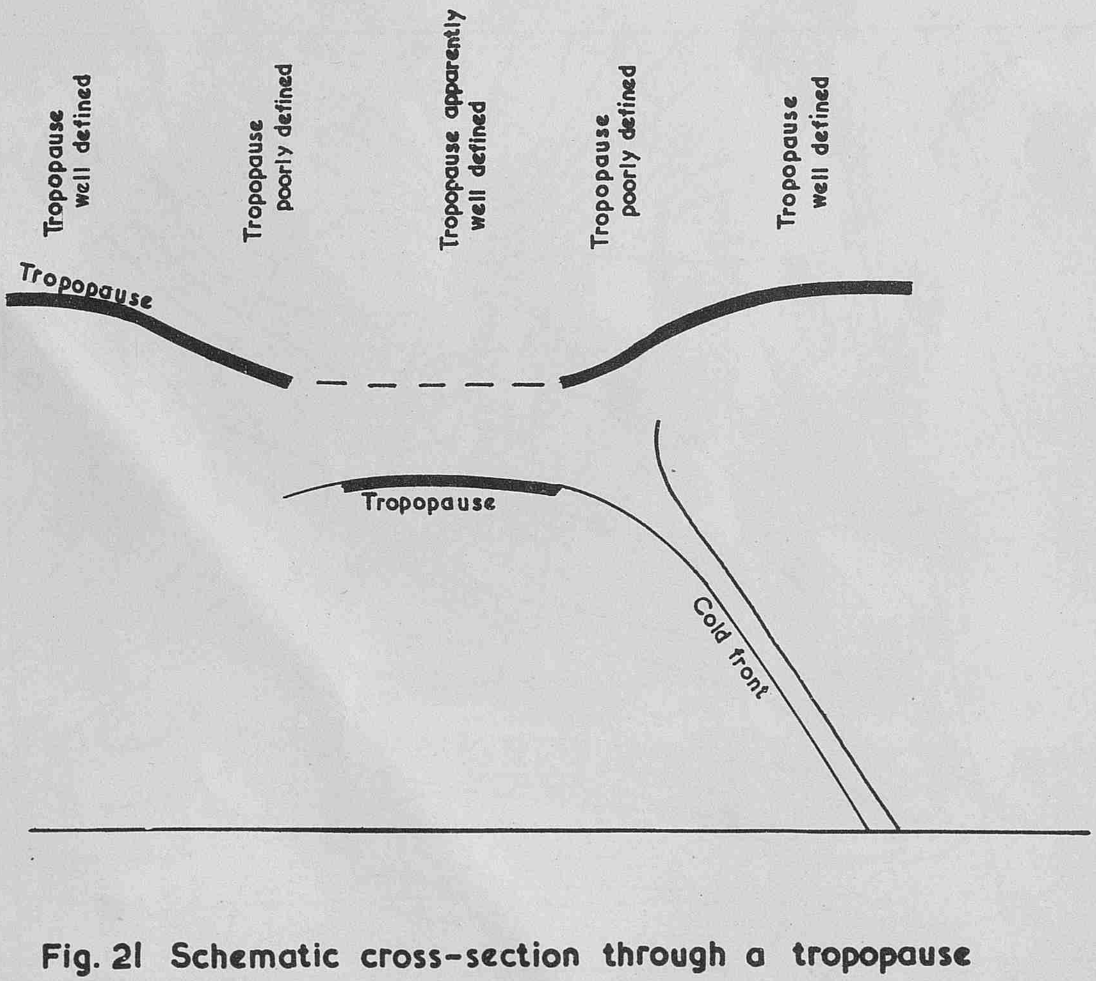
Tropopause well defined
Tropopause poorly defined
Tropopause apparently well defined
Tropopause poorly defined
Tropopause well defined
Tropopause
Tropopause
Cold front

Fig. 21 Schematic cross-section through a tropopause funnel.

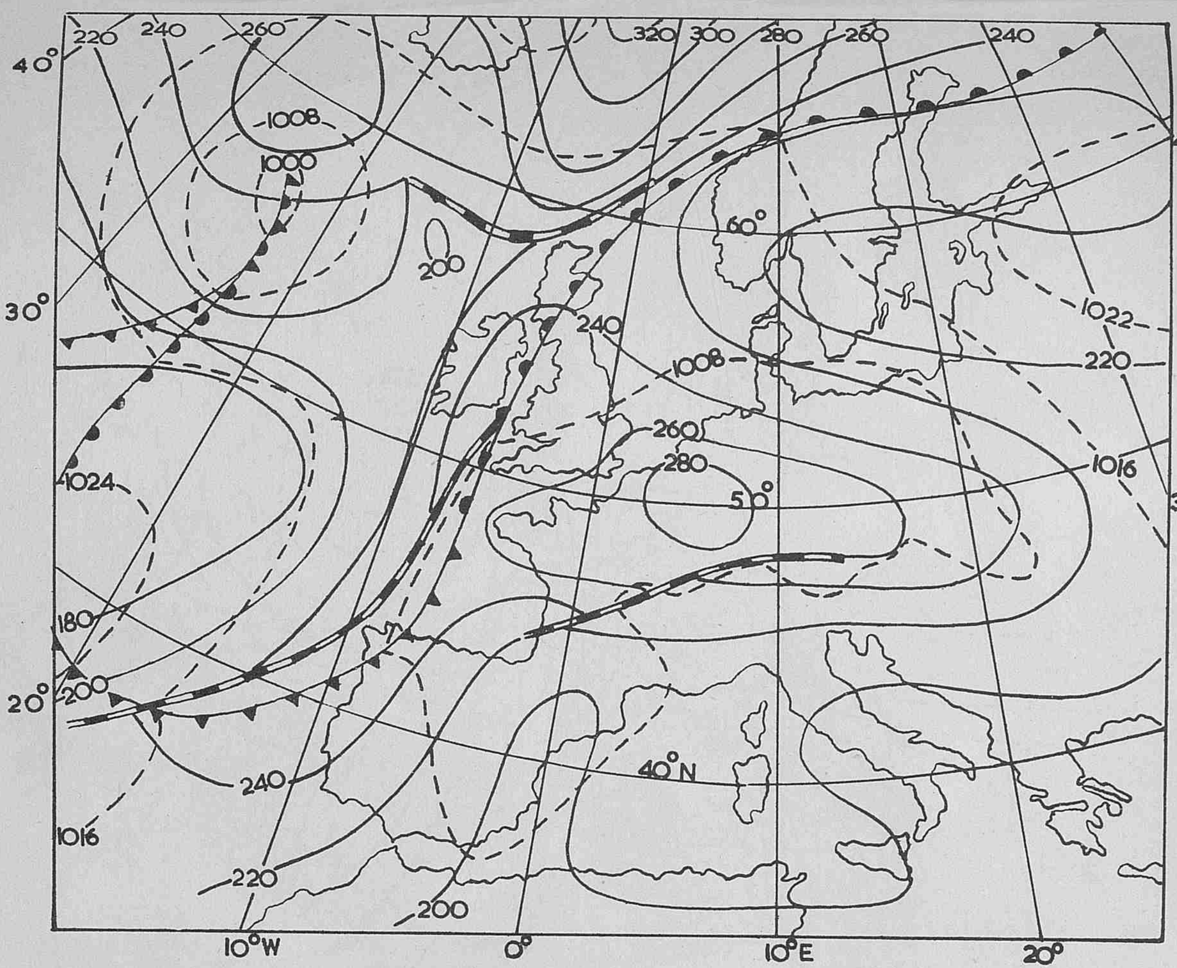
220
240
260
320
300
280
260
240
40°
1008
1000
200
60°
30°
1022
220
240
1008
260
280
50°
1016
1024
30°
180
20°
200
240
40°N
1016
220
200
10°W
0°
10°E
20°

Fig. 22(a) Isobars on the tropopause.
0300 G.M.T. 15 MAY 1949

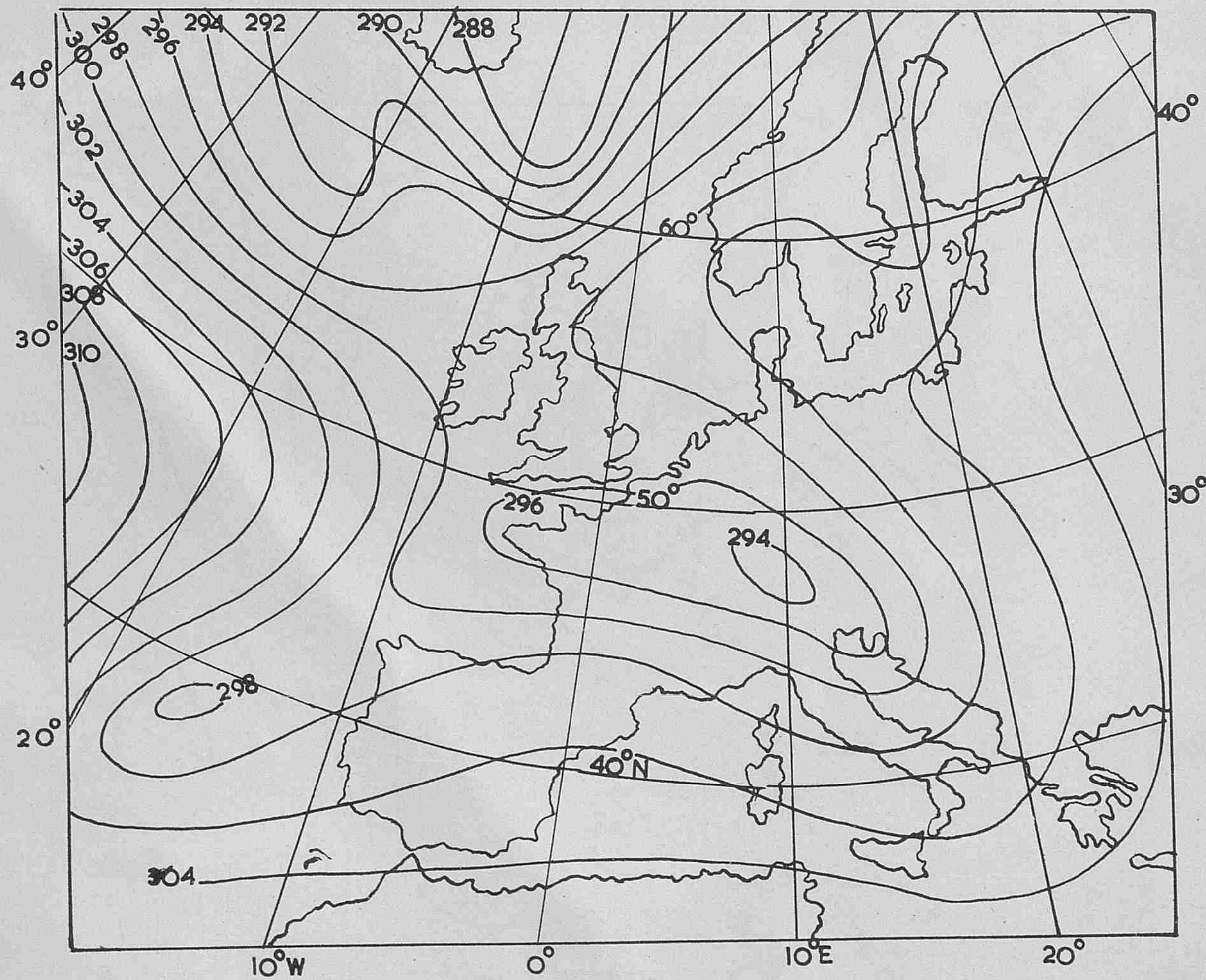
300
298
296
294
292
290
288
40°
302
304
306
308
310
30°
60°
40°
296
50°
294
30°
298
20°
40°N
304
10°W
0°
10°E
20°

Fig. 22(b) Contours of the 300 mb. surface.
0300 G.M.T. 15 MAY 1949

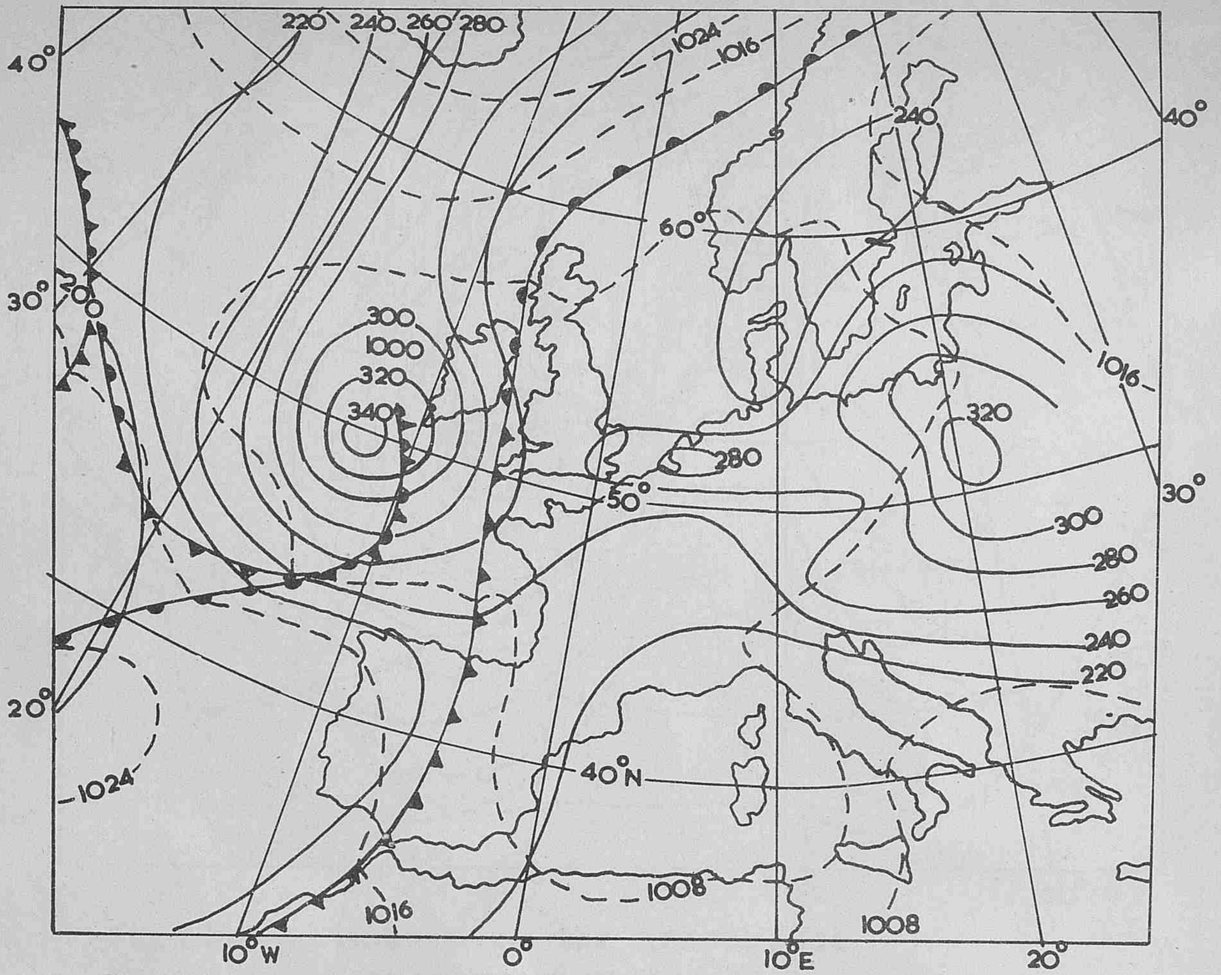
220
240
260
280
1024
1016
240
40°
60°
300
1000
320
340
280
50°
320
1016
300
280
260
240
220
30°
20°
1024
40°N
1008
1016
1008
10°W
0°
10°E
20°

Fig. 23(a) Isobars on the tropopause
0300 G.M.T. 16 MAY 1949

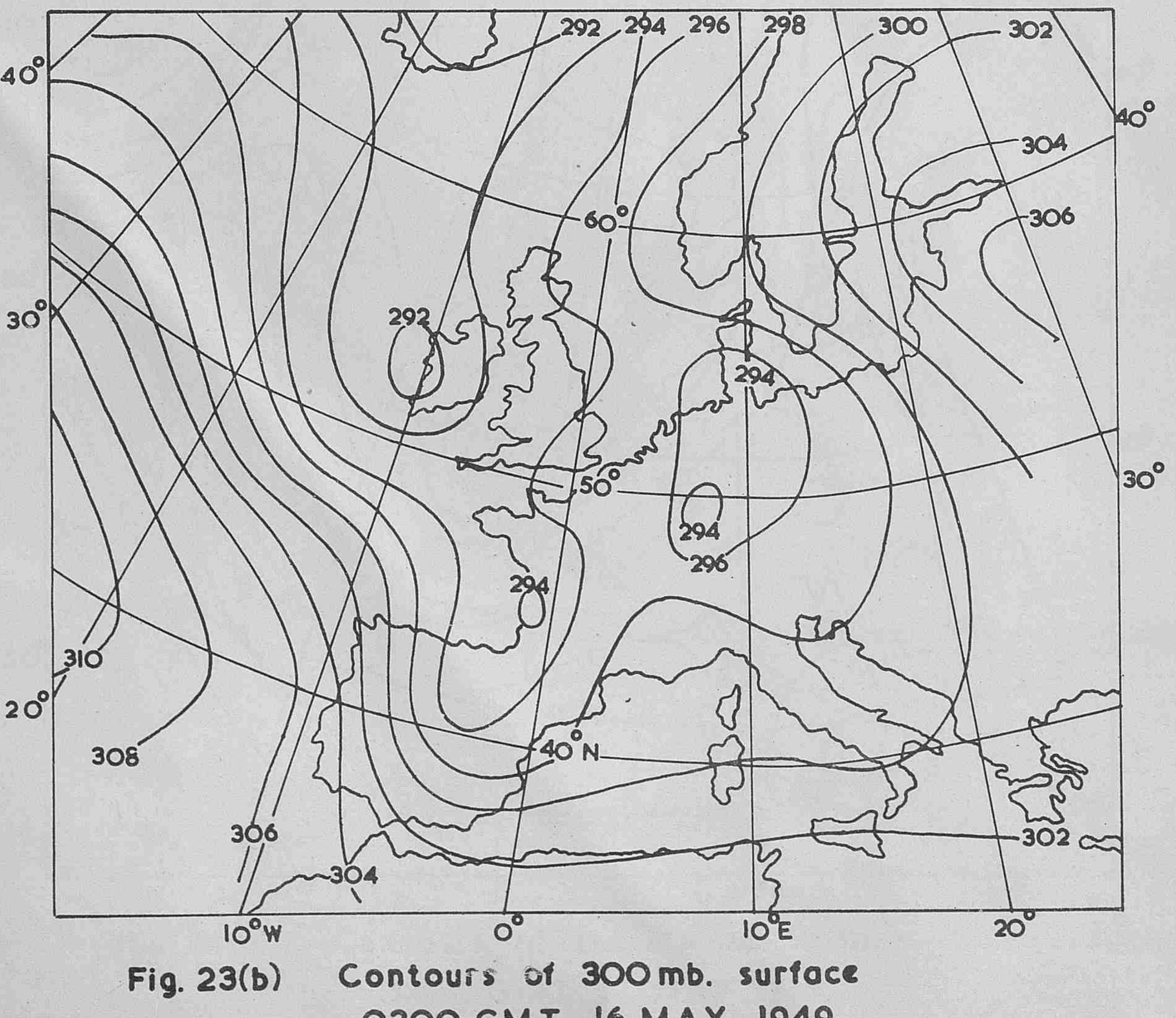
292
294
296
298
300
302
40°
304
306
60°
292
294
30°
50°
294
296
294
310
20°
308
40°N
306
302
304
10°W
0°
10°E
20°

Fig. 23(b) Contours of 300 mb. surface
0300 G.M.T. 16 MAY 1949

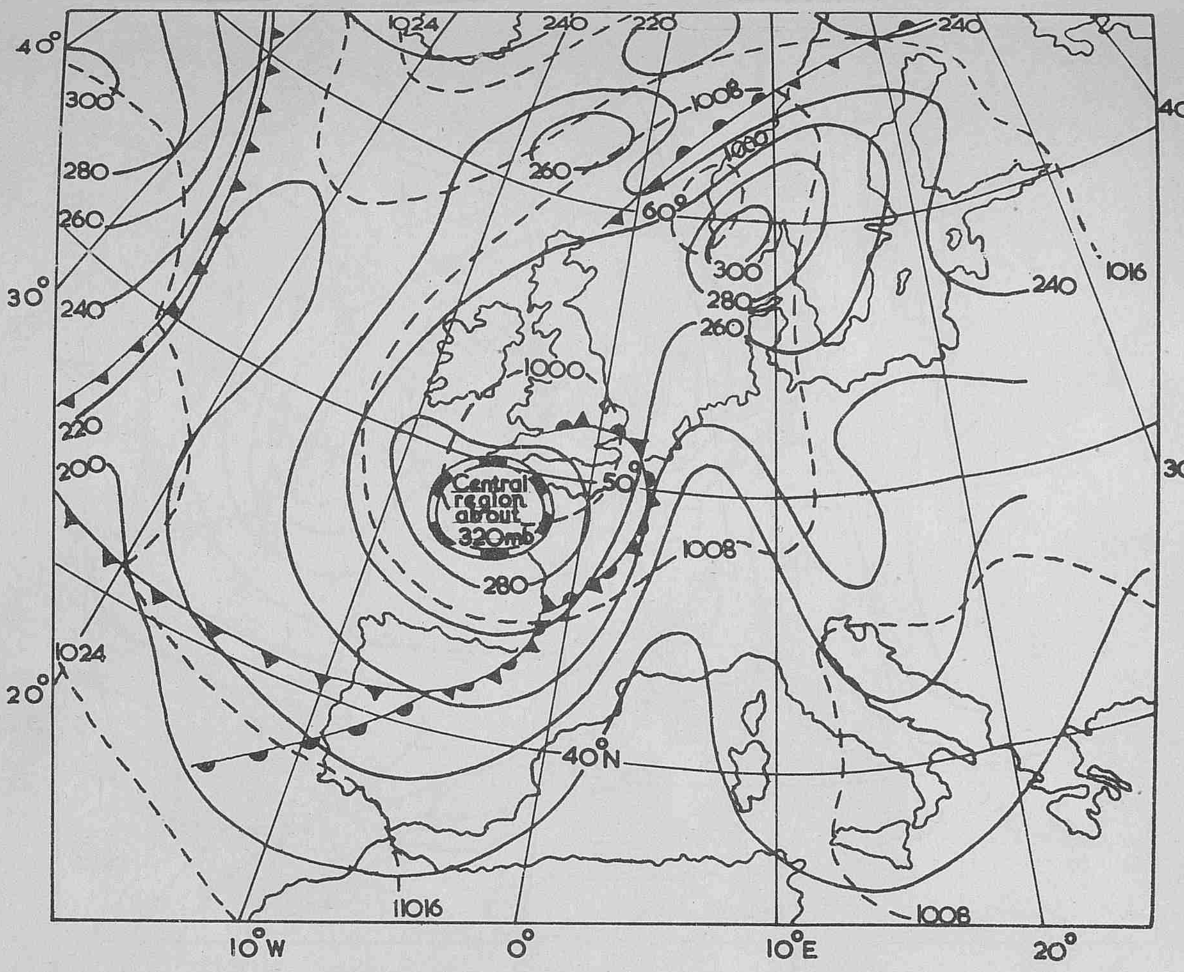
40°
1024
240
220
240
300
280
260
30°
240
220
200
1024
20°
1008
1000
260
60°
300
280
260
40°
1016
240
1000
Central region about 320mb
50°
30°
1008
280
40°N
1016
1008
10°W
0°
10°E
20°

Fig. 24(a) Isobars on the tropopause
0300 G.M.T. 17 MAY 1949

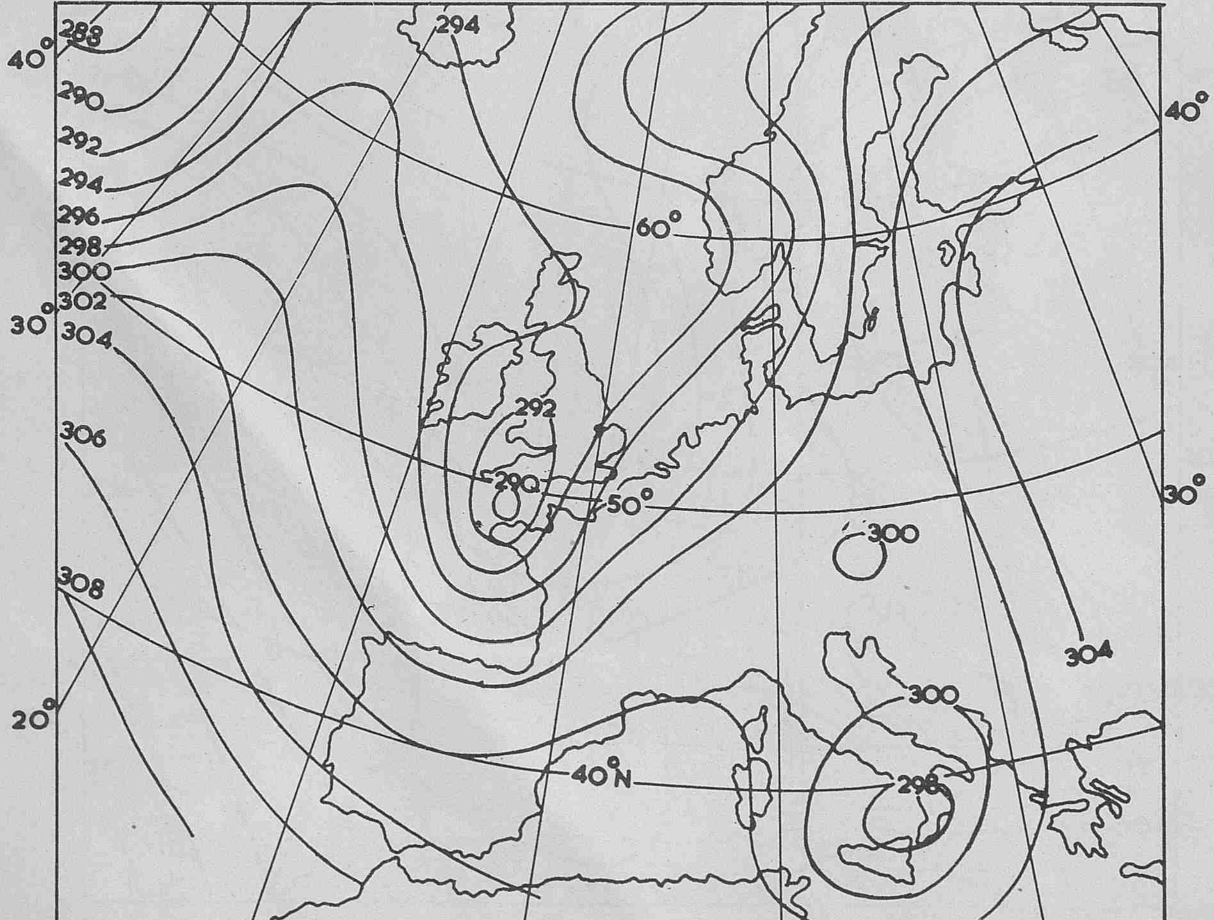
288
40°
290
292
294
296
298
300
302
30°
304
306
308
20°
294
60°
40°
292
290
50°
30°
300
304
300
298
40°N
10°W
0°
10°E
20°

Fig. 24(b) Contours of the 300 mb surface
0300 G.M.T. 17 MAY 1949

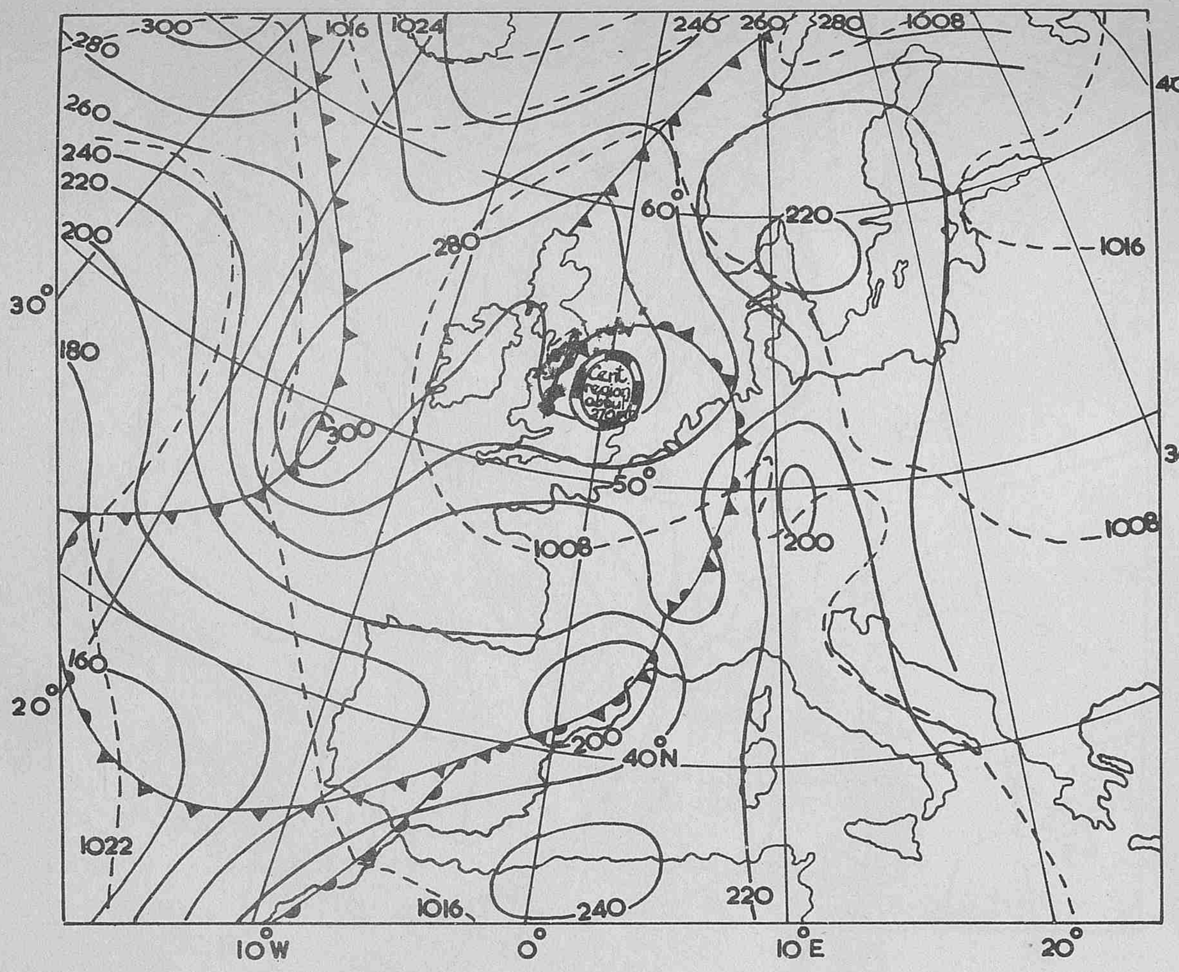
280
300
1016
1024
240
260
280
1008
40°
260
240
220
200
60°
220
1016
280
30°
180
Cent. region about 270mb
300
30°
50°
1008
1008
200
20°
160
200
40°N
1022
1016
240
220
10°W
0°
10°E
20°

Fig. 25(a) Isobars on the tropopause
0300 G.M.T. 18 MAY 1949

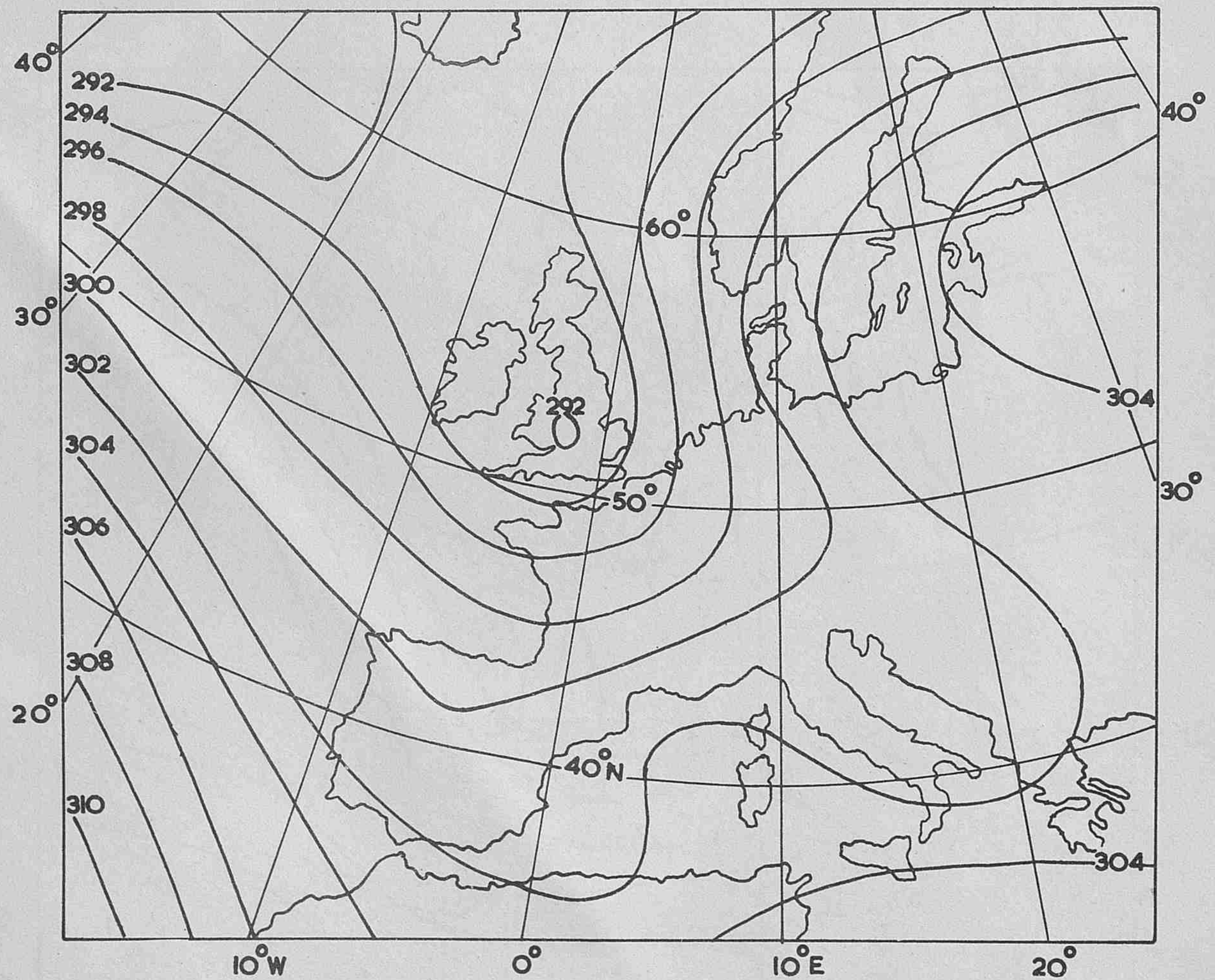
40°
292
294
296
298
300
30°
302
304
306
308
20°
310
40°
60°
292
304
50°
30°
40°N
304
10°W
0°
10°E
20°

Fig. 25(b) Contours of the 300mb surface
0300 G.M.T. 18 MAY 1949

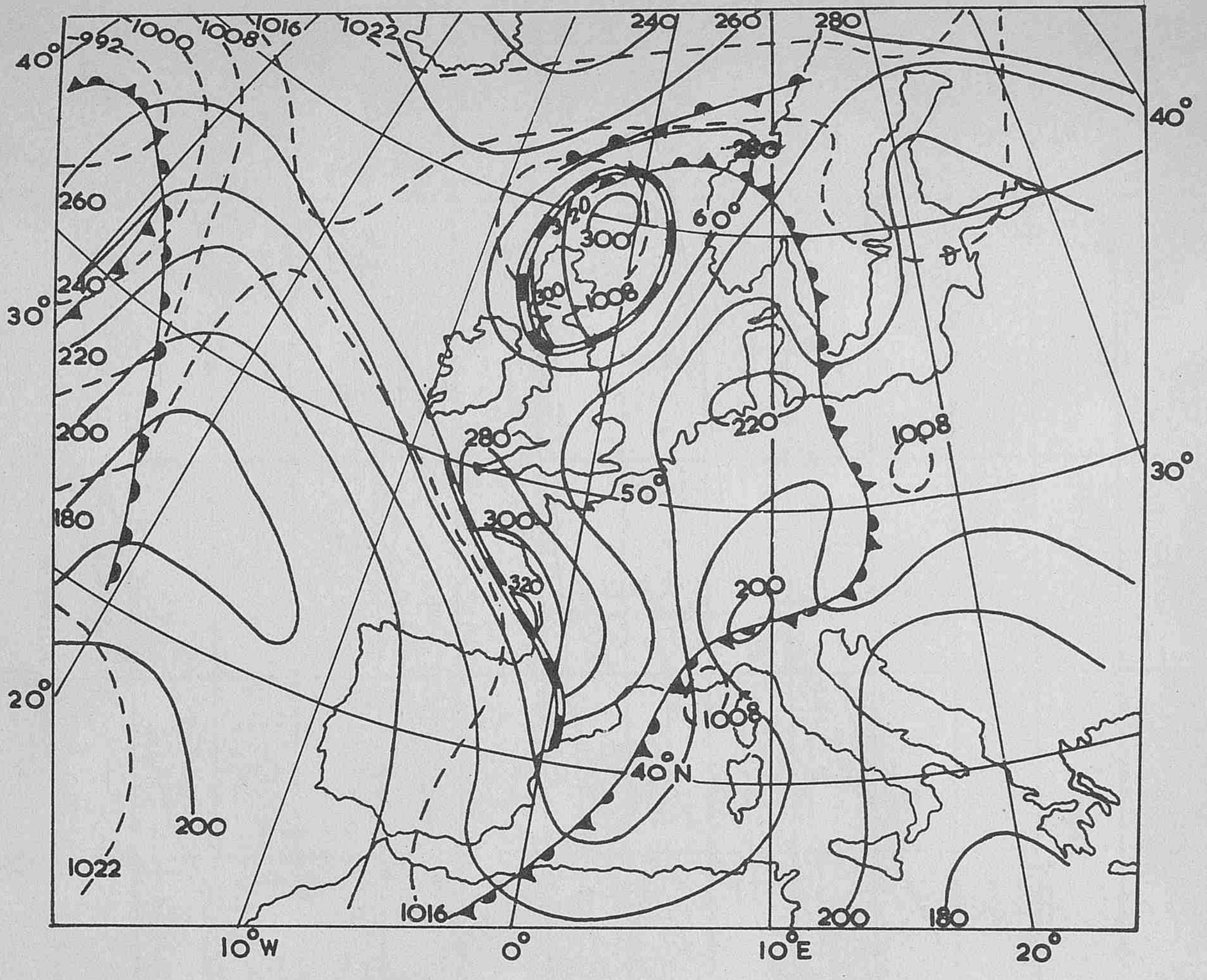

992
1000
1008
1016
1022
240
260
280
40°
260
240
30°
220
200
180
20°
280
320
300
300
1008
60°
220
1008
280
50°
300
320
200
1008
40°N
200
1022
1016
200
180
10°W
0°
10°E
20°
40°
30°

Fig. 26(a) Isobars on the tropopause
0300 G.M.T. 19 MAY 1949

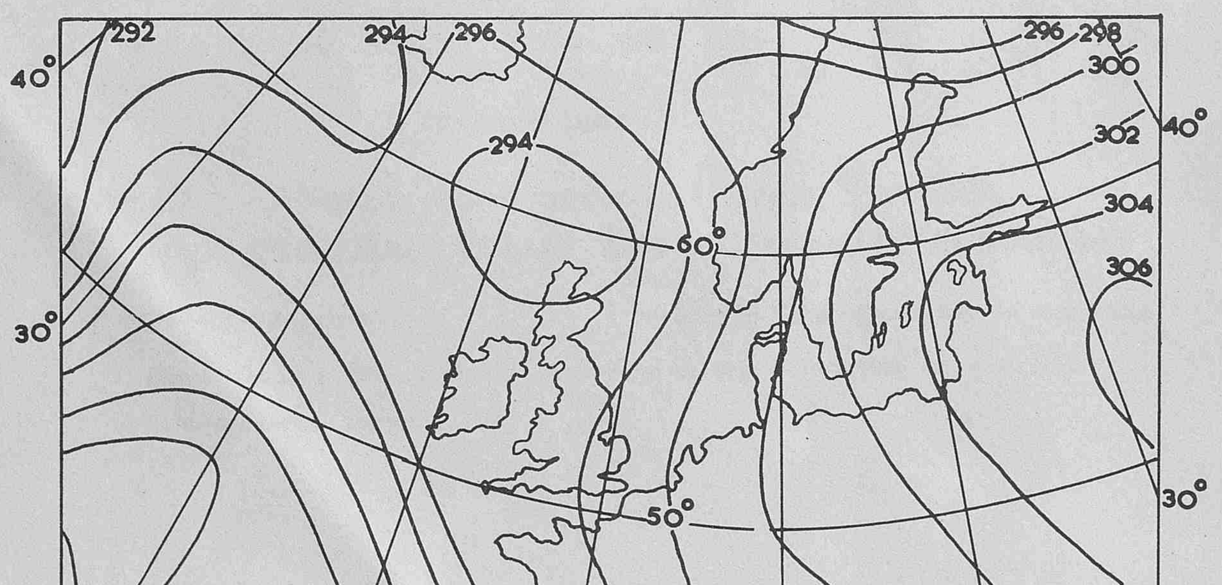

292
294
296
296
298
300
302
304
306
40°
30°
20°
294
60°
50°
40°N
306
304
10°W
0°
10°E
20°
40°
30°

Fig 26(b) Contours of the 300mb. surface
0300 G.M.T. 19 MAY 1949

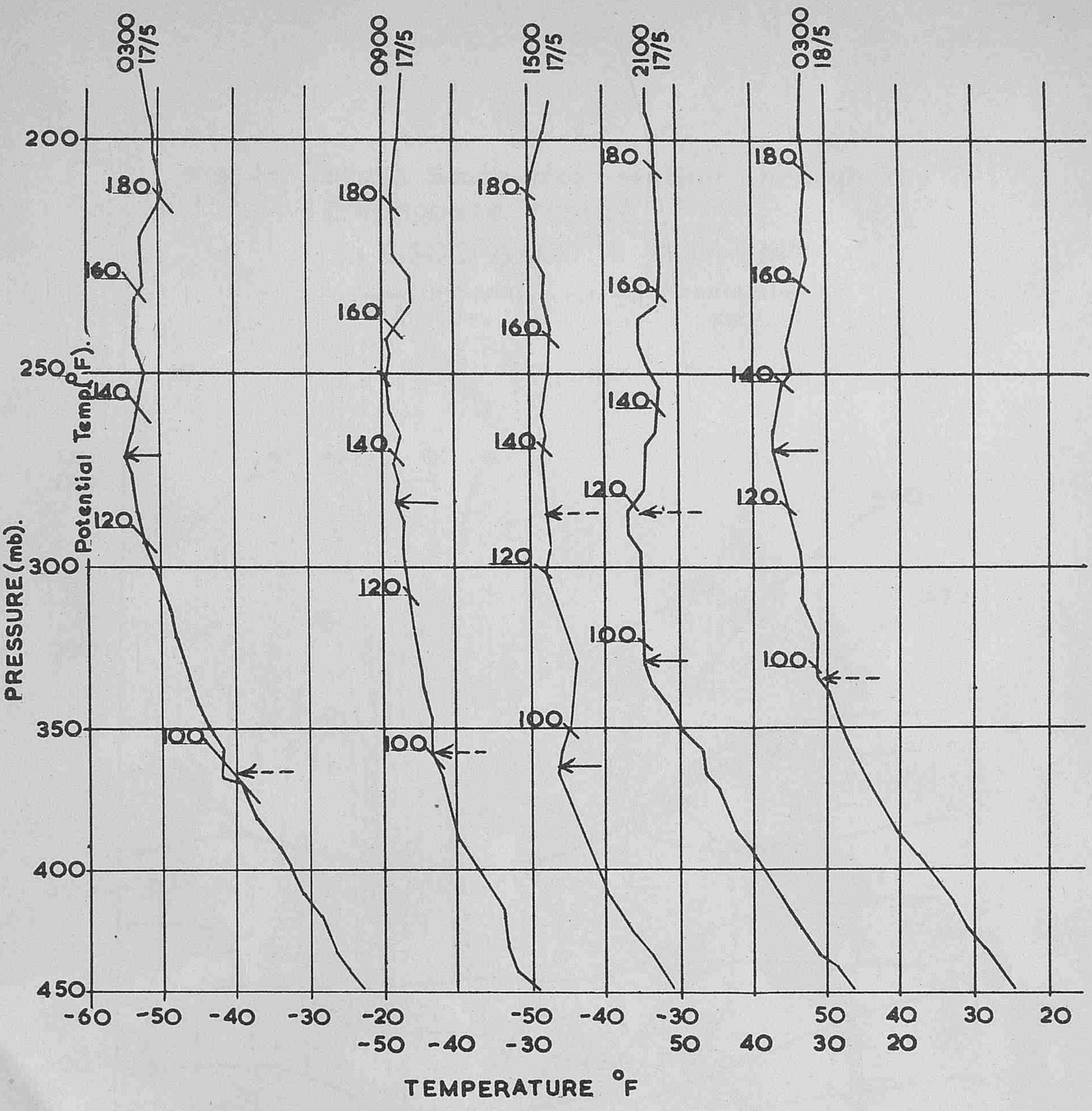

Fig. 27 Temperature soundings from Larkhill
0300 G.M.T. 17 MAY 1949 to 0300 G.M.T. 18 MAY 1949

⟵ Tropopause ⇠ – – Other discontinuity in lapse rate

Short sloping lines indicate segments of dry adiabatics at potential temperatures shown.

Fig. 28 North South cross-section through the tropopause funnel.

0300 G.M.T. 18 MAY 1949

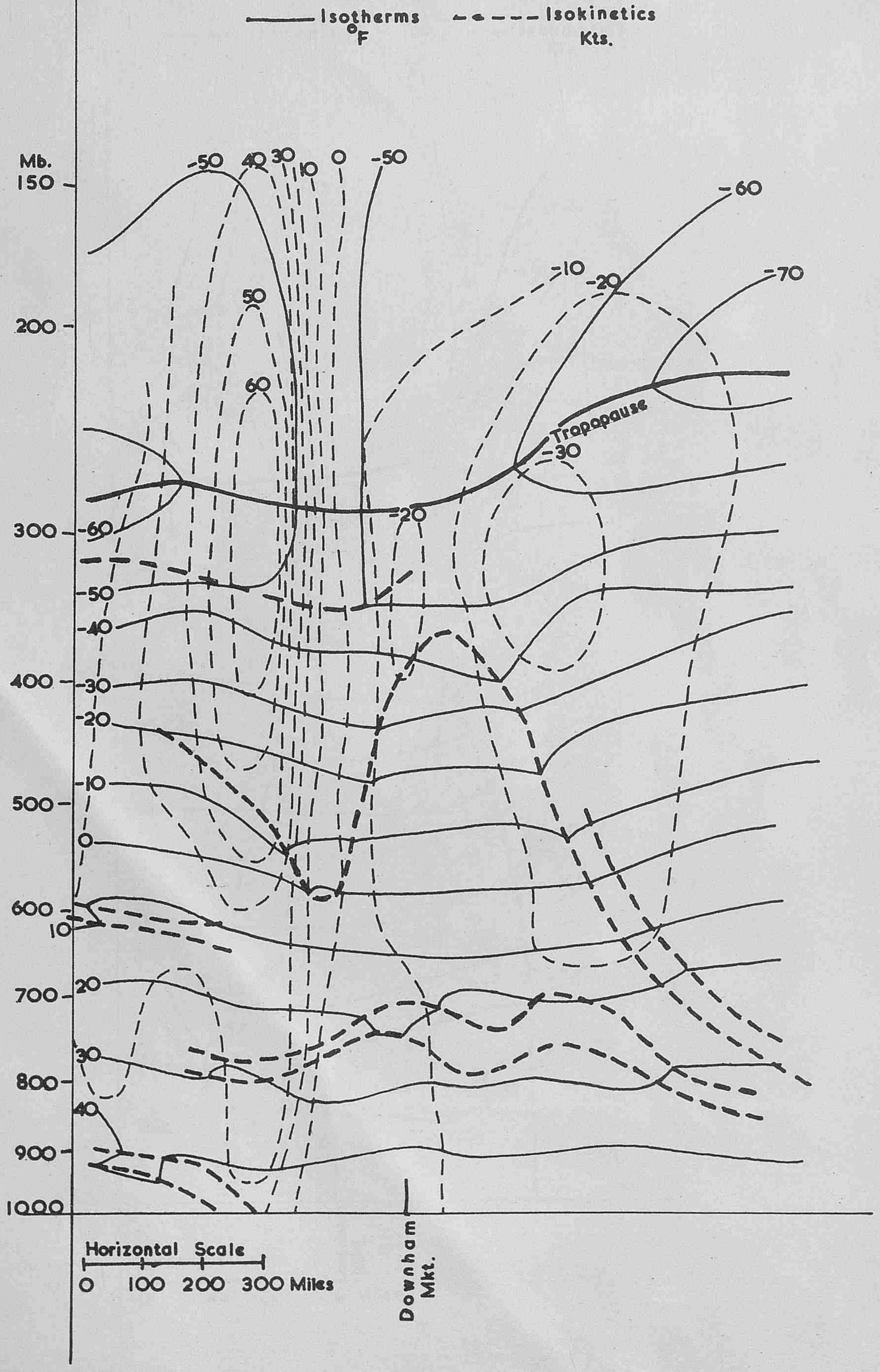

Fig. 29 East-West cross-section through the tropopause funnel
0300 G.M.T. 18 MAY 1949

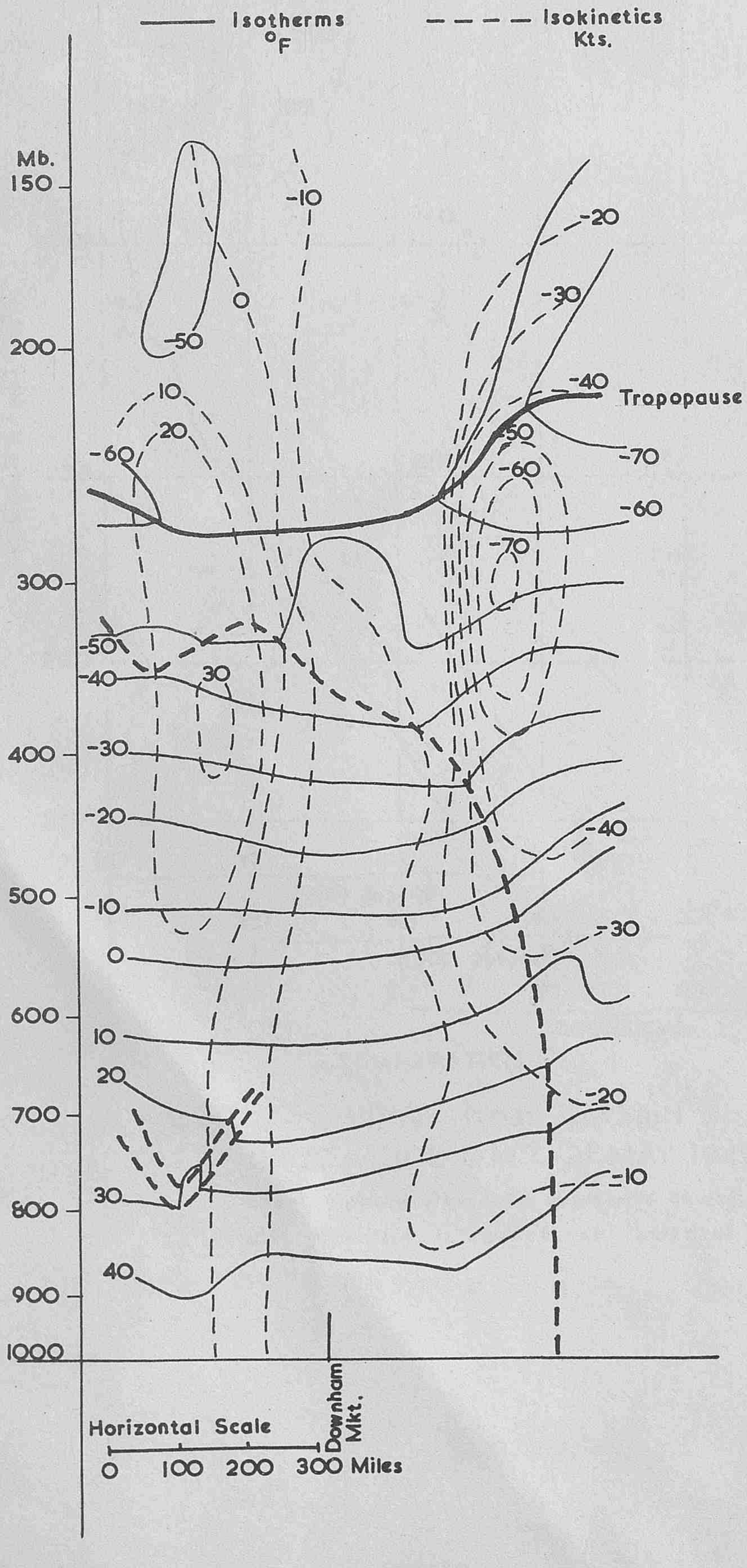

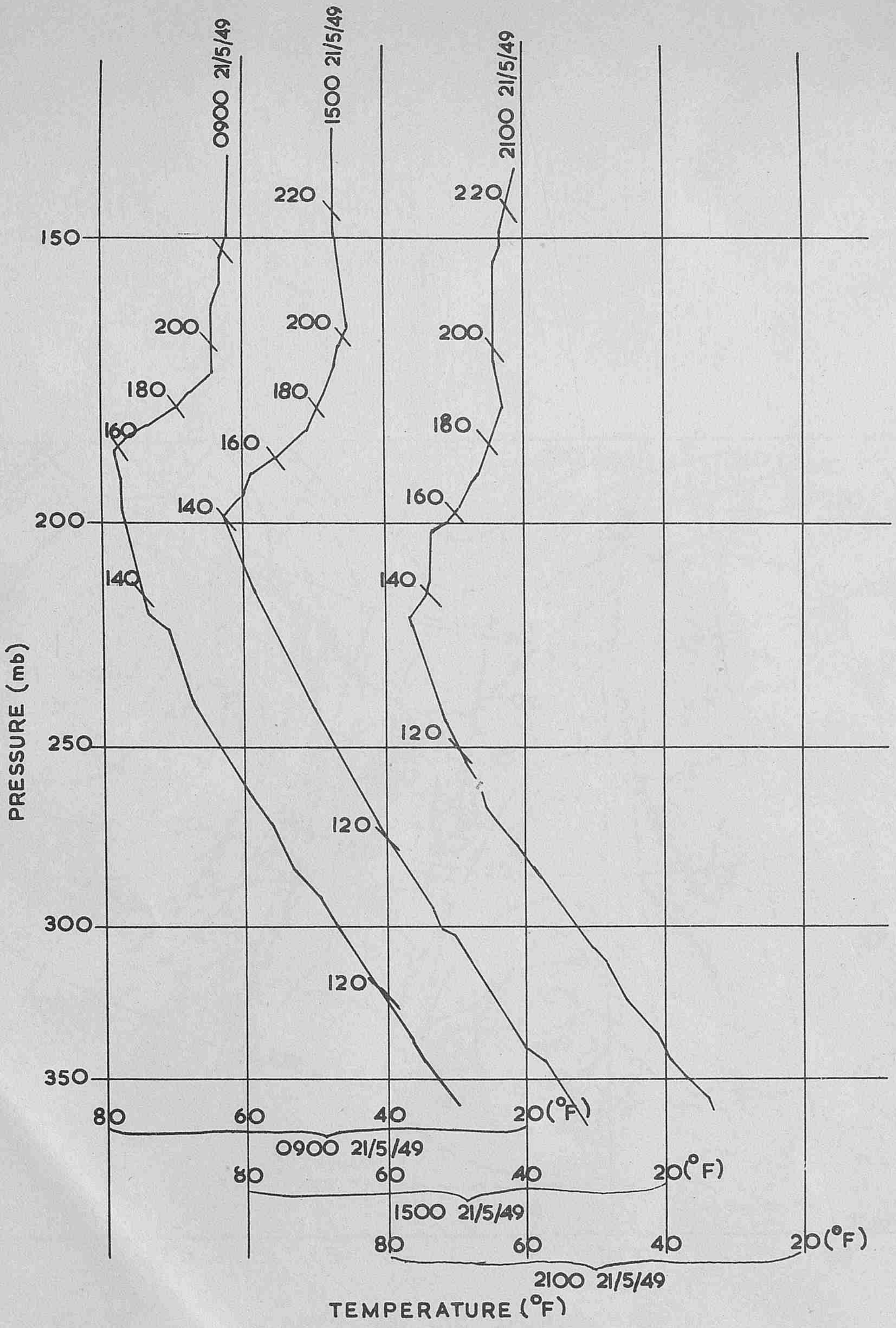

Fig. 30 Soundings from Larkhill
0900 to 2100 G.M.T. 21 MAY 1949

Short sloping lines are segments of dry adiabatics with potential temperatures indicated

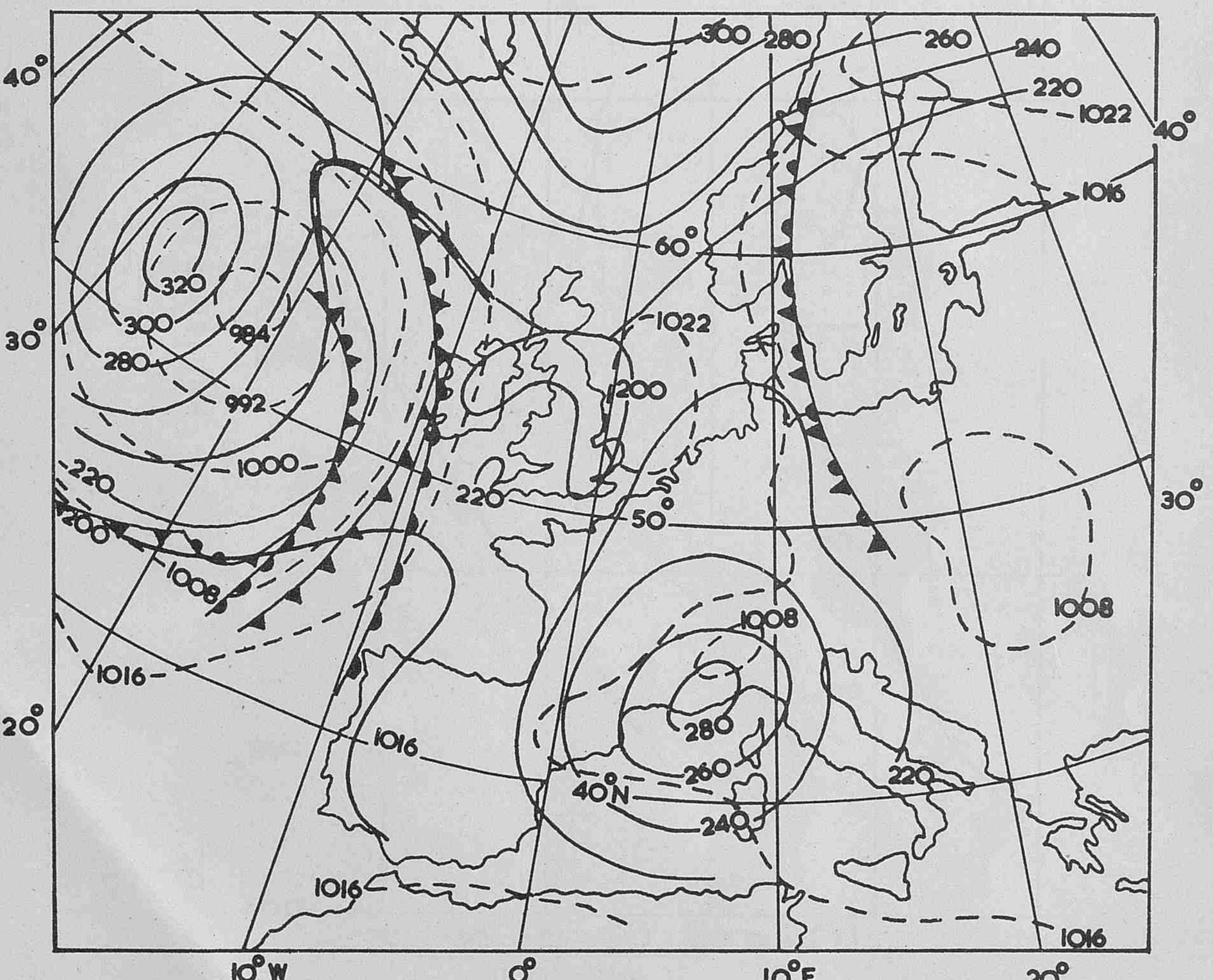

300
280
260
240
220
1022
40°
1016
60°
320
300
984
280
992
1000
220
200
1008
1016
1022
200
220
50°
30°
1008
1008
280
260
240
220
40°N
1016
1016
1016
20°
30°
40°
10°W
0°
10°E
20°

Fig. 31 Isobars on the tropopause

1500 G.M.T. 21 MAY 1949

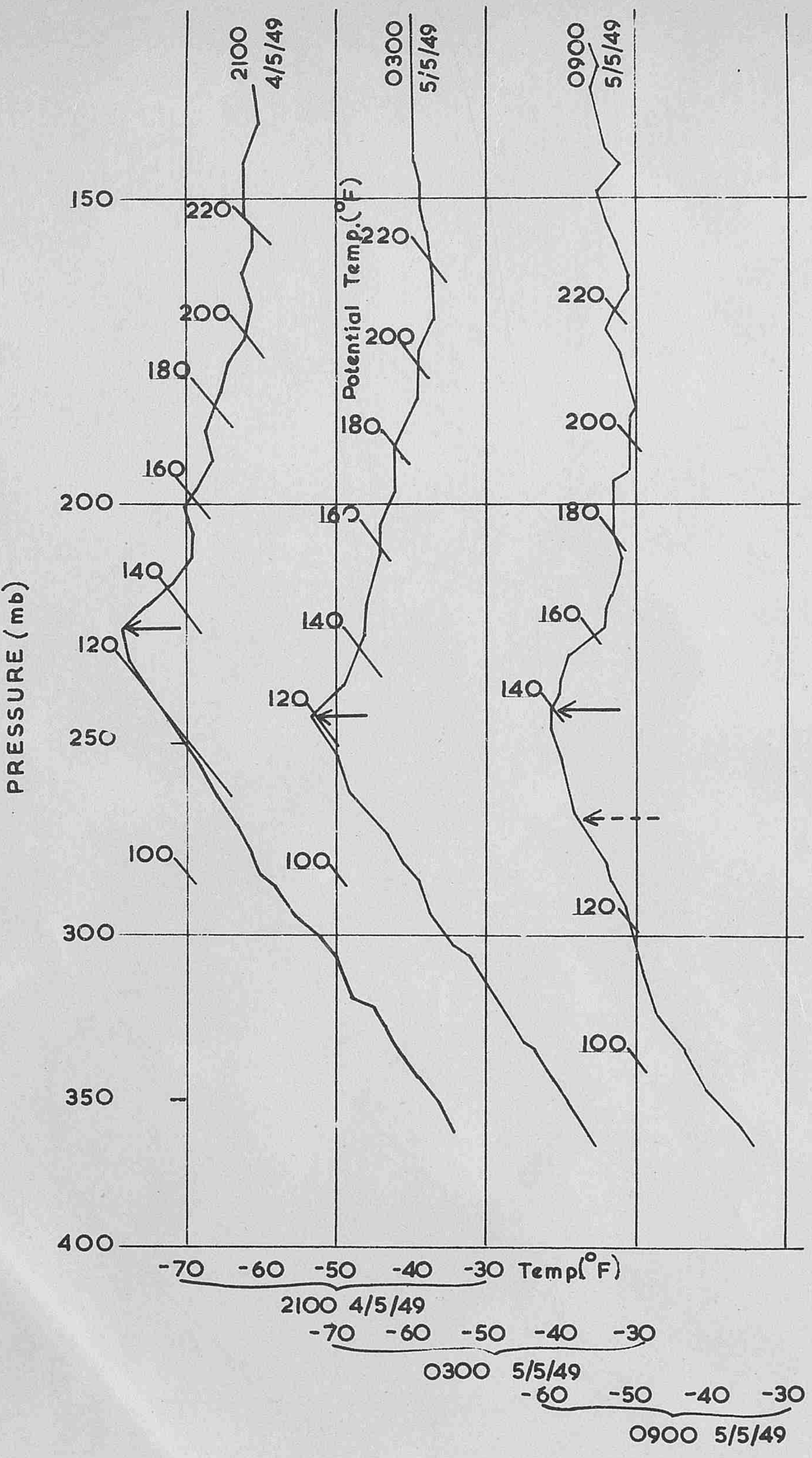

Fig. 32 Soundings at Larkhill
2100 4 MAY 1949 to 0900 5 MAY 1949

Short sloping lines are segments of dry adiabatics with the potential temperature indicated

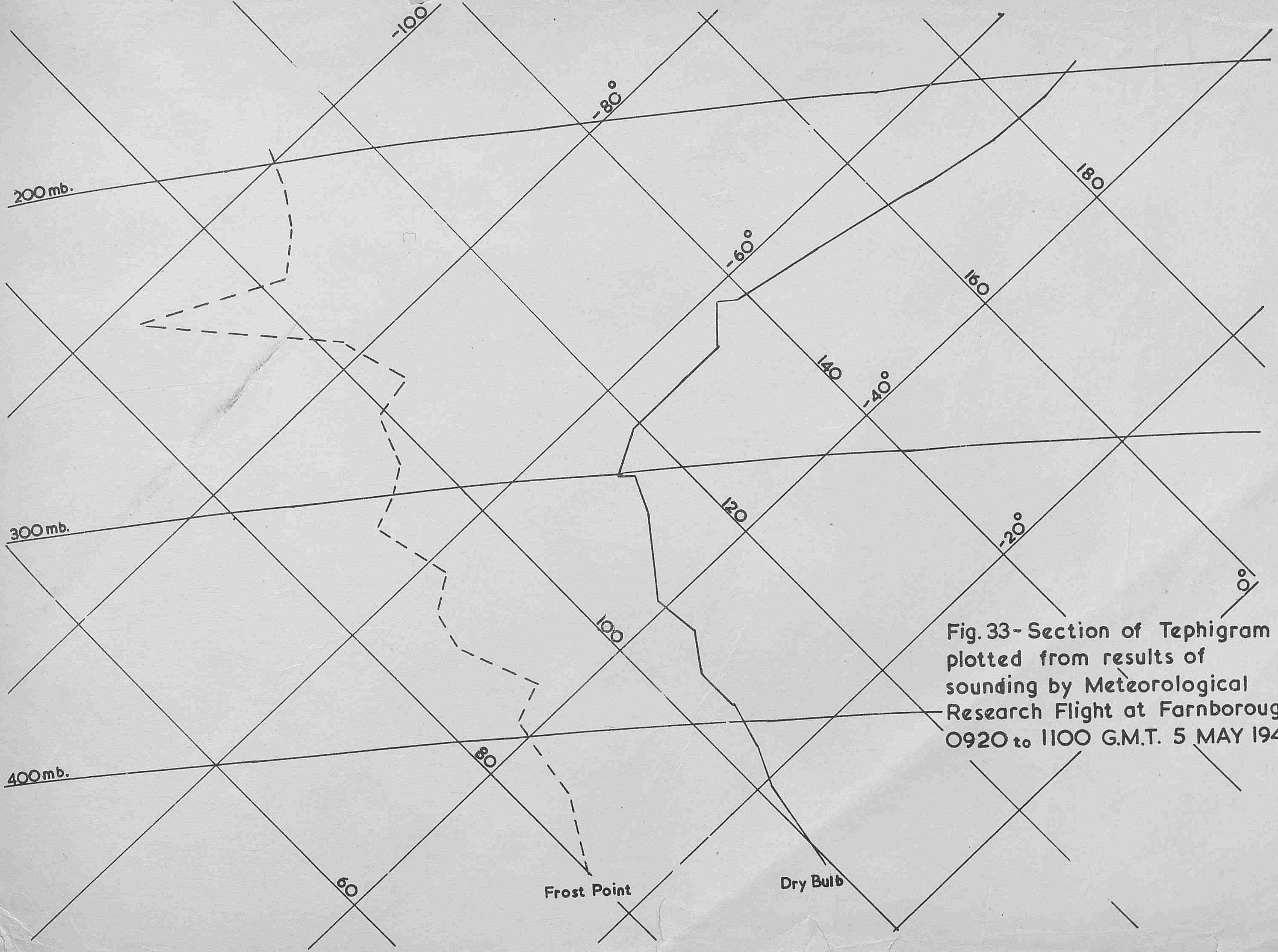

Fig. 33 - Section of Tephigram plotted from results of sounding by Meteorological Research Flight at Farnborough 0920 to 1100 G.M.T. 5 MAY 1949.

AIR WEATHER SERVICE
TECHNICAL REFERENCE FILES
DEC 11 1951

A.881287/46/Pt.II/M.O.15.

To Members of M.R.C. and S.C.III.

Amendment to M.R.P.613

Will you please amend your copy of M.R.P.613 as follows:-

Fig.I Delete the words "Wet Bulb" where they occur in the key (3 occasions) and substitute "Dew Point" in each case.

J K Bannon

17th August, 1951 for Secretary, M.R.C.

G.303633/JW/8/51/160

---

radar echoes become so widespread and complicated that it is impossible to follow the life history of individual storms within the general thundery outbreaks, but on this occasion the storms remained relatively isolated and compact and gave greater opportunity for the study of individual cells. In the present paper the development of five individual storms is discussed.

Photographic illustrations are provided, the photographs being numbered P.1, P.2, P.3 etc. for P.P.I. photographs 1, 2, 3 etc. and H.1, H.2, H.3 etc. for H.R.T. photographs 1, 2, 3 etc. References in the text to these photographs will be by these numbers omitting the word "photograph" e.g. (P.5) will mean "see P.P.I. photograph No. 5" and H.4 will refer to H.R.T. photograph 4.

2. Synoptic situation

A shallow depression was centred at 1200 G.M.T. over the Bay of Biscay and a very light E - SE airstream covered the southern half of the country. The air was unstable for surface temperatures around 83 - 85°F or higher but very dry in the higher layers and only a few isolated thunderstorms were expected, and in fact occurred. There was little difference between the radiosonde soundings for 1500 G.M.T. at Larkhill and Downham Market (Fig. I) and at both stations the winds were 10 kt or less up to at least 30,000 feet. An aircraft ascent in the neighbourhood of Maidstone, Kent at 1415 G.M.T. gave similar readings (Fig. I) to the Downham Market and Larkhill ascents and reported 3/8 Cu and Cb from 850 mb to 430 mb with 2/8 Cs not reached at 300 mb. Cumulonimbus tops in the west were estimated to extend higher than 25,000 ft. and were probably associated with the first storm observed by radar (see below).

From the upper air information therefore it appeared that any locality in the southern half of England at which the surface temperature reached about 83 - 85°F. was liable to experience a thunderstorm and it is of interest to examine where in fact the isolated storms did occur. The relevant Daily Weather Report shows that on this day maximum temperatures of 83°F. or higher were recorded at Kew, London Airport, Mildenhall and Cranfield, within the range of 65 miles used for most of the day on the radar sets at East Hill. Conditions within radar range were therefore probably favourable for thunderstorm formation in the area west of London and in parts of East Anglia and the South Midlands. In fact it will be seen (Section 3) that thunderstorms did occur in the area west of London, but not, up to 1615 G.M.T., in East Anglia or the South Midlands.

3. The localities in which thunderstorms first appeared

Photographs of the P.P.I. tube of the 10 cm. radar equipment at East Hill are available for the period 1403 to 1615 G.M.T. Prior to 1345 G.M.T. no radar weather echoes were observed and after 1615 G.M.T. observations ceased owing to a fault in the set.

/ It

To file

been published. Any author desiring to quote this paper should refer to it as "A paper of the Meteorological Research Committee (London), M.R.P. No .... by Mr.................. A copy is available in the Library of the Meteorological Office."

AF351884

DPL/1 112

M.R.P. 613
S.C.III/86
22nd February, 1951.

AIR MINISTRY

METEOROLOGICAL RESEARCH COMMITTEE

[redacted]

Thunderstorms of 5th June, 1950, as seen by radar

by

R.F. Jones (Meteorological Office)

1. Introduction

Isolated thunderstorms which developed in Southern England on the afternoon of 5th June, 1950, provided an unique opportunity of examining by radar the life history of the storms, from the time of their first appearance on the radar screens to their time of dissipation. Frequently thunderstorm radar echoes become so widespread and complicated that it is impossible to follow the life history of individual storms within the general thundery outbreaks, but on this occasion the storms remained relatively isolated and compact and gave greater opportunity for the study of individual cells. In the present paper the development of five individual storms is discussed.

Photographic illustrations are provided, the photographs being numbered P.1, P.2, P.3 etc. for P.P.I. photographs 1, 2, 3 etc. and H.1, H.2, H.3 etc. for H.R.T. photographs 1, 2, 3 etc. References in the text to these photographs will be by these numbers omitting the word "photograph" e.g. (P.5) will mean "see P.P.I. photograph No. 5" and H.4 will refer to H.R.T. photograph 4.

2. Synoptic situation

A shallow depression was centred at 1200 G.M.T. over the Bay of Biscay and a very light E - SE airstream covered the southern half of the country. The air was unstable for surface temperatures around 83 - 85°F or higher but very dry in the higher layers and only a few isolated thunderstorms were expected, and in fact occurred. There was little difference between the radiosonde soundings for 1500 G.M.T. at Larkhill and Downham Market (Fig. I) and at both stations the winds were 10 kt or less up to at least 30,000 feet. An aircraft ascent in the neighbourhood of Maidstone, Kent at 1415 G.M.T. gave similar readings (Fig. I) to the Downham Market and Larkhill ascents and reported 3/8 Cu and Cb from 850 mb to 430 mb with 2/8 Cs not reached at 300 mb. Cumulonimbus tops in the west were estimated to extend higher than 25,000 ft. and were probably associated with the first storm observed by radar (see below).

From the upper air information therefore it appeared that any locality in the southern half of England at which the surface temperature reached about 83 - 85°F. was liable to experience a thunderstorm and it is of interest to examine where in fact the isolated storms did occur. The relevant Daily Weather Report shows that on this day maximum temperatures of 83°F. or higher were recorded at Kew, London Airport, Mildenhall and Cranfield, within the range of 65 miles used for most of the day on the radar sets at East Hill. Conditions within radar range were therefore probably favourable for thunderstorm formation in the area west of London and in parts of East Anglia and the South Midlands. In fact it will be seen (Section 3) that thunderstorms did occur in the area west of London, but not, up to 1615 G.M.T., in East Anglia or the South Midlands.

3. The localities in which thunderstorms first appeared

Photographs of the P.P.I. tube of the 10 cm. radar equipment at East Hill are available for the period 1403 to 1615 G.M.T. Prior to 1345 G.M.T. no radar weather echoes were observed and after 1615 G.M.T. observations ceased owing to a fault in the set.

/ It

It will be seen (P.1) that at some time between 1345 G.M.T. and 1403 G.M.T. a radar weather echo developed on a bearing of 212 - 214° Magnetic from East Hill at a range of 40 - 45 miles. The echo was first observed on the height-range tube at 1359 G.M.T. (H.1) and it is probable that the time of first appearance (which was certainly after 1345 G.M.T.) was about 1355 G.M.T. The area of first appearance was a region over the River Blackwater about three miles west of Sandhurst (Fig.II). This storm moved from a mean direction of about 097° True at a speed of about 8 kt. The nearest upper winds, reported at Larkhill at 1500 G.M.T., to this movement are at 1000 mb. (680 ft.) where the wind was 103°T 8kt. and at 700 mb. (10,500 ft.) where the wind was 103°T 6 kt, but with the wind so light and variable any correlation is of doubtful significance. However above 650 mb (12,500 ft) the wind veered progressively with height from 116°T 5 kt at 650 mb to 272°T 15 kt at 250 mb (about 35,500 ft) so that it seems probable that the movement of the storm was governed by the wind at some level below 650 mb. Radar responses from this storm had completely disappeared by 1511 G.M.T. (P.8) and were already becoming weak at 1446 G.M.T. (H.7), some 6 miles from the locality where it first developed.

The second storm (referred to hereafter as Storm II) was first observed on the height-range tube as two separate narrow columns of echo at 1459 G.M.T. on bearings of 186½° Mag 25 miles (H.8) and 182° Mag 27 miles (H.9), in the vicinity of Uxbridge and Hayes respectively (Fig.II). These two columns had grown but maintained their separate identity at 1503 G.M.T. (P.6). After about 1507 G.M.T. (P.7) the two echoes amalgamated and the echo grew considerably (Fig. III). Growth of the echo obscured its slow movement so that accurate speed and direction of movement cannot be determined before 1541 G.M.T. (P.10), but after this time the echo appeared to move from 113°T at a speed of 10 kt until 1607 G.M.T. (P.12) after which time this storm had decayed considerably. Correlation of the movement is again with the winds at some level below 650 mb.

By 1541 G.M.T., however, there were signs (P.10) that this storm was developing a new centre of activity (Storm III) at its western edge (Fig. III) and this development became more marked on subsequent photographs, while the original storm centre (Storm II) declined, until by 1615 G.M.T. Storm II had largely disappeared (P.13). Storm III would appear to have originated close to the River Thames about 3 miles N.N.E. of Maidenhead (Fig. II).

Development of this storm was probably an example of the generation of a new cell on the perimeter of an existing cell by forced uplift due to the descending air of the original cell.(1,2)

The fourth storm (Storm IV) is in evidence on the photograph for 1541 G.M.T. (P.10) on a bearing of 236½° Mag and had clearly developed between this time and the time of the previous photograph at 1515 G.M.T. (P.9). It is noteworthy (Fig. II) that this storm, as well as Storm III and Storm V (see below), developed approximately on the line of movement of Storm II and ahead of it (no storm developed to the rear of Storm II even though its speed of movement was very slow). The locality in which Storm IV developed was about 2 miles south of Wallingford in the neighbourhood of the river Thames and some 28 miles from the origin of Storm II. As development of this storm took place probably only about half an hour after Storm II, it seems unlikely that its growth can be ascribed to any influence of that storm. The storm had disappeared again by 1558 G.M.T. (P.11).

Finally a fifth storm (Storm V) appeared between 1541 and 1558 G.M.T. (P.10 and P.11) on a bearing of 225° Mag, also approximately on the line of movement of Storm II and about 8 miles ahead of Storm III but 8 miles to the rear of Storm IV (Fig. II). This storm grew rapidly in the following 9 minutes and was the dominant storm of the family by 1615 G.M.T. (P.13). Height-range tube photographs (H.29 to H.41) suggest that it reached its maximum development about 1618 G.M.T. (H.39). The area in which this storm developed was about 2 miles north of Henley near the River Thames and its growth was such as to mask its movement.

It is of interest to note that although conditions, as mentioned in Section 2, were generally favourable for isolated thunderstorm development in parts of East Anglia and the South Midlands as well as the area west of London, no such development in the former areas occurred up to 1615 G.M.T. It appears that some especially favourable conditions for thunderstorm formation existed in the area immediately to the west of London which were not in evidence from the meteorological data available. Some possibilities are indicated below:-

(i) For some hours prior to thunderstorm formation the air had been drifting slowly westwards across the built up area of London and more or less along the Thames valley.

(ii) All the storms appeared to develop near rivers and with slowly moving air the moisture content may have been increased locally. However there are other rivers in the general area above which thunderstorm formation did not occur.

(iii) The topography may have been particularly favourable.

(iv) Temperatures near to the maximum temperatures may have been maintained in the area west of London for a longer period than elsewhere.

(v) Some minor discontinuity in the upper air may have occurred in a narrow belt which was not in evidence at either Larkhill or Downham Market.

The first storm to develop did not grow to the same extent as the second and subsequent storms nor did it appear to trigger off any strong new cells on its perimeter. This was probably an isolated storm which developed around the time of maximum temperature but was unable for some reason to maintain its source of supply of warm and moist air. The maximum temperature at Farnborough, 5 miles to the southeast of the area of origin, was 85°F and it may be significant that at 1400 G.M.T. the dew point was 66°F, which is higher than those at other stations in the neighbourhood at 1200 and 1800 G.M.T.

The remaining storms all developed in the Thames valley area(Fig. II). Although the original storm (Storm II) in the Uxbridge area was somewhat removed from the river, (although close to the River Colne and some canals) the remaining storms originated very close to the river. Storm II spread N.W. and moved about W.N.W. until its outer edge, as shown on the P.P.I., reached high ground some 300 - 400 ft. high (Fig. III). When this occurred movement in the direction of the high ground ceased and Storm II began to disperse. The new development, Storm III, then occurred to the south of the high ground and close to the river in a direction slightly south of west from the main centre of activity of Storm II (Fig. III). This storm also avoided the high ground and seemed to follow the bend of the river keeping always a mile or two from the north bank. At the same time Storm IV developed on the same side of the river further along its course, while a short time later Storm V developed near Henley, again on the same side of the river. The Henley storm grew considerably but still appeared reluctant to cross the river to the south or the high ground to the west and northwest. Subsequent movement of this storm, however, could not be observed.

It is noteworthy that Storms II and V, which moved over areas where the high ground was further removed from the river than the areas over which Storms III and IV moved (Fig. II), grew to a greater horizontal extent.

Fig. II shows that the places where Storms II, III, IV and V first developed lie exactly on a straight line which, when projected eastwards, crosses London north of the Thames and then passes out to sea along the

Thames Estuary. This line is oriented along the direction 093°T. If this is the direction from which the air in the lowest layers moved, as seems likely, it is clear that the air which finally ascended into the storms had a long traverse (in time and distance) near to a water supply and would therefore be expected to have a significantly greater moisture content than the air further north which would have had no such opportunities for increasing its moisture content.

A significant feature in the development of these storms can therefore be found in the previous history of the air, the movement of which was such that for a long period it was able to travel close to a fairly large river and gain additional moisture therefrom. The river however was too small to exercise any marked effect on the temperature distribution so that the air experienced the full effect of the heating of the land.

As regards the detailed movement of the storms, once they had formed, there would appear to be a tendency, in the light winds prevailing, to keep close to the river and follow the minor variations of its course. There is also the possibility that the ground higher than about 400 ft. exercised a damping effect on the spread or movement of the storms across it.

4. Area covered by precipitation and its rate of change

From the P.P.I. photographs it is possible to find the area covered by echo at the time of the photographs for Storm II (P.6 to P.13 and Fig. III) and Storm V (P.11 to P.13).

The P.P.I. photograph however is the projection on an almost horizontal plane of the whole of the radar echo and in some circumstances will not therefore accurately represent the area of the earth which is experiencing rainfall of a sufficient intensity to give a radar echo. An exaggerated picture of the area experiencing precipitation is given (a) in the initial stages of radar echo formation when the echo has not yet reached to the ground and (b) when the echo, as sometimes happens around the time of its maximum development, becomes wider at high levels than near to the ground. In case (a) a P.P.I. echo will be observed even though no appreciable precipitation is yet reaching the ground and in case (b) the P.P.I. echo received will be larger in horizontal extent than the echo near to the ground since responses will also be received from the greater width of echo at high levels. When the storm is decaying the residual precipitation from the cloud may lead to a greater area of light precipitation on the ground than at any time during the stage when the precipitation was heavy.

It is desirable therefore to use the P.P.I. photographs in conjunction with the vertical cross-section photographs and to limit measurements to the times when the P.P.I. photograph is truly representative of the area of the ground experiencing heavy precipitation.

In the case of Storm II it will be seen from the sequence of H.R.T. photographs (H.8 to H.28) that prior to about 1504 G.M.T. (H.12) appreciable precipitation was not reaching to a lower height than 5,000 ft. and that appreciable precipitation probably did not reach the ground until 1505 - 1506 G.M.T. (H.13, H.20). From this time until about 1521 G.M.T. (H.22) the P.P.I. picture probably represented accurately the area of ground covered by heavy precipitation, but after 1521 G.M.T. the spreading out of the echo at higher levels caused the P.P.I. to give an exaggerated impression of the area of precipitation on the ground, which exaggeration probably persisted until the storm was well into the decaying stage. The three P.P.I. pictures (P.7, P.8, P.9) at 1507, 1511 and 1515 G.M.T. only are therefore used to gain an idea of the area of heavy precipitation on the ground and its growth with time.

At these times the areas of the P.P.I. echo were respectively 26.8, 30.8 and 36.8 sq. miles (equivalent to circles of diameters 5.8, 6.3 and 6.8 miles respectively) giving a mean rate of growth of 1¼ sq. miles per minute.

For Storm V only the P.P.I. photograph at 1607 G.M.T. (P.12) is truly representative and this shows the area covered by precipitation to be 27.5 sq. miles (equivalent to a circle of diameter 5.9 miles). An estimate however of the area of precipitation at 1615 G.M.T. (P.13) can be made from the fact that the width of the H.R.T. echo at that time (H.38) at 30,000 feet (the widest part) is 1.35 times as great as the echo near the ground. This suggests that the dimensions of the P.P.I. echo may be increased in this ratio and the area therefore in the ratio $1.35^2 : 1$ or $1.82 : 1$. The area of the P.P.I. echo is 47.5 sq. miles so that the area of precipitation on the ground may be approximately

$$\frac{47.5}{1.82} \text{ sq. miles} = 26.1 \text{ sq. miles.}$$

i.e. Storm V had probably reached its maximum area of heavy precipitation on the ground by about 1607 G.M.T.

5. Development of the radar echoes in the vertical plane

Height-range tube photographs giving some evidence of the change of the echo in the vertical plane are available for Storm I (H.1 to H.7), Storm II (H.8 to H.28) and Storm V (H.29 to H.41).

It is clear that, with storms which may extend over several degrees of azimuth, it is impossible to get a complete picture of the vertical structure on a photograph taken on one particular bearing. The photographs, however, were taken on the bearing which gave the highest top determined by swinging the aerial from side to side through the whole spread of the storm. In addition the beam width in the horizontal plane of the equipment used was 7½°. It is likely therefore that photographs of the most active part of the storm on each occasion have been obtained. The bearing on which the photograph was taken and the time are given beneath each photograph.

Storm I. Photographs H.1 to H.7 give vertical cross-sections through this storm at the times and on the bearings indicated.

No observations were taken prior to 1359 G.M.T. but the storm was certainly not giving a radar echo at 1345 G.M.T. and the time of first appearance of an echo was probably about 1355 G.M.T.

At 1359 G.M.T. (H.1) a column of echo extended from the surface to 26,300 ft, while there was evidence of a second column at its side extending to 14,700 ft. 3½ minutes later (H.2) the main top had reached 27,900 ft. while the second column top had attained 17,800 ft. By 1412 G.M.T. (H.3) the main column reached to 30,000 ft. and there is a suggestion that the second column had reached 28,800 ft. Yet another column appears on this photograph with a top at 16,800 ft. At 1421 G.M.T. (H.4) the photograph suggests that the first two columns were dissipating leaving a weak and diffuse echo while the third column had reached 27,800 ft. This column reached 32,900 ft. by 1425 G.M.T. (H.5). At this time a fourth column was in evidence to 21,500 ft. and reached 30,000 ft. by 1433 G.M.T. (H.6) by which time the third column was in the dissipating stage. By 1446 G.M.T. (H.7) the whole echo had decayed considerably and only a faint trace of the echo remained by 1457 G.M.T., about one hour after its first appearance.

Mean rates of growth of the tops of the four columns are given in Table I below:-

/ TABLE I

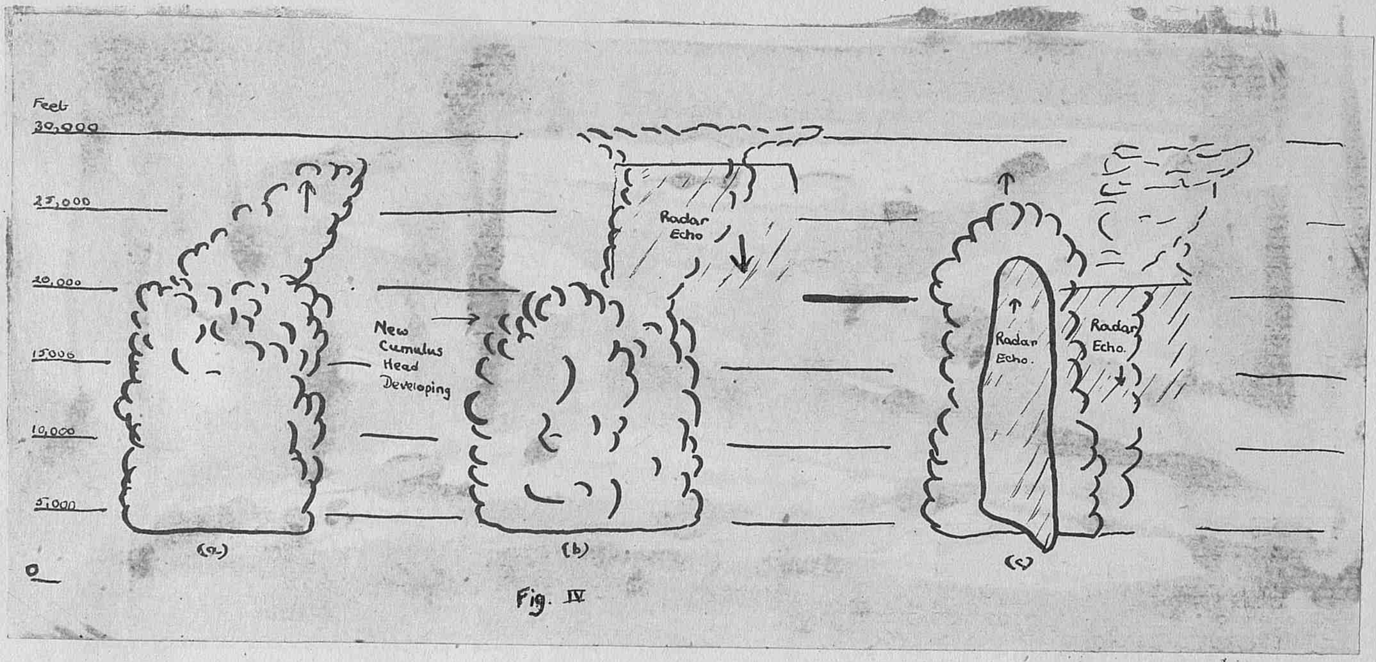

Fig. IV

In (a) of this figure is shown the cloud as it may have existed prior to the appearance of any weather echo, having been in existence for some time and still growing slowly. The effect of wind shear above 20,000 ft. is demonstrated by the leaning away of the cloud above this level from the perpendicular through the base. In (b) the cloud has now reached the 30,000 ft. level with the formation of ice crystals and the growth of large enough crystals to give a radar echo. The vertical component of the air current in this region has now decreased to zero and the large ice crystals are falling giving a radar echo over some height interval. In the meantime the vertical currents below 20,000 ft. have increased and a new development of cloud is taking place, but without a radar echo as yet. This corresponds to the position at the time of H.8. In (c) the echo from the ice crystals has fallen further and the cloud top has descended, with this part of the cloud dissipating. Meanwhile the new development has continued its rapid growth and raindrops have formed within the ascending current producing a column of radar echo. The growth of this new cumulus is so rapid (the echo top rose at 8½ m./sec. between 1504 and 1506) that the effect of wind shear is not so noticeable. This corresponds to the position at the time of H.19 and H.12. Rapid growth of the new cumulus continues until it finally reaches 41,000 ft. while the precipitation from the old cumulus head falls to the ground. The rate of fall of this precipitation (8 m./sec.) suggests that it was probably assisted on its way by the down-current surrounding the strong up-current of the newly developing cumulus - possibly also reinforced by the close proximity of the second cell to the southeast.

Having reached its maximum development at 41,000 ft. this cell in its turn begins to decay.

Development of the second of the two cells of Storm II - the one to the southeast (P.6) - was somewhat different. In this case also the first echo was probably from ice crystal precipitation (H.9) but after falling some distance a new development from beneath probably swept it up or occurred so close to the descending ice crystals that radar discrimination was impossible. On H.10 there is a suggestion of a stronger column developing from 10,000 to 22,000 ft. at 25½ miles which by the time of H.12 extends from near the ground to 27,000 ft. Meanwhile it will be noticed that the higher top, originally to 30,000 ft, attributed to ice crystals, has descended and is weakly in evidence on H.12 at 26,500 ft. at a slightly greater range than the developing column. After this time development of the stronger column masked any return from the original ice crystal precipitation. This interpretation is reinforced by the fact that the rate of growth of this column from 22,000 ft. to a final height of 40,500 ft. correlates almost exactly with the rates of growth of the northwestern cell, being 8 m./sec. between 22,000 and 29,000 ft. from 1501 to 1505 ($8\frac{1}{2}$ m./sec. between 23,000 and 27,000 ft. from 1504 to 1506 for the northwestern cell) and 5 m./sec. as the mean rate between 22,000 and 40,500 ft. from 1501 to 1521 (5 m./sec. between 23,000 and 41,000 ft. from 1504 to 1522 for the northwestern cell).

It seems possible therefore that, although the first signs of radar echo were received from the 30,000 ft. region, the strong subsequent development was connected with the growth from below of strong new cumulus columns.

Storm V. Height-range tube photographs of the development of this storm are shown in H.29 to H.41 at the times and on the bearings indicated.

From the P.P.I. photographs P.10 to P.13 it is clear that the radar echo from this storm was already in existence at 1558 G.M.T. (P.11) but had developed at some time after 1541 G.M.T. (P.10). The first vertical cross-section of this echo was obtained at 1600 G.M.T. (H.29) and compared with similar photographs for Storm II suggests that the echo had probably been in existence at that time for about 4 - 5 minutes.

Development of this storm would appear to have followed similar lines to that of Storm I with the growth and decay of more than one column within the general echo from the storm. This is particularly marked in photographs H.32 to H.34 and the column there developing at furthest range is probably the one which finally attained the maximum height of 41,000 ft. in H.39. If this is so the mean rate of ascent of the column top between 1607 and $1617\frac{1}{2}$ G.M.T. was 5.7 m./sec. which is very similar to the mean rate of ascent over such a height interval of the columns in Storm II.

6. The significance of the rate of rise of echo top

It is clear that, since the radar reflecting particles within the cloud must grow to a certain size and concentration before a measurable radar echo is received with the equipment used, the radar echo received does not come from the whole volume of the cloud. There will be parts of the cloud, in which the concentration and size of the particles is too small, from which no measurable radar echo is received. It does not follow therefore that the radar echo top bears any fixed relation to the cloud top nor that the rate of rise of the echo top is related to the rate of rise of the cloud top, except that the cloud top must always be at least as high as the radar echo top. (This point is also referred to in the report of the American Thunderstorm Project (5. page 92)).

If we assume, however,

(a) that the radar reflecting particles in a growing cumulonimbus cloud are waterdrops of raindrop size(4) with a terminal velocity of the order of 5 m./sec. or greater and

(b) that once formed the top and bottom of a radar echo move by virtue of the movement of the drops causing the echo (i.e. that drops do not grow to echo size in other parts of the column) then it is possible to make the following deductions concerning the up-currents and precipitation fall speeds from the records of Storm II.

(i) The vertical component of the air current between 23,000 and 27,000 ft. was about $13\frac{1}{2}$ m./sec. ($8\frac{1}{2}$ + 5) upwards and had a mean value of about 9 m./sec. from 27,000 to 41,000 ft.

(The echo top rose at $8\frac{1}{2}$ m./sec. from 23,000 to 27,000 ft. and at a mean rate of 5 m./sec. from 23,000 to 41,000 ft. - implying a mean rate of ascent of 4 m./sec. from 27,000 to 41,000 ft).

(ii) The vertical component of the air current decreased to about 5 m./sec. at 41,000 ft. (the final echo top).

(iii) As the tropopause height from the Larkhill ascent at 1500 G.M.T. (Fig. I) was 40,400 ft. it would seem that the cloud top and echo top almost coincided (since there is no evidence to suppose that the cloud tops will penetrate into the stratosphere) and that a rapid reduction in the vertical component of the air current from about 5 m./sec. to zero took place in the top few hundred feet at most of the cloud. (The discrepancy between the 41,000 ft. observed for the radar echo top and the 40,400 ft. for the tropopause height can probably be attributed to normal inaccuracies in the absolute determination of height by radar).

(iv) The rate of fall of the precipitation from about 10,000 ft. to the ground was $9\frac{1}{2}$ m./sec. (echo base descended at $9\frac{1}{2}$ m./sec). This speed is about the terminal velocity of the largest water drops which can exist without disruption so that the up-currents between the ground and 10,000 ft. were small at this time in this part of the cloud.

Up-currents of about 13 m./sec. or greater have been measured on about 20% of all draft measurements at 25,000 ft. in Ohio and on about 10% at 26,000 ft. in Florida in the American Thunderstorm Project ((5) page 40, Table 7) and have also been inferred in England (6) from aircraft accelerometer records on one occasion at 14,000 ft. out of a total of five detailed integrations of such records.

It is significant that the temperature difference between the assumed ascent curve, i.e., the wet adiabatic through the cloud base (see Fig. I), and the environment curve is greater than elsewhere (10°F or higher) between 19,000 and 35,500 ft. with the maximum difference (14°F) between 25,000 and 31,000 ft, while the temperature difference from 10,000 ft. downwards is almost constant at the much smaller value of 5°F. The greatest energy to maintain and increase the vertical current speed is therefore available between 19,000 and 35,500 ft, between which levels the radar evidence suggests that the vertical current reached its maximum value.

7. Other points of interest

(a) Time from first appearance of radar echo to time of maximum altitude of echo top.

This can be measured with reasonable accuracy for Storms I, II and V by using the height-range tube photographs.

For Storm I the time is 30 min., for Storm II 23 min. and for Storm V 22 - 23 min. In addition the P.P.I. photographs indicate that the whole radar echo life of Storm IV was less than 43 minutes.

The significance of these times in relation to the whole life of the cloud is in doubt, since it is not known how long the cloud had been in existence before the first radar echo appeared. In the case of Storm II, for example, it is certain that some part of the cloud, although probably not the part which became the most active, had already reached to about 30,000 ft. before a radar echo was received.

All that is known is that some 20 - 30 minutes after the first appearance of precipitation (not necessarily reaching to the ground) within the clouds, the clouds had reached their maximum vertical development.

(b) Time when thunder was first heard

Development of Storm II took place very close to Northolt aerodrome, the eastern edge of the radar echo was over Northolt until 1515 G.M.T. and then moved away to the W.N.W. about 2 miles by 1541 G.M.T. (Fig. III).

Observations at Northolt reported 6/8 Cu, Sc base 3,500 ft. at 1500 G.M.T. and 6/8 cumulonimbus at 1505 G.M.T. Thunder was heard at the station at 1535 G.M.T., 13 mins after the radar echo top had attained its maximum altitude of 41,000 ft. Thunder was still reported here and at London Airport, 6½ miles from the nearest part of the echo, at 1600 G.M.T. when the echo was well into the decaying stage (H.28). No "Sferics" were reported from this area at any time.

Observations collected, and kindly made available, by the Thunderstorm Census Organisation, however, show that thunder was first heard in the area of Storm II at 1510 G.M.T. at Slough, about 1½ miles south of the nearest edge of the radar echo at this time (Fig. III) and at 1515 G.M.T. at Pinner, about 2½ miles N.E. of the nearest edge of the radar echo. Thunder and lightning were also recorded ½ mile S.E. of Gerrards Cross at 1517 G.M.T. and therefore from a point within the radar echo at this time. Photographs H.21 and H.16 show the stage of development the radar echoes had attained at the time when thunder was first heard at Slough and Gerrards Cross respectively and it is clear that the radar echo had not yet attained its maximum vertical development when lightning first occurred.

It has been suggested elsewhere(4) that the occurrence of lightning is associated with the introduction of large supercooled waterdrops into a volume containing large numbers of ice crystals, and it is significant that in both H.16 and H.21 the radar echo top had already ascended through (within the preceding minute in the case of H.21) the 30,000 ft. level, at which height the Larkhill radiosonde (Fig. I) indicated the temperature to have been -40°F. At this temperature large numbers of ice crystals may be expected to have been formed.(3)

American evidence ((7) page 89), (8) has suggested that maximum cell height and maximum lightning frequency occurred together and it may be noted that, without evidence of maximum lightning frequency for Storm II, the evidence here presented is not incompatible with this idea, in that lightning was first observed some 12 minutes before maximum echo top height was attained (at 1522 G.M.T., H.23) and was still being reported 13 and 38 minutes afterwards.

(c) Characteristics of successive echo columns in a storm

In each of the storms (Storms I, II and V), for which a series of vertical cross-sections is available, the first column of echo when first detected had a much higher top than the succeeding columns on first appearance. On or more of these succeeding columns eventually outstripped the original column in size and height. Thus growth to raindrop size in the second and following cloud columns probably occurred before the cloud top in these columns had reached as great a height as the original cloud column and, since these columns finally outstripped the original column, it is probable that their vertical currents were greater. This latter suggestion is borne out by the fact that in Storm I (Table I) the rate of growth of the radar echo associated with the second and subsequent columns was greater than that of the original column.

The initial cloud column therefore "smoothed the way" for succeeding columns making it easier for them to grow and produce precipitation.

The fact that the second and subsequent columns usually rose to a greater height than the first has been reported by the Thunderstorm Project ((5) page 94) and the explanation there given is based on the concept of entraining of environment air. The air entrained in the first column is relatively dry air from the environment and a greater amount of evaporation of water drops is required to maintain saturation in the mixed air than is required when the environment air, as in subsequent columns, already includes a proportion of saturated air from the original cloud column. Greater energy is therefore available to accelerate the air in the second column than in the first.

The fact that the column top of the second and following columns on first appearance is lower than the original column top on its first appearance suggests that raindrop formation first takes place more rapidly and at a lower height when the vertical current is stronger.

8. Summary

A study of the radar life history of five isolated thunderstorms on 5th June, 1950, leads to the conclusion that the localities most favoured for thunderstorm development are those over which the air in the lowest layers arrives, about the time of maximum surface temperature, after a considerable period close to a supply of moist air. The existence of a river valley lying parallel to the direction of the wind in the lowest layers is particularly favourable by supplying the moisture while still allowing the air to be heated over the neighbouring land.

If the winds are light there appears to be a tendency for the storms to keep close to the river and follow its minor variations in course, while there is a possibility that high ground exercises a damping effect on the spread or movement of storms across it.

The relation between the rate of rise of echo top and the vertical currents within the cloud is discussed and suggests that, in the developing stage, the vertical currents may exceed 40 ft./sec.

The time from first appearance of precipitation within the thunderstorm cell (not necessarily reaching the ground) to the time of maximum vertical development of the cell is of the order of 20 - 30 mins. and thunder is first heard before the storm has reached its maximum vertical development.

/ 9.

9. References

1. Byers and Braham: Thunderstorm structure and circulation. J.Met., Milton, Mass., Vol. 5, No. 3, June, 1948.

2. Jones, R.F.: The horizontal dimensions of cumulonimbus clouds at various heights. M.R.P. No. 535, Air Ministry, Meteorological Research Committee, London, 1950.

3. Cwilong, B.M.: Proc. Roy. Soc., London, A, 190, p.137.

4. Jones, R.F.: The temperatures at the tops of radar echoes associated with various cloud systems. Quart. J.R. Met. Soc., London, 76, p.312, July, 1950.

5. Byers and Braham: The Thunderstorm. Report of the Thunderstorm Project. Washington, D.C., June, 1949.

6. Jones, R.F.: The relation between the radar echoes from cumulus and cumulonimbus clouds and the turbulence within those clouds. Part II. M.R.P.593, 1950.

7. Workman, E.J. and Reynolds, S.E.: Electrical Activity as related to thunderstorm cell growth, Bul. Am. Met. Soc., Vol. 30, p.142, April, 1949

G.278688/JMB/1/51/40

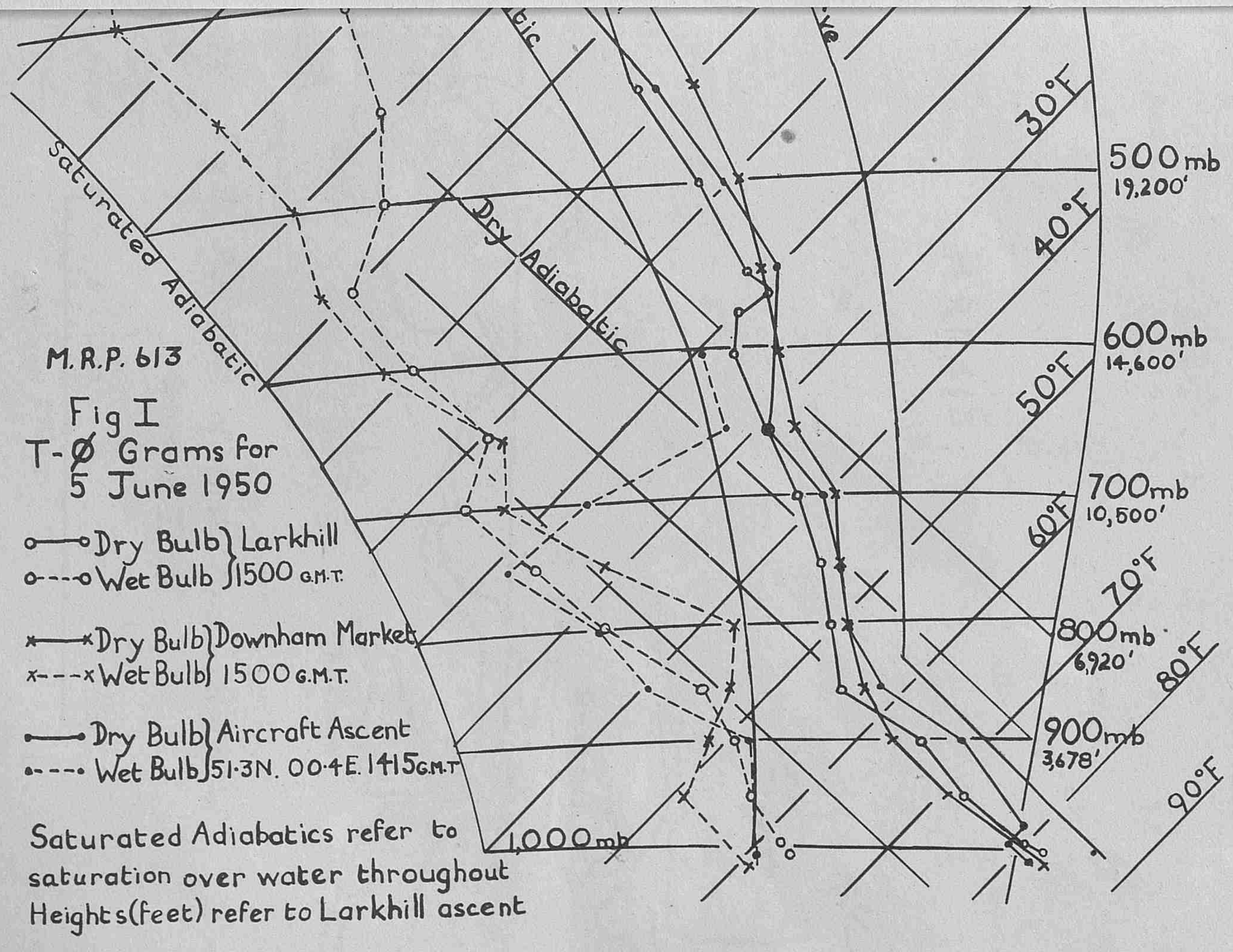

M.R.P. 613

Fig I
T-Ø Grams for
5 June 1950

Saturated Adiabatics refer to
saturation over water throughout
Heights (feet) refer to Larkhill ascent

M.R.P. 613

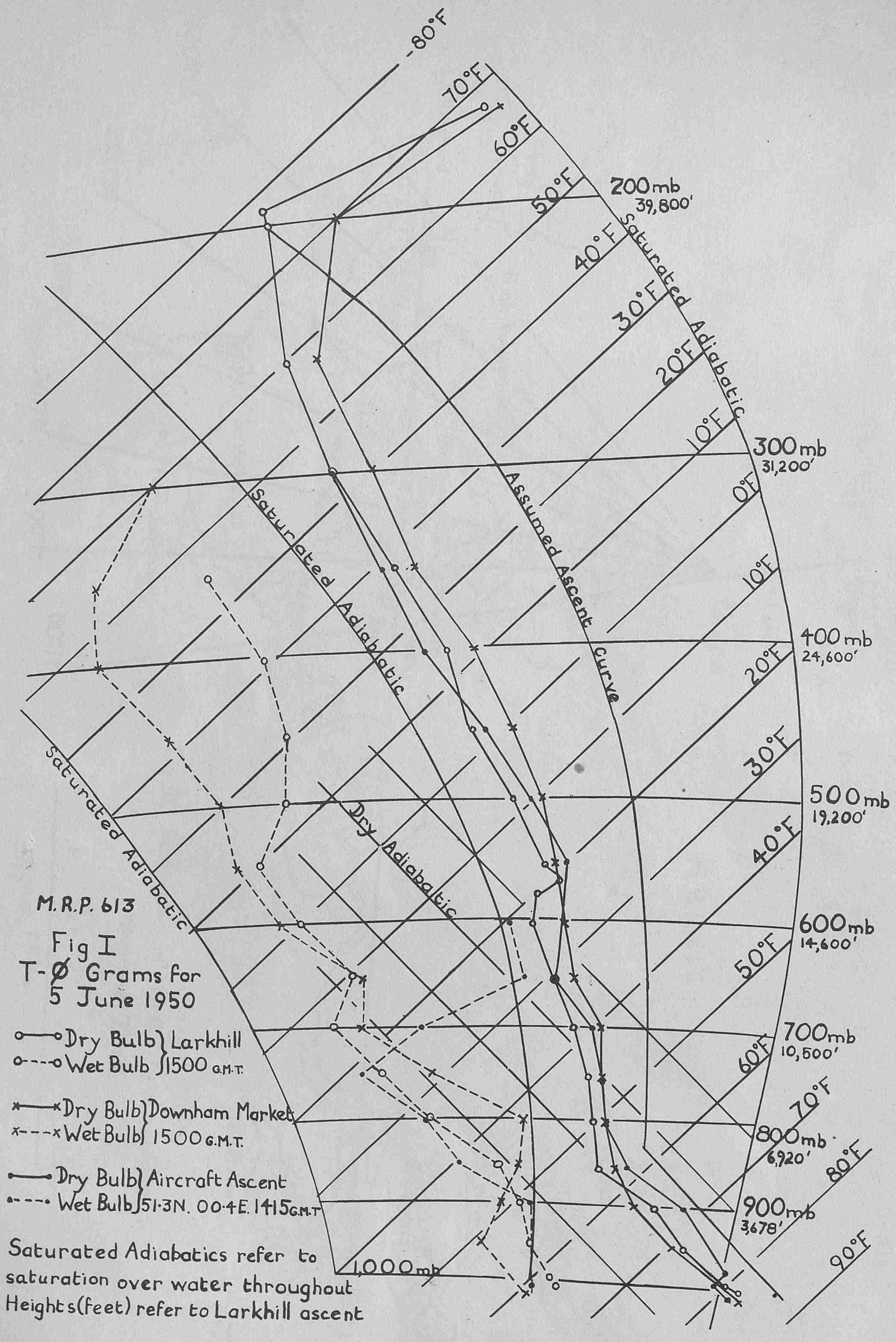

Fig I
T-φ Grams for
5 June 1950

Saturated Adiabatics refer to saturation over water throughout
Heights (feet) refer to Larkhill ascent

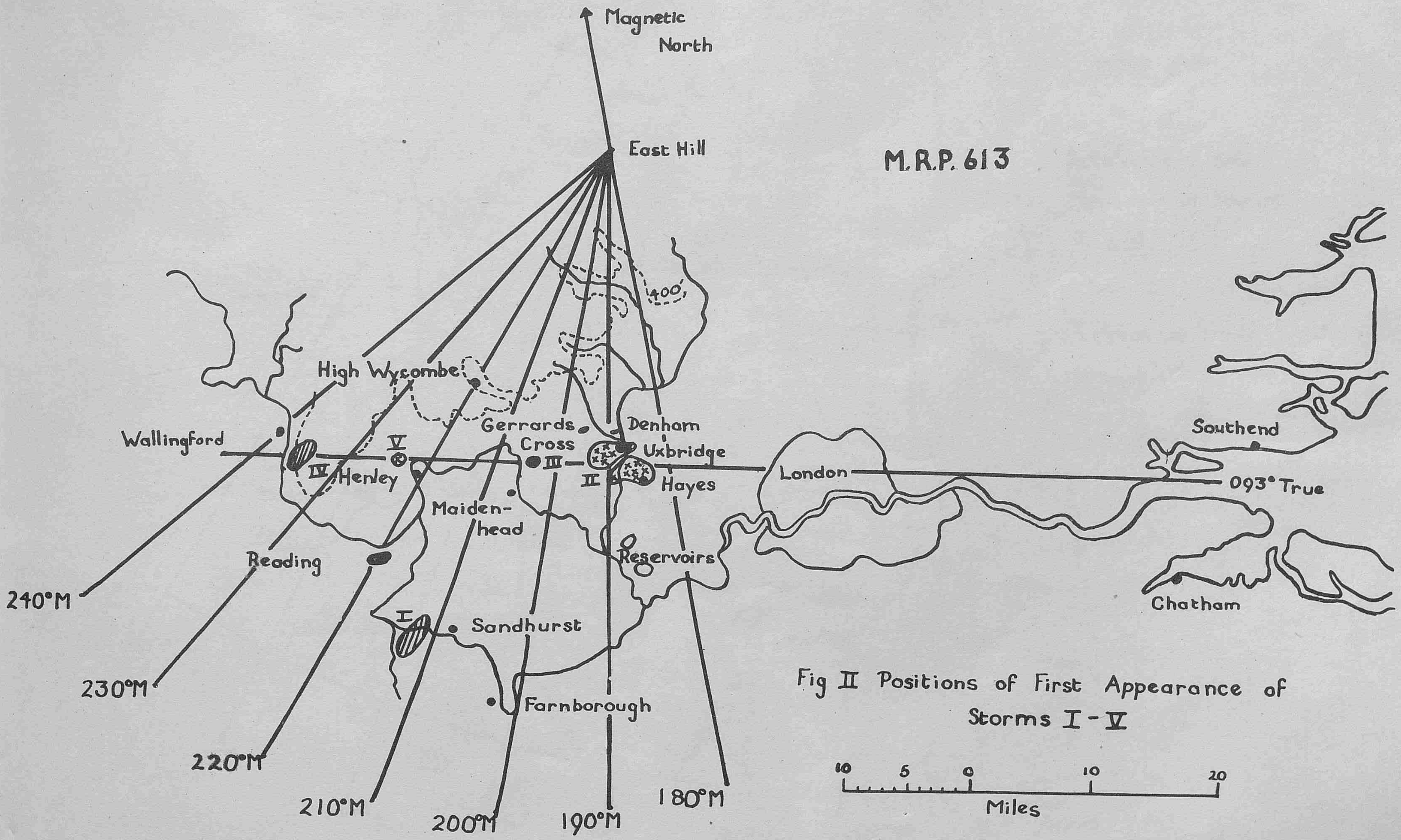
Magnetic North
East Hill
400'
High Wycombe
Wallingford
V
IV
Henley
Gerrards Cross
III
II
Denham
Uxbridge
Hayes
Maiden-head
Reading
Reservoirs
London
093° True
Southend
Chatham
I
Sandhurst
Farnborough
240°M
230°M
220°M
210°M
200°M
190°M
180°M
10
5
0
10
20
Miles

Fig II Positions of First Appearance of Storms I - V

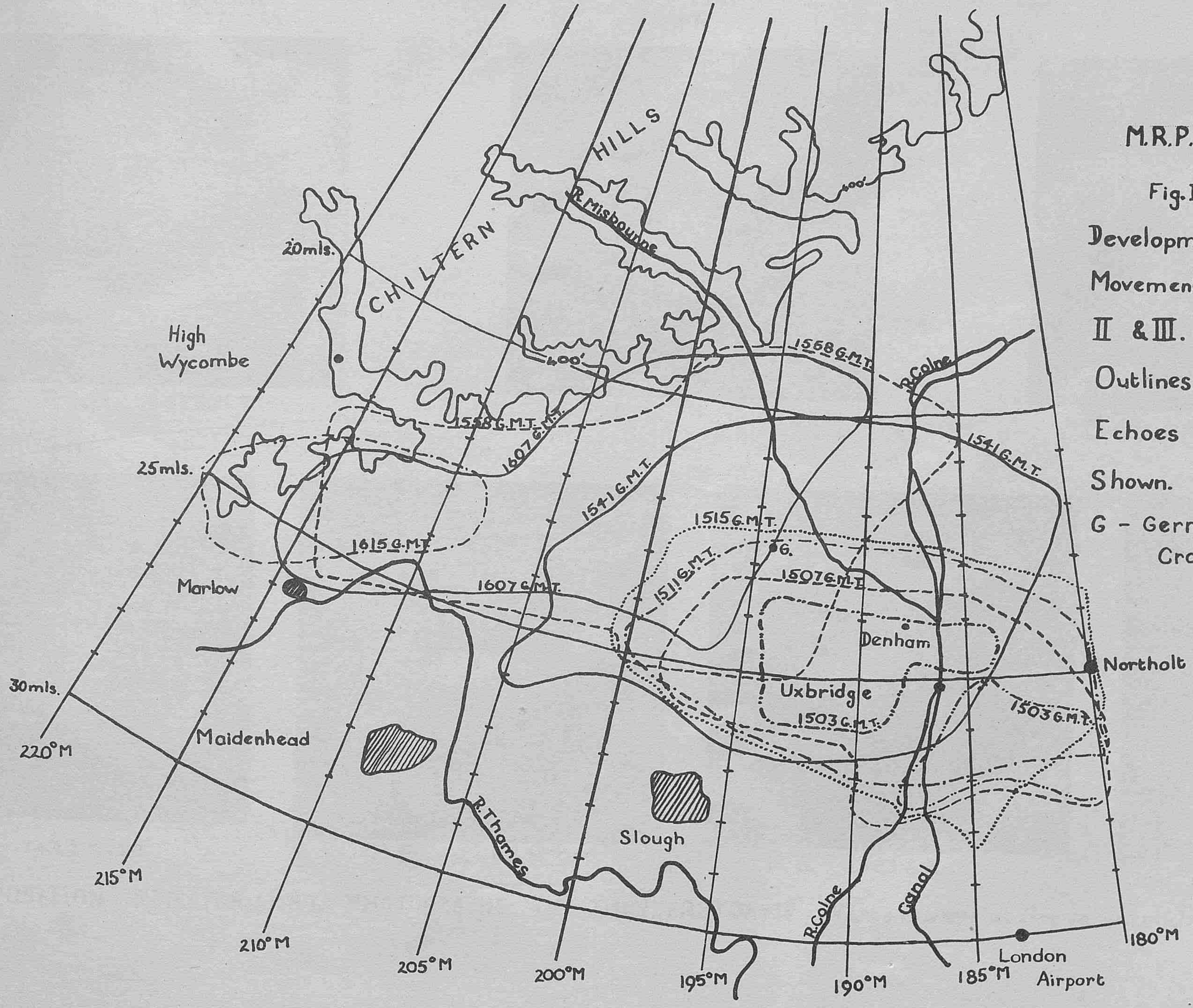
CHILTERN HILLS
R. Misbourne
400'
400'
20mls.
25mls.
30mls.
High Wycombe
Marlow
Maidenhead
Slough
R. Thames
R. Colne
R. Colne
Canal
Denham
Uxbridge
Northolt
London Airport
G.
1568 G.M.T.
1558 G.M.T.
1607 G.M.T.
1607 G.M.T.
1615 G.M.T.
1541 G.M.T.
1541 G.M.T.
1515 G.M.T.
1511 G.M.T.
1507 G.M.T.
1503 G.M.T.
1503 G.M.T.
220°M
215°M
210°M
205°M
200°M
195°M
190°M
185°M
180°M

M.R.P. 613

Fig. III

Development and Movement of Storms II & III.

Outlines of P.P.I. Echoes at Times Shown.

G - Gerrards Cross

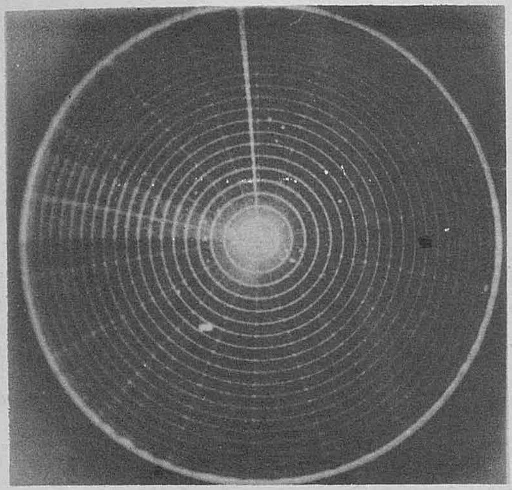
↑ Magnetic North
Thunderstorm I
→
22-214° Mag
40-45 miles

P. 1. 1403 G.M.T.

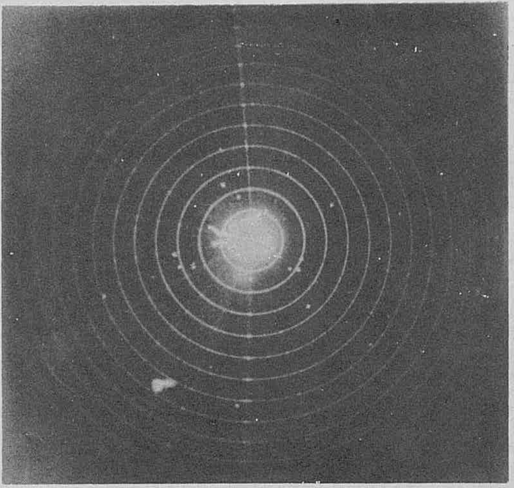

P. 2. 1408 G.M.T.

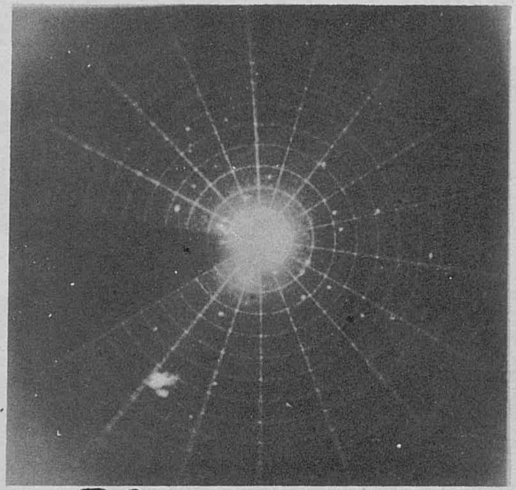

P. 3. 1422 G.M.T.

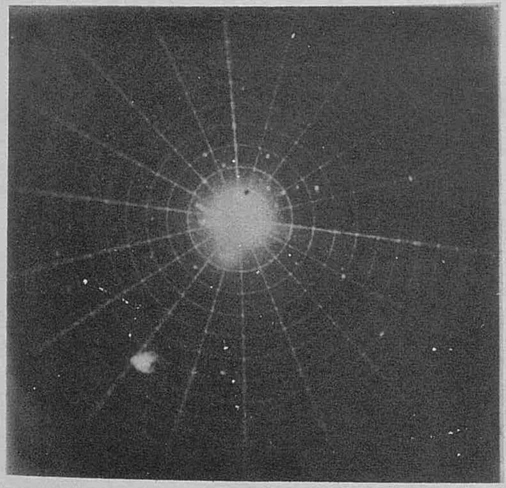

P. 4. 1429 G.M.T.

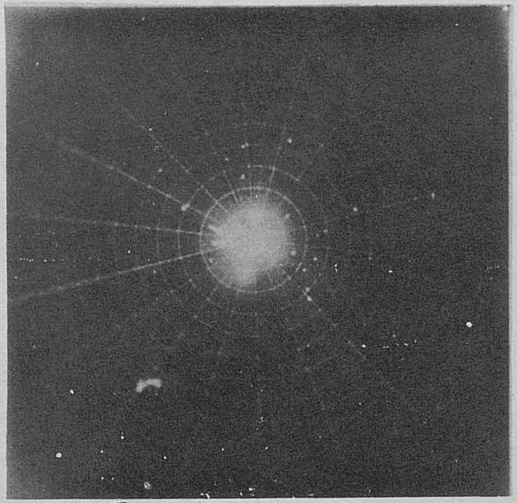

P. 5. 1441 G.M.T.

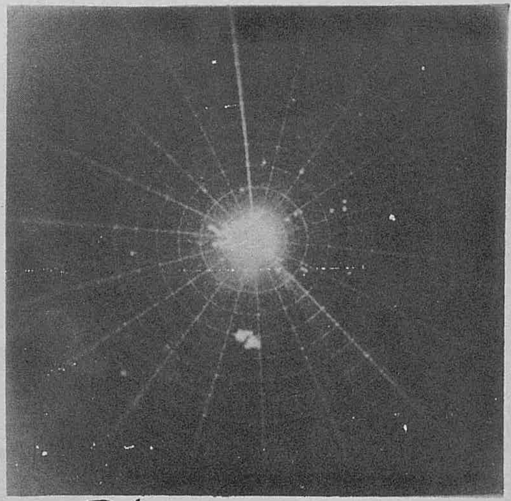

P. 6. 1503 G.M.T.

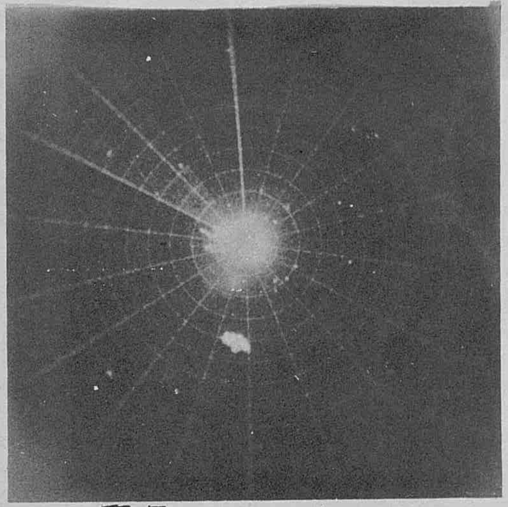

P. 7. 1507 G.M.T.

PLAN POSITION INDICATOR (P.P.I.) PHOTOGRAPHS OF THUNDERSTORMS (Range markers at 5-mile intervals)

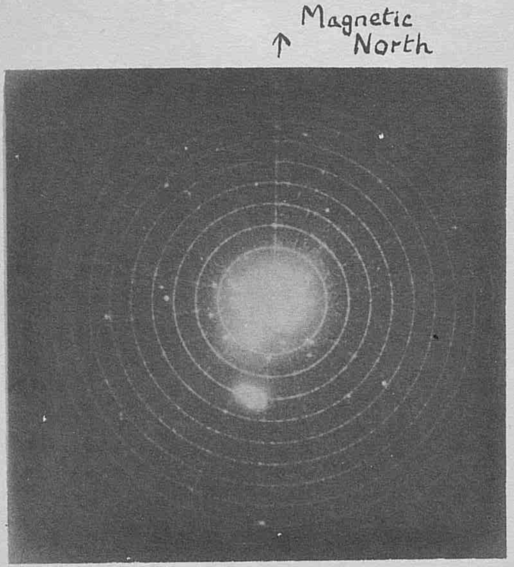
↑ Magnetic North

P. 8. 1511 G.M.T.

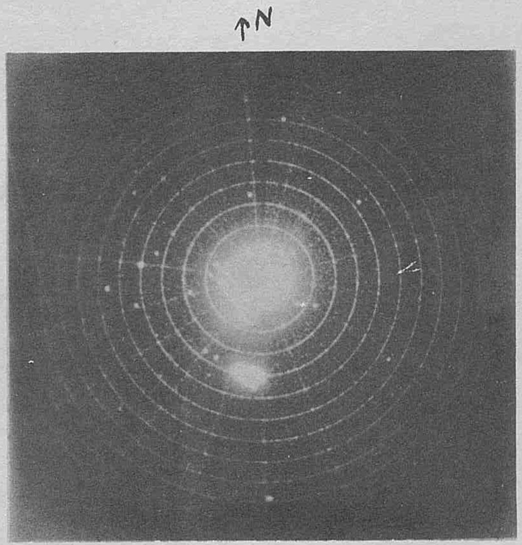

P. 9. 1515 G.M.T.

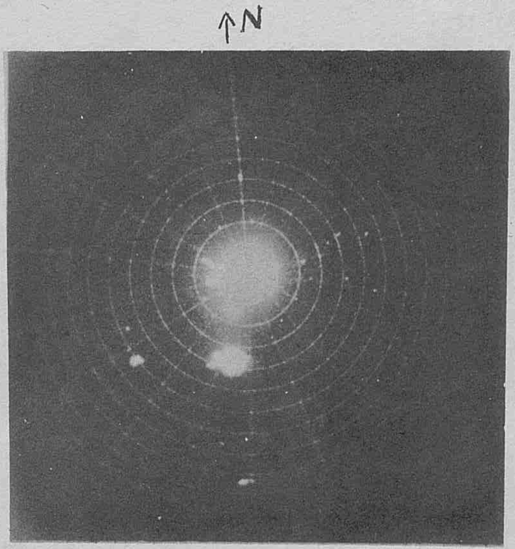

P.10. 1541 G.M.T.

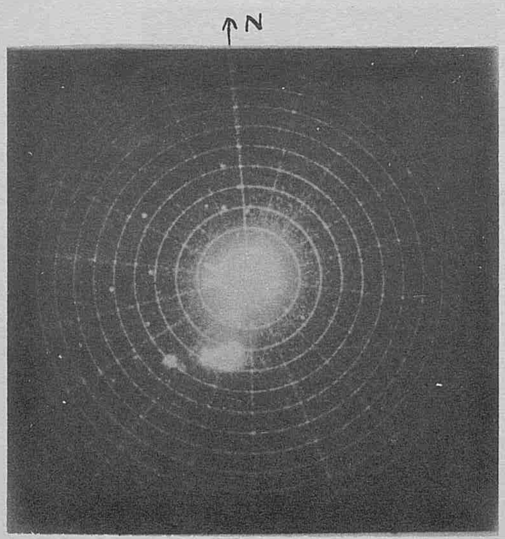

P. 11. 1558 G.M.T.

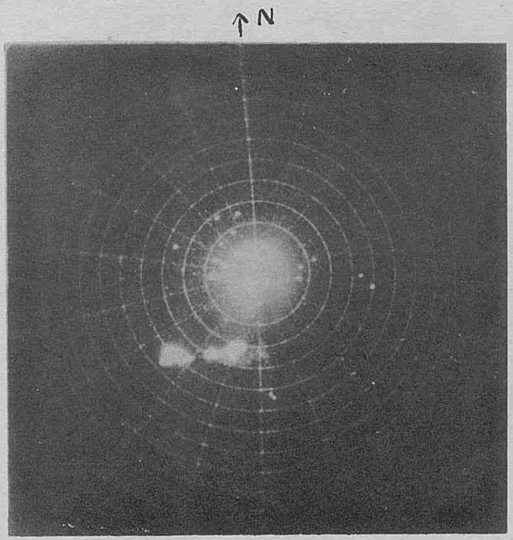

P. 12. 1607 G.M.T.

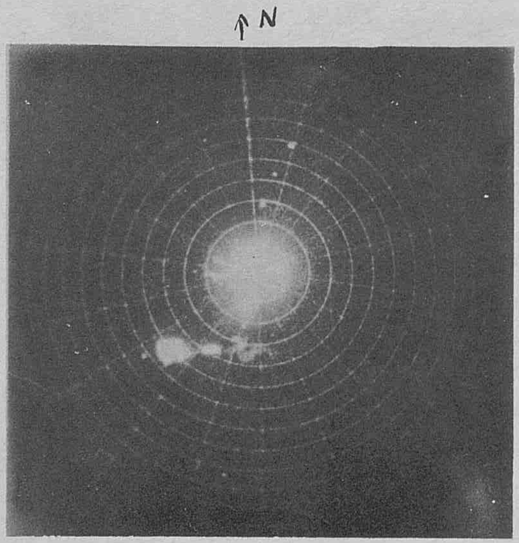

P. 13. 1615 G.M.T.

PLAN POSITION INDICATOR (P.P.I.) PHOTOGRAPHS OF THUNDERSTORMS (Range markers at 5-mile intervals)

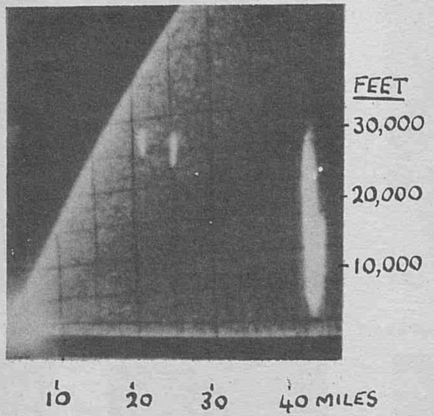
FEET
30,000
20,000
10,000
10
20
30
40 MILES

H. 1.

1359 G.M.T. 213½° Mag.

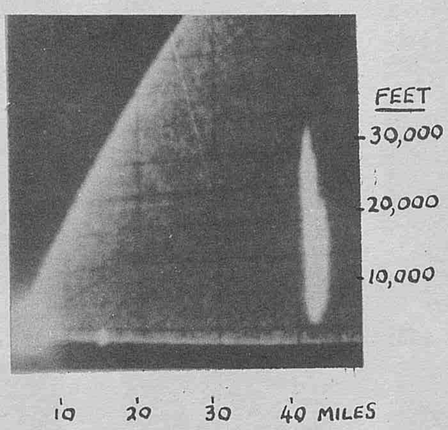
FEET
30,000
20,000
10,000
10
20
30
40 MILES

H. 2.

1402½ G.M.T. 213° Mag.

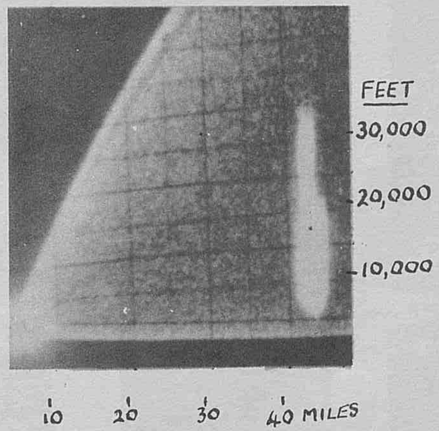
FEET
30,000
20,000
10,000
10
20
30
40 MILES

H. 3.

1412 G.M.T. 216° Mag.

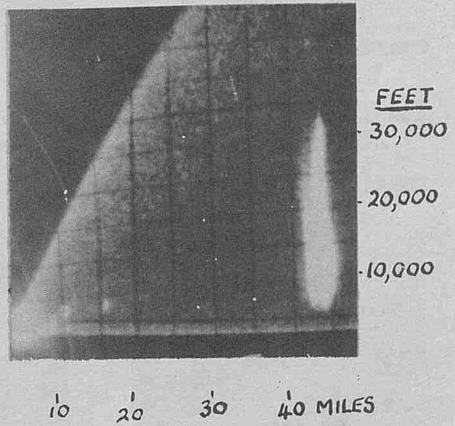
FEET
30,000
20,000
10,000
10
20
30
40 MILES

H. 4.

1421 G.M.T. 218½° Mag.

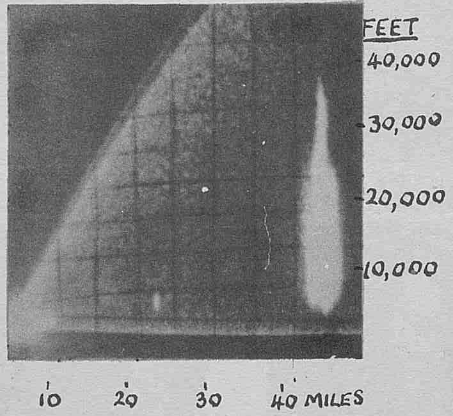
FEET
40,000
30,000
20,000
10,000
10
20
30
40 MILES

H. 5.

1425 G.M.T. 218° Mag.

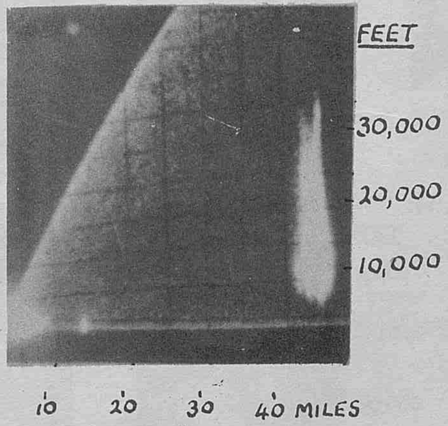
FEET
30,000
20,000
10,000
10
20
30
40 MILES

H. 6.

1433 G.M.T. 217½° Mag.

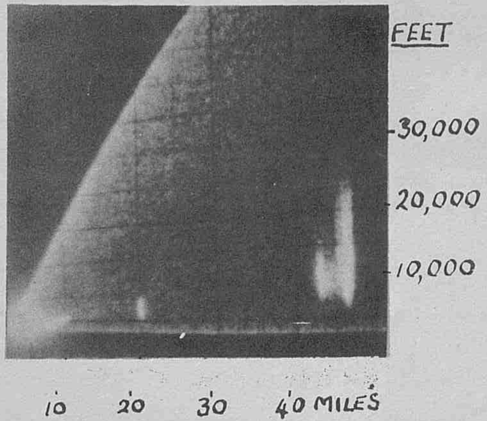
FEET
30,000
20,000
10,000
10
20
30
40 MILES

H. 7.

1446 G.M.T. 221° Mag.

HEIGHT-RANGE TUBE (H.R.T.) PHOTOGRAPHS OF THUNDERSTORMS – STORM I

(Time and bearing indicated beneath each photograph)

M.R.P. 613.

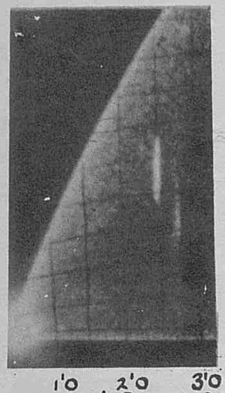

1459.08 H.8. 186½°

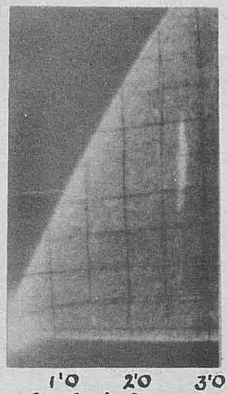

1459.45 H.9. 182°

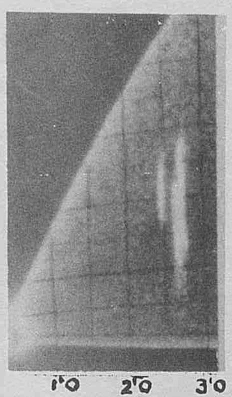

1500.50 H.10. 186°

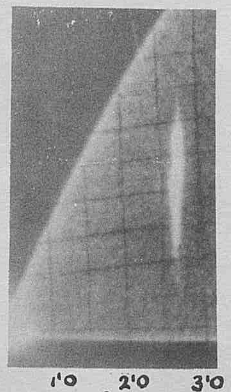

1501.20 H.11. 182½°

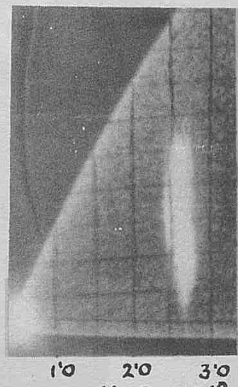

1504.00 H.12. 186°

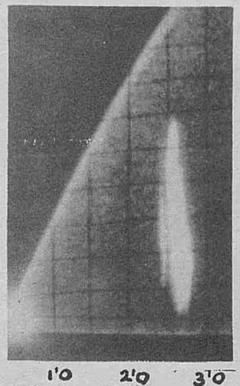

1505.27 H.13. 187°

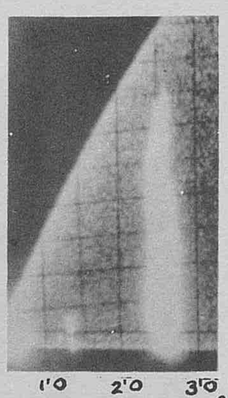

1512.25 H.14. 188½°

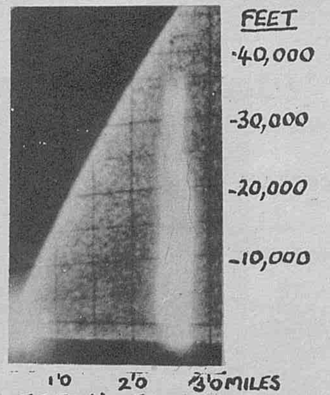
FEET
40,000
-30,000
-20,000
-10,000
1'0
2'0
3'0 MILES

1513.50 H.15. 188½°

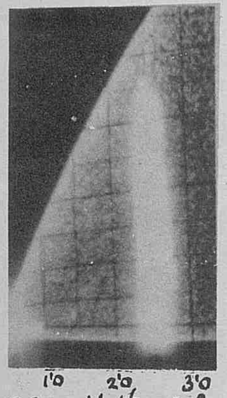

1518.20 H.16. 189°

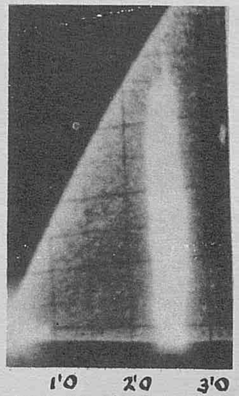

1519.25 H.17. 189°

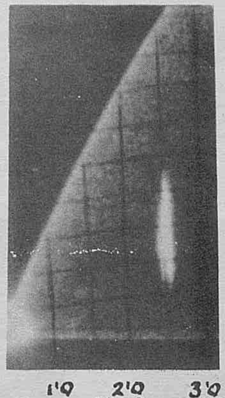

1502.20 H.18. 194½°

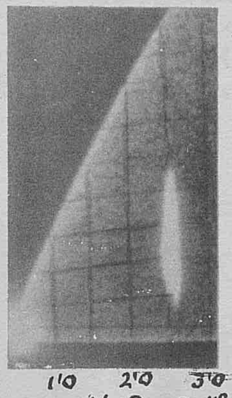

1503.45 H.19. 194½°

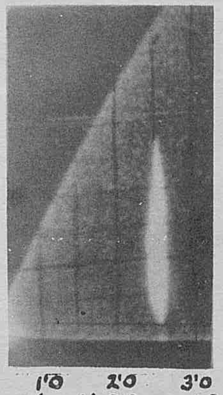

1506.10 H.20. 194½°

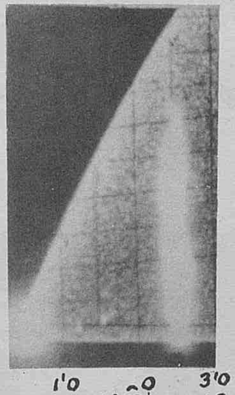

1511.35 H.21. 194½°

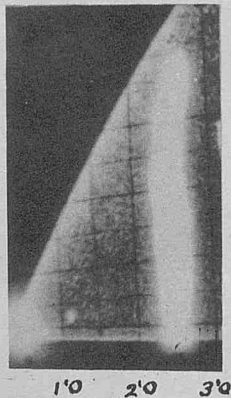

1520.50 H.22. 193°

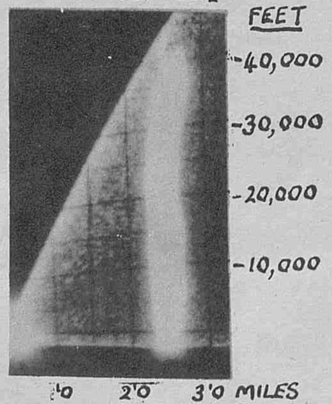
FEET
-40,000
-30,000
-20,000
-10,000
1'0
2'0
3'0 MILES

1521.50 H.23. 194½°

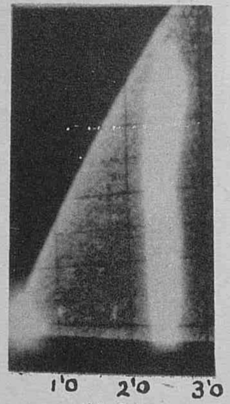

1524.50 H.24. 195°

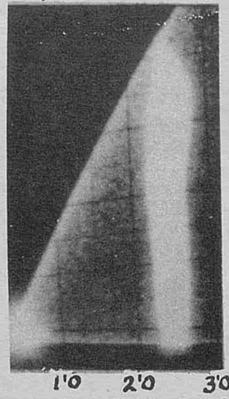

1526.15 H.25. 194½°

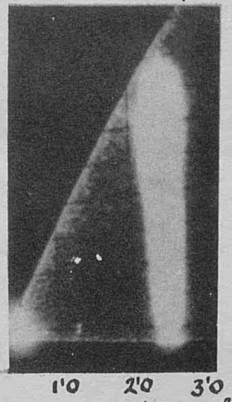

1534.20 H.26. 194½°

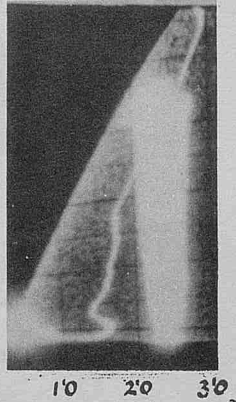

1539.25 H.27. 194½°

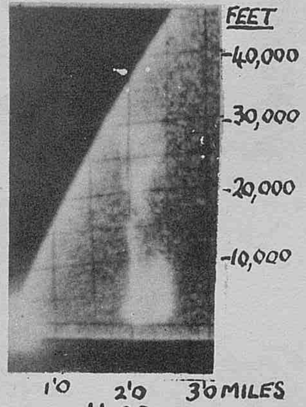
FEET
-40,000
-30,000
-20,000
-10,000
1'0
2'0
3'0 MILES

1606.20 H.28. 198°

HEIGHT-RANGE TUBE (H.R.T.) PHOTOGRAPHS OF THUNDERSTORMS — STORM II

(Time (G.M.T.) to nearest second and bearing (degrees Magnetic) indicated beneath each photograph).

Bright irregular line on H. 27. is due to fault on equipment.

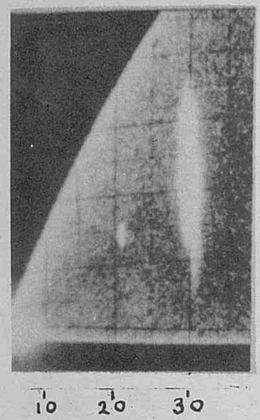

H.29.

1600.15 225°

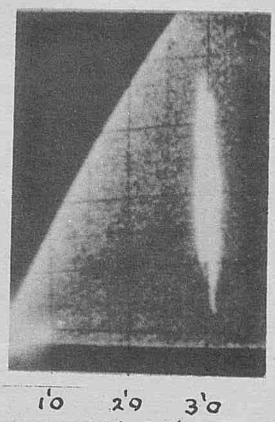

H.30

1601.50 225°

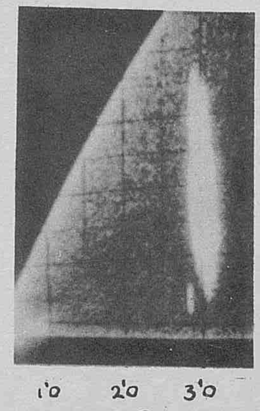

H.31.

1602.45 227°

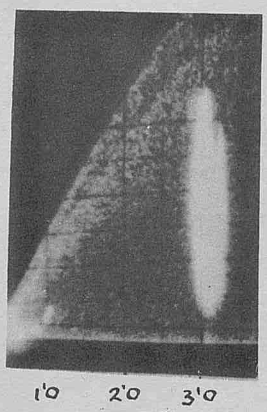

H.32.

1604.30 230°

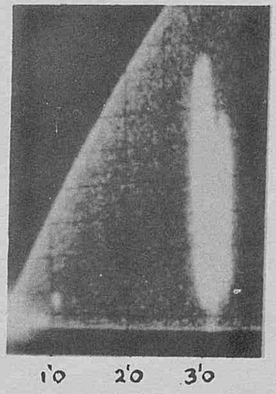

H.33.

1606.55 230°

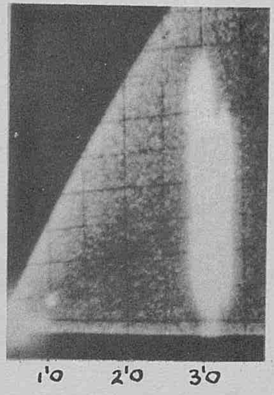

H.34.

1608.00 230°

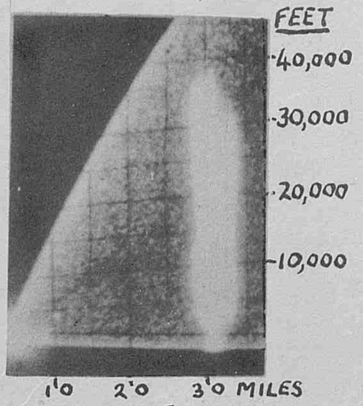

H.35.

1609.30 230°

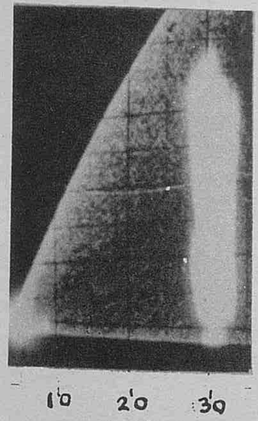

H.36.

1610.55 230°

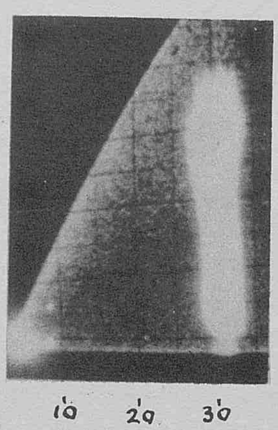

H.37.

1613.50 230°

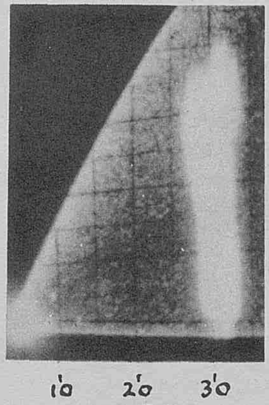

H.38.

1615.50 230°

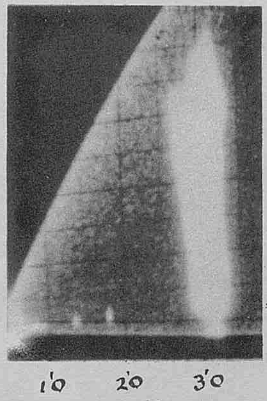

H.39.

1617.35 232°

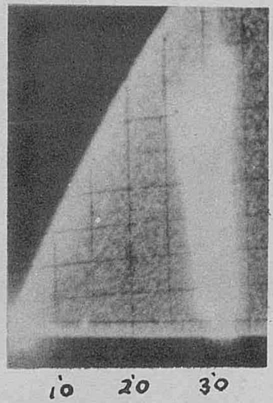

H.40.

1621.30 234½°

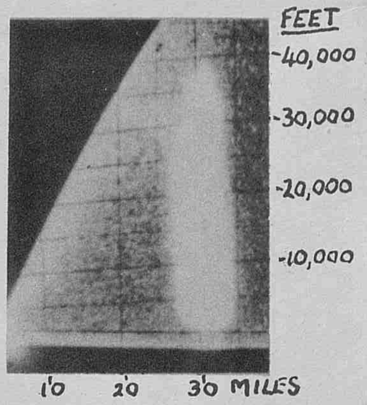

H.41.

1631.15 235½°

HEIGHT-RANGE TUBE (H.R.T.) PHOTOGRAPHS OF THUNDERSTORMS - STORM V. (Time (G.M.T.) to nearest second and bearing (degs. Mag.) indicated beneath each photograph).

paper of the Meteorological Research
Committee (London).
M.R.P. No............ by Mr...............................
A copy is available in the Library of
the Meteorological Office."

M.R.P. 622
S.C.II/73
13th March, 1951.

AIR MINISTRY

METEOROLOGICAL RESEARCH COMMITTEE

Second Report arising from Charney and Eliassen's method of computing forecast 500 mb. contour charts

by

F.H. Bushby (Meteorological Office)

AIR WEATHER SERVICE
TECHNICAL REFERENCE FILE
JUL 6 1951

1. Introduction

In M.R.P. 566 an account was given of a test made of the Charney and Eliassen (1) one-dimensional method of computing a forecast 500 mb. contour profile along a parallel of latitude. The method consists basically of assuming that the flow in a barotropic atmosphere would be equivalent to the flow in the actual baroclinic atmosphere at the 500 mb. level and that this flow can be considered as consisting of small perturbations superimposed upon a zonal west-east current constant with respect to time and longitude. There are some theoretical refinements to the basic assumption, but these have little practical significance. As such, the method ignores "development" in the sense used by Sutcliffe (2) and may therefore seem fundamentally inadequate even as a first step, but Charney's analysis purports to show that in spite of baroclinic development there is one level in the atmosphere at which there is "equivalent barotropic flow".

A test was made of the method in latitudes 45° North and 60° North, and the agreement between prediction and actuality seemed promising - better than could be expected if the method was fundamentally unsound. That was the conclusion of the first test and justified further work which is reported here.

2. The second test

Basic coefficients were calculated, so that Charney and Eliassen's formula could be used in latitudes 40°, 50°, and 60° North. These coefficients are given in the appendix. They permitted the computation of forecast contour profiles for 24 hours ahead and such profiles were computed for 34 days in June and July, 1950 from longitude 80° W to 20° E. Forecast charts were prepared by combining the profiles for latitudes 40°, 50° and 60° North. In estimating the zonal current, a 20° latitude band was used. In M.R.P. 566 it was stated that in certain synoptic situations the computed forecast value for the contour height would necessarily be unreliable, because some of the basic assumptions were unfulfilled. In drawing the forecast charts in the present experiment, the computed value was treated with circumspection if it occurred in a region dominated by one of those synoptic situations.

In order to test the success and value of the Charney and Eliassen method of forecasting the 500 mb. zonal profile, four different methods were adopted. These were as follows:-

(1) The forecast change of 500 mb. height was correlated with the actual change of the 500 mb. height and regression coefficients were calculated for the best fitting straight line giving the actual change (Y feet) in terms of the forecast change (X feet) in the form

$$Y = aX + b \quad \ldots\ldots\ldots\ldots (1)$$

/ (2)

JUL 2 1951

(2) The average error (without regard to sign) and the root mean square error in the forecast 500 mb. heights were calculated.

(3) The forecast movements of the trough and ridge lines at 50° North were correlated with the actual movement and regression coefficients were calculated for the best fitting straight line giving the actual movement (N degrees of longitude) in terms of the forecast movement (M degrees of longitude) in the form

$$N = cM + d \qquad (2)$$

(4) The average error and the root mean square error in the forecast movement of trough and ridge lines at 50° North were calculated.

In order to provide a basis for the comparison of the success of Charney's forecasting method with that of other methods, the comparisons (1) (2) (3) and (4) were made in respect of some or all of the following methods of forecasting.

Forecast A	Computation, using Charney's formula.
Forecast B	From forecast charts, primarily based on the computed values obtained by forecast A.
Forecast C	Movement forward of actual 500 mb. heights at the speed of the zonal current (constant with respect to longitude from 120° West to 40° East).
Forecast D	From forecast charts prepared by conventional methods in the Forecast Research Division at Dunstable.
Forecast E	Assuming no change.

The results of this statistical analysis are set out in Tables I - IV in which the various forecasts are identified by the letters given above.

Table I

Correlation of forecast change of 500 mb. height with actual change

r = correlation coefficient

a and b (in feet) = regression coefficients of equation (1)

Forecast compared with actuality	40° North			50° North			60° North		
	r	a	b	r	a	b	r	a	b
Forecast A	.35	.46	28	.54	.72	33	.24	.38	15
Forecast B	.28	.36	22	.52	.73	4	.19	.30	7
Forecast C	.34	.28	12	.55	.48	10	.27	.28	4
Forecast D				.70	.89	-16			

/ Table II

Table II

Average errors and root mean square errors (in feet) of the forecast 500 mb. height

	40° North		50° North		60° North	
	Average	Root Mean Square	Average	Root Mean Square	Average	Root Mean Square
Errors of forecast A	110	140	150	200	160	210
Errors of forecast B	110	140	150	200	150	200
Errors of forecast C	130	190	210	270	210	270
Errors of forecast D			130	170		
Errors of forecast E	120	150	190	250	160	230

TABLE III

Correlation of forecast movement of trough and ridge lines at 50° North with their actual movement.

r = correlation coefficient

c and d (in degrees of longitude) = regression coefficients of equation (2)

Forecast compared with actuality	r	c	d
Forecast A	.49	.54	2.9
Forecast B	.64	.79	1.3
Forecast C	.18	.61	0
Forecast D	.60	.69	2.3

Table IV

Average errors and root mean square errors (in degrees of longitude) of the forecast movement of troughs and ridges at 50° North.

	Average	Root mean square
Errors of forecast A	3.4	4.1
Errors of forecast B	2.5	3.2
Errors of forecast C	5.0	5.9
Errors of forecast D	3.1	3.6
Errors of forecast E	7.8	8.8

/ 3.

3. Interpretation of Results

Charney's formula gives a better result in latitude 50° North than in latitudes 40° and 60° North. This is mainly due to the zonal current in the latitude band about 50° North being stronger than in the latitude bands about 40° and 60° North. As Charney's formula is based on small perturbations on the zonal current, one would expect it to give better results when the zonal current is strong than when it is weak, for when the zonal current is strong the motion in the N - S direction will, in general, be relatively small.

Tables II and IV clearly show that forecasts A and B were better than assuming no change had occurred, but were generally not as good as the conventional methods of forecasting. However, forecast B predicts the movement of the trough and ridge lines more successfully than forecasts A and D. This is the only case in which forecast A or forecast B is not less successful than forecast D, and in which forecast B improved upon forecast A.

The change in the 500 mb. height forecast by Charney's method consists of two essentially independent parts; the first representing a displacement of the existing profile eastward with the zonal current and the second representing the contribution of various terms in which the variation of the Coriolis parameter with latitude plays an important part. The question arises as to whether the second set of terms do contribute significantly to the success of the method. In order to investigate this, corresponding forecasts were made on the basis of the first term only - viz. on the assumption that the 500 mb. profile moves eastward with the zonal current. If Tables II and IV are examined it will be seen that the Charney method does achieve greater success than a forecast which simply moves the 500 mb. profile eastward with the zonal current. This applies both to the forecast height of the 500 mb. surface and to the position of trough and ridge lines. On the other hand it will be seen from Table I that the correlation coefficients between the forecast and actual height changes are no less for the forecasts based on the zonal current alone than for those based on Charney's method. This implies that an empirical linear formula (the regression equation) involving the heights obtained from the zonal current method will give no greater a mean square error in the forecast 500 mb. height than any similar formula using the Charney forecasts. This fact might have some relevance if it was proposed to adopt either method in practice, but the regression equations themselves have no physical interpretation and it would be incorrect to argue from these correlation coefficients that moving the actual 500 mb. profile eastward with the zonal current gives as good a solution as the Charney formula.

4. Conclusions and proposed further work

These tests corroborate the conclusions reached in the first report. Although the method is based on treating the 500 mb. flow as if it consisted of small perturbations on a uniform zonal current, the method is more successful than simply moving the actual 500 mb. contour pattern at the speed of the zonal current. The method shows significant success, but the standard is rather less than that achieved by conventional methods. It is therefore not proposed to continue with the direct testing of the Charney method at present.

A report will shortly be available on a mathematical extension of the analysis to include some terms omitted by Charney and related with baroclinic development. It appears at present that it can be shown that these terms are just as important as those included by Charney, so that Charney's method is not, in general, a legitimate first approximation.

The object of introducing computational methods into synoptic forecasting must, however, be kept in mind, and a rather different approach is now being explored.

/ 5.

5. References

1. Charney J.G. and Eliassen A. A numerical method for predicting the perturbations of the middle latitude westerlies. Tellus, Vol. 1, No. 2, 1949, p.38.

2. Sutcliffe R.C. A contribution to the problem of development. Q.J.R. Met. Soc. Vol. 73, 1947, p.370.

30	-0.16	0.55	-0.17	0.38	-0.14	0.23
40	-0.03	0.34	-0.06	0.22	-0.06	0.14
50	-0.01	0.20	-0.02	0.13	-0.01	0.07
60	0.00	0.12	0.00	0.07	0.00	0.03
70	0.00	0.08	0.00	0.04	0.00	0.02
80	0.00	0.04	0.00	0.02	0.00	0.00
90	0.00	0.03	0.00	0.01	0.00	0.00
100	0.00	0.01	0.00	0.00	0.00	0.00
110	0.00	0.01	0.00	0.00	0.00	0.00
120	0.00	0.00	0.00	0.00	0.00	0.00
130	0.00	0.00	0.00	0.00	0.00	0.00
140	0.00	0.00	0.00	0.00	0.00	0.00
150	0.00	0.00	0.00	0.00	0.00	0.00
160	0.00	0.00	0.00	0.00	0.00	0.00
170	0.00	0.00	0.00	0.00	0.00	0.00
180	0.00	0.00	0.00	0.00	0.00	0.00

/ Now

APPENDIX

Charney and Eliassen's one dimensional formula can be written

$$z(x+Ut,t) = z(x,0) + \int_{x-x_1}^{x+x_2} z(\alpha,0)\, I_{a^2}(x-\alpha,t)\, d\alpha \qquad (1)$$

$$\text{where} \quad I_{a^2}(x,t) = \frac{1}{2\pi}\sum_{-\infty}^{\infty}\left(\exp\frac{inbt}{n^2+a^2} - 1\right)\exp inx \qquad (2)$$

Values of $I_{18}(x,1)$ for latitudes 40°, 50° and 60° North have been interpolated from values given by Charney in Journal of Meteorology Vol. 6 No. 6 and are tabulated in Table I. Parameter b = 3.8, 5.9 and 8.2 for latitudes 40°, 50° and 60° North respectively.

Table I

x	40° North		50° North		60° North	
	$I_{18}(x,1)$	$I_{18}(-x,1)$	$I_{18}(x,1)$	$I_{18}(-x,1)$	$I_{18}(x,1)$	$I_{18}(-x,1)$
0	-4.82	2.13	-3.77	1.83	-2.61	1.36
10	-1.75	1.39	-1.27	1.08	-0.78	0.73
20	-0.55	0.90	-0.50	0.66	-0.42	0.42
30	-0.16	0.55	-0.17	0.38	-0.14	0.23
40	-0.03	0.34	-0.06	0.22	-0.06	0.14
50	-0.01	0.20	-0.02	0.13	-0.01	0.07
60	0.00	0.12	0.00	0.07	0.00	0.03
70	0.00	0.08	0.00	0.04	0.00	0.02
80	0.00	0.04	0.00	0.02	0.00	0.00
90	0.00	0.03	0.00	0.01	0.00	0.00
100	0.00	0.01	0.00	0.00	0.00	0.00
110	0.00	0.01	0.00	0.00	0.00	0.00
120	0.00	0.00	0.00	0.00	0.00	0.00
130	0.00	0.00	0.00	0.00	0.00	0.00
140	0.00	0.00	0.00	0.00	0.00	0.00
150	0.00	0.00	0.00	0.00	0.00	0.00
160	0.00	0.00	0.00	0.00	0.00	0.00
170	0.00	0.00	0.00	0.00	0.00	0.00
180	0.00	0.00	0.00	0.00	0.00	0.00

Now $\int_{x-x_1}^{x+x_2} z(a,0)\, I_{18}(x-a,1)\, da$ can be evaluated by Simpson's rule, giving $\sum_{-x_2/10}^{x_1/10} A_N\, z(x+10N,0)$. For latitudes 40° and 50° North the limits of integration were $x_2 = 100°$, $x_1 = 40°$, but it was found that A_{-4}, A_8, A_9 and A_{10} were negligible in each case. For latitude 60° North, the limits of integration were $x_2 = 80°$, $x_1 = 40°$, and it was found that A_{-4}, A_6, A_7, and A_8 were negligible. Coefficients A_N are given in Table II.

Table II

N	A_N		
	40° North	50° North	60° North
-3	-.036	-.035	-.031
-2	-.068	-.056	-.047
-1	-.393	-.285	-.175
0	-.151	-.109	-.071
1	.312	.243	.164
2	.101	.074	.047
3	.124	.085	.052
4	.038	.025	.016
5	.045	.029	.016
6	.013	.008	-
7	.009	.009	-

paper of the Meteorological Research
Committee (London),
M.R.P. No.......... by Mr.........................
A copy is available in the Library of
the Meteorological Office."

M.R.P.624
SC.II/74
16th April, 1951.

AIR MINISTRY

METEOROLOGICAL RESEARCH COMMITTEE

AIR WEATHER SERVICE
TECHNICAL REFERENCE FILES

Forecasting the Formation of Radiation Fog - A preliminary approach.

by J.M. Craddock and Dorothy Pritchard (Meteorological Office)

Summary.

This note describes the development of an experimental method of forecasting whether radiation fog will form at a station during a particular night, taking account only of the mean cloud amount and gradient wind speed expected during the night and of the temperature and dewpoint at midday on the day before. The forecast made depends on the predicted values of the night minimum temperature (on the assumption that fog does not form) and fog point on the night in question; these quantities are first estimated by means of regression equations from the midday temperature and dewpoint and then corrected to allow for the expected mean gradient wind speed and cloud amount. The regression equations are chosen to give almost the least possible mean square error when applied to all of 13 or 16 inland stations in England on every night during the year 1949 on which the air mass over the area covered by these stations did not change materially during the 24-hour period from one midday to the next, and the corrections prescribed for wind speed and cloud amount are close to the average values found for the same body of data. The prediction formulae were tested on an independent larger body of similar data obtained from 25 inland stations during 1948, and found to give results similar to those obtained for 1949. In each case the night minimum temperature could be predicted with a mean square error of about $3\frac{1}{2}$°F., and the fog point with a mean square error of about 4°F.

A forecast whether fog would form or not, based on the predicted values of the fog point and the night minimum temperature, was made for each station for each night considered during 1948 and 1949, and was checked against the event. The comparison suggested that if used in practice, the experimental method of forecasting would enable nights of more or less widespread fog to be distinguished in advance in most cases from those on which there was little or no fog. A further test was made, using the same formula for predicting the night minimum temperature and the fog point estimated by a method proposed by Saunders. This appeared to attain about the same level of success as the first method.

Introduction.

The problem of producing an entirely satisfactory method for forecasting the formation of radiation fog, which is receiving attention in the Forecasting Research Division of the Meteorological Office, does not appear capable of easy or quick solution, owing, partly, to our incomplete understanding of the physical processes involved. The background of the problem has been discussed at length in M.R.P.557, where the view is expressed that the approach having most immediate promise is one which uses physical arguments to suggest parameters sufficient to control the general course of events, and capable of observation or estimation in advance, and then relates these parameters statistically to quantities whose value we wish to forecast. The present work was directed, not to solving the problem as a whole, but to finding a method, simple and easy to use, and of wide applicability, to serve as a standard from which future progress can be measured. It makes use only of four parameters, a representative temperature and dewpoint during the preceding day, and the mean cloud amount and gradient wind speed during the night. The standard of accuracy and reliability attained are high enough to make the method worth consideration by any forecaster who is dissatisfied with his present technique.

The method, which can be used on any night during which no considerable change of air mass is expected, is a very familiar one, and consists in estimating during the preceding afternoon the night minimum temperature to be expected if there is no fog and the fog point (i.e. the temperature at which fog is expected to form), and forecasting fog if the point is higher than or equal to the night minimum temperature and no fog when the fog point is the lower. The novelty in the present work lies in the prediction formulae used, which are based on data collected from a variety of stations, and the extensive test of reliability carried out on independent data. Since data from several stations are lumped together, the prediction formulae depend on the atmospheric processes which act alike at all the stations (i.e. on those connections between parameters and quantities predicted which are the same at all stations) and ignores those which operate differently at different stations. Hence the measure of success attained by the present method throws some light on the importance of universal atmospheric processes as against purely local effects in leading to the formation of fog.

The description of the method falls into three parts, dealing with the development and testing (1) of the formula for the night minimum temperature, (2) the formula for the fog point and (3) with the forecasts to be made on the basis of these.

1. Notation.

If T is an observed quantity which we wish to forecast, then T' is the estimated values obtained by some specified forecasting method, T" a revised estimate found by applying a correction to T' and so on. The residuals T-T', T-T" etc. are denoted by Δ_1 , Δ_2 etc. The difference between an estimated fog point and an estimated night minimum temperature is denoted by E. All temperatures are in degrees Fahrenheit. The initials F.R.D. are used to indicate formulae developed in this investigation in the Forecasting Research Division.

2. Estimation of the night minimum temperature.

It is a matter of common experience that when there is no change in air mass the night minimum temperature is affected and largely determined by the four parameters mentioned in the introduction. For the present purpose a method of forecasting the night minimum temperature must be of wide application and reasonably sensitive to variations in these parameters, and a careful search of the literature failed to reveal any suitable. A method was therefore developed, using a straightforward process similar to one first used by Angström. The Daily Weather Reports for 1949 were examined, and every occasion noted on which no considerable change of air mass took place in a 24 hour period ending at noon. The criterion of admission was that during the 24 hours the sum of the absolute values of the change in dewpoint at three stations (Kew, Bristol and Manchester) should be less than 9°F, and that no noticeable front should have crossed England during that period. There were 91 such nights, with more or less extensive fog formation on 53 of them. The other 38, on which fog did not form, were used as basis for the formula for the night minimum temperature.
16 stations were used, chosen to cover the part of England not close to the sea, as follows:-

Kew
London Airport
Boscombe Down
Mildenhall
Cranfield
Honiley
Wittering
Watnall
Little Rissington
Ross-on-Wye
Shawbury
Bristol
Exeter
Manchester
Finningley
Leeming

For each night the following elements were extracted, using, where necessary, the 1:2,000,000 charts analysed at the Central Forecasting Office:-

/T

T min the night minimum temperature.
G min the grass minimum temperature.
T_{12} the temperature at 1200 hours the previous day.
D_{12} the dewpoint at 1200 hours the previous day.
C the mean cloud amount at 1800, 2400, and 0600 hours.
G the mean gradient wind velocity at the same hours.

The parameters T_{12} and D_{12} are strongly correlated with one another, a fact which introduces complications in the statistical work, so they were used to calculate two other parameters $\frac{T_{12} + D_{12}}{2}$ and $(T_{12} - D_{12})$ which are not highly correlated. A scatter diagram was then plotted, with T min and $\frac{T_{12} + D_{12}}{2}$ as variables, and showed a strong association, the correlation, based on 606 observations, being ·91, and the regression of T min on $\frac{T_{12} + D_{12}}{2}$ was

$$T'_{min} = .864\ (T_{12} + D_{12})/2 + .68 \quad\text{.......} (1)$$

The residual $\Delta_1 = T\ min - T'\ min$ was then found for each case, and correlated with $T_{12} - D_{12}$.

The correlation was only - .19, but nevertheless is significant, the regression equation for Δ_1 being

$$\Delta_1' = -.116\ (T_{12} - D_{12}) + 1.44 \quad\text{.......} (2)$$

Adding this correction to Eqn.(1) gives a second estimate for T_{min}

$$T''_{min} = .316\ T_{12} + .548\ D_{12} + 2.12 \quad\text{.......} (3)$$

The relation between the second residual $\Delta_2 = T_{min} - T''_{min}$ with the wind speed and cloud amount does not appear to be linear, so we cannot expect good results from linear regression methods. Instead, the data were divided into blocks, depending on these parameters lying within particular ranges, and the average value of Δ_2 was found for each block. The smallest suitable size of block is dependent on the accuracy with which it is possible to forecast these parameters in advance and the requirement that a reasonable number of cases should appear in each block. In fact four ranges of wind speed (0-14, 15-29, 30-44 and 45-60 mph) were used, and four of mean cloud amount (0-2, $2\frac{1}{3}$-4, $4\frac{1}{3}$-6 and $6\frac{1}{3}$-8 oktas) giving 16 blocks, and the mean value of Δ_2 found for each block is stated in Table 1.

Table 1. Mean value of $\Delta_2 = T_{min} - T''_{min}$ for different values of the mean gradient wind speed and cloud amount.

Mean gradient wind speed

	C \ G	0-14 mph	15-29 mph	30-44 mph	45-59 mph
Mean cloud amount	0-2 okt.	-4.26 (39)	-1.74 (62)	-1.14 (42)	1.85 (13)
	$2\frac{1}{3}$-4 okt.	-2.83 (30)	-0.20 (97)	-0.21 (43)	5.00 (6)
	$4\frac{1}{3}$-6 okt.	-1.33 (18)	1.58 (62)	1.00 (52)	4.00 (6)
	$6\frac{1}{3}$-8 okt.	0.05 (19)	2.31 (61)	1.74 (51)	

The figure in brackets in each block is the number of observations from which the mean value in question is calculated.

This table demonstrates the dependence of the night minimum temperatures on gradient wind speed and cloud amount. It shows a few minor irregularities, which were not thought to merit further investigation at this stage. The values were smoothed and amended to give a correction, to be added to T''_{min}, which is set out in Table 2.

Table 2. Correction to be added to T" to get the final estimate T'''_{min} of the night minimum temperature.

	G C	0-14 mph	15-29 mph	30-44 mph	45-59 mph
Mean cloud amount during night	0-2 okt.	-4	-2	-1	2
	$2\frac{1}{3}$-4 okt.	-3	0	0	3
	$4\frac{1}{3}$-6 okt.	-1	1	1	5
	$6\frac{1}{3}$-8 okt.	0	2	2	

The corrected estimate T'''_{min} has been used in all that follows. The value of the residual error $T_{min} - T'''_{min}$ was found for each station for each suitable night during 1949, (the test of suitability being that on that night there should be no material change of air mass and no fog). The distribution of the sample of 605 cases is shown in Fig.1. The mean error is less than 0.2°F, so that the prediction formulae are free from appreciable bias, while the mean square error is 3.40°F. The frequency diagram does not appear to depart seriously from the normal form, although there are perhaps a few more extreme errors than should arise with a normal variate.

The least possible value of the mean square error, given the actual observational error of the parameters used in making the estimate, is perhaps 1°F, and the difference between this and the 3.4°F actually found measures the ground to be covered by further improvements in forecasting method.

Besides its use in the present connection an estimate of the night minimum temperature is usually used when considering the risk of air or ground frosts. When the estimated night minimum temperature falls below freezing, and fog is not expected, air frost will be forecast, but the risk of ground frost also arises when the estimated night minimum temperature is above freezing. To throw light on the amount by which the ground temperature may fall below the air temperature, given the values of the wind speed and cloud amount used in this note, mean values of the difference T min-G min for the 16 stations and 38 cases already used are given in Table 3.

Table 3. Mean value of T min - G min under stated conditions.

G C	0-14 mph	15-29 mph	30-44 mph	45-60 mph
0-2 oktas	7.2 (36)	7.6 (58)	5.9 (41)	4.8 (12)
2-4 oktas	+8.8 (28)	+6.7 (90)	+5.6 (42)	+4.4 (5)
$4\frac{1}{3}$-6 oktas	+6.7 (16)	+5.4 (54)	+4.7 (52)	+4.2 (5)
6-8 oktas	+7.2 (18)	+3.7 (59)	+4.5 (48)	5 (1)

The figure in brackets in each block is the number of observations from which the mean value in question is calculated.

An independent check of the formula was made by applying it on each of the 70 nights during 1948 which satisfied the same criteria of no frontal passage and no significant change in air mass at each of 25 inland stations in England. The means and standard deviations of the discrepancy $\Delta_3 = T_{min} - T'''_{min}$ for each night on which fog did not form at the station concerned are given in Table 4.

Table 4. Values of $\Delta_3 = T_{min} - T'''_{min}$ for 25 stations on all suitable nights during 1948.

Station	No. of obs.	Mean	S.D.	Station	No. of obs.	Mean	S.D.
Leeming	46	-2.00	3.97	Manchester	47	-0.87	3.54
Watnall	48	-1.27	2.84	Swinderby	38	-1.95	2.85
Ch. Fenton	42	-2.64	2.99	Defford	52	-1.75	3.56
Waddington	47	-1.91	2.80	Hullavington	49	-2.22	3.11
Oakington	52	-1.46	3.48	South Cerney *	20	-0.40	4.02
Mildenhall	54	-1.67	3.64	L. Rissington	49	0.42	2.88
Abingdon	47	-2.06	3.94	Boscombe D.	52	-1.73	3.05
Benson	54	-0.59	3.20	Bovingdon	46	-1.11	2.97
Whitchurch	54	-1.56	3.31	London Airport	47	-0.23	3.40
Lyneham	51	-1.84	3.18	Finningley	43	-1.39	3.70
Northolt	39	0.08	2.86	S. Farnborough	38	-1.02	3.68
Croydon	50	0.66	2.69	Shawbury	49	-0.63	3.67
Exeter	27	-0.37	3.73	Total	1141	-1.22	3.40

In interpreting this Table, differences exceeding 1°F between the mean for all stations and the mean for one station found from about 50 observations are probably significant, so that it appears that in 1948, for similar values of the parameters, the night minimum temperature at two stations (Church Fenton and Hullavington) was significantly below the general value, while at Northolt, Croydon, Little Rissington and possibly London Airport it was significantly above the general value. It may be desirable to work out special formulae for these exceptional stations, but, at any rate on this evidence, the prediction formula which ignores local features seems to be applicable over most of the country.

The most interesting feature of the Table is that at nearly all stations, for similar values of the parameters, the night minimum temperature during 1948 was consistently below its value during 1949. This consistent difference points to some omitted parameter, such as the hydrolapse, or the soil conductivity having markedly different mean values in the two years; the various possibilities offer avenues for future research, but in the meantime, discrepancies of this kind must be expected if the experimental method is used in practice.

A similar analysis of Δ_3 for the 1949 data on which the prediction formula is based is summarised in Table 5.

Table 5. Values of $\Delta_3 = T_{min} - T'''_{min}$ for 16 stations on all suitable nights during 1949.

Station	No. of obs.	Mean	S.D.	Station	No. of obs.	Mean	S.D.
Leeming	66	0.22	3.38	Boscombe D.	64	-0.72	2.99
Watnall	56	0.36	2.60	London Airport	61	0.43	3.65
Mildenhall	55	-0.78	3.05	Finningley	61	-0.49	3.48
Bristol	67	0.00	2.94	Shawbury	62	0.34	3.20
Exeter	67	-0.32	3.59	Cranfield	53	-0.13	3.45
Manchester	72	-1.15	3.49	Wittering	56	-0.66	3.21
L. Rissington	59	1.80	3.89	Total	799	-0.11	3.40

/It

---

* Data from South Cerney refers to 6 months only.

It seems that in 1949 also, Little Rissington had night minimum temperatures above the general value, while the impression given by the 1948 data that London Airport is exceptional in the same way receives further support.

It is interesting to compare these prediction formulae with results obtained by Franssila (1948) and Faust (1949). The method used by Franssila is the same as that in the present work except that he uses afternoon wet bulb temperature as a parameter instead of dewpoint. For a station in South Finland (Malmi) he obtains a formula almost equivalent to

$$T'_{min} = .25\ T + .50D - k \qquad (4)$$

where k may depend on wind speed, cloud amount, time of year, upper air conditions or the hour at which the parameters are observed. The standard deviation of the residual discrepancy is about 2.7° to 3.8°F, varying from one month to another. These are comparable with the values found in the present work. Franssila concludes that while k depends considerably on wind speed and cloud amount, it was not significantly affected by the upper air conditions, the history of the air mass or the hour at which the parameters were observed.

The method used by Faust is rather different. He selected 60 nights of fairly clear sky and light wind at Iserlohn, and represented each on a graph by a point whose co-ordinates were the screen temperature and vapour pressure at 1400 hours on the previous day. The points representing nights of ground frost were well separated from the rest, and he draws a line of demarcation between the two sets for use in forecasting. A comparable graph can be prepared from Equation (3), taking T_{12} and D_{12} as co-ordinates, and giving corresponding values of T''_{min} by a series of straight isopleths. If the isopleth corresponding, under the conditions of wind and cloud accepted by Faust, to a ground temperature of 32°F is transformed into the co-ordinates used by Faust, it will be found to separate the "frost" points from the rest, although it differs from the line chosen by him.

It seems therefore that a relation of the type given in Equation (3) may be valid elsewhere than in the British Isles with values of the constants not differing much from those given.

3. Estimation of the fog point.

The fog point, unlike the night minimum temperature, is not a regularly observed meteorological quantity, and before setting out to forecast it an effort was made to study its variations over the country. To do this, a selection was made of 29 inland stations which make hourly observations during the night, as follows:-

Leeming
Watnall
Church Fenton
Waddington
Marham
Cranfield
Oakington
Mildenhall
Lakenheath
Abingdon
Benson
Bristol
Lyneham
Northolt
Croydon
Exeter
Manchester
Finningley
Swinderby
Shawbury
Wittering
Defford
Hullavington
South Cerney
Little Rissington
Boscombe Down
South Farnborough
Bovingdon
London Airport

For each of these, on each of the 53 nights in 1949 during which there was no material change in air mass, and more or less widespread fog, the time and temperature of fog formation was extracted from the hourly records. These were plotted on a chart for each night, on which isopleths of fog point were drawn. A typical chart, for a night of widespread fog (27th - 28th January, 1949) is shown in Fig.2. A survey of this series of charts showed, of course, that widespread fog, affecting nearly every station, was comparatively rare, and that the time and temperature at which fog formed were apt to vary considerably, even among stations quite close together. There did seem to be some tendency towards uniformity of behaviour, with regard to fog formation, in geographical areas up to about the size of East Anglia, but even in such areas, the fog point at individual stations was often 2-3°F different from the mean value, while the time of formation might vary among the stations by several hours. The inference is that a forecast of fog point should apply to a single station only, and take account of conditions at that station. If instead a single fog point is assumed to apply to an area, then the area should be the appropriate geographical district, such as East Anglia, the Upper Thames basin or Lincolnshire and East Yorkshire, and the forecast should be worded to suggest degrees of fog incidence, so as to allow for the local variations which will certainly occur.

A formula for the fog point was developed using the same four parameters (two of which are observed at the particular station concerned) which had been used for forecasting the night minimum temperature.

13 stations were used, the same as those used for the night minimum temperature, excluding three (Kew, Ross-on-Wye and Honiley or Elmdon) where no hourly observations were made during the night.

The days considered were the 53 during 1949 on which there was no material change in air mass (by the criterion already stated) and more or less widespread fog. The statistical work followed that for the night minimum temperature. The total number of observations of fog point was 372, there being many cases where fog did not form at a particular station although present elsewhere in the country.

The correlation between T_F and $(T_{12} + D_{12})/2$ was .90, and the regression equation

$$T'_F = .88\,\frac{(T_{12} + D_{12})}{2} - .71 \quad\ldots\ldots\ldots\ldots\ldots\ldots(5)$$

The first residual $\Delta_1 = T_F - T'_F$ has a correlation of -0.52 with $T_{12} - D_{12}$, giving the regression equation

$$\Delta'_1 = -.400\,(T_{12} - D_{12}) + 3.31 \quad\ldots\ldots\ldots\ldots(6)$$

which, when combined with Eqn. (5), gives

$$T''_F = 0.044\,T_{12} + .844 D_{12} + 2.60 \quad\ldots\ldots\ldots\ldots\ldots\ldots(7)$$

It appeared that scarcely any fogs formed with mean gradient wind speed of 30 mph or more, so the final correction was found only for lower wind speeds, and is given in Table 6.

Table 6. Mean value of $\Delta_2 = T_F - T''_F$ for different values of the mean gradient wind speed and cloud amount.

G C	0-14 mph	15-29 mph
0-2 okt.	-.26 (76)	-2.9 (49)
2-4 okt.	0.10 (75)	-0.1 (31)
4-6 okt.	1.7 (40)	0.8 (26)
6-8 okt.	2.6 (44)	0.8 (22)

The figure in brackets in each block is the number of observations from which the mean value in question is calculated.

These were rounded to the nearest unit to give the correction to be added to T''_F to get the final estimate T'''_F which is used in all that follows.

The value of the residual error, $\Delta_3 = T_F - T'''_F$, was found for each of 363 cases from those already used, and the frequency distribution is shown in Fig.3. This is nearly a normal distribution, with mean value about -0.02°F, and standard deviation 3.31°F.

An independent check of this formula was made as before at 25 stations on all eligible nights during 1948, and the results are summarised in Table 7.

Table 7. Values of $\Delta_3 = T_F - T'''_F$ for 25 stations on all suitable nights during 1948.

Station	No. of obs.	Mean	S.D.	Station	No. of obs.	Mean	S.D.
Leeming	13	-1.39	4.23	Manchester	17	-0.76	3.17
Watnall	12	0.08	4.41	Swinderby	17	-2.18	3.43
Ch. Fenton	18	-2.56	3.76	Defford	12	-3.67	5.01
Waddington	14	-0.50	2.93	Hullavington	7	-0.57	4.08
Oakington	10	-3.00	3.12	South Cerney *	15	-1.20	3.45
Mildenhall	10	-4.00	3.52	L. Rissington	15	-0.73	3.42
Abingdon	15	-2.73	4.77	Boscombe D.	9	-0.44	3.89
Benson	6	-0.83	4.79	Bovingdon	16	-2.25	4.94
Whitchurch	7	-0.57	3.60	London Airport	13	-0.69	3.90
Lyneham	11	-0.36	3.12	Finningley	18	-0.78	3.73
Northolt	19	0.36	4.49	S. Farnborough	22	0.18	5.39
Croydon	13	0.69	2.52	Shawbury	15	1.00	3.96
Exeter	29	1.65	4.90	Total	353	-0.85	4.25

With the smaller number of observations, this Table affords less reliable ground for inference than does Table 4, although there is little doubt that for given values of the parameters under conditions like 1948 the fog point at Oakington, Mildenhall and Defford was significantly below the general level, and that at Exeter and perhaps Croydon and Shawbury significantly above. It appears too that the fog point was fairly consistently lower during 1948 than it was with similar values of the parameters during 1949, by about .8°F, so that discrepancies of this kind must be expected if the fog point is used in practice. The bias in the estimated fog point is in the same direction as that in the estimated night minimum temperature, so that effect on the experimental forecasts made was comparatively slight.

A similar analysis of $\Delta_3 = T_F - T'''_F$ for 1949 is summarised in Table 8.

Table 8. Values of $\Delta_3 = T_F - T'''_F$ for 13 stations on 53 suitable nights during 1949.

Station	No. of obs.	Mean	S.D.	Station	No. of obs.	Mean	S.D.
Leeming	21	-0.24	3.21	Boscombe D.	27	-0.78	3.80
Watnall	33	0.18	2.44	London Airport	28	1.30	3.10
Mildenhall	35	-0.56	3.00	Finningley	29	-0.76	3.83
Bristol	24	-0.67	3.46	Shawbury	28	1.25	2.80
Exeter	24	-1.46	3.81	Cranfield	38	-0.61	3.27
Manchester	20	-0.15	2.99	Wittering	35	0.14	2.70
L. Rissington	32	1.41	3.42	Total	374	-0.02	3.31

The variations of individual stations from the mean differ considerably from those observed in 1948, and it is difficult to decide the significance of any of them. Possibly the most definite indication is that the method is comparatively unreliable when applied on these days at Exeter, perhaps because Exeter lies considerably outside the triangle Bristol-Manchester-London used in selecting the days.

4. Experimental forecasts of fog formation.

If we find T'''_{min} and T'''_F for a station for a particular night, then we expect fog unless T'''_{min} is higher than T'''_F. If we define a quantity $E=T'''_F-T'''_{min}$ we expect fog when E is positive or zero, and no fog if E is

/negative

---

* Data for South Cerney for 6 months only.

negative. An experimental forecast was made, based on the value of E, for each suitable case during 1948 and 1949. For 1948, forecasts were made at each of the 25 stations on each of the 70 nights on which there was no material change in air mass, while for 1949 forecasts were made for each of the 13 stations used in obtaining the fog point formula on each of the 91 nights of no material change in air mass. Cases where the mean gradient wind speed during the night exceeded 30 mph were excluded, as it was clear that a forecast of no fog on such nights was nearly always correct. All the other cases were sorted according to the event, and the values of E tabulated, the notation E_F implying a case where fog (including fog patches and ground fog) formed on that night, as shown by the hourly observations up to 0800 hours the following morning, and E_N implying a night on which fog did not form. The frequency distributions of E_F and E_N in 1948 and 1949 are given in Table 9 and Fig.4.

Table 9. Frequencies of the difference $E = T'''_F - T'''_{min}$ during 1948 and 1949.

1948			1949		
Value	fqcy of E_N	fqcy of E_F	Value	fqcy of E_N	fqcy of E_F
10			10		1
9			9		
8			8		
7			7		
6			6		
5	2	6	5	4	7
4	29	32	4	15	8
3	29	42	3	44	42
2	58	36	2	65	62
1	103	48	1	59	57
0	121	66	0	90	46
-1	157	63	-1	102	51
-2	133	33	-2	85	36
-3	104	25	-3	69	36
-4	45	8	-4	32	9
-5	16	4	-5	29	4
-6	4		-6	8	1
-7	5		-7	2	
	806	363		604	360

The forecaster, before the event, has only the value of E to go on in making his forecast. Fig. 4 shows on the one hand that there is a definite association between the value of E found for a particular night and the expectation that fog will form on that night (the greater the value of E, the larger the risk of fog) but on the other hand, that there is no critical value of E separating the cases of fog from those of no fog. However, a forecast of no fog whenever E is negative (i.e. whenever T'''_{min} is higher than T'''_F) will be right on 75 per cent of occasions, while the corresponding forecast, that fog will form whenever T'''_{min} is equal to or lower than T'''_F, would have been right about 40 per cent of the time in 1948 and 50 per cent of the time in 1949. In each year about two thirds of the fogs actually occurring would have been forecast. By raising the threshold and forecasting fog, say, only when E is +2 or more, the percentage success of a forecast of fog will be improved, but the proportion of fogs occurring which are forecast will be less.

For practical use, it is suggested that a forecaster who is concerned with an area (for which he has assumed uniform values of the parameters) should forecast "little or no fog" whenever E is less than 0, and "more or less widespread fog" when E is greater than or equal to 0. Only when E takes extreme values, such as -6 or +5, will his forecast be quite definite. A forecaster who is concerned with a single station has the difficulty that a risk of fog, falling short of a 50 per cent expectation, is still a hazard which the recipient of the forecast may not wish to ignore. He may prefer to forecast "fog" only when E is +2 or more, "more or less serious risk of fog" when E lies in the range +1 to -3 and "negligible risk of fog" when E is -4 or less. These are suggestions only; a forecaster may arrive at other commonsense interpretations of Table 9 appropriate to his own circumstances, and can if he wishes construct a similar Table based entirely on data from his own station.

Whichever variant of the forecasting method is chosen, it is objective in the sense that, once the right night and the right values of the parameters have been chosen, any operator using the method blindly will arrive at the same forecast. If practice, however, a skilful forecaster may expect to improve on the objective forecast. The residual errors of mean square value between 3° and 4°F are not wholly unpredictable, but depend mainly on two things:- (1) variations in parameters, such as the hydrolapse, the soil conductivity or the atmospheric pollution, which being ignored in the prediction formulae are effectively treated as always having their average values and (2) the fact that the mean corrections for wind speed and cloud amount refer strictly to parameters having the mean values in the respective ranges, so that a somewhat different correction is appropriate when the forecast value of the parameter is near the extreme of that range. A forecaster who knows his case under consideration to be exceptional in either of these respects should make a suitable empirical correction to allow for this, but generally not more than 7°F (i.e. twice the M.S.E. of the prediction formulae).

The use of this or any similar method does not absolve the forecaster from using his judgment, but simply puts on a firm statistical basis the adjustment for some of the variables he would otherwise have to consider, and allows him to exercise his judgment within the narrower range indicated by the mean square error.

5. An example of the use of the experimental method as a datum.

One of the more reasonable methods which have been suggested for estimating the fog point is that proposed by Saunders (1950). This, which is explained in full detail in Saunders' own work, is obtained by means of a simple construction on the afternoon tephigram. The parameters which determine the fog point are a representative temperature and dewpoint and the hydrolapse in the lowest 50 mbs.

On each of the 91 nights of no material change in air mass during 1949 the fog point was found by this method from the afternoon upper air soundings at Downham Market, Larkhill and Liverpool. Estimates were then made of the fog point at each of 13 inland synoptic reporting stations (the same ones as were used in developing the Forecasting Research Division experimental formula for the fog point), taking into account the fog points at the three upper air stations and the direction of the airflow. All the estimates were made by one of us (Dorothy Pritchard) in the rough, commonsense way that a practising forecaster would use, and on all occasions when fog actually formed, the estimated fog point was compared with that observed. The mean error (actual minus forecast fog point) for 368 comparisons was almost exactly -3°F, while the mean square departure of this error from its mean was 4.6°F. There is thus some reason to think that Saunders' formula, which was mostly tested by its author against London data, gives higher values than those observed in most parts of the country.

This test suggests that Saunders' fog point when estimated in this way is subject to larger errors than the F.R.D. formula, which is much simpler and quicker to estimate. However, we are really interested, not in the accuracy of a forecast fog point, but on whether it can be used as a basis of good forecasts of the occurrence of fog. A further test was made, on the 1949 data, taking the night minimum temperature estimated with the F.R.D. formula and the fog point estimated by Saunders' formula, as above, and finding E for each occasion. The values of E, divided into E_F, and E_N, are given in Fig.5, which refers to the same cases and is properly comparable with the second half of Fig.4. It seems that the separation of the cases of fog formation from those /

of no fog is even more incomplete than in Fig.4. If Saunders' formula is to be used so as to forecast two thirds of the cases of fog which actually occur (a reasonable requirement) then fog must be forecast whenever E is -3°F or more, and about 46 per cent of such forecasts will be correct. This is below the standard of success obtained with the F.R.D. fog point for 1949, but above that obtained with the F.R.D. fog point for 1948. We may conclude that there is little to be gained by using Saunders' fog point in this way, instead of the F.R.D. fog point which is easier to calculate and available at an earlier hour. On the other hand Saunders' formula used with a different formula for the night minimum temperature, or subject to more stringent restrictions as to the place and occasion of use, may perhaps be made the basis of a more successful forecasting method, or the effect of variations in the hydrolapse may be allowed for in a different way if, for example, it can be shown to be correlated with the residuals left after applying the F.R.D. formulae. Possibilities of this kind offer a wide field for future research.

6. Conclusion.

This F.R.D. experimental forecasting method is primarily intended to serve as a datum, from which progress resulting from further research can be measured, and the degree of success attained suggests that it will be satisfactory for this purpose. Any method which, by adequate statistical trial, is shown to have noticeably higher accuracy will be of immediate practical value, and conversely, there is no reason to devote time to developing any method which does not, on preliminary trial, offer advantages in accuracy or ease of use when compared with this datum. The prediction formulae for the night minimum temperature and for the fog point are of course quite independent: either can be used with any other proposed formula for predicting the other element.

Looked at as a tool for the practical forecaster, the method has neither the detail nor the reliability to be expected in a finished product. Nevertheless, it places on a firm statistical basis adjustments which most practical forecasters have been accustomed to make subjectively, so that practical forecasters, or at least those who are dissatisfied with their present methods, may find it worth a trial. The simulated forecasting experiment was not made under actual working conditions, because the fact that no material change in air mass would take place, and the mean cloud amount and gradient wind speed during the night were known in advance. The working forecaster has to forecast these, and his errors in using the formulae on the wrong night or with wrong values of the parameters are added to the inherent errors analysed above. These, however, are matters of general synoptic meteorology, which must be dealt with when using any method of fog forecasting, and it is not thought that the demands made by the present method on the forecaster's general technique are unreasonable. Against additional errors arising this way must be set the gain which may be made by a forecaster who uses his judgment to reduce the residual errors, as indicated in Section 4, and on balance the percentage success may be as good if not better than that achieved in this experiment.

References.

Franssila, M. 1949. Geophysica (Helsinki) Vol.3 pp.102-113.

Faust, R. 1949. Ann. d. Met. Bd. 2 Nr. pp.105-111.

Saunders, W.E. 1950. Met. Mag. Vol.79 pp.213-219.

FIG. I. FREQUENCY DISTRIBUTION OF THE RESIDUAL ERROR OF T'''_{MIN} FOR 1949 DATA.

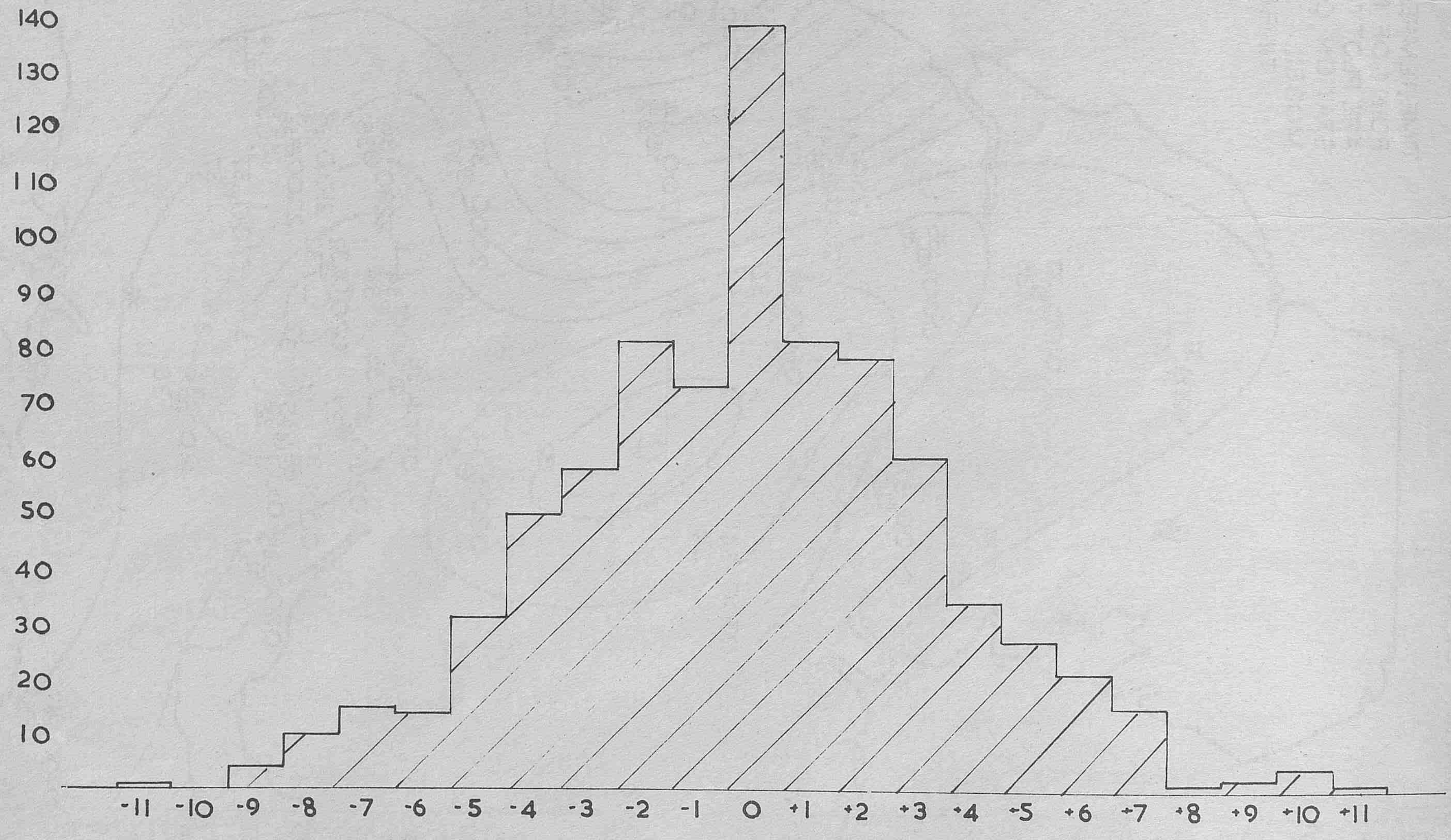

]

FIG 2. SPECIMEN MAP TO SHOW VARIATION OF TEMPERATURE OF FOG FORMATION 27 - 28 JANUARY 1950.

TIME, TEMPERATURE AND DEWPOINT OF FOG FORMATION ARE PLOTTED FOR EACH STATION ON THE FOLLOWING MODEL.

TIME G.M.T. ⊕ TEMPERATURE.
DEWPOINT.

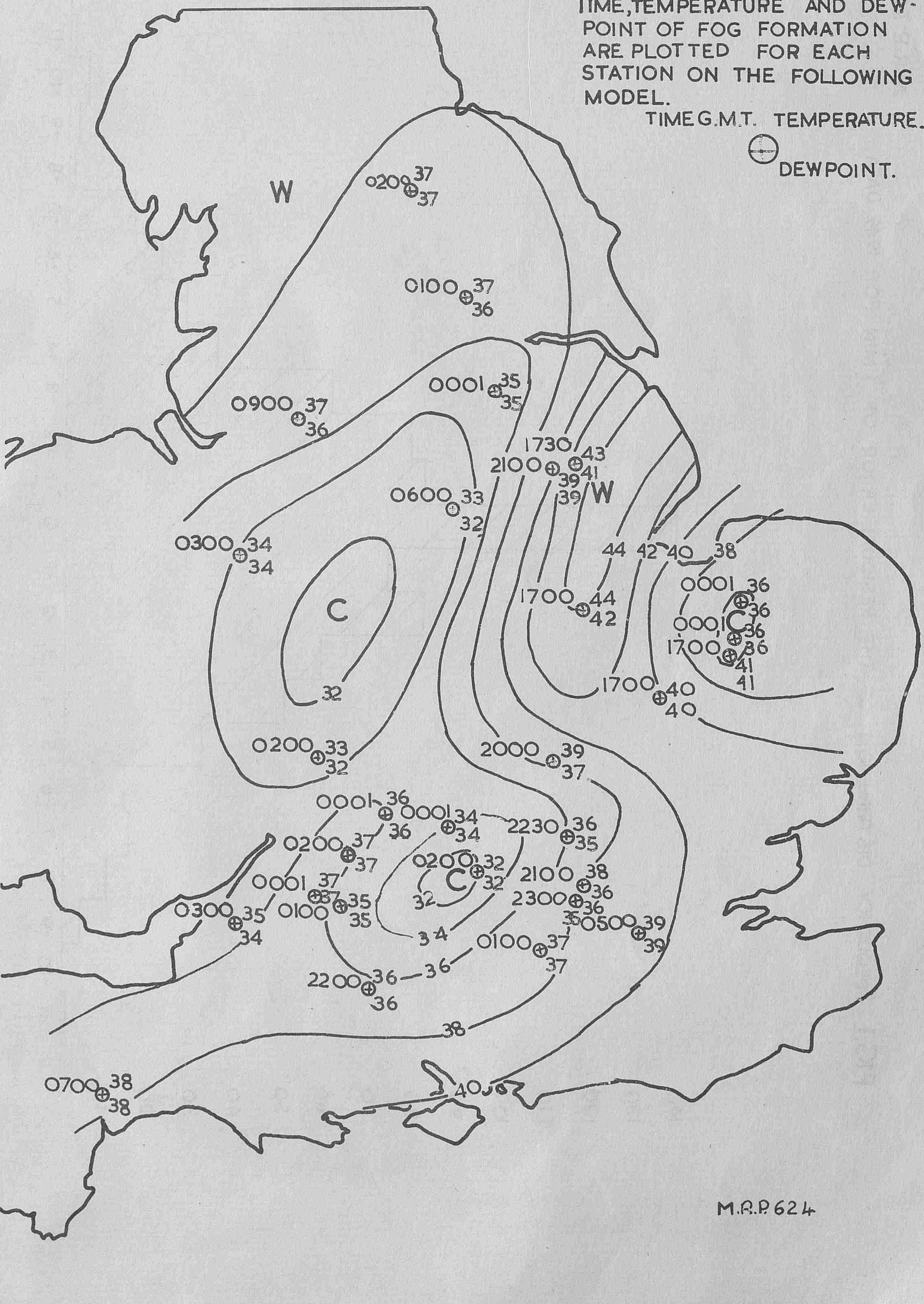
W
0200 37 37
0100 37 36
0001 35 35
0900 37 36
1730 43 41
2100 39 39
W
0600 33 32
0300 34 34
44
42
40
38
0001 36 36
0001 36 36
1700 41 41
1700 44 42
C
C
32
1700 40 40
0200 33 32
2000 39 37
0001 36 36
0001 34 34
2230 36 35
0200 37 37
0200 32 32
C
32
2100 38 36
0001 37 37
0100 35 35
0300 35 34
2300 36 36
36
0500 39 39
34
0100 37 37
2200 36 36
36
38
0700 38 38
40

M.A.P. 624

FIG.3 FREQUENCY DISTRIBUTION OF THE RESIDUAL ERROR OF T_F''' FOR 1949 DATA.

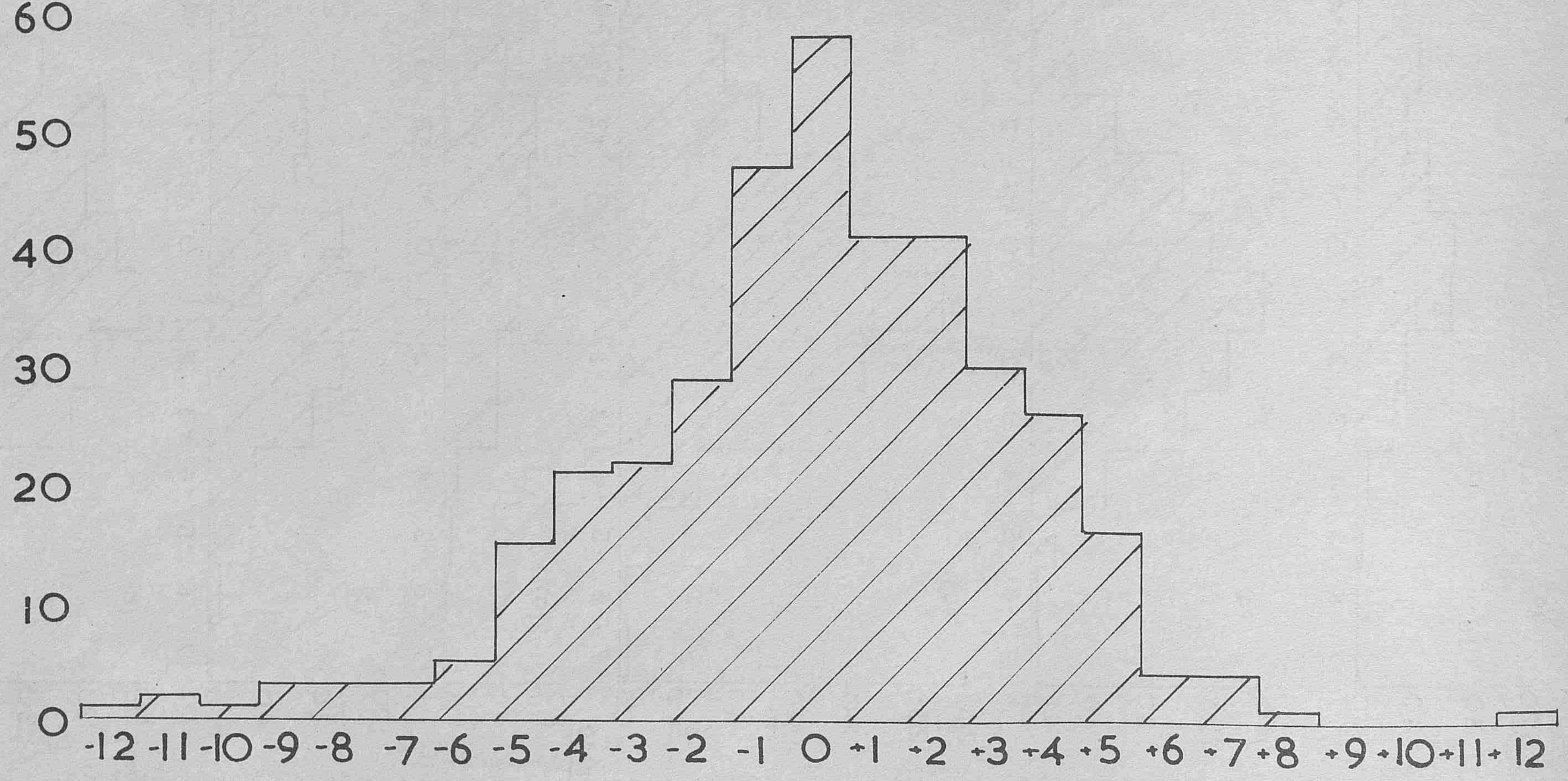

Fig. 4. Dissected frequency distribution of the difference $T_F''' - T_{MIN}'''$, given by the F.R.D. Fog forecasting formulae for 1948 and 1949: (a) cases when fog formed, (b) cases when fog did not form (c) all cases taken together.

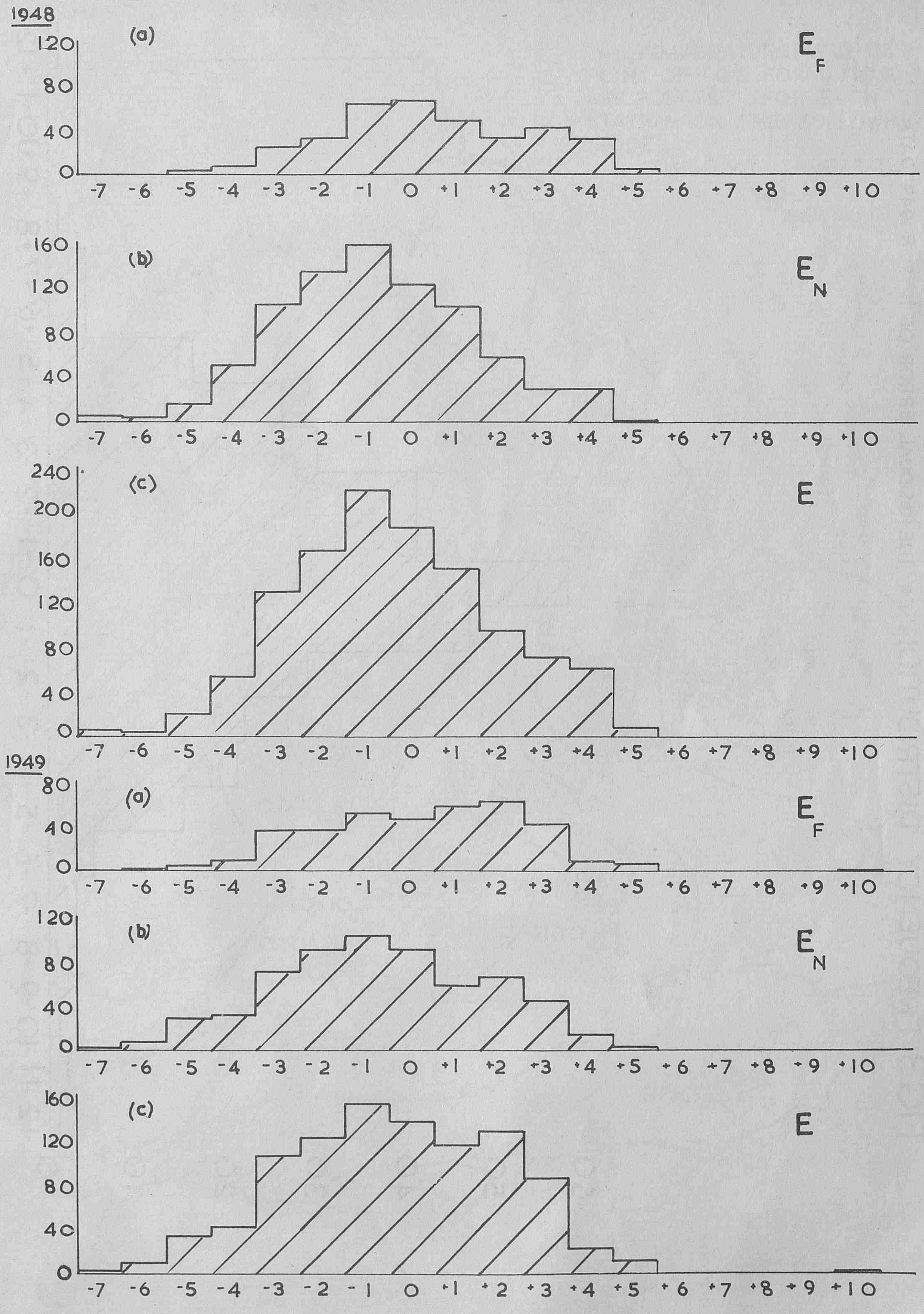

M.R.P. 624

Fig. 5. Dissected frequency distribution of the difference between Saunders' fog point and the night minimum temperature T_{MIN} given by the F.R.D. formulae for 1949: (a) cases when fog formed (b) cases when fog did not form (c) all cases taken together.

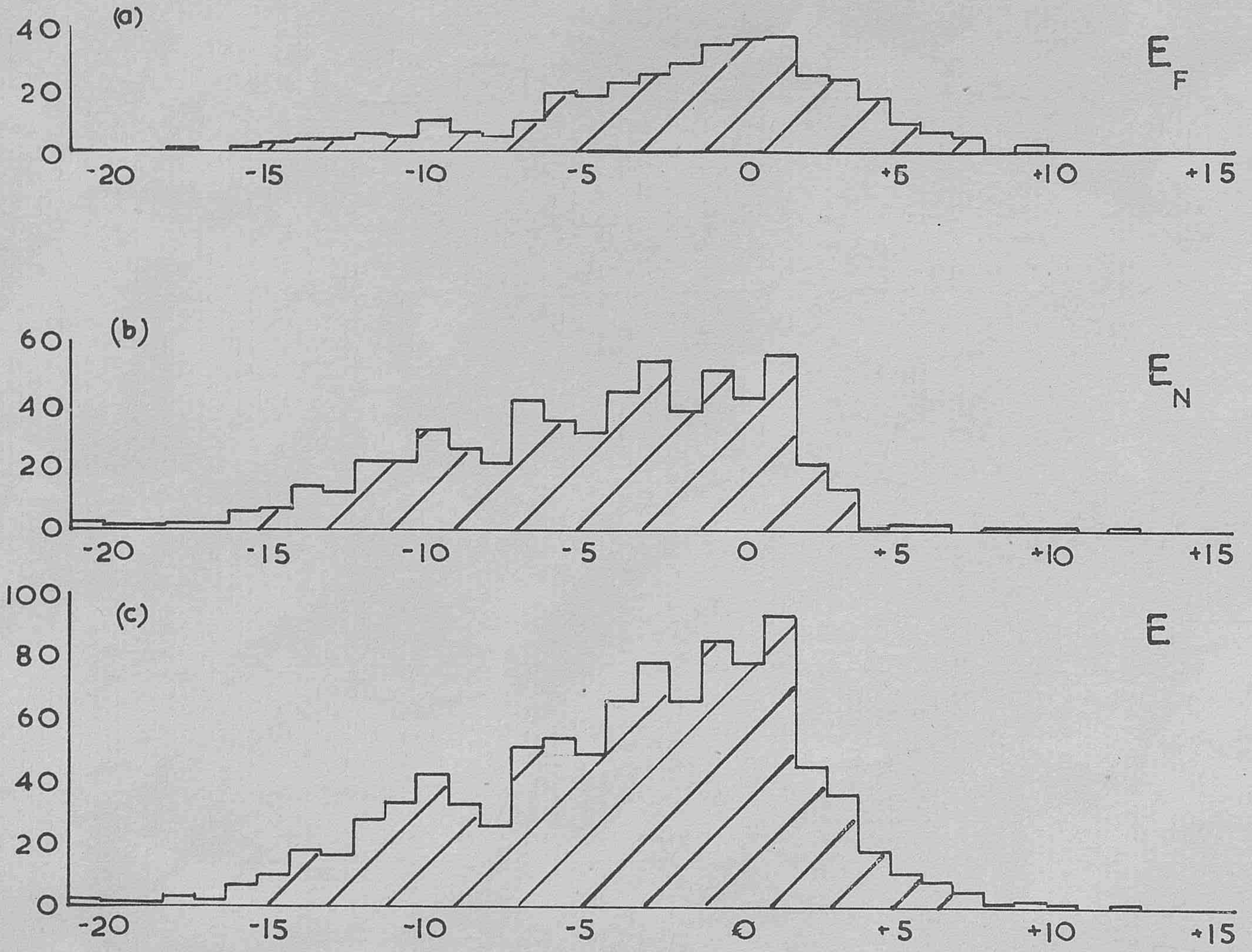

~~quote this paper should refer to it as "A paper of the Meteorological Research Committee (London).
M.R.P. No .... by Mr ....
A copy is available in the Library of the Meteorological Office."~~

SEP 26 1955

M.R.P. 626.
S.C.III/89
9 th April, 1951

ATI-145270

AIR MINISTRY

METEOROLOGICAL RESEARCH COMMITTEE

A study of the relation between aerodynamic drag and wind profile over grassland.

by

N. E. Rider.
(Meteorological Office.)

Summary.

An account is given of measurements of the aerodynamic drag of a short grass surface and the simultaneous determination of the wind and temperature profiles up to a height of two metres. The drag plate apparatus was an improved version of that employed by Pasquill (1950). The measurements were conducted over a band of atmospheric stability represented by a variation in the Richardson Number at a height of 75 cm. from 0.18 to -0.04. Pasquill's result that the empirical laboratory law

$$u_z = \frac{1}{k}\left(\frac{\tau_o}{\rho}\right)^{1/2}\log\left(\frac{z-d}{z_o}\right)$$

where u_z is the wind velocity at a height z above the ground, τ_o is the drag, k is von Kármán's constant, z_o is the roughness parameter, ρ is the density of the air, and d is the zero plane displacement is applicable to the lowest layers of the atmosphere in neutral conditions is confirmed. The determined value of k is 0.38. Values of the dimensionless quantity $\tau_o/\rho z^2(\partial u/\partial z)^2$ (= k^2 in neutral conditions) are calculated and shown to have a tenfold variation over the range of stability experienced in the observations. Values of the index β in the Deacon (1948) wind profile law are determined by two methods, and some observations are made on the normally accepted variation of β with stability when applied to individual occasions. Finally it is pointed out that the results are potentially capable of demonstrating the validity or otherwise of the equation

$$\frac{\tau_o}{\rho z^2\left(\frac{\partial u}{\partial z}\right)^2} = k^2\left(\frac{z}{z_o}\right)^{2\beta-2}$$

which follows from the Deacon wind profile law. Unfortunately the scatter in the values of $\tau_o/\rho z^2(\partial u/\partial z)^2$ makes a definite conclusion impossible.

1. Introduction.

The aerodynamic drag of a natural surface was first measured by Pasquill (1950) who followed a technique previously employed by Sheppard (1947) in measuring the aerodynamic drag experienced on an isolated metal plate in the centre of an extensive concrete area. Pasquill, in particular, was concerned with establishing the explicit validity of an empirical laboratory law relating the drag exerted on an artificially roughened surface in fully developed turbulent flow to the fluid velocity above the surface, when applied to the atmosphere. This law established by Nikuradse (1933) and Schlichting (1936) may be written in the form

$$u_z = \frac{1}{k}\left(\frac{\tau_o}{\rho}\right)^{1/2}\log_e\left(\frac{z}{z_o}\right) \quad \ldots\ldots\ldots\ldots\ldots\ldots\ldots(1)$$

where u_z = the fluid velocity at a distance z from the pipe wall.
τ_o = the shearing stress per unit area of the pipe wall.
ρ = the fluid density.
z_o = a constant for each type of roughness: in meteorological applications usually known as the roughness parameter.
k = a dimensionless constant, usually known as von Kármán's constant.

When the height of the roughness elements attached to the solid boundary is comparable to the distance between the boundary and the point of measurement of the fluid velocity it is necessary to consider this latter distance to be reduced by an amount d which in meteorological applications is known as the zero plane displacement. In these circumstances equation 1 becomes

$$u_z = \frac{1}{k}\left(\frac{\tau_o}{\rho}\right)^{1/2}\log_e\left(\frac{z-d}{z_o}\right) \quad \ldots\ldots\ldots\ldots\ldots\ldots\ldots(2)$$

It is apparent that equation 1 can only be functionally true as long as

$$u_z \propto \log_e\left(\frac{z}{z_o}\right)$$

The researches of Best (1935) and Deacon (1948) on the form of the wind velocity profile over natural surfaces indicate that this is only true under certain conditions in the atmosphere, namely in neutral or adiabatic conditions of flow. In non-adiabatic conditions Deacon has suggested a wind profile law of the form

$$\frac{\partial u}{\partial z} = az^{-\beta} \quad \ldots\ldots\ldots\ldots\ldots\ldots\ldots\ldots\ldots\ldots\ldots(3)$$

where a and β are constants, and β takes values < 1, 1 and > 1 according to the stability of the atmosphere. Recently it has become the custom to regard the stability of the atmosphere as not to be defined by the vertical temperature gradient alone ($\partial T/\partial z$), but to be modified by the horizontal shearing stress ($\partial u/\partial z$). The Richardson Number, defined by

$$R_i = \frac{\frac{g}{T}\left(\frac{\partial T}{\partial z} + \Gamma\right)}{\left(\frac{\partial u}{\partial z}\right)^2}$$

where g = acceleration due to gravity.
T = absolute temperature.
Γ = the dry adiabatic lapse rate, -1×10^{-4}.

is now regarded as the best indicator of the degree of departure from neutral conditions. The index β in the Deacon wind profile law (equation 3) takes values

$$\begin{array}{l} >1 \text{ when Ri is negative} \\ 1 \text{ when Ri} = 0 \\ <1 \text{ when Ri is positive} \end{array}$$

and therefore indicates that $u_z \propto \log_e (z/z_o)$ when Ri = 0 i.e. in neutral conditions only. We should therefore expect equation 1 to hold, if at all, only when Ri = 0. Pasquill was able to confirm the explicit truth of equation 2 in these conditions, and further his determined value of k, von Kármán's constant, was very close to the laboratory determined value of 0.4. The investigation to be described here extends Pasquill's measurements to a range of atmospheric stabilities over which the Deacon wind velocity profile law could be expected to hold.

2. The apparatus.

A drag plate apparatus similar to that described by Pasquill (1950) was used to measure the aerodynamic drag. His apparatus consisted essentially of two containers or metal circular pans with vertical sides, one being slightly larger in diameter than the other. The larger pan contained water in which the smaller pan floated. A sample of the natural surface was cut out and supported in the inner pan on a false bottom, the level of water in the outer pan being adjusted until the sample was exposed at its natural level, the outer pan having been let into the ground. Movement of the inner pan carrying the sample was controlled by a metal strip which was firmly held at its far end. Movement of the inner pan as a result of the drag on the sample was gauged by means of a long pointer which moved over a suitable scale, the pointer being attached to the inner pan at a position diametrically opposite to the point of attachment of the control strip. The main differences between the present apparatus and that used by Pasquill (1950), together with an account of the method of calibration etc., are set out below:

(a) The effective area of the drag plate was increased approximately eight times, thus enabling a larger area sample to be used. By this increase in size it was hoped to obtain in one position a sample of the natural surface which could be considered typical of the whole surface on which measurements were made.

(b) The control strip was of phosphor bronze and its fixed end was held in a brass vice of heavy construction.

(c) The control strip and pointer were linked to the moving plate in such a way that they could be contained in perspex covered boxes below the level of the lip of the inner movable container which takes the sample. In the field this enabled the boxes to be let into the surface, so eliminating as far as possible any disturbance to the air flow about and over the apparatus.

(d) The apparatus was made to record the deflections experienced by the inner floating container by attaching a light syphon type pen and ink-well to the pointer and allowing the pen to rest on a chart on a clockwork drum mounted on a horizontal axis, the axis being at right angles to the line of symmetry of the apparatus. The time scale of the drum was adjustable over a fairly wide range and a remotely operated electromagnetic device was constructed to provide time marks at one minute intervals on the chart. It was found that the time scale remained linear throughout the series of experiments. The whole recording unit was mounted in a box which was let into the ground with its perspex-covered top level with the ground surface. The necessity to have an observer near the position of the apparatus during the course of an experiment was thus eradicated. The syphon type pen was provided with counter balance weights so that adjustment of the pressure of the pen on the chart was possible. It was found that by adjusting these weights the condition could be reached in which the pen was held in contact with the chart by the surface tension of the ink. There was thus little frictional drag introduced by the adoption of this recording method.

(e) The only parts of the apparatus exposed to the air flow (other than the sample of the surface when in position) were the edges of the links from the control strip and pointer to the inner moving container carrying the sample. Since these were made from 22 s.w.g. material and had a length of about 3 cm. the exposed area was very small. Further, in the field, these links were well below the top of the grass cover.

(f) Calibration of the drag plate apparatus was undertaken in the laboratory by attaching light weights to the centre of the inner container by a human hair passing over a pulley. Stops were provided to restrict the movement of the inner container to the range over which the calibration was found to be linear. From time to time check calibrations were performed in the field. For this operation, and for providing a zero line at the start and finish of an experiment, a bottomless draught-tight box was made which could be placed over the apparatus, so excluding air movement from its surface. The check calibrations were obtained by positioning this box over the apparatus and attaching weights to the centre of the inner container as in the laboratory, the hair in this case passing through a small hole in the side of the box. The weights were situated a few cm. below ground level in a 3 cm. diameter hole made with a soil sampler close to the outer container. This hole was in such a position that, when the apparatus was in use, the air passed over the sample before passing over the hole. The grass and soil could be replaced so maintaining a uniform surface. It was found that repeated calibration in the laboratory after dismantling and reassembling the apparatus indicated no detectable variation in the calibration factor i.e. in the reflection produced per unit applied force. The check calibrations performed in the field throughout the period of exposure yielded results which were within 5% of the laboratory value. In view of the difficulties attendant upon field calibration it was decided to employ the laboratory calibration factor in reducing the measurements.

(g) In use the plate was critically damped by adjusting the depth to which a light vane, attached to the pointer, was immersed in an oil bath. A full deflection to an applied force was obtained in approximately 30 sec. with the sample in position and the inner container floating at its operating depth. The apparatus was exposed in the one position for a period of about three months and it was not posible to preserve in a healthy condition one sample of the grass surface on the false bottom of the inner pan over this period. A new sample was cut and inserted every two weeks. Further, since the boxes containing the control strip etc. were embedded in the surface it was not possible to rotate the apparatus which had the result of severely restricting the number of occasions on which measurements could be made since it was desired to have wind directions within a small arc centred about the normal to the axis of symmetry of the apparatus.

3. A distant reading thermo electric temperature gradient apparatus similar to that used by Pasquill (1949 a) and Rider and Robinson (1949) was used to obtain the dry bulb temperature profile. Temperatures were obtained at heights of 200, 150, 100, 50, 37.5 and 25 cm. above the surface and a temperature at each height could be obtained in about 45 sec.

4. A light vane which was capable of recording the wind direction for periods of 3 min. was mounted on a mast at a height of 125 cm. to obtain the mean wind direction at intervals during the course of each observation.

5. The wind velocity profile was measured by using sensitive cup anemometers of the Sheppard type. These were exposed during all but the first two observations (7/6/50) at heights of 200, 150, 100, 50, 37.5, 25, 17.5 and 10 cm. above the ground. During the first two observations the lowest two anemometers were not available. It was found impossible to mount all the anemometers on one mast and provide each with a satisfactory exposure. This resulted in certain difficulties in deciding the height of exposure of each anemometer with reference to a single 'ground level'. This will be discussed later. Further, the lowest two anemometers had to be set up with their recording mechanisms below the surface. This was achieved by mounting them in circular holes extracted by a soil sampler to appropriate depths, the diameter of the holes being 10 cm. The disturbance to the surface caused by this method of mounting was considered not to lead to errors in the anemometer indications as the holes were within the area swept out by the anemometer cups. It will be seen later that for certain reasons the readings of the anemometers at 200 and 150 cm. were not finally used in arriving at the form of the wind velocity profile.

6 The Site.

The site used for the present measurements on Downing College Sports Ground was covered with short grass which was kept mown to a length of 2 to 3 cm. throughout the period of the experiments. The dimensions of the field were about 225 m. (N. to S.) by 150 m. (E. to W.), and its boundaries ran approximately N,S,E and W. The field was bordered by a hawthorn hedge which varied in height from 2 m. to 1 m. Beyond this hedge to the E, S and W the land was open and level and free from large obstacles. However, to the N immediately beyond the hawthorn hedge was a second hedge about 4 m. high and beyond this, further still to the N., was a belt of tall trees with tops extending to the 25 m. level. After a survey of the effect of the hawthorn hedge on the wind velocity profile had been completed (Rider (1951)) it was decided to site the apparatus towards the NE corner of the field, 50 m. from the N. boundary and 20 m. from the E. boundary. The apparatus was set out along a roughly NW-SE line and experiments were restricted to occasions on which southwesterly wind directions occurred. In this position, with southwesterly winds there was a uniform grass surface for 200 m. upwind and 60 m. downwind from the apparatus. The results of the survey mentioned above indicated that the hawthorn hedge should have no influence on the shape of the wind velocity profile in the position chosen, and this was believed to be the case. However it will be seen later that the anemometers at the heights of 200 and 150 cm. provided indications of wind speed below that which was expected. During the survey mentioned above it was found that a hawthorn hedge exerted an influence on the measured wind velocity at 200 cm. some 15 hedge heights upwind from the hedge. How far this result can be multiplied in scale and applied to the influence of the belt of trees situated some 125 m. to the N. of the apparatus is by no means certain. It will be appreciated that the apparatus was 7 to 10 barrier heights from this belt of trees and their presence could well have the result of reducing the wind speed below that appropriate to an infinite grass surface above a height of 100 cm. at the position of measurement.

7 Experimental Procedure.

As far as possible observations were only made on occasions of southwesterly winds having a mean direction within 20 degrees of the normal to the axis of the drag plate apparatus. In addition it was hoped to restrict observations to times with reasonably uniform skies in the hope that a satisfactory temperature profile would be obtained having regard to the frequency with which individual temperature determinations at the various heights could be made with the available apparatus. Some preliminary measurements showed that a minimum time of 15 min. was generally required to obtain a satisfactory profile under uniform radiation conditions, and with this in mind, together with the fact that only two observers could be relied upon to be present at any one time, 15 min. was adopted as the period for one observation. It will be seen that the desired conditions of weather and wind direction were not always present and on some occasions it was not possible to draw a satisfactory temperature profile from the results.
During the 15 min. period the following records and readings were taken:

(a) A 15 min. observation of the temperature at the various heights (generally twenty to twenty five individual temperature determinations were obtained at each height).

(b) A 15 min. observation of the total run of wind at the various heights.

(c) A 10 min. record of the deflection of the drag plate centred about the mean time of the observation.

(d) Two 3 min. records of wind direction, the first ending 1 min. before the mid time of the observation and the second starting 1 min. after this time.

Method of Treatment of the Observations.

8 Aerodynamic Drag.

Three typical records from the drag plate apparatus are shown in Fig. 1. a b and c. Fig. 1. a is an occasion of light wind (observation No. 9) and b and c are occasions of stronger wind (observation Nos. 18 and 3). Sections AB and FG of the records are zero lines obtained at the start and finish of the plate exposures with the draught tight box in position. D is the mid time of the observation and CD and DE are two five minute records with which are associated the two separate determinations of the mean wind direction. A planimeter was employed to find the total area enclosed by each of the two 5 min. sections of every record. These areas when divided by the corresponding base lengths yielded the mean deflection of the plate and hence the mean force on the plate during each five minute period when the calibration factor was applied. Several separate determinations of each area were made and the mean used as that required. It is convenient here to note the degree of reproduceability of the individual determinations of the areas. When dealing with large deflection records the differences between individual determinations were never greater than 3 °/o, but with small deflection records the differences were sometimes as large as 8°/o. By taking the mean of several determinations we may expect the areas obtained to be within 1 to 2°/o of the true areas for large deflections and about 5°/o for small deflections. To calculate the aerodynamic drag τ_0 per unit area of the sample surface during each half of the observation from the force per unit area experienced, as found above, it was necessary to know the angle between the mean wind direction and the axis of symmetry of the drag plate apparatus during the time of exposure. This was obtained from the records provided by the light vane. If this angle is θ then the force per unit area of the sample is $F = \tau_0 \sin \theta$. τ_0 was obtained for each half of a single observation and the mean taken as the aerodynamic drag over the ten minute interval of exposure. It may be objected that here we are associating the drag measured over 10 min. with a determination of the mean temperature and wind velocity profile taken over a period of 15 min. centred about the mean time of the drag determination. As has already been stated the number of observers was limited and the process of starting and stopping the anemometers demanded the presence of an observer in the immediate vicinity of the drag plate apparatus which may well have led to false readings at the commencement and finish of the records had the apparatus been recording over the whole 15 min. period.

9. Wind Speed Profile.

The total run of wind at each height over the 15 min. period was converted to the mean wind speeds by means of the anemometer calibration curves. These results were then plotted against the corresponding heights and the best freehand curve drawn through them. It soon became evident that
(a) The wind speeds indicated by the 200 and 150 cm. anemometers always appeared to be too small.
(b) The amount of scatter of the various points about the best mean curve was greater than previous experience suggested should be present.
With regard to (a) a possible explanation of the failure of the two highest anemometers to provide a convincing result has already been advanced (para. 6), and the magnitude of the effect can be seen by a study of Fig.5. With regard to (b) it has already been stated that it was found impossible to mount all the anemometers on one mast and they were mounted on a number of masts set out in a line approximately across wind. Examination of even the smoothest natural surface will show irregularities in the ground in the form of small-amplitude 'bumps'. Examination of the sports field surface showed that, since the heights of the individual anemometers were set with reference to the ground at the base of the individual masts, the heights adopted for the mid points of the anemometer cups could well have been in error by ± 2.5 cm. with reference to any one of the heights.

10. In order to examine this point more fully a series of subsidiary experiments was performed in which the velocity profile was investigated in more detail. 15 anemometers were exposed at various heights in the range 200 to 25 cm. on individual masts on the same site, there being two anemometers exposed at the heights of 25, 75 and 100 cm.
A 15 min. run was taken and the anemometers were then interchanged and the experiment repeated. The method of exposure and of interchanging the anemometers together with the results of one of these experiments will be seen in Table 3 and Fig. 2 a. Fig. 2 b is plot of the results given in Table 3 against the logarithms of the heights. The degree of scatter of the points will be seen to reduce very closely to the mean curve drawn

on the figure if a height 'error' of ± 2.5 cm. is allowed. Further it should be noted that the 25 cm. anemometers even when interchanged indicate a higher wind speed in one position, (N), and the anemometer exposed at 30 cm. indicated a wind velocity approximately equal to the mean at the two 25 cm. positions. The same effect can be seen by comparing the results given by the instruments at 100 and 75 cm. These effects are considered to be due to the height errors introduced by the small scale 'bumpiness' of the surface rather than a genuine variation in the mean wind speed from place to place over a short distance (13 m.) during a period of exposure as long as 15 min. It will also be seen that the wind velocities at 200 and 150 m. appear low.

11. The results of the mean wind speed measurements during the drag experiments were plotted against a linear height scale for each observation and the best freehand curve drawn through the points bearing in mind the considerations set out above. Tangents were then constructed to these curves at the heights of 100, 75, 50, 37.5, 25 and 15 cm. and the slopes of the curves ($\partial u/\partial z$) found at these heights.

12. Dry Bulb Temperature Profiles.

The mean air temperature at each height was obtained for the observational period of 15 min. The sensitivity and construction of the apparatus was such that the temperature differences between the temperature bulb at 200 cm. and those at the other heights were obtained to 0.01°F and the absolute temperature of the 200 cm. bulb could be read to 0.1°F. Having found the mean temperature at each height over the period of the observation these were plotted against the height and the best freehand curve drawn through the points. On the majority of occasions the curve was well defined and no difficulty was experienced. However there were a few occasions (observations Nos. 26, 29, 30 and 39), particularly when a substantial and changing amount of cloud was present, when a satisfactory profile could not be drawn. No attempt was made to construct the profile when this was found and the temperatures at 200 cm. and 25 cm. were joined with a straight line which was assumed to represent the gradient of the profile at 75 cm., i.e. the mean logarithmic height. This is equivalent to assuming a logarithmic variation of temperature with height, an assumption which cannot lead to a large error in the gradient at 75 cm. On the other occasions on which the profile was well defined tangents were constructed to the curves at 100, 75, and 37.5 cm. so that the gradient of the curves ($\partial T/\partial z$) at these heights could be measured.

13. The observed values of the wind speed and temperatures are set out in Table 1, together with the values of ($\partial u/\partial z$) and ($\partial T/\partial z$) found in the manner already indicated. The values of the force per unit area of the exposed sample surface, the values of θ the angle between the mean wind and the axis of symmetry of the drag apparatus, the calculated value of the aerodynamic drag per unit area of sample surface, τ_0 , and the Richardson Numbers at the heights of 100, 75, 37.5 cm. (in a few instances at 75 cm. only) form part of Table 2. Fig. 3 shows three examples of the mean wind speed profiles and Fig. 4 three examples of the temperature profiles.

Analysis and discussion of the results.

14. In neutral conditions.

Of the 39 observations set out in the tables 7 were on occasions with a Richardson Number numerically less than 0.01 at 75 cm. The details of these observations have been abstracted from the main tables and set out in Table 4 which also contains values of the ratio u_z/u_{100} together with various other appropriate data. Plots of the individual results show some departure from smooth u, log z profiles and it is intended to discuss these variations later. A plot of the mean values of the ratio show an approximation to a smooth profile if the results above 100 cm. are neglected. (see para. 9). This profile is convex to the u_z/u_{100} axis. If, however, a zero plane displacement (d) is introduced a good approach to a linear profile is obtained with d = 2cm.

As already stated the grass cover had a length of 2 to 3 cm. throughout the experimental period which suggests that the value adopted for d is reasonable. Fig. 5 shows a plot of u_z/u_{100} against log (z-d) for (a) d = 0 and (b) d=2 cm. The equation of the latter line is

$$\frac{u_z}{u_{100}} = \frac{1}{2.76}\left[\log_{10}(z-d) + 0.8\right] \quad \ldots\ldots\ldots\ldots\ldots(4)$$

and this has to be compared with equation 2 arranged in the form

$$\frac{u_z}{u_{100}} = \frac{2.303}{ku_{100}}\left(\frac{\tau_o}{\rho}\right)^{1/2}\left[\log_{10}(z-d) - \log_{10}z_o\right] \quad \ldots\ldots(5)$$

which provides a value of $\underline{z_o = 0.16 \text{ cm.}}$

Further the mean value of $u_{100}/(\tau_o)^{1/2}$ is 4.77×10^2 and if this is associated with the second condition for the identity of equations 4 and 5, namely

$$\frac{2.303}{ku_{100}}\left(\frac{\tau_o}{\rho}\right)^{1/2} = \frac{1}{2.76}$$

we obtain $\underline{k = 0.38}$

The degree of agreement between the laboratory determined value of von Kármán's constant and the value given above is gratifying, but it must be regarded as fortunate having regard to the various difficulties and inaccuracies attendant on field observations of this type. Nevertheless it is considered that the applicability of equation 2 to the lower atmosphere in neutral conditions has now been sufficiently demonstrated since it has been confirmed for two different surfaces having very different roughness characteristics (Pasquill's value of z_o and d were 0.66 cm. and 8.0 cm. respectively, and his determined value of k was 0.37). It must be noted that the mean value of $u_{100}/(\tau_o)^{1/2}$ can vary considerably without having a very marked influence on the corresponding value of k. Indeed, if one plots values of u_{100} against $\tau_o^{1/2}$ and draws two lines through the origin, one such that all the points are below the line and the other such that all the points are above the line, the values of k corresponding to the slopes of the two lines are 0.47 and 0.32 respectively.

15. In stable and unstable conditions.

We are here concerned with the relationship between the aerodynamic drag and the form of the wind profile. Deacon's generalised wind profile law has already been stated (equation 3). By integrating this equation and applying his result that as the ground is approached the stability effect, as represented by the Richardson Number, becomes small owing to the increasing wind gradient Deacon obtained the relationship

$$u_z = \frac{1}{k(1-\beta)}\left(\frac{\tau_o}{\rho}\right)^{1/2}\left[\left(\frac{z}{z_o}\right)^{1-\beta} - 1\right] \quad \ldots\ldots\ldots\ldots\ldots\ldots(6)$$

which, when z is small and β is approximately equal to unity, reduces to equation 1. Now the eddy diffusivity for momentum, K_m, consistent with equation 1 is

$$K_m = k^2z^2\left(\frac{\partial u}{\partial z}\right)_z \quad \ldots\ldots\ldots\ldots\ldots\ldots\ldots\ldots\ldots\ldots\ldots\ldots(7)$$

which, if equation 6 is true, is modified by the factor $\left(\frac{z}{z_o}\right)^{2\beta-2}$ such that

$$K_m = k^2z^2\left(\frac{\partial u}{\partial z}\right)_z\left(\frac{z}{z_o}\right)^{2\beta-2}$$

which re-arranged gives

$$\frac{K_m}{z^2\left(\frac{\partial u}{\partial z}\right)_z} = k^2\left(\frac{z}{z_0}\right)^{2\beta-2} \quad\ldots\ldots\ldots\ldots\ldots\ldots\ldots\ldots(8)$$

in the general case. The eddy diffusivity for momentum, K_m, can be defined by the relationship

$$\tau_0 = \rho K_m \left(\frac{\partial u}{\partial z}\right)_z$$

or

$$K_m = \frac{\tau_0}{\rho\left(\frac{\partial u}{\partial z}\right)_z} \quad\ldots\ldots\ldots\ldots\ldots\ldots\ldots\ldots(9)$$

if constancy of the horizontal shearing stress in the first few metres of the atmosphere is assumed. From equations 7 and 9 we have (for neutral conditions)

$$k^2 = \frac{\tau_0}{\rho z^2\left(\frac{\partial u}{\partial z}\right)^2_z} \quad\ldots\ldots\ldots\ldots\ldots\ldots\ldots\ldots(10)$$

and, if equation 6 holds, in the general case

$$k^2\left(\frac{z}{z_0}\right)^{2\beta-2} = \frac{\tau_0}{\rho z^2\left(\frac{\partial u}{\partial z}\right)^2_z} \quad\ldots\ldots\ldots\ldots\ldots\ldots\ldots\ldots(11)$$

Equation 11 has not been verified explicitly and it is the purpose here to first investigate the variation of the dimensionless quantity $\tau_0/\rho z^2(\partial u/\partial z)^2_z$ with stability and further to see how far the values of β derived from the wind speed profiles will satisfy equation 11.

For the reason indicated above (para. 9) it was decided to use the measurements of wind speed up to 100 cm. in arriving at values of β. There are a number of methods available, the most direct and theoretically satisfactory being to construct tangents to the wind speed profiles as already explained and then to plot graphs of log $(\partial u/\partial z)_z/(\partial u/\partial z)_{z_1}$ against log (z/z_1) which should yield a straight line if the profile is a power law. Further, if the straight line results, the slope of the line provides a value of β. This was done for all the observations and, with the exception of a few doubtful cases, a straight line was clearly indicated [*]. Fig. 6(a) and (b) show some examples of these plots for stable and unstable conditions respectively. It will be noted that all the straight lines drawn on the plots do not pass through the origins of the axes, in spite of the fact that there is no possibility of experimental or other error in determining this point. However, as far as the determination of the slope of a particular plot is concerned, and hence the value of β_1, it is considered that the origin should not be given more weight than any other point. The failure of a line to pass through the origin must be regarded as a result of the presence of experimental and computational error.

A second method, used by Deacon himself, requires a knowledge of the wind speed at three heights. If equation 3 is integrated we obtain

$$u_z = \frac{az^{1-\beta}}{1-\beta} + b \quad\ldots\ldots\ldots\ldots\ldots\ldots\ldots\ldots(12)$$

---

[*] Strictly the z in the equations of para 15 should be replaced by (z-d). This is also true when determining β_1. If this substitution were made the values of all the β_1's would be reduced, but using a value of d of 2 cm. (para. 14) the reduction in the values of the β_1's is insignificant having regard to the errors inherent in the method.

and considering the wind speed u_1, u_2 and u_3, at three heights z_1, z_2 and z_3 respectively it follows that

$$\frac{u_3 - u_2}{u_2 - u_1} = \frac{z_3^{1-\beta} - z_2^{1-\beta}}{z_2^{1-\beta} - z_1^{1-\beta}} \quad \dots\dots\dots\dots\dots\dots(13)$$

The value of the right hand side of 13 was evaluated using values of z = 100 cm, z = 50 cm, and z = 25 cm. for a range of likely values of β, and a curve of these values was constructed against the appropriate values of β. The values of β corresponding to the left hand side of equation 13 found using the observed values of the wind speeds could then be obtained from this curve. It soon became evident that the value of β so obtained was very sensitive to errors in u_2, the wind speed at 50 cm. An example will illustrate this point. Assuming u_{100}, u_{50} and u_{25} to have values of 334, 295 and 258 cm./sec. respectively, which are reasonable values, β takes the value 0.96. If u_{50} is now increased by 1°/₀ the value of β becomes 1.19 and if u_{50} is decreased by 1°/₀ the corresponding value of β is 0.79. Even if the wind speeds are read from the smooth profiles they can hardly be expected to be within more than 1°/₀ of the true values, and with this in mind the method was not pursued further.

A third method is to employ the value of z_o obtained in neutral conditions and substitute it in the equation

$$\frac{u_{100}}{u_{37.5}} = \frac{100^{1-\beta} - z_o^{1-\beta}}{37.5^{1-\beta} - z_o^{1-\beta}} \quad \dots\dots\dots\dots\dots\dots(14)$$

which is derived from equation 6. We already have a value of z_o obtained from the plot of u_z/u_{100} against $\log_{10}(z-d)$ in the neutral case. A further value of z_o may be obtained by plotting the ratio $u_{100}/u_{37.5}$ against the Richardson Number at say, 75 cm., drawing a smooth curve through the points and extracting the value of the ratio appropriate to $Ri_{75} = 0$. This value was found to be 1.172 at Ri = 0 (see Fig. 7) which with equation 1, gave a value of z_o equal to 0.13 to be compared with the value 0.16 found previously. Using the value of $z_o = 0.13$ the right hand side of equation 14 was evaluated for a range of values of β and a curve of β against the ratio $u_{100}/u_{37.5}$ drawn. By combining this curve with that already drawn for the variation of $u_{100}/u_{37.5}$ with the Richardson Number a curve relating β and the Richardson Number was obtained. This is shown as Fig. 8. It should be noted that this method leads to a smoothed variation of β with Richardson Number which results directly from the smoothing introduced in drawing the curve of Fig. 7. It may be thought that the curve of this latter figure could be replaced by another curve which would be as good a representation of the observations. This is true and the general scatter of the points, particularly in very stable conditions, leaves much to be desired.

18. Table 2 contains values of β_1, the β obtained from the first method and of β_2, those obtained as explained immediately above. While the values of β_2 will of necessity follow the Deacon variation of β with stability the same is not true of the β_1, where we have cases of $\beta > 1$ in stable conditions. Further a plot of β_1 against the Richardson Number at 75 cm. shows considerable scatter and indicates that β_1 does not become < 1 until the Richardson Number at that height exceeds +0.04. It is considered that the variations in β_1 are real and not a result of any inability to draw tangents to a curve. Rider and Robinson (1949) working in the height range up to 40 cm. noticed similar departures from the normally accepted variation of β with stability. Indeed Deacon in arriving at the variation of β with stability groups his observations into stability ranges, each group containing from 120 to 6 separate observations (his tables 12 and 13) and gives a mean value of β appropriate to the range. The present writer prefers to consider that,

(a) The wind velocity is invariably proportional to a power of the height.

(b) The index β in the power law, whilst varying with stability in the manner indicated by Deacon over a number of occasions, may, on individual occasions, depart from this normal variation; i.e. the statement

$\beta > 1$ for $Ri < 0$
$\beta = 1$ for $Ri = 0$
$\beta < 1$ for $Ri > 0$

is a mean result not necessarily applicable to any one occasion, and has only a statistical significance.

19. Values of the dimensionless quantity $\tau_o/\rho z^2(\partial u/\partial z)_z^2$ are set out in table 2 for values of z of 100, 75 and 37.5 cm., together with values of the Richardson Number at the three heights. (On a few occasions the Richardson Number at 75 cm. only is given - see para 12 above). These results form the basis of Fig. 9. As can be readily seen there would be a considerable scatter of these points about any smooth curve drawn through them. However there is no doubt that the quantity $\tau_o/\rho z^2(\partial u/\partial z)_z^2$ varies with stability, becoming greater as one passes from stable to unstable conditions, and the variation is of the order of ten times over the range of stability experienced here. The full line in Fig. 9 is a plot of $k^2(z/z_o)^{2\beta_2-2}$ against the Richardson Number using values of $z_o = 0.13$ cm., $z = 75$ cm. and $k = 0.4$. It must be emphasized that the shape of this full line is entirely dependent on the assumed variation of the ratio $u_{100}/u_{37.5}$ (and hence of β_2) with the Richardson Number. On the other hand the plots of $\tau_o/\rho z^2(\partial u/\partial z)_z^2$ are not smoothed in any way and are more closely associated with the individual values of β, β_1, determined for each separate occasion by the tangent drawing method.

20. Pasquill (1949b) in his study of the eddy diffusivity and conductivity near the ground gives observed values of the quantity $-E/z^2\,(\partial\psi/\partial z)_z(\partial u/\partial z)_z$ where $(\partial\psi/\partial z)$ is the gradient of the curve of absolute humidity against height and E is the measured rate of natural evaporation. He found in neutral stability conditions that

$$\frac{-E}{z^2\left(\frac{\partial\psi}{\partial z}\right)_z\left(\frac{\partial u}{\partial z}\right)_z} = \frac{K_v}{z^2\left(\frac{\partial u}{\partial z}\right)_z} = k^2$$

where K_v is the eddy diffusivity for matter (in this case water vapour). Throughout a range of stability the value of $-E/z^2(\partial\psi/\partial z)_z(\partial u/\partial z)_z$ varied in a systematic manner. He was able to obtain values of $k^2(z/z_o)^{2\beta-2}$ using a similar method to that used here to obtain β_2 which, by assuming the validity of equation 6, he set equal to $K_m/z^2(\partial u/\partial z)_z$. His results showed that in unstable conditions there was good agreement between the observed values of

$$\frac{-E}{z^2\left(\frac{\partial\psi}{\partial z}\right)_z\left(\frac{\partial u}{\partial z}\right)_z} = \left[\frac{K_v}{z^2\left(\frac{\partial u}{\partial z}\right)_z}\right]$$

and the computed values of

$$k^2\left(\frac{z}{z_o}\right)^{2\beta-2} = \left[\frac{K_m}{z^2\left(\frac{\partial u}{\partial z}\right)_z}\right]$$

but that in stable conditions a discrepancy appeared which can be regarded as an indication that either

(a) equation 6 and hence equation 11 is not a true representation of the state of affairs in stable conditions of flow

or

(b) the identity $K_m = K_v$ is not true in stable conditions.

Now, if the plot of $k^2(z/z_o)^{2\beta_2-2}$ in Fig. 9 is regarded as a fair representation of the variation of $\tau_o/\rho z^2(\partial u/\partial z)_z^2$ with stability then equation 6 must be regarded as verified. This, considered in conjunction with Pasquill's results, leads to the conclusion $K_m \neq K_v$ in stable conditions.

21. A broken line, representing Pasquill's observed values of $-E/z^2(\partial\psi/\partial z)_z(\partial u/\partial z)_z$ has been added to Fig. 9. It will be seen that this line does not lie along the full line even in unstable conditions as Pasquill's results might lead one to expect since he has shown that

$$\frac{-E}{z^2\left(\frac{\partial\psi}{\partial z}\right)_z\left(\frac{\partial u}{\partial z}\right)_z} = \frac{K_v}{z^2\left(\frac{\partial u}{\partial z}\right)_z} = k^2\left(\frac{z}{z_0}\right)^{2\beta-2}$$

in these conditions. However it must be remembered that Pasquill's observations were made over a much rougher natural surface than those which form the basis of this paper, and the discrepancy between his values of $k^2(z/z_0)^{2\beta-2}$ and those found here may result from the likelihood that there is not one general relationship between β and the Richardson Number which can be applied to all natural surfaces. If there were such a relationship, then for any given Richardson Number there would have to be a relationship between z_0 and β.

22. It is considered that the inaccuracies inherent in the observations and the computation of the results cannot explain all the scatter of the plots of $\tau_0/\rho z^2(\partial u/\partial z)_z^2$ about the curve of $k^2(z/z_0)^{2\beta_2-2}$, and some of this scatter must be regarded as real. If the observations could be repeated with better apparatus the writer believes that the individual determinations of $\tau_0/\rho z^2(\partial u/\partial z)_z^2$ would not lie very much more closely to a smooth curve than those presented above. Indeed this scatter must be regarded as associated with the departure of the wind velocity profile on individual occasions from the normally accepted smooth variation with stability.

References.

Best, A.C. 1935 Geophysical Memoir No. 65.
Deacon, E.L. 1948 Porton Technical Paper No. 39.
Nikuradse, J. 1933 Met. Z. 50,386.
Pasquill, F. 1950 Proc. Roy. Soc. A. 202, 143
Pasquill, F. 1949a Quart. J. R. Met. Soc. 75, 239.
Pasquill, F. 1949b Proc. Roy. Soc. A. 198, 208.
Rider, N.E. 1951 M.R.P. 602.
Rider, N.E. and Robinson, G.D. 1949 M.R.P. 547.
Schlichting, H. 1936 Ingen. Arch. 7, 1.
Sheppard, P.A. 1947 Proc. Roy. Soc. A. 188, 208.

Table 1.

Observation No.		1	2	3	4	5	6	7	8	9	10	11	12	13	14	15	16	17	18	19	20
Date		7/6/50	7/6/50	19/6/50 ---								---19/6/50	20/6/50---		---21/6/50-	1/8/50---					---1/8/50
G.M.T.		2030	2200	1505	1530	1600	1630	1845	2110	2145	2215	2300	1030	1300	1330	1020	1050	1510	1540	1802	1830
Wind Velocity u in cm./sec. at heights z cm.	200	249	270	320	266	315	352	110	97	177	162	90	375	474	389	364	454	209	241	313	159
	150	231	254	311	257	308	340	102	84	170	150	81	360	455	378	351	428	205	238	305	152
	100	220	244	299	240	295	325	93	76	156	138	71	343	429	361	334	407	193	227	290	137
	50	190	218	260	210	258	280	80	60	134	118	55	310	392	320	298	371	164	201	256	116
	37.5	180	204	254	209	254	276	76	58	131	115	54	298	370	311	288	349	162	196	245	109
	25	166	187	223	187	224	243	69	47	108	96	45	262	331	280	258	319	140	175	225	96
	17.5	-	-	222	175	207	229	65	45	104	94	41	255	315	260	236	299	126	160	202	88
	10	-	-	178	146	170	191	50	32	82	73	30	216	266	221	203	254	100	129	171	67
Air Temp. T in °F at heights z cm.	200	66.7	66.8	67.4	71.4	70.5	71.4	66.5	59.8	60.3	59.8	58.8	68.8	62.9	62.9	64.1	65.8	66.2	67.6	66.4	63.6
	150	66.62	66.70	67.56	71.50	70.54	71.45	66.36	59.70	60.22	59.70	58.65	68.93	63.13	63.11	64.24	65.89	66.21	67.66	66.37	63.43
	100	66.48	66.61	67.69	71.58	70.61	71.52	66.23	59.58	60.11	59.53	58.52	69.14	≠	63.15	64.38	66.20	66.06	67.74	66.28	63.17
	50	66.25	66.47	68.28	71.74	70.68	71.71	66.03	59.37	59.87	59.27	58.33	69.51	64.05	63.64	64.63	66.62	65.96	67.97	66.14	62.71
	37.5	66.16	66.45	68.43	71.86	70.72	71.81	65.91	59.26	59.76	59.16	58.23	69.59	64.16	63.68	64.68	66.79	65.86	68.09	66.11	62.50
	25	65.98	66.27	68.64	72.01	70.91	71.90	65.75	59.12	59.57	58.97	58.13	70.27	64.44	64.03	64.87	67.13	65.84	68.56	66.01	62.18
$\frac{(\partial u)}{(\partial z)} \times 10^2$ cm./sec./cm. at heights z cm.	100	39.5	38.7	44.4	39.8	45.2	51.2	22.1	25.2	28.8	29.3	23.5	51.7	60.0	51.0	48.0	62.4	30.4	29.1	43.5	30.6
	75	54.0	57.7	66.0	51.5	64.2	81.7	29.7	30.4	39.2	39.0	28.7	68.3	82.1	72.5	69.7	84.7	57.0	44.5	69.6	42.6
	50	85.2	95.7	102.	79.0	83.2	117.	35.9	40.1	68.8	55.7	36.8	103.	134.	109.	108.	131.	84.0	78.4	97.3	62.1
	37.5	107.	132.	130.	102.	136.	151.	44.6	50.8	91.5	72.2	45.5	140.	188.	146.	148.	178.	113.	113.	131.	79.8
	25	146.	181.	189.	151.	205.	213.	63.5	69.4	140.	110.	67.2	218.	287.	240.	230.	262.	180.	184.	196.	109.
	15	-	-	321.	291.	382.	380.	114.	114.	226.	203.	108.	415.	683.	508.	524.	562.	320.	316.	434.	192.
$\frac{(\partial T)}{(\partial z)} \times 10^4$ °F/cm. at heights z cm.	100	36^+	26^+	72^-	24^-	15^-	24^-	33^+	29^+	34^+	40^+	35^+	54^-	86^-	49^-	37^-	66^-	19^+	26^-	21^+	66^+
	75	45	35	98	37	17	34	44	39	44	50	48	77	97	74	46	77	22	42	26	89
	37.5	90	56	148	124	33	72	107	99	106	97	79	322	121	173	99	185	33	120	54	209

≠ Open circuit in temperature profile apparatus.

Table 1 (continued).

Observation No.		21	22	23	24	25	26	27	28	29	30	31	32	33	34	35	36	37	38	39
Date		1/8/50				8/8/50		10/8/50									10/8/50	11/8/50		11/8/50
G.M.T.		1900	1930	2100	2130	1030	1100	1350	1420	1450	1520	1550	2100	2125	2200	2300	2330	1320	1350	1430
Wind velocity	200	182	102	138	125	370	346	444	364	398	444	416	116	179	183	164	116	478	503	537
u in cm./sec.	150	175	89	129	114	354	332	425	350	381	425	398	100	164	168	149	103	470	494	524
at heights z	100	157	72	115	99	339	317	405	335	362	406	381	87	148	151	133	92	450	474	500
cm.	50	133	52	97	80	293	270	368	304	333	372	351	69	127	130	115	72	405	422	448
	37.5	126	47	92	73	286	267	349	290	312	357	331	67	124	125	110	68	390	408	432
	25	115	40	81	63	259	242	328	270	293	333	312	58	112	113	100	63	356	375	394
	17.5	104	35	74	55	233	218	300	245	266	300	283	46	96	101	89	50	324	341	306
	10	79	26	59	42	182	166	263	220	235	270	250	42	85	86	76	42	278	290	306
Air Temp. T	200	61.8	59.1	57.3	56.2	73.4	74.1	66.2	67.1	67.9	69.7	71.2	54.0	53.8	53.6	53.4	52.6	63.5	63.9	64.1
in °F at	150	61.59	58.83	57.14	56.17	73.61	74.29	66.30	67.31	68.09	69.87	#	53.61	53.67	53.44	53.25	52.38	63.59	63.99	64.20
heights z	100	61.31	58.83	56.92	55.82	73.67	74.40	66.37	67.44	68.13	69.69	71.37	53.29	53.57	53.25	53.13	52.10	63.68	64.06	64.28
cm.	50	60.77	57.79	56.57	55.42	73.61	74.52	66.44	67.56	68.10	69.84	71.62	52.71	53.16	52.88	52.74	51.66	63.81	64.14	64.38
	37.5	60.55	57.50	56.45	55.26	73.57	74.59	66.46	67.64	68.07	69.71	71.72	52.51	53.06	52.74	52.65	51.50	63.86	64.15	64.40
	25	60.22	57.07	56.32	55.00	73.45	74.59	66.48	67.65	67.95	70.15	71.92	52.19	52.67	52.47	52.30	51.20	63.94	64.19	64.46
$(\partial u) \times 10^2$	100	35.1	34.2	30.1	31.8	53.6	51.0	59.9	45.8	50.7	55.0	50.6	30.0	31.8	36.1	32.9	29.5	57.4	58.5	72.6
(∂z)	75	43.5	39.8	37.0	38.4	69.0	73.4	72.6	62.8	62.0	68.3	70.9	33.1	39.6	45.9	42.0	41.2	86.8	91.0	102.
cm./sec./cm.	50	89.8	47.2	47.8	50.4	113.	117.	104.	92.0	101.	90.0	113.	42.2	57.7	60.6	57.6	56.0	136.	142.	163.
at heights z	37.5	79.8	54.7	60.4	66.0	156.	146.	152.	128.	143.	143.	148.	58.9	83.6	81.8	72.2	71.1	176.	204.	212.
cm.	25	127.	72.6	85.0	92.6	224.	225.	285.	192.	261.	288.	216.	79.5	113.	109.	98.0	94.0	276.	352.	323.
	15	237.	109.	152.	151.	441.	477.	454.	428.	446.	510.	427.	114.	177.	186.	151.	116.	588.	670.	544.
$(\partial T) \times 10^4$	100	73^+	93^+	55^+	58^+	-5	-	14^-	30^-	-	-	34^-	97^+	46^+	52^+	45^+	68^+	22^-	15^-	-
(∂z)	75	100	127	68	76	+ 9	56	14	35	3	25	53	104	66	61	65	85	24	15	15
°F/cm. at	37.5	205	234	102	150	+63		15	41			90	194	145	160	145	141	46	27	
heights z																				
cm.																				

Open circuit in temperature profile apparatus.

Table 2.

Observation No.		1	2	3	4	5	6	7	8	9	10	11	12	13	14	15	16	17	18	19	20
Angle θ between Mean Wind and axis of Drag Plate Apparatus. 1st half / 2nd half.		66 / 75	90 / 87	83 / 65	73 / 60	87 / 76	86 / 90	85 / 83	80 / 69	82 / 76	69 / 70	80 / 71	73 / 72	88 / 86	78 / 89	66 / 75	68 / 85	87 / 67	81 / 90	73 / 89	80 / 81
Force on Drag Plate dynes/cm² x 10³ 1st half / 2nd half.		213 / 277	345 / 330	366 / 378	286 / 226	433 / 417	626 / 401	22 / 12	16 / 8	58 / 57	37 / 49	16 / 15	231 / 165	270 / 428	421 / 474	318 / 746	913 / 1110	235 / 144	203 / 210	237 / 443	79 / 59
Mean Drag τ_0 dynes/cm² x 10³		260	338	393	280	431	515	17	13	58	46	16	208	350	452	560	1048	196	208	246	70
$\tau_o/\rho z^2\left(\frac{\partial u}{\partial z}\right)^2_z$ x 10³	100	139	188	166	147	176	163	29	17	58	45	24	65	81	145	203	224	177	205	153	62
at heights	75	132	150	133	156	155	114	29	21	56	45	29	66	77	127	171	216	89	156	106	57
z cm.	37.5	135	115	137	160	138	134	51	30	41	52	46	63	59	126	152	196	91	97	117	65
Richardson No. $\frac{g}{T}\left(\frac{\partial T}{\partial z}+\Gamma\right)\Big/\left(\frac{\partial u}{\partial z}\right)^2$ x 10³		+	+	-	-	-	-	+	+	+	+	+	-	-	-	-	-	+	-	+	+
	100	41	29	70	29	15	18	117	81	65	83	113	38	46	36	32	33	35	61	19	130
at heights	75	28	18	42	27	8	10	88	77	51	60	107	33	24	28	19	21	11	41	9	89
z cm.	37.5	14	5	16	22	6	6	98	71	24	35	71	31	6	15	9	11	4	18	6	61
β_1 from curves of log $(\partial u/\partial z)_z/(\partial u/\partial z)_{50}$ v. log $(z/50)$		1.01	1.21	1.02	1.05	1.18	1.01	0.82	0.72	1.10	0.97	0.78	1.03	1.15	1.11	1.08	1.06	1.01	1.24	1.02	0.96
β_2 from curve of β v. Richardson No. at 75 cm.		0.97	0.98	1.05	1.03	1.01	1.01	0.86	0.89	0.93	0.92	0.84	1.04	1.03	1.04	1.02	1.03	0.99	1.05	0.99	0.87
$k^2\left(\frac{z}{z_o}\right)^{2\beta_2-2}$ x 10⁴	100	1074	1227	3110	2384	1827	1827	254	371	631	554	191	2668	2384	2668	2086	2384	1401	3110	1401	284
at heights	75	1092	1241	3021	2343	1818	1818	270	395	657	579	209	2589	2343	2589	2063	2343	1409	3021	1409	306
z cm.	37.5	1140	1276	2819	2248	1793	1793	356	461	724	646	261	2517	2248	2517	2006	2248	1429	2819	1429	367

Table 2 (continued).

Observation No.		21	22	23	24	25	26	27	28	29	30	31	32	33	34	35	36	37	38	39
Angle θ between Mean Wind and axis of Drag Plate Apparatus. 1st half / 2nd half.		89 / 81	73 / 77	66 / 69	84 / 79	77 / 83	82 / 76	83 / 80	81 / 76	89 / 80	69 / 73	85 / 76	80 / 66	75 / 81	83 / 84	76 / 74	80 / 70	89 / 78	78 / 76	76 / 77
Force on Drag Plate dynes/cm² x 10³ 1st half / 2nd half.		40 / 73	13 / 8	30 / 25	38 / 48	477 / 243	477 / 432	1050 / 1020	656 / 766	877 / 784	1100 / 1130	1450 / 991	13 / 19	59 / 83	65 / 65	95 / 66	32 / 17	1050 / 1020	656 / 766	1340 / 1150
Mean Drag τ_o dynes/cm² x 10³		67	11	30	44	367	464	1050	727	837	1180	1240	17	72	65	83	25	1050	730	1210
$\tau_o/\rho z^2\left(\frac{\partial u}{\partial z}\right)^2$ x 10³	100	45	8	28	36	106	149	244	289	271	325	404	16	59	42	64	24	266	178	191
at heights	75	53	10	31	44	114	127	295	274	323	375	366	18	68	46	70	22	207	131	172
z cm.	37.5	62	22	49	60	89	129	271	264	243	342	337	29	61	58	95	30	201	104	160
Richardson No.		+	+	+	+		−	−	−	−	−	−	+	+	+	+	+	−	−	−
$\frac{g}{T}\left(\frac{\partial T}{\partial z}+\Gamma\right)\Big/\left(\frac{\partial u}{\partial z}\right)^2$ x 10³	100	109	145	110	101	−4		8	28			27	203	82	74	76	147	13	9	
at heights	75	99	150	92	95	+3	20	6	17	3	11	20	179	78	58	68	93	6	4	3
z cm.	37.5	60	147	53	65	+5		1	6			8	106	39	45	53	53	3	1	
β_1 from curves of $\log(\partial u/\partial z)_z/(\partial u/\partial z)_{50}$ v. $\log(z/50)$		0.92	0.53	0.86	0.77	1.11	1.02	1.10	1.16	1.21	1.18	1.04	0.81	0.94	0.86	0.79	0.85	1.08	1.22	1.05
β_2 from curves of β v. Richardson No. at 75 cm.		0.86	0.71	0.86	0.86	1.00	1.03	1.01	1.02	1.01	1.01	1.03	0.56	0.89	0.92	0.90	0.86	1.01	1.01	1.00
$k^2\left(\frac{z}{z_o}\right)^{2\beta_2-2}$ x 10⁴	100	249	34	249	249	1600	2384	1827	2086	1827	1827	2384	5	371	554	423	249	1827	1827	1600
at heights	75	270	40	270	270	1600	2343	1817	2064	1817	1817	2343	6	395	579	449	270	1817	1817	1600
z cm.	37.5	238	60	328	328	1600	2248	1792	2006	1792	1792	2248	11	460	646	515	328	1792	1792	1600

Table 3.

Results of Two Wind Velocity Profile Determinations over 15 min. at Downing College Sports Ground

Position across wind (see Fig. 2a)	Height (cm.)	Run 1. Anemometer No.	Run 1. Wind velocity (cm/sec.)	$u_z/u_{100}(C)$	Run 2. Anemometer No.	Run 2. Wind Velocity (cm/sec.)	$u_z/u_{100}(C)$	Mean u_z/u_{100}
A	200	1	491	1.128	10	472	1.124	1.126
B	150	2	449	1.032	11	437	1.041	1.037
C	100	3	435	1.000	4	420	1.000	1.000
D	100	4	439	1.009	3	425	1.012	1.011
E	80	5	400	.912	12	402	.957	.935
F	75	6	395	.908	7	382	.910	.909
G	75	7	404	.929	6	394	.938	.934
H	70	8	400	.912	13	392	.933	.923
I	60	9	378	.869	9	369	.879	.874
J	50	10	369	.848	1	370	.881	.865
K	40	11	353	.812	2	357	.843	.828
L	37.5	12	347	.798	5	333	.793	.796
M	30	13	306	.703	8	300	.714	.709
N	25	14	310	.713	15	299	.712	.713
O	25	15	306	.703	14	292	.695	.699

Table 4.

Results in Near Neutral Conditions (Downing College Sports Ground)

Observation No.	θ 1st. half/2nd. half	u_{100} cm/sec	u_z/u_{100} Height z in cm. 200	150	100	50	37.5	25	17.5	10	τ_0 dynes/cm^2	Temp at -400 cm °F.	$\frac{u_{100}}{100\tau_0^{1/2}}$	$10^3 R_{75}$
5	87/76	295	1.068	1.043	1.000	.875	.861	.739	.702	.576	.43	70.6	4.50	-8
19	73/89	290	1.078	1.051	1.000	.883	.845	.776	.697	.590	.35	66.1	4.90	+9
25	77/83	339	1.092	1.044	1.000	.864	.844	.764	.688	.537	.37	73.7	5.57	+3
27	83/80	405	1.096	1.050	1.000	.908	.862	.810	.741	.650	1.05	66.4	3.95	-6
37	89/78	450	1.062	1.044	1.000	.900	.867	.792	.720	.618	1.05	63.7	4.39	-6
38	78/76	474	1.061	1.042	1.000	.892	.861	.791	.720	.612	.73	64.1	5.55	-4
39	76/77	500	1.073	1.047	1.000	.896	.864	.788	.718	.612	1.21	64.3	4.55	-3
Means			1.076	1.046	1.000	.888	.858	.783	.712	.599			4.77	-2

$\rho = 1.2 \times 10^{-3}$ gm./cm^3 throughout

FIG. 1.
EXAMPLES OF RECORDS FROM DRAG PLATE APPARATUS

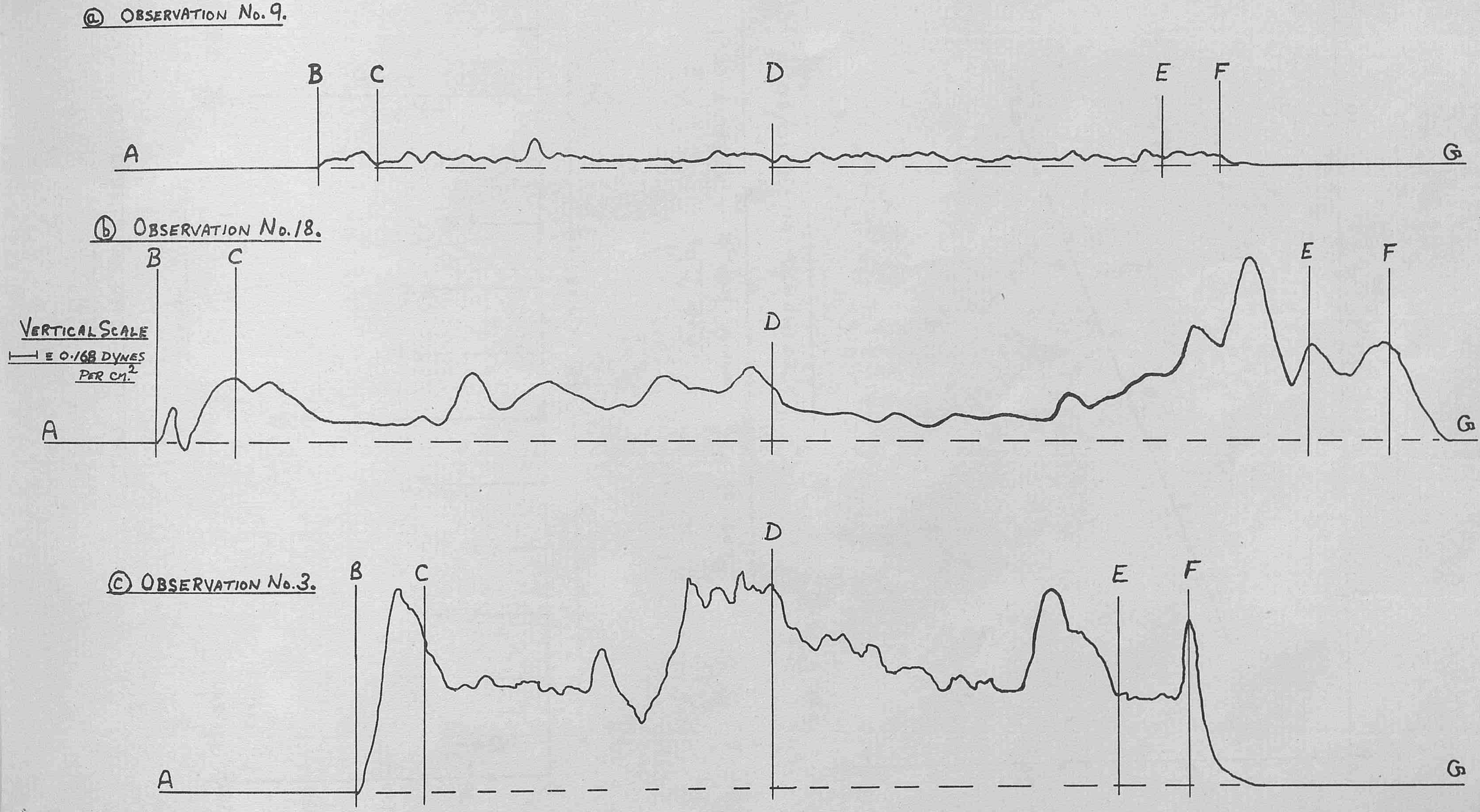

FIG 2 a.

METHOD OF EXPOSURE OF ANEMOMETERS

ACROSS WIND.

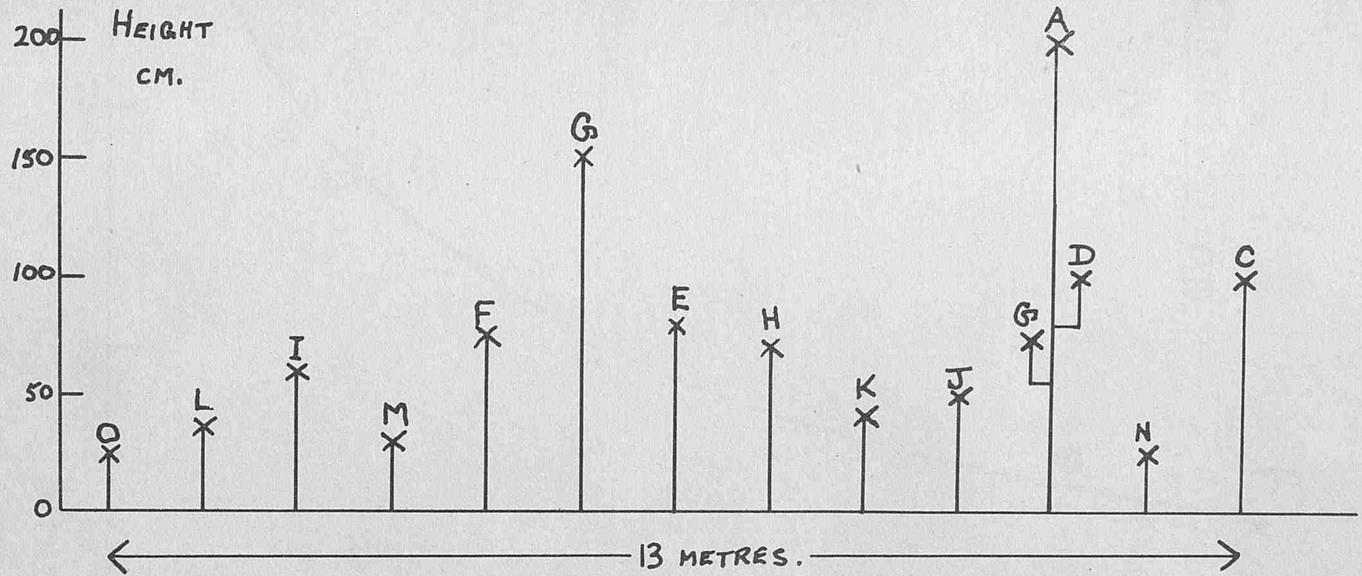
HEIGHT
CM.
200
150
100
50
0
O
L
I
M
F
G
E
H
K
J
G
A
D
N
C
13 METRES.

FIG 2 b.

PLOT OF u_z/u_{100} AGAINST $\log_{10} z$ — RESULTS OF TWO EXPERIMENTS ON 4/10/50

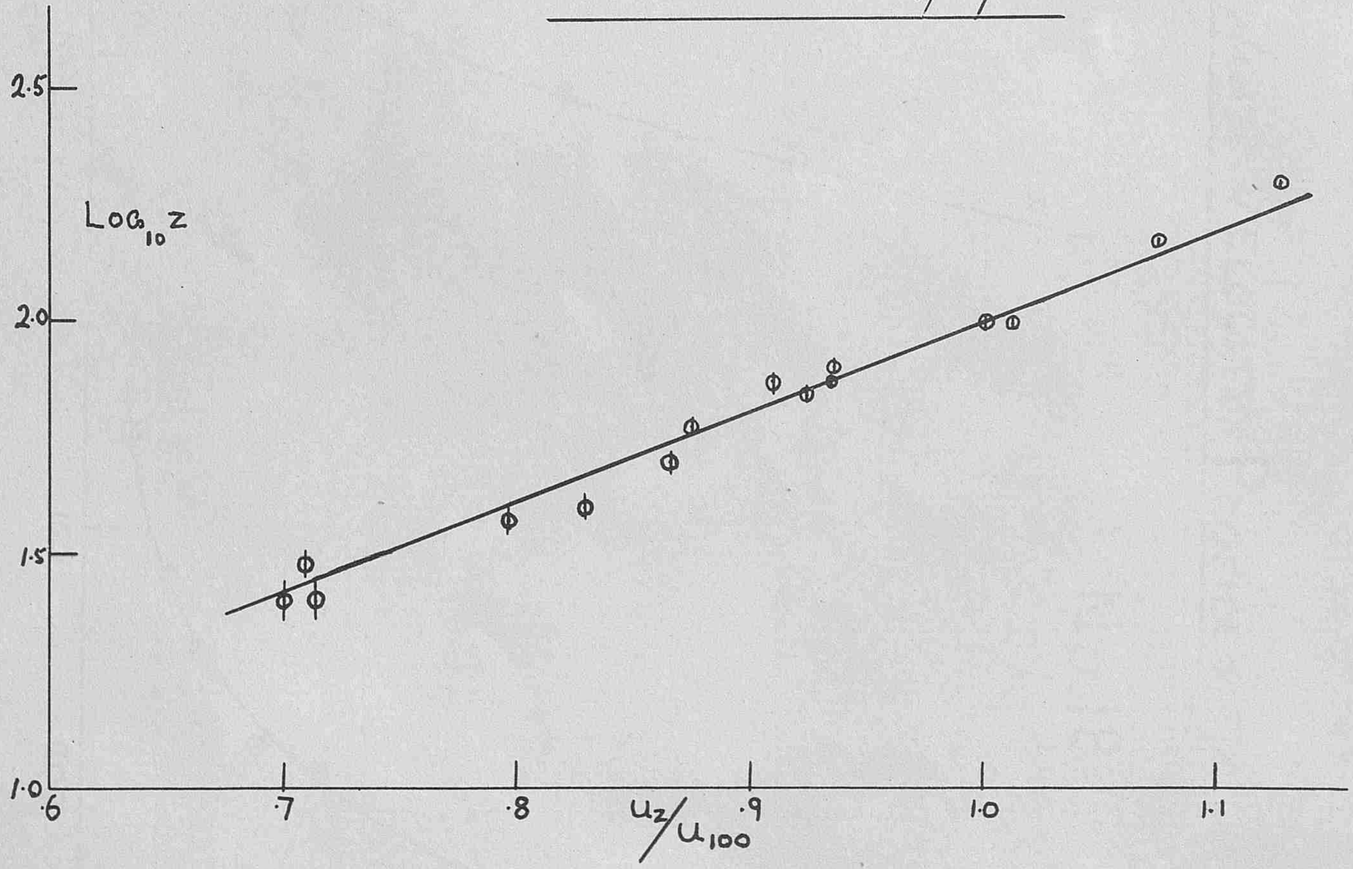

FIG. 3.

EXAMPLES OF WIND VELOCITY PROFILES

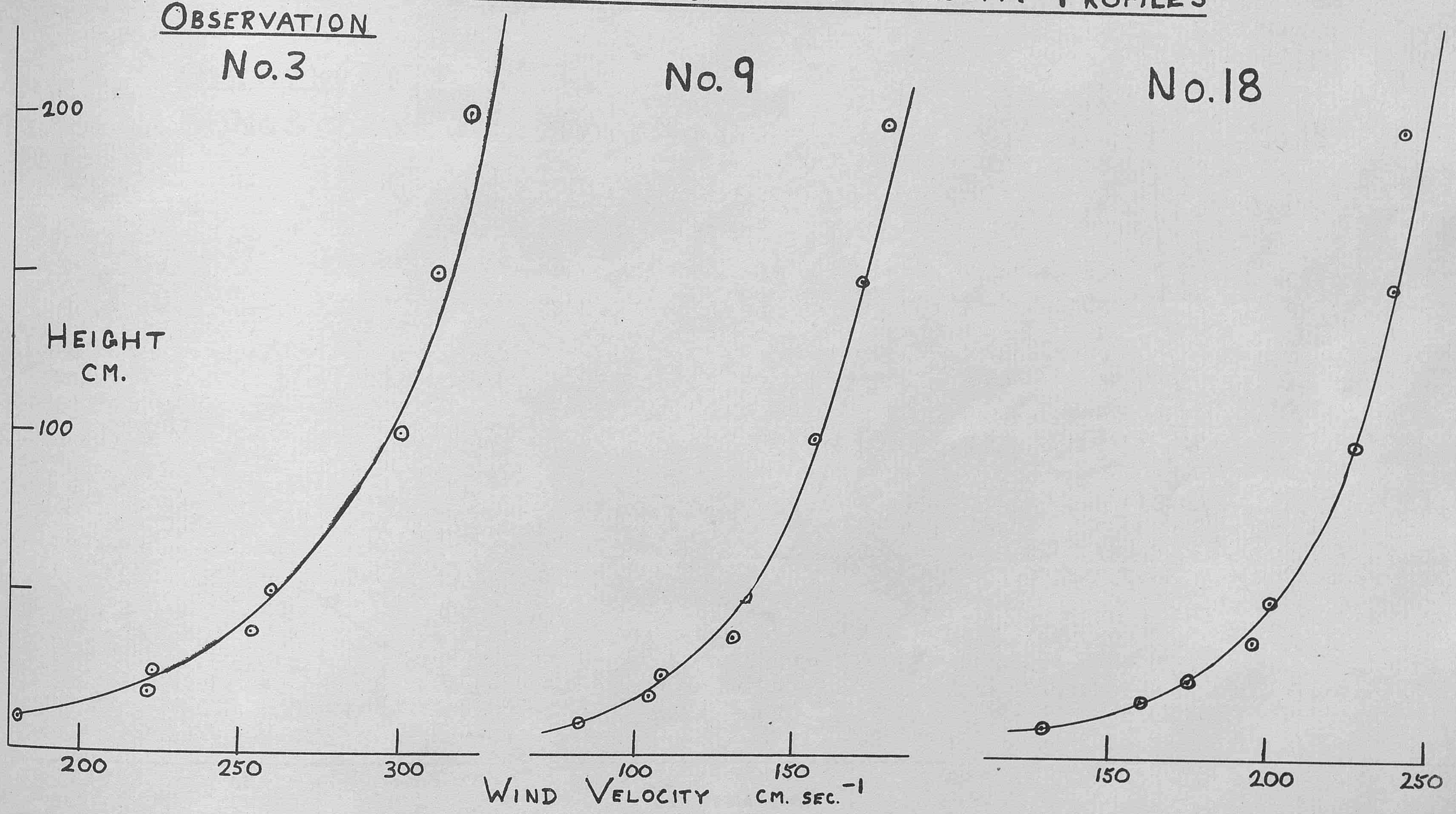

FIG 4.

EXAMPLES OF AIR TEMPERATURE PROFILES

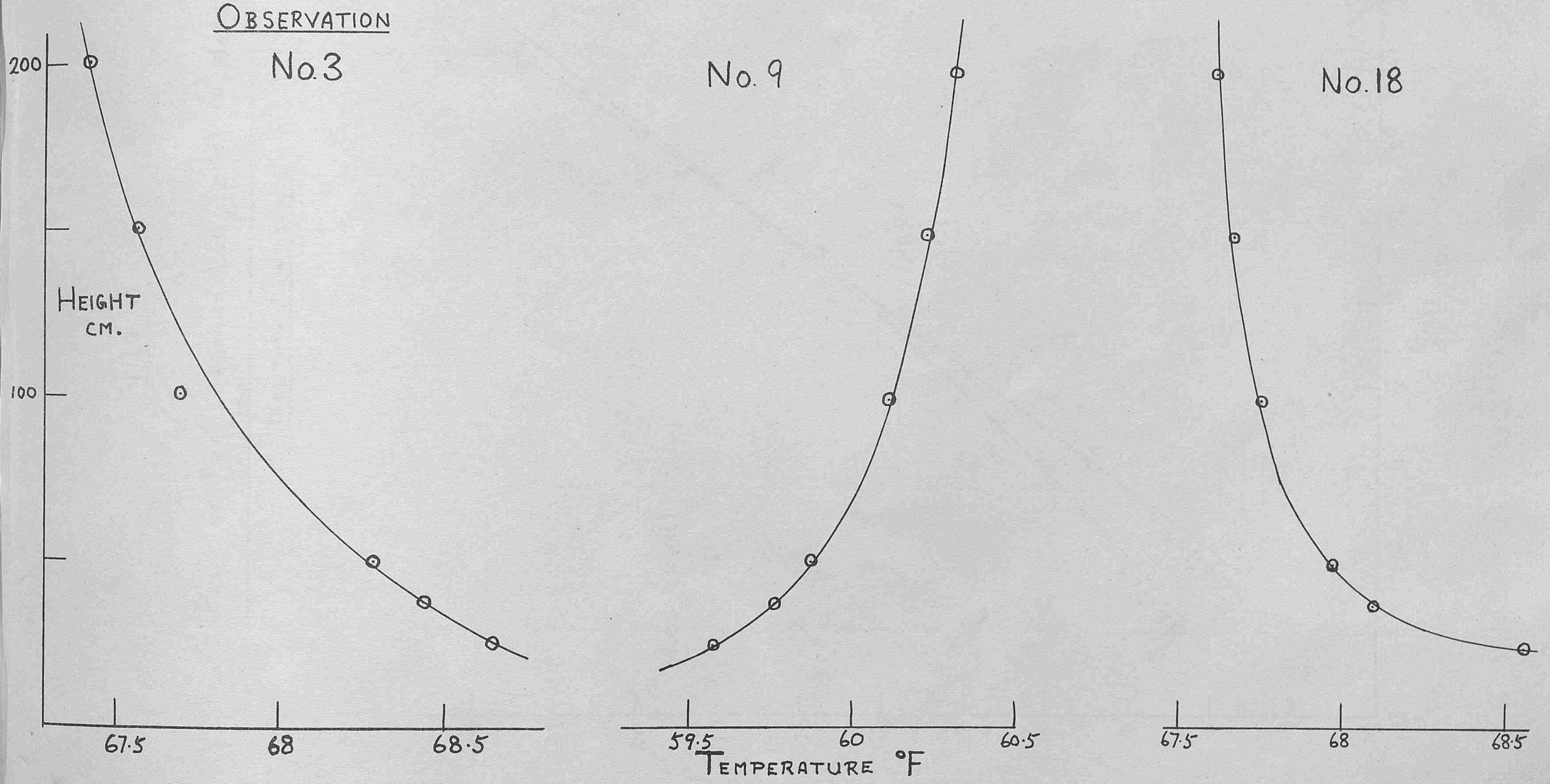

FIG. 5

PLOT OF u_z/u_{100} AGAINST $\text{LOG}_{10}(z-d)$ IN NEAR NEUTRAL CONDITIONS

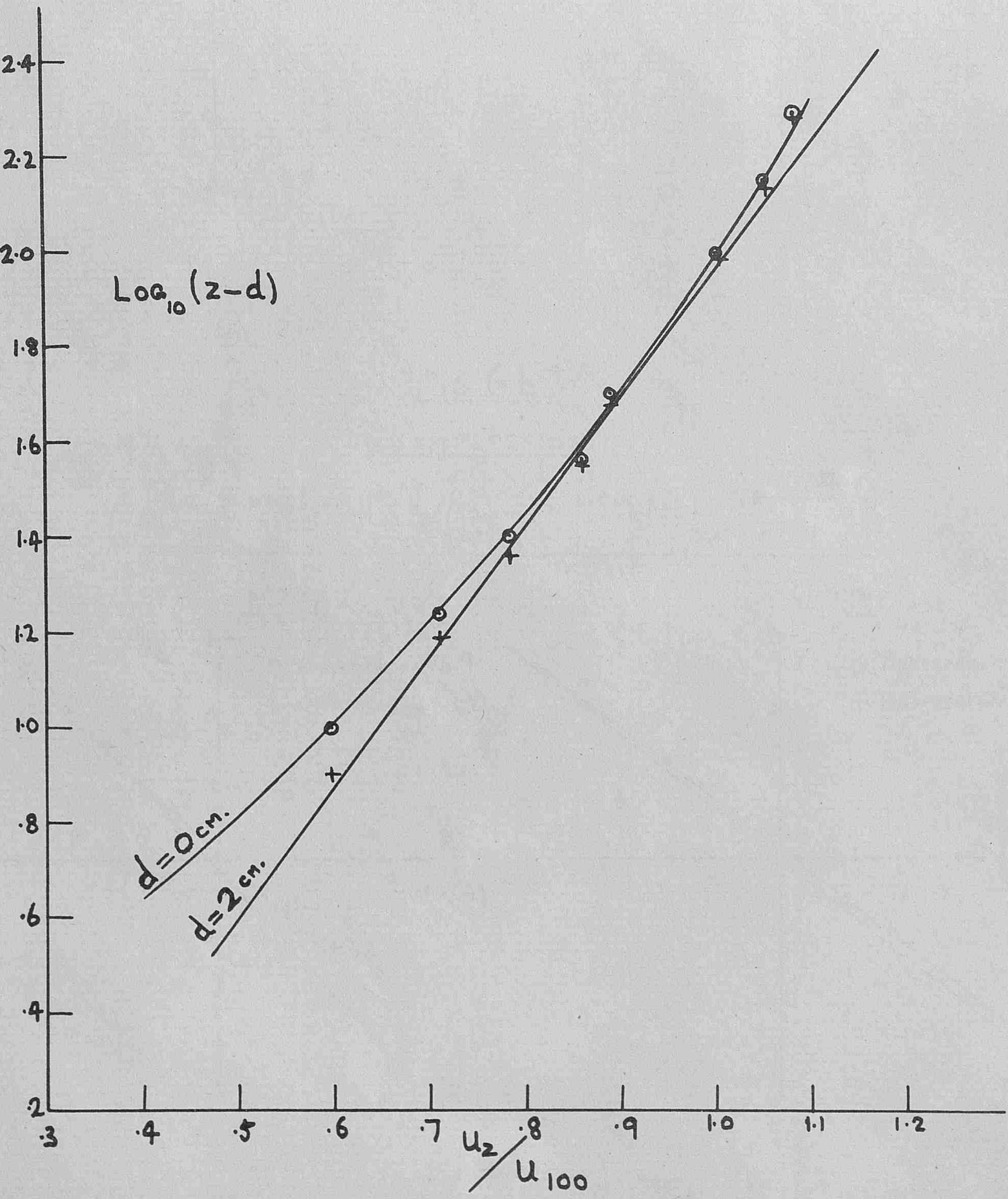

FIG. 6a.

EXAMPLES OF

PLOTS OF $\mathrm{LOG}_{10}\left(\frac{\partial u}{\partial z}\right)_z \Big/ \left(\frac{\partial u}{\partial z}\right)_{50}$ v. $\mathrm{LOG}_{10}\left(\frac{z}{50}\right)$ FOR $Ri < 0$

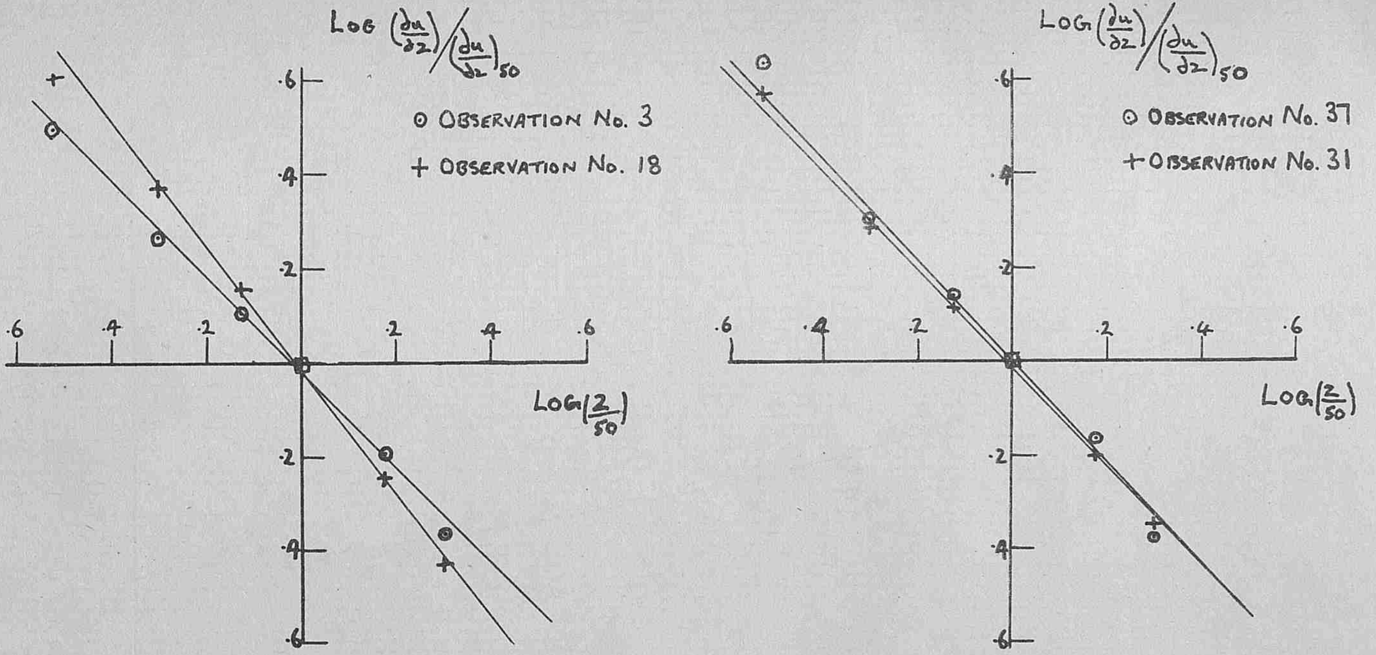

FIG. 6b.

EXAMPLES OF

PLOTS OF $\mathrm{LOG}_{10}\left(\frac{\partial u}{\partial z}\right)_z \Big/ \left(\frac{\partial u}{\partial z}\right)_{50}$ v. $\mathrm{LOG}_{10}\left(\frac{z}{50}\right)$ FOR $Ri > 0$

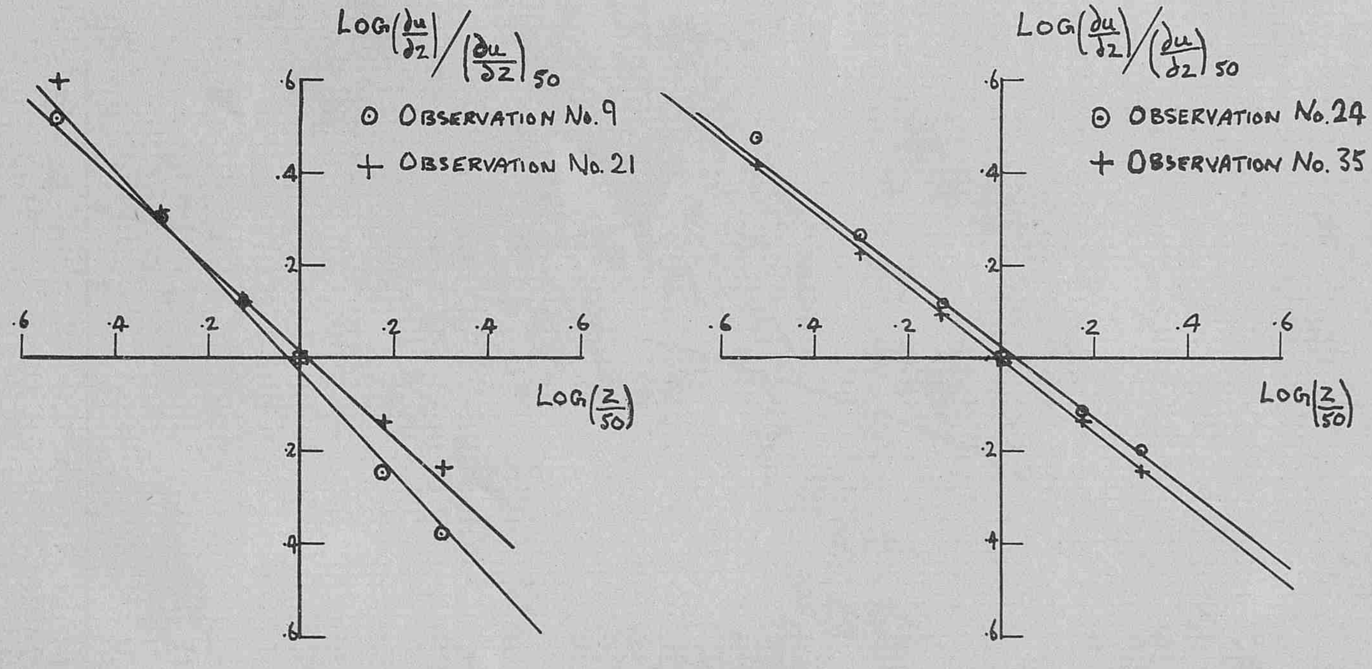

FIG. 7

PLOT OF THE RATIO $u_{100}/u_{37.5}$ AGAINST THE RICHARDSON NUMBER AT 75 CM.

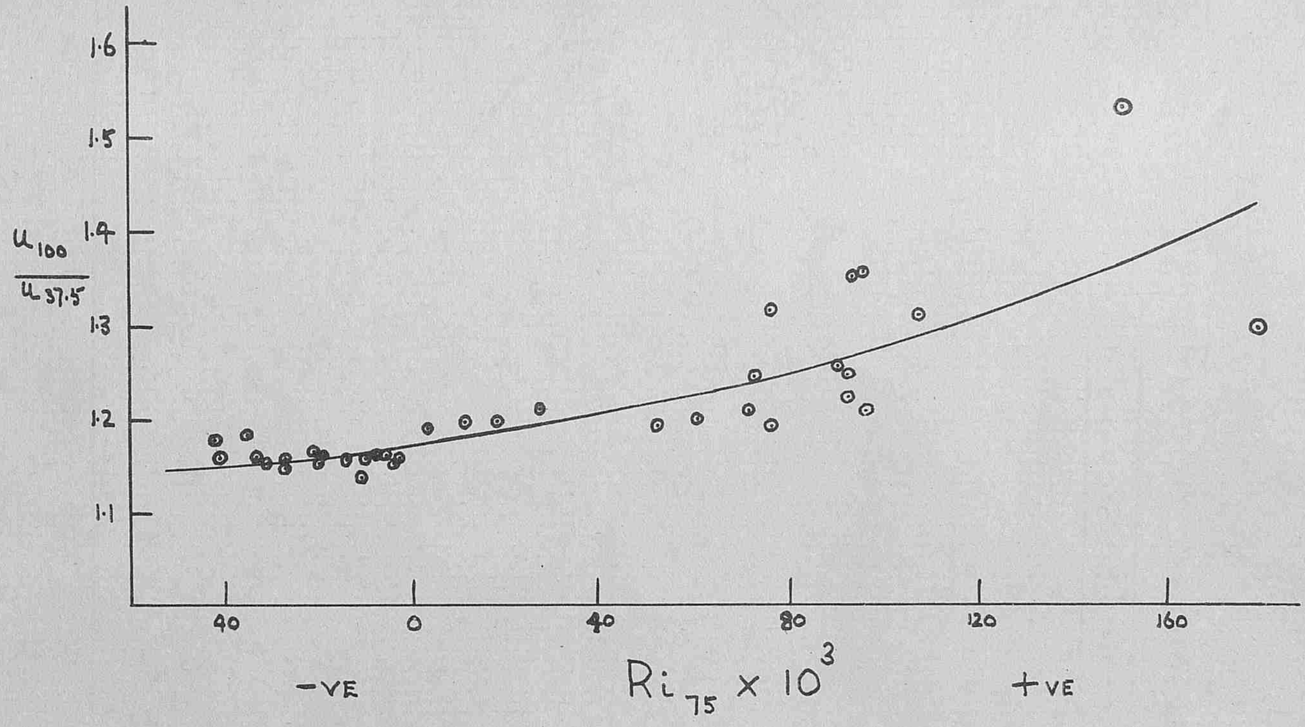

FIG. 8

VARIATION OF β_2 WITH RICHARDSON NUMBER AT 75 CM.

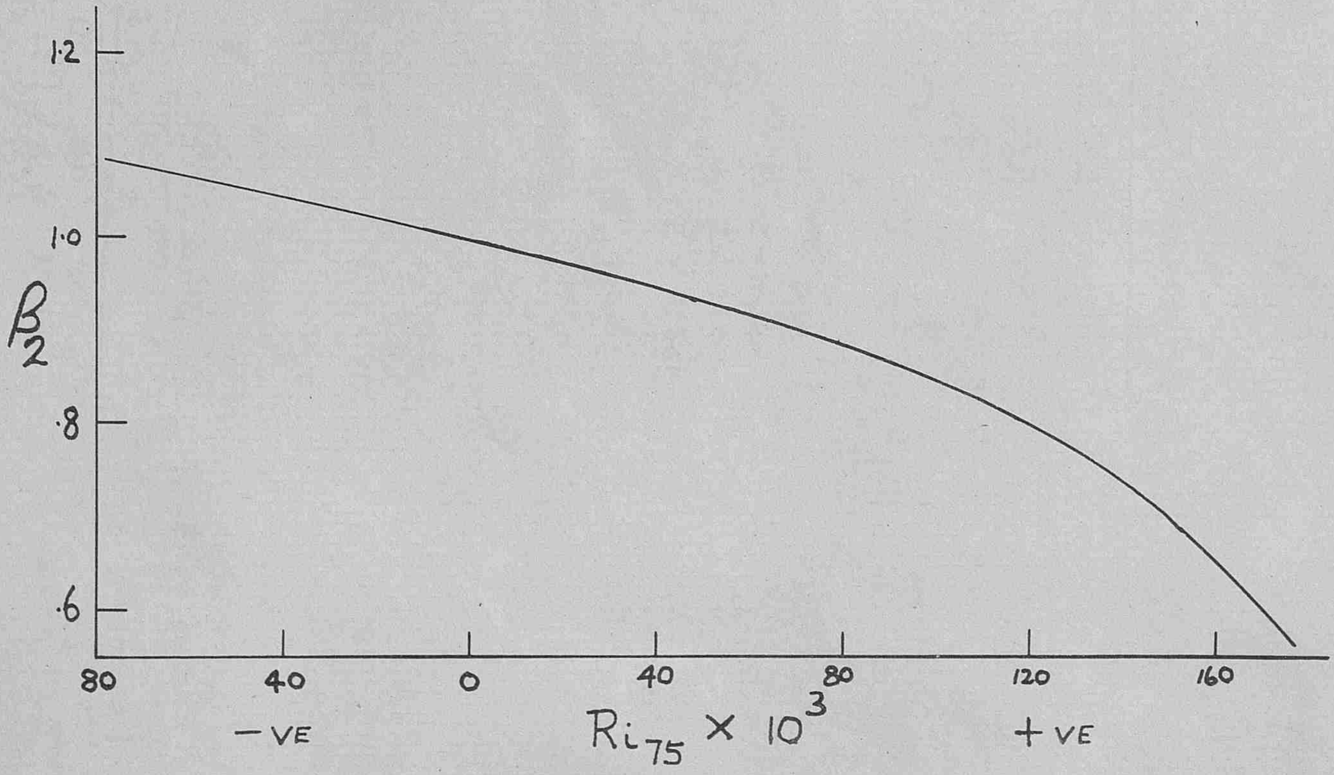

FIG. 9

PLOT OF THE DIMENSIONLESS QUANTITY $\tau_0 / \rho . z^2 . \left(\frac{\partial u}{\partial z}\right)_z^2$ AGAINST THE RICHARDSON NUMBER FOR $Z = 100, 75,$ AND 37·5 CM.

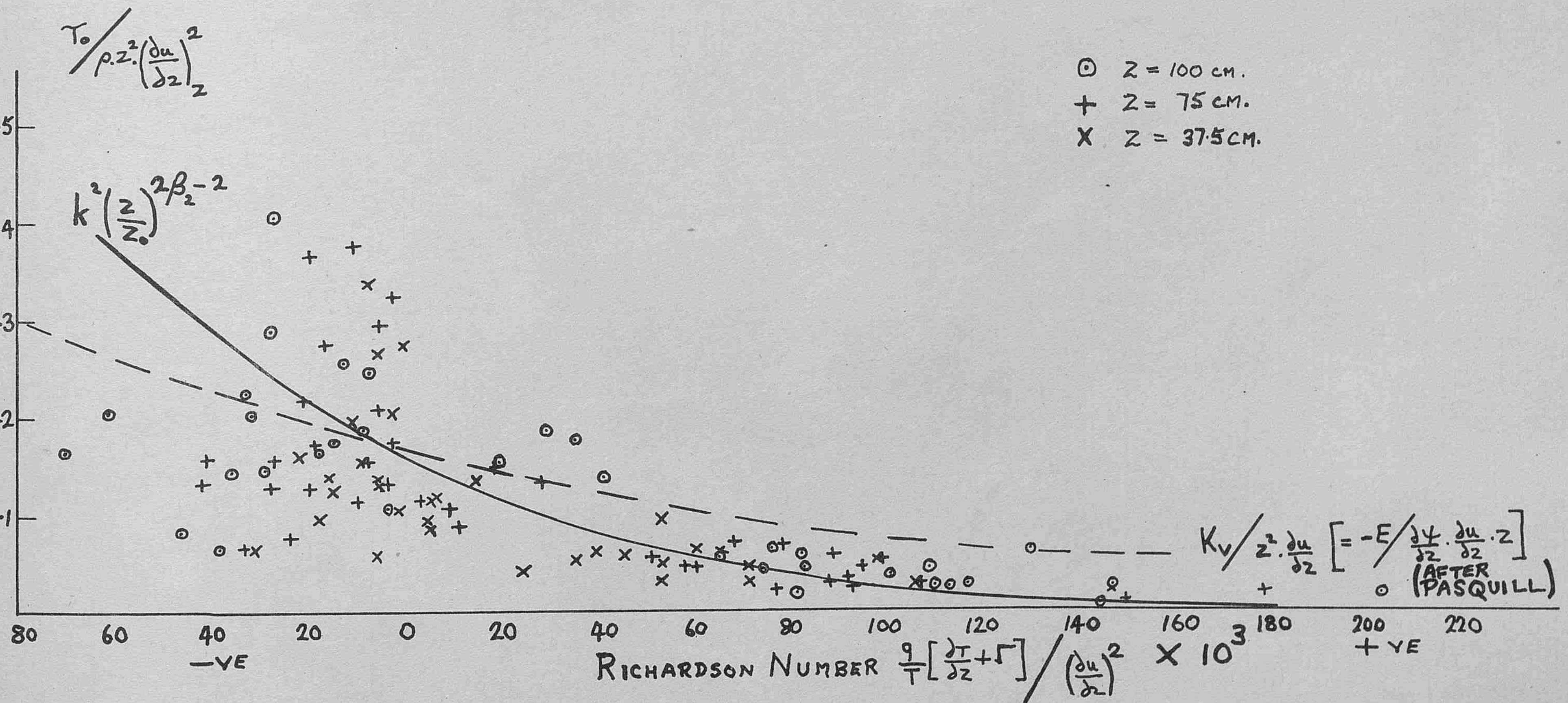

been published. Any author desiring to quote this paper should refer to it as "A paper of the Meteorological Research Committee (London), M.R.P. No........... by Mr.......................... A copy is available in the Library of the Meteorological Office."

AF323744

M.R.P. 627
S.C.III/90
6th February, 1951.

AD 223 008

AW

AIR MINISTRY

METEOROLOGICAL RESEARCH COMMITTEE

Effect of turbulence on drop size distribution in cloud.

by

A. C. Best.

(Meteorological Office)

AIR WEATHER SERVICE
TECHNICAL REFERENCE FILES
AUG 3 1951

mata-2

Summary.

With the assumption that drop size distribution in a cloud is governed by rate of condensation on the drops in the cloud and rate of turbulent diffusion of the drops out of the cloud it is shown that the fractional volume of water comprised by drops smaller than a specified size is expressible in terms of an Incomplete Gamma function. In this Incomplete Gamma function the argument is 1.5 and the upper limit to the integral varies as the square of the drop size and is also proportional to a quantity which depends upon the degree of turbulence and upon parameters connected with the rate of condensation. It is shown that this theoretical formula approximates closely to a simpler formula already established empirically and that reasonable values for the coefficient of turbulence and the condensation parameters lead to a mean drop size which agrees closely with measured values.

1. Introduction.

In an earlier paper (Best, 1950 (a)) it was shown that the average size of cloud particles is consistent with the assumption that this size is determined by the condensation processes operating for the average time during which an individual cloud droplet remains in the cloud before being ejected under the influence of turbulent diffusion. In a second paper (Best, 1950 (b)) it was shown that measured drop size distributions in cloud conform with reasonably close approximation to the formula

$$1 - F = \exp\left(-(x/b)^n\right) \quad \ldots\ldots\ldots\ldots\ldots\ldots\ldots(1)$$

where F is the fraction of liquid water comprised by drops having diameter less than x and b and n are constants. The value found empirically for the distributive index n was 3.20; the value of the scale diameter b was of the order 20μ but varied with the liquid water content of the cloud. It is a natural sequel to this work to consider whether the turbulent diffusion and the condensation processes can explain the form of the drop size distribution formula found empirically.

2. The differential equation.

Consider a cloud layer which is uniform in the horizontal direction. At any point in the cloud denoted by the vertical coordinate z let the number of drops per unit volume and with radius between r and $r+\Delta r$ be $f(r,z)\Delta r$ or, more shortly, $f\ \Delta r$.

If we neglect sedimentation the factors which govern f are

(a) All drops are growing by condensation so that drops within the range r to $r+\Delta r$ tend to grow out of this range and smaller drops tend to grow into it.

(b) f varies with distance from the (horizontal) boundary surface of the cloud. Accordingly turbulent diffusion is continuously transporting drops of all sizes from inside the cloud to the boundary and thence into the clear air where they evaporate.

When a steady state has been reached the loss of drops in any one size class by diffusion and growth out of the class must be balanced by growth of drops into the same class by condensation.

The condensation processes are described by the equation (see e.g. Fuchs, 1934)

$$r\frac{\partial r}{\partial t} = G \quad \ldots\ldots\ldots\ldots\ldots\ldots\ldots\ldots\ldots(2)$$

where

$$G = \frac{MD}{R\theta}(hp_a - p') \quad \ldots\ldots\ldots\ldots\ldots(3)$$

r = drop radius.
M = molecular weight of water (18).
D = coefficient of diffusion of water vapour in air ($cm^2\ sec^{-1}$).
R = gas constant per gram molecule ($= 8.314\ 10^7$ erg $deg^{-1}\ mol^{-1}$).
θ = absolute temperature.
$(hp_a - p')$ = vapour pressure excess of water in atmosphere over drop.

For convenience we shall write $(hp_a - p') = sp_\theta$ where p_θ is the saturation vapour pressure at temperature θ.

Thus G is independent of r and we shall also assume that it is independent of z.

In a small time Δt the number of drops, originally smaller than r, which grow sufficiently to enter the r class is the number of drops with radius between r and $r - \frac{\partial r}{\partial t}\Delta t$, i.e. $f\frac{\partial r}{\partial t}\Delta t$. Similarly the number which grow bigger than $r + \Delta r$ is $(1 + \Delta r\frac{\partial}{\partial r})(f\frac{\partial r}{\partial t}\Delta t)$. Thus the number per unit volume lost to the r class is $\Delta r\frac{\partial}{\partial r}(f\frac{\partial r}{\partial t})\Delta t$ and the rate of loss is $\Delta r\frac{\partial}{\partial r}(f\frac{\partial r}{\partial t})$. But we have seen in equation 2 that $\partial r/\partial t = G/r$ where G is independent of r so that the rate of loss of drops from the r class is $\Delta r\frac{\partial}{\partial r}(\frac{fG}{r})$.

If we regard the r class drops as constituting a cloud the density (grams/cm^3) of the suspended matter will be $4\pi r^3\sigma f\Delta r/3 = \rho$ say (where σ is density of water $= 1$) and we have

$$\frac{\partial\rho}{\partial t} = -\frac{4}{3}\pi r^3\sigma\ \Delta r\frac{\partial}{\partial r}\left(\frac{fG}{r}\right) \quad \ldots\ldots\ldots\ldots\ldots(4)$$

to represent the effect of the condensation processes only upon ρ.

The density of the cloud of r class particles varies from the centre of the cloud to the boundary because f varies. Let us measure z from the centre of the cloud towards the boundary. Then in the usual way by considering an elementary volume composed of two areas dA perpendicular to the z direction and separated by a distance dz we have

$$\text{Rate of mass transfer across first area} \quad = \quad - K \frac{\partial\rho}{\partial z} dA$$

where K is the usual eddy coefficient of diffusion and has a value about 10^5 cm^2 sec^{-1}. Similarly the rate of transfer across the second area is $- K(1 + \frac{\partial}{\partial z} dz) \frac{\partial\rho}{\partial z} dA$ and the rate of loss of mass from the elementary volume is $- K \frac{\partial^2\rho}{\partial z^2} dz\, dA$. The rate of gain of density is $K\, \partial^2\rho/\partial z^2$ or $K \frac{4}{3} \pi r^3 \sigma \Delta r \frac{\partial^2 f}{\partial z^2}$. This is the effect of turbulent diffusion upon ρ and combining with equation 4 we find that in the steady state

$$K \frac{\partial^2 f}{\partial z^2} \quad = \quad G \frac{\partial}{\partial r}\left(\frac{f}{r}\right) \quad \ldots\ldots\ldots\ldots\ldots\ldots\ldots(5)$$

3. Solution of the equation.

Equation 5 is the differential equation for f as a function of z and r. The boundary conditions which any solution must satisfy are

(a) $f = 0$ when $r = \infty$
(b) $f = 0$ when $z = l$ where l is the semi thickness of the cloud.
(c) $\partial f/\partial z = 0$ when $z = 0$.

and of course the solution must be intuitively reasonable.

Suppose we put

$$f \quad = \quad \phi(r)\, \psi(z)$$

Then ϕ and ψ must satisfy

$$\frac{1}{\psi} \frac{\partial^2\psi}{\partial z^2} \quad = \quad \frac{G}{K} \frac{1}{\phi} \frac{\partial}{\partial r} \left(\frac{\phi}{r}\right) \quad \ldots\ldots\ldots\ldots\ldots\ldots\ldots(6)$$

Put each side of equation 6 equal to $-A^2$ where A is a constant. The solution of

$$\frac{\partial^2\psi}{\partial z^2} \quad = \quad - A^2 \psi$$

is $\qquad \psi \quad = \quad B \cos Az + C \sin Az$

where B and C are constants. The boundary conditions give

$$0 \quad = \quad B \cos Al + C \sin Al$$
$$0 \quad = \quad C A$$

whence $C = 0$ and $Al = (2p + 1)\, \pi/2$ where p is an integer. Strictly we now need another boundary condition in z in order to complete the solution. It is not easy to see what other boundary condition could be formulated without assuming some knowledge of the constitution of the cloud. However physically it seems reasonable to assume that ψ decreases steadily as z varies from 0 to l and as a first approximation we therefore restrict the solution to $p = 0$ giving $A = \pi/2l$ and thus

$$\psi \quad = \quad B \cos \frac{\pi z}{2l}$$

We then have from equation 6

$$- \frac{\pi^2}{4l^2} \quad = \quad \frac{G}{K} \frac{1}{\phi} \frac{\partial}{\partial r} \left(\frac{\phi}{r}\right)$$

The solution to this equation is

$$\phi \quad = \quad H\, r \exp(- K\pi^2 r^2/8l^2 G)$$

where H is a constant. Thus the full solution of equation 5 is

$$f = J \cos \frac{\pi z}{2l}\, r \exp(-Qr^2) \quad \ldots\ldots\ldots\ldots\ldots(7)$$

where

$$Q = K\pi^2/8Gl^2 \quad \ldots\ldots\ldots\ldots\ldots\ldots\ldots\ldots\ldots\ldots(8)$$

and J is an undetermined constant.

4. Cumulative size distribution of drops.

If the drop size distribution is described by equation 7 then at any point in the cloud the amount of water per unit volume comprised by drops having radius less than r

$$= J \cos \frac{\pi z}{2l} \frac{4\pi}{3} \int_0^r r^4 e^{-Qr^2}\, dr$$

and the total amount of water per unit volume is represented by a similar expression but with the upper limit in the integral replaced by infinity. Thus the fraction of liquid water comprised by drops with radius less than r is

$$F = \int_0^r r^4 e^{-Qr^2}\, dr \Bigg/ \int_0^\infty r^4 e^{-Qr^2}\, dr$$

Making the substitution $Qr^2 = v$ we then get

$$F = \frac{\int_0^{Qr^2} v^{3/2} e^{-v}\, dv}{\Gamma(2.5)} \quad \ldots\ldots\ldots\ldots\ldots\ldots\ldots\ldots(9)$$

5. Comparison between the Incomplete Gamma Function and empirical formula for drop size distribution.

In Pearson's tables (Pearson 1946) the function I(u,p) is tabulated against u and p where

$$I(u,p) = \frac{\int_0^{u\sqrt{p+1}} e^{-v} v^p\, dv}{\Gamma(p+1)}$$

From these tables $\log \log_{10}(1/(1 - I))$ has been plotted against $\log_{10} u$ for $p = 1.5$. The result is shown in the figure. It is clear that the points represented by circles (and which cover values of I from I = 0.1 to 0.9) approximate reasonably closely to a straight line. The straight line drawn in the figure has been computed from these points by the method of least squares and yields the equation

$$\log \log_{10}(1/(1 - I)) = 1.770 \log_{10} u - 0.7875 \quad \ldots\ldots(10)$$

We may identify the F in equation 9 with the I in equation 10 provided we put

$$u\sqrt{2.5} = Qr^2 \quad \ldots\ldots\ldots\ldots\ldots\ldots\ldots(11)$$

Doing this and writing x for 2r we find that equation 10 can be rewritten

$$1 - F = \exp\left(-(x\sqrt{Q}/3.317)^{3.54}\right) \quad \text{.........(12)}$$

Equation 12 is in the same form as equation 1 and we see that the theoretical value of the distributive index n is 3.54, in good agreement with the empirical value 3.20. It is rather remarkable that the value of this index should be independent of the numerical values of the usual meteorological parameters. This probably explains why no systematic variation in n was found in the previous paper (Best, 1950 (b)).

Comparing equations 1 and 12 we see that

$$b\sqrt{Q} = 3.317 \quad \text{........................(13)}$$

Now from equations 3 and 8 we have

$$Q = \frac{R\pi^2}{8M} \frac{K\theta}{Dsp_\theta l^2} \quad \text{...................(14)}$$

and it has been shown previously (Best, 1950 (b)) that the mean drop diameter is proportional to b. Thus the mean drop size is directly proportional to the thickness of the cloud and to the square root of the supersaturation and inversely proportional to the square root of the turbulence coefficient K. Substituting in equation 14 the numerical values (c.g.s. units)
$M = 18$, $\theta = 273$, $D = 0.219$, $R = 8.314\ 10^7$,
$p_\theta = 6.108\ 10^3$, $s = 10^{-4}$, $K = 10^5$, $l = 2\ 10^4$.
we get $Q = 2.907\ 10^6$ cm^{-2} and $b = 19.5\mu$. This value is in good agreement with the values found from observations (Best, 1950 (b)) but of course a very considerable range of values is possible by varying the values of the individual parameters in Q. Two of these parameters in particular, K and s, are very difficult to assess. Nevertheless it does appear that the considerations outlined in sections 2 and 3 do account reasonably well for the observed facts about drop size distribution in cloud. It is rather interesting also to note that the smaller value of K associated with fogs should lead to smaller values of Q and hence to a larger average drop size.

References.

Best, A. C.	(a)	1950	M.R.P. 538.
	(b)	1950	M.R.P. 559.
Fuchs, N.		1934	Phys. Zs. Sov. Union, Kharkov, 6, p.224.
Pearson, K.		1946	Tables of the Incomplete Gamma Function, Biometrika.

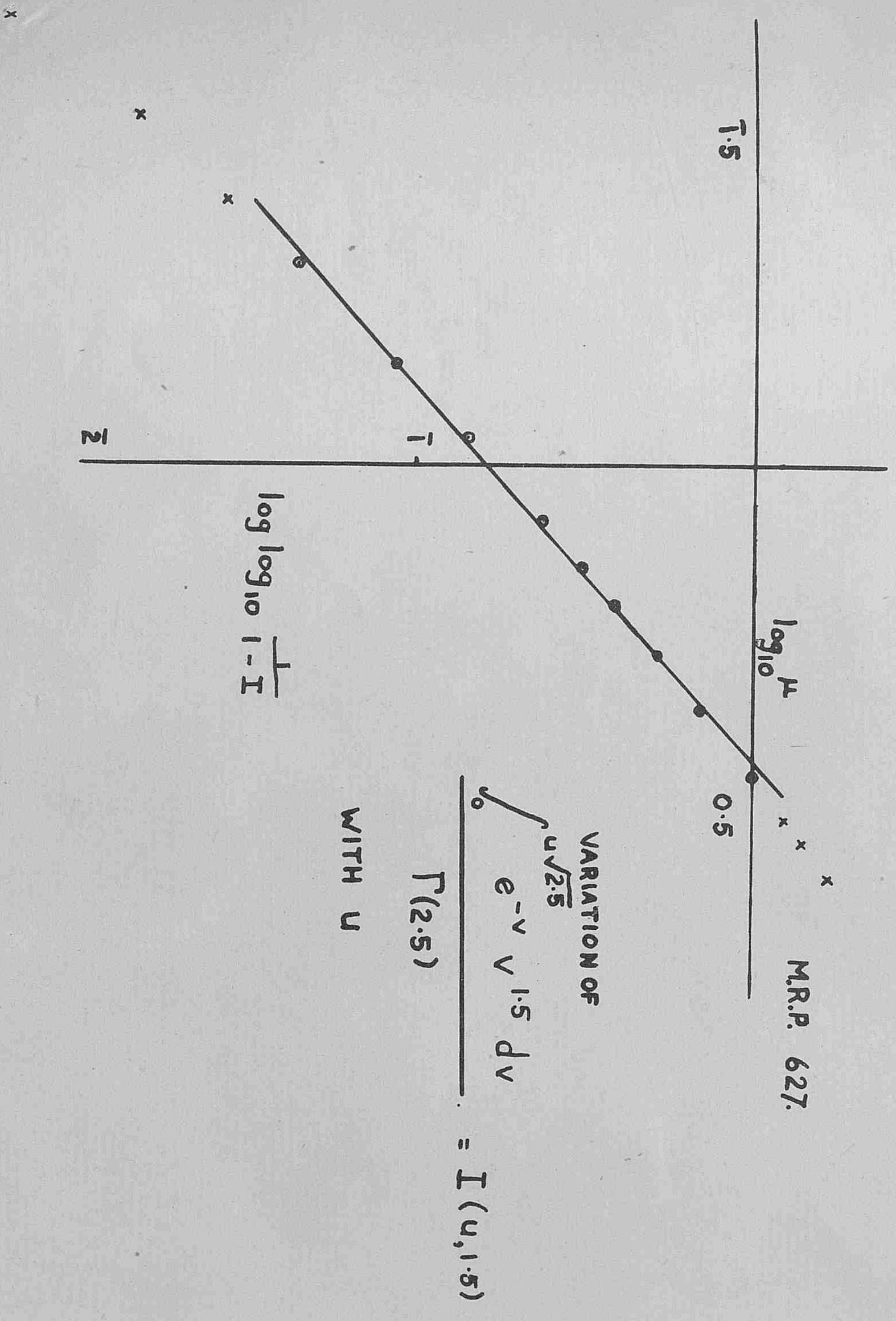

651
/92
ruary, 1951.

onditions on
bulence
arge shear just

in the
these two
incident
ail below.

s flying at
.A.S.) of
perienced
s varying
e frequency
to an eddy
lerometer may
celerations
ivalent gust
agnitude to
ays research
, however,
945,
ments

time of the
height
cloud but
he turbulence,

course was immediately altered northwards, smooth air being reached when over the cumulus cloud. The air temperature in the smooth air over the cumulus was 6°C lower than when the turbulence was first met. There is no information as to the distance flown during this temperature fall.

(b) Meteorological situation

Figure 1 shows the synoptic situation at midday on 2nd November, 1950; the contours of the 300 mb. pressure surface apply to time 14.30 hours G.M.T. approximately and indicate the nature of the flow at about 30,000 ft. The shallow depression over the North Sea was filling up rapidly while the depression over south east Ireland continued to deepen and moved east over Southern England reaching London at 18.00 hours and being over the Ruhr the following morning.

/ Associated

≠ All heights quoted in this note are pressure heights in the I.C.A.N. atmosphere. (For details of the I.C.A.N. atmosphere see e.g. M.O.470, Meteorological Air Observers Handbook, H.M.S.O. 1945).

T.F

paper of the Meteorological Research Committee (London), M.R.P. No........... by Mr..........................
A copy is available in the Library of the Meteorological Office."

M.R.P. 631
S.C.III/92
1st February, 1951.

AWS

ATI-200024

AIR MINISTRY

APR 21 1952
AIR WEATHER SERVICE
TECHNICAL INFORMATION FILES

mete 2

METEOROLOGICAL RESEARCH COMMITTEE

Severe clear air turbulence experienced at high altitude on 2nd and 7th November, 1950

by

J.K. Bannon (Meteorological Office)

1. Introduction

The writer (1) has previously described the meteorological conditions on one occasion of exceptional turbulence at high altitude; the turbulence occurred between 34,000 and 38,000 ft. and was in the region of large shear just above the axis of a well marked jet stream.

Exceptional turbulence was encountered recently on two days in the neighbourhood of jet streams. The meteorological conditions on these two days were in many ways similar to those of the earlier turbulence incident and have many points of interest; they are discussed in some detail below.

2. Incident on 2nd November, 1950.

(a) Description of the turbulence

At about 12.50 hours G.M.T. a De Havilland Comet aircraft was flying at 35,000 ft ≠ over Flushing (Holland) at an equivalent air speed (E.A.S.) of 250 knots, (true air speed 434 knots). Severe turbulence was experienced during which the visual accelerometer in the cockpit gave readings varying from over 2g to 0.5g, i.e. increments of over 1g and - 0.5 g; the frequency of the bumps was about 1.5 cycles per second and this corresponds to an eddy diameter of 500 ft. approximately. The indications of this accelerometer may be in some doubt, (see reference 2), but it is likely that the accelerations experienced by the aircraft were of the order of ± 1g and the equivalent gust velocities therefore of the order of 20 ft./sec. and of similar magnitude to the greatest (26 ft./sec.) observed by the British European Airways research flights at high altitudes (see reference 3). The turbulence was, however, not so severe as that encountered by a Comet on 14th November, 1949, (reference 2) when the accelerometer indicated acceleration increments between 2g and - 2.6 g.

On 2nd November the aircraft was flying in clear air at the time of the incident on a course of 300° magnetic; below the aircraft, at a height estimated to be 20,000 ft, was a continuous sheet of alto-stratus cloud but northwards could be seen broken cumulus cloud. On encountering the turbulence, course was immediately altered northwards, smooth air being reached when over the cumulus cloud. The air temperature in the smooth air over the cumulus was 6°C lower than when the turbulence was first met. There is no information as to the distance flown during this temperature fall.

(b) Meteorological situation

Figure 1 shows the synoptic situation at midday on 2nd November, 1950; the contours of the 300 mb. pressure surface apply to time 14.30 hours G.M.T. approximately and indicate the nature of the flow at about 30,000 ft. The shallow depression over the North Sea was filling up rapidly while the depression over south east Ireland continued to deepen and moved east over Southern England reaching London at 18.00 hours and being over the Ruhr the following morning.

/ Associated

≠ All heights quoted in this note are pressure heights in the I.C.A.N. atmosphere. (For details of the I.C.A.N. atmosphere see e.g. M.O.470, Meteorological Air Observers Handbook, H.M.S.O. 1945).

T.F.

Associated with the frontal surface of the depression over south east Ireland was a well marked jet stream; the approproximate position of the axis of this jet is indicated in Figure 1. Figure 2 shows a cross section of this jet stream at right angles to the general wind direction at 30,000 ft. On this diagram are given the isopleths of the wind velocity component normal to this cross section; these isopleths were constructed from the observed wind velocities. Also shown on Figure 2 are the isopleths of potential temperature, which are also isentropics (lines of equal entropy). If lateral mixing is taking place it will tend to act along the isentropic surfaces; (see e.g. Haurwitz (4); the development of the use of isentropic surfaces in this connection is due to Shaw and Rossby). The closer the isopleths of potential temperature are together the greater the static stability of the air (in the vertical); when the isopleths are far apart the air is approaching instability.

Frontal and tropopause surfaces are also indicatedon the cross section.

As is often the case when constructing cross section diagrams use has had to be made of observations which were not on the line of the cross section. Thus the Liverpool observations are plotted on the cross section at the point down-wind from Liverpool at 30,000 ft. This probably accounts for some of the variation in the slope of the warm front surface as drawn on the diagram. As no upper air observations were made over the North Sea the observations at Leuchars were taken as representing the cold (tropospheric) air there and were plotted on the diagram; they may not give an accurate description of conditions over that point on the cross section but the writer is confident they give a reasonable representation of the general nature of the temperature and wind structure there. The wind observations at Camborne ceased above the level 23,600 ft; those given at higher levels on the diagram, in brackets, were the speeds observed at the same time at Velentia, upwind from Camborne. (The winds at 23,600 ft. at the two places were very similar). The positions of the upper air stations are shown in Figure 1.

(c) Analysis

The wind observation at about 14.30 hours G.M.T. at Downham Market, which was upwind and slightly to the left of the area in which the turbulence was found at 12.50 hours, showed large shear of wind in the vertical in the region of 35,000 ft, i.e. just above the level of maximum wind. The wind speeds evaluated over layers approximately 1,500 ft. thick (i.e. over 1 minute intervals of the balloon ascent), showed rather erratic variations. (See Figure 2). As the wind direction did not change appreciably the errors in speed derivations were probably less than 3 knots, (see reference 5), and these erratic variations were, therefore, real. Table I gives the wind shear, temperature lapse rate and Richardson number over 2,000 ft. layers between 30,000 and 40,000 ft. The wind shears are smoothed values derived by drawing a smooth curve to represent the wind speed distribution with height (direction constant); since the balloon ascent may well have been subject to turbulent velocities in this region above the level of maximum wind, (the erratic variations in velocity also point to this), these smoothed values of the shear are probably more appropriate to our problem than unsmoothed values.

/ Table I

Table I

Wind shear in the vertical, temperature lapse rate and Richardson number: Downham Market 14.30 hours, 2nd November, 1950.

Layer (1,000's of ft.)	Wind shear in the vertical (Smoothed) (kt./1,000 ft.)	Temperature lapse rate (°F/1,000 ft.)	Richardson number
30-32	1.5	2.7	32.4
32-34	8.5	2.7	1.02
34-36	12.0	1.7	0.72
36-38	7.5	1.7	1.9
38-40	3.9	1.5	3.9

It will be noted that the Richardson number had a minimum in the layer which includes the height (35,000 ft.) at which the turbulence was experienced. In fact, from the evidence available it seems likely that the turbulence was associated with large shear in the vertical and small Richardson number. (The significance of Richardson number in such turbulence is discussed briefly in reference 6; Richardson number was also used as a parameter in reference 1). The fall in temperature noted when flying out of the turbulent zone also points to considerable shear in the vertical (See reference 3).

It was not possible to estimate the wind shear in the horizontal in the neighbourhood of Flushing at 14.30 hours; at 08.30 hours the horizontal shear evaluated between Larkhill and Downham Market at 34,000 ft. was 0.3 hours^{-1} (cyclonic), i.e. it was much larger than normal (about 0.08 hours^{-1}) Because of the motion of the weather systems eastwards it is likely that a horizontal shear of similar order of magnitude existed in the turbulent zone at 12.50 hours. (The relation between horizontal shear and turbulence is discussed in reference 6).

This turbulence near Flushing occurred in much the same place relative to the jet stream as the incident on 14th November, 1949, reported in references 1 and 2.

3. Incidents on 7th November, 1950.

(a) Description of the turbulence

(i) A meteor aircraft in the Leicester area at approximately 14.00 hours G.M.T. experienced turbulence between 28,000 and 32,000 ft. and again between 39,000 and 41,000 ft. The aircraft was flying at 220 knots E.A.S. and the pilot described the bumpiness as exceptionally severe; the rate of climb varied between 1,000 and 3,000 ft. per minute and the air speed fluctuated 30 knots because of the turbulence. There was no cloud in the vicinity at these heights.

(ii) An American type F.86 aircraft made a climb to 45,000 ft. between Cromer and Skegness at approximately 14.30 hours and found violent turbulence between 33,000 and 38,000 ft, in clear air, both on ascent and descent. Aircraft speed was about 280 knots, E.A.S.

(iii) Between 14.30 and 15.00 hours a Meteor aircraft flying in the region 30 miles to north and south of West Raynham (Norfolk) experienced what was described as 'considerable' turbulence at 23,000 ft, 'very considerable' turbulence between 29,000 and 34,000 ft. and smooth flying between 34,000 ft. and 40,000 ft., the greatest height reached. Air speed varied between 200 and 300 knots E.A.S. The turbulence occurred in clear air.

(iv) Other pilots on training flights in the area West Raynham - Spalding at approximately 13.45 hours reported turbulence (in clear air) in the layer 28,000 - 34,000 ft. with a maximum intensity between 29,000 and 31,000 ft. The greatest height reached was 35,000 ft.

(b) Meteorological situation

The synoptic chart for midday on 7th November is shown in Figure 3; the contours of the 300 mb. pressure surface at 14.30 hours are also shown. The depression centred west of Iceland moved little during the next 24 hours and the associated frontal system moved east and south east across the British Isles, becoming partly occluded. The northerly jet stream over the west of Great Britain (axis marked in Figure 3) moved east and became much less intense. Figure 4 shows a cross section at right angles to the general northerly stream, (normal to direction 350° true). As in Figure 2 isopleths of wind speed component normal to the section and isopleths of potential temperature are given and the frontal and tropopause surfaces marked. The positions of the upper air stations are indicated in Figure 3.

(c) Analysis

The turbulence incidents described in 3(a) above occurred in different places at slightly different times; they were all associated with the same jet stream. Wind shear, temperature lapse rate and Richardson number all vary rapidly with distance (horizontal and vertical) in the neighbourhood of such jet streams and radio-sonde observations were not available which could be associated with each of the turbulence incidents exactly in space and time. Never-the-less, within the limits imposed by lack of simultaneity in measurements of turbulence and shear, the analysis of these incidents given below using available radio-sonde information does show good agreement between turbulent zones and zones of shear in the vertical (small Richardson number).

(i) The incident noted in 3 (a) (i) above was roughly 90 miles upwind from Larkhill where an upper air observation (temperature and wind) was made approximately 1/2 hour later. Of all available upper air observations this observation at Larkhill probably best represents the conditions over Leicester at the time in question. The Larkhill observation was not shown on Figure 4 as its position was well off the line of the section and movement and development of the weather features were taking place. (In fairly static situations where fronts etc. are moving only slowly it is often legitimate to utilise observations well off the line of section, projected up or down-wind onto the section. In this case the Larkhill observations if plotted on the cross section show good general agreement with the other observations except that the frontal surface is displaced). The warm frontal surface (or zone) was clearly marked at Larkhill between 28,000 and 30,000 ft. by an inversion of temperature and a sharp increase of wind with height; the increase of wind continued upwards above the frontal surface. Table II gives details of the wind between 20,000 and 43,000 ft. evaluated over layers approximately 1,300 ft. thick and it will be noted that there is strong shear in the vertical both below and above the level of maximum wind. Wind shear, lapse rate and associated Richardson number are also given for various layers.

/ Table II

Table II

Upper wind observations at Larkhill, 14.30 hours 7th November, 1950 and related parameters

Height (1,000's ft.)	Wind Direction (°)	Speed (kt.)	Layer (1,000's of ft.)	Wind shear (kt/1,000 ft.)	Lapse rate (°F per 1,000 ft.)	Richardson number	Turbulent layers Leicester 14.30 hr.
20.3	332	39					
26.2	334	32	20.3-26.2	1.2	4.0	25.3	
27.7	334	41	26.2-27.7	6.0	3.5	1.4	
29.1	003	60	28.3 to				28,000 -
30.8	010	96	30.0	21.0	-0.6	0.37	32,000 ft.
32.4	010	130	30.0-32.4	21.5	3.7	0.10	
34.2	017	102	32.4-34.2	16.9	3.7	0.17	
35.8	013	102	34.2-35.8	4.7	3.5	2.4	
37.3	003	81	35.8-37.3	17.3	2.7	0.26	
39.0	001	77	37.3-39.0	2.6	1.0	18.8	39,000 -
41.2	351	61	39.0-41.2	9.1	0.6	1.7	41,000 ft.
43.0	354	45	41.2-43.0	9.2	-1.0	2.2	

The lower turbulent layer would appear to have been associated with the frontal zone and the layer above it, below the level of meximum wind; the Richardson number was considerably less than 1 in this turbulent layer.

Above the level of maximum wind the wind speed fell off rather erratically; between 32,400 and 39,000 ft. the Richardson number was sometimes quite small though there was no corresponding turbulence over Leicester. The upper turbulent layer over Leicester was associated with a minimum of Richardson number at Larkhill; whether this is significant is not certain though it seems likely. This upper turbulent layer, 39,000 to 41,000 ft., was above the tropopause which was at 36,000 ft. at Larkhill and 38,600 ft. at Downham Market.

Table III gives the shear in the horizontal at various levels over the Midlands at 14.30 hours. At 26,600 ft. and below, the shear refers to the cold air beneath the warm frontal surface; at 30,000 ft. and above, the shear refers to the warm air. Owing to difficulty in estimating the radius of curvature of the stream-lines the values of the horizontal shear are liable to error; in this case the error is probably less than 0.07 hours^{-1}. The layer just above the warm frontal surface, where turbulence occurred, was a layer of strong cyclonic shear in the horizontal. The shear in the horizontal in the upper turbulent layer does not appear to have been large.

/ Table III

Table III

Shear in the horizontal over the Midlands, 14.30 hours 7th November, 1950

Height (ft.)	Shear ($Hours^{-1}$)
20,800	-0.09
23,600	-0.15
26,600	-0.08
30,000	0.47
34,000	0.41
38,600	0.37
42,000	0.0

(ii) The upper air observation most applicable to the area and time of the turbulent incidents described in 3(a) (ii), (iii) and (iv) was that made at Downham Market (West Norfolk) at about 14.30 hours. (See Figure 4 for details). Table IV gives values of wind shear, temperature lapse rate and Richardson number for various layers. The observed wind directions fluctuated by a few degrees, apart from the apparently systematic changes with height. Such fluctuations may well have been caused by the errors of observation (see reference 5) and accordingly the wind directions were smoothed (maximum smoothing 3°) before evaluating the wind shear.

Table IV

Shears, lapse rates and Richardson numbers; Downham Market, 14.30 hours 7th November, 1950

Layer (1,000's of ft.)	Shear (kt./ 1,000 ft.)	Lapse rate (°F per 1,000 ft.)	Richardson number	Turbulence
19.8 - 21.2	0.7	3.9	78.0	
21.2 - 22.6	1.4	3.3	27.5	West Raynham: considerable at 14.30 -15.00 hrs. at 23,000 ft.
22.6 - 24.1	2.7	3.5	6.8	
24.1 - 25.5	5.0	4.0	1.5	
25.5 - 27.0	0.7	3.8	87.4	West Raynham: very considerable 29-34,000 ft. at 14.30-1500 hrs.
27.0 - 28.4	7.3	3.2	1.1	
28.4 - 29.5	11.5	0.0	1.1	West Raynham to Spalding at 1345 hrs 28-34,000 ft, max at 29-31,000 ft.
29.5 - 30.9	17.5	1.6	0.34	
30.9 - 32.4	26.7	2.7	0.10	
32.4 - 34.0	15.6	2.7	0.31	
34.0 - 35.6	15.9	1.9	0.39	Cromer to Skegness: violent 33-38,000 ft. at 14.30 hrs.
35.6 - 37.0	5.9	1.9	2.8	
37.0 - 38.8	0.6	1.8	283.0	
38.8 - 40.4	0.0	-0.3	∞	
40.4 - 42.0	8.4	-0.3	2.1	
42.0 - 43.5	7.0	0.2	3.0	
43.5 - 44.9	2.9	0.2	17.7	

The turbulence near West Raynham at 23,000 ft. had no markedly small value of Richardson number associated with it; the wind shear in the layer22,600 - 24,100 ft. was almost reversed in the layer above (wind at 24,100 ft. was a minimum), so that the Richardson number over the layer 22,600 - 25,500 ft. was 51.6.

The next layer of turbulence near West Raynham described as very considerable between 29,000 and 34,000 ft., was in and above the warm frontal zone and the Richardson number from the Downham Market radio-sonde data was small in this layer. The turbulent layer experienced earlier (13.45 hours approximately) between 28,000 and 34,000 ft. was presumably also associated with the frontal surface and the layer of strong shear in the vertical above it; as this flight was westwards into Lincolnshire the frontal surface was probably met at a slightly lower height than over West Norfolk and hence the bottom of the turbulent layer was also lower.

The violent turbulence found between 33,000 and 38,000 ft. on the flight between Cromer and Skegness was also associated with small Richardson number at Downham Market over much of the layer; as the flight was over a distance of 45 miles normal to the jet stream the radio-sonde observations at one spot cannot be expected to apply to all of this incident and this is, presumably, partly the explanation of the disagreement of this observation of turbulence with the others.

The values of shear in the horizontal given in Table III are of interest in these cases of turbulence over East Anglia; the main turbulent zones were in the layers of large horizontal shear.

These incidents also service to demonstrate the rapid variation of turbulence both in time and space which can occur. Only one of the flights experienced turbulence at 23,000 ft, (that in the West Raynham area), and though three of the flights (including that over Leicester) reached 40,000 ft. or more on only one was turbulence experienced above 38,000 ft, though the flights were within 100 miles of each other. It must be remembered, of course, that other meteorological parameters such as shear, Richardson number, also change markedly in short distances in the neighbourhood of jet streams.

This series of observations confirms that high altitude turbulence can be quite severe and also can have permanence in the neighbourhood of jet streams as was also shown by the incidents reported in reference 1. It is known, (see references 3 and 6), that high altitude turbulence, not necessarily associated with a jet stream, is often 'patchy' and impermanent.

4. Conclusions

These experiences of severe turbulence provide further evidence in support of the contention put forward in reference 6 and also suggested tentatively in reference 3, namely, that severe turbulence (apart from that which may occur in association with cumulonimbus cloud) occurs at high altitude in temperature latitudes only in the region of sharply marked jet streams.

The observations of turbulence on 7th November illustrate the permanence of some zones of turbulence associated with jet streams but also show the rapid variation in height and depth of such zones with distance, a variation matched by other meteorological parameters, temperature, shear etc.

From the upper air observations available it seems very probable that each of the turbulent zones reported on these two days, with the exception of the shallow layer at 23,000 ft. on 7th November, (see 3 (a)(iii)), was associated with strong shear of wind in the vertical and small Richardson number.

/ Acknowledgement

Acknowledgement

The details of the incident on 2nd November, 1950 were kindly supplied by the De Havilland Aircraft Company.

References

1. Bannon J.K. A note on the meteorological conditions associated with the exceptional turbulence encountered by the DH Comet aircraft, 14th November, 1949. A.R.C. No. 12,877 (January, 1950).

2. Hislop G.S. Clear air turbulence incident encountered by DH Comet aircraft, 14th November, 1949. A.R.C. No. 12,833 (December, 1949).

3. Hislop G.S. and Davies D.M. Final report of the Clear Air Gust Research Project. A.R.C. No. 13,316 (June, 1950).

4. Haurwitz B. Dynamic Meteorology, New York, 1941, P.231.

5. Bannon J.K. Errors in winds measured by GL III Radar Equipment. Met. Off. London, Met. Res. Paper No. 406, 1948.

6. Bannon J.K. Meteorological aspects of turbulence affecting aircraft at high altitude. Prof. Notes, Met. Off, London, No. 104, 1951 (in the press) or Met. Res. Paper, No. 510, 1949.

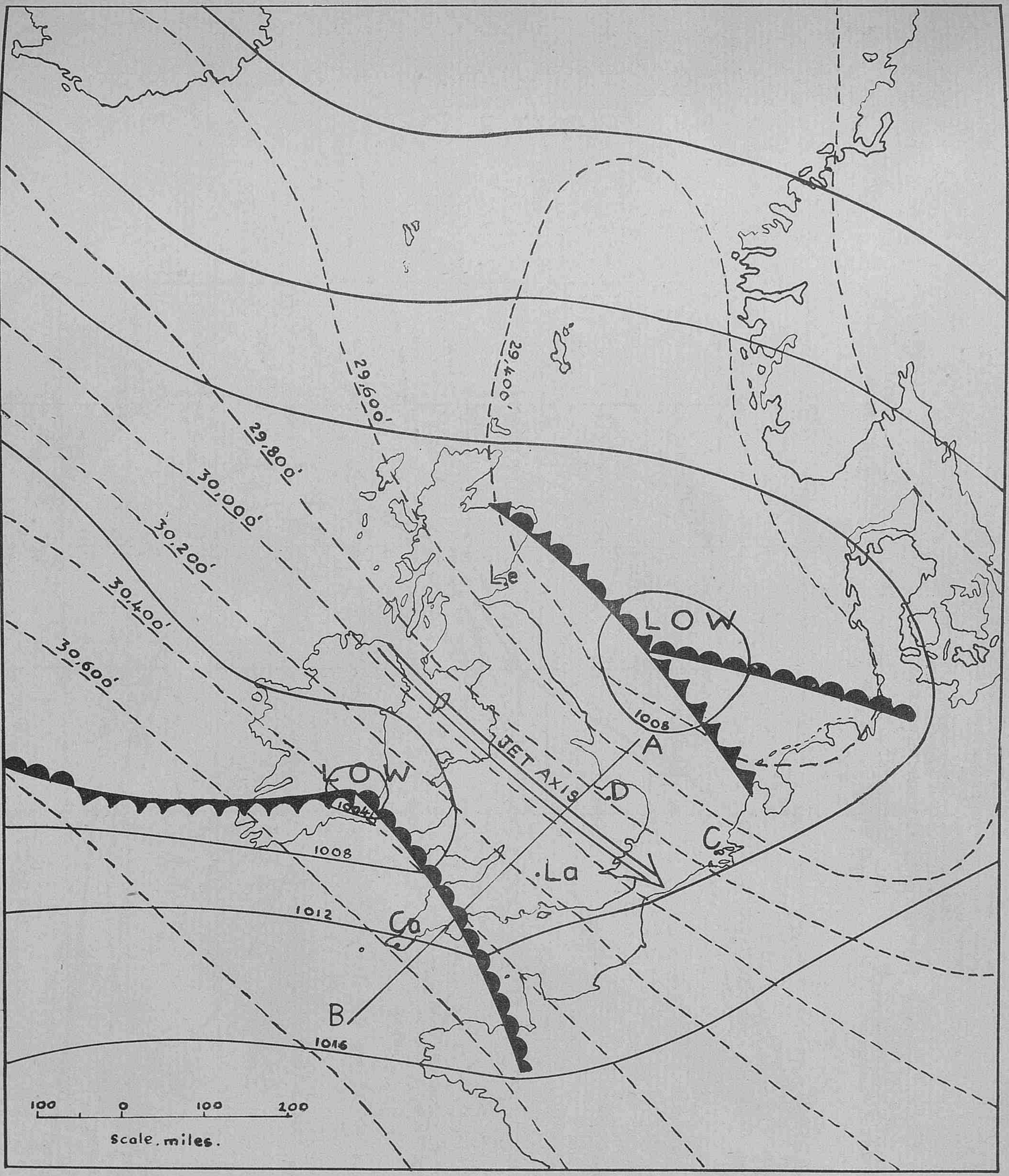
29,400'
29,600'
29,800'
30,000'
30,200'
30,400'
30,600'
LOW
LOW
1008
1004
1008
1012
1016
JET AXIS
A
B
C
D
La
Ca
Le
100
0
100
200
Scale. miles.

Figure 1.

Weather Situation Midday 2nd November 1950.

—— Sea level isobars at 1200 hours; pressure in millibars.

- - - - Contours of 300 mb. surface at 14:30 hours; heights in feet

◓◓◓ Warm front

▲▲▲ Cold front ◓▲◓▲ Occluded front

A B Approximate line of section to which Figure 2 applies.

C Area where turbulence occurred.

Radio Sonde Stations.

D	Downham Market	Ca	Cambourne
La	Larkhill	Le	Leuchars

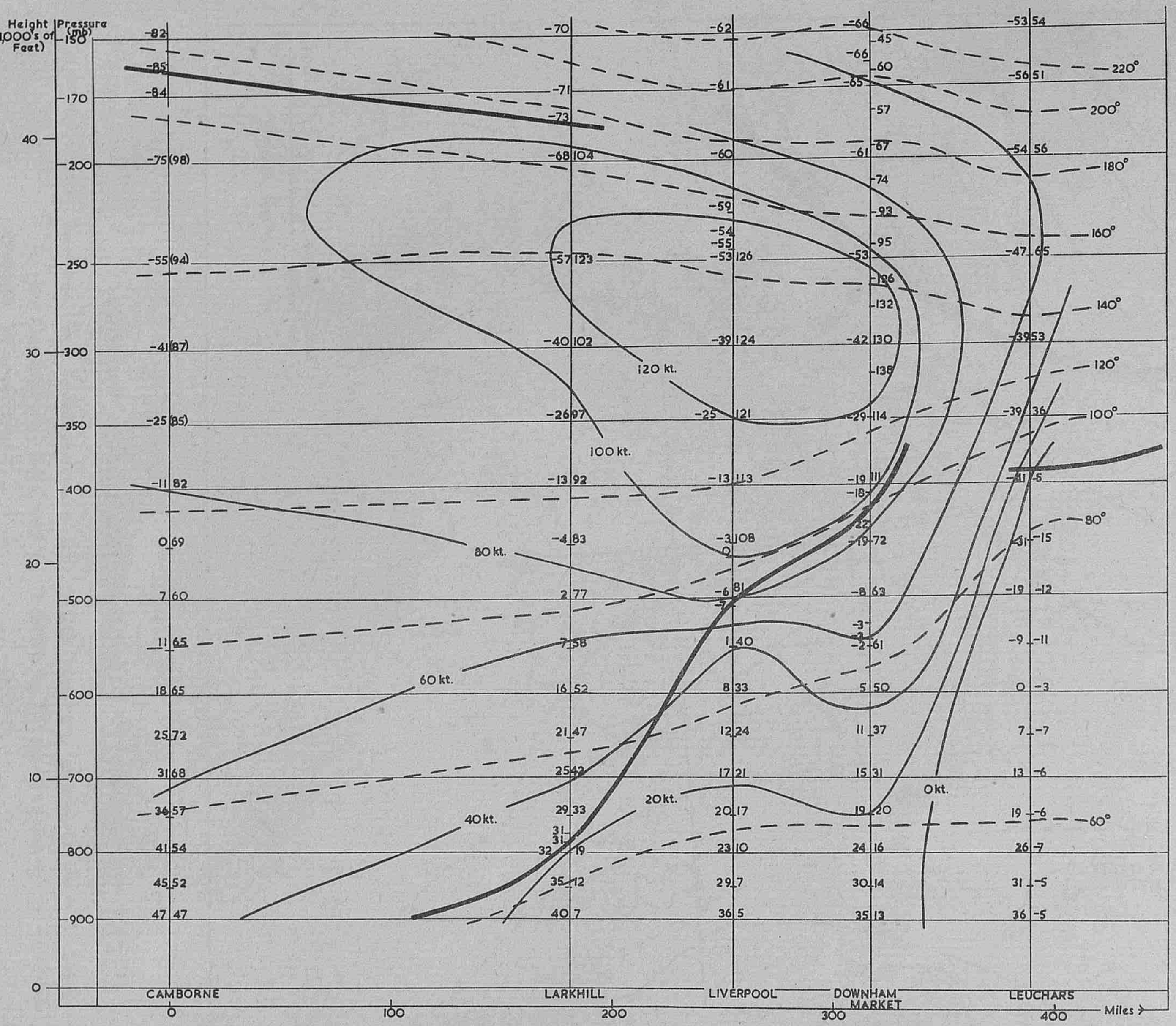

FIGURE 2. CROSS SECTION OF JET STREAM 1430hrs, 2nd NOVEMBER, 1950.

M.R.P. 631.

—— Isopleths of wind velocity component from 310°.

– – – Isopleths of potential temperature °F. (Referred to 1,000mb. pressure).

▬ Frontal or tropopause surface.

For each ascent the temperature (°F.) is given on the left, and the component of the wind velocity from the direction 310° on the right, at the specified levels.

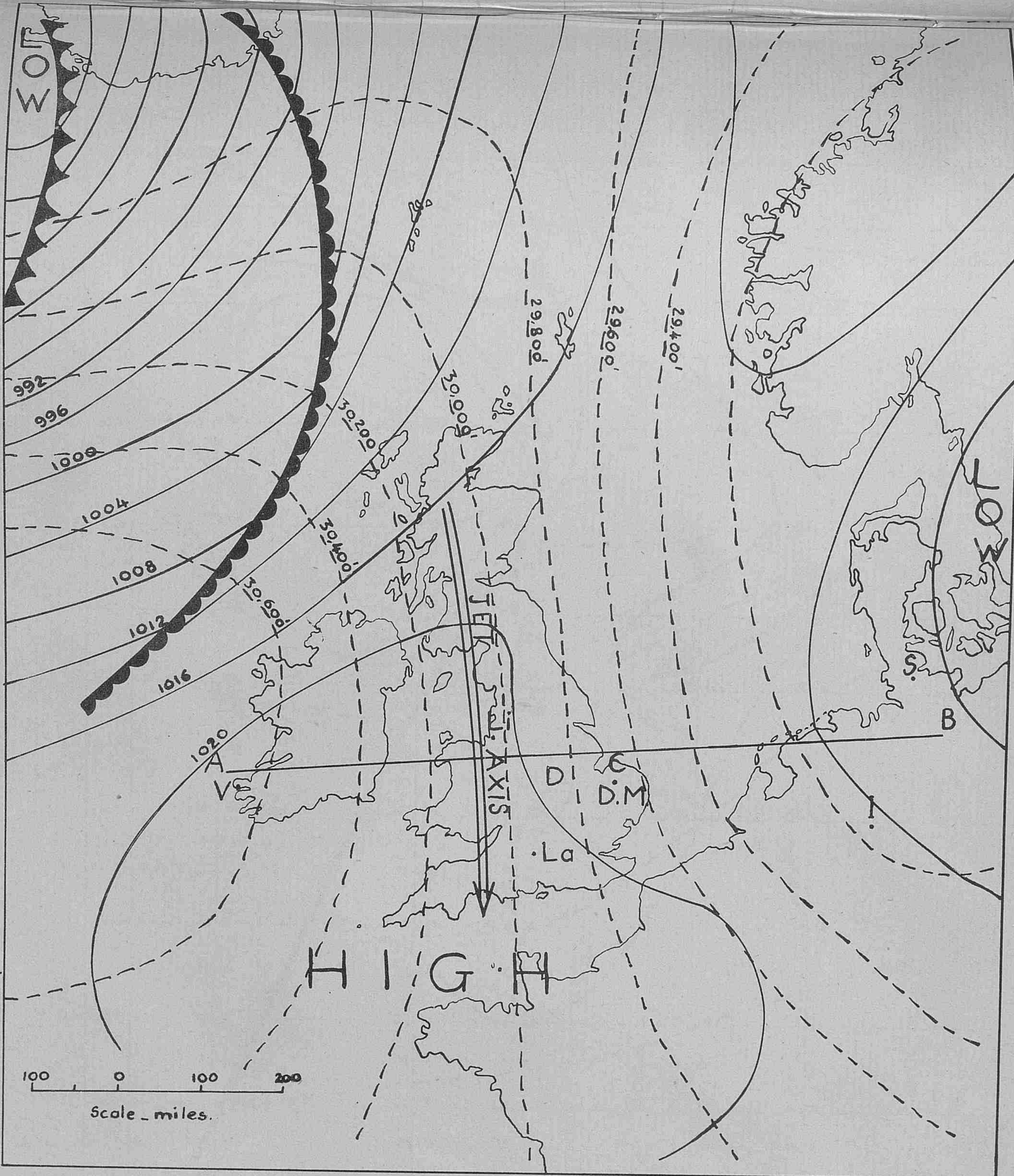
LOW
992
996
1000
1004
1008
1012
1016
1020
30,600
30,400
30,200
30,000
29,800
29,600
29,400
JET AXIS
Li
A
V
D
C
D.M
La
B
I
S.
LOW
HIGH
100
0
100
200
Scale _ miles.

Figure 3.

Weather Situation Midday 7th November 1950.

——— Sea level isobars at 1200 hours; pressure in millibars.

– – – Contours of 300 mb. surface at 14:30 hours; heights in feet.

◠◠◠ Warm front.

▲▲▲ Cold front.

A–B	Approximate line of section to which Figure 4 applies.
C, D	Areas where turbulence occurred.

Radio Sonde Stations.

D.M.	Downham Market
I	Iserlohn
La	Larkhill
Li	Liverpool
S	Schleswig
V	Valentia

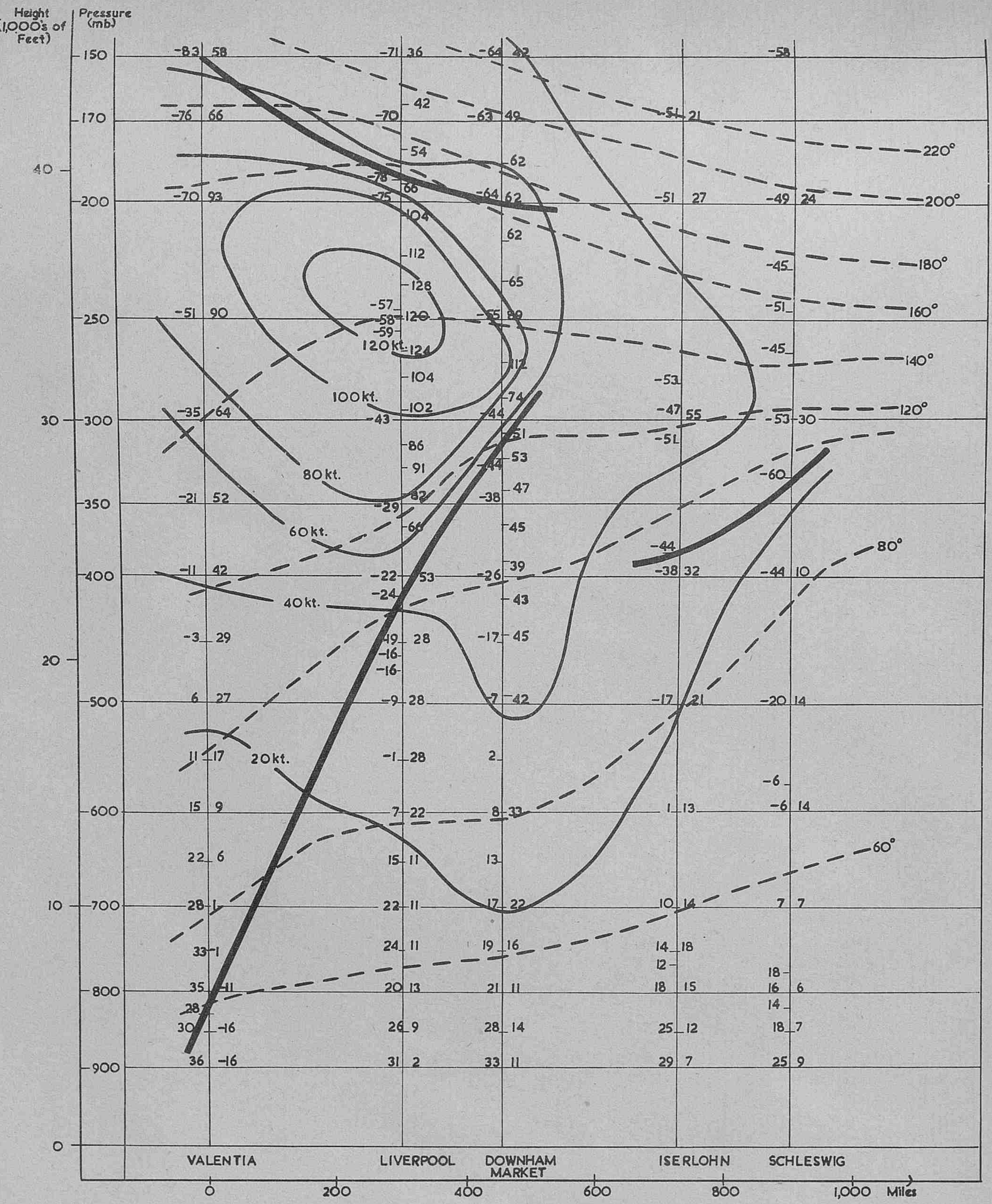

FIGURE 4. CROSS SECTION OF JET STREAM 1430hrs, 7th. NOVEMBER, 1950. M.R.P. 631.

—— Isopleths of wind velocity component from 350°.
– – – Isopleths of potential temperature °F. (Referred to 1,000 mb. pressure).
▬ Frontal or tropopause surface.

For each ascent the temperature, (°F.) is given on the left, and the component of the wind velocity from the direction 350°, on the right, at the specified levels.

ASTIA FILE COPY

A copy is available in the Library of the Meteorological Office."

AF359488

R.P.632
S.C.II/75
20th April, 1951.

ATI-200023

AF359488

AIR MINISTRY

METEOROLOGICAL RESEARCH COMMITTEE

Hemisphere-Wide Circulation Patterns and Type-Classification

by

H.H. Lamb (Meteorological Office)

NOV 5 1951

AIR WEATHER SERVICE
TECHNICAL REFERENCE FILES

1. Introductory.

Research under this heading, as part of the Meteorological Research Programme (Item II. 6(a)), was carried on from October, 1948 to January, 1950. The basic idea was that there are other circulation models beside the one suggested by the long-period (e.g. annual) mean pressure distribution. The atmosphere may strive to establish and settle down into one or other of these models at various times.

The so-called normal sea-level pressure and wind distribution, represented by the annual mean figures, is the average of all the individual distributions which occur, and not necessarily itself a possible circulation model at all. This point has received rather little attention in recent years.* In spite of the fact that various other patterns of circulation (some quite unlike the climatological normal) can easily be recognised and are found to persist for days at a time, the various individual circulation patterns occurring have been treated mainly as departures from the mean.

The physical processes at work in the atmospheric circulation and the energy sources which directly or indirectly agitate them may indeed be lost sight of in such treatment. Dr. R.C. Sutcliffe (1) has pointed out that, on the basis of various workers' estimates, the amount of kinetic energy possessed by the entire atmosphere would be destroyed, or at all events radically lowered, by friction in something between one and ten days, if it were not maintained by energy fed into the atmosphere. The estimates of time required for the circulation to run down have been the subject of inconclusive discussion, but about 5 days seems most reasonable as a provisional figure. The troposphere, as is well known, gains heat primarily from the earth's surface, in sensible form by radiation and conduction, and in latent form by evaporation of moisture; heat is lost by radiation, particularly from condensed moisture wherever it is present, and by such other processes as carry heat from the troposphere into the higher levels. In the language of thermodynamics, the general circulation of the lower atmosphere, meaning in this case the sum of all the large and small-scale circulations and eddies, serves to convey heat from source to sink in accord with the pattern of sources of heat-gain and regions of heat-loss prevailing at any given time. If therefore a given circulation pattern lasts for more than about five days, it must be specifically maintained by its own pattern of energy sources and sinks.

2. Classification of the individual circulation patterns occurring over the hemisphere.

A difficulty which must arise in any attempted classification of patterns covering an area of the size of a hemisphere is the need to suppress detail in order to make the broad features classifiable to all. Over long periods this can be achieved objectively by considering mean maps covering the duration of predominance of a given type (spell), but if individual daily maps are to be classified, subjectivity may creep in: it is not to be expected that different

/workers

---

* See however (1), (2), (3), (4).

workers will agree exactly on what detail may legitimately be disregarded nor that every day's map will conform to any of the defined types. The experiment suggested that any given worker would consider about 50 per cent of the days classifiable according to the scheme chosen but that only about half of these would be fully agreed by different workers.

Nine types of circulation pattern were defined. Of these nine, six were more or less orderly geometrical patterns around the hemisphere and three were fundamentally geographical, one of the latter ((ii) below) being discovered in the course of the experiment. The types were:-

(i) Z Zonal circulation, approximating to the climatological mean maps.

(ii) Z' Winter-modified zonal circulation, in which the sub-tropical high-pressure belt spirals from low latitudes in the Atlantic E.N.E. towards the N.E. corner of Asia, and thence (in the most highly developed cases) to Alaska.

(iii) D Double-structure zonal circulation, with two main high-pressure belts (one sub-tropical and the other in 60-70°N) and two main belts of travelling depressions (one in middle latitudes and one in the polar basin).

(iv) S Slanting-axis circulation with high-pressure axes and depression tracks orientated SW to NE.

(v) M Meridional patterns with N'ly and S'ly components predominant in the surface windstreams.

(vi) SI Slanting inverted patterns characterised by high pressure centres about 60°N with axes extending NW to SE or WNW to ESE, normal W to E depression track in low latitudes; but minor cyclonic features travelling from SE to NW in middle latitudes. Cyclonic features also travel SE or ESE on the poleward side of the northern anticyclones and feed into major stationary depressions in certain longitudes about 70°N.

(vii) I Inverted or zonal easterly circulations in middle latitudes; sub-divided according to whether the situation north of 70°N was anticyclonic or cyclonic.

(viii) MW Monsoonal winter patterns dominated by continental high pressure and oceanic lows.

(ix) MS Monsoonal summer patterns dominated by continental low pressure and oceanic highs.

To these nine types were added (x) a category of weak circulations (W), characterized by lack of pattern and small overall pressure differences in the hemisphere (the largest range allowed being about 40 mb.), representing an extreme state which never persists for long and occurs only in summer. (The full definitions are set out in the Appendix.)

Middle latitudes blocking (the term used by Elliott and Smith (5) to describe the situation with the main anticyclones displaced from the subtropical belt to about 50°N) did not seem to produce a type of conformity around the hemisphere except insofar as type (iv) fits the definition. Other cases might be classified as (vii), which is the least persistent of our hemisphere types and most inclined to appear in incomplete form. The longer-lasting high-latitude blocking (i.e. dominant highs north of 55°N) could be associated with patterns (vi) and (viii), which were also found to be more persistent than the other hemisphere types and liable to occur in association with each other in spells. Further consideration suggests that there is a geographical element (winter - monsoon) in type (vi) as well as in types (ii) and (viii). The centres of action in these types as well as the N'ly airstreams in the meridional type (v) seem to have preferred geographical positions.

/Six

Six years' northern hemisphere weather maps (1899, 1911, 1923, 1935, 1948 and 1949) were classified according to this scheme. About 50 per cent of the days showed a sufficient degree of order to be classifiable; near-misses in which the chaotic element was limited to about one major system in the hemisphere accounted for a further 10 per cent.

An experiment was made in classifying more limited sectors, but about the same proportion of unclassifiable cases arose. Classification in geographical regions appears, however, to yield a much higher proportion of conformity (over 90% in tests of appropriate regional classifications applied to the polar basin, Canadian Arctic, British Isles and Siberia).

Comparison was made with a sample period of 4½ summer and autumn months for which a similar classification could be applied to the southern hemisphere, where it was found that a much smaller range of types, comprising only (i), (iv) and (v), and possibly (iii), occurred. There were, however, hints of a special long-wavelength type in the southern hemisphere, characterised by anticyclonic cells and depression tracks in neighbouring sectors orientated alternately NW to SE and SW to NE - a sort of combination of types (iv) and (vi).

Much longer periods of years would need to be classified to establish thoroughly all the significant associations of types with each other and with the thermal patterns occurring at each time of the year.

In the five years 1899, 1911, 1923, 1935 and 1948, the order of frequency with which the above defined northern hemisphere types occurred was as follows:-

Chaotic	X	43.9%
Slanting	S	11.2%
Meridional	M	9.4%
Zonal or Winter-modified zonal	Z or Z'	8.8%
Monsoonal Winter	MW	6.4%
Slanting Inverted	SI	5.1%
Monsoonal Summer	MS	4.7%
Double	D	4.3%
Inverted	I	4.2%
Weak	W	2.1%

3. Dimensions of systems.

Observed dimensions of the systems suggest that certain limits exist. More than two main zonal belts of high pressure apparently never occur. The distance separating neighbouring belts of low pressure varied between about 40 and 72° latitude. This implies that double-structure types (e.g. (iii) or (vi)) might not require the existence of external agencies favouring cyclogenesis in more than one belt around the hemisphere; the second belt might be an induced effect appearing as a necessary consequence of the atmospheric circulations set up in much higher or much lower latitudes. The concentration of thermal gradient in summer around the fringe of the polar basin, and in winter in low latitudes, may give rise to double-structure circulations (iii) and (vi).

/4.

4. Seasonal effects.

The frequency distributions showed the commonest types to be quite different in different months, though based on too few years for reliance. The monsoonal types (viii) and (ix) headed the lists (about 20%) in June, December and February. The geometrical type (iv) came out commonest (about 11%) in most years over the year as a whole, chiefly because it occasionally crops up in any month, and is common in July (23%), September (17%), and April (15%). It is accompanied 88% by either W'ly, anticyclonic or NW'ly weather in the British Isles. The highest proportions of chaotic maps were found in March, September, May and December (50 to 60%), the lowest in July, August, June, November and February (under 40%). During December, oscillations between the zonal types ((i) and (ii)) dominant in November, and the monsoonal type prominent later in the winter, were commonly in progress. The full list of frequencies month by month are given in Table I.

Table I. Monthly Frequencies (%) of Individual Types: five years 1899, 1911, 1923, 1935, 1948.

	Z or Z'	D	S	M	SI	I	MW	MS	X	W
J	11.6	1.3	9.0	12.9	7.7	1.9	10.3	0	45.2	0
F	9.9	0	4.9	2.1	9.9	7.1	27.0	0	39.0	0
M	2.6	0	11.0	9.7	8.4	7.1	1.9	0	59.4	0
A	10.0	2.0	14.7	12.7	6.7	8.0	2.0	0	44.0	0
M	3.2	5.8	7.1	20.0	0	10.3	0	0.6	52.3	0.6
J	8.7	6.7	12.7	5.3	0.7	4.0	0	20.7	36.0	5.3
J	5.2	11.6	22.6	0	1.9	1.3	0	21.9	24.5	11.0
A	9.0	12.9	13.5	2.6	1.9	5.8	0	12.3	35.5	6.5
S	6.0	8.7	17.3	12.7	0.7	0	0.7	0	52.7	1.3
O	12.3	2.6	9.7	14.2	5.2	1.9	7.1	0	47.1	0
N	17.3	0	9.3	10.7	12.0	2.0	10.7	0	38.0	0
D	10.3	0	2.6	9.0	6.5	1.3	18.1	0	52.3	0

In this table the maximum frequency values for each type are heavily underlined and the minimum values lightly underlined.

Classification of a much longer period of years would be needed to study frequencies over shorter ranges of dates than a month, which is undoubtedly necessary for a full knowledge of the seasonal process. (Full northern hemisphere surface weather maps are now available for just over 40 years between 1899 and 1950.)

5. Persistences of types; spell durations.

Persistence tables showed that the monsoonal types were the most persistent or recurrent once established, but examples of unbroken spells of 7 days or more of each type except (vi), (vii), (viii) and (x) were found in the 6 years classified; and there were also a good many examples of types (vi) and (viii) occurring together in hybrid spells of 7 or more days' duration without a break.

In the same period 520 days (23.7% of the time) came within spells of 7 or more days of dominance (as defined below) of some hemisphere-wide pattern or of types (vi) and (viii) in combination. Breakdowns to chaos, often caused by the occurrence of just one major system not fitting the pattern, were much commoner than direct transitions from type to type. Eventual recoveries (reversions from chaos) to the original type were quite common ($\frac{1}{4}$ to $\frac{1}{3}$ of the cases). Many of the chaotic patterns represented appearances of unlike hemisphere types in different sectors sometimes protracted over several days with neither type achieving mastery around the hemisphere. (However, the longest run of chaotic or unclassifiable situations lasted only 15 days).

Table II. Persistencies and Transitions

Type on given day T	No. of occurrences of T	Type next day (Percentage of number in second column)									
		Z or Z'	D	S	M	SI	I	MW	MS	W	X
Z or Z'	174	52.3	0	5.7	0	0	0	0	1.7	0.6	39.7
D	86	3.5	41.9	4.7	1.2	2.3	1.2	0	4.7	7.0	33.7
S	231	9.5	3.5	44.1	4.3	0	0.4	1.7	1.3	0.9	34.2
M	222	0.9	1.4	3.2	43.2	4.1	2.3	2.3	0	0.5	42.3
SI	100	0	1.0	1.0	11.0	44.0	9.0	11.0	1.0	1.0	21.0
I	83	0	2.4	0	8.4	4.8	32.5	9.6	3.6	1.2	37.3
MW	119	0	0	4.2	2.5	6.7	3.4	59.7	0	0	23.5
MS	111	1.8	2.7	2.7	1.8	0	1.8	0	65.8	7.2	16.2
W	40	5.0	7.5	10.0	0	0	7.5	0	15.0	30.0	25.0
X	959	5.4	3.1	9.9	9.7	3.4	3.2	2.1	1.9	0.8	60.4

Table II gives the frequencies of persistence and of direct transitions from one type to another between one day and the next.

A better measure of the duration of spells of dominance of one type or another over the hemisphere as a whole is probably given by Table III, showing the frequency of spells in which minor interruptions of chaos or of another type are allowed as follows:

(a) an interruption of one day in a 4-day spell

(b) an interruption of one or two days in a 5-day spell

(c) interruptions of not more than three consecutive days in the longer spells.

This may be considered as a systematic allowance for disregarding discordant detail in cases where reversion to the original type soon takes place. In the longer spells repeated reversions to type after minor interruptions were quite common. On this rating spells of dominance of one or another hemisphere type lasting 4 days or more were in progress 47.3% of the time, most frequent being spells of 5 days' duration (32 cases in 6 years, i.e. 8.8% of the time).

/Table III

Table III. Spells of dominance of one or another type of hemisphere circulation pattern, allowing interruptions of not more than 3 days (number of cases).

1899, 1911, 1923, 1935, 1948, 1949.

Duration (days) / Type	4	5	6	7	8	9	10	11	12	13	14	17	18	20	22	25	45
Z or Z'	7	5	8	2	3				2								
D	2	2		2	3						1						
S	4	3	2	8	4	3			1								
M	6	6	4	2		2			2						1		
SI	1	4	2	1		1		1									
I	1	3	1	1													
MW	2	6	1		2					1				1			
MS	2	3		1	1			1									1
W	2			1	1												
Total all types % of time in 6 years.	5.9	8.8	5.9	6.9	6.1	3.0	0	1.2	3.3	0.7	0.8	0	0	1.1	1.1	0	2.5
Hybrids * SI + MW		2		2	1		1					1	1	1	1	1	
MS + W		1		1					1								

* Most of these cases of allowed hybrids merely result in lengthening periods already counted as spells of either SI, MW, MS or W.

(No cases arose of spells lasting 15, 16, 19, 21, 23, 24 or 26-44 days).

6. Corresponding patterns in the upper air.

Comparison with a classification of nine months' upper air (500 mb. level) maps between 120°W and 60°E (the half-hemisphere excluding most of Asia and the Pacific), by Mr. E.J. Sumner, revealed certain strong correspondences in cases where the patterns persisted for 4 days or more. Most of these correspondences were of types that would have been expected, e.g. no cases of blocked zonal flow in the upper westerlies over the half-hemisphere considered when the surface map was classified as zonal (i) or (ii); 80% of blocked zonal flow aloft when the surface maps showed monsoonal winter character (viii), the remaining 20% being accounted for by wavy patterns of varying degrees of distortion in the upper flow. It was noted, however, that meridional flow (v) at sea-level corresponded only 47% to blocked zonal flow aloft , 26% to sinusoidal waves, and 27% to other patterns. The slanting axis pattern (iv) at the ground corresponded to very various patterns at 500 mb. However, the number of examples was rather small, and none were available for some types in the particular 9-month period.

/7.

7. Corresponding weather types in the British Isles.

Comparison with the local types of surface weather occurring in the British Isles revealed of course no rigid correspondence with the hemisphere pattern. The Levick-Lamb type definitions were used for the comparison (6). Nevertheless, zonal types of hemisphere pattern gave 80% W'ly weather, 10% NW'ly, and 6% anticyclonic (in all 96% W + NW + AC) in the British Isles. On the other hand, the winter monsoonal hemisphere type gave only 30% anticyclonic weather over our islands, but 34% S'ly and 6% E'ly (together 70% AC + S + E, probably all cold types); as expected, N'ly weather in the British Isles was rare with this type of hemisphere circulation, but the Atlantic W'ly type penetrated as far as the North Sea 26%. An interesting surprise was that meridional circulations over the hemisphere as a whole rarely, if ever, were accompanied by S'ly weather in Britain, probably because the Norwegian Sea is a strongly preferred channel for the N'lies; the meridional type gave almost equally frequently N'ly, W'ly or anticyclonic weather over this country (together 82%), the nearest depression being often between Scotland, Iceland and S. Norway.

Table IV. Corresponding Weather in the British Isles.

Hemisphere Type	British Isles Type (%)						Cyclonic features over the mainland (%)
	Anti-cyclonic	W'ly	NW'ly	N'ly	E'ly	S'ly	
Z or Z'	6	80	10	0	0	4	30
D	30	26	26	6	6	6	22
S	34	42	12	6	2	4	14
M	26	30	12	26	6	0	26
SI	32	18	10	8	18	14	20
I	42	4	2	18	26	8	12
NW	30	26	0	4	6	34	32
MS	45	25	12	14	2	2	30

Table IV gives the full list of correspondences found between local weather types in the British Isles and the hemisphere circulation pattern type. The percentage frequency of the British Isles weather type most often accompanying each hemisphere type is underlined boldly in this table; the lowest frequencies are lightly underlined.

8. Conclusion.

The investigation was abandoned at this stage. It was obvious that no immediate contribution to the problem of forecasting four days ahead in the British Isles was likely to come from continuing this study. It seemed rather that prolonged effort involving the classification of many more years' weather maps would gradually lead to a better understanding of the general circulation and its seasonal evolution, but that this might not be the quickest way of achieving this desired background knowledge. Lack of rigid correspondence between the hemisphere circulation model and the type of weather in the British Isles was to be explained by the fact that local details cannot be rigidly determined by the broad pattern of flow; nevertheless we must seek to understand the broad features and the generalized patterns of flow preferred by the atmosphere in various circumstances and at various points of the seasonal evolution, if our detailed interpretation in the region of the British Isles is at all times to be reasonable.

References

(1) R.C. Sutcliffe, London, 1949. "The general circulation of the atmosphere" Q.J., R. Met. Soc., 75, pp.417-443

(2) H.C. Willett, Boston, Mass., 1947 approx. "Final Report of the Weather Bureau - M.I.T. Extended Forecasting Project for the Fiscal Year 1946/47"

(3) H.C. Willett, Lancaster, Pa., 1949. "Long-period fluctuations of the general circulation of the atmosphere" J. Met., Amer. Met. Soc., 6, No.1, pp.34-50.

(4) D. Brunt, Cambridge, 1939. "Physical and Dynamical Meteorology" (2nd edition) (p. 408 commenting on Jeffreys)

(5) R.D. Elliott and T.B. Smith, Lancaster, Pa., 1949. "A study of the effects of large blocking highs on the general circulation in the northern hemisphere westerlies" J. Met., Amer. Met. Soc., 6, pp.67-85.

(6) H.H. Lamb, London, 1950. "Types and spells of weather around the year in the British Isles - Annual trends, seasonal structure of the year, singularities" Q.J., R. Met. Soc., 76, pp.393-438.

---

anticyclonic with this type of circulation pattern. In some cases the low pressure systems developed on the polar front in middle to sub-polar latitudes are so large and intense as to leave no room for a high-pressure centre near the Pole. A rather slack region of relatively higher pressure will, however, be found.

The wind circulation defined by these axes of high and low pressure is largely zonal. Tropical or subtropical easterlies, middle-latitudes westerlies, and polar easterlies are the main features at the ground. In the upper troposphere the westerlies extend to lower and higher latitudes than in the bottom layers. The upper westerlies reach their greatest strength in jet streams in middle latitudes associated with the polar front surface aloft.

Average pressure profiles worked out for spells of this type gave maximum surface pressure near 40°N and minimum near 70°N, with strongest mean pressure gradient around the hemisphere between 45 and 65°N.

/(ii)

Appendix. Type definitions; hemisphere-wide circulation patterns.

(i) Z. The standard zonal circulation. Often considered as the normal circulation because of its approximation to the model presented by the annual mean (climatological) map, this type was found to occur less frequently than either S or M (defined below).

A belt of high pressure encircles the Earth, largely in subtropical latitudes, averaging about 30°N over much of the Pacific and western N. Atlantic but 30 - 40°N towards the eastern sides of these oceans and about 50°N over Asia north of the great mountain chains.

Separate anticyclonic cells exist within the high-pressure belt, but are often mobile, travelling along the axis of the belt. The cell divisions are less noticeable than with most of the other types.

An ideal zonal circulation with perfectly W to E axes and no breaks in the continuity of the high pressure belt or the depression belt to the north of it seems to be dynamically and geographically impossible. We have to permit a minor slant in the axis to place the anticyclones just north of the mountains of Asia, presumably because the circulations could not be complete if centred over the mountain-land. At least some of the individual anticyclonic cells often have a distinctly greater slant than the axis of the high pressure girdle itself and lie almost WSW to ENE. Breaks in the continuity of the anticyclonic belt are common near the east coasts of Asia and America, high pressure re-appearing over the western Pacific and western Atlantic at a distinctly lower latitude. A more or less well-developed exchange of air takes place across the parallels of latitude in the region of the break. No charts at all could be classified as zonal or "normal", if we were not to overlook these local features which depart from the zonal ideal.

North of the high-pressure girdle are regions of lower pressure, characterised by travelling depressions which commonly reach their greatest depth over the northeastern portions of the great oceans, notably between the Iceland region and the Barents Sea and between the Aleutian Isles and the Gulf of Alaska. The mean latitude of lowest pressure appears to be 65 - 70°N, being a few degrees farther north in the Atlantic than in the Pacific sector, where the Alaskan Rockies set a limit to the free circulation.

Over the polar ice conditions are generally, but not always, anticyclonic with this type of circulation pattern. In some cases the low pressure systems developed on the polar front in middle to sub-polar latitudes are so large and intense as to leave no room for a high-pressure centre near the Pole. A rather slack region of relatively higher pressure will, however, be found.

The wind circulation defined by these axes of high and low pressure is largely zonal. Tropical or subtropical easterlies, middle-latitudes westerlies, and polar easterlies are the main features at the ground. In the upper troposphere the westerlies extend to lower and higher latitudes than in the bottom layers. The upper westerlies reach their greatest strength in jet streams in middle latitudes associated with the polar front surface aloft.

Average pressure profiles worked out for spells of this type gave maximum surface pressure near 40°N and minimum near 70°N, with strongest mean pressure gradient around the hemisphere between 45 and 65°N.

(ii) Z'. A winter-modified zonal circulation commonly occurs in the season when the continents are cold.

The monsoonal effect induces a modification of the zonal flow, whereby the main belt of high pressure spirals around the Earth from subtropical latitudes in the Atlantic sector gradually into higher latitudes across Asia, reaching the Anadir peninsula in NE Asia at its eastern end and sometimes continuing into northern Alaska. Offshoot high pressure centres travel southeastwards from there across North America as polar anticyclones. The circulation over America is typically confused or meridional. This sector is the cradle of disturbances possessing great potential energy with this type of general circulation pattern.

The transition along the high pressure belt from warm to cold anticyclones is believed to be a matter of increasing intensity of the surface radiation cooling (continentality) eastwards and as the belt progresses into higher latitudes. The occurrence of subsidence accompanied by dynamical warming and inversions in the middle and lower troposphere in these anticyclones is probably not affected but merely masked in the "total" thickness values by the intense surface cooling and initial coldness of the air masses involved in the upper convergence; all the anticyclones in the belt are in this sense warm anticyclones.

In the Pacific a separate sub-tropical high-pressure belt exists in the usual latitudes, isolated from the main portion of the high-pressure belt spiralling around the hemisphere, the eastern end of which overlaps in high latitudes in the Pacific sector. Occasional linkages with the Azores - Bermuda anticyclone may be achieved by the Pacific anticyclone spreading across the southern Rockies and centres passing on from there across the U.S.A.

The Iceland depression is usually vigorously developed in this type of circulation with deep, travelling centres dominating the northeastern Atlantic and circulating around much of the polar basin. The normal zonal regime exists in isolation over the N. Pacific, modified only in so far as the Aleutian and Gulf of Alaska depressions may be forced a few degrees further south by the high pressure established over the Behring Strait.

This winter-modified zonal circulation is the most asymmetrical type recognized. Asymmetry reduces the significance of the latitude profiles of surface pressure and thickness (mean air-column temperatures of the troposphere), but the effects of temperature and surface pressure distribution appear to cancel one another out to give a largely symmetrical and unmodified zonal circulation model in the upper troposphere. Moreover, the outstanding intensity of the depressions and anticyclones occurring in spells of this type produced the most extreme ranges of pressure found in the latitude profiles of any type, in spite of the asymmetry.

(iii) D. Double-structure zonal circulation pattern.

Cases arise in which the zonal axes of high and low pressure are practically repeated twice over in the hemisphere.

Depression families travel from W to E around the fringe of the polar basin and also in lower latitudes across the United States, through the Mediterranean or over Europe, across central Asia and in the mid-Pacific.

The high-pressure belts in sub-tropical latitudes and around 60°N-70°N are on the whole less intense and more broken up into individual cells than the single high-pressure belt in the simple zonal circulation type. The sub-tropical belt is displaced a few degrees south of the climatological mean. The systems in both belts of high pressure are warm anticyclones.

The thermal distribution over the hemisphere shows concentrations of gradient in high latitudes as well as in the lower middle latitudes associated with the respective depression families. Correspondingly the zonal circulation of the upper westerlies shows twin concentrations giving a split jet-stream effect. Observational details do not appear adequate for a comparison of the strengths of these jet streams.

Mean profiles for spells of this type showed pressure maxima near 35 and 60 - 65°N and minima in 50°N - 55°N and near the North Pole.

(iv) S. Slanting-axis circulation pattern.

The axes of the main high-pressure systems and depression paths approximate to a SW to NE orientation.

The main depressions travel NE and reach their greatest development in high latitudes, but smaller cyclonic features may be seen to break away southeastwards from the major systems and travel around the southern limit of the polar airstream at the eastern extremity of the anticyclonic axis.

The cell-divisions, which are marked by cold troughs and polar outbreaks, take on much greater importance with this type than with types Z, Z', or D. This may be used as a criterion to distinguish the type from a simple zonal circulation. Longitudinal differences of weather-type are pronounced.

The slanting axes of high and low pressure and the polar outbreaks between may occur in any longitude, but various geographical locations seem to be preferred. Patterns with SW to NE orientated anticyclones over the eastern N. Pacific and N. Atlantic oceans, thrusting into the northwestern U.S.A. (between the coast of Washington-Oregon and the Great Basin, west of the main Rocky Mountains watershed) and towards southern England respectively, are common; also a similarly orientated axis stretching across central Asia from Turkestan towards Yakutsk along the edge of the great mountain region.

Other longitudinal dispositions do occur, and the regions liable to polar outbreaks with this pattern are probably less clearly marked than in the case of meridional circulations.

The slanting axis circulation pattern implies a wavy pattern in the upper westerlies, the ridges and troughs of which lie somewhat to the west of the corresponding features in the surface pressure distribution.

The main anticyclones are warm anticyclones, which project into higher latitudes than in the zonal circulation type.

Pressure profiles are weaker than for types Z or Z' (though not D) on account of the tilted axes.

/(v)

(v) M. Meridional circulation type.

The main surface wind streams have stronger northerly and southerly components than zonal components.

Correspondingly the axes of high pressure are orientated nearly N to S.

Occluding wave depressions tend to travel on meridional tracks.

High and low pressure regions alternate with one another in most latitudes around the world. Both high and low pressure systems tend to reach their most intense development in sub-polar latitudes, between 50° and 70°N.

Many different longitudinal dispositions of the pattern occur, but some paths seem to be preferred for the polar outbreaks, those in the Norwegian Sea and Davis Strait being well-known at certain seasons of the year. In regard to the former channel both topography and the common north Greenland anticyclones probably play important parts in determining the favoured path. Northerly outbreaks on either side of the Urals, in the White Sea basin and in the neighbourhood of the great Siberian rivers, as well as through the Behring Strait and along the eastern flank of the Rockies, are also sufficiently well-known and appear to be favoured by topographical factors at least. (A general tendency is evident on the hemisphere thickness maps for topographical features to guide the cold outbreaks, a tendency which even increases towards lower latitudes in most cases as the cold air becomes shallower.)

The wind and temperature distribution in the upper troposphere shows waves of great amplitude with this type of circulation. Latitudinal pressure profiles are very weak and featureless.

(vi) SI. Slanting inverted circulations.

This type of pattern is defined by axes of high pressure and depression paths orientated NW to SE. The high pressure systems are generally centred about 60°N at the western ends of the respective axes. These circulation patterns resemble the double-structure zonal type in that depressions move around the fringe of the polar basin, but may be distinguished by

(a) departure of the depression paths from the zonal orientation, and

(b) occurrence of some (often rather minor) inverted frontal cyclonic features with a tendency to travel from SE to NW (or from SSE to NNW) along the southern limits of the sub-polar warm anticyclones.

Farther south fragments of another depression belt with systems advancing from W to E are usually found more or less well developed. The travelling systems in this sub-tropical depression belt are commonly frontal waves, first formed in quite low latitudes and often hard to detect or follow in detail owing to the sparse observational network available over the tropical oceans and deserts. These wave disturbances travel E or NE and usually culminate in rather deep, stationary, occluded lows about 40 - 50°N, which they feed. These depressions are normally more intense than the rather minor inverted systems which ultimately depend upon them for a supply of cold air.

Any high pressure occurring in the tropics south of the subtropical belt of travelling disturbances forms a rather fragmentary belt represented by (mostly) rather weak anticyclones in notably low latitudes.

The depressions in high latitudes are usually intense and considerable high- and low-pressure systems alternate with one another in much the same latitude band. Frontal wave disturbances in high latitudes travel SE and ultimately occlude and deepen as they feed into the more or less stationary cyclonic circulations, which they help to maintain.

Large amplitude and often greatly distorted wave patterns characterize the temperature and wind distributions in the upper troposphere with this circulation type. Cut-off warm and cold circulations, in high and low latitudes respectively, are also typical.

The upper wind flow shows some likeness to the double zonal structure circulation in that jet streams occur in both high and low latitudes, but with the slanting inverted type appreciable easterly components will be found throughout the troposphere at some points in middle latitudes. Over some limited regions we may speak of an easterly jet in the upper levels. Of the two westerly jet streams, either the one in the far north or the one in low latitudes may be the stronger with this circulation type. The orientations of the air streams slant strongly away from the true zonal directions at all levels in the troposphere.

Very variable pressure profiles occur.

(vii) I. Simple inverted (zonal easterly) circulation type.

The main high pressure belt is in high latitudes, north of 60°N in the Siberian sector and north of 50°N elsewhere, the individual anti-cyclones being characteristically intense though separated from one another by fairly low pressures and even minor low-pressure systems in the same latitude zone at the cell divisions.

The main low-pressure systems are further south, mainly between 30 and 50°N, and are not outstandingly deep. Some inverted warm sectors are generally to be seen and some of the low-pressure centres show a tendency to move from E to W. As in the case of the slanting inverted type any inverted systems are typically rather weak and might indeed be dismissed as mere details of only local interest on the northern or northeastern fringe of the bigger cyclonic circulations of middle latitudes.

There is usually no well-marked belt of high pressure in the lower latitudes, although here and there individual anticyclones may be found south and west of the mean positions of the subtropical anticyclones known to climatology. These anticyclones are mostly rather weak, but not always so.

This type of circulation pattern represents the greatest departure from the climatological mean which occurs.

Easterly surface winds prevail in middle latitudes, more variable winds in the tropics where the normal trade wind circulation is disturbed. In the polar basin either easterly or westerly surface winds may prevail, and the type may be subdivided:-

/(i)

(i) I_A - conditions in the polar basin anticyclonic.

(ii) I_C - conditions in the polar basin cyclonic.

Accordingly the maximum of the pressure profile may lie either near the Pole or about 60°N. The anticyclones near 60°N are warm anticyclones, the individual centres being subject to more or less regular replacement by new development with subsidence behind shallow invading cold fronts, if the type is to persist for many days; this process sometimes results in a net westward drift of the cells, even though the individual centres more commonly move from W to E.

The middle-latitudes easterlies are found throughout the troposphere, with local concentrations forming easterly jet-streams in the higher levels.

In other latitudes there is considerable variability of direction of the upper winds. Notably strong westerly jet streams may be found in low latitudes in some cases. Appreciable meridional air currents also occur over restricted regions.

The simple inverted type is rarer than the slanting inverted and is perhaps the rarest of the types recognised. Its occurrence in the Pacific sector seems rarest of all. Examples in the Atlantic sector are not uncommon, and similar patterns often spread to Europe and North America. Some cases of inverted type first appear over Asia, and spread to cover most of the hemisphere. The subpolar warm* anticyclones are mostly established over regions with a notably cold undersurface, consisting of snow-covered land, ice, or near-freezing melt-water on the ocean surface. Perhaps it is this geographical factor which is missing in the Pacific sector, with the result that truly hemisphere-wide examples of this type are hard to find and often rather ill-formed when they do occur.

Longitudinal differences of weather are more prominent than with the zonal westerly circulation types.

(viii) MW. Monsoonal winter circulation.

This type is characterized by rather weak overall zonal westerly flow around the hemisphere and dominant effect of the cold continents. It displays some similarity therefore with the meridional and inverted types of circulation pattern, and may be related particularly with the slanting inverted type which seems often to occur in association with the winter monsoon pattern in the longer spells.

High pressure dominates all the continental land areas and may spread over the northern parts of the oceans (where the oceans are narrowest). Nowhere are any important depressions to be found over the land (no centres below 995 - 1,000 mb.).

In late winter conditions are generally anticyclonic also over the fast ice covering the polar seas when the monsoonal winter type is recognized, but not always so.

We use the designations MW_a and MW_c for the cases where the polar basin is predominantly anticyclonic and cyclonic respectively.

---

* Called warm because of the subsidence and dynamical warming above the bottom layer.

Over the warmer oceans various patterns may occur, but deep depressions are commonly found over the wide stretches of ocean in middle latitudes, especially between 25 and 55°N. This activity may be associated with the strong thermal gradients and air mass instability which prevail, thanks to the specially cold air coming over the sea from the continental regions. The deepest centres move only slowly, and individual depressions sometimes survive over long periods.

An extremely cold troposphere develops over the continental anticyclones, in which surface radiational heat-loss more than offsets the dynamical warming of the middle troposphere levels where subsidence takes place. (The mean temperature aloft in the region of the Siberian winter anticyclones (Yakutsk, Chita) show an inversion of the order of 10°C up to about 1.7 km and above that temperatures similar, level for level, to Spitzbergen and Franz Josefs Land, which lie admittedly in much higher latitudes but only 300 - 400 miles from open water.) These anticyclones differ from warm anticyclones therefore mainly in virtue of the intensely cold bottom layers. Their very high central pressures ensure that at least a ridge in the pressure and wind-flow pattern extends up to considerable heights, except in the case of the more northerly centres, which are liable to be surrounded by warmer air at most levels. In general the flow patterns in the upper troposphere with this type are distorted, but much less distorted than at the ground. Strong westerly jet streams occur in low latitudes, particularly over the southeastern sectors of the continents; elsewhere the zonal flow is rather weak.

This type should not be confused with the winter-modified zonal circulation type Z' in which similar monsoonal effects are seen at work only where they are most readily superimposed on an intense zonal circulation in the regions farthest downstream from the warm oceans. Nevertheless it may be noted that some of the most intense Siberian anticyclones of all occur in the Lake Baikal region of SE Siberia and the borders of Mongolia, precisely with the Z' circulation. The monsoonal winter pattern corresponds to anticyclones in higher latitudes; the anticyclones are intense for those latitudes, but no more intense than some of the Lake Baikal highs with the Z' type.

(ix) MS. Monsoonal summer type.

This type is characterized by weak overall zonal westerly flow around the hemisphere and dominant effect of the heated continents. Like the MW type, its onset seems to be associated with the meridional and inverted types, and may be particularly related with the slanting inverted type.

Low pressure, on the whole marked by only weak circulations and shallow centres, though not entirely so, covers the continents, and no important high-pressure system is found anywhere over the strongly heated land. (Northern tundras with continuing snow-cover, high mountains and enclosed seas may be excepted from this qualification. Elsewhere no centres over 1,020 mb. should be allowed for recognition of this type). South of 50°N over America and about 60°N over Asia the monsoonal depressions tend to stagnate, but over the northern tundras travelling systems may occur.

Various patterns arise over the oceans, but the most typical show anticyclones displaced north of the annual mean position, perhaps most commonly between 40 and 50°N, and above average intensity.

We use the designations MS_a and MS_c for the cases where the polar basin is predominantly anticyclonic and cyclonic respectively.

The thermal distribution patterns show rather weak gradients generally except near the continental margins and strong gradients near the limits of the polar ice. The spread of cold melt-water also over the ocean surface doubtless has a fleeting importance while a given area is affected but is itself subject to atmospheric control.

Geographical and longitudinal differences may give rise to considerable and important differences of weather type over wide areas in different cases of monsoonal summer type.

The high-level winds show no very strong features, their distribution and concentrations following the thermal pattern.

(x) W. Weak circulation.

This type is patternless and without well-developed circulation systems anywhere in the hemisphere. It is rare, seems to occur only in summer when thermal gradients are weak, and is most closely related to summer-monsoon situations.

In extreme cases the overall range of sea-level pressures in the hemisphere is only 30 to 40 mb. (most commonly with values between 990 and 1,030 mb.).

It very seldom occurs for more than one or two days at a time.

paper of the Meteorological Research
Committee (London),
M.R.P. No .... by Mr...........................
A copy is available in the Library of
the Meteorological Office."

TECHNICAL REFERENCE FILE

M.R.P. 633
S.C. II/76
26th April, 1951.

ATI 113149

AIR MINISTRY

METEOROLOGICAL RESEARCH COMMITTEE

The distribution of medium and high cloud near the jet stream

by J.S. Sawyer and Betty Ilett. (Meteorological Office)

1. Introduction

Narrow belts of strong winds are a recognised feature of synoptic charts for levels in the upper troposphere and have come to be known as "jet streams". The best defined maxima of wind appear to occur in relatively straight stretches of the meandering belt of the upper westerly current of the hemisphere. These narrow bands of strong upper winds persist from one chart to the next and must form stable dynamical systems. It might therefore be expected that features of the flow in the upper troposphere and associated cloud systems would show a closer relation to the position and movement of the axis of the jet stream than to the synoptic systems of the surface pressure field.

The present investigation was undertaken in order to ascertain whether the distribution of high and medium cloud near the jet stream followed a recognisable pattern. If such a pattern existed it would be of value in the analysis of high level charts when few upper air soundings were available; it might also permit the navigator of an aircraft to recognise his position with respect to the jet stream from the state of the sky.

The available data consisted of the synoptic reports received at C.F.O. (both surface observations and upper air soundings) together with the analysed charts. On the basis of those observations some uncertainty will exist regarding the position of the axis of the jet stream; even over the British Isles it would not be expected that one could place the axis with a much smaller error than the average distance between upper air soundings, 200 miles; in other areas the errors would be greater. A less obvious uncertainty arises from reports of medium and high cloud. The estimation of the amount of high cloud is not easy, nor is the classification of the medium and high clouds according to the international code entirely unambiguous. No doubt cirrus and medium cloud structure varies considerably from place to place, but reported amounts and types differ between stations so close together that the observers must be viewing the same clouds over at least part of the sky.

For these reasons it seems unlikely that a direct examination of synoptic charts will give a true picture of the distribution of upper cloud around the jet stream on individual occasions. Two methods of approach to the study therefore seem possible: the first, by the detailed reanalysis of all available observations, and the making of special observations of cloud etc. in relation to individual jet streams: the second, the statistical approach, in which a large number of jet streams are examined and cloud observations tabulated in relation to their position with regard to the jet. The second approach has been adopted in the present work in the hope that any relationships between the cloud and the jet stream which are sufficiently regular to be of interest will be brought out statistically despite errors in individual cases.

/2.

2. Method of analysis

The period covered by the analysis was the year 1949. Occasions of jet streams passing over or within about 500 miles of the British Isles were noted by examination of the 300 mb. contour charts drawn as routine at C.F.O. For this purpose a belt of approximately straight flow with a maximum wind speed at 300 mb. (observed or geostrophic) of 70 kt. or more was taken as defining a "jet stream". The axis of the jet, viz. the line of greatest velocity, was noted on the charts for 1500 G.M.T. each day and the distribution of medium and high cloud examined in relation to this.

All available observations of medium and high cloud for 1500 G.M.T. were plotted on charts together with the axis of the jet stream. The type and amount of the medium and high cloud were recorded. The present scheme of synoptic reporting does not make provision for reports of the amount of the medium and high cloud layers on all occasions. However an estimate of the amount of both medium and high cloud was made and plotted on the basis of the total amount of cloud reported and the amounts reported in lower cloud layers. If the amount of low cloud was less than 4 eighths and no upper cloud was reported both cirrus and medium cloud were assumed to be absent. Occasions of 4 eighths of low cloud or more and no medium cloud or cirrus observed were not plotted nor were they included in the statistical summaries.

3. Statistical Results

In order to analyse the distribution of cloud with relation to the axis of the jet, the area around the jet was divided into 8 sectors as indicated in Figure 1. The division was firstly into bands parallel to the jet and 200 miles wide and secondly by a line perpendicular to the axis through its mid-point, dividing the jet into two equal sections longitudinally from the entrance to the mid-point and from the mid-point to the exit. The letters in Fig. 1 have been used to define the sectors in the tabular results.

The results of the statistical analysis are given in Tables I to IV. The number of occasions of particular amounts and types of high and medium cloud is expressed as a percentage of the number of occasions for which observations of high and medium cloud respectively or their absences were available for the particular sectors. It must be remembered in considering these figures that observation of medium and high cloud was prevented by low cloud on a considerable number of occasions and that with broken low cloud (4 eighths or more) observations of medium and high cloud have been included but observations of their absence under these circumstances have been omitted. However the purpose of the present investigation was to establish if any pronounced relation between the jet and upper cloud existed, and statistical corrections for the unrepresentative nature of some of the data have not been attempted.

The most noteworthy feature of Tables I to IV are the following:

(a) Amounts of cirrus of 4 eighths or more are considerably more frequent to the right of the axis of the jet (sectors C, D, G and H) than to the left (sectors A, B, E and F). This is brought out in table V which gives the percentage frequency of cloud 4 eighths or more to the right and left of the jet axis.

There is little difference between the sectors longitudinally along the jet in respect of high cloud amount, but this is not to be interpreted as indicating no difference between the entrance and exit to the jet - probably only a few of the observations are really close to either the exit or entrance; the observations are mainly typical of the central region.

The more or less corresponding increase of cirrus amounts from sector A to D and from E to H lends support to the reality of the distribution of high cloud found.

(b) Medium cloud amounts appear to be less in sectors A and B i.e. the left entrance to the jet but the amounts in other sectors show little variation.

(c) The statistics of cirrus types show, as would be expected, a dominance of cirrus type 3 (anvil cirrus) to the left of the jet stream and a relative abundance of the frontal and layer types of cirrus to the right. In order to bring out the difference between the character of the cirrus cloud table VI gives (i) the total frequencies of the layer types of cirrus (types 4 to 8) and (ii) the frequency of no cirrus and anvil cirrus (type 3) added together for the various sectors.

(d) The statistics of medium cloud type show a remarkable dominance of type 6 (altocumulus formed by spreading out of cumulus) to the left of the jet. Altostratus, frontal types of altocumulus and altocumulus castillatus are more common to the right of the jet.

4. Notes on individual jet streams

For several jet streams fairly complete sets of observations of cirrus cloud were available. It was noteworthy that on most occasions when a clear limit to an area of cirrus could be defined, this limit lay close to the axis of the jet stream. These were mainly the cases in which the jet stream was associated with an active front. On the other hand there were a number of jets through surface ridges of high pressure in which upper cloud amounts were small or zero in all sectors for which observations were available.

5. Conclusions

There is statistical evidence that cirrus cloud is considerably more frequent and extensive to the right of the axis of the jet stream than to the left. The frontal and layer types of cirrus and medium cloud are more common to the right of the jet; anvil cirrus and altocumulus from the spreading out of cumulus are more common to the left.

There is some suggestion from the study of individual cases that when a well defined boundary to the frontal cirrus occurs the axis of the jet stream is found close to this boundary, but the evidence is insufficient to establish this with certainty. It might be profitable to carry out a more detailed examination by means of specially made observations from the ground or from aircraft in association with a jet stream crossing the country.

There is little evidence for any variation of the cloud distribution along the length of the jet except for the relatively low frequency of medium cloud in the left entrance. However, the mode of analysis was not suitable to bring out features which affect only small areas near the exit or entrance of the jet.

/- 4 -

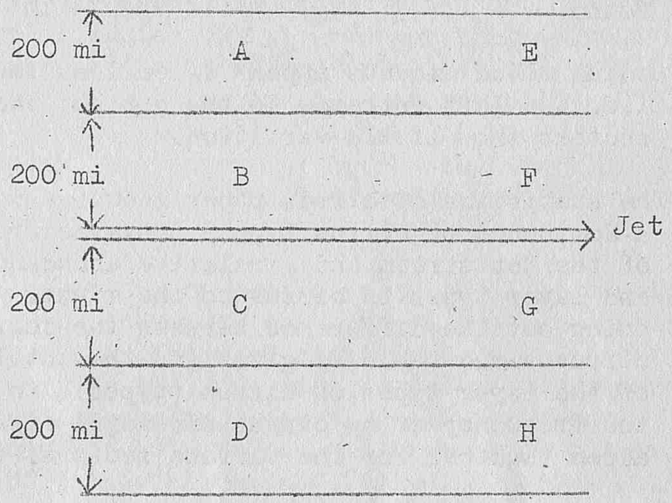
200 mi
A
E
200 mi
B
F
Jet
200 mi
C
G
200 mi
D
H

Fig. 1. Sectors used for study of cloud distribution in relation to the jet stream.

Fig. 23

Table I. Frequency of high cloud amounts in various sectors of the jet stream expressed as a percentage of the total number of observations of high cloud together with observations of no high cloud and low cloud less than 4 oktas.

(a) All jet streams - greater than 70 kts.

Amount (oktas)	0	1-3	4	5-7	8	Total No. of obs.	Amount (oktas)	0	1-3	4	5-7	8	Total No. of obs.
Sector A	37	44	12	6	1	95	Sector E	37	46	10	5	2	205
Sector B	45	30	16	7	2	201	Sector F	58	27	5	8	1	308
Sector C	22	49	19	8	2	192	Sector G	31	35	18	12	4	458
Sector D	19	32	23	11	5	104	Sector H	29	36	17	17	1	369

(b) Strong jets - greater than 120 kts.

Amount (oktas)	0	1-3	4	5-7	8	Total No. of obs.	Amount (oktas)	0	1-3	4	5-7	8	Total No. of obs.
Sector A	41	36	18	5	0	39	Sector E	46	39	5	9	0	56
Sector B	55	23	12	8	2	119	Sector F	59	26	8	6	1	123
Sector C	20	45	12	19	5	65	Sector G	29	34	16	15	6	168
Sector D	0	33	28	22	17	18	Sector H	17	43	19	18	3	111

Table II. Frequency of high cloud types in various sectors of the jet stream expressed as a percentage of the total number of observations of high cloud together with observations of no high cloud and low cloud less than 4 oktas.

(a) All jet streams - greater than 70 kts.

Type *	0	1	2	3	4	5	6	7	8	9	Total No. of obs.	Type*	0	1	2	3	4	5	6	7	8	9	Total No. of obs.
Sect. A	37	9	15	23	5	2	2	2	0	4	95	Sect. E	37	11	15	22	1	3	4	2	3	2	205
Sect. B	45	9	9	15	3	3	9	1	4	2	201	Sect. F	58	5	5	15	2	4	5	2	3	1	308
Sect. C	22	21	17	8	2	5	10	4	6	5	192	Sect. G	31	15	18	6	2	7	6	4	4	5	458
Sect. D	29	15	22	2	5	8	6	7	4	3	104	Sect. H	29	19	19	3	3	6	8	2	5	5	369

* International code figure as used in 1949 (see M.O. 510b pp. 20-21)

/- 6 -

(b) Strong jets - greater than 120 kts.

Type *	0	1	2	3	4	5	6	7	8	9	Total No. of obs.	Type *	0	1	2	3	4	5	6	7	8	9	Total No. of obs
Sect.A	41	3	15	21	10	0	3	3	0	5	39	Sect.E	46	11	5	23	0	4	5	0	5	0	56
Sect.B	55	6	7	12	2	3	10	1	2	3	119	Sect.F	59	2	3	19	4	5	5	0	1	1	123
Sect.C	20	19	5	12	0	6	17	8	5	9	65	Sect.G	29	17	16	8	3	5	5	7	4	6	168
Sect.D	0	22	28	0	6	6	11	22	0	6	18	Sect.H	17	19	19	3	5	8	12	5	7	6	111

* International code figure as used in 1949 (see M.O.510b pp. 20-21)

Table III. Frequency of medium cloud amounts in various sectors of the jet streams expressed as a percentage of the total number of observations of medium cloud together with observations of no medium cloud and low cloud less than 4 oktas.

(a) All jet streams - greater than 70 kts.

Amount (oktas)	0	1-3	4	5-7	8	Total No. of obs.	Amount (oktas)	0	1-3	4	5-7	8	Total No. of obs.
Sector A	38	23	17	16	6	154	Sector E	34	16	15	20	16	335
Sector B	5	21	12	11	5	256	Sector F	34	21	12	18	15	574
Sector C	30	25	15	21	10	334	Sector G	36	16	12	20	16	764
Sector D	31	17	14	24	14	177	Sector H	34	12	13	23	17	641

(b) Strong jets - greater than 120 kts.

Amount (oktas)	0	1-3	4	5-7	8	Total No. of obs.	Amount (oktas)	0	1-3	4	5-7	8	Total No. of obs.
Sector A	45	21	15	15	4	53	Sector E	39	13	14	21	13	92
Sector B	62	18	10	8	2	134	Sector F	35	20	14	21	10	205
Sector C	25	22	16	21	17	126	Sector G	28	17	13	22	19	318
Sector D	14	12	14	35	26	43	Sector H	24	10	12	27	26	225

/Table IV

Table IV. Frequency of medium cloud types in various sectors of the jet streams expressed as a percentage of the total number of observations of medium cloud together with observations of no medium cloud and low cloud less than 4 oktas.

(a) All jet streams - greater than 70 kts.

Type *	0	1	2	3	4	5	6	7	8	9	Total No. of obs.	Type *	0	1	2	3	4	5	6	7	8	9	Total No. of obs.
Sect.A	38	2	6	7	9	2	26	9	1	1	154	Sect.E	34	5	14	7	7	1	9	13	1	0	335
Sect.B	50	2	5	10	7	2	14	9	0	0	256	Sect.F	34	4	12	9	7	1	20	12	1	0	574
Sect.C	30	4	6	13	11	2	8	22	3	1	334	Sect.G	36	5	12	9	10	2	10	15	5	4	764
Sect.D	31	5	12	9	9	2	0	21	7	3	177	Sect.H	34	6	12	11	11	2	4	19	1	1	641

(b) Strong jets - greater than 120 kts.

Type *	0	1	2	3	4	5	6	7	8	9	Total No. of obs.	Type *	0	1	2	3	4	5	6	7	8	9	Total No. of obs.
Sect.A	45	0	6	4	13	0	26	6	0	0	53	Sect.E	39	5	14	4	8	0	16	13	0	0	92
Sect.B	62	1	2	10	7	3	7	7	0	0	134	Sect.F	35	3	9	8	9	1	23	11	0	0	205
Sect.C	25	5	8	13	10	2	11	25	0	0	126	Sect.G	28	7	15	9	9	2	13	16	1	0	318
Sect.D	14	12	23	7	5	2	0	33	0	5	43	Sect.H	24	8	18	12	7	1	4	25	0	0	225

* International code figure as used in 1949 (see M.O. 510b pp. 20-21)

Table V. Percentage of high and medium cloud 4 eighths or more to the left and right of jet stream.

(a) All jet streams - greater than 70 kts.

(b) Strong jets - greater than 120 kts.

To the Left of jet. Sectors A, B, E and F	To the Right of jet. Sectors C, D, G and H.
High Cloud (a) 19	34
(b) 18	39
Medium Cloud (a) 41	50
(b) 37	60

Table VI. Percentage frequency of (i) no cirrus or anvil cirrus and (ii) layer type cirrus in various sectors.

No cirrus or anvil cirrus

(a) All jet streams - greater than 70 kts.

Sect.A	60	Sect.E	59
Sect.B	51	Sect.F	72
Sect.C	30	Sect.G	37
Sect.D	31	Sect.H	32

(b) Strong jets - greater than 120 kts.

Sect.A	62	Sect.E	70
Sect.B	67	Sect.F	79
Sect.C	32	Sect.G	37
Sect.D	0	Sect.H	19

Cirrus types 4 - 8

(a) All jet streams - greater than 70 kts.

Sect.A	12	Sect.E	14
Sect.B	20	Sect.F	16
Sect.C	27	Sect.G	24
Sect.D	29	Sect.H	24

(b) Strong jets - greater than 120 kts.

Sect.A	15	Sect.E	14
Sect.B	18	Sect.F	15
Sect.C	35	Sect.G	24
Sect.D	44	Sect.H	36

been published. Any author desiring to
quote this paper should refer to it as "A
paper of the Meteorological Research
Committee (London),
M.R.P. No .... by Mr.........................
A copy is available in the Library of
the Meteorological Office."

c 8

M.R.P. 639
S.C.III/97
28th March, 1951

AD 223 001

AIR MINISTRY

METEOROLOGICAL RESEARCH COMMITTEE

Coalescence as a factor in drop size distribution in cloud.

by

A. C. Best.
(Meteorological Office)

AIR WEATHER SERVICE
TECHNICAL REFERENCE FILE
AUG 7 1951

Summary

Equations are developed to represent the rate of change of the number of drops of a given size in a cloud owing to condensation and to coalescence respectively. Numerical computation from these equations shows that condensation is much more effective than coalescence in determining drop size distribution in clouds with small average drop size, with small liquid water content or with a large degree of supersaturation.

1. Introduction

In a previous paper (1) a formula for drop size distribution in cloud was deduced from the assumption that the governing factors are rate of growth of drops owing to condensation and rate of diffusion of the drops out of the cloud under the action of turbulence. In particular the effects, if any, of coalescence were ignored. In the present paper we propose to examine the magnitude of the effect of coalescence on size distribution of cloud drops and to compare it with the magnitude of the effect of condensation.

We shall assume that two drops coalesce when they touch though possibly this is controversial. We shall also assume a collection efficiency of unity for a cloud drop falling through a group of smaller drops. This will lead to an overestimation of the effects of coalescence.

2. The equations

At any time t let the number of drops per unit volume and having radius between r and r+Δr be f(r,t) Δr. Every cloud droplet grows by absorbing smaller droplets until it ceases to exist because it is itself absorbed by a larger droplet. Thus the quantity f will vary with time for three reasons, viz.

(a) Some drops with radius previously smaller than r will grow into the r class by absorbing smaller drops.
(b) Some drops previously in the r class will grow out of the class by absorbing smaller drops.
(c) Some drops previously in the r class will disappear because they have been absorbed by larger drops.

Factors (a) and (b) are related to the rate of growth of a droplet as follows. Let the terminal velocity of a drop of radius r be u(r). In time Δt the swept volume of contact for drops of radius r and of radius x ($< r$) is $\pi(r+x)^2\left[u(r) - u(x)\right] \Delta t$. Since the falling drop is assumed to collect all smaller drops lying in its path we have

$$\frac{\partial}{\partial t}\left(\frac{4\pi r^3}{3}\right) \Delta t = \int_0^r f(x,t)\, \frac{4\pi x^3}{3}\, \pi(r+x)^2 \left[u(r) - u(x)\right] dx\, \Delta t$$

or

$$\frac{\partial r}{\partial t} = \frac{\pi}{3r^2} \int_0^r x^3 \, f(x,t) \, (r+x)^2 \left[u(r) - u(x)\right] dx \quad \ldots.(1)$$

Equation 1 represents the rate of growth of an individual droplet owing to coalescence during the period before it is in turn absorbed by a larger drop. In time Δt the number of drops per unit volume, with radius originally smaller than r, which grow sufficiently to come into the r class is the number of drops with radius between r and $r-\Delta t \, \partial r/\partial t$, i.e. $f(r,t) \, \Delta t \, \partial r/\partial t$. Similarly the number which grow out of the class is $(1+\Delta r \, \partial/\partial r)(f(r,t) \, \Delta t \, \partial r/\partial t)$ and thus we get

$$f'_a = \left(\frac{\partial f}{\partial t}\right)_a = -\frac{\partial}{\partial r}\left(f(r,t) \frac{\partial r}{\partial t}\right) \quad \ldots\ldots\ldots\ldots\ldots.(2)$$

where $\partial r/\partial t$ is defined by equation 1 and the suffix a indicates the time variation of f owing to absorption of smaller drops.

A similar line of reasoning in M.R.P. 627 led to a similar expression for f'_n, the time variation of f owing to condensation, viz.

$$f'_n = \left(\frac{\partial f}{\partial t}\right)_n = -\frac{\partial}{\partial r}\left(f(r,t) \frac{G}{r}\right) \quad \ldots\ldots\ldots\ldots\ldots\ldots.(3)$$

where

$$G = \frac{MD}{R\theta} \, s \, p_\theta \quad \ldots\ldots\ldots\ldots\ldots\ldots\ldots\ldots\ldots.(4)$$

M = molecular weight of water (=18).
D = coefficient of diffusion of water vapour in air ($cm^2 \, sec^{-1}$).
R = gas constant per gram molecule (= 8.314 10^7 erg deg^{-1} mol^{-1}).
θ = absolute temperature.
sp_θ = vapour pressure excess of water in atmosphere over drop.
p_θ = saturation vapour pressure (dynes cm^{-2}) of water at temperature θ.

(Except for very small drops 100s is practically the excess of relative humidity over 100 per cent.)

Turning now to the rate of disappearance of drops owing to absorption by larger drops we easily get

$$f'_d = \left(\frac{\partial f}{\partial t}\right)_d = -\int_r^\infty f(x,t) \, f(r,t) \, \pi (x+r)^2 \left[u(x) - u(r)\right] dx \quad ..(5)$$

where the suffix d denotes the time variation of f owing to absorption by larger drops.

The complete time rate of variation of f is given by the sum of f'_a, f'_d and f'_n. It would obviously be a complicated problem to solve the above equations for f. Instead we shall compute $(f'_a + f'_d)$, the effect of coalescence, and compare it with f'_n, the effect of condensation. To do this we shall assume that the drop size distribution is defined by

$$1 - F = \exp\left[-(r/b)^n\right] \quad \ldots\ldots\ldots\ldots\ldots\ldots\ldots\ldots.(6)$$

where F is the fraction of liquid water in the air comprised by drops with radius less than r and b and n are constants with approximate values 10 microns and 3.25 respectively. Equation 6 has been justified on empirical grounds elsewhere (2). From equation 6 it easily follows that

$$f = \frac{3Wnr^{n-4}}{4\pi b^n} \, e^{-(r/b)^n} \quad \ldots\ldots\ldots\ldots\ldots\ldots.(7)$$

where W is the concentration of liquid water in the air (cm^3/cm^3). We shall also assume the formula obtained from Stokes' law for the terminal velocity of a drop. Neglecting air density in comparison with the density of water this gives

$$u(r) = \frac{2gr^2}{9\mu} \quad \ldots\ldots\ldots\ldots\ldots\ldots\ldots\ldots\ldots (8)$$

where μ is the coefficient of viscosity of air.

3 Numerical computation.

Substituting from (7) and (8) in (1) and (2) we obtain after a little algebraic manipulation

$$f_a' = -f\frac{Wgb}{18k^2\mu}P \quad \ldots\ldots\ldots\ldots\ldots\ldots\ldots\ldots (9)$$

where

$$k = r/b$$

$$P = A_o(1 - e^{-k^n}) + A_1\,\Gamma(1 + \tfrac{1}{n})\,I(\frac{k^n}{\sqrt{(1+1/n)}}, \tfrac{1}{n}) + A_3\,\Gamma(1 + \tfrac{3}{n})\,I(\frac{k^n}{\sqrt{(1+3/n)}}, \tfrac{3}{n}) + A_4\,\Gamma(1 + \tfrac{4}{n})\,I(\frac{k^n}{\sqrt{(1+4/n)}}, \tfrac{4}{n})$$

$$I(u,p) = \int_o^{u\sqrt{(p+1)}} e^{-v}\,v^p\,dv \,/\, \Gamma(p+1)$$

$$A_o = k^3(n - 2 - nk^n)$$

$$A_1 = 2k^2(n - 3 - nk^n)$$

$$A_3 = -2(n - 5 - nk^n)$$

$$A_4 = -\frac{1}{k}(n - 6 - nk^n)$$

(The particular form chosen for the function P was selected in order to facilitate the use of Pearson's tables of the Incomplete Gamma Function)
From equations (3) and (7) we get

$$f_n' = f\frac{A_3G}{2b^2k^2} \quad \ldots\ldots\ldots\ldots\ldots\ldots\ldots\ldots (10)$$

Similarly from equations (5) and (7) we obtain

$$f_d' = -f\frac{Wgb}{6\mu}Z \quad \ldots\ldots\ldots\ldots\ldots\ldots\ldots (11)$$

where

$$Z = \int_{k^n}^{\infty} e^{-y}(y^{1/n} + 2k - 2k^3\,y^{-2/n} - k^4\,y^{-3/n})\,dy$$

The numerical evaluation of Z depends upon the value of n. It is easily verified that

$$n = 1 \qquad Z = \frac{e^{-k}}{2}(4k - 5k^2 + k^3) + \Gamma(2)(1 - I(k/\sqrt{2}, 1)) - \frac{k^3}{2}\,Ei(-k)(4 - k)$$

$$n = 2 \qquad Z = 2ke^{-k^2}(1 - k^2 - 2k^4) + \Gamma(3/2)(1 + 4k^4)(1 - I(k^2/\sqrt{3/2}, 1/2)) + 2k^3\,Ei(-k^2)$$

$$n = 3 \qquad Z = 2ke^{-k^3}(1 + 3k^3) + \Gamma(4/3)(1 - 6k^3)(1 - I(k^3/\sqrt{4/3}, 1/3)) + k^4\,Ei(-k^3)$$

$$n = 4 \qquad Z = 2ke^{-k^4}(1 + 4k^4) + \Gamma(5/4)(1 - 4k^4)(1 - I(k^4/\sqrt{5/4}, 1/4)) - 4k^3\,\Gamma(3/2)(1 - I(k^4/\sqrt{3/2}, 1/2))$$

where $Ei(-x)$ is the exponential integral $\int^{x} e^{-y}/y\,dy$. It is to be noted that the radius of the droplet is now given by k, the unit being the scale radius b.

4 Numerical results for specified conditions.

From equations (9), (10) and (11) we see that

$$\frac{f'_n}{f} = \frac{AsG}{2b^2k^2} \quad \ldots\ldots\ldots\ldots\ldots\ldots\ldots\ldots\ldots\ldots (12)$$

$$\frac{f'_a + f'_d}{f} = -\frac{Wgb}{6\mu}\left[\frac{P}{3k^2} + Z\right] \quad \ldots\ldots\ldots\ldots\ldots\ldots (13)$$

The fractional rate of increase of f owing to condensation (equation 12) depends upon the values of the constants representing the physical characteristics of air and water, upon the concentration of liquid water W, upon the parameters b and n in the assumed drop size distribution and upon the radius k (=r/b) of the drop. We are primarily interested here in the ratio of the condensation term to the coalescence term

$$\frac{f'_n}{f'_a + f'_d} = -\frac{\mu G}{Wb^3} \; \frac{3As}{gk^2\left(\frac{P}{3k^2} + Z\right)} \quad \ldots\ldots\ldots\ldots (14)$$

the significant question being whether this ratio differs substantially from unity. Let us select values of the physical constants appropriate to layer type cloud. It has been shown elsewhere (3) that in layer type cloud $W < 0.2\ 10^{-6}$ g cm^{-3} in slightly over 50 per cent of measurements and that the predominant drop diameter is less than 12 microns in about half the measurements. Moreover a predominant radius of 6 microns (with n = 3.25) corresponds to $b = 6\ 10^{-4}/0.9 = 6.7\ 10^{-4}$ cm. (see reference 2). If we assume also that the cloud temperature is 5°C and that the supersaturation is 0.01 per cent we have the following values for the constants.

$M = 18$, $D = 0.226$ cm^2 sec^{-1}, $R = 8.314\ 10^7$, $\theta = 273°$A
$s = 10^{-4}$, $p_\theta = 8719$ dynes cm^{-2}, $W = 0.2\ 10^{-6}$ cm^3/cm^3
$b = 6.7\ 10^{-4}$ cm, $g = 981$ cm sec^{-2}, $\mu = 1.74\ 10^{-4}$ g cm^{-1} sec^{-1}

These lead to

$$G = 1.535\ 10^{-10} \qquad \frac{Wgb}{6\mu} = 1.259\ 10^{-4}$$

With these values the table has been compiled to show f'_n/f, $(f'_a + f'_d)/f$, $f'_n/(f'_a + f'_d)$ and the fraction of liquid water comprissed by drops smaller than k for various values of k and n.

The first part of the table shows that the number of drops per unit volume of a given size increases by about 0.2 per cent per second owing to the condensation processes. The second part shows that the effect of coalescence is very dependent upon the drop size. At the smaller sizes coalescence diminishes the number of drops by about 0.01 to 0.02 per cent per second but at the larger sizes coalescence leads to an increase in the number of drops at a rate which reaches about 0.03 per cent per second for k = 1.3 and n = 3.0. The values of f'_a and f'_d have not been tabulated separately but it is of interest to note that the computations showed that Z is always positive (and so f'_d is negative). At small values of k, Z is larger than $P/3k^2$ (and with the same sign) by a factor of 3 to 20. For large values of k however Z diminished to zero and $P/3k^2$ became large and negative.

The relative importance of condensation and coalescence is measured by the numerical values of the entries in the third part of the table and we see that unless k exceeds 1.3 condensation is far more effective in determining the size distribution of the drops than is coalescence (in the conditions postulated). The last part of the table shows that the predominant influence of condensation (for $k < 1.3$) applies to approximately 90 per cent of the liquid water in the cloud even with the assumptions mentioned in the introduction. The net positive value of f' is of course balanced by turbulent diffusion as shown elsewhere (1).

Table

Fractional rate of increase of number of drops of specified size owing to condensation or to coalescence.

k n	0.5	0.8	1.0	1.1	1.3	2.0
			$10^4\ f'_n/f$			
1	62	26	17	14	11	6.0
2	48	23	17	15	13	9.4
3	32	19	17	17	17	22
4	17	14	17	19	25	56
			$10^4\ (f'_a + f'_d)/f$			
1	-1.6	-1.2	-0.85	-0.62	-0.11	1.8
2	-1.6	-1.1	-0.54	-0.10	1.1	9.4
3	-1.8	-1.4	-0.61	0.12	2.7	30
4	-1.8	-1.5	-0.75	0.32	5.4	84
			$f'_n/(f'_a + f'_d)$			
1	-39	-21	-20	-23	-94	3.3
2	-29	-21	-32	-150	12	1.0
3	-18	-14	-28	140	6.5	0.74
4	-9	-10	-23	60	4.7	0.66
			$1 - \exp(-k^n)$			
1	0.39	0.55	0.63	0.67	0.73	0.86
2	0.22	0.47	0.63	0.70	0.82	0.98
3	0.12	0.40	0.63	0.74	0.89	1.0
4	0.06	0.34	0.63	0.77	0.94	1.0

Let us now consider conditions typical of a well developed convective cloud. We note first that the signs of P, A_3 and Z depend only upon n and k so that changes in the values of θ, b and W will not affect the sign of any term in the table. From reference 3 we may assume $W = 0.3\ 10^{-6}\ cm^3/cm^3$ and predominant drop diameter = 20 microns leading to $b = 11.1\ 10^{-4}$ cm. We shall also assume $\theta = 268°A$, $\mu = 1.69\ 10^{-4}\ g.\ cm^{-1}\ sec^{-1}$ and $D = 0.211\ cm^2\ sec^{-1}$, $p_\theta = 4215$ dynes cm^{-2}. The choice of a suitable value for s presents some difficulties but Howell's calculations (4) suggest that in a vigorous convective cloud $s = 1.5\ 10^{-3}$ may not be an overestimate. With these values for the constants the entries in parts 1, 2 and 3 of the table should be multiplied by 2.56, 2.56 and 1.0 respectively. Of course it is coincidence that the first two factors should be identical. The precise value of s is subject to considerable uncertainty. Nevertheless it seems reasonable to conclude that if the supersaturation in a vigorous convective cloud is of the order $1.5\ 10^{-3}$ condensation will be more important than coalescence in determining the drop size distribution. It might even be legitimate to argue that since the drop size distribution in convective cloud has been found experimentally (2) to agree with a formula which was deduced by assuming condensation and turbulence to be the governing factors (1) (though that deduction was made primarily with reference to layer type cloud) then the agreement is evidence that the value of s must be of the order $1.5 \; 10^{-3}$. The larger value found for f_n' in convective cloud would then imply a larger coefficient of turbulent diffusion, a very reasonable result.

References

1. Best, A. C. 1951. M.R.P. 627.
2. .. .. 1950. M.R.P. 559.
3. .. .. 1951. M.R.P. 610.
4. Howell, W. E. 1949. J. Met. Amer. Met. Soc., Boston, Mass. 6, p. 134.

paper of the Meteorological Research
Committee London).
M.R.P. No .... by Mr..........................
A copy is available in the Library of
the Meteorological Office."

AD 223 009

M.R.P.645
S.C.III/99
9th May, 1951.

AIR MINISTRY [illegible]
TECHNICAL REFERENCE [illegible]
AUG 7 1951

AIR MINISTRY

METEOROLOGICAL RESEARCH COMMITTEE

Some statistics of rate of rainfall in Southern England

by A.C. Best (Meteorological Office).

1. Introduction. Although statistics of amount of rainfall have been collected over a number of years and have been analysed in various ways and for various purposes, comparatively little attention has been given to statistics of rate of rainfall except with regard to the higher rates which are "noteworthy" "rare", etc. Undoubtedly one reason for this is that the usual recording raingauge is very unsuitable for recording rate of rainfall since this is measured by the slope of the record. There are some problems of long standing, e.g. problems connected with drainage of storm water, for which information about rate of rainfall would be very useful. Other problems are arising as a result of developments in other fields of activity. For example, radar is now used as an aid to flying control offices. But the effectiveness of radar in locating aircraft may be seriously hampered by heavy precipitation and the extent to which the radar operator is handicapped is obviously dependent upon the frequency of heavy precipitation, the size of the area covered and the length of period during which the precipitation persists. The size of areas of storm precipitation is also important in aircraft navigation.

At a few stations in the British Isles Jardi rate of rainfall recorders are installed. On records from these instruments the height of the trace above the zero line is proportional to the rate of rainfall. The type of record is far from ideal for extracting statistics of rate of rainfall. For example, the scale is rather small and it is not easy to estimate durations of the order of a few minutes. Furthermore, the number of such instruments in use in this country is so small that, unless the records are supplemented by records from the more numerous recording raingauges, no information can be obtained about the area covered by precipitation of a specified rate. Nevertheless, in view of the need for statistics about rate of rainfall, an attempt has been made in this note to compile such information.

The data given below are based primarily upon records from the Jardi rate of rainfall recorder at Kew Observatory. The statistics of paragraph 2 relate to a period of 18 years but the detailed analysis of paragraphs 3, 4 and 5 refer to records gathered over a period of only six months. A period of this length is, of course, far too short to lead to reliable statistics. Even for this short period, however, a very large amount of labour was involved in reducing the data. This note should therefore be regarded rather as an attempt to obtain orders of magnitude and to indicate the type of information which could be obtained if a sufficient number of suitable rate of rainfall recorders were distributed about the country.

2. Frequency of occurrence of specified rates of rainfall.

Table 1 is self explanatory. It is based upon the Kew Jardi type records and has been compiled from the data obtained from the routine analysis of the records. It refers to the period 1933 to 1950.

/ TABLE I

TABLE I

Average number of falls of any duration with precipitation rate exceeding specified values

Rate (mm/hr)	Jan.	Feb.	Mch.	Apl.	May	June	July	Aug.	Sept.	Oct.	Nov.	Dec.
>10	9.1	6.3	4.6	7.2	11.4	16.1	18.3	22.3	15.1	15.7	10.3	7.2
>25	2.3	1.5	0.7	1.9	3.7	6.7	8.1	9.4	6.6	5.3	3.2	1.7
>50	0.7	0.4	0.1	0.4	1.1	2.3	3.4	3.6	2.3	1.2	0.9	0.3

Percentage frequency of days with rain with maximum rate exceeding specified values

>10	21.8	18.6	23.7	30.1	40.4	42.0	43.6	48.1	36.7	42.1	25.5	22.4
>25	6.3	7.5	4.5	9.3	16.6	24.8	22.4	26.0	21.2	20.4	9.9	7.6
>50	2.9	2.1	1.0	2.4	5.3	8.6	12.2	11.6	8.4	6.4	2.6	1.9

Maximum rate of rainfall recorded (mm/hr)

128	69	147	111	137	129	200	171	160	148	115	79

3. Duration and frequency of rainfalls exceeding specified amounts. For the period January to June, 1948 (6 months) the duration of each period of rain at Kew during which the rate of rainfall exceeded specified values was assessed from the records. The results of this analysis are shown in tables 2 and 3.

TABLE 2

Total duration (minutes) during 6 months of rainfalls, each of which lasted for more than t minutes during which rate of precipitation exceeded p mm/hr

t mins.	p (mm/hr) 6	10	25	50	75	100
0	785	184	61	20	7	3
2	681	137	44	9	3	
5	463	75	14			
10	254	12				
20	75					

TABLE 3

Number of rainfall periods during 6 months each of which lasted for more than t minutes, during which rate of precipitation exceeded p mm/hr

t mins.	p (mm/hr) 6	10	25	50	75	100
0	159	52	21	11	4	2
2	100	27	11	3	1	
5	42	10	2			
10	14	1				
20	2					

If the periods covered by the statistics of tables 1 and 3 were the same there would be a relation between the first part of table 1 and table 3. Thus the mean of the first six entries in the first line of part 1 of table 1 would be (from table 3) 52/6. From table 1 it is 54.7/6.

/ 4.

4. The size of area affected by rainfall with a specified rate. Sections 2 and 3 above have dealt only with rainfall at a single station. For some purposes, however, it is necessary to know the probability that the specified rate of rainfall will cover a specified area. To obtain information about this aspect use has been made of the recording raingauges maintained by various authorities within a radius of 20 miles of Kew. The charts from these instruments (there were 39 such instruments) were borrowed and examined for each of the 159 occasions on which Kew recorded a rate of rainfall exceeding 6 mm/hour. The times of the Kew rainfalls had been noted and each of the 39 charts was scrutinised to decide whether the simultaneous rate of rainfall at the corresponding station was less than 6 mm/hr, or greater than 6, 10, 25 or 50 mm/hr. Some tolerance was necessary in interpreting the word "simultaneous". The instruments were maintained by different authorities and in some instances the standard of time marking was not as high as that required at Meteorological Office stations. After examination of the charts it was decided to count as "simultaneous" a rainfall which, according to the chart, occurred within 30 minutes of the beginning or end of the Kew period. Having extracted these data the results were plotted on maps and, for each of the 159 occasions, isopleths were drawn for p = 6, 10, 25 and 50 mm/hr. Obviously the isopleths of higher values will enclose smaller areas than those for lower values. On some occasions the 6 mm/hr isopleth (and very occasionally the 10 mm/hr isopleth) was not closed because charts from only those instruments within 20 miles of Kew had been examined. If the shape of these open isopleths suggested that they would close just outside the 20 mile circle they were completed by guesswork. If they did not appear to justify extrapolation in this fashion they were left open and no further use made of them. The tolerance of 30 minutes in assessing simultantaneity of observations at the various stations would tend to enlarge the area of the isopleths in the direction of travel of the storm, the effect being more important for the smaller areas of high rates of precipitation.

The next step was to estimate the diameter of a circle of equivalent area for each closed isopleth. This was done by eye. The results are a measure of the area covered by precipitation at rates exceeding 6, 10, 25 and 50 mm/hr. The cumulative percentage frequency of equivalent diameters less than certain values is shown in fig. 1 for the four values of p. Some values read from the smoothed curves, the mean diameters and standard deviations about the mean are given in table 4. Occasions of high rates of precipitation must coincide, to a large extent, with occasions on which radar echoes will be received from the storm. In this connection it is interesting to note that the mean diameters quoted in table 4 are of the same order of magnitude as the mean width of radar echoes received from multiple cell convective storms (see table II of M.R.P.535 by R.F. Jones).

TABLE 4

Data relating to frequency of certain values of diameter (in miles) of circle equivalent to isopleths of specified rate of rainfall.

	Rate of Precipitation (mm/hr)			
	6	10	25	50
Diameter exceeded on 10% occasions	17.8	13.8	11.6	6.3
" " " 25% "	11.5	9.2	6.6	4.6
" " " 50% "	7.5	5.7	4.2	3.1
" " " 75% "	4.6	3.8	2.8	2.1
" " " 90% "	3.3	2.5	2.1	1.6
Mean diameter	9.2	7.1	5.5	3.6
Standard deviation about mean	5.9	4.8	4.1	2.2
Number of areas measured	197	217	148	73

/ In

In view of the inadequacy of the original data forming the basis of table 4 the values in that table must be regarded as indicating order of magnitudes only. Nevertheless, it is of interest to note that there is some similarity between the shape of the frequency curves for the four different rates of precipitation. Table 5 shows the ratio of the various diameters to the mean diameter for the same rate of precipitation, the nomenclature being obvious.

TABLE 5

Precipitation rate (mm/hr)	6	10	25	50	Mean
D_{10}/D_m	1.935	1.943	2.110	1.750	1.935
D_{25}/D_m	1.250	1.295	1.200	1.278	1.256
D_{50}/D_m	0.815	0.802	0.763	0.861	0.810
D_{75}/D_m	0.500	0.535	0.509	0.584	0.532
D_{90}/D_m	0.358	0.352	0.382	0.444	0.384
(S.D.)/D_m	0.641	0.675	0.745	0.611	0.668

The values in table 5 show no systematic variation with rate of precipitation and it appears that the values in the last column of that table might be adopted irrespective of the rate of rainfall.

In figure 2 log p (p = rate of precipitation) has been plotted against log D_m. To a close approximation it appears that D_m (in miles) and p (in mm/hr) are related by the equation.

$$D_m \, p^{0.425} = 19.5$$

5. Cross sections of rainstorms. Finally an attempt has been made to construct idealized cross sections of the rainstorms. Inspection of the data showed that a closed isopleth for 10 mm/hour could be constructed more frequently than any of the other three isopleths - the 6 mm/hour isopleth was sometimes missing because it went outside the area of country from which reports were collected and rates of rainfall of 25 and 50 mm/hour are of course less frequent than 10 mm/hour. Accordingly this part of the work was restricted to occasions when a 10 mm/hour isopleth was constructed.

On those occasions when two (or more) isopleths for 25 mm/hour were enclosed within one 10 mm/hour isopleth the two 25 mm/hr isopleths (or rather their equivalent circles) were replaced by one circle of equal area. The 50 mm/hour isopleths were treated similarly.

Denoting the diameter of the 6, 10, 25 and 50 mm/hr circles by d_6, d_{10}, d_{25} and d_{50} the ratios d_6/d_{10}, d_{25}/d_{10} and d_{50}/d_{10} were then computed. Table 6 shows the mean values of these ratios, the standard deviations about the mean, the mean value of d_{10} and the number of occasions.

TABLE 6

Cross sections of rainstorms

Quantity	Mean Value	Standard Deviation	Mean d_{10} (miles)	No. of Cases
d_6/d_{10}	1.77	0.48	9.4	51
d_{25}/d_{10}	0.44	0.19	12.2	63
d_{50}/d_{10}	0.28	0.13	13.5	13

When constructing table 6 only occasions when d_{10} exceeded 5 miles were included. To the scale on which the isopleths were drawn 5 miles was represented by 12.5 mm. and it was considered that the standard deviation would be unduly affected by the impossibility of assessing accurately the small areas if these areas were included.

In fig. 3 log (d_p/d_{10}) has been plotted against log p, the standard deviations also being indicated. To the accuracy justified by the nature of the data it appears that d_p varies inversely as p. The ratios d_6/d_{10} and d_{25}/d_{10} have also been plotted against d_{10}. The results showed considerable scatter of the points but no systematic relationship and are not reproduced here.

G.291456/JDG/4/51/40

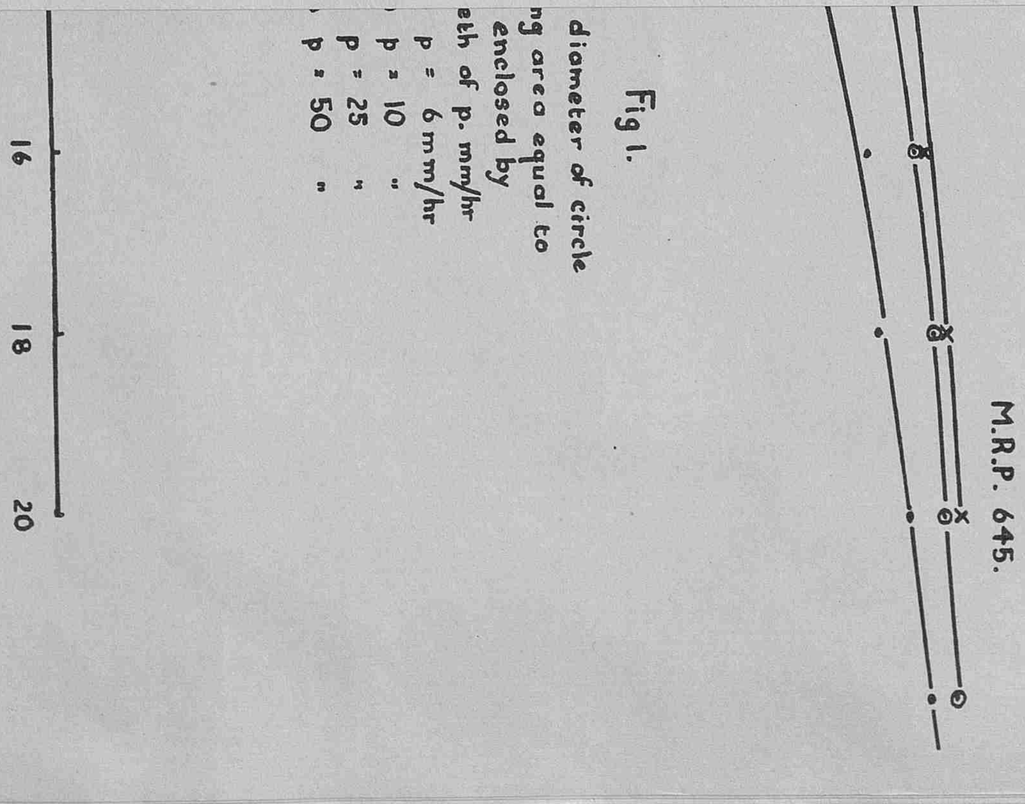

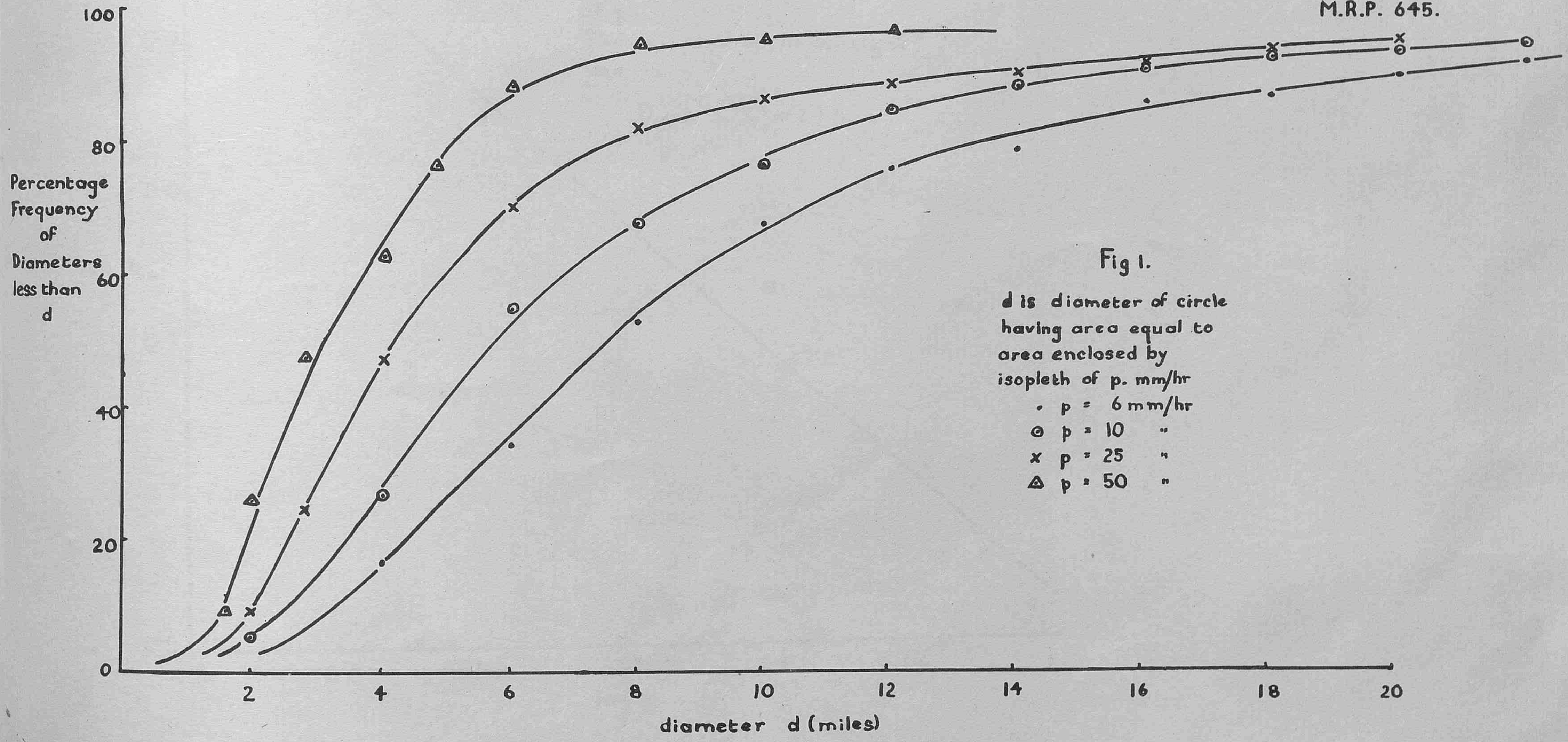

Fig 1.

d is diameter of circle having area equal to area enclosed by isopleth of p. mm/hr

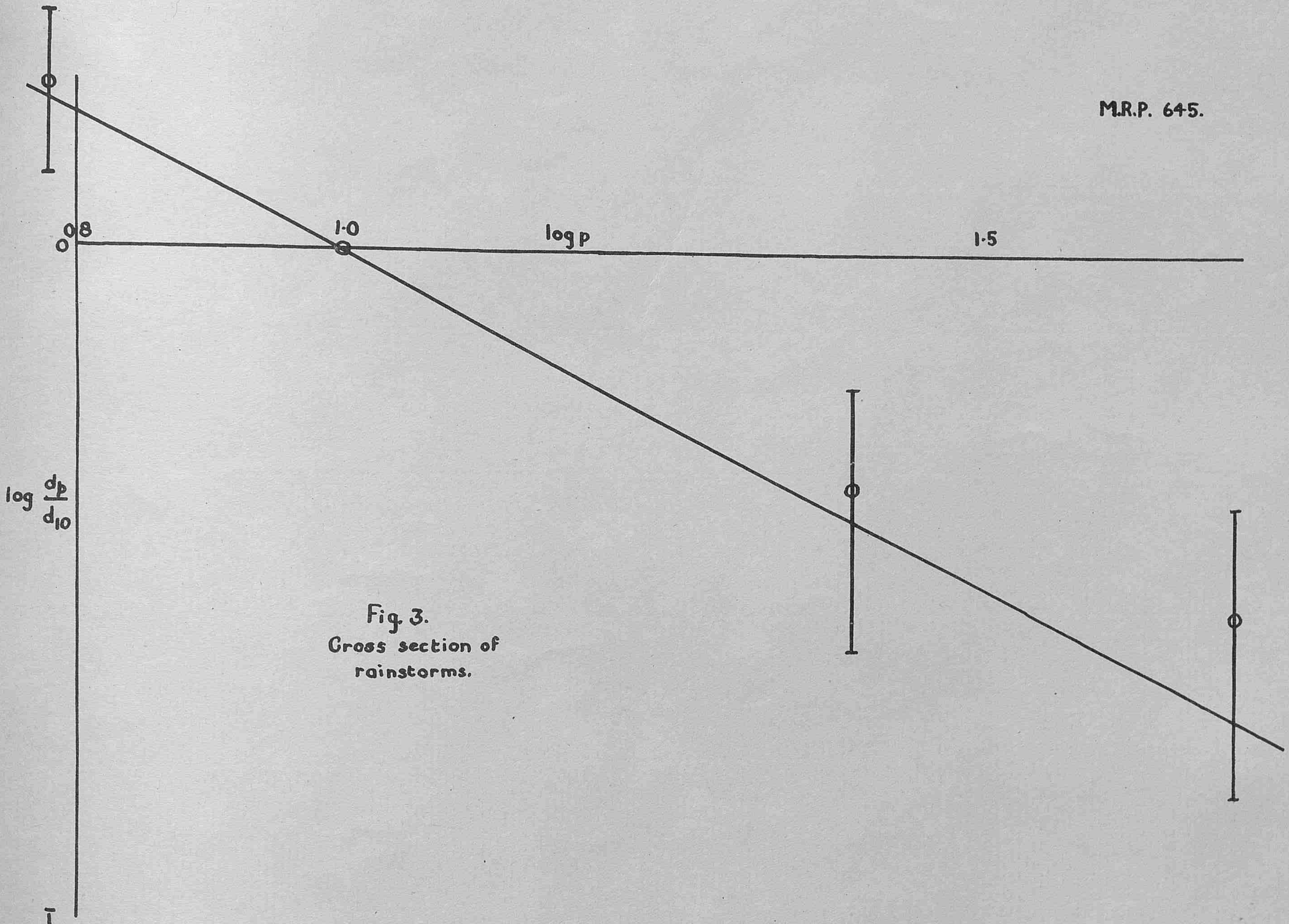

Fig. 3.
Cross section of rainstorms.

quote this paper should refer to it as "A paper of the Meteorological Research Committee London), M.R.P. No .... by Mr.............................
A copy is available in the Library of the Meteorological Office."

TECHNICAL REFERENCE FILES
AUG 23 1951

M.R.P. 646
S.C. II/80
5th May, 1951.

AD 223018

AIR MINISTRY
METEOROLOGICAL RESEARCH COMMITTEE

Seasonal Changes in the Mean Pressure Distribution over the World and some Inferences about the General Circulation

by A.H. Gordon (Meteorological Office)

1. Introduction

Atmospheric surface pressure is a measure of the weight of a vertical column of air of unit area cross-section extending to the outer limits of the earth's atmosphere. A change in atmospheric surface pressure at a given place therefore represents a net mass transfer of air per unit area to or from that place. The convergences and divergences which may occur at various levels within a column of air usually cancel out to a large extent and it is only the relatively small residual which appears as a change in surface pressure. It is difficult to assess the particular level or levels at which convergence or divergence may occur; but it follows that if there is a change in surface pressure, then there must be a net gain or loss of air within the column as a whole. A study of the seasonal changes in the mean pressure distribution over the earth's surface should, therefore, give useful evidence of the seasonal net mass transfer of air from one region of the globe to another. The seasonal net mass transfer may be partly an exchange between continent and ocean and partly an exchange between the two hemispheres. From the net mass transfer pattern over the globe inferences may be drawn about the importance of non-geostrophic flow as an inherent part of the mean general circulation.

2. Data and techniques of representation of seasonal changes of mean pressure distribution over the oceans.

The climatic charts of the oceans prepared in the Meteorological Office include monthly charts of the mean pressure distribution over the oceans. The isobars, which have been smoothed by eye, are based on mean pressure values computed for two-degree squares in the North Atlantic and five-degree squares elsewhere. The pressure observations from which the charts have been compiled cover the following periods:

North Atlantic	1921-1938
South Atlantic	1855-1899, 1921-1938
Indian Ocean	1855-1943 north of 30°S 1921-1943 south of 30°S
Eastern Pacific to 160°E	1921-1938
Western Pacific to 160°E	1921-1938

To obtain mean pressure values for 2° squares over these oceans, 2° grids were placed over the mean pressure charts in the atlases, and pressure values interpolated for each such square; pressure values obtained in this way were meaned over each 2° belt in each ocean. These means were used to construct isopleths in which the ordinates and abscissae were latitude and time (months) respectively, and the distribution of the mean belt of pressure was represented by contours.

Subsequently the pressure values for each two-degree square were subtracted from the corresponding values for the following month and the mean monthly tendencies so obtained plotted on charts of the oceans. The marine data were supplemented over land by mean tendencies obtained in the same way from pressure data in World Weather Records (1920-1940). Mean isallobaric charts were then drawn up for the whole world, excluding the region south of 50° South latitude where data were scarce, for each two consecutive months of the year. Finally the mean tendencies were converted into units of relative change of mass and integrated round the globe for each ten degrees of latitude, excluding the region south of 50° South latitude. The net changes in relative mass were plotted as a function of latitude for each month of the year and isopleths drawn.

As a whole the periods covered by the different sets of observations are fairly consistent, except in the South Atlantic Ocean and Indian Ocean north of 30°S where observations for an earlier period are also included. However, the inclusion of such earlier observations is not expected to affect seriously the broad pattern of the changes in mean pressure from month to month.

3. Mean pressure distribution over the oceans

Figures 1-4 represent the mean pressure distribution throughout the year as a function of latitude for the Atlantic, Indian, East and West Pacific Oceans respectively. The main features of the patterns are changes in mean pressure in the doldrum, subtropical anticyclone and polar low belts and northward and southward movements of these belts with the seasons.

(a) Atlantic Ocean (52°S - 60°N). In the North Atlantic there are two main seasonal maxima and minima of pressure in the subtropical anticyclonic belt; the maxima are in January and July and the minima in March and October. The range of pressure along the axis of highest pressure is 4.5 mb. In the corresponding belt of the South Atlantic there is only one main maximum, in July and August, and no well defined minimum although pressure is generally lowest from November to April inclusive. The range of pressure is 5.2 mb. The westerly belt in the North Atlantic is characterised by a minimum in December and January and a maximum in May. The westerly belt at 50°S is characterised by relatively low pressure from November to June inclusive and by relatively high pressure from July to October inclusive but these values are based on a much smaller number of observations. The doldrum belt is characterised by a minimum in December and maximum in June, July and August. The range along the axis of lowest pressure is 3.3 mb.

(b) Indian Ocean (48°S - 20°N). North of the equator the mean pressure distribution is dominated almost entirely by the effect of the continent of Asia. The maximum is in mid-winter and the minimum in mid-summer. The range is 14.5 mb. South of the equator there is a maximum in July and August and a minimum in December in the subtropical anticyclonic belt. The range here along the axis of highest pressure is 7.1 mb. In the belt of westerlies there is little evidence of a significant seasonal variation of mean pressure.

(c) East Pacific Ocean (57°S - 53°N). In the northern hemisphere in the subtropical anticyclonic belt there is a maximum in July and a minimum in October; these extremes are reflected in the polar belt of westerlies where they occur in the same months. The range along the axis of highest pressure is 6.3 mb. In the southern hemisphere the maximum in the subtropical anticyclonic belt occurs in September and an ill defined minimum from April to July. The range is 4.4 mb. There is no significant variation of pressure in the belt of westerlies. Pressure in the doldrum belt is fairly uniform but a weak maximum occurs in August and weak minima in April and May and in December. The range is 2.0 mb.

(d) West Pacific Ocean (40°S - 50°N). In the northern hemisphere in the subtropical anticyclonic belt there are maxima in July and April and minima in February and June. The range is 3.1 mb. In the belt of westerlies there is a maximum in July and minimum in January. In the southern hemisphere in the subtropical belt there are maxima in April and September; the chief minimum occurs in January and a secondary minimum in June; the range is 4.6 mb. In the doldrums the maximum occurs in October and the minimum in January; the range is 2.1 mb.

The patterns in Figures 1-4 are common to all oceans in respect of certain broad features. Ignoring the partial effect of the Asian monsoon on the distribution in the West Pacific ocean pressure is highest in the northern hemisphere anticyclonic belt in July and lowest in February and March and again in October. In the corresponding belt in the southern hemisphere pressure is highest from July to September and lowest from November to April. In the northern hemisphere "westerly belt", pressure is highest from May to July and lowest from October to January. In the doldrum belt it is highest from June to October and lowest from December to May. The mean range of pressure along the axis of highest pressure is 4.6 mb. in the northern hemisphere and 5.3 mb. in the southern hemisphere. The mean range along the axis of lowest pressure in the doldrum belt is 2.5 mb.

Pressure distribution charts along the lines of Figs. 1-4 have been drawn by Lettan (10) for three chosen meridians, North America, mid-Atlantic and East Europe, respectively for the polar year 1932-33. This technique yields information of the general trend of the changing pressure field throughout the course of the year.

4. Relative Mass of Air over the Oceans

We may convert pressure into units of mass. Thus $M = p\ n \cos \phi\ l^2$ where M is the mass across a two-degree belt of latitude of the ocean, p is the mean pressure in millibars, n is the number of two-degree squares along the belt, ϕ is the mid-latitude of the two-degree belt, and l is the length of a side of a two-degree square at the equator.

Figures 5-8 represent the seasonal changes of mass as departures from the mean for the Atlantic, Indian, East Pacific and West Pacific Oceans respectively within the areas covered by Figures 1-4.

Figures 5-8 show certain features common to all oceans. In the northern hemisphere, excluding the Indian Ocean, there is excess of air in spring or summer and a general deficit in autumn or winter. In the southern hemisphere there is an excess reaching a maximum generally in August and September and a deficit in the summer months. The trend in the northern hemisphere appears to be followed in the mean by a similar trend one month later in the southern hemisphere. The seasonal changes in the relative mass of air shown in Figures 5-8 suggest that the dominant feature is a seasonal exchange of air between the northern hemisphere land masses and the oceans of both hemispheres.

5. Distribution of Mean Monthly Isallobars

Figures 9-10 show the distribution of the change in mean pressure from April - May and from October - November by means of isallobars. These two pairs of months are chosen for illustration as representing the highest rates of change. The outstanding features for each month throughout the year will, however, be discussed briefly in turn.

December - January An extensive isallobaric low is centred over the Western Pacific in temperate latitudes; another low extends from Iceland to the Barents Sea. The summer isallobaric low is beginning to appear over Southern Asia. Isallobaric highs cover extreme northeast Asia, Alaska and Central Europe. In the southern hemisphere there is an isallobaric low in the Indian Ocean.

January - February An isallobaric low covers the United States and Alaska and also extends eastwards from mid-Atlantic to the Pacific coast of Asia, chiefly between 20° and 50° latitude. Isallobaric highs are centred over Northern Scandinavia and the Northwest Pacific Ocean.

February - March A deep isallobaric low covers Siberia and extends southwards to the Indian Ocean and westwards across Europe, North Africa and the North Atlantic Ocean south of 50° to the Pacific Coast of the North American continent. An intense isallobaric high covers the whole of the Arctic while a second high covers the whole of the Pacific Ocean north of the tropics. In the southern hemisphere a high covering southern Australia appears to extend southwards.

March - April The extensive isallobaric low over the Eurasian continent is maintained while a low of less extent covers that part of the East Pacific Ocean bordering the United States and Central America. An extensive high centred near Iceland extends southwards over the North Atlantic while another high is centred over the West Pacific Ocean in temperate latitudes.

April - May (see Fig.9) An extension of the Asian isallobaric low covers the Arctic and also that part of the West Pacific Ocean bordering the Asian coast. An extensive high covers Europe and the North Atlantic Ocean. In the southern hemisphere small highs cover the major land masses.

May - June The Asian low extends into the whole of the Arctic and also into the West Pacific Ocean while an extension from the Arctic covers the North American continent. Relatively small highs cover the Atlantic Ocean west of France and the British Isles and also the Gulf of Alaska. In the southern hemisphere a high covers the South Atlantic Ocean, South Africa and the Indian Ocean.

June - July The Asian isallobaric low has become less extensive. A second low now extends from the Arctic north of the Bering Sea across Northern Canada, Greenland and Iceland to the British Isles. Highs cover the central North Atlantic and the whole of the North Pacific Oceans. In the southern hemisphere there is a belt of isallobaric high across the Atlantic and Indian Oceans and a low to the west of Chile.

July - August An isallobaric high has replaced the low over the Asian continent. A low covers the Arctic and the Central North Atlantic and North Pacific Oceans. Highs cover the South Pacific and Indian Oceans.

August - September An intense isallobaric high covers the Eurasian land mass while lows cover the North Atlantic and North Pacific Oceans and the Barents Sea.

September - October The intense isallobaric high is maintained over Asia. An extensive low covers the North Atlantic Ocean from 30° to the Arctic and an intense low is centred in the Gulf of Alaska. In the southern hemisphere a belt of low extends round the globe, mainly north of 40°.

October - November (see Fig.10) The Asian high extends northeastwards across the Arctic to Alaska. A low extends from Greenland to the British Isles and another covers the Western Pacific in temperate latitudes. A belt of low extends around the globe in the southern hemisphere.

November - December A high remains over Asia and an extension from it stretches across North Africa and the North Atlantic Ocean south of 30°. An intense low is centred in the North Atlantic Ocean south of Greenland and another low covers the North Pacific Ocean in temperate latitudes. A belt of low almost encircles the globe in the southern hemisphere.

Although no attempt will be made to explain in detail the patterns described interesting inferences may be drawn from them. The main feature that becomes evident is the vast seasonal exchange of air from continent to ocean and from hemisphere to hemisphere. In the northern hemisphere the flow from the continents to the oceans begins in February and continues through July while the reverse process begins in August and continues through January. The exchange is most pronounced at the equinoxes when the rate of change of mean temperature is probably a maximum. The North American continent appears to play an insignificant part in the seasonal exchange of air as compared with the Eurasian land mass. Figure 11 shows the annual range of mean pressure. Maxima occur in the region of Iceland, the Aleutians and over the central Asian land mass.

Becker (3) confirms that whilst the distribution of pressure over the continents of both hemispheres shows a strong annual variation (high pressure in winter, low pressure in summer of the hemisphere in question) the marine subtropical areas of high pressure have their strongest development in both hemispheres in the northern summer. This fact is explained thus that the run off of air masses from the large continents of the northern hemisphere caused by the summerly decrease of pressure does not only lead to an enlargement of the marine high pressure areas of the northern hemisphere, but encroaches also on the southern hemisphere, causing there too an enlargement of the marine subtropical areas of high pressure.

6. Seasonal exchange of air between the hemispheres

The changes in mean pressure from one month to the next for each ten-degree square were converted into units of relative mass and integrated around the globe. If the total of mass so obtained is plotted for each month of the year as a function of latitude, isopleths may be drawn as in Figure 12. The pattern which appears shows net relative mass divergence and convergence and indicates the magnitude of the net exchange of air between the hemispheres. The greatest net divergence and the greatest net convergence occur in subtropical latitudes. In the northern hemisphere maximum net divergence occurs from April to May and maximum net convergence from October to November; both occur at 30° latitude. In the southern hemisphere maximum net divergence occurs from October to November and maximum net convergence from April to May; both occur at 20° latitude. The latitude at which the net annual transfer of air is greatest is also 30° in the northern hemisphere and 20° in the southern hemisphere.

If we confine the net mass divergence to a layer from the surface to 1 km. the net transfer which occurs during the months and over the 10° belt where divergence is greatest is equivalent to an unbalanced net meridional circulation of about 1 metre/sec.

/References

References

1. Hohn, H. — Eine equatoriale Westwind zone als Glied der allgemeinen Zirkulation. Z.M. 3, 1949, pp. 240-246.

2. Widger W.K. — A study of the flow of angular momentum in the atmosphere. J. Met. Amer. Met. S. 6, 1949, pp. 291-299.

3. Becker R. — Der planetärische Jahresgang der maritim - sub tropischen Hochdrückkerne. Hamburg, A. Met., 2, 1949, pp. 48-51 (English Abs. p.48).

4. Stewart H.J. — Periodic properties of the semi-permanent atmospheric pressure systems. Q. Appl. Math., 1, 1943, pp. 262-267.

5. Glenn. A.H. — Circulation and convergence in the equatorial zone between 95°E and 160°E. December - February. B. Amer. Met. S., 28, 1947, pp. 453-464.

6. Burkhart, K. — Eine statistische Untersüchung atmosphärischer Zirkulations - schwarkurgen. A. Hydr., 68, 1940. pp. 1 - 13 (Abs. B. Amer. Met. S., 23, 1942, p.316).

7. Ramanathan K.R. and K.P. Ramakrishnan. The general circulation of the atmosphere over India and its neighbourhood. Ind. Met. Mem., 26, PG X. 1939, pp. 189-245.

8. Reuter F. — Die halbjährige Luftzirkulation im NO - Passatgebiet des Nordatlantischen Ozeans über Teneriffa. A. Hydr. 67, 1939, pp. 67-70.

9. Dalldorf H. — Troposphärischer Meridionalaustausch in den gemässigtem Breiten. Hamburg. Arch. Seewarte, Marine obs., 57, Nr. 10, 1937, p. 21.

10. Lettau H. — Luftmassen - und Energieaustausch zwischen niederen und hohen Breiten der Nordhalbkugel wahrend des Polarjahres 1932/33. Beit. Phys. Atm., 23, 1935, pp.45-84.

11. Jaw, J.J., — S.Y. Tao and Y.S. Kao. Statistical studies on the general circulation in middle latitudes. Nanking, J. Chinese Geoph. S., 1, 1949, pp. 140-158.

12. Rossby C. - G. — Air displacements and intensity changes of atmosphere vortices. New Haven. J. Mar. Res., 7, 1948, pp. 175-187.

13. Namias J. & P.F. Clapp. Normal fields of convergence and divergence at 10,000 ft. level. J. Met. Amer. Met. S., 3, 1946, pp. 14-22.

M.R.P 646

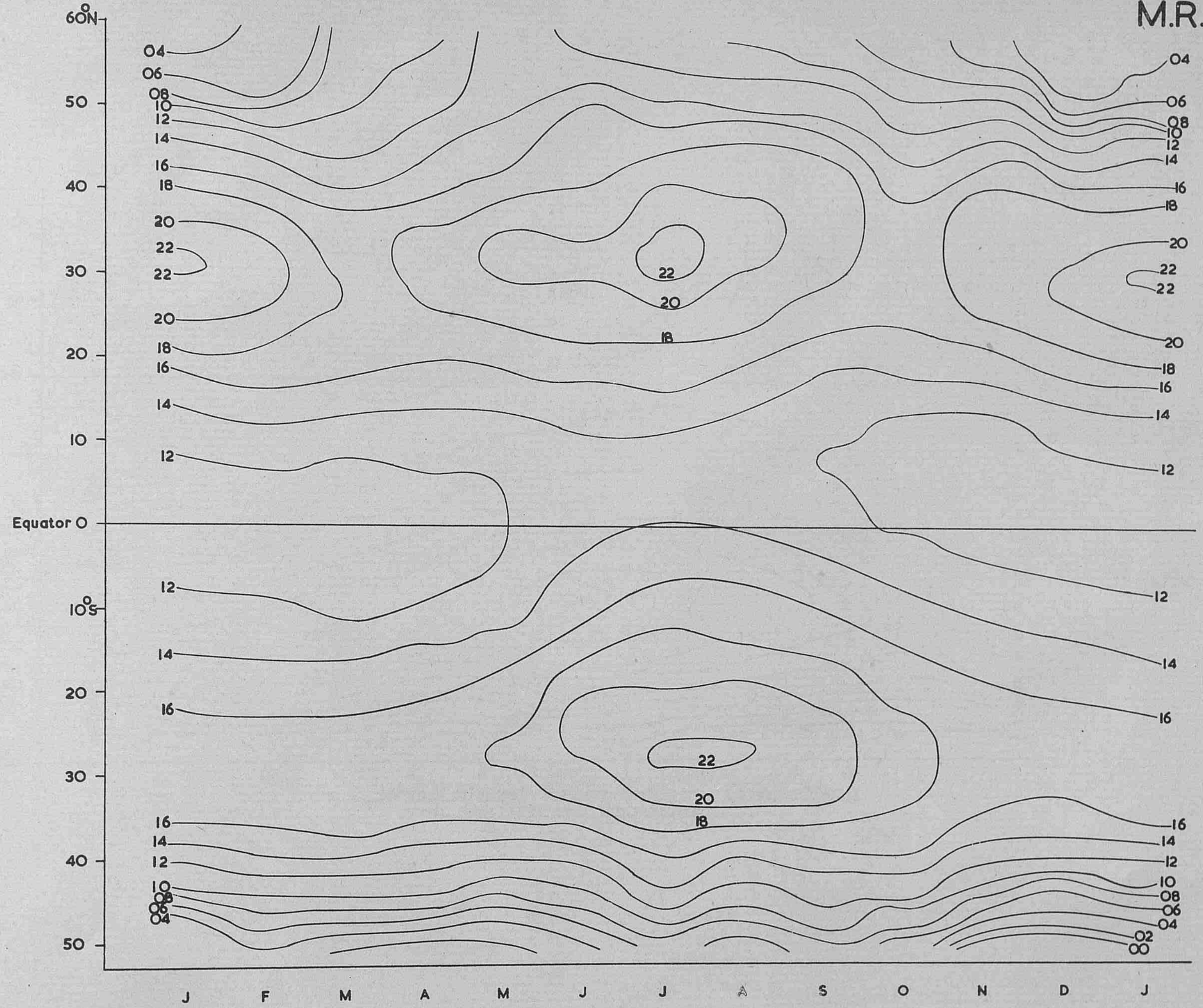

Fig. I Mean Latitudinal Pressure Pattern (Atlantic Ocean) in mb. with first two figs. omitted.

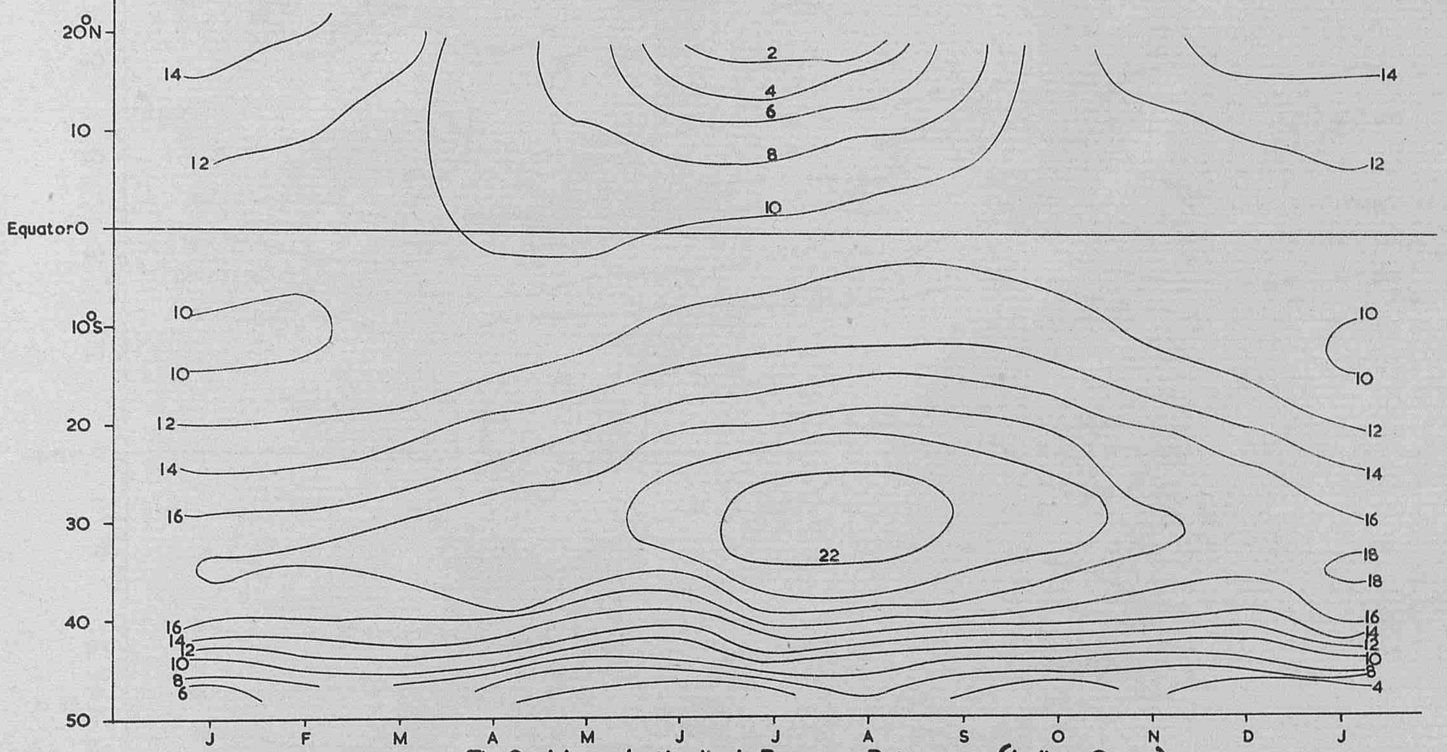

Fig. 2 Mean Latitudinal Pressure Pattern (Indian Ocean) in mb. with first two figs. omitted

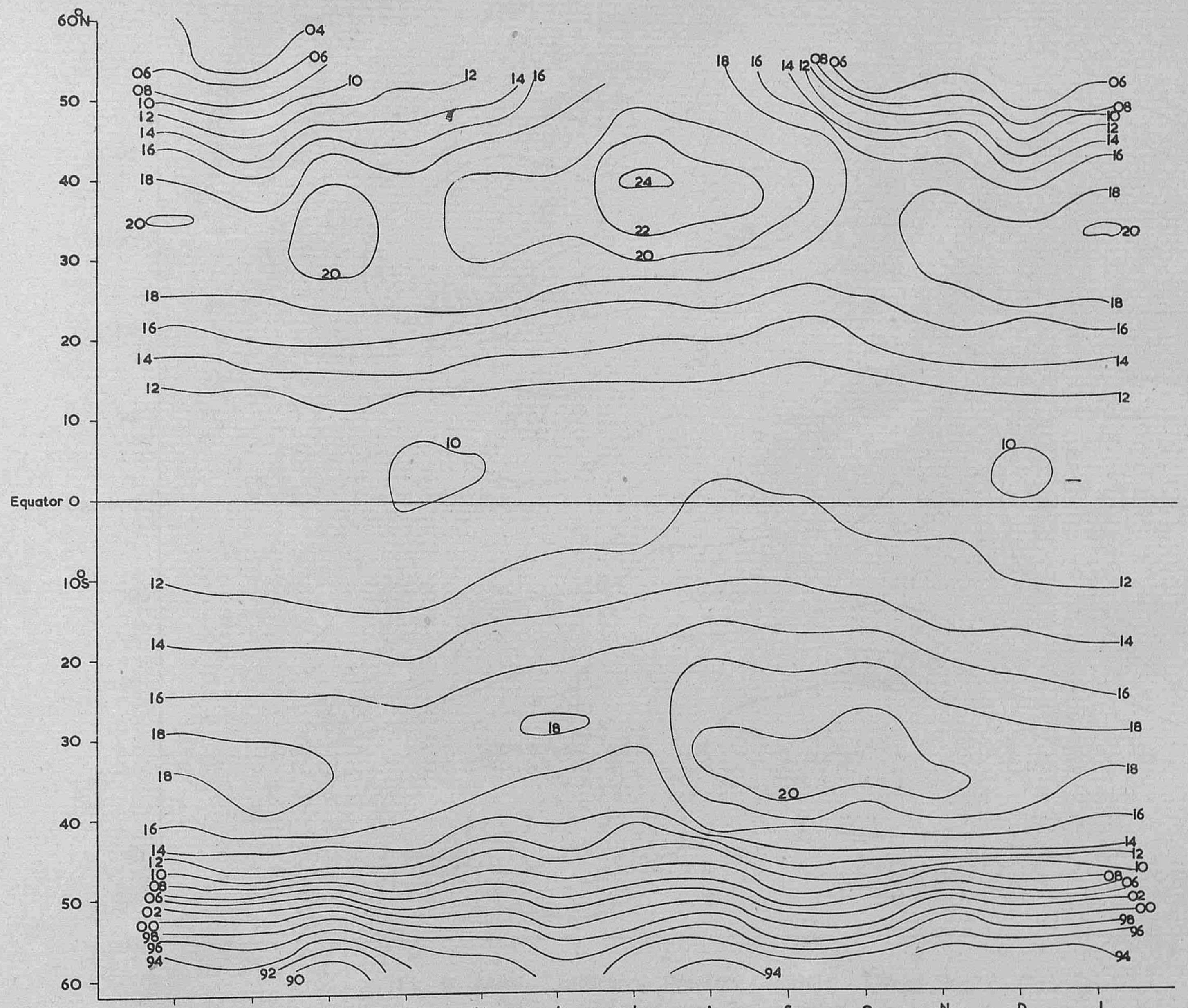

Fig.3 Mean Latitudinal Pressure Pattern (East Pacific Ocean)
in mb. with first two figs. omitted

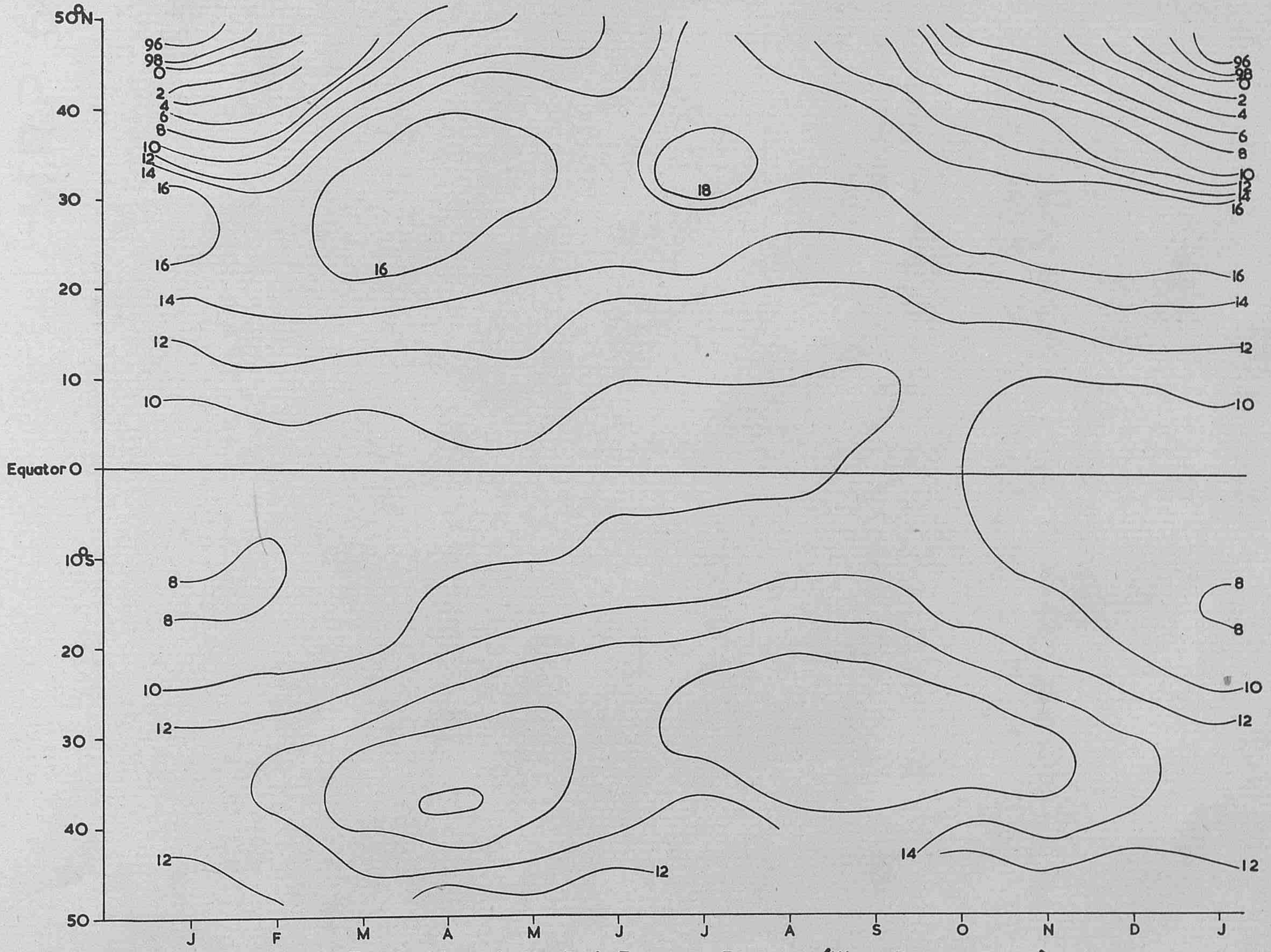

Fig. 4 Mean Latitudinal Pressure Pattern (West Pacific Ocean) in mb. with first two figs. omitted

M.R.P 646

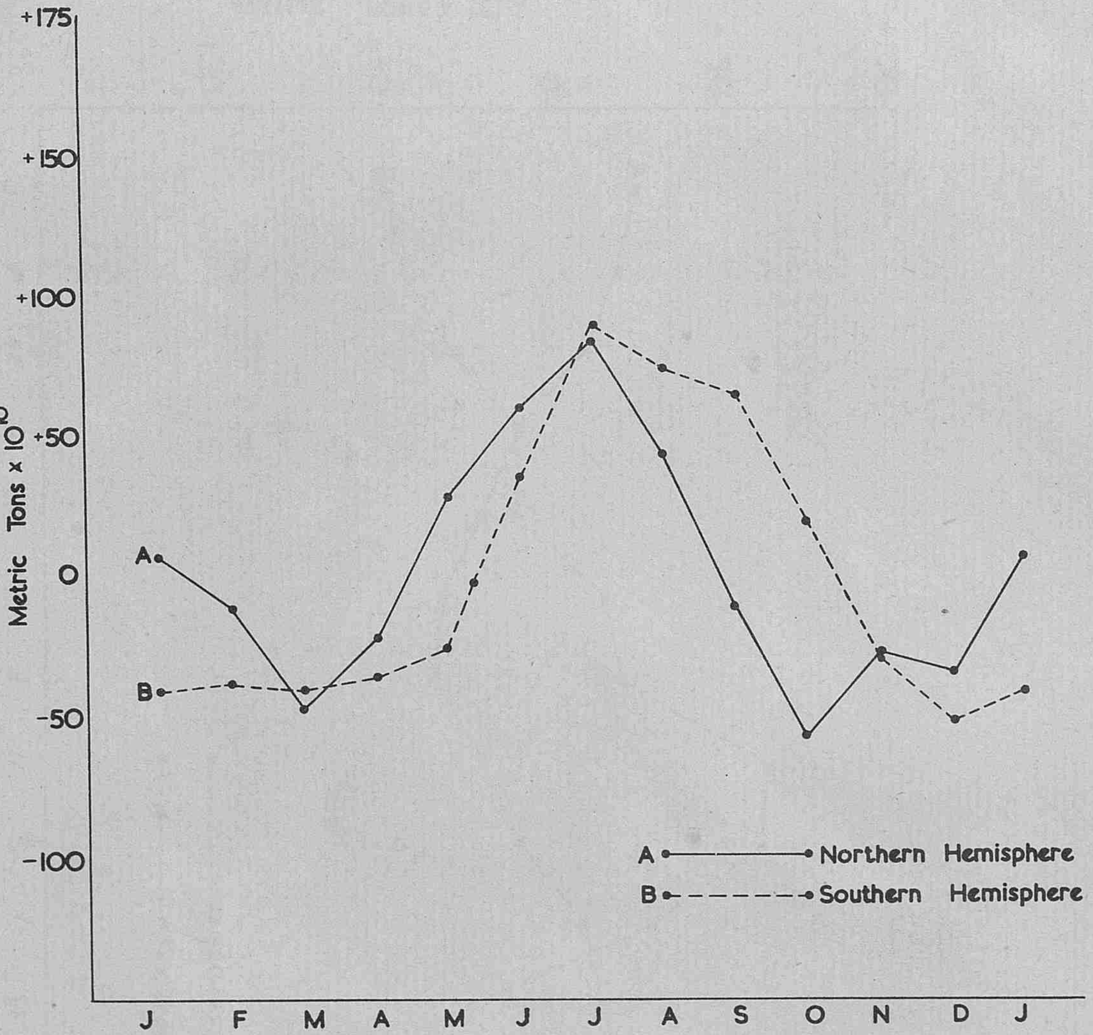

Fig. 5 Seasonal Change of Mass Departure from Normal (Atlantic Ocean)

M.R.P 646

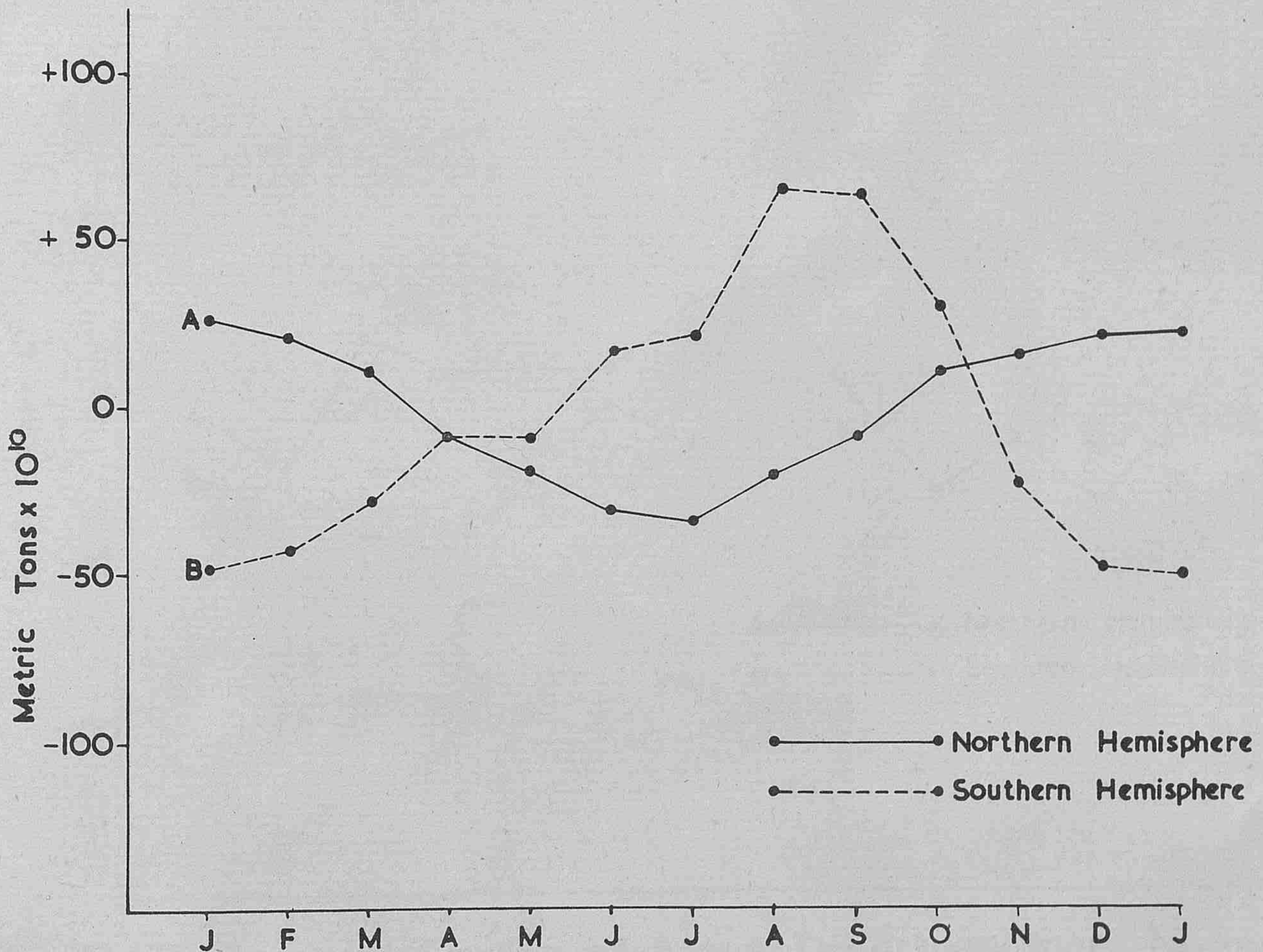

Fig. 6 Seasonal Change of Mass Departure from Normal (Indian Ocean)

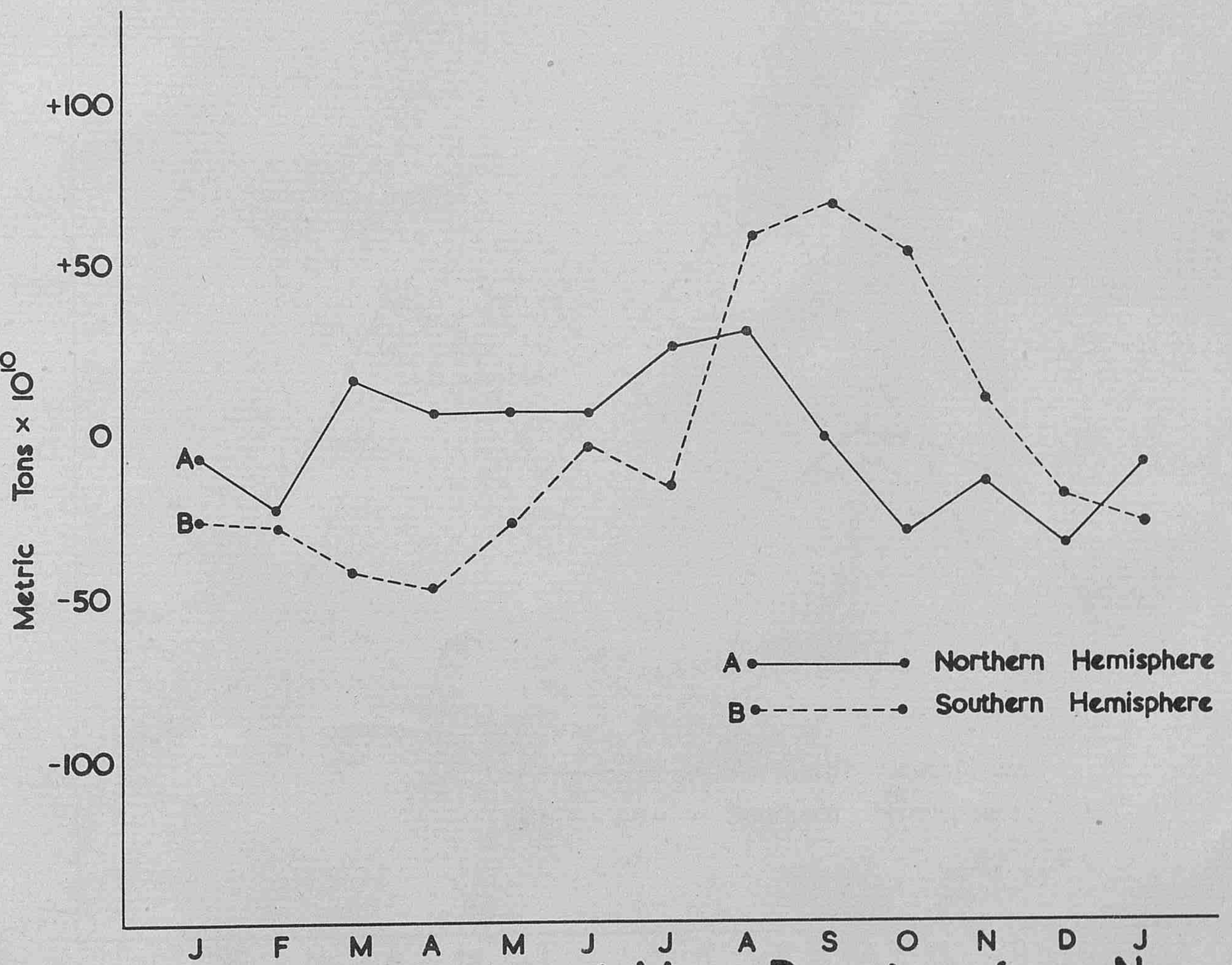

Fig. 7 Seasonal Change of Mass Departure from Normal (East Pacific Ocean)

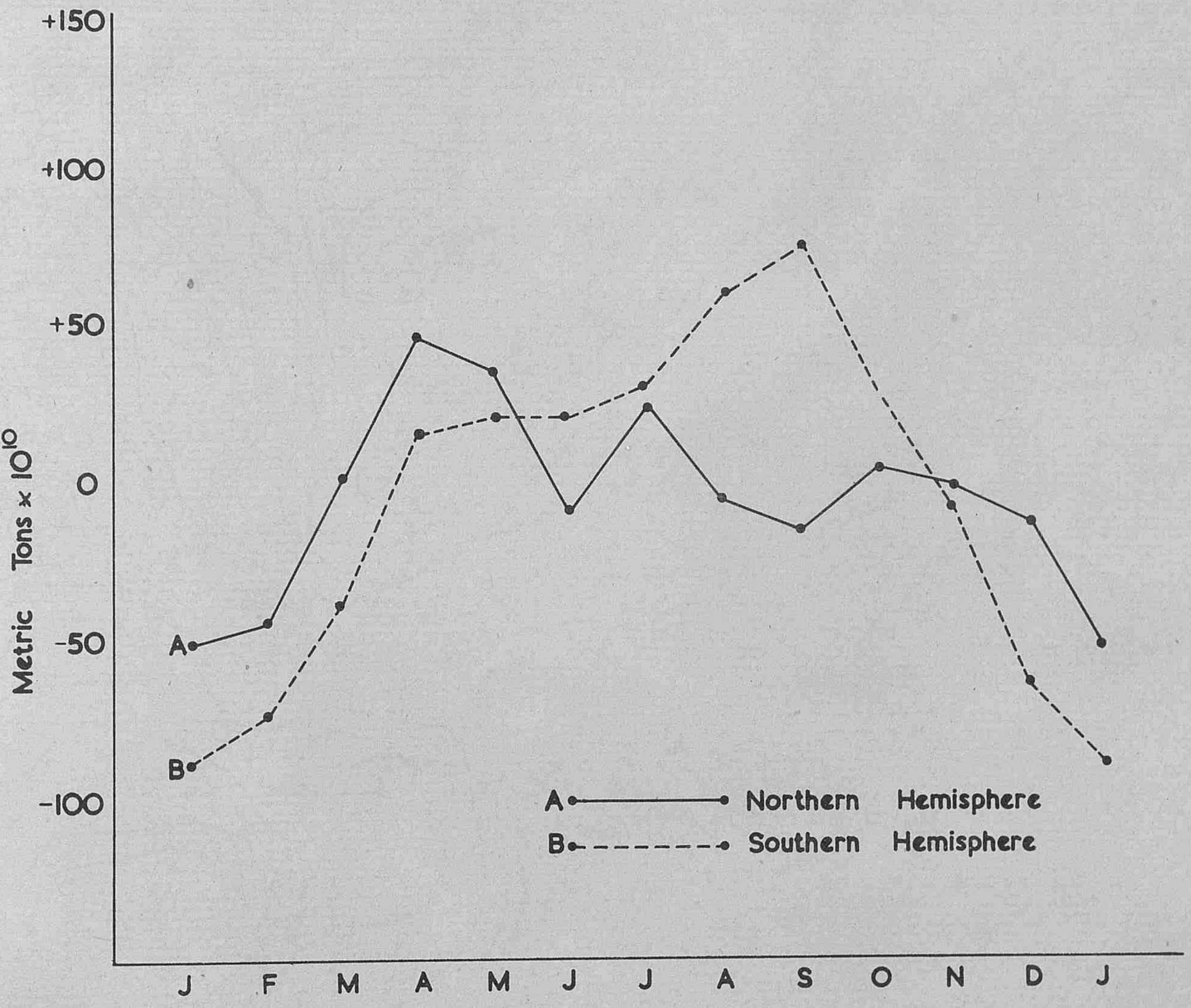

Fig.8 Seasonal Change of Mass Departure from Normal (West Pacific Ocean)

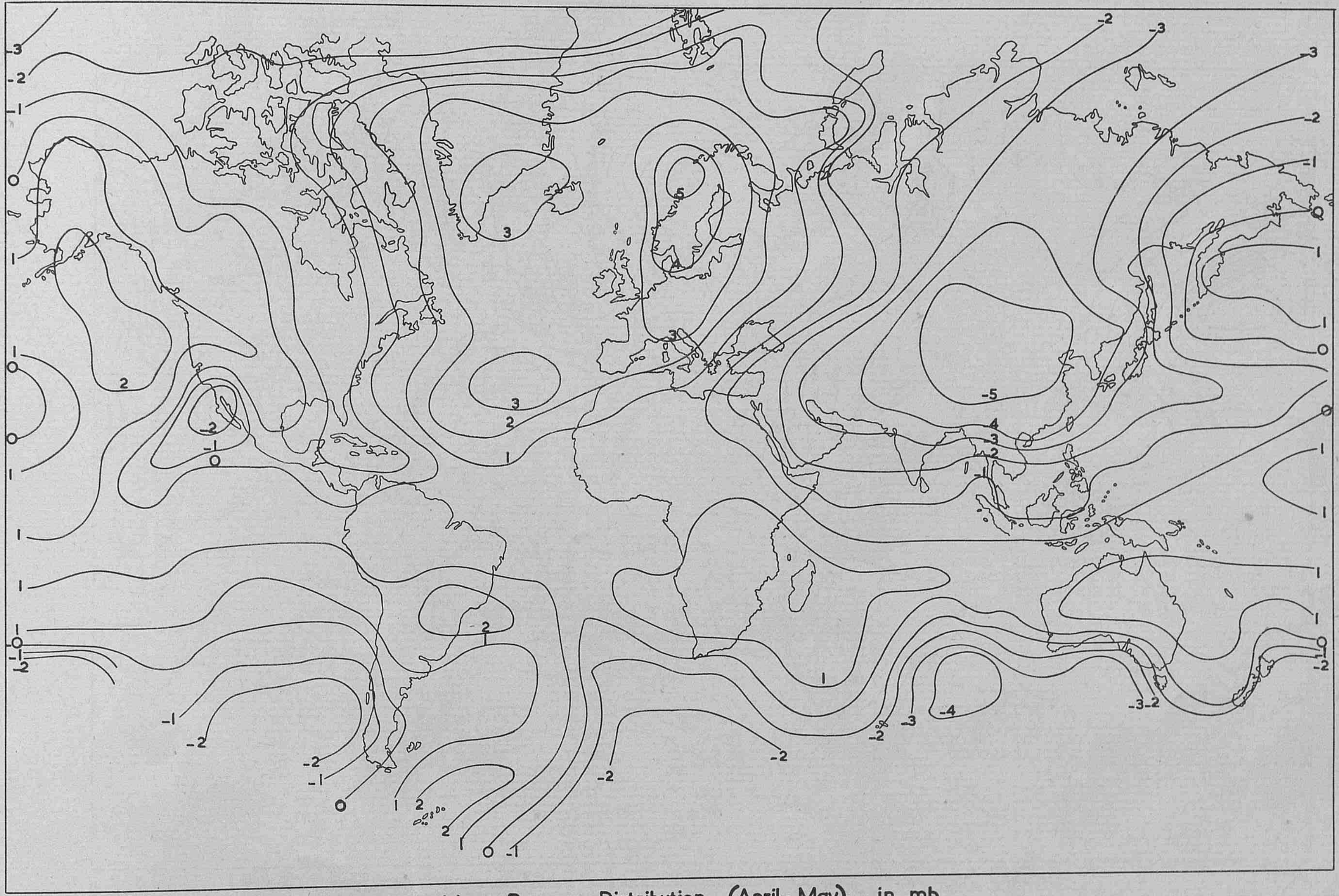
-3
-2
-1
0
1
2
3
-5
-4
-3
-2
-1
0
1
2
3
-5
-4
-3
-2
1
0
1
2
-1
-2
-2
-3
-3-2
-4
-2
-2
-1
0
1
2
2
1
0
-1

Fig. 9 Seasonal Change of Mean Pressure Distribution (April- May) in mb.

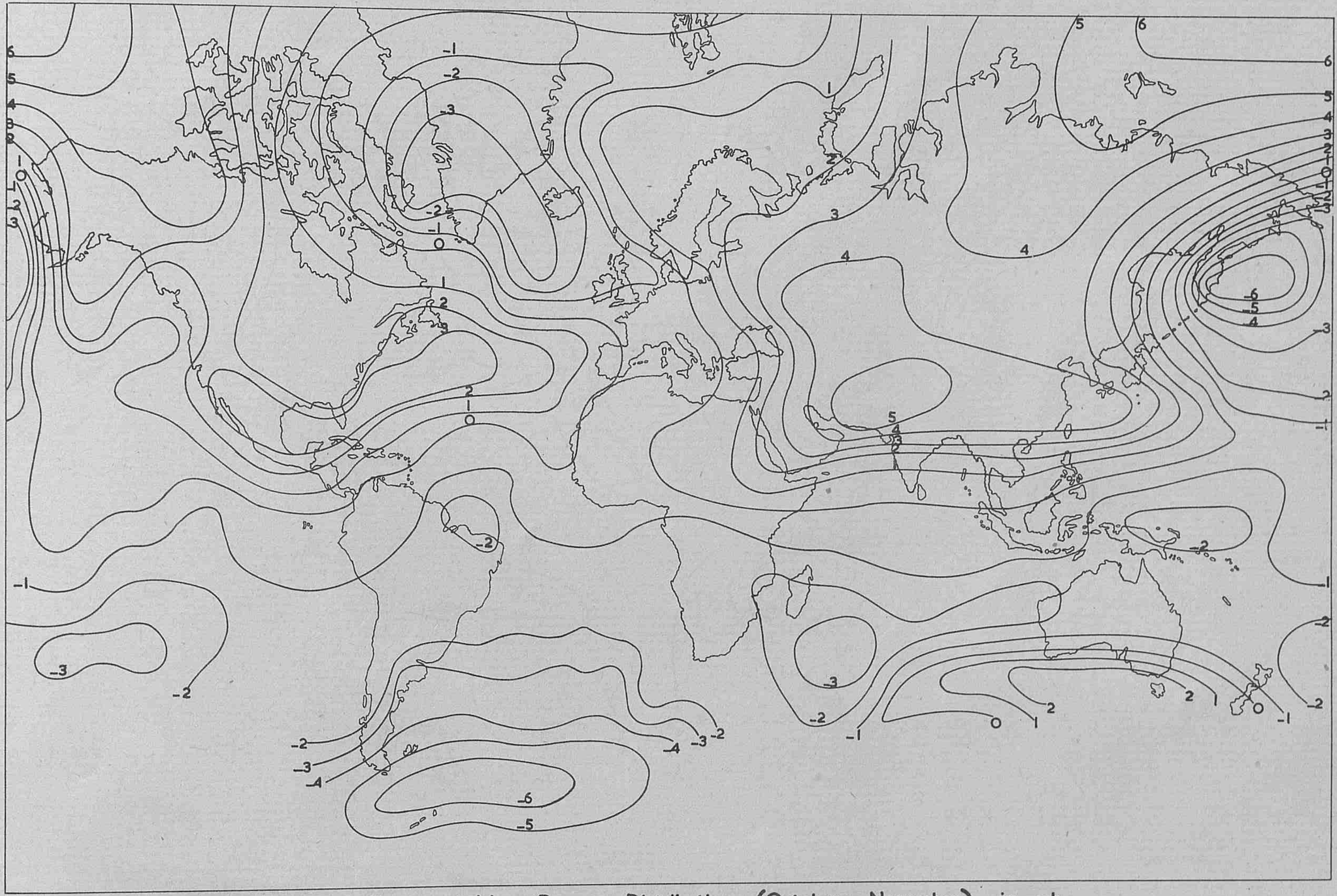
6
5
4
3
2
1
0
-1
-2
-3
-1
-2
-3
-2
-1
0
1
2
3
2
1
0
-2
1
2
3
4
4
5
4
3
2
5
6
6
5
4
3
2
1
0
-1
-2
-3
-6
-5
-4
-3
-2
-1
-2
-1
-2
-3
-2
-2
-3
-4
-6
-5
-4
-3
-2
-3
-2
-1
0
1
2
2
1
0
-1
-2
-2
-1

Fig. 10 Seasonal Change of Mean Pressure Distribution (October – November) in mb.

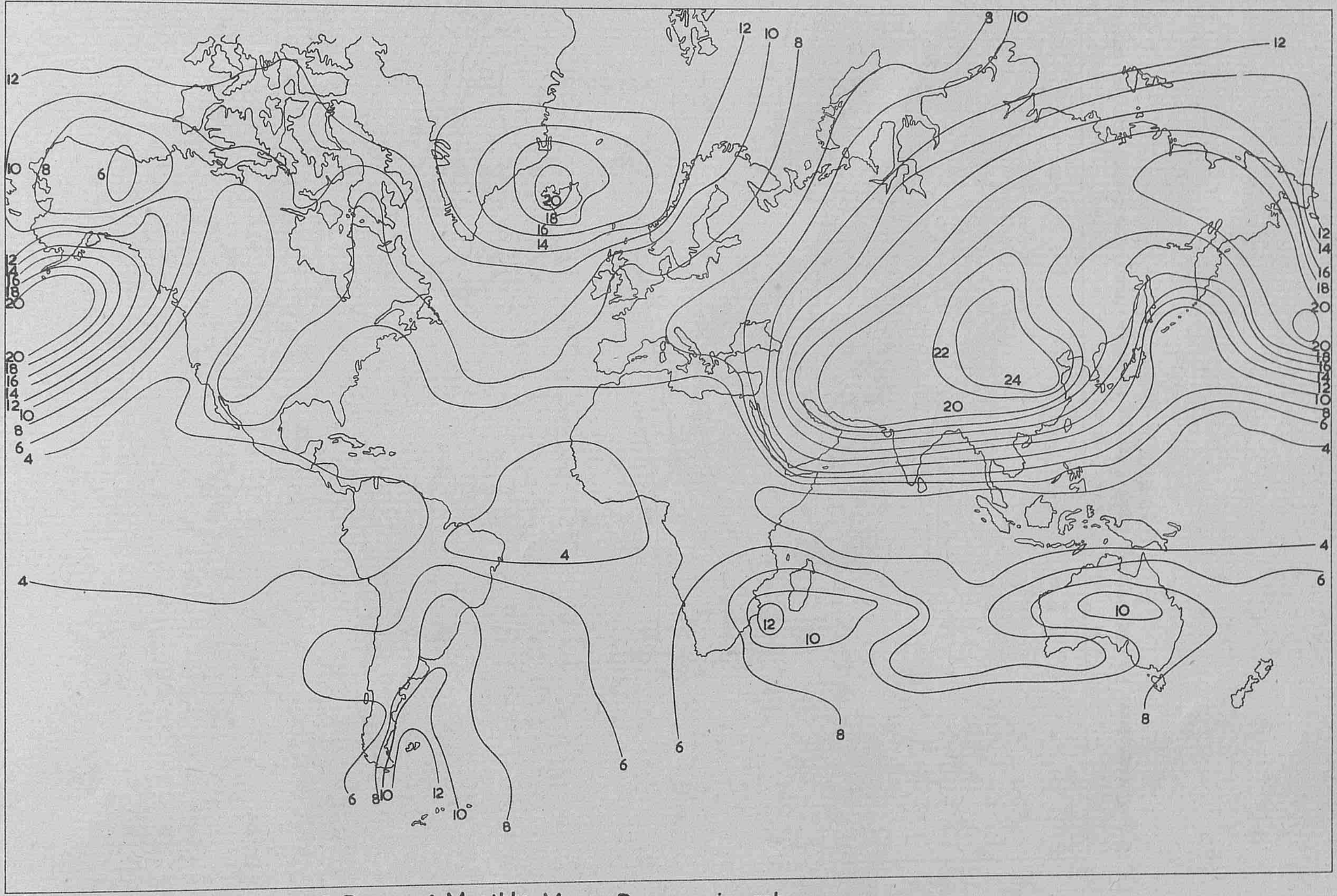
12
10
8
6
12
14
16
18
20
20
18
16
14
12
10
8
6
4
20
18
16
14
12
10
8
12
10
8
4
4
6
12
10
8
6
6
8
6
8
10
12
10
8
22
24
20
12
14
16
18
20
20
18
16
14
12
10
8
6
4
4
6
10
8

Fig. 11 Annual Range of Monthly Mean Pressure in mb.

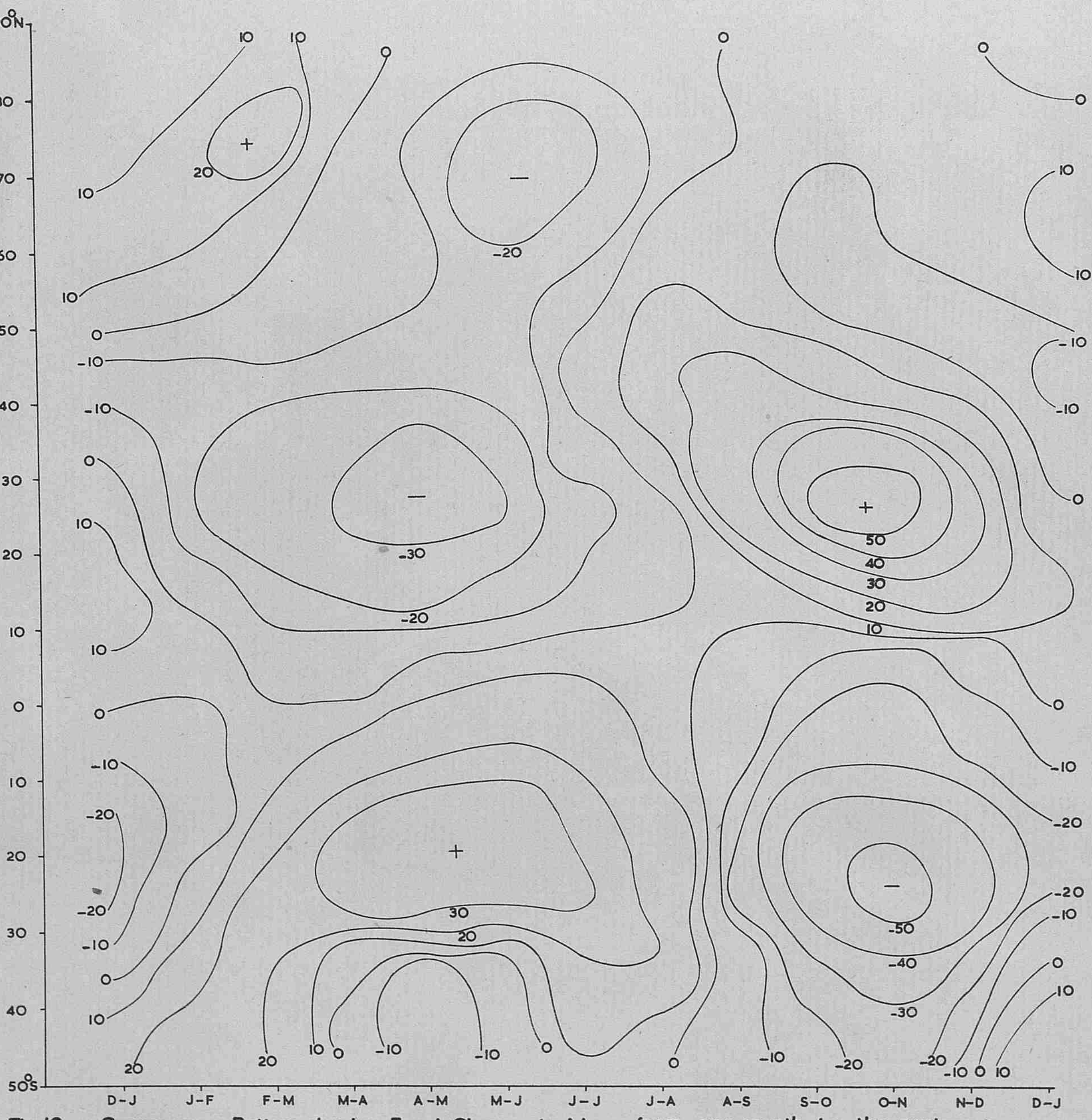

Fig. 12 Convergence Pattern showing Zonal Changes in Mass from one month to the next X ($1{\cdot}25 \times 10^{10}$) metric tons.

paper of the Meteorological Research
Committee (London).
M.R.P. No.......... by Mr..........................
A copy is available in the Library of
the Meteorological Office."

TECHNICAL REFERENCE FILE

M.R.P. 650
S.C. II/83
7th June, 1951

ATI - 145271

AIR MINISTRY
METEOROLOGICAL RESEARCH COMMITTEE

A study of the rainfall of two selected synoptic situations

by J.S. Sawyer (Meteorological Office)

INTRODUCTION

A great wealth of information is recorded on the rainfall of each day over the British Isles. This consists of daily measurements of rainfall and records of recording rain gauges at an extensive network of places over the country. The information is of a much more detailed character than is used in synoptic analysis and forecasting practice, and because of the labour of collecting and analysing the material it is doubtful if it can be used even in research when a large number of occasions are to be studied. However, as a preliminary to research into the problem of forecasting frontal rainfall, it was decided to analyse in detail the rainfall from two selected frontal systems, making full use of the available material.

The purpose of the investigation was:

(a) to establish with some certainty the rainfall distribution in the selected cases and to ascertain whether it could be explained by physical and dynamical principles.

(b) to ascertain to what extent the rainfall distribution could be correctly inferred from the more limited set of rainfall observations available in synoptic practice.

The two cases selected were chosen to be typical of steady warm front rain over England, although the choice was also guided by the need to be able to separate the rainfall of the disturbance from the rain of preceding and following rain areas in the records of gauges read at 24 hour intervals. The two situations studied were:

(a) that of 14th March, 1949, when a small depression moved east-south-eastward over England and Wales.

(b) that of 14th-15th February, 1950, when an active warm front moved north-eastward over the whole of the British Isles.

PART I

The depression of 14th March, 1949

1. The synoptic situation

At midnight on 14th March, 1949, a deep depression over Norway was moving slowly east and an anticyclone was almost stationary near the Azores. Between these two systems a belt of strong thermal gradient extended from west-northwest to east-southeast over the British Isles. The synoptic situation is illustrated in figure 1. A small depression, LN, was situated about 600 miles west of Scotland, and this depression subsequently moved quickly east-southeast across Northern Ireland and Central England, closely following the direction of the thickness lines and causing little distortion in them. The depression was analysed as possessing a warm front, cold front and "trailing occlusion". Some evidence can be found for the passage of these fronts across England, but with the exception of some sections of the occlusion, the fronts were poorly defined - the cold front was particularly difficult to place. However, the centre of the depression, LN, could be followed without difficulty, moving along a track from County Mayo, to near

Dublin and thence to Felixstowe, at about 40 kt. It was accompanied by an extensive area of rain.

2. The rainfall distribution in the moving rain area

The rainfall distribution within the rain area has been reconstructed from the records of some 50 autographic rain gauges maintained at official meteorological stations in England, Wales and Northern Ireland. (Records from privately maintained autographic gauges were not used for this purpose but a few such records were subsequently obtained and used to study the time-sequence of rain in the hilly areas of Wales and Devon). The rate of rainfall has been measured from the slope of the rain gauge trace and approximate plots of rate of rainfall against time have been constructed for each station.

It was clear from an inspection of these diagrams that a broad similarity existed in the time-distribution of rainfall at stations similarly situated with respect to the track of the depression. A composite chart has therefore been constructed in which rate of rainfall is plotted for each station as a function of time along a line placed at a distance from the x-axis corresponding to the distance of the station from the track of the depression. In this diagram mean rates of rainfall over hourly periods have been plotted and mean values have been formed for each area of the diagram. In this way a composite picture of the rate of rainfall in the depression can be built up from which the differences between individual records due to orographic influence, site or exposure, have been eliminated. Such a picture is presented in figure 2; small adjustments have been made to bring the time of occurrence of cold front or occlusion rain into coincidence, but general agreement between different stations regarding the limits of the rain area is good. In this form of diagram it is not possible to show adequately the rainfall in the right hand rear sector where short periods of intense rainfall (reaching a rate equivalent to 10 mm/hr. over periods of 10 minutes with the passage of the occlusion) occurred at some stations but not at others. The cold front also produced sporadic rain of a less intense nature.

The main features of the rain area as analysed from the records of the autographic gauges are:

(a) A centre of maximum intensity of about 2 mm/hr on the track of the depression and about 200 miles ahead of the centre, with a secondary maximum of about 1 mm/hr just behind the centre.

(b) A broad area of rainfall exceeding 0.5 mm/hr extending about 100 mi to the left of the track of the centre and reaching about 540 miles ahead of the depression and 150 miles behind it.

(c) An area of fairly uniform rainfall exceeding 1 mm/hr in the forward right hand sector; this was not associated at all closely with the surface warm front.

(d) A series of belts of sporadic and rather heavy rain extending rearward and to the right of the track from the central region of the depression.

The onset of the measurable rain appeared to have been abrupt at most stations - at no station would the curves have been better described by a gradually increasing rate of rainfall. However, it is not possible to identify a single moving line representing the onset of rain. As indicated in fig. 1 the rain area appears to have possessed three distinct boundaries which advanced across the country in echelon. The isochrones of the position of these three boundaries are shown in fig. 3. At some stations (e.g. Chivenor) the passage of two of the boundaries can be identified with a cessation of rain between; at others (e.g. Croydon) an increase of the rate of rainfall takes place as the station is passed by the extension of a boundary line into the rain area. It may be significant that the southern limit of the two northern boundaries occurs near a break in the high ground along the western seaboard; the more northerly at the gap between Pennines and Welsh Mountains and the more southerly at the gap between the Welsh Mountains and the hills of Devon.

The broad belt of rain in the right-forward sector appears to have maintained a reasonably constant position with respect to the depression as it moved across the country. The warm front itself did not do this. Thus we find that most of the rain fell behind the warm front at Chivenor and Bristol but ahead of the warm front at Croydon and Lympne. The subsidiary maximum of rainfall at the southern end of this belt of rain is probably not significant. The only stations in this region were St. Eval and Plymouth, and they may both have been subject to orographic increase of the rain. The rear edge of this rain belt was quite clearly defined by the autographic records although slight rain or drizzle continued with less than measurable intensity after the indicated rain area had passed. Isochrones of the end of continuous measurable rain are given in figure 4.

In the right hand rear sector of the depression most stations experienced one or more short periods of rain of moderate or heavy intensity. It is possible to define without difficulty the last of these; this was analysed as associated with the trailing occlusions which moved south in the rear of the depression. Isochrones of the position of this rain belt are given in figure 5. Only a band from South Wales to Sussex and Kent was affected. To the southwest of this no measurable precipitation fell except possibly over Dartmoor and to the northeast no well defined separation occurred between the occlusion rainfall and that of the main rain area. Amounts of rain from the occlusion varied irregularly (see figure 5) but most stations had two bursts of moderate or heavy rain about 15 minutes apart.

It is uncertain from the autographic records whether the other short bursts of rain behind the main rain belt were arranged along linear belts of a frontal type or not. There is some suggestion of two such belts as suggested in figure 2, but if they existed many stations escaped rain from one or other of them. The original cold front of the system was so diffuse that it cannot be placed with any certainty although it must have been present in this sector of the depression if it still existed at all.

The mean value of the rate of rainfall was evaluated over all stations for a period of 11 hours during which the depression passed. The mean value obtained was 0.67 mm/hr and the root mean square departure from this was 0.57 mm/hr. A calculation was also made of the departure of the rainfall from the smoothed average value appropriate to the particular sector of the depression as presented in figure 2. The root mean square departure was 0.39 mm/hr. A comparison of this figure with the departure from the overall mean shows that a large part of the variation of rainfall is accounted for by the structure of the rain area shown in figure 2. Noteworthy positive departures of the rates of rainfall from the values appropriate to the distribution in figure 2, occurred at some west coast stations and in East Anglia. The positive excesses at Aberporth (+5.6mm) and Chivenor (+3.7mm) might be expected from the onshore wind and lifting by the hills only a short distance inland. The positive excesses at West Raynham (+3.2mm) and Wittering (+3.4mm) are less easy to explain. Negative departures are found at stations east of the Welsh mountains but also over Wiltshire and the Thames valley reaching -3.3mm at South Farnborough. These differences are presumably due to orographic effects and there is no clear sign that they operated differently in different sectors of the depression. Most of the places with an orographic increase had rainfall for much the same period as stations with amounts nearer to the average, but the intensity appears to have been increased. However, at Princetown, 1,360 ft. above sea level on Dartmoor, the rainfall commenced 5 hours earlier and was more continuous in the rear sector of the depression than at low level stations in the same area. However, only about 20% of the rainfall fell at Princetown before rain commenced at neighbouring low level stations.

/3.

3. The total rainfall from the depression

A chart of the rainfall distribution resulting from the depression has been drawn on the basis of all 24 hour rainfall observations available in the Climatology branch of the Meteorological Office. This provides a network of observations at about 10 mile intervals over most of the country except the less populated hilly areas of Wales, Pennines, Devon and Cornwall. The resulting chart is shown in figure 6. Reports are available only to 0.1 inches but isopleths have been drawn on the basis of these figures at intervals of 5 mm (0.2 in.approx.). In order to include all the rain from the depression the isohyets are based on the rainfall from 0900 14th March to 0900 15th March over most of England, but from 0900 13th March to 0900 15th March over Northern Ireland, Wales and N.W. England. Little rainfall is included other than that associated with the depression.

The most striking features of this detailed rainfall chart are the maxima of rainfall over Wales and over Dartmoor and Exmoor, where orographic effects are pronounced. However, this should not obscure the general distribution of precipitation resulting from the depression. This leads to a band of high rainfall along the track of the centre of the depression from North Wales to Essex. This band is clearly defined over Eastern England where orographic effects are small. Rainfall falls off fairly rapidly to the north and less rapidly to the south of this band. The effects of various orographic features can be identified by maxima in the rainfall distribution, e.g. the Mendip Hills, the South Downs and the higher ground of East Anglia. The location of the rainfall minima, presumably rain shadows, is more surprising. The small dry area east of Dartmoor is to be expected, and the low rainfall round Gloucester and Hereford, but the dry areas in central Hampshire and the Vale of the White Horse are more difficult to explain.

It is interesting to note the relatively small variability of rainfall from place to place over eastern England where orographic influences are not on a large scale. This is illustrated by the detailed plot of rainfall amounts in the Home Counties (figure 7). It is also useful to compare figure 6 with a rainfall chart solely on those observations received telegraphically (figure 8). This latter chart was drawn independently. It brings out the broad features of the rainfall distribution from the depression but underemphasises the orographic features because of the absence of telegraphic reporting stations in the hilly districts.

4. Distribution of rain as observed by radar at East Hill

A comprehensive set of photographs is available for this occasion from the meteorological radar at East Hill (near Dunstable). These confirm in some detail the horizontal structure of the rain area of the depression as deduced from the autographic rainfall records. Photographs of the P.P.I. tube from 1100 to 1130 show the boundary of the rain area approaching from the west with an alignment from NNW to ESE closely corresponding to the appropriate section of figure 2. East Hill remained in the rain area until 1530, but from 1200 to 1300 the radar photographs show that the rainfall fell off southward rather sharply at a distance of 25-30 miles corresponding to the section X of figure 2. The echo again extends further southward from 1310 until 1400 and this is presumably an indication of the extensive belt of rain to the south.

A clearance of the main precipitation echo is clearly shown as moving over East Hill from the northwest at 1530. This agrees closely with the rear edge of the main rain belt as deduced from the autographic records both in the time of clearance and alignment of the edge of the rain area. Prior to this clearance, the radar photographs from East Hill had shown a more patchy structure than before, with bands of relatively intense echo and intermediate weaker bands aligned parallel to the rear edge of the rain area. Subsequent photographs of the P.P.I. tube up to 1630 show a number of small echoes scattered over the area but with no tendency to form into bands, except for one rather more extensive area of rain which appears to have formed over East Hill about 20 miles behind the main rain area and moved southeast behind it. This echo developed a definite alignment parallel to the preceding rain edge.

5. Rainfall of 14th March in relation to Sutcliffe's theory of development

R.C. Sutcliffe (Q.J. Vol. 73, 1947, p.370) has made considerable use of the idea of cyclonic development, and shown how it should be theoretically possible to compute the rate of development from the distribution of the 1000 mb heights and the thickness distribution for an appropriate layer of the troposphere. Cyclonic development, defined by Sutcliffe as the difference between the divergence at two levels in the troposphere, is intimately related to the large scale vertical air movements and consequently to the rate of rainfall, if the air is saturated. If several rather crude assumptions are made it is possible to derive the rate of rainfall from the value of Sutcliffe's expression for the rate of development together with the temperature of the air column assumed saturated. The theoretical basis of this calculation is given in an unpublished note by J.S. Sawyer (M.O.21 Technical Note No. 20). The most important assumptions are the absences of vertical movement at the tropopause, the constancy of the thermal wind direction with height, and neutral stability of the air columns.

Further work by E.J. Summer (Q.J. Vol. 76, 1950, p.384) and by F.H. Bushby (unpublished) has shown that if the stable stratification of the atmosphere is taken into account the vertical velocities will be reduced, and the numerical solution of the problem by Mr. Bushby in selected cases suggests that damping by a factor of about 4 is normal.

In order to make an approximate assessment of the amount of rainfall which would have been expected if these theoretical ideas were valid, Sutcliffe's expression for the development was evaluated for 6 hour intervals during the passage of the depression. The expression used was

$-V'\frac{\partial}{\partial s}(\zeta' + 2\zeta_0)$ where V' is the thermal wind velocity, ζ' is the vorticity of the thermal wind field. ζ_0 is the vorticity of the geostrophic wind field at a low level (1,000 mb) and $\frac{\partial}{\partial s}$ denotes differentiation in the direction of the thermal wind. This expression was evaluated for the layer 1,000-500 mb, and is shown in figures 9(a) to (d). The positive areas indicated cyclonic development and upward motion. In order to estimate the total effect of upward motion in producing rainfall the positive contributions have been added together and the rainfall which should have been expected indicated in figure 10. For this purpose it has been assumed that if the expression $-V'\frac{\partial}{\partial s}(\zeta' + 2\zeta_0)$ had been evaluated up to the tropopause (200 mb. approx) it would have been increased in proportion to the depth of the layer, i.e. approximately by a factor of 2. On the other hand it is assumed that the damping effect of stability would have been as indicated above (i.e. to reduce the vertical velocity to a quarter of that in atmosphere of neutral stability). It will be seen that the direct application of the development principles leads to the expectation of a broad band of precipitation across the British Isles of about the correct intensity. The axis of heaviest rainfall in fact occurred about 100 mi south of the position which would have been expected. It is unlikely that the appropriate vorticity gradients could have been evaluated sufficiently accurately on the 1,000 mb and thickness charts to place the maximum of development with an error less than 100 mi but it is interesting to note that the numerical solution of Mr. F.H. Bushby of the equation representing the damping effect of vertical stability does suggest that the maximum of vertical velocity should have occurred slightly to the south of the maximum of Sutcliffe's expression for development.

/6.

6. Orographic influences on the rainfall

It is interesting to note that the autographic records from Aberporth, Swansea and Chivenor show that, although these stations received considerably heavier rainfall than places inland, the duration of the significant rainfall was much the same. This is also true at higher level stations on Snowden (Cym Dyli) and at Taf Fechan (Pontsticill) in South Wales. However, as noted earlier, rain commenced earlier at Princetown than at low level stations in Devon. These facts suggest that the effect of lifting by the hills further inland has been principally to increase the intensity of the rain in the dynamically produced rain areas, rather than to produce additional orographic rainfall within the air masses themselves. Douglas and Glasspoole (Quart. J.R.Met.Soc.Vol.73,p.11) have pointed out the need for a deep damp layer of air for heavy orographic rainfall to result. Such conditions certainly exist in the rain areas of the depression, but it may be that elsewhere the orographically produced cloud is often too thin, or physically too stable, to cause effective precipitation. Within the pre-existing rain areas we can expect that any additional droplets produced by orographic lifting will be swept up by the falling rain and so increase the rainfall. If rain is not already falling, however, this may not necessarily occur.

It is interesting to form an estimate of the additional orographic rainfall which would be expected if all additional condensation during the passage of the rain area reached the ground as rain. We follow the method adopted by Douglas and Glasspoole (Quart. J.R. Met.Soc.Vol.73,p.11). It is reasonable to assume that the motion at some level is undisturbed by the topography, that the air near the ground follows the outline of the hills and that the air at intermediate levels is lifted in proportion. If we further assume that the same amount of water is carried as cloud and rain drops thoughout, it is a simple matter to compute the amount of water which must fall out of a given vertical column during its ascent of a windward slope. This calculation has been made for a lifting of 1,000 and 2,000 feet, an air column saturated and with a lapse rate following the saturated adiabat for a wet bulb potential temperature of 50°F (this is close to the actual conditions in the rain area on 14th March); various assumptions have been tried regarding the height of the undisturbed level.

Depth of water that would be precipitated from an air column saturated along the 50°F saturated adiabat when lifted over a ridge of hills

Height of Hills	Undisturbed level assumed to be		
	850 mb	700 mb	500 mb
1000 feet	.05 cm	.08 cm	.12 cm
2000 feet	.08 cm	.15 cm	.25 cm

The amount of orographic rainfall which falls at individual places depends on the slope of the barrier or hills and on the area over which the rainfall is spread. Over Exmoor on figure 6 the area of marked orographic rainfall probably only extends 25 miles from east to west. We treat Exmoor as a barrier 1000 feet high and assume that lifting extends to 500 mb. The wind at 800 mb during the rain period was about 280 deg. and 40 kt and the rain area took about 5 hours to pass (at Chivenor) so that .12 cm of water from an air mass 200 miles long was deposited over an area of 25 miles long - the total orographic fall should therefore have been about 0.96 cm. This appears to be of the correct order as the maximum fall observed was 0.8 inches of which about 0.6 can be regarded as an orographic increment. Over the Dartmoor-Bodmin Moor area the rain was spread over about 35 miles depth and the duration may have been slightly less, but as the barrier is probably rather higher the maximum rainfall was about the same. The amounts of orographic rain in South Wales can be broadly explained in the same way. The maximum of about 40 mm near Plynlymon in central Wales of which about 30 mm was probably due to orographic lifting requires a barrier of 2,000 feet and the rainfall deposited on an area of only 20 mi depth - not an unreasonable expectation on this section of the Welsh coast.

It is not possible to discuss the orographic rainfall in North Wales where the winds were irregular and variable but it is noteworthy that very little orographic increase is observed on the South Pennines where low level winds were light during the rain period.

Poulter (Quart. Journal R.Met.Soc.Vol. 62,p.49) has demonstrated that the orographic effect is less on cold front rain than on warm front rain. In view of the small contribution of the cold front and occlusion to the total rainfall at low level stations, it therefore seemed reasonable to omit the orographic increment to the rain in the cold sector in making the estimates of orographic rainfall given in the preceding paragraphs. Although this assumption has sufficed to obtain crude estimates of the rainfall in the hill districts (probably correct within 50%), nevertheless the rain in the cold sector of the depression was very much greater at the high level stations of Princetown and Taf Fechan than at adjacent low level stations. At Princetown the cold sector rain provided about 20% of the total, at Taf Fechan rather less.

It is not the purpose of this paper to analyse in detail the pattern of orographic rainfall. This would require a detailed study of the local topography. However, it is clear that the broader features of the rainfall over the hilly districts can be explained on the simple hypothesis of the lifting of the saturated air of the rain area as it crosses the hills.

The distribution and intensity of the "rain shadows" in the lee of the high ground is less easily explained. It has been indicated above that a barrier 1000 feet high would be expected to have condensed from the air an additional depth of about 1 mm of water. This represents about an hour's rainfall on level ground as measured in most parts of the rain area ($\frac{1}{2}$ hour's rain near the centre) and we might therefore have expected a completely dry area of 30-40 miles east of the Welsh mountains and Dartmoor or an area of reduced rainfall of much greater extent. In fact no such substantial reduction of rainfall can be noted. There are small dry areas east of Dartmoor and between Monmouth and Hereford but the relatively dry areas extending across Salisbury Plain from Bath to Southampton and Guildford and that between Swindon and Oxford are not related to the main orographic barriers in any obvious way.

PART II

The warm front rain of 14th February, 1950

1. The synoptic situation

At 1200 on 14th February, 1950, a deep depression was centred about 60 mi SW of Iceland and was moving north-eastward. Its warm front extended from north-west to south-east across the south-west Approaches to the British Isles. The warm front moved north-eastward across the country with only small irregularities and by 1200 15th February, it had reached the central North Sea. The warm front was preceded by the well defined rain belt which was selected for study. The cold front of the system came southward only as far as the Scottish Border before returning as a warm front into a following wave depression, but the warm sector was in process of rapid occlusion as it crossed Scotland. (The synoptic situation is illustrated in figure 11.) The main depression was associated with a strong twisting of the 1000-500 mb. thickness lines and the warm sector was accompanied by a well defined thermal ridge. A strong thermal contrast existed across the warm front; this amounted to over 20°F at the 700 mb level.

/2.

2. The rainfall distribution in the moving rain area

The records from 66 autographic rain-gauges at stations in the British Isles have been examined and the rate of rainfall plotted as a function of time during the passage of the frontal system.

The passage of the belt of warm front rain was clearly shown by all the records in England and Wales and most of the rain occurred in advance of the warm front. Except at high level stations there were only small amounts of rain in the warm sector and at most stations the amounts were insufficient to be recorded. At high level stations in Wales and on Dartmoor rainfall continued irregularly in the warm sector with an intensity of about 1 mm/hr. (rather less on Dartmoor). Over Scotland the rainfall distribution was more complex because of the occlusion process which was going on rapidly and also on account of the strong orographic influences.

At most stations measurable warm front rain lasted about 4 hours. The intensity increased irregularly to a maximum one to two hours before the passage of the front as analysed from the surface charts, and measurable rain ceased in most cases a little before the arrival of the front. The intensity of the rain varied considerably from place to place, presumably as a result of orographic influences. However, the plotting of rates of rainfall in position relative to the front (as was done in figure 1 for the depression of 14th March, 1949) and the calculation of average values over all of the stations in various sectors showed that there was little systematic variation in intensity along the length of the front over England and Wales. However, stations near the west coast had a maximum intensity of about 2 mm/hr whereas some stations in eastern England did not reach 1 mm/hr. There is also an indication that the duration of the warm front rain was less at the stations with lighter rainfall suggesting that situations relative to the front which gave only light rain on the west coast gave none at all at some eastern stations. We may compare the plots of rate of rainfall against time at Chivenor on the west coast and Cranfield in eastern England (figure 12). A rough approximation to the Cranfield curve would be obtained by reducing all of the Chivenor ordinates by 1 mm/hr (omitting the short spasm of heavy rain which occurred early in the rain area at Chivenor).

At stations in SW Scotland the distribution of rainfall with respect to the warm front was similar to that in England but the rainfall was much heavier. However, at Renfrew and Eskdalemuir heavy continued at a rate of 3 to 4 mm/hr in most of the warm sector. Further to the north the rain appears to have been less intense, and on the east coast at Dyce, Lossiemouth and Wick amounts were similar to those in England but the rain area was displaced ahead of the warm front as analysed on the surface charts by a period of about 2 hours.

The average rate of rainfall for periods $\frac{1}{2}$, $1\frac{1}{2}$, $2\frac{1}{2}$ etc. hours ahead of the frontal passage have been calculated over all stations in England and Wales and they are as follows:-

Hours before warm front passage	$\frac{1}{2}$	$1\frac{1}{2}$	$2\frac{1}{2}$	$3\frac{1}{2}$	$4\frac{1}{2}$	$5\frac{1}{2}$	$6\frac{1}{2}$
Rainfall (mm/hr)	0.32	0.89	0.94	0.60	0.25	0.01	0

The average rate of rainfall for all stations in England and Wales over the 6 hours preceding the frontal passage was 0.50 mm/hr and the standard departure of the hourly rates from this mean was 0.51 mm/hr. The standard departure from the average rate appropriate to the distance from the warm front as given in the preceding table was also calculated. This was 0.34 mm/hr showing that the variation of intensity with the approach of the front does account for a substantial part of the variation of rate of rainfall at individual stations.

/3.

3. The total rainfall of February 14th

Isohyets for the period 0900 14th February, 1950, to 0900 15th February, 1950, are given in figure 13 based on all available raingauge readings.

It is seen that about 5 mm rainfall was received in places on the western coasts of England and Wales and in Northern Ireland. Rather less than 5 mm fell in eastern and central districts of England and some districts of northeast Scotland.

Pronounced orographic maxima of rainfall are found over the Welsh mountains, Dartmoor, the Lake District and the mountains of West Scotland. The orographic effect is less well marked over the Pennines, possibly because the air had only recently crossed the Welsh mountains. Increase of rainfall may also be noted over the Mendip Hills and the South and North Downs.

The most striking maximum of rainfall, however, is that centred a little southeast of Greenock. As well as including the high ground in that area this heavy rainfall also fell at stations on the banks of the Firth of Clyde. The autographic records from Renfrew and Eskdalemuir suggest that much of this rain fell in the warm sector.

4. Radar observations of rainfall distribution

The East Hill meteorological radar station did not operate during the passage of this rain belt.

5. Rainfall of 14th February in relation to Sutcliffe's theory of development

A chart of the integrated value of the cyclonic development has been computed for the period 0900 14th February, 1950, to 0900 15th February, 1950, as was done for the depression of 14th March, 1949. Figure 14 shows the rainfall which would have been expected based on this calculation. It shows values of a little under 5 mm over eastern and southern England increasing to about 12 mm in the region of the Hebrides. The values for England agree well with those found at places where there is no significant orographic effect.

It is difficult to make a satisfactory comparison over Scotland because of the widespread orographic effects, but the amounts of 12 mm measured on Colonsay and Islay, and 10 mm on Iona and Tiree suggest that the band of heaviest precipitation was again south of the area in which it would have been expected.

6. Orographic effects in the rainfall of 14th February

On this occasion, also, the warm air mass had a wet-bulb potential temperature of about 50°F, and it is possible again to take a saturated adiabat through 50°F as a representative sounding in the frontal rain area. When the frontal rain area crossed Wales and southwest England the wind at 900 mb was about 260 degrees 40 kt and the duration of the frontal rain was about 4 hours at coastal stations in SW England and 5 hours on the Welsh coast. In the warm sector the wind at 900 mb was about 240 deg. 50 kt and although there was little rain in the warm sector at low level stations, a further 7 or 8 hours' rain occurred at high level stations before the raingauges were read at 0900. About 55% of the total rain at high level stations fell in the frontal rain area and most of the remainder in the warm sector (some showers had occurred in the Welsh hills early on 14th and were included in the total for the day).

We first compute the probable orographic addition to the frontal rain in a manner similar to that adopted in the preceding example. If we treat Devon as a barrier 1,000 feet high and assume the rain spread over 35 miles, we obtain an additional orographic component of 6 mm. Similarly, if we treat Wales as a barrier of 2,000 ft and again assume the rain to be spread over a depth of 35 miles we obtain an orographic increment to the frontal rain of 12 mm. It is not certain how much of the observed rainfall fell in the frontal rain belt and how much in the warm sector but from the autographic records it seems that practically all the rain fell in the frontal belt at low level stations and about 55% at high levels - say an overall percentage of 80%. On this basis an average of about 7 mm of rain fell in the frontal rain area over the Devonshire hills of which about 3 mm can be regarded as the orographic increment. Over the Welsh hills an average of about 12 mm fell in the frontal rain area of which about 8 mm should be regarded as due to orographic effect. It thus appears that the preceding computation has over-estimated the effect of the orographic lifting - a closer agreement would have been achieved if the lifting had been assumed to extend up to only 700 mb instead of 500 mb.

An examination of the radio-soundings at Camborne and Larkhill in the warm sector shows that the air was moist up to about 800 mb but above that level it was relatively dry. It is probable that further north the moist air was deeper. However, taking the Camborne soundings as typical of the warm air we find that if the undisturbed layer is assumed to be 500 mb orographic lifting of the lower layers by 1,000 ft would result in the condensation of approximately .06 cm of water and orographic lifting by 2,000 feet would result in condensation of 0.12 cm of water. With an undisturbed layer at 700 mb the figures are about 0.04 and 0.08 cm of water. Taking the undisturbed layer as 700 mb, a wind of 50 kt, and a spread of orographic rain over a depth of 35 miles at a 1,000 foot barrier we obtain a rate of rainfall of about 0.5 mm/hr or at a 2,000 foot barrier of about 1.1 mm/hr. At Princetown (1,360 ft) the average rate of rainfall in the warm sector was about 0.5 mm/hr during the period in which measurable rain fell (about 2/3 of the warm sector). At the Welsh stations Taf Fechan, Lake Vyrnwy and Cym Dyli the rainfall averaged about 1 mm/hr in the warm sector; these figures conform closely with the preceding estimates.

The absence of any marked orographic effect on the southern Pennines is noteworthy; the air had already been lifted to a similar height over Wales. The absence of any marked rain shadow between the two masses of hills suggests that the air did not descend significantly between them.

The general rainfall over the Lake District can be adequately explained in a manner similar to that over Devon and Cornwall but the very heavy rainfall in the centre of the area would require a study of local topography to be fully understood.

The rainfall distribution over SW Scotland, however, is unexpected and difficult to interpret. The maximum of over 40 mm fell at Greenock, which is close to sea level, as well as on higher ground to the southeast. The point of occlusion passed near to this area and the analysis of the rainfall is therefore complicated. Moreover, it seems unlikely that the explanation is to be sought on dynamical grounds. The role of the fronts seems rather to have been to maintain a deep damp air mass and general rainfall over the area for a longer period than elsewhere, thus enabling a heavy orographic fall to accumulate. C.K.M. Douglas and Glasspoole (Quart. J.R.Met.Soc.Vol.73, p.11) have emphasised the importance of deep damp layers of air and continued rain in a warm sector as factors in producing heavy orographic falls. Rain continued at both Renfrew and Eskdalemuir for over 10 hours. At Prestwick also, where the total fall was quite small, and orographic effects presumably not important, the rain was spread over a similar period. However, although the total amount of rain which fell over southwest Scotland could probably be adequately explained on the same lines as those adopted for Devon and Wales but assuming a duration of 10 hours, the peculiar concentration around

Greenock would probably need a careful study of local winds and other similar cases before any definite conclusions could be reached.

The areas deficient in rainfall are again not distributed in any very obvious relationship to the high ground. Their location over England are, however, rather similar to those which occurred on 14th March, 1949; there are dry areas round Gloucester and eastward from Bristol to the Thames Valley and Salisbury Plain. The small dry areas east of Stoke-on-Trent and near Hemel Hempstead are surprising.

PART III - CONCLUSIONS

The study of the rainfall distribution on these two occasions suggests that despite minor irregularities in the recorded rainfall the general distribution over the British Isles on these occasions can be analysed into two components - dynamical and orographic. The occasions were selected to exclude, as far as possible, rainfall of a convectional or instability character; the results can therefore be regarded only as suggestive of the structure of steady rains.

The dynamical component moves across the country with the pressure system with which it is associated and appears to maintain a broadly recognisable structure. The total amount of the rainfall can be adequately explained on the basis of Sutcliffe's theory of development.

The orographic component of the rainfall arises from lifting of the moist air by ranges of hills. In association with the lower hills (not exceeding 1,000 ft), and on the approaches to the higher ranges the orographic component occurs primarily within the rain areas already established by dynamical causes and augments the rainfall there. The amount of this orographic rain is consistent with orographic lifting extending upward to a level between 700 and 500 mb. On the hills the rainfall within the warm air mass becomes of increasing importance and the amounts are broadly consistent with the orographic lifting extending upward to a level of 700 or 500 mb. These conclusions are in general agreement with those of Douglas and Glasspoole.

The distribution of areas deficient in rainfall (rain shadows) is not easily explained in relation to the high ground masses. However, the diminution of rainfall east of the main barriers appears to be less than would be expected if the air descended again to the extent to which it had been lifted. The study of these rain shadows and the smaller features of the rainfall distribution would require the detailed analysis of the rainfall amounts from a larger number of disturbances similar in structure and with the same wind directions.

It is also concluded that the dynamical component of the rainfall is depicted in charts based on the observations of telegraphic reporting stations with sufficient accuracy for study in relation to the synoptic situation. Such charts are, however, misleading in regard to the amount of rain which falls over the hilly areas.

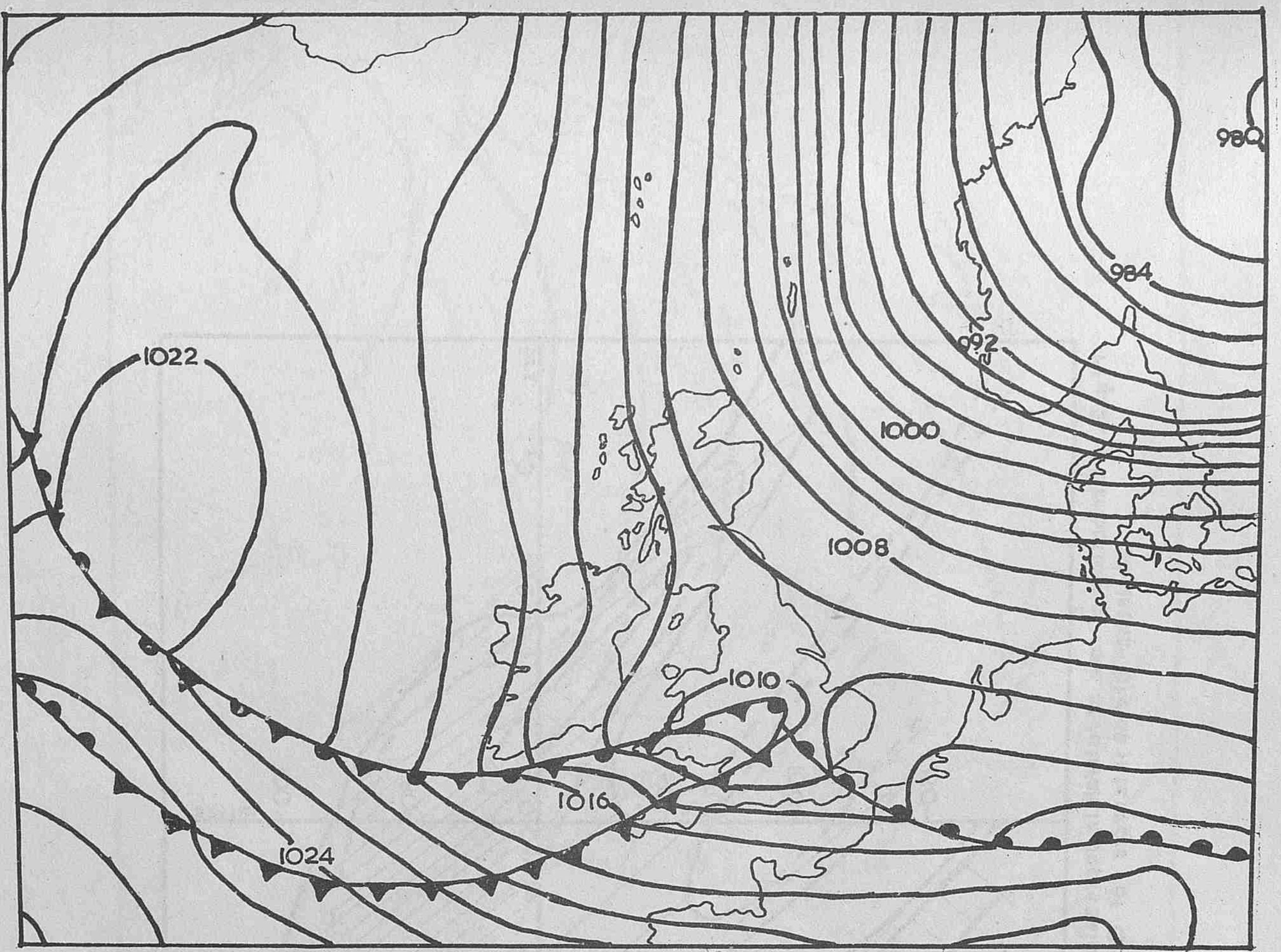
980
984
992
1000
1008
1010
1016
1022
1024

Fig. 1(a). Synoptic situation 1500 14 March 1949.

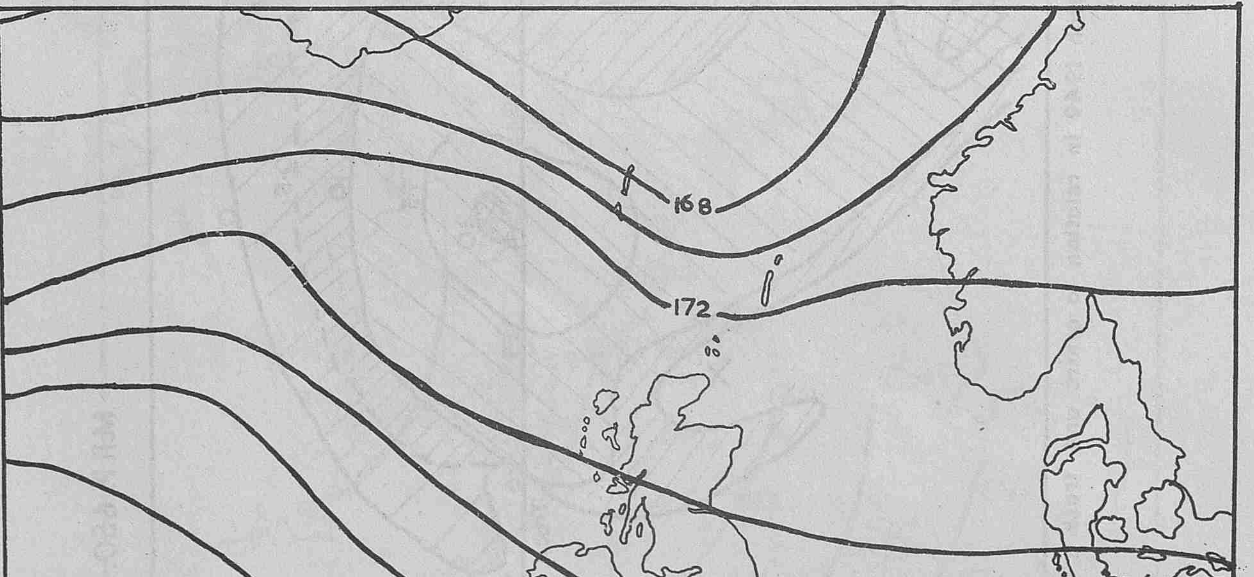
168
172
176
180

Fig. 1(b). 1000–500 mb. thickness lines. 1500 14 March 1949. (unit 100's ft.)

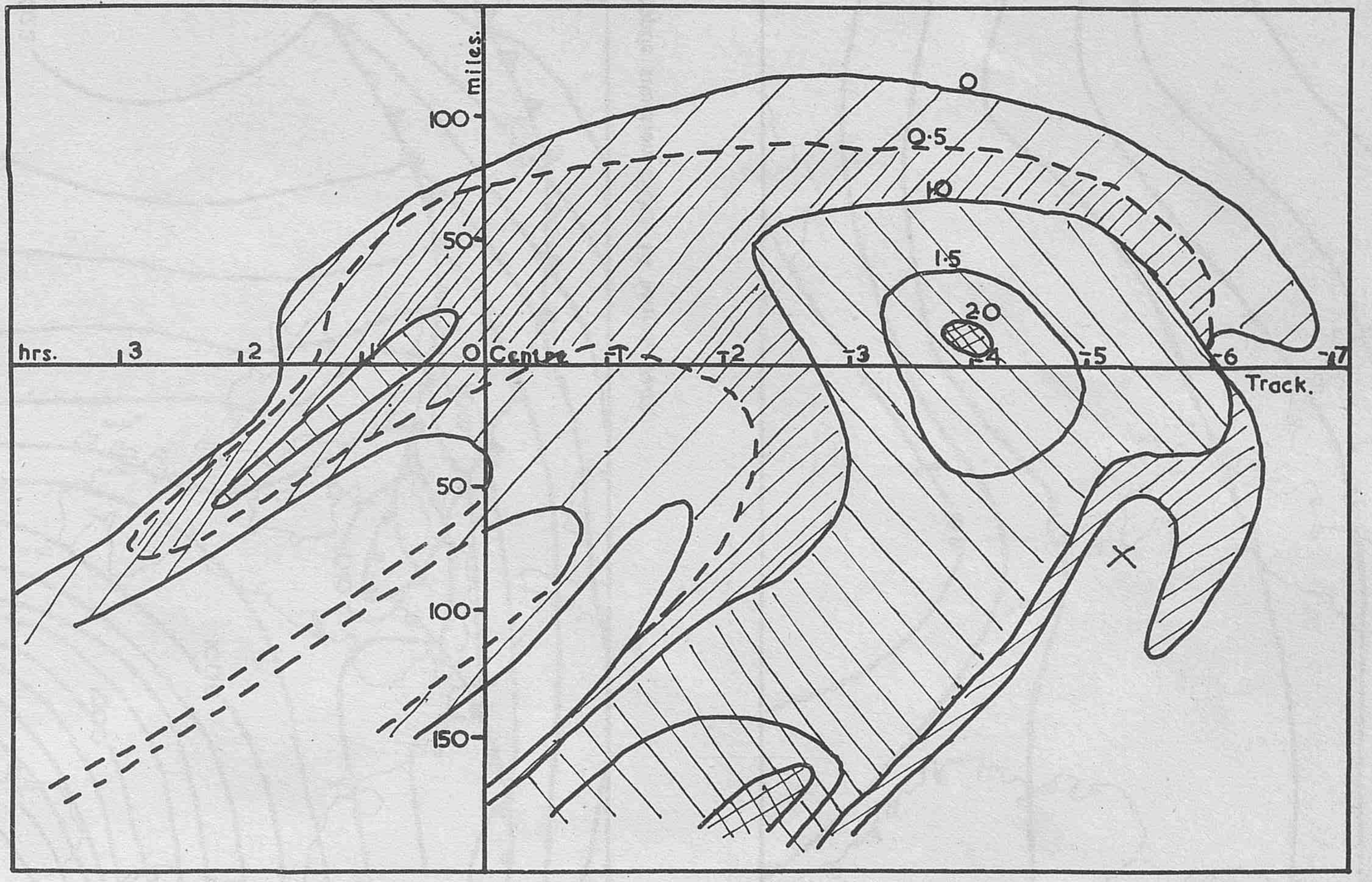

Fig. 2. Distribution of rate of rainfall in depression of 14 March 1949 in relation to centre and track. Isopleths are at intervals of 0·5 mm/hr..

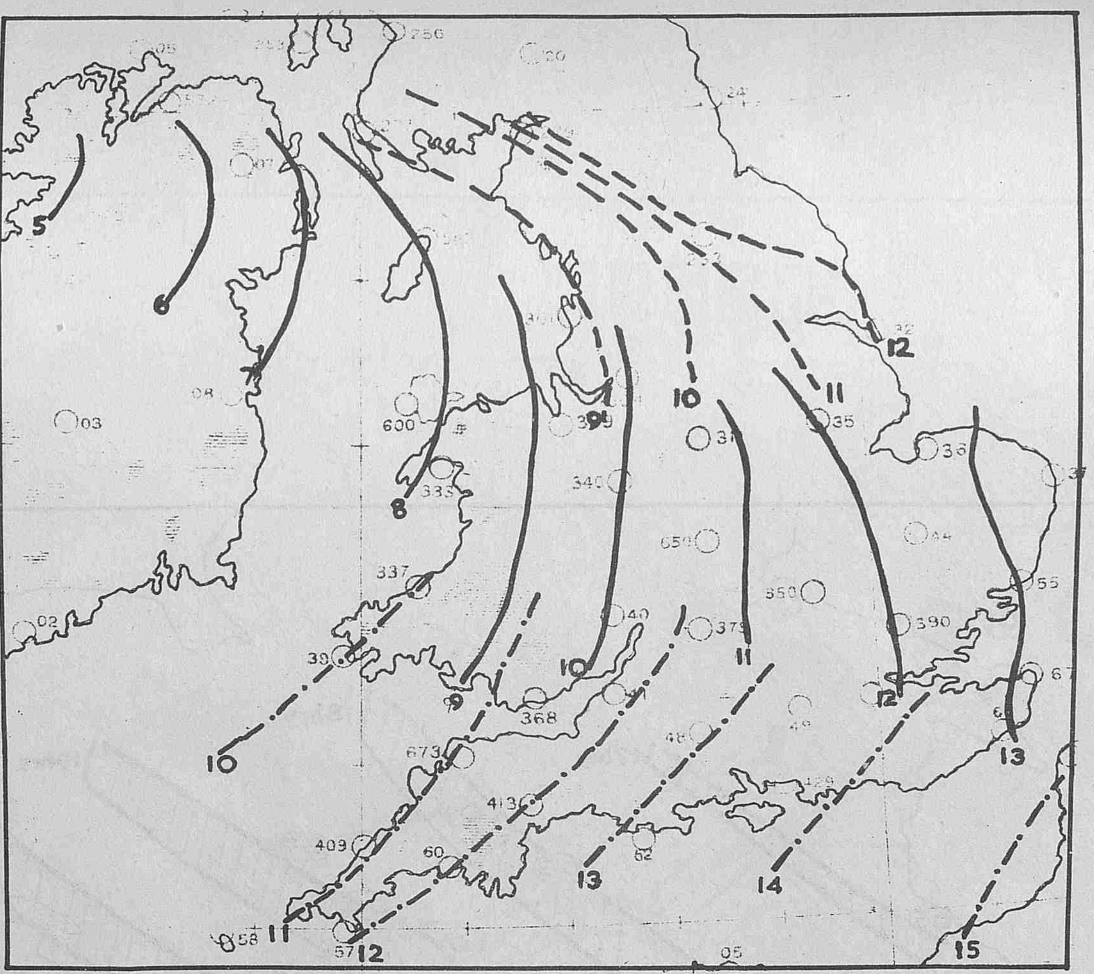
5
6
7
8
9
10
11
12
13
14
15
05
253
256
20
24
572
07
08
03
02
600
309
340
31
35
36
37
333
337
39
650
350
40
379
390
44
55
67
368
673
413
409
60
62
48
49
129
58
57
05

Fig. 3. Isochrones of front edges of rain area.

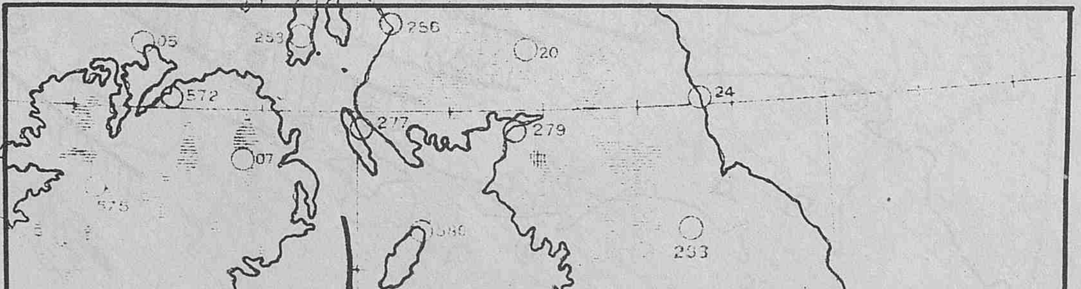
05
253
256
20
24
572
277
279
07
575
586
293
301
32
08
03
600
304
309
311
35
36
37
333
340
650
44
12
13
14
15
16
17
337
350
55
02
40
390
368
41
51
67
673
48
49
66
129
413
409
60
62
58
57
05

Fig.4. Isochrones of rear edges of rain area.

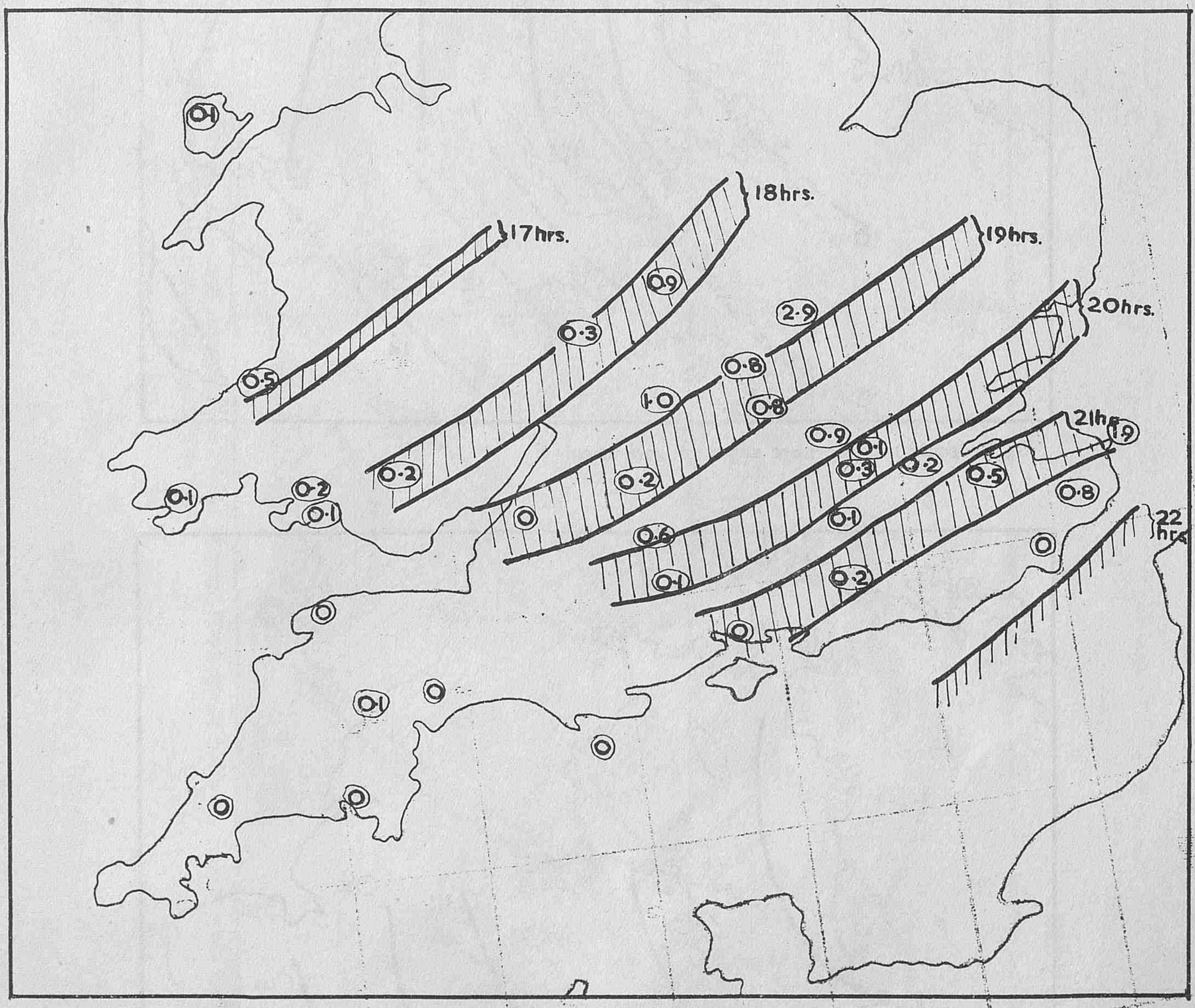
17hrs.
18hrs.
19hrs.
20hrs.
21hrs
22 hrs
0·1
0·5
0·9
0·3
2·9
0·8
1·0
0·8
0·2
0·9
0·1
0·3
0·2
1·9
0·5
0·8
0·1
0·2
0·1
0·2
0·6
0·1
0
0·2
0
0
0·1
0
0
0
0

Fig. 5. Isochrones of occlusion rain area. Amount of rain from occlusion in mm. thus ○.

M.R.P. 650.

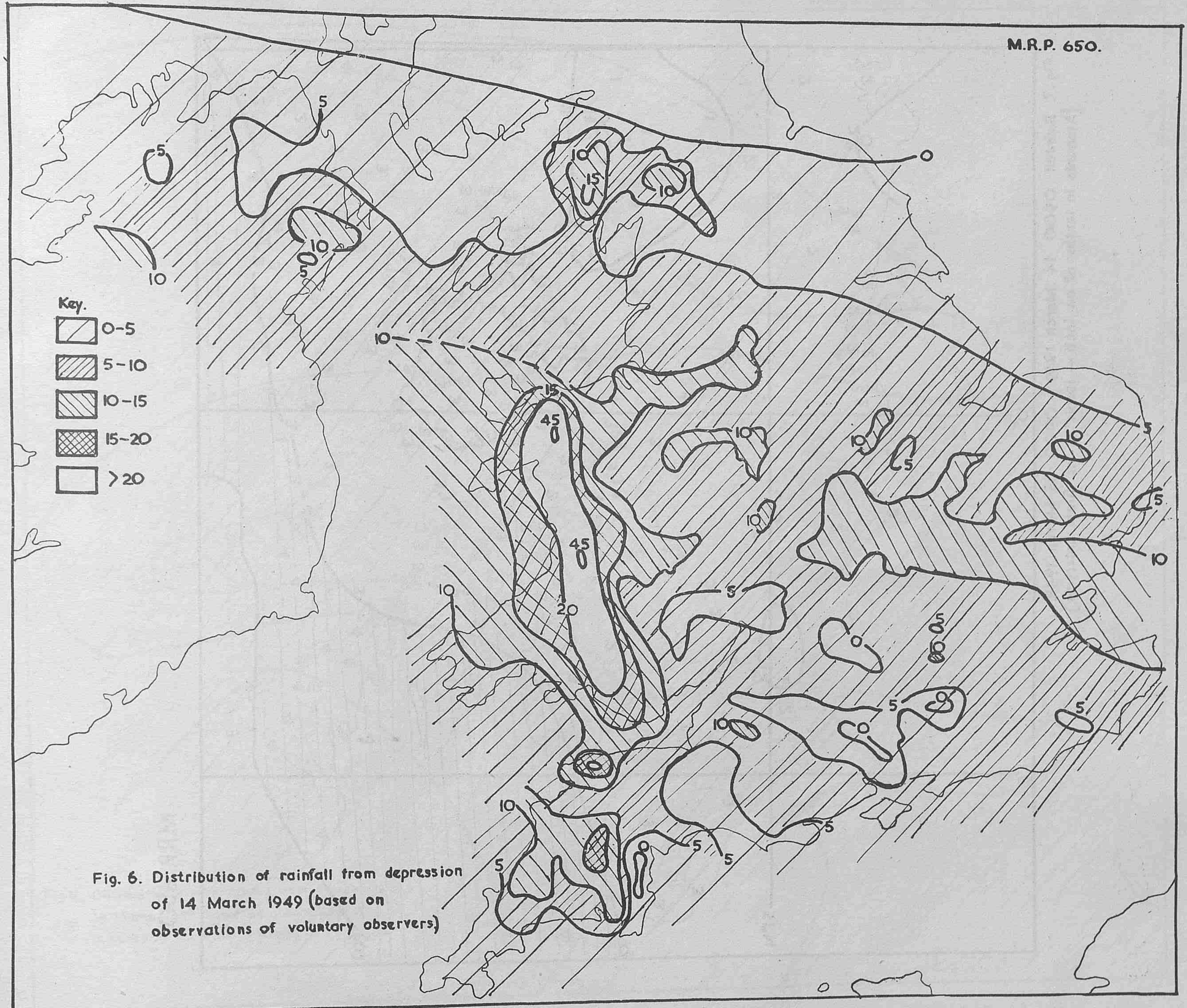
Key.
0-5
5-10
10-15
15-20
>20
45
45
20
15
10
5
0

Fig. 6. Distribution of rainfall from depression of 14 March 1949 (based on observations of voluntary observers)

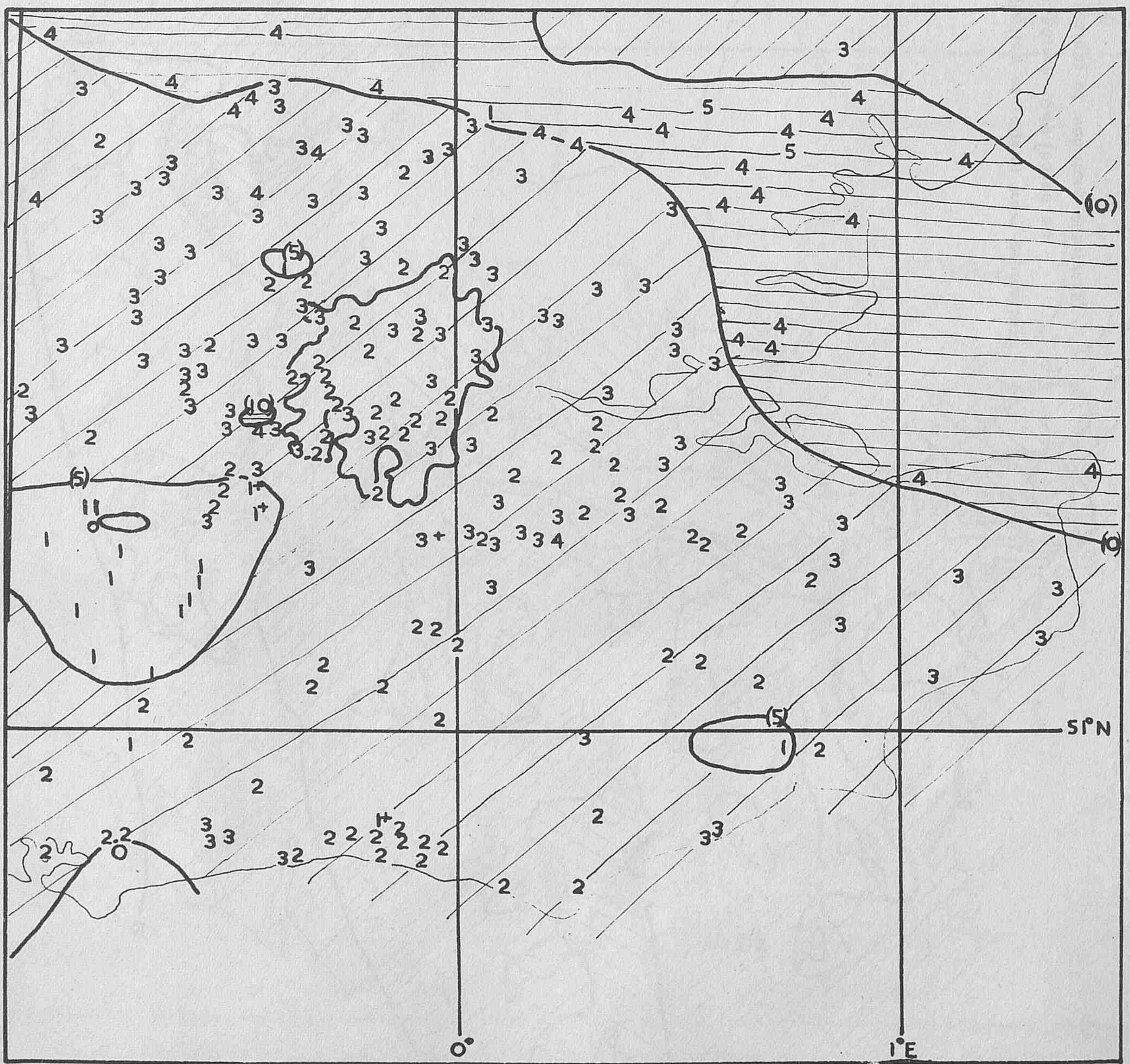

Fig. 7. Rainfall 0900 14 March 1949 – 0900 15 March 1949.
(Amounts in tenths of an inch — isopleths at 5mm intervals.)

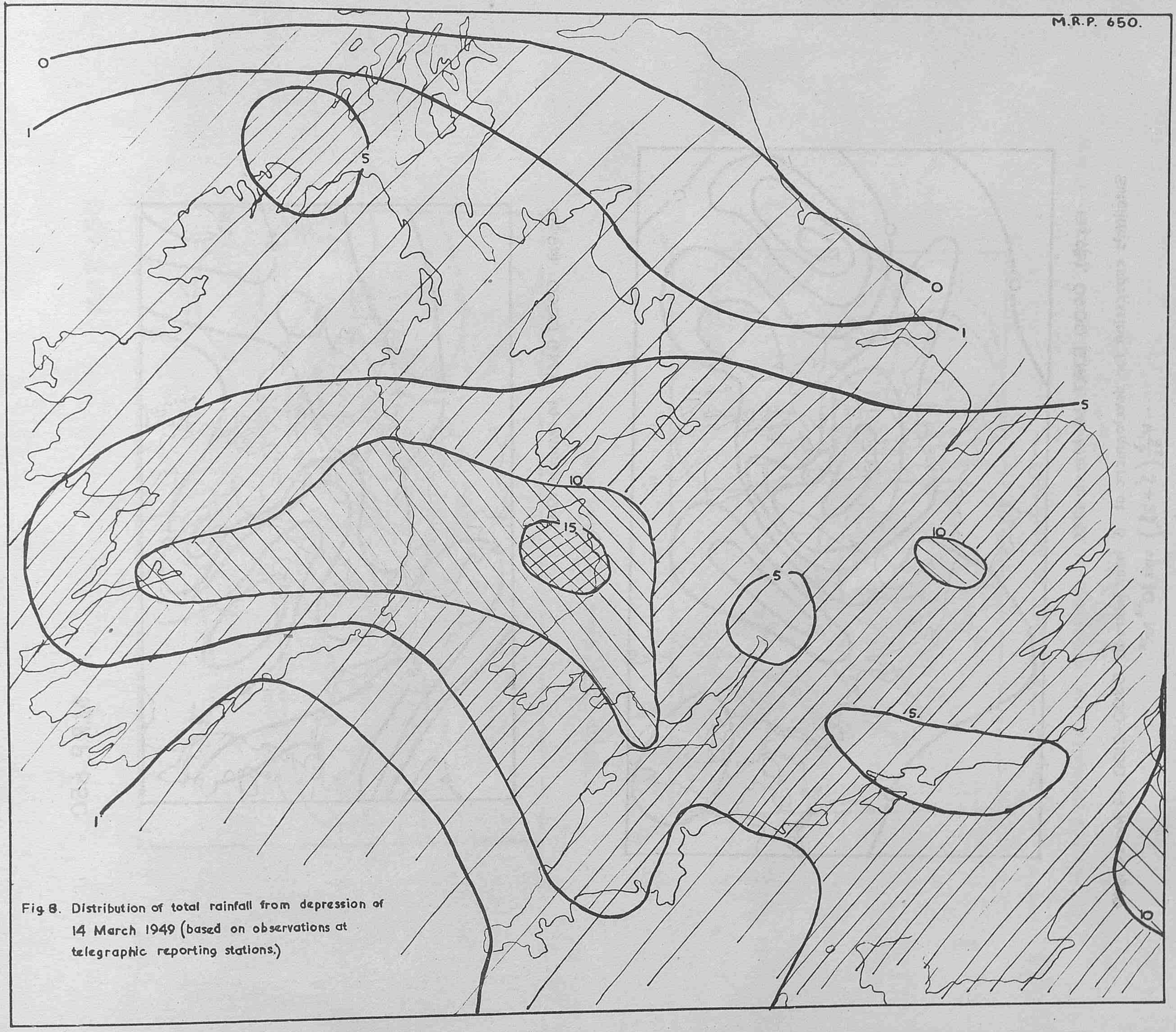
0
1
5
10
15
5
5
10
5.
10
0
1
5
1

Fig. 8. Distribution of total rainfall from depression of 14 March 1949 (based on observations at telegraphic reporting stations.)

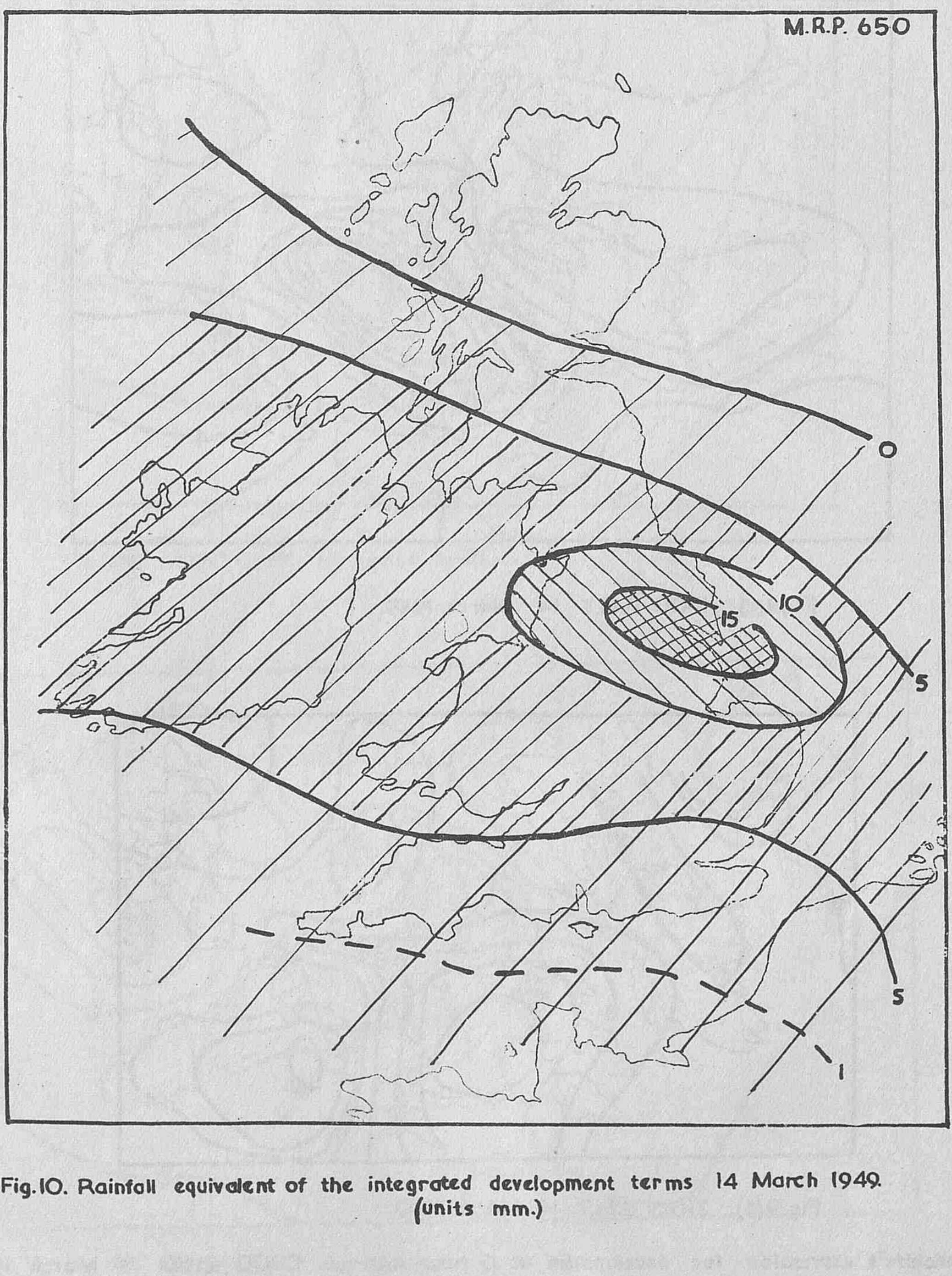
M.R.P. 650
0
5
10
15
5
5
1

Fig. 10. Rainfall equivalent of the integrated development terms 14 March 1949.
(units mm.)

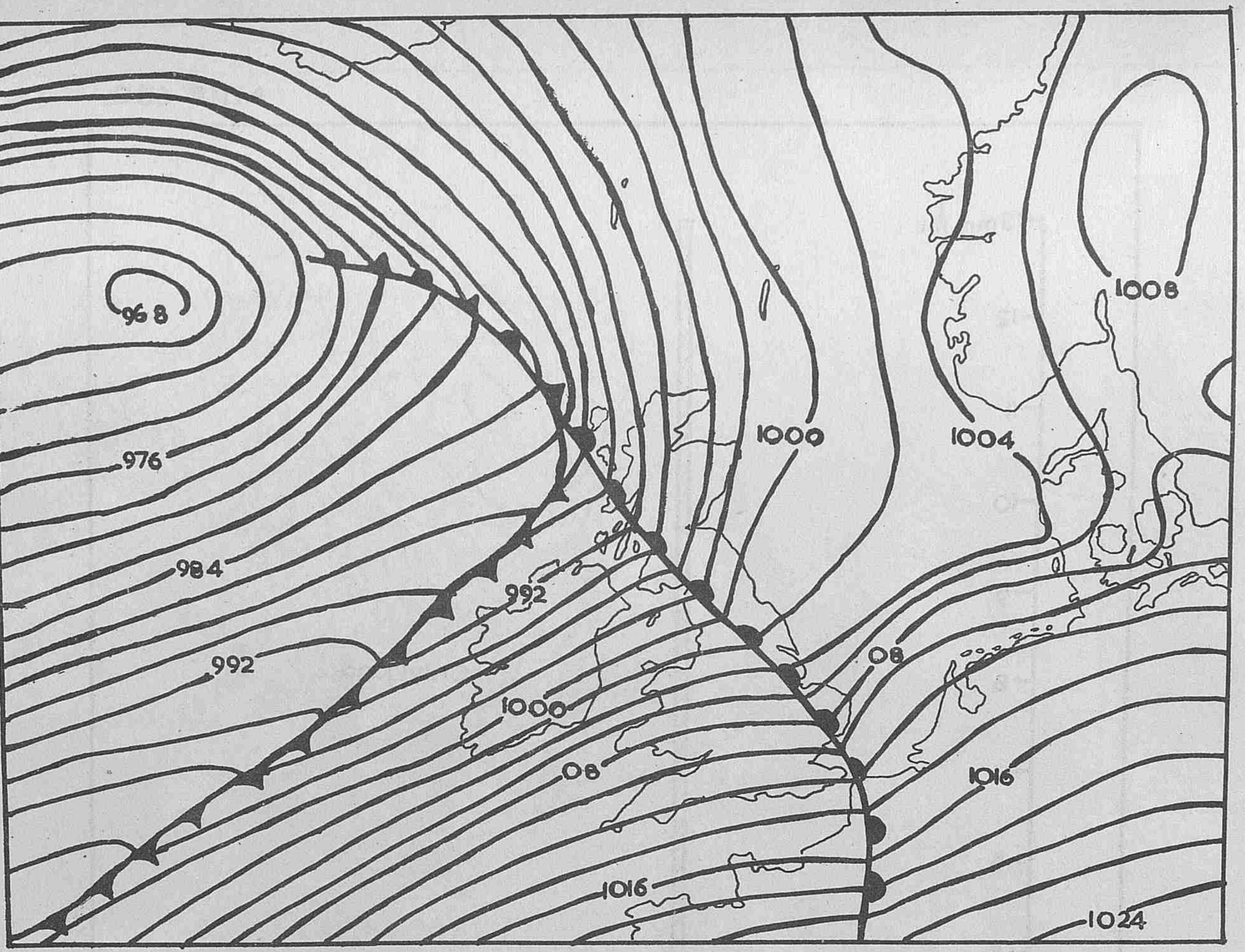
968
976
984
992
992
992
1000
1000
08
1016
1000
1004
1008
08
1016
1024

Fig. 11(a). Synoptic situation 0300 G.M.T. 15 February 1950.

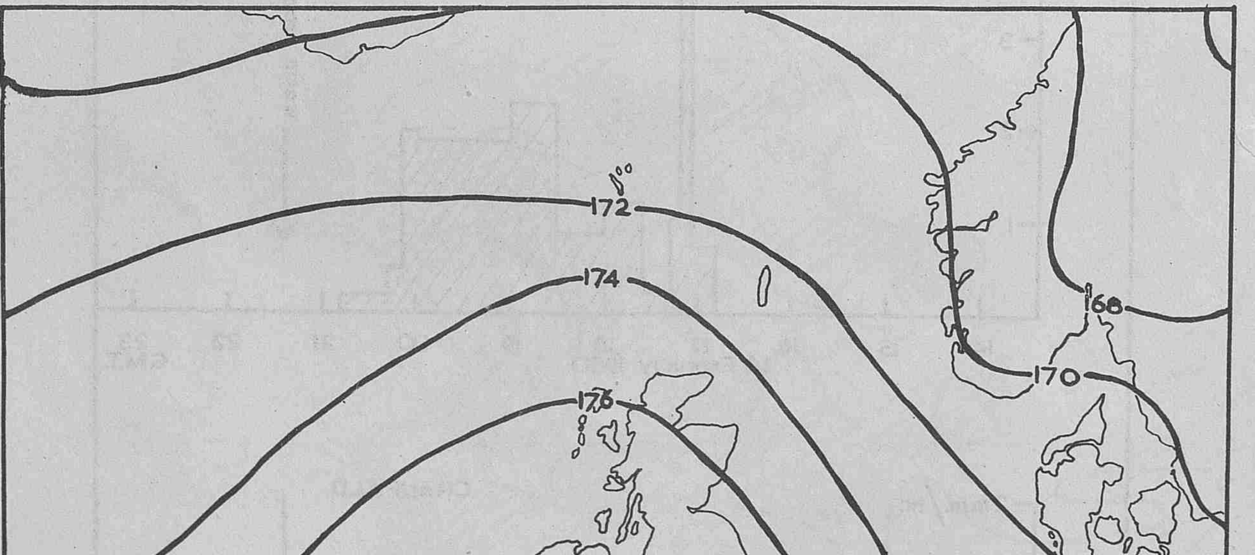
172
174
176
178
180
168
170

Fig. 11(b). 1000-500 mb. thickness lines 0300 G.M.T. 15 February 1950. (units 100's ft.)

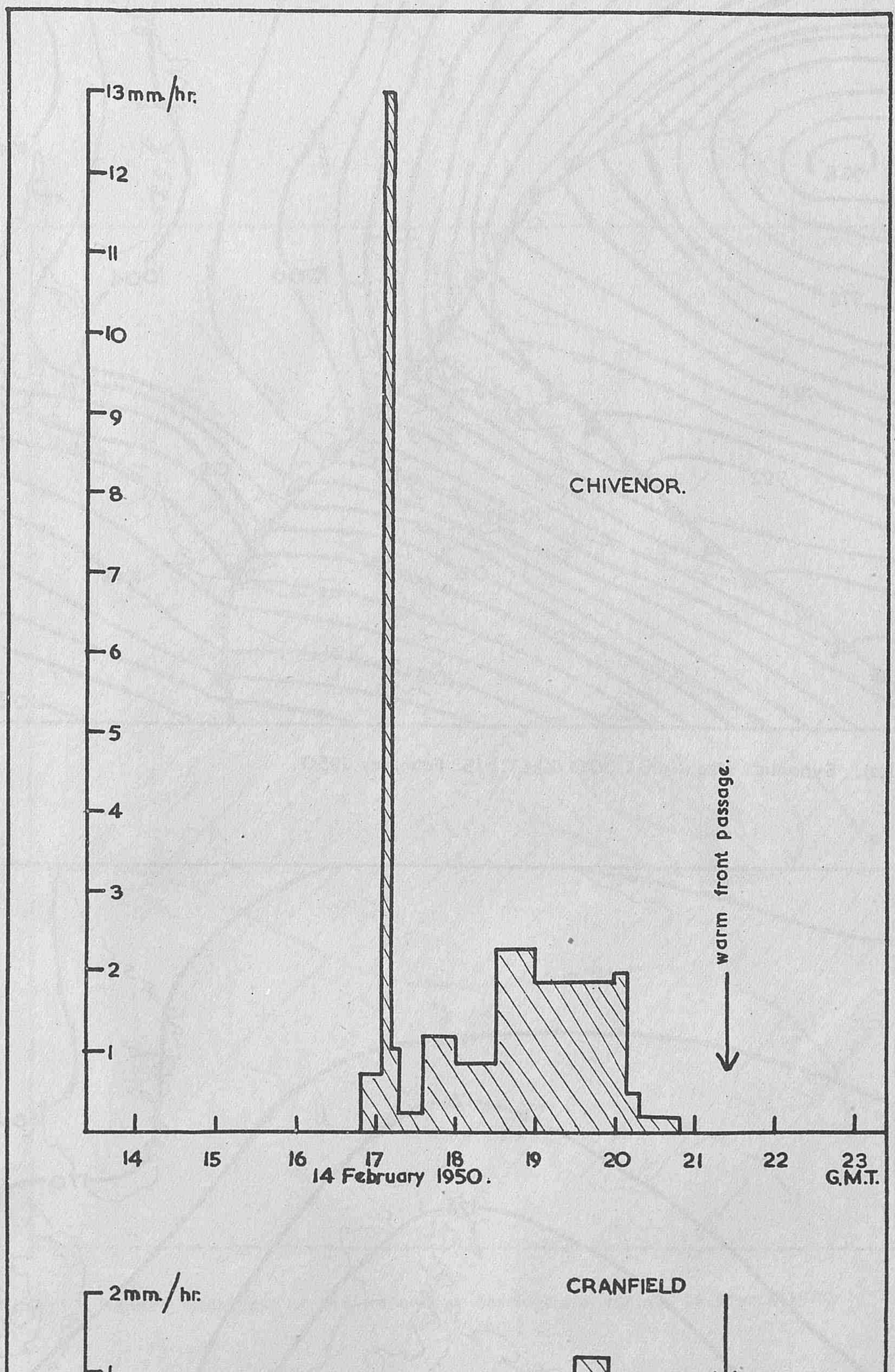

Fig. 12. Rate of rainfall at Chivenor and Cranfield.

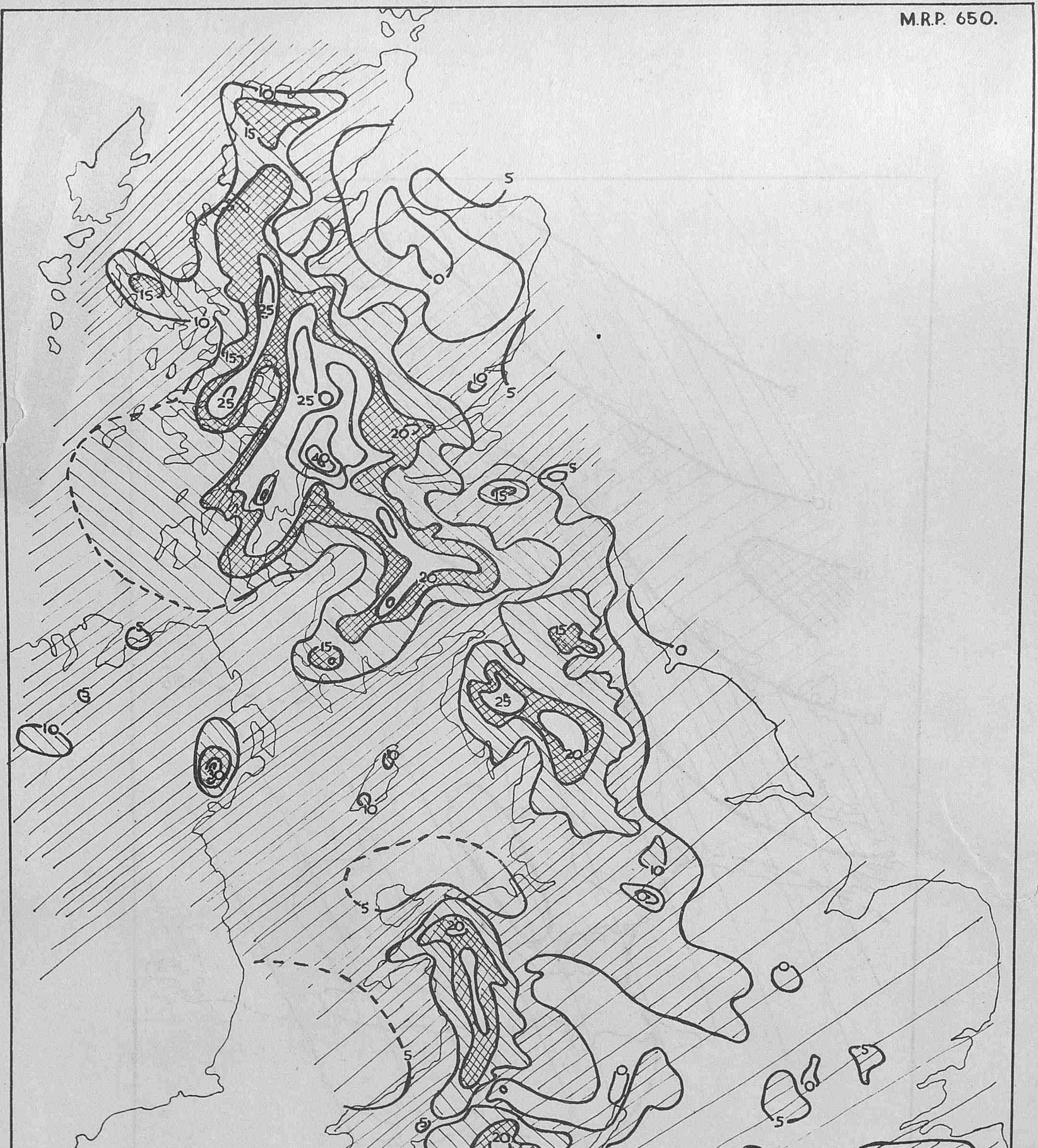
10
15
5
15
10
25
15
25
25
0
10
5
20
40
5
15
20
0
15
15
25
20
5
5
10
10
30
10
10
5
20
5
0
5
0
5
20
10
10
5
5
10
5
5
10
5

Fig. 13. Rainfall of 14 February 1950 (based on observations of voluntary observers.) 0900 14 February to 0900 15 February.

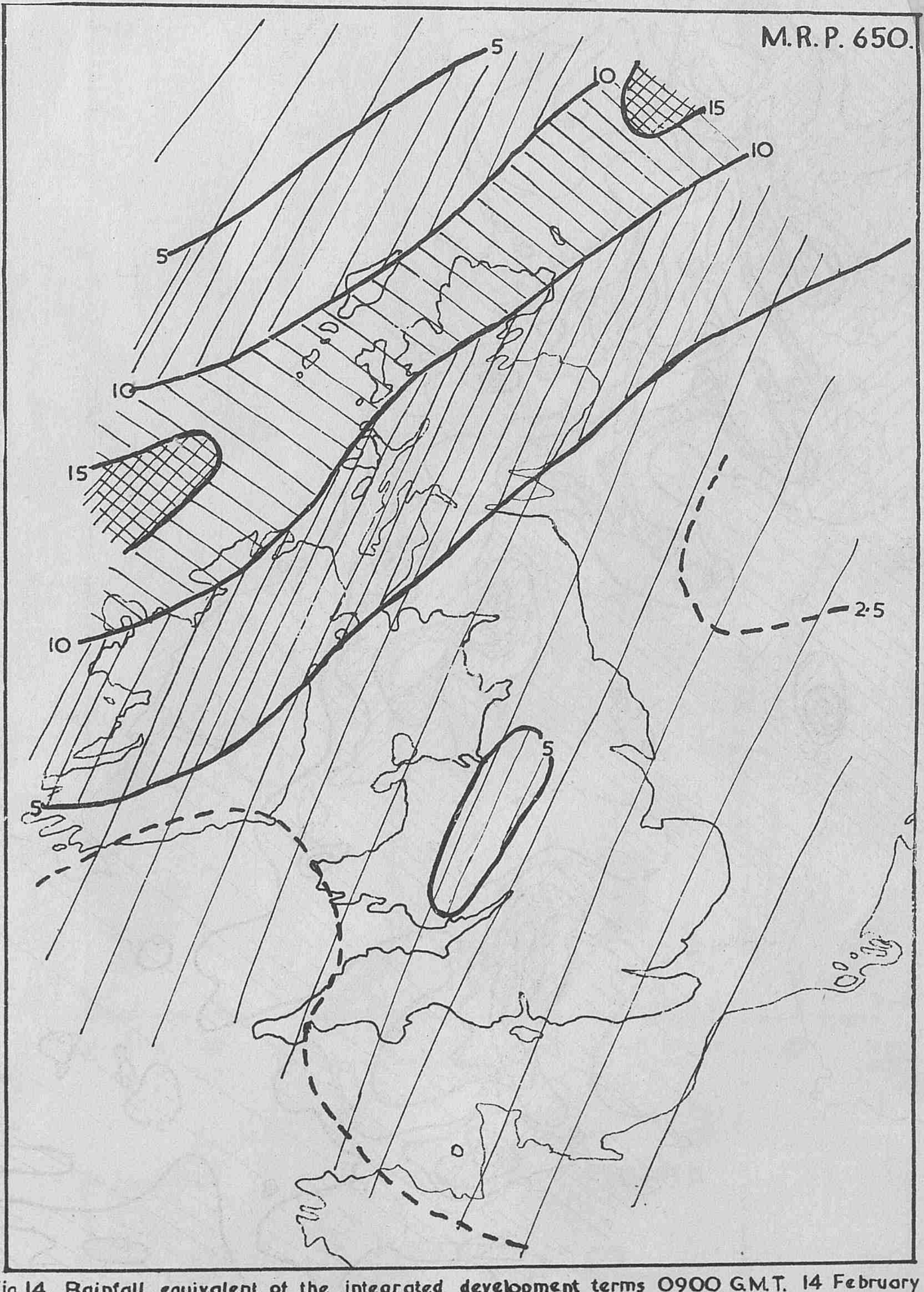
M.R.P. 650.
5
5
10
15
10
10
15
10
5
2·5
5

Fig. 14. Rainfall equivalent of the integrated development terms 0900 G.M.T. 14 February 1950 to 0900 G.M.T. 15 February 1950.